frontiers | Research Topics

New mechanisms for anti-cancer drugs

Edited by
Ayaz Shahid and Pranav Kumar Prabhakar

Coordinated by
Ajit Prakash and Saad Mustafa

Published in
Frontiers in Pharmacology
Frontiers in Oncology

ISSN 1664-8714
ISBN 978-2-8325-4784-7
DOI 10.3389/978-2-8325-4784-7

About Frontiers

Frontiers is more than just an open access publisher of scholarly articles: it is a pioneering approach to the world of academia, radically improving the way scholarly research is managed. The grand vision of Frontiers is a world where all people have an equal opportunity to seek, share and generate knowledge. Frontiers provides immediate and permanent online open access to all its publications, but this alone is not enough to realize our grand goals.

Frontiers journal series

The Frontiers journal series is a multi-tier and interdisciplinary set of open-access, online journals, promising a paradigm shift from the current review, selection and dissemination processes in academic publishing. All Frontiers journals are driven by researchers for researchers; therefore, they constitute a service to the scholarly community. At the same time, the *Frontiers journal series* operates on a revolutionary invention, the tiered publishing system, initially addressing specific communities of scholars, and gradually climbing up to broader public understanding, thus serving the interests of the lay society, too.

Dedication to quality

Each Frontiers article is a landmark of the highest quality, thanks to genuinely collaborative interactions between authors and review editors, who include some of the world's best academicians. Research must be certified by peers before entering a stream of knowledge that may eventually reach the public - and shape society; therefore, Frontiers only applies the most rigorous and unbiased reviews. Frontiers revolutionizes research publishing by freely delivering the most outstanding research, evaluated with no bias from both the academic and social point of view. By applying the most advanced information technologies, Frontiers is catapulting scholarly publishing into a new generation.

What are Frontiers Research Topics?

Frontiers Research Topics are very popular trademarks of the *Frontiers journals series*: they are collections of at least ten articles, all centered on a particular subject. With their unique mix of varied contributions from Original Research to Review Articles, Frontiers Research Topics unify the most influential researchers, the latest key findings and historical advances in a hot research area.

Find out more on how to host your own Frontiers Research Topic or contribute to one as an author by contacting the Frontiers editorial office: frontiersin.org/about/contact

New mechanisms for anti-cancer drugs

Topic editors

Ayaz Shahid – Western University of Health Sciences, United States

Pranav Kumar Prabhakar – Lovely Professional University, India

Topic coordinators

Ajit Prakash – University of North Carolina at Chapel Hill, United States

Saad Mustafa – Jamia Millia Islamia, India

Citation

Shahid, A., Prabhakar, P. K., Prakash, A., Mustafa, S., eds. (2024). *New mechanisms for anti-cancer drugs*. Lausanne: Frontiers Media SA.

doi: 10.3389/978-2-8325-4784-7

Table of contents

frontiers | Frontiers in Pharmacology

TYPE Editorial
PUBLISHED 05 April 2024
DOI 10.3389/fphar.2024.1387942

OPEN ACCESS

EDITED AND REVIEWED BY
Antonella D'Anneo,
University of Palermo, Italy

*CORRESPONDENCE
Ayaz Shahid,
ashahid@westernu.edu

RECEIVED 18 February 2024
ACCEPTED 25 March 2024
PUBLISHED 05 April 2024

CITATION
Shahid A, Prakash A, Mustafa S and Prabhakar PK (2024), Editorial: New mechanisms for anti-cancer drugs.
Front. Pharmacol. 15:1387942.
doi: 10.3389/fphar.2024.1387942

Editorial: New mechanisms for anti-cancer drugs

Ayaz Shahid[1]*, Ajit Prakash[2], Saad Mustafa[3] and Pranav Kumar Prabhakar[4]

[1]Department of Biotechnology and Pharmaceutical Sciences, College of Pharmacy, Western University of Health Sciences, Pomona, CA, United States, [2]Department of Biochemistry and Biophysics, School of Medicine, University of North Carolina at Chapel Hill, Chapel Hill, NC, United States, [3]Department of Geriatric Medicine, All India Institute of Medical Science, New Delhi, India, [4]Department of Research Impact and Outcome, Division of Research and Development, Lovely Professional University, Phagwara, India

KEYWORDS

anti-cancer drug, nanotechnology-based drug delivery systems, natural product, biomarker, cell signaling

Editorial on the Research Topic
New Mechanisms for Anti-Cancer Drugs

Cancer is one of the leading causes of death globally (Siegel et al., 2023). Ongoing investigations aim to discover and develop new drugs for treating cancer (Debela et al., 2021). However, identifying and evaluating the effectiveness of drugs poses a significant challenge. The Research Topic of "New Mechanisms for Anti-Cancer Drugs" is focused on gathering different studies that highlight innovative chemical or natural compounds with unique modes of action to target cell signaling pathways and exert cytotoxic effects on cancer cells. This Research Topic is an amalgamation of preclinical and clinical studies and review articles.

Overall, the studies presented in this Research Topic are significant in advancing our knowledge of cancer biology, biomarkers, and possible therapeutic approaches. The use of natural compounds, nanotechnology, and repurposed drugs represents the multifaceted efforts made to combat cancer. Together, these studies represent a promising step forward in the fight against cancer.

In a groundbreaking series of studies, investigators have discovered new insights into the potential of various compounds and plant extracts to combat different types of cancer. A study by (Petronek et al.) discovered that sirtinol, an intracellular iron chelator, can cause metabolic changes in non-small cell lung cancer (NSCLC) cells. Sirtinol also reduces labile iron pools and triggers an adaptive response that increases iron uptake and decreases storage, particularly in KRAS/STK11/KEAP1 mutant cells. This study demonstrated that sirtinol exhibits cytotoxic effects on NSCLC cells, which is attributed to its iron-chelating function. However, these effects are context-dependent and vary based on the genetic background differences in iron regulation and dependency between KRAS/STK11/KEAP1 mutant and wild-type cells. In another study, (Reddy et al.) found that Terminalia chebula fruit extract (TCF) has anti-proliferative effects against MCF-7 breast cancer cells by inducing cell cycle arrest at the G2/M phase and inhibiting EGFR signaling pathways. TCF phytochemical saccharopine shows potential as an anti-cancer agent, but further studies are needed to evaluate its efficacy and safety. A study by (Chandrasekaran et al.) discovered that cumin seed extracts are highly effective against bone cancer cell line MG63, showing an LC50 of 86 µg/mL. Cumin seed extracts have

potential anti-cancer and antimicrobial properties with key compounds identified as phthalic acid, propanal, and methyl esters. In another study, (Rong et al.) suggest that vitamin D3 may prevent colorectal cancer by targeting mainly 10 proteins. It regulates biological processes and affects signaling pathways that control cancer mechanisms. Molecular docking analysis suggests it can directly bind to the predicted 10 proteins. Vitamin D3 anti-cancer properties were validated through bioinformatics analysis and animal experiments. These findings offer new prevention and treatment strategies for colorectal cancer. Wu et al. conducted a study that found curcumin can inhibit colon cancer cell growth and movement. The authors identified 3,505 genes upregulated in colon cancer cells treated with curcumin, including 37 genes acting as tumor suppressors. Molecular docking analysis showed that curcumin may disrupt the ARHGEF12-RhoA complex, suppressing cancer cell invasion. Another study by (Han et al.) revealed that maltol has anti-cancer properties against melanoma cells. It reduces melanin production and hinders the growth of cancer cells by inducing a pause in their cell cycle. Maltol also boosts apoptosis or programmed cell death and has a synergistic anti-cancer effect when combined with chemotherapy drugs. Additionally, maltol suppresses PD-L1 expression in melanoma cells, which can decrease immunotherapy resistance and enhance tumor cell killing. A study by (Chen et al.) aimed to investigate the influence of Danshen, a Chinese herbal medicine, on the clinical outcomes of bladder cancer patients. The study gathered data from Taiwan's National Health Insurance database. Patients treated with Danshen had a lower incidence of major adverse cardiac events and improved survival rates. It was linked to a 44% reduction in MACE risk and a 40% decrease in mortality risk compared to non-Danshen patients, suggesting its potential to lower cardiovascular risks and improve outcomes. Together, these studies offer a multifaceted approach to cancer treatment and prevention, showcasing the diverse therapeutic potential of natural compounds in combating various cancer types.

An investigation led by Zhang and colleagues (Zhang et al.) has discovered that GLS, an overexpressed protein in multiple types of cancer, including breast cancer, can differentiate breast cancer cells from normal tissue samples. The reduction of GLS protein promotes the growth and spread of breast cancer cells, and its expression is associated with the immune system's response to breast cancer. Therefore, GLS may serve as a useful diagnostic biomarker with potential functional implications for the diagnosis and treatment of breast cancer. Expanding on this theme, (Zhang et al.) identified 14 genes as prognostic markers for lung adenocarcinoma (LUAD) that are related to the basement membrane (BM). These genes are part of pathways that contribute to cancer progression. The study also established a link between the BM gene signature and immune cell infiltration. The authors developed a risk model based on these genes with good predictive ability. Additionally, the study identified 12 small-molecule drugs that have inhibitory effects against LUAD and suggested that cyclopamine and docetaxel could be more beneficial for low-risk patients. At the same time, Jamal and colleagues (Jamal et al.) found that the chemokine receptor CCR9 promotes the infiltration of T-ALL cells into tissues, leading to increased cholesterol biosynthesis and disease progression. It showed that statins could be beneficial in treating aggressive forms of breast cancer. To sum up, GLS is a diagnostic biomarker for breast cancer, while genes linked to the basement membrane are prognostic markers for lung adenocarcinoma. CCR9 promotes T-ALL cell infiltration, and statins may be used for treatment. These findings can enhance the accuracy of diagnosis and lead to personalized treatment options. In conclusion, these studies highlight the significance of ongoing research and collaboration in the battle against cancer.

Various studies also have shown that nanotechnology-based drug delivery systems can be effective in targeted cancer therapy, and these systems may have the potential to be further developed in the future. One such study by (Hussein et al.) aimed to determine the effectiveness of two types of niosomes in fighting cancer in breast cancer cell lines. The two types of niosomes tested were carnosine-loaded niosomes (Car-NIO) and melittin-loaded niosomes (Mel-NIO). The study showed that Mel-NIO has a stronger anti-cancer activity against breast cancer cells than Car-NIO. However, both Car-NIO and Mel-NIO are able to reduce lipid peroxidation and stop the progression of the cell cycle in cancer cells. In a similar vein, (Akbar et al.) developed nanoparticles of a metal-organic framework (MOF) coated with chitosan that is conjugated with folic acid (FC). The MOFs are bi-metallic FeCo-based MOFs (bi-MIL-88B), which selectively deliver an anti-cancer drug, 5-fluorouracil (5-FU), to FR-overexpressing cancer cells. The FC coating allows for pH-responsive and sustained release of 5-FU in the tumor microenvironment. This system has the potential for combined chemo and hemodynamic therapy. In conclusion, nanotechnology-based drug delivery systems have shown promising results in targeted cancer therapy. Both Car-NIO and Mel-NIO were able to reduce lipid peroxidation and stop the progression of the cell cycle in cancer cells. However, Mel-NIO was found to have stronger anti-cancer activity against breast cancer cells compared to Car-NIO. Akbar et al. developed MOFs coated with chitosan and conjugated with folic acid, which have the potential for combined chemo and hemodynamic therapy. These findings provide hope for developing more effective cancer treatments in the future.

Several review articles have highlighted the potential of natural products, such as flavonoids, alkaloids, and phytochemicals, in treating different cancers. A review article by (Khan et al., 2023) discussed the potential of plant-based compounds in reversing abnormal epigenetic changes in cancer cells. These plant-based compounds can alter DNA methylation, histone modifications, and microRNA expression. For example, compounds such as curcumin, EGCG, genistein, quercetin, and resveratrol can regulate the expression of genes involved in apoptosis, cell cycle control, DNA repair, etc., which are often dysregulated in cancer. However, their bioavailability and clinical evidence are still limited. Another review by (Zhou et al.) emphasized the potential of natural products such as flavonoids and alkaloids in treating endometrial cancer. These natural products have anti-cancer effects on endometrial cancer cells by regulating apoptosis. They act on signaling pathways that play a role in apoptosis, including the mitochondrial pathway, MAPK pathway, PI3K/AKT/mTOR pathway, and NF-κB pathway. Combining natural products with chemotherapeutic agents may have synergistic effects, but developing natural product-based therapies faces challenges of toxicity and bioavailability. (Zhan et al.) highlighted the numerous phytochemicals present in medicinal plants that can

impede glycolysis and the Warburg effect in colorectal cancer cells. These phytochemicals target various enzymes, transporters, and pathways to affect glycolysis. Inhibition of the glycolytic pathway reduces proliferation and metastasis and increases sensitivity to chemotherapeutics in colorectal cancer. Furthermore, (Zhang et al.) discussed the potential of natural products to inhibit tumor growth and enhance cell death. These products target the endoplasmic reticulum stress (ERS) pathway, which promotes apoptosis in tumor cells. The authors summarized 69 natural products that can regulate ERS and induce apoptosis in various cancers. However, more research is needed to fully understand mechanisms, conduct clinical trials, and evaluate safety. In another review article by (Cao et al.), the alkaloid leonurine demonstrated anti-tumor properties in preclinical studies. It has been shown to inhibit cancer cell proliferation, induce apoptosis and autophagy, and reduce invasion and migration. However, further clinical research is necessary to validate the safety, pharmacology, and potential of leonurine as an anti-cancer agent or drug. In conclusion, plant-based compounds and natural products can target various aspects of cancer biology. However, challenges like bioavailability, toxicity, and clinical evidence persist, necessitating further research. These findings offer promising avenues for developing novel anti-cancer strategies based on natural products.

One study by (Wang et al.) found that abnormal lipid metabolism is a significant characteristic of cancer, especially hepatocellular carcinoma (HCC). Using statins, such as simvastatin, can reduce the risk of HCC and improve outcomes with immunotherapy in cancer patients. Combining statins with ICIs may improve immunotherapy in HCC, but determining the optimal dose and managing side effects remains challenging. Natural compounds and repurposed drugs are being explored as potential therapeutic strategies, but further research is needed to implement these approaches. Another review by (Zhang and Yu) explores the interaction between Wnt signaling and DNA damage response (DDR) pathways. These pathways, which comprise several components, including β-catenin, APC, Axin, GSK-3β, and p53, are crucial factors impacting cancer development and its resistance to therapy. Targeting the Wnt and DDR pathways simultaneously could help overcome therapy resistance in cancer. However, more research is needed to understand the molecular mechanisms involved in their interaction fully. Riccardi et al. explain how Antibody-drug conjugates (ADCs) work to deliver chemotherapy directly to cancer cells, reducing the damage to healthy cells. ADCs consist of a monoclonal antibody, a stable linker, and a cytotoxic payload. Their mechanism involves binding specific antigens on the surface of cancer cells, which triggers internalization and drug release. There are approved ADCs for cancer treatment, but they have toxicities related to cytotoxic payloads. Combination therapies and further research can expand their use. Buczyńska et al. highlight the therapeutic landscape beyond traditional boundaries, showing that medications used for treating diabetes, such as DPP-IV and SGLT2 inhibitors, can potentially be effective in treating papillary thyroid cancer (PTC). These drugs target glucose metabolism and the Warburg effect, which may help reduce PTC tumor growth and cell migration. However, further research is required to identify biomarkers for patient stratification and carry out well-designed clinical trials to evaluate the safety and efficacy of these drugs. Emerging therapies like Wnt/DDR inhibitors and natural products like leonurine hold potential, but more research is needed to realize their clinical promise.

This editorial concludes that various chemical compounds such as sirtinol, TCF, cumin seed extract, and Vitamin D3 have potential anti-cancer properties. It also discussed the anti-cancer effect of carnosine, melittin-loaded niosomes, and folic acid-coated metal-organic framework nanoparticles. Furthermore, it explains how GLS can be used as a diagnostic biomarker for diagnosing and treating breast cancer. Several review articles have also discussed prevention and treatment strategies for different types of cancers. All these findings bring hope for the future of cancer treatment as various anti-cancer compounds with unique mechanisms of action have shown potential for future cancer treatments.

Author contributions

AS: Conceptualization, Writing–original draft, Writing–review and editing. AP: Writing–review and editing. SM: Writing–review and editing. PP: Writing–review and editing.

Funding

The author(s) declare that no financial support was received for the research, authorship, and/or publication of this article.

Acknowledgments

We thank the authors, editors, and reviewers who contributed to this Research Topic.

Conflict of interest

The authors declare that the research was conducted in the absence of any commercial or financial relationships that could be construed as a potential conflict of interest.

Publisher's note

References

Debela, D. T., Muzazu, S. G., Heraro, K. D., Ndalama, M. T., Mesele, B. W., Haile, D. C., et al. (2021). New approaches and procedures for cancer treatment: current perspectives. *SAGE Open Med.* 9, 20503121211034366. doi:10.1177/20503121211034366

Khan, A., Khan, A., Khan, M. A., Malik, Z., Massey, S., Parveen, R., et al. (2023). Directional preference for glioblastoma cancer cell membrane encapsulated nanoparticle population: a probabilistic approach for cancer therapeutics. *Front. Pharmacol.* 14, 1257289. doi:10.3389/fimmu.2023.1162213

Siegel, R. L., Miller, K. D., Wagle, N. S., and Jemal, A. (2023). Cancer statistics, 2023. *CA Cancer J. Clin.* 73 (1), 17–48. doi:10.3322/caac.21763

frontiers | Frontiers in Pharmacology

TYPE Original Research
PUBLISHED 05 May 2023
DOI 10.3389/fphar.2023.1185380

OPEN ACCESS

EDITED BY
Ayaz Shahid,
Western University of Health Sciences, United States

REVIEWED BY
Jogendra Singh Pawar,
The Ohio State University, United States
Nashrah Sharif Khan,
University of Delhi, India

*CORRESPONDENCE
Li Wang,
394004312@qq.com

RECEIVED 13 March 2023
ACCEPTED 24 April 2023
PUBLISHED 05 May 2023

CITATION
Zhang Y, Li T, Liu H and Wang L (2023), Function and prognostic value of basement membrane -related genes in lung adenocarcinoma.
Front. Pharmacol. 14:1185380.
doi: 10.3389/fphar.2023.1185380

Function and prognostic value of basement membrane -related genes in lung adenocarcinoma

Yurong Zhang[1], Tingting Li[2], Huanqing Liu[3] and Li Wang[1]*

[1]Department of Scientific Research, The First Affiliated Hospital, Xi'an Medical University, Xi'an, Shaanxi, China, [2]Department of Pharmacy, Xi'an Chest Hospital, Xi'an, Shaanxi, China, [3]Information Construction and Management Office, Northwest Polytechnical University, Xi'an, Shaanxi, China

Background: Lung adenocarcinoma (LUAD) has become a common cause of cancer-related death. Many studies have shown that the basement membrane (BM) is associated with the development of cancer. However, BM-related gene expression and its relationship to LUAD prognosis remains unclear.

Methods: BM-related genes from previous studies were used. Clinical and mRNA expression information were obtained from TCGA database. Cox, minimum absolute contraction, and selection operator regression were applied to analyze the selected genes affecting LUAD prognosis. A prognostic-risk model was then established. Furthermore, this study applied Kaplan-Meier analysis to assess the outcomes of high- and low-risk groups, then explored their differences in drug sensitivity. The DSigDB database was used to screen for therapeutic small-molecule drugs.

Results: Fourteen prognostic models based on BM-related genes were successfully constructed and validated in patients with LUAD. We also found that independence was a prognostic factor in all 14 BM-based models. Functional analysis showed that the enrichment of BM-related genes mainly originated from signaling pathways related to cancer. The BM-based model also suggested that immune cell infiltration is associated with checkpoints. The low-risk patients may benefit from cyclopamine and docetaxel treatments.

Conclusion: This study identified a reliable biomarker to predict survival in patients with LUAD and offered new insights into the function of BM-related genes in LUAD.

KEYWORDS

basement membrane, LUAD, prognosis, potential drug candidate, risk score

Abbreviations: LUAD, lung adenocarcinoma; bm, basement membrane; TCGA, The Cancer Genome Atlas; LC, lung cancer; NSCLC, non-small cell lung cancer; LASSO, The least absolute shrinkage and selection operator; GO, Gene Ontology; CC, Cell Composition; MF, Molecular Functionality; BP, Biological Process; KEGG, Kyoto Encyclopedia of Genes and Genomes; STRING, the Search Tool for the Retrieval of Distant Genes Database; CMAP, Connectivity MAP database; ROC, receiver operating characteristic; GSEA, Gene Set Enrichment Analysis; GDSC, Genomics of Drug Sensitivity in Cancer; EMT, epithelial-Mesenchymal transition.

1 Introduction

Served as a common cancer, lung cancer (LC) has become one of the leading causes in humans, with an estimated 5-year survival rate of 19% (Siegel et al., 2020). Non-small cell lung cancer (NSCLC) accounts for about 90% of the total number of LC cases, of which lung adenocarcinoma (LUAD) is considered to be one of the most common histological subtypes of LC. According to statistics, the incidence of LUAD is increasing year by year. Although the prognosis of LUAD continues to improve with the advancement of targeted molecular therapy and immunotherapy, the improvement in LUAD therapeutic outcomes is limited to some patients with specific molecular characteristics, such as driver gene mutations in EGFR (Herbst et al., 2018; Duma et al., 2019). Therefore, an accurate and individualized assessment and the improvement of survival in patients with LUAD remain major challenges.

The basement membrane (BM) plays a crucial role in normal tissues (Yurchenco, 2011), and its proteins participate in the formation, invasion, as well as metastasis of cancer cells. Relevant reports have proposed that stromal cell invasion is essential for the division and growth of tumor cells. BM-related genes have a significant influence on the invasiveness of cancer cells in the oral cavity (Celentano et al., 2021), breast (Liu et al., 2018), ovary (Januchowski et al., 2016), etc. Serving as one of the most destructive types of malignancy, the progression of lung cancer is strongly related to the interaction between cells and their matrix environments. Matric stiffness associated with enhanced collagen crosslinking may affect the motility of lung cancer cells (Götte and Kovalszky, 2018). XIX collagen, with certain relevance to types XVIII and XV in the BM zone, has been shown to enhance several types of cancer, distinguishing NSCLC from healthy controls (Liu et al., 2016). XVII collagen has been shown to be essential for maintaining epithelial-Mesenchymal transition (EMT) phenotypes and metastasis in lung cancer stem-like cells. Col XVII inhibits ubiquitination degradation in snails by activating the FAK/AKT/GSK3β pathway by stabilizing laminin-5. Col XVII and Laminin-5 were overexpressed in patients with LC resection, and the prognosis was the worst (Liu et al., 2016). Laminin, the main structural component of BM, is a strong promoter that promotes cell adhesion, migration, differentiation and proliferation through integrins and other cell receptors on the surface. Studies have supported the importance of serum laminin levels as a diagnostic marker in LC patients. Laminin ɣ2 is different melamine adhesion protein 332 a unique subunit, the level in patients with NSCLC was found to be enhanced. Laminin ɣ2 with NSCLC was significantly associated with poor prognosis, especially for the early cases (Tas et al., 2016; Teng et al., 2016). Therefore, the speculation that BM-related genes may be closely related to the occurrence and development of LUAD is worth further study, and these proteins have been identified as biomarkers that can be used to predict, diagnose, or treat LUAD.

In recent decades, great strides have been made in the field of BM, from understanding basic BM-related cancer characteristics to identify the underlying genetic changes that drive unique gene expression programs and promote tumor development. Therefore, it is necessary to better understand the effects of BM on the progression and treatment of LUAD to lay the foundation for further research. However, few studies mentioned the relationship between BM related genes and progression of LUAD. This study investigated changes in BM-related gene expression in both LUAD and normal lung tissues and their prognostic value for LUAD based on bioinformatics methods. Using statistical methods, a prognostic feature was successfully constructed and verified based on 14 BM-related genes, which may predict the prognosis of LUAD in an effective way. Additionally, we also demonstrated the prognostic characteristics of LUAD were correlated with the immune microenvironment, offering a theoretical basis for the application of immune checkpoint in LUAD therapy. Subsequently, Twelve small molecule drugs that may participate in LUAD therapy were found, opening a new path for the development of drugs to treat LUAD.

2 Materials and methods

2.1 Acquire data and patient samples

The study acquired clinicopathological data and mRNA expression of LUAD patients from TCGA database (https://cancergenome.nih.gov/), namely, sex, age, staging status, TMN type, survival status, and survival duration. Finally, the relevant information of normal lung tissues of 19 patients and LUAD tissues of 414 patients were screened from the TCGA database. Total of 224 BM-related genes were identified through a literature search (Jayadev et al., 2022).

2.2 Identify differentially expressed BM

The R package was applied for the normalization of the collected mRNA expression profiles. And BM-related differentially expressed genes were screened using Limma package of R software within the scope of $|\log FC| > 1$ and FDR < 0.05.

2.3 Functional enrichment analyses

ClusterProfiler software packages were utilized for performing gene ontology (GO) analyses, including Cell Composition (CC), Molecular Functionality (MF), and Biological Process (BP). Kyoto Encyclopedia of Genes and Genomes (KEGG) pathway analyses were carried out using the same software. These were regarded as significantly enriched (FDR and $p < 0.05$).

2.4 Establish PPI network

This study submitted varying expressed BM-related genes to the Search Tool for the Retrieval of Distant Genes Database (STRING) (https://cn.string-db.org/) to obtain information about protein-protein interaction, and visualized the PPI network through Cytoscape software (Ver. 3.7.1). Molecular Complex Detection (MCODE) (Ver. 1.6.1) is a Cytoscape plug-in that identifies regions with dense connections and selects statistically significant models. The key modules with MCODE were identified, of which MCODE score>5, degree cut-off =2, node cut-off = 0.2, maximum depth = 100, and K-score =2.

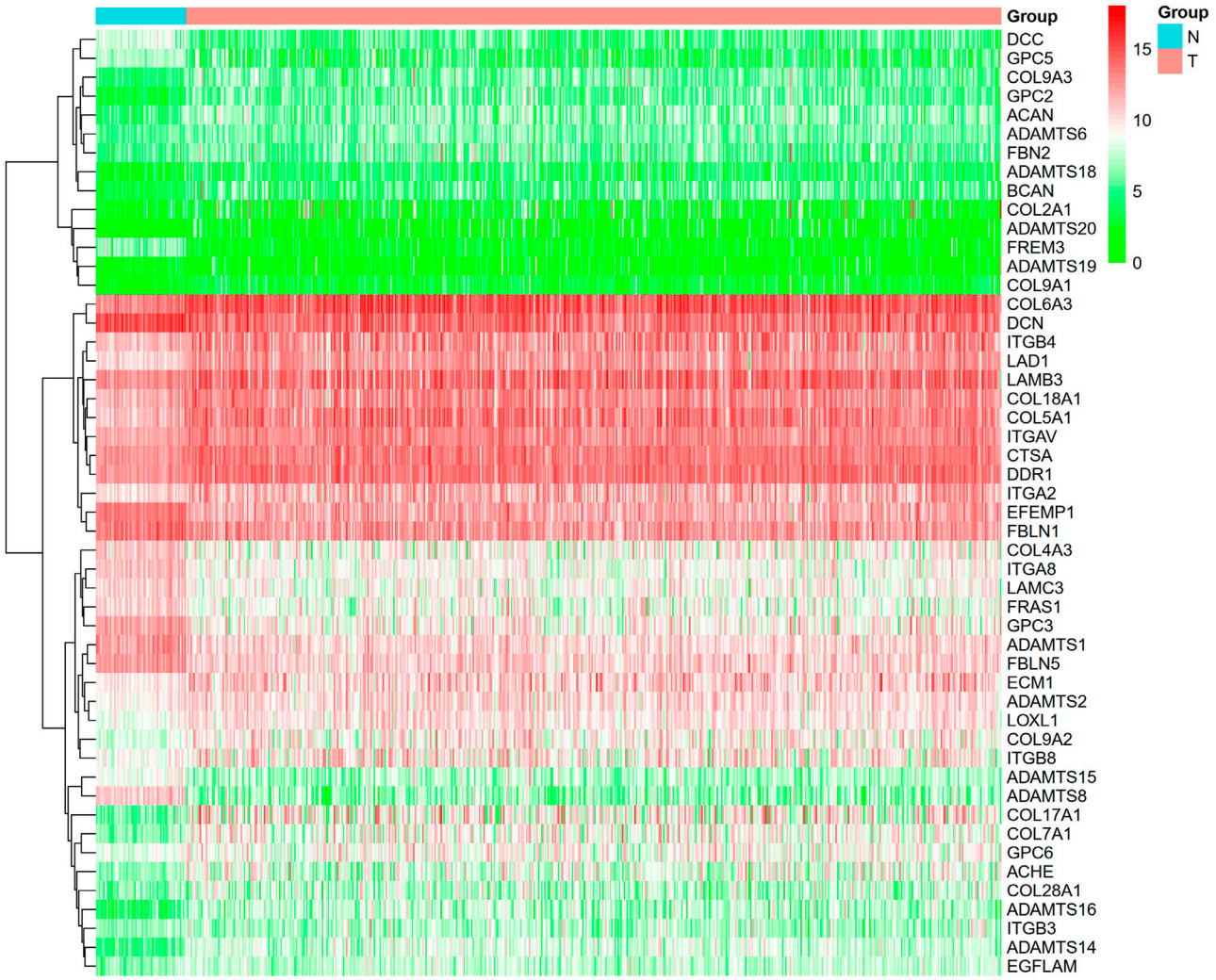

FIGURE 1
Heatmap revealed BM with differential expressions. (green color: low expression; red color: high expression).

2.5 Screen out potential small molecule medication

The differentially expressed genes were updated to the Connectivity MAP database (CMAP) (https://portals.broadinstitute.org/cmap/) to screen out potential BM-related small molecule drugs, which may be used for treating patients with LUAD. The proximity ($-1<p<1$) of compounds associated with the uploaded genes was evaluated accordingly. Thus, it can be concluded that negative drugs can inhibit cancer cells. The threshold values were as follows: $p < 0.01$, N ≥ 3%, non-null =100, and enrichment < −0.8.

2.6 Develop and verify the prognosis model based on BM

The prognostic value of BM-related genes was preliminarily assessed using univariate COX regression. Multivariate COX proportional hazards regression model was applied to access those obtained data. The prognostic value of BM-related genes was first assessed by univariate COX regression. Genes obtained from univariate COX regression model and clinical factors were used in multivariate COX proportional hazard regression model. Only BM genes and clinical factors in the univariate and multivariate COX analyses with $p < 0.05$ were deemed as prognosis factors of LUAD. Then LASSO analysis was employed for constructing prognostic risk model via the glmnet R package. Calculation of risk scores was done through utilization tools with the formula as follows:

$$\begin{aligned} \textit{Risk score} = {} & (\textit{coefficient mRNA1} \times \textit{expression of mRNA1}) \\ & + (\textit{coefficient mRNA2} \times \textit{expression of mRNA2}) \\ & + \cdots + (\textit{coefficient mRNAn} \times \textit{expression mRNAn}) \end{aligned}$$

Patients with LUAD were divided into two groups (high- and low-risk) according to their median risk score. This study used Kaplan-Meier analysis to analyze and compare OS times and applied the surviving ROC package to plot time-dependent receiver operating characteristic (ROC) curves and predict the accuracy of

prognostic indicators. To verify the prognostic value of BM-based characteristics, we randomly selected 30% of TCGA sample data for validation using the same method.

2.7 Conduct gene set enrichment analysis

Gene Set Enrichment Analysis (GSEA) has been applied for exploring potential molecular mechanisms in low- and high-risk populations. Those with $p < 0.05$ and FDR < 25% should be thought to be differences with statistical significance.

2.8 Nomogram construction

The relationship between signatures based on BM-related genes and clinical features was investigated. The univariate and multivariate COX regression analyses were conducted to investigate whether risk scores had independent prognostic value among with LUAD suffers. Clinical characteristics with BM-based signature risk scores were deployed to establish nomogram prognostic maps for LUAD patients with OS of 3 and 5 years.

2.9 Immune cell infiltration analysis

Many algorithms, including McP-counter, ciber-SORT, Cibersor-ABS, QUANTISEQ, XCELL, etc. were applied to assess immune cell infiltration levels in the two groups. To predict the efficacy of immune checkpoints in blocking therapy, we examined the expression of immune checkpoints, such as BTLA, BTNL2, CD27, CD28, CD40LG, and TNFSF15. In addition, the connection between immune cells and 14 BM-related genes was identified through TIMER database (https://cistrome.shinyapps.io/timer/), improving our acquaintance of the functionality of BM-related genes in LUAD.

2.10 Medication sensitivity analyses

The Genomics of Drug Sensitivity in Cancer (GDSC) database (http://www.Cancerxgene.org/) was applied to investigate differences in drug sensitivity, then analyzed the half-maximal inhibitory concentration (IC50) of medication, aiming to predict its sensitivity through the package (pRRophetic). Those with $p < 0.05$ had statistical significance.

2.11 Statistical analyses

Univariate analysis of variance was used to compare gene expression levels in normal lung tissue and LUAD tissue, and Pearson Chi-square test was used to compare categorical variables. To compare OS in different subgroups, Kaplan-Meier method and two-sided log-rank test were used. To assess the independent prognostic value of the risk model, univariate and multivariate Cox regression models were used. Through using Wilcoxon test, distinctions between the two groups were contrasted. $p < 0.05$ meant statistical significance. The Mann-Whitney test was used to compare the immune cell infiltration and immune pathway activation between the two groups. The statistical analysis was performed by using R software (Ver.4.0.5).

3 Results

3.1 Establish and validate BM-based signature

This study identified 93 differentially expressed BM-related genes, of which 31 were downregulated BM related genes and 62 were upregulated in the TCGA-LUAD dataset. The expression of the identified BM related genes is presented as heat maps in Figure 1. According to the abnormal expression value of BM related genes obtained, univariate COX regression analysis was used to probe the prognostic value of BM related genes in LUAD. The results suggested that only 20 genes had prognostic value (Figure 2). The LASSO COX regression analysis was carried out to establish the prognostic significance in LUAD patients. It should be mentioned that a risk model was constructed with a total of 14 genes (TENM3, ADAMTS8, ADAMTS6, TINAG, ITGB4, LAMB3, TIMP1, ITGA8, COL7A1, FBLN5, COL4A3, PAPLN, SPARCL1, and ITGA2) (Figures 3A,B). Calculation of the risk score was conducted using the corresponding coefficients of the 14 BM genes according to the following formula (see Table 1):

$$\begin{aligned}\textit{Risk Score} = {} & (1.60E-04 \times \textit{TENM3 expression}) \\ & + (-3.23E-04 \times \textit{ADAMTS8 expression}) \\ & + (6.64E-05 \times \textit{ADAMTS6 expression}) \\ & + (1.30E-04 \times \textit{TINAG expression}) \\ & + (2.46E-06 \times \textit{ITGB4 expression}) \\ & + (1.49E-06 \times \textit{LAMB3 expression}) \\ & + (4.70E-05 \times \textit{TIMP1 expression}) \\ & + (-6.51E-05 \times \textit{ITGA8 expression}) \\ & + (2.9E-06 \times \textit{COL7A1 expression}) \\ & + (3.54E-05 \times \textit{FBLN5 expression}) + (-3.63E \\ & -05 \times \textit{COL4A3 expression} + (-1.12E \\ & -04 \times \textit{PAPLN expression} + (-8.54E \\ & -06 \times \textit{SPARCL1 expression} \\ & + (1.39E-05 \times \textit{ITGA2 expression})\end{aligned}$$

The results showed that the mortality rate of high-risk patients was significantly higher than that of low-risk patients ($p < 0.001$), suggesting risk scores showed a negative correlation with prognosis (Figures 3C–E). The study used time-dependent ROC analysis to evaluate the specific with sensitive features in prognostic model. And AUCs were 0.676, 0.687, and 0.703 for 1-year, 3-year, and 5-year survival, respectively (Figure 3F). Additionally, we plotted a heatmap of the 14 BM-related genes in patients in the high-risk and low-risk TCGA groups (Figure 3G). To verify the prognostic value of BM-based characteristics, we randomly selected 30% of TCGA sample data for validation using the same method (Figure 4).

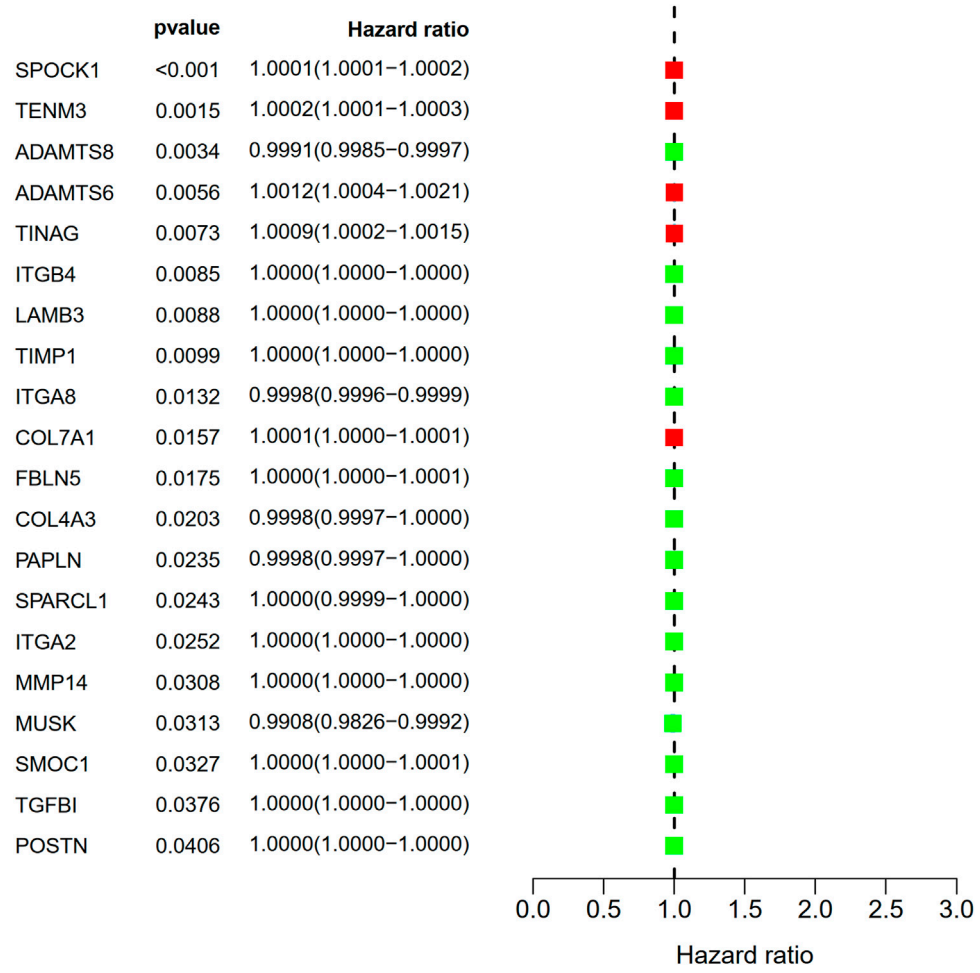

FIGURE 2
Identification of prognostic BM related genes by univariate Cox regression analysis.

3.2 Independent prognosis values of the risk model

The study carried out univariate and multivariate COX analyses to screen out signatures that may be used as independent prognostic indicators. The former indicated that two factors, including risk score and pathologic stage showed a significant correlation with the survival of patients with LUAD ($p < 0.001$) (Figure 5A). The latter showed that these two factors were closely associated with prognosis ($p < 0.05$) (Figure 5B). The above mentioned results suggested BM-based signatures are independent prognostic indicators in patients with LUAD.

3.3 Relationship between clinical characteristics and signatures

The study used Chi-square test to probe into whether the prognostic signature was involved in LUAD progression and development. According to the results, sex ($p < 0.05$), pathologic stage ($p < 0.001$), T stage ($p < 0.05$), M stage ($p < 0.05$), and N stage ($p < 0.005$) were statistically significant, whereas there was no difference statistical in age ($p > 0.05$) (Figures 6A,B). Furthermore, this study conducted a stratified analysis to explore its prognostic significance in some subgroups, such as age, sex, and TNM stage. The results showed that BM-based signatures performed well in those with age>65 years ($p < 0.001$), with female $p = 0.025$ and male $p = 0.043$, together with T1–T2 $p = 0.043$, T3–T4 $p = 0.011$, N0–N1 $p = 0.01$, and M0 $p < 0.001$. However, the BM-based signature had poor predictive ability in age ≤ 65 years ($p = 0.460$), stages I–II ($p = 0.062$), stages III–IV ($p = 0.357$), and N2–N3 ($p = 0.0.952$) (Figure 7).

3.4 Establish a nomogram

The nomogram includes multiple prognostic indicators and can be used to graphically assess individual survival likelihood, which aimed to predict the survival of patients with LUAD. Its indicators included sex, smoking status, age, pathological stage, and risk score (Figure 8A). The results indicated that actual survival was fitted with the predicted value (Figure 8B).

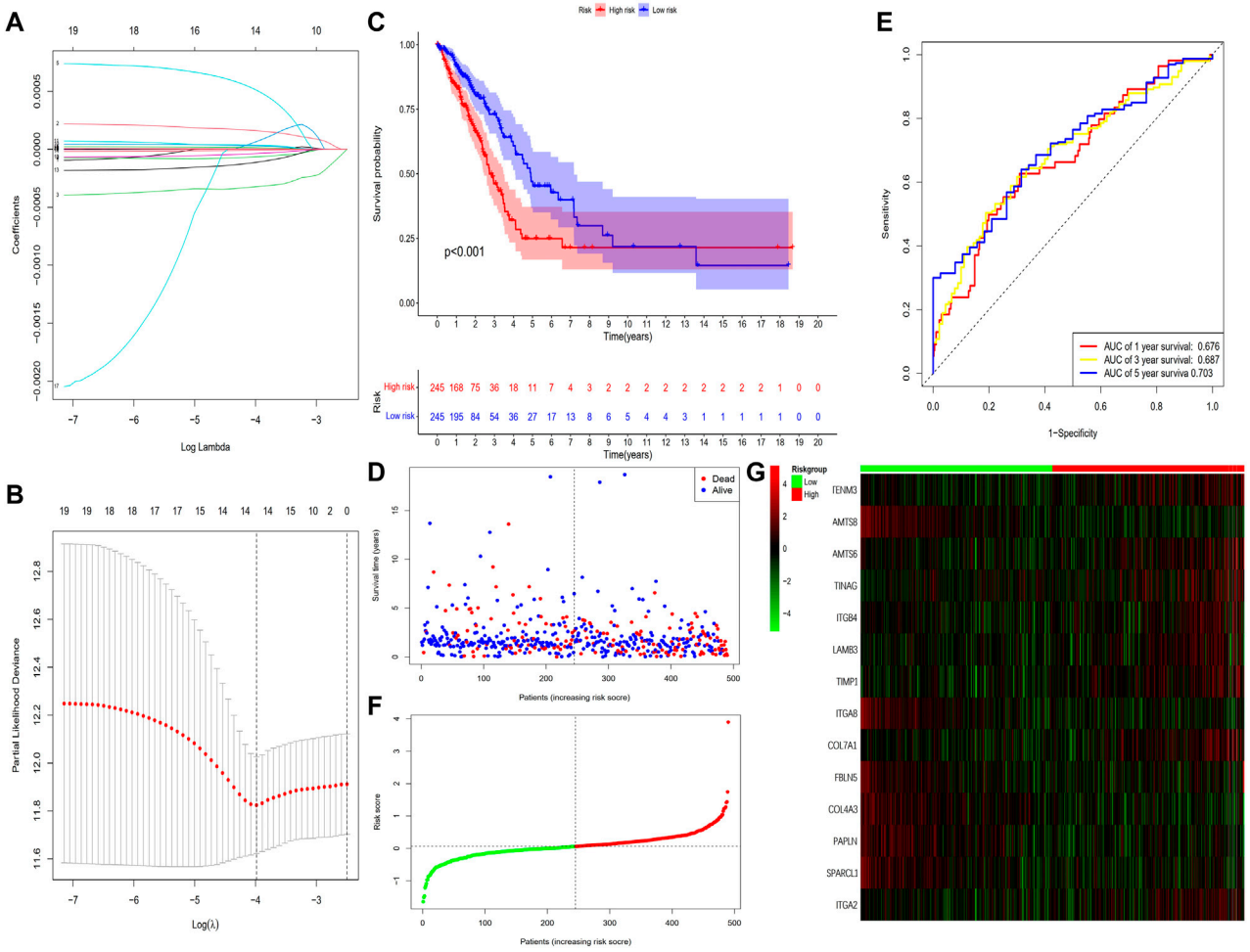

FIGURE 3
Construction of the prognostic BM-based signature in TCGA cohort. **(A)** Identification of prognostic BM related genes by univariate Cox regression analyses. **(B)** LASSO regression of the 14 BM-related genes. **(C)** Cross-validation of the parameter selection adjustment in the LASSO regression. **(D)** Kaplan-Meier survival analysis of LUAD patients between high-risk groups and low-risk groups. **(E)** Distribution of survival status based on the median risk score. **(F)** ROC analysis of risk scores predicting the OS. **(G)** Heatmap showed the differences of 14 BM related genes between high and low-risk patients.

3.5 Functional enrichment analysis and protein-protein interaction (PPI)

GO is a bioinformatics tool for the annotation of functional studies, which is widely applied in Molecular Function (MF), Biological Process (BP), and Cellular Components (CC), whereas KEGG is a repository of genetic network information generated by high-throughput experimental techniques. The potential functions of BM-related genes with different expression levels among the subgroups of the risk model classification were explored using GO and KEGG analyses. We identified 93 BM genes from the two groups in TCGA cohort. BP analysis showed these genes remarkably participated in an extracellular matrix organization and structure organization as well as external encapsulating structure organization; According to CC analyses, collagen with the extracellular matrix, basement membrane and endoplasmic reticulum lumen was commonly enriched; the result of MF analyses showed 93 BM-related genes were primly related to extracellular matrix structural constituent, metalloendopeptidase activity, and metallopeptidase activity (Figure 9A). According to KEGG pathway analysis, ECM–receptor interaction, PI3K–Akt signaling pathway were mainly involved (Figure 9B). The STRING database indicated that the BM PPI network with differential expression consisted of 93 nodes and 582 edges (Figure 9C).

3.6 GSEA analysis

The molecular mechanism of BM-based signature was clarified based on GSEA analysis. The results indicated that the Fc epsilon RI signaling pathway, linoleic acid metabolism, phagosomes, *Salmonella* infection, and spliceosome got main enrichment in high-risk group (Figure 10).

TABLE 1 Gene list and coefficient.

Gene symbol	Coefficient
TENM3	1.60E-04
ADAMTS8	−3.23E-04
ADAMTS6	6.64E-05
TINAG	5.10E-04
ITGB4	2.46E-06
LAMB3	1.49E-06
TIMP1	4.70E-06
ITGA8	−6.51E-05
COL7A1	2.90E-05
FBLN5	3.54E-05
COL4A3	−3.63E-05
PAPLN	−1.1E-04
SPARCL1	−8.54E-06
ITGA2	1.39E-05

3.7 Immune infiltration level analysis on BM-based signature

We explored the connection between BM-based signature and immunity infiltration based on these following analyses; namely, CIBERSORT, TIMER, CIBERSORT, CIBERSORT-ABS, XCELL, EPIC, and MCP-counter analyses, and the outcomes were demonstrated in the heatmap (Figure 11). According to the results of CIBERSORT, the low-risk group patients had higher proportions of B cells, CD4+ T cells, monocytes, myeloid dendritic cells, and mast cells, whereas the high-risk group patients had higher ratios of M0 macrophages and neutrophils. Considering the importance of checkpoint inhibitor immunotherapy, this study carried out the analysis on the relation between key immune checkpoints and risk score (Danilova et al., 2019). More importantly, there exited a great difference in the expression of BTLA, CD28, CD40LG, CD48, CD200R1, CD276, HHLA2, IDO2, TNFSF4, and TNFSF15 between patients in the two groups. Additionally, immune checkpoints were all expressed in high-risk patients, indicating immunosuppressive and failure phenotypes (Figure 12).

3.8 Identify small molecule drugs

This study acquired 12 potential small molecule drugs based on BM from the DsigDB database, including 1 h-pyrazolo[3,4-d] pyrimidine, progesterone, phenytoin, 8-Bromo-cAMP Na, Indeno[1,2,3-cd] pyrene, LAMININ BOSS, LY-294002 PC3 UP, aspirin, Aflodac, anthracene, lamivudine and fluoranthene (Table 2).

3.9 TIMER analysis

The relationship between immune cells and 14 prognostic BM-related genes is crucial and was explored in this study based on the TIMER database. ADAMTS6, ADAMTS8, COL4A3, FBLN5, ITGA2, ITGA8, PAPLN, and TINAG showed positively correlation with immune cells, such as CD4+ T cells, B cells, CD8+ T cells, macrophages, dendritic cells, and neutrophils, whereas TINAG had negative correlation to these immune cells. COL7A1, ITGB4, and LAMB3 were negatively correlated with B cells and CD8+ T cells but had positive associations with CD4+ T cells, neutrophils, and dendritic cells, while COL7A1 was negatively associated with macrophages (Figure 13).

3.10 Drug sensitivity analysis

The study conducted a further investigated the differences in sensitivity to commonly used chemotherapy agents between high-risk and low-risk groups, to improve treatment effects. According to the GDSC database analysis, patients in the later group (high-risk) showed lower IC50 values of Cyclopamine and Docetaxel than those in the former group (low-risk), suggesting patients in the former group were more sensitive to the drugs (Figure 14).

4 Discussion

NSCLC accounts for approximately 85% of all LC cases worldwide. Most of them cannot be cured because of their complex nature and slow progression. Despite advances in molecular targeted therapy and immunotherapy, drug-based chemotherapy may modestly prolong the survival of these patients. However, current treatment outcomes appear to be stagnating, with little significant improvement in response rates or median survival status (Schiller et al., 2002; Scagliotti et al., 2008).

Many studies in recent years have focused on the importance of BM proteins, which are primarily involved in tumorigenesis and evolution. The pore size of transfer membranes may determine BM's stiffness of the BM, which is dependent on the ratio of netrin-4 (NET-4) to laminin molecules. A larger ratio indicates softer BM, thus downregulating the invasive activity of cancer cells (Reuten et al., 2021). Meanwhile, its epithelial-mesenchymal transition enhances epithelial phenotype cells to be transformed into mesenchymal phenotype cells and metastasized through lymphatic vasculature via the metastatic cascade of intravenous and exosmosis, assisting cancer cells in spreading to remote organs from the tumor location (Banyard and Bielenberg, 2015). BM mainly consists of laminin, collagen, and integrins, all of which contribute to the metastasis of tumor cells, making them ideal targets for anticancer drugs (Xiao et al., 2015a; Rousselle and Scoazec, 2020; Su et al., 2020). Some recent studies have discovered that BM-related genes play a variety of functions during tumorigenesis; however, few have analyzed BM-related genes and comprehensively explored the clinical significance of BM in LUAD.

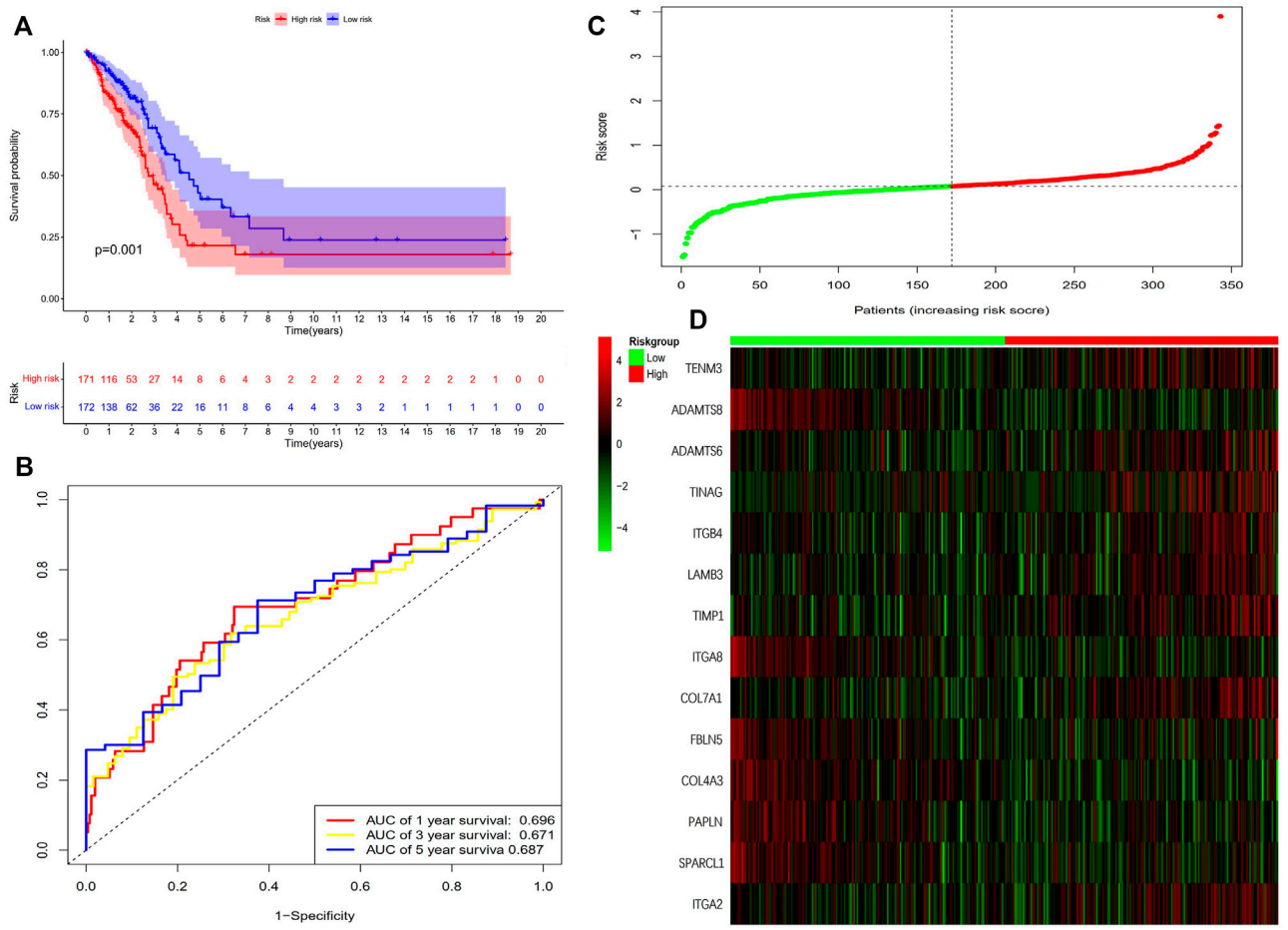

FIGURE 4
Validation of the prognostic BM-based signature. **(A)** Kaplan-Meier survival analysis of LUAD patients between high-risk groups and low-risk groups; **(B)** Time-independent receiver operating characteristic (ROC) analysis of risk scores predicting the overall survival; **(C)** Distribution of survival status based on the median risk score; **(D)** Heatmap showed the differences of 14 BM related genes between high and low-risk patients.

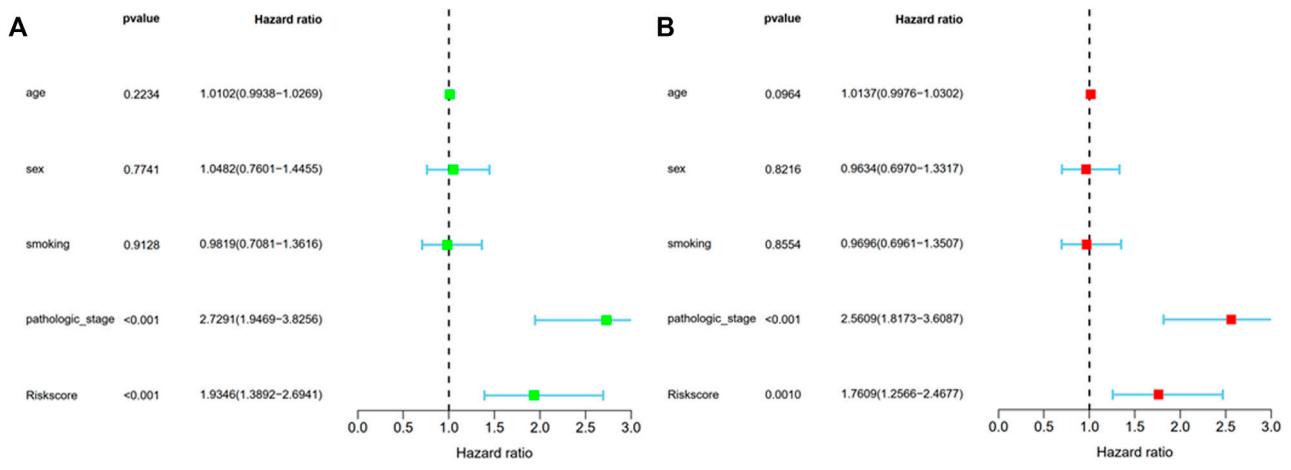

FIGURE 5
Prognosis factor with independency for LUAD in the TCGA cohort. **(A)** The correlations of the risk score for OS with clinical pathology factors through Univariate Cox regression analyses; **(B)** The correlations of the risk score for OS with clinical pathology factors through Multivariate Cox regression analyses.

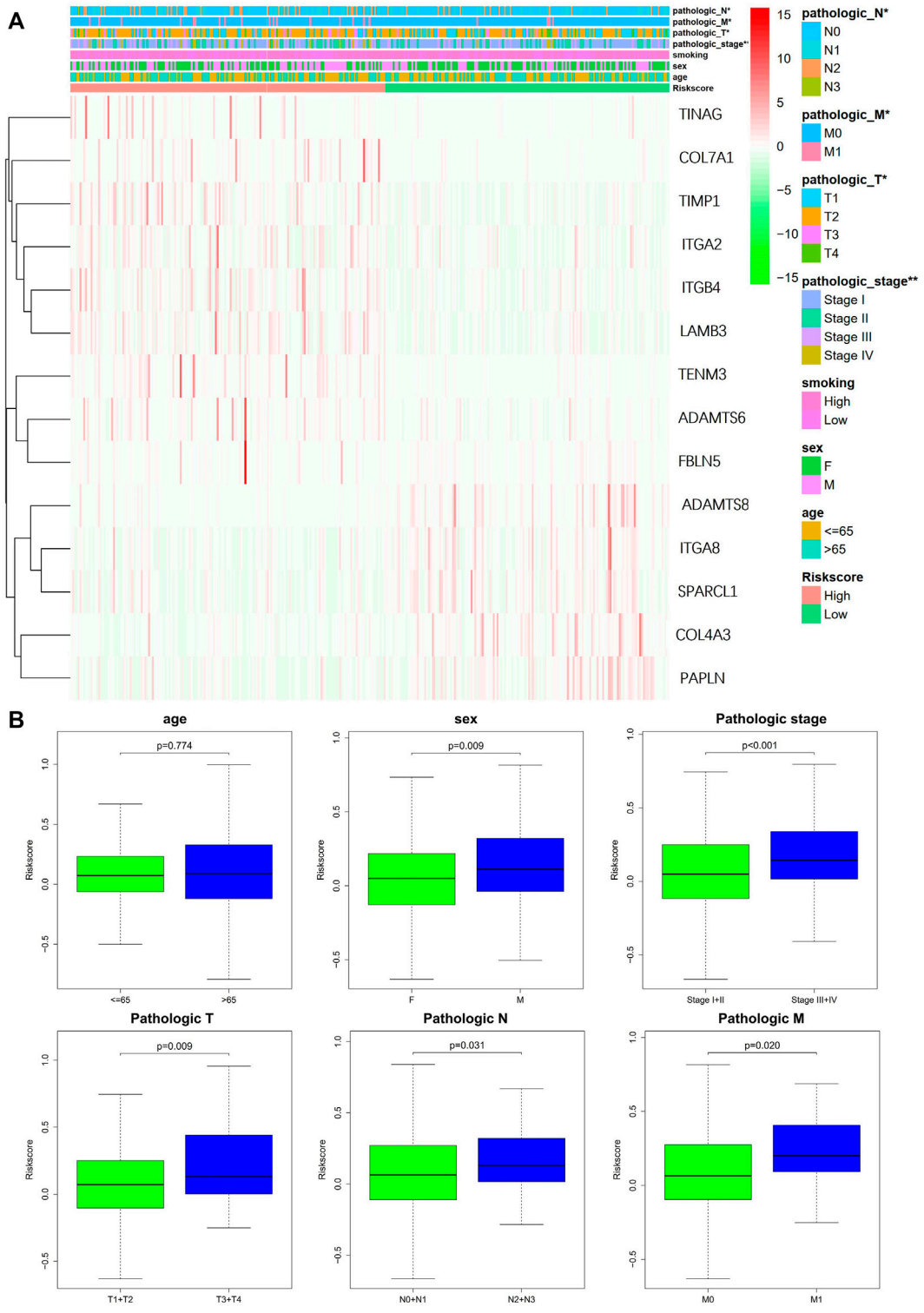

FIGURE 6
Correlation of signature with clinical features. **(A)** Chi-square test of LUAD patients between high- and low-risk groups. **(B)** Stratified analysis of clinical subgroups: prognostic significance of age, sex, and TNM stage.

This study acquired 93 BM-related genes with different expressions in LUAD tissues and normal lung ones from TCGA database, and then conducted COX and LASSO regression analyses to assess the prognostic value of these BM-related genes and identified 14 genes associated with LUAD prognosis: TENM3, ADAMTS8, ADAMTS6, TINAG, ITGB4, LAMB3, TIMP1, ITGA8, COL7A1, FBLN5, COL4A3, PAPLN, SPARCL1, and ITGA2. Subsequently, a risk model which had association with

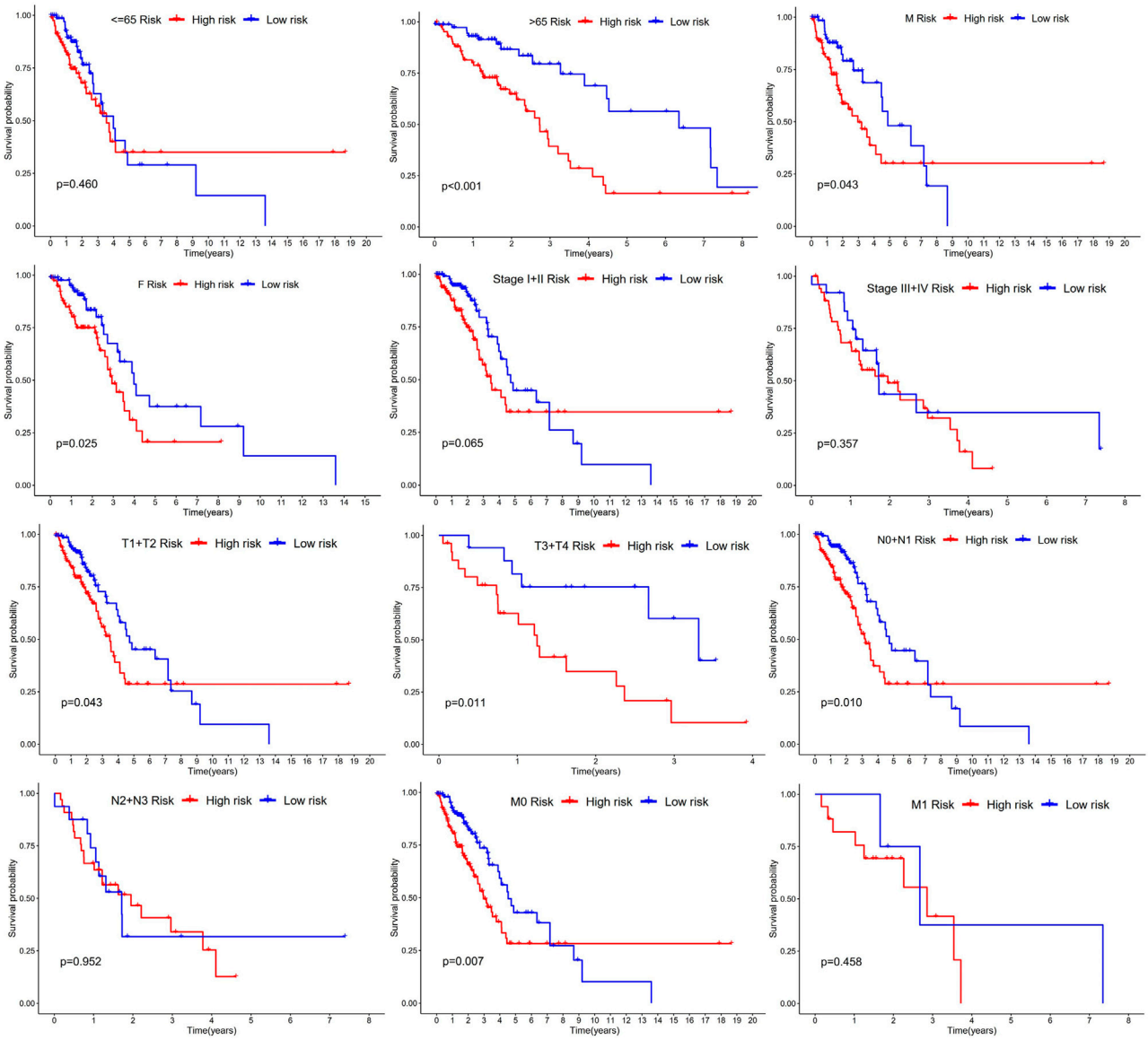

FIGURE 7
Kaplan-Meier curves of OS differences through stratification of age, gender, grade, and TNM stage between the high-risk groups and low-risk groups.

the outcome was established and validated according to the 14 BM related genes. The survival and ROC analyses indicated a good predictive ability of this risk model. Results of AUCs with 1-, 3- and 5-year survival were 0.676, 0.687, and 0.703, respectively. Cox analysis determined that risk scores based on 14 BM-related genes could be an independent prognostic factor for LUAD. In addition, it was found that this signature was related to immune cell infiltration. Simultaneously, 12 small-molecule drugs have been discovered to treat LUAD.

The GO and KEGG analyses were conducted through the "limma" R package, aiming to probe into the potential mechanism of these BM genes in the risk model. Based on the GO enrichment analysis, differential expression was mainly connected with some process terms, namely, extracellular matrix organization and structure organization, together with external encapsulating structure organization. In accordance with KEGG enrichment analysis, BM related genes were involved in ECM– interactions and the PI3K–Akt signaling pathway. It should be mentioned that ECM is identified as one of the major components in the tumor microenvironment. It has been found Collagen is closely associated with ECM function, which may affect the biological behaviors of tumor cells (Riegler et al., 2018). Epithelial functions, including cell differentiation, migration, and invasion, are mediated by physical interactions with the ECM (Lu et al., 2012). Su et al. (2021) used a bioinformatics method to use microarray data and enriched differentially expressed genes in lung cancer via the ECM-receptor interaction pathway. This is consistent with our

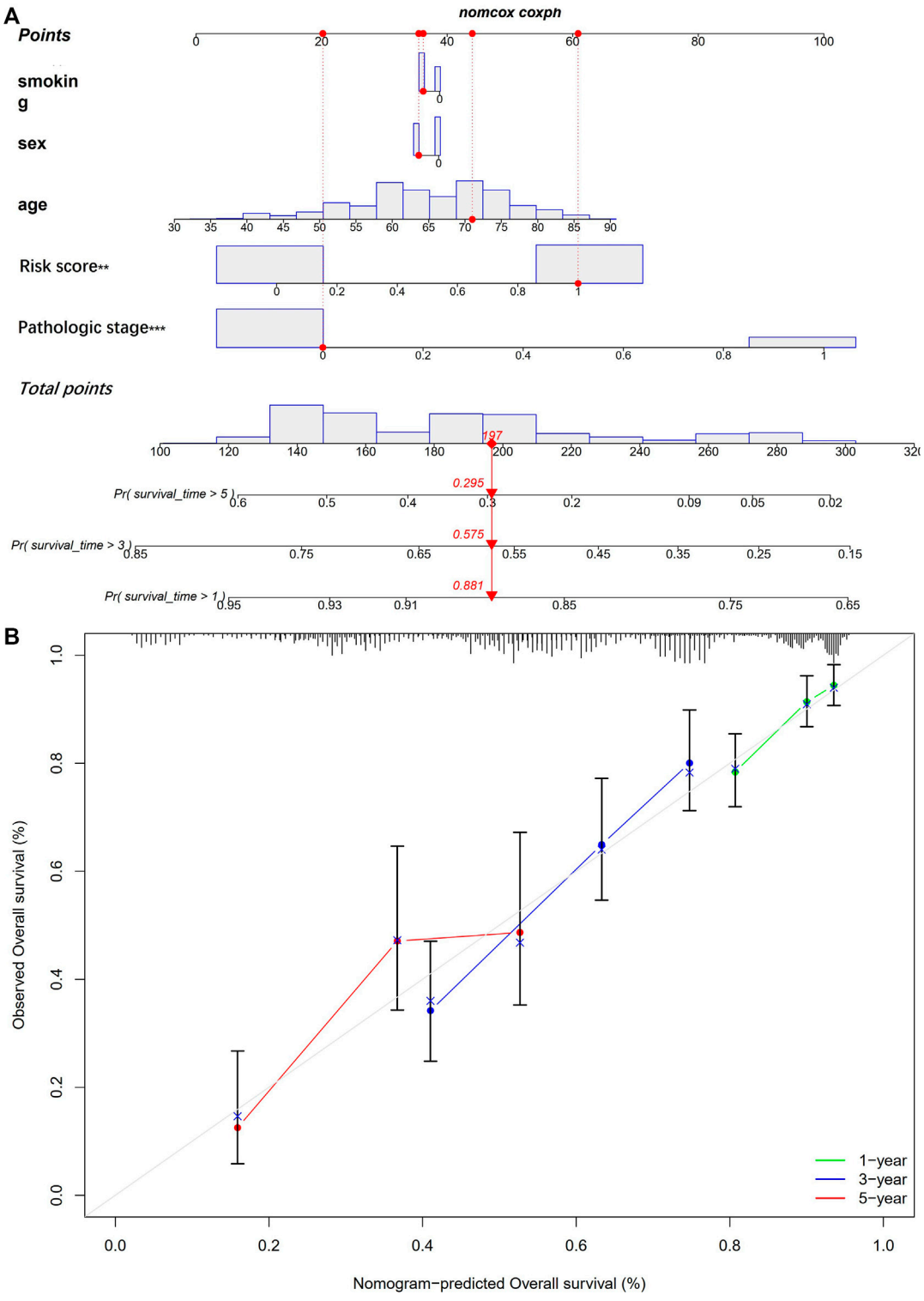

FIGURE 8
Establishment of a nomogram. **(A)** nomogram for prediction of 1-, 3- and 5-year OS; **(B)** The calibration plots for prediction of 1-, 3- and 5-year OS.

results, which indicate that this pathway is crucial for the development and occurrence of LUAD. The PI3K-AKT pathway, a classic cancer-related signaling pathway, increases endothelial tube formation and survival when activated (Cheng et al., 2017). These pathways are closely related to the malignant phenotype of many cancers, suggesting that BM-related genes play key roles in tumorigenesis and development. In addition, 14 BM-related genes of prognostic value were associated with

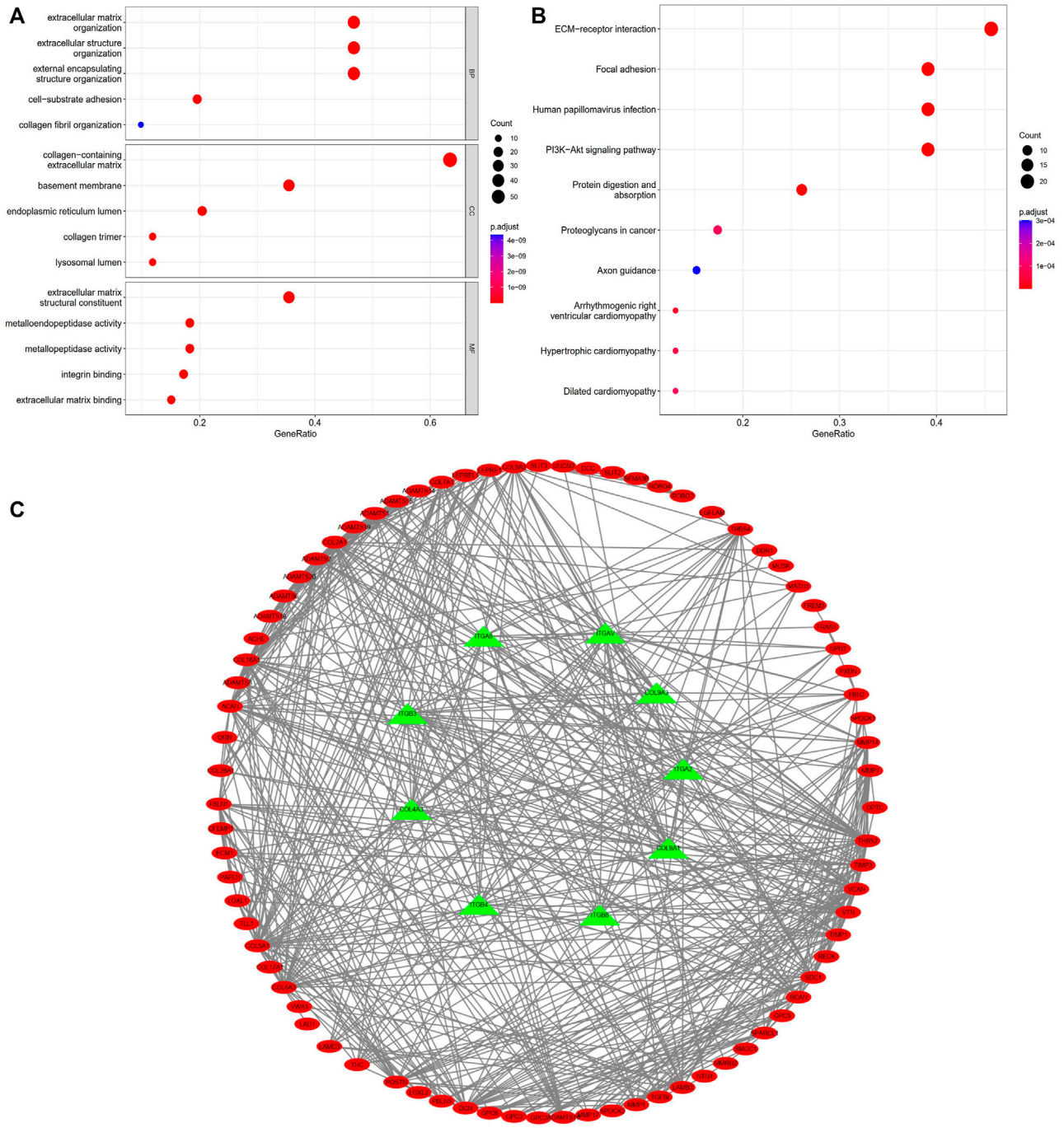

FIGURE 9
Enrichment analyses of differentially expressed BM related genes. **(A)** GO analysis; **(B)** KEGG analysis. **(C)** PPI network of BM related genes with differential expression.

immune cell infiltration, according to TIMER database analysis, suggesting that BM-related genes may promote cancer progression by regulating immune infiltration.

This study identified 14 BM-related genes: TENM3, ADAMTS8, ADAMTS6, TINAG, ITGB4, LAMB3, TIMP1, ITGA8, COL7A1, FBLN5, COL4A3, PAPLN, SPARCL1, and ITGA2), and concluded that these genes may be capable of predicting the OS of patients with LUAD.

TENM3, a member of the conserved Teneurin family, is a highly conserved transmembrane glycoprotein receptor associated with tumor development and drug resistance (Ziegler et al., 2012). The relationship between TENM3 and neuroblastoma has been reported by Hiwatari et al. (Hiwatari et al., 2022), who suggested that TENM3 acts as a novel ALK partner in young adults at high risk for stage 4 neuroblastoma. However, few research has been conducted on this gene in LC, the only studies found that the mutation

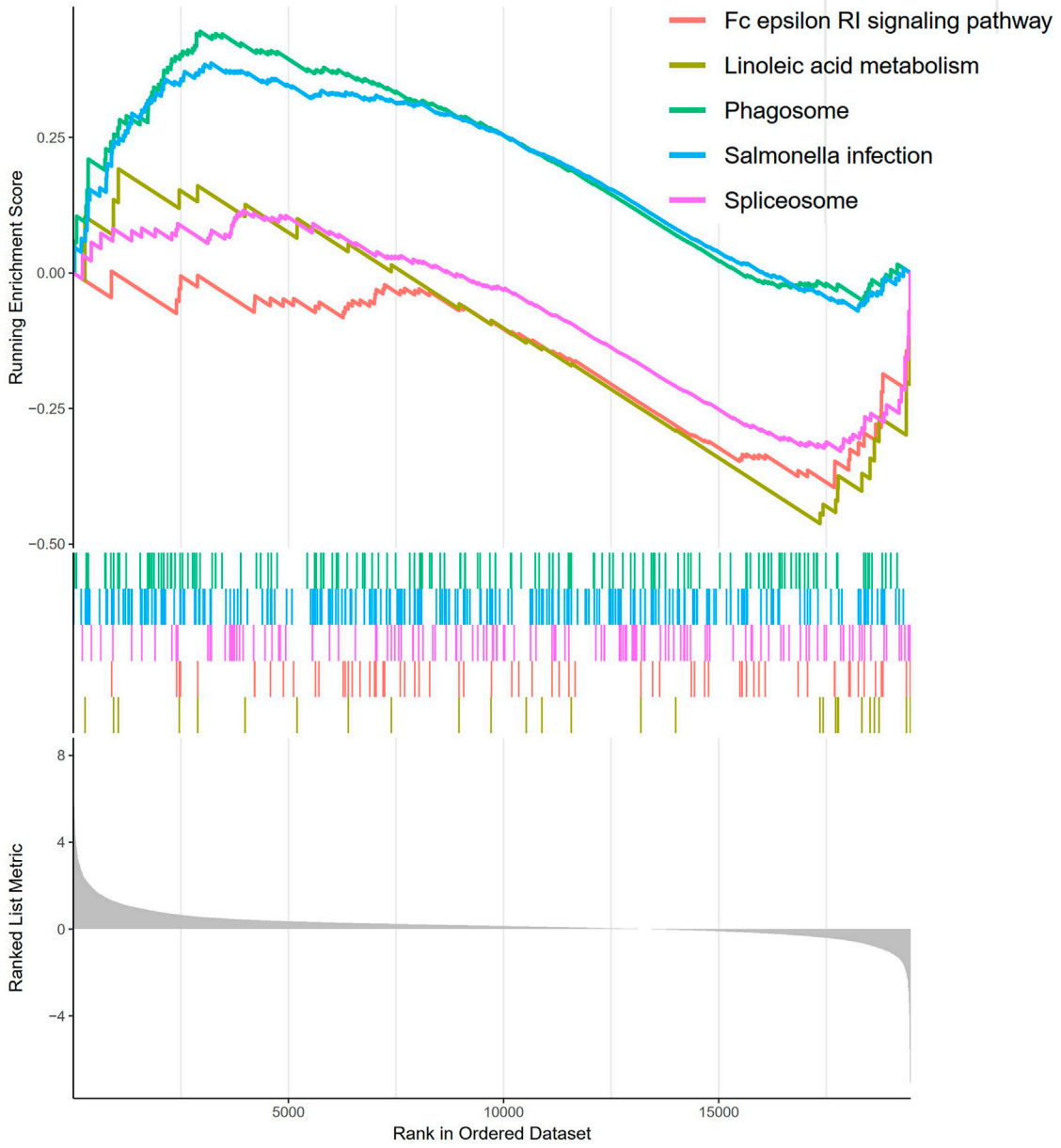

FIGURE 10
GSEA analysis of BM-based signature.

frequency of TENM3 increased significantly in patients with stage III (Liu et al., 2023). Our results can provide clues for future basic and clinical research related to LUAD treatment.

ADAMTS8 serves as a suppressor or oncogene in numerous cancers (Zhong and Khalil, 2019). In breast cancer, its overexpression may be associated with longer OS and progression-free survival, which may take part in cell cycle regulation, and may be related to the EGFR/Akt signaling pathway (Zhang et al., 2022a). Based on some findings, it was lower in NSCLC tissues compared with normal tissues (Dunn et al., 2004). Zhang et al. (2022b) reported that high ADAMTS8 levels had association with higher survival in LC patients. Moreover, it was abnormally downregulated in NSCLC cells. The upregulated proteins may inhibit cell proliferation and promote apoptosis by suppressing VEGFA. Lee et al. (2022) found that ADAMTS8 expression was positively correlated with the recruitment of anti-cancer NKT cells, patients with higher ADAMTS8 levels in wild-type EGFR or low PD-L1 groups survived longer than with low levels of LUAD, suggesting that ADAMTS8 may be a treatment option for patients with lung adenoma who lack effective targeted or immunotherapy. ADAMTS8 acts as a secretory protease to inhibit the EGFR signaling pathway, while phosphorylating MEK and ERK levels are reduced. ADAMTS8 also acts as a functional tumor suppressor by antagonizing EGFR-MEK-ERK signaling to disrupt actin stressed fibrous tissue and inhibit

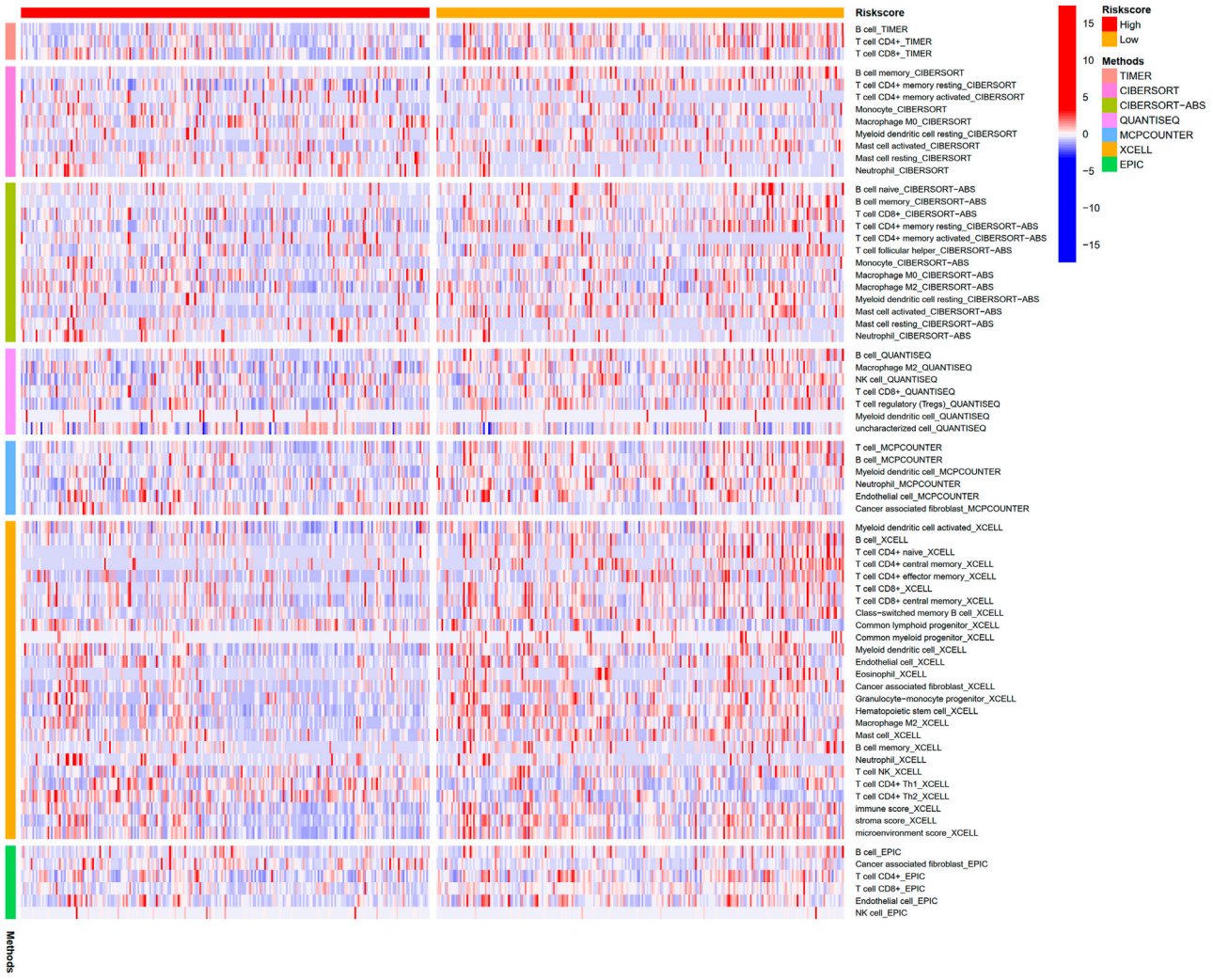

FIGURE 11
Immunity cells infiltration amid high-risk groups and low-risk groups.

tumor cell motility, which is often methylated in common tumors (Choi et al., 2014).

ADAMTS6 is one of members in the ADAMTS family, playing a key role in regulating the progression of many cancers spanning several organ systems, such as breast cancer (Xu et al., 2021) and colorectal cancer (Xiao et al., 2015b). A study using TCGA and RNA-seq data showed that its high expression may be related to poor clinical outcomes in patients with gastric cancer (Zhu et al., 2021). In our analysis, ADAMTS6 was highly expressed in tissues of LUAD patients, mainly in high-risk patients. Luu et al. (2020) found that ADAMTS6 is associated with NSCLC by modulating AGR2, a recently discovered oncogene related to p53. The relationship between ADAMTS6 and NSCLC was further described by Lachat et al. (2020) chromatin immunoprecipitation and qRT-PCR analysis showed that ADAMTS6 expression was upregulated more than 60-fold during EMT and was associated with deletion of the promoter H3K27me3.

TINAG encodes extracellular matrix proteins that are expressed in the tubular BM. Through a literature search, we found that TINAG plays a major role in regulating kidney-related diseases; however, there are few studies on cancer. Zhang et al. (2018) reported TINAG was highly expressed in hepatocellular carcinoma, which was related to three factors: pathological metastasis, pathological stage, and pathological node. It has also been confirmed that PI3K/AKT activation plays a major role in promoting TINAG-mediated migration, proliferation, and invasion. TINAG is a key gene related to the prognosis of pancreatic cancer (Liu et al., 2019). Our results showed that TINAG is highly expressed in LUAD, which is the first time that this gene has been reported in LUAD. Further studies and verifications are required.

Integrins regulate a variety of cellular behaviors in response to cytokines and growth factors by forming transmembrane connections between the extracellular matrix (ECM) and actin cytoskeleton (Thuveson et al., 2019). ITGB4 was upregulated in various tumor types (Mercurio et al., 2001; Thuveson et al., 2019) and was linked to poor prognosis or aggressive behavior (Kurokawa et al., 2008). Mohanty et al. (2020) recently reported that high ITGB4 expression has association with poor prognosis in LUAD

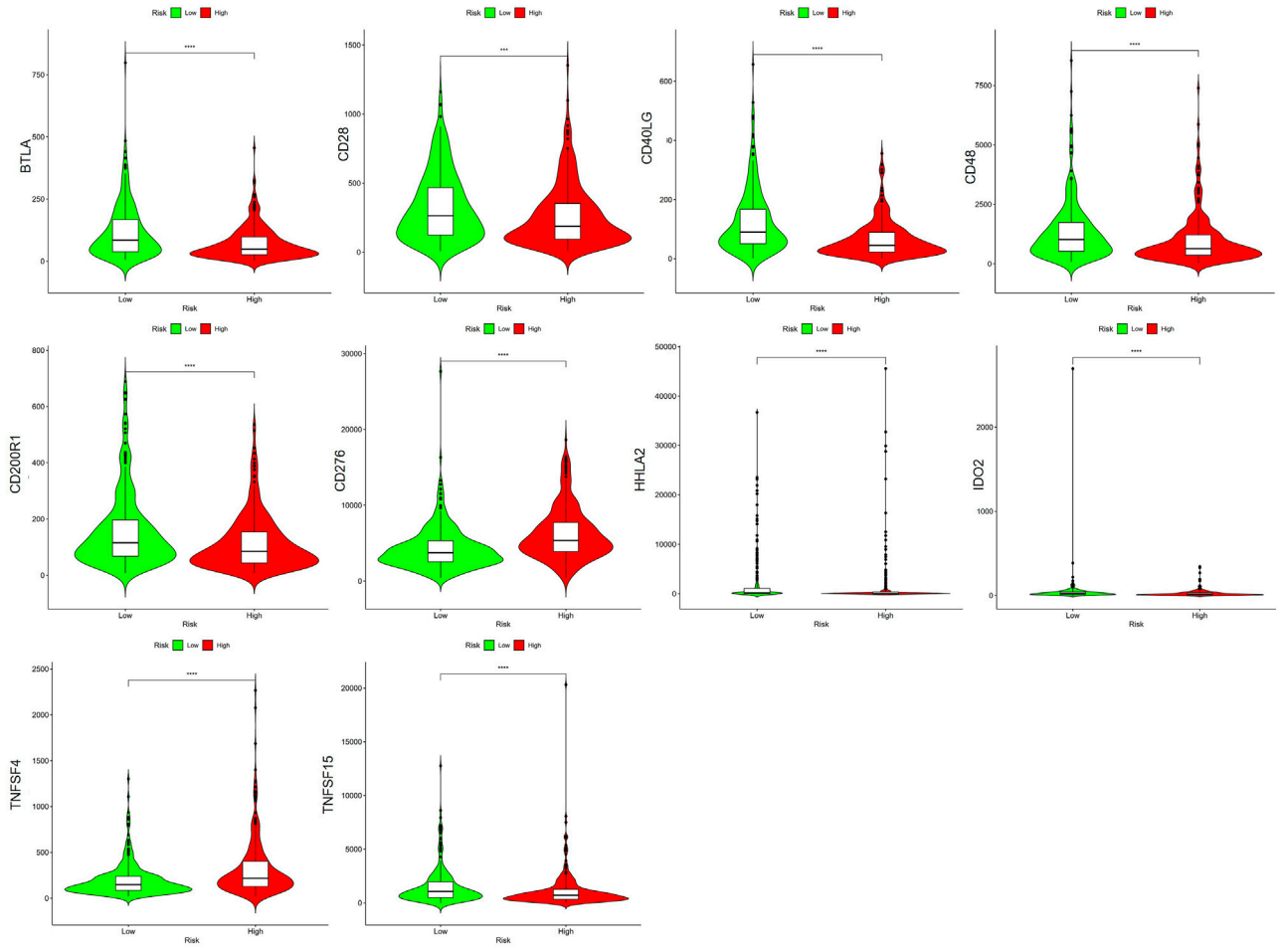

FIGURE 12
The relationship of prognosis feature with immunity checkpoints.

TABLE 2 The 12 small molecular medication of DsigDB database analysing outcomes.

Term	*p*-value	Odds ratio	Combined score
1 h-pyrazolo[3,4-d]pyrimidine	9.59E-06	93.70532915	1082.71
progesterone	1.23E-05	12.64044747	142.89
phenytoin	5.49E-05	51.14922813	501.81
8-Bromo-cAMP Na	5.68E-05	16.60570153	162.33
Indeno[1,2,3-cd]pyrene	2.09E-04	114.6954023	971.76
LAMININ BOSS	3.16E-04	27.82380506	224.23
LY-294002 PC3 UP	4.43E-04	77.29844961	596.93
aspirin	4.90E-04	13.95260323	106.34
Aflodac	5.23E-04	23.32349469	176.22
Benz[a]anthracene	1.04E-03	49.54975124	340.37
lamivudine	1.19E-03	46.09722222	310.25
Benzo[k]fluoranthene	0.0011941.19E-03	46.09722222	310.25

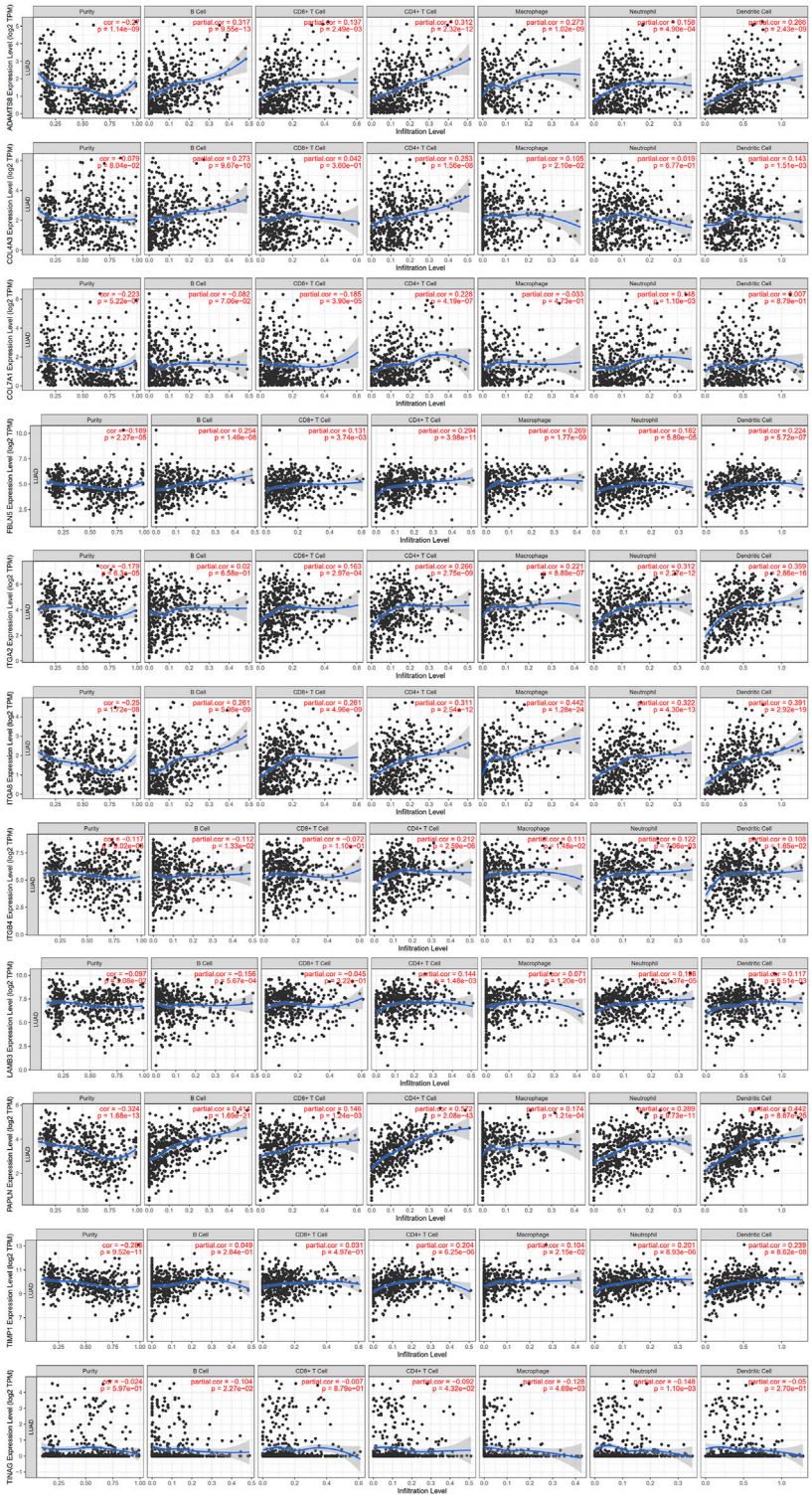

FIGURE 13
Immune cells infiltration by TIMER database.

patients, which is consistent with our results. Ning et al. (2022) found that ZBM-H, a HOCl probe, inhibited the migration of A549 cells by inducing autophagy to negatively regulate ITGB4 protein levels, suggesting that ITGB4 might act as a diagnostic biomarker of LUAD. As a transmembrane receptor for collagen and related proteins, ITGA2 has been shown to influence cancer progression through multiple pathways (Ghosh et al., 2016). The upregulation and relocalization of ITGA2 may promote tumor

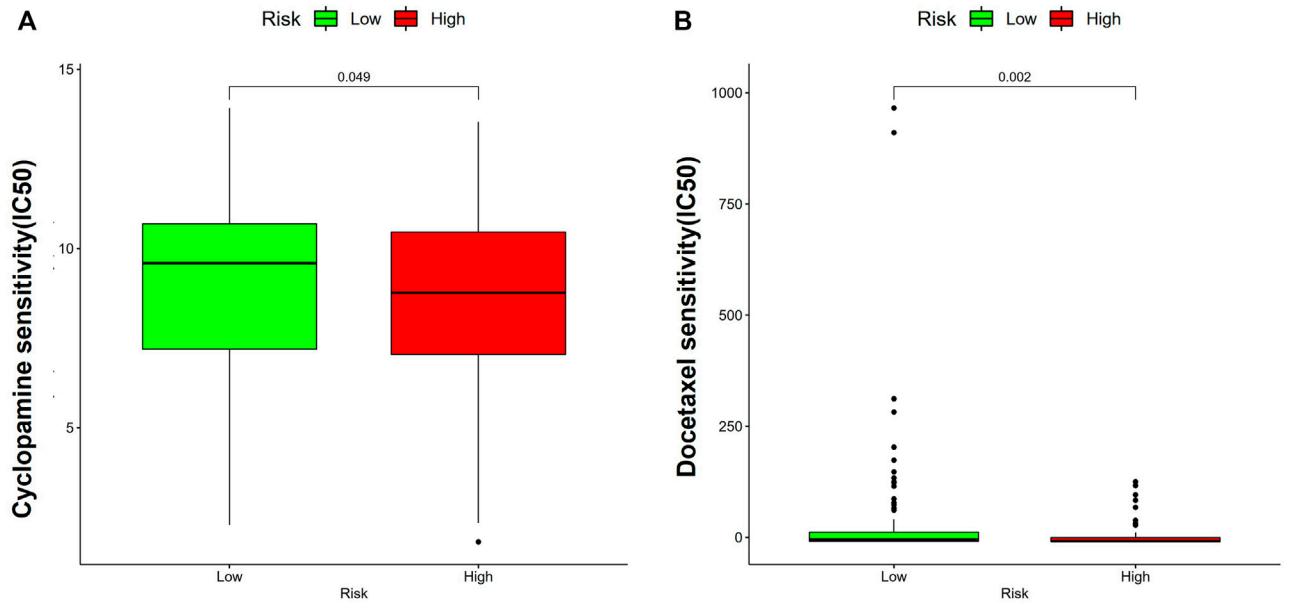

FIGURE 14
Drug sensitivity analysis. **(A)** Cyclopamine; **(B)** Docetaxel.

metastasis by increasing adhesion to the ECM and inhibiting local adhesion kinase activation. Studies have demonstrated that transient ITGA2 knockdown in NSCLC inhibits TNBC proliferation by inducing a G1 block (Adorno-Cruz et al., 2020). Chen et al. (2021) demonstrated that long non-coding RNA SLC25A25-AS1 plays a carcinogenic role in NSCLC by regulating the miRNA-195-5p/ITGA2 axis, suggesting the involvement of ITGA2 in the progression of NSCLC. To date, several studies have linked ITGA8 to tumorigenesis (Matsushima et al., 2020), and Lu et al. (2016) used bioinformatics methods to demonstrate that low ITGA8 expression had association with poor disease-free prognosis and survival in clear cell RCC patients. Similarly, through multivariate Cox regression analysis, Cui et al. (2022) discovered that ITGA8 had connection with poor prognosis in NSCLC and could considered as an independent predictor. Li et al. (2023) found that miR-17-5p could regulate the expression of ITGA8. Therefore, the regulatory network of ITGA8 may be a new therapeutic target to improve the prognosis of LC patients.

Studies have found that LAMB3 may participate in invasion and metastasis ability of some cancers, like thyroid, liver, and lung cancers (Wang et al., 2013; Wang et al., 2017; Hou et al., 2018). Zhang et al. (2019) verified that LAMB3 mediates apoptosis, proliferation, invasion, and metastasis of pancreatic cancers through the regulation of the PI3K/Akt signaling pathway. As a key gene involved in the progression of lung cancer, it showed high expression in LC tissues compared with normal ones (Wang et al., 2013).

Type VII collagen is encoded by COL7A1. Any changes in collagen under the tumor microenvironment will be reflected in the aspects of new collagen, density, direction, length, and cross-linking, which may influence many aspects through the regulation of epithelial-mesenchymal transformation, immunity, and mesenchymal cells, namely, tumor cell metabolism, macromolecular transport, gene expression, angiogenesis, as well as tumor invasion and metastasis (Peng et al., 2016). It was confirmed in this study that COL7A1 served as an oncogene in LUAD because its expression was upregulated compared to that in normal tissues. Li et al. (2020) claimed that COL7A1 may act as a crucial gene affecting the progression of hypoxia-related LUAD via DNA methylation. Unlike COL7A1, COL4A3 is expressed at low levels in lung cancer tissue. Metodieva et al. (2011) found that the expression of COL4A3 genes was upregulated in early NSCLC, while in another study, patients with lower COL4A3 expression shared a longer median OS (Jiang et al., 2013), confirming that it may act as a biomarker of LC. It has been reported that DNA repair can be weakened by blocking the interaction between COL4A3 proteins (Stabuc-Silih et al., 2009).

FBLN5, as a member of the fibulin family, is of great importance in angiogenesis and elastic fiber assembly. FBLN5 is often silenced by promoter hypermethylation in NSCLC, which is the main reason why it is often downregulated in more than 50% of lung cancers (Yue et al., 2009). FBLN5 may slow down the metastasis and invasion of lung cancer by inhibiting MMP-7 expression and promoting tumor metastasis through BM degradation. At the same time, it may also act as a barrier for surrounding tissues (Yue et al., 2009; Chen et al., 2014), and Chen et al. (2015) demonstrated that this process may be conducted by regulating the Wnt/β-catenin pathway. Little research has been conducted on the link between PAPLN and cancer. In studying cell-cell crosstalk in extramedullary infiltration of acute myeloid leukemia, Lv et al. (2018) found that PALPN showed a protective effect against the disease, thereby prolonging the overall survival. It was found that SPARCL1 is downregulated in many histological types of human epithelial cancers, including NSCLC (Sullivan and Sage, 2004). The role of SPARCL1 in NSCLC biology has been widely discussed. By cloning and mapping human SPARCL1 genomic loci and using FISH technology, Isler et al. (2001) found that SPARCL1 acts as a tumor suppressor. Zhou and Zhang (2021) found that differences in SPARCL1 expression in

NSCLC was connected with clinical stage, and the low expression rate of SPARCL1 in the TNM stage (I-II) was higher than that in the TNM stage (III-IV). Patients with higher SPARCL1 expression had higher 5-year survival rates. The above evidence indicated FBLN5 plays a major role in the prognosis and development of NSCLC. However, it has been previously reported that SPARCL1 activates typical WNT/β-catenin signaling by stabilizing the Wnt-receptor complex, inhibiting osteosarcoma metastasis and recruiting macrophages (Zhao et al., 2018), but the signaling pathway through which SPARCL1 is involved in the LUAD process remains unknown.

In accordance with the GSEA analysis, BM-related genes were mainly involved in metabolism-related pathways, including the Fc epsilon RI signaling pathway, which also plays a role in linoleic acid metabolism, Phagosome, *Salmonella* infection, and spliceosome, with main enrichment in the high-risk group. Therefore, BM-based markers were demonstrated to be able to predict the prognosis of LUAD patients and might have a significant function in LUAD treatment.

$CD4^+$T cells indicated an excellent prognosis and outstanding response to pembrolizumab, which had same results in this study. That is, patients in the former group had less $CD4^+$ T cells, while those in the latter group had higher expression of CD276, HHLA2, and TNFSF4, indicating that poor prognosis may be related to the immunosuppressive microenvironment. Besides, patients in low-risk populations may benefit from checkpoint inhibitor immunotherapy. Additionally, according to our findings, LUAD suffers in the low-risk group may profit by Cyclopamine and Docetaxel.

In this study, 14 BM-related genes involved in LUAD process were found, and the variation of these genes is the basis of human diseases. The BM protein is the target of autoantibodies in immune diseases. BM proteins are targets of autoantibodies in immune disorders and defects in BM protein expression and turnover are a key pathogenic aspect of cancer. Although we used bioinformatics to identify prognostic BM-related genes involved in LUAD, the limitations in our study should be seen. The proposed verification cohort was based on the retrospective TCGA data. Therefore, additional validation of the model should be performed in massive-sample clinical research. We expect that this will ultimately facilitate early disease detection, improve prognostic prediction, and inform the treatment of BM-associated cancers, including LUAD.

5 Conclusion

Overall, this study identified differentially expressed BM-related genes, which may be involved in cancer, together with progression of NSCLC. These genes are valuable to predict the prognosis of NSCLC patients. At the same time, targeting BM-related genes is expected to be an effective treatment for NSCLC. It shall be mentioned that this study may be further confirmed by other research in the future.

Data availability statement

The original contributions presented in the study are included in the article/Supplementary Material, further inquiries can be directed to the corresponding author.

Author contributions

YZ performed statistical analysis, and was responsible for the quality control of data and algorithms. TL performed literature research and data interpretation. HL helped data discussion. LW contributed to the study concept and study design. All authors contributed to writing of the manuscript and approved the final version.

Acknowledgments

We thank all colleagues involved in the study for their contributions. We acknowledge TCGA database for providing their platforms and contributors for uploading their meaningful datasets.

Conflict of interest

The authors declare that the research was conducted in the absence of any commercial or financial relationships that could be construed as a potential conflict of interest.

Publisher's note

References

Adorno-Cruz, V., Hoffmann, A. D., Liu, X., Dashzeveg, N. K., Taftaf, R., Wray, B., et al. (2020). ITGA2 promotes expression of ACLY and CCND1 in enhancing breast cancer stemness and metastasis. *Genes Dis.* 8 (4), 493–508. doi:10.1016/j.gendis.2020.01.015

Banyard, J., and Bielenberg, D. R. (2015). The role of EMT and MET in cancer dissemination. *Connect. Tissue Res.* 56 (5), 403–413. doi:10.3109/03008207.2015.1060970

Celentano, A., Yap, T., Paolini, R., Yiannis, C., Mirams, M., Koo, K., et al. (2021). Inhibition of matrix metalloproteinase-2 modulates malignant behaviour of oral squamous cell carcinoma cells. *J. Oral Pathol. Med.* 50 (3), 323–332. doi:10.1111/jop.12992

Chen, J., Gao, C., and Zhu, W. (2021). Long non-coding RNA SLC25A25-AS1 exhibits oncogenic roles in non-small cell lung cancer by regulating the microRNA-195-5p/ITGA2 axis. *Oncol. Lett.* 22 (1), 529. doi:10.3892/ol.2021.12790

Chen, X., Meng, J., Yue, W., Yu, J., Yang, J., Yao, Z., et al. (2014). Fibulin-3 suppresses Wnt/β-catenin signaling and lung cancer invasion. *Carcinogenesis* 35 (8), 1707–1716. doi:10.1093/carcin/bgu023

Chen, X., Song, X., Yue, W., Chen, D., Yu, J., Yao, Z., et al. (2015). Fibulin-5 inhibits Wnt/β-catenin signaling in lung cancer. *Oncotarget* 6 (17), 15022–15034. doi:10.18632/oncotarget.3609

Cheng, H.-W., Chen, Y.-F., Wong, J.-M., Weng, C.-W., Chen, H.-Y., Yu, S.-L., et al. (2017). Cancer cells increase endothelial cell tube formation and survival by activating the PI3K/Akt signalling pathway. *J. Exp. Clin. Cancer Res.* 36 (1), 27. doi:10.1186/s13046-017-0495-3

Choi, G.-C., Li, J., Wang, Y., Li, L., Zhong, L., Ma, B., et al. (2014). The metalloprotease ADAMTS8 displays antitumor properties through antagonizing EGFR-MEK-ERK signaling and is silenced in carcinomas by CpG methylation. *Mol. Cancer Res.* 12 (2), 228–238. doi:10.1158/1541-7786.MCR-13-0195

Cui, S., Lou, S., Feng, J., Tang, X., Xiao, X., Huang, R., et al. (2022). Identification of genes and pathways leading to poor prognosis of non-small cell lung cancer using integrated bioinformatics analysis. *Transl. Cancer Res.* 11 (4), 710–724. doi:10.21037/tcr-21-1986

Danilova, L., Ho, W.-J., Zhu, Q., Vithayathil, T., DeJesus-Acosta., A., Azad, N. S., et al. (2019). Programmed cell death ligand-1 (PD-L1) and CD8 expression profiling identify an immunologic subtype of pancreatic ductal adenocarcinomas with favorable survival. *Cancer Immunol. Res.* 7 (6), 886–895. doi:10.1158/2326-6066.CIR-18-0822

Duma, N., Santana-Davila, R., and Molina, J. R. (2019). Non-small cell lung cancer: Epidemiology, screening, diagnosis, and treatment. *Mayo Clin. Proc.* 94 (8), 1623–1640. doi:10.1016/j.mayocp.2019.01.013

Dunn, J. R., Panutsopulos, D., Shaw, M. W., Heighway, J., Dormer, R., Salmoal., E. N., et al. (2004). METH-2 silencing and promoter hypermethylation in NSCLC. *Br. J. Cancer* 13 (6), 1149–1154. doi:10.1038/sj.bjc.6602107

Ghosh, S., Shinogle, H. E., Galeva, N. A., Dobrowsky, R. T., and Blagg, B. S. (2016). Endoplasmic reticulum-resident heat shock protein 90 (HSP90) isoform glucose-regulated protein 94 (GRP94) regulates cell polarity and cancer cell migration by affecting intracellular transport. *J. Biol. Chem.* 291 (16), 8309–8323. doi:10.1074/jbc.M115.688374

Götte, M., and Kovalszky, I. (2018). Extracellular matrix functions in lung cancer. *Matrix Biol.* 73, 105–121. doi:10.1016/j.matbio.2018.02.018

Herbst, R. S., Morgensztern, D., and Boshoff, C. (2018). The biology and management of non-small cell lung cancer. *Nature* 553 (7689), 446–454. doi:10.1038/nature25183

Hiwatari, M., Seki, M., Matsuno, R., Yoshida, K., Nagasawa, T., Sato-Otsubo, A., et al. (2022). Novel TENM3-ALK fusion is an alternate mechanism for ALK activation in neuroblastoma. *Oncogene* 41 (20), 2789–2797. doi:10.1038/s41388-022-02301-1

Hou, J., Wang, L., and Wu, D. (2018). The root of Actinidia chinensis inhibits hepatocellular carcinomas cells through LAMB3. *Cell Biol. Toxicol.* 34 (4), 321–332. doi:10.1007/s10565-017-9416-7

Isler, S. G., Schenk, S., Bendik, I., Schraml, P., Novotna, H., Moch, H., et al. (2001). Genomic organization and chromosomal mapping of SPARC-like 1, a gene down regulated in cancers. *Int. J. Oncol.* 18 (3), 521–526. doi:10.3892/ijo.18.3.521

Januchowski, R., Świerczewska, M., Sterzyńska, K., Wojtowicz, K., Nowicki, M., and Zabel, M. (2016). Increased expression of several collagen genes is associated with drug resistance in ovarian cancer cell lines. *J. Cancer* 7 (10), 1295–1310. doi:10.7150/jca.15371

Jayadev, R., Morais, M. R. P. T., Ellingford, J. M., Srinivasan, S., Naylor, R. W., Lawless, C., et al. (2022). A basement membrane discovery pipeline uncovers network complexity, regulators, and human disease associations. *Sci. Adv.* 20 (20), eabn2265. doi:10.1126/sciadv.abn2265

Jiang, C.-P., Wu, B.-H., Chen, S.-P., Fu, M.-Y., Yang, M., Liu, F., et al. (2013). High COL4A3 expression correlates with poor prognosis after cisplatin plus gemcitabine chemotherapy in non-small cell lung cancer. *Tumour Biol.* 34 (1), 415–420. doi:10.1007/s13277-012-0565-2

Kurokawa, A., Nagata, M., Kitamura, N., Noman, A. A., Ohnishi, M., Ohyama, T., et al. (2008). Diagnostic value of integrin alpha3, beta4, and beta5 gene expression levels for the clinical outcome of tongue squamous cell carcinoma. *Cancer* 112 (6), 1272–1281. doi:10.1002/cncr.23295

Lachat, C., Bruyère, D., Etcheverry, A., Aubry, M., Mosser, J., Warda, W., et al. (2020). EZH2 and KDM6B expressions are associated with specific epigenetic signatures during EMT in non small cell lung carcinomas. *Cancers (Basel)* 12 (12), 3649. doi:10.3390/cancers12123649

Lee, H.-C., Chang, C.-Y., Wu, K.-L., Chiang, H.-H., Chang, Y.-Y., Liu, L.-X., et al. (2022). The therapeutic potential of ADAMTS8 in lung adenocarcinoma without targetable therapy. *J. Pers. Med.* 12 (6), 902. doi:10.3390/jpm12060902

Li, H., Tong, L., Tao, H., and Liu, Z. (2020). Genome-wide analysis of the hypoxia-related DNA methylation-driven genes in lung adenocarcinoma progression. *Biosci. Rep.* 40 (2), BSR20194200. doi:10.1042/BSR20194200

Li, X., Zhu, G., Li, Y., Huang, H., Chen, C., Wu, D., et al. (2023). LINC01798/miR-17-5p axis regulates ITGA8 and causes changes in tumor microenvironment and stemness in lung adenocarcinoma. *Front. Immunol.* 23 (14), 1096818. doi:10.3389/fimmu.2023.1096818

Liu, C.-C., Lin, J.-H., Hsu, T.-W., Hsu, J.-W., Chang, J.-W., Su, K., et al. (2016). Collagen XVII/laminin-5 activates epithelial-to-mesenchymal transition and is associated with poor prognosis in lung cancer. *Oncotarget* 9 (2), 1656–1672. doi:10.18632/oncotarget.11208

Liu, J., Shen, J.-X., Wu, H.-T., Li, X.-L., Wen, X.-F., Du, C.-W., et al. (2018). Collagen 1A1 (COL1A1) promotes metastasis of breast cancer and is a potential therapeutic target. *Discov. Med.* 25 (139), 211–223.

Liu, Y., Duan, J., Zhang, F., Liu, F., Luo, X., Shi, Y., et al. (2023). Mutational and transcriptional characterization establishes prognostic models for resectable lung squamous cell carcinoma. *Cancer Manag. Res.* 17 (15), 147–163. doi:10.2147/CMAR.S384918

Liu, Y., Zhu, D., Xing, H., Hou, Y., and Sun, Y. (2019). A 6-gene risk score system constructed for predicting the clinical prognosis of pancreatic adenocarcinoma patients. *Oncol. Rep.* 41 (3), 1521–1530. doi:10.3892/or.2019.6979

Lu, P., Weaver, V. M., and Werb, Z. (2012). The extracellular matrix: A dynamic niche in cancer progression. *J. Cell Biol.* 196 (4), 395–406. doi:10.1083/jcb.201102147

Lu, X., Wan, F., Zhang, H., Shi, G., and Ye, D. (2016). ITGA2B and ITGA8 are predictive of prognosis in clear cell renal cell carcinoma patients. *Tumour Biol.* 37 (1), 253–262. doi:10.1007/s13277-015-3792-5

Luu, T.-T., Bach, D. H., Kim, D., Hu, R., Park, H. J., and Lee, S. K. (2020). Overexpression of AGR2 is associated with drug resistance in mutant non-small cell lung cancers. *Anticancer Res.* 40 (4), 1855–1866. doi:10.21873/anticanres.14139

Lv, C., Sun, L., Guo, Z., Li, H., Kong, D., Xu, B., et al. (2018). Circular RNA regulatory network reveals cell-cell crosstalk in acute myeloid leukemia extramedullary infiltration. *J. Transl. Med.* 16 (1), 361. doi:10.1186/s12967-018-1726-x

Matsushima, S., Aoshima, Y., Akamatsu, T., Enomoto, Y., Meguro, S., Kosugi, ., et al. (2020). CD248 and integrin alpha-8 are candidate markers for differentiating lung fibroblast subtypes. *BMC Pulm. Med.* 21 (1), 21. doi:10.1186/s12890-020-1054-9

Mercurio, A. M., Bachelder, R. E., Rabinovitz, I., O'Connor, K. L., Tani, T., and Shaw, L.-M. (2001). The metastatic odyssey: The integrin connection. *Surg. Oncol. Clin. N. Am.* 10 (2), 313–328. doi:10.1016/s1055-3207(18)30067-x

Metodieva, S. N., Nikolova, D. N., Cherneva, R. V., Dimova, I. I., Petrov, D. B., Toncheva, D. I., et al. (2011). Expression analysis of angiogenesis-related genes in Bulgarian patients with early-stage non-small cell lung cancer. *Tumor* 97 (1), 86–94. doi:10.1177/030089161109700116

Mohanty, A., Nam, A., Pozhitkov, A., Yang, L., Srivastava, S., et al. (2020). A non-genetic mechanism involving the integrin β4/paxillin Axis contributes to chemoresistance in lung cancer. *Science* 23 (9), 101496. doi:10.1016/j.isci.2020.101496

Ning, J., Cui, X., Li, N., Li, N., Zhao, B., Miao, J., et al. (2022). Activation of GRP78 ATPase suppresses A549 lung cancer cell migration by promoting ITGB4 degradation. *Cell Adh Migr.* 16 (1), 107–114. doi:10.1080/19336918.2022.2130415

Peng, D.-H., Ungewiss, C., Tong, P., Byers, L. A., Wang, J., Canales, J. R., et al. (2016). ZEB1 induces LOXL2-mediated collagen stabilization and deposition in the extracellular matrix to drive lung cancer invasion and metastasis. *Oncogene* 36 (14), 1925–1938. doi:10.1038/onc.2016.358

Reuten, R., Zendehroud, S., Nicolau, M., Fleischhauer, L., Laitala, A., Kiderlen, S., et al. (2021). Basement membrane stiffness determines metastases formation. *Nat. Mater* 20 (6), 892–903. doi:10.1038/s41563-020-00894-0

Riegler, J., Labyed, Y., Rosenzweig, S., Javinal, V., Castiglioni, A., et al. (2018). Tumor elastography and its association with collagen and the tumor microenvironment. *Clin. Cancer Res.* 24 (18), 4455–4467. doi:10.1158/1078-0432.CCR-17-3262

Rousselle, P., and Scoazec, J. Y. (2020). Laminin 332 in cancer: When the extracellular matrix turns signals from cell anchorage to cell movement. *Semin. Cancer Biol.* 62, 149–165. doi:10.1016/j.semcancer.2019.09.026

Scagliotti, G. V., Parikh, P., von Pawel, J., Biesma, B., Vansteenkiste, J., Manegold, C., et al. (2008). Phase III study comparing cisplatin plus gemcitabine with cisplatin plus pemetrexed in chemotherapy-naive patients with advanced-stage non-small-cell lung cancer. *J. Clin. Oncol.* 26 (21), 3543–3551. doi:10.1200/JCO.2007.15.0375

Schiller, J. H., Harrington, D., Belani, C. P., Langer, C., Sandler, A., Krook, J., et al. (2002). Comparison of four chemotherapy regimens for advanced non-small-cell lung cancer. *N. Engl. J. Med.* 346 (2), 92–98. doi:10.1056/NEJMoa011954

Siegel, R. L., Miller, K. D., and Jemal, A. (2020). Cancer statistics, 2020. *CA Cancer J. Clin.* 70 (1), 7–30. doi:10.3322/caac.21590

Stabuc-Silih, M., Ravnik-Glavac, M., Glavac, D., Hawlina, M., and Strazisar, M. (2009). Polymorphisms in COL4A3 and COL4A4 genes associated with keratoconus. *Mol. Vis.* 15, 2848–2860.

Su, C.-Y., Li, J.-Q., Zhang, L.-L., Wang, H., Wang, F.-H., Tao, Y.-W., et al. (2020). The biological functions and clinical applications of integrins in cancers. *Front. Pharmacol.* 11, 57906. doi:10.3389/fphar.2020.579068

Su, C., Liu, W.-X., Wu, L.-S., Dong, T.-J., and Liu, J.-F. (2021). Screening of hub gene targets for lung cancer via microarray data. *Comb. Chem. High. Throughput Screen* 24 (2), 269–285. doi:10.2174/1386207323666200808172631

Sullivan, M. M., and Sage, E. H. (2004). Hevin/SC1, a matricellular glycoprotein and potential tumor-suppressor of the SPARC/BM-40/Osteonectin family. *Int. J. Biochem. Cell Biol.* 36 (6), 991–996. doi:10.1016/j.biocel.2004.01.017

Tas, F., Bilgin, E., Tastekin, D., Erturk, K., and Duranyildiz, D. (2016). Serum IGF-1 and IGFBP-3 levels as clinical markers for patients with lung cancer. *Biomed. Rep.* 4 (5), 609–614. doi:10.3892/br.2016.629

Teng, Y., Wang, Z., Ma, L., Zhang, L., Guo, Y., Gu, M., et al. (2016). Prognostic significance of circulating laminin gamma2 for early-stage non-small-cell lung cancer. *Onco Targets Ther.* 7 (9), 4151–4162. doi:10.2147/OTT.S105732

Thuveson, M., Gaengel, K., Collu, G. M., Chin, M. L., Singh, J., and Mlodzik, M. (2019). Integrins are required for synchronous ommatidial rotation in the Drosophila eye linking planar cell polarity signalling to the extracellular matrix. *Open Biol.* 9 (8), 190148. doi:10.1098/rsob.190148

Wang, X.-M., Li, J., Yan, M.-X., Liu, L., Jia, D.-S., Geng, Q., et al. (2013). Integrative analyses identify osteopontin, LAMB3 and ITGB1 as critical pro-metastatic genes for lung cancer. *PLoS One* 8 (2), e55714. doi:10.1371/journal.pone.0055714

Wang, Y., Jin, Y., Bhandari, A., Yao, Z., Yang, F., Pan, Y., et al. (2017). Upregulated LAMB3 increases proliferation and metastasis in thyroid cancer. *Onco Targets Ther.* 21 (11), 37–46. doi:10.2147/OTT.S149613

Xiao, Q., Jiang, Y., Liu, Q., Yue, J., Liu, C., Zhao, X., et al. (2015a). Minor type IV collagen α5 chain promotes cancer progression through discoidin domain receptor-1. *PLoS Genet.* 11 (5), e1005249. doi:10.1371/journal.pgen.1005249

Xiao, Q., Qu, X.-L., Li, X.-M., Sun, Y.-L., Zhao, H.-X., Wang, S., et al. (2015b). Identification of commonly dysregulated genes in colorectal cancer by integrating analysis of RNA-Seq data and qRT-PCR validation. *Cancer Gene Ther.* 22 (5), 278–284. doi:10.1038/cgt.2015.20

Xu, X., Li, N., Wang, Y., Yu, J., and Mi, J. (2021). Calcium channel TRPV6 promotes breast cancer metastasis by NFATC2IP. *Cancer Lett.* 28 (519), 150–160. doi:10.1016/j.canlet.2021.07.017

Yue, W., Sun, Q., Landreneau, R., Wu, C., Siegfried, J. M., Yu, J., et al. (2009). Fibulin-5 suppresses lung cancer invasion by inhibiting matrix metalloproteinase-7 expression. *Cancer Res.* 69 (15), 6339–6346. doi:10.1158/0008-5472.CAN-09-0398

Yurchenco, P. D. (2011). Basement membranes: Cell scaffoldings and signaling platforms. *Cold Spring Harb. Perspect. Biol.* 3 (2), a004911. doi:10.1101/cshperspect.a004911

Zhang, H., Pan, Y.-Z., Cheung, M., Cao, M., Yu, C., Chen, L., et al. (2019). LAMB3 mediates apoptotic, proliferative, invasive, and metastatic behaviors in pancreatic cancer by regulating the PI3K/Akt signaling pathway. *Cell Death Dis.* 10 (3), 230. doi:10.1038/s41419-019-1320-z

Zhang, M.-H., Niu, H., Li, Z., Huo, R.-T., Wang, J.-M., and Liu, J. (2018). Activation of PI3K/AKT is involved in TINAG-mediated promotion of proliferation, invasion and migration of hepatocellular carcinoma. *Cancer Biomark.* 23 (1), 33–43. doi:10.3233/CBM-181277

Zhang, Q., Hu, K., Qu, Z., Xie, Z., and Tian, F. (2022b). ADAMTS8 inhibited lung cancer progression through suppressing VEGFA. *Biochem. Biophys. Res. Commun.* 2 (598), 1–8. doi:10.1016/j.bbrc.2022.01.110

Zhang, Q., Kanyomse, Q., Luo, C., Mo, Q., Zhao, X., Wang, L., et al. (2022a). The prognostic value of ADAMTS8 and its role as a tumor suppressor in breast cancer. *Cancer Invest.* 11, 119–132. doi:10.1080/07357907.2022.2128367

Zhao, S.-J., Jiang, Y.-Q., Xu, N.-W., Li, Q., Zhang, Q., Wang, S.-Y., et al. (2018). SPARCL1 suppresses osteosarcoma metastasis and recruits macrophages by activation of canonical WNT/β-catenin signaling through stabilization of the WNT-receptor complex. *Oncogene* 37 (8), 1049–1061. doi:10.1038/onc.2017.403

Zhong, S., and Khalil, R. A. (2019). A Disintegrin and Metalloproteinase (ADAM) and ADAM with thrombospondin motifs (ADAMTS) family in vascular biology and disease. *Biochem. Pharmacol.* 164, 188–204. doi:10.1016/j.bcp.2019.03.033

Zhou, Y., and Zhang, Q. (2021). Association of tumor suppressor Sparcl1 with clinical staging and prognosis of NSCLC. *Ann. Clin. Lab. Sci.* 51 (6), 756–765.

Zhu, Y.-Z., Liu, Y., Liao, X.-W., and Luo, S.-S. (2021). Identified a disintegrin and metalloproteinase with thrombospondin motifs 6 serve as a novel gastric cancer prognostic biomarker by bioinformatics analysis. *Biosci. Rep.* 41 (4), BSR20204359. doi:10.1042/BSR20204359

Ziegler, A., Corvalán, A., Roa, I., Brañes, J. A., and Wollscheid, B. (2012). Teneurin protein family: An emerging role in human tumorigenesis and drug resistance. *Cancer Lett.* 326 (1), 1–7. doi:10.1016/j.canlet.2012.07.021

frontiers | Frontiers in Pharmacology

TYPE Original Research
PUBLISHED 17 May 2023
DOI 10.3389/fphar.2023.1192210

OPEN ACCESS

EDITED BY
Ayaz Shahid,
Western University of Health Sciences, United States

REVIEWED BY
Bingyan Li,
Soochow University, China
Tingyuan Lang,
Chongqing University, China

*CORRESPONDENCE
Huang Huang,
haohuanghuang@126.com
Pengyuan Zheng,
pyzheng@zzu.edu.cn

†These authors have contributed equally to this work

RECEIVED 23 March 2023
ACCEPTED 05 May 2023
PUBLISHED 17 May 2023

CITATION
Rong K, He Q, Chen S, Yu Y, Mei L, Mi Y, Mu L, Zhu M, Nan M, Zhang X, Wan Z, Huang H and Zheng P (2023), The mechanism of vitamin D3 in preventing colorectal cancer through network pharmacology.
Front. Pharmacol. 14:1192210.
doi: 10.3389/fphar.2023.1192210

The mechanism of vitamin D3 in preventing colorectal cancer through network pharmacology

Kang Rong[1,2†], Qingmin He[1,2†], Shu Chen[3†], Yong Yu[1,2], Lu Mei[1,2], Yang Mi[1,2], Liufan Mu[1,2], Mingyang Zhu[1,2], Mengjiao Nan[1,2], Xiaoyang Zhang[1,2], Zhaoyang Wan[1,2], Huang Huang[1,2*] and Pengyuan Zheng[1,2*]

[1]Henan Key Laboratory of Helicobacter Pylori and Microbiota and Gastrointestinal Cancer, Marshall B. J. Medical Research Center of Zhengzhou University, The Fifth Affiliated Hospital of Zhengzhou University, Zhengzhou, China, [2]Department of Gastroenterology, The Fifth Affiliated Hospital of Zhengzhou University, Zhengzhou, China, [3]The First Clinical Medical School of Henan University of Chinese Medicine, Zhengzhou, China

Objective: Colorectal cancer (CRC) is a common cancer that cannot be detected at an early stage and is a major challenge in oncology research. Studies have shown that vitamin D3 has some anti-cancer and preventive effects on colorectal cancer, but the exact anti-cancer mechanism is not clear. We applied the relevant research methods of network pharmacology to speculate and validate the possible potential pharmacological mechanisms of vitamin D3 for the prevention of colorectal cancer, and to provide more theoretical support for the clinical anticancer effects of vitamin D3.

Methods: The relevant targets for vitamin D3 and CRC were obtained from the database of drug and disease targets, respectively. The target of vitamin D3 and the target of colorectal cancer were taken to intersect to obtain common targets. Then, the PPI network was constructed. In addition, the pathways of drug-disease interactions were predicted by GO and KEGG enrichment analysis. Finally, the obtained results were verified to ensure the reliability of the experiments.

Results: 51 targets of vitamin D3 for the prevention of colorectal cancer were obtained. The 10 core targets were obtained from the PPI network. The 10 core targets include: ALB, SRC, MMP9, PPARG, HSP90AA1, IGF1, EGFR, MAPK1, MAP2K1 and IGF1R. The core targets were further validated by molecular docking and animal experiments. The results suggest that vitamin D3 plays a key role in the prevention of CRC through core targets, PI3K-Akt pathway, HIF-1 pathway, and FoxO pathway.

Conclusion: This study will provide more theoretical support for vitamin D3 to reduce the incidence of CRC and is important to explore more pharmacological effects of vitamin D3.

KEYWORDS

vitaminD3, CRC, chemoprevention, network pharmacology, molecular docking

1 Introduction

Colorectal cancer (CRC) is a malignant tumor that has the third highest incidence rate among cancers and the second highest mortality rate among malignant tumors (Sung et al., 2021). In China, CRC ranks fifth in the incidence of malignant tumors in men and fourth in the incidence of malignant tumors in women. CRC ranks fifth in both male malignancy mortality and female malignancy mortality (Chen et al., 2016). Despite extensive research, the pathogenesis of CRC remains unclear (Thanikachalam and Khan, 2019). With the improvement of treatment methods and medical devices, the risk of CRC has already decreased, but the disease burden of CRC is still heavy, and more prevention strategies are needed (Schoen et al., 2012; Nishihara et al., 2013; Shaukat et al., 2013; Fakih, 2015; Doubeni et al., 2018; Levin et al., 2018). The concept of chemoprevention was first introduced in 1976. Chemoprevention of cancer usually involves the use of synthetic drugs to reduce the incidence of cancer and even reverse pre-cancerous and carcinogenic processes (Sporn, 1976). Currently, drugs that can have a chemopreventive effect on CRC include statins, drugs that target metabolic pathways, aspirin,non-aspirin non-steroidal anti-inflammatory drugs, and vitamins and minerals (Katona and Weiss, 2020). Vitamin D maintains relatively stable levels of calcium in the body's serum, and calcium salts deposited in certain areas contribute to the formation of bone. Several epidemiological studies have shown that patients with inadequate vitamin D intake have an increased risk of developing cancer (Holick, 2004; Bikle, 2016; Wang et al., 2017). In addition, studies have shown that vitamin D has a specific inhibitory effect on cancer (Harris and Go, 2004; Fleet et al., 2012; Feldman et al., 2014; Giammanco et al., 2015). The vitamin D receptor is expressed in a variety of cells in the body. By targeting the vitamin D receptor to initiate intracellular signaling regulatory mechanisms, it regulates complex intracellular signaling and ultimately inhibits CRC (Leyssens et al., 2013; Baron JA et al., 2015). Studies have shown that patients with low levels of vitamin D in the serum are more likely to develop CRC. Thus, vitamin D supplementation has a role in improving patient prognosis and preventing the development of CRC (Terry et al., 2002; Mccullough et al., 2003; Ma et al., 2011), although these results are based primarily on studies of the distal

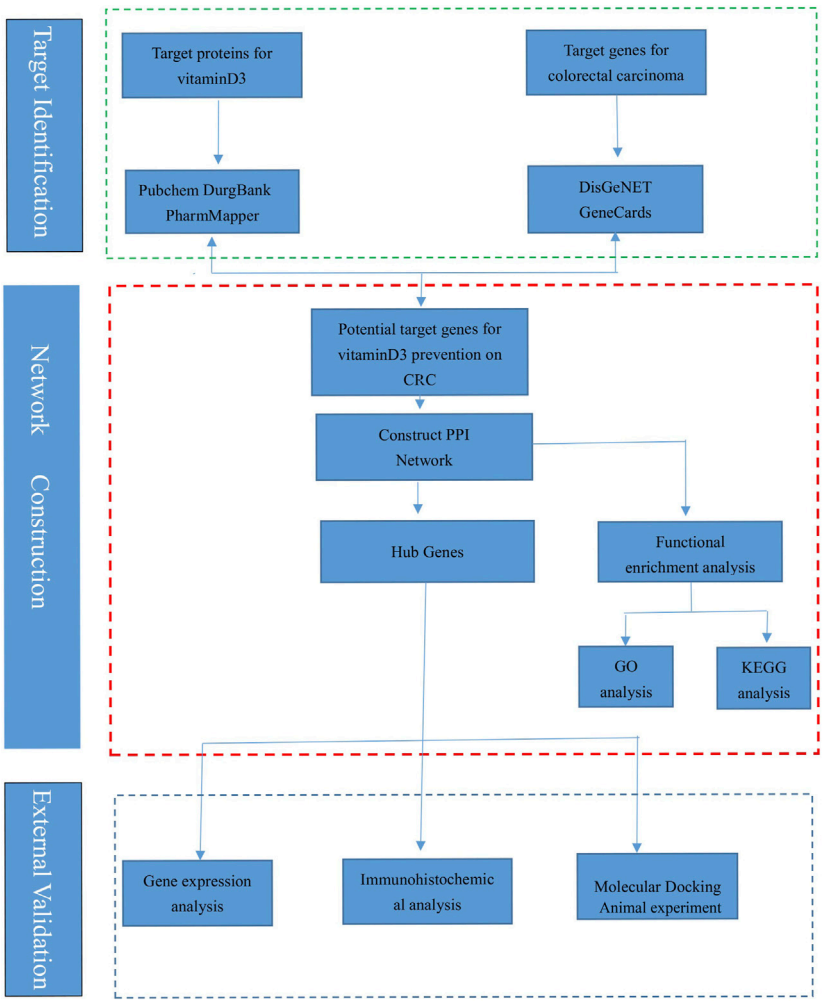

FIGURE 1
The flow chart of this research.

TABLE 1 Website information of the database involved in the study of vitamin D3 prevention of colorectal cancer.

Name	URL
PubChem	https://pubchem.ncbi.nlm.nih.gov/
PharmMapper	http://lilab-ecust.cn/pharmmapper/
Drugbank	https://go.drugbank.com/
Targetnet	http://targetnet.scbdd.com/
DisGeNET	https://www.disgenet.org/
GeneCards	https://www.genecards.org/
GEPIA	http://gepia.cancer-pku.cn/
HPA	https://www.proteinatlas.org/
Uniprot	https://www.uniprot.org/
STRING	https://cn.string-db.org/
DAVID	https://david.ncifcrf.gov/
Venny 2.1.0	https://bioinfogp.cnb.csic.es/tools/venny/index.html
RCSB PDB	https://www.rcsb.org/
Bioinformatics	http://www.bioinformatics.com.cn/
Cytoscape	https://cytoscape. org/
cBioPortal	https://www.cbioportal.org/
Kaplan-Meier Plotter	https://kmplot.com/analysis/

TABLE 2 Detailed molecular properties of vitamin D3 in PubChem.

Name	Details
PubChem CID	5280795
Molecular Formula	$C_{27}H_{44}O$
Synonyms	cholecalciferol
Molecular Weight	384.6
CAS	67–97–0
XLogP3-AA	7.9
Hydrogen Bond Donor Count	1
Hydrogen Bond Acceptor Count	1
Rotatable Bond Count	6
Topological Polar Surface Area	20.2 $Å^2$
Heavy Atom Count	28
Complexity	610
Covalently-Bonded Unit Count	1

colon and rectum (Zheng et al., 1998; Wu et al., 2002). This study reviewed the literature related to vitamin D and CRC and ultimately concluded that vitamin D has an inhibitory effect on CRC. However, the pathway is still unclear and more research is needed.

2 Materials and methods

2.1 Overview of the present study

The research process is shown (Figure 1), and the databases involved are listed (Table 1).

2.2 Molecular properties of vitaminD3

Vitamin D3 is a class of steroid hormones that are usually synthesized by the body in response to UV radiation or supplemented by food. Studies have shown that vitamin D3 is necessary to maintain calcium homeostasis and bone mineralization in the body. Binding of vitamin D3 and its receptors can regulate specific gene expression and signal transduction in the body, exerting biological effects. The properties of vitamin D3 are shown (Table 2), and the data are from PubChem.

2.3 Target of vitamin D3 was obtained

The English name of the drug was input to get its details in PubChem (https://pubchem. ncbi.nlm.nih.gov/) (Kim et al., 2021). The SDF format file of the drug was obtained from PubChem and then imported into PharmMapper (http://lilab-ecust.cn/pharmmapper/) (Liu et al., 2010). In PharmMapper, the screening criteria are as follows: Generate Conformers:Yes, Maximum Generated Conformations:300, Number of Reserved Matched Targets (Max 1,000):300. The canonical smiles of the drug was searched to obtain the target of vitamin D3 in Targetnet (http://targetnet.scbdd.com/) (Yao et al., 2016), and the English name of the drug was searched to obtain the target of vitamin D3 in Drugbank (https://go.drugbank.com/) (Wishart et al., 2018). The targets of the drug were converted into gene names in UniProt (https://www.uniprot.org/) (UniProt Consortium, 2021). Finally, the gene names were merged and de-duplicated to obtain the potential targets of vitamin D3.

2.4 CRC-related targets were obtained

The targets were obtained in DisGeNET (https://www.disgenet.org/) (Pinero et al., 2020) and GeneCards (https://www.genecards.org/) (Stelzer et al., 2016). The targets were merged and de-duplicated to be the related targets of CRC.

2.5 Screening of intersection targets and construction of PPI network

The targets of vitamin D3 and CRC-related targets were taken intersected in Venny 2.1.0 (https://bioinfogp.cnb.csic.es/tools/venny/index.html). Finally, the intersecting targets obtained are potential targets of vitamin D3 for CRC prevention. The intersection targets are imported into String (https://cn.string-db.org/) to construct the PPI network. The tsv file of the PPI network

TABLE 3 Primer sequences corresponding to core targets.

Gene name	Forward primer (5′→3′)	Reverse primer (5′→3′)
GAPDH	TGACCTCAACTACATGGTCTACA	CTTCCCATTCTCGGCCTTG
ALB	TCCAAACCTCCGTGAAAACTATG	TGTGTTGCAGGAAACATTCGT
SRC	GAACCCGAGAGGGACCTTC	GAGGCAGTAGGCACCTTTTGT
MMP9	GCAGAGGCATACTTGTACCG	TGATGTTATGATGGTCCCACTTG
PPARG	GGAAGACCACTCGCATTCCTT	GTAATCAGCAACCATTGGGTCA
HSP90AA1	GACGCTCTGGATAAAATCCGTT	TGGGAATGAGATTGATGTGCAG
IGF1	CTGGACCAGAGACCCTTTGC	GGACGGGGACTTCTGAGTCTT
EGFR	ATGAAAACACCTATGCCTTAGCC	TAAGTTCCGCATGGGCAGTTC
MAPK1	GGTTGTTCCCAAATGCTGACT	CAACTTCAATCCTCTTGTGAGGG
MAP2K1	AACGGTGGAGTGGTCTTCAAG	CGGATTGCGGGTTTGATCTC
IGF1R	CTTCTACAACTACGCACTGGTC	TCGGCGTTCTTCTCAATCCTG

was obtained and imported into Cytoscape 3.9.0 (https://cytoscape.org/; Version 3.9.0) (Doncheva et al., 2019) for analysis and visualization. In cytohubba, the core targets are obtained according to the importance of the nodes. The core targets were visualized.

2.6 GO and KEGG enrichment analysis

Core targets were imported into David (https://david.ncifcrf.gov/) (Huang et al., 2007) to obtain the results of GO and KEGG enrichment analysis (Ashburner et al., 2000; Kanehisa et al., 2021). The screening criteria were $p < 0.05$ and the enriched signaling pathway contained multiple core targets. The first 10 entries of BP, CC and MF were selected in this study, respectively. The collated data were imported into the bioinformatics (http://www.bioinformatics.com.cn/) for visualization and analysis.

2.7 Construction of drug-target-pathway network

$p < 0.05$ was used as a screening criterion, and the top 20 signaling pathways were selected based on the ranking of *p*-values from smallest to largest. Data of vitamin D3, signaling pathways and core targets were made into network.xlsx and type.xlsx and the files were imported into Cytoscape for visualization. The vitamin D3-core target-pathway network was constructed. The red triangle represents vitamin D3, the blue diamond represents the core target, and the green circle represents the signaling pathway.

2.8 Molecular docking

2.8.1 The process of molecular docking

To explore the possible mechanisms of vitamin D3 action on CRC. The strength and pattern of interactions between vitamin D3 and core targets were assessed by molecular docking in this study. The PDB ID of the core target was obtained from the RCSB PDB and its 3D structure was downloaded in PDB format. Molecular docking was performed using Discovery studio (2019 version) and the "Prepare Ligands" module was used to obtain 3D structures in this study. After removing the water of crystallization, the "Prepare Protein" module is used to remove multiple conformations of the target protein by adding hydrogen atoms. Then, the fast molecular docking option is selected in the "LibDock" module. The software calculates the corresponding docking scores in the columns of the LibDockScore. The docking score as a judgment criterion was used to evaluate the affinity of the target protein and the drug.

2.8.2 Reliability of molecular docking was verified

To verify the reliability of molecular docking, the original ligands of 10 target protein complexes were separated and then reattached to the pockets of the complexes in this study. The root-means-square deviation (RMSD) of the ligand conformation after ligand docking and the ligand conformation in the original crystal structure were calculated. The RMSD value less than 2.0Å indicates that the docking method can well reproduce the original ligand-receptor binding mode and the docking parameters are reasonably set.

2.9 External validation of core targets

2.9.1 Expression at the gene level

In GEPIA (http://gepia.cancer-pku.cn), the expression information of the core targets were obtained. The relevant information of core targets for different populations and different stages of cancer were obtained in the "Expression DIY" module (Tang et al., 2017).

2.9.2 Expression at the protein level

Differences of core targets were studied at the protein expression level. The relevant data from the Human Protein

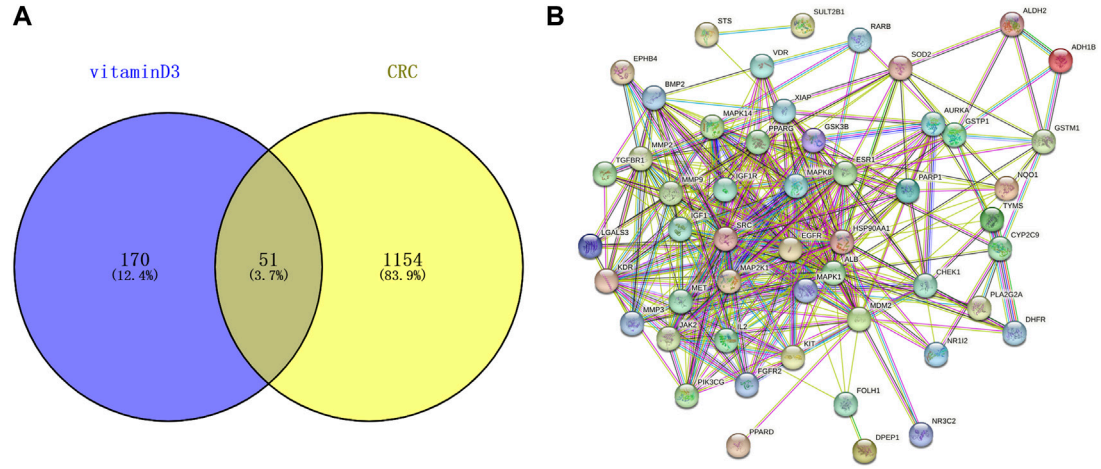

FIGURE 2
Information related to CRC chemoprevention. **(A)** Venn diagram of intersection targets between vitamin D3 and CRC **(B)** Establishment of PPI network for intersection targets.

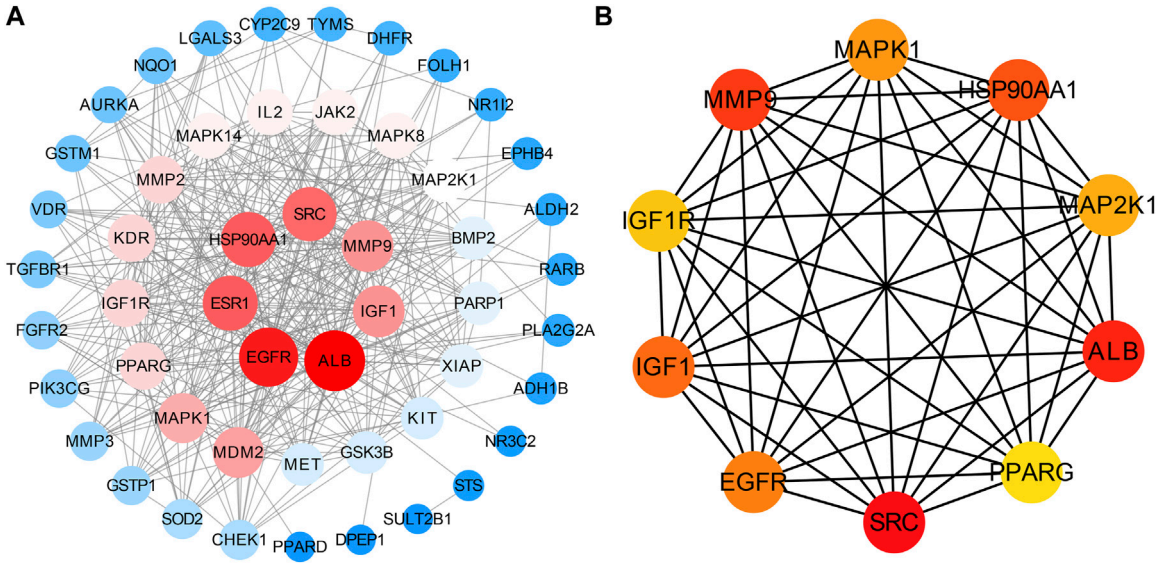

FIGURE 3
Visual results of intersection and core targets. **(A)** Graphical display of intersection targets **(B)** Visualization of core target genes.

Atlas database (https://www.proteinatlas.org/) (Uhlen et al., 2015) were analyzed. The core targets were analyzed and compared using the relevant data from this database to make further conclusions.

2.9.3 Alteration of genetic information in CRC

The 105 colon cancer (CPTAC - 2 prospective, cell 2019) samples in the database were analyzed using cBioPortal (https://www.cbioportal.org/) (Wu et al., 2019). We obtained the genetic information of the core targets (He et al., 2023). In addition, the mutation sites and mutation types of the core targets were obtained from this database.

2.9.4 Presence of core target proteins in other cancers

In GEPIA, the "General" module was selected and the core targets were entered to obtain the distribution and expression levels of the core targets in different cancers. The obtained results were presented in the form of a dot plot.

2.9.5 The effect of core targets on survival in CRC

To explore the impact of core targets on overall survival in CRC, Kaplan-Meier Plotter (https://kmplot.com/analysis/) was accessed. After the core targets were entered, the results of the overall survival of each target were obtained in this database.

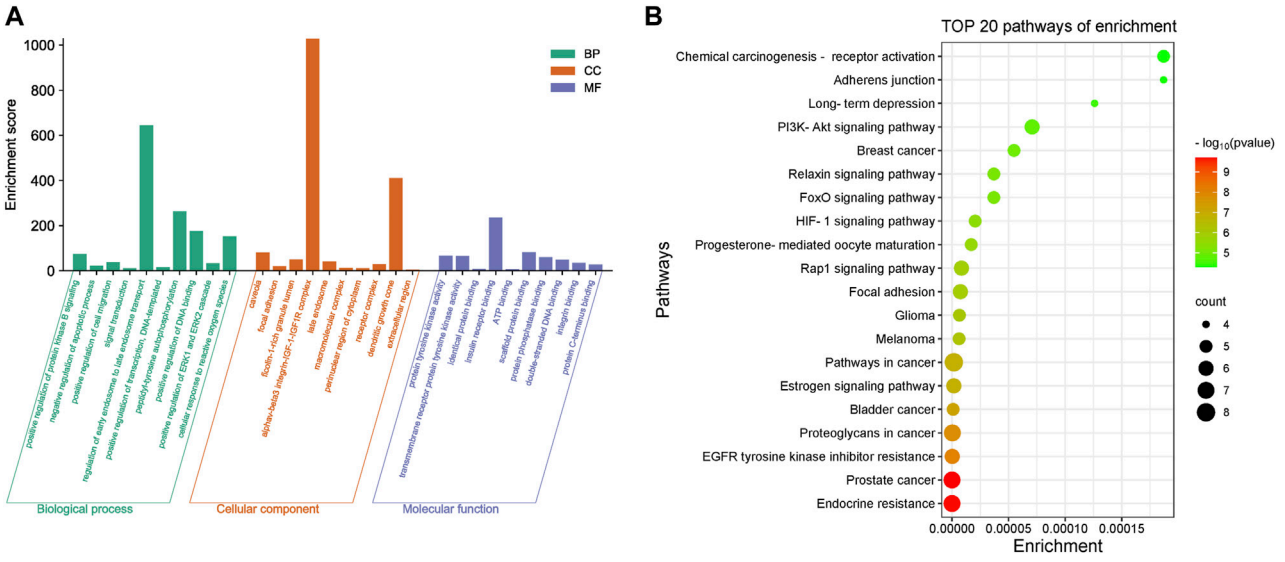

FIGURE 4
Enrichment results of core targets **(A)**. Visualization results of GO enrichment analysis. **(B)** Visualization results of KEGG enrichment analysis.

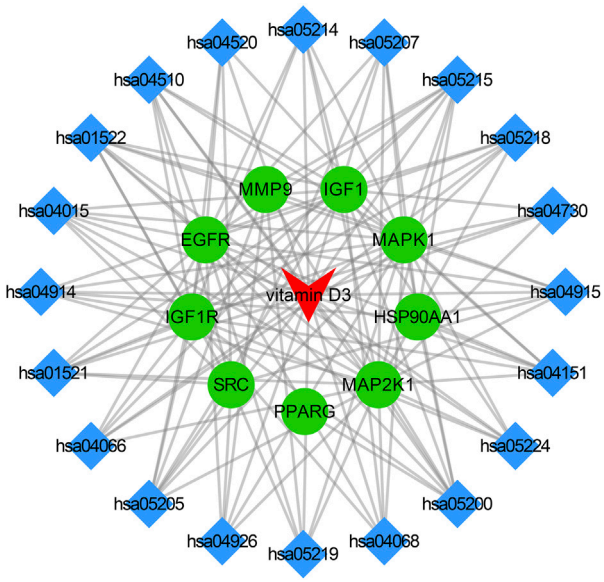

FIGURE 5
Visualization results of drug-pathway-target relationship network.

2.9.6 Animal experimental verification

2.9.6.1 Experimental animals

Eighteen 7-week-old male C57BL/6N mice were procured from Beijing Weitong Lihua Experimental Animal Technology Co. The mice were randomly divided into control group, model group and vitamin D3 intervention group, 6 mice in each group. The experimental conditions included constant temperature, pressure and humidity, and 12 h of light per day. Mice were fed with Co60 irradiated sterilized maintenance feed. The animal experiments were approved by the Animal Ethics Committee of the Fifth Affiliated Hospital of Zhengzhou University (Ethics No: KY2023007).

2.9.6.2 Reagents

Vitamin D3 (Item No.: B2065) was purchased from APExBIO(Houston,TX). Azoxymethane (AOM, item number: 0218397125) was purchased from Abe Medical Device Trading (Shanghai) Co., LTD., and Dextran sulfate sodium (DSS, item number MB5535) was purchased from Meilan Biotechnology (Dalian) Co., LTD. RNAiso Plus was purchased from Takara bio, Japan, and RIPA cell lysate and protease inhibitors were purchased from Dingguo Changsheng Biotechnology (Beijing) Co., LTD. Protein phosphatase inhibitors were purchased from bimake Biotechnology Co., LTD. HiScript®II 1st Strand cDNA Synthesis Kit and ChamQ universal SYBR qPCR Master Mix were purchased from Novizam Biotechnology (Nanjing) Co., LTD. The corresponding primers of the core target were synthesized by Sangon Biotech (Shanghai).

2.9.6.3 Animal grouping and modeling methods

A completely randomized design was used to divide the mice into three groups. Physiological saline control group (Nacl): 6 mice, model group (AOM + DSS): 6 mice, vitamin D3 intervention group (AOM + DSS + vitaminD3): 6 mice. After 1 week of adaptive feeding, the mice were gavaged with vitamin D for 2 continuous weeks at a dose of 60 IU/g per week, 3 times per week. At week 4, mice of the model and vitamin D3 intervention groups were given a single intraperitoneal injection of

TABLE 4 Information about core target proteins.

Targets	PDB ID	Method	Resolution (Å)	R-Value free	R-Value work	R-Value observed
ALB	6A7P	X-RAY DIFFRACTION	2.28	0.255	0.207	0.211
SRC	6QL3	X-RAY DIFFRACTION	1.35	0.156	0.116	0.12
MMP9	5UE4	X-RAY DIFFRACTION	1.80	0.224	0.199	0.2
PPARG	4XUH	X-RAY DIFFRACTION	2.22	0.23	0.186	0.189
HSP90AA1	2BZ5	X-RAY DIFFRACTION	1.90	0.254	0.195	0.198
IGF1	3O23	X-RAY DIFFRACTION	2.10	0.278	0.238	——
EGFR	5D41	X-RAY DIFFRACTION	2.31	0.207	0.174	0.175
MAPK1	5K4I	X-RAY DIFFRACTION	1.76	0.232	0.181	0.183
MAP2K1	4U7Z	X-RAY DIFFRACTION	2.81	0.214	0.161	0.163
IGF1R	2OJ9	X-RAY DIFFRACTION	2.00	0.276	0.214	0.217

TABLE 5 Results of data related to the docking of vitamin D3 with core target molecules.

Molecular name	Targets	PDB ID	LibDockScore	RMSD(Å)
VitaminD3	ALB	6A7P	159.048	1.32
VitaminD3	SRC	6QL3	120.344	1.29
VitaminD3	MMP9	5UE4	115.312	0.39
VitaminD3	PPARG	4XUH	135.064	0.70
VitaminD3	HSP90AA1	2BZ5	102.392	1.68
VitaminD3	IGF1	3O23	131.303	1.76
VitaminD3	EGFR	5D41	142.962	0.50
VitaminD3	MAPK1	5K4I	135.699	0.41
VitaminD3	MAP2K1	4U7Z	123.954	0.68
VitaminD3	IGF1R	20J9	125.226	1.67

AOM (10 mg/kg). At weeks 5, 8 and 11, the model and vitamin D3 intervention groups were given drinking water containing 2% DSS for 5 days and normal drinking water for the rest of the day. The mice were weighed twice a week. Mice were sacrificed at week 15, and colorectal tissues were collected for RT-qPCR experiments.

2.9.6.4 RT-qPCR

Gene expression of the core targets were detected in colorectal tissue by RT-qPCR. Total RNA was extracted from mouse intestinal tissue following the tissue RNA extraction protocol. The purity of RNA was detected by NanoDrop ND-2000 spectrophotometer and the ratio of A260/A280 was recorded. The reverse transcription reactions were performed on a common PCR instrument using the HiScript®II 1st Strand cDNA Synthesis Kit. Real-time fluorescence quantitative PCR was performed on a Light Cycler 480II real-time fluorescence quantitative PCR instrument. The $2^{-\Delta\Delta CT}$ method was used to calculate the expression of core targets. The corresponding primer sequences of the core targets were listed (Table 3).

3 Results

3.1 Target identification and analysis

221 targets of vitamin D3 were obtained in PharmMapper, DrugBank and Targetnet databases. 1205 CRC-related targets were obtained in the DisGeNET and GeneCards databases. The targets of vitamin D3 and CRC-related targets were imported into Venny 2.1.0, and 51 intersecting targets were obtained (Figure 2A).

3.2 Establishment of PPI network and selection of core targets

51 intersecting targets were input to String, and a PPI network (Figure 2B) containing 51 nodes and 369 edges was established. The tsv file of the PPI network was downloaded and imported into Cytoscape 3.9.0 for visualization and analysis (Figure 3A). The intersecting targets were ranked from largest to smallest

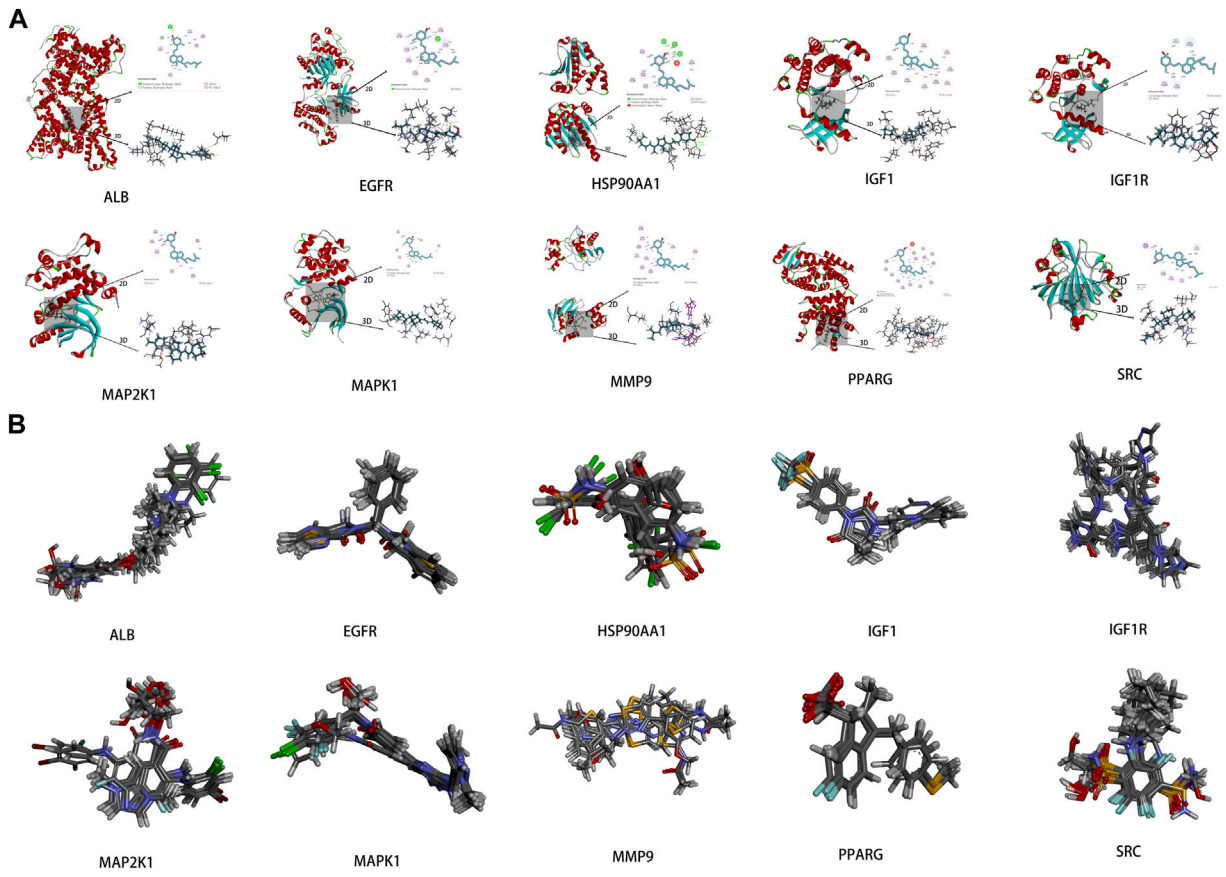

FIGURE 6
Results of molecular docking **(A)**. Schematic diagram of molecular docking of the core targets with vitamin D3 **(B)**. Visualization results of molecular docking RMSD validation.

according to the degree value using the Cytohubba plugin. The top 10 intersecting targets were selected as core targets for vitamin D3 prevention of CRC. The core targets are visualized (Figure 3B). The circles represent the core targets for screening, and the redder the color of the circle, the greater the importance (Chin et al., 2014). The 10 core targets include ALB, SRC, MMP9, PPARG, HSP90AA1, IGF1, EGFR, MAPK1, MAP2K1 and IGF1R.

3.3 Results of enrichment analysis

Core targets were imported into DAVID for GO and KEGG enrichment analysis. The results of GO enrichment analysis of core targets included 134 entries, BP(Biological Process):90, CC(Cellular Component):23, MF(Molecular Function):21. The top 10 items in each category were selected for visual analysis (Figure 4A). The biological processes involved in the 10 core targets were mainly endosome transport, peptidyl-tyrosine autophosphorylation, and positive regulation of DNA binding. They mainly act on the alphav-beta3 integrin-IGF-1-IGF1R complex, dendritic growth cone. They are involved in molecular functions including insulin receptor binding, scaffold protein binding, protein tyrosine kinase activity, etc. 80 signaling pathways were identified by KEGG enrichment analysis of core targets, and 20 important signaling pathways were visualized and analyzed (Figure 4B). The main signaling pathways involved include the HIF-1 signaling pathway, PI3K-Akt signaling pathway, etc. The results of KEGG enrichment analysis suggest that vitamin D3 may prevent CRC mainly through the above pathway.

3.4 Drug-target-pathway network

The core targets, vitamin D3 and KEGG enrichment pathways were categorized and organized to construct the drug-target-pathway network in Cytoscape 3.9.0 (Figure 5). In Figure 5, the triangle represents vitamin D3, the circle represents the core target, and the diamond represents the pathway in which the core target was enriched.

3.5 Results of molecular docking

To investigate the interaction between the 10 core targets and vitamin D3, molecular docking was used. The relevant information of 10 core target proteins was downloaded from the PDB database (Table 4). First, the 3D structure file of vitaminD3 was uploaded to Discovery Studio 2019; then, its docking potential with ALB, SRC, MMP9, PPARG, HSP90AA1, IGF1, EGFR, MAPK1, MAP2K1 and IGF1R were analyzed. The results of molecular docking scores were

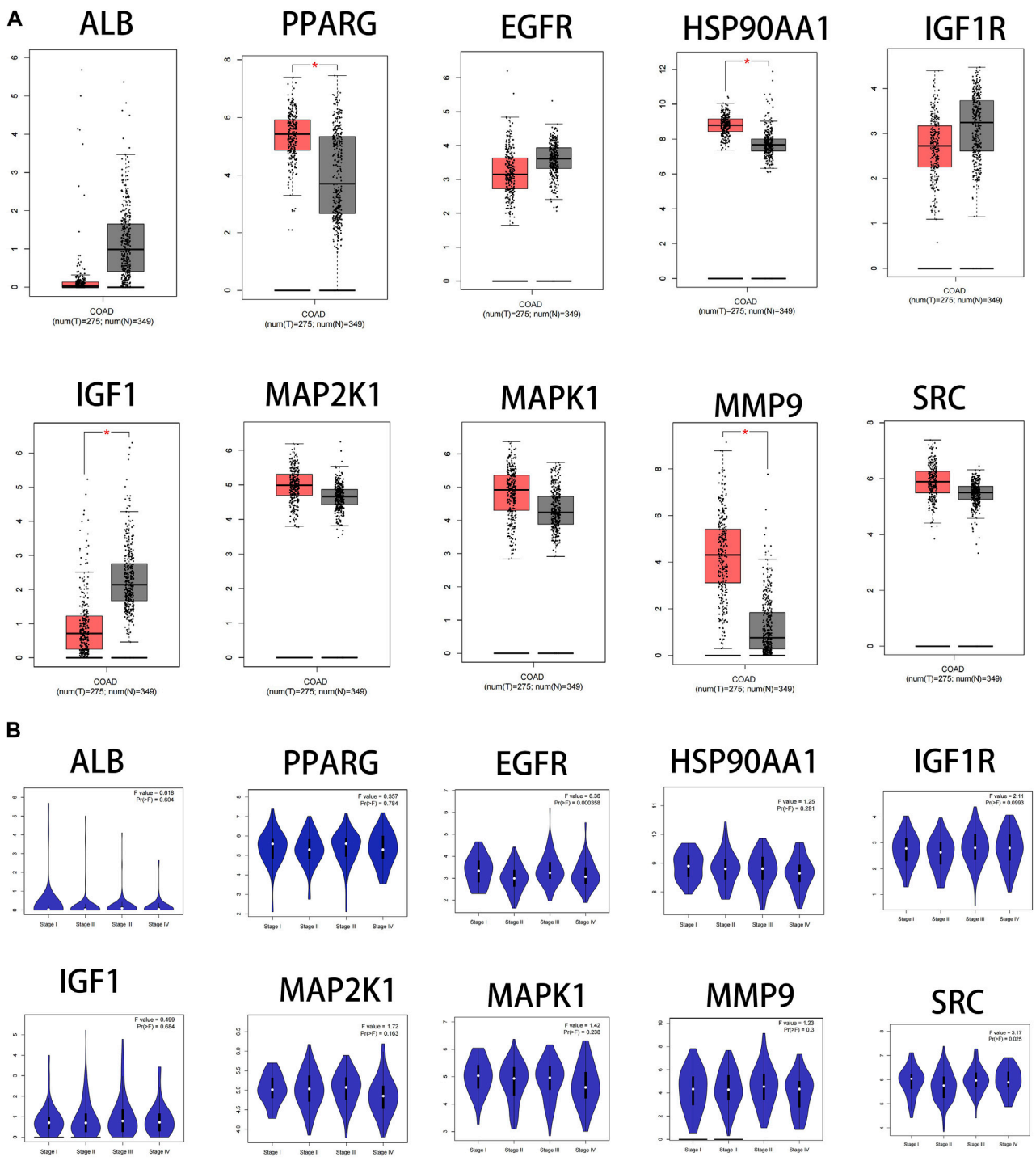

FIGURE 7
Fact sheet of the core targets on the GEPIA website. **(A)** Boxplot results of mRNA expression levels of core targets. Tumor tissue is shown in red and normal tissue is shown in gray. **(B)** Diagram of the relationship between core target gene expression and CRC cancer stage.

obtained. The root-mean-square deviation (RMSD) of the ligand conformation after docking and the ligand conformation of the original crystal structure were calculated. It is generally considered that when the RMSD value is less than 2.0, it proves that the docking method can better reproduce the original ligand-receptor binding mode and the docking parameters are reasonably set (Table 5). All results of RMSD are displayed. The results of core target docking with vitamin D3 are shown, the relationship between vitamin D3 and docking sites was represented in two and three dimensions, respectively (Figure 6A). RMSD validates the molecular docking reliability. In the 2D and 3D structure diagrams, we can observe the type of interaction forces between vitamin D3 and amino acid residues, and the length of the

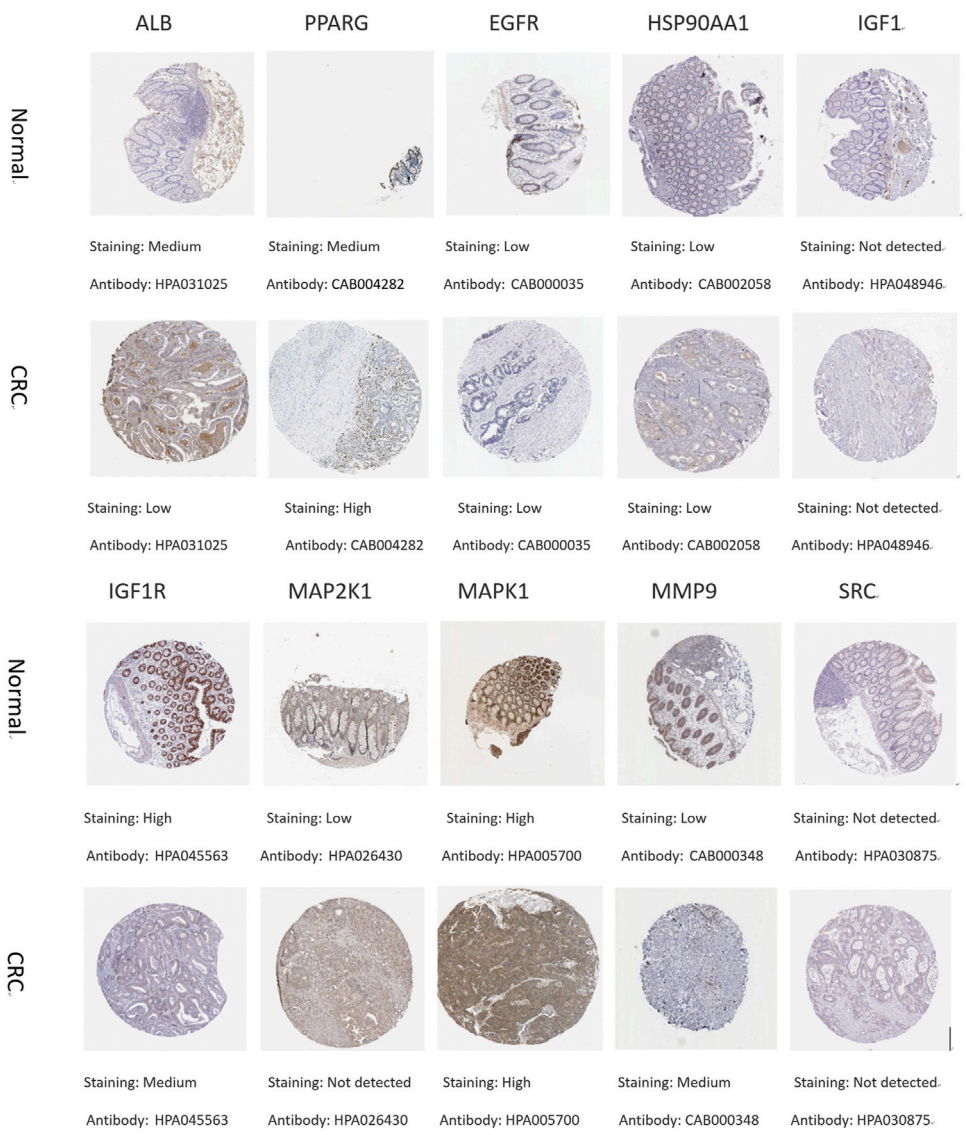

FIGURE 8
Immunohistochemical pictures of core target proteins in normal and CRC patients from the HPA database.

bonds. Validation of the reliability of molecular docking results (Figure 6B). The higher the degree of overlap of different conformations of the same protein, the more reliable the molecular docking results. The RMSD value is generally considered to be less than 2, and molecular docking is more reliable.

3.6 External validation of core targets

3.6.1 The mRNA expression levels of core targets

The results showed that the mRNA expression levels of PPARG, HSP90AA1and MMP9 were higher than normal in CRC($p < 0.05$). The mRNA expression level of IGF1 was lower than normal in CRC ($p < 0.05$) (Figure 7A). The mRNA expression levels of EGFR and SRC correlated with the stages of CRC($p < 0.05$) (Figure 7B).

3.6.2 The protein expression level of core targets

To understand the expression of core targets in CRC, the relevant immunohistochemical images were analyzed by HPA database. The protein levels of PPARG and MMP9 were found to be high in CRC by comparative analysis. The protein expression of ALB, IGF1R, and MAP2K1 was higher in normal tissues than in CRC. The protein expression of EGFR, HSP90AA1, and MAPK1 was equal in normal and CRC. Immunohistochemical data of IGF1 and SRC were not found in the HPA database (Figure 8).

3.7 Genetic alteration of core targets

Among the samples with mutation and CNA data (105 samples/patient), a total of 36 samples (34%) had mutations in the relevant genes,

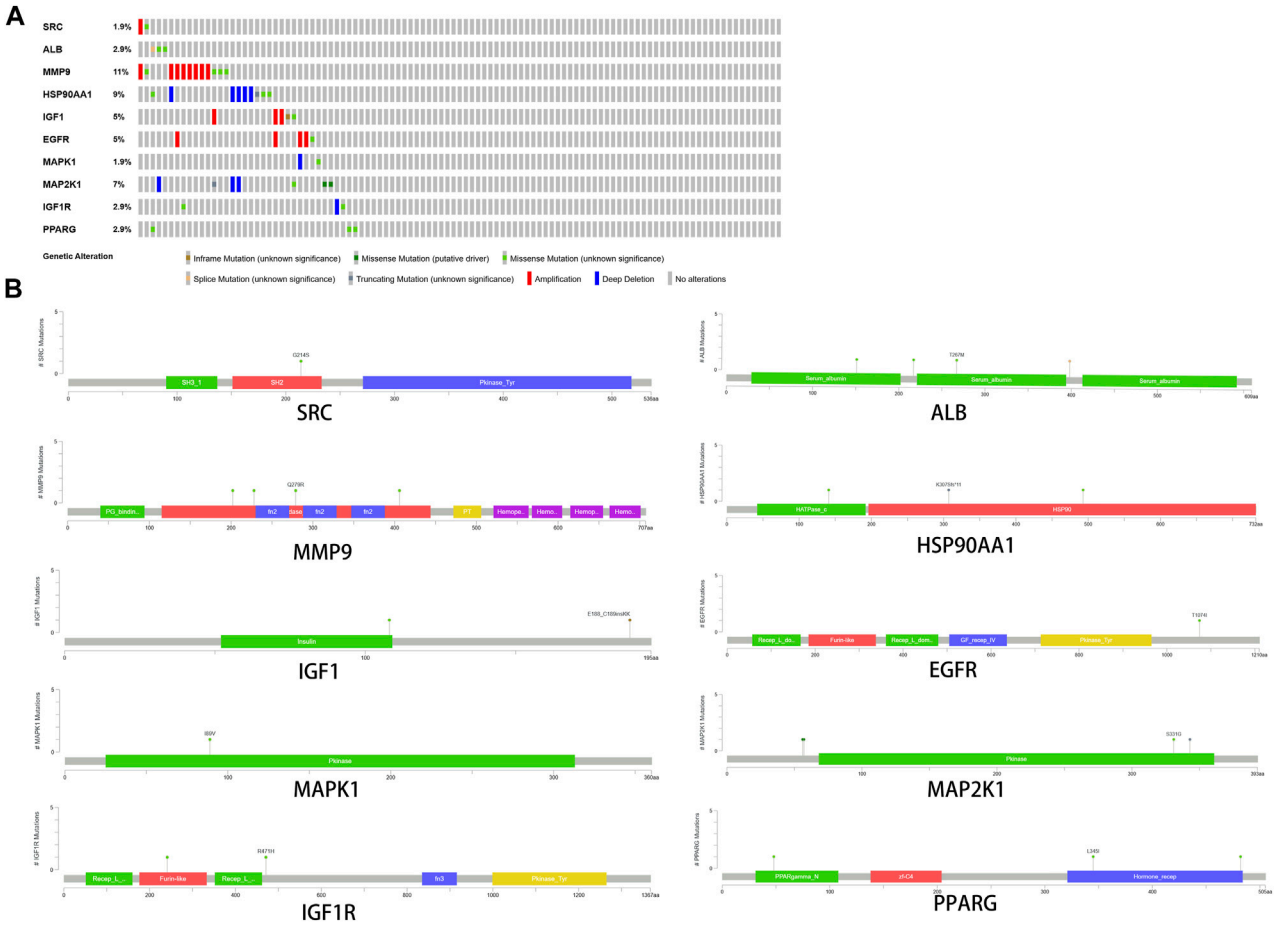

FIGURE 9
Genetic data on core targets. **(A)** The data suggested that 34 of 105 patients (36%) had a heritable variation on core target genes. **(B)** Information on the site and type of gene mutations on core targets in CRC patients.

TABLE 6 Detailed information about mutations on core target genes.

Gene name	Sample ID	Protein change	Mutation type	Variant type	Start pos	End pos
SRC	11CO018	G214S	Missense	SNP	36024651	36024651
ALB	11CO070	X398_splice	Splice	SNP	74281975	74281975
MMP9	11CO051	A202T	Missense	SNP	44639644	44639644
HSP90AA1	05CO041	T141M	Missense	SNP	102552660	102552660
IGF1	05CO050	Y108N	Missense	SNP	102813367	102813367
EGFR	14CO003	T1074I	Missense	SNP	55270268	55270268
MAPK1	11CO036	I89V	Missense	SNP	22161990	22161990
MAP2K1	11CO019	Q56P	Missense	SNP	66727451	66727451
IGF1R	20CO003	A241T	Missense	SNP	99434634	99434634
PPARG	05CO015	V48M	Missense	SNP	12421262	12421262

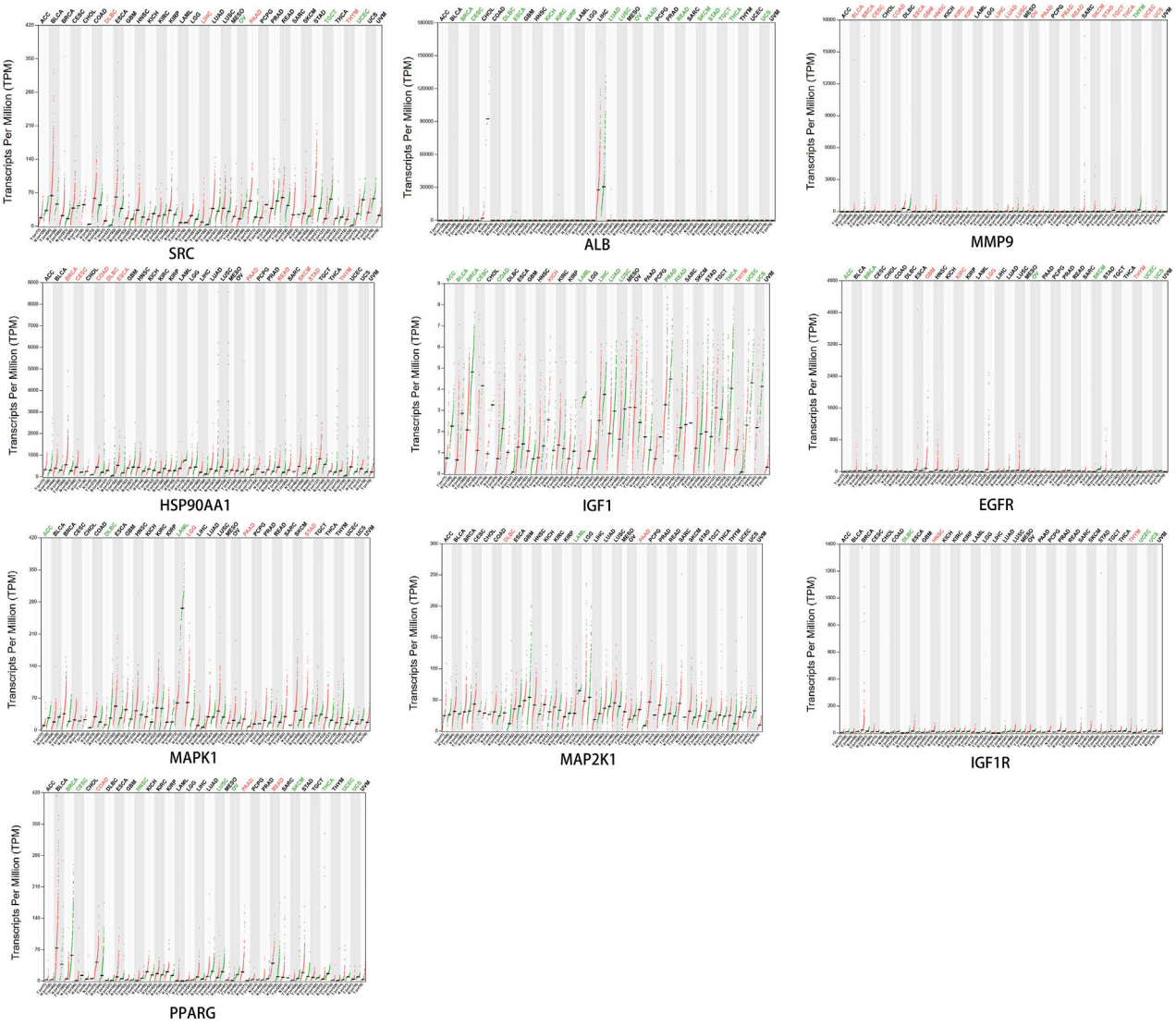

FIGURE 10
Expression of core target proteins in different cancers.

including 10 core targets (Figure 9A). It also shows the site and type of mutations in the core target genes in CRC patients (Figure 9B). Some details of the mutations in the core target genes are shown (Table 6).

3.8 The expression of core targets in different cancers

Dot plots of core target protein distribution were obtained in different cancers in the GEPIA database. The results showed that the expression levels of core target proteins differed in different cancers (Figure 10).

3.9 Effect of core targets on overall survival

The core targets were entered into Kaplan-Meier Plotter for analysis. The effect of expression levels of 10 targets on the overall survival of CRC patients were obtained (Figure 11). The results of survival analysis showed that patients with high expression of ALB,HSP90AA1, PPARG and MAPK1 had a longer survival period than those with low expression, and the difference was statistically significant. Patients with low expression of EGFR,IGF1, IGF1R and SRC in CRC patients had a longer survival time than those with high expression, and the difference was statistically significant. Patients with higher expression of MAP2K1 and MMP9 in CRC had longer survival, but the difference was not statistically significant.

3.10 RT-qPCR results

Through the experiment, the following findings were obtained:SRC, IGF1, IGF1R, HSP90AA1, MAPK1 and

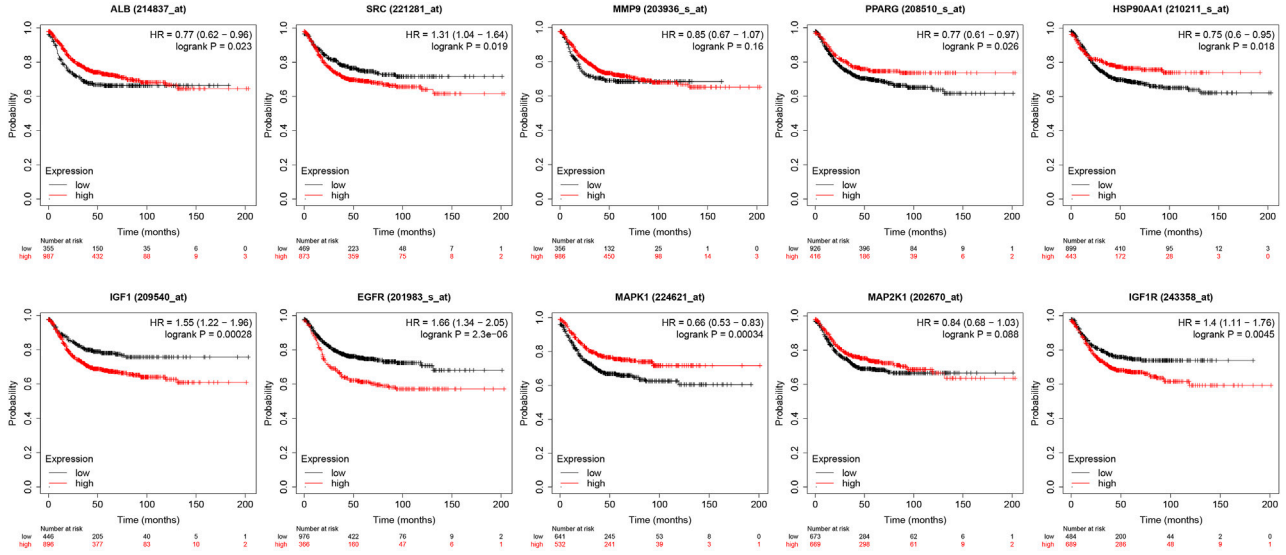

FIGURE 11
Presentation of results from survival analysis.

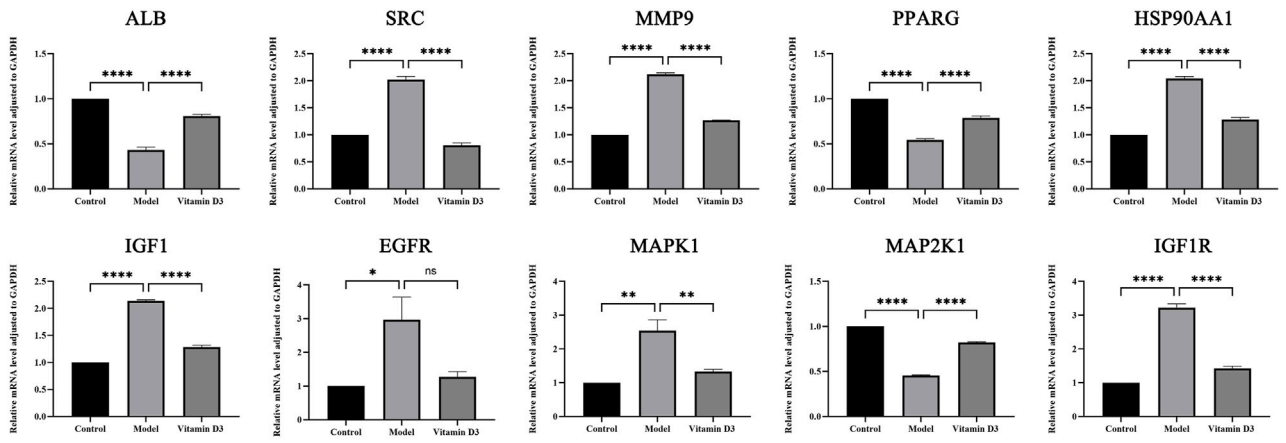

FIGURE 12
Results of RT-qPCR statistical analysis.

MMP9 are high expression in CRC tissues and after the intervention of vitamin D3, the expression of these genes was reduced in cancer tissues, and the differences were statistically significant ($p < 0.05$). The expression of EGFR is high in CRC tissues and decreased in CRC tissues after vitamin D3 intervention, but the difference was not statistically significant ($p > 0.05$). ALB, MAP2K1, and PPARG are low expression in CRC tissues, and their expression levels increased after the intervention of vitamin D3, which indicates that the treatment of vitamin D3 is effective and the difference is statistically significant ($p < 0.05$). The results of statistical analysis of RT-qPCR experiments are shown (Figure 12).

4 Discussion

The disease burden of CRC has been high and has increased in Asia in recent years (Onyoh et al., 2019). Vitamin D3 is a small molecule compound. More and more epidemiological studies have shown that vitamin D3 has a more prominent role in preventing cancer, especially CRC. The chemopreventive effect of vitamin D3 on CRC has been reported (Lamprecht and Lipkin, 2003). However, the pathogenesis of cancer is complex and the chemical nature of the drug is not fully clear, so the molecular mechanism of the interaction between vitamin D3 and CRC needs to be further investigated.

In this study, we further investigated the molecular mechanism of vitamin D3 in the prevention of CRC through network pharmacology and animal experimental studies. The results of the enrichment analysis suggest that vitamin D3 may play a role in the prevention of CRC through the PI3K-Akt signaling pathway and the HIF signaling pathway. A study showed that vitamin D3 can inhibit cell proliferation, invasion, and metastasis and promote apoptosis through the PI3K-Akt pathway (Songyang et al., 2021). Vitamin D3 can also interfere with the metabolism of cancer cells, inhibit the growth and proliferation of cancer cells, and play an anti-cancer role through the HIF signaling pathway (Gkotinakou et al., 2022).

The mechanisms of action of vitamin D include inhibition of VDR-mediated IGF1, HIF1, NF-κB and PI3K/AKT activities, or activation of MAPK family-related genes, downregulation of cell cycle progression, anti-inflammation, inhibition of angiogenesis, induction of apoptosis, and other anti-tumor effects (Skrajnowska and Bobrowska-Korczak, 2019). Solid tumor cells usually exhibit reduced oxygen levels depending on the rate of cell proliferation, vascular abnormalities, and the distance to the area surrounding the oxygen-containing vessels (Semenza, 2021). The growth and reproduction of cancer cells depend on a moderate supply of oxygen, so a hypoxic microenvironment would significantly affect the biological behavior of cancer cells during their life course. Under hypoxic conditions, the HIF signaling pathway is activated, causing transcription of the corresponding target genes and promoting the development of tumors. Thus, overexpression of HIF-1α can induce increased mortality in many common cancers (Keith et al., 2011). Activation of HIFs induces a series of cascade responses, including alteration of the metabolism of cancer cells and inhibition of the apoptosis of cancer cells. Under the combined effect of these factors, the proliferation, angiogenesis, immune escape, epithelial-mesenchymal transition and the ability of extracellular matrix remodeling of cancer cells are enhanced (Mylonis et al., 2021; Semenza, 2021). The existing evidence suggests that ossifying triol can act on the signaling process of HIF pathway, blocking signal transduction, promoting apoptosis of cancer cells and exerting tumor suppressive effects (Gkotinakou et al., 2022). Mitogen-activated protein kinase (MAPK) is an important member of the serine-threonine kinase family and is the main cell proliferation signaling pathway from the cell surface to the nucleus (Dong et al., 2002).

A growing number of evidences suggest that activation of ERK MAPK pathway is closely associated with the occurrence, development and oncogenic behavior of human CRC (Wang et al., 2004). The antitumor effects of vitamin D in CRC are achieved through various pathways such as promoting cell cycle arrest in the G1 phase, reducing the synthesis of vascular endothelial growth factor (VEGF), and decreasing the ability of cell migration and angiogenesis. Meanwhile, IGF1 and IGF1R can induce cell proliferation, promote the transcription and expression of vascular endothelial growth factor genes, promote angiogenesis, provide more nutrients for tumor growth, and promote the further development of CRC to advanced stages. The effect of vitamin D on the G1/S cell cycle transition is opposite to that of IGF-1 and also has antagonistic effects on angiogenesis and the tumor microenvironment. Therefore, this evidence may provide new ideas on the mechanism of the prevention of vitamin D in CRC (Ciulei et al., 2020). The results of RT-qPCR from animal experiments in this study also indicated that vitamin D has a therapeutic and preventive effect on CRC.

These results suggest that vitamin D may be an effective chemical for the prevention of CRC. In summary, ALB, SRC, MMP9, PPARG, HSP90AA1, IGF1, EGFR, MAPK1, MAP2K1 and IGF1R play important roles in the pathogenesis of CRC. Therefore, based on the network pharmacological analysis, it is expected to discover more novel compounds that can prevent cancer or play an anti-cancer role. This study provides additional theoretical basis for the prevention of CRC with vitamin D3.

In this study, vitamin D was found to be a multi-target medicine for the prevention of CRC. We predict that the main mechanism of vitamin D for the prevention of CRC is the regulation of tumor cell proliferation, apoptosis, migration and angiogenesis through signaling pathways such as HIF-1, FoxO and PI3K-Akt, thus playing a role in the prevention of CRC.

5 Conclusion

Based on network pharmacological analysis, this study predicted 10 potential core targets of vitamin D3 for the prevention of CRC, suggesting that vitamin D3 is a single-component, multi-target, multi-pathway small molecule compound. Network pharmacological analysis suggests that vitamin D3 may play a role in CRC chemoprevention by regulating different targets, such as MAPK, IGF1 and IGF1R. Graphene oxide analysis of the core targets ALB, SRC, MMP9, PPARG, HSP90AA1, IGF1, EGFR, MAPK1, MAP2K1 and IGF1R showed that vitamin D3 exerts pharmacological effects by affecting different biological processes, such as endosomal transport and positive regulation of protein kinase B signaling. The analysis of KEGG pathway in this study suggests that vitamin D3 may exert pharmacological effects by simultaneously regulating different CRC-related signaling pathways, such as FoxO signaling pathway, HIF-1 signaling pathway, PI3K-Akt signaling pathway, etc. These results support that vitamin D3 may mediate the inhibition of HIF-1 through inhibition of the upstream PI3K-AKT pathway.

In summary, vitamin D3 may be a new safe, effective, multi-targeted medicine for the prevention of CRC. This study concludes from a network pharmacological analysis that vitamin D3 may play a preventive role in CRC by regulating cell metabolism, proliferation and apoptosis through multiple targets, pathways and biological processes. However, the clinical efficacy of vitamin D3 in the prevention of CRC and its mechanism of action need to be further validated.

Data availability statement

The original contributions presented in the study are included in the article/Supplementary Material, further inquiries can be directed to the corresponding author.

Ethics statement

The animal study was reviewed and approved by the Ethics Committee of the Fifth Affiliated Hospital of Zhengzhou University (KY2023007). Written informed consent was obtained from the individual(s) for the publication of any potentially identifiable images or data included in this article.

Author contributions

Conception and design KR and SC; Administrative support HH; Provision of study materials or patients: KR and SC; Collection and assembly of data KR, SC, LM, and MN; Data analysis and interpretation KR, SC, and LM; Manuscript writing. All authors listed have made a substantial, direct, and intellectual contribution to the work and approved it for publication.

Funding

Medical Science and Technology Research Program of Henan Province (No: 2018020228).

Acknowledgments

We like to thank the editors and the reviewers for their valuable comments and suggestions to improve the quality of the paper.

Conflict of interest

The authors declare that the research was conducted in the absence of any commercial or financial relationships that could be construed as a potential conflict of interest.

Publisher's note

Supplementary material

The Supplementary Material for this article can be found online at: https://www.frontiersin.org/articles/10.3389/fphar.2023.1192210/full#supplementary-material

References

Ashburner, M., Ball, C. A., Blake, J. A., Botstein, D., Butler, H., Cherry, J. M., et al. (2000). Gene ontology: Tool for the unification of biology. The gene ontology consortium. *Nat. Genet.* 25 (1), 25–29. doi:10.1038/75556

Baron, J. .A., Barry, E. L., Mott, L. A., Rees, J. R., Sandler, R. S., Snover, D. C., et al. (2015). A trial of calcium and vitamin D for the prevention of colorectal adenomas. *N. Engl. J. Med.* 373 (16), 1519–1530. doi:10.1056/NEJMoa1500409

Bikle, D. D. (2016). Extraskeletal actions of vitamin D. *Ann. N. Y. Acad. Sci.* 1376 (1), 29–52. doi:10.1111/nyas.13219

Chen, W., Zheng, R., Baade, P. D., Zhang, S., Zeng, H., Bray, F., et al. (2016). Cancer statistics in China, 2015. *CA Cancer J. Clin.* 66 (2), 115–132. doi:10.3322/caac.21338

Chin, C. H., Chen, S. H., Wu, H. H., et al. (2014). cytoHubba: identifying hub objects and sub-networks from complex interactome [J]. *BMC Syst. Biol.* 8 (Suppl. 4), s11.

Ciulei, G., Orasan, O. H., Coste, S. C., Cozma, A., Negrean, V., and Procopciuc, L. M. (2020). Vitamin D and the insulin-like growth factor system: Implications for colorectal neoplasia. *Eur. J. Clin. Invest.* 50 (9), e13265. doi:10.1111/eci.13265

Doncheva, N. T., Morris, J. H., Gorodkin, J., and Jensen, L. J. (2019). Cytoscape StringApp: Network analysis and visualization of proteomics data. *J. Proteome Res.* 18 (2), 623–632. doi:10.1021/acs.jproteome.8b00702

Dong, C., Davis, R. J., and Flavell, R. A. (2002). MAP kinases in the immune response. *Annu. Rev. Immunol.* 20, 55–72. doi:10.1146/annurev.immunol.20.091301.131133

Doubeni, C. A., Corley, D. A., Quinn, V. P., Jensen, C. D., Zauber, A. G., Goodman, M., et al. (2018). Effectiveness of screening colonoscopy in reducing the risk of death from right and left colon cancer: A large community-based study. *Gut* 67 (2), 291–298. doi:10.1136/gutjnl-2016-312712

Fakih, M. G. (2015). Metastatic colorectal cancer: Current state and future directions. *J. Clin. Oncol.* 33 (16), 1809–1824. doi:10.1200/JCO.2014.59.7633

Feldman, D., Krishnan, A. V., Swami, S., Giovannucci, E., and Feldman, B. J. (2014). The role of vitamin D in reducing cancer risk and progression. *Nat. Rev. Cancer*. 14 (5), 342–357. doi:10.1038/nrc3691

Fleet, J. C., Desmet, M., Johnson, R., and Li, Y. (2012). Vitamin D and cancer: A review of molecular mechanisms. *Biochem. J.* 441 (1), 61–76. doi:10.1042/BJ20110744

Giammanco, M., Di Majo, D., La Guardia, M., Aiello, S., Crescimannno, M., Flandina, C., et al. (2015). Vitamin D in cancer chemoprevention. *Pharm. Biol.* 53 (10), 1399–1434. doi:10.3109/13880209.2014.988274

Gkotinakou, I. M., Mylonis, I., and Tsakalof, A. (2022). Vitamin D and hypoxia: Points of interplay in cancer. *Cancers (Basel)* 14 (7), 1791. doi:10.3390/cancers14071791

Harris, D. M., and Go, V. L. (2004). Vitamin D and colon carcinogenesis. *J. Nutr.* 134, 3463S–3471S. doi:10.1093/jn/134.12.3463S

He, Q., Liu, C., Wang, X., Rong, K., Zhu, M., Duan, L., et al. (2023). Exploring the mechanism of curcumin in the treatment of colon cancer based on network pharmacology and molecular docking. *Front. Pharmacol.* 14, 1102581. doi:10.3389/fphar.2023.1102581

Holick, M. F. (2004). Sunlight and vitamin D for bone health and prevention of autoimmune diseases, cancers, and cardiovascular disease. *Am. J. Clin. Nutr.* 80, 1678S–88S. doi:10.1093/ajcn/80.6.1678S

Huang, D. W., Sherman, B. T., Tan, Q., Kir, J., Liu, D., Bryant, D., et al. (2007). DAVID bioinformatics resources: Expanded annotation database and novel algorithms to better extract biology from large gene lists. *Nucleic Acids Res.* 35, W169–W175. doi:10.1093/nar/gkm415

Kanehisa, M., Furumichi, M., Sato, Y., Ishiguro-Watanabe, M., and Tanabe, M. (2021). KEGG: Integrating viruses and cellular organisms. *Nucleic Acids Res.* 49 (D1), D545–D551. doi:10.1093/nar/gkaa970

Katona, B. W., and Weiss, J. M. (2020). Chemoprevention of colorectal cancer. *Gastroenterology* 158 (2), 368–388. doi:10.1053/j.gastro.2019.06.047

Keith, B., Johnson, R. S., and Simon, M. C. (2011). HIF1α and HIF2α: Sibling rivalry in hypoxic tumour growth and progression. *Nat. Rev. Cancer.* 12 (1), 9–22. doi:10.1038/nrc3183

Kim, S., Chen, J., Cheng, T., Gindulyte, A., He, J., He, S., et al. (2021). PubChem in 2021: New data content and improved web interfaces. *Nucleic Acids Res.* 49 (D1), D1388–D1395. doi:10.1093/nar/gkaa971

Lamprecht, S. A., and Lipkin, M. (2003). Chemoprevention of colon cancer by calcium, vitamin D and folate: Molecular mechanisms. *Nat. Rev. Cancer*. 3 (8), 601–614. doi:10.1038/nrc1144

Levin, T. R., Corley, D. A., Jensen, C. D., Schottinger, J. E., Quinn, V. P., Zauber, A. G., et al. (2018). Effects of organized colorectal cancer screening on cancer incidence and mortality in a large community-based population. *Gastroenterology* 155 (5), 1383–1391. doi:10.1053/j.gastro.2018.07.017

Leyssens, C., Verlinden, L., and Verstuyf, A. (2013). Antineoplastic effects of 1,25(OH)2D3 and its analogs in breast, prostate and colorectal cancer. *Endocr. Relat. Cancer* 20 (2), R31–R47. doi:10.1530/ERC-12-0381

Liu, X., Ouyang, S., Yu, B., Liu, Y., Huang, K., Gong, J., et al. (2010). PharmMapper server: A web server for potential drug target identification using pharmacophore mapping approach. *Nucleic Acids Res.* 38, W609–W614. doi:10.1093/nar/gkq300

Ma, Y., Zhang, P., Wang, F., Yang, J., Liu, Z., and Qin, H. (2011). Association between vitamin D and risk of colorectal cancer: A systematic review of prospective studies. *J. Clin. Oncol.* 29 (28), 3775–3782. doi:10.1200/JCO.2011.35.7566

Mccullough, M. L., Robertson, A. S., Rodriguez, C., Jacobs, E. J., Chao, A., Carolyn, J., et al. (2003). Calcium, vitamin D, dairy products, and risk of colorectal cancer in the Cancer Prevention Study II Nutrition Cohort (United States). *Cancer Causes Control* 14 (1), 1–12. doi:10.1023/a:1022591007673

Mylonis, I., Chachami, G., and Simos, G. (2021). Specific inhibition of HIF activity: Can peptides lead the way? *Cancers (Basel)* 13 (3), 410. doi:10.3390/cancers13030410

Nishihara, R., Wu, K., Lochhead, P., Morikawa, T., Liao, X., Qian, Z. R., et al. (2013). Long-term colorectal-cancer incidence and mortality after lower endoscopy. *N. Engl. J. Med.* 369 (12), 1095–1105. doi:10.1056/NEJMoa1301969

Onyoh, E. F., Hsu, W. F., Chang, L. C., Lee, Y. C., Wu, M. S., and Chiu, H. M. (2019). The rise of colorectal cancer in Asia: Epidemiology, screening, and management. *Curr. Gastroenterol. Rep.* 21 (8), 36. doi:10.1007/s11894-019-0703-8

Pinero, J., Ramirez-Anguita, J. M., Sauch-Pitarch, J., Ronzano, F., Centeno, E., Sanz, F., et al. (2020). The DisGeNET knowledge platform for disease genomics: 2019 update. *Nucleic Acids Res.* 48 (D1), D845–D855. doi:10.1093/nar/gkz1021

Schoen, R. E., Pinsky, P. F., Weissfeld, J. L., Yokochi, L. A., Church, T., Laiyemo, A. O., et al. (2012). Colorectal-cancer incidence and mortality with screening flexible sigmoidoscopy. *N. Engl. J. Med.* 366 (25), 2345–2357. doi:10.1056/NEJMoa1114635

Semenza, G. L. (2021). Heritable disorders of oxygen sensing. *Am. J. Med. Genet. A* 185 (8), 2576–2581. doi:10.1002/ajmg.a.62250

Shaukat, A., Mongin, S. J., Geisser, M. S., Lederle, F. A., Bond, J. H., Mandel, J. S., et al. (2013). Long-term mortality after screening for colorectal cancer. *N. Engl. J. Med.* 369 (12), 1106–1114. doi:10.1056/NEJMoa1300720

Skrajnowska, D., and Bobrowska-Korczak, B. (2019). Potential molecular mechanisms of the anti-cancer activity of vitamin D. *Anticancer Res.* 39 (7), 3353–3363. doi:10.21873/anticanres.13478

Songyang, Y., Song, T., Shi, Z., Li, W., Yang, S., and Li, D. (2021). Effect of vitamin D on malignant behavior of non-small cell lung cancer cells. *Gene* 768, 145309. doi:10.1016/j.gene.2020.145309

Sporn, M. B. (1976). Approaches to prevention of epithelial cancer during the preneoplastic period. *Cancer Res.* 36 (7 PT 2), 2699–2702.

Stelzer, G., Rosen, N., Plaschkes, I., Zimmerman, S., Twik, M., Fishilevich, S., et al. (2016). The GeneCards suite: From gene data mining to disease genome sequence analyses. *Curr. Protoc. Bioinforma.* 54, 1.30.1–1.30.33. doi:10.1002/cpbi.5

Sung, H., Ferlay, J., Siegel, R. L., Laversanne, M., Soerjomataram, I., Jemal, A., et al. (2021). Global cancer statistics 2020: GLOBOCAN estimates of incidence and mortality worldwide for 36 cancers in 185 countries. *CA Cancer J. Clin.* 71 (3), 209–249. doi:10.3322/caac.21660

Tang, Z., Li, C., Kang, B., Gao, G., Li, C., and Zhang, Z. (2017). GEPIA: A web server for cancer and normal gene expression profiling and interactive analyses. *Nucleic Acids Res.* 45 (W1), W98–W102. doi:10.1093/nar/gkx247

Terry, P., Baron, J. .A., Bergkvist, L., Holmberg, L., and Wolk, A. (2002). Dietary calcium and vitamin D intake and risk of colorectal cancer: A prospective cohort study in women. *Nutr. Cancer.* 43 (1), 39–46. doi:10.1207/S15327914NC431_4

Thanikachalam, K., and Khan, G. (2019). Colorectal cancer and nutrition. *Nutrients* 11 (1), 164. doi:10.3390/nu11010164

Uhlen, M., Fagerberg, L., Hallstrom, B. M., Lindskog, C., Oksvold, P., Mardinoglu, A., et al. (2015). Proteomics. Tissue-based map of the human proteome. *Science* 347 (6220), 1260419. doi:10.1126/science.1260419

UniProt Consortium (2021). UniProt: The universal protein knowledgebase in 2021. *Nucleic Acids Res.* 49 (D1), D480–D489. doi:10.1093/nar/gkaa1100

Wang, X., Wang, Q., Hu, W., and Evers, B. M. (2004). Regulation of phorbol ester-mediated TRAF1 induction in human colon cancer cells through a PKC/RAF/ERK/NF-kappaB-dependent pathway. *Oncogene* 23 (10), 1885–1895. doi:10.1038/sj.onc.1207312

Wang, H., Chen, W., Li, D., Yin, X., Zhang, X., Olsen, N., et al. (2017). Vitamin D and chronic diseases. *Aging Dis.* 8 (3), 346–353. doi:10.14336/AD.2016.1021

Wishart, D. S., Feunang, Y. D., Guo, A. C., Lo, E. J., Marcu, A., Grant, J. R., et al. (2018). DrugBank 5.0: A major update to the DrugBank database for 2018. *Nucleic Acids Res.* 46 (D1), D1074–D1082. doi:10.1093/nar/gkx1037

Wu, K., Willett, W. C., Fuchs, C. S., Colditz, G. A., and Giovannucci, E. L. (2002). Calcium intake and risk of colon cancer in women and men. *J. Natl. Cancer Inst.* 94 (6), 437–446. doi:10.1093/jnci/94.6.437

Wu, P., Heins, Z. J., Muller, J. T., Katsnelson, L., de Bruijn, I., Abeshouse, A. A., et al. (2019). Integration and analysis of CPTAC proteomics data in the context of cancer genomics in the cBioPortal. *Mol. Cell. Proteomics*. 18 (9), 1893–1898. doi:10.1074/mcp.TIR119.001673

Yao, Z. J., Dong, J., Che, Y. J., Zhu, M. F., Wen, M., Wang, N. N., et al. (2016). TargetNet: A web service for predicting potential drug-target interaction profiling via multi-target SAR models. *J. Comput. Aided Mol. Des.* 30 (5), 413–424. doi:10.1007/s10822-016-9915-2

Zheng, W., Anderson, K. E., Kushi, L. H., Sellers, T. A., Greenstein, J., Hong, C. P., et al. (1998). A prospective cohort study of intake of calcium, vitamin D, and other micronutrients in relation to incidence of rectal cancer among postmenopausal women. *Cancer Epidemiol. Biomarkers Prev.* 7 (3), 221–225.

frontiers | Frontiers in Pharmacology

TYPE Review
PUBLISHED 08 June 2023
DOI 10.3389/fphar.2023.1209412

OPEN ACCESS

EDITED BY
Ayaz Shahid,
Western University of Health Sciences, United States

REVIEWED BY
Suryaa Manoharan,
Bharathiar University, India
Muhammad Khan,
University of the Punjab, Pakistan

*CORRESPONDENCE
Jinzhu Huang,
huangjinzhu@cdutcm.edu.cn
Yulan Ren,
renxg2468@163.com

†These authors have contributed equally to this work and share first authorship

RECEIVED 20 April 2023
ACCEPTED 30 May 2023
PUBLISHED 08 June 2023

CITATION
Zhou X, Zeng Y, Zheng R, Wang Y, Li T, Song S, Zhang S, Huang J and Ren Y (2023), Natural products modulate cell apoptosis: a promising way for treating endometrial cancer.
Front. Pharmacol. 14:1209412.
doi: 10.3389/fphar.2023.1209412

Natural products modulate cell apoptosis: a promising way for treating endometrial cancer

Xin Zhou[1†], Yiwei Zeng[1†], Runchen Zheng[2], Yuemei Wang[1], Tao Li[1], Shanshan Song[2], Su Zhang[1], Jinzhu Huang[3,4]* and Yulan Ren[2]*

[1]School of Acupuncture-Moxibustion and Tuina, Chengdu University of Traditional Chinese Medicine, Chengdu, China, [2]School of Chinese Classics, Chengdu University of Traditional Chinese Medicine, Chengdu, China, [3]School of Nursing, Chengdu University of Traditional Chinese Medicine, Chengdu, China, [4]Department of Gynecology, School of Clinical Medicine, Chengdu University of Traditional Chinese Medicine, Chengdu, China

Endometrial cancer (EC) is a prevalent epithelial malignancy in the uterine corpus's endometrium and myometrium. Regulating apoptosis of endometrial cancer cells has been a promising approach for treating EC. Recent *in-vitro* and *in-vivo* studies show that numerous extracts and monomers from natural products have pro-apoptotic properties in EC. Therefore, we have reviewed the current studies regarding natural products in modulating the apoptosis of EC cells and summarized their potential mechanisms. The potential signaling pathways include the mitochondria-dependent apoptotic pathway, endoplasmic reticulum stress (ERS) mediated apoptotic pathway, the mitogen-activated protein kinase (MAPK) mediated apoptotic pathway, NF-κB-mediated apoptotic pathway, PI3K/AKT/mTOR mediated apoptotic pathway, the p21-mediated apoptotic pathway, and other reported pathways. This review focuses on the importance of natural products in treating EC and provides a foundation for developing natural products-based anti-EC agents.

KEYWORDS

natural products, endometrial cancer, apoptosis, signal pathway, anti-cancer effects

1 Introduction

Endometrial cancer (EC) refers to a prevalent epithelial malignancy occurring in the endometrium and myometrium of the uterine corpus. It is the most common gynecological malignancy in developed countries and the second most common in developing countries (Sung et al., 2021; Akazawa and Hashimoto, 2022). The morbidity of EC is estimated to increase by more than 50% worldwide by 2040 (Moore and Brewer, 2017; Zhang S. et al., 2019; Brooks et al., 2019). EC typically occurs in postmenopausal women, while a rising incidence is observed in the premenopausal population due to the increasing onset of obesity globally (Moore and Brewer, 2017). Conventional treatments for EC include surgical resection, radiotherapy, chemotherapy, and hormonotherapy, depending on the cancer stage (An et al., 2021). Though these treatment regimens benefit the patients, the outcomes and prognosis of those at the advanced and recurrent stage or with metastasis remain poor (Lu and Broaddus, 2020).

On the other hand, these options are often accompanied by adverse consequences. For example, a hysterectomy is recommended for patients with higher-grade EC or myometrium invasion, while these patients have to lose their childbearing ability (Lu and Broaddus, 2020). For patients receiving chemotherapy, the issue of drug resistance would not be ignored,

which could compromise the therapeutic effects of the agents leading to treatment failure (Hashem et al., 2022). Various side effects during the treatments pose multiple challenges to the patients; they would suffer from a functional loss in different behavioral and life domains and psychosocial distress (Concin et al., 2021). Hence, it presents an urgent need to explore new treatment alternatives for EC to improve patient outcomes and prognosis.

The specific pathogenesis of EC remains to be fully elucidated. Several physical, clinical, and genetic variables, including age, race, proximity to the metabolic syndrome, unopposed estrogen exposure, and genetic predispositions, are thought to have a role in the unique etiology of EC (Cai et al., 2019; Passarello et al., 2019). EC can be typically categorized into type-I and type-II due to their molecular and histopathology features, based on a classification system produced by Bokhman in 1983. Type-I accounts for most EC cases (70%–80%). In the endometrium, periodic hyperplasia is delicately controlled by programmed cell growth and death. The long-term effects of estrogen without progestin antagonism, which cause endometrial hyperplasia and atypical hyperplasia, followed by carcinogenesis, may cause type-I EC. Endometrial hyperplasia is a significant problem, and also the associated risk factors include hyperinsulinemia, obesity, high estradiol levels, and advanced age. Endometrial hyperplasia without atypical has a low (5%) risk of progression to endometrial cancer over 20 years. However, atypical glandular hyperplasia has a 27.5% risk of progression over 20 years and up to 43% of such patients (Hutt et al., 2019). Atypical hyperplasia, related to abnormal growth and proliferation of endometrial cells, is a precursor lesion for type-I EC (Armstrong et al., 2012; Braun et al., 2016; Urick and Bell, 2019), while its molecular basis is still unclear (Terzic et al., 2021). Apoptosis is a multistep programmed cell death process critical in clearing senescent and aberrant cells. Studies have demonstrated that inhibited cellular apoptosis is closely associated with the pathogenesis of EC. Dysfunction or inhibition of cellular apoptosis in the endometrium causes uncontrolled cell proliferation, aberration, and carcinogenesis (Fisher, 1994; Zhang et al., 2020). Given this situation, regulating apoptosis of EC cells would be a promising target for developing effective anti-EC agents.

In recent years, natural products (NPs) have become a research hotspot in cancer treatment (Huang et al., 2019; Atanasov et al., 2021; Kim et al., 2021; Anjum et al., 2022; Liu et al., 2022; Huang et al., 2023; Yuan et al., 2023). NPs refer to components, isolated metabolites, and extracts from natural plants and be of multiple bioactivities, such as regulating oxidative stress, inflammatory response, and cellular apoptosis. These agents also reveal therapeutic effects on various cancers (Shanmugam et al., 2016) with low toxicity and few side effects (Torquato et al., 2017). The detailed mechanisms underlying the anti-cancer properties of NPs need to be further explored to facilitate the development of NP-based anti-cancer agents. Both *in-vitro* and *in-vivo* studies demonstrate that many NPs could effectively suppress EC cells' growth, proliferation, and differentiation via regulating apoptosis (Liu et al., 2012), indicating the apoptosis-regulatory properties of NPs would be a promising direction for further exploration.

Therefore, we have performed a comprehensive search in Google Scholar, PubMed, China National Knowledge Infrastructure (CNKI), Wanfang Database, and VIP database, from the inception to 31 December 2022, for studies regarding NPs for the treatment of EC via inducing apoptosis, and have reviewed the relevant pathways including mitochondria-dependent apoptotic pathway, endoplasmic reticulum stress (ERS) mediated apoptotic pathway, mitogen-activated protein kinase (MAPK) mediated apoptotic pathway, NF-κB mediated apoptotic pathway, PI3K/Akt mediated apoptotic pathway, p21-mediated apoptotic pathway and others. We hope our work could provide inspiration and valuable references for future studies.

2 Overview of apoptosis

Cellular apoptosis is a genetically-regulated programmed cell death process that plays an essential role in cellular metabolism (Hengartner, 2000). Inadequate apoptosis could cause pathological changes like carcinogenesis, autoimmune diseases, and diabetes (Nair et al., 2014). It was first reported by Kerr et al., in 1972, describing it as characteristic morphological changes and a series of enzyme-dependent biochemical processes (Kerr et al., 1972). Apoptosis can be divided into the exogenous death receptor and endogenous mitochondrial apoptosis pathways (Ricci and El-Deiry, 2007; Zhang et al., 2022).

The intrinsic pathway refers to apoptotic cascades triggered by intracellular signals, such as DNA damage, aberrant cell metabolism, calcium overload, chemotherapeutic drugs, radiation, high levels of reactive oxygen species, and detachment from the extracellular matrix (Chaudhry and Asselin, 2009). In a typical situation, there is a dynamic balance between the expression of pro-apoptotic protein and anti-apoptotic protein, which regulates physiological apoptosis. Decreased expression of anti-apoptotic protein BCL-2 family members or increased expression of pro-apoptotic proteins in response to the various stimulus signals described previously leads to an unbalance in the BCL/BAX ratio, which in turn initiates the endogenous pathway. The intrinsic pathway is mainly mediated by the B Cell lymphoma-2 (BCL-2) gene family (Ashkenazi, 2008; Nair et al., 2014). Interactions between the BCL-2 protein family determine mitochondrial outer membrane permeability (Green, 2022). The pro-apoptotic BCL-2 effectors, such as BAX, BAK, BIM, BID, and PUMA, promote apoptosis by causing mitochondrial outer membrane permeabilization (MOMP), whereas anti-apoptotic BCL-2 effectors inhibit this process, such as BCL-2, BCL-XL, BCL-W, BCL-2-A1 and MCL1 (Carneiro and El-Deiry, 2020; Wolf et al., 2022). When BAX/BAK is inserted into the mitochondrial membrane, cytochrome c (Cyt-c) is released into the cytosol from the outer mitochondrial membrane. Cytochrome c's release is critical in cell apoptosis (Santucci et al., 2019). Cytosolic cytochrome c combines with apoptotic protease activating factor-1 (Apaf–1) and recruit pro-caspase-9 to form the apoptosome, a multiprotein complex (Li et al., 2017). Apoptosome is a multiprotein platform of caspase-9 activation to execute apoptosis (Malladi et al., 2009; Bratton and Salvesen, 2010; Dorstyn et al., 2018; Avrutsky and Troy, 2021). Once activated, caspase-9 could cleave and activate downstream pro-caspase-3 and -7 in the apoptosome, which in turn triggers the activation of further caspase-9 (Qin et al., 1999, 1; McComb et al., 2019, 7). If caspase-9 successfully processes some caspase-3 or caspase-7 in this situation, XIAP can bind to and suppress these active effector caspases (Bratton and Salvesen, 2010).

The extrinsic pathway is mainly triggered by extracellular stimuli (Jan and Chaudhry, 2019; Kashyap et al., 2021). The extracellular ligands such as tumor necrosis factor (TNF), Fas ligand (Fas-L), death receptor3 ligand (DR3L), and TNF-related apoptosis-inducing ligand (TRAIL) recognize and bind to their cognate death receptors (such as TNFR, Fas, DR3, DR4 or DR5) (Mandal et al., 2020). Procaspase-8 binds to the exposed DED of death receptor-related FADD through a pocket in its DED1 to form a death-inducing signaling complex (DISC) (Jiang M. et al., 2021) and subsequently activate pro-caspase-8. It can cleave and activate the downstream targeted molecules, including executor caspase-3 and caspase-7 and turn on the exogenous apoptotic cell death response (Jiang M. et al., 2021). Activated caspase-8 is a crucial protein of cross-talk signal way and could cleave Bid into tBid. Bid is generally thought to be inactive as an apoptosis inducer. tBid could induce mitochondrial outer membrane permeabilization (MOMP) in cells and induce the release of cytochrome c (CytC) and Smac/DIABLO from the mitochondria. Eventually, tBid can initiate the mitochondrial apoptosis pathway and makes significant in the endogenous apoptotic pathway by activating caspase-9 (Kantari and Walczak, 2011).

3 Endometrial carcinogenesis

Carcinogenesis in the endometrium is a complex and multistep process. The specific mechanisms remain elusive while several physical, pathological, and genetic factors are considered to be involved, such as age, race, concomitance with metabolic syndrome, unopposed estrogen exposure, and genetic predispositions (Cai et al., 2019; Passarello et al., 2019). Dysregulation of cellular apoptosis in the endometrium causes uncontrolled cell proliferation, aberration, and carcinogenesis (Fisher, 1994; Mirakhor Samani et al., 2018; Zhang et al., 2020).

EC can be typically categorized into type-I and type-II due to their molecular and histopathological features (Rodríguez-Palacios et al., 2022; Karia et al., 2023), based on a classification system produced by Bokhman in 1983. The type-I EC, endometrioid tumors, accounts for most EC cases (70%–80%). The type-I EC is derived from a precancerous condition called endometrial hyperplasia, whereas the type-II is hormone-independent pathogenesis without known precursor lesions (Huvila et al., 2013). Hyperplasia is a significant problem, and the associated risk factors include hyperinsulinemia, obesity, high estradiol levels, and increasing age (Singh et al., 2020). Endometrial hyperplasia without atypical has a low (5%) risk of progression to endometrial cancer over 20 years. However, atypical glandular hyperplasia has a 27.5% risk of progression over 20 years and up to 43% of such patients (Hutt et al., 2019). Atypical hyperplasia may further evolve into complex atypical hyperplasia (CAH). CAH is a precursor lesion for endometrioid-type endometrial cancer and is related to abnormal growth and proliferation of endometrial cells (Armstrong et al., 2012; Braun et al., 2016; Urick and Bell, 2019).

Clinical studies have found that the normal apoptotic mechanisms of many malignant cells are inhibited, preventing the body from early clearance of cells that may be at risk of cancer. Endometrial periodic hyperplasia is under delicate control by programmed cell growth and death. Apoptosis typically occurs between the human endometrium's late secretory and menstrual stages (Otsuki, 2001). Compared to the proliferating phase, the expression of BCL-2 and the activation of caspase-3, -8, and -9 are higher in secretory to menstruating stages (Otsuki, 2001). It is reported that EC patients are resistant to apoptosis due to the unbalance of the anti- and pro-apoptotic molecules. Increasing evidence has suggested that anti-apoptotic mediators, such as BCL-2, Mcl-2, and IAP (Ai et al., 2006), are downregulated in EC patients, whereas the pro-apoptotic proteins, such as tumor necrosis factor-related apoptosis-inducing ligand (TRAIL), p53 (Kohlberger et al., 1996; Geisler et al., 1999; Edmondson et al., 2017) upregulated modulator.

Cellular apoptosis is crucial in endometrial hyperplasia, atypical hyperplasia, complex atypical hyperplasia, and eventually endometrial cancer. Given this situation, regulating apoptosis of EC cells would be a promising target for developing effective anti-EC agents and could provide a possible direction for developing anti-EC drugs. In almost all cases, detailed information of NPs and their potential effects with mechanisms on modulating apoptosis in EC is illustrated in Table 1, and the chemical structures of isolated metabolites are summarized in Table 2.

4 Effects and mechanisms of NPs on apoptosis in EC

4.1 Mitochondria-dependent apoptotic pathway

Mitochondria is the core organelle for energy synthesis and supply, thereby maintaining cellular function and managing cell life and death (Abate et al., 2020; Wang and Roh, 2020). Mitochondrial malfunction often triggers stress-mediated apoptosis. Since resistance to apoptosis is decisive for degenerative diseases and is a hallmark of cancer, the basis of cellular health is the correct functioning of mitochondria. Internal apoptotic signals, such as p53-PUMA or death receptor signal pathways, could alter the mitochondrial membrane permeability (MMP), releasing Cyto-c and other apoptosis-related factors into the cytosol to form the apoptosome. The apoptosome recruits and activates caspase-9, which in turn activates the effector caspases (caspase-3, -6, -7, *etc.*). Subsequently, the down-stream cascades by cleaving poly ADP-ribose polymerase (PARP) and actin substrates. Current studies demonstrate that some NPs effectively treat EC by modulating the mitochondria-dependent apoptotic pathway. All the relevant NPs that activate apoptosis via the mitochondria-dependent pathway are listed in Figure 1.

4.1.1 Extracts from NPs

In early 2009, Li et al. studied the anti-EC effects of the Tian-Long compound (TL compound) *in vitro*. They found that TL compound (0.05%–0.5%) could significantly suppress the proliferation of Ishikawa cells by activating the mitochondrial-dependent apoptotic pathway. The potential mechanisms could be the upregulation of caspase-9 and caspase-3 and the downregulation of BCL-2 (Li et al., 2009). Liu et al. reported that a Steam Distilled Extract of Ginger (SDGE, 0.025–12.50 μg/ml) could induce apoptosis in Ishikawa and ECC-1 cells. The possible

TABLE 1 Potential effects and mechanisms of natural products on modulating apoptosis in EC.

Potential pathways	Detailed mechanisms	Extracts/monomers (dose/concentration)	Cell/Animal model	Related targets	Refs
Mitochondria-dependent pathway	Up-regulating caspase-9, -3; Down-regulating bcl-2	Tian-Long compound (0.05%–0.5%)	Ishikawa cell	Caspase-9, -3, bcl-2	Li et al. (2009)
	Increasing p53 phosphorylation; Decreasing bcl-2	SDGE (0.025–12.50 μg/ml)	Ishikawa, ECC-1 cells	p53, bcl-2	Liu et al. (2012)
	Up-regulating bad, bak, bax; Up-regulating bcl-2, bcl-xL, caspase-9, -3, -8	SOE (50–150 μg/ml)	RL95-2 cell	bad, bak, bax, bcl-2, bcl-xL, caspase-9, -3, -8	Chang et al. (2014)
	Up-regulating caspase-3, bax; Down-regulating bcl-2	Zedoary Turmeric Oil (120–960 mg/L)	HEC-1B	caspase-3, bax, bcl-2	Li et al. (2021)
	Increasing DR5, bim, PUMA; Decreasing survivin	Flavokawain B (1.1–8.8 μM)	SK-LMS-1, ECC-1, T-HESC cells	DR5, bim, p53, survivin	Eskander et al. (2012)
	Incuding Ca2+ influx; Down-regulating bcl-2; Up-regulating bax, caspase-3, -9	Hyperin (0–500 μM)	RL95-2 cell	Bcl-2, bax, caspase-3, -9	Li et al. (2012)
	Decreasing bcl-2, bcl-xL; Increasing caspase-3, -9, PARP	Cucurbitacin D (0.5–4 μM)	Ishikawa, HHUA, HEC59	Bcl-2, bax, caspase-3, -9, PARP	Ishii et al. (2013)
	Decreasing bcl-2; Increasing p53, caspase-9, -3	Triptolide (10–320 nM)	HEC-1 B Cell	Bcl-2, p53, caspase-9, -3	Wang et al. (2014)
	Increasing ROS, caspase-9, -8, -3, cyto-c	α-terthienylmethanol (0–2 μM)	HEC-1A, Ishikawa cells	ROS, caspase-9, -8, -3, cyto-c	Lee et al. (2015)
	Decreasing bcl-2; Increasing caspase-3, PARP	Ginsenoside Rh2 (20, 40 μM)	Ishikawa, HEC-1A	Bcl-2, caspase-3, PARP	Kim et al. (2017b)
	Up-regulating caspase-3, bax; Down-regulating bcl-2; Increasing ROS, PARP, p-ERK1/2	Hinokitiol (1–50 μM)	Ishikawa, HEC-1A, KLE cells	Caspase-3, bax, bcl-2, PARP, ERK	Chen et al. (2021)
	Increasing cyto-c, caspase-3, -9, bax, bim; Decreasing bcl-xL XIAP, survivin	Curcusone C (0.1nM-100 μM)	HEC-1A, hESCs	Cyto-c, caspase-3, -9, bax, bim, bcl-xL XIAP, survivin	An et al. (2021)
ERS mediated stress	Activating GPR78; Increasing CHOP	Realgar quantum dots (0–30 μg/ml)	JEC cells	GPR78, CHOP	Li et al. (2009)
	Increasing Ca2+ influx, caspase-3, -7, CHOP, PARP	Cannabinoids (0.01–25 μM)	Ishikawa, Hec50co	Caspase-3, -7, CHOP, PARP	Fonseca et al. (2018)
	Increasing PERK, p-eIF2a, ATF4; Activating Hippo signaling pathway	Wogonoside (50μM, 80 mg/kg)	Ishikawa	PERK, p-eIF2a, ATF4, Hippo	Chen et al. (2019)
			BALB/c-nu mice		
	Up-regulating caspase-3, PARP, JNK, p38; Down-regulating ERK; Activating Akt	ProEGCG (20, 40, 60 μM)	AN3 CA, RL95–2 cells	Caspase-3, JNK, p38, ERK,Akt	Man et al. (2020)
MAPK mediated pathway	Activating ERK, JNK	Ellipticine (1–10 μM)	RL95-2 cell	ERK, JNK, caspase-7, -8, -9, -3, bid, XIAP, AIF, cyt-c	Kim et al. (2011)
	Up-regulating caspase-7, -8, -9. –3; Down-regulating Bid, XIAP				
	Increasing bax, ERK1/2; Decreasing bcl-2	Icaritin (0–10 μM)	HeC-1A	ERK, bax, bcl-2	Tong et al. (2011)
	Decreasing p-ERK; Increasing caspase-3	Annonacin (0.2–100 μg/ml)	ECCs cells	ERK, caspase-3	Chung et al. (2017)
	Up-regulating caspase-3, bax, bik; Down regulating bcl-2, ESR1	Hesperidin (5–50 μM)	ECC-1 cells	Caspase-3, bax, bik, blc-2, ESR1	Cincin et al. (2018)
	Up-regulating caspase-3, bax, p38, ERK, JNK, ROS; Down-regulating bcl-2, Akt	Emodin (1.25, 2.5, 5 μM)	KLE cells	Caspase-3, bax, bcl-2, p38, ERK, JNK, Akt	Jiang et al. (2019)

(Continued on following page)

TABLE 1 (*Continued*) Potential effects and mechanisms of natural products on modulating apoptosis in EC.

Potential pathways	Detailed mechanisms	Extracts/monomers (dose/concentration)	Cell/Animal model	Related targets	Refs
	Inhibiting ERK1/2 phosphorylation, c-Jun	Curcumin (10–80 μM)	Ishikawa	ERK, c-Jun	Zhang et al. (2019b)
NF-κB mediated pathway	Decreasing NF-κBp50; Up-regulating IκBα, caspase-3	Scutellaria baicalensis; Fritillaria cirrhosa (1.5–500 μg/ml)	EM-E6/E7/TERT, Ishikawa, HEC-1B Cells	NF-κBp50, IκBα, caspase-3	Kavandi et al. (2015)
	Inhibiting NF-κB; Down-regulating caspase-3	Curcumin (0–150 μM)	Ishikawa, HEC-1	NF-κB, caspase-3	Xu et al. (2018)
	Inhibiting VEGF/PI3K/Akt pathway	Panaxnotoginsengsaponins (50–200 μg/ml)	Ishikawa, HEC-1A cells	VEGF, Akt	Tan et al. (2016)
P13K/Akt/mTOR pathway	Decreasing p-AKT; Up-regulating caspase-3; Regulating Akt/mTOR pathway	Resveratrol (0.1, 100 μg); (25–200 μmol)	HeLa, Hec-1A, KLE, RL95-2, Ishikawa and EN1078D cells	p-AKT, caspase-3, mTOR, p38-AMPK	(Sexton et al., 2006) (Xu et al., 2020)
	Decreasing p-AKT, p-ERK1/2; Increasing caspase-3	Pseudolaric acid B (0.5–10 μmol/l)	Ishikawa cells	AKT, ERK, caspase-3	Wang et al. (2017)
	Modulating miR-106b/PTEN/AKT/mTOR pathway; Up-regulating caspase-3, bax; Down-regulating bcl-2	Shikonin ((10–20μM; 0.3–0.7 μg/ml)	Ishikawa, HEC-1A, KLE, RL95-2 cells	miR-106b, PTEN, AKT, mTOR, caspase-3, bax, bcl-2	Yin, 2016; Huang and Hu (2018)
	Increasing bax, Decreasing bcl-2, p-mTOR, p-Akt, p-P13K	Kaempferol (0–20 μM)	MFE-280	Bax, bcl-2, P13K, Akt, mTOR	Lei et al. (2019)
	Up-regulating bax; Down-regulating bcl-2, P13K, Akt, mTOR	Amygdalin (8–128 mg/L)	EECs, RL95-2, HEC-1B	Bax, bcl-2, P13K, Akt, mTOR	Ye et al. (2020)
	Decreasing P13K, Akt, mTOR Up-regulating bax, bak, bad, cyto-c, caspase-3, -9; Down-regulating bcl-xL	Asparanin A (6–18 μM)	Ishikawa cells Female BALB/c-nu mice	P13K, Akt, mTOR, bax, bak, bad, cyto-c, caspase-3, -9, bcl-xL	Zhang et al. (2020)
	Up-regulating bax, caspase-3, -9, PARP, PETN; Down-regulating P13K, Akt	Osthole (25–200 μM)	EC-KLE, Ishikawa cells	P13K, Akt, PETN, bax, caspase-3, -9, PARP	Liang et al. (2021)
p21-mediated pathway	Regulating p53-independent pathway	Psammaplin A (1–10 μg/ml)	Ishikawa cells	$p21^{WAF1}$, p53	Ahn et al. (2008)
	Down-regulating cyclin A, cyclin D3, bcl-2 and bcl-xL; Up-regulating $p21^{WAF1}$, caspase-9	Bufalin (1 ng/ml)	Ishikawa, HHUS, HEC-1B, NHEEC cells	Cyclin A, cyclin D3, bcl-2 and bcl-xL, $p21^{WAF1}$, caspase-9	Takai et al. (2008)
	Up-regulating p21; Down-regulating CDK4, MMP2, MMP9	Cinnamaldehyde (3.75, 7.5, 15 μg/ml)	Ishikawa cells	p21, CDK4, MMP2, MMP9	Dong and Li (2021)
Other	Not concluded	Rice bran fraction (100, 200, 300 μg/ml)	Sawano cell	Not concluded	Fan et al. (2000)
	Up-regulating BAG3, caspase-4, -5	PCAE (0–4 mg/ml)	Ishikawa cells	BAG3, caspase-4, -5	Tsai et al. (2015)
	Increasing ROS, bax; Decreasing bcl-2; Inhibiting pSTAT1, pSTAT2, pJAK1, pJAK2	Tanshinone I (0–40 μM)	HEC-1-A cells	Bax, bcl-2, STAT, JAK	Li et al. (2018)
	Up-regulating caspase-3, -7, PARP	Isoliquiritigenin (5–100 μM)	HEC-1-A, Ishikawa	Caspase-3, -7, PARP	Wu et al. (2016a)
	Inhibiting STAT3; Decreasing bcl-2, survivin	Silibinin (100, 150, 200 μM)	Ishikawa, RL-952	STAT3, bcl-2, survivin	Shi et al. (2019)
	Increasing miR-424 caspase-3, -9; Decreasing CPEB2	Osthole (50, 100, 200 μM)	Ishikawa, KLE	miR-424, CPEB2, caspase-3, -9	Lu et al. (2020)
	Increasing caspase-3	Gallic Acid (5–100 μg/ml)	Ishikawa cells	Caspase-3	Bulbul et al. (2021)

(Continued on following page)

TABLE 1 (*Continued*) Potential effects and mechanisms of natural products on modulating apoptosis in EC.

Potential pathways	Detailed mechanisms	Extracts/monomers (dose/concentration)	Cell/Animal model	Related targets	Refs
	Down-regulating XIAP, bcl-xL, pAKT via hnRNPA1	Esculetin (0–120 μM)	HEC-1B, Ishikawa cells	hnRNPA1, XIAP, bcl-xL, pAKT	Jiang et al. (2021b)
	Up-regulating caspase-3	Silymarin (6 μg/ml)	Ishikawa cells	caspase-3	Chen et al. (2019)

DR5, death receptor 5; PUMA, p53 Upregulated Modulator of Apoptosis; SDGE, steam distilled extract of ginger; SOE, siegesbeckia orientalis ethanol extract; CHOP, C/EBP, homologous protein; GPR78, G-protein coupled receptor 78; ERK, extracellular-signal-regulated kinase; JNK, c-Jun N-terminal kinase; ProEGCG, prodrug of (−)-epigallocatechin-3-gallate; AMPK, AMP-activated protein kinase; XIAP, X-linked inhibitor of apoptosis protein; AIF, apoptosis inducing factor; ESR1, estrogen receptor I; Cyto-c, cytochrome-c; β-HIVS, β-Hydroxyisovalerylshikonin; PARP, poly-ADP, ribose polymerase; BAG3, BCL-associated athanogene 3; VEGF, vascular endothelial growth factor; PCAE, pogostemon cablin aqueous extract.

mechanisms are closely related to up-regulating p53 phosphorylation and down-regulating BCL-2 (Liu et al., 2012, 5). Later in 2014, Chang et al. investigated the pro-apoptotic effects of Siegesbeckia orientalis Ethanol Extract (SOE, 50–150 μg/ml) on Human Endometrial RL-95 Cancer Cells and found that SOE was of significant anti-proliferative and apoptotic effects in RL95-2 cells via activating both intrinsic and extrinsic signaling pathways. A study on its specific mechanisms revealed that SOE could upregulate the expression of Bad, Bak, and Bax, caspase-3, -9, and -8, whereas downregulate that of BCL-2 and BCL-xL (Chang et al., 2014). In 2021, Li et al. reported that Zedoary Turmeric Oil (120–960 mg/L) could significantly inhibit the proliferation of HEC-1-B cells and induce apoptosis by up-regulating the expressions of Bax and caspase-3 and down-regulating the expression of BCL-2 (Li et al., 2021).

4.1.2 Monomers from NPs

In 2012, Zhou et al. reported that Flavokawain B (FKB, 1.1–8.8 μM) could significantly inhibit the growth of SK-LMS-1 and ECC-1 cell lines compared to non-malignant human endometrium fibroblast-like cells. The potential mechanisms might be associated with G2/M arrest and induction of mitochondrial-dependent apoptosis via upregulation of the pro-apoptotic proteins DR5, Puma, and Bim and downregulation of survivin, an inhibitor of apoptosis protein (IAP) (Eskander et al., 2012) and a promising therapeutic target as a new therapy for cancer treatment (Martínez-García et al., 2019). In 2012, Li et al. studied the anti-proliferative activity of Hyperin on RL952 cells. The results showed that Hyperin (0–200 μM) could suppress the viability of RL952 cells by inducing apoptosis, which would attribute to the regulation of Ca2+ influx, downregulation of BCL-2, and up-expression of bax, caspase-3,-8, and -9 (Li et al., 2012). In 2013, Cucurbitacin D (0.5–4 μM), extracted from Extrasynthese, proved the effect of induction of apoptosis via decreasing BCL-2, BCL-xL, and increasing caspase-3, caspase −9, PARP (Ishii et al., 2013). Triptolide (TP, 10–320 nM), a validated component purified from Tripterygium wilfordii Hook. f. showed to promote apoptosis via a p53-independent mitochondrial pathway. The possible mechanisms are closely related to the reactivation of the p53 to induce apoptosis via downregulation of the expression of BCL-2, and upregulation of caspase-9,-3 in HEC-1B Cells. In 2015, an *in vitro* study by Lee et al. suggested that α-terthienylmethanol (0–2 μM), isolated from Eclipta prostrata, and could induce apoptosis in HEC-1A and Ishikawa cells via increasing expression of Pro-caspase-3, 8, 9, and Cyto-c in a time-dependent manner and increasing ROS generation. The author also suggested that the apoptosis would be likely mediated by both the intrinsic and extrinsic pathways in ECCs (Lee et al., 2015). Later in 2017, Kim et al. found that the Ginsenoside Rh2 (20, 40 μM) could induce apoptosis in Ishikawa and HEC-1A cells via activation of caspase-3, PARP, and inhibition of BCL-2 (Kim J. H. et al., 2017). In 2021, Chen et al. observed that Hinokitiol (1–50 μM) could induce ROS-Mediated Apoptosis and p53-Driven Cell-Cycle Arrest in Endometrial Cancer Cell Lines (Ishikawa, HEC-1A, KLE) through up-regulating ROS,bax,caspase-3, PARP, p-ERK1/2, whereas down-regulating BCL-2 (Chen et al., 2021). In 2021, an *in vivo* study by Junxia et al. demonstrated that the Curcusone C (0.1 nM–100 μM) treatment caused significant anti-proliferative and apoptotic effects in Ishikawa and HEC-1A cells by inducing the release of Cytochrome c and increasing caspase-3,-9, Bax and bim, whereas decreasing X-linked inhibitor of apoptosis protein (XIAP), survivin, and BCL-xL (An et al., 2021).

4.2 Endoplasmic reticulum stress mediated pathway

The endoplasmic reticulum (ER) is the central subcellular region for protein synthesis, folding, and transport. It also plays a vital role in intracellular Ca2+ homeostasis and various metabolic processes (Clarke et al., 2014; Wang et al., 2019). Cellular stress conditions can activate endoplasmic reticulum stress (ERS) to restore endoplasmic reticulum homeostasis and normal cellular function. In response to ER stress stimuli, such as the accumulation of unfolded/misfolded proteins in the ER above a critical threshold, the unfolded protein response (UPR) is initiated through three signaling cascades involving the protein kinase RNA-like ER kinase (PERK), inositol-requiring enzyme-1 (IRE1), and activating transcription factor-6 (ATF6) (Ron and Walter, 2007; Wang and Kaufman, 2016; Marciniak, 2019). However, if it fails, UPR triggers cell death (Wu F.-L. et al., 2016). ER stress and UPR have been shown to play critical roles in cancer pathogenesis, progression, and therapeutic response (Oakes et al., 2015). Increasing attention has been paid to ER stress's essential role in endometrial carcinogenesis and the drug-resistance during chemotherapy. Several studies have demonstrated that NPs would be promising anti-cancer effects on EC via targeting ERS-mediated apoptosis. The potential effectiveness and mechanism of NPs on ERS-mediated apoptosis are summarized in Figure 2.

TABLE 2 Detailed information and chemical structures of natural products.

Monomers	Origin	Systematic name	Chemical structures
Flavokawain B	Piper methysticum	(2E)-1-(2-Hydroxy-4,6-dimethoxyphenyl)-3-phenyl-2-propen-1-one	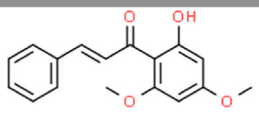
Hyperin	Rhododendron dauricum L.	2-(3,4-Dihydroxyphenyl)-5,7-dihydroxy-4-oxo-4H-chromen-3-yl β-D-galactopyranoside	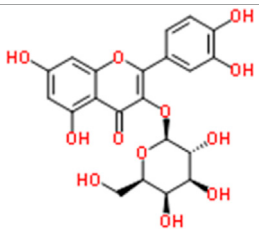
Cucurbitacin D	Pyrus communis subsp. communis	(2S,4R,9β,16α,23E)-2,16,20,25-Tetrahydroxy-9,10,14-trimethyl-4,9-cyclo-9,10-secocholesta-5,23-diene-1,11,22-trione	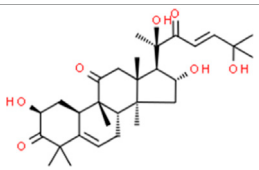
Triptolide	Tripterygium wilfordii Hook.f.	(3bS,4aS,5aS,6R,6aR,7aS,7bS,8aS,8bS)-6-Hydroxy-6a-isopropyl-8b-methyl-3b,4,4a,6,6a,7a,7b,8b,9,10-decahydrotrisoxireno [6,7:8a,9:4b,5]phenanthro [1,2-c]furan-1(3H)-one	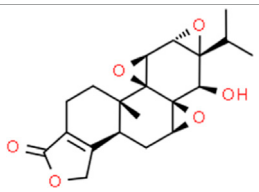
alpha-Terthienylmethanol	Eclipta prostrata (L.) L.	2,2':5′,2″-Terthiophen-5-ylmethanol	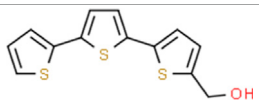
Ginsenoside Rh2	Panax ginseng C.A.Mey.	(3β,12β)-12,20-Dihydroxydammar-24-en-3-yl β-D-glucopyranoside	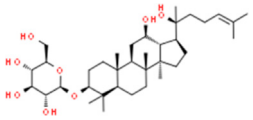
Hinokitiol	Chamaecyparis obtusa var. formosana (Hayata) Hayata	2-Hydroxy-4-isopropyl-2,4,6-cycloheptatrien-1-one	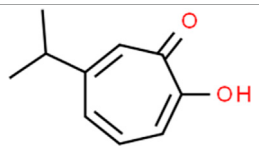
Curcusone C	Jatropha curcas L.	(2S,6aS)-2-Hydroxy-7-isopropenyl-2,5-dimethyl-10-methylene-2,3,6a,7,8,9,10,10a-octahydrobenzo [e]azulene-1,4-dione	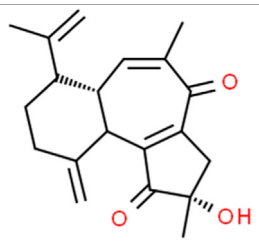

(Continued on following page)

TABLE 2 (*Continued*) Detailed information and chemical structures of natural products.

Monomers	Origin	Systematic name	Chemical structures
Wogonoside	Scutellaria baicalensis Georgi	5-Hydroxy-8-methoxy-4-oxo-2-phenyl-4H-chromen-7-yl β-D-glucopyranosiduronic acid	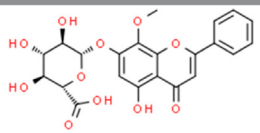
Ellipticine	*Ochrosia elliptica* Labill.	5,11-Dimethyl-6H-pyrido [4,3-b]carbazole	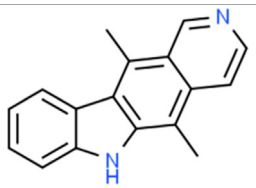
Icaritin	Epimedium brevicornu Maxim.	3,5,7-Trihydroxy-2-(4-methoxyphenyl)-8-(3-methyl-2-buten-1-yl)-4H-chromen-4-one	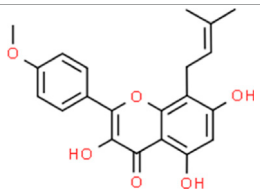
Annonacin	Annona muricata L.	(5S)-5-Methyl-3-[(2R,8R,13R)-2,8,13-trihydroxy-13-{(2R,5R)-5-[(1R)-1-hydroxytridecyl]tetrahydro-2-furanyl}tridecyl]-2(5H)-furanone	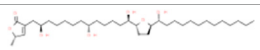
Hesperidin	Citrus × aurantium L.	(2S)-5-Hydroxy-2-(3-hydroxy-4-methoxyphenyl)-4-oxo-3,4-dihydro-2H-chromen-7-yl 6-O-(6-deoxy-α-L-mannopyranosyl)-β-D-glucopyranoside	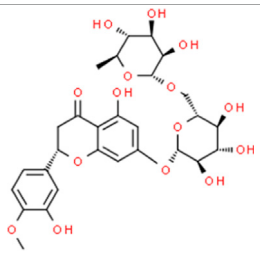
Emodin	Rheum palmatum L.	1,3,8-Trihydroxy-6-methyl-9,10-anthraquinone	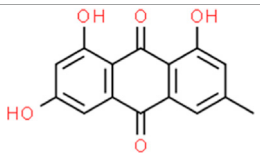
Curcumin	Curcuma longa L.	(1Z,6Z)-1,7-Bis(4-hydroxy-3-methoxyphenyl)-1,6-heptadiene-3,5-dione	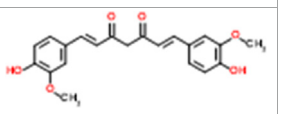
Scutellaria baicalensis	Scutellaria baicalensis Georgi	3-(9,9-Dimethyl-10(9H)-acridinyl)-N,N-dimethyl-1-propanamine	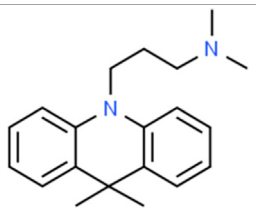

(Continued on following page)

TABLE 2 (*Continued*) Detailed information and chemical structures of natural products.

Monomers	Origin	Systematic name	Chemical structures
Resveratrol	Red wine	5-[(E)-2-(4-Hydroxyphenyl)vinyl]-1,3-benzenediol	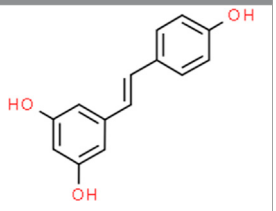
Pseudolaric acid B	Larix kaempferi (Lamb.) Carrière	(2E,4E)-5-[(1R,7S,8S,9R)-7-Acetoxy-4-(methoxycarbonyl)-9-methyl-11-oxo-10-oxatricyclo [6.3.2.01,7]tridec-3-en-9-yl]-2-methyl-2,4-pentadienoic acid	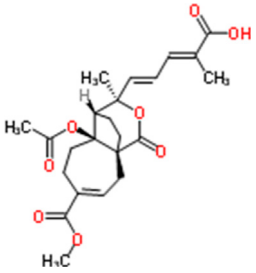
Shikonin	Lithospermum erythrorhizon Siebold & Zucc.	5,8-Dihydroxy-2-[(1R)-1-hydroxy-4-methyl-3-penten-1-yl]-1,4-naphthoquinone	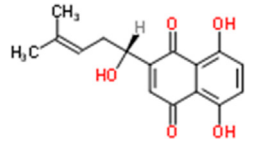
Kaempferol	Kaempferia galanga L.	3,5,7-Trihydroxy-2-(4-hydroxyphenyl)-4H-chromen-4-one	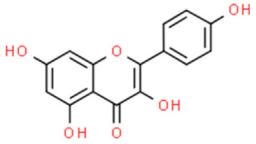
Amygdalin	Prunus amygdalus Batsch	(2R)-{[6-O-(β-D-Glucopyranosyl)-β-D-glucopyranosyl]oxy}(phenyl) acetonitrile	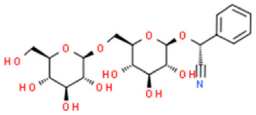
Asparanin A	Asparagus officinalis L.	(3β,5β,25S)-Spirostan-3-yl 2-O-β-D-glucopyranosyl-β-D-glucopyranoside	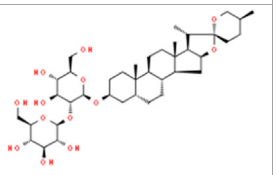
Osthole	Cnidium monnieri (L.) Cusson	7-Methoxy-8-(3-methyl-2-buten-1-yl)-2H-chromen-2-one	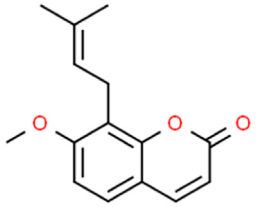
Isoliquiritigenin	Glycyrrhiza glabra L.	(2E)-1-(2,4-Dihydroxyphenyl)-3-(4-hydroxyphenyl)-2-propen-1-one	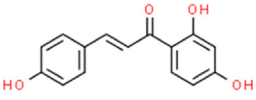

(Continued on following page)

TABLE 2 (*Continued*) **Detailed information and chemical structures of natural products.**

Monomers	Origin	Systematic name	Chemical structures
Esculetin	Fraxinus chinensis subsp. rhynchophylla (Hance) A.E.Murray	6,7-Dihydroxy-2H-chromen-2-one	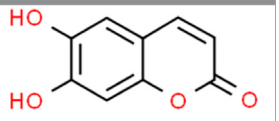
Silymarin	Silybum marianum (L.) Gaertn.	3,5,7-trihydroxy-2-[3-(4-hydroxy-3-methoxyphenyl)-2-(hydroxymethyl)-2,3-dihydro-1,4-benzodioxin-6-yl]-2,3-dihydrochromen-4-one	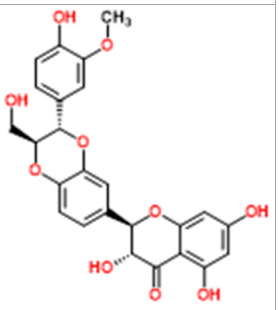

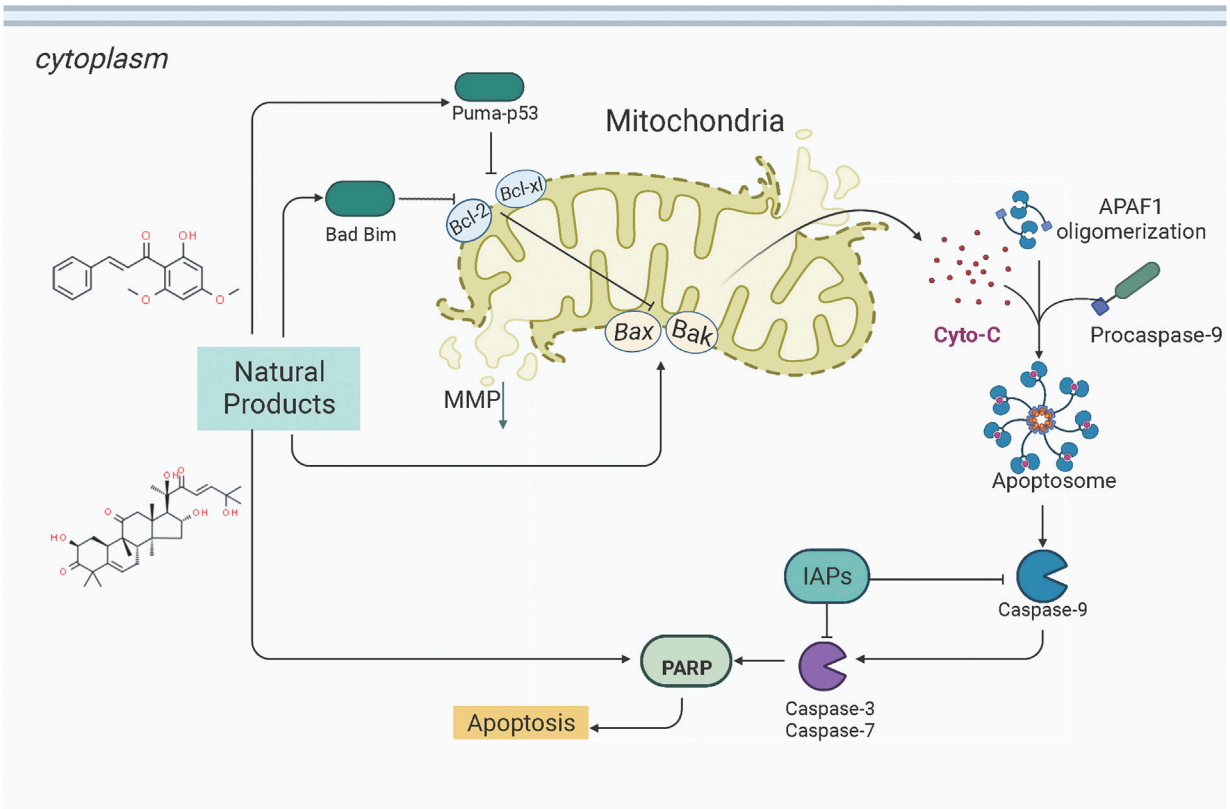

FIGURE 1
Natural products modulate apoptosis of ECCs through mitochondria-dependent pathway.

4.2.1 Extracts from NPs

In 2015, Wang et al. found that Realgar quantum dots (RQDs, 0–80 μg/ml) can induce apoptosis *in vitro* by increasing the expression level of GRP78 (BIP) and GADD153 (CHOP). Their studies demonstrated that RQDs could activate ER stress and mitochondrial pathways (Wang et al., 2015). Later in 2018, Fonseca et al. reported that Cannabinoids (0.01–25 μM) could induce apoptosis *in vitro* by activating TRPV1 and increasing caspase-3,-7, Ca2+ influx, CHOP, and cleaved PARP (Fonseca et al., 2018).

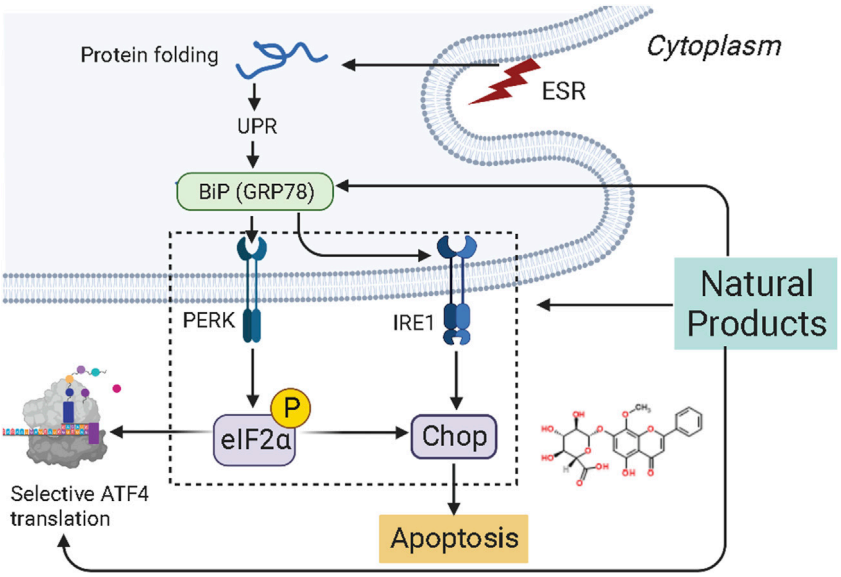

FIGURE 2
Natural products modulate apoptosis of ECCs through ERS-mediated pathway.

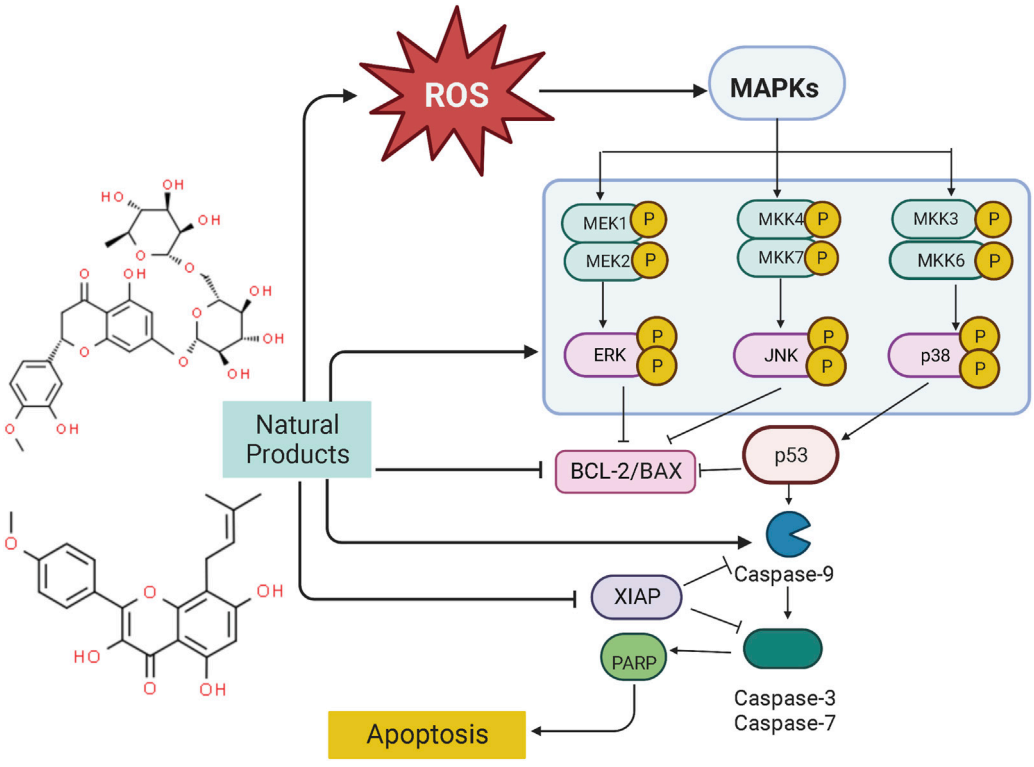

FIGURE 3
Natural products modulate apoptosis of ECCs through MAPK mediated pathway.

4.2.2 Monomers from NPs

In 2019, Chen et al. found that Wogonoside (50 μM, 80 mg/kg), a bioactive flavonoid component derived from Scutellaria baicalensis Georgi, can induce apoptosis and inhibit cell proliferation depending on the ER stress-Hippo signaling axis *in vitro* and *in vivo* (in Ishikawa and BALB/c-nu mice) via increasing the

expression of protein kinase-like endoplasmic reticulum kinase (PERK), binding protein (Bip), p-eIF2a, and transcription factor 4 (TCF4) (Chen et al., 2019).

4.3 MAPK-mediated apoptotic pathway

Mitogen-activated protein kinase (MAPK) pathway is an important signal transduction pathway in eukaryotic organisms. MAPK signaling pathways are involved in cell growth, migration, proliferation, differentiation, and apoptosis (Kim and Choi, 2010). Each MAPK signaling cascade consists of at least three layers of protein kinases: MAP3K, MAPKK, and MAPK. These cascades can be divided into extracellular signal-regulated kinase (ERK)1/2, c-Jun N-terminal kinase (JNK), P38 MAPK (P38), ERK3/4, and ERK7/8 (Chuderland and Seger, 2005; Dhillon et al., 2007). Among them, the JNK and p38 MAPK pathways are mainly related to cell stress and apoptosis, while ERK/MAPK signaling pathway is the most intensively studied MAPK signaling pathway, which is closely associated with cell proliferation and differentiation (Chuderland and Seger, 2005). However, the abnormal regulation of the MAPK signaling pathway plays a significant role in carcinogenesis. It is abundantly reported that NPs could be a promising way to treat EC to induce apoptosis through the MAPK pathway. The potential effectiveness and mechanism of NPs on MAPK-mediated apoptosis are summarized in Figure 3.

4.3.1 Extracts from NPs

In another study by Man GCW et al., in 2020, the apoptotic effects of a prodrug of (−)-epigallocatechin-3-gallate (ProEGCG, 20, 40, 60 μM) showed a highly anti-proliferative activity on tumor cells in both EC xenografts cultured *in vivo* and RL95–2 and AN3 CA EC cells *in vitro* via promoting apoptosis, which was associated with activation of Akt, Up-regulating caspase-3, PARP, JNK, p38 whereas down-regulating ERK (Man et al., 2020).

4.3.2 Monomers from NPs

Ellipticine (5,11-dimethyl-6H-pyrido [4,3-b]carbazole) is a bioactive component of Ochrosia elliptical, which has been demonstrated to be of pro-apoptotic effect on EC-RL95-2 cells (0.1–20 μM), and the potential mechanisms are related to the activation of ERK, JNA, as well as the increase of ROS generation. Ellipticine can also regulate the XIAP transcription and mediate the caspase cascade reaction to induce cellular apoptosis (Kim et al., 2011). In 2011, Tong et al. reported that Icaritin (0–10 μM), a compound from Epimedium Genus, possessed significant anti-proliferative and apoptosis-inducing activities in Hec1A cells, the potential mechanisms are correlated to increasing bax, ERK1/2 whereas decreasing BCL-2 (Tong et al., 2011). Another investigation in 2017 by Chung et al. studied the anti-proliferative effects of Annonacin (0.2–100 μg/ml) on both EC cell lines (ECC-1 and HEC-1A) and primary cells (EC6-ept and EC14-ept) and found that Annonacin has significant anti-proliferative activity via inhibition of ERK signaling pathway through down-regulating p-ERK whereas increasing caspase-3 (Chung et al., 2017). Hesperidin (Hsd) is the most active flavanone glycoside in citrus flavonoids. Studies in 2018 found that Hsd (5–50 μM) could downregulate MAPK, PI3K, STAT, and mTOR signal transduction pathways for regulating apoptotic and autophagic responses. The underlying mechanism may be related to up-regulating caspase-3, bax, and bik, whereas downregulate BCL-2 and ESR1 (Cincin et al., 2018). In 2018, Jiang et al. found that Emodin (1.25, 2.5, 5 μM), a significant component of rhubarb, can induce apoptosis *in vivo* (Xenograft Tumor Models) and *in vitro* in a time- and dose-dependent manner via inhibiting the PI3K/Akt pathways while activating MAPK signaling, and after Emodin treatment, caspase-3, bax, p38, ERK, JNK, and ROS were significantly upregulated whereas BCL-2 and Akt were downregulated (Jiang et al., 2019). Curcumin (10–80 μM), reported to have antioxidant, anti-inflammatory, liver protection, analgesia and antiarthritis, lipid modification, immune regulation, and anti-diabetic properties, could induce apoptosis via Inhibiting the Phosphorylation of ERK/c-Jun pathway via reducing mRNA expression of ERK2 and JUN genes (Zhang Z. et al., 2019).

4.4 NF-κB mediated apoptotic pathway

NF-κB is a transcription factor that usually exists as a dimer. p65/relA and p50 are the most common dimeric forms of NF-κB, and its dimers have two states: inactivation and activation. In the "resting" state of cell c, NF-κB is inactive and binds to the inhibitor IκBα on the cell membrane, preventing it from entering the nucleus to activate genes. When external signals stimulate the cell, IκBα is degraded, NF-κB is released, and its nuclear localization sequence (NLS) is exposed. NF-κB rapidly enters the nucleus from the cell membrane and binds to specific sequences on nuclear DNA to initiate or enhance transcription of related genes, which can control protein transcription and participate in physiological processes such as cell proliferation and apoptosis, stress response, and cytokine release. Recently, the NF-κB pathway has been considered a promising therapeutic target for EC therapy. Studies have shown NPs can induce apoptosis in ECCs and prevent endometrial hyperplasia. The potential mechanisms of NPs on NF-κB mediated apoptosis are summarized in Figure 4.

In 2015, it was reported by Kavandi et al. found that the anti-proliferative properties of the herbs Scutellaria baicalensis (SB) and Fritillaria cirrhosa (FC,1.5–500 μg/ml) on EM-E6/E7/TERT, Ishikawa, and HEC-1B Cells closely related to NF-κB pathway via regulation of decreasing NF-κB p50 whereas up-regulating IκBα and caspase-3 (Kavandi et al., 2015). Afterward, Xu et al., in 2018 recorded that Curcumin (0–150 μM) extracted from the rhizome of the plant Curcuma longa could induce apoptosis through negative regulation of the NF-κB pathway *in vitro in vivo*, and the molecular mechanisms might be related to inhibiting NF-κB and down-regulating caspase-3 (Xu et al., 2018).

4.5 PI3K/AKT/mTOR pathway

PI3K, or phosphatidylinositol 3-kinase, is a family of lipid kinases that control different processes in mammalian cells, including cell proliferation, survival, differentiation, activation of effector functions, and metabolism (Ali et al., 2015). The PI3K family consists of three classes of PI3Ks (I-III) (Narita et al., 2002). Class I can be further divided into class IA and class IB enzymes, and

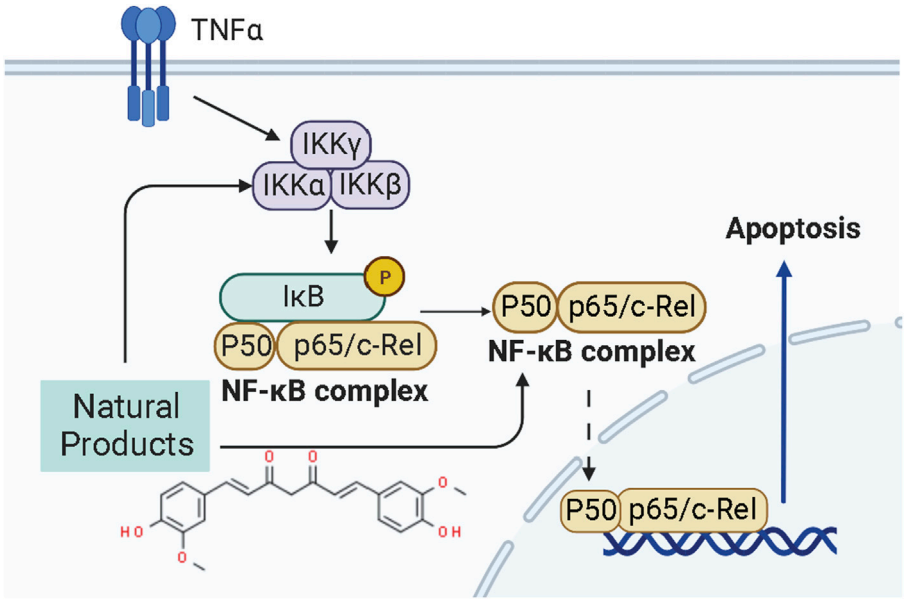

FIGURE 4
Natural products modulate apoptosis of ECCs through NF-κB mediated pathway.

Class IA PI3K enzymes include a catalytic (p110) and a regulatory subunit (p85 or p101) (Hennessy et al., 2005; Sujobert and Sujobert, 2005; Fruman, 2008, 110; Piddock et al., 2017). Akt, also known as protein kinase B (PKB), is a serine/threonine-specific protein kinase (Yip, 2015). Signaling pathways determined by PI3K, AKT, and the mammalian target of rapamycin (mTOR) are critical for many features of cancer, such as cell growth, survival, metabolism, apoptosis, and angiogenesis (Ediriweera et al., 2019; Fattahi et al., 2020; Miricescu et al., 2020; Mirza-Aghazadeh-Attari et al., 2020). The PI3K/Akt/mTOR intracellular signaling cascade begins with activating RTKs and cytokine receptors, which generate phosphorylated tyrosine residues that provide anchor sites for recruiting PI3K to membrane translocation. Class IA PI3Ks can be activated by receptor tyrosine kinases (RTKs), G protein-coupled receptors (GPCRs) located on the cell surface membrane (Darici et al., 2020). Upon activation, The P110 catalytic subunit of PI3Ks could convert phosphorylate PI(4,5)P2 to PI(3,4,5)P3 (Denley et al., 2009), a second messenger. And then, PIP3 induces the activation of phosphoinositide-dependent kinase-1 (PDK1) and downstream targets of AKT (Pothongsrisit and Pongrakhananon, 2021). The levels of PI(3,4,5)P3 and PI(4,5)P2 could be regulated by PTEN (Chalhoub and Baker, 2009; Blanco et al., 2020). The PI3K/AKT/mTOR signaling pathway is the essential cell signaling pathway in animals, involved in regulating physiological processes such as cell growth, survival, proliferation, metabolism, and apoptosis. Alterations in the PI3K/AKT/mTOR pathway are now thought to be strongly associated with the carcinogenesis and progression of endometrial cancer (Slomovitz and Coleman, 2012; Chen et al., 2014). The pathway most frequently damaged in endometrial cancer is the PI3K/AKT/mTOR pathway (Crosbie et al., 2022). In recent years, it has been abundantly reported that NPs could exert pro-apoptosis via the PI3K/AKT/mTOR pathway (Mirza-Aghazadeh-Attari et al., 2020). The potential mechanisms of NPs on PI3K/AKT/mTOR mediated apoptosis are summarized in Figure 5.

4.5.1 Extracts from NPs

In 2016, Tan et al. reported that the intervention of Panaxnotoginsengsaponins (PNS, 50–200 μg/ml) could induce apoptosis in Ishikawa and HEC-1A cells via inhibiting the expression of VEGF, which may be related to inhibiting PI3K/AKT/mTOR signaling pathway (Tan et al., 2016).

4.5.2 Monomers from NPs

Resveratrol (3, 4, 5-trihydroxy-trans-stilbène), a natural phytoalexin present in grape skins, has considerable anti-proliferation effects and can induce apoptotic cell death in various types of cancers cell *in vitro*. In 2006, Émilie Sexton et al. reported that high-dose of resveratrol (0,10, and 100 μM) could inhibit cell growth and trigger apoptotic cell death *in vitro* via decreasing p-Akt, whereas up-regulating caspase-3 (Sexton et al., 2006). Another study in 2020 by Xu et al. also suggested that the anti-proliferative and pro-apoptotic effect of resveratrol might attribute to the regulation of the Akt/mTOR signaling pathway (Xu et al., 2020). Pseudolaric acid B (PAB) is the major bioactive component of Pseudolarix kaempferi Gorden. Studies in 2017 by Wang et al. have found that PAB (0.5–10 μmol/l) could inhibit Ishikawa cell proliferation and induces apoptosis *in vitro*. Its related molecular mechanisms may involve Akt-GSK-3β and ERK1/2 signaling pathways via decreasing p-Akt and p-ERK1/2 whereas increasing caspase-3 and p-GSK3β (Wang et al., 2017). Shikonin, an active biological component derived from the roots of the herb Lithospermu erythrorhizon, has considerable antitumor effects, including antioxidation, anti-inflammation, and anti-apoptosis. Studies reported in 2016 by Yin et al. and in 2017 by Huang et al. suggested that Shikonin could promote apoptosis *in vitro*

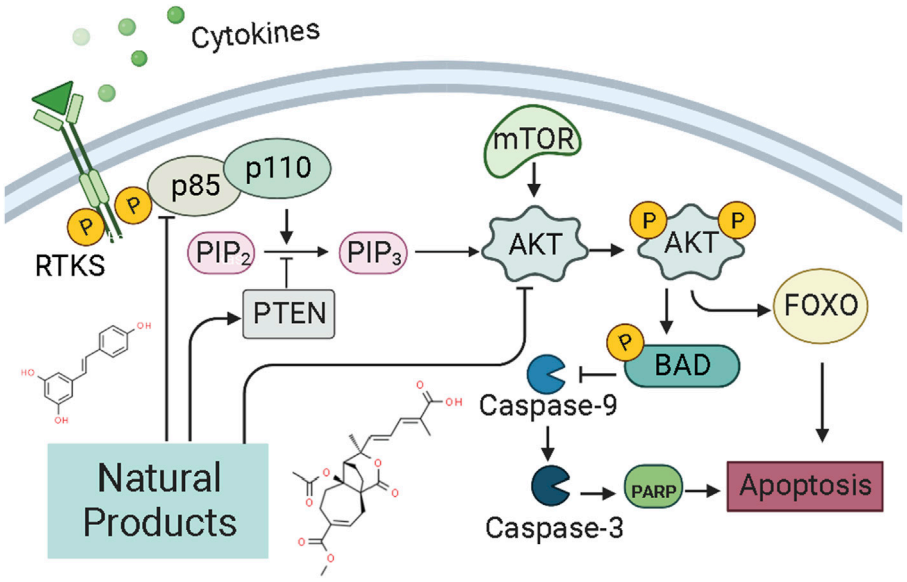

FIGURE 5
Natural products modulate apoptosis of ECCs through PI3K/AKT/mTOR pathway.

by modulating the miR-106b/PTEN/Akt/mTOR pathway (Yin, 2016; Huang and Hu, 2018). In 2019, a study by Xia et al. suggested that Kaempferol (0–20 μM) can promote apoptosis via increasing bax whereas decreasing p-PI3K p-mTOR, p-Akt, and BCL-2 (Lei et al., 2019). Besides, from the results of Ye et al., Amygdalin (8–128 mg/L) could also induce apoptosis *in vitro* via regulation of the proteins related to the PI3K-Akt signal (Ye et al., 2020). Another study in 2020 by Zhang et al. first reported that Asparanin A (AA, 6–18 μM) could promote apoptosis *in vitro* and *in vivo* by activating the mitochondrial pathway and inhibiting PI3K/Akt signaling pathway (Zhang et al., 2020). Recently, a study by Liang et al., in 2021 showed that Osthole (25–200 μM) could suppress the growth *in vitro* and *in vivo*, which was associated with up-regulating bax, caspase-3, -9, PARP, PETN, whereas down-regulating PI3K and Akt (Liang et al., 2021).

4.6 P21-mediated pathway

P21, also called $P21^{WAF1}$/CIP1 or P21/CDKN 1a, is a small protein with 165 amino acids related to cell cycle progression (Karimian et al., 2016). In 1993, a finding found that P21, or wild-type p53-activated fragment 1 (WAF1), is directly regulated by P53 and can suppress tumor cell growth in culture (El-Deiry et al., 1993). However, P21 is a downstream mediator of the P53 transcription factor and can interact directly with P53 (Kim E. M. et al., 2017). Thus, P21 may be an essential p53 growth suppression pathway component. Some findings indicate that the p53/p21 complex regulates cell apoptosis by targeting Bcl-2 proteins (Kim et al., 2022). P21 protein, a cyclin-dependent kinase inhibitor (CKI), can bind to and inhibit the activity of CDK1, CDK2, and CDK4/6 enzyme complexes (Marchetti et al., 1996), thereby acting as a cell cycle regulator at the G1 and S phases (Kikuchi et al., 2022). When DNA is damaged, the increased expression of p53 could activate the transcription of gene p21 by binding to its response element within its promoter. $P21^{WAF1}$ can decrease kinase activity and may be a key regulator of G0/G1 accumulation and G1 cell cycle arrest. Consequently, cell apoptosis was induced by p21. Several studies have shown that NPs can regulate the cell cycle of ECCs by mediating P21, thereby promoting the induction of apoptosis in EC. The potential effectiveness and mechanism of NPs on P21-mediated apoptosis are summarized in Figure 6.

In 2008, after the human endometrial Ishikawa cancer cell line was prepared, Mee et al. investigated the effect of the Psammaplin A (0.1–10 μg/ml), a natural histone deacetylase inhibitor, induces on the Ishikawa cells. They found that Psammaplin A (5 μg/ml) can notably inhibit the proliferation and induced cell cycle arrest or apoptosis *in vitro*. The molecular mechanisms might be related to the increased expression of p21WAF1 through a p53-independent pathway (Ahn et al., 2008). In the same year, Takai et al. first demonstrated that Bufalin (1 ng/ml) could inhibit proliferation and induce apoptosis *in vitro*. The mechanism may be related to an increase in cleaved caspase-9 expression caused by up-regulating the levels of p21WAF1 protein and down-regulating cyclin A, cyclin D3, BCL-2, and BCL-xL (Takai et al., 2008). Recently, Dong et al. investigated the effect of Cinnamaldehyde (3.75, 7.5, 15 μg/ml) on Ishikawa cells. The results showed that Cinnamaldehyde has notable pro-apoptotic effects via up-regulating p21WAF1, whereas down-regulating CDK4, MMP2, and MMP9 (Dong and Li, 2021).

4.7 Other reported pathways

In addition to the apoptotic pathways mentioned above, there are NPs reported to exert pro-apoptotic effects on EC through other mechanisms.

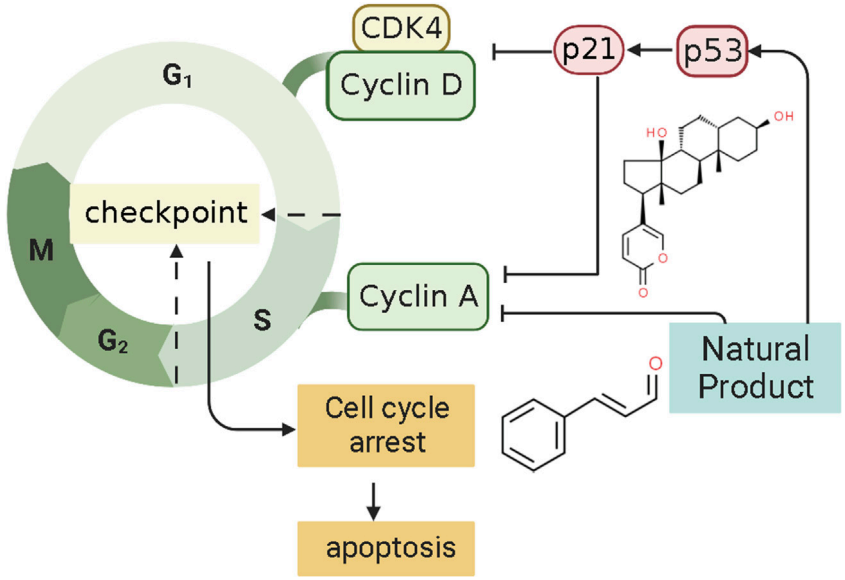

FIGURE 6
Natural products modulate apoptosis of ECCs through P21-mediated pathway.

4.7.1 Extracts from NPs

In 2000, the Rice bran fraction (100, 200, 300 μg/ml) was reported to be a lipoprotein fraction that could induce apoptosis of the Sawano cells (Fan et al., 2000). In 2015, Tsai et al. studied the influence of Pogostemon cablin Aqueous Extract (PCAE, 0–4 mg/ml) on the induction of apoptosis. The results showed that PCAE induced apparent apoptosis in Ishikawa cells. In addition, further investigation revealed that the mechanism might be related to up-regulating BAG3,caspase-4, and caspase-5 (Tsai et al., 2015). In 2018, it was also reported that Tanshinone l (0–40 μM) could induce apoptosis and can increase ROS, bax. In contrast, downregulate BCL-2 and inhibit the phosphorylation of pSTAT1, pSTAT-2, pJAK1, and pJAk, inhibiting JAK/STAT pathway signal pathway and mitochondrial-mediated apoptosis in HEC-1-A cells (Li et al., 2018).

4.7.2 Monomers from NPs

In 2016, Wu et al. studied the inhibitory effect of Isoliquiritigenin (ISL, 5–100 μM), a licorice flavonoid, which was shown to could induce apoptosis and cell growth inhibition *in vitro* and *in vivo* via up-regulating caspase-3, caspase −7 and PARP (Wu C.-H. et al., 2016). Later in 2019, Shi et al. found that the Silibinin (SB, 100, 150, 200 μM), extracted from milk thistle seeds, can significantly inhibit the proliferation and promote apoptosis in a dose- and time-dependent manner via blocking pathways of STAT3 activation and SREBP1-mediated lipid accumulation, which is closely related to inhibiting STAT3, whereas decreasing BCL-2 and survivin (Shi et al., 2019). Lu et al., in 2019 recorded that Osthole (50, 100, 200 μM) could induce apoptosis in the Ishikawa and KLE cells, and after Osthole treatment,caspase-3, -9,miR-424 were significantly upregulated, and the CPEB2 were downregulated (Lu et al., 2020). A report in 2021 by Bulbul et al. studied the effect of Gallic Acid (3,4,5-tri hydroxybenzoic acid; GA; 5–100 μg/ml) and found it could induce apoptosis in Ishikawa cells by mitochondrial pathway via up-regulating caspase-3 (Bulbul et al., 2021). In 2021, Jiang reported that Esculetin (0–120 μM) could result in apoptosis and an arrest in proliferation in the HEC-1B, Ishikawa cells, and can target hnRNPA1, thereby downregulate the expression level BCL-XL, XIAP, and pAkt protein (Jiang R. et al., 2021). Recently, Hua et al. suggested that Silymarin (6 μg/ml) could induce apoptosis in Ishikawa cells via up-regulating caspase-3 (Chen et al., 2019).

5 Perspectives and conclusion

NPs are a wide range of bioactive components isolated from natural organisms, including plants, animals, insects, marine organisms (Manoharan and Perumal, 2022), and microorganisms. NPs are attractive sources for developing new medicinal and therapeutic agents (Thomford et al., 2018; Thompson and Lutsiv, 2023; Rao et al., 2019). For a long time, NPs have been regarded as a rich source of the active ingredients in new drugs. Moreover, the structural complexity and functional diversity of NPs are irreplaceable advantages compared to chemical drugs. These bioactive elements exert remarkable therapeutic effects on various diseases. NPs possess anti-cancer, anti-inflammatory, antioxidant, anti-bacterial, analgesic, anti-diabetic, and enzyme-inhibitory activities (Hassan et al., 2022). In recent years, the anti-cancer effects of NPs have drawn increasing attention (Hassan et al., 2022; Islam, 2022; Nuzzo et al., 2022), and we focus on their apoptosis-regulatory effect. Existing studies suggest that NPs can promote EC cell apoptosis through multiple pathways and thus exert anti-EC effects. Although existing research has reached a depth, some issues have not been well addressed and cannot be ignored to advance the development of NP-based anti-EC drugs.

First, the material basis of NPs for preventing and treating diseases is their active ingredients. Limited sources or meager

amounts of bioactive molecules raw material is considered one of the most important obstacles to developing NPs into drugs. Many unexplored natural resources, especially uncultured marine organisms, will expand the sources of NPs because they can provide complex molecules with biologically active pharmacophores (Bilal and Iqbal, 2020). To better develop NPs, two different aspects may be involved: isolating additional structures directly from NPs, and modifying or improving these structures by chemical or biochemical methods (Li and Lou, 2018). These pathways may be helpful to facilitate the production of candidate molecules with lower costs, better efficacy, and less toxic side effects. Furthermore, the difficulty of extracting bioactive molecules is considered one of the significant obstacles to developing NPs into chemotherapeutic agents. Conventional extraction techniques frequently include preparatory fractionation of the parent material or crude extract, which limits their practical adoption on a large scale. Traditional extraction techniques also have other drawbacks, such as long extraction times, solvent purity issues, excessive solvent consumption and evaporation, shortened extraction yields, and thermal degradation of thermally degraded compounds. These limitations limit the development of NPs. Numerous modern extraction methods have been created and used, taking into account the structural and compositional characteristics of target sources, such as enzyme-assisted extraction (EAE), supercritical-fluid extraction (SFE), and microwave-assisted extraction (MAE), *etc.* (Bilal and Iqbal, 2020). Second, most studies have only focused on a single certain NP, and the combination of multiple NPs may help improve the efficacy and further explore the role of these NPs in the overall regulation of apoptosis, as well as their drug interrelationships. Third, the above studies were almost carried out via *in vitro* and *in vivo* approaches. Not all papers conducted *in vivo* experiments, so further investigation is suggested. Besides, the experimental data above almost explored a single pathway targeting the pro-apoptotic effects of NPs, and only a few NPs targeting cross-talk are available in studies. This may lead to the failure of drugs if this mechanism is interrupted or altered due to various cancer-related phenomena. This may also be a limitation and cause drug resistance to cancer. Clinical trials are also necessary to demonstrate whether the *in vitro* and *in vivo* animal data are reproduced in humans and to allow the application of NPs in cancer prevention and treatment. Most articles have analyzed their mechanism of action at the cellular and/or molecular level (Ekiert and Szopa, 2022). Fourth, NPs that are well tolerated and have less toxicity will help patients to achieve better treatment outcomes and improve their quality of life. The toxicity and pharmacokinetic selectivity of NPs should be further explored to validate their safety, which is a key step in the development of new drugs and can provide a strong basis for their translation to the clinic. Despite efforts to improve the therapeutic outcome for EC over the past decades, chemoresistance and side effects remain significant problems. The following clinical research stage must include a rational combination of agents that activate apoptotic signaling pathways and block pro-survival mechanisms while minimizing off-target toxicities. Furthermore, NPs that can treat various symptoms related to chemotherapeutics, such as nausea and vomiting, should be investigated. Exploration of the combination NPs with classical chemotherapeutic agents may be a possible way to enhance the susceptibility of cancer cells. Moreover, a study (Li et al., 2022) suggests that acupoint stimulation involves synergy with chemotherapy and can alleviate chemotherapeutic agents side effects.

NPs with anti-EC effects were classified and systematically organized by their inducing-apoptosis mechanisms and the sources in the review. The cell line, animal model, dose, efficacy, and mechanism of the NPs in each paper were covered clearly. The main related signal pathways are the mitochondrial-dependent apoptotic pathway, endoplasmic reticulum stress (ERS) mediated apoptotic pathway, mitogen-activated protein kinase (MAPK) mediated apoptotic pathway, NF-κB mediated apoptotic pathways, PI3K-Akt mediated apoptotic pathway, P21-mediated apoptotic pathway, and other reported pathways. In conclusion, we summarized the experiment-based molecular mechanisms and regulatory networks of NPs for EC. Hopefully, this review focuses on the importance of natural medicines in treating EC and provides a foundation for developing potential anti-EC drugs from natural therapies. There are more and more studies about NPs, and the depth of the research is increasing (Kirchmair, 2020; Naeem et al., 2022). NPs and their biological activities are currently a subject of great interest in the pharmaceutical (Ekiert and Szopa, 2020). Hopefully, the information presented in this review might be significant for further preclinical and clinical investigation.

Author contributions

All authors contributed to the article and approved the submitted version. JH, YZ, and YR conceived and designed this paper. XZ, YZ, RZ, YW, TL, SS, and SZ summarized and analyzed the data. XZ and YW drafted, revised, and edited the paper.

Funding

This research was supported by the Xinglin Scholar Research Promotion Project of Chengdu University of TCM (Grant no. QJRC2021019), and NSFC (National Natural Science Foundation of China, Grant no. 82004415).

Acknowledgments

We would like to acknowledge the assistance and contributions from our colleagues. I also would like to thank Xiang Zhang for helping me to export images on biorender.

Conflict of interest

The authors declare that the research was conducted in the absence of any commercial or financial relationships that could be construed as a potential conflict of interest.

Publisher's note

All claims expressed in this article are solely those of the authors and do not necessarily represent those

of their affiliated organizations, or those of the publisher, the editors and the reviewers. Any product that may be evaluated in this article, or claim that may be made by its manufacturer, is not guaranteed or endorsed by the publisher.

Supplementary material

The Supplementary Material for this article can be found online at: https://www.frontiersin.org/articles/10.3389/fphar.2023.1209412/full#supplementary-material

References

Abate, M., Festa, A., Falco, M., Lombardi, A., Luce, A., Grimaldi, A., et al. (2020). Mitochondria as playmakers of apoptosis, autophagy and senescence. *Semin. Cell Dev. Biol.* 98, 139–153. doi:10.1016/j.semcdb.2019.05.022

Ahn, M. Y., Jung, J. H., Na, Y. J., and Kim, H. S. (2008). A natural histone deacetylase inhibitor, Psammaplin A, induces cell cycle arrest and apoptosis in human endometrial cancer cells. *Gynecol. Oncol.* 108, 27–33. doi:10.1016/j.ygyno.2007.08.098

Ai, Z., Yin, L., Zhou, X., Zhu, Y., Zhu, D., Yu, Y., et al. (2006). Inhibition of survivin reduces cell proliferation and induces apoptosis in human endometrial cancer. *Cancer* 107, 746–756. doi:10.1002/cncr.22044

Akazawa, M., and Hashimoto, K. (2022). Development and validation of machine learning models for the prediction of overall survival and cancer-specific survival in patients with endometrial cancer: An analysis of the surveillance, epidemiology, and end results (SEER) database by munetoshi Akazawa, kazunori Hashimoto SSRN. Available at: https://papers.ssrn.com/sol3/papers.cfm?abstract_id=4191367 (Accessed December 11, 2022).

Ali, A. K., Nandagopal, N., and Lee, S.-H. (2015). IL-15-PI3K-AKT-mTOR: A critical pathway in the life journey of natural killer cells. *Front. Immunol.* 6, 355. doi:10.3389/fimmu.2015.00355

An, J., Li, L., and Zhang, X. (2021). Curcusone C induces apoptosis in endometrial cancer cells via mitochondria-dependent apoptotic and ERK pathway. *Biotechnol. Lett.* 43, 329–338. doi:10.1007/s10529-020-03027-4

Anjum, J., Mitra, S., Das, R., Alam, R., Mojumder, A., Emran, T. B., et al. (2022). A renewed concept on the MAPK signaling pathway in cancers: Polyphenols as a choice of therapeutics. *Mol. Cell Biochem.* 477, 106398. doi:10.1016/j.phrs.2022.106398

Armstrong, A. J., Hurd, W. W., Elguero, S., Barker, N. M., and Zanotti, K. M. (2012). Diagnosis and management of endometrial hyperplasia. *J. Minim. Invasive Gynecol.* 19, 562–571. doi:10.1016/j.jmig.2012.05.009

Ashkenazi, A. (2008). Targeting the extrinsic apoptosis pathway in cancer. *Cytokine & Growth Factor Rev.* 19, 325–331. doi:10.1016/j.cytogfr.2008.04.001

Atanasov, A. G., Zotchev, S. B., Dirsch, V. M., and Supuran, C. T. (2021). Natural products in drug discovery: Advances and opportunities. *Nat. Rev. Drug Discov.* 20, 200–216. doi:10.1038/s41573-020-00114-z

Avrutsky, M. I., and Troy, C. M. (2021). Caspase-9: A multimodal therapeutic target with diverse cellular expression in human disease. *Front. Pharmacol.* 12, 701301. doi:10.3389/fphar.2021.701301

Bilal, M., and Iqbal, H. M. N. (2020). Biologically active macromolecules: Extraction strategies, therapeutic potential and biomedical perspective. *Int. J. Biol. Macromol.* 151, 1–18. doi:10.1016/j.ijbiomac.2020.02.037

Blanco, J., Cameirao, C., López, M. C., and Muñoz-Barroso, I. (2020). Phosphatidylinositol-3-kinase-Akt pathway in negative-stranded RNA virus infection: A minireview. *Arch. Virol.* 165, 2165–2176. doi:10.1007/s00705-020-04740-1

Bratton, S. B., and Salvesen, G. S. (2010). Regulation of the apaf-1-caspase-9 apoptosome. *J. Cell Sci.* 123, 3209–3214. doi:10.1242/jcs.073643

Braun, M. M., Overbeek-Wager, E. A., and Grumbo, R. J. (2016). Diagnosis and management of endometrial cancer. *Am. Fam. Physician* 93, 468–474.

Brooks, R. A., Fleming, G. F., Lastra, R. R., Lee, N. K., Moroney, J. W., Son, C. H., et al. (2019). Current recommendations and recent progress in endometrial cancer. *CA A Cancer J. Clin.* 69, 258–279. doi:10.3322/caac.21561

Bulbul, M., Karabulut, S., Kalender, M., and Keskin, I. (2021). Effects of gallic acid on endometrial cancer cells in two and three dimensional cell culture models. *Asian Pac J. Cancer Prev.* 22, 1745–1751. doi:10.31557/APJCP.2021.22.6.1745

Cai, J., Huang, S., Yi, Y., and Bao, S. (2019). Downregulation of PTPN18 can inhibit proliferation and metastasis and promote apoptosis of endometrial cancer. *Clin. Exp. Pharmacol. Physiol.* 46, 734–742. doi:10.1111/1440-1681.13098

Carneiro, B. A., and El-Deiry, W. S. (2020). Targeting apoptosis in cancer therapy. *Nat. Rev. Clin. Oncol.* 17, 395–417. doi:10.1038/s41571-020-0341-y

Chalhoub, N., and Baker, S. J. (2009). PTEN and the PI3-kinase pathway in cancer. *Annu. Rev. Pathol. Mech. Dis.* 4, 127–150. doi:10.1146/annurev.pathol.4.110807.092311

Chang, C.-C., Hsu, H.-F., Huang, K.-H., Wu, J.-M., Kuo, S.-M., Ling, X.-H., et al. (2014). Anti-proliferative effects of Siegesbeckia orientalis ethanol extract on human endometrial RL-95 cancer cells. *Molecules* 19, 19980–19994. doi:10.3390/molecules191219980

Chaudhry, P., and Asselin, E. (2009). Resistance to chemotherapy and hormone therapy in endometrial cancer. *Endocrine-Related Cancer* 16, 363–380. doi:10.1677/ERC-08-0266

Chen, H.-Y., Cheng, W.-P., Chiang, Y.-F., Hong, Y.-H., Ali, M., Huang, T.-C., et al. (2021). Hinokitiol exhibits antitumor properties through induction of ROS-mediated apoptosis and p53-driven cell-cycle arrest in endometrial cancer cell lines (Ishikawa, HEC-1A, KLE). *Int. J. Mol. Sci.* 22, 8268. doi:10.3390/ijms22158268

Chen, J., Zhao, K.-N., Li, R., Shao, R., and Chen, C. (2014). Activation of PI3K/Akt/mTOR pathway and dual inhibitors of PI3K and mTOR in endometrial cancer. *Curr. Med. Chem.* 21, 3070–3080. doi:10.2174/0929867321666140414095605

Chen, S., Wu, Z., Ke, Y., Shu, P., Chen, C., Lin, R., et al. (2019). Wogonoside inhibits tumor growth and metastasis in endometrial cancer via ER stress-Hippo signaling axis. *Acta Biochim. Biophys. Sin. (Shanghai)* 51, 1096–1105. doi:10.1093/abbs/gmz109

Chuderland, D., and Seger, R. (2005). Protein–protein interactions in the regulation of the extracellular signal-regulated kinase. *Mol. Biotechnol.* 29, 57–74. doi:10.1385/MB:29:1:57

Chung, I., Yap, C., Subramaniam, K., and Khor, S. (2017). Annonacin exerts antitumor activity through induction of apoptosis and extracellular signal-regulated kinase inhibition. *Phcog Res.* 9, 378–383. doi:10.4103/pr.pr_19_17

Cincin, Z. B., Kiran, B., Baran, Y., and Cakmakoglu, B. (2018). Hesperidin promotes programmed cell death by downregulation of nongenomic estrogen receptor signalling pathway in endometrial cancer cells. *Biomed. Pharmacother.* 103, 336–345. doi:10.1016/j.biopha.2018.04.020

Clarke, H. J., Chambers, J. E., Liniker, E., Marciniak, S. J., Clarke, H. J., Chambers, J. E., et al. (2014). Endoplasmic reticulum stress in malignancy. *Cancer Cell* 25, 563–573. doi:10.1016/j.ccr.2014.03.015

Concin, N., Creutzberg, C. L., Vergote, I., Cibula, D., Mirza, M. R., Marnitz, S., et al. (2021). ESGO/ESTRO/ESP Guidelines for the management of patients with endometrial carcinoma. *Virchows Arch.* 478, 153–190. doi:10.1007/s00428-020-03007-z

Crosbie, E. J., Kitson, S. J., McAlpine, J. N., Mukhopadhyay, A., Powell, M. E., and Singh, N. (2022). Endometrial cancer. *Lancet* 399, 1412–1428. doi:10.1016/S0140-6736(22)00323-3

Darici, S., Alkhaldi, H., Horne, G., Jørgensen, H. G., Marmiroli, S., and Huang, X. (2020). Targeting PI3K/Akt/mTOR in AML: Rationale and clinical evidence. *J. Clin. Med.* 9, 2934. doi:10.3390/jcm9092934

Denley, A., Gymnopoulos, M., Kang, S., Mitchell, C., and Vogt, P. K. (2009). Requirement of phosphatidylinositol(3,4,5)Trisphosphate in phosphatidylinositol 3-kinase-induced oncogenic transformation. *Mol. Cancer Res.* 7, 1132–1138. doi:10.1158/1541-7786.MCR-09-0068

Dhillon, A. S., Hagan, S., Rath, O., and Kolch, W. (2007). MAP kinase signalling pathways in cancer. *Oncogene* 26, 3279–3290. doi:10.1038/sj.onc.1210421

Dong, Y., and Li, W. (2021). Effects of cinnamaldehyde on proliferation, apoptosis and invasion of endometrial carcinoma cell line Ishikawa (China). *Prog. Anatomical Sci.* 27, 248–251. doi:10.16695/j.cnki.1006-2947.2021.02.030

Dorstyn, L., Akey, C. W., and Kumar, S. (2018). New insights into apoptosome structure and function. *Cell Death Differ.* 25, 1194–1208. doi:10.1038/s41418-017-0025-z

Ediriweera, M. K., Tennekoon, K. H., and Samarakoon, S. R. (2019). Role of the PI3K/AKT/mTOR signaling pathway in ovarian cancer: Biological and therapeutic significance. *Seminars Cancer Biol.* 59, 147–160. doi:10.1016/j.semcancer.2019.05.012

Edmondson, R. J., Crosbie, E. J., Nickkho-Amiry, M., Kaufmann, A., Stelloo, E., Nijman, H. W., et al. (2017). Markers of the p53 pathway further refine molecular profiling in high-risk endometrial cancer: A trans portec initiative. *Gynecol. Oncol.* 146, 327–333. doi:10.1016/j.ygyno.2017.05.014

Ekiert, H. M., and Szopa, A. (2020). Biological activities of natural products. *Molecules* 25, 5769. doi:10.3390/molecules25235769

Ekiert, H. M., and Szopa, A. (2022). Biological activities of natural products II. *Molecules* 27, 1519. doi:10.3390/molecules27051519

El-Deiry, W. S., Tokino, T., Velculescu, V. E., Levy, D. B., Parsons, R., Trent, J. M., et al. (1993). WAF1, a potential mediator of p53 tumor suppression. *Cell* 75, 817–825. doi:10.1016/0092-8674(93)90500-P

Eskander, R. N., Randall, L. M., Sakai, T., Guo, Y., Hoang, B., and Zi, X. (2012). Flavokawain B, a novel, naturally occurring chalcone, exhibits robust apoptotic effects

and induces G2/M arrest of a uterine leiomyosarcoma cell line. *J. Obstet. Gynaecol. Res.* 38, 1086–1094. doi:10.1111/j.1447-0756.2011.01841.x

Fan, H., Morioka, T., and Ito, E. (2000). Induction of apoptosis and growth inhibition of cultured human endometrial adenocarcinoma cells (Sawano) by an antitumor lipoprotein fraction of rice bran. *Gynecol. Oncol.* 76, 170–175. doi:10.1006/gyno.1999.5669

Fattahi, S., Amjadi-Moheb, F., Tabaripour, R., Ashrafi, G. H., and Akhavan-Niaki, H. (2020). PI3K/AKT/mTOR signaling in gastric cancer: Epigenetics and beyond. *Life Sci.* 262, 118513. doi:10.1016/j.lfs.2020.118513

Fisher, D. E. (1994). Apoptosis in cancer therapy: Crossing the threshold. *Cell* 78, 539–542. doi:10.1016/0092-8674(94)90518-5

Fonseca, B. M., Correia-da-Silva, G., and Teixeira, N. A. (2018). Cannabinoid-induced cell death in endometrial cancer cells: Involvement of TRPV1 receptors in apoptosis. *J. Physiol. Biochem.* 74, 261–272. doi:10.1007/s13105-018-0611-7

Fruman, D. (2008). *Faculty Opinions recommendation of the p110beta isoform of phosphoinositide 3-kinase signals downstream of G protein-coupled receptors and is functionally redundant with p110gamma*, 575678.

Geisler, J. P., Geisler, H. E., Wiemann, M. C., Zhou, Z., Miller, G. A., and Crabtree, W. (1999). p53 expression as a prognostic indicator of 5-year survival in endometrial cancer. *Gynecol. Oncol.* 74, 468–471. doi:10.1006/gyno.1999.5482

Green, D. R. (2022). The mitochondrial pathway of apoptosis Part II: The BCL-2 protein family. *Cold Spring Harb. Perspect. Biol.* 14, a041046. doi:10.1101/cshperspect.a041046

Hashem, S., Ali, T. A., Akhtar, S., Nisar, S., Sageena, G., Ali, S., et al. (2022). Targeting cancer signaling pathways by natural products: Exploring promising anti-cancer agents. *Biomed. Pharmacother.* 150, 113054. doi:10.1016/j.biopha.2022.113054

Hassan, S. S. U., Abdel-Daim, M. M., Behl, T., and Bungau, S. (2022). Natural products for chronic diseases: A ray of hope. *Molecules* 27, 5573. doi:10.3390/molecules27175573

Hengartner, M. O. (2000). The biochemistry of apoptosis. *Nature* 407, 770–776. doi:10.1038/35037710

Hennessy, B. T., Smith, D. L., Ram, P. T., Lu, Y., Mills, G. B., Hennessy, B. T., et al. (2005). Exploiting the PI3K/AKT pathway for cancer drug discovery. *Nat. Rev. Drug Discov.* 4, 988–1004. doi:10.1038/nrd1902

Huang, C., and Hu, G. (2018). Shikonin suppresses proliferation and induces apoptosis in endometrioid endometrial cancer cells via modulating miR-106b/PTEN/AKT/mTOR signaling pathway. *Biosci. Rep.* 38, BSR20171546. doi:10.1042/BSR20171546

Huang, X., Yang, Z., Xie, Q., Zhang, Z., Zhang, H., and Ma, J. (2019). Natural products for treating colorectal cancer: A mechanistic review. *Biomed. Pharmacother.* 117, 109142. doi:10.1016/j.biopha.2019.109142

Huang, Y., Hou, Y., Qu, P., and Dai, Y. (2023). Editorial: Combating cancer with natural products: Non-coding RNA and RNA modification. *Front. Pharmacol.* 14, 1149777. doi:10.3389/fphar.2023.1149777

Hutt, S., Tailor, A., Ellis, P., Michael, A., Butler-Manuel, S., and Chatterjee, J. (2019). The role of biomarkers in endometrial cancer and hyperplasia: A literature review. *Acta Oncol.* 58, 342–352. doi:10.1080/0284186X.2018.1540886

Huvila, J., Talve, L., Carpén, O., Edqvist, P.-H., Pontén, F., Grénman, S., et al. (2013). Progesterone receptor negativity is an independent risk factor for relapse in patients with early stage endometrioid endometrial adenocarcinoma. *Gynecol. Oncol.* 130, 463–469. doi:10.1016/j.ygyno.2013.06.015

Ishii, T., Kira, N., Yoshida, T., and Narahara, H. (2013). Cucurbitacin D induces growth inhibition, cell cycle arrest, and apoptosis in human endometrial and ovarian cancer cells. *Tumor Biol.* 34, 285–291. doi:10.1007/s13277-012-0549-2

Islam, M. S. (2022). Natural products and disease prevention, relief and treatment. *Nutrients* 14, 2396. doi:10.3390/nu14122396

Jan, R., and Chaudhry, G.-S. (2019). Understanding apoptosis and apoptotic pathways targeted cancer therapeutics. *Adv. Pharm. Bull.* 9, 205–218. doi:10.15171/apb.2019.024

Jiang, J., Zhou, N., Ying, P., Zhang, T., Liang, R., and Jiang, X. (2019). Emodin promotes apoptosis of human endometrial cancer through regulating the MAPK and PI3K/AKT pathways. *Open Life Sci.* 13, 489–496. doi:10.1515/biol-2018-0058

Jiang, M., Qi, L., Li, L., Wu, Y., Song, D., and Li, Y. (2021a). Caspase-8: A key protein of cross-talk signal way in "PANoptosis" in cancer. *Int. J. Cancer* 149, 1408–1420. doi:10.1002/ijc.33698

Jiang, R., Su, G., Chen, X., Chen, S., Li, Q., Xie, B., et al. (2021b). Esculetin inhibits endometrial cancer proliferation and promotes apoptosis via hnRNPA1 to downregulate BCLXL and XIAP. *Cancer Lett.* 521, 308–321. doi:10.1016/j.canlet.2021.08.039

Kantari, C., and Walczak, H. (2011). Caspase-8 and Bid: Caught in the act between death receptors and mitochondria. *Biochimica Biophysica Acta* 1813, 558–563. doi:10.1016/j.bbamcr.2011.01.026

Karia, P. S., Huang, Y., Tehranifar, P., Wright, J. D., Genkinger, J. M., Karia, P. S., et al. (2023). Racial and ethnic differences in type II endometrial cancer mortality outcomes: The contribution of sociodemographic, clinicopathologic, and treatment factors. *Gynecol. Oncol.* 168, 119–126. doi:10.1016/j.ygyno.2022.11.015

Karimian, A., Ahmadi, Y., Yousefi, B., Karimian, A., Ahmadi, Y., and Yousefi, B. (2016). Multiple functions of p21 in cell cycle, apoptosis and transcriptional regulation after DNA damage. *DNA Repair* 42, 63–71. doi:10.1016/j.dnarep.2016.04.008

Kashyap, D., Garg, V. K., and Goel, N. (2021). Intrinsic and extrinsic pathways of apoptosis: Role in cancer development and prognosis. *Adv. Protein Chem. Struct. Biol.* 125, 73–120. doi:10.1016/bs.apcsb.2021.01.003

Kavandi, L., Lee, L. R., Bokhari, A. A., Pirog, J. E., Jiang, Y., Ahmad, K. A., et al. (2015). The Chinese herbs*Scutellaria baicalensis*and*Fritillaria cirrhosa*target NFκB to inhibit proliferation of ovarian and endometrial cancer cells. *Mol. Carcinog.* 54, 368–378. doi:10.1002/mc.22107

Kikuchi, K., Haneda, M., Hayashi, S., Maeda, T., Nakano, N., Kuroda, Y., et al. (2022). P21 deficiency exhibits delayed endochondral ossification during fracture healing. *Bone* 165, 116572. doi:10.1016/j.bone.2022.116572

Kim, A., Ha, J., Kim, J., Cho, Y., Ahn, J., Cheon, C., et al. (2021). Natural products for pancreatic cancer treatment: From traditional medicine to modern drug discovery. *Nutrients* 13, 3801. doi:10.3390/nu13113801

Kim, E. K., and Choi, E.-J. (2010). Pathological roles of MAPK signaling pathways in human diseases. *Biochimica Biophysica Acta* 1802, 396–405. doi:10.1016/j.bbadis.2009.12.009

Kim, E. M., Jung, C.-H., Kim, J., Hwang, S.-G., Park, J. K., and Um, H.-D. (2017a). The p53/p21 complex regulates cancer cell invasion and apoptosis by targeting bcl-2 family proteins. *Cancer Res.* 77, 3092–3100. doi:10.1158/0008-5472.CAN-16-2098

Kim, J. H., Kim, M., Yun, S.-M., Lee, S., No, J. H., Suh, D. H., et al. (2017b). Ginsenoside Rh2 induces apoptosis and inhibits epithelial-mesenchymal transition in HEC1A and Ishikawa endometrial cancer cells. *Biomed. Pharmacother.* 96, 871–876. doi:10.1016/j.biopha.2017.09.033

Kim, J. Y., Lee, S. G., Chung, J.-Y., Kim, Y.-J., Park, J.-E., Koh, H., et al. (2011). Ellipticine induces apoptosis in human endometrial cancer cells: The potential involvement of reactive oxygen species and mitogen-activated protein kinases. *Toxicology* 289, 91–102. doi:10.1016/j.tox.2011.07.014

Kim, U., Kim, K. S., Park, J.-K., and Um, H.-D. (2022). Involvement of the p53/p21 complex in p53-dependent gene expression. *Biochem. Biophysical Res. Commun.* 621, 151–156. doi:10.1016/j.bbrc.2022.07.022

Kirchmair, J. (2020). Molecular informatics in natural products research. *Mol. Inf.* 39, e2000206. doi:10.1002/minf.202000206

Kohlberger, P., Gitsch, G., Loesch, A., Tempfer, C., Kaider, A., Reinthaller, A., et al. (1996). p53 protein overexpression in early stage endometrial cancer. *Gynecol. Oncol.* 62, 213–217. doi:10.1006/gyno.1996.0218

Lee, J.-S., Ahn, J.-H., Cho, Y.-J., Kim, H.-Y., Yang, Y.-I., Lee, K.-T., et al. (2015). α-Terthienylmethanol, isolated from Eclipta prostrata, induces apoptosis by generating reactive oxygen species via NADPH oxidase in human endometrial cancer cells. *J. Ethnopharmacol.* 169, 426–434. doi:10.1016/j.jep.2015.04.029

Lei, X., Guo, J., Wang, Y., Cui, J., Feng, B., Su, Y., et al. (2019). Inhibition of endometrial carcinoma by Kaempferol is interceded through apoptosis induction, G2/M phase cell cycle arrest, suppression of cell invasion and upregulation of m-TOR/PI3K signalling pathway. *J. BUON* 24, 1555–1561.

Li, F.-R., Yu, F.-X., Yao, S.-T., Si, Y.-H., Zhang, W., and Gao, L.-L. (2012). Hyperin extracted from manchurian Rhododendron leaf induces apoptosis in human endometrial cancer cells through a mitochondrial pathway. *Asian Pac. J. Cancer Prev.* 13, 3653–3656. doi:10.7314/apjcp.2012.13.8.3653

Li, G., and Lou, H.-X. (2018). Strategies to diversify natural products for drug discovery. *Med. Res. Rev.* 38, 1255–1294. doi:10.1002/med.21474

Li, P., Zhou, L., Zhao, T., Liu, X., Zhang, P., Liu, Y., et al. (2017). Caspase-9: Structure, mechanisms and clinical application. *Oncotarget* 8, 23996–24008. doi:10.18632/oncotarget.15098

Li, Q., Zhang, J., Liang, Y., Mu, W., Hou, X., Ma, X., et al. (2018). Tanshinone l exhibits anticancer effects in human endometrial carcinoma HEC-1-A cells via mitochondrial mediated apoptosis, cell cycle arrest and inhibition of JAK/STAT signalling pathway. *J. BUON* 23, 1092–1096.

Li, S., Zhao, S., Guo, Y., Yang, Y., Huang, J., Wang, J., et al. (2022). Clinical efficacy and potential mechanisms of acupoint stimulation combined with chemotherapy in combating cancer: A review and prospects. *Front. Oncol.* 12, 864046. doi:10.3389/fonc.2022.864046

Li, W., Tian, L., and Liu, J. (2021). The effects of zedoary turmeric Oil on proliferation and apoptosis and expressions of caspase-3 and bax and bcl-2 in HEC-1B (China). *Henan Tradit. Chin. Med.* 41, 384–387.

Li, Z.-L., Morishima, S., Tang, J.-T., and Otsuki, Y. (2009). Apoptotic effects of Tian-Long compound on endometrial adenocarcinoma cells *in vitro*. *Med. Mol. Morphol.* 42, 32–39. doi:10.1007/s00795-008-0424-9

Liang, L., Yang, B., Wu, Y., and Sun, L. (2021). Osthole suppresses the proliferation and induces apoptosis via inhibiting the PI3K/AKT signaling pathway of endometrial cancer JEC cells. *Exp. Ther. Med.* 22, 1171. doi:10.3892/etm.2021.10605

Liu, C., Zeng, Y., Wen, Y., Huang, X., and Liu, Y. (2022). Natural products modulate cell apoptosis: A promising way for the treatment of ulcerative colitis. *Front. Pharmacol.* 13, 806148. doi:10.3389/fphar.2022.806148

Liu, Y., Whelan, R. J., Pattnaik, B. R., Ludwig, K., Subudhi, E., Rowland, H., et al. (2012). Terpenoids from Zingiber officinale (Ginger) induce apoptosis in endometrial cancer cells through the activation of p53. *PLoS One* 7, e53178. doi:10.1371/journal.pone.0053178

Lu, K. H., and Broaddus, R. R. (2020). Endometrial cancer. *N. Engl. J. Med.* 383, 2053–2064. doi:10.1056/NEJMra1514010

Lu, K., Lin, J., and Jiang, J. (2020). Osthole inhibited cell proliferation and induced cell apoptosis through decreasing CPEB2 expression via up-regulating miR-424 in endometrial carcinoma. *J. Recept. Signal Transduct.* 40, 89–96. doi:10.1080/10799893.2019.1710846

Malladi, S., Challa-Malladi, M., Fearnhead, H. O., and Bratton, S. B. (2009). The Apaf-1·procaspase-9 apoptosome complex functions as a proteolytic-based molecular timer. *EMBO J.* 28, 1916–1925. doi:10.1038/emboj.2009.152

Man, G. C. W., Wang, J., Song, Y., Wong, J. H., Zhao, Y., Lau, T. S., et al. (2020). Therapeutic potential of a novel prodrug of green tea extract in induction of apoptosis via ERK/JNK and Akt signaling pathway in human endometrial cancer. *BMC Cancer* 20, 964. doi:10.1186/s12885-020-07455-3

Mandal, R., Barrón, J. C., Kostova, I., Becker, S., and Strebhardt, K. (2020). Caspase-8: The double-edged sword. *Biochimica Biophysica Acta* 1873, 188357. doi:10.1016/j.bbcan.2020.188357

Manoharan, S., and Perumal, E. (2022). Potential role of marine bioactive compounds in cancer signaling pathways: A review. *Eur. J. Pharmacol.* 936, 175330. doi:10.1016/j.ejphar.2022.175330

Marchetti, A., Doglioni, C., Barbareschi, M., Buttitta, F., Pellegrini, S., Bertacca, G., et al. (1996). P21 RNA and protein expression in non-small cell lung carcinomas: Evidence of p53-independent expression and association with tumoral differentiation. *Oncogene* 12, 1319–1324.

Marciniak, S. J. (2019). Endoplasmic reticulum stress: A key player in human disease. *FEBS J.* 286, 228–231. doi:10.1111/febs.14740

Martínez-García, D., Manero-Rupérez, N., Quesada, R., Korrodi-Gregório, L., and Soto-Cerrato, V. (2019). Therapeutic strategies involving survivin inhibition in cancer. *Med. Res. Rev.* 39, 887–909. doi:10.1002/med.21547

McComb, S., Chan, P. K., Guinot, A., Hartmannsdottir, H., Jenni, S., Dobay, M. P., et al. (2019). Efficient apoptosis requires feedback amplification of upstream apoptotic signals by effector caspase-3 or -7. *Sci. Adv.* 5, eaau9433. doi:10.1126/sciadv.aau9433

Mirakhor Samani, S., Ezazi Bojnordi, T., Zarghampour, M., Merat, S., Fouladi, D. F., Mirakhor Samani, S., et al. (2018). Expression of p53, bcl-2 and bax in endometrial carcinoma, endometrial hyperplasia and normal endometrium: A histopathological study. *J. Obstetrics Gynaecol.* 38, 999–1004. doi:10.1080/01443615.2018.1437717

Miricescu, D., Totan, A., Stanescu-Spinu, I.-I., Badoiu, S. C., Stefani, C., and Greabu, M. (2020). PI3K/AKT/mTOR signaling pathway in breast cancer: From molecular landscape to clinical aspects. *Int. J. Mol. Sci.* 22, 173. doi:10.3390/ijms22010173

Mirza-Aghazadeh-Attari, M., Ekrami, E. M., Aghdas, S. A. M., Mihanfar, A., Hallaj, S., Yousefi, B., et al. (2020). Targeting PI3K/Akt/mTOR signaling pathway by polyphenols: Implication for cancer therapy. *Life Sci.* 255, 117481. doi:10.1016/j.lfs.2020.117481

Moore, K., and Brewer, M. A. (2017). Endometrial cancer: Is this a new disease? *Am. Soc. Clin. Oncol. Educ. Book* 37, 435–442. doi:10.1200/EDBK_175666

Naeem, A., Hu, P., Yang, M., Zhang, J., Liu, Y., Zhu, W., et al. (2022). Natural products as anticancer agents: Current status and future perspectives. *Molecules* 27, 8367. doi:10.3390/molecules27238367

Nair, P., Lu, M., Petersen, S., and Ashkenazi, A. (2014). "Chapter five - apoptosis initiation through the cell-extrinsic pathway," in Methods in enzymology *regulated cell death Part A: Apoptotic mechanisms*. Editors A. Ashkenazi, J. Yuan, and J. A. Wells (Cambridge: Academic Press), 99–128.

Narita, M., Ohnishi, O., Nemoto, M., Yajima, Y., and Suzuki, T. (2002). Implications of phosphoinositide 3-kinase in the μ- and δ-opioid receptor-mediated supraspinal antinociception in the mouse. *Neuroscience* 113, 647–652. doi:10.1016/S0306-4522(02)00197-5

Nuzzo, G., Senese, G., Gallo, C., Albiani, F., Romano, L., d'Ippolito, G., et al. (2022). Antitumor potential of immunomodulatory natural products. *Mar. Drugs* 20, 386. doi:10.3390/md20060386

Oakes, S. A., Papa, F. R., Oakes, S. A., and Papa, F. R. (2015). The role of endoplasmic reticulum stress in human pathology. *Annu. Rev. Pathol. Mech. Dis.* 10, 173–194. doi:10.1146/annurev-pathol-012513-104649

Otsuki, Y. (2001). Apoptosis in human endometrium: Apoptotic detection methods and signaling. *Med. Electron Microsc.* 34, 166–173. doi:10.1007/s007950100011

Passarello, K., Kurian, S., and Villanueva, V. (2019). Endometrial cancer: An overview of pathophysiology, management, and care. *Seminars Oncol. Nurs.* 35, 157–165. doi:10.1016/j.soncn.2019.02.002

Piddock, R., Bowles, K., and Rushworth, S. (2017). The role of PI3K isoforms in regulating bone marrow microenvironment signaling focusing on acute myeloid leukemia and multiple myeloma. *Cancers* 9, 29. doi:10.3390/cancers9040029

Pothongsrisit, S., and Pongrakhananon, V. (2021). Targeting the PI3K/AKT/mTOR signaling pathway in lung cancer: An update regarding potential drugs and natural products. *Molecules* 26, 4100. doi:10.3390/molecules26134100

Qin, H., Srinivasula, S. M., Wu, G., Fernandes-Alnemri, T., Alnemri, E. S., and Shi, Y. (1999). Structural basis of procaspase-9 recruitment by the apoptotic protease-activating factor 1. *Nature* 399, 549–557. doi:10.1038/21124

Rao, T., Tan, Z., Peng, J., Guo, Y., Chen, Y., Zhou, H., et al. (2019). The pharmacogenetics of natural products: A pharmacokinetic and pharmacodynamic perspective. *Pharmacol. Res.* 146, 104283. doi:10.1016/j.phrs.2019.104283

Ricci, M. S., and El-Deiry, W. S. (2007). "The extrinsic pathway of apoptosis," in *Apoptosis, senescence, and cancer* (New York City: Springer), 31–54.

Rodríguez-Palacios, D. Á., Colorado-Yohar, S. M., Velten, M., Vaamonde-Martín, R. J., Ballesta, M., Chirlaque, M.-D., et al. (2022). Incidence and trend of type I and II endometrial cancer in women from two population-based European cancer registries (1998–2012). *Int. J. Environ. Res. Public Health* 19, 3789. doi:10.3390/ijerph19073789

Ron, D., and Walter, P. (2007). Signal integration in the endoplasmic reticulum unfolded protein response. *Nat. Rev. Mol. Cell Biol.* 8, 519–529. doi:10.1038/nrm2199

Santucci, R., Sinibaldi, F., Cozza, P., Polticelli, F., and Fiorucci, L. (2019). Cytochrome c: An extreme multifunctional protein with a key role in cell fate. *Int. J. Biol. Macromol.* 136, 1237–1246. doi:10.1016/j.ijbiomac.2019.06.180

Sexton, É., Van Themsche, C., Leblanc, K., Parent, S., Lemoine, P., and Asselin, E. (2006). Resveratrol interferes with AKT activity and triggers apoptosis in human uterine cancer cells. *Mol. Cancer* 5, 45. doi:10.1186/1476-4598-5-45

Shanmugam, M. K., Lee, J. H., Chai, E. Z. P., Kanchi, M. M., Kar, S., Arfuso, F., et al. (2016). Cancer prevention and therapy through the modulation of transcription factors by bioactive natural compounds. *Seminars Cancer Biol.* 40–41, 35–47. doi:10.1016/j.semcancer.2016.03.005

Shi, Z., Zhou, Q., Gao, S., Li, W., Li, X., Liu, Z., et al. (2019). Silibinin inhibits endometrial carcinoma via blocking pathways of STAT3 activation and SREBP1-mediated lipid accumulation. *Life Sci.* 217, 70–80. doi:10.1016/j.lfs.2018.11.037

Singh, S., Pavuluri, S., Jyothi Lakshmi, B., Biswa, B. B., Venkatachalam, B., Tripura, C., et al. (2020). Molecular characterization of Wdr13 knockout female mice uteri: A model for human endometrial hyperplasia. *Sci. Rep.* 10, 14621. doi:10.1038/s41598-020-70773-w

Slomovitz, B. M., and Coleman, R. L. (2012). The PI3K/AKT/mTOR pathway as a therapeutic target in endometrial cancer. *Clin. Cancer Res.* 18, 5856–5864. doi:10.1158/1078-0432.CCR-12-0662

Sujobert, P., Sujobert, P., Cornillet-Lefebvre, P., Hayflick, J. S., Prie, N., Verdier, F., et al. (2005). Essential role for the p110delta isoform in phosphoinositide 3-kinase activation and cell proliferation in acute myeloid leukemia. *Blood* 106, 1063–1066. doi:10.1182/blood-2004-08-3225

Sung, H., Ferlay, J., Siegel, R. L., Laversanne, M., Soerjomataram, I., Jemal, A., et al. (2021). Global cancer statistics 2020: GLOBOCAN estimates of incidence and mortality worldwide for 36 cancers in 185 countries. *CA A Cancer J. Clin.* 71, 209–249. doi:10.3322/caac.21660

Takai, N., Ueda, T., Nishida, M., Nasu, K., and Narahara, H. (2008). Bufalin induces growth inhibition, cell cycle arrest and apoptosis in human endometrial and ovarian cancer cells. *Int. J. Mol. Med.* 21, 637–643. doi:10.3892/ijmm.21.5.637

Tan, H., Chu, G., Hu, C., and Zhang, E. (2016). Effects of Panaxnotoginsengsaponins on proliferation, invasion, apoptosis of endometrial cancercell lines Ishikawa and HEC-1A (China). *China Med. Her.* 13, 13–16.

Terzic, M., Aimagambetova, G., Kunz, J., Bapayeva, G., Aitbayeva, B., Terzic, S., et al. (2021). Molecular basis of endometriosis and endometrial cancer: Current Knowledge and future perspectives. *Int. J. Mol. Sci.* 22, 9274. doi:10.3390/ijms22179274

Thomford, N., Senthebane, D., Rowe, A., Munro, D., Seele, P., Maroyi, A., et al. (2018). Natural products for drug discovery in the 21st century: Innovations for novel drug discovery. *Int. J. Mol. Sci.* 19, 1578. doi:10.3390/ijms19061578

Thompson, H. J., and Lutsiv, T. (2023). Natural products in precision oncology: Plant-based small molecule inhibitors of protein kinases for cancer chemoprevention. *Nutrients* 15, 1192. doi:10.3390/nu15051192

Tong, J.-S., Zhang, Q.-H., Huang, X., Fu, X.-Q., Qi, S.-T., Wang, Y.-P., et al. (2011). Icaritin causes sustained ERK1/2 activation and induces apoptosis in human endometrial cancer cells. *PLoS ONE* 6, e16781. doi:10.1371/journal.pone.0016781

Torquato, H., Goettert, M., Justo, G., and Paredes-Gamero, E. (2017). Anti-cancer phytometabolites targeting cancer stem cells. *Curr. Genomics* 18, 156–174. doi:10.2174/1389202917666160803162309

Tsai, C.-C., Chang, Y.-H., Chang, C.-C., Cheng, Y.-M., Ou, Y.-C., Chien, C.-C., et al. (2015). Induction of apoptosis in endometrial cancer (Ishikawa) cells by Pogostemon cablin aqueous extract (PCAE). *Int. J. Mol. Sci.* 16, 12424–12435. doi:10.3390/ijms160612424

Urick, M. E., and Bell, D. W. (2019). Clinical actionability of molecular targets in endometrial cancer. *Nat. Rev. Cancer* 19, 510–521. doi:10.1038/s41568-019-0177-x

Wang, D., Tian, Y., Feng, W., Zhao, L., Zhao, M., Liu, J., et al. (2017). Pseudolaric acid B induces endometrial cancer Ishikawa cell apoptosis and inhibits metastasis through

AKT-GSK-3β and ERK1/2 signaling pathways. *Anti-Cancer Drugs* 28, 603–612. doi:10.1097/CAD.0000000000000500

Wang, F., and Roh, Y. S. (2020). Mitochondrial connection to ginsenosides. *Arch. Pharm. Res.* 43, 1031–1045. doi:10.1007/s12272-020-01279-2

Wang, H., Liu, Z., Gou, Y., Qin, Y., Xu, Y., Liu, J., et al. (2015). Apoptosis and necrosis induced by novel realgar quantum dots in human endometrial cancer cells via endoplasmic reticulum stress signaling pathway. *Int. J. Nanomedicine* 10, 5505–5512. doi:10.2147/IJN.S83838

Wang, M., and Kaufman, R. J. (2016). Protein misfolding in the endoplasmic reticulum as a conduit to human disease. *Nature* 529, 326–335. doi:10.1038/nature17041

Wang, X.-F., Zhao, Y.-B., Wu, Q., Sun, Z.-H., and Li, H.-J. (2014). Triptolide induces apoptosis in endometrial cancer via a p53-independent mitochondrial pathway. *Mol. Med. Rep.* 9, 39–44. doi:10.3892/mmr.2013.1783

Wang, Y., Wang, K., Jin, Y., and Sheng, X. (2019). Endoplasmic reticulum proteostasis control and gastric cancer. *Cancer Lett.* 449, 263–271. doi:10.1016/j.canlet.2019.01.034

Wolf, P., Schoeniger, A., and Edlich, F. (2022). Pro-apoptotic complexes of BAX and BAK on the outer mitochondrial membrane. *Biochim. Biophys. Acta Mol. Cell Res.* 1869, 119317. doi:10.1016/j.bbamcr.2022.119317

Wu, C.-H., Chen, H.-Y., Wang, C.-W., Shieh, T.-M., Huang, T.-C., Lin, L.-C., et al. (2016a). Isoliquiritigenin induces apoptosis and autophagy and inhibits endometrial cancer growth in mice. *Oncotarget* 7, 73432–73447. doi:10.18632/oncotarget.12369

Wu, F.-L., Liu, W.-Y., Van Poucke, S., Braddock, M., Jin, W.-M., Xiao, J., et al. (2016b). Targeting endoplasmic reticulum stress in liver disease. *Expert Rev. Gastroenterology Hepatology* 10, 1041–1052. doi:10.1080/17474124.2016.1179575

Xu, H., Gong, Z., Zhou, S., Yang, S., Wang, D., Chen, X., et al. (2018). Liposomal Curcumin targeting endometrial cancer through the NF-κB pathway. *Cell Physiol. Biochem.* 48, 569–582. doi:10.1159/000491886

Xu, H., Zhang, J., Wang, Q., Li, Y., and Zhang, B. (2020). Effect of resveratrol on the expression of molecules related to the mTOR signaling pathway in endometrial cancer. *Chin. J. Birth Health Hered.* 28, 533–536+577. doi:10.13404/j.cnki.cjbhh.2020.05.003

Ye, Wenwei, Pan, Dan, and Yang, Jingjin (2020). Effects of Amygdalin on proliferation, invasion and apoptosis of endometrial cancer cells through inhibiting PI3K/Akt/mTOR pathway (China). *Zhejiang JITCWM* 30, 795–799.

Yin, W. (2016). Effects and mechanism of Shikonin on the proliferation and apoptosis of endometrial Ishikawa cancer cell (China). *Mod. J. Integr. Traditional Chin. West. Med.* 25, 3548–3551.

Yip, P. Y. (2015). Phosphatidylinositol 3-kinase-AKT-mammalian target of rapamycin (PI3K-Akt-mTOR) signaling pathway in non-small cell lung cancer. *Transl. Lung Cancer Res.* 4, 165–176. doi:10.3978/j.issn.2218-6751.2015.01.04

Yuan, Y., Long, H., Zhou, Z., Fu, Y., and Jiang, B. (2023). PI3K–AKT-Targeting breast cancer treatments: Natural products and synthetic compounds. *Biomolecules* 13, 93. doi:10.3390/biom13010093

Zhang, F., Zhang, Y.-Y., Sun, Y.-S., Ma, R.-H., Thakur, K., Zhang, J.-G., et al. (2020). Asparanin A from *Asparagus officinalis* L. Induces G0/G1 cell cycle arrest and apoptosis in human endometrial carcinoma Ishikawa cells via mitochondrial and PI3K/AKT signaling pathways. *J. Agric. Food Chem.* 68, 213–224. doi:10.1021/acs.jafc.9b07103

Zhang, S., Gong, T.-T., Liu, F.-H., Jiang, Y.-T., Sun, H., Ma, X.-X., et al. (2019a). Global, regional, and national burden of endometrial cancer, 1990–2017: Results from the global burden of disease study, 2017. *Front. Oncol.* 9, 1440. doi:10.3389/fonc.2019.01440

Zhang, S., Rao, S., Yang, M., Ma, C., Hong, F., and Yang, S. (2022). Role of mitochondrial pathways in cell apoptosis during He-patic ischemia/reperfusion injury. *Int. J. Mol. Sci.* 23, 2357. doi:10.3390/ijms23042357

Zhang, Z., Yi, P., Tu, C., Zhan, J., Jiang, L., and Zhang, F. (2019b). Curcumin inhibits ERK/c-Jun expressions and phosphorylation against endometrial carcinoma. *BioMed Res. Int.* 2019, 8912961. doi:10.1155/2019/8912961

frontiers | Frontiers in Oncology

TYPE Original Research
PUBLISHED 15 June 2023
DOI 10.3389/fonc.2023.1185715

OPEN ACCESS

EDITED BY
Pranav Kumar Prabhakar,
Lovely Professional University, India

REVIEWED BY
Hiu Chuen Lok,
The University of Sydney, Australia
Miranda Lynch,
Hauptman-Woodward Medical Research Institute, United States

*CORRESPONDENCE
Michael S. Petronek
michael-petronek@uiowa.edu
Charvann K. Bailey
baileych@grinnell.edu

RECEIVED 13 March 2023
ACCEPTED 25 May 2023
PUBLISHED 15 June 2023

CITATION
Petronek MS, Bayanbold K, Amegble K, Tomanek-Chalkley AM, Allen BG, Spitz DR and Bailey CK (2023) Evaluating the iron chelator function of sirtinol in non-small cell lung cancer.
Front. Oncol. 13:1185715.
doi: 10.3389/fonc.2023.1185715

Evaluating the iron chelator function of sirtinol in non-small cell lung cancer

Michael S. Petronek[1*], Khaliunaa Bayanbold[1], Koffi Amegble[2], Ann M. Tomanek-Chalkley[1], Bryan G. Allen[1], Douglas R. Spitz[1] and Charvann K. Bailey[2*]

[1]Department of Radiation Oncology, Division of Free Radical and Radiation Biology, University of Iowa, Iowa City, IA, United States, [2]Department of Biology, Grinnell College, Grinnell, IA, United States

A distinctive feature of cancer is the upregulation of sirtuin proteins. Sirtuins are class III NAD+-dependent deacetylases involved in cellular processes such as proliferation and protection against oxidative stress. SIRTs 1 and 2 are also overexpressed in several types of cancers including non-small cell lung cancer (NSCLC). Sirtinol, a sirtuin (SIRT) 1 and 2 specific inhibitor, is a recent anti-cancer agent that is cytotoxic against several types of cancers including NSCLC. Thus, sirtuins 1 and 2 represent valuable targets for cancer therapy. Recent studies show that sirtinol functions as a tridentate iron chelator by binding Fe3+ with 3:1 stoichiometry. However, the biological consequences of this function remain unexplored. Consistent with preliminary literature, we show that sirtinol can deplete intracellular labile iron pools in both A549 and H1299 non-small cell lung cancer cells acutely. Interestingly, a temporal adaptive response occurs in A549 cells as sirtinol enhances transferrin receptor stability and represses ferritin heavy chain translation through impaired aconitase activity and apparent IRP1 activation. This effect was not observed in H1299 cells. Holo-transferrin supplementation significantly enhanced colony formation in A549 cells while increasing sirtinol toxicity. This effect was not observed in H1299 cells. The results highlight the fundamental genetic differences that may exist between H1299 and A549 cells and offer a novel mechanism of how sirtinol kills NSCLC cells.

KEYWORDS

cancer therapy, iron metabolism, non-small cell lung cancer (NSCLC), iron, cancer biology

Introduction

Globally, lung cancer is one of the leading causes of cancer deaths. Approximately 80%–85% of all lung cancer diagnoses are non-small cell lung cancer (NSCLC), and the 5-year overall survival remains approximately 28% (1). Such a despondent figure indicates a

need for more effective treatment. Historically, treatments for cancer consisted of radiotherapy and chemotherapy, which have had limited success, treating NSCLC (2, 3). More contemporary techniques like targeted therapy allow researchers to exploit distinctive characteristics of cancer cells for more precise treatment (4). One consistent attribute of lung cancer cells is the overexpression of sirtuin 1 and 2 (SIRT1/2) proteins compared to normal human bronchial epithelial cells where enhanced SIRT1/2 expression has been correlated with a poor prognosis in NSCLC patients (5, 6). SIRTs are class III nicotinamide adenine dinucleotide $(NAD)^+$-dependent histone deacetylases that modulate senescence, cell cycle regulation, apoptosis, and oxidative stress response (7). By using NAD^+ as a cosubstrate for their modulation of histone deacetylation, targets such as H3K9ac or non-histone targets like Foxo3a and sirtuins are critical for mediating cell survival (8). Current literature reveals that targeted inhibition of SIRT1 and 2 proteins in cancer is beneficial for constraining their growth and defense mechanisms—making them more susceptible to apoptosis.

Sirtinol is a SIRT 1 and 2 pharmacological inhibitor that was discovered during cell-based screening of *Saccharomyces cerevisiae* yeast by accessing Sir2p inhibition (9). Its potent inhibition of SIRT1 and 2 and has been investigated as an anticancer agent (10). Sirtinol induces senescence and apoptosis in MCF-7 breast cancer cells and H1299 NSCLCs (11, 12). Although sirtinol is not currently a mainline therapeutic used to treat NSCLCs, several studies show its potential for use in the clinic. For example, Fong et al. showed that sirtinol is cytotoxic to NSCLC cells in a dose-dependent manner after 24 and 48 h treatment (13). This study also showed that sirtinol reduces the proliferation of cancer cells by pausing the cell in the G1 phase of the cell cycle. Sirtinol also enhances the cytotoxicity of traditional chemotherapeutic agents like gemcitabine and cisplatin (14, 15), while reducing inflammation in normal epithelial cells, suggesting selective sensitization (16).

Recently, sirtinol was also discovered to be an intracellular iron chelator (17). This observation evolved from evaluating the chemical structure of sirtinol relative to other iron-chelating molecules [*e.g.*, desferrioxamine (DFO) or deferasirox] (7). Sirtinol's structure contains a 2-hydroxynaphthalenyl moiety that is connected to a benzamide through an aldiminic nitrogen atom (Figures 1A, B). This group can provide a tridentate O – N – O donor moiety that is often observed in other iron-chelating molecules. Crystallography analysis showed that sirtinol can function as a tridentate iron chelator by binding a single Fe^{3+} atom with 3:1 (sirtinol:Fe^{3+}) stoichiometry to form an octahedral, high-spin (S = 5/2) Fe^{3+} complex comprised of five donor oxygen atoms and one donor nitrogen atom (Figure 1C) (17). This is a critical finding as iron chelation may serve as an important drug effect associated with the cytotoxicity of sirtinol. However, the biological significance of sirtinol's iron-chelator function remains unclear. Thus, it was hypothesized that sirtinol can impair iron metabolism in NSCLC cells and this study aimed to evaluate the biological significance of the chelator function of sirtinol in NSCLC.

Iron metabolism is a critical feature of a multitude of cellular functions central to cancer progression (18). It is altered in a wide array of cancer types with cancer cells typically harboring an iron dependency as compared to their normal tissue counterparts. Iron metabolism is altered in human NSCLC tumor tissue with increased hepcidin expression (19). Increased transferrin receptor (TfR) expression has also been observed in human NSCLC tumors (20). These data suggest that NSCLC tumors accumulate iron preferentially. Iron chelation therapy may be an attractive anticancer therapeutic strategy. For example, deferoxamine has recently been shown to selectively induce mitochondrial dysfunction in cancer cells (21).

In this study, A549 and H1299 NSCLC cells were used to evaluate the chelator function of sirtinol. These cells represent two widely used NSCLC *in vitro* models with varying clinically relevant genetic backgrounds (Table 1). Importantly, A549 cells harbor mutations that have been observed in aggressive lung tumors. STK11 comutations as observed in the A549 cells are relatively frequent with both KRAS (54%) and KEAP1 (27%), where STK11 comutations are associated with worse clinical outcomes (27). Thus, A549 cells provide an *in vitro* model of an aggressive NSCLC tumor.

Results

First, the proposed chelator function was evaluated in this *in vitro* NSCLC model. Consistent with this function, a 72 h treatment of sirtinol caused decrease in intracellular labile iron in both H1299 and A549 cells (Figure 2). Importantly, the decrease in labile iron by sirtinol is the same effect as observed by DFO. An interesting observation was that this effect was greater in the A549 cells (79.2%

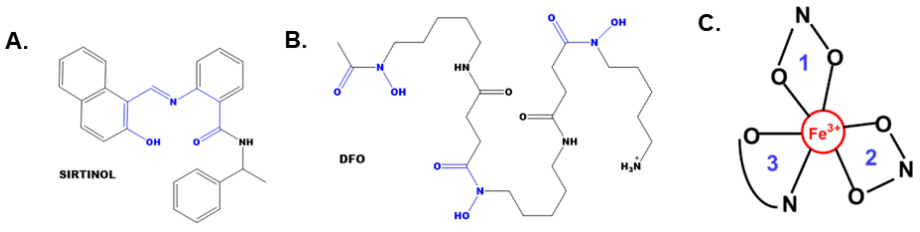

FIGURE 1
The structures of sirtinol and desferrioxamine (DFO) and its iron coordination sites. **(A, B)** The structures of sirtinol **(A)** and DFO **(B)**. The putative iron coordination site within both structures are highlighted in blue. **(C)** Tridentate, octahedral, high-spin Fe^{3+} complex formed from the binding of sirtinol to a free Fe atom. Blue numbers represent independent sirtinol molecules bound to the Fe atom.

TABLE 1 Genetic differences in cell lines used in this study.

Genetic Background (mutant frequency, %)	A549	H1299
KRAS (17%) (22)	G12S mutant (23)	Wild type
STK11 (27%) (22)	Q37 mutant (24)	Wild type
KEAP1 (15%) (25)	G333C mutant (26)	Wild type

decrease) as compared to the H1299 (36.3% decrease). Thus, we have been able to recapitulate the ability of sirtinol to serve as an iron chelator to a differential effect in these genetic subtypes of NSCLC.

Sirtinol alters iron metabolic features in non-small cell lung cancer cells

Because of the initial validation of the sirtinol iron chelator function, it was hypothesized that this would result in metabolic alterations associated with labile iron regulation. Aconitase was first interrogated as it is an iron-dependent tricarboxylic acid (TCA)-cycle intermediate that utilizes a complete $[4Fe\text{-}4S]^{2+}$ cluster for the isomerization of citrate to isocitrate (28). Under conditions of limited intracellular iron availability, the cluster will be in an incomplete $[3Fe\text{-}4S]^{+}$ form leading to enzyme inactivation (29). In both A549 and H1299 cell lines, a significant decrease in aconitase activity (>50% reduction in enzymatic activity, $p< 0.05$) was observed (Figure 3A), further indicating that sirtinol's chelator activity can sequester iron to impair the activity of iron-dependent enzymes.

Converse to its TCA-cycle function, in an inactive $[3Fe\text{-}4S]^{+}$ form, aconitase can function as iron-responsive protein-1 (IRP1). IRP1 responds to intracellular Fe levels to promote either stabilization or degradation of TfR and ferritin heavy-chain (FtH) mRNAs (30). When there is limited intracellular iron availability, IRP1 binds to iron response elements (IREs) to maintain homeostasis by binding at the 3' end of TfR mRNA to enhance stability and promote translation (31–33) or the 5' end of FtH to repress translation (34, 35). Interestingly, a sirtinol concentration–dependent increase in TfR protein levels and FtH repression cells was observed in A549 cells that was not apparent in H1299 cells (Figures 3B, C). This further supports the hypothesis that the chelator function of sirtinol disrupts iron metabolism by limiting intracellular iron availability, although the biological effects appear to present as a cell type–dependent effect. Therefore, it appears that sirtinol may be able to impair the IRP-IRE system through its chelator function; however, this requires further validation. Based on the observed iron metabolic perturbations, the temporal-dependent changes in intracellular iron were interrogated. Using this colorimetric assay, sirtinol was observed to chelate iron in both H1299 and A549 cell lines, as relative labile iron concentrations were decreased in both cell lines acutely (Figure 3D). In A549 cells, the labile iron pool was decreased acutely (within 6 h) while noticeable decreases did not occur in H1299 cells until 24 h sirtinol treatment was used. Interestingly, after the acute decrease in labile iron in A549, there was an apparent adaptive response where labile iron continued to increase above the basal level until 72 h. A similar trend was not observed in the H1299 cells as labile iron was decreased through 48 h until a slight increase from 48 to 72 h occurred but remained below the basal level. These results are consistent with the cell type–specific adaptive response that occurred in the A549 cells. These results further support the iron chelator function of sirtinol, and these observations may represent a fundamental difference in iron metabolic regulation and response to perturbations between NSCLC cell lines with variable genetic backgrounds.

Sirtinol impairs iron-dependent colony formation in A549 cells

Based upon sirtinol's induced iron-metabolic shifts, the biological relevance of these findings was interrogated by

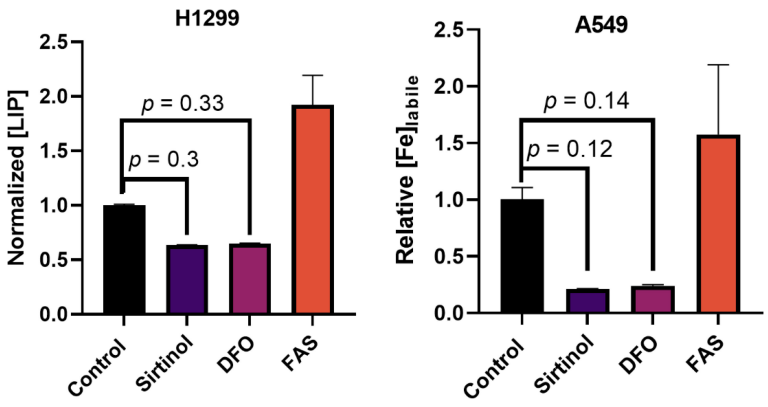

FIGURE 2
Sirtinol behaves like DFO to chelate iron in non-small cell lung cancer (NSCLC). Effects on labile iron in H1299 and A549 cells by a 50 μM 72 h treatment of sirtinol and DFO using a calcein–AM flow cytometry probe. Conversely, 3 h, 50 μM ferrous ammonium sulfate was used as a positive control. Error bars represent the mean ± SEM of $n = 3$ replicates. Statistical analysis was done using a one-way ANOVA with a *post-hoc* Tukey's test for individual comparisons.

10.3389/fonc.2023.1185715

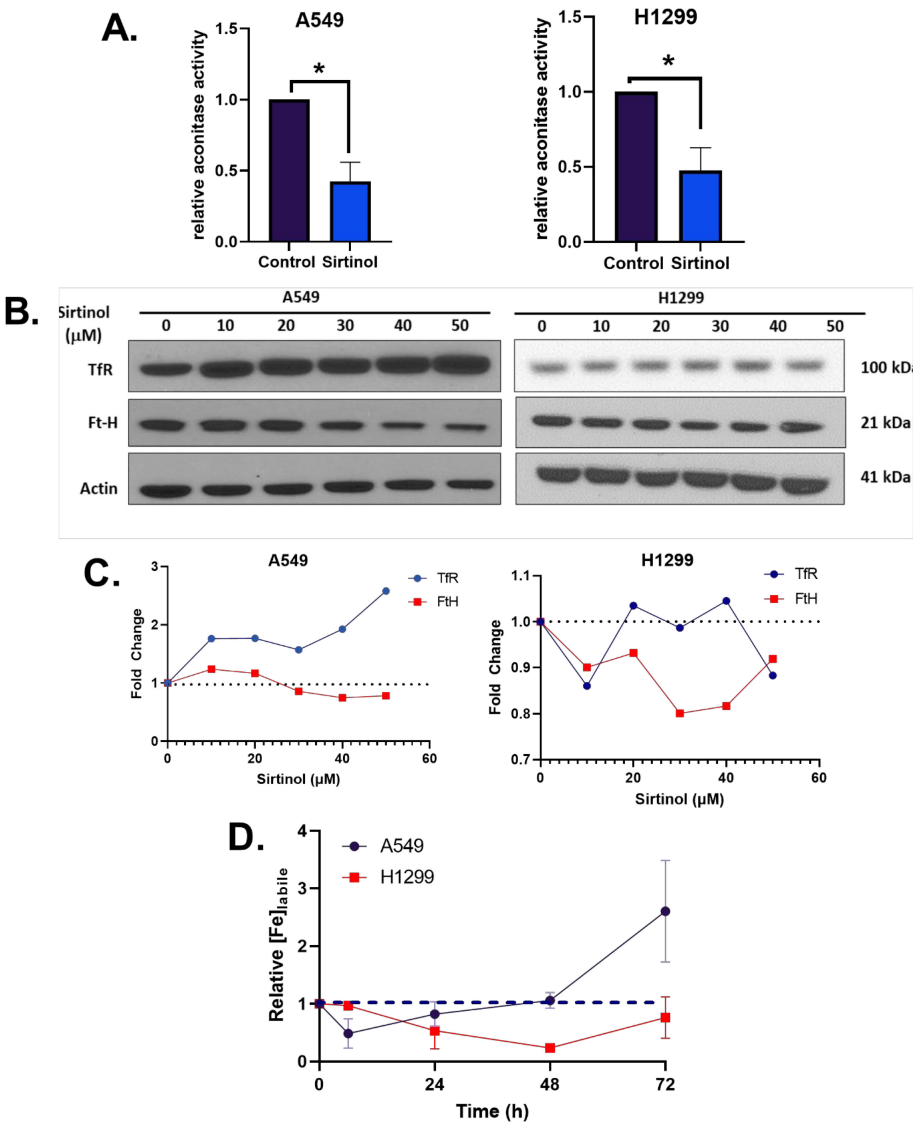

FIGURE 3
Sirtinol alters iron metabolic features. **(A)** Relative aconitase activity in A549 and H1299 cells following a 24 h treatment of 50 μM sirtinol. Aconitase activity was evaluated by measuring the rate of appearance of nicotinamide adenine dinucleotide phosphate (NADPH) at 340 nm in the presence of citrate and isocitrate dehydrogenase. Error bars represent the mean ± SEM of n = 3–4 experiments where *p< 0.05 using an unpaired, Welch's T-test. **(B)** A549 and H1299 NSCLC cells were treated for 24 h with 0–50 μM sirtinol and then harvested for evaluation of the transferrin receptor (TfR) and ferritin (FtH) expression using a Western blot approach. **(C)** Western blot quantification TfR and FtH changes in A549 and H1299 cells. **(D)** A549 and H1299 NSCLC cells were treated for 6, 24, 48, or 72 h with 50 μM sirtinol and then harvested for evaluation of labile iron pool concentrations using a colorimetric ferrozine-based assay. Each timepoint was normalized to an untreated control. Dashed black line indicates baseline measures. Error bars represent mean ± SD from triplicate measures.

investigating its effects on iron-dependent colony formation. First, the effects of holo-transferrin [hTf; di-ferric transferrin; Tf-$(Fe^{3+})_2$] on NSCLC plating efficiency were assessed. Interestingly, a significant increase in plating efficiency (40%–60%) was observed in A549 cells following a 24 h supplementation of cell culture media with hTf while there was no effect in H1299 cells (Figure 4A). Thus, A549 cells exhibit a pattern of iron dependency to facilitate colony formation, while H1299 cells do not. Similarly, sirtinol enhanced cell-killing in A549 cells supplemented with hTf but had little to no effect in H1299 cells (Figure 4B). Therefore, the chelator function of sirtinol appears to play a role in sirtinol's cytotoxicity but is largely context dependent.

Discussion

This study has shown that sirtinol can function as an intracellular iron chelator to induce iron metabolic changes. Importantly, the chelator function of sirtinol has been further validated in NSCLC cells as sirtinol exhibited the same effects on labile iron as DFO. The ability of sirtinol to deplete intracellular labile iron is consistent with the previous literature that sirtinol can function as a tridentate iron chelator (17). Furthermore, sirtinol has been observed to deplete intracellular labile iron acutely leading to an adaptive response; however, the adaptive response is cell line dependent. The adaptive response that we observed, primarily in

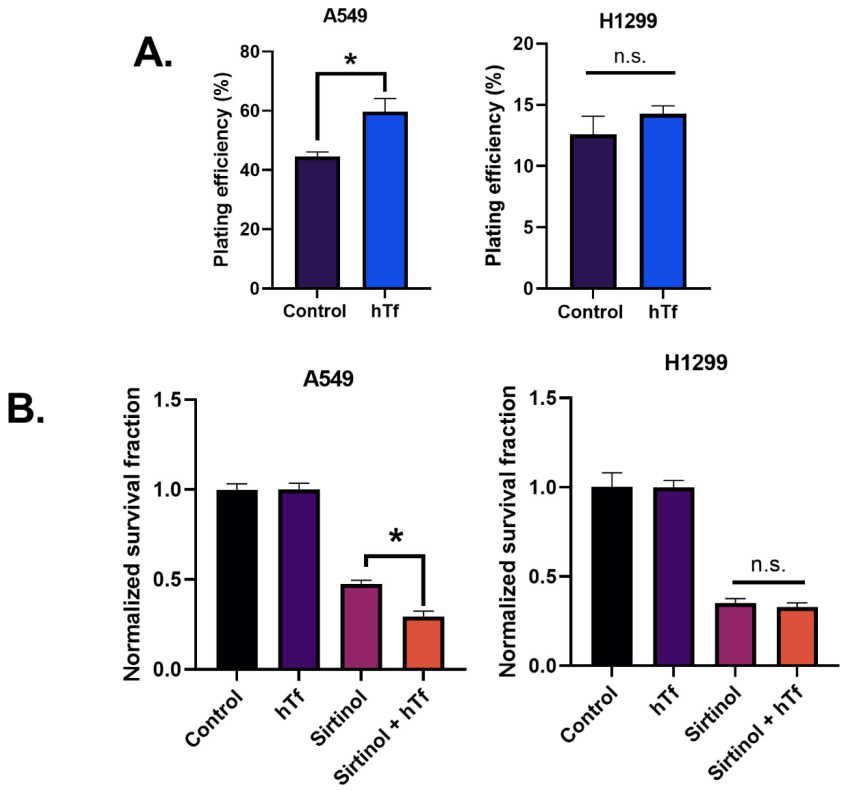

FIGURE 4
Sirtinol impairs iron-dependent colony formation in A549 cells. **(A)** Plating efficiency (%) of A549 and H1299 cells following a 24 h supplement of 200 μg ml^{-1} holo-transferrin (hTf). Error bars represent mean ± SD (n = 3) with *p< 0.05 using a paired, two-tailed Welch's T-test. **(B)** Clonogenic survival of A549 and H1299 cells treated for 24 h ± sirtinol (50 μM) ± hTf (200 μg ml^{-1}). Error bars represent mean ± SD (n = 3) with *p< 0.05 using a one-way ANOVA test.

A549 cells, is consistent with decreased aconitase activity (i.e., enhanced IRP1 activation) leading to increased TfR stability and decreased FtH translation. This is likely due to the sequestering of iron leading to an incomplete $[3Fe\text{-}4S]^{+}$ cluster in aconitase (30). Thus, it can be hypothesized that a disruption in the IRP-IRE system results in an increase in TfR stability leading to increased iron uptake *via* receptor-mediated endocytosis (36, 37). Meanwhile, the decrease in FtH expression indicates decreased iron storage capacity, as ferritin is the primary iron storage enzyme of the cell (38). Further experiments are required to elucidate the effects of sirtinol on the IRP-IRE system. However, an adaptive response to increase iron uptake and decrease storage would explain the temporally dependent increases in labile iron observed for extended sirtinol treatments in A549 cells. The increase in labile iron at 72 h observed using ferrozine is slightly contradictory to the calcein-AM results. This is likely due to the nature of each individual assay as calcein-AM can bind iron irrespective of its oxidation state but is unable to remove iron from other complexes, while ferrozine is Fe^{2+}-dependent and utilizes ascorbic acid to convert all of the iron in a highly acidic (pH ≈ 4–4.5) solution to convert all of the iron to Fe^{2+}. Thus, the ferrozine results at 72 h may be more reflective of the total iron accumulated within the cells in addition to the iron bound to sirtinol, while the calcein-AM results are more likely to reflect the amount of iron remaining to be chelated after treatment. This hypothesis is based on the notion that sirtinol iron binding permits iron recycling allowing for the iron to be reduced to Fe^{2+} under the acidic conditions. This would be consistent with previously reported literature that a sirtinol-Fe^{3+} complex can enhance oxidation of the DCFH fluorescent probe, indicating that this is a redox-active chelator capable of catalyze redox reactions (39). Based on these observations, the iron-chelator capacity of sirtinol previously described chemically appears to have biological importance and is a drug effect that should be considered when evaluating the therapeutic effects of sirtinol (17).

An unexpected discovery is the iron-dependent differences observed between A549 and H1299 NSCLC cells. Consistently, a more pronounced iron-metabolic disruption has been observed in the A549 cells throughout this study. A major, correlative difference between these two cell lines is their KRAS/STK11/KEAP-1 mutational status. A549 cells are KRAS/STK11/KEAP-1 mutant cells resulting in constitutive activation of NRF2 (40, 41) while H1299 cells are not (42). This is of particular interest because KEAP-1 mutant NSCLC cells, such as A549, are particularly aggressive and exhibit therapy resistance as patients with tumors harboring this mutational profile appear to have worse clinical outcomes (42–44). A recent retrospective study of NSCLC patients showed that KEAP-1 was a negative prognostic marker in advanced-stage (stage IIIB–IV) tumors (HR = 1.40, 95% CI: 1.23–1.61, p< 0.001, N = 4,779) (44). Therefore, strategies aimed at enhancing clinical responses in mutant tumors may be of critical

importance in managing NSCLC. Interestingly, we have observed that STK11/KRAS/KEAP-1 mutant A549 cells exhibit a pattern of iron-dependent clonogenicity that the chelator function of sirtinol can exploit while the H1299 tumors do not. While this finding is intriguing, it also represents a significant limitation of our study. Because of the concurrent mutations observed in the A549, it is currently unclear to what extent each mutation contributes to the differential iron metabolic regulation observed in these cells. Future studies should be designed to evaluate each of these mutations independently and assess their impacts on iron metabolic regulation.

Conclusions

In summary, it has been observed that the chemical iron-chelator function of sirtinol has biological consequences. It has been shown that sirtinol can chelate iron in NSCLC cells leading to a decrease in labile iron acutely and a cell line–specific adaptive response characterized by a decrease in aconitase activity leading to a shift toward IRP1 activation, enhanced TfR stability, and repressed FtH translation. Intriguingly, KRAS/STK11/KEAP-1 mutant cells exhibit iron-dependent colony formation that can be inhibited by sirtinol, which does not occur in H1299 cells. Overall, it can be concluded that the chelator function of sirtinol has context-dependent biological consequences that may contribute to its toxicity in NSCLC.

Materials and methods

Cell culture

A549 and H1299 cells were grown to 80% confluence before experimentation at 21% O_2. Cells were treated with sirtinol prepared in 50mM stocks in DMSO and stored at −80°C for the appropriate concentration and time. For iron supplementation, 10 mg ml^{-1} of human holo-transferrin (T0665 Sigma-Aldrich, St. Louis, MO) prepared in H_2O was added directly to the cell culture media at a concentration of 200 μg ml^{-1}. For experiments testing the combination, both sirtinol and holo-transferrin were added simultaneously. For colony formation assays, cells were treated, washed, and trypsinized. Following trypsinization, cells were counted and plated as single cells in a 6-well dish (≈500 cells per well). Cells were left undisturbed for 7–10 days to allow for colony formation. Colonies were then washed with 70% EtOH for fixation and stained with Coomassie blue. Stained colonies (≥50 cells) were counted under a microscope.

Labile iron pool measures with flow cytometry

Intracellular labile iron pool measures were performed using a Calcein-AM fluorescent dye. Cells were harvested by trypsinization. After cell harvesting, cell pellets were washed in phosphate buffered saline (PBS) and then resuspended in 500 nM Calcein-AM diluted in PBS. Samples were incubated for 15 min at 4% O_2 (37°C, 5% CO_2). Following incubation, extracellular Calcein-AM was removed by washing with PBS, and cells were resuspended in 1 ml PBS. Following incubation 10,000 cells were analyzed on an LSR II Flow Cytometer (BD Biosciences; λ_{ex} = 488 nm, λ_{em} = 515/20 nm). The labile iron pool was quantified using the following formula:

$$\text{relative LIP (A . U .)} = \left(\frac{MFI_{treatment}}{MFI_{control}}\right)^{-1}$$

An inverse normalization was done to approximate the labile iron pool because calcein-AM functions as a "turn-off" probe.

Colorimetric labile iron assay

Labile iron and total iron concentrations were done using a ferrozine-based colorimetric assay. Cells were homogenized in 1X RIPA lysis buffer (Sigma-Aldrich; R0278). Cells were centrifuged at maximum speed for 10 min to remove cell debris, and 100 μl of the supernatant was then diluted 1:1 in ferrozine buffer (5 mM ferrozine, 1.25 M ammonium acetate, and 10 mM ascorbate) and centrifuged again at maximum speed for 10 min to remove any protein aggregates. This step is critical as the acidic nature of the buffer (pH ≈ 4–4.5) will result in protein aggregation that can cause the samples to become cloudy and alter the absorbance profile, resulting in an experimental artifact. Thus, samples with remaining protein aggregates were removed from analysis. The supernatant was then placed in a single well of a clear 96-well plate. Following dilution, the 96-well plate was evaluated for the formation of a Fe2+-ferrozine complex by monitoring the absorbance at 562 nm and Fe concentration was calculated using Beer's Law:

$$A_{562}(\text{A . U . }) = \epsilon_{562} * [\text{Fe}] * \text{L}$$

where A_{562} is the measured absorbance at 562 nm, ϵ562 is the molar extinction coefficient for a Fe^{2+}-ferrozine complex = 27,900 M^{-1} cm^{-1}, [Fe] is the calculated Fe concentration (M), and L is the pathlength for 200 μl of liquid ≈ 0.55 cm.

Western blotting

Total protein (25 μg) was electrophoresed on a 4%–20% gradient gel (Bio-Rad) at 150 V for approximately 1.5 h. The separated proteins were transferred onto polyvinylidene difluoride (PVDF) membranes (Millipore, Billerica, CA) and non-specific binding was blocked using 5% non-fat dry milk in PBS-Tween (0.2%) for 1 h at room temperature. The membranes were incubated with primary antibodies (ferritin-heavy chain, 1:1,000 from Abcam, Cambridge, MA, TfR, 1:1,000, Invitrogen, Camarillo, CA) at 4°C overnight. B-actin served as a loading control (1:4,000; Sigma-Aldrich). Following three 5 min TBS-Tween washes, the membranes were probed with secondary antibodies (mouse anti-rabbit; 1:10,000; Sigma-Aldrich, St. Louis, MO) that were

conjugated with horseradish peroxidase for 45 min. The washed membranes were incubated with a Super Signal West Pico Chemiluminescent Substrate (Thermo Scientific, Rockford, IL) and exposed to CareStream BioMax MR Film (CareStream Health, Rochester, NY). Quantification of Western blots were performed in ImageJ.

Aconitase activity

Exponentially growing cells were scraped and frozen as dry pellets until assayed for total aconitase activity adapted from as previously described (45). Briefly, cell pellets were resuspended in 50 mM Tris-HCl, pH 7.4 with 0.6 mM $MnCl_2$, and 5 mM Na-citrate and sonicated 3 × 10 s each. Protein was quantified by the Lowry method (46). Aconitase activity was measured as the rate of appearance of NADPH (at 340 nm; Beckman DU 800 spectrophotometer, Brea, CA) for 45 min during the reaction of 200 µg total sample protein with 200 µM NADP+ and 10 U isocitrate dehydrogenase.

Data availability statement

The original contributions presented in the study are included in the article/supplementary material. Further inquiries can be directed to the corresponding authors.

Author contributions

MP and CB performed study designs; MP, CB, KB, KA, and AT-C performed experiments; MP, CB, KB, KA, AT-C, BA, and DS performed data analysis; MP and CB prepared the manuscript; MP, CB, KB, KA, AT-C, BA, and DS contributed to editing. All authors contributed to the article and approved the submitted version.

Funding

This work was supported by NIH grants, P01 CA217797, P01 CA244091, and the Gateway for Cancer Research grant G-17-1500. Core facilities were supported in part by the Carver College of Medicine and the Holden Comprehensive Cancer Center, NIH P30 CA086862.

Conflict of interest

The authors declare that the research was conducted in the absence of any commercial or financial relationships that could be construed as a potential conflict of interest.

Publisher's note

All claims expressed in this article are solely those of the authors and do not necessarily represent those of their affiliated organizations, or those of the publisher, the editors and the reviewers. Any product that may be evaluated in this article, or claim that may be made by its manufacturer, is not guaranteed or endorsed by the publisher.

Author disclaimer

The content is solely the responsibility of the authors and does not represent the views of the National Institutes of Health.

References

1. Siegel RL, Miller KD, Wagle NS, Jemal A. Cancer statistics, 2023. *CA: A Cancer J Clin* (2023) 73:17–48. doi: 10.3322/caac.21763

2. Parashar B, Arora S, Wernicke A. Radiation therapy for early stage lung cancer. *Semin interventional Radiol* (2013) 30:185–90. doi: 10.1055/s-0033-1342960

3. Zhang J-G, Hong D-F, Zhang C-W, Sun X-D, Wang Z-F, Shi Y, et al. SIRT1 facilitates chemoresistance of pancreatic cancer cells by regulating adaptive response to chemotherapy-induced stress. *Cancer Sci* (2014) 105(4):445–54. doi: 10.1111/cas.12364

4. Reyes-Habito C, Roh E. Cutaneous reactions to chemotherapeutic drugs and targeted therapy for cancer: part II. targeted therapy. *J Am Acad Dermatol* (2014) 71:217.e1–217.e11. doi: 10.1016/j.jaad.2014.04.013

5. Zheng M, Hu C, Wu M, Chin Y. Emerging role of SIRT2 in non-small cell lung cancer (Review). *Oncol Lett* (2021) 22:731. doi: 10.3892/ol.2021.12992

6. Grbesa I, Pajares MJ, Martínez-Terroba E, Agorreta J, Mikecin A-M, Larráyoz M, et al. Expression of sirtuin 1 and 2 is associated with poor prognosis in non-small cell lung cancer patients. *PloS One* (2015) 10:e0124670. doi: 10.1371/journal.pone.0124670

7. Chalkiadaki A, Guarente L. The multifaceted functions of sirtuins in cancer. *Nat Rev Cancer* (2015) 15:608–24. doi: 10.1038/nrc3985

8. Wang F, Chan C-H, Chen K, Guan X, Lin H-K, Tong Q, et al. Deacetylation of FOXO3 by SIRT1 or SIRT2 leads to Skp2-mediated FOXO3 ubiquitination and degradation. *Oncogene* (2012) 31:1546–57. doi: 10.1038/onc.2011.347

9. Bedalov A, Chowdhury S, Simon JA. Chapter nine - biology, chemistry, and pharmacology of sirtuins. In: Marmorstein R, editor. *Enzymes of Epigenetics, Part B*, Methods in Enzymology, vol. 574 . Academic Press (2016). p. 183–211.

10. Hu J, Jing H, Lin H. Sirtuin inhibitors as anticancer agents. *Future Medicinal Chem* (2014) 6:945–66. doi: 10.4155/fmc.14.44

11. Wang J, Kim T-H, Ahn MY, Lee J, Jung JH, Choi WS, et al. Sirtinol, a class III HDAC inhibitor, induces apoptotic and autophagic cell death in MCF-7 human breast cancer cells. *Int J Oncol* (2012) 41:1101–9. doi: 10.3892/ijo.2012.1534

12. Ota H, Tokunaga E, Chang K, Hikasa M, Iijima K, Eto M, et al. Sirt1 inhibitor, sirtinol, induces senescence-like growth arrest with attenuated ras–MAPK signaling in human cancer cells. *Oncogene* (2006) 25:176–85. doi: 10.1038/sj.onc.1209049

13. Fong Y, Lin Y-C, Wu C-Y, Wang H-MD, Lin L-L, Chou HL, et al. The antiproliferative and apoptotic effects of sirtinol, a sirtuin inhibitor on human lung cancer cells by modulating akt/β-Catenin-Foxo3A axis. *Sci World J* (2014) 2014:937051. doi: 10.1155/2014/937051

14. Jin KL, Park J-Y, Noh EJ, Hoe KL, Lee JH, Kim J-H, et al. The effect of combined treatment with cisplatin and histone deacetylase inhibitors on HeLa cells. *J Gynecol Oncol* (2010) 21:262–8. doi: 10.3802/jgo.2010.21.4.262

15. Gong D-J, Zhang J-M, Yu M, Zhuang B, Guo Q-Q. Inhibition of SIRTI combined with gemcitabine therapy for pancreatic carcinoma. *Clin Interventions Aging* (2013) 8:889–97. doi: 10.2147/CIA.S45064

16. Orecchia A, Scarponi C, Di Felice F, Cesarini E, Avitabile S, Mai A, et al. Sirtinol treatment reduces inflammation in human dermal microvascular endothelial cells. *PloS One* (2011) 6:e24307. doi: 10.1371/journal.pone.0024307

17. Gautam R, Akam EA, Astashkin AV, Loughrey JJ, Tomat E. Sirtuin inhibitor sirtinol is an intracellular iron chelator. *Chem Commun* (2015) 51:5104–7. doi: 10.1039/C5CC00829H

18. Petronek MS, Spitz DR, Buettner GR, Allen BG. Linking cancer metabolic dysfunction and genetic instability through the lens of iron metabolism. *Cancers (Basel)* (2019) 11:1077. doi: 10.3390/cancers11081077

19. Chen Q, Wang L, Ma Y, Wu X, Jin L, Yu F, et al. Increased hepcidin expression in non-small cell lung cancer tissue and serum is associated with clinical stage. *Thorac Cancer* (2014) 5:14–24. doi: 10.1111/1759-7714.12046

20. Kukulj S, Jaganjac M, Boranic M, Krizanac S, Santic Z, Poljak-Blazi M, et al. Altered iron metabolism, inflammation, transferrin receptors, and ferritin expression in non-small-cell lung cancer. *Med Oncol* (2010) 27:268–77. doi: 10.1007/s12032-009-9203-2

21. Sandoval-Acuña C, Torrealba N, Tomkova V, Jadhav SB, Blazkova K, Merta L, et al. Targeting mitochondrial iron metabolism suppresses tumor growth and metastasis by inducing mitochondrial dysfunction and mitophagy. *Cancer Res* (2021) 81:2289–303. doi: 10.1158/0008-5472.CAN-20-1628

22. Blanco R, Iwakawa R, Tang M, Kohno T, Angulo B, Pio R, et al. A gene-alteration profile of human lung cancer cell lines. *Hum Mutat* (2009) 30:1199–206. doi: 10.1002/humu.21028

23. Acunzo M, Romano G, Nigita G, Veneziano D, Fattore L, Laganà A, et al. Selective targeting of point-mutated KRAS through artificial microRNAs. *Proc Natl Acad Sci U.S.A.* (2017) 114:E4203–12. doi: 10.1073/pnas.1620562114

24. Matsumoto S, Iwakawa R, Takahashi K, Kohno T, Nakanishi Y, Matsuno Y, et al. Prevalence and specificity of LKB1 genetic alterations in lung cancers. *Oncogene* (2007) 26:5911–8. doi: 10.1038/sj.onc.1210418

25. Chen X, Su C, Ren S, Zhou C, Jiang T. Pan-cancer analysis of KEAP1 mutations as biomarkers for immunotherapy outcomes. *Ann Trans Med* (2019) 8(4):141. doi: 10.21037/atm.2019.11.52

26. Taguchi K, Yamamoto M. The KEAP1-NRF2 system in cancer. *Front Oncol* (2017) 7:85. doi: 10.3389/fonc.2017.00085

27. Malhotra J, Ryan B, Patel M, Chan N, Guo Y, Aisner J, et al. Clinical outcomes and immune phenotypes associated with STK11 co-occurring mutations in non-small cell lung cancer. *J Thorac Dis* (2022) 14(6):1772–83. doi: 10.21037/jtd-21-1377

28. Lushchak OV, Piroddi M, Galli F, Lushchak VI. Aconitase post-translational modification as a key in linkage between Krebs cycle, iron homeostasis, redox signaling, and metabolism of reactive oxygen species. *null* (2014) 19:8–15. doi: 10.1179/1351000213Y.0000000073

29. Volz K. The functional duality of iron regulatory protein 1. *Curr Opin Struct Biol* (2008) 18:106–11. doi: 10.1016/j.sbi.2007.12.010

30. Casey JL, Hentze MW, Koeller DM, Caughman SW, Rouault TA, Klausner RD, et al. Iron-responsive elements: regulatory RNA sequences that control mRNA levels and translation. *Science* (1988) 240:924–8. doi: 10.1126/science.2452485

31. Erlitzki R, Long JC, Theil EC. Multiple, conserved iron-responsive elements in the 3′-untranslated region of transferrin receptor mRNA enhance binding of iron regulatory protein 2 *. *J Biol Chem* (2002) 277:42579–87. doi: 10.1074/jbc.M207918200

32. Müllner EW. & kühn, l. c. a stem-loop in the 3′ untranslated region mediates iron-dependent regulation of transferrin receptor mRNA stability in the cytoplasm. *Cell* (1988) 53:815–25. doi: 10.1016/0092-8674(88)90098-0

33. Casey JL, Koeller DM, Ramin VC, Klausner RD, Harford JB. Iron regulation of transferrin receptor mRNA levels requires iron-responsive elements and a rapid turnover determinant in the 3′ untranslated region of the mRNA. *EMBO J* (1989) 8:3693–9. doi: 10.1002/j.1460-2075.1989.tb08544.x

34. Hentze Matthias W, Caughman SW, Rouault TA, Barriocanal JG, Dancis A, Harford JB, et al. Identification of the iron-responsive element for the translational regulation of human ferritin mRNA. *Science* (1987) 238:1570–3. doi: 10.1126/science.3685996

35. Leibold EA, Munro HN. Cytoplasmic protein binds *in vitro* to a highly conserved sequence in the 5' untranslated region of ferritin heavy- and light-subunit mRNAs. *Proc Natl Acad Sci USA* (1988) 85:2171. doi: 10.1073/pnas.85.7.2171

36. Hentze MW, Muckenthaler MU, Andrews NC. Balancing acts: molecular control of mammalian iron metabolism. *Cell* (2004) 117:285–97. doi: 10.1016/S0092-8674(04)00343-5

37. Gammella E, Buratti P, Cairo G, Recalcati S. The transferrin receptor: the cellular iron gate. *Metallomics* (2017) 9:1367–75. doi: 10.1039/C7MT00143F

38. Harrison PM, Arosio P. The ferritins: molecular properties, iron storage function and cellular regulation. *Biochim Biophys Acta (BBA) - Bioenergetics* (1996) 1275:161–203. doi: 10.1016/0005-2728(96)00022-9

39. Akam EA, Gautam R, Tomat E. Metal-binding effects of sirtuin inhibitor sirtinol. *Supramol Chem* (2016) 28:108–16. doi: 10.1080/10610278.2015.1092537

40. Singh A, Misra V, Thimmulappa RK, Lee H, Ames S, Hoque MO, et al. Dysfunctional KEAP1–NRF2 interaction in non-Small-Cell lung cancer. *PloS Med* (2006) 3:e420. doi: 10.1371/journal.pmed.0030420

41. Taguchi K, Yamamoto M. The KEAP1–NRF2 system in cancer. *Front Oncol* (2017) 7. doi: 10.3389/fonc.2017.00085

42. Gong M, Li Y, Ye X, Zhang L, Wang Z, Xu X, et al. Loss-of-function mutations in KEAP1 drive lung cancer progression via KEAP1/NRF2 pathway activation. *Cell Communication Signaling* (2020) 18:98. doi: 10.1186/s12964-020-00568-z

43. Vollrath V, Wielandt AM, Iruretagoyena M, Chianale J. Role of Nrf2 in the regulation of the Mrp2 (ABCC2) gene. *Biochem J* (2006) 395:599–609. doi: 10.1042/BJ20051518

44. Saleh MM, Scheffler M, Merkelbach-Bruse S, Scheel AH, Ulmer B, Wolf J, et al. Comprehensive analysis of TP53 and KEAP1 mutations and their impact on survival in localized- and advanced-stage NSCLC. *J Thorac Oncol* (2022) 17:76–88. doi: 10.1016/j.jtho.2021.08.764

45. Case AJ, McGill JL, Tygrett LT, Shirasawa T, Spitz DR, Waldschmidt TJ, et al. Elevated mitochondrial superoxide disrupts normal T cell development, impairing adaptive immune responses to an influenza challenge. *Free Radic Biol Med* (2011) 50:448–58. doi: 10.1016/j.freeradbiomed.2010.11.025

46. Lowry OH, Rosebrough NJ, Farr AL, Randall RJ. PROTEIN MEASUREMENT WITH THE FOLIN PHENOL REAGENT. *J Biol Chem* (1951) 193:265–75. doi: 10.1016/S0021-9258(19)52451-6

frontiers | Frontiers in Pharmacology

TYPE Review
PUBLISHED 02 August 2023
DOI 10.3389/fphar.2023.1230822

OPEN ACCESS

EDITED BY
Ayaz Shahid,
Western University of Health Sciences, United States

REVIEWED BY
Pengcheng Wang,
Capital Medical University, China
Mohammad Ashhar I. Khan,
University of North Carolina at Chapel Hill, United States

*CORRESPONDENCE
Xiaofeng Yu,
yanke110112@163.com

RECEIVED 29 May 2023
ACCEPTED 20 July 2023
PUBLISHED 02 August 2023

CITATION
Zhang X and Yu X (2023), Crosstalk between Wnt/β-catenin signaling pathway and DNA damage response in cancer: a new direction for overcoming therapy resistance.
Front. Pharmacol. 14:1230822.
doi: 10.3389/fphar.2023.1230822

Crosstalk between Wnt/β-catenin signaling pathway and DNA damage response in cancer: a new direction for overcoming therapy resistance

Xixia Zhang and Xiaofeng Yu*

Department of Otolaryngology Head and Neck Surgery, Shengjing Hospital of China Medical University, Shenyang, China

Wnt signaling plays an important role in regulating the biological behavior of cancers, and many drugs targeting this signaling have been developed. Recently, a series of research have revealed that Wnt signaling could regulate DNA damage response (DDR) which is crucial for maintaining the genomic integrity in cells and closely related to cancer genome instability. Many drugs have been developed to target DNA damage response in cancers. Notably, different components of the Wnt and DDR pathways are involved in crosstalk, forming a complex regulatory network and providing new opportunities for cancer therapy. Here, we provide a brief overview of Wnt signaling and DDR in the field of cancer research and review the interactions between these two pathways. Finally, we also discuss the possibility of therapeutic agents targeting Wnt and DDR as potential cancer treatment strategies.

KEYWORDS

Wnt, DNA damage response, cancer, therapy, drug resistance

1 Introduction

The Wnt signaling pathway is a complex protein regulatory network cascade, which participates in various biological processes, including embryonic development, tissue development and regeneration, and cancer development and progression. The abnormal activation of Wnt signaling will result in many pathological processes, such as cancer, inflammatory and immune diseases, and metabolic diseases (Clevers and Nusse, 2012; Nusse and Clevers, 2017).

DNA damage response (DDR) is a hierarchical signaling pathway that functions to maintain the genome integrity and stability and is coordinated by a variety of proteins. Numerous studies have demonstrated that DDR deficiency is closely associated with several diseases (Jackson and Bartek, 2009; Ciccia and Elledge, 2010; Lee and Paull, 2021; Stoof et al., 2021; Ye et al., 2021), among which cancer has become a focus of research. DDR has been extensively involved in regulation of cell senescence, carcinogenesis, and cancer progression as well as influencing the efficacy of cancer radiotherapy and chemotherapy. As the majority of anti-tumor therapies primarily target the genomic DNA of cancer cells, enhancement of DDR is closely related to their therapeutic efficacy (Lord and Ashworth, 2012; Su et al., 2023; Traphagen et al., 2023).

Previous studies have reported that Wnt signaling can affect DDR by regulating a variety of factors (Lento et al., 2014; Tao et al., 2015; Liang et al., 2018). In this review, we first introduce the Wnt/β-catenin and DDR signaling pathways and focus on the role of signaling in the regulation of DDR. Wnt/β-catenin pathway and DDR pathway members are potential therapeutic targets for many types of cancer (Lord and Ashworth, 2012; Krishnamurthy and Kurzrock, 2018; Pilié et al., 2019; Wang et al., 2021a). Could this possibly shed new light on clinical decision-making? We describe the molecular mechanisms and associations of the Wnt and DDR pathways with the biological processes involved in cancer and the treatment of cancer and their potential impact on the development of new treatment regimens.

2 Wnt signaling pathway

The Wnt signaling can be activated through the binding of Wnt family member ligand to the membrane receptors like Frizzled (FZD) family receptors, low-density lipoprotein receptor-related protein 5/6 (LRP5/6), and receptor tyrosine kinase-like orphan receptors (ROR1/2). Wnt signaling activation leads to transcriptional activation of multiple downstream effectors (Clevers and Nusse, 2012), and extracellular signals are transmitted through this pathway into the cell via activation of the intracellular segments of receptors on the cell surface, which in turn activates β-catenin-dependent or -independent Wnt signaling cascades. There are several separate Wnt pathways which can engage in crosstalk with one another; these have been summarized as canonical (β-catenin-dependent) and non-canonical signaling (Wnt/Ca^{2+} (calcium) pathway and Wnt/PCP (planar cell polarity) pathway) pathways (Figure 1). Generally, the canonical Wnt signaling pathway mainly participates in regulating progenitor cell self-renewal, proliferation, or differentiation, while the non-canonical signaling pathway is primarily responsible for the maintenance of cell stemness, cell motility, or antagonism of the canonical pathway (Fodde and Brabletz, 2007; Clevers and Nusse, 2012; Nusse and Clevers, 2017).

2.1 The canonical Wnt/β-catenin pathway

The key members of the canonical Wnt signaling pathway include the Wnt family proteins, FZD/LRP6, disheveled protein (Dvl), β-catenin, T lymphocytokine/lymphoenhancer factor (TCF), human lymphoid enhancer factor (LEF), and the β-catenin destruction complex which comprises adenomatous polyposis coli (APC), axin, glycogen synthase kinase-3β (GSK-3β), and casein kinase 1α (CK1α). In the absence of a Wnt signal, β-catenin binds to the destruction complex, resulting in its ubiquitination via proteasomal degradation mediated by β-TrCP. In the presence of Wnt signal, Wnt binds to the FZD and LRP5/6 receptors to activate Dvl protein and inhibit the destruction complex, resulting in the accumulation of free unphosphorylated β-catenin in the cytoplasm, which is then transported to the nucleus where it can combine with TCF/LEF to induce transcription of downstream Wnt signaling genes (Clevers and Nusse, 2012; Nusse and Clevers, 2017).

2.2 The non-canonical Wnt pathway

2.2.1 The Wnt/Ca^{2+} pathway

The Wnt proteins could bind to the FZD receptors on the cell transmembrane and participate in several cellular processes that are involved in stimulating the isotrimer G protein to further activate PLC. PLC activation could result in elevated release of intracellular Ca^{2+}, reduced cyclic guanosine (cGMP) levels, and activation of Ca^{2+}/calmodulin-dependent protein kinase-II (CaMKII) and PKC; these processes can stimulate NFAT and other transcription factors such as CREB1 (De, 2011).

2.2.2 Wnt/PCP signaling

In Wnt/PCP signaling (Wang et al., 2021a), PCP mainly regulates cell movement direction and cell morphology. Wnt ligands bind to the ROR–FZD receptor complex to recruit and activate Dvl which binds to the small GTPase Rho. Then, the small GTPase Rac1 and Rho together trigger ROCK (Rho kinase) and JNK, thereby contributing to the regulation of cytoskeletal and transcriptional responses.

3 DDR regulators and signaling pathways

Under physiological conditions, DNA damage can be caused by various environmental stimuli and intracellular stress. After suffering DNA damage, cells can have three possible fates: recovering to the normal physiological state, initiation of apoptosis, or survival with damage. Through various regulatory pathways, cells can efficiently recognize DNA damage lesions, activate the DDR, and initiate the corresponding repair mechanism. The DDR involves a series of complex and elaborate regulatory events, including the identification of lesions, activation of checkpoints, remodeling of chromatin, DNA damage repair, cell cycle arrest, and apoptosis.

The DNA repair pathways vary in response to different types of DNA damage, which can be classified as follows: base excision repair (BER), nucleotide excision repair (NER), mismatch repair (MMR), homologous recombination (HR; where another nucleotide chain is required as a repair template), and non-homologous end-joining (NHEJ, where the broken ends are directly connected to the DNA strand). HR and NHEJ are the main repair ways for double-strand breaks (DSBs). HR always occurs in G2 and S phases, during which sister chromatids are present and can provide a template strand, while NHEJ is cell cycle phase-independent. For eukaryotes, NHEJ repairs most DSBs, and HR is preferentially used when the lesion occurs at DNA replication forks.

DDR is majorly regulated by two protein families: the phosphatidylinositol 3-kinase-like protein kinase (PIKK) family (including ATM, ATR, and DNA-PK) and the 16-member poly (ADP) ribose polymerase (PARP) family. Generally speaking, ATM, ATR, DNA-PK, and PARP mainly function as sensors for DNA damage. ATM is recruited by the MRN (MRE11/RAD50/NBS1) complex following recognition of DSBs (Rupnik et al., 2010; Blackford and Jackson, 2017), and ATM is the kinase typically responsible for modulation of cellular responses to DSBs, which comprise DNA repair, checkpoint activation, apoptosis, senescence,

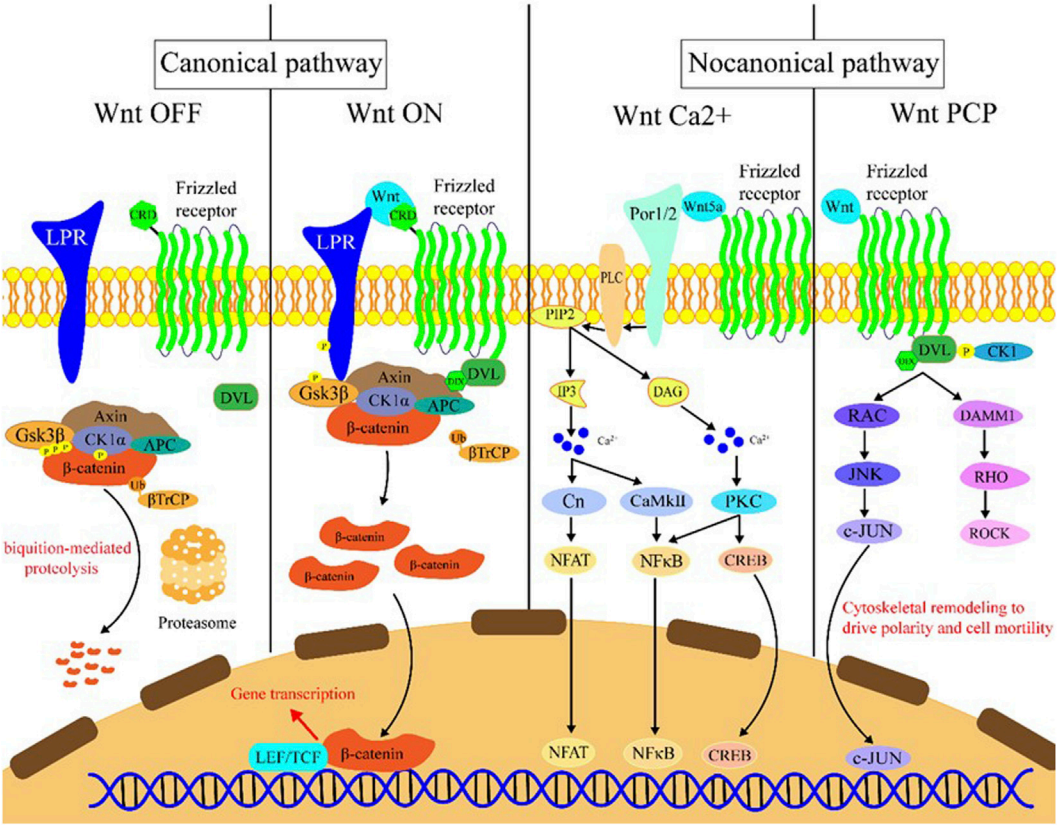

FIGURE 1
Introduction of the Wnt signaling pathway. Wnt OFF: In the absence of Wnt ligand, β-catenin binds to the destruction complex which comprises AXIN, CK1α, GSK-3β, and APC. Subsequently, a series of phosphorylation events occur to create a docking site on β-catenin for β-TrCP, and then β-catenin is ubiquitinated by β-TrCP and subjected to ubiquitin-proteasomal degradation. Wnt ON: In the presence of Wnt ligands, Frizzled receptors and the co-receptors LRP5/6 multimerize at the cell surface. This leads to recruitment of the cytoplasmic protein Dvl to the cell membrane by interacting with cytoplasmic domains of Frizzled receptors. The Frizzled-bound Dvl recruits the destruction complex through Dvl and axin, GSK-3β in the destruction complex initiates phosphorylation of the LRP5/6 and subsequent phosphorylation by CK1s, and more destruction complexes are recruited to the cell membrane that further phosphorylate LRP5/6 as a positive feedback loop. Wnt Ca^{2+}: Wnt/Frizzled ligand receptor interaction with the participating co-receptor ROR1/2 leads to the activation of PLC and then hydrolyzes PIP2 into products IP3 and DAG. IP3 causes the release of Ca^{2+} from the endoplasmic reticulum, and two kinases CaMKII and Cn are activated, which in turn activate NFAT and NF-κB. DAG is activated by released calcium from the endoplasmic reticulum. Subsequently, PKC is activated which then activates NF-κB and CREB. These factors translocate to the nucleus where downstream gene expression is regulated. Wnt PCP: In the planar cell polarity pathway, after binding to Frizzled receptors and recruiting Dvl, which forms a complex with DAAM1, Wnt then activates the small GTPase Rho, which in turn activates ROCK. Alternatively, Dvl could also form a complex with RAC to activate JNK and then increase JNK-dependent c-JUN transcription activity.

and alterations in the chromatin structure (Shiloh and Ziv, 2013; Blackford and Jackson, 2017). ATR is recruited by 9-1-1 (RAD9–RAD1–HUS1) complex to extend tracts of ssDNA (Blackford and Jackson, 2017). ATR is the DNA replication stress response kinase which could phosphorylate numerous substrates under the stimulation of genotoxic stresses. Following detection of DSBs, DNA-PK is recruited by Ku to initiate NHEJ (Graham et al., 2016). Among PARP family proteins, the structure and function of PARP-1 have been well elucidated by researchers. PARP plays a multifaceted role in cellular response to DNA damage. For example, PARP acts as a sensor in DDR that catalyzes the addition of poly (ADP-ribose) chains to histones and other nuclear proteins to recruit DDR factors to chromatin at breakpoints (Amé et al., 2004). PARP could also cause chromatin remodeling and recruit DNA-repair-associated proteins (Haince et al., 2008). In Figure 2, we summarize the DDR processes involving these different sensors, namely, ATM, ATR, DNA-PK, and PARP.

The downstream effects of these repair processes involve activation of various substrates to elicit appropriate responses involved in cell fate determination. These downstream effectors include H2AX, CHK1, CHK2, and p53, among others. H2AX is phosphorylated to form γH2AX, which is one of the earliest events in DDR. γH2AX not only generates a signaling cascade to amplify the signal of DDR and recruits the DDR proteins but also regulates chromatin relaxation (Rogakou et al., 1998). CHK1 and CHK2, coordinating DDR by arresting the cell cycle (Abraham, 2001), can phosphorylate p53 at Ser20 (Bode and Dong, 2004). P53 plays an important role in activating repair proteins to promote DNA repair, arresting the cell cycle in G1/S to provide ample time to repair damage, and initiating apoptosis to prevent abnormal genetic information from dividing and growing if the damage proves to be irreparable (Shiloh and Ziv, 2013; Li et al., 2016). Several characteristics of p53 are particularly notable. In the normal physiological state, p53 is presented at low levels in cells because of proteasome-mediated degradation, which is closely related to complex

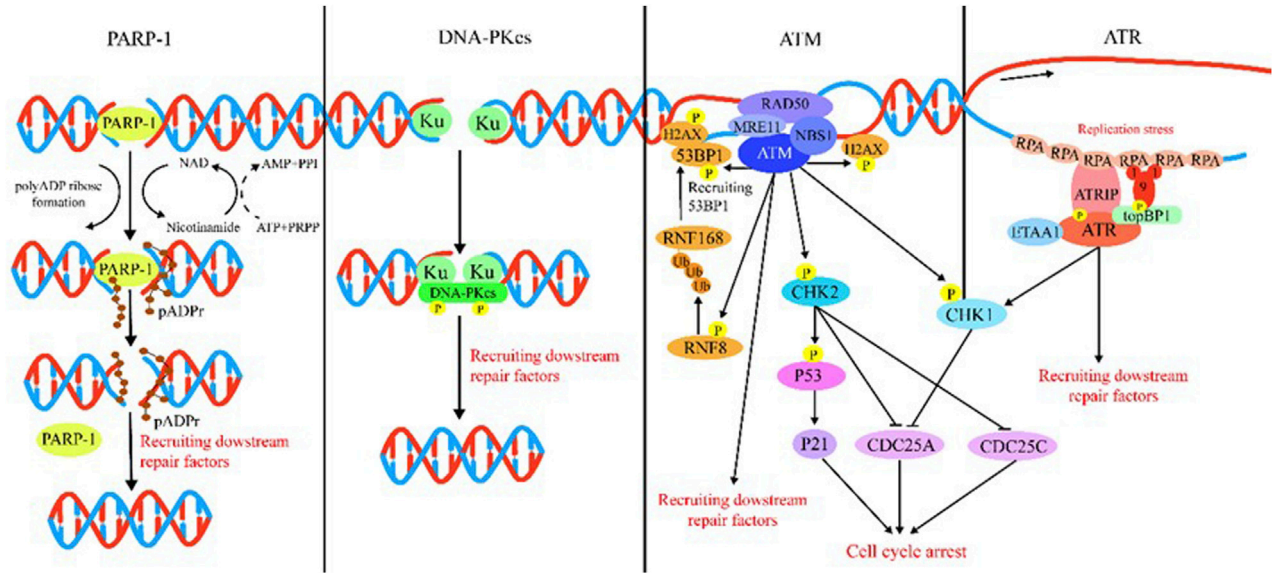

FIGURE 2
Introduction of DDR. PARP-1: PARP-1 detects and binds to damaged DNA and subsequently synthesizes poly (ADP) ribose (pADPr) on acceptor proteins. The high-density negative charge of pADPr gradually accumulates, leading to PARP-1 release from DNA simultaneously with the recruitment of DNA repair protein complex. Lastly, after the DNA break is repaired, the repair complex is dissociated from DNA and poly (ADP-ribose) glycohydrolase (PARG), and ADP-ribose hydrolase 3 (ARH3) hydrolyzes pADPr into ADP-ribose molecules and free pADPr. DNA-PKcs: DSBs are rapidly bound by the Ku heterodimer (Ku70 and Ku80) and loads onto DSB ends. Within seconds, Ku loads and activates DNA-PKcs to initiate NHEJ. Additional NHEJ core factors are subsequently recruited for the ends to be closely aligned and ligated. ATM: The MRN complex recruits ATM to DNA lesions and stimulates ATM kinase activity in response to DSBs. ATM phosphorylates histone H2AX and MDC1 in response to DSBs and lays the foundation for the chromatin-based signaling cascade involving phosphorylation and ubiquitination, which are mediated by RNF8 and RNF168 that results in ubiquitination of H2A to promote recruitment of 53BP1, which recruits its effectors to repair lesion. In addition, ATM phosphorylation activates Chk1/2, which in turn influences downstream factor cell to arrest the cell cycle. ATR: After suffering various forms of damaged DNA or helicase-polymerase uncoupling at stalled replication forks, RPA coats the ssDNA protecting it from degradation. ATR is recruited to RPA-ssDNA by its partner protein ATRIP and activated by TopBP1 or ETAA1; TopBP1 plays a role in ATR activation, which requires interaction with the RAD9–HUS1–RAD1 (9-1-1) clamp complex. ETAA1 is recruited to RPA-ssDNA via direct binding to RPA. In the downstream, ATR signaling activates the CHK1 kinase. CHK1 activation causes CDC25A degradation and slowing of cell cycle progression to arrest the cell cycle.

formation with various types of E3 ubiquitin ligases, the most important of which is Mdm2 (Brooks and Gu, 2006). HIPK2, a p53 Ser46 kinase, is retained in an inactive status because of the targeted proteolysis by E3 ubiquitin ligases in unstressed cells, making it an important regulator of stress signaling and DDR (Matt and Hofmann, 2016). When DNA damage is encountered, ATM and ATR kinases could phosphorylate Siah1, resulting in the dissociation of the HIPK2–Siah1 complex and increased stability of the HIPK2 protein (Winter et al., 2008).

4 Wnt and its crosstalk with DDR

Numerous studies have shown that Wnt signaling is highly intertwined with DDR (Zhang et al., 2011; Karimaian et al., 2017; Zhao et al., 2018b). In this section, we elaborate on these specific connections by outlining the roles of key factors (Figure 3).

4.1 The role of β-catenin in DDR

β-catenin is implicated in the regulation of DDR (Xu et al., 2008; Zhang et al., 2011; Priolli et al., 2013; Tavana et al., 2013; Chandra et al., 2015; Serebryannyy et al., 2017). Activation of downstream target genes of β-catenin such as cyclin D1 and c-myc proto-oncogenes leads to cell proliferation, differentiation, and maturation (Tulac et al., 2003). Notably, there is a growing list of Wnt/β-catenin target genes which have been found in various species and have been cataloged at: http://www.stanford.edu/group/nusselab/cgi-bin/wnt/target_genes. Based on these data, we have summarized the target genes closely related to DDR and briefly describe their roles in DDR.

4.2 The role of APC in DDR

APC is a key effector of the canonical Wnt signaling pathway involved in downregulating the β-catenin level. Many previous studies have shown that the loss of APC function can cause chromosomal instability (Fodde et al., 2001; Kaplan et al., 2001; Bienz, 2002). Clarke et al. found that APC loss leads to DNA damage and genomic instability in the live cell in a process closely associated with p53 (Méniel et al., 2015). In addition, there have been reports that APC is involved in the BER (Jaiswal and Narayan, 2008; Jaiswal and Narayan, 2011). Moreover, APC loss decreases cancer cell sensitivity to chemotherapy by reducing phosphorylation of ATM/Chk1/Chk2, which in turn influences DDR (Stefanski et al., 2019). APC loss can also increase STAT3 activation, leading to chemotherapy resistance (VanKlompenberg et al., 2017). STAT3 has

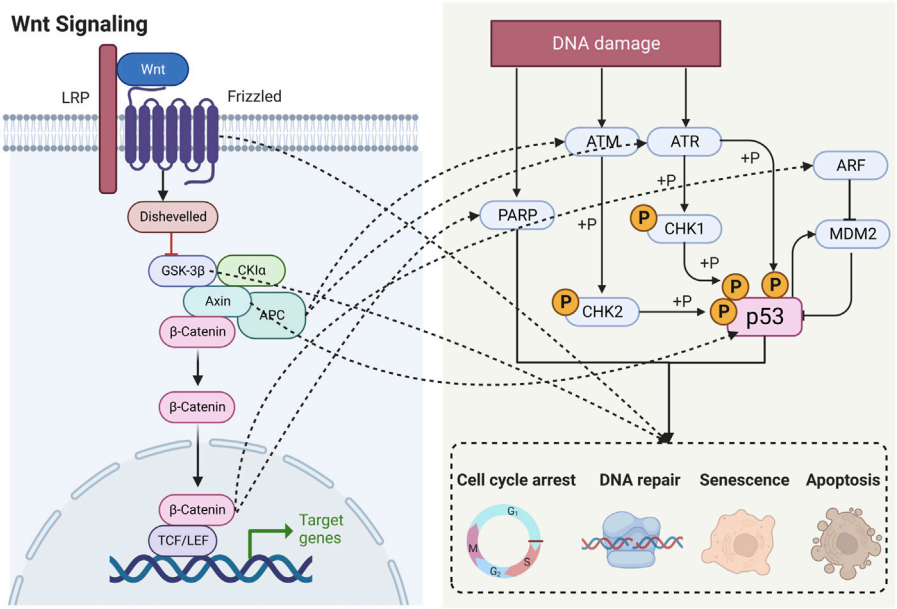

FIGURE 3
Schematic diagram showing that Wnt signaling is highly intertwined with DDR. LRP, lipoprotein receptor-related protein; APC, adenomatous polyposis coli; GSK-3β, glycogen synthase kinase-3β; CK1α, casein kinase 1α; TCF, T lymphocytokine/lymphoenhancer factor; LEF, human lymphoid enhancer factor; PARP, poly (ADP) ribose polymerase; ATM, ataxia telangiectasia mutated proteins; ATR, ataxia telangiectasia and Rad3-related protein; CHK, checkpoint kinase; ARF, ADP-ribosylation factor; MDM2, murine double minute 2.

been shown to take part in DNA repair, as low STAT3 levels can reduce ATM and ATR signaling through MDC1 (Barry et al., 2010).

4.3 Regulation of Axin on DDR

Axin, a key scaffolding protein, is responsible for the formation of the β-catenin destruction complex. Stability of axin protein is regulated by the ubiquitin-proteasome system, and enhancing axin stabilization is a common method of inhibiting Wnt/β-catenin signaling. In DDR, axin interacts with PML to regulate p53-dependent apoptosis in response to DNA damage (Li et al., 2011). Axin is involved in regulating phosphorylation of p53 Ser46 by forming a p53–axin–HIPK2 complex (Rui et al., 2004). Additionally, Lin et al. found that Tip60 interacts with axin in an ATM/ATR/CHK1-dependent way and abrogates Pirh2–axin binding, forming an axin–Tip60–HIPK2–p53 complex and leading to p53 phosphorylation in response to genotoxic stress during radiochemotherapy (Li et al., 2009).

4.4 Regulation of FZD on DDR

FZD is the seven-pass transmembrane receptor of Wnt. FZD5 is a member of the FZD family. Zhao et al. revealed that FZD5 has been involved in triple-negative breast cancer (TNBC) cell G1/S transition and DNA damage repair partially dependent on Wnt7B (Sun et al., 2020). Moreover, FZD5 modulates the downstream effecter FOXM1 in a Wnt/β-catenin-dependent manner to regulate the cell cycle, DNA replication, and DNA damage repair (Sun et al., 2020). In addition, a study on ovarian cancer found that another FZD family member, FZD7, can protect cells from chemotherapy-induced oxidative stress through the FZD7–β-catenin–Tp63–GPX4 pathway (Wang et al., 2021b). Similarly, another study showed that FZD10 can regulate Wnt signaling in BRCA-mutated epithelial ovarian cancers, ultimately contributing to increased HR activity (Fukumoto et al., 2019).

4.5 The effects of GSK-3β on DDR

GSK-3β is involved in multiple intracellular signaling pathways and is a component of the β-catenin destruction complex in Wnt signaling, which determines β-catenin stabilization. In DDR, GSK-3β can phosphorylate several DNA repair factors and affect their interaction with chromatin. For instance, through phosphorylating cyclin D1, CDC25A, and CRY2, GSK-3β can tune DNA repair and cell cycle (Diehl et al., 1998; Harada et al., 2005; Kang et al., 2008). Furthermore, GSK-3β can also phosphorylate B-Myb, leading to the dissociation of B-Myb from the MRN-mediated response to DNA damage (Henrich et al., 2017). Translin-associated protein X (TRAX) is a DNA/RNA-binding protein that participates in various functions, including DNA repair and physical interaction with GSK-3β and other DNA repair factors, to further influence NHEJ-mediated repair (Weng et al., 2018). In the cytoplasm, GSK-3β could phosphorylate targets to trigger proteasomal degradation and promote activation of NF-κB activity to evade apoptosis (Lin et al., 2020). On radiation exposure, GSK-3β translocates from the cytoplasm to the nucleus and phosphorylates 53BP1, an important regulator for DNA repair (Yang et al., 2018). There is strong evidence that GSK-3β plays an important role in DDR; however, whether those functions of GSK-3β depend on Wnt/β-catenin signaling requires further investigation.

TABLE 1 Function of Wnt target genes in DDR.

Gene	Function in DDR
c-myc	Regulates the cell cycle, telomere homeostasis, and c-myc target genes are involved in DDR, DNA synthesis, and apoptosis
n-myc	Regulates DDR
Cyclin D1	Regulates cell cycle and DNA repair
uPAR	Activates DNA repair signaling pathway
MMP-7	DNA repair
Endothelin-1	Enhances DNA repair
Jagged1	DNA repair
iNOS	Product NO causes DNA damage and inhibits DNA repair proteins
Telomerase	Sustains DNA damage signals in senescent cells, regulates apoptosis, and protects the cell against DNA damage
Sox9	Increases cell survival and regulates the cell cycle
Sox17	Downregulation of DDR genes
Runx2	Regulates the cell cycle, DNA repair, and apoptosis
SALL4	Activates the critical ATM-dependent cellular responses and chromatin remodeling
Osteoprotegerin	Reduces UV-induced apoptosis
CCN1 (Cyr61)	Regulates the cell cycle
Sox2	Regulates the cell cycle
PTTG (securin)	Regulates cell cycle, activates DDR, and modulates DDR gene expression
Nanog	Deregulates DDR and chromatin remodeling
OCT-4	Regulates the homologous recombination, regulates the cell cycle, and modulation of p53
Fibronectin	Regulates the cell cycle and priming and potentiation of DDR
Wnt3a	Regulates the cell cycle
Connexin43	Regulates the cell cycle
RARγ	Involved in DNA damage-induced necroptosis and extrinsic apoptosis
MITF	DNA repair, activates DDR signaling cascade, and regulates the cell cycle
Stra6	Apoptosis
Autotaxin	Involved in DDR and DNA repair
WISP	Apoptosis
COX-2	Prevents DNA damage
Nkx2.2	Regulates ATM activity
WISP-1	Regulates p53-mediated apoptosis
Periostin	Periostin-deficient embryos could be linked to improve DNA damage repair and regulates the cell cycle
β-TrCP	Regulates the cell cycle and DNA repair
CDC25A	Regulates the cell cycle
P16	Regulates the cell cycle and induces DDR

4.6 The role of p53 in DDR

In DDR, p53 can be activated in various ways. For example, ATM and ATR can phosphorylate p53 on Ser15 which is thought to inhibit interaction of p53 with the ubiquitin ligase, MDM2, leading to its dissociation from MDM2, thereby contributing to p53 stabilization (Shiloh and Ziv, 2013). Likewise, the p53 co-factor, hnRNPK, can be phosphorylated by ATM and protect p53 from MDM2-mediated degradation (Moumen et al., 2013). In the Wnt pathway, Wnt/β-catenin can promote the expression of ARF, which binds to MDM2 leading to its inactivation (Kubbutat et al., 1997). In contrast, the activation of p53 could trigger the Siah/SIP/Skp1/Ebi pathway for β-catenin ubiquitination degradation and then reduce activity of TCF/LEF (Matsuzawa and Reed, 2001). Accordingly, p53 is a key factor in the crosstalk between the Wnt/β-catenin signaling pathway and DDR.

4.7 Regulation of PARP on DDR

In general, PARP, a DNA damage sensor, is activated by recognizing damaged DNA fragments. DNA damage would induce auto-polyADP-ribosylation of the PARP-1 protein to inhibit the functional interaction of PARP-1 with TCF-4 and participate in the transcriptional regulation of TCF-4/β-catenin complex target genes, such as *cyclin D1* and *c-myc* (Idogawa et al., 2005). In addition, Ku70 is an inhibitor of the β-catenin/TCF-4 transcriptional complex, and PARP-1 could compete with Ku70 for binding to TCF-4, thereby modifying transcriptional activity of TCF-4 (Idogawa et al., 2007). Moreover, there is considerable evidence that Wnt/β-catenin signaling activation can promote resistance to PARP inhibitors (Fukumoto et al., 2019; Yamamoto et al., 2019; Zhu et al., 2021). Therefore, PARP may provide a novel linkage between Wnt/β-catenin signaling and DDR.

In summary, there are many connections between Wnt and DDR (Table 1); however, whether these factors regulate DDR directly via Wnt signaling or independent of the Wnt signaling pathway warrants further investigation.

5 Potential treatment strategies

At present, initiation and increase of DNA damage in cancer cell is a commonly exploited strategy for treating cancer and plays an effective therapeutic role; however, some cancer cells can develop resistance to DNA damage drugs by activating DDR. Increased DNA repair leads to resistance of cancer cells to targeted local (radiotherapy) or systemic (chemotherapy) treatments. Numerous kinds of drugs used for cancer chemotherapy, such as Adriamycin, etoposide, bleomycin, and cisplatin, are characterized as intense inducers of DNA damage and could effectively activate the intracellular DDR (Jackson and Bartek, 2009). All parts of DDR require proper coordination to maintain genome stability, and they can all influence the effects of cancer treatment. Therefore, DDR

TABLE 2 Drug target and clinical trials on Wnt/β-catenin-targeted agents in cancer.

Target	Mechanism of action	Compound name	Cancer type	Trial identifier	Reference
PORCN	Porcupine inhibitor	LGK974 (Wnt974)	Pancreatic cancer, BRAF mutant colorectal cancer, melanoma, triple-negative breast cancer, head and neck squamous cell cancer, cervical squamous cell cancer, esophageal squamous cell cancer, and lung squamous cell cancer	NCT01351103	Rodon et al. (2021)
			Metastatic colorectal cancer	NCT02278133	Tabernero et al. (2023)
		ETC-159 (ETC-1922159)	Solid tumors	NCT02521844	Katoh (2018)
		RXC004	Colorectal cancer	NCT04907539	
			Advanced solid tumors	NCT04907851	Phillips et al. (2022)
			Cancer and solid tumors	NCT03447470	
		CGX1321	Colorectal adenocarcinoma, gastric adenocarcinoma, pancreatic adenocarcinoma, bile duct carcinoma, hepatocellular carcinoma, esophageal carcinoma, and gastrointestinal cancer	NCT03507998	Li et al., 2019; Goldsberry et al., 2020; Shah et al., 2021
Wnt	Preventing Wnt binding to FZD	Ipafricept (OMP-54F28)	Hepatocellular cancer and liver cancer	NCT02069145	Jimeno et al., 2017
			Ovarian cancer	NCT02092363	Moore et al. (2019)
			Pancreatic cancer and stage IV pancreatic cancer	NCT02050178	
			Solid tumors	NCT01608867	
	Wnt5a agonist	Foxy-5	Metastatic breast cancer, colorectal cancer, and prostate cancer	NCT02020291 and NCT02655952	Säfholm et al., 2008; Canesin et al., 2017; Osman et al., 2019
			Colon cancer	NCT03883802	
FZD	Inhibits Wnt signaling by binding FZD 1, 2, 5, 7, 8	Vantictumab (OMP-18R5)	Solid tumors	NCT01345201 and NCT01957007	
			Pancreatic cancer and stage IV pancreatic cancer	NCT02005315	Davis et al., 2020; Diamond et al., 2020
			Metastatic breast cancer	NCT01973309	
	FZD10 antagonist	OTSA101-DTPA-90Y	Synovial sarcoma	NCT01469975	Goswami and Patel (2021)
	FZD8 decoy receptor	Ipafricept (OMP-54F28)	Solid tumors	NCT01608867	
			Hepatocellular cancer and liver cancer	NCT02069145	Jimeno et al., 2017; Moore et al., 2019; Dotan et al., 2020
			Ovarian cancer	NCT02092363	
			Pancreatic cancer	NCT02050178	
ROR1	Anti-ROR1 antibody	Cirmtuzumab (UC-961)	Chronic lymphocytic leukemia	NCT02860676	
				NCT02222688 and NCT03088878	
			Metastatic castration-resistant prostate cancer	NCT05156905	Choi et al., 2015; Choi et al., 2018
			Chronic lymphocytic leukemia	NCT04501939, NCT02860676, and NCT02222688	
			Breast neoplasms	NCT02776917	

(Continued on following page)

TABLE 2 (*Continued*) Drug target and clinical trials on Wnt/β-catenin-targeted agents in cancer.

Target	Mechanism of action	Compound name	Cancer type	Trial identifier	Reference
			B-cell chronic lymphocytic leukemia, small lymphocytic lymphoma, and mantle cell lymphoma	NCT03088878	
		NBE-002	Advanced solid tumor, advanced cancer, and triple-negative breast cancer	NCT04441099	
	Overexpressing ROR1	Zilovertamab vedotin (VLS-101 and MK-2140)	Hematologic malignancies	NCT03833180	
			Solid tumors	NCT04504916	Kipps, 2021; Vaisitti et al., 2021
			Relapsed or refractory diffuse large B-cell lymphoma	NCT05139017	
		NVG-111 (RP2D)	Chronic lymphocytic leukemia and mantle cell lymphoma	NCT04763083	
	Targeting of genetically engineered autologous T-lymphocytes to ROR1$^+$ tumors	Anti-ROR1 CAR	ROR1$^+$ tumors	NCT02706392	
ROR2	Targeting of genetically engineered autologous T-lymphocytes to ROR2$^+$ tumors	CCT301CAR (CCT301-38 and CCT301-59)	Renal cell carcinoma	NCT03393936	
			Solid tumor, soft tissue sarcoma, gastric cancer, pancreatic cancer, and bladder cancer	NCT03960060	
	Conditionally active biologic anti-ROR2 antibody drug conjugate	Ozuriftamab vedotin (CAB-ROR2-ADC and BA3021)	Non-small cell lung cancer, triple-negative breast cancer, melanoma, and head and neck cancer	NCT03504488	
			Recurrent or metastatic squamous cell cancer of the head and neck	NCT05271604	
			Ovarian cancer	NCT04918186	
			Non-small cell lung cancer	NCT04681131	
CBP	CBP/β-catenin antagonist	PRI-724	Colorectal cancer	NCT02413853 and NCT04351009	
			Advanced or metastatic pancreatic cancer	NCT01764477	
			Advanced myeloid malignancies	NCT01606579	
			Advanced solid tumors	NCT01302405	
β-catenin	Degrading β-catenin	CWP232291	Acute myeloid leukemia and chronic myelomonocytic leukemia	NCT01398462	Pak et al., 2019; Lee et al., 2020; Wang et al., 2022
			Acute myeloid leukemia	NCT03055286	
			Multiple myeloma	NCT02426723	

components can serve as radiation and chemical sensitization targets in cancer treatment. Knowledge of the DDR defects that are present in cancer can also allow for the selection of optimal treatments that can efficiently kill the cancer cells (Goldstein and Kastan, 2015). Currently, many drugs targeting the DDR have been developed to treat tumors, which are shown in Schedule 1. A summary of clinical trials on Wnt/β-catenin-targeted agents is presented in Table 2.

Theoretically, targeting both DDR and Wnt signaling could serve as potential treatment strategies for cancer. Another common denominator of them is that DDR and Wnt signaling have been associated with therapeutic resistance (Martin-Orozco et al., 2019). Alterations in Wnt signaling are also closely associated with maintenance of cancer stem cell (CSCs) proliferation, as hyperactivation of the Wnt signaling pathway is critical in supporting cancer cell survival in the context of treatment with anti-cancer drugs and ultimately leads to cancer progression. Therefore, the design and development of appropriate anti-cancer strategies based on Wnt targets may have important therapeutic value in treating cancer cells, thereby enhancing the therapeutic efficacy of these strategies (Mukherjee and Panda, 2020; Zhang and Wang, 2020). The formation of drug resistance could be attributed to some different mechanisms such as the acquisition of quiescence, the interaction with the microenvironment, drug efflux capacity, increased resistance to apoptosis, and increased DNA repair. For example, FZD5 enhances DNA damage repair and chemoresistance (Sun et al., 2020). GSK-3β promotes

resistance of cancer cells to DNA damage chemotherapeutic agents and radiation through regulating DNA repair and stemness of cancer cells (Lin et al., 2020). YAP/TAZ is a Wnt regulator that can be activated to protect cancer cells from DNA damage (de Lau et al., 2014). Furthermore, the role of Wnt signaling in promoting DNA damage repair and inhibiting apoptosis contributes to cancer resistance to radiation (Jun et al., 2016; Zhao et al., 2018a).

Most current anti-cancer chemotherapy approaches function by killing highly proliferating cells, which in many cancers are mostly non-CSCs. However, small CSC populations present in cancer have a higher repair mechanism and are also highly resistant to chemotherapy. In addition, radiotherapy and chemotherapy may trigger a series of cellular stress response mechanisms that enhance stem cell properties of non-CSCs, thereby improving their adaptation and survival. Therefore, compared with previous therapies, new combination therapies, which can kill both CSCs and non-CSCs while preventing the transition from non-CSCs to CSCs, require consideration. It would be possible to develop a therapeutic strategy which combines DDR-targeting drugs with Wnt-targeting drugs to increase sensitivity of cytotoxic drugs while contributing anti-CSC effects. Importantly, the connection points between the DDR and Wnt warrant further investigation, as drugs targeting these points are likely to inhibit both DDR and CSCs simultaneously.

6 Discussion and conclusion

In the context of cancer, increased Wnt signaling is beneficial and reflected in enhancement of DDR, endowing cancer cells with increased ability to repair themselves during radiation or chemotherapy. The association between Wnt signaling and DDR in the post-carcinogenesis stage have been well studied, but the relationship between these two pathways during the process of carcinogenesis requires further investigation. There is a strong correlation between carcinogenesis and inadequate repair of DNA damage; however, whether Wnt signaling is involved in this process remains unknown. Future studies are required to investigate whether Wnt signaling can influence carcinogenesis via regulation of DDR.

Although Wnt signaling and the DDR are closely related, the effects generated by different specific points of crosstalk are unknown. Identification of an appropriate regulator as a therapeutic target may be beneficial to cancer treatment. Compared with single-drug chemotherapy or radiotherapy, drug combination may achieve double efficacy with half the input. From another perspective, a triple therapy including DDR-targeting drugs and Wnt-targeting drugs has the potential to enhance the efficacy of radiotherapy and chemotherapy. Although our theory may be considered oversimplified, identification of crosstalk between the Wnt signaling pathway and DNA damage recognition has potential to provide novel insights into cancer therapy.

Author contributions

XZ and XY: conceptualization. XZ: data curation and writing–original draft preparation. XY: visualization and investigation. XZ and XY: supervision. XZ and XY: writing–reviewing and editing. All authors contributed to the article and approved the submitted version.

Funding

This work was supported by the 345 Talent Project of Shengjing Hospital of China Medical University.

Acknowledgments

The authors thank the Department of Otolaryngology, Head, and Neck Surgery, Shengjing Hospital of China Medical University. This work was supported by the 345 Talent Project of Shengjing Hospital of China Medical University. The authors also thank biorender.com for creating Figure 3.

Conflict of interest

The authors declare that the research was conducted in the absence of any commercial or financial relationships that could be construed as a potential conflict of interest.

Publisher's note

References

Abraham, R. T. (2001). Cell cycle checkpoint signaling through the ATM and ATR kinases. *Genes & Dev.* 15 (17), 2177–2196. doi:10.1101/gad.914401

Amé, J.-C., Spenlehauer, C., and de Murcia, G. (2004). The PARP superfamily. *BioEssays news Rev. Mol. Cell. Dev. Biol.* 26 (8), 882–893. doi:10.1002/bies.20085

Barry, S. P., Townsend, P. A., Knight, R. A., Scarabelli, T. M., Latchman, D. S., and Stephanou, A. (2010). STAT3 modulates the DNA damage response pathway. *Int. J. Exp. Pathology* 91 (6), 506–514. doi:10.1111/j.1365-2613.2010.00734.x

Bienz, M. (2002). The subcellular destinations of APC proteins. *Nat. Rev. Mol. Cell Biol.* 3 (5), 328–338. doi:10.1038/nrm806

Blackford, A. N., and Jackson, S. P. (2017). ATM, ATR, and DNA-PK: The trinity at the heart of the DNA damage response. *Mol. Cell* 66 (6), 801–817. doi:10.1016/j.molcel.2017.05.015

Bode, A. M., and Dong, Z. (2004). Post-translational modification of p53 in tumorigenesis. *Nat. Rev. Cancer* 4 (10), 793–805. doi:10.1038/nrc1455

Brooks, C. L., and Gu, W. (2006). p53 ubiquitination: Mdm2 and beyond. *Mol. Cell* 21 (3), 307–315. doi:10.1016/j.molcel.2006.01.020

Canesin, G., Evans-Axelsson, S., Hellsten, R., Krzyzanowska, A., Prasad, C. P., Bjartell, A., et al. (2017). Treatment with the WNT5A-mimicking peptide Foxy-5 effectively

reduces the metastatic spread of WNT5A-low prostate cancer cells in an orthotopic mouse model. *PLoS One* 12 (9), e0184418. doi:10.1371/journal.pone.0184418

Chandra, A., Lin, T., Zhu, J., Tong, W., Huo, Y., Jia, H., et al. (2015). PTH1-34 blocks radiation-induced osteoblast apoptosis by enhancing DNA repair through canonical Wnt pathway. *J. Biol. Chem.* 290 (1), 157–167. doi:10.1074/jbc.M114.608158

Choi, M. Y., Widhopf, G. F., 2nd, Ghia, E. M., Kidwell, R. L., Hasan, M. K., Yu, J., et al. (2018). Phase I trial: Cirmtuzumab inhibits ROR1 signaling and stemness signatures in patients with chronic lymphocytic leukemia. *Cell Stem Cell* 22 (6), 951–959.e3. doi:10.1016/j.stem.2018.05.018

Choi, M. Y., Widhopf, G. F., 2ndWu, C. C., Cui, B., Lao, F., Sadarangani, A., et al. (2015). Pre-clinical specificity and safety of UC-961, a first-in-class monoclonal antibody targeting ROR1. *Clin. Lymphoma Myeloma Leuk.* 15, S167–S169. doi:10.1016/j.clml.2015.02.010

Ciccia, A., and Elledge, S. J. (2010). The DNA damage response: Making it safe to play with knives. *Mol. Cell* 40 (2), 179–204. doi:10.1016/j.molcel.2010.09.019

Clevers, H., and Nusse, R. (2012). Wnt/β-catenin signaling and disease. *Cell* 149 (6), 1192–1205. doi:10.1016/j.cell.2012.05.012

Davis, S. L., Cardin, D. B., Shahda, S., Lenz, H. J., Dotan, E., O'Neil, B. H., et al. (2020). A phase 1b dose escalation study of Wnt pathway inhibitor vantictumab in combination with nab-paclitaxel and gemcitabine in patients with previously untreated metastatic pancreatic cancer. *Invest. New Drugs* 38 (3), 821–830. doi:10.1007/s10637-019-00824-1

De, A. (2011). Wnt/Ca2+ signaling pathway: A brief overview. *Acta biochimica biophysica Sinica* 43 (10), 745–756. doi:10.1093/abbs/gmr079

de Lau, W., Peng, W. C., Gros, P., and Clevers, H. (2014). The R-spondin/lgr5/rnf43 module: Regulator of Wnt signal strength. *Genes & Dev.* 28 (4), 305–316. doi:10.1101/gad.235473.113

Diamond, J. R., Becerra, C., Richards, D., Mita, A., Osborne, C., O'Shaughnessy, J., et al. (2020). Phase Ib clinical trial of the anti-frizzled antibody vantictumab (OMP-18R5) plus paclitaxel in patients with locally advanced or metastatic HER2-negative breast cancer. *Breast Cancer Res. Treat.* 184 (1), 53–62. doi:10.1007/s10549-020-05817-w

Diehl, J. A., Cheng, M., Roussel, M. F., and Sherr, C. J. (1998). Glycogen synthase kinase-3beta regulates cyclin D1 proteolysis and subcellular localization. *Genes & Dev.* 12 (22), 3499–3511. doi:10.1101/gad.12.22.3499

Dotan, E., Cardin, D. B., Lenz, H. J., Messersmith, W., O'Neil, B., Cohen, S. J., et al. (2020). Phase ib study of Wnt inhibitor ipafricept with gemcitabine and nab-paclitaxel in patients with previously untreated stage IV pancreatic cancer. *Clin. Cancer Res.* 26 (20), 5348–5357. doi:10.1158/1078-0432.Ccr-20-0489

Fodde, R., and Brabletz, T. J. C. (2007). Wnt/beta-catenin signaling in cancer stemness and malignant behavior. *Wnt/β-catenin Signal. cancer stemness malignant Behav.* 19 (2), 150–158. doi:10.1016/j.ceb.2007.02.007

Fodde, R., Kuipers, J., Rosenberg, C., Smits, R., Kielman, M., Gaspar, C., et al. (2001). Mutations in the APC tumour suppressor gene cause chromosomal instability. *Nat. Cell Biol.* 3 (4), 433–438. doi:10.1038/35070129

Fukumoto, T., Zhu, H., Nacarelli, T., Karakashev, S., Fatkhutdinov, N., Wu, S., et al. (2019). N^6-Methylation of adenosine of *FZD10* mRNA contributes to PARP inhibitor resistance. *Cancer Res.* 79 (11), 2812–2820. doi:10.1158/0008-5472.CAN-18-3592

Goldsberry, W. N., Meza-Perez, S., Londoño, A. I., Katre, A. A., Mott, B. T., Roane, B. M., et al. (2020). Inhibiting WNT ligand production for improved immune recognition in the ovarian tumor microenvironment. *Cancers (Basel)* 12 (3), 766. doi:10.3390/cancers12030766

Goldstein, M., and Kastan, M. B. (2015). The DNA damage response: Implications for tumor responses to radiation and chemotherapy. *Annu. Rev. Med.* 66, 129–143. doi:10.1146/annurev-med-081313-121208

Goswami, V. G., and Patel, B. D. (2021). Recent updates on Wnt signaling modulators: A patent review (2014-2020). *Expert Opin. Ther. Pat.* 31 (11), 1009–1043. doi:10.1080/13543776.2021.1940138

Graham, T. G. W., Walter, J. C., and Loparo, J. J. (2016). Two-stage synapsis of DNA ends during non-homologous end joining. *Mol. Cell* 61 (6), 850–858. doi:10.1016/j.molcel.2016.02.010

Haince, J.-F., McDonald, D., Rodrigue, A., Déry, U., Masson, J.-Y., Hendzel, M. J., et al. (2008). PARP1-dependent kinetics of recruitment of MRE11 and NBS1 proteins to multiple DNA damage sites. *J. Biol. Chem.* 283 (2), 1197–1208. doi:10.1074/jbc.M706734200

Harada, Y., Sakai, M., Kurabayashi, N., Hirota, T., and Fukada, Y. (2005). Ser-557-phosphorylated mCRY2 is degraded upon synergistic phosphorylation by glycogen synthase kinase-3 beta. *J. Biol. Chem.* 280 (36), 31714–31721. doi:10.1074/jbc.M506225200

Henrich, S. M., Usadel, C., Werwein, E., Burdova, K., Janscak, P., Ferrari, S., et al. (2017). Interplay with the Mre11-Rad50-Nbs1 complex and phosphorylation by GSK3β implicate human B-Myb in DNA-damage signaling. *Sci. Rep.* 7, 41663. doi:10.1038/srep41663

Idogawa, M., Masutani, M., Shitashige, M., Honda, K., Tokino, T., Shinomura, Y., et al. (2007). Ku70 and poly(ADP-ribose) polymerase-1 competitively regulate beta-catenin and T-cell factor-4-mediated gene transactivation: Possible linkage of DNA damage recognition and Wnt signaling. *Cancer Res.* 67 (3), 911–918. doi:10.1158/0008-5472.CAN-06-2360

Idogawa, M., Yamada, T., Honda, K., Sato, S., Imai, K., and Hirohashi, S. (2005). Poly(ADP-ribose) polymerase-1 is a component of the oncogenic T-cell factor-4/beta-catenin complex. *Gastroenterology* 128 (7), 1919–1936. doi:10.1053/j.gastro.2005.03.007

Jackson, S. P., and Bartek, J. (2009). The DNA-damage response in human biology and disease. *Nature* 461 (7267), 1071–1078. doi:10.1038/nature08467

Jaiswal, A. S., and Narayan, S. (2008). A novel function of adenomatous polyposis coli (APC) in regulating DNA repair. *Cancer Lett.* 271 (2), 272–280. doi:10.1016/j.canlet.2008.06.024

Jaiswal, A. S., and Narayan, S. (2011). Assembly of the base excision repair complex on abasic DNA and role of adenomatous polyposis coli on its functional activity. *Biochemistry* 50 (11), 1901–1909. doi:10.1021/bi102000q

Jimeno, A., Gordon, M., Chugh, R., Messersmith, W., Mendelson, D., Dupont, J., et al. (2017). A first-in-human phase I study of the anticancer stem cell agent ipafricept (OMP-54F28), a decoy receptor for Wnt ligands, in patients with advanced solid tumors. *Clin. Cancer Res.* 23 (24), 7490–7497. doi:10.1158/1078-0432.Ccr-17-2157

Jun, S., Jung, Y.-S., Suh, H. N., Wang, W., Kim, M. J., Oh, Y. S., et al. (2016). LIG4 mediates Wnt signalling-induced radioresistance. *Nat. Commun.* 7, 10994. doi:10.1038/ncomms10994

Kang, T., Wei, Y., Honaker, Y., Yamaguchi, H., Appella, E., Hung, M.-C., et al. (2008). GSK-3 beta targets Cdc25A for ubiquitin-mediated proteolysis, and GSK-3 beta inactivation correlates with Cdc25A overproduction in human cancers. *Cancer Cell* 13 (1), 36–47. doi:10.1016/j.ccr.2007.12.002

Kaplan, K. B., Burds, A. A., Swedlow, J. R., Bekir, S. S., Sorger, P. K., and Näthke, I. S. (2001). A role for the Adenomatous Polyposis Coli protein in chromosome segregation. *Nat. Cell Biol.* 3 (4), 429–432. doi:10.1038/35070123

Karimaian, A., Majidinia, M., Baghi, H. B., and Yousefi, B. J. D. (2017). The crosstalk between Wnt/β-catenin signaling pathway with DNA damage response and oxidative stress: Implications in cancer therapy. *DNA Repair* 51, 14–19. doi:10.1016/j.dnarep.2017.01.003

Katoh, M. (2018). Multi-layered prevention and treatment of chronic inflammation, organ fibrosis and cancer associated with canonical WNT/β-catenin signaling activation (Review). *Int. J. Mol. Med.* 42 (2), 713–725. doi:10.3892/ijmm.2018.3689

Kipps, T. J. (2021). Mining the microenvironment for therapeutic targets in chronic lymphocytic leukemia. *Cancer J.* 27 (4), 306–313. doi:10.1097/ppo.0000000000000536

Krishnamurthy, N., and Kurzrock, R. (2018). Targeting the Wnt/beta-catenin pathway in cancer: Update on effectors and inhibitors. *Cancer Treat. Rev.* 62, 50–60. doi:10.1016/j.ctrv.2017.11.002

Kubbutat, M. H., Jones, S. N., and Vousden, K. H. (1997). Regulation of p53 stability by Mdm2. *Nature* 387 (6630), 299–303. doi:10.1038/387299a0

Lee, J. H., Faderl, S., Pagel, J. M., Jung, C. W., Yoon, S. S., Pardanani, A. D., et al. (2020). Phase 1 study of CWP232291 in patients with relapsed or refractory acute myeloid leukemia and myelodysplastic syndrome. *Blood Adv.* 4 (9), 2032–2043. doi:10.1182/bloodadvances.2019000757

Lee, J. H., and Paull, T. T. (2021). Cellular functions of the protein kinase ATM and their relevance to human disease. *Nat. Rev. Mol. Cell Biol.* 22 (12), 796–814. doi:10.1038/s41580-021-00394-2

Lento, W., Ito, T., Zhao, C., Harris, J. R., Huang, W., Jiang, C., et al. (2014). Loss of β-catenin triggers oxidative stress and impairs hematopoietic regeneration. *Genes & Dev.* 28 (9), 995–1004. doi:10.1101/gad.231944.113

Li, C., Liang, Y., Cao, J., Zhang, N., Wei, X., Tu, M., et al. (2019). The delivery of a Wnt pathway inhibitor toward CSCs requires stable liposome encapsulation and delayed drug release in tumor tissues. *Mol. Ther.* 27 (9), 1558–1567. doi:10.1016/j.ymthe.2019.06.013

Li, Q., He, Y., Wei, L., Wu, X., Wu, D., Lin, S., et al. (2011). AXIN is an essential co-activator for the promyelocytic leukemia protein in p53 activation. *Oncogene* 30 (10), 1194–1204. doi:10.1038/onc.2010.499

Li, Q., Lin, S., Wang, X., Lian, G., Lu, Z., Guo, H., et al. (2009). Axin determines cell fate by controlling the p53 activation threshold after DNA damage. *Nat. Cell Biol.* 11 (9), 1128–1134. doi:10.1038/ncb1927

Li, T., Liu, X., Jiang, L., Manfredi, J., Zha, S., and Gu, W. (2016). Loss of p53-mediated cell-cycle arrest, senescence and apoptosis promotes genomic instability and premature aging. *Oncotarget* 7 (11), 11838–11849. doi:10.18632/oncotarget.7864

Liang, Y., Feng, Y., Zong, M., Wei, X.-F., Lee, J., Feng, Y., et al. (2018). β-catenin deficiency in hepatocytes aggravates hepatocarcinogenesis driven by oncogenic β-catenin and MET. *Hepatol. Baltim. Md* 67 (5), 1807–1822. doi:10.1002/hep.29661

Lin, J., Song, T., Li, C., and Mao, W. (2020). GSK-3β in DNA repair, apoptosis, and resistance of chemotherapy, radiotherapy of cancer. *Biochimica biophysica acta. Mol. Cell Res.* 1867 (5), 118659. doi:10.1016/j.bbamcr.2020.118659

Lord, C. J., and Ashworth, A. (2012). The DNA damage response and cancer therapy. *Nature* 481 (7381), 287–294. doi:10.1038/nature10760

Martin-Orozco, E., Sanchez-Fernandez, A., Ortiz-Parra, I., and Ayala-San Nicolas, M. (2019). WNT signaling in tumors: The way to evade drugs and immunity. *Front. Immunol.* 10, 2854. doi:10.3389/fimmu.2019.02854

Matsuzawa, S. I., and Reed, J. C. (2001). Siah-1, SIP, and Ebi collaborate in a novel pathway for beta-catenin degradation linked to p53 responses. *Mol. Cell* 7 (5), 915–926. doi:10.1016/s1097-2765(01)00242-8

Matt, S., and Hofmann, T. G. (2016). The DNA damage-induced cell death response: A roadmap to kill cancer cells. *Cell. Mol. life Sci. CMLS* 73 (15), 2829–2850. doi:10.1007/s00018-016-2130-4

Méniel, V., Megges, M., Young, M. A., Cole, A., Sansom, O. J., and Clarke, A. R. (2015). Apc and p53 interaction in DNA damage and genomic instability in hepatocytes. *Oncogene* 34 (31), 4118–4129. doi:10.1038/onc.2014.342

Moore, K. N., Gunderson, C. C., Sabbatini, P., McMeekin, D. S., Mantia-Smaldone, G., Burger, R. A., et al. (2019). A phase 1b dose escalation study of ipafricept (OMP54F28) in combination with paclitaxel and carboplatin in patients with recurrent platinum-sensitive ovarian cancer. *Gynecol. Oncol.* 154 (2), 294–301. doi:10.1016/j.ygyno.2019.04.001

Moumen, A., Magill, C., Dry, K. L., and Jackson, S. P. (2013). ATM-dependent phosphorylation of heterogeneous nuclear ribonucleoprotein K promotes p53 transcriptional activation in response to DNA damage. *Cell cycleGeorget. Tex.)* 12 (4), 698–704. doi:10.4161/cc.23592

Mukherjee, N., and Panda, C. K. (2020). Wnt/β-Catenin signaling pathway as chemotherapeutic target in breast cancer: An update on pros and cons. *Clin. Breast Cancer* 20 (5), 361–370. doi:10.1016/j.clbc.2020.04.004

Nusse, R., and Clevers, H. (2017). Wnt/β-Catenin signaling, disease, and emerging therapeutic modalities. *Cell* 169 (6), 985–999. doi:10.1016/j.cell.2017.05.016

Osman, J., Bellamkonda, K., Liu, Q., Andersson, T., and Sjölander, A. (2019). The WNT5A agonist Foxy5 reduces the number of colonic cancer stem cells in a xenograft mouse model of human colonic cancer. *Anticancer Res.* 39 (4), 1719–1728. doi:10.21873/anticanres.13278

Pak, S., Park, S., Kim, Y., Park, J. H., Park, C. H., Lee, K. J., et al. (2019). The small molecule WNT/β-catenin inhibitor CWP232291 blocks the growth of castration-resistant prostate cancer by activating the endoplasmic reticulum stress pathway. *J. Exp. Clin. Cancer Res.* 38 (1), 342. doi:10.1186/s13046-019-1342-5

Phillips, C., Bhamra, I., Eagle, C., Flanagan, E., Armer, R., Jones, C. D., et al. (2022). The Wnt pathway inhibitor RXC004 blocks tumor growth and reverses immune evasion in Wnt ligand-dependent cancer models. *Cancer Res. Commun.* 2 (9), 914–928. doi:10.1158/2767-9764.Crc-21-0095

Pilié, P. G., Tang, C., Mills, G. B., and Yap, T. A. (2019). State-of-the-art strategies for targeting the DNA damage response in cancer. *Nat. Rev. Clin. Oncol.* 16 (2), 81–104. doi:10.1038/s41571-018-0114-z

Priolli, D. G., Canelloi, T. P., Lopes, C. O., Valdívia, J. C. M., Martinez, N. P., Açari, D. P., et al. (2013). Oxidative DNA damage and β-catenin expression in colorectal cancer evolution. *Int. J. colorectal Dis.* 28 (5), 713–722. doi:10.1007/s00384-013-1688-7

Rodon, J., Argilés, G., Connolly, R. M., Vaishampayan, U., de Jonge, M., Garralda, E., et al. (2021). Phase 1 study of single-agent WNT974, a first-in-class Porcupine inhibitor, in patients with advanced solid tumours. *Br. J. Cancer* 125 (1), 28–37. doi:10.1038/s41416-021-01389-8

Rogakou, E. P., Pilch, D. R., Orr, A. H., Ivanova, V. S., and Bonner, W. M. (1998). DNA double-stranded breaks induce histone H2AX phosphorylation on serine 139. *J. Biol. Chem.* 273 (10), 5858–5868. doi:10.1074/jbc.273.10.5858

Rui, Y., Xu, Z., Lin, S., Li, Q., Rui, H., Luo, W., et al. (2004). Axin stimulates p53 functions by activation of HIPK2 kinase through multimeric complex formation. *EMBO J.* 23 (23), 4583–4594. doi:10.1038/sj.emboj.7600475

Rupnik, A., Lowndes, N. F., and Grenon, M. (2010). MRN and the race to the break. *Chromosoma* 119 (2), 115–135. doi:10.1007/s00412-009-0242-4

Säfholm, A., Tuomela, J., Rosenkvist, J., Dejmek, J., Härkönen, P., and Andersson, T. (2008). The Wnt-5a-derived hexapeptide Foxy-5 inhibits breast cancer metastasis *in vivo* by targeting cell motility. *Clin. Cancer Res.* 14 (20), 6556–6563. doi:10.1158/1078-0432.Ccr-08-0711

Serebryannyy, L. A., Yemelyanov, A., Gottardi, C. J., and de Lanerolle, P. (2017). Nuclear α-catenin mediates the DNA damage response via β-catenin and nuclear actin. *J. Cell Sci.* 130 (10), 1717–1729. doi:10.1242/jcs.199893

Shah, K., Panchal, S., and Patel, B. (2021). Porcupine inhibitors: Novel and emerging anti-cancer therapeutics targeting the Wnt signaling pathway. *Pharmacol. Res.* 167, 105532. doi:10.1016/j.phrs.2021.105532

Shiloh, Y., and Ziv, Y. (2013). The ATM protein kinase: Regulating the cellular response to genotoxic stress, and more. *Nat. Rev. Mol. Cell Biol.* 14 (4), 197–210. doi:10.1038/nrm3546

Stefanski, C. D., Keffler, K., McClintock, S., Milac, L., and Prosperi, J. R. (2019). APC loss affects DNA damage repair causing doxorubicin resistance in breast cancer cells. *Neoplasia (New York, N.Y.)* 21 (12), 1143–1150. doi:10.1016/j.neo.2019.09.002

Stoof, J., Harrold, E., Mariottino, S., Lowery, M. A., and Walsh, N. (2021). DNA damage repair deficiency in pancreatic ductal adenocarcinoma: Preclinical models and clinical perspectives. *Front. Cell Dev. Biol.* 9, 749490. doi:10.3389/fcell.2021.749490

Su, Y. L., Xiao, L. Y., Huang, S. Y., Wu, C. C., Chang, L. C., Chen, Y. H., et al. (2023). Inhibiting WEE1 augments the antitumor efficacy of Cisplatin in urothelial carcinoma by enhancing the DNA damage process. *Cells* 12 (11), 1471. doi:10.3390/cells12111471

Sun, Y., Wang, Z., Na, L., Dong, D., Wang, W., and Zhao, C. (2020). FZD5 contributes to TNBC proliferation, DNA damage repair and stemness. *Cell Death Dis.* 11 (12), 1060. doi:10.1038/s41419-020-03282-3

Tabernero, J., Van Cutsem, E., Garralda, E., Tai, D., De Braud, F., Geva, R., et al. (2023). A phase ib/II study of WNT974 + encorafenib + cetuximab in patients with BRAF V600e-mutant KRAS wild-type metastatic colorectal cancer. *Oncologist* 28 (3), 230–238. doi:10.1093/oncolo/oyad007

Tao, S., Tang, D., Morita, Y., Sperka, T., Omrani, O., Lechel, A., et al. (2015). Wnt activity and basal niche position sensitize intestinal stem and progenitor cells to DNA damage. *EMBO J.* 34 (5), 624–640. doi:10.15252/embj.201490700

Tavana, O., Puebla-Osorio, N., Kim, J., Sang, M., Jang, S., and Zhu, C. (2013). Ku70 functions in addition to nonhomologous end joining in pancreatic β-cells: A connection to β-catenin regulation. *Diabetes* 62 (7), 2429–2438. doi:10.2337/db12-1218

Traphagen, N. A., Schwartz, G. N., Tau, S., Roberts, A. M., Jiang, A., Hosford, S. R., et al. (2023). Estrogen therapy induces receptor-dependent DNA damage enhanced by PARP inhibition in ER+ breast cancer. *Clin. Cancer Res.* 23, 488. doi:10.1158/1078-0432.Ccr-23-0488

Tulac, S., Nayak, N. R., Kao, L. C., Van Waes, M., Huang, J., Lobo, S., et al. (2003). Identification, characterization, and regulation of the canonical Wnt signaling pathway in human endometrium. *J. Clin. Endocrinol. metabolism* 88 (8), 3860–3866. doi:10.1210/jc.2003-030494

Vaisitti, T., Arruga, F., Vitale, N., Lee, T. T., Ko, M., Chadburn, A., et al. (2021). ROR1 targeting with the antibody-drug conjugate VLS-101 is effective in Richter syndrome patient-derived xenograft mouse models. *Blood* 137 (24), 3365–3377. doi:10.1182/blood.2020008404

VanKlompenberg, M. K., Leyden, E., Arnason, A. H., Zhang, J.-T., Stefanski, C. D., and Prosperi, J. R. (2017). APC loss in breast cancer leads to doxorubicin resistance via STAT3 activation. *Oncotarget* 8 (61), 102868–102879. doi:10.18632/oncotarget.22263

Wang, J., Feng, D., and Gao, B. (2021a). An overview of potential therapeutic agents targeting WNT/PCP signaling. *Handb. Exp. Pharmacol.* 269, 175–213. doi:10.1007/164_2021_533

Wang, J., Zhao, G., Condello, S., Huang, H., Cardenas, H., Tanner, E. J., et al. (2021b). Frizzled-7 identifies platinum-tolerant ovarian cancer cells susceptible to ferroptosis. *Cancer Res.* 81 (2), 384–399. doi:10.1158/0008-5472.CAN-20-1488

Wang, W., Cho, U., Yoo, A., Jung, C. L., Kim, B., Kim, H., et al. (2022). Wnt/β-Catenin inhibition by CWP232291 as a novel therapeutic strategy in ovarian cancer. *Front. Oncol.* 12, 852260. doi:10.3389/fonc.2022.852260

Weng, Y.-T., Chien, T., Kuan, I. I., and Chern, Y. (2018). The TRAX, DISC1, and GSK3 complex in mental disorders and therapeutic interventions. *J. Biomed. Sci.* 25 (1), 71. doi:10.1186/s12929-018-0473-x

Winter, M., Sombroek, D., Dauth, I., Moehlenbrink, J., Scheuermann, K., Crone, J., et al. (2008). Control of HIPK2 stability by ubiquitin ligase Siah-1 and checkpoint kinases ATM and ATR. *Nat. Cell Biol.* 10 (7), 812–824. doi:10.1038/ncb1743

Xu, M., Yu, Q., Subrahmanyam, R., Difilippantonio, M. J., Ried, T., and Sen, J. M. (2008). Beta-catenin expression results in p53-independent DNA damage and oncogene-induced senescence in prelymphomagenic thymocytes *in vivo*. *Mol. Cell. Biol.* 28 (5), 1713–1723. doi:10.1128/MCB.01360-07

Yamamoto, T. M., McMellen, A., Watson, Z. L., Aguilera, J., Ferguson, R., Nurmemmedov, E., et al. (2019). Activation of Wnt signaling promotes olaparib resistant ovarian cancer. *Mol. Carcinog.* 58 (10), 1770–1782. doi:10.1002/mc.23064

Yang, Y., Lei, T., Du, S., Tong, R., Wang, H., Yang, J., et al. (2018). Nuclear GSK3β induces DNA double-strand break repair by phosphorylating 53BP1 in glioblastoma. *Int. J. Oncol.* 52 (3), 709–720. doi:10.3892/ijo.2018.4237

Ye, Z., Shi, Y., Lees-Miller, S. P., and Tainer, J. A. (2021). Function and molecular mechanism of the DNA damage response in immunity and cancer immunotherapy. *Front. Immunol.* 12, 797880. doi:10.3389/fimmu.2021.797880

Zhang, D., Wang, H., and Tan, Y. (2011). Wnt/β-catenin signaling induces the aging of mesenchymal stem cells through the DNA damage response and the p53/p21 pathway. *PloS one* 6 (6), e21397. doi:10.1371/journal.pone.0021397

Zhang, Y., and Wang, X. (2020). Targeting the Wnt/β-catenin signaling pathway in cancer. *J. Hematol. Oncol.* 13 (1), 165. doi:10.1186/s13045-020-00990-3

Zhao, Y., Tao, L., Yi, J., Song, H., and Chen, L. (2018a). The role of canonical Wnt signaling in regulating radioresistance. *Cell. physiology Biochem. Int. J. Exp. Cell. physiology, Biochem. Pharmacol.* 48 (2), 419–432. doi:10.1159/000491774

Zhao, Y., Yi, J., Tao, L., Huang, G., Chu, X., Song, H., et al. (2018b). Wnt signaling induces radioresistance through upregulating HMGB1 in esophageal squamous cell carcinoma. *Cell Death Dis.* 9 (4), 433. doi:10.1038/s41419-018-0466-4

Zhu, X., Chen, L., Huang, B., Li, X., Yang, L., Hu, X., et al. (2021). Efficacy and mechanism of the combination of PARP and CDK4/6 inhibitors in the treatment of triple-negative breast cancer. *J. Exp. Clin. Cancer Res.* 40 (1), 122. doi:10.1186/s13046-021-01930-w

frontiers | Frontiers in Oncology

TYPE Original Research
PUBLISHED 18 August 2023
DOI 10.3389/fonc.2023.1220038

OPEN ACCESS

EDITED BY
Ayaz Shahid,
Western University of Health Sciences, United States

REVIEWED BY
Runtian Wang,
Nanjing Medical University, China
Pengcheng Wang,
Capital Medical University, China

*CORRESPONDENCE
Geng Wang
12190816@qq.com

RECEIVED 12 May 2023
ACCEPTED 31 July 2023
PUBLISHED 18 August 2023

CITATION
Zhang D, Wang M, Huang X, Wang L, Liu Y, Zhou S, Tang Y, Wang Q, Li Z and Wang G (2023) GLS as a diagnostic biomarker in breast cancer: in-silico, in-situ, and in-vitro insights.
Front. Oncol. 13:1220038.
doi: 10.3389/fonc.2023.1220038

GLS as a diagnostic biomarker in breast cancer: in-silico, in-situ, and in-vitro insights

Danfeng Zhang[1], Man Wang[2], Xufeng Huang[3], Longbin Wang[4], Ying Liu[5], Shujing Zhou[6], Yidan Tang[6], Qi Wang[7], Zhengrui Li[8] and Geng Wang[1]*

[1]Departments of Breast Thyroid Vascular Surgery, Taihe Hospital, Hubei University of Medicine, Shiyan, Hubei, China, [2]Departments of Outpatient Department, Taihe Hospital, Hubei University of Medicine, Shiyan, Hubei, China, [3]Faculty of Dentistry, University of Debrecen, Debrecen, Hungary, [4]Faculty of Life Science, Huazhong Agricultural University, Wuhan, China, [5]Department of Cardiology, Sixth Medical Center, PLA General Hospital, Beijing, China, [6]Faculty of Medicine, University of Debrecen, Debrecen, Hungary, [7]Faculty of Medicine, Jiangsu University, Zhenjiang, China, [8]Faculty of Dentistry, Shanghai Jiaotong University, Shanghai, China

Background: Recently, a novel programmed cell death mechanism, Cuproptosis, has been discovered and found to play an important role in the development and progression of diverse tumors. In the present study, we comprehensively investigated the core gene of this mechanism, GLS, in breast cancer.

Materials and methods: Bulk RNA sequencing data were curated from the TCGA repository to investigate the aberrant expression of GLS over diverse cancer types. Then, we examined its efficacy as a diagnostic biomarker in breast cancer by Area Under Curve (AUC) of the Receiver Operative Characteristic (ROC) curve. Furthermore, by applying siRNA technique, we knocked down the GLS expression level in cancerous cell lines, measuring the corresponding effects on cell proliferation and metastasis. Afterward, we explored the potential implications of GLS expression in the tumor immune microenvironment quantitatively by using several R packages and algorithms, including ESTIMATE, CIBERSORT, etc.

Results: Pan-cancer analysis suggested that GLS was aberrantly over-expressed in many cancer types, with breast cancer being typical. More in-depth analyses revealed the expression of GLS exerted a high ROC-AUC value in breast cancer diagnosis. Through the knock-down of GLS expression, it was found that GLS expression was strongly relevant to the growth and metastasis of tumor. Furthermore, it was also found to be correlated with the immune tumor microenvironment.

Conclusion: We highlighted that GLS expression might be applicable as a diagnostic biomarker in breast cancer and possess significant implications in the growth and metastasis of tumor and the immune tumor microenvironment, sharing new insights into ontological and personalized medicine.

KEYWORDS

breast cancer, bioinformatics, cuproptosis, biomarker, EMT pathway

Introduction

Breast cancer is the most common malignant tumor in women and one of the main causes of disease burden worldwide (1). Despite the significant advances in diagnosis and prognosis, treating patients with advanced stages remains challenging (2–5). To improve the prognosis, early detection, and timely treatment are of great significance. Therefore, revealing new and highly sensitive molecular biomarkers remains critical. Cuproptosis, a newly discovered cell death mechanism, serves an important role in the modification of specific mitochondrial metabolic enzymes, through which it triggers a series of intracellular signaling events and ultimately leads to cellular caseation (6). Earlier studies have also shown that the aberration of copper levels in the serum and tissues of patients with different solid tumors indicates poor clinical outcomes in a fair number of cases (7–10). Indeed, copper as a basic metal ion in most aerobic organisms serves as a structural and catalytic cofactor for many essential biological enzymes (11). Furthermore, in some studies, certain copper chelators were applied in anticancer therapies, such as tetrathiomolybylate, which has shown a clear survival benefit for high-risk triple-negative breast cancer (12, 13). Therefore, it is of ration that utilizing Cuproptosis-related genes to assist in the early screening of breast cancer. GLS, one of the 10 Cuproptosis-related genes, is an encoding gene of glutaminase which is the enzyme catalyzing the hydrolysis of L-β-glutamine into L-glutamate and ammonia. As glutamine metabolism plays an important role in various tumors, GLS has also become a promising therapeutic target in cancer treatment (14, 15). However, back to date, the utilization of GLS in breast cancer diagnosis remains in need. From this end, it is of interest to explore the role of GLS from this aspect. In the present study, by integrating bioinformatics analytics and immunohistochemical (IHC) staining of real-world patient samples from the HPA database, as well as the siRNA technique, we proposed the idea that GLS may serve as a valuable diagnostic biomarker for breast cancer. Figure 1 demonstrates the general design of the present study.

Materials and methods

Data curation

The sequencing data of 10,534 TCGA pan-cancer samples and 15,776 GTEx normal samples were downloaded from the UCSC Xena database. In particular, for breast cancer, raw transcriptomic count data and the normalized mRNA profile fragments per kilobase of exon per million reads (FPKM) of 115 TNBC patients and 113 normal tissues were retrieved.

Logistics modeling and diagnostic nomogram construction

The logistics algorithm was used to model the data so that the predictive ability of GLS expression for breast cancer could be further improved. Subsequently, we established a nomogram for predicting the diagnostic probability of breast cancer using the expression of GLS.

Estimation of the tumor microenvironment condition

The tumor microenvironment condition was assessed quantitatively by calculating the levels of stromal and immune cell infiltration using the expression profiles obtained from the TCGA dataset. This was done by the R package "ESTIMATE" in which the stromal score, immune score, and ESTIMATE score were calculated (16).

Screening of immune cell infiltration

For the analysis of immune cell infiltration, we used the CIBERSORT algorithm which is a strong and robust immunoinformatic method to evaluate the immune cell population based on bulk RNA transcriptome. This was achieved by the R package "immunedeconv" (17).

Single-cell analysis

The single-cell transcriptomic profile of the GSE114727 dataset (18) was recorded in the Gene Expression Omnibus (GEO) database. The visualization was done by the online toolkit TISCH (http://tisch.comp-genomics.org/) (19).

Cell culturing and transfection

The breast cancer cell line, MCF7, was cultured in Huazhong University (April 2023). The medium was specially designed (i.e., DMEM + 10% FBS + 20ng/ml EGF + 0.5ug/mL Hydrocortisone + 10ug/mL Insulin + 1% NEAA + 1% P/S) and regularly changed when the medium colour turned yellowish. The culturing flasks were saved consistently at 37°C in a humidified incubator containing 5% CO2.

The vectors, si-NC and si-GLS were transfected into MCF7 cell line by Liposome 2000 transfection agent (Invitgen, USA) according to the manufacturer's protocol. Sequences of si-NC was: UUCUCCGAACGUGUCACGUTT ACGUGACACGUUCG GAGAATT, and sequences of si-GLS was: GAUGGUGUCAU GCUAGACAAATT UUUGUCUAGCAUGACACCAUCTT.

CCK8 assay

The siRNA-transfected MCF7 cells were fully digested, inoculated into 96-well culture plates at 2 x 10^3 cells per well and incubated at 37° C. The absorptivity was measured every day using the CCK-8 kit, for a total of seven days of incubation. The above procedures were carried out at 450 nm on the advice of the reagent supplier and four secondary wells were retained for the experimental sessions.

Western blotting

We treated the MCF7 cell line with cell lysis buffer at 100°C for a total of 10 min with cells that had been previously rinsed with cold PBS to extract total protein. Prepared proteins were added to a 10% SDS/PAGE grid system and equal amounts of proteins were electrolysed at constant pressure (i.e., 200V) and then transferred to a PVDF membrane. After sealing the membrane with 5% skimmed milk powder for 1h, we incubated it overnight at 4°C with primary antibodies, followed by 1.5h incubation with secondary antibodies. Then, the PVDF membrane strips were washed and visualized, the relative protein abundance was assessed using Image Lab analysis software and ImageJ.

Statistical analysis

R Studio software (v 4.1.0) was used for bioinformatics analytics and GraphPad Prism 5.0 (GraphPad Software, Inc., San Diego, CA) was used for semi-quantification of the real-time PCR and western blot results. The software was also used to generate the relevant charts. The Chi-square test or the Wilcoxon signed-rank test was conducted to calculate the P-values. The correlation analyses were done under the Spearman method. The area under the curve (AUC) and the receiver operating characteristic (ROC) curve were analyzed to determine the predictive accuracy. P-value < 0.05 was deemed statistically significant.

Results

Pan-cancer analysis of GLS expression across various cancer types

Pan-cancer analysis is a widely used and efficient approach to identify the diagnostic value of a specific gene in regard of human tumors (20, 21). Therefore, we first conducted a pan-cancer analysis based on the transcriptomic data from the TCGA database, the result of which revealed that the expression of the GLS gene was significantly down-regulated in diverse cancer types, including but not limited to GBM, KICH, KIRC, and KIRP, etc. (Figure 2A), particularly in the breast cancer (abbreviation: BRCA or BC, Figure 2B). As the TCGA database lacks normal controls, we further combined the transcriptomic data from the GTEx repository for comparison. As a result, the previous observations were confirmed (Figures 2C, D).

Evaluation of the reliability of GLS expression as a diagnostic biomarker in breast cancer

We used the TCGA dataset alone (Figure 3A) and combined it with the GTEx database data (Figure 3B) to plot the receiver operating curves (ROC curves), through which we found that the ROC-AUC values were high (in the case of solely used TCGA dataset, ROC-AUC value = 0.68, and in the case of TCGA-GTEx combination, ROC-AUC value = 0.75), suggesting that GLS may serve as an important diagnostic biomarker breast cancer. Then, we used the logistics algorithm to optimize a model aiming for better diagnostic prediction and constructed a GLS-based nomogram (Figure 3C), with a C-index = 0.680, hindering it possessed a very good clinical diagnostic ability, which once again supported our idea.

By knocking down the GLS expression *via* the siRNA techinique, we found that the down expression of GLS promoted the vitality of tumor cells (Figure 3D).

As we know, the emt pathway has a very important role in cancer deterioration. From the very general aspect, the up regulation of emt pathway is regarded as one of the potential bases of tumor metastasis. On the other hand, E-adherin and N-cadherin, the 2 key proteins in the emt pathway are thought as the most active players that anchor the tumor tissues to their place of origin. Namely, when the 2 proteins are down regulated, the emt

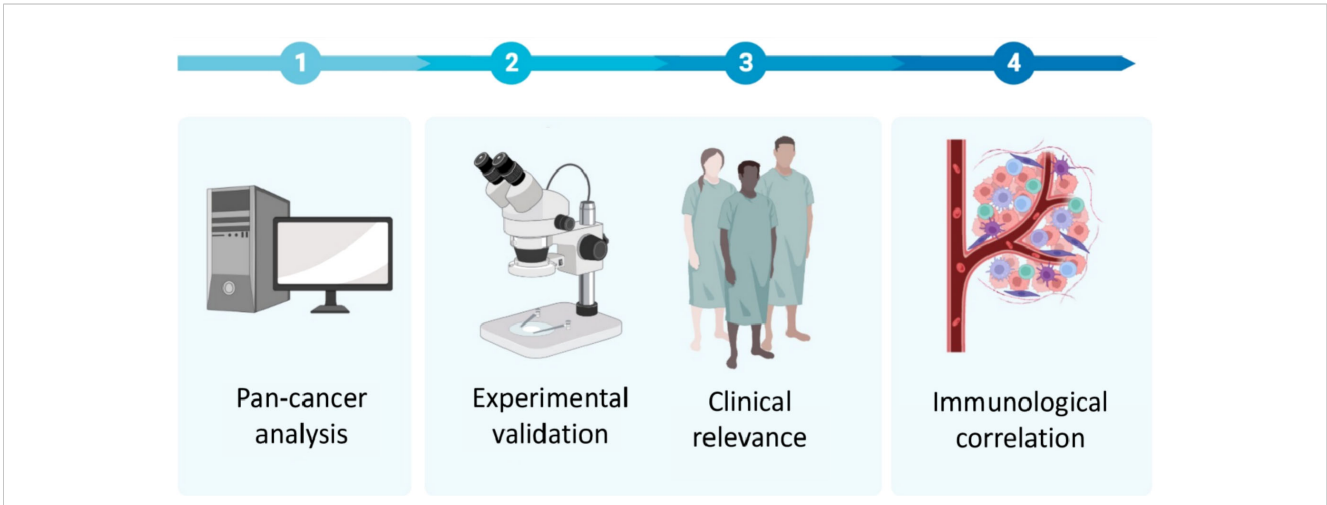

FIGURE 1
Graphical abstract of the present study.

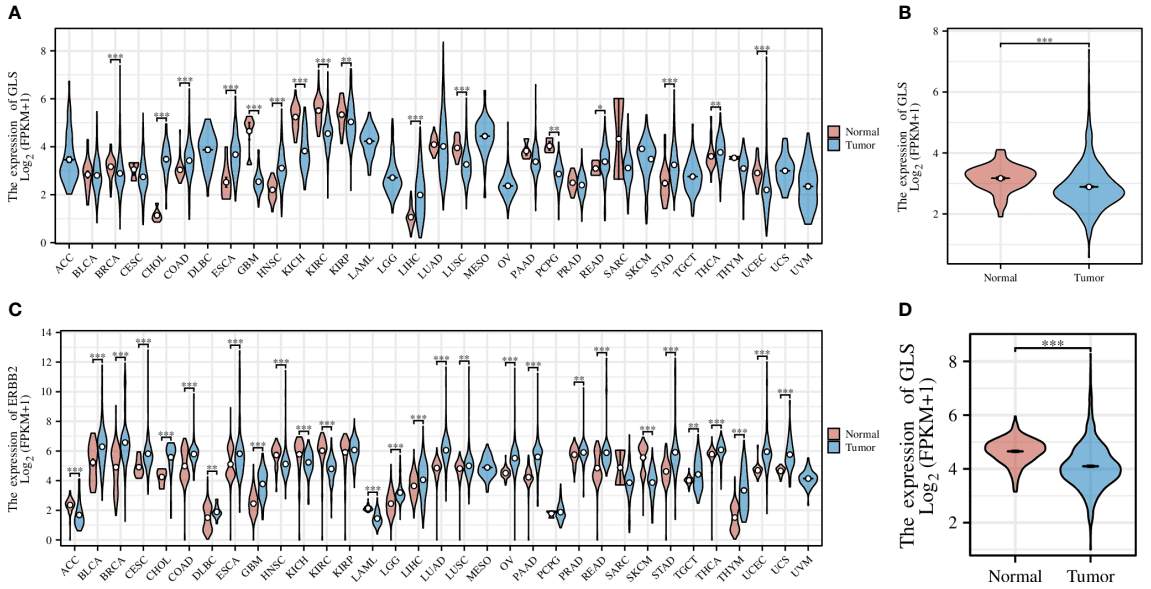

FIGURE 2
Pan-cancer analysis of GLS expression across various cancer types, with the **(A)** TCGA dataset alone and **(C)** combined it with the GTEx data. **(B, D)** Demonstrate the comparison of GLS expression in normal samples and tumor samples, respectively. *P < 0.05, **P < 0.01, ***P < 0.001.

pathway will be activated, and so more likely to have tumor metastasis occurred. Our observation showed that after intervening with si-GLS, the expression levels of both E-cadherin and N-cadherin were significantly decreased, indicating a promoting effect on the pathway, and so the metastasis of the tumor (Figures 3E, F).

The expression of GLS was tightly associated with multiple clinical characteristics of breast cancer

A genetic signature coined as PAM50 composed of 50 genes is commonly used clinically to divide breast cancer into several different molecular subtypes, and even now is still being a critical indicator in the treatment of breast cancer (22). Here we used GLS instead of this signature (Figure 4A) and found that the classification can be performed more efficiently, although the classification is somehow rougher (Luminal type A, Luminal type B, and Her2 type were indistinguishable, thus hereby we termed it as mixed type). The ROC analyses of the comparison between Basal type and mixed type (Figure 4B), between Basal type and Normal type (Figure 4C), and between Normal type and mixed type (Figure 4D) were also conducted. As a result, we found that such GLS-based distinguishments were of high accuracy with high ROC-AUC values, especially in the case of Basal type and mixed type, the ROC-AUC value was up to 0.854.

PR-positive cancer cells may require progesterone to grow. Consequently, these cells may stop growing or die when treated with substances that block the binding and action of progesterone. Therefore, patients with positive PR in the short term have better treatment prospects. In this study, we found that GLS expression was significantly reduced in PR-positive patients than in PR-negative patients (Figure 4E). This conjecture was then confirmed by the subsequent ROC analysis results (AUC-value = 0.681, Figure 4F).

Similar to PR status, ER-positive cancer cells may require estrogen to grow. These cells may stop growing or die when treated with substances that block the binding and action of estrogen. Therefore, patients who are ER-positive in the short term have better treatment prospects. We found that GLS expression was also significantly less in ER-positive patients than in PR-negative patients (Figure 4G). This conjecture was also confirmed by the subsequent ROC analysis results (AUC-value = 0.757, Figure 4H).

Taking them altogether, based on the PR/ER status, it seems that the low expression of GLS may exert adverse effects on the treatment in the short term. In addition, its expression level in breast cancer is lower than that in normal tissues, as such, finding ways to increase its expression level may be a new adjuvant treatment strategy.

Exploration of the immune implications of GLS in breast cancer

We first assessed the association of GLS with the tumor microenvironment by using the ESTIMATE algorithm and found that it was significantly associated with the stromal cells and immune cells (Figure 5A). This conclusion was further

10.3389/fonc.2023.1220038

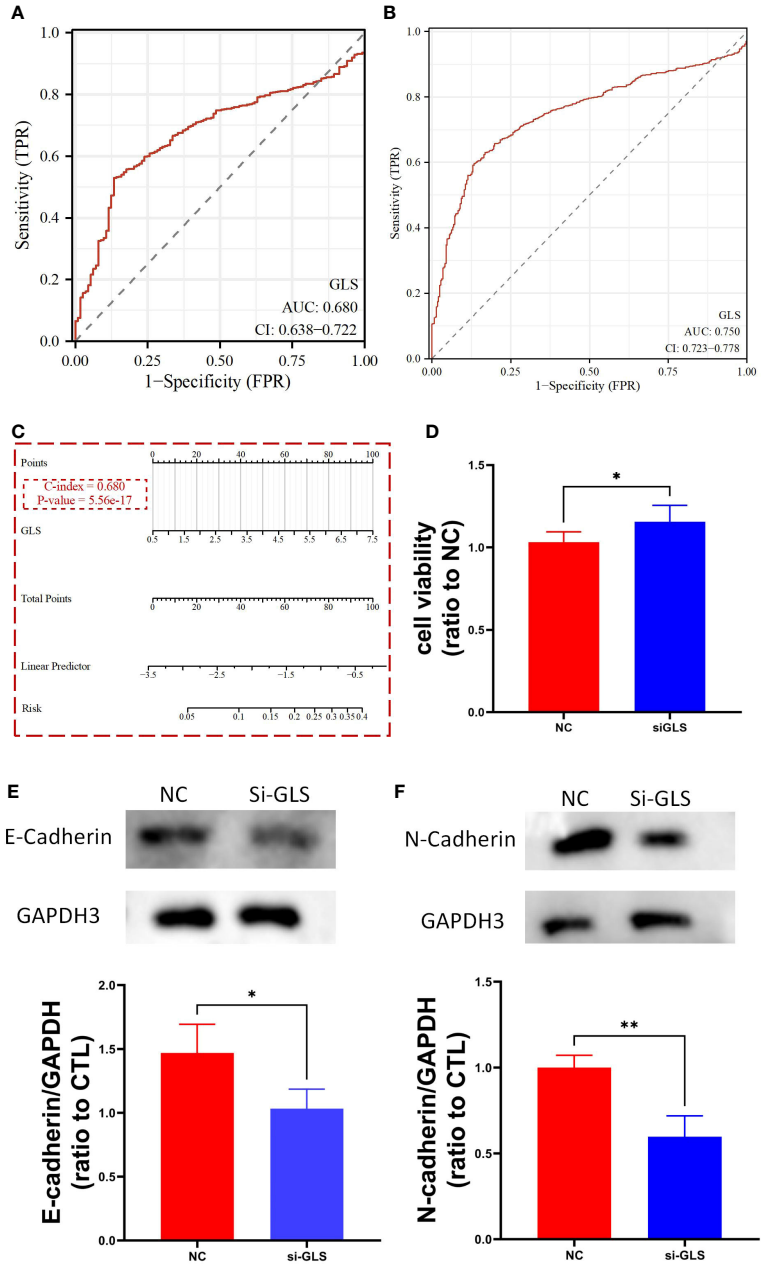

FIGURE 3
GLS expression might serve as a diagnostic biomarker for breast cancer. **(A, B)** Demonstrate the reliability of using GLS expression as a diagnostic biomarker in breast cancer by ROC curves, respectively. **(C)** Diagnostic nomogram utilizing GLS expression as an indicator for breast cancer. **(D)** Is the cck8 result demonstrating the comparison of controlled group (i.e., NC) and siRNA group (i.e., si-GLS) from the aspect of cell viability. In contrast with the controlled group, when GLS expression was impaired, cell viability was significantly better. **(E, F)** Are the western blot images of the 2 key emt pathway proteins (i.e., E-cadherin and Ecadherin) with semi-quantification, respectively. *P < 0.05, **P < 0.01.

strengthened by the group comparison between high- and low-GLS expression (Figure 5B). Then, we performed ssGSEA analysis on a variety of immune cells and the expression of GLS. Subsequently, it was found that GLS extensively affected the infiltration of almost all immune cell types (Figure 5C). This conclusion was also further strengthened by the group comparison of the expression level of GLS (Figure 5D), as well as its visualization at single-cell transcriptome (Figure 5E), which further highlighted the important impact of GLS on the immune microenvironment of breast cancer.

Functional analysis

Through the ssGSEA algorithm, we investigated the functionalities of GLS in breast cancer. It was found that except for DNA repair (Figure 6H), its expression was positively associated with the rest pathways (Figures 6A-G, I).

In addition, we supplemented an analysis of drug sensitivity targeting the GLS gene based on the GDSC repository (Supplementary Figure S1), from that we found KIN001−102, Phenformin, WZ3105, Vinorelbine, and SB52334 were positively

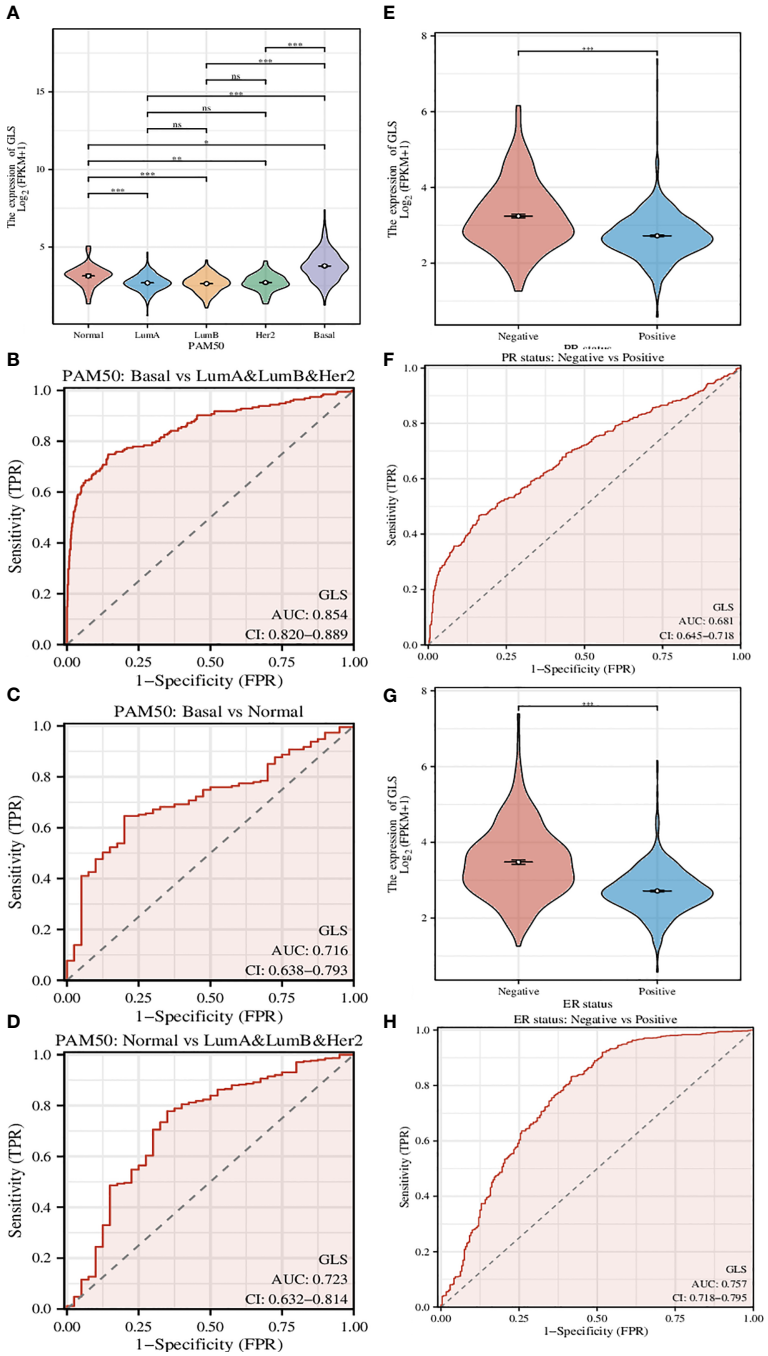

FIGURE 4
Investigation of the correlation between different clinical characteristics and the GLS expression. **(A)** Utilization of GLS expression to classify the molecular subtypes of breast cancer. **(B-D)** ROC curves to assess the reliability of **(A)**. **(E, F)** Utilization of GLS expression to classify the PR positive and negative subtypes of breast cancer, and the ROC curve to assess the reliability. **(G, H)** Utilization of GLS expression to classify the ER positive and negative subtypes of breast cancer, and the ROC curve to assess the reliability. *P < 0.05, **P < 0.01, ***P < 0.001.

related to GLS expression. They might have certain value to be tested in the future.

Discussion

Breast cancer is a life-threatening disease that poses a significant challenge to the world and has been becoming a pivotal cause of global women's cancer death (1). Although the survival outcomes have significantly improved over the past decades, patients with metastatic breast cancer still show poor prognoses (2–5). As such, early detection and genetic screening of breast cancer are of great interest to public health.

On the other hand, Cuproptosis, a novel cell death mechanism induced by copper ion imbalance, has been shown to play a significant role in the development and deterioration of various

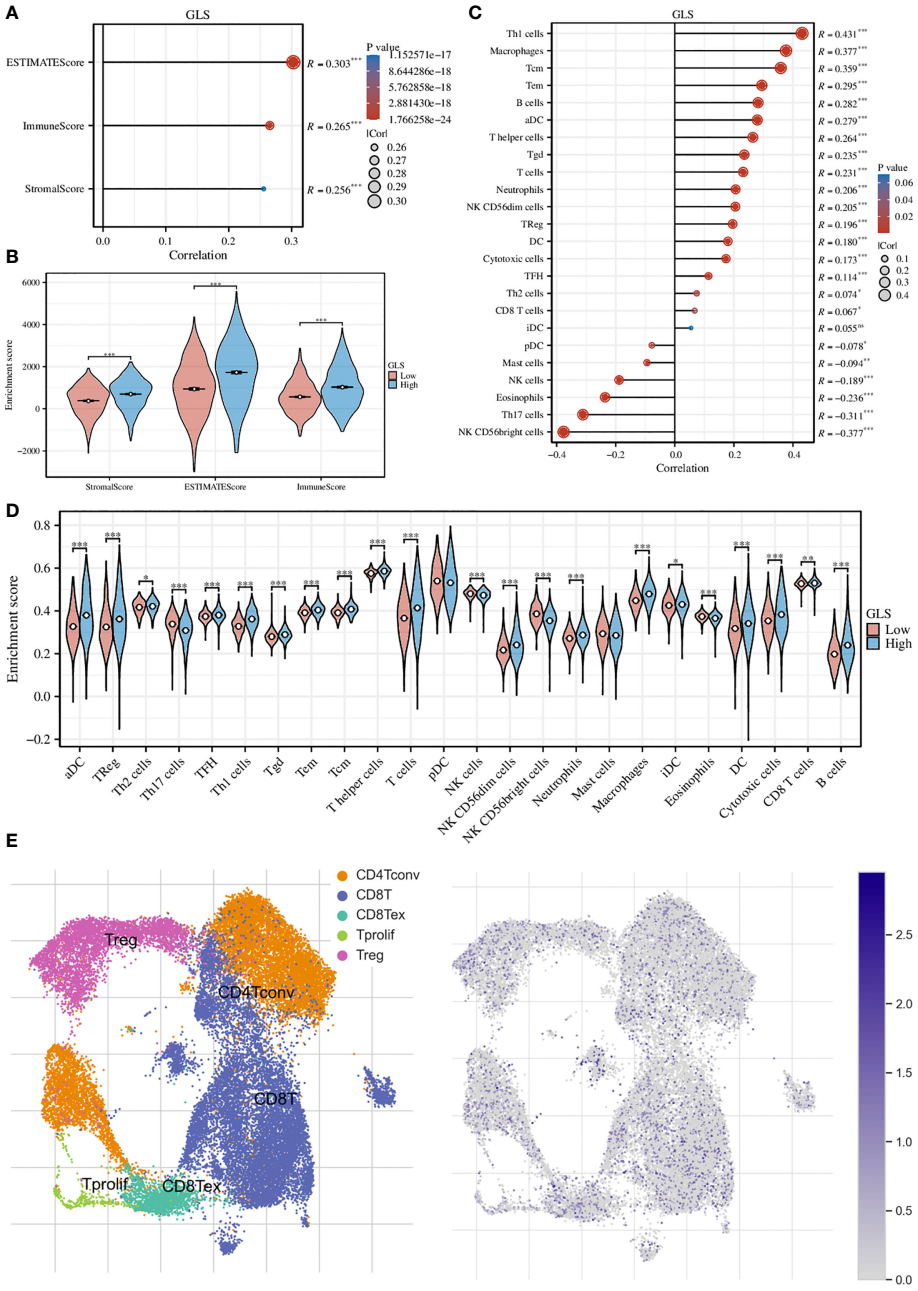

FIGURE 5
Exploration of the immunological implications. **(A)** Correlation analysis of GLS expression and the ESTIMATE, stromal, and immune scores. **(B)** Comparison of the ESTIMATE, stromal, and immune scores in high and low GLS expression groups. **(C)** Correlation analysis of GLS expression and the infiltration of different immune cell types. **(D)** Comparison of immune cell infiltration in high and low GLS expression groups. **(E)** Visualization of the expression of GLS in various immune cells at the single-cell level. The left panel demonstrated the cell populations in the GSE114727 dataset which described the general tumor immune microenvironment in breast cancer, and the right panel showed the GLS expression of each cell within the dataset. *P < 0.05, **P < 0.01, ***P < 0.001.

cancers, indicating that it could serve as a potential biological target for diagnosing or treating these illnesses (6–13). Meanwhile, GLS, the gene encoding glutaminase, is an important Cuproptosis-related gene. The dependence of a plethora of malignancies on glutaminase has prompted the proposition of glutaminase inhibitors as a viable therapeutic strategy for cancer (14, 15).

To date, although previous studies have shown that imbalanced copper metabolism can significantly impact the tumor microenvironment, adjusting the immunotherapy responsiveness, and several researchers even established GLS-involved signatures associated with human cancer cell proliferation and metastasis, there is still a lack of focus on the correlation between GLS and breast cancer. From this end, the present study explored the possibility of using GLS as a diagnostic biomarker for breast cancer and further clarified the underlying mechanisms by the bioinformatics method combined with clinical investigations on real-world samples.

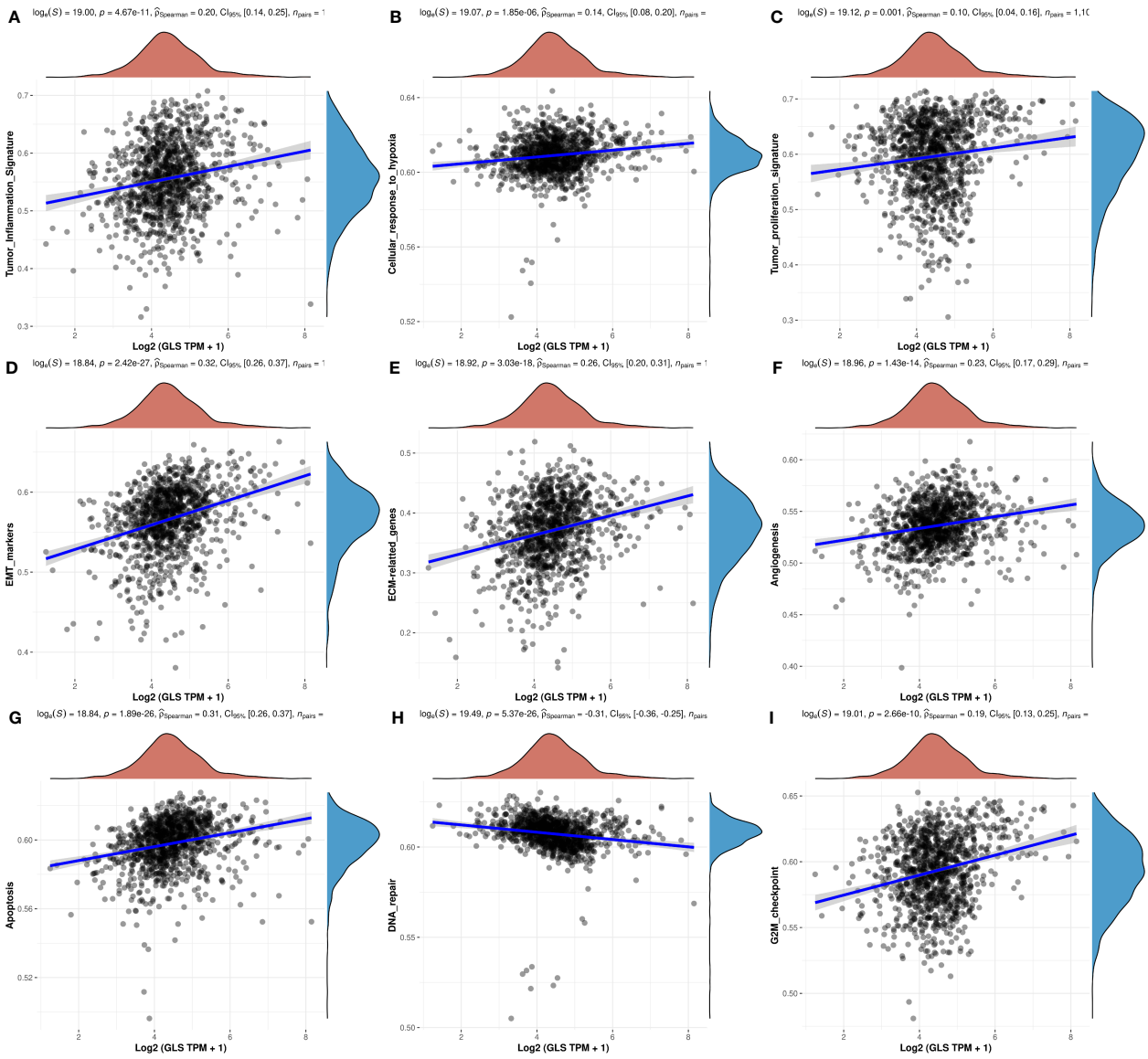

FIGURE 6
Investigation of the functionalities of GLS in breast cancer. Correlation between GLS expression and Tumor Infiltration Signature **(A)**, Cellular response to hypoxia **(B)**, Tumor proliferation signature **(C)**, EMT markers **(D)**, ECM-related genes **(E)**, Angiogenesis **(F)**, Apoptosis **(G)**, DNA repair **(H)**, G2M checkpoint **(I)**, respectively.

We first conducted a pan-cancer analysis, reviewing its expressions in different cancers. As a result, its aberrant expressions were observed in diverse cancer types, especially breast cancer. In breast cancer, it was found that GLS was abnormally expressed which raised our interest in the possibility of utilizing it as a diagnostic biomarker in the future. In fact, the ROC-AUC values in the TCGA cohort alone and combination with GTEx data were surprisingly satisfying. Therefore, we further modeled a diagnostic nomogram aiming to assist physicians in making clinical decisions in their daily practice. More important, we surprisingly found that the expression of GLS could be used for a more efficient classification of molecular subtypes in breast cancer, although certain more exact subtypes were not applicable.

Given that nowadays the detailed interplays of the tumor immune microenvironment (TIME) have been unraveled drastically, its major component, namely the vast diversity of immune cell populations such as regulatory T cells, cytotoxic T cells, helper T cells, B cells, monocytes, etc. are deemed to play a critical role regarding various diseases, including cancers (23–26). Therefore, it was of huge interest to investigate the TIME in the present study. To the best of our knowledge, this is the very first time to explore the relationship between GLS expression and the TIME in breast cancer. We first utilized the ESTIMATE algorithm to examine the association of GLS expression with the TIME. Through quantitatively measuring the stromal and immune landscapes by the ssGSEA method, we found that the expression

of GLS possessed statistically significant impacts in both regards, which was further supported by the comparison of high and low GLS expression groups. More importantly, at the single-cell level, we found its expression was enriched in various immune cells including CD8+ and CD4+ T cells, B cells, and more. These findings suggested that GLS might extensively involve in the shaping of the tumor microenvironment in breast cancer.

In conclusion, in the present study, we performed in-depth bioinformatics analytics of GLS expression in breast cancer, based on which we established a practically useful diagnostic monogram, which to a large extent, cross-supporting the previous research, although form a different aspect (27). Collectively speaking, the idea of using GLS as a biomarker for breast cancer is convincing. Moreover, we provided significant mechanistic insights into GLS's impacts on the tumor microenvironment, focusing on the immune aspect.

Data availability statement

The original contributions presented in the study are included in the article/Supplementary Material. Further inquiries can be directed to the corresponding author.

Author contributions

Conceptualization: XH, DZ, QW, ZL, and GW. Data curation: XH, DZ, MW, SZ, LW, and YT. Formal analysis: XH and DZ. Visualization: XH, YL, SZ, QW and ZL. Writing – original draft: XH, DZ, MW, LW, SZ, YT, QW, ZL, YT, and YL. Writing - review and edition: YL and GW. All authors contributed to the article and approved the submitted version.

Acknowledgments

We want to express our deep gratitude to the public databases, including the TCGA and HPA repositories, and more, for providing open-accessible and high-quality research resources. We also sincerely thank the Fundamental Research Funds for the Central Universities of China for their financial support of our present study.

Conflict of interest

The authors declare that they have no known competing financial interests or personal relationships that could have appeared to influence the work reported in the present study.

Publisher's note

All claims expressed in this article are solely those of the authors and do not necessarily represent those of their affiliated organizations, or those of the publisher, the editors and the reviewers. Any product that may be evaluated in this article, or claim that may be made by its manufacturer, is not guaranteed or endorsed by the publisher.

Supplementary material

The Supplementary Material for this article can be found online at: https://www.frontiersin.org/articles/10.3389/fonc.2023.1220038/full#supplementary-material

SUPPLEMENTARY FIGURE S1
Chemosensitivity test targeting GLS gene expression.

References

1. Sung H, Ferlay J, Siegel RL, Laversanne M, Soerjomataram I, Jemal A, et al. Global cancer statistics 2020: GLOBOCAN estimates of incidence and mortality worldwide for 36 cancers in 185 countries. *CA: Cancer J Clin* (2021) 71(3):209–49. doi: 10.3322/caac.21660

2. Li L, Duns GJ, Dessie W, Cao Z, Ji X, Luo X. Recent advances in peptide-based therapeutic strategies for breast cancer treatment. *Front Pharmacol* (2023) 14:1052301. doi: 10.3389/fphar.2023.1052301

3. Den J, Sisti A. Recent advances in breast cancer diagnosis, treatment, psychology, management, and reconstruction. *Medicina (Kaunas Lithuania)* (2023) 59(2):212. doi: 10.3390/medicina59020212

4. Swain SM, Shastry M, Hamilton E. Targeting HER2-positive breast cancer: advances and future directions. *Nat Rev Drug Discovery* (2023) 22(2):101–26. doi: 10.1038/s41573-022-00579-0

5. Ge J, Zuo W, Chen Y, Shao Z, Yu K. The advance of adjuvant treatment for triple-negative breast cancer. *Cancer Biol Med* (2021) 19(2):187–201. doi: 10.20892/j.issn.2095-3941.2020.0752

6. Tsvetkov P, Coy S, Petrova B, Dreishpoon M, Verma A, Abdusamad M, et al. Copper induces cell death by targeting lipoylated TCA cycle proteins. *Sci (New York NY)* (2022) 375(6586):1254–61. doi: 10.1126/science.abf0529

7. Kahlson MA, Dixon SJ. Copper-induced cell death. *Sci (New York NY)* (2022) 375 (6586):1231–2. doi: 10.1126/science.abo3959

8. Cobine PA, Brady DC. Cuproptosis: Cellular and molecular mechanisms underlying copper-induced cell death. *Mol Cell* (2022) 82(10):1786–7. doi: 10.1016/j.molcel.2022.05.001

9. Jiang Y, Huo Z, Qi X, Zuo T, Wu Z. Copper-induced tumor cell death mechanisms and antitumor theragnostic applications of copper complexes. *Nanomed (London England)* (2022) 17(5):303–24. doi: 10.2217/nnm-2021-0374

10. Duan WJ, He RR. Cuproptosis: copper-induced regulated cell death. *Sci China Life Sci* (2022) 65(8):1680–2. doi: 10.1007/s11427-022-2106-6

11. Chen L, Min J, Wang F. Copper homeostasis and cuproptosis in health and disease. *Signal Transduct Target Ther* (2022) 7(1):378. doi: 10.1038/s41392-022-01229-y

12. Emami F, Aliomrani M, Tangestaninejad S, Kazemian H, Moradi M, Rostami M. Copper-curcumin-bipyridine dicarboxylate complexes as anticancer candidates. *Chem Biodivers* (2022) 19(10):e202200202. doi: 10.1002/cbdv.202200202

13. Ishida S, McCormick F, Smith-McCune K, Hanahan D. Enhancing tumor-specific uptake of the anticancer drug cisplatin with a copper chelator. *Cancer Cell* (2010) 17(6):574–83. doi: 10.1016/j.ccr.2010.04.011

14. Chen Y, Tan L, Gao J, Lin C, Wu F, Li Y, et al. Targeting glutaminase 1 (GLS1) by small molecules for anticancer therapeutics. *Eur J Medicinal Chem* (2023) 252:115306. doi: 10.1016/j.ejmech.2023.115306

15. Jin H, Wang S, Zaal EA, Wang C, Wu H, Bosma A, et al. A powerful drug combination strategy targeting glutamine addiction for the treatment of human liver cancer. *eLife* (2020) 9:e56749. doi: 10.7554/eLife.56749

16. Yoshihara K, Shahmoradgoli M, Martínez E, Vegesna R, Kim H, Torres-Garcia W, et al. Inferring tumour purity and stromal and immune cell admixture from expression data. *Nat Commun* (2013) 4:2612. doi: 10.1038/ncomms3612

17. Sturm G, Finotello F, Petitprez F, Zhang JD, Baumbach J, Fridman WH, et al. Comprehensive evaluation of transcriptome-based cell-type quantification methods for immuno-oncology. *Bioinf (Oxford England)* (2019) 35(14):i436–45. doi: 10.1093/bioinformatics/btz363

18. Azizi E, Carr AJ, Plitas G, Cornish AE, Konopacki C, Prabhakaran S, et al. Single-cell map of diverse immune phenotypes in the breast tumor microenvironment. *Cell* (2018) 174(5):1293–1308.e36. doi: 10.1016/j.cell.2018.05.060

19. Han Y, Wang Y, Dong X, Sun D, Liu Z, Yue J, et al. TISCH2: expanded datasets and new tools for single-cell transcriptome analyses of the tumor microenvironment. *Nucleic Acids Res* (2023) 51(D1):D1425–31. doi: 10.1093/nar/gkac959

20. Xie J, Zhang J, Tian W, Zou Y, Tang Y, Zheng S, et al. The pan-cancer multi-omics landscape of FOXO family relevant to clinical outcome and drug resistance. *Int J Mol Sci* (2022) 23(24):15647. doi: 10.3390/ijms232415647

21. Pan S, Sun S, Liu B, Hou Y. Pan-cancer Landscape of the RUNX Protein Family Reveals their Potential as Carcinogenic Biomarkers and the Mechanisms Underlying their Action. *J Trans Internal Med* (2022) 10(2):156–74. doi: 10.2478/jtim-2022-0013

22. Xie J, Zou Y, Gao T, Xie L, Tan D, Xie X. Therapeutic landscape of human epidermal growth factor receptor 2-positive breast cancer. *Cancer Control J Moffitt Cancer Center* (2022) 29:10732748221099230. doi: 10.1177/10732748221099230

23. Alok A, Seok K, Wesolow J. A case of abdominal pain and diarrhea post immunotherapy: hypophysitis associated with immune checkpoint inhibitors. *J Trans Internal Med* (2022) 10(2):178–80. doi: 10.2478/jtim-2022-0030

24. Tang Y, Tian W, Xie J, Zou Y, Wang Z, Li N, et al. Prognosis and dissection of immunosuppressive microenvironment in breast cancer based on fatty acid metabolism-related signature. *Front Immunol* (2022) 13:843515. doi: 10.3389/fimmu.2022.843515

25. Luo Y, Tian W, Lu X, Zhang C, Xie J, Deng X, et al. Prognosis stratification in breast cancer and characterization of immunosuppressive microenvironment through a pyrimidine metabolism-related signature. *Front Immunol* (2022) 13:1056680. doi: 10.3389/fimmu.2022.1056680

26. Zou Y, Ye F, Kong Y, Hu X, Deng X, Xie J, et al. The single-cell landscape of intratumoral heterogeneity and the immunosuppressive microenvironment in liver and brain metastases of breast cancer. *Adv Sci (Weinheim Baden-Wurttemberg Germany)* (2023) 10(5):e2203699. doi: 10.1002/advs.202203699

27. Budczies J, Pfitzner BM, Györffy B, Winzer KJ, Radke C, Dietel M, et al. Glutamate enrichment as new diagnostic opportunity in breast cancer. *Int J Cancer* (2015) 136(7):1619–28. doi: 10.1002/ijc.29152

frontiers | Frontiers in Pharmacology

TYPE Review
PUBLISHED 24 August 2023
DOI 10.3389/fphar.2023.1257450

OPEN ACCESS

EDITED BY
Pranav Kumar Prabhakar,
Lovely Professional University, India

REVIEWED BY
Jinjun Wu,
Guangzhou University of Chinese Medicine, China
Ali AbdelWahab,
Cairo University, Egypt

*CORRESPONDENCE
Yu Chen,
735405661@qq.com
Xiao Ma,
tobymaxiao@cdutcm.edu.cn
Jinhao Zeng,
zengjinhao@cdutcm.edu.cn

†These authors have contributed equally to this work

RECEIVED 12 July 2023
ACCEPTED 10 August 2023
PUBLISHED 24 August 2023

CITATION
Zhan L, Su F, Li Q, Wen Y, Wei F, He Z, Chen X, Yin X, Wang J, Cai Y, Gong Y, Chen Y, Ma X and Zeng J (2023), Phytochemicals targeting glycolysis in colorectal cancer therapy: effects and mechanisms of action.
Front. Pharmacol. 14:1257450.
doi: 10.3389/fphar.2023.1257450

Phytochemicals targeting glycolysis in colorectal cancer therapy: effects and mechanisms of action

Lu Zhan[1†], Fangting Su[1†], Qiang Li[1†], Yueqiang Wen[2], Feng Wei[1], Zhelin He[3], Xiaoyan Chen[3], Xiang Yin[3], Jian Wang[3], Yilin Cai[1], Yuxia Gong[1], Yu Chen[1*], Xiao Ma[4*] and Jinhao Zeng[5,6*]

[1]Department of Oncology, Hospital of Chengdu University of Traditional Chinese Medicine, Chengdu, China, [2]School of Basic Medicine, Chengdu University of Traditional Chinese Medicine, Chengdu, China, [3]Guang'an Hospital of Traditional Chinese Medicine, Guang'an, China, [4]State Key Laboratory of Southwestern Chinese Medicine Resources, School of Pharmacy, Chengdu University of Traditional Chinese Medicine, Chengdu, China, [5]Department of Gastroenterology, Hospital of Chengdu University of Traditional Chinese Medicine, Chengdu, China, [6]TCM Regulating Metabolic Diseases Key Laboratory of Sichuan Province, Hospital of Chengdu University of Traditional Chinese Medicine, Chengdu, China

Colorectal cancer (CRC) is the third most common malignant tumor in the world, and it is prone to recurrence and metastasis during treatment. Aerobic glycolysis is one of the main characteristics of tumor cell metabolism in CRC. Tumor cells rely on glycolysis to rapidly consume glucose and to obtain more lactate and intermediate macromolecular products so as to maintain growth and proliferation. The regulation of the CRC glycolysis pathway is closely associated with several signal transduction pathways and transcription factors including phosphatidylinositol 3-kinases/protein kinase B/mammalian target of rapamycin (PI3K/AKT/mTOR), adenosine 5′-monophosphate (AMP)-activated protein kinase (AMPK), hypoxia-inducible factor-1 (HIF-1), myc, and p53. Targeting the glycolytic pathway has become one of the key research aspects in CRC therapy. Many phytochemicals were shown to exert anti-CRC activity by targeting the glycolytic pathway. Here, we review the effects and mechanisms of phytochemicals on CRC glycolytic pathways, providing a new method of drug development.

KEYWORDS

colorectal cancer, warburg effect, glycolysis, phytochemicals, molecular pathways

1 Introduction

Colorectal cancer (CRC) ranks third among the globally most prevalent cancers, in terms of incidence and mortality (Sheng et al., 2020). The morbidity and mortality of CRC are consistently increasing, which poses a serious threat to the general population's health (Jian et al., 2020). After initial CRC diagnosis, 20% of the patients develop metastatic disease, and an additional 25% of the patients with initially localized disease will subsequently develop metastasis (Biller and Schrag, 2021). At present, surgical resection and chemo-radiotherapy are the most common treatment options for CRC patients (Liang et al., 2019). Surgery is the only curative treatment of CRC, however, even after radical surgery, a high recurrence rate remains (van der Stok et al., 2017). Further, there is considerable resistance to CRC to

chemotherapy (Van der Jeught et al., 2018). Therefore, the current treatment of CRC is in urgent need of novel and more effective avenues.

The Warburg effect of cancer cells dictates that even under aerobic conditions, cancer cells require glycolysis for energy, which is a hallmark of tumor metabolism (Salimian Rizi et al., 2015). Normal cells generate energy primarily through mitochondrial oxidative phosphorylation, and glycolysis is increased only under hypoxia (Leung et al., 2015). The glucose uptake by cancer cells is markedly higher than that of normal cells, and most of the pyruvate produced is converted to lactic acid through lactate dehydrogenase (LDH). Compared with 36 ATP molecules produced by oxidative metabolism, glycolysis yields only 2 ATP plus 2 lactic acid molecules from 1 molecule of glucose (Gatenby and Gillies, 2004). Although the efficiency of ATP production through glycolysis is lower, the ATP generation rate through glycolysis is nearly 100-fold faster, compared to oxidative phosphorylation (Zhou et al., 2012). Further, rapid aerobic glycolysis produces many intermediates that are conducive to the growth of tumor cells, and these intermediates maintain the proliferation, invasion, and metastasis of tumor cells (Lunt and Vander Heiden, 2011). The metabolic pathway of the Warburg effect has become the focus of tumor treatment in recent years, and its related targeted pathways will be used as an important approach for researching treatment options for colorectal malignancies.

Phytochemicals are an important source of medicines, and plant drugs still play an important role in the treatment of diseases in developing countries (Tamene and Endale, 2019). Despite the rapid development of synthetic drugs, natural compounds remain one of the main sources of drugs (Kazantseva et al., 2022). Approximately 25% of anti-cancer drugs are derived from phytochemicals and contain one or more plant-active ingredients (Kopaskova et al., 2011). At present, many anticancer drugs are derived from phytochemicals, such as vinblastine, paclitaxel, and camptothecin (Wang H. et al., 2018). With the wide application of phytochemicals in cancer treatment and synthetic drug development becoming more difficult, research on anticancer drugs is focused on the development and utilization of phytochemicals and their active substances (Tong et al., 2019), and phytochemicals targeting tumor metabolism have been extensively studied. Moreover, the synergistic effects of phytochemical drugs and anticancer drugs have been attracting attention, as a combination of the two drugs can inhibit the recurrence and metastasis of cancer and reduce the resistance of tumor cells to chemotherapy (Lee et al., 2021). Therefore, it is vital to accelerate the development and utilization of phytochemical drugs for cancer treatment.

Here, we review research on phytochemicals and their active components acting on the glycolysis pathway of CRC cells, and we discuss the molecular mechanisms of phytochemicals targeting the glycolysis pathway to treat CRC. This review will provide a clue for further research on the treatment of CRC targeting the glycolysis pathway.

2 Aerobic glycolysis in CRC

Substantial evidence suggests that metabolic enzymes and transporters associated with the glycolytic pathway are highly expressed in CRC, and these changes may be related to the regulation of several signaling pathways and transcription factors (As shown in Figure 1).

2.1 Upregulation of the glycolytic pathways in CRC

The glycolytic metabolism of CRC cells is closely associated with particular transporters and key enzymes of the glycolytic pathway. Glucose metabolism in cells is mediated by glucose transporters (GLUTs), which occur in the cell membrane. There are 14 subtypes of the GLUT gene (Ancey et al., 2018), of which GLUT1, as one of the most intensively studied membrane transporters, is a key speed-limiting factor of glucose metabolism (Thorens and Mueckler, 2010). This transporter is highly expressed in various cancer tissues, including CRC (Younes et al., 1995; Baer et al., 1997; Mori et al., 2007; Feng et al., 2017), and it has been confirmed to be related to the progress and metastasis of CRC (Younes et al., 1996; Haber et al., 1998). Hexokinase (HK) is a catalytic enzyme that converts glucose into glucose-6-phosphate and is the first rate-limiting enzyme in the glycolysis pathway. There are four types of HK isoenzymes, among which HK2 is abnormally highly expressed in the metabolic pathway of tumor cells, and its expression is closely associated with CRC proliferation and metastasis (Shinohara et al., 1994; Wilson, 2003; Katagiri et al., 2017; Huang et al., 2021). Phosphofructokinase-1, as a catalytic enzyme for the synthesis of 1,6-fructose-diphosphate from fructose-6-phosphate, is one of the key rate-limiting enzymes in the glycolytic pathway. Genes encoding phosphofructokinase-1 activity are highly expressed in CRC (Houddane et al., 2017). The key regulatory enzyme of the pyruvate kinase (PK) glycolysis pathway is responsible for the dephosphorylation of phosphoenolpyruvate to pyruvate and ATP. There are four PK isoenzymes, of which PKM2 is highly expressed in many malignant tumors, including colorectal tumors (Wong et al., 2014; Cui and Shi, 2015; Han et al., 2016). PKM2 maintains the high glycolysis rate of tumor cells and regulates the proliferation of tumor cells (Yu et al., 2015). In the process of tumor glycolysis, most pyruvate is converted into lactic acid by LDH (Li et al., 2020b). LDHA is highly expressed in colorectal and other malignant tumors and is closely related to tumor proliferation and metastasis (Wang et al., 2015; Xian et al., 2015; Cui et al., 2017; Zhao et al., 2017).

Monocarboxylic acid transporters (MCTs) are lactic acid transporters located on the cell membrane, which are responsible for transporting intracellular lactic acid to the exterior of the cell to maintain the pH in tumor cells; further, they are highly expressed in primary CRC and are associated with CRC metastasis and prognosis (Martins et al., 2016). Pyruvate can be converted to acetyl coenzyme A (CoA) under the action of the pyruvate dehydrogenase complex, and enter mitochondria for metabolism through the oxidative phosphorylation pathway (Saunier et al., 2016). Pyruvate dehydrogenase complex acts as the gatekeeper of the oxidative phosphorylation pathway, and the respective enzymes are inhibited in CRC to maintain the high glycolysis rate of CRC and its proliferation and invasion (Hamabe et al., 2014; Ho and Coomber, 2015). Therefore, targeting pyruvate dehydrogenase complex may be a new direction for CRC treatment. The above

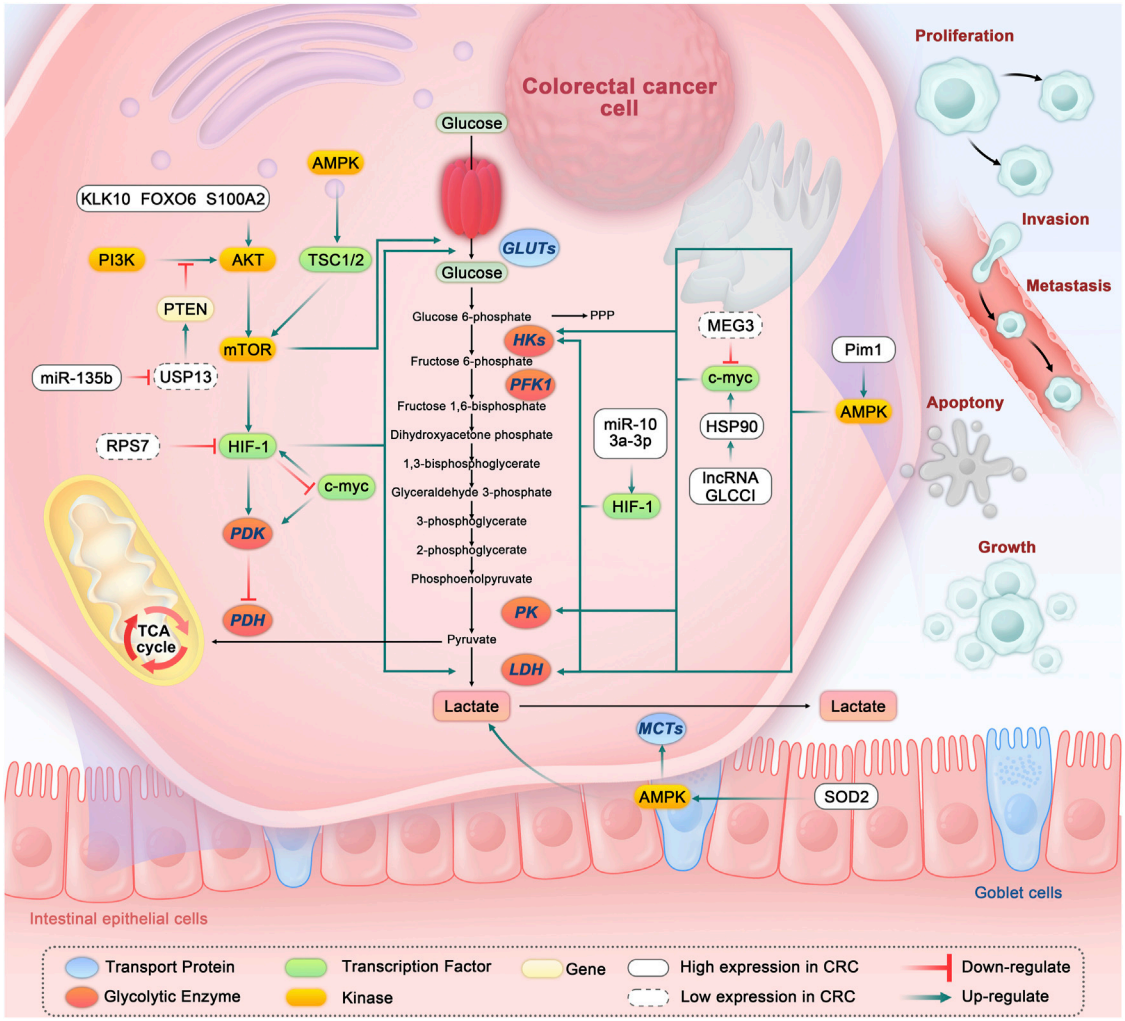

FIGURE 1
Glycolysis in colorectal cancer cells and the related regulatory pathways. Abbreviation: GLUTs, Glucose transporters; HKs, Hexokinases; PFK1, Phosphofructokinase-1; PK, Pyruvate kinase; LDH, Lactate dehydrogenase; PDK, Pyruvate dehydrogenase kinase; PDH, Pyruvate dehydrogenase; AMPK, Adenosine 5′-monophosphate-activated protein kinase; TSC1/2, Tuberous sclerosis complex1/2; AKT, Protein kinase B; mTOR, Mammalian target of rapamycin; HIF-1, Hypoxia-inducible factor-1; PI3K, Phosphatidylinositol 3-kinases; PTEN, Phosphatase and tensin homolog; USP13, Ubiquitin-specific peptidase 13; RPS7, ribosomal protein S7; TCA, Tricarboxylic acid; PPP, Pentose phosphate pathway; HSP90, Heat shock protein 90; MCTs, Monocarboxylic acid transporters; MEG3, lncRNA maternally expressed gene 3; SOD2, Superoxide dismutase 2.

glycolytic metabolic pathways are abnormally expressed in CRC cells and have exacerbating effects on the occurrence and development of CRC.

2.2 Regulatory mechanisms of glycolytic pathways in CRC

Enzymes and transporters related to the CRC glycolysis pathway are abnormally expressed by different molecular regulatory mechanisms, thus leading to the occurrence and development of CRC.

2.2.1 PI3K/AKT/mTOR

PI3K/AKT/mTOR signaling pathway is a cellular signal transduction pathway, which affects cell growth, proliferation, angiogenesis, and other processes (Coutte et al., 2012; He et al., 2022; Hu et al., 2023). Activation of the PI3K/AKT signal pathway plays an important role in maintaining the glucose metabolism of cells, as it can increase glucose intake by increasing the expression of GLUT and upregulate the expression of glycolysis-related enzymes to promote cell glycolysis (Chang et al., 2015; Prabakaran et al., 2018). AKT is frequently overexpressed in most CRC, whereas phosphatase and tensin homolog (PTEN) expression is lost (Robey and Hay, 2009). As a tumor suppressor gene, PTEN negatively regulates the PI3K/AKT/mTOR pathway (Hollander et al., 2011), and deletion of PTEN can specifically increase the protein level of HIF-1α through PI3K signaling (Jiang et al., 2001), mTOR is closely related to cell growth and mTOR expression is regulated by a variety of factors, including the energy regulator AMPK. mTOR can also regulate the expression of HIF-1α by sensing the intracellular level of hypoxia (Martin and Hall, 2005).

Kallikrein-related peptidase, forkhead box class O6, and S100 calcium-binding protein A2 are highly expressed in CRC and play an activating role in glycolysis by activating PI3K/AKT/mTOR pathway and up-regulating GLUT1 expression (Li et al., 2019; Li C. et al., 2020; Wei et al., 2020). MicroRNAs are non-coding RNA molecules that play a central part in cell differentiation, proliferation, and survival (Rupaimoole and Slack, 2017). MiR-135b is highly expressed in CRC cells, which can activate PI3K pathway and promote glycolysis of CRC cells by down-regulating the expression of ubiquitin-specific peptidase 13 and reducing the stability of PETN (Xiang et al., 2015).

2.2.2 AMPK

AMPK is a conservative Ser/Thr protein kinase, which regulates cell metabolism and maintains the dynamic balance of cell metabolism, thus it is referred to as a regulator of energy homeostasis (Faubert et al., 2013; Narayanankutty, 2019). AMPK is activated by sensing the increase of AMP and ATP (Tokunaga et al., 2019). Once activated, AMPK will immediately block the energy consumption process of cells, and turn to increase the ATP decomposition process (Wang and Guan, 2009). AMPK is an important kinase of cell metabolism and has been widely studied in many metabolic diseases (Towler and Hardie, 2007).

Superoxide dismutase 2 (SOD2) is a key antioxidant enzyme that is highly expressed in CRC. The reduction of SOD2 can significantly downregulate AMPK phosphorylation and the expression of MCT4 and L-lactate and ultimately inhibit the migration and glycolytic metabolism of CRC cells (Zhou C. et al., 2020). Pim1 is an oncogene promoting the growth and metastasis of CRC, which is highly expressed in CRC cells, and it has been found that pim1 can upregulate the expression of HK2 and LDHA in CRC cells, which may be related to the activation of the AMPK pathway under glucose deprivation (Zhang et al., 2018).

2.2.3 HIF-1

Compared with normal cells, the oxygen consumption of tumor cells is markedly increased to maintain cancer cells rapid proliferation, thus leading to relative hypoxia in the local microenvironment (Georges et al., 2018). HIF plays a critical role in driving tumor growth, invasion, and metastasis and is found to be highly expressed in most solid tumors (Kumar and Gabrilovich, 2014; Jiang et al., 2020). HIF - 1 has been demonstrated to participate in regulating key transcription factors of EMT and indirectly promotes EMT by Notch, TGF-β, Wnt, and Hedgehog signal pathways, thereby promoting tumor invasive metastasis (Rankin and Giaccia, 2016). HIF-1 can also induce the expression of the epidermal growth factor receptor (EGFR), transforming growth factor-β, insulin-like growth factor 2 to promote tumor angiogenesis (Bui et al., 2022). HIF has been confirmed to be involved in the glycolytic pathway of tumor cells, and it can directly upregulate the expression of glycolysis-related transporters and key enzymes such as GLUT, PFK, LDH, HK, etc. (Song et al., 2016). At the same time, HIF can also be activated by PI3K/AKT (Yeh et al., 2018), YAP/TAZ (Simula et al., 2022), hippo/YAP1 (Sun et al., 2020) and other signaling pathways to further promote the glycolytic process of tumor cells.

miR-103a-3p is an oncogene that is highly expressed in CRC tissues and cell lines and promotes the glycolysis pathway and proliferation, invasion, and migration of CRC cells by up-regulating the transcription of HK2, LDHA, and PKM1 through the Hippo/YAP1/HIF1α axis (Sun et al., 2020). The ribosomal protein S7 gene (RPS7), as a tumor suppressor gene plays a role in inhibiting glycolysis of CRC cells by inhibiting the expression of HIF-1α, GLUT4, and LDHB (Zhang et al., 2016).

2.2.4 Myc

Myc is highly overexpressed in human cancers, thus providing energy for tumor growth and proliferation and the synthesis of substrates required for the respective metabolism pathways (Dang et al., 2006; Miller et al., 2012). c-myc can directly upregulate the expression of LDHA and promote the conversion of pyruvate to lactic acid, and it can upregulate the expression of enzymes related to glycolytic pathways, such as HK2 and phosphoinositide-dependent protein kinase 1, and promote the glycolytic metabolism of cells (Dang et al., 2006; Miller et al., 2012). Myc is inhibited by HIF-1α, however, the two show synergistic effects in regulating the expression of glycolysis-related enzymes including HK2 and PDK1 (Yeung et al., 2008).

Long non-coding RNAs (lncRNAs) are commonly involved in tumor metabolic rewiring and immune cell infiltration and functioning (Zhang Y. et al., 2021). The lncRNA maternally expressed gene 3 (MEG3) reduces glycolytic levels in CRC cells by degrading the expression of c-myc, including down-regulating the expressions of glycolysis-related enzymes such as LDHA, PKM2, and HK2 (Zuo et al., 2020). Thus, MEG3 expression is inhibited in CRC cells (Zuo et al., 2020). Glycolysis-associated lncRNA of colorectal cancer (lncRNA GLCC1) interacts with heat shock protein90 (HSP90) to stabilize c-myc transcription and thus target c-myc-mediated LDHA expression (Tang et al., 2019).

3 Targeting glycolysis in colorectal cancer therapy

Increasing evidence suggests that metabolic reprogramming is closely related to the occurrence and development of most tumors, including CRC (Nenkov et al., 2021). Cancer cells show a significant increase in aerobic glycolysis in their metabolism, making them potentially more susceptible to inhibition of glycolytic pathways than normal cells. Numerous studies on CRC metabolic pathways attempted to identify new therapeutic directions, including the glycolysis pathway, and the drug-targeting glycolysis pathway is an attractive strategy for CRC therapy.

lncRNAs play an important role in the epigenetic regulation of cancer progression by regulating cell function and development (Zheng et al., 2021). Some lncRNAs are highly expressed in CRC, and they exert anti-tumor effects by regulating the glycolytic pathway (Wang Y. et al., 2019; Liu et al., 2020; Li C. et al., 2021). Chemotherapeutic resistance is a major challenge in CRC treatment, and reprogramming of glucose metabolism is also associated with chemical drug resistance, and high glycolysis levels found in human CRC drug-resistant models (Wang T. et al., 2018). Targeted inhibition of the glycolytic pathway can increase the sensitivity of CRC cells to chemotherapy drugs (Cao et al., 2018; An and Ha, 2022). 5-FU is an important drug in first-line

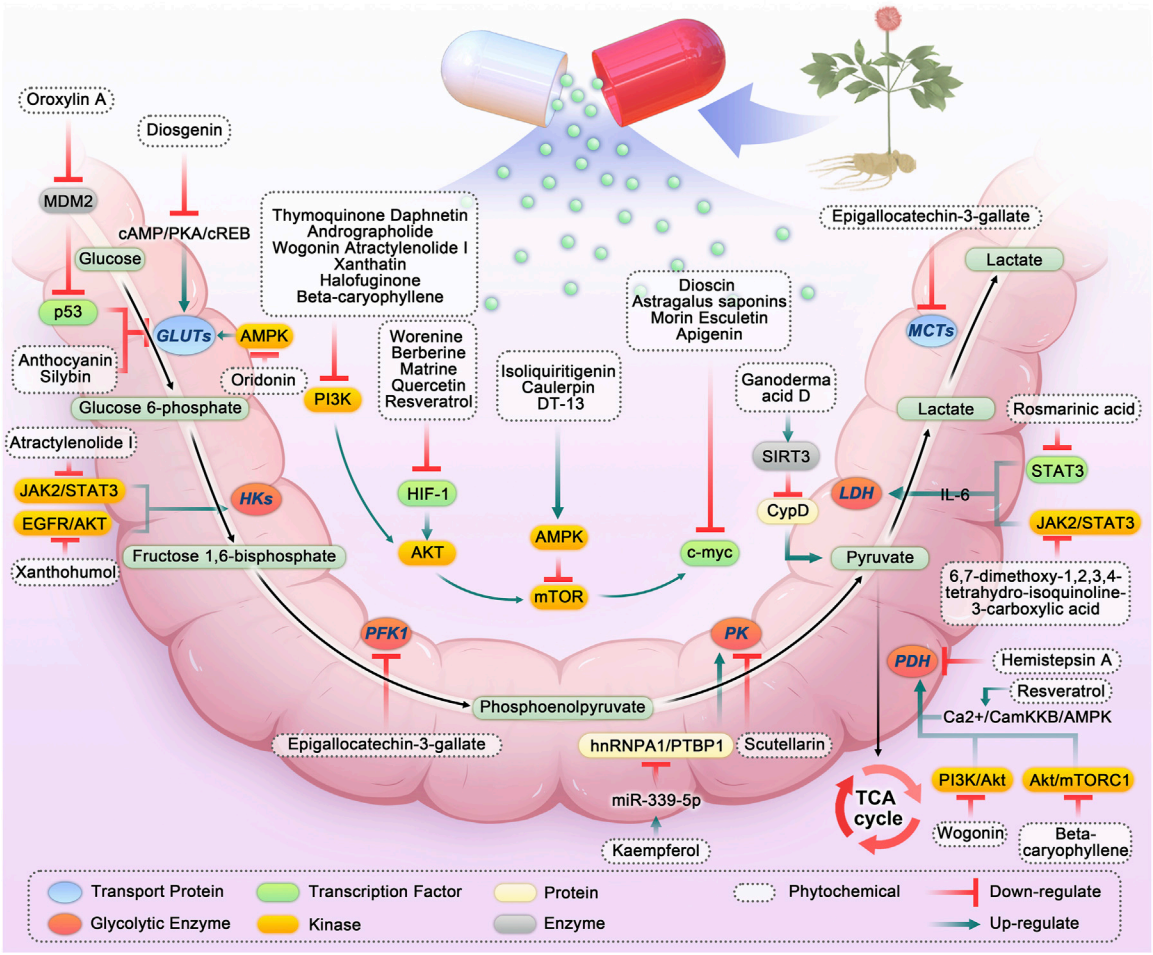

FIGURE 2
Phytochemicals targeting glycolysis in colorectal cancer. Abbreviation: HKs, Hexokinases; PFK1, Phosphofructokinase-1; PK, Pyruvate kinase; LDH, Lactate dehydrogenase; MCTs, Monocarboxylic acid transporters; PDH, Pyruvate dehydrogenase; TCA, Tricarboxylic acid; IL-6, Interleukin 6; SIRT3, Sirtuin-3; JAK2/STAT3, Janus kinase 2/signal transducer and activator of transcription 3; PI3K, Phosphatidylinositol 3-kinases; AKT, Protein kinase B; HIF-1, Hypoxia-inducible factor-1; AMPK, Adenosine 5′-monophosphate-activated protein kinase; hnRNPA1, Heterogeneous nuclear ribonucleoprotein A1; PTBP1, polypyrimidine tract-binding protein 1; PTEN, Phosphatase and tensin homolog.

chemotherapy for CRC. In CRC cells resistant to 5-FU, glucose uptake and lactic acid production increase, and glycolysis-related enzymes and GLUT1 and MCT1/4 are significantly upregulated, which may be related to the activation of PI3K/AKT and the Wnt/β-catenin signaling pathway by upregulation of HIF-1α (Dong et al., 2022). The onset of CRC is closely associated with intestinal environment disorders caused by lifestyle and dietary habits, thus probiotics show promising prospects in the treatment of CRC (Donovan et al., 2017; Eslami et al., 2020). Butyrate, a short-chain fatty acid produced by bacterial fermentation of dietary fibers in the colon, was the first probiotic identified as a histone deacetylase inhibitor, which may be related to the inhibition of the Warburg effect in CRC (Hamer et al., 2008; Donohoe et al., 2012; Eslami et al., 2020).

In conclusion, the glycolytic pathway can affect the occurrence and development of CRC through various processes. Therefore, studying the mechanism of CRC and reprogramming glucose metabolism in tumor cells may provide a new research strategy for CRC treatment (Vasaikar et al., 2019).

4 Methods

We conducted a comprehensive literature search using the Web of Science, PubMed, Embase, SpringerLink, ScienceDirect, and EBSCO databases from the beginning of the database to 30 September 2022 and collated and analyzed the literature for this review. The literature search was conducted by two authors independently and separately to minimize potential oversights. This review evaluates and summarizes all previous scientific studies on the effects of phytochemicals on CRC glycolysis pathways. In PubMed, we used MeSH search terms such as "colorectal neoplasm," "colorectal cancer," "glycolysis," "Embden Meyerhof pathway," "Warburg effect," "phytochemicals" and "natural product." We excluded non-experimental articles and repeated articles in the search process.

Through screening and summarizing plant chemicals targeting the CRC glycolytic pathway, we found that numerous *in vitro* and *in vivo* studies confirmed that plant chemicals can target the CRC glycolytic pathway and exert anti-cancer effects (As shown in

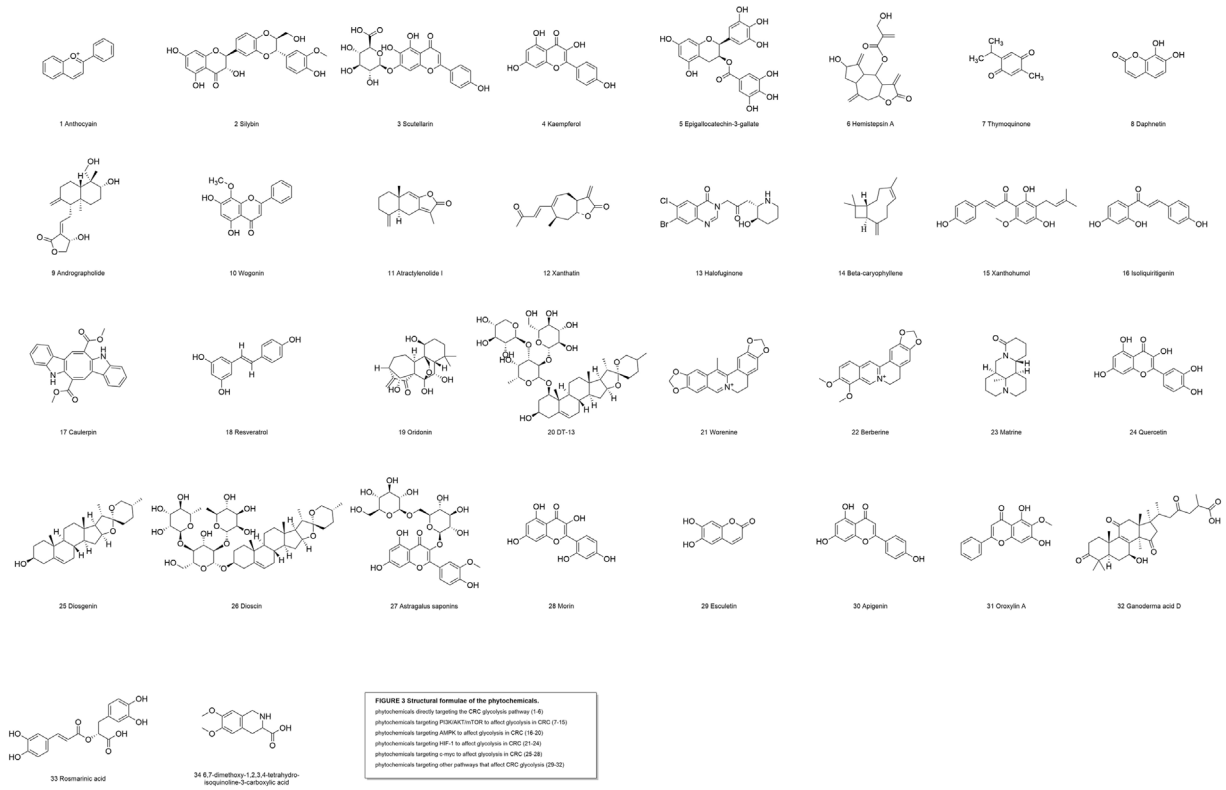

FIGURE 3
Structural formulae of the phytochemicals.

Figures 2, 3; Table 1). Here, the targets affecting the glycolytic pathway are divided into 1) phytochemicals directly targeting the CRC glycolysis pathway; 2) phytochemicals targeting PI3K/AKT/mTOR to affect glycolysis in CRC; 3) phytochemicals targeting AMPK to affect glycolysis in CRC; 4) phytochemicals targeting HIF-1 to affect glycolysis in CRC; 5) phytochemicals targeting c-myc to affect glycolysis in CRC; 6) phytochemicals targeting other pathways that affect CRC glycolysis.

5 Phytochemicals targeting signal pathways and transcription factors in the CRC glycolysis pathway

5.1 Phytochemicals directly targeting CRC glycolysis pathway

5.1.1 Anthocyanin

Anthocyanin (ANC) is a flavonoid that is common in plants (McGhie and Walton, 2007). And after glycosylation, ANC glycosides can be rapidly absorbed by the human body (McGhie et al., 2003). Cyanidin-3-glucoside, a member of the anthocyanin family, is found in purple or red vegetables and fruits (Shan et al., 2021). A comparative study using cyanidin-3-glucoside and its anthocyanidin aglycone showed that cyanidin-3-glucoside significantly inhibited the expression of GLUT1 in MC38 (mouse colon cancer cells), and it can disturb glucose transport, inhibit energy metabolism, and cause mitochondrial damage and apoptosis in CRC cells (Jing et al., 2020).

5.1.2 Silybin

Silybin is the major component of silymarin, a flavonolignan mixture extracted from the fruits of *Silybum marianum* (L.) Gaertner displays antioxidant, anti-inflammatory, immunomodulatory and hepatoprotective properties (Chambers et al., 2017). Compared with doxorubicin-sensitive LoVo cells (LoVo WT), doxorubicin-resistant LoVo cells (LoVo DOX) show higher mRNA and protein expression levels of glycolysis-related enzymes, such as GLUT1 and MCT4 (Catanzaro et al., 2018). Further, it also shows a tendency for metabolic transfer from the oxidative phosphorylation pathway to the glycolysis pathway. After treatment of cells with silybin 10–50 μM, glucose uptake and GLUT1 expression is downregulated in sensitive and drug-resistant LoVo cells in silybin 10 μM, and silybin 50 μM resulted effective only in resistant cells (Catanzaro et al., 2018).

5.1.3 Scutellarin

Scutellarin is a flavonoid drug derived from the plant *Erigeron breviscapus* (Vant.) Hand.-Mazz. (Chen et al., 2006; Dong and Qu, 2022). *Erigeron breviscapus* (Vant.) Hand.-Mazz. is a Chinese herbal medicine that was first recorded in South Yunnan Materia Medica with multiple pharmacological effects and clinical applications, such as detoxification, inflammation reduction and pain relief (Chen et al., 2006; Dong and Qu, 2022). Studies have found that Oxaliplatin-resistant CRC cells (OR-SW480 and OR-HT29)

TABLE 1 Phytochemicals targeting glycolysis for colorectal cancer therapy.

Signal pathways and transcription factors in glycolysis	Compound	Source	Experimental model		Efficacy	Mechanism	Experimental dosage	References
			In vitro	*In vivo*				
GLUT1	Anthocyanin (Flavonoids)	*grape, mulberry, and raspberry*	MC38	—	Disturbtion of glucose transport; inhibition of energy metabolism	↓GLUT1	500,1000, 2000 μM (24 h)	Jing et al. (2020)
	Silybin (Flavonoids)	*Silybum marianum* (L.) *Gaertner*	LoVo	—	Downregulation of the glucose uptake	↓GLUT1	5, 10, 50 μM (24/48/72 h)	Catanzaro et al. (2018)
PKM2	Scutellarin (Flavonoids)	*Erigeron breviscapus* (Vant.) Hand.-Mazz.	SW480 HT29	OR-SW480 cells mouse model	Induction of apoptosis; reduction of ATP product; inhibition of glycolysis	↓PKM2	2 μM 10 μg/kg	Sun et al. (2021)
	Kaempferol (Flavonoids)	*Acacia nilotica* (L.) Delile, *Aloe vera* (L.) Burm.f., *Crocus sativus* L.	HCT116 DLD1	—	Inhibition of glycolysis and ATP product; induction of apoptosis	↑miR-339-5p; ↓hnRNPA1; ↓PTBP1; ↓PKM2	0, 50, 100 μM (48 h)	Wu et al. (2021)
MCT4	Epigallocatechin-3-gallate (Polyphenols)	*green tea*	HCT116; HT29	—	Inhibition of the proliferation, migration and metastasis; Inhibition of glycolysis	↓PFK; ↓MCT4	25, 50, 100 μM	Chen et al. (2022)
PDH	Hemistepsin A (Sesquiterpene lactone)	*Hemistepta lyrata*	DLD1 CT26	CT26 cells xenograft tumors	Inhibition of cell growth; inhibition of glycolysis; induction of apoptosis	↓PDK1; ↓PDHA1	0,5,7.5.10 μM(4 h) 1 mg/kg, 10 mg/kg	Jin et al. (2020)
PI3K/AKT/mTOR	Thymoquinone (Quinones)	*Nigella sativa*	HCT116; SW480	—	Inhibition of proliferation and migration; induction of apoptosis; inhibition of glycolysis and ATP product	↓PI3K; ↓AKT; ↓HK2	21.71 μM, 20.53 μM	Karim et al. (2022)
	Daphnetin (Coumarins)	*Daphne Korean Nakai*	SW480 HT29	—	Inhibition of proliferation and migration; induction of apoptosis; inhibition of glycolysis	↓PI3K; ↓AKT; ↓HK2; ↓GLUT1	0, 25, 50 μM (24 h)	He et al. (2018)
	Andrographolide (Diterpenoids)	*Andrographis paniculata*	HCT116	—	inhibition of glycolysis and ATP product	↓HK2; ↓PFK1; ↓GLUT1; ↓PI3K; ↓AKT; ↓mTOR	20 μM	Li et al. (2020c)
	Wogonin (Flavonoids)	*Scutellaria baicalensis*	HCT116	HCT116 cells xenograft mice	inhibition of glycolysis and ATP product; Inhibition of tumor growth	↓PI3K/AKT; ↓HIF-1α; ↓HK2; ↓PDHK1; ↓LDHA; ↓GLUT1	20, 40, 60, 80, 100 μM(24 h) 30, 60 mg/kg; 0, 10, 20, 40 μM	Wang et al. (2014) Zhao et al. (2018)
	Atractylenolide I (Sesquiterpene lactones)	*Atractylodis macrocephalus*	HCT116 Colo205	HCT116 xenograft nude mice	Disruption of glucose metabolism; induction of apoptosis; inhibition of invasion and glycolysis; Inhibition of tumor growth	↓AKT/mTOR→↓GLUT1; ↓LDH; ↓HK2; ↓PKM2; ↓JAK2/STAT3 → ↓HK2	0, 80, 150, 200 μM (24 h) 25, 75 mg/kg; 0, 100, 200 μM (24 h) 50 mg/kg	Wang et al. (2020b) Li et al. (2020d)

(Continued on following page)

10.3389/fphar.2023.1257450

TABLE 1 (*Continued*) Phytochemicals targeting glycolysis for colorectal cancer therapy.

Signal pathways and transcription factors in glycolysis	Compound	Source	Experimental model		Efficacy	Mechanism	Experimental dosage	References
			In vitro	*In vivo*				
	Xanthatin (Sesquiterpene lactones)	*Xanthium strumarium* L.	HT-29 HCT-116	—	inhibition of glycolysis and ATP product	↓mTOR→↓GLUT1; ↓HK1; ↓MCT4	0, 20, 30, 40 μM (24 h)	Li et al. (2022a)
	Halofuginone (Alkaloids)	*Dichroa febrifuga*	SW480 HCT116	HCT116 xenograft nude mice	induction of apoptosis; inhibition of glycolysis; Inhibition of tumor growth	↓AKT/mTORC1→↓P70S6K; ↑4EBP1→↓ HK2; ↓GLUT1	0, 5, 10, 20 nM 0.1 mg/kg	Chen et al. (2015)
	Beta-caryophyllene (Sesquiterpenes)	*Syzygium aromaticum*	CT26	diabetic Balb/c mice	Inhibition of proliferation and glycolysis; induction of apoptosis	↓p-AKT; ↓p-mTOR; ↓c-myc; ↓PDK1; ↓LDHA	50 μM 200 mg/kg	Zhou et al. (2018)
	Xanthohumol (Polyphenol)	*Humulus lupulus* L.	HCT116 SW620 HT29	HT29 and HCT116 cells xenotransplantation mice	Inhibition of proliferation and glycolysis; induction of apoptosis; Inhibition of tumor growth	↓EGFR/AKT→↓ERK1/2→↓HK2	0,2,4,8 μM 10 mg/kg	Liu et al. (2019)
AMPK	Isoliquiritigenin (Flavonoids)	*Glycyrrhiza uralensis, Mongolian glycyrrhiza, Glycyrrhiza glabra*	HCT116	—	Inhibition of proliferation, glycolysis and ATP product; induction of apoptosis	↑AMPK→↓AKT/mTOR→↓ENO1; ↓ALDOA; ↓LDHA; ↓MCT4; ↓c-myc; ↓HIF-1α	12.5, 25, 50, 100 μM	Wang et al. (2020a)
	Caulerpin (Alkaloids)	*Caulerpa racemosa, C. serrulata*	LoVo SW480	SW480 xenograft nude mice	Disturbtion of glycolysis Delay the tumor growth	↑AMPK→↓mTORC1; ↓GLUT1	5,10,20 μM 30 mg/kg	Yu et al. (2017)
	Resveratrol (Polyphenols)	*pomegranates, berries, peanuts,* and *red wine*	Caco2 HCT116 CT26 HT29	CT26 tumor bearing mice	inhibition of glycolysis; Inhibition of tumor growth	↑Ca2+/CamKKB/AMPK→↑PDH; ↓HIF-1α	10 μM (48 h); 50 μM; 50 μM	Saunier et al. (2017) Jung et al. (2015) Jung et al. (2013)
	Oridonin (Diterpenoid)	*Rabdosia rubescens*	SW480	SW480 xenograft tumors	Inhibition of proliferation and glycolysis; Inhibition of tumor growth	↓AMPK; ↓GLUT1; ↓MCT1	5,10,15,20.25 μM	Yao et al. (2017)
	DT-13 (Saponins)	*Liriope muscari* (Decne.) Bailey	HT29 HCT116 HCT15 COLO205	HCT-15 orthotopic nude mice	Inhibition of proliferation and glycolysis; Inhibition of tumor growth	↑AMPK→↓mTOR→↓GLUT1; ↓HK2; ↓PFKM; ↓LDHA	2.5, 5, 10 μM (72 h) 0.625, 1.25, 2.5 mg/kg	Wei et al. (2019)
HIF-1	Worenine (Alkaloids)	*Coptis chinensis*	HCT116 SW620	—	inhibition of glycolysis	↓HIF-1α→↓GLUT3; ↓HK2; ↓PFK-L; ↓PKM2; ↓LDHA; ↓PKM	50,10,20 μM (24 h)	Ji et al. (2021)
	Berberine (Alkaloids)	*Rhizoma coptidis*	HCT116 KM12C	—	inhibition of glycolysis	↓mTOR; ↓HIF-1α→↓GLUT1; ↓LDHA; ↓HK2	0,6.25,12.5, 25,50,100 μM	Mao et al. (2018)
	Matrine (Alkaloids)	*Sophora flavescens*	HCT116 SW620	—	inhibition of glycolysis	↓HIF-1α→↓GLUT1; ↓HK2; ↓LDHA	0,2,4,6,8 μM	Hong et al. (2019)

(Continued on following page)

10.3389/fphar.2023.1257450

TABLE 1 (*Continued*) Phytochemicals targeting glycolysis for colorectal cancer therapy.

Signal pathways and transcription factors in glycolysis	Compound	Source	Experimental model		Efficacy	Mechanism	Experimental dosage	References
			In vitro	*In vivo*				
	Quercetin (Flavonoids)	*apples, cabbage, cauliflower, and berries*	HCT116	F344 rats	induction of apoptosis; inhibition of glycolysis; upregulation of the mitochondrial fatty acid degradation	↓AMPK→↓HIF-1α→↓VEGF; ↓GLUT1 ↓F-1,6-BP; ↓GAPDH; ↓ENO1; ↓PK ↑3-hydroxy-3-methylglutaryl-CoA synthase 2; ↑acetyl-CoA acyltransferase 1; ↑acyl-CoA dehydrogenase short-chain	100 μM; 10 g/kg	Kim et al. (2012) Dihal et al. (2008).
c-myc	Diosgenin (Saponins)	*legumes, fenugreek, yams*	SW1116 RKO	SW1116 cells xenograft mice	Inhibition of proliferation, invasion and metastasis; induction of apoptosis; inhibition of glycolysis; Inhibition of tumor growth	↓cAMP/PKA/CREB→↓GLUT3; ↓GLUT2; ↓PC	20 μM	Li et al. (2021b)
	Dioscin (Saponins)	*Dioscoreae rhizome, Paridis rhizome*	HT29 HCT116 SW480 SW620	HCT116 and HT29 xenograft mice; HT29 and SW620 xenograft mice	Inhibition of proliferation and glycolysis; Inhibition of tumor growth	↓c-myc; ↓Skp2; ↓Cdh1→↓HK2	0, 1, 2, 5 μM, 5 mg/kg; 0,1,2,4 μM, 10 mg/kg	Zhou et al. (2020b), Wu et al. (2020)
	Astragalus saponins (Saponins)	*Astragalus membranaceus*	SW620	DSS-induced colitis mouse model	induction of apoptosis; Inhibition of proliferation and glycolysis	↓c-myc→↓HK2; ↓LDHA	50 μg/mL (0, 12, 24 and 48 h) 0.1 mg/g	Guo et al. (2019)
	Morin (Flavonoids)	*mulberry figs, fustic*	SW480	DMH induce colon cancer model	Reduce the incidence of tumors; inhibition of glycolysis and ATP production; induction of apoptosis	↓β-cateinin/c-myc; ↓GLUT1; ↓HK2; ↓PKM2; ↓LDHA	50 μg/kg 150, 200, and 250 μM (48 h)	Sharma et al. (2017), Sithara et al. (2017)
	Esculetin (Coumarins)	*Fraxinus rhynchophylla* Hance	—	DMH induce colon cancer model	Reduce the incidence of tumors; downregulate the expression of proto-oncogenes; affect tumor metabolism	↓β-cateinin/c-myc ↓GLUT1; ↓HK2; ↓PKM2; ↓LDHA	50 μg/kg	Sharma et al. (2017)
	Apigenin (Flavonoids)	*parsley, celery, chamomile*	HCT116 HT29 DLD1	—	inhibition of the cell survival and colony formation; inhibition of glycolysis	↓β-catenin/c-myc/polypyrimidine tract binding protein 1; ↓PKM2	0, 20, 40 μM	Shan et al. (2017)
p53	Oroxylin A (Flavonoids)	*Scutellaria baicalensis Georgi.*	HCT116	HCT116 xenograft mice	inhibition of glycolysis; Inhibition of tumor growth	↑p53; ↑TIGAR; ↑SIRT3 ↓PGM; ↓GLUT4; ↓MDM2	200 μM (48 h) 100 mg/kg	Zhao et al. (2015)
SIRT3/Cypd	Ganoderma acid D (Triterpenoids)	*Ganoderma lucidum*	HT29 SW620	—	inhibition of glycolysis	↓CypD→↑SIRT3	0,50,100,200 μmol/L	Liu et al. (2018)

(Continued on following page)

10.3389/fphar.2023.1257450

TABLE 1 (*Continued*) Phytochemicals targeting glycolysis for colorectal cancer therapy.

Signal pathways and transcription factors in glycolysis	Compound	Source	Experimental model		Efficacy	Mechanism	Experimental dosage	References
			In vitro	*In vivo*				
IL/STAT3	Rosmarinic acid (Phenylpropanoids)	*Rosmarinus officinalis* L. (Lamiaceae)	HCT8 HCT116	—	inhibition of glycolysis	↓miR-155-5p→↓IL-6/STAT3→↓LDH; ↓HIF-1α	075,150 μmol/L (24 h)	Xu et al. (2016)
	6,7-dimethoxy-1,2,3,4-tetrahydro-isoquinoline-3-carboxylic acid (Alkaloids)	*Mucuna pruriens*	—	DMH induce CRC rats	inhibition of glycolysis	↓IL-6→↓JAK2/STAT3→↓LDH	25 mg/kg	Mishra et al. (2018)

exhibit higher glycolysis rate and high mRNA and protein expression of PKM2, while scutellarin can inhibit the glucose metabolism rate and ATP production of cells by decreasing the PKM2 expression of OR-SW480 and OR-HT29 cells, leading to mitochondrial dysfunction and finally inducing cell apoptosis (Sun et al., 2021). This previous study established an *in vivo* model using OR-SW480 cells injected into 4-week-old female immunodeficient nude BALB/c mice, showing that 10 mg/kg scutellarin reversed the drug resistance of oxaliplatin in the OR-SW480 mouse model, increased apoptosis induced by oxaliplatin, and significantly reduced protein expression of PKM2 and ATP production in the tumor (Sun et al., 2021).

5.1.4 Kaempferol

Kaempferol is a flavonoid compound that occurs in many plants such as *Acacia nilotica* (L.) Delile, *Aloe vera* (L.) Burm.f., and *Crocus sativus* L, and has been shown to be cardioprotective, anti-inflammatory, antidiabetic, antioxidant, antitumor, and have anticancer activities (Devi et al., 2015; Imran et al., 2019). Studies have shown that kaempferol can exert anticancer effects by inducing apoptosis of cancer cells, causing cell cycle arrest and autophagy (Wu et al., 2018). Studies have shown that after Kaempferol treatment, the cell cycle of HCT116 and DLD1 cells is delayed, and apoptosis is upregulated (Wu et al., 2021). In addition, glucose consumption, lactic acid production, and ATP level exhibit a downward trend. Kaempferol can also upregulate the expression of miR-339-5p in HCT116 and DLD1 cells, reducing the expression of hnRNPA1 and PTBP1, leading to the downregulation of PKM2 expression, thereby inhibiting glycolysis of CRC (Wu et al., 2021).

5.1.5 Epigallocatechin-3-gallate

Green tea, which originated in China, is one of the most popular drinks in the world and was used in traditional Chinese medicine to treat many illnesses (Akbarialiabad et al., 2021). Epigallocatechin-3-gallate (EGCG) is mainly sourced from green tea (Nagle et al., 2006). EGCG inhibits the proliferation, migration, and metastasis of HCT116 and HT29 cells (Chen et al., 2022). In addition, in cancer-associated fibroblasts (CAFs) co-cultured with HCT116 and HT29 cells, 50 μM EGCG significantly decreased lactate production, PFK, and MCT4 expression (Chen et al., 2022). After further silencing the expression of MCT4, it was found that the above inhibitory effect of EGCG was reversed. Therefore, it is speculated that EGCG may inhibit the glycolysis of CAFs through MCT4.

5.1.6 Hemistepsin A

Hemisteptia lyrata is a kind of Chinese herb, its leaves and flowers are used for the treatment of sore throat and treatment of tumor (Jang et al., 1999). Hemistepsin A (HsA) is a sesquiterpene lactone isolated from *Hemistepta lyrata* Bunge, which exerts various pharmacological effects including anti-hepatotoxic, anti-inflammatory, and anti-cancer activities (Park et al., 2020). Treatment of various CRC cell lines with HsA showed that HsA had significant cytotoxicity, and significantly inhibited cell growth, but had no significant effect on normal cells (Jin et al., 2020). Further, after treatment with HsA, the extracellular acidification rate (ECAR) of DLD1 and CT26 cells decreased in a dose-dependent manner. Further study of its internal mechanism found that HsA

inhibited the activity of PDK1 by interfering with the interaction between PDK1 protein and lipoamide binding domains of PDH-E2 (L1 and L2), reduced the phosphorylation of PDHA1, and thus inhibited the formation of lactic acid. *In vivo*, experiments showed that HsA (1, 10 mg/kg/day) treated for 10d inhibited the growth of BALB/c mice bearing CT26 cells in a dose-dependent manner, upregulated the expression of apoptosis-related genes, and reduced the phosphorylation of PDHA1, which was consistent with the results of *in vitro* experiments (Jin et al., 2020).

5.2 Phytochemicals targeting PI3K/AKT/mTOR to affect glycolysis in CRC

5.2.1 Thymoquinone

Nigella sativa is a flowering plant that belongs to the Ranunculaceae family, native to south and southwest Asia, and is used to treat a variety of ailments such as diarrhea, asthma, headaches, cough, eczema, and more (Ciesielska-Figlon et al., 2023). Thymoquinone is a bioactive constituent derived from the seeds of *N. sativa* and has shown significant anticancer activity in various tumors (Phua et al., 2021). Thymoquinone significantly inhibits the proliferation, invasion, and metastasis of HCT116 and SW480 cells, induces cell apoptosis, and downregulates the lactic acid production, glucose uptake, and ATP levels of tumor cells (Karim et al., 2022). Furthermore, it exerts anti-CRC effects by inhibiting HK2 expression under the PI3K/AKT pathway, thus affecting the glycolysis pathway of CRC cells (Karim et al., 2022).

5.2.2 Daphnetin

Daphnetin, a coumarin derivative, was first isolated from *Daphne Korean Nakai*, and it exerts various pharmacological activities such as anticoagulation, anti-inflammatory, heart protection, and anti-cancer effects (Hang et al., 2022; Javed et al., 2022). After daphnetin treatment for 24 h, the proliferation and migration of SW480 and HT29 cells are inhibited, apoptosis is increased, glucose uptake and lactic acid production are inhibited, and the protein expression levels of HK2 and GLUT1 are downregulated (He et al., 2018). In addition, the phosphorylated expression of PI3K and AKT is significantly downregulated in SW480 cells treated with daphnetin, LY294002 (a PI3K/AKT inhibitor) could enhance the inhibitory effect of daphnetin on the glycolysis pathway in SW480 cells. Thus daphnetin may exert anti-cancer effects by targeting the PI3K/AKT pathway to affect glycolysis in CRC cells (He et al., 2018).

5.2.3 Andrographolide

Andrographis paniculata belongs to the genus Andrographis, widely distributed in Asian countries such as India, China, and Malaysia, and has been often used to treat inflammatory diseases (Li et al., 2022c). Andrographolide is the principal active ingredient of *Andrographis paniculate* extract, which has shown great potential in the treatment of a variety of inflammatory diseases as well as tumors (Zhang H. et al., 2021; Qu et al., 2022). Andrographolide not only inhibits glucose uptake and lactic acid production in HCT116 cells, decreases ATP levels, and inhibits the expression of glycolysis proteins and enzymes, such as PFK1, HK2, and GLUT1, but also inhibits the phosphorylation of the PI3K/AKT/mTOR pathway (Li et al., 2020c). Further, IGF-1 (a PI3K activator) can reverse the downregulated expression of PI3K, p-AKT, and p-mTOR by andrographolide, and andrographolide shows similar inhibitory effects on HCT116 as LY294002 (a PI3K inhibitor). Therefore, andrographolide may inhibit CRC by targeting PI3K/AKT signal pathway. Interestingly, andrographolide may also improve the radio sensitivity of HCT116 cells through the PI3K/AKT pathway (Li et al., 2020c).

5.2.4 Wogonin

Scutellaria Baicalensis, belonging to the Lamiaceae family, is a commonly used Chinese herb for clearing heat and detoxification (Yang et al., 2022). Wogonin is a flavonoid from *Scutellaria baicalensis*, which has anti-tumor, anti-inflammatory, antiviral, and other pharmacological effects (Banik et al., 2022). Wogonin at 20, 40, 60, 80, and 100 mM for 24 h can downregulate the expressions of HK2, PDHK1, and LDHA by inhibiting the transcriptional activity of PI3K/AKT and the expression of HIF-1α, thus affecting the glucose uptake and lactic acid production of HCT116 cells under hypoxia (Wang et al., 2014). Meanwhile, an *in vivo* study showed that 30 and 60 mg/kg wogonin could significantly reduce the tumor weight of male BALB/c nude mice, and decreased the expression of HIF-1α, glycolysis-related proteins, and PI3K/AKT (Wang et al., 2014). In another study, wogonin inhibited the survival of HCT116 cells and the glycolysis of HCT116 expressing wild type in a dose-dependent manner (Zhao et al., 2018). Wogonin increased the protein level as well as mRNA level of p53 and TIGAR in HCT116 cells, and decreased the protein and mRNA level of PGM, HK2, GLUT1, PDHK1, and LDHA, however, in p53-null and mt-p53 HCT-116 cells the expression and transcription of the glycolysis regulator barely changed. The experiment showed that the inhibitory effect of wogonin on cancer cell glycolysis was dependent on wt-p53. (Zhao et al., 2018).

5.2.5 Atractylenolide I

Atractylodes macrocephala Koidz., which has been used for thousands of years in China, is mainly used to treat gastrointestinal diseases such as loss of appetite, abdominal distension and diarrhea, has the functions of invigorating the spleen for strengthening the stomach, and dispelling dampness for diuresis (Li et al., 2022b). Atractylenolide I (AT-I) is a sesquiterpenoid lactone derivative of *Atractylodis macrocephalus* (Zhu et al., 2018). AT-I downregulates the phosphorylation of proteins related to the AKT/mTOR pathway and the protein expression of GLUT1, LDH, HK2, and PKM2 in a dose-dependent manner in HCT116 and Colo205 cells, thus disrupting the glucose metabolism of colorectal tumors, followed by induction of apoptosis and reduced cell invasion (Wang K. et al., 2020). In Balb/c nude mice were xenografted with HCT116 cells treated with 25 and 75 mg/kg AT-I, the tumor growth and the expression of glycolysis-related proteins were significantly inhibited, it is consistent with the *in vitro* experimental results (Wang K. et al., 2020). In addition, AT-I downregulates the expression of HK2 in HCT116 cells by inhibiting the JAK2/STAT3 pathway and reduces glucose consumption and lactate production in HCT116 cells, thus exerting anti-CRC effects (Li Y. et al., 2020). Similar results were also shown *in vivo* using an HCT116 transplanted mouse model treatment with AT-I at 50 mg/kg/day for 3 weeks. JAK2/STAT3,

as a signaling network pathway, is responsible for transducing the signals conveyed by many cytokines from the cell membrane to the nucleus, and extensive studies have confirmed that JAK2/STAT3 plays an important role in the occurrence and development of tumors and drug resistance (Mengie Ayele et al., 2022).

5.2.6 Xanthatin

Xanthium strumarium L (Asteraceae) is a commonly traditional Chinese herb have been applied for treating various diseases, including rhinitis, headache, arthritis, etc. (Fan et al., 2019). Xanthatin is a bioactive sesquiterpene lactone isolated from *X. strumarium* L. (Fan et al., 2019), which suppresses the growth of many tumors, such as lung cancer (Tao et al., 2016), glioma (Ma et al., 2020), and melanoma (Li et al., 2013). In addition, xanthatin downregulates ATP levels, lactic acid production, and glucose uptake in HCT116 and HT29 cells by inhibiting the mTOR pathway, and the mRNA and protein levels expression of GLUT1, MCT4 and the protein levels expression of HK1 is also inhibited (Li L. et al., 2022). Interestingly, elevated oxygen consumption rates (OCR) and downregulated succinic acid expression were observed in xanthatin-treated HT29 cells, which may be related to xanthatin-induced oxidative phosphorylation (Li L. et al., 2022). These results suggest that xanthatin may inhibit the glycolytic pathway of CRC cells by targeting the mTOR signaling pathway, in compensation for the activation of oxidative phosphorylation metabolism in cells, thereby causing mitochondrial dysfunction and ultimately inhibiting the growth and metastasis of CRC cells.

5.2.7 Halofuginone

Chang Shan (*Dichroa febrifuga Lour*) is a traditional Chinese medicine as a treatment for malaria, dating back about 2000 years of history (Zhou et al., 2013). Halofuginone is a natural quinazolinone alkaloid extracted from the plant *Dichroa febrifuga* (Jain et al., 2021). Halofuginone is less toxic to normal cells, but it significantly inhibits the growth of CRC and induces reactive oxygen species (ROS) production and cell apoptosis in a dose-dependent manner (Chen et al., 2015). Moreover, halofuginone downregulates the phosphorylation of AKT, mTORC1, and downstream p70S6K in SW480 and HCT116 cells, while the phosphorylation of 4EBP1 is increased in a dose-dependent manner. P70S6K is one of the effectors of mTORC1, which can activate the pentose phosphate pathway, and 4EBP1 inhibits glucose uptake and glycolysis. Halofuginone also significantly decreases the protein expression of HK2 and GLUT1 and the production of tricarboxylic acid cycle intermediates, indicating that halofuginone inhibits the glycolysis pathway of CRC, which may be mediated by the AKT/mTORC1 signaling pathway. A vivo experiment showed that halofuginone at 0.1 mg/kg for 14 days downregulated the tumor weight and AKT/mTORC1 expression in female BALB/c nude mice xenotransplanted with HCT116 cells, which was consistent with the results of an *in vitro* experiment (Chen et al., 2015).

5.2.8 Beta-caryophyllene

Beta-caryophyllene (BCP) is a bicyclic sesquiterpene that is a common constituent of essential oils, such as clove oil obtained from the dried flower-buds of *Syzygium aromaticum* (Machado et al., 2018). Arginine-specific-mono-ADP-ribosyltransfer 1 (ART1) is highly expressed in CRC and inhibits CRC proliferation, invasion, and metastasis (Yang et al., 2016). The glycolytic pathway is upregulated in ART1-expressing CT26 cells, while BCP can inhibit the expression of ART1-influenced glycolysis-related expression, such that of p-AKT, p-mTOR, c-Myc, PDK1 and LDHA, and it reduces lactate concentrations and ATP levels in CT26 cells, as shown using *in vivo* and *in vitro* models (Zhou et al., 2018) This suggests that BCP may inhibit ART1-induced glycolysis through the AKT/mTOR pathway, and it may play a role in inhibiting CRC cell proliferation and inducing apoptosis.

5.2.9 Xanthohumol

Xanthohumol is a natural polyphenol chalcone from flowers of the common hop (*Humulus lupulus* L.) (Vicente de Andrade Silva et al., 2022). Xanthohumol has a variety of pharmacological activities, including antioxidant, anti-inflammatory, and anti-tumor effects (Jiang et al., 2018). The proliferation of HCT116, SW620, and HT29 cells is significantly inhibited and apoptosis is increased after treatment with xanthohumol (Liu et al., 2019); at the same time, glucose consumption, lactic acid production, and HK2 expression in cells are inhibited, and cell pH is decreased. In addition, xanthohumol inhibits the epidermal growth factor receptor (EGFR) and AKT signaling in a dose-dependent manner, and active Akt, Myr-Akt1 can rescued xanthohumol-induced HK2 suppression (Liu et al., 2019). Therefore, xanthohumol may downregulate HK2 expression by inhibiting the activation of the EGFR/AKT pathway, thus affecting the glycolytic pathway and inducing apoptosis in CRC cells. After xenotransplantation of HT29 and HCT116 cells into female athymic nude mice, the tumor weight of 10 mg/kg every 2 days in xanthohumol-treated mice was significantly reduced, and expression of Ki-67, p-AKT, and HK2 was downregulated, which was consistent with the results of *in vitro* experiment (Liu et al., 2019).

5.3 Phytochemicals targeting AMPK to affect glycolysis in CRC

5.3.1 Isoliquiritigenin

Isoliquiritigenin (ISL) is one of the bioactive ingredients isolated from the roots of plants including *Glycyrrhiza uralensis*, *Mongolian glycyrrhiza*, and *Glycyrrhiza glabra* (Peng et al., 2015). ISL has a variety of biological activities, such as anti-inflammatory, antioxidant, nerve protection, and anti-tumor growth effects (Wang et al., 2021). ISL and ISL-loaded nanoparticles (ISL-NLs) inhibit proliferation, increase apoptosis, inhibit glucose uptake and lactate production, downregulate OCR and ATP levels, and decrease basal ECAR and maximum ECAR in HCT116 cells (Wang G. et al., 2020). Further, the respective study showed that the cell membrane potential was decreased, ROS levels were significantly increased, and the mRNA and protein levels of molecules enolase 1 (ENO1), aldolase, fructose-bisphosphate A (ALDOA), LDHA, MCT4, c-myc, and HIF-1α were also significantly decreased. The authors found that ISL and ISL-NLS could though activate AMPK and downregulate the expression of AKT and mTOR in HCT116 cells,

thereby affecting cellular glucose metabolism. Compared with ISL, ISL-NLs have a stronger inhibitory effect on CRC (Wang G. et al., 2020).

5.3.2 Caulerpin

Caulerpin is a bis-indole alkaloid, which has been isolated from *Caulerpa racemosa* and *C. serrulata* (Canché Chay et al., 2014). It has been proven to have anti-diabetic, anti-inflammatory, anti-tumor, anti-tuberculosis, and antibacterial effects (Lunagariya et al., 2019). A previous study found that caulerpin regulation of glucose metabolism in CRC cells depended on treatment time (Yu et al., 2017). After 8 h of caulerpin treatment, glucose metabolism in CRC cells was upregulated; GLUT1 was downregulated in LoVo and SW480 cells after 48 h; and p-AMPK increased during the first 30 min and decreased after 60 min. The downstream targets of mTORC1 4E-BP1 and S6 were also found to be inhibited. The above results may be related to the inhibition of ROS by caulerpin, resulting in reduced intracellular ATP levels and activation of the energy sensor AMPK. Once activated, AMPK promotes glycolysis to compensate for the loss of ATP. However, long-term activation of AMPK by caulerpin disrupts glycolysis and glucose metabolism in colorectal cells, ultimately leading to cell death (Yu et al., 2017). In mice transplanted with SW480, caulerpin (30 mg/kg) slowed tumor growth.

5.3.3 Resveratrol

Resveratrol is a natural polyphenol occurring in a wide variety of fruits and vegetables, including peanuts, pistachios, and grapes (Ren et al., 2021), and it has biological activities such as antioxidation and antiproliferation effects (Jang et al., 1997). Studies have shown that in Caco^2 and HCT116 cells, resveratrol by targeting the Ca^{2+}/CamKKB/AMPK pathway, activates PDH, increasing the oxidative capacity of colorectal cancer cells, reducing glycolysis, and changing the metabolic pattern of tumor cells (Saunier et al., 2017). Resveratrol-loaded polymeric nanoparticles suppress glucose metabolism and tumor growth of CT26 cells *in vitro* and *in vivo* (Jung et al., 2015). In addition, resveratrol can also reduce F-FDG uptake and glycolytic metabolism in HT29 cells by downregulating HIF-1α (Jung et al., 2013).

5.3.4 Oridonin

Rabdosia rubescens is a Chinese medicine to treat sore throat, gingivitis, and rheumatoid arthritis and is widely distributed in China (Abdullah et al., 2021). Oridonin, which is purified from *R. rubescens*, is an active diterpenoid compound with significant anticancer activity (Fujita et al., 1976; Yang et al., 2017). The inhibition of cell growth and apoptosis induction refers to various cancers, including prostate cancer, non-small cell lung cancer, and glioblastoma (Ikezoe et al., 2003). Oridonin not only showed anti-CRC cell activity *in vivo* and *in vitro* but also related to p53. This study further confirmed that oridonin could reduce glucose consumption and extracellular lactate concentration, down-regulating the mRNA and protein expression of GLUT1 and MCT1 in SW480 cells, thereby affecting cancer cell metabolism, and similar results were observed in SW480 xenograft BALB/c nude mice (Yao et al., 2017). However, interestingly, the increased ATP level in the CRC cells treated with oridonin was found, which may be related to the deactivation of AMPK, downregulate the expression of GLUT1 caused by oridonin, metabolic disorder of CRC cells, and thus induced autophagy (Yao et al., 2017).

5.3.5 DT-13

Ophiopogonis Radix (Maidong in Chinese), the root of Ophiopogon japonicus, is widely used as a medicine in East Asia, with functions such as nourishing yin, promoting fluid production, and moistening the lungs (Chen et al., 2016). DT-13 is a saponin monomer of *Liriope muscari* (Decne.) Bailey has significant anti-tumor, anti-inflammatory, and heart protection effects (Zhang et al., 2015; Khan et al., 2018). DT-13 can inhibit the growth of HT29, HCT116, HCT15, and COLO205 cells (Wei et al., 2019). DT13 significantly inhibited glucose uptake, lactate production, and the expression of GLUT1 in HCT15 and HT29 cells, and also downregulated glycolysis-related mRNA and protein expressions such as HK2, PFK, and LDHA. Blocking GLUT1 attenuated the effects of DT13 on glucose uptake and cell proliferation in CRC cells (Wei et al., 2019). The *in vivo* study showed that DT-13 at dosages of 0.625, 1.25, and 2.5 mg/kg not only reduced tumor size and weight but also downregulated GLUT1 expression in HCT-15 orthotopic nude mice. Meanwhile, this study also found that DT13 could inhibit the proliferation of CRC cells by activating AMPK and inhibiting mTOR and its downstream phosphorylation. Treatment with an AMPK inhibitor (Compound C) alleviated the proliferation inhibition of DT13 (Wei et al., 2019).

5.4 Phytochemicals targeting HIF-1 to affect glycolysis in CRC

5.4.1 Worenine

Coptis Chinensis (Huanglian in Chinese), a famous traditional herbal medicine used for clearing heat and detoxification, is widely used to treat inflammatory and other diseases (Wang J. et al., 2019; Yang et al., 2021). Worenine is one of the bioactive components in the dried rhizomes of *Coptis Chinensis* (Meng et al., 2018), and it inhibits cell viability and induces cell cycle arrest of HCT116 and SW620 cells *in vitro* (Ji et al., 2021). Worenine-treated HCT116 and SW620 cells, the production of lactic acid and the uptake and consumption of glucose is significantly inhibited, the protein and mRNA levels of GLUT3, HK2, PFK-L, PKM2, and LDHA in HCT116 cells are reduced, and PKM activity is also knockdown. The above changes were achieved by reducing the level of HIF-1α, desferrioxamine (stabilize HIF-1α) treatment for HCT116 cells reversed worenine-induced effects on the Warburg effect (Ji et al., 2021).

5.4.2 Berberine

Berberine is a botanical alkaloid from the Ranunculaceae and Papaveraceae plant families (Mao et al., 2018). It is the active component of the Chinese medicine *Rhizoma coptidis* (Xiong et al., 2022), and it has shown anticancer activity in a variety of cancers, such as breast cancer (Zhong et al., 2022), lung cancer (Achi et al., 2022), gastric cancer (Liu et al., 2022), liver cancer (Wang et al., 2010), CRC (Sun Q. et al., 2022). Berberine significantly inhibits the growth and glucose uptake of HCT116 and KM12C cells in a

dose-dependent manner and inhibited the mRNA levels of GLUT1, LDHA, and HK2. Further investigation of the underlying mechanism revealed that berberine inhibited glucose metabolism by suppressing mTOR-dependent HIF-1α protein synthesis in CRC cells (Mao et al., 2018).

5.4.3 Matrine

Sophora flavescens (Fabaceae), which has the effect of killing insects and dispelling dampness, has a long history of use for thousands of years (Sun P. et al., 2022). Matrine is a natural quinoline alkaloid that occurs in the traditional Chinese medicine *Sophora flavescens* (Lai et al., 2003; Zhang et al., 2020a). A study on the anti-tumor effects of matrine in CRC showed that glucose uptake and lactic acid production in HCT116 and SW620 after matrine treatment decreased, inhibiting the Warburg effect in CRC (Hong et al., 2019). Mechanistically, the transcription and expression of HIF-1α and its downstream related proteins GLUT1, HK2, and LDHA are significantly inhibited by matrine treatment, and knockdown of HIF-1α or overexpression of HIF-1α could reverse matrine's effect on glucose uptake and lactate production (Hong et al., 2019).

5.4.4 Quercetin

Quercetin is a flavonoid extract that is common in fruits and vegetables and which exerts anticancer effects by inhibiting cell proliferation, inducing cell apoptosis, and delaying the invasion and metastasis of cancer cells (Wang et al., 2022; Xia et al., 2022). Quercetin can induce apoptosis of HCT116 cells by inhibiting the activity of AMPK under hypoxia, down-regulating the expression of HIF-1α and its downstream vascular endothelial growth factor and GLUT1 (Kim et al., 2012). A previous study analyzed the effects of quercetin on the transcriptome and protein change in the discretion-rate colon mucosa of F344 rats and found that quercetin downregulated the expressions of glycolysis-related enzymes such as F-1,6-BP, glyceraldehyde-3-phosphate dehydrogenase (GAPDH), ENO1, PK, and upregulated the expression of genes related to mitochondrial fatty acid degradation, such as 3-hydroxy-3-methylglutaryl-CoA synthase 2, acetyl-CoA acyltransferase 1, and acyl-CoA dehydrogenase short-chain (Dihal et al., 2008). Quercetin may transform the glycolysis of CRC into the degradation of mitochondrial fatty acid in F334 rats, causing mitochondrial dysfunction and inhibiting the development of CRC (Dihal et al., 2008).

5.5 Phytochemicals targeting c-myc to affect glycolysis in CRC

5.5.1 Diosgenin and dioscin

Diosgenin (DSG) is a bioactive steroidal sapogenin, abundant in fenugreek seeds (Raju and Mehta, 2009). DSG not only showed inhibitory effects on the proliferation, invasion, and metastasis of CRC cells but also induced apoptosis (Li S. Y. et al., 2021). In SW1116 cells, DSG showed inhibitory effects on cancer cells glycolysis, including reduction of ECAR, OCR, lactate production, glucose uptake, and expression of GLUT2, GLUT3, and PC (Li S. Y. et al., 2021). Mechanistically, DSG regulated the expression of proteins involved in apoptosis, migration, invasion, and metabolic phenotypes of CRC cells by inhibiting the cAMP/PKA/CREB pathway in SW1116 and RKO cells. On xenograft tumor model of nude mice with SW1116 cells showed that 30 mg/kg DSG can reduce the weight of tumors *in vivo*, and inhibit the expression of Ki67 and proliferating cell nuclear antigen, Consistent with previous results in cells, DSG also inhibited the cAMP/PKA/CREB signaling pathway in tumor of nude mice (Li S. Y. et al., 2021). The cAMP/PKA/CREB pathway has been confirmed to regulate the growth, migration, invasion, and metabolism of cancer cells, and it is closely related to CRC metastasis (Zhang et al., 2020b; Fujishita et al., 2022).

Dioscin, a structural analog of DSG, is also a steroid saponin isolated from *Dioscoreae rhizome* and *Paridis rhizome,* among others. Dioscin downregulates CRC cells (HT-29, HCT-116, and SW480) proliferation and colony formation by promoting FBW-7-mediated c-myc ubiquitination, leading to the downregulation of c-myc and HK2 expression, reduced lactate consumption and glucose absorption, and inhibition of glycolysis. In xenograft models of HCT116 and HT29, tumor growth was inhibited after 5 mg/kg dioscin every 2 days treatment, and expression of c-myc, Ki-67, and HK2 was significantly reduced, and apoptosis was upregulated (Wu et al., 2020). In addition, Dioscin was shown to downregulate S-phase kinase-associated protein 2 (Skp2) protein levels and inhibit the expression of HK2 and aerobic glycolysis in CRC cells *in vitro* and *in vivo* by inhibiting Skp2 S72 phosphorylation and enhancing Skp2 ubiquitination and degradation in a cadherin 1(Cdh1) dependent manner (Zhou L. et al., 2020). As an oncogene, the Skp2 gene is closely related to the pathogenesis of CRC and is essential for the growth of CRC cells.

5.5.2 Astragalus saponins

Astragalus membranaceus is a well-known Chinese tonic, that is used as an immune stimulant, antioxidant, diuretic, etc. (Fu et al., 2014). Astragalus saponins (AST), are extracted from the medicinal plant *Astragalus membranaceus*. Studies have shown that AST downregulates the mRNA expression and enzyme activities of LDHA and HK2 in SW620 cells, inhibits glucose uptake and lactate production, induces apoptosis, and inhibits cell growth and proliferation (Guo et al., 2019). The authors speculated that this may be related to the downregulation of c-myc expression in SW620 cells by AST. In DSS-induced colitis mice, AST attenuates DSS-induced body weight loss and inflammatory response and downregulated the mRNA expression of c-myc and glycolysis-related enzymes, such as LDHA, GLUT, and HK2, which was consistent with the *in vitro* results (Guo et al., 2019).

5.5.3 Morin and esculetin

Morin is a polyphenol compound originally isolated from members of the Moraceae family such as *mulberry figs* and *fustic* (Chung et al., 2016). Esculetin is the principal bioactive ingredient of *Fraxinus rhynchophylla* Hance (Zhang et al., 2022). In a rat colon cancer model induced by 1,2-dimethylhydrazine (DMH), Morin and esculetin at a dose of 50 mg/kg were shown to reduce the incidence of DMH-induced tumors and down-regulating the expression of related proto-oncogenes. It also affects tumor metabolism through the β-cateinin/c-myc signaling pathway, including inhibiting the protein expression of GLUT, HK2, PKM2, LDHA and other glycolysis-related proteins, and promoting glutaminolysis (Sharma et al., 2017).

Morin also downregulated GLUT1 expression and glucose uptake, inhibited ATP production of SW480 cells, and induced ROS production, affecting mitochondrial function and promoting SW480 cells apoptosis (Sithara et al., 2017).

5.5.4 Apigenin

Apigenin is a natural flavonoid compound, which is common in vegetables and fruits (Sharma et al., 2019) and which significantly restrains cell survival and colony formation of HCT116, HT29, and DLD1 (Shan et al., 2017). Further studies showed that apigenin inhibited the mRNA and protein levels of PKM2 by specifically targeting the allosteric FBP binding site of PKM2 and blocking β-catenin/c-myc/PTBP1 signaling pathway to HCT116 cells, reducing the extracellular acidification rate, glucose consumption, and lactate production, blocking the glycolytic metabolism of HCT116 cells (Shan et al., 2017).

5.6 Phytochemicals targeting other pathways that affect CRC glycolysis

5.6.1 Oroxylin A

Oroxylin A (OA) is a flavonoid isolated from the root of *S. baicalensis* Georgi., which exerts various functions including cell growth inhibition and apoptosis induction in various cancer cells (Wei et al., 2013). A previous study showed that OA significantly inhibited glucose uptake and lactate production of HCT116 cells, and it significantly increased the protein level of p53 and the expression of TIGAR in cells and inhibited downstream the mRNA and protein levels of PGM and GLUT4; these inhibitory effects were confirmed to be mediated by p53 (Zhao et al., 2015). Mechanism studies showed that OA by promoting the deacetylation of sirtuin-3(SIRT3), increases the lipid phosphatase activity of PTEN and negatively regulates the transcription of MDM2, thus reducing the degradation of P53 (Zhao et al., 2015). An *in vivo* study showed that 100 mg/kg OA inhibited the growth of nude mice xenograft tumor-inoculated HCT116 cells by down-regulating MDM2 level and glycolytic protein mediated by p53. As one of the widely studied tumor suppressor genes, the p53 gene plays an important role in inhibiting the growth of tumor cells, inducing apoptosis, and regulating metabolism (Komarova and Gudkov, 1998; Vogelstein et al., 2000). SIRT3 is a member of the SIRT family of proteins and has been considered to be related to genomic stability, tumorigenesis, and energy metabolism (Finkel et al., 2009). As a tumor suppressor gene, PTEN has been demonstrated in previous studies to inhibit p53 degradation by controlling MDM2 P1 promoter activity through its lipid phosphatase activity (Freeman et al., 2003).

5.6.2 Ganoderma acid D

Ganoderma lucidum is a type of mushroom that grows on plum trees in Asia and is believed to protect body functions, regulate immunity, and promote health and longevity (Jin et al., 2016). Ganoderma acid D (GAD) is a kind of triterpene compound, which is the main active component of *G. lucidum* (Yuan et al., 2022). Studies have shown that GAD can reduce glucose uptake, lactic acid production, pyruvate production, and acetyl COA level of HT29 and SW620 cells by upregulating the expression of SIRT3 protein, inactivating acetylation cyclophilin D (CypD), thus playing a role in regulating CRC energy metabolism (Liu et al., 2018). SIRT3 is a mitochondrial deacetylase, and SIRT3 plays a key role in ROS and limiting cell oxidative damage (Torrens-Mas et al., 2017). SIRT3 can cause cell death under stress conditions, thus acting as a tumor suppressor (Torrens-Mas et al., 2017). CypD is one of the SIRT3-modified target proteins in mitochondria.

5.6.3 Rosmarinic acid

Rosmarinus officinalis L. is a plant of the Lamiaceae family native to the Mediterranean region, which has anti-inflammatory, antioxidant, anti-proliferation and other pharmacological effects (de Oliveira et al., 2019). As a water-soluble polyphenol compound, rosmarinic acid (RA) was first isolated from *R. officinalis* L. (Lamiaceae) (Khojasteh et al., 2020). RA inhibits the inflammatory response to the tumor microenvironment by inhibiting the expression of miR-155-5p in HCT8 and HCT116 cells, down-regulating the levels of transcription factor STAT3 and inflammatory factor Interleukin 6(IL-6), resulting in the inhibition of glucose consumption and lactic acid production in CRC cells, and the down-regulating expression of LDH and HIF-1α, and play the role of anti-Warburg effect (Xu et al., 2016). After further intervention with a miR-155-5p agomir drug, it was found that the above inhibitory effects of RA were reversed (Xu et al., 2016). Recent studies have shown that miR-155 plays an important role in immunity, inflammation, cardiovascular disease, and tumors (Elton et al., 2013). IL-6 is an inflammatory molecule that is highly expressed in tumor tissues and closely related to tumor cell proliferation (Kumari et al., 2016).

5.6.4 6,7-dimethoxy-1,2,3,4-tetrahydro-isoquinoline-3-carboxylic acid

The isoquinoline alkaloids 6,7-dimethoxy-1,2,3,4-tetrahydro-isoquinoline-3-carboxylic acid (M1) are isolated from the seeds of *Mucuna pruriens(Kumar et al., 2016)*. The cytotoxicity of M1 was determined by the cell growth inhibition (MTT) method, which showed its antiproliferative activity against Huh-7 (human hepatoma cell line) (Kumar et al., 2016). M1 also shows anticancer effects in CRC. A study showed that M1 at 10 and 25 mg/kg doses for 15 days inhibited the high expression of inflammatory cells such as IL-6 in DMH-induced CRC cells and inhibited the activation of the JAK2/STAT3 pathway mediated by IL-6 (Mishra et al., 2018); further, it downregulated the expression of enzymes such as LDH in CRC liver metastasis and inhibited the high uptake of lactic acid and glucose in CRC cells (Mishra et al., 2018).

6 Critical considerations

6.1 Potential side-effects of phytochemicals

Although some phytochemicals show specific cytotoxicity to tumor cells, they may elicit adverse effects in humans, depending on the dosage and preparation. Studies have shown that the semi-lethal concentration (LC50) of quercetin is 448.45 ± 0.46 mg/L, and low oral dosages of quercetin (128 mg/kg) do not cause any significant changes in body appearance and general behavior in mice (Pal and Tripathi, 2020).

However, higher dosages of quercetin (450 mg/kg) showed mild toxic effects, including weight loss and liver function impairment (Pal and Tripathi, 2020). Oral dosages of quercetin-magnesium were recommended to be restricted to less than 130 mg/kg to avoid possible toxic effects (Ghosh et al., 2017). Andrographolide show toxic side effects in a time-dependent manner, and they can significantly inhibit the proliferation of human renal tubular epithelium cells, induce cell apoptosis and inflammation, and increase nephrotoxicity (Zeng et al., 2022). Meanwhile, it has been reported that with andrographolide (PN355, Paracelsian, Inc.) in a phase-I clinical trial with HIV-positive patients, adverse effects such as anaphylaxis, fatigue, headache, rash, diarrhea, dry mouth, and decreased taste occurred with increasing dosage, and the adverse events disappeared 6 weeks after trial interruption (Calabrese et al., 2000). Determining the safe dosage of phytochemicals *in vivo* and balancing the relationship between their therapeutic effects and toxic side effects is a prominent difficulty in the development of phytochemical drugs.

6.2 Bioavailability

Some phytochemicals have been demonstrated to inhibit the glycolytic pathway of CRC *in vitro* and *in vivo* studies, however, due to their poor water solubility, low bioavailability, low cell uptake, etc., their further application in clinical practice is limited (Mohapatra et al., 2022). How to prepare such drugs so that they can be effectively utilized by humans is one of the bottlenecks of drug development. Therefore, one main objective of drug development is to improve the absorption and pharmacokinetics of drugs *in vivo* (Estrela et al., 2017). Piperine, a component of black pepper (Piper spp.), can improve the bioavailability of curcumin, the tea polyphenol (-)-Epigallocatechin-3-gallate, and other phytochemicals by inhibiting their glucuronidation (Lambert et al., 2004; Shaikh et al., 2009).

A further prominent avenue to improve the bioavailability of phytochemical drugs is novel drug delivery systems such as nanocarriers, which can alter the pharmacokinetics and improve the stability and half-life of drugs (Aqil et al., 2013). Quercetin has shown promising anticancer activity in current studies, however, its applicability is limited due to its poor water solubility *in vivo*, poor deliverability, and unstable molecular structure. Nano-conjugated quercetin can overcome the limitations of quercetin and enhance its anticancer effect, thus offering development prospects (Vinayak and Maurya, 2019). Liposome nanocarriers of apigenin can improve its bioavailability, and dual-drug-loaded liposomes with apigenin and 5-FU show higher cytotoxicity, stronger inhibition of angiogenesis and cell proliferation, and increased apoptosis. This delivery mode also showed upregulation of AMPK and downregulation of downstream HIF-1 activity and stronger reversal of the Warburg effect in CRC cells, compared to the single agent (Sen et al., 2019).

6.3 Synergistic interactions of phytochemicals with other treatments

The combination of various phytochemicals can improve the blood concentrations and bioavailability of drugs. Therefore, identifying the synergistic effects of drugs is an important aspect of drug development. The synergistic effect of phytochemical drugs combined with chemoradiotherapy is thus a key direction of treatment research. HF and artemisinin (ATS) show synergistic effects in CRC, manifested as synergistic induction of apoptosis and autophagy by HF-ATS (Gong et al., 2022). Quercetin can be used in combination with 5-FU (Boersma et al., 1994), doxorubicin (Atashpour et al., 2015), and other chemotherapy drugs to enhance its anti-cancer effect and to reduce the cytotoxicity of chemotherapy drugs. Furthermore, quercetin also played a significant role in reducing the mechanism of CRC chemoresistance (Zhou Y. et al., 2020). Oroxylin A and wogonin can synergistically inhibit MCF-7 proliferation and induce cell apoptosis, and baicalein also shows increased gastric cancer AGS cells sensitivity to 5-FU by inhibiting glycolytic flux (Cheng et al., 2018). Currently used phytochemicals have shown great potential in the treatment of cancer, and synergistic effects of phytochemicals and other drugs are a key aspect of drug development.

6.4 Clinical transformation of phytochemicals

Numerous clinical trials have been conducted to develop phytochemical drugs. In a double-blind, randomized, placebo-controlled trial on berberine and patients who had undergone colorectal polypectomy within 6 months before recruitment, the experimental group received berberine (0.3 g, twice per day) and were followed for 2 years; the results showed that the berberine treatment group had a lower incidence of recurrent adenomas (Chen et al., 2020). As a well-known proprietary Chinese medicine, Kangai injection consists of extracts of Astragalus, Ginseng, and Matrine. In a randomized trial, Kangai injection and platinum combination therapy have been shown to have a greater benefit than chemotherapy alone in patients with advanced non-small cell lung cancer, which can enhance the body's immunity and reduce the toxicity of chemotherapy drugs (Cheng et al., 2018). Aidi injection plays a role of advantages in the treatment of liver cancer (Liu et al., 2021). In CRC patients, the combined use of FOLFOX with Chinese herbal medicines such as Delisheng and Xiaoaiping shows higher safety and improved body functioning than treatment with FOLFOX alone (Zhang et al., 2019). Further evidence also suggests that the use of chemotherapeutic drugs combined with Chinese patent medicine may be more beneficial, and some studies have shown that phytochemicals have significant anticancer properties, however, further research is needed (Thomasset et al., 2007).

7 Summary and prospect

In the past few decades, CRC screening has become increasingly common, and treatment methods have been developed, however, death and incidence rates of CRC are still increasing. At present, there is a lack of effective targeted therapy for CRC. Aerobic glycolysis, as one of the characteristics of tumors, is considered a therapeutic target. It has been found that many malignant tumors, including CRC, have higher glycolysis rates to maintain the proliferation, invasion, and metastasis of cancer cells. In CRC, glycolysis-related enzymes and transporters (e.g., GLUT1, HK2, LDHA, PKM2) are highly expressed, and the upregulation of

HIF-1, AMPK, c-Myc, PI3K/Akt/mTOR and other related pathways and transporters also promote the glycolysis process of CRC. This review focuses on phytochemicals that target the glycolytic pathway in CRC. There is *in vitro* and *in vivo* evidence that some phytochemicals can affect the growth, invasion, and metastasis of CRC and induce CRC apoptosis by targeting the glycolytic pathway.

The results compiled for this review were classified according to different mechanism pathways targeted, including phytochemicals targeting PI3K/AKT/mTOR pathway (e.g., Thymoquinone and Daphnetin), AMPK pathway (e.g., Isoliquiritigenin and Resveratrol), HIF-1 (e.g., Worenine and Berberine), and c-myc (e.g., Astragalus saponins and Morin), and some phytochemicals directly affecting the glycolytic pathway of CRC without involving the above pathways. Examples include phytochemicals that directly target GLUT1 (e.g., Scutellarin and Kaempferol), PKM2 (e.g., Anthocyanin and Silybin), and MCT4 (e.g., Epigallocatechin-3-gallate). Although the phytochemicals mentioned above affect CRC cells through different pathways, they all suggest bright prospects for targeting CRC glycolytic pathways in the treatment of CRC.

Tumor metabolism is highly complex. Some phytochemicals have complex and diverse molecular targets, and further experiments are needed to verify their anticancer effects. We introduce several phytochemicals targeting CRC glycolysis metabolic pathways, which appears to be a promising direction; however, further research is required, including on how to maintain the stability of plant chemicals in the body, how to prepare plant chemicals that can be transmitted directly to the lesion site, and how to improve blood concentrations of phytochemicals. Therefore, exploiting synergistic effects of phytochemicals with other drugs may provide new ideas for further research and development of anticancer drugs. In addition to the regulation of glucose metabolism, some phytochemicals have shown the therapeutic action of multi-target and multi-pathway, and their anticancer mechanisms need further verification. Although some phytochemicals have shown potential therapeutic effects on colorectal cancer, but long-term evaluation for their possible toxic and side effects is required. In the future, more researches on phytochemicals targeting glycolysis can provide evidence for the drug development in CRC therapy.

Author contributions

LZ: Writing–review and editing, Data curation, Formal Analysis, Writing–original draft. FS: Writing–original draft, Formal Analysis. QL: Writing–original draft, Investigation. YW: Data curation, Methodology, Writing–review and editing. FW: Data curation, Writing–review and editing, Formal Analysis. ZH: Writing–review and editing, Resources, Software. XC: Software, Resources, Writing–review and editing. XY: Writing–review and editing, Formal Analysis, Visualization. JW: Writing–review and editing, Project administration, Resources. YiC: Writing–review and editing, Data curation, Visualization. YG: Visualization, Writing–review and editing. YuC: Writing–review and editing, Funding acquisition, Supervision. XM: Funding acquisition, Supervision, Writing–review and editing, Methodology. JZ: Funding acquisition, Supervision, Writing–review and editing, Conceptualization.

Funding

The author(s) declare financial support was received for the research, authorship, and/or publication of this article. This work was supported by the Program of Science and Technology Department of Sichuan Province (Grant Nos. 2023YFS0476, 2023YFQ0016, and 2023NSFSC0039), the Project of Traditional Chinese Medicine Administration of Sichuan Province (Grant Nos.MS461), "Hundred Talents Program" of the Hospital of the Chengdu University of Traditional Chinese Medicine (Grant Nos. 20-Q03 and 22-B09), Xinglin Scholar Research Promotion Project of Chengdu University of TCM (Grant Nos. QJJJ2022010 and QJRC2022028).

Conflict of interest

The authors declare that the research was conducted in the absence of any commercial or financial relationships that could be construed as a potential conflict of interest.

Publisher's note

References

Abdullah, N. A., Md Hashim, N. F., Ammar, A., and Muhamad Zakuan, N. (2021). An insight into the anti-angiogenic and anti-metastatic effects of oridonin: current knowledge and future potential. *Molecules* 26 (4), 775. doi:10.3390/molecules26040775

Achi, I. T., Sarbadhikary, P., George, B. P., and Abrahamse, H. (2022). Multi-target potential of berberine as an antineoplastic and antimetastatic agent: a special focus on lung cancer treatment. *Cells* 11 (21), 3433. doi:10.3390/cells11213433

Akbarialiabad, H., Dahroud, M. D., Khazaei, M. M., Razmeh, S., and Zarshenas, M. M. (2021). Green tea, A medicinal food with promising neurological benefits. *Curr. Neuropharmacol.* 19 (3), 349–359. doi:10.2174/1570159x18666200529152625

An, J., and Ha, E. M. (2022). Extracellular vesicles derived from Lactobacillus plantarum restore chemosensitivity through the PDK2-mediated glucose metabolic pathway in 5-FU-resistant colorectal cancer cells. *J. Microbiol.* 60 (7), 735–745. doi:10.1007/s12275-022-2201-1

Ancey, P. B., Contat, C., and Meylan, E. (2018). Glucose transporters in cancer - from tumor cells to the tumor microenvironment. *Febs J.* 285 (16), 2926–2943. doi:10.1111/febs.14577

Aqil, F., Munagala, R., Jeyabalan, J., and Vadhanam, M. V. (2013). Bioavailability of phytochemicals and its enhancement by drug delivery systems. *Cancer Lett.* 334 (1), 133–141. doi:10.1016/j.canlet.2013.02.032

Atashpour, S., Fouladdel, S., Movahhed, T. K., Barzegar, E., Ghahremani, M. H., Ostad, S. N., et al. (2015). Quercetin induces cell cycle arrest and apoptosis in CD133(+) cancer stem cells of human colorectal HT29 cancer cell line and enhances anticancer effects of doxorubicin. *Iran. J. Basic Med. Sci.* 18 (7), 635–643.

Baer, S. C., Casaubon, L., and Younes, M. (1997). Expression of the human erythrocyte glucose transporter Glut1 in cutaneous neoplasia. *J. Am. Acad. Dermatol* 37 (4), 575–577. doi:10.1016/s0190-9622(97)70174-9

Banik, K., Khatoon, E., Harsha, C., Rana, V., Parama, D., Thakur, K. K., et al. (2022). Wogonin and its analogs for the prevention and treatment of cancer: a systematic review. *Phytother. Res.* 36 (5), 1854–1883. doi:10.1002/ptr.7386

Biller, L. H., and Schrag, D. (2021). Diagnosis and treatment of metastatic colorectal cancer: a review. *Jama* 325 (7), 669–685. doi:10.1001/jama.2021.0106

Boersma, H. H., Woerdenbag, H. J., Bauer, J., Scheithauer, W., Kampinga, H. H., and Konings, A. W. (1994). Interaction between the cytostatic effects of quercetin and 5-fluorouracil in two human colorectal cancer cell lines. *Phytomedicine* 1 (3), 239–244. doi:10.1016/s0944-7113(11)80071-1

Bui, B. P., Nguyen, P. L., Lee, K., and Cho, J. (2022). Hypoxia-inducible factor-1: a novel therapeutic target for the management of cancer, drug resistance, and cancer-related pain. *Cancers (Basel)* 14 (24), 6054. doi:10.3390/cancers14246054

Calabrese, C., Berman, S. H., Babish, J. G., Ma, X., Shinto, L., Dorr, M., et al. (2000). A phase I trial of andrographolide in HIV positive patients and normal volunteers. *Phytother. Res.* 14 (5), 333–338. doi:10.1002/1099-1573(200008)14:5<333::aid-ptr584>3.0.co;2-d

Canché Chay, C. I., Gómez Cansino, R., Espitia Pinzón, C. I., Torres-Ochoa, R. O., and Martínez, R. (2014). Synthesis and anti-tuberculosis activity of the marine natural product caulerpin and its analogues. *Mar. Drugs* 12 (4), 1757–1772. doi:10.3390/md12041757

Cao, Y., Lin, Y., Wang, D., Pan, D., Zhang, Y., Jin, Y., et al. (2018). Enhancing 5-fluorouracil efficacy through suppression of PKM2 in colorectal cancer cells. *Cancer Chemother. Pharmacol.* 82 (6), 1081–1086. doi:10.1007/s00280-018-3676-7

Catanzaro, D., Gabbia, D., Cocetta, V., Biagi, M., Ragazzi, E., Montopoli, M., et al. (2018). Silybin counteracts doxorubicin resistance by inhibiting GLUT1 expression. *Fitoterapia* 124, 42–48. doi:10.1016/j.fitote.2017.10.007

Chambers, C. S., Holečková, V., Petrásková, L., Biedermann, D., Valentová, K., Buchta, M., et al. (2017). The silymarin composition and why does it matter??? *Food Res. Int.* 100(3), 339–353. doi:10.1016/j.foodres.2017.07.017

Chang, R. C., Shi, L., Huang, C. C., Kim, A. J., Ko, M. L., Zhou, B., et al. (2015). High-fat diet-induced retinal dysfunction. *Invest. Ophthalmol. Vis. Sci.* 56 (4), 2367–2380. doi:10.1167/iovs.14-16143

Chen, G. Q., Tang, C. F., Shi, X. K., Lin, C. Y., Fatima, S., Pan, X. H., et al. (2015). Halofuginone inhibits colorectal cancer growth through suppression of Akt/mTORC1 signaling and glucose metabolism. *Oncotarget* 6 (27), 24148–24162. doi:10.18632/oncotarget.4376

Chen, M. H., Chen, X. J., Wang, M., Lin, L. G., and Wang, Y. T. (2016). Ophiopogon japonicus--A phytochemical, ethnomedicinal and pharmacological review. *J. Ethnopharmacol.* 181, 193–213. doi:10.1016/j.jep.2016.01.037

Chen, S., Nishi, M., Morine, Y., Shimada, M., Tokunaga, T., Kashihara, H., et al. (2022). Epigallocatechin-3-gallate hinders metabolic coupling to suppress colorectal cancer malignancy through targeting aerobic glycolysis in cancer-associated fibroblasts. *Int. J. Oncol.* 60 (2), 19. doi:10.3892/ijo.2022.5309

Chen, X., Cui, L., Duan, X., Ma, B., and Zhong, D. (2006). Pharmacokinetics and metabolism of the flavonoid scutellarin in humans after a single oral administration. *Drug Metab. Dispos.* 34 (8), 1345–1352. doi:10.1124/dmd.106.009779

Chen, Y. X., Gao, Q. Y., Zou, T. H., Wang, B. M., Liu, S. D., Sheng, J. Q., et al. (2020). Berberine versus placebo for the prevention of recurrence of colorectal adenoma: a multicentre, double-blinded, randomised controlled study. *Lancet Gastroenterol. Hepatol.* 5 (3), 267–275. doi:10.1016/s2468-1253(19)30409-1

Cheng, C. S., Chen, J., Tan, H. Y., Wang, N., Chen, Z., and Feng, Y. (2018). Scutellaria baicalensis and cancer treatment: recent progress and perspectives in biomedical and clinical studies. *Am. J. Chin. Med.* 46 (1), 25–54. doi:10.1142/s0192415x18500027

Chung, S. S., Oliva, B., Dwabe, S., and Vadgama, J. V. (2016). Combination treatment with flavonoid morin and telomerase inhibitor MST-312 reduces cancer stem cell traits by targeting STAT3 and telomerase. *Int. J. Oncol.* 49 (2), 487–498. doi:10.3892/ijo.2016.3546

Ciesielska-Figlon, K., Wojciechowicz, K., Wardowska, A., and Lisowska, K. A. (2023). The immunomodulatory effect of Nigella sativa. *Antioxidants (Basel)* 12 (7), 1340. doi:10.3390/antiox12071340

Coutte, L., Dreyer, C., Sablin, M. P., Faivre, S., and Raymond, E. (2012). [PI3K-AKT-mTOR pathway and cancer]. *Bull. Cancer* 99 (2), 173–180. doi:10.1684/bdc.2011.1384

Cui, R., and Shi, X. Y. (2015). Expression of pyruvate kinase M2 in human colorectal cancer and its prognostic value. *Int. J. Clin. Exp. Pathol.* 8 (9), 11393–11399.

Cui, X. G., Han, Z. T., He, S. H., Wu, X. D., Chen, T. R., Shao, C. H., et al. (2017). HIF1/2α mediates hypoxia-induced LDHA expression in human pancreatic cancer cells. *Oncotarget* 8 (15), 24840–24852. doi:10.18632/oncotarget.15266

Dang, C. V., O'Donnell, K. A., Zeller, K. I., Nguyen, T., Osthus, R. C., and Li, F. (2006). The c-Myc target gene network. *Semin. Cancer Biol.* 16 (4), 253–264. doi:10.1016/j.semcancer.2006.07.014

de Oliveira, J. R., Camargo, S. E. A., and de Oliveira, L. D. (2019). Rosmarinus officinalis L. (rosemary) as therapeutic and prophylactic agent. *J. Biomed. Sci.* 26 (1), 5. doi:10.1186/s12929-019-0499-8

Devi, K. P., Malar, D. S., Nabavi, S. F., Sureda, A., Xiao, J., Nabavi, S. M., et al. (2015). Kaempferol and inflammation: from chemistry to medicine. *Pharmacol. Res.* 99, 1–10. doi:10.1016/j.phrs.2015.05.002

Dihal, A. A., van der Woude, H., Hendriksen, P. J., Charif, H., Dekker, L. J., Ijsselstijn, L., et al. (2008). Transcriptome and proteome profiling of colon mucosa from quercetin fed F344 rats point to tumor preventive mechanisms, increased mitochondrial fatty acid degradation and decreased glycolysis. *Proteomics* 8 (1), 45–61. doi:10.1002/pmic.200700364

Dong, S., Liang, S., Cheng, Z., Zhang, X., Luo, L., Li, L., et al. (2022). ROS/PI3K/Akt and Wnt/β-catenin signalings activate HIF-1α-induced metabolic reprogramming to impart 5-fluorouracil resistance in colorectal cancer. *J. Exp. Clin. Cancer Res.* 41 (1), 15. doi:10.1186/s13046-021-02229-6

Dong, X., and Qu, S. (2022). Erigeron breviscapus (vant) hand-mazz: a promising natural neuroprotective agent for alzheimer's disease. *Front. Pharmacol.* 13, 877872. doi:10.3389/fphar.2022.877872

Donohoe, D. R., Collins, L. B., Wali, A., Bigler, R., Sun, W., and Bultman, S. J. (2012). The Warburg effect dictates the mechanism of butyrate-mediated histone acetylation and cell proliferation. *Mol. Cell* 48 (4), 612–626. doi:10.1016/j.molcel.2012.08.033

Donovan, M. G., Selmin, O. I., Doetschman, T. C., and Romagnolo, D. F. (2017). Mediterranean diet: prevention of colorectal cancer. *Front. Nutr.* 4, 59. doi:10.3389/fnut.2017.00059

Elton, T. S., Selemon, H., Elton, S. M., and Parinandi, N. L. (2013). Regulation of the MIR155 host gene in physiological and pathological processes. *Gene* 532 (1), 1–12. doi:10.1016/j.gene.2012.12.009

Eslami, M., Sadrifar, S., Karbalaei, M., Keikha, M., Kobyliak, N. M., and Yousefi, B. (2020). Importance of the microbiota inhibitory mechanism on the Warburg effect in colorectal cancer cells. *J. Gastrointest. Cancer* 51 (3), 738–747. doi:10.1007/s12029-019-00329-3

Estrela, J. M., Mena, S., Obrador, E., Benlloch, M., Castellano, G., Salvador, R., et al. (2017). Polyphenolic phytochemicals in cancer prevention and therapy: bioavailability versus bioefficacy. *J. Med. Chem.* 60 (23), 9413–9436. doi:10.1021/acs.jmedchem.6b01026

Fan, W., Fan, L., Peng, C., Zhang, Q., Wang, L., Li, L., et al. (2019). Traditional uses, botany, phytochemistry, pharmacology, pharmacokinetics and toxicology of *Xanthium strumarium* L: a review. *Molecules* 24 (2), 359. doi:10.3390/molecules24020359

Faubert, B., Boily, G., Izreig, S., Griss, T., Samborska, B., Dong, Z., et al. (2013). AMPK is a negative regulator of the Warburg effect and suppresses tumor growth *in vivo*. *Cell Metab.* 17 (1), 113–124. doi:10.1016/j.cmet.2012.12.001

Feng, W., Cui, G., Tang, C. W., Zhang, X. L., Dai, C., Xu, Y. Q., et al. (2017). Role of glucose metabolism related gene GLUT1 in the occurrence and prognosis of colorectal cancer. *Oncotarget* 8 (34), 56850–56857. doi:10.18632/oncotarget.18090

Finkel, T., Deng, C. X., and Mostoslavsky, R. (2009). Recent progress in the biology and physiology of sirtuins. *Nature* 460 (7255), 587–591. doi:10.1038/nature08197

Freeman, D. J., Li, A. G., Wei, G., Li, H. H., Kertesz, N., Lesche, R., et al. (2003). PTEN tumor suppressor regulates p53 protein levels and activity through phosphatase-dependent and -independent mechanisms. *Cancer Cell* 3 (2), 117–130. doi:10.1016/s1535-6108(03)00021-7

Fu, J., Wang, Z., Huang, L., Zheng, S., Wang, D., Chen, S., et al. (2014). Review of the botanical characteristics, phytochemistry, and pharmacology of Astragalus membranaceus (Huangqi). *Phytother. Res.* 28 (9), 1275–1283. doi:10.1002/ptr.5188

Fujishita, T., Kojima, Y., Kajino-Sakamoto, R., Mishiro-Sato, E., Shimizu, Y., Hosoda, W., et al. (2022). The cAMP/PKA/CREB and TGF-β/SMAD4 pathways regulate stemness and metastatic potential in colorectal cancer cells. *Cancer Res.* 82, 4179–4190. doi:10.1158/0008-5472.Can-22-1369

Fujita, E., Nagao, Y., Node, M., Kaneko, K., Nakazawa, S., and Kuroda, H. (1976). Antitumor activity of the isodon diterpenoids: structural requirements for the activity. *Experientia* 32 (2), 203–206. doi:10.1007/bf01937766

Gatenby, R. A., and Gillies, R. J. (2004). Why do cancers have high aerobic glycolysis? *Nat. Rev. Cancer* 4 (11), 891–899. doi:10.1038/nrc1478

Georges, L. M., Verset, L., Zlobec, I., Demetter, P., and De Wever, O. (2018). Impact of the microenvironment on tumour budding in colorectal cancer. *Adv. Exp. Med. Biol.* 1110, 101–111. doi:10.1007/978-3-030-02771-1_7

Ghosh, N., Sandur, R., Ghosh, D., Roy, S., and Janadri, S. (2017). Acute, 28days sub acute and genotoxic profiling of Quercetin-Magnesium complex in Swiss albino mice. *Biomed. Pharmacother.* 86, 279–291. doi:10.1016/j.biopha.2016.12.015

Gong, R. H., Yang, D. J., Kwan, H. Y., Lyu, A. P., Chen, G. Q., and Bian, Z. X. (2022). Cell death mechanisms induced by synergistic effects of halofuginone and artemisinin in colorectal cancer cells. *Int. J. Med. Sci.* 19 (1), 175–185. doi:10.7150/ijms.66737

Guo, H., Wan, B., Wang, J., Zhang, J., Yao, W., and Shen, Z. (2019). Astragalus saponins inhibit cell growth, aerobic glycolysis and attenuate the inflammatory response in a DSS-induced colitis model. *Int. J. Mol. Med.* 43 (2), 1041–1048. doi:10.3892/ijmm.2018.4036

Haber, R. S., Rathan, A., Weiser, K. R., Pritsker, A., Itzkowitz, S. H., Bodian, C., et al. (1998). GLUT1 glucose transporter expression in colorectal carcinoma: a marker for poor prognosis. *Cancer* 83 (1), 34–40. doi:10.1002/(sici)1097-0142(19980701)83:1<34::aid-cncr5>3.0.co;2-e

Hamabe, A., Yamamoto, H., Konno, M., Uemura, M., Nishimura, J., Hata, T., et al. (2014). Combined evaluation of hexokinase 2 and phosphorylated pyruvate

dehydrogenase-E1α in invasive front lesions of colorectal tumors predicts cancer metabolism and patient prognosis. *Cancer Sci.* 105 (9), 1100–1108. doi:10.1111/cas.12487

Hamer, H. M., Jonkers, D., Venema, K., Vanhoutvin, S., Troost, F. J., and Brummer, R. J. (2008). Review article: the role of butyrate on colonic function. *Aliment. Pharmacol. Ther.* 27 (2), 104–119. doi:10.1111/j.1365-2036.2007.03562.x

Han, J., Meng, Q., Xi, Q., Zhang, Y., Zhuang, Q., Han, Y., et al. (2016). Interleukin-6 stimulates aerobic glycolysis by regulating PFKFB3 at early stage of colorectal cancer. *Int. J. Oncol.* 48 (1), 215–224. doi:10.3892/ijo.2015.3225

Hang, S., Wu, W., Wang, Y., Sheng, R., Fang, Y., and Guo, R. (2022). Daphnetin, a coumarin in genus stellera chamaejasme linn: chemistry, bioactivity and therapeutic potential. *Chem. Biodivers.* 19 (9), e202200261. doi:10.1002/cbdv.202200261

He, L., Lv, S., Ma, X., Jiang, S., Zhou, F., Zhang, Y., et al. (2022). ErbB2 promotes breast cancer metastatic potential via HSF1/LDHA axis-mediated glycolysis. *Med. Oncol.* 39 (4), 45. doi:10.1007/s12032-021-01641-4

He, Z., Dong, W., Yao, K., Qin, C., and Duan, B. (2018). Retracted article: daphnetin inhibits proliferation and glycolysis in colorectal cancer cells by regulating the PI3K/Akt signaling pathway. *RSC Adv.* 8 (60), 34483–34490. doi:10.1039/c8ra05583a

Ho, N., and Coomber, B. L. (2015). Pyruvate dehydrogenase kinase expression and metabolic changes following dichloroacetate exposure in anoxic human colorectal cancer cells. *Exp. Cell Res.* 331 (1), 73–81. doi:10.1016/j.yexcr.2014.12.006

Hollander, M. C., Blumenthal, G. M., and Dennis, P. A. (2011). PTEN loss in the continuum of common cancers, rare syndromes and mouse models. *Nat. Rev. Cancer* 11 (4), 289–301. doi:10.1038/nrc3037

Hong, X., Zhong, L., Xie, Y., Zheng, K., Pang, J., Li, Y., et al. (2019). Matrine reverses the Warburg effect and suppresses colon cancer cell growth via negatively regulating HIF-1α. *Front. Pharmacol.* 10, 1437. doi:10.3389/fphar.2019.01437

Houddane, A., Bultot, L., Novellasdemunt, L., Johanns, M., Gueuning, M. A., Vertommen, D., et al. (2017). Role of Akt/PKB and PFKFB isoenzymes in the control of glycolysis, cell proliferation and protein synthesis in mitogen-stimulated thymocytes. *Cell Signal* 34, 23–37. doi:10.1016/j.cellsig.2017.02.019

Hu, Q., Chen, Y., Deng, X., Li, Y., Ma, X., Zeng, J., et al. (2023). Diabetic nephropathy: focusing on pathological signals, clinical treatment, and dietary regulation. *Biomed. Pharmacother.* 159, 114252. doi:10.1016/j.biopha.2023.114252

Huang, C. Y., Weng, Y. T., Li, P. C., Hsieh, N. T., Li, C. I., Liu, H. S., et al. (2021). Calcitriol suppresses Warburg effect and cell growth in human colorectal cancer cells. *Life (Basel)* 11 (9), 963. doi:10.3390/life11090963

Ikezoe, T., Chen, S. S., Tong, X. J., Heber, D., Taguchi, H., and Koeffler, H. P. (2003). Oridonin induces growth inhibition and apoptosis of a variety of human cancer cells. *Int. J. Oncol.* 23 (4), 1187–1193. doi:10.3892/ijo.23.4.1187

Imran, M., Salehi, B., Sharifi-Rad, J., Aslam Gondal, T., Saeed, F., Imran, A., et al. (2019). Kaempferol: a key emphasis to its anticancer potential. *Molecules* 24 (12), 2277. doi:10.3390/molecules24122277

Jain, P. P., Zhao, T., Xiong, M., Song, S., Lai, N., Zheng, Q., et al. (2021). Halofuginone, a promising drug for treatment of pulmonary hypertension. *Br. J. Pharmacol.* 178 (17), 3373–3394. doi:10.1111/bph.15442

Jang, D. S., Yang, M. S., Ha, T. J., and Park, K. H. (1999). Hemistepsins with cytotoxic activity from Hemisteptia lyrata. *Planta Med.* 65 (8), 765–766. doi:10.1055/s-2006-960863

Jang, M., Cai, L., Udeani, G. O., Slowing, K. V., Thomas, C. F., Beecher, C. W., et al. (1997). Cancer chemopreventive activity of resveratrol, a natural product derived from grapes. *Science* 275 (5297), 218–220. doi:10.1126/science.275.5297.218

Javed, M., Saleem, A., Xaveria, A., and Akhtar, M. F. (2022). Daphnetin: a bioactive natural coumarin with diverse therapeutic potentials. *Front. Pharmacol.* 13, 993562. doi:10.3389/fphar.2022.993562

Ji, L., Shen, W., Zhang, F., Qian, J., Jiang, J., Weng, L., et al. (2021). Worenine reverses the Warburg effect and inhibits colon cancer cell growth by negatively regulating HIF-1α. *Cell Mol. Biol. Lett.* 26 (1), 19. doi:10.1186/s11658-021-00263-y

Jian, X., He, H., Zhu, J., Zhang, Q., Zheng, Z., Liang, X., et al. (2020). Hsa_circ_001680 affects the proliferation and migration of CRC and mediates its chemoresistance by regulating BMI1 through miR-340. *Mol. Cancer* 19 (1), 20. doi:10.1186/s12943-020-1134-8

Jiang, B. H., Jiang, G., Zheng, J. Z., Lu, Z., Hunter, T., and Vogt, P. K. (2001). Phosphatidylinositol 3-kinase signaling controls levels of hypoxia-inducible factor 1. *Cell Growth Differ.* 12 (7), 363–369.

Jiang, C. H., Sun, T. L., Xiang, D. X., Wei, S. S., and Li, W. Q. (2018). Anticancer activity and mechanism of xanthohumol: a prenylated flavonoid from hops (humulus lupulus L). *Front. Pharmacol.* 9, 530. doi:10.3389/fphar.2018.00530

Jiang, X., Wang, J., Deng, X., Xiong, F., Zhang, S., Gong, Z., et al. (2020). The role of microenvironment in tumor angiogenesis. *J. Exp. Clin. Cancer Res.* 39 (1), 204. doi:10.1186/s13046-020-01709-5

Jin, L., Kim, E. Y., Chung, T. W., Han, C. W., Park, S. Y., Han, J. H., et al. (2020). Hemistepsin A suppresses colorectal cancer growth through inhibiting pyruvate dehydrogenase kinase activity. *Sci. Rep.* 10 (1), 21940. doi:10.1038/s41598-020-79019-1

Jin, X., Ruiz Beguerie, J., Sze, D. M., and Chan, G. C. (2016). Ganoderma lucidum (Reishi mushroom) for cancer treatment. *Cochrane Database Syst. Rev.* 4 (4), Cd007731. doi:10.1002/14651858.CD007731.pub3

Jing, N., Song, J., Liu, Z., Wang, L., and Jiang, G. (2020). Glycosylation of anthocyanins enhances the apoptosis of colon cancer cells by handicapping energy metabolism. *BMC Complement. Med. Ther.* 20 (1), 312. doi:10.1186/s12906-020-03096-y

Jung, K. H., Lee, J. H., Park, J. W., Quach, C. H. T., Moon, S. H., Cho, Y. S., et al. (2015). Resveratrol-loaded polymeric nanoparticles suppress glucose metabolism and tumor growth *in vitro* and *in vivo*. *Int. J. Pharm.* 478 (1), 251–257. doi:10.1016/j.ijpharm.2014.11.049

Jung, K. H., Lee, J. H., Thien Quach, C. H., Paik, J. Y., Oh, H., Park, J. W., et al. (2013). Resveratrol suppresses cancer cell glucose uptake by targeting reactive oxygen species-mediated hypoxia-inducible factor-1α activation. *J. Nucl. Med.* 54 (12), 2161–2167. doi:10.2967/jnumed.112.115436

Karim, S., Burzangi, A. S., Ahmad, A., Siddiqui, N. A., Ibrahim, I. M., Sharma, P., et al. (2022). PI3K-AKT pathway modulation by thymoquinone limits tumor growth and glycolytic metabolism in colorectal cancer. *Int. J. Mol. Sci.* 23 (4), 2305. doi:10.3390/ijms23042305

Katagiri, M., Karasawa, H., Takagi, K., Nakayama, S., Yabuuchi, S., Fujishima, F., et al. (2017). Hexokinase 2 in colorectal cancer: a potent prognostic factor associated with glycolysis, proliferation and migration. *Histol. Histopathol.* 32 (4), 351–360. doi:10.14670/hh-11-799

Kazantseva, L., Becerra, J., and Santos-Ruiz, L. (2022). Traditional medicinal plants as a source of inspiration for osteosarcoma therapy. *Molecules* 27 (15), 5008. doi:10.3390/molecules27155008

Khan, G. J., Rizwan, M., Abbas, M., Naveed, M., Boyang, Y., Naeem, M. A., et al. (2018). Pharmacological effects and potential therapeutic targets of DT-13. *Biomed. Pharmacother.* 97, 255–263. doi:10.1016/j.biopha.2017.10.101

Khojasteh, A., Mirjalili, M. H., Alcalde, M. A., Cusido, R. M., Eibl, R., and Palazon, J. (2020). Powerful plant antioxidants: a new biosustainable approach to the production of rosmarinic acid. *Antioxidants (Basel)* 9 (12), 1273. doi:10.3390/antiox9121273

Kim, H. S., Wannatung, T., Lee, S., Yang, W. K., Chung, S. H., Lim, J. S., et al. (2012). Quercetin enhances hypoxia-mediated apoptosis via direct inhibition of AMPK activity in HCT116 colon cancer. *Apoptosis* 17 (9), 938–949. doi:10.1007/s10495-012-0719-0

Komarova, E. A., and Gudkov, A. V. (1998). Could p53 be a target for therapeutic suppression? *Semin. Cancer Biol.* 8 (5), 389–400. doi:10.1006/scbi.1998.0101

Kopaskova, M., Hadjo, L., Yankulova, B., Jovtchev, G., Galova, E., Sevcovicova, A., et al. (2011). Extract of Lillium candidum L. can modulate the genotoxicity of the antibiotic zeocin. *Molecules* 17 (1), 80–97. doi:10.3390/molecules17010080

Kumar, P., Rawat, A., Keshari, A. K., Singh, A. K., Maity, S., De, A., et al. (2016). Antiproliferative effect of isolated isoquinoline alkaloid from Mucuna pruriens seeds in hepatic carcinoma cells. *Nat. Prod. Res.* 30 (4), 460–463. doi:10.1080/14786419.2015.1020489

Kumar, V., and Gabrilovich, D. I. (2014). Hypoxia-inducible factors in regulation of immune responses in tumour microenvironment. *Immunology* 143 (4), 512–519. doi:10.1111/imm.12380

Kumari, N., Dwarakanath, B. S., Das, A., and Bhatt, A. N. (2016). Role of interleukin-6 in cancer progression and therapeutic resistance. *Tumour Biol.* 37 (9), 11553–11572. doi:10.1007/s13277-016-5098-7

Lai, J. P., He, X. W., Jiang, Y., and Chen, F. (2003). Preparative separation and determination of matrine from the Chinese medicinal plant Sophora flavescens Ait by molecularly imprinted solid-phase extraction. *Anal. Bioanal. Chem.* 375 (2), 264–269. doi:10.1007/s00216-002-1675-2

Lambert, J. D., Hong, J., Kim, D. H., Mishin, V. M., and Yang, C. S. (2004). Piperine enhances the bioavailability of the tea polyphenol (-)-epigallocatechin-3-gallate in mice. *J. Nutr.* 134 (8), 1948–1952. doi:10.1093/jn/134.8.1948

Lee, D. Y., Song, M. Y., and Kim, E. H. (2021). Role of oxidative stress and nrf2/KEAP1 signaling in colorectal cancer: mechanisms and therapeutic perspectives with phytochemicals. *Antioxidants (Basel)* 10 (5), 743. doi:10.3390/antiox10050743

Leung, C. O., Wong, C. C., Fan, D. N., Kai, A. K., Tung, E. K., Xu, I. M., et al. (2015). PIM1 regulates glycolysis and promotes tumor progression in hepatocellular carcinoma. *Oncotarget* 6 (13), 10880–10892. doi:10.18632/oncotarget.3534

Li, C., Chen, Q., Zhou, Y., Niu, Y., Wang, X., Li, X., et al. (2020a). S100A2 promotes glycolysis and proliferation via GLUT1 regulation in colorectal cancer. *Faseb J.* 34 (10), 13333–13344. doi:10.1096/fj.202000555R

Li, C., Wang, P., Du, J., Chen, J., Liu, W., and Ye, K. (2021a). LncRNA RAD51-AS1/miR-29b/c-3p/NDRG2 crosstalk repressed proliferation, invasion and glycolysis of colorectal cancer. *IUBMB Life* 73 (1), 286–298. doi:10.1002/iub.2427

Li, L., Liu, P., Xie, Y., Liu, Y., Chen, Z., Geng, Y., et al. (2022a). Xanthatin inhibits human colon cancer cells progression via mTOR signaling mediated energy metabolism alteration. *Drug Dev. Res.* 83 (1), 119–130. doi:10.1002/ddr.21850

Li, Q., Tang, H., Hu, F., and Qin, C. (2019). Silencing of FOXO6 inhibits the proliferation, invasion, and glycolysis in colorectal cancer cells. *J. Cell Biochem.* 120 (3), 3853–3860. doi:10.1002/jcb.27667

Li, S. Y., Shang, J., Mao, X. M., Fan, R., Li, H. Q., Li, R. H., et al. (2021b). Diosgenin exerts anti-tumor effects through inactivation of cAMP/PKA/CREB signaling pathway in colorectal cancer. *Eur. J. Pharmacol.* 908, 174370. doi:10.1016/j.ejphar.2021.174370

Li, W. D., Wu, Y., Zhang, L., Yan, L. G., Yin, F. Z., Ruan, J. S., et al. (2013). Characterization of xanthatin: anticancer properties and mechanisms of inhibited murine melanoma *in vitro* and *in vivo*. *Phytomedicine* 20 (10), 865–873. doi:10.1016/j.phymed.2013.03.006

Li, X., Rao, Z., Xie, Z., Qi, H., and Zeng, N. (2022b). Isolation, structure and bioactivity of polysaccharides from atractylodes macrocephala: a review. *J. Ethnopharmacol.* 296, 115506. doi:10.1016/j.jep.2022.115506

Li, X., Sun, J., Xu, Q., Duan, W., Yang, L., Wu, X., et al. (2020b). Oxymatrine inhibits colorectal cancer metastasis via attenuating PKM2-mediated aerobic glycolysis. *Cancer Manag. Res.* 12, 9503–9513. doi:10.2147/cmar.S267686

Li, X., Tian, R., Liu, L., Wang, L., He, D., Cao, K., et al. (2020c). Andrographolide enhanced radiosensitivity by downregulating glycolysis via the inhibition of the PI3K-Akt-mTOR signaling pathway in HCT116 colorectal cancer cells. *J. Int. Med. Res.* 48 (8), 300060520946169. doi:10.1177/0300060520946169

Li, X., Yuan, W., Wu, J., Zhen, J., Sun, Q., and Yu, M. (2022c). Andrographolide, a natural anti-inflammatory agent: an Update. *Front. Pharmacol.* 13, 920435. doi:10.3389/fphar.2022.920435

Li, Y., Wang, Y., Liu, Z., Guo, X., Miao, Z., and Ma, S. (2020d). Atractylenolide I induces apoptosis and suppresses glycolysis by blocking the JAK2/STAT3 signaling pathway in colorectal cancer cells. *Front. Pharmacol.* 11, 273. doi:10.3389/fphar.2020.00273

Liang, Z., Li, X., Liu, S., Li, C., Wang, X., and Xing, J. (2019). MiR-141-3p inhibits cell proliferation, migration and invasion by targeting TRAF5 in colorectal cancer. *Biochem. Biophys. Res. Commun.* 514 (3), 699–705. doi:10.1016/j.bbrc.2019.05.002

Liu, Q., Tang, J., Chen, S., Hu, S., Shen, C., Xiang, J., et al. (2022). Berberine for gastric cancer prevention and treatment: multi-step actions on the Correa's cascade underlie its therapeutic effects. *Pharmacol. Res.* 184, 106440. doi:10.1016/j.phrs.2022.106440

Liu, R., Zhu, L. L., Yu, C. Y., Shuai, Y. P., Sun, L. L., Bi, K. S., et al. (2021). Quantitative evaluation of the compatibility effects of aidi injection on the treatment of hepatocellular carcinoma using targeted metabolomics: a new strategy on the mechanism study of an anticancer compound in traditional Chinese medicine. *World J. Tradit. Chin. Med.* 7 (1), 111–119. doi:10.4103/wjtcm.wjtcm_86_20

Liu, S., Huang, F., Ye, Q., Li, Y., Chen, J., and Huang, H. (2020). SPRY4-IT1 promotes survival of colorectal cancer cells through regulating PDK1-mediated glycolysis. *Anim. Cells Syst. Seoul.* 24 (4), 220–227. doi:10.1080/19768354.2020.1784274

Liu, W., Li, W., Liu, H., and Yu, X. (2019). Xanthohumol inhibits colorectal cancer cells via downregulation of Hexokinases II-mediated glycolysis. *Int. J. Biol. Sci.* 15 (11), 2497–2508. doi:10.7150/ijbs.37481

Liu, Z., Li, L., and Xue, B. (2018). Effect of ganoderic acid D on colon cancer Warburg effect: role of SIRT3/cyclophilin D. *Eur. J. Pharmacol.* 824, 72–77. doi:10.1016/j.ejphar.2018.01.026

Lunagariya, J., Bhadja, P., Zhong, S., Vekariya, R., and Xu, S. (2019). Marine natural product bis-indole alkaloid caulerpin: chemistry and biology. *Mini Rev. Med. Chem.* 19 (9), 751–761. doi:10.2174/1389557517666170927154231

Lunt, S. Y., and Vander Heiden, M. G. (2011). Aerobic glycolysis: meeting the metabolic requirements of cell proliferation. *Annu. Rev. Cell Dev. Biol.* 27, 441–464. doi:10.1146/annurev-cellbio-092910-154237

Ma, Y. Y., Di, Z. M., Cao, Q., Xu, W. S., Bi, S. X., Yu, J. S., et al. (2020). Xanthatin induces glioma cell apoptosis and inhibits tumor growth via activating endoplasmic reticulum stress-dependent CHOP pathway. *Acta Pharmacol. Sin.* 41 (3), 404–414. doi:10.1038/s41401-019-0318-5

Machado, K. D. C., Islam, M. T., Ali, E. S., Rouf, R., Uddin, S. J., Dev, S., et al. (2018). A systematic review on the neuroprotective perspectives of beta-caryophyllene. *Phytother. Res.* 32 (12), 2376–2388. doi:10.1002/ptr.6199

Mao, L., Chen, Q., Gong, K., Xu, X., Xie, Y., Zhang, W., et al. (2018). Berberine decelerates glucose metabolism via suppression of mTOR-dependent HIF-1α protein synthesis in colon cancer cells. *Oncol. Rep.* 39 (5), 2436–2442. doi:10.3892/or.2018.6318

Martin, D. E., and Hall, M. N. (2005). The expanding TOR signaling network. *Curr. Opin. Cell Biol.* 17 (2), 158–166. doi:10.1016/j.ceb.2005.02.008

Martins, S. F., Amorim, R., Viana-Pereira, M., Pinheiro, C., Costa, R. F., Silva, P., et al. (2016). Significance of glycolytic metabolism-related protein expression in colorectal cancer, lymph node and hepatic metastasis. *BMC Cancer* 16, 535. doi:10.1186/s12885-016-2566-9

McGhie, T. K., Ainge, G. D., Barnett, L. E., Cooney, J. M., and Jensen, D. J. (2003). Anthocyanin glycosides from berry fruit are absorbed and excreted unmetabolized by both humans and rats. *J. Agric. Food Chem.* 51 (16), 4539–4548. doi:10.1021/jf026206w

McGhie, T. K., and Walton, M. C. (2007). The bioavailability and absorption of anthocyanins: towards a better understanding. *Mol. Nutr. Food Res.* 51 (6), 702–713. doi:10.1002/mnfr.200700092

Meng, F. C., Wu, Z. F., Yin, Z. Q., Lin, L. G., Wang, R., and Zhang, Q. W. (2018). Coptidis rhizoma and its main bioactive components: recent advances in chemical investigation, quality evaluation and pharmacological activity. *Chin. Med.* 13, 13. doi:10.1186/s13020-018-0171-3

Mengie Ayele, T., Tilahun Muche, Z., Behaile Teklemariam, A., Bogale Kassie, A., and Chekol Abebe, E. (2022). Role of JAK2/STAT3 signaling pathway in the tumorigenesis, chemotherapy resistance, and treatment of solid tumors: a systemic review. *J. Inflamm. Res.* 15, 1349–1364. doi:10.2147/jir.S353489

Miller, D. M., Thomas, S. D., Islam, A., Muench, D., and Sedoris, K. (2012). c-Myc and cancer metabolism. *Clin. Cancer Res.* 18 (20), 5546–5553. doi:10.1158/1078-0432.Ccr-12-0977

Mishra, P., Raj, V., Bhadauria, A. S., Singh, A. K., Rai, A., Kumar, P., et al. (2018). 6,7-dimethoxy-1,2,3,4-tetrahydro-isoquinoline-3-carboxylic acid attenuates colon carcinogenesis via blockade of IL-6 mediated signals. *Biomed. Pharmacother.* 100, 282–295. doi:10.1016/j.biopha.2018.02.009

Mohapatra, P., Singh, P., Singh, D., Sahoo, S., and Sahoo, S. K. (2022). Phytochemical based nanomedicine: a panacea for cancer treatment, present status and future prospective. *OpenNano* 7, 100055. doi:10.1016/j.onano.2022.100055

Mori, Y., Tsukinoki, K., Yasuda, M., Miyazawa, M., Kaneko, A., and Watanabe, Y. (2007). Glucose transporter type 1 expression are associated with poor prognosis in patients with salivary gland tumors. *Oral Oncol.* 43 (6), 563–569. doi:10.1016/j.oraloncology.2006.06.006

Nagle, D. G., Ferreira, D., and Zhou, Y. D. (2006). Epigallocatechin-3-gallate (EGCG): chemical and biomedical perspectives. *Phytochemistry* 67 (17), 1849–1855. doi:10.1016/j.phytochem.2006.06.020

Narayanankutty, A. (2019). PI3K/Akt/mTOR pathway as a therapeutic target for colorectal cancer: a review of preclinical and clinical evidence. *Curr. Drug Targets* 20 (12), 1217–1226. doi:10.2174/1389450120666190618123846

Nenkov, M., Ma, Y., Gaßler, N., and Chen, Y. (2021). Metabolic reprogramming of colorectal cancer cells and the microenvironment: implication for therapy. *Int. J. Mol. Sci.* 22 (12), 6262. doi:10.3390/ijms22126262

Pal, A., and Tripathi, A. (2020). Toxicological and behavioral study of two potential antibacterial agents:4-chloromercuribenzoic acid and quercetin on Swiss-albino mice. *Drug Chem. Toxicol.* 43 (6), 645–655. doi:10.1080/01480545.2018.1517774

Park, C., Lee, H., Noh, J. S., Jin, C. Y., Kim, G. Y., Hyun, J. W., et al. (2020). Hemistepsin A protects human keratinocytes against hydrogen peroxide-induced oxidative stress through activation of the Nrf2/HO-1 signaling pathway. *Arch. Biochem. Biophys.* 691, 108512. doi:10.1016/j.abb.2020.108512

Peng, F., Du, Q., Peng, C., Wang, N., Tang, H., Xie, X., et al. (2015). A review: the pharmacology of isoliquiritigenin. *Phytother. Res.* 29 (7), 969–977. doi:10.1002/ptr.5348

Phua, C. Y. H., Teoh, Z. L., Goh, B. H., Yap, W. H., and Tang, Y. Q. (2021). Triangulating the pharmacological properties of thymoquinone in regulating reactive oxygen species, inflammation, and cancer: therapeutic applications and mechanistic pathways. *Life Sci.* 287, 120120. doi:10.1016/j.lfs.2021.120120

Prabakaran, A. D., Karakkat, J. V., Vijayan, R., Chalissery, J., Ibrahim, M. F., Kaimala, S., et al. (2018). Identification of early indicators of altered metabolism in normal development using a rodent model system. *Dis. Model Mech.* 11 (3), dmm031815. doi:10.1242/dmm.031815

Qu, J., Liu, Q., You, G., Ye, L., Jin, Y., Kong, L., et al. (2022). Advances in ameliorating inflammatory diseases and cancers by andrographolide: pharmacokinetics, pharmacodynamics, and perspective. *Med. Res. Rev.* 42 (3), 1147–1178. doi:10.1002/med.21873

Raju, J., and Mehta, R. (2009). Cancer chemopreventive and therapeutic effects of diosgenin, a food saponin. *Nutr. Cancer* 61 (1), 27–35. doi:10.1080/01635580802357352

Rankin, E. B., and Giaccia, A. J. (2016). Hypoxic control of metastasis. *Science* 352 (6282), 175–180. doi:10.1126/science.aaf4405

Ren, B., Kwah, M. X., Liu, C., Ma, Z., Shanmugam, M. K., Ding, L., et al. (2021). Resveratrol for cancer therapy: challenges and future perspectives. *Cancer Lett.* 515, 63–72. doi:10.1016/j.canlet.2021.05.001

Robey, R. B., and Hay, N. (2009). Is Akt the "Warburg kinase"? Akt-energy metabolism interactions and oncogenesis. *Semin. Cancer Biol.* 19 (1), 25–31. doi:10.1016/j.semcancer.2008.11.010

Rupaimoole, R., and Slack, F. J. (2017). MicroRNA therapeutics: towards a new era for the management of cancer and other diseases. *Nat. Rev. Drug Discov.* 16 (3), 203–222. doi:10.1038/nrd.2016.246

Salimian Rizi, B., Caneba, C., Nowicka, A., Nabiyar, A. W., Liu, X., Chen, K., et al. (2015). Nitric oxide mediates metabolic coupling of omentum-derived adipose stroma to ovarian and endometrial cancer cells. *Cancer Res.* 75 (2), 456–471. doi:10.1158/0008-5472.Can-14-1337

Saunier, E., Antonio, S., Regazzetti, A., Auzeil, N., Laprévote, O., Shay, J. W., et al. (2017). Resveratrol reverses the Warburg effect by targeting the pyruvate dehydrogenase complex in colon cancer cells. *Sci. Rep.* 7 (1), 6945. doi:10.1038/s41598-017-07006-0

Saunier, E., Benelli, C., and Bortoli, S. (2016). The pyruvate dehydrogenase complex in cancer: an old metabolic gatekeeper regulated by new pathways and pharmacological agents. *Int. J. Cancer* 138 (4), 809–817. doi:10.1002/ijc.29564

Sen, K., Banerjee, S., and Mandal, M. (2019). Dual drug loaded liposome bearing apigenin and 5-Fluorouracil for synergistic therapeutic efficacy in colorectal cancer. *Colloids Surf. B Biointerfaces* 180, 9–22. doi:10.1016/j.colsurfb.2019.04.035

Shaikh, J., Ankola, D. D., Beniwal, V., Singh, D., and Kumar, M. N. (2009). Nanoparticle encapsulation improves oral bioavailability of curcumin by at least 9-fold when compared to curcumin administered with piperine as absorption enhancer. *Eur. J. Pharm. Sci.* 37 (3-4), 223–230. doi:10.1016/j.ejps.2009.02.019

Shan, S., Shi, J., Yang, P., Jia, B., Wu, H., Zhang, X., et al. (2017). Apigenin restrains colon cancer cell proliferation via targeted blocking of pyruvate kinase M2-dependent glycolysis. *J. Agric. Food Chem.* 65 (37), 8136–8144. doi:10.1021/acs.jafc.7b02757

Shan, X., Lv, Z. Y., Yin, M. J., Chen, J., Wang, J., and Wu, Q. N. (2021). The protective effect of cyanidin-3-glucoside on myocardial ischemia-reperfusion injury through ferroptosis. *Oxid. Med. Cell Longev.* 2021, 8880141. doi:10.1155/2021/8880141

Sharma, A., Ghani, A., Sak, K., Tuli, H. S., Sharma, A. K., Setzer, W. N., et al. (2019). Probing into therapeutic anti-cancer potential of apigenin: recent trends and future directions. *Recent Pat. Inflamm. Allergy Drug Discov.* 13 (2), 124–133. doi:10.2174/1872213x13666190816160240

Sharma, S. H., Thulasingam, S., Chellappan, D. R., Chinnaswamy, P., and Nagarajan, S. (2017). Morin and Esculetin supplementation modulates c-myc induced energy metabolism and attenuates neoplastic changes in rats challenged with the procarcinogen 1,2 - dimethylhydrazine. *Eur. J. Pharmacol.* 796, 20–31. doi:10.1016/j.ejphar.2016.12.019

Sheng, Q. S., He, K. X., Li, J. J., Zhong, Z. F., Wang, F. X., Pan, L. L., et al. (2020). Comparison of gut microbiome in human colorectal cancer in paired tumor and adjacent normal tissues. *Onco Targets Ther.* 13, 635–646. doi:10.2147/ott.S218004

Shinohara, Y., Yamamoto, K., Kogure, K., Ichihara, J., and Terada, H. (1994). Steady state transcript levels of the type II hexokinase and type 1 glucose transporter in human tumor cell lines. *Cancer Lett.* 82 (1), 27–32. doi:10.1016/0304-3835(94)90142-2

Simula, L., Alifano, M., and Icard, P. (2022). How phosphofructokinase-1 promotes PI3K and YAP/TAZ in cancer: therapeutic perspectives. *Cancers (Basel)* 14 (10), 2478. doi:10.3390/cancers14102478

Sithara, T., Arun, K. B., Syama, H. P., Reshmitha, T. R., and Nisha, P. (2017). Morin inhibits proliferation of SW480 colorectal cancer cells by inducing apoptosis mediated by reactive oxygen species formation and uncoupling of Warburg effect. *Front. Pharmacol.* 8, 640. doi:10.3389/fphar.2017.00640

Song, K., Li, M., Xu, X., Xuan, L. I., Huang, G., and Liu, Q. (2016). Resistance to chemotherapy is associated with altered glucose metabolism in acute myeloid leukemia. *Oncol. Lett.* 12 (1), 334–342. doi:10.3892/ol.2016.4600

Sun, P., Zhao, W., Wang, Q., Chen, L., Sun, K., Zhan, Z., et al. (2022a). Chemical diversity, biological activities and Traditional uses of and important Chinese herb Sophora. *Phytomedicine* 100, 154054. doi:10.1016/j.phymed.2022.154054

Sun, Q., Yang, H., Liu, M., Ren, S., Zhao, H., Ming, T., et al. (2022b). Berberine suppresses colorectal cancer by regulation of Hedgehog signaling pathway activity and gut microbiota. *Phytomedicine* 103, 154227. doi:10.1016/j.phymed.2022.154227

Sun, W., Ge, Y., Cui, J., Yu, Y., and Liu, B. (2021). Scutellarin resensitizes oxaliplatin-resistant colorectal cancer cells to oxaliplatin treatment through inhibition of PKM2. *Mol. Ther. Oncolytics* 21, 87–97. doi:10.1016/j.omto.2021.03.010

Sun, Z., Zhang, Q., Yuan, W., Li, X., Chen, C., Guo, Y., et al. (2020). MiR-103a-3p promotes tumour glycolysis in colorectal cancer via hippo/YAP1/HIF1A axis. *J. Exp. Clin. Cancer Res.* 39 (1), 250. doi:10.1186/s13046-020-01705-9

Tamene, D., and Endale, M. (2019). Antibacterial activity of coumarins and carbazole alkaloid from roots of clausena anisata. *Adv. Pharmacol. Sci.* 2019, 5419854. doi:10.1155/2019/5419854

Tang, J., Yan, T., Bao, Y., Shen, C., Yu, C., Zhu, X., et al. (2019). LncRNA GLCC1 promotes colorectal carcinogenesis and glucose metabolism by stabilizing c-Myc. *Nat. Commun.* 10 (1), 3499. doi:10.1038/s41467-019-11447-8

Tao, L., Sheng, X., Zhang, L., Li, W., Wei, Z., Zhu, P., et al. (2016). Xanthatin anti-tumor cytotoxicity is mediated via glycogen synthase kinase-3β and β-catenin. *Biochem. Pharmacol.* 115, 18–27. doi:10.1016/j.bcp.2016.06.009

Thomasset, S. C., Berry, D. P., Garcea, G., Marczylo, T., Steward, W. P., and Gescher, A. J. (2007). Dietary polyphenolic phytochemicals--promising cancer chemopreventive agents in humans? A review of their clinical properties. *Int. J. Cancer* 120 (3), 451–458. doi:10.1002/ijc.22419

Thorens, B., and Mueckler, M. (2010). Glucose transporters in the 21st century. *Am. J. Physiol. Endocrinol. Metab.* 298 (2), E141–E145. doi:10.1152/ajpendo.00712.2009

Tokunaga, R., Cao, S., Naseem, M., Battaglin, F., Lo, J. H., Arai, H., et al. (2019). AMPK variant, a candidate of novel predictor for chemotherapy in metastatic colorectal cancer: a meta-analysis using tribe, mavericc and FIRE3. *Int. J. Cancer* 145 (8), 2082–2090. doi:10.1002/ijc.32261

Tong, J., Shen, Y., Zhang, Z., Hu, Y., Zhang, X., and Han, L. (2019). Apigenin inhibits epithelial-mesenchymal transition of human colon cancer cells through NF-κB/Snail signaling pathway. *Biosci. Rep.* 39 (5), BSR20190452. doi:10.1042/bsr20190452

Torrens-Mas, M., Oliver, J., Roca, P., and Sastre-Serra, J. (2017). SIRT3: oncogene and tumor suppressor in cancer. *Cancers (Basel)* 9 (7), 90. doi:10.3390/cancers9070090

Towler, M. C., and Hardie, D. G. (2007). AMP-activated protein kinase in metabolic control and insulin signaling. *Circ. Res.* 100 (3), 328–341. doi:10.1161/01.Res.0000256090.42690.05

Van der Jeught, K., Xu, H. C., Li, Y. J., Lu, X. B., and Ji, G. (2018). Drug resistance and new therapies in colorectal cancer. *World J. Gastroenterol.* 24 (34), 3834–3848. doi:10.3748/wjg.v24.i34.3834

van der Stok, E. P., Spaander, M. C. W., Grünhagen, D. J., Verhoef, C., and Kuipers, E. J. (2017). Surveillance after curative treatment for colorectal cancer. *Nat. Rev. Clin. Oncol.* 14 (5), 297–315. doi:10.1038/nrclinonc.2016.199

Vasaikar, S., Huang, C., Wang, X., Petyuk, V. A., Savage, S. R., Wen, B., et al. (2019). Proteogenomic analysis of human colon cancer reveals new therapeutic opportunities. *Cell* 177 (4), 1035–1049.e19. doi:10.1016/j.cell.2019.03.030

Vicente de Andrade Silva, G., Demaman Arend, G., Antonio Ferreira Zielinski, A., Di Luccio, M., and Ambrosi, A. (2022). Xanthohumol properties and strategies for extraction from hops and brewery residues: a review. *Food Chem.* 404, 134629. doi:10.1016/j.foodchem.2022.134629

Vinayak, M., and Maurya, A. K. (2019). Quercetin loaded nanoparticles in targeting cancer: recent development. *Anticancer Agents Med. Chem.* 19 (13), 1560–1576. doi:10.2174/1871520619666190705150214

Vogelstein, B., Lane, D., and Levine, A. J. (2000). Surfing the p53 network. *Nature* 408 (6810), 307–310. doi:10.1038/35042675

Wang, G., Yu, Y., Wang, Y. Z., Yin, P. H., Xu, K., and Zhang, H. (2020a). The effects and mechanisms of isoliquiritigenin loaded nanoliposomes regulated AMPK/mTOR mediated glycolysis in colorectal cancer. *Artif. Cells Nanomed Biotechnol.* 48 (1), 1231–1249. doi:10.1080/21691401.2020.1825092

Wang, H., Zhao, L., Zhu, L. T., Wang, Y., Pan, D., Yao, J., et al. (2014). Wogonin reverses hypoxia resistance of human colon cancer HCT116 cells via downregulation of HIF-1α and glycolysis, by inhibiting PI3K/Akt signaling pathway. *Mol. Carcinog.* 53 (1), E107–E118. doi:10.1002/mc.22052

Wang, H., Zhao, W., Zhou, L., Wang, J., Liu, L., Wang, S., et al. (2018a). Soft particles of gemini surfactant/conjugated polymer for enhanced anticancer activity of chemotherapeutics. *ACS Appl. Mater Interfaces* 10 (1), 37–41. doi:10.1021/acsami.7b16396

Wang, J., Wang, H., Liu, A., Fang, C., Hao, J., and Wang, Z. (2015). Lactate dehydrogenase A negatively regulated by miRNAs promotes aerobic glycolysis and is increased in colorectal cancer. *Oncotarget* 6 (23), 19456–19468. doi:10.18632/oncotarget.3318

Wang, J., Wang, L., Lou, G. H., Zeng, H. R., Hu, J., Huang, Q. W., et al. (2019a). Coptidis rhizoma: a comprehensive review of its traditional uses, botany, phytochemistry, pharmacology and toxicology. *Pharm. Biol.* 57 (1), 193–225. doi:10.1080/13880209.2019.1577466

Wang, K., Huang, W., Sang, X., Wu, X., Shan, Q., Tang, D., et al. (2020b). Atractylenolide I inhibits colorectal cancer cell proliferation by affecting metabolism and stemness via AKT/mTOR signaling. *Phytomedicine* 68, 153191. doi:10.1016/j.phymed.2020.153191

Wang, K. L., Yu, Y. C., and Hsia, S. M. (2021). Perspectives on the role of isoliquiritigenin in cancer. *Cancers (Basel)* 13 (1), 115. doi:10.3390/cancers13010115

Wang, M., Chen, X., Yu, F., Zhang, L., Zhang, Y., and Chang, W. (2022). The targeting of noncoding RNAs by quercetin in cancer prevention and therapy. *Oxid. Med. Cell Longev.* 2022, 4330681. doi:10.1155/2022/4330681

Wang, N., Feng, Y., Zhu, M., Tsang, C. M., Man, K., Tong, Y., et al. (2010). Berberine induces autophagic cell death and mitochondrial apoptosis in liver cancer cells: the cellular mechanism. *J. Cell Biochem.* 111 (6), 1426–1436. doi:10.1002/jcb.22869

Wang, T., Ning, K., Sun, X., Zhang, C., Jin, L. F., and Hua, D. (2018b). Glycolysis is essential for chemoresistance induced by transient receptor potential channel C5 in colorectal cancer. *BMC Cancer* 18 (1), 207. doi:10.1186/s12885-018-4123-1

Wang, W., and Guan, K. L. (2009). AMP-activated protein kinase and cancer. *Acta Physiol. (Oxf)* 196 (1), 55–63. doi:10.1111/j.1748-1716.2009.01980.x

Wang, Y., Lu, J. H., Wu, Q. N., Jin, Y., Wang, D. S., Chen, Y. X., et al. (2019b). LncRNA LINRIS stabilizes IGF2BP2 and promotes the aerobic glycolysis in colorectal cancer. *Mol. Cancer* 18 (1), 174. doi:10.1186/s12943-019-1105-0

Wei, H., Dong, C., and Shen, Z. (2020). Kallikrein-related peptidase (KLK10) cessation blunts colorectal cancer cell growth and glucose metabolism by regulating the PI3K/Akt/mTOR pathway. *Neoplasma* 67 (4), 889–897. doi:10.4149/neo_2020_190814N758

Wei, L., Zhou, Y., Dai, Q., Qiao, C., Zhao, L., Hui, H., et al. (2013). Oroxylin A induces dissociation of hexokinase II from the mitochondria and inhibits glycolysis by SIRT3-mediated deacetylation of cyclophilin D in breast carcinoma. *Cell Death Dis.* 4 (4), e601. doi:10.1038/cddis.2013.131

Wei, X., Mao, T., Li, S., He, J., Hou, X., Li, H., et al. (2019). DT-13 inhibited the proliferation of colorectal cancer via glycolytic metabolism and AMPK/mTOR signaling pathway. *Phytomedicine* 54, 120–131. doi:10.1016/j.phymed.2018.09.003

Wilson, J. E. (2003). Isozymes of mammalian hexokinase: structure, subcellular localization and metabolic function. *J. Exp. Biol.* 206 (12), 2049–2057. doi:10.1242/jeb.00241

Wong, N., Yan, J., Ojo, D., De Melo, J., Cutz, J. C., and Tang, D. (2014). Changes in PKM2 associate with prostate cancer progression. *Cancer Invest.* 32 (7), 330–338. doi:10.3109/07357907.2014.919306

Wu, H., Cui, M., Li, C., Li, H., Dai, Y., Cui, K., et al. (2021). Kaempferol reverses aerobic glycolysis via miR-339-5p-mediated PKM alternative splicing in colon cancer cells. *J. Agric. Food Chem.* 69 (10), 3060–3068. doi:10.1021/acs.jafc.0c07640

Wu, P., Meng, X., Zheng, H., Zeng, Q., Chen, T., Wang, W., et al. (2018). Kaempferol attenuates ROS-induced hemolysis and the molecular mechanism of its induction of apoptosis on bladder cancer. *Molecules* 23 (10), 2592. doi:10.3390/molecules23102592

Wu, Z., Han, X., Tan, G., Zhu, Q., Chen, H., Xia, Y., et al. (2020). Dioscin inhibited glycolysis and induced cell apoptosis in colorectal cancer via promoting c-myc ubiquitination and subsequent hexokinase-2 suppression. *Onco Targets Ther.* 13, 31–44. doi:10.2147/ott.S224062

Xia, L. M., Zhang, A. P., Zheng, Q., Ding, J., Jin, Z., Yu, H., et al. (2022). Quercetin-3-O-β-D-glucuronide inhibits mitochondria pathway-mediated platelet apoptosis via the phosphatidylinositol-3-kinase/AKT pathway in immunological bone marrow failure. *World J. Tradit. Chin. Med.* 8 (1), 115–122. doi:10.4103/wjtcm.wjtcm_44_21

Xian, Z. Y., Liu, J. M., Chen, Q. K., Chen, H. Z., Ye, C. J., Xue, J., et al. (2015). Inhibition of LDHA suppresses tumor progression in prostate cancer. *Tumour Biol.* 36 (10), 8093–8100. doi:10.1007/s13277-015-3540-x

Xiang, S., Fang, J., Wang, S., Deng, B., and Zhu, L. (2015). MicroRNA-135b regulates the stability of PTEN and promotes glycolysis by targeting USP13 in human colorectal cancers. *Oncol. Rep.* 33 (3), 1342–1348. doi:10.3892/or.2014.3694

Xiong, R. G., Huang, S. Y., Wu, S. X., Zhou, D. D., Yang, Z. J., Saimaiti, A., et al. (2022). Anticancer effects and mechanisms of berberine from medicinal herbs: an update review. *Molecules* 27 (14), 4523. doi:10.3390/molecules27144523

Xu, Y., Han, S., Lei, K., Chang, X., Wang, K., Li, Z., et al. (2016). Anti-Warburg effect of rosmarinic acid via miR-155 in colorectal carcinoma cells. *Eur. J. Cancer Prev.* 25 (6), 481–489. doi:10.1097/cej.0000000000000205

Yang, I. H., Shin, J. A., Lee, K. E., Kim, J., Cho, N. P., and Cho, S. D. (2017). Oridonin induces apoptosis in human oral cancer cells via phosphorylation of histone H2AX. *Eur. J. Oral Sci.* 125 (6), 438–443. doi:10.1111/eos.12387

Yang, L., Xiao, M., Li, X., Tang, Y., and Wang, Y. L. (2016). Arginine ADP-ribosyltransferase 1 promotes angiogenesis in colorectal cancer via the PI3K/Akt pathway. *Int. J. Mol. Med.* 37 (3), 734–742. doi:10.3892/ijmm.2016.2473

Yang, X., Zheng, S., Wang, X., Wang, J., Ali Shah, S. B., Wang, Y., et al. (2022). Advances in pharmacology, biosynthesis, and metabolic engineering of Scutellaria-specialized metabolites. *Crit. Rev. Biotechnol.* 29, 1–17. doi:10.1080/07388551.2022.2149386

Yang, Y., Vong, C. T., Zeng, S., Gao, C., Chen, Z., Fu, C., et al. (2021). Tracking evidences of Coptis chinensis for the treatment of inflammatory bowel disease from pharmacological, pharmacokinetic to clinical studies. *J. Ethnopharmacol.* 268, 113573. doi:10.1016/j.jep.2020.113573

Yao, Z., Xie, F., Li, M., Liang, Z., Xu, W., Yang, J., et al. (2017). Oridonin induces autophagy via inhibition of glucose metabolism in p53-mutated colorectal cancer cells. *Cell Death Dis.* 8 (2), e2633. doi:10.1038/cddis.2017.35

Yeh, Y. H., Hsiao, H. F., Yeh, Y. C., Chen, T. W., and Li, T. K. (2018). Inflammatory interferon activates HIF-1α-mediated epithelial-to-mesenchymal transition via PI3K/AKT/mTOR pathway. *J. Exp. Clin. Cancer Res.* 37 (1), 70. doi:10.1186/s13046-018-0730-6

Yeung, S. J., Pan, J., and Lee, M. H. (2008). Roles of p53, MYC and HIF-1 in regulating glycolysis - the seventh hallmark of cancer. *Cell Mol. Life Sci.* 65 (24), 3981–3999. doi:10.1007/s00018-008-8224-x

Younes, M., Brown, R. W., Mody, D. R., Fernandez, L., and Laucirica, R. (1995). GLUT1 expression in human breast carcinoma: correlation with known prognostic markers. *Anticancer Res.* 15 (6), 2895–2898.

Younes, M., Lechago, L. V., and Lechago, J. (1996). Overexpression of the human erythrocyte glucose transporter occurs as a late event in human colorectal carcinogenesis and is associated with an increased incidence of lymph node metastases. *Clin. Cancer Res.* 2 (7), 1151–1154.

Yu, G., Yu, W., Jin, G., Xu, D., Chen, Y., Xia, T., et al. (2015). PKM2 regulates neural invasion of and predicts poor prognosis for human hilar cholangiocarcinoma. *Mol. Cancer* 14, 193. doi:10.1186/s12943-015-0462-6

Yu, H., Zhang, H., Dong, M., Wu, Z., Shen, Z., Xie, Y., et al. (2017). Metabolic reprogramming and AMPKα1 pathway activation by caulerpin in colorectal cancer cells. *Int. J. Oncol.* 50 (1), 161–172. doi:10.3892/ijo.2016.3794

Yuan, H., Xu, Y., Luo, Y., Zhang, J. R., Zhu, X. X., and Xiao, J. H. (2022). Ganoderic acid D prevents oxidative stress-induced senescence by targeting 14-3-3ε to activate CaM/CaMKII/NRF2 signaling pathway in mesenchymal stem cells. *Aging Cell* 21 (9), e13686. doi:10.1111/acel.13686

Zeng, B., Wei, A., Zhou, Q., Yuan, M., Lei, K., Liu, Y., et al. (2022). Andrographolide: a review of its pharmacology, pharmacokinetics, toxicity and clinical trials and pharmaceutical researches. *Phytother. Res.* 36 (1), 336–364. doi:10.1002/ptr.7324

Zhang, D., Wu, J., Duan, X., Wang, K., Ni, M., Liu, S., et al. (2019). Network meta-analysis of Chinese herbal injections plus the FOLFOX regimen for the treatment of colorectal cancer in China. *Integr. Cancer Ther.* 18, 1534735419827098. doi:10.1177/1534735419827098

Zhang, H., Chen, L., Sun, X., Yang, Q., Wan, L., and Guo, C. (2020a). Matrine: a promising natural product with various pharmacological activities. *Front. Pharmacol.* 11, 588. doi:10.3389/fphar.2020.00588

Zhang, H., Kong, Q., Wang, J., Jiang, Y., and Hua, H. (2020b). Complex roles of cAMP-PKA-CREB signaling in cancer. *Exp. Hematol. Oncol.* 9 (1), 32. doi:10.1186/s40164-020-00191-1

Zhang, H., Li, S., Si, Y., and Xu, H. (2021a). Andrographolide and its derivatives: current achievements and future perspectives. *Eur. J. Med. Chem.* 224, 113710. doi:10.1016/j.ejmech.2021.113710

Zhang, L., Xie, Q., and Li, X. (2022). Esculetin: a review of its pharmacology and pharmacokinetics. *Phytother. Res.* 36 (1), 279–298. doi:10.1002/ptr.7311

Zhang, M., Liu, T., Sun, H., Weng, W., Zhang, Q., Liu, C., et al. (2018). Pim1 supports human colorectal cancer growth during glucose deprivation by enhancing the Warburg effect. *Cancer Sci.* 109 (5), 1468–1479. doi:10.1111/cas.13562

Zhang, W., Tong, D., Liu, F., Li, D., Li, J., Cheng, X., et al. (2016). RPS7 inhibits colorectal cancer growth via decreasing HIF-1α-mediated glycolysis. *Oncotarget* 7 (5), 5800–5814. doi:10.18632/oncotarget.6807

Zhang, Y., Mao, Q., Xia, Q., Cheng, J., Huang, Z., Li, Y., et al. (2021b). Noncoding RNAs link metabolic reprogramming to immune microenvironment in cancers. *J. Hematol. Oncol.* 14 (1), 169. doi:10.1186/s13045-021-01179-y

Zhang, Y., Sun, M., Han, Y., Zhai, K., Tang, Y., Qin, X., et al. (2015). The saponin DT-13 attenuates tumor necrosis factor-α-induced vascular inflammation associated with Src/NF-κB/MAPK pathway modulation. *Int. J. Biol. Sci.* 11 (8), 970–981. doi:10.7150/ijbs.11635

Zhao, J., Huang, X., Xu, Z., Dai, J., He, H., Zhu, Y., et al. (2017). LDHA promotes tumor metastasis by facilitating epithelial-mesenchymal transition in renal cell carcinoma. *Mol. Med. Rep.* 16 (6), 8335–8344. doi:10.3892/mmr.2017.7637

Zhao, K., Zhou, Y., Qiao, C., Ni, T., Li, Z., Wang, X., et al. (2015). Oroxylin A promotes PTEN-mediated negative regulation of MDM2 transcription via SIRT3-mediated deacetylation to stabilize p53 and inhibit glycolysis in wt-p53 cancer cells. *J. Hematol. Oncol.* 8, 41. doi:10.1186/s13045-015-0137-1

Zhao, Y., Zhang, L., Wu, Y., Dai, Q., Zhou, Y., Li, Z., et al. (2018). Selective anti-tumor activity of wogonin targeting the Warburg effect through stablizing p53. *Pharmacol. Res.* 135, 49–59. doi:10.1016/j.phrs.2018.07.011

Zheng, Y., Wang, Y., Liu, Y., Xie, L., Ge, J., Yu, G., et al. (2021). N6-Methyladenosine modification of PTTG3P contributes to colorectal cancer proliferation via YAP1. *Front. Oncol.* 11, 669731. doi:10.3389/fonc.2021.669731

Zhong, X. D., Chen, L. J., Xu, X. Y., Liu, Y. J., Tao, F., Zhu, M. H., et al. (2022). Berberine as a potential agent for breast cancer therapy. *Front. Oncol.* 12, 993775. doi:10.3389/fonc.2022.993775

Zhou, C., Lyu, L. H., Miao, H. K., Bahr, T., Zhang, Q. Y., Liang, T., et al. (2020a). Redox regulation by SOD2 modulates colorectal cancer tumorigenesis through AMPK-mediated energy metabolism. *Mol. Carcinog.* 59 (5), 545–556. doi:10.1002/mc.23178

Zhou, H., Sun, L., Yang, X. L., and Schimmel, P. (2013). ATP-directed capture of bioactive herbal-based medicine on human tRNA synthetase. *Nature* 494 (7435), 121–124. doi:10.1038/nature11774

Zhou, L., Yu, X., Li, M., Gong, G., Liu, W., Li, T., et al. (2020b). Cdh1-mediated Skp2 degradation by dioscin reprogrammes aerobic glycolysis and inhibits colorectal cancer cells growth. *EBioMedicine* 51, 102570. doi:10.1016/j.ebiom.2019.11.031

Zhou, L., Zhan, M. L., Tang, Y., Xiao, M., Li, M., Li, Q. S., et al. (2018). Effects of β-caryophyllene on arginine ADP-ribosyltransferase 1-mediated regulation of glycolysis in colorectal cancer under high-glucose conditions. *Int. J. Oncol.* 53 (4), 1613–1624. doi:10.3892/ijo.2018.4506

Zhou, Y., Tozzi, F., Chen, J., Fan, F., Xia, L., Wang, J., et al. (2012). Intracellular ATP levels are a pivotal determinant of chemoresistance in colon cancer cells. *Cancer Res.* 72 (1), 304–314. doi:10.1158/0008-5472.Can-11-1674

Zhou, Y., Zhang, J., Wang, K., Han, W., Wang, X., Gao, M., et al. (2020c). Quercetin overcomes colon cancer cells resistance to chemotherapy by inhibiting solute carrier family 1, member 5 transporter. *Eur. J. Pharmacol.* 881, 173185. doi:10.1016/j.ejphar.2020.173185

Zhu, B., Zhang, Q. L., Hua, J. W., Cheng, W. L., and Qin, L. P. (2018). The traditional uses, phytochemistry, and pharmacology of atractylodes macrocephala Koidz.: a review. *J. Ethnopharmacol.* 226, 143–167. doi:10.1016/j.jep.2018.08.023

Zuo, S., Wu, L., Wang, Y., and Yuan, X. (2020). Long non-coding RNA MEG3 activated by vitamin D suppresses glycolysis in colorectal cancer via promoting c-myc degradation. *Front. Oncol.* 10, 274. doi:10.3389/fonc.2020.00274

Glossary

AMPK	Adenosine 5′-monophosphate (AMP)-activated protein kinase
ALDOA	Aldolase, fructose-bisphosphate A
Cdh1	Cadherin 1
CamKKB	Calmodulin-dependent protein kinase beta
CAFs	Cancer-associated fibroblasts
CoA	Coenzyme A
CRC	Colorectal cancer
cAMP	cyclic adenosine monophosphate
CREB	Cyclic-AMP response binding protein
CypD	Cyclophilin D
DMH	1,2-dimethylhydrazine
ENO1	Enolase 1
EGFR	Epidermal growth factor receptor
ECAR	Extracellular acidification rate
ERK (1/2)	Extracellular regulated protein kinases (1/2)
5-FU	5-Fluorouracil
GLUTs	Glucose transporters
GAPDH	Glyceraldehyde-3-phosphate dehydrogenase
hnRNPA1	heterogeneous nuclear ribonucleoprotein A1
HK(2)	Hexokinase (2)
HIF-1(α)	Hypoxia-inducible factor-1(α)
IL-6	Interleukin 6
JAK2/STAT3	Janus kinase 2/signal transducer and activator of transcription 3
LDH (A/B)	Lactate dehydrogenase (A/B);
LncRNA GLCC1	glycolysis-associated lncRNA of colorectal cancer
LncRNAs	Long non-coding RNAs
mTOR	mammalian target of rapamycin
MCTs	Monocarboxylic acid transporters
OCR	Oxygen consumption rates
PTEN	Phosphatase and tensin homolog
PI3K/AKT	Phosphatidylinositol 3-kinases/protein kinase B
PGM	Phosphoglucomutase
PTBP1	Polypyrimidine tract-binding protein 1
PKA	Protein kinase A
PDK1	Pyruvate dehydrogenase kinase 1
PK(M2)	Pyruvate kinase (M2)
ROS	Reactive oxygen species
SIRT3	Sirtuin-3
Skp2	S-phase kinase associated protein 2
SOD2	Superoxide dismutase 2
TIGAR	TP53-induced glycolysis and apoptosis regulator
YAP1	Yes-associated protein 1

frontiers | Frontiers in Oncology

TYPE Original Research
PUBLISHED 29 August 2023
DOI 10.3389/fonc.2023.1221275

OPEN ACCESS

EDITED BY
Ayaz Shahid,
Western University of Health Sciences, United States

REVIEWED BY
Shahina Akhter,
University of Science and Technology Chittagong, Bangladesh
Pengcheng Wang,
Capital Medical University, China

*CORRESPONDENCE
Chandan Shivamallu
chandans@jssuni.edu.in
Shiva Prasad Kollur
shivachemist@gmail.com
Raghu Ram Achar
rracharya@jssuni.edu.in

†These authors have contributed equally to this work and share first authorship

RECEIVED 12 May 2023
ACCEPTED 06 July 2023
PUBLISHED 29 August 2023

CITATION
Reddy P, Pradeep S, S. M. G, Dharmashekar C, G. D, M. R. SC, Srinivasa C, Shati AA, Alfaifi MY, Elbehairi SEI, Achar RR, Silina E, Stupin V, Manturova N, Shivamallu C and Kollur SP (2023) Cell cycle arrest and apoptotic studies of *Terminalia chebula* against MCF-7 breast cancer cell line: an *in vitro* and *in silico* approach. *Front. Oncol.* 13:1221275. doi: 10.3389/fonc.2023.1221275

Cell cycle arrest and apoptotic studies of *Terminalia chebula* against MCF-7 breast cancer cell line: an *in vitro* and *in silico* approach

Pruthvish Reddy[1†], Sushma Pradeep[2†], Gopinath S. M.[1], Chandan Dharmashekar[2], Disha G.[3], Sai Chakith M. R.[4], Chandrashekar Srinivasa[5], Ali A. Shati[6], Mohammad Y. Alfaifi[6], Serag Eldin I. Elbehairi[6], Raghu Ram Achar[7*], Ekaterina Silina[8], Victor Stupin[8], Natalia Manturova[8], Chandan Shivamallu[2*] and Shiva Prasad Kollur[9*]

[1]Department of Biotechnology, Acharya Institute of Technology, Bengaluru, Karnataka, India, [2]Department of Biotechnology and Bioinformatics, School of Life Sciences, JSS Academy of Higher Education and Research, Mysuru, Karnataka, India, [3]Department of Neurochemistry, National Institute of Mental Health and Neiurosciences, Bangalore, Karnataka, India, [4]Department of Pharmacology, JSS Medical College, JSS Academy of Higher Education and Research, Mysuru, Karnataka, India, [5]Department of Studies in Biotechnology, Davangere University, Davangere, Karnataka, India, [6]Biology Department, Faculty of Science, King Khalid University, Abha, Saudi Arabia, [7]Division of Biochemistry, School of Life Sciences, JSS Academy of Higher Education and Research, Mysuru, Karnataka, India, [8]Department of Hospital Surgery, N.I. Pirogov Russian National Research Medical University (RNRMU), Moscow, Russia, [9]School of Physical Sciences, Amrita Vishwa Vidyapeetham, Mysuru, Karnataka, India

Breast cancer is a leading cause of mortality in women, and alternative therapies with fewer side effects are actively being explored. Breast cancer is a significant global health concern, and conventional treatments like radiotherapy and chemotherapy often have side effects. Medicinal plant extracts offer a promising avenue for the development of effective and safe anticancer therapies. *Terminalia chebula*, a plant known for its medicinal properties, was selected for investigation in this study. We aimed to assess the antiproliferative effects of TCF extract on breast cancer cells and explore the potential role of saccharopine, a phytochemical found in TCF, as an anticancer agent. MCF7 breast cancer cell lines were exposed to TCF extract, and cell viability and apoptosis assays were performed to evaluate the antiproliferative and apoptogenic effects. Molecular docking studies were conducted to assess the binding affinity of saccharopine with EGFRs. Molecular dynamics simulations and binding energy calculations were employed to analyze the stability of the EGFR-saccharopine complex. The TCF extract exhibited significant antiproliferative effects on MCF7 breast cancer cells and induced apoptosis in a dose-dependent manner. Molecular docking analysis revealed that saccharopine demonstrated a higher binding affinity with EGFR compared to the reference compound (17b-estradiol). The subsequent MDS simulations indicated stable binding patterns and conformation of the EGFR-saccharopine complex, suggesting a potential role in inhibiting EGFR-mediated signaling pathways. The investigation of Terminalia chebula fruit extract and its phytochemical saccharopine has revealed promising antiproliferative effects and a strong binding affinity with EGFR. These findings

provide a foundation for future research aimed at isolating saccharopine and conducting in vivo studies to evaluate its potential as a targeted therapy for breast cancer. The development of novel anticancer agents from plant sources holds great promise in advancing the field of oncology and improving treatment outcomes for breast cancer patients.

KEYWORDS

breast cancer, apoptosis, phytocompounds, EGFR, hemolysis

1 Introduction

Cancer is one of the deadliest illnesses worldwide. The global disease burden in 2018 was estimated to be 18.1 million new malignant cases (1). In India, there were approximately 2.25 million recorded cases and over 784,000 deaths in the year 2020 as per the National Institute of Disease Avoidance and Research.

Carcinoma, sarcoma, lymphoma, melanoma, and leukemia are the five major types of cancer, with carcinoma being the most extensively studied (2). Carcinomas predominantly affect organs such as the lungs, breasts, skin, glands, and pancreas. The treatment of cancer involves various approaches, including surgery, chemotherapy, hormonal therapy, radiation therapy, and immunotherapy (3). However, these treatments have certain limitations, including high costs, physical and mental side effects, frequent hospital visits, and avoidable complications. Cancer conditions can lead to an increased production of free radicals by the immune system, resulting in oxidative stress, impaired cell function, and a compromised immune state (4).

Breast cancer is the most common cancer among women and ranks second overall when considering both genders (5). Globally, over 1 million women are diagnosed with breast cancer annually, and more than 410,000 lose their lives to this disease, accounting for 14% of female cancer deaths. Furthermore, the prevalence of breast cancer is projected to increase by up to 5% per year in several non-industrialized countries (6). It is estimated that by 2030, 192,370 women will be diagnosed with breast cancer, and 40,170 women will succumb to the disease. In India, breast cancer is the second most common cancer after cervical cancer, contributing to 19% of the total cancer burden in women (7). Approximately 80,000 women are diagnosed with breast cancer, and 40,000 lose their lives to the disease annually in India (3).

Breast cancer is characterized by the abnormal growth of cancer cells in the epithelial cells lining the lobules or ducts of the breast (ductal epithelium). The primary tumor originates in the breast itself but can become invasive and spread beyond the breast to regional lymph nodes or other organs, leading to a systemic disease (8). Metastatic spread, which is the main cause of breast cancer-related deaths, is often facilitated by tumor cells utilizing lymphatic routes for early dissemination. Tumor cells that remain in the lymph nodes can proliferate and eventually breach the node's capsule. Lymph nodes can also serve as a source from which tumor cells enter the bloodstream, spreading to distant organ sites such as the bones, liver, brain, and lungs (9).

India, known for its rich ecological diversity, has provided abundant resources, including plants, with potential therapeutic properties for various diseases. Plants are known to contain phytoconstituents that possess pharmacological qualities, such as anti-diabetic, anticancer, and cardioprotective effects. However, before identifying the biologically active compounds responsible for these properties, it is crucial to evaluate their antiproliferative characteristics. Once the anticancer properties of a plant have been established, dried forms of the plant can be used for patient treatment. However, it is necessary to isolate and concentrate the therapeutically significant molecules while eliminating any toxic compounds present (10).

Terminalia chebula Retzius (*T. chebula* Retz.), also known as black Myroblans, is a plant from the *Terminalia* genus that is widely distributed in tropical regions worldwide. It has been traditionally used in folk medicine and studied for its various properties, including homeostatic, antitussive, laxative, diuretic, and cardiotonic effects. Several *Terminalia* species, including *T. chebula*, have been investigated for their potential in treating cancer. Fruit extracts from *T. chebula* have shown memory-enhancing effects by improving neurotransmission in the central cholinergic system, which may be beneficial for Alzheimer's disease patients. Alcoholic root extracts from the plant have demonstrated local analgesic properties and can be used in oral surgeries at low concentrations. Furthermore, these extracts have shown potential in treating depression by interacting with dopamine and adrenergic receptors, leading to increased levels of noradrenaline and dopamine in the rat brain (11). Owing to its remarkable healing abilities, *T. chebula* is often referred to as the "king of medicines" in Ayurveda. It is believed to have broad-spectrum therapeutic effects, promoting tissue growth, and overall health while eliminating diseases and toxins from the body. *T. chebula* has been utilized in traditional formulations for its anti-diabetic, anti-inflammatory, laxative, antibacterial, antifungal, cardiotonic, diuretic, hyperlipidemic, jaundice, anti-helminthic, aphrodisiac, and restorative properties (12).

Nowadays, it is common to use bioinformatics tools to identify drugs for treating various diseases. One such tool is structure-based drug design, which allows for virtual screening of compounds to identify potential therapeutic candidates by examining their binding affinities with protein receptors before conducting *in vitro* and *in vivo* experiments. In this study, the performance of

integrated computational approaches involving molecular docking (MD), molecular dynamics simulation (MDS), and binding energy calculations was evaluated during interaction with protein receptors to identify potential anti-carcinogenic properties of TCF extracts against breast cancer cell line. Cytotoxicity analysis was performed using MTT (3-(4,5-Dimethylthiazol-2-yl)-2,5-diphenyltetrazolium bromide) assay of the ethanolic extract of TCF conducted on the MCF7 breast cancer cell line, and the bioactive compounds of TCF were further evaluated for their anticancer properties using MD, MDS, and binding energy calculation studies. Epidermal growth factor receptor (EGFR), also known as ErbB1 or HER1, is a cell surface receptor that plays a crucial role in various cellular processes, including cell growth, proliferation, and survival. It belongs to the ErbB family of receptor tyrosine kinases and is expressed on the surface of many cell types, particularly in epithelial tissues. Activation of EGFR occurs upon binding of specific ligands, such as epidermal growth factor (EGF) or transforming growth factor alpha (TGF-α). This binding leads to receptor dimerization and autophosphorylation of tyrosine residues in the intracellular domain, initiating downstream signaling cascades. The activation of EGFR triggers various intracellular pathways, such as the Ras/MAPK pathway and the PI3K/Akt pathway, which regulate cell proliferation, survival, and differentiation. Dysregulation of EGFR signaling is associated with numerous diseases, including cancer, where overexpression or mutations in EGFR can lead to uncontrolled cell growth and tumor progression. Therefore, EGFR has become an important target for therapeutic interventions, and drugs that inhibit EGFR signaling, such as tyrosine kinase inhibitors and monoclonal antibodies, have been developed for the treatment of certain cancers. The study of EGFR and its signaling pathways continues to provide valuable insights into cellular biology and potential avenues for targeted therapies.

2 Materials and methods

The chemicals required for the study were obtained from Loba chemicals (Bangalore, India). Demineralized water was collected from an ELGA RO system and was used throughout the experiments (Elga Veolia, Lane End, UK). Breast cancer cells (MCF-7) were procured from the ATCC and cultured in Dulbecco's Modified Eagle Medium (DMEM) with 10% fetal bovine serum (FBS), penicillin (100 IU/ml), and streptomycin (100 µg/ml) in 5% CO_2 at 37°C until confluence.

2.1 Preparation of *T. chebula* fruit extract

The sample was ordered from the Amruth Kesari depot, and it was dried in the shade for 3 days in a row on hot, sunny days. After that, the sample was ground into powder. After that, it was weighed and kept in a cool, dark room. To begin the ethanol extraction process, a 10-g sample was weighed, and 50 ml of 100% ethanol was added one at a time. The sample was kept in a water bath with the temperature set at 50°C for 4 h. Whatman filter paper was used to filter the samples after the incubation period of 4 h. The filtrate was then held at 80°C to allow the ethanol to evaporate (ethanol has a boiling point of 78.3°C) and produce the concentrated dried plant extract that can be utilized right away in various dilutions to analyze the apoptosis of MCF7 cells (13).

2.2 Phytochemical screening of the prepared plant extract

The presence of many substances, including alkaloids, phenols, flavonoids, tannins, saponins, glycosides, and many more, was determined using a qualitative phytochemical assay. The plant extract was dissolved in ethanol at a concentration of 100 mg/ml. It was then kept for dissolving in vortex at 50°C for 10 min. Each phytochemical assay was then conducted using it (12). The below-described assays were performed.

a. Screening for Alkaloids (Dragendroff's test)

Twenty microliters of concentrated HCl was added to 200 µl of the plant extract and then mixed properly. To the obtained solution, 100 µl of Dragendroff's reagent was added and then mixed well. Red precipitate appeared, indicating the presence of alkaloids (14).

b. Screening for carbohydrate (Molish's test)

A few drops of Molish's reagent were added to 200 µl of plant extract taken in a test tube. After mixing properly, a few drops of concentrated HCl were added slowly. Formation of red or violet ring at the junction of layer in tube indicated the presence of carbohydrates (15).

c. Screening for tannins

In 200 µl of extract, a few drops of 1% $FeCl_3$ solution were added while stirring. Formation of green precipitate points the presence of tannins (16).

d. Screening for terpenoid (Salkowski s test)

Two hundred microliters of chloroform and three to four drops of concentrated HCl were added to 200 µl of plant extract. It was then mixed well and kept for a few minutes. The formation of yellow precipitate indicated the presence of terpenoids (17).

e. Screening for glycoside (Liebermann's test)

In a glass test tube, 200 µl of plant extract was taken; later, chloroform and acetic acid were added and mixed. The mixture was then cooled in ice and concentrated HCl was added. The color change from violet to blue to green indicated the presence of glycosides (14).

f. Screening for steroid

To 200 µl of plant extract, 200 µl of chloroform and concentrated HCl were added. Presence of red color on the top layer indicated the presence of steroids in the sample (15).

g. Screening for saponin

Two hundred microliters of distilled water was added to 200 µl of plant extract solution. It was then shaken and warmed. Formation of stable foam indicated the presence of saponins (17).

h. Screening for flavonoids

Two hundred microliters of 10% lead acetate was added to equal volume of plant extract solution. The appearance of yellow-colored precipitate indicated the presence of flavonoids (16).

i. Screening for amino acid (ninhydrin test)

Two hundred microliters of the plant extract was mixed in 200 µl of 0.2% ninhydrin, which, upon reduction, resulted in a violet color, indicating the presence of amino acids (16).

j. Screening for mucilage

Two hundred microliters of the plant extract was dissolved in 500 µl of absolute alcohol and then allowed to dry. The absence of precipitate solution indicated the presence of mucilage (16).

k. Screening for volatile oils

Two hundred microliters of plant extract sample was mixed with dilute HCl. White precipitate indicated the presence of volatile oils (17).

2.3 Quantitative phytochemical analysis

2.3.1 DPPH radical scavenging assay

Antioxidants scavenge DPPH (2,2-diphenylpicrylhydrazyl) radicals by donating an electron, resulting in the reduction of DPPH. Its decrease in absorbance at wavelength 517 nm can be used to measure how quickly the color changed from purple to yellow after reduction. Different concentrations (20, 40, 60, 80, and 100 µg/ml) of gallic acid and plant sample were added to multiple test tubes. Methanol was added for the volume to reach 500 µl. Five milliliters of a 0.1 mM DPPH methanolic solution was added to each test tube, which was then vortexed. For 20 min, the tubes were left to stand at room temperature. Methanol was utilized for the baseline correction, and the control was made in the same way as the sample but without any extract. At 517 nm, changes in the sample's absorbance were detected (17). The inhibition percentage was used to express the radical scavenging activity. Gallic acid was used as standard. The relationship between concentration and percentage inhibition was plotted, and the IC50 value, the concentration needed to inhibit radicals by 50%, was calculated.

2.3.2 ABTS radical scavenging assay

The (18) method was used to determine the ABTS [2,2′-azino-bis(3-ethylbenzothiazoline-6-sulfonic acid)] radical scavenging assay. The relative ability of antioxidants to squelch the radical cation $ABTS^+$ served as the basis for the test. The ABTS decolorization assay involves the oxidation of ABTS with ammonium persulfate to produce the $ABTS^+$ chromophore. Both hydrophilic and lipophilic molecules can use it. At 734 nm, the plant extract's capacity to scavenge ABTS radical cation was determined. The reaction was started by adding 0.1 ml of diluted ABTS to 10 µl of variously concentrated aqueous extracts from the sample and 10 µl of methanol to act as the control, each of which had a different concentration. At 734 nm, the absorbance was measured (19).

2.4 MCF7 cell line preparation

The frozen MCF7 cell cryovials were taken from the liquid nitrogen storage and were thawed at a 37°C water bath by gentle shaking for less than 1 min until 70% of the culture is thawed. The vial was wiped with 70% ethanol to maintain aseptic conditions and then taken into the laminar air flow hood. Thawed cells were transferred into a 15-ml falcon tube and the required volume of incomplete DMEM media was added. Cell suspension was centrifuged at 11 rcf (*g*-value) for 5 min. The supernatant was discarded aseptically and DMEM medium was added to the cell pellet and resuspended in it. The number of viable cells was counted under the inverted microscope using Neubaur's counting chamber after staining it with Trypan blue dye. The cell suspension was transferred to a 25-cm^2 T flask and incubated at 37°C in a 5% CO_2 incubator (20).

2.4.1 Trypan blue viable cell counting method

No viable cells lose their membrane integrity; thus, trypan blue dye enters the dead cells, then they appear blue under the microscope. In contrast, viable cells that do not take up the dye appear white; 0.4% trypan blue solution was prepared by adding trypan blue in phosphate buffer saline, maintaining the pH at 7.4. Trypan blue solution and cell suspension were mixed in equal proportion. Cell suspension (20 µl) was loaded onto a hemacytometer and the cells were observed under low magnification. The number of viable cells and the total number of cells were counted (21).

2.4.2 Hemocytometer

Total number of cells in a given cell suspension was determined by counting the number of cells in the four squares and then taking their average using the following formula (21):

$$\textbf{Total number of cells/ml} = \textbf{Average no. of cells} \times 10^4$$

2.4.2.1 MTT cell cytotoxicity assay

Three rows of 96-well plates with an average cell density of 50,000 per well were seeded with cells on the first day and was kept overnight in a CO_2 incubator at 37°C, while a stock solution of plant extract in DMSO with a 32 mg/ml concentration was created on the second day. It was spun for 5 min to remove any debris. Six different dilutions (10, 20, 40, 80, 160, and 320 µg/ml) of the plant extract were prepared in the entire DMEM medium using the stock solution. A 96-well plate seeded with medium was removed, and media with various plant extract dilutions were added. Complete media to the reference wells and 1% DMSO-treated media to the control wells were added. The culture plate was incubated overnight in a CO_2 incubator at 37°C. The treated cells were examined using an inverted microscope on the third day. MTT powder in phosphate

buffer saline (pH 7.2) at a concentration of 5 mg/10 ml was used to prepare MTT reagent. Media was removed and the 96-well plates were filled with 100 µl of MTT reagent followed by incubation for 3–4 h at 37°C. The obtained formazan was dissolved by adding 100 µl of pure DMSO after removing the MTT reagent. Microplate reader was used to measure the absorbance at 570 nm after thoroughly shaking the plate (22). Inhibition percentage was calculated by the following formula:

$$\%\ \textbf{Inhibition} = \textbf{100} - (\textbf{OD of sample}/\textbf{OD of control}) \times \textbf{100}$$

2.4.2.2 Hemolysis assay

Blood (5 ml) was collected from healthy individuals, added to a vial containing EDTA, and mixed properly. The cells were centrifuged at 8 rcf for 10 min at 4°C. The supernatant plasma and white buffy layer were removed using a pipette while the collected erythrocytes were washed with 1×PBS thrice and the cells were diluted 10 times. Collected cells (100 µl) were added into 900 µl of 1×PBS. For positive control, 100 µl of 1% SDS was added to 50 µl of cells. For negative control, 100 µl of 1×PBS was added to 50 µl of cells. For treatment, 100 µl of 10 µg/ml and 15 µg/ml dilution of each sample was added to 50 µl of cells to different Eppendorf tubes and incubated at 37°C for 1 h. The reaction volume was adjusted to 1 ml by adding 850 µl of 1×PBS. Each reaction was centrifuged at 1 rcf for 5 min. Finally, 100 µl of supernatant of each reaction was transferred to the microtiter plate and measured for absorbance at 590 nm (23). Percentage hemolysis was calculated by the formula:

$$\%\ \textbf{Hemolysis} = (\textbf{Control} - \textbf{Sample}) \times \textbf{100}/\textbf{Control}$$

2.4.2.3 G2M phase studies

MCF-7 cells were cultured in a six-well plate with 2 ml of complete medium, with a cell density of roughly 1 million per well. Cells were incubated in a CO_2 incubator at 37°C for 24 h. The cells were treated with the samples at a concentration of 10 and 15 µg/ml, respectively, with 1% DMSO as control and incubated in a CO_2 incubator at 37°C for 24 h. Trypsin treatment was used to separate the cells in each vial before collecting them. The cell suspension was centrifuged at 18 rcf for 5 min. Once the supernatant was carefully discarded, the cell pellet was thoroughly washed in 1× PBS. While blending the cell pellet, 200 ml of PBS and 1 ml of the fixing solution (70% EtOH) was added drop by drop. After that, immediately 1 ml of the fixing solution was added. The cell was maintained at 4°C for overnight fixation. Later, the cells were centrifuged at 125 rcf for 10 min at room temperature. The supernatant was removed with care, without disrupting the particle, and the pellet was washed twice in cold PBS. The cell pellet was dissolved in 500 µl of a propidium iodide (PI) solution containing 0.05 mg/ml of PI and RNaseA in PBS. FACS Calibur (BD Biosciences, San Jose, CA) was used to record the cells at different cell cycle stages (24).

2.4.2.4 Apoptotic studies

In a six-well DMEM cell culture plate, 1×10^6 MCF-7 cells were seeded per well and incubated overnight in a CO_2 incubator at 37°C. The cells were treated with the supplied samples at concentrations of 10 and 15 µg/ml in DMEM basic medium while leaving one control untreated. This was then incubated overnight in a CO_2 incubator at 37°C. The cells were collected from the well and placed in several vials with medium. Cell suspension was centrifuged at 71 rcf for 10 min, and the supernatant was carefully discarded without disrupting the cell pellet. Cells should be washed twice with cold PBS before being resuspended in 1 × PBS at a concentration of approximately 1×10^6 cells/ml. A total of 1×10^5 cells in 100 µl of cells are transferred to a 5-ml FACS tube (or 12 × 75 mm tube). To this, 5 µl each of PI and Annexin V was added. Cells were carefully mixed and left to incubate for 15 min at room temperature in the dark. Each tube was filled with 400 µl of 1 × binding buffer before being analyzed by flow cytometry as quickly as feasible (within an hour) (25). The sequential identification and refinement of a population of cells with the target molecule were visualized using fluorescence studies.

2.5 LDH assay

MCF7 cells were plated on 96-well cell culture plates at a density of 1×10^4 cells per well, and they were then left to incubate for 24 h. Following medium changes and treatments with TCF concentrations of 10, 20, 40, and 80 µg/ml, the cells were cultivated for 24 h at 37°C. A cytoplasmic enzyme known as LDH (lactate dehydrogenase) was retained by healthy cells with intact plasma membranes but released by necrotic cells with damaged membranes. The Cytotoxicity Detection Kit was used to measure the released LDH in the media following incubation (26).

2.6 AO/EtBr staining assay

MCF7 cells were seeded on 96-well cell culture plates at a density of 1×10^4 cells per well, and they were then left to incubate for 24 h. Both living and dead cells were stained by the necessary dye acridine orange. Ethidium bromide can only stain cells that have lost the integrity of their membranes. Live cells would all be the same color of green. In a microcentrifuge tube, 25 µl (approximately 1×10^5 cells) of treated and untreated cells were collected individually and stained with 5 µl of AO-EtBr (acridine orange and ethidium bromide) for approximately 2 min before being gently mixed. A glass coverslip was placed over a microscopic slide containing 10 µl of cell suspension, and the slide was then studied using a fluorescence microscope with a fluorescein filter (27). (Depending on the type of cell, a higher or lower magnification may be preferred. Nuclear morphology ought to be apparent.)

2.7 ROS determination

In a six-well DMEM cell culture plate, 1×10^6 MCF-7 cells were seeded per well and incubated overnight in a CO_2 incubator at 37°C. The cell monolayer was washed with fresh media and cells were supplemented with fresh media and incubated for 2 h before

proceeding with the treatment. DCFDA (2′-7′-dichloro dihydrofluorescein diacetate) solution at 25 µM was prepared in DMEM media and 100 µl of the solution was added to each well and incubated for 45 min in the above-mentioned conditions. DCFDA solution was removed carefully, and cell monolayer was briefly washed with 1×PBS once without affecting the cell monolayer. Cells were then treated with and without test compounds of various concentrations for 2 h, and NAC (N-acetyl-L-cysteine) at 5 mM was used as a positive control (ROS inhibitor). After 2 h of incubation, the cells were then treated with H_2O_2 at 500 µM and incubated for further for 2 h. The fluorescent signal was read at 485 nm.

2.8 *In silico* studies

2.8.1 Protein and ligand preparation

The Protein Data Bank (PDB) tool (https://www.rcsb.org/) was used to retrieve the structure of EGFR receptor with PDB ID: 3W2S (27–29). After modeling the structure, the PDB coordinate file was submitted to the Procheck server. The most favored portions of the server plot, which is a graphical depiction of protein 3D structure, were confirmed. The protein model was confirmed, and the sections were identified by distinct colors. Furthermore, the binding sites of the modeled proteins were taken from the CASTp webserver (Figure 1) (30–33).

The IMPPAT database (https://cb.imsc.res.in/imppat/basicsearchauth) (34) was used to obtain the phytocompounds of TCF. This database includes more than 1,700 Indian medicinal plants with 1,100 therapeutic uses. The phytocompounds were identified based on their ADMET properties (35). The library of 20 molecules was made and the structure of the top five molecules that showed good and comparatively least binding affinity towards the selected proteins is depicted in Table 1. The study used 17β-estradiol as a reference compound because the estrogen receptor alpha is a significant biological target that mediates the development of breast cancer driven by this compound. The 3D and 2D structures of the compounds were obtained from the PubChem database (https://pubchem.ncbi.nlm.nih.gov/) in structure data file (SDF) format. The 2D structures were then converted into 3D coordinates and geometries using Open Babel, an open-source chemical toolbox. Subsequently, these structures were converted into PDB format (36, 37).

2.8.2 Molecular docking

The interaction of various phytocompounds with EGFR cancer target was investigated using molecular docking studies. The compounds were evaluated based on their binding free energies, binding affinity, and ability to form hydrogen bonds and exhibit high hydrophobic interactions. To understand the protein–ligand complex behavior, the docking studies were performed using PyRx

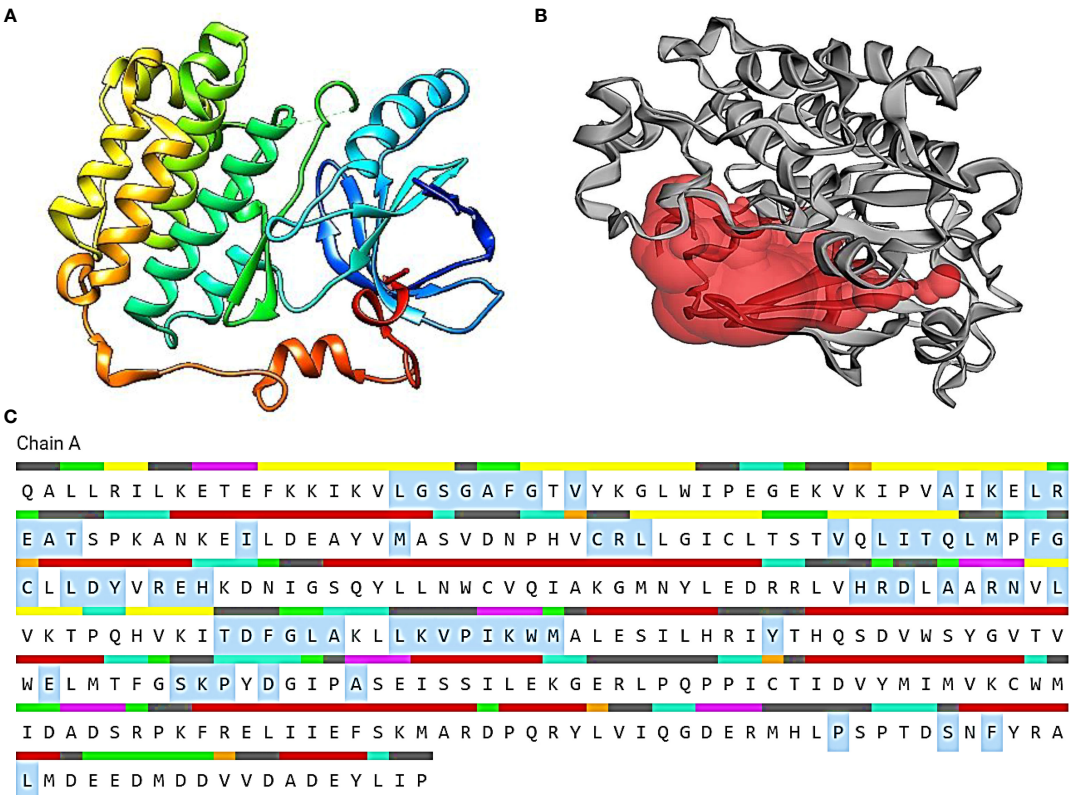

FIGURE 1
(A) The 3D representation of the 3W2S receptor. **(B)** The red pocket represents the binding pocket of the receptor. **(C)** The amino acid residues highlighted in gray specifies the amino acids present in the binding pocket of the 3W2S receptor.

10.3389/fonc.2023.1221275

TABLE 1 The structures of the top five molecules and standard drug docked with the 3W2S receptor.

Sl No.	Name of the molecule	Binding energy in kcal/mol 3W2S	Structure of the molecule
1	Phthalamic acid	−8.4	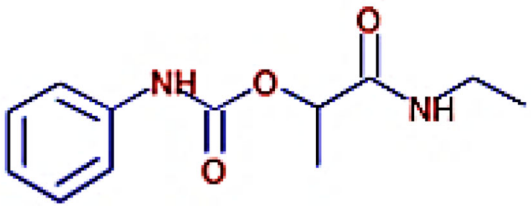
2	Saccharopine	−9.7	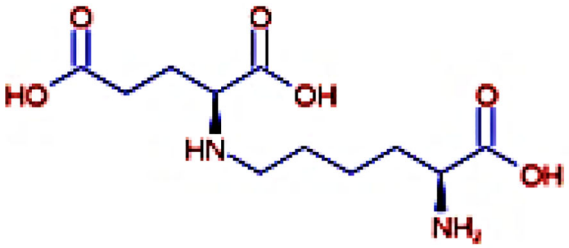
3	Mauritianin	−8.1	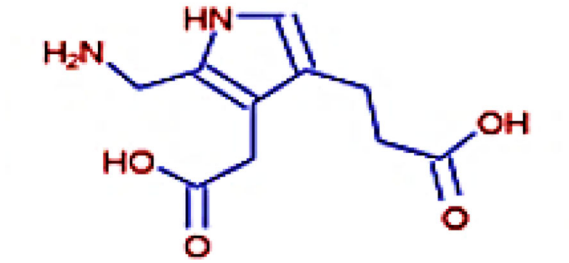
4	Carbetamide	−7.3	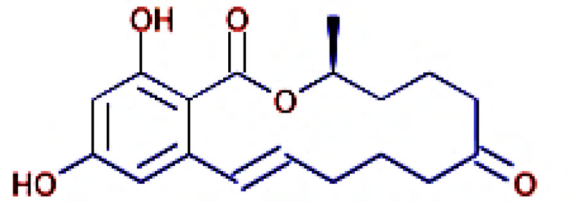
5	Silibinin	−5.4	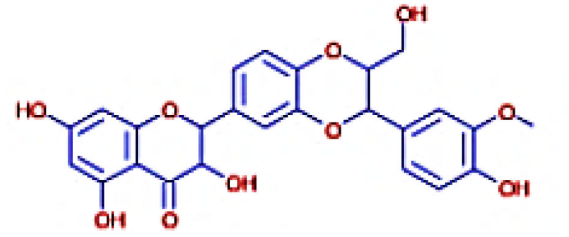
6	17β-estradiol	−4.4	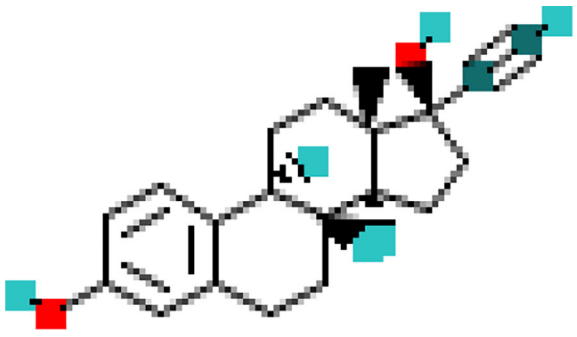

v0.8 (https://pyrx.sourceforge.io/), an open-access software (20, 38–40). The grid box was designed for the selected binding site residues to provide the best trajectory with the highest binding affinity values, shielding the active binding site residues for the selected binding site residues (41).

2.8.3 Molecular dynamics simulation studies

In this study, the stability of the conformers was evaluated by performing MD simulation analysis on ligands that showed the best binding energies according to the docking and cross-docking results. Traditional MD simulations of each system were performed using the GROMACS v5.1.4 program and the CHARMM36 all-atom force field, and the topology of the phytocompounds was created by the SwissParam website. The intermolecular complex from docking experiments, which serves as the starting structure for each system, was used in the independent MD simulations. The TIP3P water model was used to neutralize each system with counter-ions in a dodecahedron box, and then the steepest descent algorithm was used to minimize energy with a force below 1,000 kJ/mol. At a temperature of 300 K, the initial equilibration was carried out for 100 ns at constant volume (NVT) and at a constant pressure (NPT) of 1 bar. The Leapfrog method was used to produce production runs of 100 ns in the NPT ensemble at an integration time of 0.2 fs since we are refining the intermolecular complex from docking investigations. Root-mean-square deviation (RMSD) values, root-mean-square fluctuation (RMSF) values, solvent-accessible surface area (SASA), and H-bond interactions were calculated from MD trajectories.

2.8.4 Binding energy calculations

The findings of the MDS run for each target protein complexed with saccharopine and 17β-estradiol were used to calculate the binding free energies using the Molecular Mechanics/Poisson-Boltzmann Surface Area (MM-PBSA) method. Again, thermodynamics and molecular dynamics simulations were performed to determine the strength of the ligand interaction with the protein. The MmPbStat.py script, which uses the GROMACS 2018.1 trajectories as input, and the mmpbsa program were used to determine the binding free energy for each ligand–protein pair. The mmpbsa program uses three separate variables to calculate the binding free energy: molecular mechanical energy, polar and a polar solvation energy, and molecular mechanical energy. The calculation is finished using MDS. The most recent 100 ns of trajectory were used to compute G with dt 1,000 frames. This was evaluated using molecular mechanical energy, polar, and polar solvation energy. Equations 1 and 2 used to calculate the free binding energy are listed below.

$$\Delta G_{Binding} = G_{Complex} - (G_{Protein} + G_{Ligand}) \quad (1)$$

$$\Delta G = \Delta E_{MM} + \Delta G_{Solvation} - T\Delta S$$

$$\Delta E_{(Bonded+nonbonded)} + \Delta G_{(Polar+nonpolar)} - T\Delta SG \quad (2)$$

Binding: binding free energy; $G_{Complex}$: total free energy of the protein–ligand complex; $G_{Protein}$ and G_{Ligand}: total free energies of the isolated protein and ligand in solvent, respectively; ΔG: standard free energy; ΔEMM: average molecular mechanics potential energy in vacuum; $\Delta G_{Solvation}$: solvation energy; ΔE: total energy of bonded as well as non-bonded interactions; ΔS: change in entropy of the system upon ligand binding; T: temperature in Kelvin.

3 Results and discussion

3.1 Qualitative and quantitative phytochemical screening

3.1.1 Phytochemical screening

The ethanolic extract of the TCF contained flavonoids, polyphenols, tannins, alkaloids, and terpenoids, according to the results of the phytochemical screening (Table 2). These phytoconstituents are a class of compounds with diverse bioactivities, including anti-diabetic, anticancer, anti-inflammatory, antibacterial, and hepatoprotective effects. Additionally, research on the antioxidants found in plant extracts was done to create the goal of creating novel functional foods and nutraceuticals.

3.1.2 DPPH radical scavenging activity

TCF exhibited significant movement in the current study DPPH scavenging, reaching up to 78% at 100 µg/ml concentration. When compared to gallic acid, Figure 2 shows the dose–response curve for the DPPH scavenging activity of TCF. TCF had an IC_{50} of 44.54 ± 0.36 µg/ml while gallic acid standard had an IC_{50} of 68.47 ± 0.81 µg/ml. One of the frequently employed crucial methods to examine the existence of antioxidant molecules in plants and plant-based substances is the DPPH scavenging test. The findings showed that when compared to the standard, the TCF had potential DPPH scavenging activity.

TABLE 2 Phytochemical assay results of TCF.

Sl. No.	Phytochemical test	Plant sample (ethanolic extract) TCF
1	Alkaloids	+
2	Carbohydrates	+
3	Tannins	+
4	Terpenoids	+
5	Glycosides	+
6	Steroids	–
7	Saponin	+
8	Flavanoids	+
9	Proteins	–
10	Mucilage	–
11	Volatile oil	–

+ means present; – means absent.

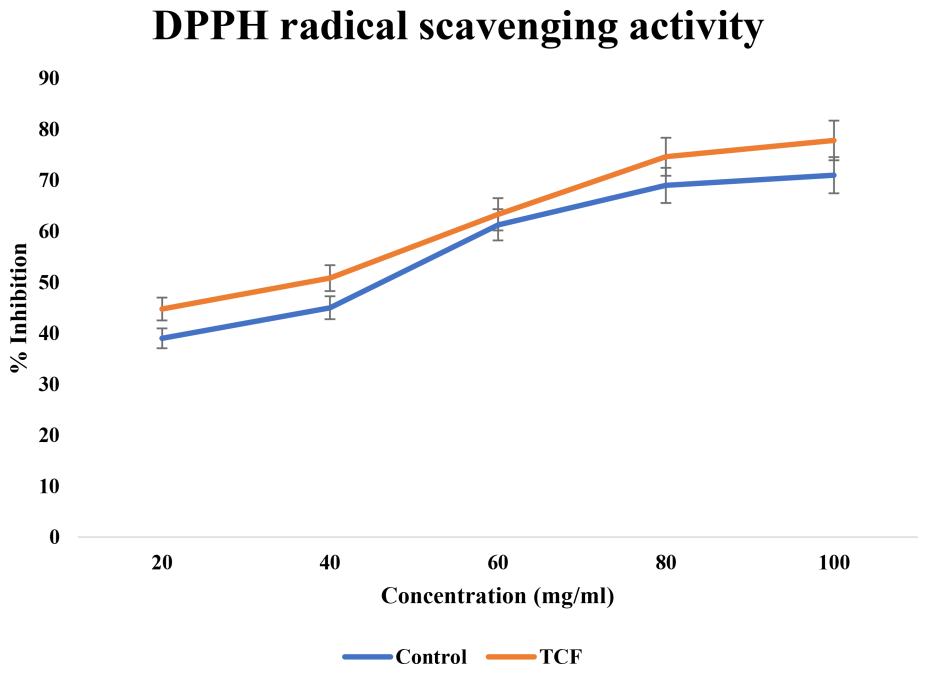

FIGURE 2
DPPH radical scavenging activity of TCF (sample) and gallic acid (control).

3.1.3 ABTS radical scavenging activity

The ascorbic acid standard verified that the TCF extract was a quick and effective ABTS scavenger (Figure 3). With an IC_{50} value of 69.73 ± 0.70 µg/ml, it demonstrated a significant scavenging activity against ABTS radicals. It had a powerful scavenging action that was significantly comparable to ascorbic acid (81.87 ± 0.15 µg/ml). TCF had an ABTS scavenging activity percentage of 96% at a dosage of 100 µg/ml, whereas ascorbic acid had a scavenging activity percentage of 81% at the same dose.

3.1.4 MTT cell cytotoxicity assay

There are various assays to measure cell viability, proliferation, and differentiation. MTT assay is one of the colorimetric, cell-based assays and is a reliable approach to quantitatively determine cell

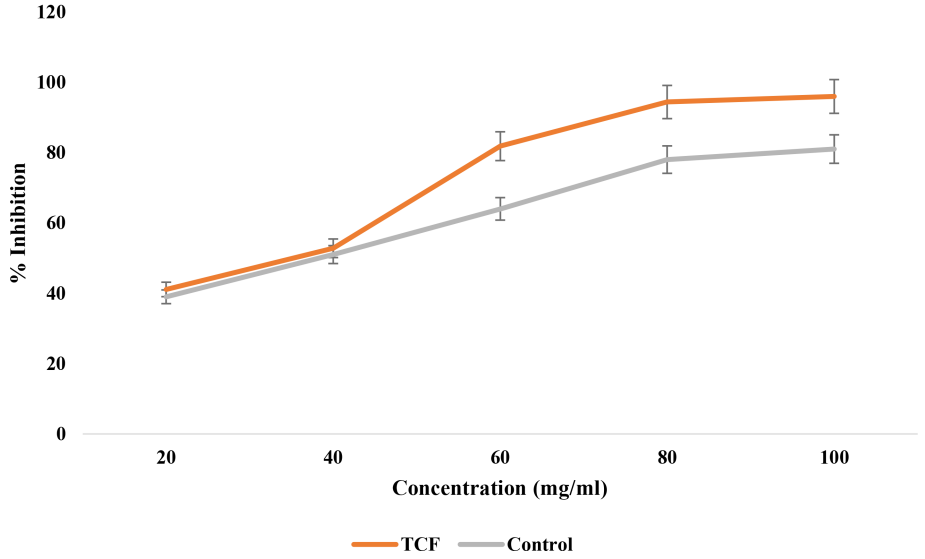

FIGURE 3
ABTS radical scavenging activity of TCF (sample) and ascorbic acid (control).

viability. Viable cells are intact and have the ability to reduce the soluble, yellow tetrazolium MTT (3-(4,5-dimethylthiazolyl-2)-2,5-diphenyltetrazolium bromide) into insoluble purple-colored formazan with the help of active mitochondrial dehydrogenase enzyme. The reaction involves reduced equivalents like NADH and NADPH as co-factors. As the formazan is insoluble, it is solubilized by cell lysis and the color intensity is measured by a colorimeter. The cells treated by drugs do not have viable cells and, hence, do not hold active enzymes to reduce MTT, and thus, they do not exhibit much change in color whose optical density is recorded and analyzed (42).

Different quantities of the TCF extract were introduced to the MCF-7 cell line, then incubated for 24 h to test their antiproliferative effect. According to the results of the MTT experiment, cell viability gradually declines as TCF concentration rises (Figure 4) with an IC_{50} of 103.2 µg/ml. Morphology of the cells was observed under an inverted microscope and was evaluated at the IC_{50} concentration of TCF.

3.1.5 Hemolysis assay

Plant extract might contain certain compounds that can induce lysis of erythrocytes. Such plant extracts are not reasonable to use for the treatment of cancer cells. To test the ability of plant extract to induce RBC's lysis, hemolysis assay is performed (Figure 5). This test involves taking RBCs from a healthy person's blood, treating them with the desired plant extract, and measuring the amount of hemoglobin produced as a result of lysis using a spectrophotometer (33). TCF was tested for its hemolytic abilities where no hemolysis of red blood cells was observed, which suggests that TCF plant extract samples can be used for G2M and apoptotic studies.

3.1.6 G2M phase studies

When cancer cells are treated with some compound, their cell cycle progression should be inhibited in order to stop their multiplication. Cell cycle studies are to be done in order to analyze the effect of drugs on tumor cells. For the determination of cell cycle distribution and progression, flow cytometry is the most favored approach in which the DNA content of the cells is measured at a moment of the cells (43). The DNA of the cell is stained with the high-affinity DNA binding dyes. The dye used must bind to DNA stoichiometrically, which means that the cells that are in G2 phase will show twice more fluorescence as seen in the G1 phase.

The treatment of cells at the concentrations of 10 µg/ml and 15 µg/ml of TCF has shown G2 phase arrest of 16.81% and 23.62%, respectively, when compared to control, which has 7.7% arrest in MCF-7 cells. TCF showed 6.13% and 4.39% S phase arrest at 10 µg/ml and 15 µg/ml in MCF-7 cells, respectively (Figures 6–8). The appearance of reddish orange fluorescence with fragmented chromatin after MCF-7 cells were treated with TCF suggests that they largely induced apoptosis in MCF-7 cells. This is because EtBr, which imparts orange color, can enter only injured or dead cells.

3.1.7 Apoptotic studies

Apoptosis is a type of cell death that is predetermined by the cell and is brought on by stimuli such as UV radiation and toxic substances. Under unfavorable circumstances, cells trigger the major physiological process of apoptosis, which leads to their own self-destruction. The process of stem cell proliferation and differentiation subsequently replaces these unhealthy cells with healthy ones, maintaining homeostasis. Cytotoxic medications can be used in chemotherapy because they cause apoptosis in cancer cells when they are administered to them (44).

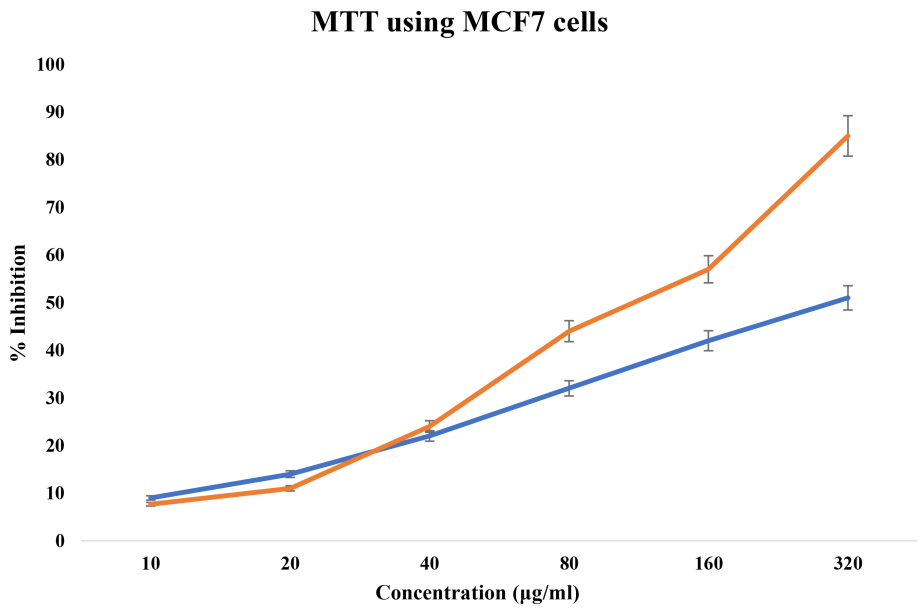

FIGURE 4
MTT cell cytotoxicity assay of TCF extract in orange and control in blue.

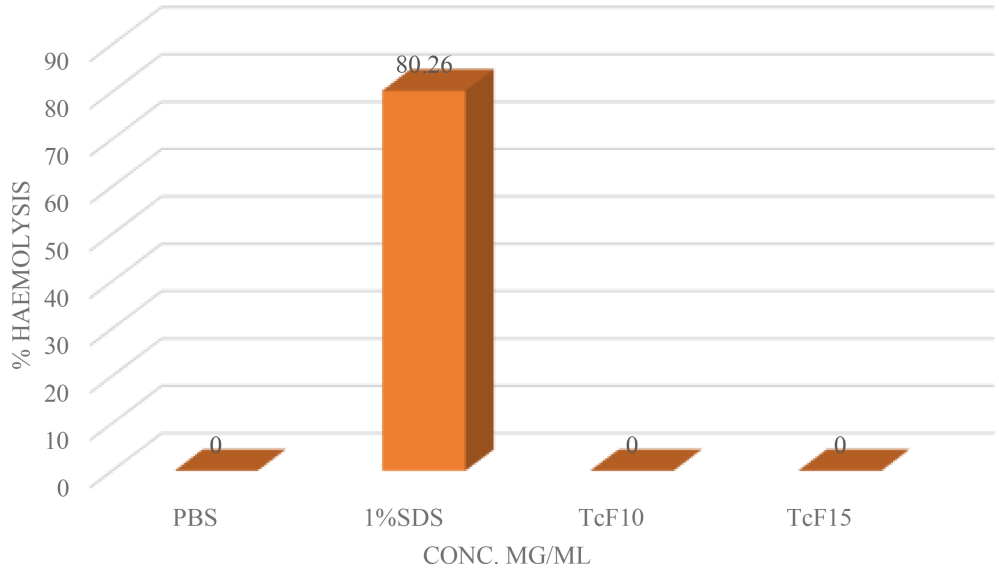

FIGURE 5
Hemolysis assay of TCF plant extract.

When a cell undergoes apoptosis, several morphological changes occur in the cell. It loses its membrane integrity, starts forming blebs, cytoplasm condenses, and nuclear DNA fragmentation occurs. The plasma membrane of the cell is made of two layers of phospholipids and various proteins. These phospholipids' bilayer arranges them as their hydrophobic tails face towards each other and hydrophilic heads face towards the extracellular fluid and cytoplasm, forming the two leaflets, outer and inner. Certain phospholipids localize themselves in any of the leaflets, e.g., phosphotidylserine is specially found in the inner leaflet of the plasma membrane. When the cell undergoes apoptosis, the phosphotidylserine becomes exposed to the outer surface of the plasma membrane, which can be used as a marker to detect whether a cell is in early apoptotic stage or not. Even the late apoptotic stages of cell can be determined by determining the DNA fragmentation in the cell, which specifically occurs in the cells that are in late apoptotic stage. Phosphatidylserine can be marked by using annexin V dye, which binds to it in the presence of Ca^{+2}. Also, annexin V bound to phosphatidylserine can be detected in the flow cytometer by conjugating annexin V with chromophore FITC (green fluorescence). DNA fragmentation can be detected by using PI (red fluorescence), which binds to double-stranded DNA. If the cell shows a positive result for both dyes, then it is in the late apoptotic stage. If it is negative for both, then it is viable and if the cell shows positive only for Annexin V-FITC, then it is in the early apoptotic stage (Shivalingaiah et al., 2022).

This investigation looked at how TCF affected the induction of apoptosis in MCF-7 cells (Figure 9). Dot-plot graphs were divided into four quadrants: the lower left quadrant displayed viable cells, the lower right quadrant showed early-phase apoptotic cells, the upper right quadrant displayed late-phase apoptotic or dead cells, and the upper right quadrant showed necrotic cells (the upper left quadrant). At 24 h, the MCF-7 lower right (LR) quadrant's early cell populations were 0.03% and 47.22%. Additionally, at a dosage of 10 and 15 µg/ml, the percentage of late apoptotic cells in the upper right quadrant of the MCF-7 sample was 15.0% and 52.38%. After the therapy was given for an additional 72 h, more than 50% of MCF-7 cells were in the late apoptotic phase.

3.2 LDH assay

The LDH activity of culture MCF-7 cells exposed to TCF was measured, and no significant changes in LDH release were seen at doses less than 20 µg/ml. Cell membrane damage causes the LDH leakage assay. After the cells were treated to the anticancer drugs, LDH levels (a sign of necrosis) in the cell media clearly increased (Figure 10). The necrotic action of TCF at high concentrations may explain the increase in LDH activity of MCF-7 cells exposed to high doses of TCF.

3.3 AO/EtBr staining assay

An increase in apoptosis-inducing cell cycle arrest was found when MCF-7 cells were treated with TCF; apoptosis-induced cell death was determined using the acridine orange/ethidium bromide dual-labeling procedure. The cells were stained with acridine orange

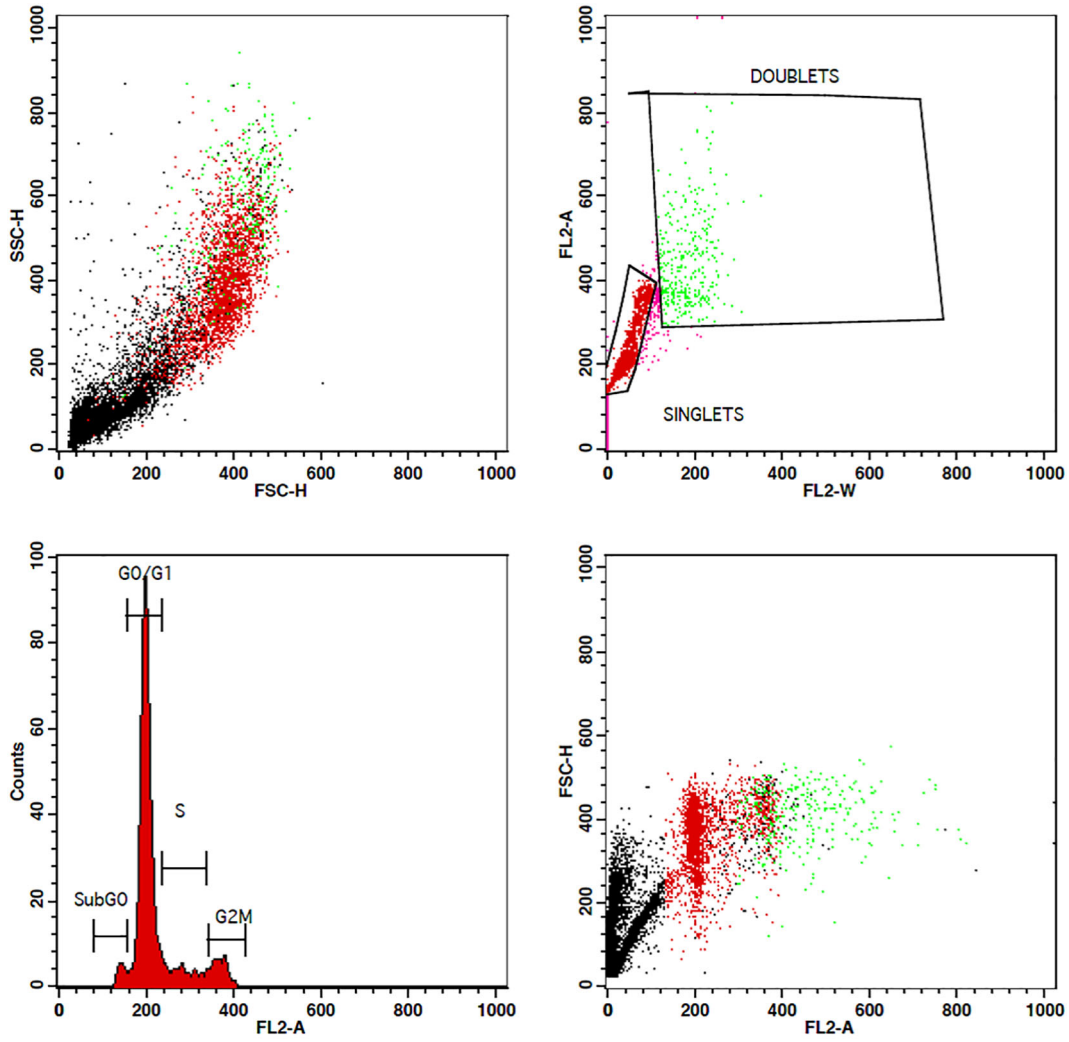

Histogram Statistics

Marker	Left, Right	Events	% Gated	% Total	Mean	CV
All	0, 1023	3000	100.00	26.92	219.20	24.39
SubG0	80, 156	95	3.17	0.85	143.43	4.66
G0/G1	156, 234	2343	78.10	21.02	198.77	6.31
S	237, 336	299	9.97	2.68	280.89	10.23
G2M	341, 427	233	7.77	2.09	365.63	3.85

FIGURE 6
Flow cytometry plots representing the cell cycle distribution of MCF-7 cells under control conditions. The plots illustrate the percentages of cells in different phases of the cell cycle, including G0/G1, S, and G2/M. The control group shows the baseline cell cycle distribution of untreated MCF-7 cells.

and ethidium bromide after being treated with escalating doses of TCF for 24 h. Under a fluorescent microscope, apoptosis-inducing cells contain compacted chromatin that takes up the ethidium bromide stain and turns orange, whereas live cells appear as green-colored entities (40×). The appearance of reddish orange fluorescence with fragmented chromatin after MCF-7 cells were treated with TCF suggests that they largely induced apoptosis in MCF-7 cells. This is because EtBr, which imparts orange color, can enter only injured or dead cells as shown in Figure 11.

3.4 ROS determination

The formation of reactive oxygen species (ROS) in MCF-7 cells exposed to TCF was observed to rise in a concentration-dependent manner. When comparing untreated MCF-7 cells to TCF exposed MCF-7 cells, fluorescence microscopic examination clearly revealed a dose-dependent increase in the intensity of green fluorescence. The highest ROS production was seen at 15 μg/ml, when it was 2.2-fold higher than the untreated control (Figure 12).

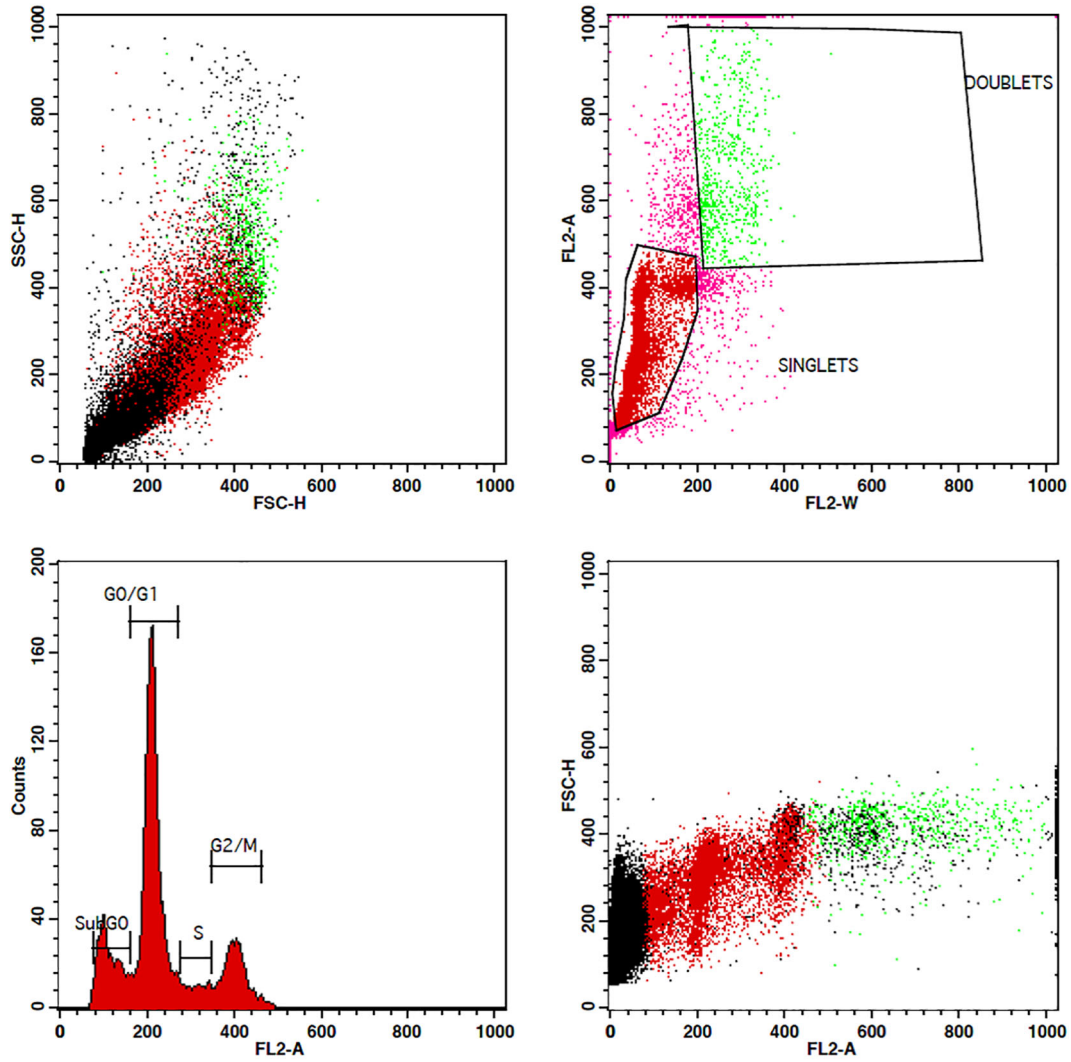

Histogram Statistics

Marker	Left, Right	Events	%Gated	%Total	Mean	CV
All	0, 1023	10000	100.00	12.48	234.04	39.22
SubG0	77, 163	1769	17.69	2.21	115.48	19.93
G0/G1	161, 273	5906	59.06	7.37	212.94	9.42
S	277, 348	613	6.13	0.77	312.79	6.85
G2/M	348, 465	1681	16.81	2.10	400.03	6.15

FIGURE 7
Flow cytometry plots representing the cell cycle distribution of MCF-7 cells treated with 10 µg/ml of TCF extract. The plots display the percentages of cells in the G0/G1, S, and G2/M phases of the cell cycle. Treatment with TcF extract at this concentration results in notable modifications in the cell cycle profile compared to the control group, indicating potential effects on cell cycle progression.

3.5 *In silico* studies

3.5.1 Molecular docking studies

Molecular docking is a computational technique used in the field of structural biology to predict the binding mode and affinity of a small molecule (ligand) to a target protein (receptor). The technique involves generating a set of possible conformations of the ligand and receptor, and then evaluating the potential interactions between them using various scoring functions. The goal is to identify the most favorable binding pose, which is the conformation of the ligand that maximizes its interactions with the receptor. Docking is widely used in drug discovery and design, as it can provide valuable insights into the binding mechanisms of potential drug candidates with their targets. It can also be used to screen large libraries of compounds to identify potential lead compounds that could be developed into drugs.

The obtained results confirm the best docking poses of all the selected ligands corresponding to their lowest binding affinity. The obtained protein–ligand interaction was further visualized and analyzed using Chimera software as it shows the binding residues that form the bonded and non-bonded interactions between the

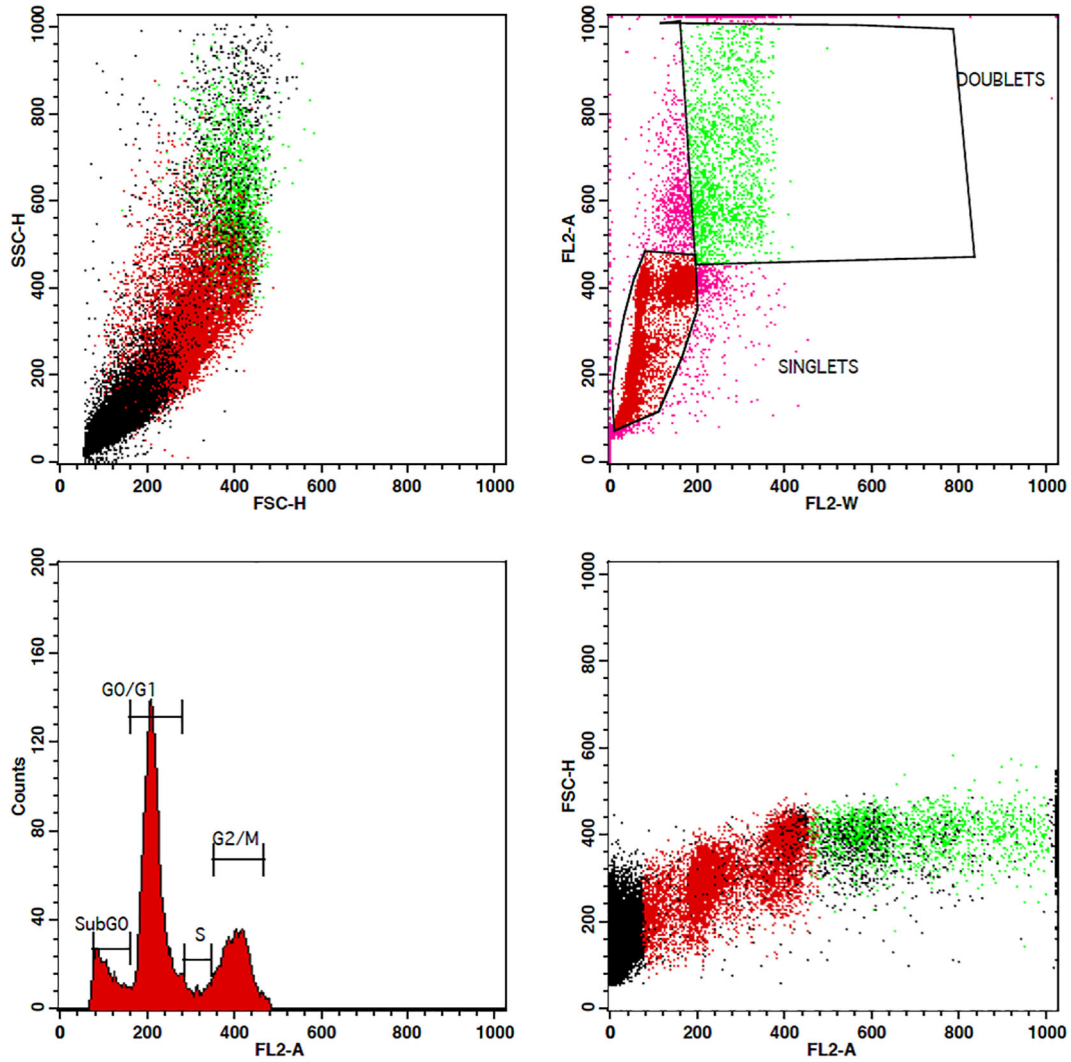

Histogram Statistics

Marker	Left, Right	Events	% Gated	% Total	Mean	CV
All	0, 1023	10080	100.00	21.31	252.52	39.01
SubG0	77, 163	1220	12.10	2.58	111.28	21.70
G0/G1	161, 281	5885	58.38	12.44	214.38	10.40
S	286, 348	443	4.39	0.94	317.11	6.05
G2/M	353, 469	2381	23.62	5.03	403.46	6.56

FIGURE 8
Flow cytometry plots depicting the cell cycle distribution of MCF-7 cells treated with 15 µg/ml of TcF extract. The plots illustrate the proportions of cells in the G0/G1, S, and G2/M phases of the cell cycle. Treatment with TCF extract at this concentration induces significant changes in the cell cycle profile compared to the control group, suggesting a pronounced effect on cell cycle progression.

protein–ligand complex. The 3D docking interaction of breast cancer protein 3W2S with ligands saccharopine and 17β-estradiol is shown in Figures 13 and 14. The saccharopine ligand exhibits a least binding affinity of −9.7 kcal/mol and GLN-791, MET-793, CYS-797, THR-854, and ASP-855 residues form the bonded interactions, whereas VAL-726, ALA-743, and LEU-844 residues form the non-bonded interactions with the 3W2S receptor. 17β-Estradiol comparatively exhibits a low binding affinity of −4.4 kcal/mol and LYS-745 residue formed one-bonded interaction, whereas LEU-718, ALA-722, VAL-726, ALA-743, ARG-841, and LEU-844 residues formed the non-bonded interactions, and it was also seen that the standard drug formed a non-favorable interaction with the MET-793 residue of the 3W2S receptor. The obtained *in silico* results infer that saccharopine molecule as the most potent phytochemical present in TCF leaf can be used as the best breast cancer inhibitor compared to the standard, as it showed very high binding affinity and very low binding energy with a good amount of bonded and non-bonded interactions.

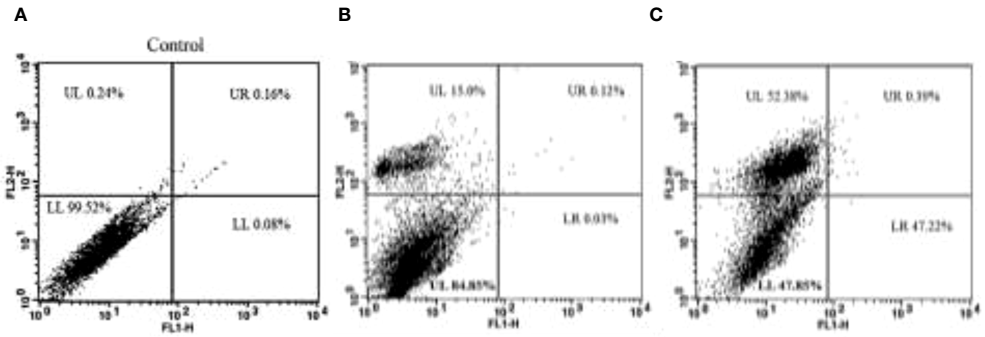

FIGURE 9
(A) The control plot represents MCF-7 cells in their untreated state, showing the baseline distribution of cell populations in the G0/G1, S, and G2/M phases of the cell cycle. **(B, C)** The plots of cells treated with 10 µg/ml and 15 µg/ml of TCF extract demonstrate the effects of the sample on the cell cycle profile. Treatment with TCF at both concentrations induces changes in the distribution of cells across the cell cycle phases, indicating potential alterations in cell cycle progression.

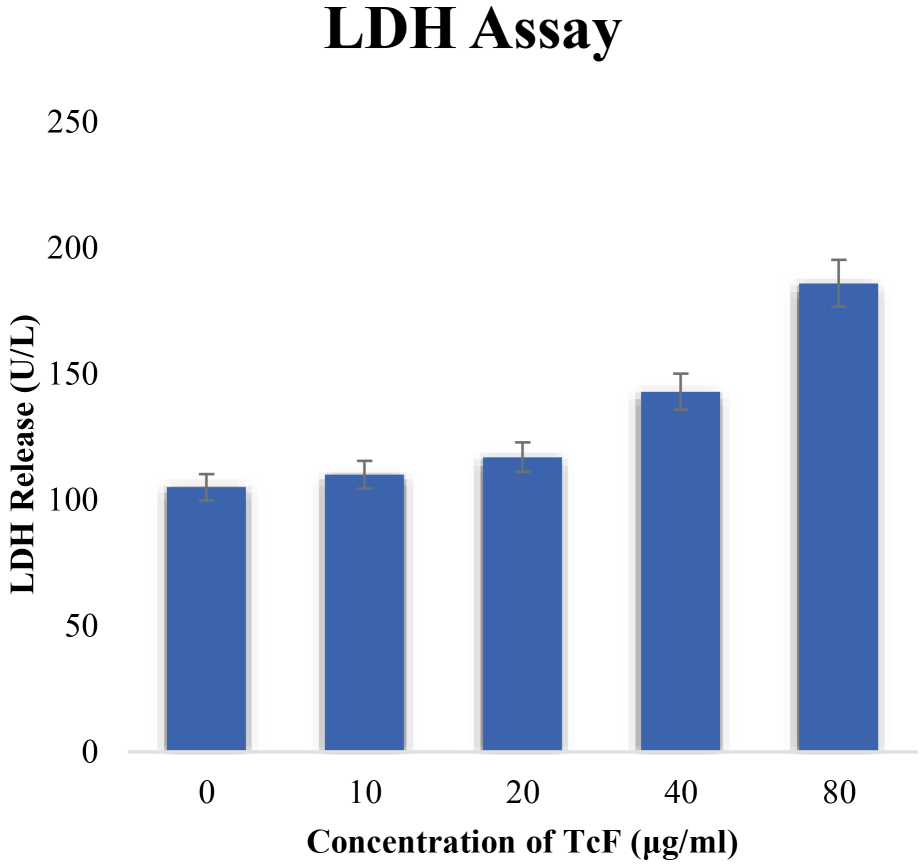

FIGURE 10
LDH activity of cultured MCF-7 cells exposed to TCF.

3.5.2 Molecular dynamics simulation studies

Molecular dynamics simulation (MDS) is a computational method used to investigate the dynamic behavior of biological macromolecules such as proteins and nucleic acids. MDS involves the application of classical mechanics equations to simulate the movements of atoms and molecules over time. It can provide valuable information on the conformational changes, flexibility, and stability of macromolecular systems in solution or at interfaces. By applying external forces and thermal fluctuations to the simulated system, MDS can mimic the behavior of biological systems in a realistic manner. MDS is widely used in drug discovery, protein engineering, and materials science to predict the behavior of

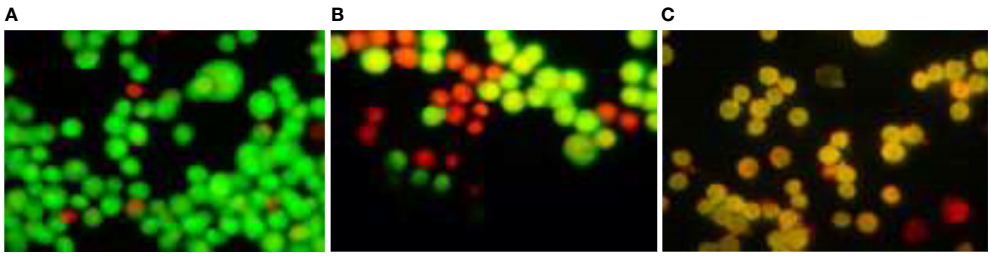

FIGURE 11
AO/EtBr staining assay. **(A)** Control, **(B)** TCF 10 µg/ml, and **(C)** TCF 15 µg/ml on the MCF7 cell line.

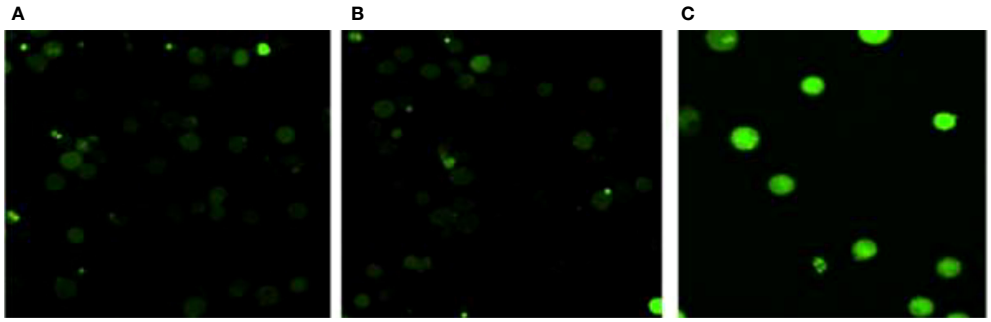

FIGURE 12
ROS determination assay. **(A)** Control, **(B)** TCF 10 µg/ml, and **(C)** TCF 15 µg/ml on the MCF7 cell line.

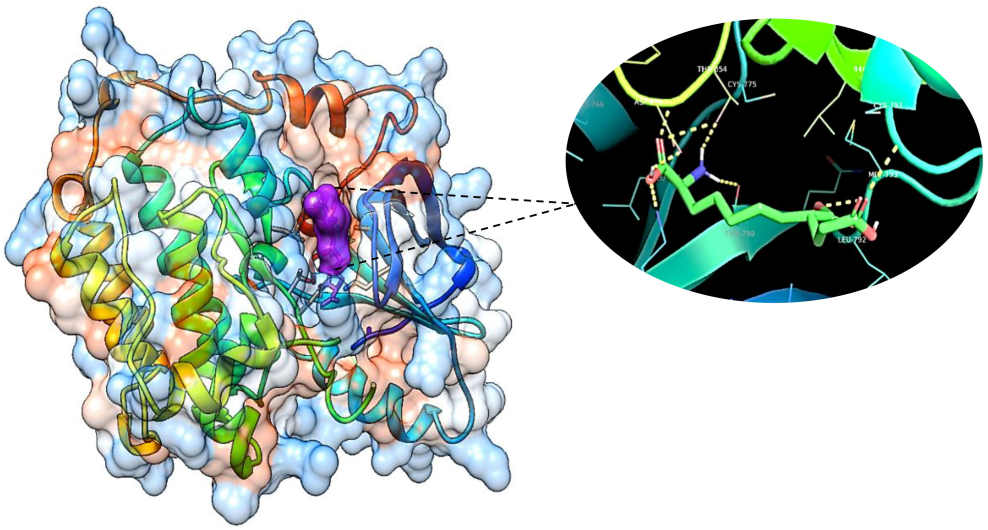

FIGURE 13
The 3D image of saccharopine (purple pocket) depicting the bonded molecular interactions (yellow dotted lines) with the 3W2S receptor (blue hydrophobic pocket).

molecules and optimize their properties. MDS is commonly used to predict and refine the binding of small molecules with proteins, as well as to assess the stability of these interactions. In this study, MD simulations were utilized to improve the predicted binding of screened phytocompounds of TCF with their individual drug targets, as well as to examine the intermolecular interactions and stability of these compounds with their targets, with the aim of discovering potential anti-lung cancer lead molecules. The predicted complexes from docking studies were used as the initial structures for the MD simulations.

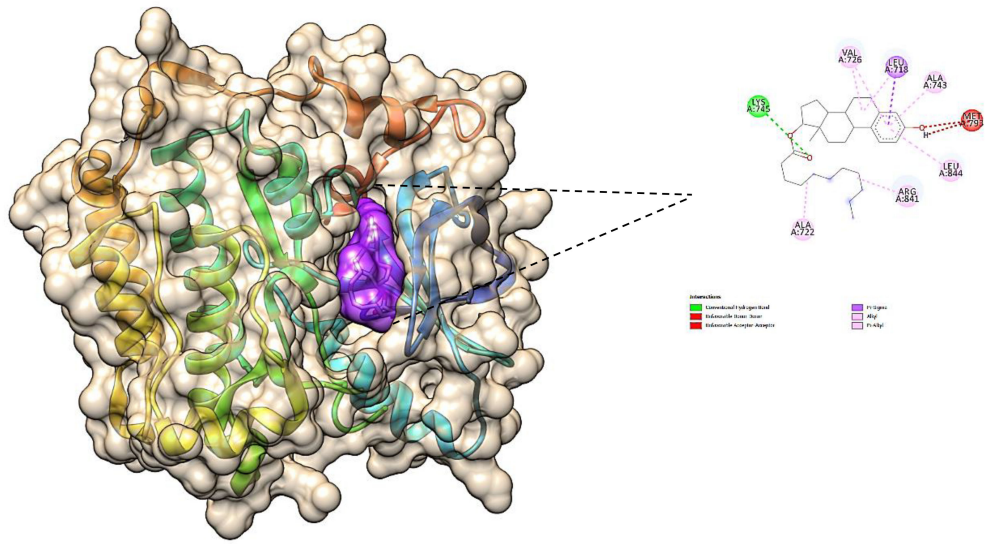

FIGURE 14
The 3D image of 17β-estradiol (purple pocket) depicting the bonded molecular interactions (yellow dotted lines) with the 3W2S receptor (brown hydrophobic pocket).

To analyze the conformational fluctuations of protein–ligand complexes, this study utilized RMSD calculations. The RMSD measures the deviation of the protein backbone and ligand coordinates from their initial docked pose coordinates. It calculates the average distance between superimposed protein and ligand structures over time, and it is a valuable metric to assess the stability of the complex. The RMSD plots were constructed using qt-Grace software and showed that the RMSD values of protein (3W2S) along with saccharopine remained stable within the range of 0.13 to 0.23 Å from 0- to 20-ns frames, and then slightly fluctuated from 70 to 85 ns in the complex. However, the 3W2S–17β-estradiol complex deviated throughout the simulation, making it an unstable molecule.

RMSF was also used to examine the regions of the protein that deviate the most/least from the mean. It calculates the root mean square distances with respect to the central axis of rotation. The RMSF plots generated from this study showed that the complexes were stable, with fluctuations only at the terminal ends and loop regions. The RMSF plots of 3W2S with saccharopine indicated that all amino acids located in the enzyme's active site had RMSF fluctuations between 0.01 and 0.35Å, indicating that the studied compounds maintained close contact with their binding pockets during the MD simulations. However, 3W2S with 17β-estradiol showed higher variations compared to saccharopine compound.

To gain a better understanding of the changes in the complex's surface area, the SASA of the simulation complex was examined. A higher SASA suggests an increase in surface volume, while a lower SASA implies a reduction in the complex's size. The SASA measures the surface area of the hydrophobic core created by protein–ligand interactions. Notably, the 3W2S protein–saccharopine complex exhibited consistent SASA values compared to other complex (Figure 15).

Additionally, hydrogen bonds were evaluated to determine the bonding and structural changes in the complex. The stability of the complex was determined by the hydrogen bonds present during the simulation. The hydrogen bonds were evaluated across the simulation duration, and the entire complex exhibited a stable trend. Hydrogen bonding is a crucial factor in molecular recognition specificity, and the hydrogen bond patterns of the complexes were investigated over the entire 100-ns simulation trajectory using GROMACS. The results showed that 3W2S with saccharopine formed more hydrogen bonds than all other conformers, while the 3W2S plus 17β-estradiol complex formed only one hydrogen bond, along with one unfavorable bond, making it an unstable molecule compared to saccharopine.

3.5.3 Binding energy calculations

Binding energy calculations are used to quantify the strength of the interactions between a ligand and a target protein. The binding energy is the amount of energy released or absorbed when the ligand and target protein interact and form a complex. It is calculated by subtracting the energy of the unbound ligand and target protein from the energy of the bound complex. A lower binding energy indicates a stronger interaction between the ligand and protein. Various energy metrics, such as van der Waals energy, electrostatic energy, polar solvation energy, SASA energy, and binding energy, can be utilized to measure the extent of ligand–target protein binding interactions during molecular dynamics simulations. These calculations can help in the design and development of new drugs by identifying compounds that have high binding affinity and stability with the target protein.

In molecular dynamics simulations, several energy metrics such as van der Waals, electrostatic, polar solvation, SASA, and binding energies are commonly used to quantify the extent of ligand–target protein binding interactions. In this study, the protein–ligand combination was primarily constructed using the electrostatic energy metric, followed by van der Waals energy, SASA energy, and binding energy. However, the polar solvation energy was not considered for

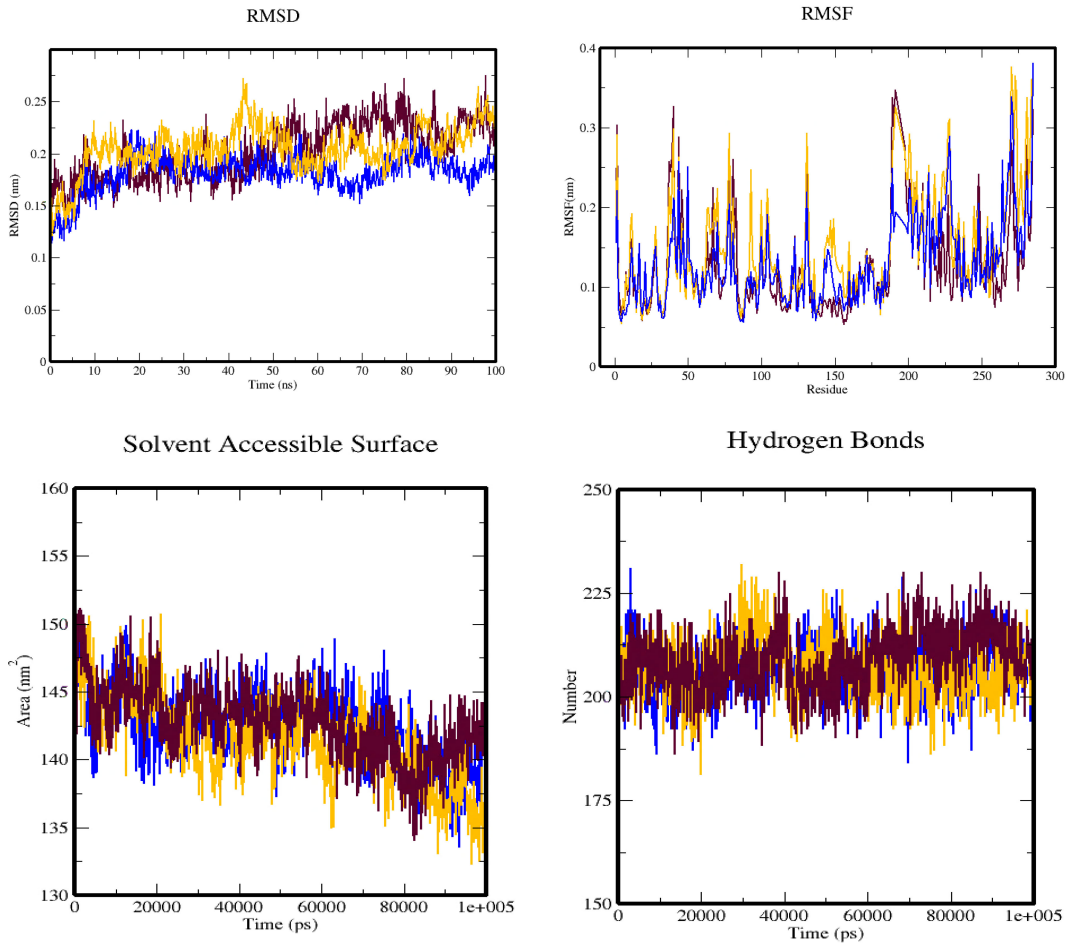

FIGURE 15
The simulation trajectories obtained from the molecular dynamics simulation over 100 ns depict four plots: **(A)** RMSD plot, **(B)** RMSF plot, **(C)** SASA plot, and **(D)** hydrogen bond plot. These plots are color-coded, with maroon representing the 3W2S alone, blue representing the 3W2S–saccharopine complex, and orange representing the 3W2S–17β-estradiol complex.

protein–ligand complex formation since its values appeared to be positive. The 3W2S complex, which was formed by saccharopine and 17β-estradiol, exhibited the highest binding affinity and was therefore chosen for the binding energy calculation studies. Moreover, the standard deviations of the protein–ligand complex were computed. A lower standard deviation suggests that the data values are close to the mean, while a higher standard deviation implies that the data values are dispersed over a broader range. However, in the complex, no high standard deviations were observed, indicating that saccharopine and 17β-estradiol bind to the protein with a high binding affinity and stable interaction. The binding free energy calculations of the protein–ligand complex are summarized in Table 3.

4 Conclusion and future prospects

As one of the top causes of death for women, breast cancer must be detected and treated as soon as possible in order to avoid

TABLE 3 Binding free energy calculations of EGFR tyrosine kinase complexed with the lead metabolite of *Trichoderma* spp. and standard inhibitor.

Category	3W2S–saccharopine complex	3W2S–17β-estradiol complex
	Values (kcal/mol)	Values (kcal/mol)
Electrostatic energy	−133.567	−95.788
Van der Waals energy	−5.682	−3.564
Polar salvation energy	17.164	26.810
SASA energy	−10.240	−2.545
Binding energy	−87.740	−18.338

metastasizing. Plant-derived bioactive chemicals have the potential to be powerful medicines; however, many plants have not yet been studied for their apoptogenic and antiproliferative effects. According to the results of the current study, *T. chebula* fruit extract has been found to be non-hemolytic and cytotoxic to the MCF-7 breast cancer cell line. As a result, the bioactive chemicals from the fruit could be exploited as a possible therapeutic agent against breast cancer. The investigation of saccharopine as a potential anticancer agent necessitates more comprehensive *in vivo* studies to assess its efficacy, safety, and therapeutic potential. Although encouraging outcomes have been observed in *in vitro* experiments, *in vivo* studies are essential for evaluating the compound's effectiveness in a complex biological system and assessing its pharmacokinetics, toxicity profile, and long-term effects. However, the isolation and testing of saccharopine pose challenges due to its limited natural occurrence and availability. Obtaining sufficient quantities of pure saccharopine for extensive *in vivo* studies may require specialized synthetic or biosynthetic approaches. Moreover, the administration and delivery of saccharopine *in vivo* present additional obstacles, such as determining the optimal dosage, route of administration, and formulation to achieve systemic distribution and tumor targeting. Additionally, understanding saccharopine's selectivity, potency, and potential limitations in its anticancer efficacy, as well as its impact on different cancer types, heterogeneity, and underlying mechanisms of action, is crucial for its further development as an anticancer therapeutic. Overall, addressing these challenges and conducting thorough *in vivo* investigations will provide valuable insights into the therapeutic potential of saccharopine and guide future preclinical and clinical studies.

The goal of the current study was to investigate and assess the efficacy of fruit in inhibiting the estrogen receptor and progesterone receptor-positive MCF-7 cell line. In preliminary antioxidant and anti-inflammatory studies, phytochemicals with anticancer potential were found. Via the induction of necrosis and cell cycle arrest, TCF extract reliably decreased MCF-7 breast cancer cell survival. In cytotoxicity testing, the phytocompounds identified in TCF were found to kill cells. The cytometric results provided strong support for the pro-apoptotic compulsions of G0/G1 phase cell cycle arrest that were responsible for the observed cytotoxicity. Based on *in silico* observations, it may be hypothesized that the MCF-7 cytotoxicity of TCF occurs via the involvement of the EGFR receptor.

Data availability statement

The datasets for this article are not publicly available due to concerns regarding participant anonymity. Requests to access the datasets should be directed to the corresponding author.

Author contributions

Conceptualization: PR and SP. Methodology: PR, SP, RA, CD, CSS, and SK. Software: SP. Validation: PR, SP, SM, and GS. Formal analysis: PR, SP, AS, MA, SE, and CS. Investigation: PR and SP. Data curation: PR, DG, ES, VS, NM, and SP. Writing—original draft preparation: PR, SP, SC, and CS. Writing—review and editing: PR, SK, and CD. Visualization: SP. All authors listed have made a substantial, direct, and intellectual contribution to the work, and approved it for publication.

Funding

The authors thank the Deanship of Scientific Research at King Khalid University under the project grant number R.G.P. 2/213/44.

Acknowledgments

The Authors acknowledge the support and infrastructure offered by the JSS Academy of Higher Education and Research (JSSAHER), Mysuru, India and the Director, Amrita Vishwa Vidyapeetham, Mysuru campus for infrastructure support. The authors acknowledge I.M. Sechenov First Moscow State Medical University (Sechenov University) and N.I. Pirogov Russian National Research Medical University (RNRMU), Russia for the support extended towards the collaboration.

Conflict of interest

The authors declare that the research was conducted in the absence of any commercial or financial relationships that could be construed as a potential conflict of interest.

Publisher's note

Supplementary material

The Supplementary Material for this article can be found online at: https://www.frontiersin.org/articles/10.3389/fonc.2023.1221275/full#supplementary-material

References

1. Rybarczyk A, Lehmann T, Iwańczyk-Skalska E. In silico and in *vitro* analysis of the impact of single substitutions within EXO-motifs on Hsa-MiR-1246 intercellular transfer in breast cancer cell. *J Appl Genet* (2023) 64:105–24. doi: 10.1007/s13353-022-00730-y

2. Wanandi SI, Limanto A, Yunita E, Syahrani RA, Louisa M, Wibowo AE, et al. In silico and in *vitro* studies on the anti-cancer activity of andrographolide targeting survivin in human breast cancer stem cells. *PloS One* (2020) 15(11):e0240020. doi: 10.1371/journal.pone.0240020

3. Henry DP, Ranjan J, Murugan RK, Deena P, Jasmine R, Rajesh KM, et al. Exploration of anti-breast cancer effects of *Terminalia Chebula* extract on DMBA-induced mammary carcinoma in sprague dawley rats. *Future J Pharm Sci* (2020) 6 (1):1–13. doi: 10.1186/s43094-020-00124-z

4. Shrihastini V, Muthuramalingam P, Adarshan S, Sujitha M, Chen JT, Shin H, et al. Plant derived bioactive compounds, their anti-cancer effects and in silico approaches as an alternative target treatment strategy for breast cancer: An updated overview. *Cancers (Basel)* (2021) 13(24):6222. doi: 10.3390/cancers13246222

5. Beyaz S, Aslan A, Gok O, Uslu H, Agca CA, Ozercan IH. *In vivo*, in *vitro* and in silico anticancer investigation of fullerene C60 on DMBA induced breast cancer in rats. *Life Sci* (2022) 291:120281. doi: 10.1016/j.lfs.2021.120281

6. Singh V, Kumar K, Purohit D, Verma R, Pandey P, Bhatia S, et al. Exploration of therapeutic applicability and different signaling mechanism of various phytopharmacological agents for treatment of breast cancer. *Biomed Pharmacother* (2021) 139:111584. doi: 10.1016/j.biopha.2021.111584

7. Rizzo LY, Longato GB, Ruiz AL, Tinti SV, Possenti A, Vendramini-Costa DB, et al. *In vitro*, in *vivo* and in silico analysis of the anticancer and estrogen-like activity of guava leaf extracts. *Curr Medicinal Chem* (2014) 21(20):2322–30. doi: 10.2174/0929867321666140120120031

8. Shendge AK, Sarkar R, Mandal N. Potent anti-inflammatory *Terminalia chebula* fruit showed in *vitro* anticancer activity on lung and breast carcinoma cells through the regulation of Bax/Bcl-2 and caspase-cascade pathways. *J Food Biochem* (2020) 44(12): e13521. doi: 10.1111/jfbc.13521

9. Muhammad TS, Muhammad JA, Muhammad I, Ijaz K, Farhan S, Shahzadi N, et al. Phytochemical profile and pro-healthy properties of *Terminalia chebula*: A comprehensive review. *Int J Food Properties* (2023) 26(1):526–51. doi: 10.1080/10942912.2023.2166951

10. Nigam M, Mishra AP, Adhikari-Devkota A, Dirar AI, Hassan MM, Adhikari A, et al. Fruits of Terminalia chebula Retz.: A review on traditional uses, bioactive chemical constituents and pharmacological activities. *Phytotherapy Res* (2020) 34 (10):2518–33. doi: 10.1002/ptr.6702

11. Tsuchida J, Rothman J, McDonald KA, Nagahashi M, Takabe K, Wakai T. Clinical target sequencing for precision medicine of breast cancer. *Int J Clin Oncol* (2019) 24:131–40. doi: 10.1007/s10147-018-1373-5

12. Rajmohamed MA, Natarajan S, Palanisamy P, Abdulkader AM, Govindaraju A. Antioxidant and Cholinesterase Inhibitory Activities of Ethyl Acetate Extract of *Terminalia chebula*: Cell-free *In vitro* and In silico Studies. *Pharmacognosy Magazine* (2017) 13(Suppl 3):S437–45. doi: 10.4103/pm.pm_57_17

13. Xu X, Zhang M, Xu F, Jiang S. Wnt signaling in breast cancer: Biological mechanisms, challenges and opportunities. *Mol Cancer* (2020) 19:165. doi: 10.1186/s12943-020-01268-7

14. Khan MI, Bouyahya A, Hachlafi NEL, Menyiy NE, Akram M, Sultana S, et al. Anticancer properties of medicinal plants and their bioactive compounds against breast cancer: a review on recent investigations. *Environ Sci pollut Res Int* (2022) 29 (17):24411–44. doi: 10.1007/s11356-021-17795-7

15. Pradeep S, Jain AS, Dharmashekara C, Prasad SK, Akshatha N, Pruthvish R, et al. Synthesis, computational pharmacokinetics report, conceptual DFT-based calculations and anti-acetylcholinesterase activity of hydroxyapatite nanoparticles derived from acorus calamus plant extract. *Front Chem* (2021) 9:741037. doi: 10.3389/fchem.2021.741037

16. Minocha T, Birla H, Obaid AA, Rai V, Sushma P, Shivamallu C, et al. Flavonoids as promising neuroprotectants and their therapeutic potential against Alzheimer's disease. *Oxid Med Cell Longevity* (2022) 13. doi: 10.1155/2022/5589425

17. Pradeep S, Patil SM, Dharmashekara C, Jain AS, Ramu R, Shirahatti PS, et al. Molecular insights into the in silico discovery of corilagin from Terminalia chebula as a potential dual inhibitor of SARS-CoV-2 structural proteins. *J Biomolecular Structure Dynamics* (2022). doi: 10.1080/07391102.2022.2011626

18. Pradeep S, Prabhuswaminath SC, Reddy P, Srinivasa SM, Shati AA, Alfaifi MY, et al. Anticholinesterase activity of Areca catechu: *In Vitro* and in silico green synthesis approach in search for therapeutic agents against Alzheimer's disease. *Front Pharmacol* (2022) 13:1044248. doi: 10.3389/fphar.2022.1044248

19. Chandrashekar S, Santosh KSR, Sushma P, Shashanka KP, Ravindra V, Mohammad AA, et al. Eco-friendly Synthesis of MnO2 Nanorods Using *Gmelina arborea* Fruit Extract and its Anticancer Potency Against MCF-7 Breast Cancer Cell Line. *Int J Nanomedicine* (2022) 17:1917–28. doi: 10.2147/IJN.S315567

20. Prasad SK, Pradeep S, Shimavallu C, Kollur SP, Syed A, Marraiki N, et al. Evaluation of *Annona muricata* acetogenins as potential anti-SARS-CoV-2 agents through computational approaches. *Front Chem* (2021) 8:624716. doi: 10.3389/fchem.2020.624716

21. Sushma P, Anisha SJ, Chandan D, Shashank KP, Shiva PK, Syed A, et al. Herbal combination therapy against Alzheimer's disease. *J Alzheimer's Dis Rep* (2020) 4 (1):417–29. doi: 10.3233/ADR-200228

22. Kollur SP, Prasad SK, Pradeep S, Veerapur R, Patil SS, Amachawadi RG, et al. Luteolin-fabricated ZnO nanostructures showed PLK-1 mediated anti-breast cancer activity. *Biomolecules* (2021) 11(3):385. doi: 10.3390/biom11030385

23. Uppar V, Chandrashekharappa S, Shivamallu C, Sushma P, Kollur SP, Ortega-Castro J, et al. Investigation of antifungal properties of synthetic dimethyl-4-bromo-1-(Substituted benzoyl) pyrrolo[1,2-a] quinoline-2,3-dicarboxylates analogues: molecular docking studies and conceptual DFT-based chemical reactivity descriptors and pharmacokinetics evaluation. *Molecules* (2021) 26(9):2722. doi: 10.3390/molecules26092722

24. Ankegowda VM, Kollur SP, Prasad SK, Pradeep S, Dhramashekara C, Jain AS, et al. Phyto-mediated synthesis of silver nanoparticles using terminalia chebula fruit extract and evaluation of its cytotoxic and antimicrobial potential. *Molecules* (2020) 25 (21):5042. doi: 10.3390/molecules25215042

25. Shivalingaiah, Thoyojaksha, Pallavi KS, Sushma P, Sai-Chakith MR, Navyashree B, et al. Computational approach in search of therapeutic for colorectal cancer. *Int J Food Nutr Sci* (2022) 4562-4576. Available at: https://ijfans.org/uploads/paper/78170eedb33d082d0bbb6a97e5bea332.pdf.

26. Patil SS, Shivamallu C, Dharmashekara C, Pradeep S, Suresh KP, Ashwini P, et al. Diversity due to mutations in circulating virus strains of SARS-CoV-2 may delay control of COVID-19. *JAppl Biol Biotech* (2022) 10(02):198–205. doi: 10.7324/JABB.2022.100223

27. Shivalingaiah, Thoyojaksha, Sai-Chakith MR, Sushma P, Pallavi KS, Kavana CP, et al. In-silico evaluation of anti-acne property of Syzygium (S.) aromaticum. *Int J Food Nutr Sci* (2022) 4577-4589. Available at: https://ijfans.org/uploads/paper/075de0507bdd4a50bf700d501d3a4868.pdf.

28. Chandrashekar S, Sharanaiah U, Sushma P, Ramith R, Mohammad AA, Shiva PK, et al. Salicylic acid-mediated enhancement of resistance in tomato plants against Xanthomonas perforans. *Saudi J Biol Sci* (2021) 29(4):2253-2261. doi: 10.1016/j.sjbs.2021.11.067

29. Vinusha HM, Shiva PK, Bindya S, Muneera B, Chandan S, Chandan D, et al. N-((1H-pyrrol-2-yl)methylene)-6-methoxypyridin-3-amine and its Co(II) and Cu(II) complexes as antimicrobial agents: Chemical preparation, in *vitro* antimicrobial evaluation, in silico analysis and computational and theoretical chemistry investigations. *Molecules* (2022) 27(7):1911. doi: 10.3390/molecules27041436

30. Prasad KS, Pillai RR, Shivamallu C, Prasad SK, Jain AS, Pradeep S, et al. Tumoricidal potential of novel amino-1,10-phenanthroline derived imine ligands: chemical preparation, structure, and biological investigations. *Molecules* (2020) 25 (12):2865. doi: 10.3390/molecules25122865

31. Heggadadevanakote KP, Shivamallu C, Shruthi G, Nagabushan CM, Pradeep S, Karunakar P, et al. In-silico screening and validation of KPHS_00890 protein of Klebsiella pneumoniae proteome: An application to bacterial resistance and pathogenesis. *J King Saud Univ - Sci* (2021) 33(6):101537. doi: 10.1016/j.jksus.2021.101537

32. Santosh KSR, Srinivasa C, Shivamallu C, Prasad KS, Pradeep S, Syed A, et al. Callus induction and shoot regeneration from the immature flower bud of Caesalpinia bonducella and its antileptospiral potential by in *vitro* and in silico analysis. *Phcog Mag* (2021) 17(S1):38–44.

33. Sharanagouda SP, Kuralayanapalya PS, Rajamani S, Raghavendra GA, Srikantiah C, Sushma P, et al. Prevalence of methicillin-resistant Staphylococcus aureus in India: A systematic review and meta-analysis. *Oman Med J* (2021) 37(4): e440. doi: 10.5001/omj.2022.22

34. Shankar A, Gopinath SM, Kollur SP, Sushma P, Jain AS, Sharanagouda SP, et al. Structural diversity and role of phytochemicals against P38-a mitogen-activated protein kinase and epidermal growth factor receptor kinase domain: A privileged computational approach. *J Pure Appl Microbiol* (2021) 15(4):2263–9. doi: 10.22207/JPAM.15.4.48

35. Vinay S, Chandan D, Sushma P, Anisha SJ, Shiva PK, Bindya S, et al. In-Silico elucidation of *Abrus precatorius* phytochemical against Diabetes mellitus. *Bull Env. Pharmacol* (2021) 10(4):118–28. Available at: https://bepls.com/bepls_march2021/13.pdf.

36. Prasad KS, Pillai RR, Ghimire MP, Ray R, Richter M, Shivamallu C, et al. Indole moiety induced biological potency in pseudo-peptides derived from 2-amino-2-(1H-indole-2-yl) based acetamides: Chemical synthesis, in *vitro* anticancer activity and theoretical studies. *J Mol Structure* (2020), 128445. doi: 10.1016/j.molstruc.2020.128445

37. Prasad KS, Shivamallu C, Gopinath SM, Srinivasa C, Dharmashekara C, Sushma P, et al. Schiff base ligands derived from 4-chloro-6-methylpyrimidin-2-amine: Chemical synthesis, bactericidal activity and molecular docking studies against targeted microbial pathogen. *Int J Health Allied Sci* (2021) 10:157–66. doi: 10.4103/ijhas.IJHAS_43_20

38. Ashwini P, Govindaraju S, Sushma P, Anisha SJ, Chandan D, Nagendra PMN, et al. Helicobacter pylori infection: A bioinformatic approach. *Int J Pharm Sci Res* (2020) 11:5469–83. doi: 10.13040/IJPSR.0975-8232.11(11).1000-15

39. Avinash KO, Sushma P, Chandan S, Gopenath TS, Kiran KMN, Kanthesh BM, et al. In silico screened flavanoids of glycyrrhiza glabra inhibit CPLA2 and SPLA2 in LPS stimulated macrophages. *Bull Environ Pharmacol* (2021) 10(5):72–80. Available at: https://bepls.com/bepls_april2021/9.pdf.

40. Pruthvish R, Gopinath SM, Sushma P, Anisha SJ, Shiva PK, Chandan S. In-silico evaluation of anti-cancerous activity of herbal plant extracts. *Bull Environ Pharmacol* (2021) 10(4):105–17. Available at: https://bepls.com/bepls_march2021/12.pdf.

41. Navyashree B, Anisha SJ, Sushma P, Chandan D, Sharagouda SP, Shiva PK, et al. Computational based approach in discovering the phytocompound based complex inhibition against *Ralstonia Solanacearum* and Root-knot nematode Meloidogyne Incognita. *Bull Environ Pharmacol* (2021) 10(11):23–34. Available at: https://bepls.com/bepls_oct2021/5.pdf.

42. Shashank MP, Sujay S, Chandana KVB, Tejaswini M, Sushma P, Prithvi SS, et al. Bioactive peptides: its production and potential role on health. *Int J Innovative Science Eng Technol* (2020) 7(1). Available at: https://ijiset.com/vol7/v7s1/IJISET_V7_I1_15.pdf.

43. Bramhadev P, Sharanagouda SP, Chandrashekar S, Raghavendra GA, Dash AP, Mahendra PY, et al. COVID-19 Pandemic: A Systematic review on the Coronaviruses of animals and SARS-CoV-2. *J Exp Biol Agric Sci* (2021) 9(2):117–30. doi: 10.18006/2021.9(2).117.130

44. Saleem A, Husheem M, Härkönen P, Pihlaja K. Inhibition of cancer cell growth by crude extract and the phenolics of *Terminalia chebula retz.* fruit. *J Ethnopharmacol* (2002) 81(3):327–36. doi: 10.1016/s0378-8741(02)00099-5

frontiers | Frontiers in Pharmacology

TYPE Original Research
PUBLISHED 05 September 2023
DOI 10.3389/fphar.2023.1255586

OPEN ACCESS

EDITED BY
Pranav Kumar Prabhakar,
Lovely Professional University, India

REVIEWED BY
Jitendra Kumar,
The University of Iowa, United States
Xiuli Yi,
Fourth Military Medical University, China

*CORRESPONDENCE
Phil-Dong Moon,
pdmoon@khu.ac.kr

RECEIVED 09 July 2023
ACCEPTED 25 August 2023
PUBLISHED 05 September 2023

CITATION
Han N-R, Park H-J, Ko S-G and Moon P-D (2023), Maltol has anti-cancer effects via modulating PD-L1 signaling pathway in B16F10 cells.
Front. Pharmacol. 14:1255586.
doi: 10.3389/fphar.2023.1255586

Maltol has anti-cancer effects via modulating PD-L1 signaling pathway in B16F10 cells

Na-Ra Han[1,2], Hi-Joon Park[3], Seong-Gyu Ko[2,4] and Phil-Dong Moon[5]*

[1]College of Korean Medicine, Kyung Hee University, Seoul, Republic of Korea, [2]Korean Medicine-Based Drug Repositioning Cancer Research Center, College of Korean Medicine, Kyung Hee University, Seoul, Republic of Korea, [3]Department of Anatomy and Information Sciences, College of Korean Medicine, Kyung Hee University, Seoul, Republic of Korea, [4]Department of Preventive Medicine, College of Korean Medicine, Kyung Hee University, Seoul, Republic of Korea, [5]Center for Converging Humanities, Kyung Hee University, Seoul, Republic of Korea

Introduction: Among skin cancers, melanoma has a high mortality rate. Recent advances in immunotherapy, particularly through immune checkpoint modulation, have improved the clinical treatment of melanoma. Maltol has various bioactivities, including anti-oxidant and anti-inflammatory properties, but the anti-melanoma property of maltol remains underexplored. The aim of this work is to explore the anti-melanoma potential of maltol through regulating immune checkpoints.

Methods: The immune checkpoint PD-L1 was analyzed using qPCR, immunoblots, and immunofluorescence. Melanoma sensitivity towards T cells was investigated via cytotoxicity, cell viability, and IL-2 assays employing CTLL-2 cells.

Results: Maltol was found to reduce melanin contents, tyrosinase activity, and expression levels of tyrosinase and tyrosinase-related protein 1. Additionally, maltol suppressed the proliferative capacity of B16F10 and induced cell cycle arrest. Maltol increased apoptotic rates by elevating cleaved caspase-3 and PARP. The co-treatment with maltol and cisplatin revealed a synergistic effect on inhibiting growth and promoting apoptosis. Maltol suppressed IFN-γ-induced PD-L1 and cisplatin-upregulated PD-L1 by attenuating STAT1 phosphorylation, thereby enhancing cisplatin's cytotoxicity against B16F10. Maltol augmented sensitivity to CTLL-2 cell-regulated melanoma destruction, leading to an increase in IL-2 production.

Discussion: These findings demonstrate that maltol restricts melanoma growth through the downregulation of PD-L1 and elicits T cell-mediated anti-cancer responses, overcoming PD-L1-mediated immunotherapy resistance of cisplatin. Therefore, maltol can be considered as an effective therapeutic agent against melanoma.

KEYWORDS

maltol, PD-L1, melanoma, cisplatin, CTLL-2 cells, B16F10 cells

Introduction

Melanoma is considered to be one of the deadliest cancers in the world (Guergueb and Akhloufi, 2021). The mortality and incidence of melanoma have increased rapidly over the past few decades, and cases are growing faster than any other type of solid cancer (Ko, 2017). Recent advances in immunotherapy have greatly improved the clinical treatment of melanoma and the blockade of immune checkpoints regulated by programmed death 1 (PD-1) and its corresponding PD ligand 1 (PD-L1) antibodies has effectively reactivated the immune-mediated elimination of melanocytes (Greil et al., 2017).

PD-1, which is a cell surface receptor on T cells, operates as a checkpoint that regulates T cell exhaustion. The binding between PD-1 and PD-L1 serves to suppress T cell activation, leading to immune suppression (Jiang et al., 2019). Interaction between PD-1 and PD-L1 subsequently inhibits the cytotoxicity of cytotoxic T lymphocytes (CTLs, Jiang et al., 2019). Atezolizumab, an anti-PD-L1 antibody, is used in melanoma patients because it is safe and has anti-tumor activity (de Azevedo et al., 2021). Notably, IFN-γ acts as a critical cytokine in tumor microenvironments, and this can contribute to tumor immune evasion by potently inducing PD-L1 expression in tumor cells and impairing CTL-immune responses (Mandai et al., 2016; Jorgovanovic et al., 2020). Unfortunately, the chronic presence of IFN-γ in inflammatory tumor microenvironments fails to contribute to tumor cell eradication and instead induces tumorigenesis (Mojic et al., 2017).

The disadvantages of conventional cancer chemotherapy and the advantages of more natural treatment options are driving the interest in the use of complementary and alternative medicines (Molassiotis et al., 2005). Accumulating evidence has revealed that phytochemical compounds hold potential as anti-cancer drugs (Chinembiri et al., 2014). Several phytochemical compounds have exhibited anti-cancer effects with promising effects on the PD-1/PD-L1 checkpoints (Xu et al., 2018; Ravindran Menon et al., 2021). Maltol, a type of phenolic compound among the phytochemicals, is typically used as a flavor enhancer and often as a marker for the quality control of various ginseng products (Jeong et al., 2015; Jin et al., 2023). Maltol is known to be effective in treating inflammation (Ahn et al., 2022), oxidation (Yang et al., 2006; Mao et al., 2022), aging (Sha et al., 2021), nephrotoxicity (Mi et al., 2018), and liver damage (Liu et al., 2018). Regarding the anti-cancer effects of maltol, anti-cancer effects of maltol-containing complexes or maltol itself in relation to promyelocytic leukemia and oral squamous cell carcinoma cell lines have been reported (Yasumoto et al., 2004; Notaro et al., 2020). However, the anti-cancer properties of maltol concerning melanoma have not been comprehensively studied.

In this work, we investigated the anti-cancer potential of maltol against melanoma cells, as well as its regulatory effects on melanogenesis. Apart from elucidating the growth-inhibiting and pro-apoptotic properties of maltol on melanoma cells by downregulating PD-L1 expression, our observations also showed that maltol was capable of enhancing T cell-regulated eradication of melanoma cells.

Materials and methods

Chemicals and reagents

Maltol (purity ≥99%) was obtained from Sigma-Aldrich Co. (St. Louis, MO, United States); cisplatin (purity ≥99.7%), α-melanocyte-stimulating hormone (α-MSH), and L-dopa from MedChemExpress (Monmouth Junction, NJ, United States); recombinant IFN-γ from R & D system Inc., (Minneapolis, MN, United States); antibodies specific for tyrosinase (sc-20035), tyrosinase related protein 1 (TYRP1, sc-166857), caspase-3 (sc-7148), PARP (sc-365315), PD-L1 (sc-518027), phosphorylated signal transducer and activator of transcription 1 (pSTAT1, sc-8394), STAT1 (sc-464), actin (sc-8432), and GAPDH (sc-32233) from Santa Cruz Biotechnology, Inc. (Dallas, Texas, United States); anti-tubulin antibody (3,873) from Cell Signaling Technology (Danvers, MA, United States); anti-mouse IgG H&L (Alexa Fluor® 647, ab150115) from abcam (Cambridge, MA, United States); anti-IL-2 antibodies (554424, 554426) from BD Biosciences (San Jose, CA, United States).

Cell culture

The B16F10 (mouse) and A375 (human) melanoma cell lines were purchased from the Korean Cell Line Bank (Seoul, Republic of Korea). The CTLL-2 cell line (# TIB-214) was purchased from the American Type Culture Collection (ATCC, Manassas, VA, United States). B16F10 and A375 cells were maintained in Dulbecco's modified Eagle's medium (Gibco, Waltham, MA, United States) supplemented with 10% fetal bovine serum (Merck Millipore, Burlington, MA, United States) and 1% penicillin/streptomycin (Gibco). CTLL-2 cells were cultured in RPMI 1,640 medium (ATCC), supplemented with 10% T cell culture supplement containing concanavalin A (T-STIM with Con A, BD Biosciences), 10% fetal bovine serum, and 1% penicillin/streptomycin.

Melanin content and tyrosinase activity assay

Melanin content and tyrosinase activity assessments were carried out as described previously (Zhou et al., 2021; Bodurlar and Caliskan, 2022). B16F10 cells (1×10^5/well) were exposed to maltol and then treated with α-MSH (100 nM) for 72 h. For the melanin content assay, the cell pellets were dissolved in 1 N NaOH containing 10% dimethyl sulfoxide (DMSO) and subjected to cell lysis for 1 h at 80°C. The optical density of melanin content was spectrophotometrically measured with a microplate reader (405 nm). In the tyrosinase activity assay, the cell pellets were lysed in PBS containing 1% Triton X-100 for 2 h at 80°C. A freshly prepared substrate (L-DOPA, 10 mM) was then added and incubated for 30 min at 37°C. The resulting absorbance was spectrophotometrically analyzed with a microplate reader (475 nm).

Cell viability assay

Cell proliferation was analyzed by using an MTT [3-(4,5-dimethylthiazol-2-yl)-2,5-diphenyltetrazolium bromide tetrazolium] assay. B16F10 cells and A375 cells were treated with maltol or cisplatin for 48 h. Following this, MTT solution (5 mg/mL) was added to each well, and the resulting formazan crystals were dissolved in DMSO. The absorbance was measured with a microplate reader (570 nm).

Flow cytometric analysis

For cell cycle analysis, maltol- or cisplatin-treated B16F10 cells were fixed in ice-cold 70% ethanol overnight at 4°C. Then, the cells were incubated in PBS buffer containing RNase (100 μg/mL) and propidium iodide (PI, 50 μg/mL) for 30 min at room temperature, utilizing a PI flow cytometry kit (abcam, Cambridge, United Kingdom). For apoptosis analysis, B16F10 cells treated with maltol or cisplatin were stained with annexin V and PI using a FITC annexin V apoptosis detection kit with PI (Biolegend, San Diego, CA, United States). Cell surface PD-L1 detection was performed with reference to previous protocols (Tang et al., 2018; Xu et al., 2018). Maltol or cisplatin-treated B16F10 cells were first blocked with anti-CD16/32 (anti-FcγIII/II receptor, clone 2.4G2, BD Biosciences, ≤ 1 μg/million cells), then incubated with PE-conjugated anti-mouse PD-L1 antibody (12-5982-83, eBioscience, San Diego, CA, United States, 1:200) in FACS buffer (PBS containing 0.1% BSA and 0.02% NaN_3) for 30 min at 4°C. Following PBS washes, the samples were resuspended in FACS buffer and analyzed through flow cytometry.

Immunoblots

Western blotting was carried out as described previously (Han et al., 2022b). The primary antibodies were used at a 1:500 dilution, and the secondary antibodies were used at a 1:10,000 dilution.

Quantitative PCR analysis

Real-time quantitative PCR (qPCR) was conducted as described previously (Han et al., 2022b). The primer sequences are as follows: mPD-L1 (For: 5′-TGCTGCATAATCAGCTACGG-3′, Rev: 5′-GCTGGTCACATTGAGAAGCA-3′) and mGAPDH (For: 5′-CCAATGTGTCCGTCGTGGATCT-3′, Rev: 5′-GTTGAAGTCGCAGGAGACAACC-3′); hPD-L1 (For: 5′-ATTTGGAGGATGTGCCAGAG-3′, Rev: 5′-CCAGCACACTGAGAATCAACA-3′) and hGAPDH (For: 5′-TCGACAGTCAGCCGCATCTTCTTT-3′, Rev: 5′-ACCAAATCCGTTGACTCCGACCTT-3′).

Immunofluorescence

Immunofluorescence was carried out as described previously (Han et al., 2022a). The antibody specific for PD-L1 was used at a 1:500 dilution, and anti-mouse IgG H&L (Alexa Fluor® 647) was used at a 1:1,000 dilution.

Co-culture experiments

After B16F10 cells (target cells, 2×10^4/well) were adhered to the plates, CTLL-2 cells (effector cells, 4×10^5/well) were added to each well. Following cell stabilization, maltol was administered to the target cells or co-cultured cells for 24 h. For the viability assay, the remaining viable target cells were exposed to an MTT solution. Cytotoxic activity against the target cells was measured in cell-free supernatants using a cell cytotoxicity assay kit (DoGenBio, Seoul, Republic of Korea). For the IL-2 release assay, the co-cultured cells were subjected to maltol and IFN-γ (10 ng/mL) treatment for 48 h. The IL-2 release from the co-cultured cells was assessed through an enzyme-linked immunosorbent assay (ELISA) according to the manufacturer's instructions. The IL-2 capture antibody was used at a 1:500 dilution, and IL-2 detection antibody was used at a 1:1,000 dilution.

Statistical analysis

The error bars in the figures represent the standard error of the mean (SEM). An unpaired Student's *t*-test was employed to compare two groups, and ANOVA followed by the Türkiye *post hoc* test was used to discern differences among several groups, all facilitated through IBM SPSS software (Armonk, NY, United States). The graphical representation was prepared using Prism—GraphPad (Boston, MA, United States). Statistical significance is denoted as $^*p < 0.05$, $^{**}p < 0.01$, and $^{***}p < 0.001$.

Results

Regulatory effect of maltol on melanin content in B16F10 melanoma cells

Melanogenesis has been linked to melanoma progression (Slominski et al., 2015). We examined whether maltol could affect the melanin content in B16F10 cells. Melanogenesis induced by α-MSH begins with tyrosine oxidation catalyzed by tyrosinase (Chen et al., 2014). As shown in Figures 1A, B, dark pigmentations were observed upon α-MSH treatment, indicating melanin synthesis, while maltol attenuated the dark pigmentations, resulting in a decrease in melanin content ($p < 0.05$). The color of the pellet was also darkened by α-MSH, while it became lighter in the maltol-treated group (Figure 1B). Maltol significantly suppressed the levels of tyrosinase activity increased by α-MSH ($p < 0.05$; Figure 1C). We further investigated whether maltol would inhibit the expression of key regulatory molecules on melanogenesis, such as tyrosinase and TYRP1 (Chen et al., 2014). The expression levels of tyrosinase and TYRP1 were also significantly decreased by maltol ($p < 0.05$; Figures 1D, E).

Growth-inhibiting effect of maltol in B16F10 melanoma cells

To examine the potential growth-inhibiting effect of maltol on melanoma, we investigated the influence of maltol on the cell proliferation of B16F10 cells. Maltol treatment decreased the propagation of B16F10 cells in a concentration-dependent manner ($p < 0.05$; Figure 2A). Notably, stronger inhibition was observed with maltol concentrations of 50 μg/mL and above. To investigate any synergistic effects between maltol and the anti-cancer drug cisplatin, cisplatin was simultaneously treated with maltol at concentrations of 50, 100, and 150 μg/ml. As expected, the results from the MTT assay revealed that co-treatment with maltol and cisplatin exhibited a more potent inhibitory effect on

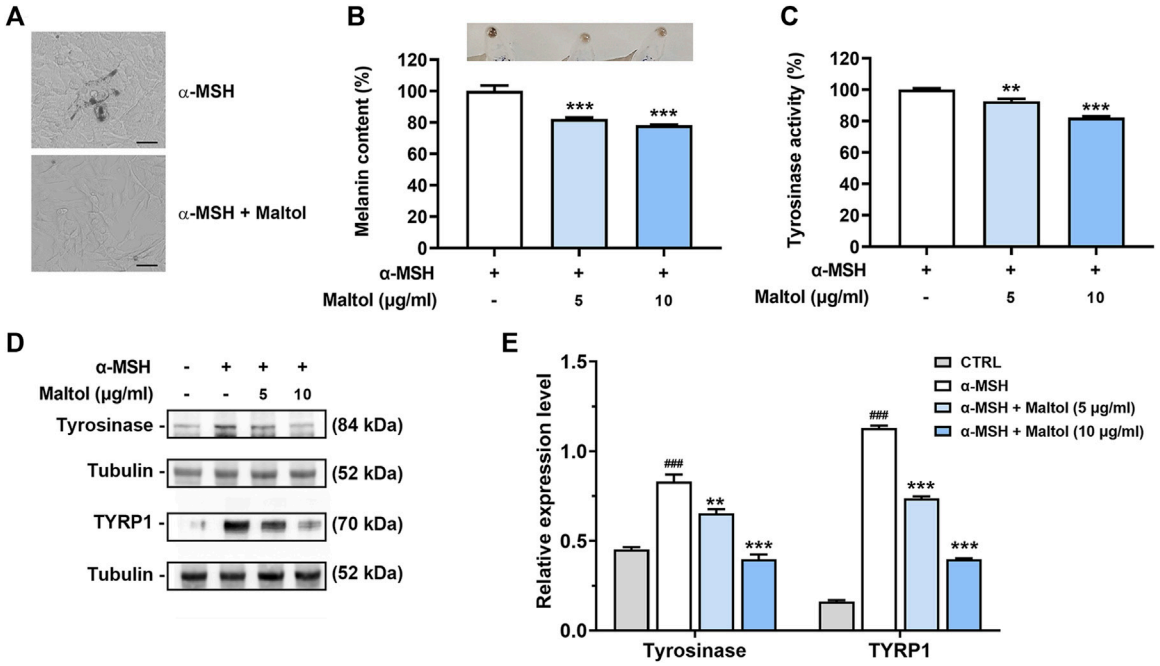

FIGURE 1
Effects of maltol on melanin content. **(A)** Maltol was pre-treated and α-MSH (100 nM) was then treated for 72 h in B16F10 cells. Representative images of dark pigmentation in α-MSH-stimulated group and α-MSH and maltol (10 μg/mL)-treated group were observed in B16F10 cells (scale bar = 50 μm). **(B)** The relative melanin content in α-MSH-stimulated B16F10 cells was measured as mentioned in the *Materials and methods* section (n = 4 per group). Pellets of B16F10 aggregates from each group were imaged above. **(C)** Intracellular tyrosinase activity in α-MSH-stimulated B16F10 cells was analyzed as mentioned in the *Materials and methods* section (n = 4 per group). **(D)** Maltol was pre-treated and α-MSH (100 nM) was then treated for 48 h in B16F10 cells. The tyrosinase and TYRP1 levels were assessed by Western blot analysis. Tubulin was a loading control. **(E)** Graphs show quantification of relative band intensities for tyrosinase and TYRP1 (n = 3 per group). $^{**}p < 0.01$ and $^{***}p < 0.001$ vs. α-MSH-stimulated group.

viability compared with the individual maltol or cisplatin treatments ($p < 0.05$; Figure 2B). Maltol caused cell cycle arrest in G2/M phase in the flow cytometric analysis of cell cycle distribution ($p < 0.05$; Figures 2C, D). In addition, the co-treatment displayed a more effective induction of G2/M phase cell cycle arrest compared to either treatment in isolation ($p < 0.05$; Figures 2C, D). Furthermore, we verified that maltol significantly suppressed the viability in A375 melanoma cells, and that the combination with cisplatin also had a synergistic effect on viability (Supplementary Figure S1).

Pro-apoptotic effect of maltol in B16F10 melanoma cells

We then performed flow cytometric analysis to assess the amount of apoptotic cells in maltol-treated melanoma cells using annexin V and PI double staining. As shown in Figures 3A, B, maltol significantly increased in the percentages of apoptotic rates ($p < 0.05$). Correspondingly, the co-treatment with maltol and cisplatin led to a significant enhancement when compared either treatment alone ($p < 0.05$). Furthermore, Western blotting analysis indicated that maltol significantly increased the cleaved caspase-3 and PARP levels compared to the control samples, indicating pro-apoptotic activities ($p < 0.05$; Figures 3C, D). Similarly, the combined treatment showed a significant synergistic effect on these levels ($p < 0.05$; Figures 3C, D).

Regulatory effect of maltol on IFN-γ-induced PD-L1 expression in B16F10 melanoma cells

Since the influence of maltol on the PD-L1 expression in tumor cells has not yet been determined, we examined the impact of maltol on the IFN-γ-induced upregulation of PD-L1 expression in B16F10 cells. As shown in Figure 4A, results from PCR experiments indicated that IFN-γ stimulated the mRNA levels of PD-L1, while maltol substantially attenuated the increase in PD-L1 ($p < 0.05$). Several studies have found that cisplatin upregulates PD-L1 expression, inducing resistance to cisplatin-induced apoptosis in tumor models (Tran et al., 2017; Hu et al., 2021). In line with previous reports, cisplatin significantly enhanced the PD-L1 mRNA expression upregulated by IFN-γ, and maltol apparently suppressed this increase ($p < 0.05$; Figure 4A). Furthermore, we detected a significant inhibition of the protein expression levels of PD-L1 from maltol-treated B16F10 cell lysates compared to the control group and the cisplatin-treated group, respectively, using Western blotting analysis ($p < 0.05$; Figures 4B, C). We next conducted immunofluorescence assays to confirm the impact of maltol on PD-L1 expression upregulated by IFN-γ. Similar to the results from the immunoblotting analysis, maltol remarkably reduced IFN-γ-induced or both IFN-γ and cisplatin-induced fluorescence signal enhancements in PD-L1 staining (Figure 4D). We next conducted flow cytometric analysis to investigate PD-L1 levels on the melanoma cell surface. Maltol significantly attenuated

10.3389/fphar.2023.1255586

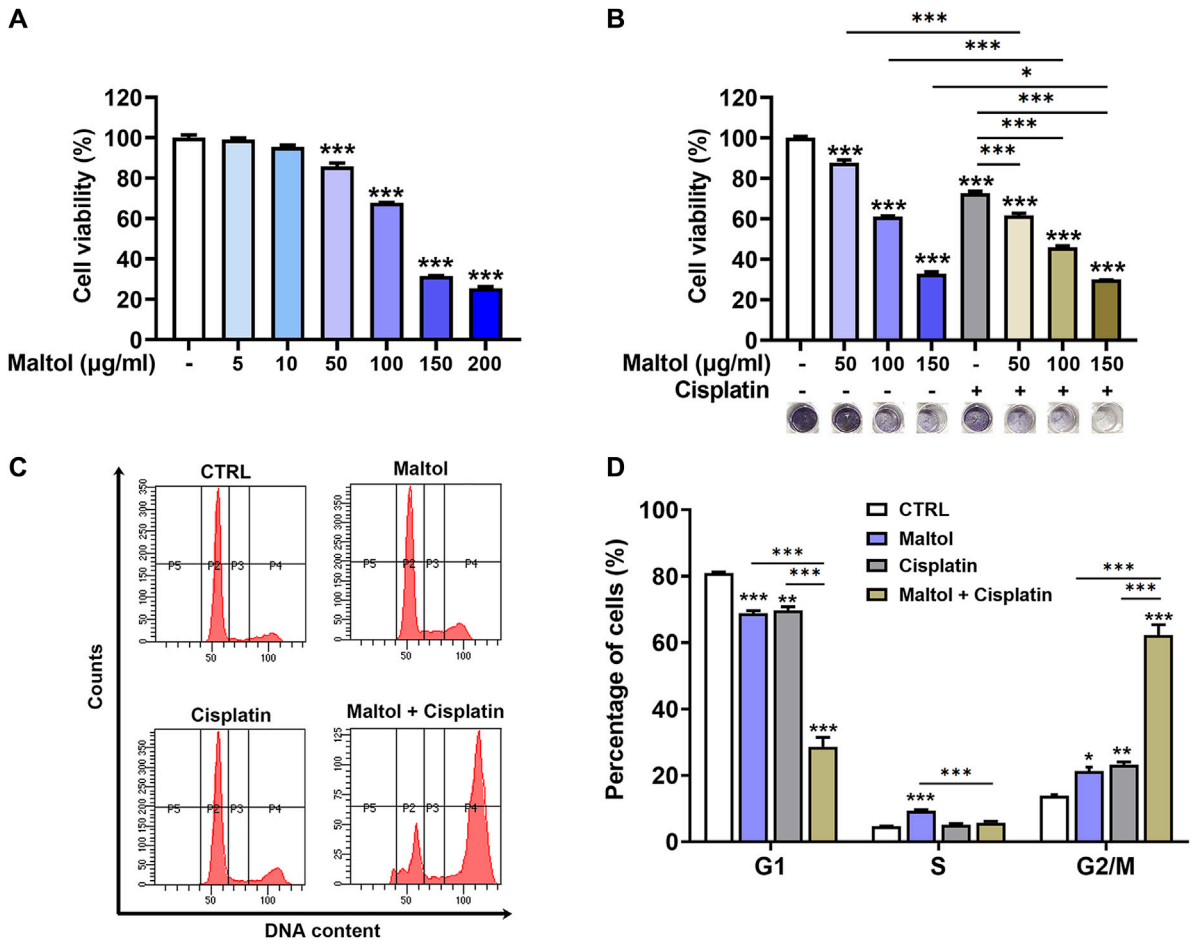

FIGURE 2
Effects of maltol on growth of B16F10 melanoma cells. **(A)** Maltol was treated in B16F10 cells at various concentrations for 48 h. The cell viability was measured with an MTT assay (n = 4 per group). **(B)** Maltol or cisplatin (20 μM) were treated in B16F10 cells for 48 h (n = 6 per group). Representative MTT-formazan from each group was imaged below. **(C)** Maltol or cisplatin were treated in B16F10 cells for 48 h. Cell cycle distribution was assessed by flow cytometry. **(D)** Cells distributed in each stage were quantified as a percentage (n = 5 per group). *p < 0.05, **p < 0.01, and ***p < 0.001 vs. CTRL (control, untreated) group.

IFN-γ-induced membrane PD-L1 expression (p < 0.05; Supplementary Figure S2). The increase in PD-L1 expression by IFN-γ is transcriptionally regulated through activation of STAT1 in tumor cells (Xu et al., 2018). As expected, results from the immunoblotting analysis showed that the STAT1 phosphorylation levels increased by IFN-γ or both IFN-γ and cisplatin were significantly inhibited by maltol (p < 0.05; Figures 4E, F). Additionally, we verified that maltol significantly suppressed the increase in PD-L1 mRNA expression by IFN-γ or both IFN-γ and cisplatin in A375 melanoma cells (Supplementary Figure S3).

Regulatory effect of maltol on T cell-regulated melanoma cell killing in CTLL-2 cells

CTLs are the most powerful effectors in anti-tumor immune responses and have the capacity to directly kill tumor cells (Raskov et al., 2021). We assessed the influence of maltol on T cell-regulated melanoma cell killing, specifically using PD-1-expressing CTLL-2 cells (Chen et al., 2021). To evaluate the modulatory effect of maltol on CTLL-2 cell-regulated melanoma cell killing, we measured the cytotoxicity exerted by CTLL-2 cells and subsequent cell viability after co-culture with B16F10 cells. Maltol significantly increased the total activity of lactate dehydrogenase (LDH) induced by CTLL-2 cells, suggesting severe damage to B16F10 cells (p < 0.05; Figure 5A). Correspondingly, the results from the cell viability assay showed that the decrease in cell viability caused by CTLL-2 cells was strongly enhanced by maltol (p < 0.05; Figure 5B). IL-2 is important for CTLs activity (Seo et al., 1993; Hidalgo et al., 2005). Thus, we further analyzed a regulatory effect of maltol on IL-2 release from the co-cultured cells. The IL-2 level was reduced in the IFN-γ-treated co-cultured cells, whereas maltol increased the diminished IL-2 levels (p < 0.05; Figure 5C).

Discussion

In the present study, we identified that maltol has anti-cancer effects via modulating the PD-L1 signaling pathway in melanoma.

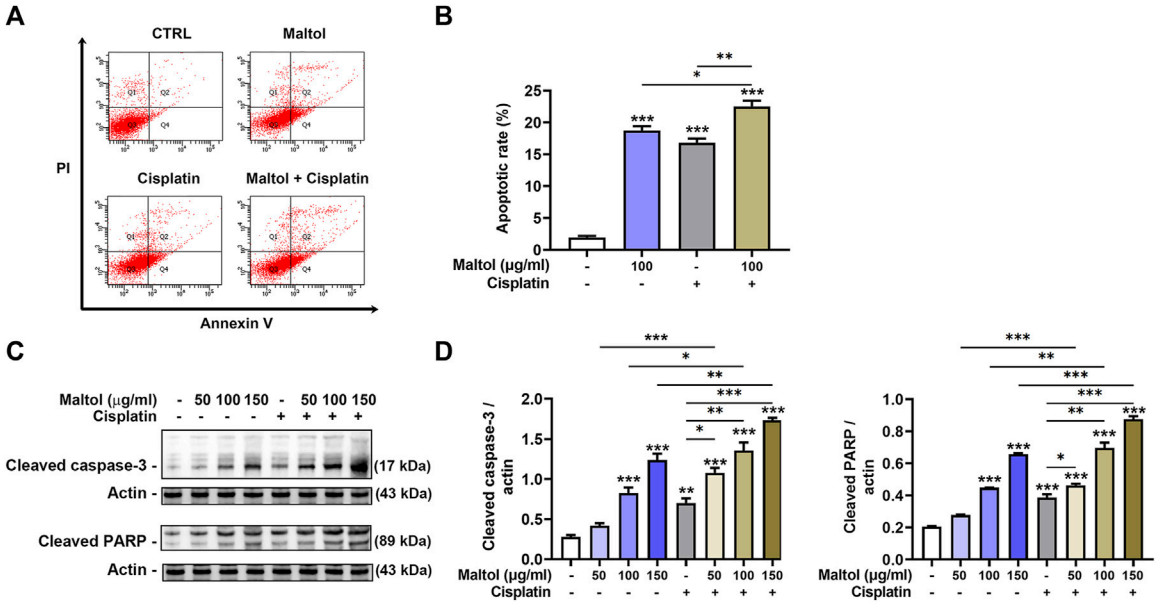

FIGURE 3
Effects of maltol on apoptosis of B16F10 melanoma cells. **(A)** Maltol or cisplatin (20 μM) were treated in B16F10 cells for 48 h. The cells were stained with annexin V and PI before flow cytometric analysis. **(B)** Apoptosis was quantified as a percentage (n = 4 per group). **(C)** Maltol or cisplatin were treated in B16F10 cells for 24 h. The cleaved caspase-3 and cleaved PARP levels were assessed by Western blot analysis. Actin was a loading control. **(D)** Graphs show quantification of relative band intensities for cleaved caspase-3 and cleaved PARP (n = 3 per group). *p < 0.05, **p < 0.01, and ***p < 0.001 vs. CTRL (control, untreated) group.

Maltol arrested the B16F10 cell cycle with a pro-apoptotic effect. Maltol inhibited IFN-γ-induced PD-L1 expression through the downregulation of STAT1 phosphorylation. In addition, maltol enhanced T cell-regulated melanoma cell eradication with an increase in IL-2 production (Figure 6).

Melanoma is the most aggressive skin cancer and originates in melanocytes. The B16 melanoma model is the most widely used metastatic melanoma model in preclinical studies (Voltarelli et al., 2017). B16F10 cells have been established to analyze the potential of immuno-oncology agents and to support the development of novel therapeutics (Nakamura et al., 2002). Growing evidence has shown the potential anti-cancer effects against melanoma by utilizing various natural products in B16F10 cells (Gao et al., 2016; Yu et al., 2020). The current work showed that maltol exhibits anti-cancer effects through suppressing the cell viability of B16F10 cells. This result may support previous reports demonstrating the inhibition of B16F10 cells progression by *Panax ginseng* extract containing maltol (Yun et al., 2015). Thus, we suggest a promising effect of maltol on melanoma that may have potential clinical implications.

The amount of cleaved caspase-3 observed in the Western blot did not align with the results from annexin V staining; however, in the present study, maltol promoted apoptotic rates with an increase in levels of cleaved caspase-3. Apoptosis is associated with multiple proteins, including PARP, Bax, Bad, p21, p53, cytochrome c, and AIF (Sim et al., 2020). The pro-apoptotic influence of maltol may involve not only caspase-3 but also a range of apoptosis-related proteins. More studies are needed to further demonstrate the entire apoptotic mechanism associated with maltol.

Immunotherapy based on PD-1/PD-L1 pathway blockade represents a groundbreaking therapeutic approach and has been demonstrated to be effective in the treatment of several cancers (Teng et al., 2018). Clinical studies have shown that the therapeutic efficacy of blockade of the PD1-PD-L1 checkpoint is related to PD-L1 expression in tumor cells (Wang et al., 2016; Zhang et al., 2018; Wang et al., 2021). High PD-L1 levels may also serve as a selective marker to stratify patients suitable for PD1-PD-L1 checkpoint blockade therapy (Yi et al., 2023). In this work, we found the suppressive effect of maltol on both mRNA and protein expression levels of PD-L1 after IFN-γ stimulation in B16F10 cells. Moreover, this work provides insight into underlying mechanisms governing maltol's effect on PD-L1 expression by showing that maltol inhibits STAT1 phosphorylation. Thus, we suggest that maltol has an anti-cancer effect by targeting PD-L1 in melanoma.

Intriguingly, our immunofluorescence experiments showed that PD-L1 was expressed in the nucleus. PD-L1, a plasma membrane multifunctional protein, can be translocated to the nucleus through interaction with multiple proteins. The nuclear presence of PD-L1 in several melanoma cell lines, including B16F10, could result from exogenous DNA damage, phosphorylation, acetylation, or other post-translational modifications (Gao et al., 2020; Kornepati et al., 2022; Lee et al., 2022). Nuclear PD-L1 accelerates tumorigenesis, confers resistance towards anti-PD1/PD-L1 therapies, and regulates cancer immune evasion and immunotherapy in the tumor microenvironment (Gao et al., 2020; Xiong et al., 2021; Yu et al., 2023). Consequently, the change in cellular localization of PD-L1 might be caused by interactions of multiple proteins in the *in vitro* environment of

10.3389/fphar.2023.1255586

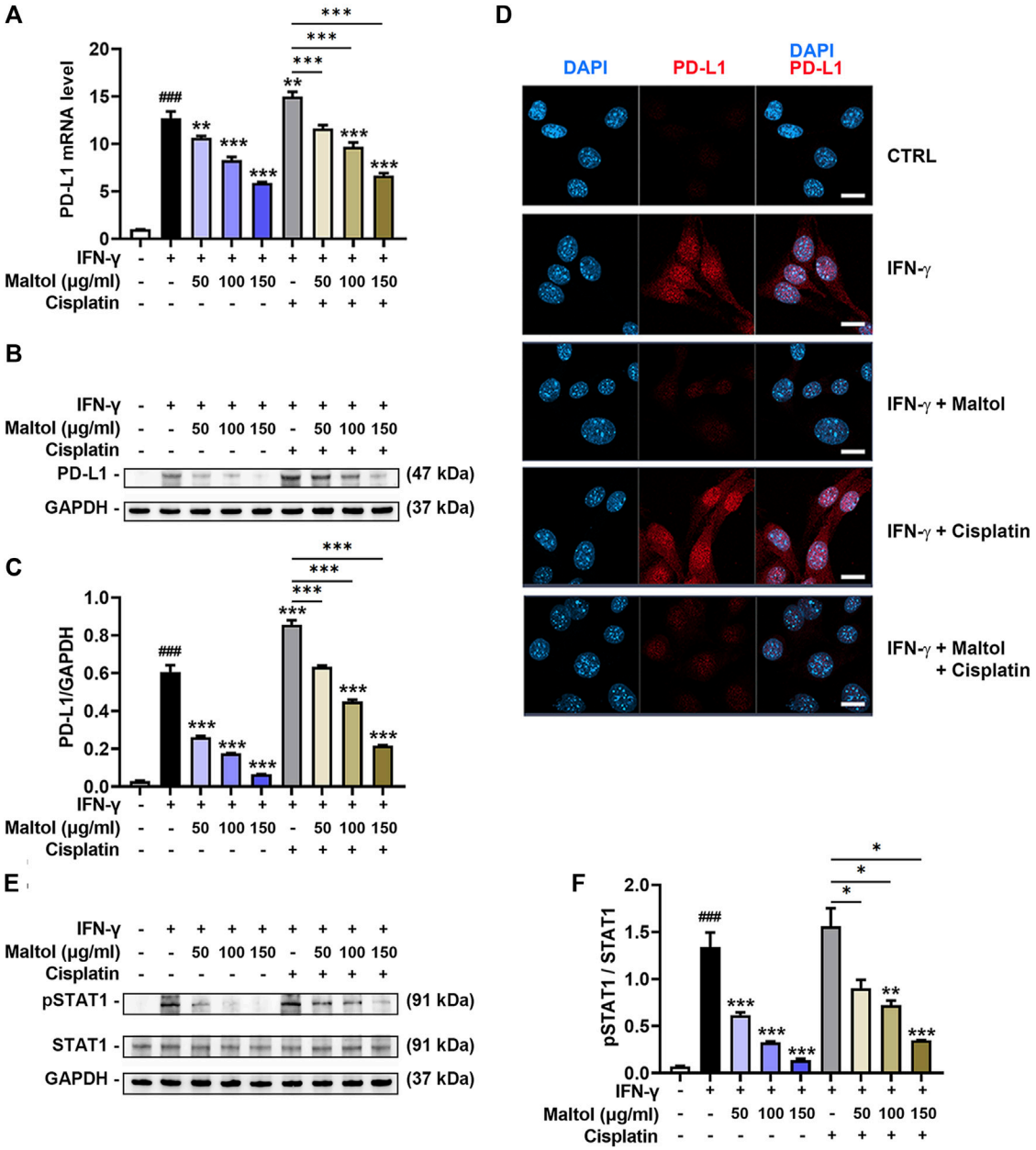

FIGURE 4
Effects of maltol on IFN-γ-induced PD-L1 expression in B16F10 melanoma cells. **(A)** Maltol or cisplatin (20 μM) was pre-treated, and IFN-γ (10 ng/mL) was then treated for 24 h in B16F10 cells. The mRNA expression was detected by real-time qPCR analysis (n = 5 per group). Each mRNA was normalized to GAPDH mRNA. **(B)** The PD-L1 level was analyzed by Western blot analysis. GAPDH was a loading control. **(C)** Graphs show quantification of relative band intensities for PD-L1 (n = 3 per group). **(D)** Representative micrographs indicate PD-L1 staining in immunofluorescence analysis (scale bar = 20 μm). **(E)** Maltol or cisplatin was pre-treated and IFN-γ was then treated for 10 min in B16F10 cells. The pSTAT1 level was analyzed by Western blot analysis. GAPDH was a loading control. **(F)** Graphs show quantification of relative band intensities for pSTAT1 (n = 3 per group). $^{###}p < 0.001$ CTRL (control, untreated) group. $^{*}p < 0.05$, $^{**}p < 0.01$, and $^{***}p < 0.001$ vs. IFN-γ treated group.

this work. However, in the future, the change in cellular localization of PD-L1 in melanoma needs to be explored more.

Cisplatin chemotherapy has formed the standard systemic therapy for various cancers (Tran et al., 2017; Grabosch et al., 2019). However, several studies have reported an increase in tumor PD-L1 expression caused by cisplatin, leading to resistance against cisplatin-induced apoptosis and subsequent immune evasion (Tran et al., 2017; Grabosch et al., 2019; Hu et al., 2021). Thus, those authors have proposed that the combination of cisplatin with anti-PD-L1 antibodies or substances down-regulating PD-L1, might enhance cisplatin's anti-cancer response (Tran et al., 2017; Grabosch et al., 2019; Hu et al., 2021). In accordance with previous evidence, we showed that the combined application of maltol and cisplatin reversed cisplatin-induced PD-L1-mediated chemotherapy and immunotherapy resistance, resulting in synergistic effects in terms of growth inhibition and pro-apoptotic action. Consequently,

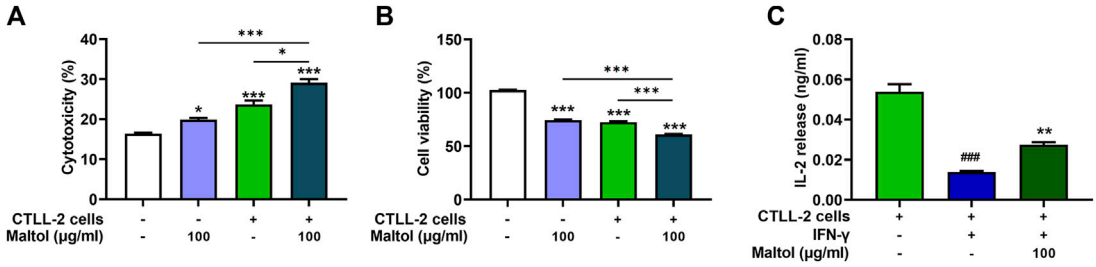

FIGURE 5
Effects of maltol on CTLL-2-mediated B16F10 killing. B16F10 cells were co-cultured with CTLL-2 cells with effector-to-target ratios of 20:1. **(A)** The cytotoxicity of CTLL-2 cells to B16F10 cells was measured with an LDH detection assay kit (n = 3 per group) and **(B)** viability of remaining B16F10 cells was assessed using an MTT assay (n = 4 per group). *p < 0.05, **p < 0.01, and ***p < 0.001 vs. CTRL (control, untreated) group. **(C)** IL-2 level secreted from co-cultured cells was measured by ELISA (n = 4 per group). $^{###}p$ < 0.001 CTRL (control, untreated) group. ***p < 0.001 vs. IFN-γ treated group.

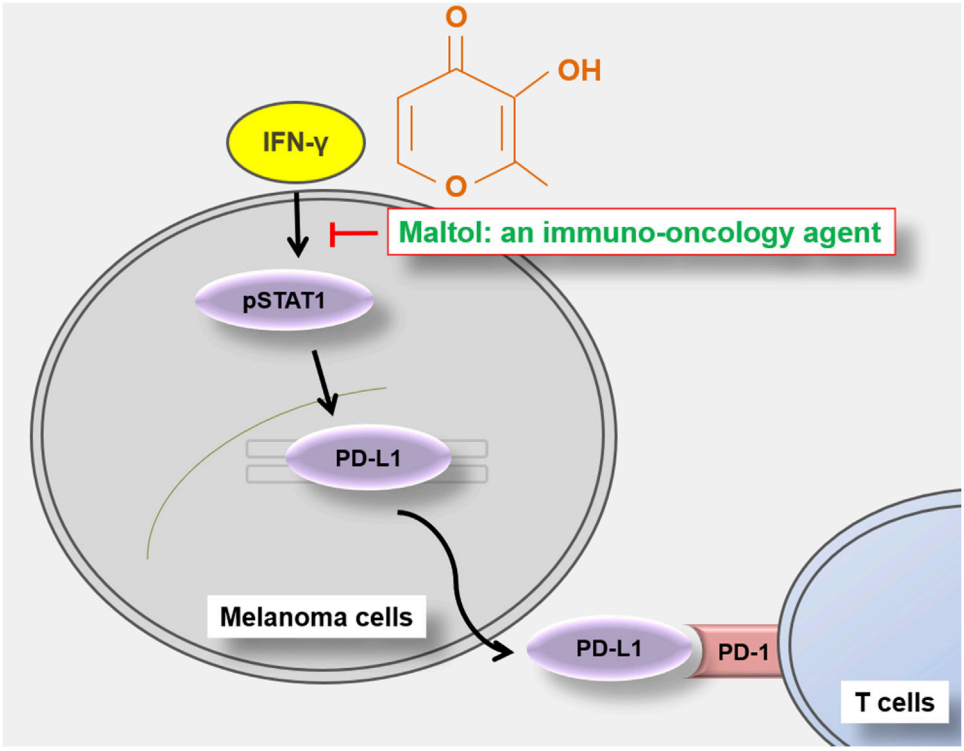

FIGURE 6
Schematic representation of maltol-mediated anti-melanoma effects in B16F10 melanoma cells.

we propose that maltol can be applied as a combinatorial agent to overcome PD-L1-related chemotherapy resistance, including in the context of cisplatin treatment.

To verify the viability of maltol as an anti-cancer agent, cell cycle arrest and apoptosis were simultaneously analyzed at equivalent concentrations. Although significant, the degree of the combination effect with cisplatin was inconsistent between the two assays. Several studies have demonstrated variable anti-cancer efficacy at the same concentration across these assays (Ghosh et al., 2018; Luo et al., 2019; Hu et al., 2020). We therefore propose the application of maltol against PD-L1-mediated resistance to cisplatin. However, a comprehensive array of growth and apoptosis-related studies on the combination is needed for better understanding.

CTLs efficiently eliminate cancer cells (Weigelin et al., 2021). High PD-L1 levels prevent CTLs from targeting tumor cells (Yi et al., 2023). The reduction of PD-L1 in melanoma cells contributes to the efficacy of CTLs-mediated cancer cell elimination (Jung et al., 2022). CTLL-2 cells, which are mouse-derived CTLs, are often used as a CTL model (Kametaka et al., 2003). An immuno-oncology agent was proposed by analyzing the effector cells (CTLL-2)-mediated cytotoxicity against target cells (B16F10) simultaneously with PD-L1 expression reduction (Jung et al., 2022). PD-L1/PD-1 checkpoint-mediated immune

suppression is accompanied by reduced IL-2 production, and blockade of the PD-L1/PD-1 interaction restores T cell functionality along with increased IL-2 levels (Xu et al., 2018). IFN-γ signaling can impair CTL function by reducing IL-2 production (Tau et al., 2001; Hidalgo et al., 2005). In this work, maltol potentiated CTLL-2 cells-regulated B16F10 killing and IL-2 production. Thus, maltol could hold promise as an immuno-oncology agent, acting by inhibiting the expression of PD-L1 while simultaneously enhancing the function of CTLs.

Conclusion

In conclusion, our findings reveal, for the first time, that maltol has an anti-melanoma effect by liberating PD-L1/PD-1 checkpoint-regulated immunosuppression, leading to more efficient T cell killing, and being effective against PD-L1-mediated immunotherapy resistance associated with cisplatin. Therefore, maltol, as an immuno-oncology agent, could be used as a potential candidate for combating melanoma. However, future studies are needed to investigate whether maltol's impact extends not only CTLs but also to PD-L1-expressing and tumor-related antigen-presenting cells.

Data availability statement

The original contributions presented in the study are included in the article/Supplementary Material, further inquiries can be directed to the corresponding author.

Ethics statement

Ethical approval was not required for the studies on animals in accordance with the local legislation and institutional requirements because only commercially available established cell lines were used.

Author contributions

N-RH: Formal Analysis, Investigation, Methodology, Writing–original draft. H-JP: Conceptualization, Validation. S-GK: Conceptualization, Validation, Funding acquisition. P-DM: Formal Analysis, Investigation, Methodology, Writing–review and editing.

Funding

This work was supported by the National Research Foundation of Korea (NRF) grant funded by the Korea government (MSIT) (No. 2020R1A5A2019413).

Conflict of interest

The authors declare that the research was conducted in the absence of any commercial or financial relationships that could be construed as a potential conflict of interest.

Publisher's note

All claims expressed in this article are solely those of the authors and do not necessarily represent those of their affiliated organizations, or those of the publisher, the editors and the reviewers. Any product that may be evaluated in this article, or claim that may be made by its manufacturer, is not guaranteed or endorsed by the publisher.

Supplementary material

The Supplementary Material for this article can be found online at: https://www.frontiersin.org/articles/10.3389/fphar.2023.1255586/full#supplementary-material

References

Ahn, H., Lee, G., Han, B. C., Lee, S. H., and Lee, G. S. (2022). Maltol, a natural flavor enhancer, inhibits NLRP3 and non-canonical inflammasome activation. *Antioxidants* 11 (10), 1923. doi:10.3390/antiox11101923

Bodurlar, Y., and Caliskan, M. (2022). Inhibitory activity of soybean (Glycine max L. Merr.) Cell Culture Extract on tyrosinase activity and melanin formation in alpha-melanocyte stimulating Hormone-Induced B16-F10 melanoma cells. *Mol. Biol. Rep.* 49 (8), 7827–7836. doi:10.1007/s11033-022-07608-6

Chen, Y. S., Lee, S. M., Lin, C. C., and Liu, C. Y. (2014). Hispolon decreases melanin production and induces apoptosis in melanoma cells through the downregulation of tyrosinase and microphthalmia-associated transcription factor (MITF) expressions and the activation of caspase-3, -8 and -9. *Int. J. Mol. Sci.* 15 (1), 1201–1215. doi:10.3390/ijms15011201

Chen, J., Chen, R., Huang, S., Zu, B., and Zhang, S. (2021). Atezolizumab alleviates the immunosuppression induced by PD-L1-positive neutrophils and improves the survival of mice during sepsis. *Mol. Med. Rep.* 23 (2), 144. doi:10.3892/mmr.2020.11783

Chinembiri, T. N., du Plessis, L. H., Gerber, M., Hamman, J. H., and du Plessis, J. (2014). Review of natural compounds for potential skin cancer treatment. *Molecules* 19 (8), 11679–11721. doi:10.3390/molecules190811679

de Azevedo, S. J., de Melo, A. C., Roberts, L., Caro, I., Xue, C., and Wainstein, A. (2021). First-line atezolizumab monotherapy in patients with advanced BRAFV600 wild-type melanoma. *Pigment. Cell. Melanoma Res.* 34 (5), 973–977. doi:10.1111/pcmr.12960

Gao, C., Yan, X., Wang, B., Yu, L., Han, J., Li, D., et al. (2016). Jolkinolide B induces apoptosis and inhibits tumor growth in mouse melanoma B16F10 cells by altering glycolysis. *Sci. Rep.* 6, 36114. doi:10.1038/srep36114

Gao, Y., Nihira, N. T., Bu, X., Chu, C., Zhang, J., Kolodziejczyk, A., et al. (2020). Acetylation-dependent regulation of PD-L1 nuclear translocation dictates the efficacy of anti-PD-1 immunotherapy. *Nat. Cell. Biol.* 22 (9), 1064–1075. doi:10.1038/s41556-020-0562-4

Ghosh, S., Jawed, J. J., Halder, K., Banerjee, S., Chowdhury, B. P., Saha, A., et al. (2018). TNFα mediated ceramide generation triggers cisplatin induced apoptosis in B16F10 melanoma in a PKCδ independent manner. *Oncotarget* 9 (102), 37627–37646. doi:10.18632/oncotarget.26478

Grabosch, S., Bulatovic, M., Zeng, F., Ma, T., Zhang, L., Ross, M., et al. (2019). Cisplatin-induced immune modulation in ovarian cancer mouse models with distinct inflammation profiles. *Oncogene* 38 (13), 2380–2393. doi:10.1038/s41388-018-0581-9

Greil, R., Hutterer, E., Hartmann, T. N., and Pleyer, L. (2017). Reactivation of dormant anti-tumor immunity - a clinical perspective of therapeutic immune checkpoint modulation. *Cell. Commun. Signal.* 15 (1), 5. doi:10.1186/s12964-016-0155-9

Guergueb, T., and Akhloufi, M. A. (2021). Melanoma skin cancer detection using recent deep learning Models<sup/>. *Annu. Int. Conf. IEEE Eng. Med. Biol. Soc.* 2021, 3074–3077. doi:10.1109/EMBC46164.2021.9631047

Han, N. R., Kim, K. C., Kim, J. S., Park, H. J., Ko, S. G., and Moon, P. D. (2022a). SBT (composed of Panax ginseng and aconitum carmichaeli) and stigmasterol enhances nitric oxide production and exerts curative properties as a potential anti-oxidant and immunity-enhancing agent. *Antioxidants* 11 (2), 199. doi:10.3390/antiox11020199

Han, N. R., Moon, P. D., Nam, S. Y., Ko, S. G., Park, H. J., Kim, H. M., et al. (2022b). TSLP up-regulates inflammatory responses through induction of autophagy in T cells. *FASEB J.* 36 (2), e22148. doi:10.1096/fj.202101447R

Hidalgo, L. G., Urmson, J., and Halloran, P. F. (2005). IFN-Gamma decreases CTL generation by limiting IL-2 production: A feedback loop controlling effector cell production. *Am. J. Transpl.* 5 (4), 651–661. doi:10.1111/j.1600-6143.2005.00761.x

Hu, K., Xie, L., Zhang, Y., Hanyu, M., Yang, Z., Nagatsu, K., et al. (2020). Marriage of black phosphorus and Cu2+ as effective photothermal agents for PET-guided combination cancer therapy. *Nat. Commun.* 11 (1), 2778. doi:10.1038/s41467-020-16513-0

Hu, W., Ma, Y., Zhao, C., Yin, S., and Hu, H. (2021). Methylseleninic acid overcomes programmed death-ligand 1-mediated resistance of prostate cancer and lung cancer. *Mol. Carcinog.* 60 (11), 746–757. doi:10.1002/mc.23340

Jeong, H. C., Hong, H. D., Kim, Y. C., Rhee, Y. K., Choi, S. Y., Kim, K. T., et al. (2015). Quantification of maltol in Korean ginseng (Panax ginseng) products by high-performance liquid chromatography-diode array detector. *Pharmacogn. Mag.* 11 (43), 657–664. doi:10.4103/0973-1296.160452

Jiang, Y., Chen, M., Nie, H., and Yuan, Y. (2019). PD-1 and PD-L1 in cancer immunotherapy: Clinical implications and future considerations. *Hum. Vaccin. Immunother.* 15 (5), 1111–1122. doi:10.1080/21645515.2019.1571892

Jin, M. H., Hu, J. N., Zhang, M., Meng, Z., Shi, G. P., Wang, Z., et al. (2023). Maltol attenuates polystyrene nanoplastic-induced enterotoxicity by promoting AMPK/mTOR/TFEB-mediated autophagy and modulating gut microbiota. *Environ. Pollut.* 322, 121202. doi:10.1016/j.envpol.2023.121202

Jorgovanovic, D., Song, M., Wang, L., and Zhang, Y. (2020). Roles of IFN-γ in tumor progression and regression: A review. *Biomark. Res.* 8, 49. doi:10.1186/s40364-020-00228-x

Jung, D., Shin, S., Kang, S. M., Jung, I., Ryu, S., Noh, S., et al. (2022). Reprogramming of T cell-derived small extracellular vesicles using IL2 surface engineering induces potent anti-cancer effects through miRNA delivery. *J. Extracell. Vesicles* 11 (12), e12287. doi:10.1002/jev2.12287

Kametaka, M., Kume, A., Okada, T., Mizukami, H., Hanazono, Y., and Ozawa, K. (2003). Reduction of CTLL-2 cytotoxicity by induction of apoptosis with a Fas-estrogen receptor chimera. *Cancer Sci.* 94 (7), 639–643. doi:10.1111/j.1349-7006.2003.tb01496.x

Ko, J. S. (2017). The immunology of melanoma. *Clin. Lab. Med.* 37 (3), 449–471. doi:10.1016/j.cll.2017.06.001

Kornepati, A. V. R., Boyd, J. T., Murray, C. E., Saifetiarova, J., de la Peña Avalos, B., Rogers, C. M., et al. (2022). Tumor intrinsic PD-L1 promotes DNA repair in distinct cancers and suppresses PARP inhibitor-induced synthetic lethality. *Cancer Res.* 82 (11), 2156–2170. doi:10.1158/0008-5472.CAN-21-2076

Lee, J. J., Kim, S. Y., Kim, S. H., Choi, S., Lee, B., and Shin, J. S. (2022). STING mediates nuclear PD-L1 targeting-induced senescence in cancer cells. *Cell. Death Dis.* 13 (9), 791. doi:10.1038/s41419-022-05217-6

Liu, W., Wang, Z., Hou, J. G., Zhou, Y. D., He, Y. F., Jiang, S., et al. (2018). The liver protection effects of maltol, a flavoring agent, on carbon tetrachloride-induced acute liver injury in mice via inhibiting apoptosis and inflammatory response. *Molecules* 23 (9), 2120. doi:10.3390/molecules23092120

Luo, Y., Feng, Y., Song, L., He, G. Q., Li, S., Bai, S. S., et al. (2019). A network pharmacology-based study on the anti-hepatoma effect of Radix Salviae Miltiorrhizae. *Chin. Med.* 14, 27. doi:10.1186/s13020-019-0249-6

Mandai, M., Hamanishi, J., Abiko, K., Matsumura, N., Baba, T., and Konishi, I. (2016). Dual faces of IFNγ in cancer progression: A role of PD-L1 induction in the determination of pro- and antitumor immunity. *Clin. Cancer Res.* 22 (10), 2329–2334. doi:10.1158/1078-0432.CCR-16-0224

Mao, Y., Du, J., Chen, X., Al Mamun, A., Cao, L., Yang, Y., et al. (2022). Maltol promotes mitophagy and inhibits oxidative stress via the Nrf2/PINK1/parkin pathway after spinal cord injury. *Oxid. Med. Cell. Longev.* 2022, 1337630. doi:10.1155/2022/1337630

Mi, X. J., Hou, J. G., Wang, Z., Han, Y., Ren, S., Hu, J. N., et al. (2018). The protective effects of maltol on cisplatin-induced nephrotoxicity through the AMPK-mediated PI3K/Akt and p53 signaling pathways. *Sci. Rep.* 8 (1), 15922. doi:10.1038/s41598-018-34156-6

Mojic, M., Takeda, K., and Hayakawa, Y. (2017). The dark side of IFN-γ: Its role in promoting cancer immunoevasion. *Int. J. Mol. Sci.* 19 (1), 89. doi:10.3390/ijms19010089

Molassiotis, A., Fernández-Ortega, P., Pud, D., Ozden, G., Scott, J. A., Panteli, V., et al. (2005). Use of complementary and alternative medicine in cancer patients: A European survey. *Ann. Oncol.* 16 (4), 655–663. doi:10.1093/annonc/mdi110

Nakamura, K., Yoshikawa, N., Yamaguchi, Y., Kagota, S., Shinozuka, K., and Kunitomo, M. (2002). Characterization of mouse melanoma cell lines by their mortal malignancy using an experimental metastatic model. *Life Sci.* 70 (7), 791–798. doi:10.1016/s0024-3205(01)01454-0

Notaro, A., Jakubaszek, M., Koch, S., Rubbiani, R., Dömötör, O., Enyedy, É. A., et al. (2020). A maltol-containing ruthenium polypyridyl complex as a potential anticancer agent. *Chemistry* 26 (22), 4997–5009. doi:10.1002/chem.201904877

Raskov, H., Orhan, A., Christensen, J. P., and Gögenur, I. (2021). Cytotoxic CD8+ T cells in cancer and cancer immunotherapy. *Br. J. Cancer* 124 (2), 359–367. doi:10.1038/s41416-020-01048-4

Ravindran Menon, D., Li, Y., Yamauchi, T., Osborne, D. G., Vaddi, P. K., Wempe, M. F., et al. (2021). EGCG inhibits tumor growth in melanoma by targeting JAK-STAT signaling and its downstream PD-L1/PD-L2-PD1 Axis in tumors and enhancing cytotoxic T-cell responses. *Pharmaceuticals* 14 (11), 1081. doi:10.3390/ph14111081

Seo, Y. J., Lee, I. K., Lee, J. Y., Oh, K. O., and Kim, H. S. (1993). Effects of cytokines on the cell proliferation of cytolytic T cell line CTLL-2. *J. Periodontal Implant Sci.* 23 (3), 454–460.

Sha, J. Y., Li, J. H., Zhou, Y. D., Yang, J. Y., Liu, W., Jiang, S., et al. (2021). The p53/p21/p16 and PI3K/Akt signaling pathways are involved in the ameliorative effects of maltol on D-galactose-induced liver and kidney aging and injury. *Phytother. Res.* 35 (8), 4411–4424. doi:10.1002/ptr.7142

Sim, W. K., Park, J. H., Kim, K. Y., and Chung, I. S. (2020). Robustaflavone induces G0/G1 cell cycle arrest and apoptosis in human umbilical vein endothelial cells and exhibits anti-angiogenic effects *in vivo*. *Sci. Rep.* 10 (1), 11070. doi:10.1038/s41598-020-67993-5

Slominski, R. M., Zmijewski, M. A., and Slominski, A. T. (2015). The role of melanin pigment in melanoma. *Exp. Dermatol.* 24 (4), 258–259. doi:10.1111/exd.12618

Tang, H., Liang, Y., Anders, R. A., Taube, J. M., Qiu, X., Mulgaonkar, A., et al. (2018). PD-L1 on host cells is essential for PD-L1 blockade-mediated tumor regression. *J. Clin. Invest.* 128 (2), 580–588. doi:10.1172/JCI96061

Tau, G. Z., Cowan, S. N., Weisburg, J., Braunstein, N. S., and Rothman, P. B. (2001). Regulation of IFN-gamma signaling is essential for the cytotoxic activity of CD8(+) T cells. *J. Immunol.* 167 (10), 5574–5582. doi:10.4049/jimmunol.167.10.5574

Teng, F., Meng, X., Kong, L., and Yu, J. (2018). Progress and challenges of predictive biomarkers of anti PD-1/PD-L1 immunotherapy: A systematic review. *Cancer Lett.* 414, 166–173. doi:10.1016/j.canlet.2017.11.014

Tran, L., Allen, C. T., Xiao, R., Moore, E., Davis, R., Park, S. J., et al. (2017). Cisplatin alters antitumor immunity and synergizes with PD-1/PD-L1 inhibition in head and neck squamous cell carcinoma. *Cancer Immunol. Res.* 5 (12), 1141–1151. doi:10.1158/2326-6066.CIR-17-0235

Voltarelli, F. A., Frajacomo, F. T., Padilha, C. S., Testa, M. T. J., Cella, P. S., Ribeiro, D. F., et al. (2017). Syngeneic B16F10 melanoma causes cachexia and impaired skeletal muscle strength and locomotor activity in mice. *Front. Physiol.* 8, 715. doi:10.3389/fphys.2017.00715

Wang, X., Teng, F., Kong, L., and Yu, J. (2016). PD-L1 expression in human cancers and its association with clinical outcomes. *Onco. Targets Ther.* 9, 5023–5039. doi:10.2147/OTT.S105862

Wang, G., Xie, L., Li, B., Sang, W., Yan, J., Li, J., et al. (2021). A nanounit strategy reverses immune suppression of exosomal PD-L1 and is associated with enhanced ferroptosis. *Nat. Commun.* 12 (1), 5733. doi:10.1038/s41467-021-25990-w

Weigelin, B., den Boer, A. T., Wagena, E., Broen, K., Dolstra, H., de Boer, R. J., et al. (2021). Cytotoxic T cells are able to efficiently eliminate cancer cells by additive cytotoxicity. *Nat. Commun.* 12 (1), 5217. doi:10.1038/s41467-021-25282-3

Xiong, W., Gao, Y., Wei, W., and Zhang, J. (2021). Extracellular and nuclear PD-L1 in modulating cancer immunotherapy. *Trends Cancer* 7 (9), 837–846. doi:10.1016/j.trecan.2021.03.003

Xu, L., Zhang, Y., Tian, K., Chen, X., Zhang, R., Mu, X., et al. (2018). Apigenin suppresses PD-L1 expression in melanoma and host dendritic cells to elicit synergistic therapeutic effects. *J. Exp. Clin. Cancer Res.* 37 (1), 261. doi:10.1186/s13046-018-0929-6

Yang, Y., Wang, J., Xu, C., Pan, H., and Zhang, Z. (2006). Maltol inhibits apoptosis of human neuroblastoma cells induced by hydrogen peroxide. *J. Biochem. Mol. Biol.* 39 (2), 145–149. doi:10.5483/bmbrep.2006.39.2.145

Yasumoto, E., Nakano, K., Nakayachi, T., Morshed, S. R., Hashimoto, K., Kikuchi, H., et al. (2004). Cytotoxic activity of deferiprone, maltol and related hydroxyketones against human tumor cell lines. *Anticancer Res.* 24 (2B), 755–762.

Yi, J., Tavana, O., Li, H., Wang, D., Baer, R. J., and Gu, W. (2023). Targeting USP2 regulation of VPRBP-mediated degradation of p53 and PD-L1 for cancer therapy. *Nat. Commun.* 14 (1), 1941. doi:10.1038/s41467-023-37617-3

Yu, X., Dai, Y., Zhao, Y., Qi, S., Liu, L., Lu, L., et al. (2020). Melittin-lipid nanoparticles target to lymph nodes and elicit a systemic anti-tumor immune response. *Nat. Commun.* 11 (1), 1110. doi:10.1038/s41467-020-14906-9

Yu, J., Zhuang, A., Gu, X., Hua, Y., Yang, L., Ge, S., et al. (2023). Nuclear PD-L1 promotes EGR1-mediated angiogenesis and accelerates tumorigenesis. *Cell. Discov.* 9 (1), 33. doi:10.1038/s41421-023-00521-7

Yun, J., Kim, B. G., Kang, J. S., Park, S. K., Lee, K., Hyun, D. H., et al. (2015). Lipid-soluble ginseng extract inhibits invasion and metastasis of B16F10 melanoma cells. *J. Med. Food* 18 (1), 102–108. doi:10.1089/jmf.2013.3138

Zhang, J., Bu, X., Wang, H., Zhu, Y., Geng, Y., Nihira, N. T., et al. (2018). Cyclin D-CDK4 kinase destabilizes PD-L1 via cullin 3-SPOP to control cancer immune surveillance. *Nature* 553 (7686), 91–95. doi:10.1038/nature25015

Zhou, S., Riadh, D., and Sakamoto, K. (2021). Grape extract promoted α-MSH-induced melanogenesis in B16F10 melanoma cells, which was inverse to resveratrol. *Molecules* 26 (19), 5959. doi:10.3390/molecules26195959

frontiers | Frontiers in Pharmacology

TYPE Original Research
PUBLISHED 05 September 2023
DOI 10.3389/fphar.2023.1218046

OPEN ACCESS

EDITED BY
Ayaz Shahid,
Western University of Health Sciences, United States

REVIEWED BY
Haibo Xu,
Chengdu University of Traditional Chinese Medicine, China
Mohammed Sikander,
The University of Texas Rio Grande Valley, United States
Pallavi Jain,
SRM Institute of Science and Technology, India

*CORRESPONDENCE
Ying Liang,
lynne3665@163.com

†These authors share first authorship

RECEIVED 06 May 2023
ACCEPTED 23 August 2023
PUBLISHED 05 September 2023

CITATION
Wu D, Fu Z, Liu W, Zhao Y, Li W, Liu Q and Liang Y (2023), Bioinformatics analysis and identification of upregulated tumor suppressor genes associated with suppressing colon cancer progression by curcumin treatment.
Front. Pharmacol. 14:1218046.
doi: 10.3389/fphar.2023.1218046

Bioinformatics analysis and identification of upregulated tumor suppressor genes associated with suppressing colon cancer progression by curcumin treatment

Dan Wu[1†], Zhenkai Fu[2†], Wenna Liu[1†], Yujia Zhao[3], Wenxuan Li[4], Qingqing Liu[1] and Ying Liang[1*]

[1]Department of Pharmacy, Drug Development Center, Precision Pharmacy, Tangdu Hospital, Fourth Military Medical University, Xi'an, Shaanxi, China, [2]School of Basic Medical Sciences, Peking University, Beijing, China, [3]Department of Oncology, the First Affiliated Hospital, School of Medicine, Xi'an Jiaotong University, Xi'an, Shaanxi, China, [4]Laboratory of RNA Epigenetics, Institutes of Biomedical Sciences, Shanghai Medical College, Fudan University, Shanghai, China

Tumor suppressor genes (TSGs) are commonly downregulated in colon cancer and play a negative role in tumorigenesis and cancer progression by affecting genomic integrity, the cell cycle, and cell proliferation. Curcumin (CUR), a Chinese herb-derived phytochemical, exerts antitumor effects on colon cancer. However, it remains unclear whether CUR exerts its antitumor effects by reactivating TSGs in colon cancer. Here, we demonstrated that CUR inhibited HT29 and HCT116 proliferation and migration by cell-counting kit-8, colony-formation, and wound-healing assays. Furthermore, the comprehensive bioinformatics analysis of mRNA sequencing revealed that 3,505 genes were significantly upregulated in response to CUR in HCT116 cells. Kyoto Encyclopedia of Genes and Genomes and Gene Ontology analyses showed that the most upregulated genes were enriched in cancer pathways containing 37 TSGs. Five (*ARHGEF12*, *APAF1*, *VHL*, *CEBPA*, and *CASP8*) of the 37 upregulated TSGs were randomly selected for real-time fluorescence polymerase chain reaction and the verification results showed that these five genes were significantly reactivated after CUR treatment, suggesting that TSGs are related to CUR-mediated colon cancer inhibition. *ARHGEF12* is a newly identified TSG and a potential therapeutic target for colon cancer. Furthermore, molecular docking was performed to predict the binding sites of CUR and ARHGEF12, suggesting that CUR can prevent colon cancer cell invasion and metastasis by inhibiting ARHGEF12 and RhoA binding. In conclusion, the present study reveals that CUR inhibits colon cancer cell proliferation and migration by reactivating TSGs, revealing a new mechanism and potential target for colon cancer treatment.

Abbreviations: CCK8, cell-counting kit-8; C/EBP, CCAAT/enhancer binding protein; CRC, Colorectal cancer; CUR, Curcumin; DEGs, Differentially expressed genes; FBS, Fetal bovine serum; GO, Gene ontology; HKII, Hexokinase II; KEGG, Kyoto Encyclopedia of Genes; NF-κB, Nuclear factor kappa-B; qPCR, Quantitative polymerase chain reaction; RNA-Seq, RNA sequencing; TLR4, Toll-like receptor 4; TSGs, Tumor suppressor genes.

KEYWORDS

tumor suppressor genes, curcumin, mRNA high-throughput sequencing, molecular docking, colon cancer

1 Introduction

Colon cancer is a malignant tumor that is considered the third most common cancer worldwide with a high morbidity and mortality rate, thereby the fourth one to cause death (Selvam et al., 2019; Tie et al., 2022). Although great progress has been made in surgical techniques and treatments for colon cancer, the 5-year relative survival rate of patients with colon cancer has not changed markedly in the past decades (Shang et al., 2023). Currently, surgical treatment, chemotherapy, and radiotherapy are the major therapeutic modalities; however, these treatments usually have side effects that damage the immune system as well as liver and kidney functions and can even contribute to drug resistance (Zhang N. et al., 2021). Chinese herbal extracts have received increasing attention for their antitumor properties via diverse mechanisms in various types of cancer (Islam et al., 2022). For instance, baicalein, a novel toll-like receptor 4 (TLR4)-targeted therapeutic drug, inhibits the development of colorectal cancer (CRC) by inhibiting the TLR4/hypoxia-inducible factor-1/vascular endothelial growth factor signaling pathway (Chen et al., 2021). Astragaloside IV inhibits the development of hepatocellular carcinoma by persistently inhibiting fibrosis by regulating the pSmad3C/3L and nuclear factor erythroid 2-related factor 2/heme oxygenase-1 pathways (Zhang C. et al., 2021). Ginsenoside Rg3 effectively suppresses human CRC cell proliferation by inhibiting the transactivation of CCAAT/enhancer binding protein (C/EBP) and nuclear factor kappa-B (NF-κB), and the interaction of C/EBPβ with p65 (Yao and Guan, 2022). Ginsenoside Rh3 induces CRC cell apoptosis by upregulating the caspase-3 gene (Cong et al., 2020). Berberine inhibits the proliferation, migration and invasion of colon cancer cells by blocking the cell cycle in the G0/G1 phase through the Hedgehog signaling cascade (Sun et al., 2023). Ursolic acid suppresses colorectal cancer by downregulation of Wnt/β-catenin signaling pathway activity (Zhao et al., 2023). Although these herbal extracts exert important therapeutic effects on tumors, their antitumor mechanisms remain to be further explored. Therefore, there is an urgent need to identify additional Chinese herbal extracts and to better understand their molecular mechanisms that inhibit tumor development.

Curcumin (CUR) is one of the most common polyphenolic compounds extracted from the rhizomes of *Curcuma longa*. It is easily soluble in acetic acid, ketones, alkali, and chloroform, whereas it is insoluble in water at acidic and neutral pH. Owing to its hydrophobic properties, it can diffuse through cell membranes into the endoplasmic reticulum, mitochondria, and nucleus, where it can exert its action (Pricci et al., 2020). The therapeutic benefits of CUR have been demonstrated in multiple chronic diseases such as inflammation, arthritis, metabolic syndrome, liver disease, obesity, neurodegenerative diseases, and certain cancers (Aggarwal and Sung, 2009; Brockmueller et al., 2023). Recently, multiple studies have confirmed that CUR exerts strong anticancer effects against various types of cancer, such as breast, lung, hematological, gastric, colon, pancreatic, and hepatic cancers. The mechanisms involved include the inhibition of cell proliferation, induction of apoptosis, and suppression of cell migration and invasion via various molecular pathways (He et al., 2023; Zhang et al., 2023). CUR is a promising candidate as an effective anticancer drug that can be used alone or in combination with other drugs. It affects different signaling pathways and molecular targets involved in the development of several cancers. It has been reported that CUR plays an important role in anti-colon cancer. For instance, CUR inhibited 1,2-dimethylhydrazine-induced rat colon carcinogenesis and the growth of the *in vitro* cultured HT29 cell line by suppressing the peroxisome proliferator-activated receptor-γ signal transduction pathway; moreover, in human colon cancer HCT116 and HT29 cells, CUR induced the dissociation of hexokinase II (HKII) from mitochondria by downregulating the expression and activity of the HKII gene, leading to mitochondria-mediated apoptosis (Giordano and Tommonaro, 2019). In HCT116 cells, it has been reported that CUR increases miR-491 expression, suppresses PEG10 expression, and consequently, silences the Wnt/β-catenin signaling pathway as a mechanism of inducing apoptosis and inhibiting cell proliferation (Wu et al., 2020). Curcumin exerts its anticancer and antiproliferative activities by inducing senescence in colon cancer cells, and curcumin-induced senescence is accompanied by autophagy (Mosieniak et al., 2012). Curcumin regulates miR-21 expression and inhibits invasion and metastasis in colorectal cancer (Mudduluru et al., 2011). Curcumin inhibits colon cancer cell proliferation by targeting CDK2 (Lim et al., 2014). Based on the important clinical role of CUR in the treatment of colon cancer, there is an urgent need to investigate its anticancer mechanisms.

Tumor suppressor genes (TSGs) play opposing roles as oncogenes in the pathological process of cancer formation. It has been shown that TSGs play an antitumor role by affecting genomic integrity, the cell cycle, and cell proliferation. TSGs can be roughly classified into five groups based on their properties: (i) TSGs that promote cancer cells to enter into a certain stage of the cell cycle; (ii) TSGs that encode for effectors or ligands of signaling pathways that have inhibitory effects on cell proliferation; (iii) TSGs that encode for checkpoint-control proteins that initiate cell cycle arrest under conditions of DNA damage or chromosomal abnormalities; (iv) TSGs that encode for pro-apoptotic proteins; and (v) TSGs that encode for proteins that are involved in the repair of DNA damage (Gao et al., 2021; Gregory and Copple, 2023). According to existing studies, TSGs play an important role in inhibiting the occurrence and development of colon cancer. Sun et al. reported that 15-lipoxygenase-1, a TSG, promoted various antitumorigenic events, including cell differentiation and apoptosis, and inhibited chronic inflammation, angiogenesis, and metastasis, especially in colon cancer, and was downregulated in human colon polyps and cancers (Il Lee et al., 2011). Yang et al. reported that miR-1253 was a novel TSG in colon cancer that inhibited cell proliferation, migration, and invasion by targeting enhancer of zeste homolog 2 (Yang and Zhang, 2021). Cheng et al. reported that mindin acted as a TSG in a CRC mouse model via the mitogen-activated protein kinase/extracellular signal-regulated kinase signaling pathway, which directly suppressed colon cancer development (Cheng

et al., 2020). Morin et al. reported that the inactivation of the adenomatous polyposis *coli* TSG initiated colonic neoplasia (Morin et al., 1997).

Based on the clinical importance of CUR in the treatment of colon cancer and its key role in colon cancer development, we explored whether CUR inhibited colon cancer by reactivating TSGs. Therefore, we verified the inhibitory effects of CUR on colon cancer by cell-counting kit-8 (CCK8), colony-formation, and wound-healing assays. The RNA sequencing (RNA-Seq) profiling of the control group and CUR-treated HCT116 cells revealed 3,505 upregulated genes. Furthermore, Kyoto Encyclopedia of Genes (KEGG) and Genomes and Gene Ontology (GO) analyses showed that among the upregulated genes, a total of 135 genes, including the largest number of differentially expressed genes (DEGs), were involved in cancer pathways. Besides, after the intersection of these 135 genes with the total TSGs downloaded from the TSGene database (https://bioinfo.uth.edu/TSGene/), we obtained 37 TSGs involved in cancer pathways that were upregulated in HCT116 cells by the action of CUR. We randomly selected five genes, *ARHGEF12*, *APAF1*, *VHL*, *CEBPA*, and *CASP8*, which were validated by quantitative polymerase chain reaction (qPCR) in HT29 and HCT116 cells. As expected, these five TSGs were significantly upregulated in both HT29 and HCT116 cells following CUR treatment. Furthermore, we predicted the binding site of ARHGEF12 and found that CUR might inhibit the invasion and migration of colon cancer cells by inhibiting the binding of ARHGEF12 to RhoA. Our results provide new insights into the use of CUR as a TSGs activator in colon cancer and suggest that TSGs play an important role in colon cancer.

2 Materials and methods

2.1 Compounds and reagents

Cur was obtained from MedChemExpress (#HY-N0005/CS-1490, purity ≥98%, CAS 458-37-7). Cell culture medium DMEM/HIGH GLUCOSE (4mML-Glutamine, 4500 mg/L Glucose) was purchased from CYTIVA (SH30022.01). CCK-8 was obtained from EnoGene Cell (E1CK-000208).

2.2 Cell lines and cell culture

Human colon cancer cell lines HT-29 and HCT-116 were obtained from the Cell Bank of the Chinese Academy of Science (Shanghai, China). All these cell lines were cultured in DMEM supplemented with 10% fetal bovine serum (FBS) and 1% penicillin-streptomycin under standard culture conditions (5% CO_2, 37°C).

2.3 Cell proliferation assay

Cell proliferation was evaluated by the CCK8 assay. HT29 and HCT116 cells were seeded in 96-well plates at 1×10^4 cells/well in a volume, and incubated overnight. Each cell line was then treated with 0, 5, 10, 20, 40 and 80 μM concentrations of CUR (dissolved in DMSO) for 24 h, the control group was treated with DMSO solvent corresponding to the experimental group. After treatment, 10 μL CCK8 reagent was added to a 96-well plate and incubated at 37 °C for 20 min, and then the absorbance was measured at a wavelength of 450 nm using an enzyme marker (M200Pro). IC50 values were obtained by nonlinear regression curve fitting analysis using GraphPad Prism 5.0.

2.4 Colony formation assay

Five thousand HT29 and HCT116 cells were inoculated in 6-well plates, respectively, and divided into control and CUR (30 μM) groups and cultured for 14 days until visible colonies appeared. The control group was treated with DMSO solvent of the same concentration as the experimental group. Then the colonies were stained with crystal violet for 20 min. The colony count was calculated using ImageJ software.

2.5 Cell migration assays

HT29 and HCT116 cells (80×10^4 cells/well) were inoculated in 6-well plates and cultured for 24 h. CUR (30 μM) was added to the experimental group before scratching and a linear scratch was formed by quickly scratching over the monolayer cell surface using a 1 mL pipette. The control group was also replaced with a medium containing the same concentration of DMSO as the experimental group before scratches. Cell migration was observed under the microscope (EVOS XL Core) at 24 h and 48h, and wound healing was observed by comparing micrographs of the experimental and control groups at different times. The gap area was analyzed using ImageJ software.

2.6 RNA extraction and RT-qPCR analysis

HCT116 cells were treated with CUR (30 μM) for 24 h. Total RNA was then extracted from cells in the administered and unadministered groups, respectively, using Trizol reagent (Sangon Biotech, B511311-0100) and reverse transcribed with a reverse transcription kit (TaKaRa, Cat# RR047A). Quantitative RT-PCR, using the FastStart Essential DNA Green Master (Roche Diagnostics GmbH, Mannheim, Germany) was performed on Qtower2.2 equipment. Gene expression was calculated using the $2^{-\Delta\Delta CT}$ method, with *GAPDH* as an internal references. Primers were synthesized as follows,

GAPDH forward: 5′-TGACTTCAACAGCGACACCCA-3′, and.

GAPDH reverse: 5′-CACCCTGTTGCTGTAGCCAAA-3′; *ARHGEF12* forward: 5′-CTATCACCGACAGATAGCTCCTCC-3′, and.

ARHGEF12 reverse: 5′-CGCTGAACAAGACCATATATC TCG; *APAF1* forward: 5′-CAAAGGCTTGGCTCATGGTTG ACA-3′, and.

APAF1 reverse: 5′-ATGATGTAGGATGTCTTGATGTCC-3′; *VHL* forward: 5′-CAGCTACCGAGTCCTCATGACT-3′, and.

VHL reverse: 5′-AGCAGGCAGGTAAGTCAATTTC-3′; *CEBPA* forward: 5′-CCGGATCTCGAGGCTTGCCCGA-3′, and.

CEBPA reverse: 5′-TCCTCGCAGGGAGAAGCCACCG-3′; *CASP8* forward: 5′-GGAGCATCTGCTGTCTGAGCAG-3′, and.

CASP8 reverse: 5′-CATAAAGATTTCTGCTGAAGTC-3′.

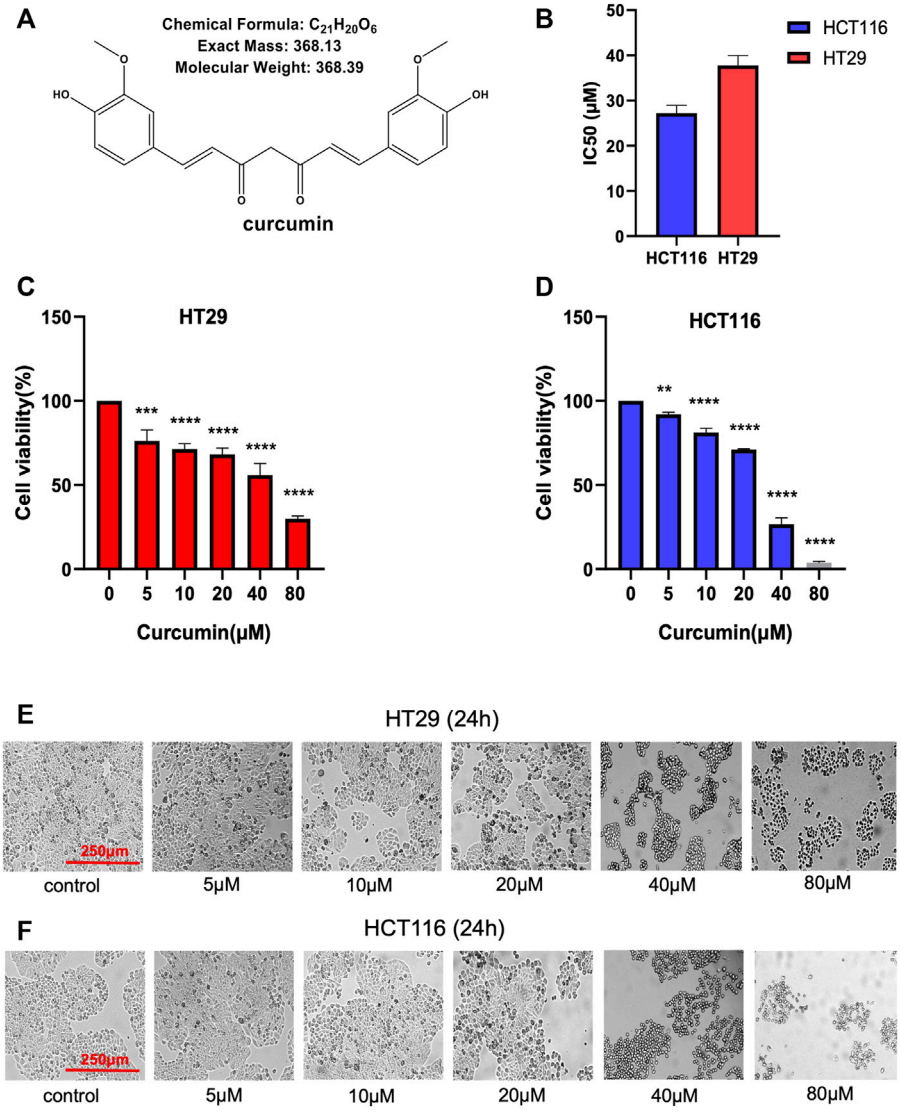

FIGURE 1
CUR inhibits the cell viability of HCT116 and HT29 cells in a dose-dependent manner. **(A)**. Chemical structure of CUR from ChemDraw. **(B)**. IC50 of CUR inhibition in colon cancer cells. **(C, D)**. The survival of HCT116 and HT29 cells was examined by CCK8 assay at 5μM, 10μM, 20μM, 40μM and 80 μM concentrations of CUR for 24 h. **(E, F)**. HCT116 and HT29 cell numbers and morphological changes were positively correlated with CUR concentrations. **** represents $p < 0.0001$, *** represents $p < 0.001$, ** represents $p < 0.01$.

2.7 RNA preparation and RNA-seq

To investigate the effect of CUR on gene expression in colon cancer cells, HCT116 cells (30×10^4 cells/well) were inoculated in 6-well plates and cultured for 24 h. The experiment was then divided into CUR (30 μM) treated and untreated groups for another 24 h. Total RNA was extracted using Trizol reagent for high-throughput sequencing. The RNA concentration and quality were determined using Nanodrop 2000 (Thermo Scientific) for library preparation. RNA-seq analysis was performed using Tophat2 (http://ccb.jhu.edu/software/tophat) to compare the sequencing reads to the human reference genome hg38. Reads were calculated using featureCounts (http://subread.sourceforge.net). Differentially expressed genes (DEGs) and statistical analyses were performed with DESeq2 (version 3.12) in R (version 4.0) (fold change >1.5, $p < 0.05$). Heat maps were created with Complex Heatmap (Bioconductor Project).

2.8 Molecular docking analysis

ARHGEF12–RhoA crystal complexes (PDB code:1X86) was obtained from the Protein Data Bank (http://www. rcsb. org/). Discovery Studio 2021 was used to perform molecular docking analysis. Before docking, CUR was prepared using "Prepare Ligands" module and CHARM force field was used for minimization, generating ten conformations. The protein was prepared using "Protein Preparation" module, allowing for the addition of hydrogen atoms and the deletion of unnecessary water. Subsequently, the proteins were optimized and

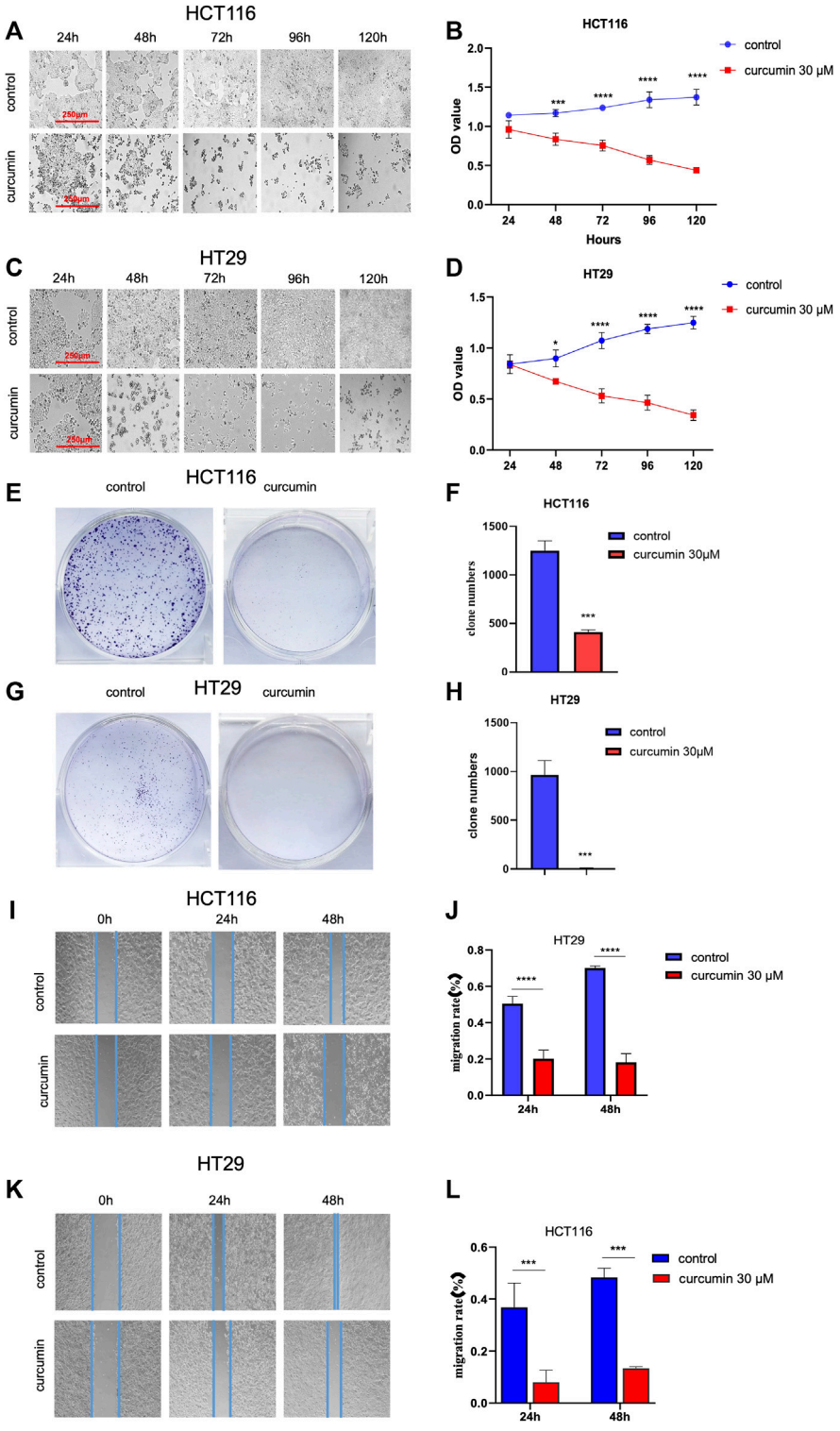

FIGURE 2
CUR inhibited the proliferation and migration abilities of HCT116 and HT29 cells in a time-dependent manner. **(A–D)**. The cell viability of 30 μM CUR was measured by CCK8 at 24h, 48h, 72h, 96 h and 120h, respectively. The viability and number of HCT116 and HT29 cells decreased in a time-dependent manner with CUR, and the cell morphology was also significantly wrinkled with the increase of drug action time. **(E–H)**. In colony formation assay, 30 μM CUR action for 24 h significantly reduced the number of clones formed by HCT116 and HT29 cells. **(I–L)**. 30 μM CUR significantly inhibited the migratory viability of HCT116 and HT29 cells at 24 h and 48 h, respectively. The cell migration pictures were gained by 200 times magnification under the microscope. **** represents $p < 0.0001$, *** represents $p < 0.001$, * represents $p < 0.05$.

minimized. Ligand binding sites are defined using the "Receptor-Ligand Pharmacophore Generation" module. The docking results were evaluated using hydrogen bond interactions and binding mode. The interaction 2D diagram of the CUR with residues of receptor was views in the "View Interaction" module. All structural figures were generated using PyMol 3.7.

2.9 Statistical analysis

All experiments were conducted in triplicate (n = 3) and the data are presented as the mean ± SEM. All statistical analyses were processed with GraphPad Prism 5.0. Differences of unpaired comparisons between two groups were analyzed using the ANOVA. p-value <0.05 was considered statistically significant.

3 Results

3.1 CUR inhibits the proliferation and migration of colon cancer cells

Figure 1A shows the chemical structure of CUR. Firstly, we calculated the IC50 values of HCT116 and HT29 cells after CUR treatment by CCK8 assay. As a result, the corresponding IC50 at 24 h was 27.21 μM and 37.76 μM in HCT116 and HT29 cells, respectively (Figure 1B). Further, we investigated the effects of CUR on the viability of colon cancer cells. Cell viability was measured by CCK8 assay after treatment with CUR at concentrations of 5, 10, 20, 40 and 80 μM for 24 h. Figure 1C, D showed that CUR reduced cell proliferation in a dose-dependent manner. As the dose of CUR increased, the number of cells gradually decreased and the morphology shrank (Figure 1E, F).

Next, we used the CCK8 method to detect the effect of CUR on the proliferation of HCT116 and HT29 cells by CCK8 assay. The results in Figure 2A–D show that cell proliferation decreased in a time-dependent manner with increasing time of CUR treatment, and cell morphology was crinkled.Elucidation of the effects of CUR on colon cancer cell proliferation and migration by colony formation and wound healing assays. In the colony formation assay, the observations showed that the colony formation capacity of HCT116 and HT29 cells was reduced after treatment with CUR at 30 μM, indicated by significantly decreased colony numbers (Figure 2E-H). Wound healing assays showed that CUR treatment inhibited cell migration from 0 to 48 h (Figure 2I-L). The migration rates of the CUR treatment group in HCT116 and HT29 cells were 39.9% and 21.79% compared with those of the corresponding control group after CUR treatment for 24 h and 25.89% and 27.64% of the control group after CUR treatment for 48 h ($p < 0.0001$), respectively.

3.2 High-throughput sequencing identifies the upregulated tumor suppressor genes through the cancer pathway after CUR treatment

To investigate the molecular mechanism of CUR inhibition of colon cancer cell proliferation and migration, we treated HCT116 cells with CUR (30 μM) for 24 h, and collected HCT116 cells from the control and CUR groups separately for mRNA high-throughput sequencing analysis to determine the curcumin-related genes. The results are shown in Figure 3A, 3,505 genes were upregulated and 3,564 genes were downregulated. Cluster analysis by the top 100 differentially expressed genes in Figure 3B showed that these differentially expressed genes clustered significantly between the control and CUR group cell samples. KEGG pathway enrichment analysis showed that these differentially expressed genes after being acted upon by CUR were enriched in the cancer pathway in Figure 3C.

TSG is a key gene involved in DNA damage repair, suppression of cell mitosis, induction of apoptosis and prevention of metastasis. Hence, downregulation of TSG will lead to cancer development and progression. Therefore, re-upregulation of TSGs that are downregulated in cancers may prevent cancer progression (Wang et al., 2018). To explore whether CUR could reactivate the TSGs that were downregulated in colon cancer, we intersected the 1,217 tumor suppressor genes that were downregulated in colon cancer from TCGA database (https://bioinfo.uth.edu/TSGene/) with 135 genes that were upregulated in cancer pathways in HCT116 under the treatment of CUR, 37 TSGs that were reactivated under the action of CUR were obtained, including *ARHGEF12*, *APAF1*, *VHL*, *CEBPA*, *CASP8 et al* (Figure 4A). The results of KEGG and GO analysis are shown in Figure 4B, C. These 37 reactivated TSGs are mainly involved in the cancer pathways, which is consistent with the results of KEGG analysis of the first 100 upregulated genes in Figure 3C. In addition, GO profiling suggested that these 37 upregulated TSGs negatively regulated the transcription of RNA polymerase II promoter and positively regulated the apoptotic process. (Figure 4C), suggesting activation of these genes can suppress cell growth and proliferation.

3.3 CUR treatment reactivates the TSGs *ARHGEF12* and *APAF1* in colon cancer cells and correlated with a good prognosis for patients with colon cancer

To further verify that TSGs were indeed reactivated by CUR, we randomly selected five of the 37 upregulated TSGs: *ARHGEF12*, *APAF1*, *VHL*, *CEBPA*, and *CASP8* for qPCR assay. The results showed that the expression of these five TSGs was upregulated in both HCT116 and HT29 cells after CUR (60 μM) treatment, with significant differences in *ARHGEF12*, *APAF1*, *VHL* three genes in HCT116 and *ARHGEF12*, *APAF1*, *VHL*, *CASP8* four genes in HT29 (Figure 5A, B). Among them, *ARHGEF12* and *APAF1* genes, which were most significantly upregulated by CUR, were preferentially selected as candidate targets for CUR in colon cancer cells.

Considering that CUR can significantly reactivate TSGs *ARHGEF12* and *APAF1*, to further investigate whether upregulated *ARHGEF12* and *APAF1* expression in colon cancer correlates with patient prognosis, we analyzed colon cancer subtypes using Kaplan-Meier survival curves. We found in Figure 5C, D that high expression of *ARHGEF12* and *APAF1* was significantly correlated with a good prognosis for patients of colon cancer. Further, we queried the pan-oncogene expression profiles of *ARHGEF12* and *APAF1* in the TCGA

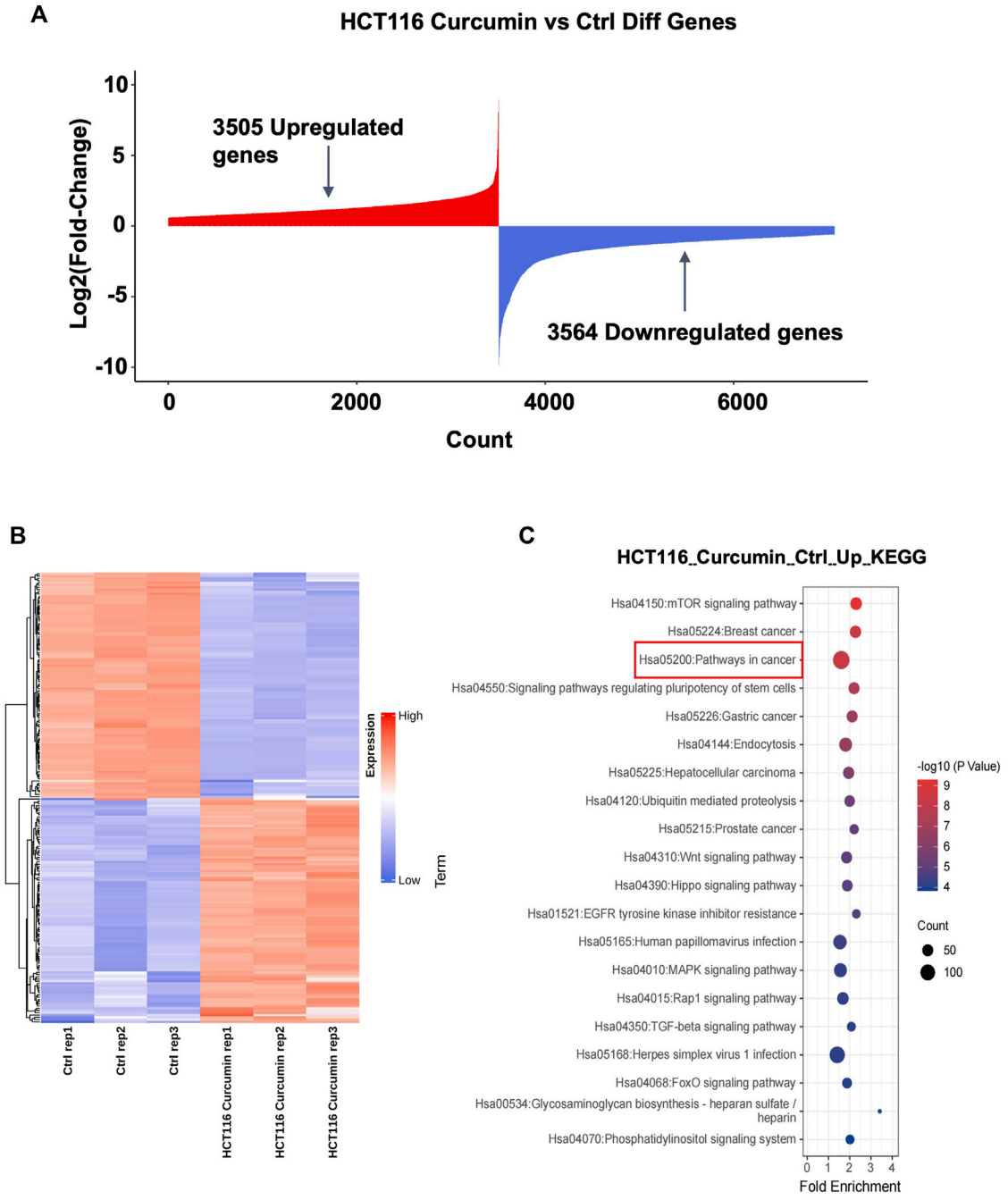

FIGURE 3
The highest number of genes involved in cancer pathways were upregulated by CUR. **(A)** A total of 3,505 upregulated genes and 3,564 downregulated genes were obtained by mRNA sequencing analysis under the effect of CUR. **(B).** Heat map of the top 100 differential genes. **(C).** KEGG enrichment analysis showed that the most upregulated of the differential genes were involved in the cancer pathway.

(https://bioinfo.uth.edu/TSGene/) database using the UALCAN database (http://ualcan.path.uab.edu/), and as shown in Figure 5E, F, *ARHGEF12* and *APAF1* were significantly downregulated in colon cancer and many other types of cancers. In summary, both TSGs *ARHGEF12* and *APAF1* expression were downregulated in colon cancer and could be reactivated by CUR, and upregulated *ARHGEF12* and *APAF1* may be associated with favorable prognosis of patients.

3.4 Interaction of CUR with ARHGEF12–RhoA complex

Since ARHGEF12 has not been reported as a therapeutic target for colon cancer, we aimed to investigate the molecular mechanism by which CUR inhibits colon cancer by acting on ARHGEF12. Based on the reported researches, ARHGEF12 binds to RhoA to shape a functional complex, thereby enhancing cancer cell migration and

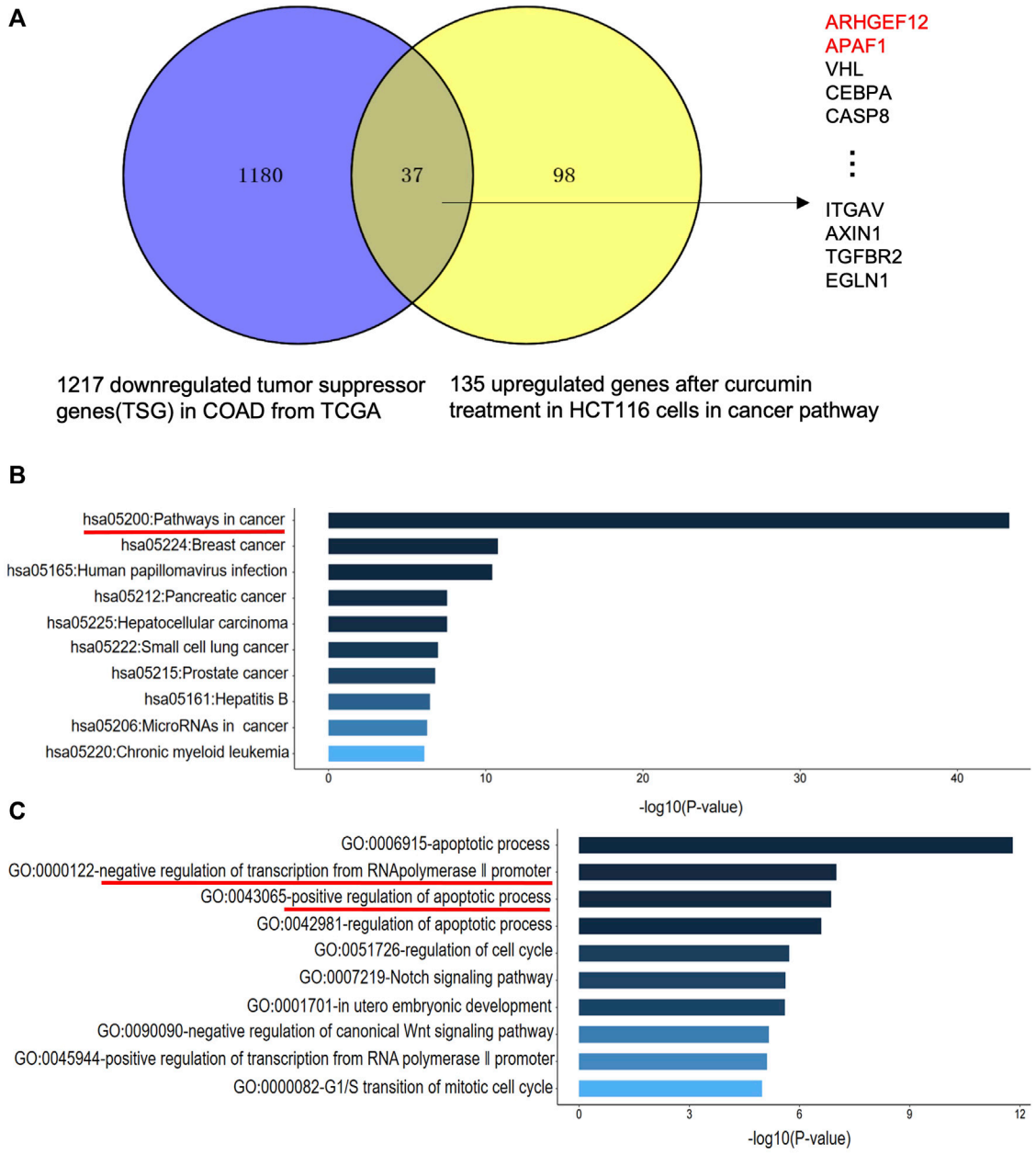

FIGURE 4
CUR may reactivate TSGs in COAD via the cancer pathway. **(A)**. CUR activated a total of 37 TSGs in the cancer pathway out of 135 upregulated genes. **(B)**. KEGG analysis of 37 upregulated TSGs treated with CUR. **(C)**. GO analysis of 37 upregulated TSGs after CUR treatment.

invasion. (Lacoste et al., 2012; Ghanem et al., 2022). We speculate that CUR may block the binding of ARHGEF12-RhoA complex to suppress colon cancer cells, providing a new therapeutic strategy for colon cancer treatment.

To verify whether CUR interacts with ARHGEF12–RhoA, we performed molecular docking to analyze its affinity and binding mode. In the structure of ARHGEF12–RhoA complexes, ARG 923 of ARHGEF12 formed multiple salt bridge interactions with ASP 45 and GLU 54 of RhoA, which was important for RhoA to be selected as a substrate (Aggarwal and Sung, 2009). In our study, we found that CUR occupied the cavity at the interface between ARHGEF12 and RhoA, indicating that CUR effectively inhibited interactions between ARHGEF12 and RhoA (Figure 6A, B). In the binding pocket, ARG 923 formed a direct hydrogen bond with the phenolic hydroxyl group of CUR at 2.8 Å. Additionally, ARG 804 of ARHGEF12 and GLU 40 of RhoA both formed stronger hydrogen bonds with CUR at 2.7 Å and 2.9 Å, respectively. ARG 936 of ARHGEF12 and TYR 42 of RhoA formed weaker hydrogen bonds with CUR at 4.0 Å and 3.7 Å. Moreover, ARG 922 of ARHGEF12 was packed in the hydrophobic core of CUR, which contributed to stabilizing the molecule at the binding site (Figure 6C, D). This suggests that CUR has a high affinity for ARHGEF12 and can effectively intervene in the interaction between ARHGEF12 and RhoA. Therefore, we hypothesized that CUR reactivated the *ARHGEF12* TSG to block colon cancer cell

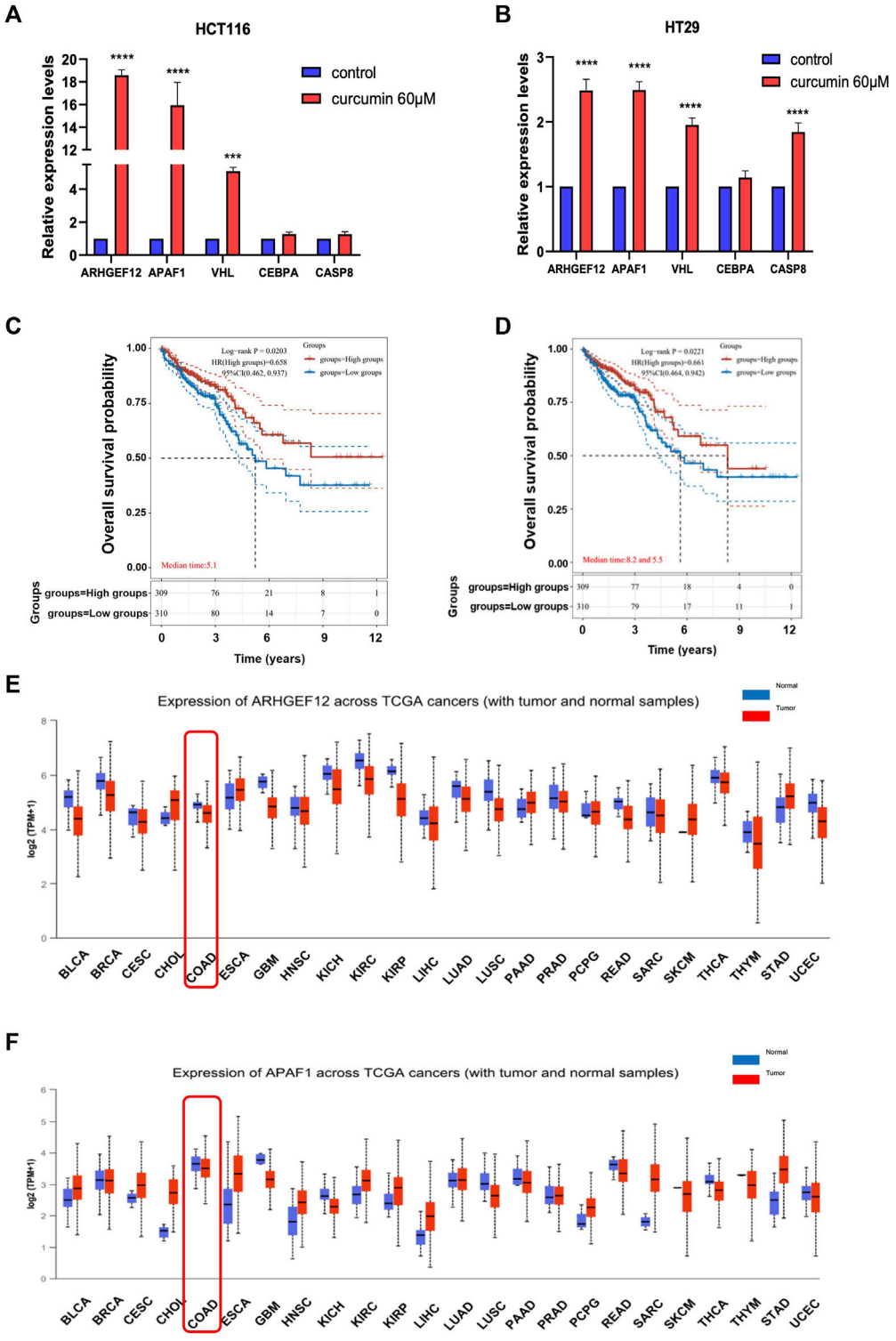

FIGURE 5
CUR increased TSGs *ARHGEF12* and *APAF1* in the cancer pathway, and these two TSGs are correlated with good patient prognosis in clinic practice. **(A, B)**. *ARHGEF12, APAF1, VHL, CEBPA* and *CASP8* were reactivated in HCT116 and HT29 cells after CUR treatment as verified by qPCR. **(C, D)**. Kaplan - Meier survival curve plots showed that activation of *ARHGEF12* and *APAF1* was positively correlated with the likelihood of patient survival time. **(E, F)**. pan-oncogene expression profiles of *ARHGEF12* and *APAF1*. **** represents $p < 0.0001$, *** represents $p < 0.001$.

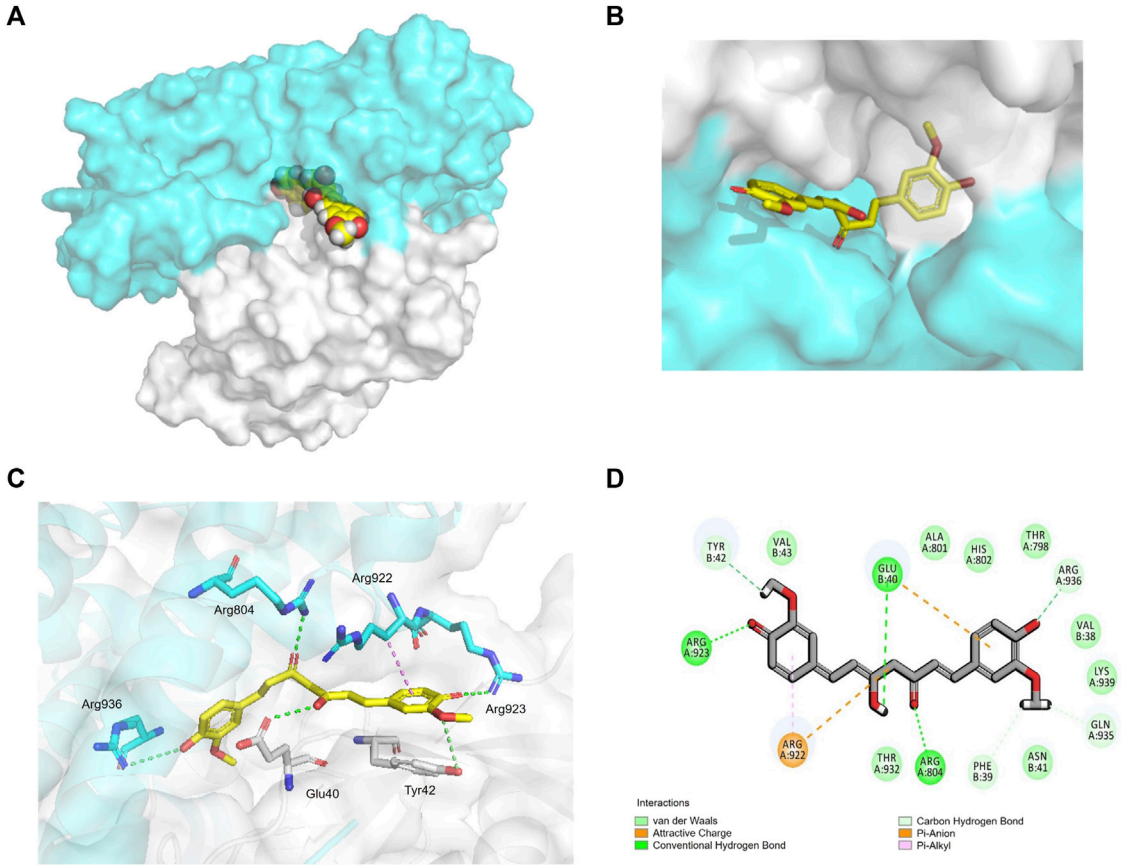

FIGURE 6
Interaction of CUR with ARHGEF12-RhoA complex. **(A, B)**. curcumin (yellow) occupied the cavity of the ARHGEF12-RhoA complex, ARHGEF12 (blue), RhoA (grey) (PDB code:1X86). **(C)**. Interactions of CUR with TYR 42 of RhoA, ARG923, ARG922, and ARG804 of ARHGEF12, respectively. **(D)**. Diagram of SantacruzaMate A interaction in the cavity formed by ARHGEF12-RhoA. The hydrogen bond is depicted as a green line, and the interaction of pi-alkyl is depicted as a purple line.

proliferation and migration via cancer pathways, whereas CUR might exert an inhibitory effect on invasion and migration by blocking the binding of ARHGEF12 to RhoA.

4 Discussion

Colon cancer ranks as the third most prevalent cancer worldwide, with an annual incidence of 1.1 million new cases. Furthermore, it is the second foremost contributor to cancer-related deaths, seriously threatening human health (Cervantes et al., 2023). The 5-year survival time has not been significantly improved by the current treatment methods; therefore, there is an urgent need to identify more treatment methods. Traditional Chinese medicine has been employed and widely acknowledged as an alternative approach in cancer treatment for centuries (Xiang et al., 2019). In particular, Chinese herbal medicine-derived phytochemicals, such as CUR, have demonstrated significant anti-tumor effects across various types of cancer (Miyazaki et al., 2023). CUR inhibits tumor development by reactivating TSGs. For instance, in lung cancer A549 and H460 cells, CUR significantly upregulates RARβ TSG expression at both the mRNA and protein levels (Jiang et al., 2015); CUR acts through the inhibition of DNA methyltransferases and the subsequent reactivation of *RASSF1A* in cancer, leading to its therapeutic effects (Dammann et al., 2017). However, it remains unknown whether CUR exerts its antitumor effects by reactivating TSGs in colon cancer.

In the present study, we performed mRNA-seq with CUR-treated or untreated colon cancer cell lines HCT116 and found 3,505 upregulated genes, among which 37 TSGs were significantly upregulated in cancer pathways, indicating that TSGs might play a critical role in colon cancer via cancer pathways. To confirm that these TSGs were indeed upregulated after CUR treatment, we selected 5 of the 37 upregulated TSGs for RT-qPCR. As expected, all five TSGs were upregulated, the most significantly upregulated TSGs were *ARHGEF12* and *APAF1* (Figure 5A, B). Furthermore, the upregulation of *ARHGEF12* and *APAF1* was found to be associated with a good prognosis in patients by Kaplan-Meier analysis (Figure 5C, D). Other researchers have also demonstrated the tumor suppressor role of these two TSGs in tumors. For example, the overexpression of *LARG* in breast and CRC cells demonstrated diminished cell proliferation and colony formation, as along with a significantly decreased cell migration rate in CRC cells, whereas *APAF1* played a key role in apoptosis and was significantly downregulated in colon cancer cells (Ong et al., 2009; Han et al., 2018). The present study provides groundbreaking evidence that CUR inhibited colon cancer development via the upregulation of

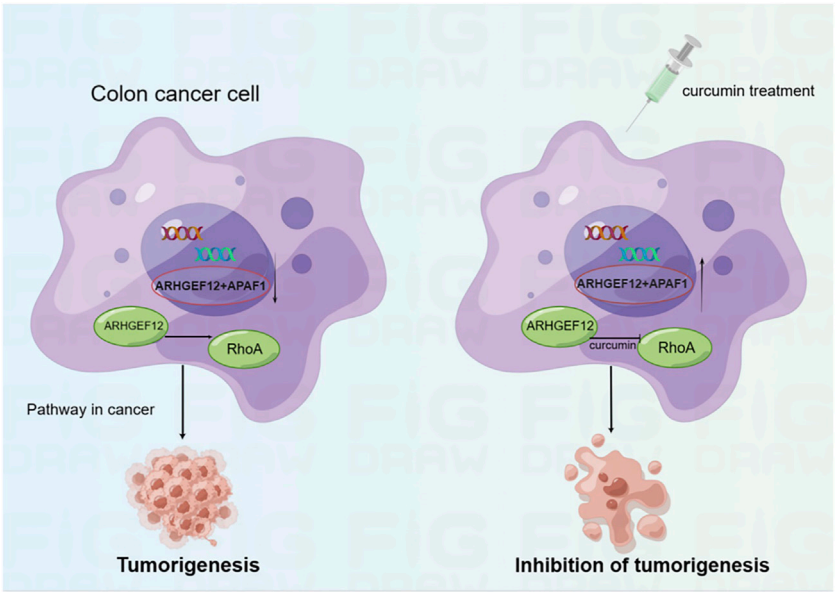

FIGURE 7
Schematic diagram showing CUR reactivates *ARHGEF12* and *APAF1* to block colon cancer cells proliferation and migration through cancer pathways. Moreover, CUR may inhibit the invasion and migration of colon cancer cells by blocking the binding of ARHGEF12 and RhoA.

the TSGs *ARHGEF12* and *APAF1*. Furthermore, we performed molecular docking and demonstrated that the curcumin can form a stable H-bond with ARHGEF12 and RhoA, respectively, indicating curcumin can bind tightly to these two proteins (Xiang et al., 2022; He et al., 2023), as shown in the schematic diagram (Figure 6, 7, by Figdraw). This, for the first time, suggested that CUR might play a role in inhibiting tumor invasion and migration by blocking the binding of ARHGEF12 and RhoA, which provided a theoretical basis for the CUR treatment of colon cancer.

5 Conclusion

We identified upregulated TSGs related to the inhibition of colon cancer progression after CUR treatment via comprehensive bioinformatics analysis and demonstrated that CUR inhibited the proliferation and migration of colon cancer cell lines by reactivating TSGs such as *ARHGEF12* and *APAF1* via cancer pathways. These TSGs are novel targets identified in the CUR-mediated inhibition of colon cancer and correlated with patient prognosis. Further, we predicted the binding sites of CUR and ARHGEF12 by molecular docking, suggesting that CUR may inhibit colon cancer invasion and migration by blocking the ARHGEF12-RhoA complex, which provides a theoretical basis for the molecular mechanism of CUR-mediated inhibition of colon cancer cells.

Data availability statement

The datasets presented in this study can be found in online repositories. The names of the repository/repositories and accession number(s) can be found in the article/Supplementary material.

Author contributions

Conceptualization, YL; methodology, YL; software, DW, WeL, and QL; validation, DW and YL; investigation, DW, ZF, YZ, and WL; data curation, YL; writing—original draft preparation, DW, YL, and QL; writing, review and editing, ZF and YL; visualization, DW and YL; supervision, YL; project administration, YL; funding acquisition, YL All authors contributed to the article and approved the submitted version.

Funding

This research was funded by the "Phoenix Introduction Plan" Talent Startover Project of Tangdu Hospital, grant number 2022YFJH001.

Acknowledgments

The authors sincerely appreciate Professor Minggao Zhao and Le Yang from Tangdu hospital of Fourth Military Medical University for their critical suggestions. We also would like to thank Editage (www.editage.cn) for the English language improvement.

Conflict of interest

The authors declare that the research was conducted in the absence of any commercial or financial relationships that could be construed as a potential conflict of interest.

Publisher's note

References

Aggarwal, B. B., and Sung, B. (2009). Pharmacological basis for the role of curcumin in chronic diseases: An age-old spice with modern targets. *Trends Pharmacol. Sci.* 30, 85–94. doi:10.1016/j.tips.2008.11.002

Brockmueller, A., Samuel, S. M., Mazurakova, A., Busselberg, D., Kubatka, P., and Shakibaei, M. (2023). Curcumin, calebin A and chemosensitization: How are they linked to colorectal cancer? *Life Sci.* 318, 121504. doi:10.1016/j.lfs.2023.121504

Cervantes, A., Adam, R., Rosello, S., Arnold, D., Normanno, N., Taieb, J., et al. (2023). Metastatic colorectal cancer: ESMO clinical practice guideline for diagnosis, treatment and follow-up. *Ann. Oncol.* 34, 10–32. doi:10.1016/j.annonc.2022.10.003

Chen, M., Zhong, K., Tan, J., Meng, M., Liu, C. M., Chen, B., et al. (2021). Baicalein is a novel TLR4-targeting therapeutics agent that inhibits TLR4/HIF-1alpha/VEGF signaling pathway in colorectal cancer. *Clin. Transl. Med.* 11, e564. doi:10.1002/ctm2.564

Cheng, X. S., Huo, Y. N., Fan, Y. Y., Xiao, C. X., Ouyang, X. M., Liang, L. Y., et al. (2020). Mindin serves as a tumour suppressor gene during colon cancer progression through MAPK/ERK signalling pathway in mice. *J. Cell. Mol. Med.* 24, 8391–8404. doi:10.1111/jcmm.15332

Cong, Z., Zhao, Q., Yang, B., Cong, D., Zhou, Y., Lei, X., et al. (2020). Ginsenoside Rh3 inhibits proliferation and induces apoptosis of colorectal cancer cells. *Pharmacology* 105, 329–338. doi:10.1159/000503821

Dammann, R. H., Richter, A. M., Jimenez, A. P., Woods, M., Kuster, M., and Witharana, C. (2017). Impact of natural compounds on DNA methylation levels of the tumor suppressor gene RASSF1A in cancer. *Int. J. Mol. Sci.* 18, 2160. doi:10.3390/ijms18102160

Gao, L., Wu, Z. X., Assaraf, Y. G., Chen, Z. S., and Wang, L. (2021). Overcoming anti-cancer drug resistance via restoration of tumor suppressor gene function. *Drug Resist Updat* 57, 100770. doi:10.1016/j.drup.2021.100770

Ghanem, N. Z., Matter, M. L., and Ramos, J. W. (2022). Regulation of leukaemia associated rho GEF (LARG/ARHGEF12). *Small GTPases* 13, 196–204. doi:10.1080/21541248.2021.1951590

Giordano, A., and Tommonaro, G. (2019). Curcumin and cancer. *Nutrients* 11, 2376. doi:10.3390/nu11102376

Gregory, G. L., and Copple, I. M. (2023). Modulating the expression of tumor suppressor genes using activating oligonucleotide technologies as a therapeutic approach in cancer. *Mol. Ther. Nucleic Acids* 31, 211–223. doi:10.1016/j.omtn.2022.12.016

Han, B., Jiang, P., Li, Z., Yu, Y., Huang, T., Ye, X., et al. (2018). Coptisine-induced apoptosis in human colon cancer cells (HCT-116) is mediated by PI3K/Akt and mitochondrial-associated apoptotic pathway. *Phytomedicine* 48, 152–160. doi:10.1016/j.phymed.2017.12.027

He, Q., Liu, C., Wang, X., Rong, K., Zhu, M., Duan, L., et al. (2023). Exploring the mechanism of curcumin in the treatment of colon cancer based on network pharmacology and molecular docking. *Front. Pharmacol.* 14, 1102581. doi:10.3389/fphar.2023.1102581

Il Lee, S., Zuo, X., and Shureiqi, I. (2011). 15-Lipoxygenase-1 as a tumor suppressor gene in colon cancer: Is the verdict in? *Cancer Metastasis Rev.* 30, 481–491. doi:10.1007/s10555-011-9321-0

Islam, M. R., Akash, S., Rahman, M. M., Nowrin, F. T., Akter, T., Shohag, S., et al. (2022). Colon cancer and colorectal cancer: Prevention and treatment by potential natural products. *Chem. Biol. Interact.* 368, 110170. doi:10.1016/j.cbi.2022.110170

Jiang, A., Wang, X., Shan, X., Li, Y., Wang, P., Jiang, P., et al. (2015). Curcumin reactivates silenced tumor suppressor gene RARβ by reducing DNA methylation. *Phytother. Res.* 29, 1237–1245. doi:10.1002/ptr.5373

Lacoste, C., Herve, J., Bou Nader, M., Dos Santos, A., Moniaux, N., Valogne, Y., et al. (2012). Iodide transporter NIS regulates cancer cell motility and invasiveness by interacting with the Rho guanine nucleotide exchange factor LARG. *Cancer Res.* 72, 5505–5515. doi:10.1158/0008-5472.CAN-12-0516

Lim, T. G., Lee, S. Y., Huang, Z., Lim, D. Y., Chen, H., Jung, S. K., et al. (2014). Curcumin suppresses proliferation of colon cancer cells by targeting CDK2. *Cancer Prev. Res. (Phila)* 7, 466–474. doi:10.1158/1940-6207.CAPR-13-0387

Miyazaki, K., Xu, C., Shimada, M., and Goel, A. (2023). Curcumin and andrographis exhibit anti-tumor effects in colorectal cancer via activation of ferroptosis and dual suppression of glutathione peroxidase-4 and ferroptosis suppressor protein-1. *Pharm. (Basel)* 16, 383. doi:10.3390/ph16030383

Morin, P. J., Sparks, A. B., Korinek, V., Barker, N., Clevers, H., Vogelstein, B., et al. (1997). Activation of beta-catenin-Tcf signaling in colon cancer by mutations in beta-catenin or APC. *Science* 275, 1787–1790. doi:10.1126/science.275.5307.1787

Mosieniak, G., Adamowicz, M., Alster, O., Jaskowiak, H., Szczepankiewicz, A. A., Wilczynski, G. M., et al. (2012). Curcumin induces permanent growth arrest of human colon cancer cells: Link between senescence and autophagy. *Mech. Ageing Dev.* 133, 444–455. doi:10.1016/j.mad.2012.05.004

Mudduluru, G., George-William, J. N., Muppala, S., Asangani, I. A., Kumarswamy, R., Nelson, L. D., et al. (2011). Curcumin regulates miR-21 expression and inhibits invasion and metastasis in colorectal cancer. *Biosci. Rep.* 31, 185–197. doi:10.1042/BSR20100065

Ong, D. C., Ho, Y. M., Rudduck, C., Chin, K., Kuo, W. L., Lie, D. K., et al. (2009). LARG at chromosome 11q23 has functional characteristics of a tumor suppressor in human breast and colorectal cancer. *Oncogene* 28, 4189–4200. doi:10.1038/onc.2009.266

Pricci, M., Girardi, B., Giorgio, F., Losurdo, G., Ierardi, E., and Di Leo, A. (2020). Curcumin and colorectal cancer: From basic to clinical evidences. *Int. J. Mol. Sci.* 21, 2364. doi:10.3390/ijms21072364

Selvam, C., Prabu, S. L., Jordan, B. C., Purushothaman, Y., Umamaheswari, A., Hosseini Zare, M. S., et al. (2019). Molecular mechanisms of curcumin and its analogs in colon cancer prevention and treatment. *Life Sci.* 239, 117032. doi:10.1016/j.lfs.2019.117032

Shang, L., Wang, Y., Li, J., Zhou, F., Xiao, K., Liu, Y., et al. (2023). Mechanism of Sijunzi Decoction in the treatment of colorectal cancer based on network pharmacology and experimental validation. *J. Ethnopharmacol.* 302, 115876. doi:10.1016/j.jep.2022.115876

Sun, Q., Tao, Q., Ming, T., Tang, S., Zhao, H., Liu, M., et al. (2023). Berberine is a suppressor of Hedgehog signaling cascade in colorectal cancer. *Phytomedicine* 114, 154792. doi:10.1016/j.phymed.2023.154792

Tie, J., Cohen, J. D., Lahouel, K., Lo, S. N., Wang, Y., Kosmider, S., et al. (2022). Circulating tumor DNA analysis guiding adjuvant therapy in stage II colon cancer. *N. Engl. J. Med.* 386, 2261–2272. doi:10.1056/NEJMoa2200075

Wang, L. H., Wu, C. F., Rajasekaran, N., and Shin, Y. K. (2018). Loss of tumor suppressor gene function in human cancer: An overview. *Cell. Physiol. Biochem.* 51, 2647–2693. doi:10.1159/000495956

Wu, R., Wang, L., Yin, R., Hudlikar, R., Li, S., Kuo, H. D., et al. (2020). Epigenetics/epigenomics and prevention by curcumin of early stages of inflammatory-driven colon cancer. *Mol. Carcinog.* 59, 227–236. doi:10.1002/mc.23146

Xiang, C., Liao, Y., Chen, Z., Xiao, B., Zhao, Z., Li, A., et al. (2022). Network pharmacology and molecular docking to elucidate the potential mechanism of ligusticum chuanxiong against osteoarthritis. *Front. Pharmacol.* 13, 854215. doi:10.3389/fphar.2022.854215

Xiang, Y., Guo, Z., Zhu, P., Chen, J., and Huang, Y. (2019). Traditional Chinese medicine as a cancer treatment: Modern perspectives of ancient but advanced science. *Cancer Med.* 8, 1958–1975. doi:10.1002/cam4.2108

Yang, D., and Zhang, D. (2021). miR-1253, a novel tumor suppressor gene in colon cancer, is associated with poor patients prognosis. *Clin. Exp. Med.* 21, 563–571. doi:10.1007/s10238-021-00706-y

Yao, W., and Guan, Y. (2022). Ginsenosides in cancer: A focus on the regulation of cell metabolism. *Biomed. Pharmacother.* 156, 113756. doi:10.1016/j.biopha.2022.113756

Zhang, C., Li, L., Hou, S., Shi, Z., Xu, W., Wang, Q., et al. (2021b). Astragaloside IV inhibits hepatocellular carcinoma by continually suppressing the development of fibrosis and regulating pSmad3C/3L and Nrf2/HO-1 pathways. *J. Ethnopharmacol.* 279, 114350. doi:10.1016/j.jep.2021.114350

Zhang, N., Gao, M., Wang, Z., Zhang, J., Cui, W., Li, J., et al. (2021a). Curcumin reverses doxorubicin resistance in colon cancer cells at the metabolic level. *J. Pharm. Biomed. Anal.* 201, 114129. doi:10.1016/j.jpba.2021.114129

Zhang, X., Zhu, L., Wang, X., Zhang, H., Wang, L., and Xia, L. (2023). Basic research on curcumin in cervical cancer: Progress and perspectives. *Biomed. Pharmacother.* 162, 114590. doi:10.1016/j.biopha.2023.114590

Zhao, H., Tang, S., Tao, Q., Ming, T., Lei, J., Liang, Y., et al. (2023). Ursolic acid suppresses colorectal cancer by down-regulation of wnt/β-catenin signaling pathway activity. *J. Agric. Food Chem.* 71, 3981–3993. doi:10.1021/acs.jafc.2c06775

frontiers | Frontiers in Pharmacology

TYPE Original Research
PUBLISHED 06 September 2023
DOI 10.3389/fphar.2023.1257289

OPEN ACCESS

EDITED BY
Ayaz Shahid,
Western University of Health Sciences, United States

REVIEWED BY
Anita Roy,
Indian Institutes of Technology (IIT), India
Shiva Prasad Kollur,
Amrita Vishwa Vidyapeetham, India

*CORRESPONDENCE
Quiping Zhang,
qpzhang@whu.edu.cn
Fuling Zhou,
zhoufuling@whu.edu.cn
Liang Shao,
zn001287@whu.edu.cn

†These authors have contributed equally to this work

RECEIVED 12 July 2023
ACCEPTED 22 August 2023
PUBLISHED 06 September 2023

CITATION
Jamal M, Lei Y, He H, Zeng X, Bangash HI, Xiao D, Shao L, Zhou F and Zhang Q (2023), CCR9 overexpression promotes T-ALL progression by enhancing cholesterol biosynthesis.
Front. Pharmacol. 14:1257289.
doi: 10.3389/fphar.2023.1257289

CCR9 overexpression promotes T-ALL progression by enhancing cholesterol biosynthesis

Muhammad Jamal[1†], Yufei Lei[1†], Hengjing He[1†], Xingruo Zeng[1], Hina Iqbal Bangash[2], Di Xiao[1], Liang Shao[3*], Fuling Zhou[3*] and Quiping Zhang[1,4*]

[1]Department of Immunology, School of Basic Medical Sciences, Wuhan University, Wuhan, China, [2]State Key Laboratory of Agricultural Microbiology, Hubei Hongshan Laboratory, College of Life Science and Technology, Huazhong Agricultural University, Wuhan, Hubei, China, [3]Department of Hematology, Zhongnan Hospital of Wuhan University, Wuhan, China, [4]Hubei Provincial Key Laboratory of Developmentally Originated Disease, Wuhan University, Wuhan, China

Introduction: T-cell acute lymphoblastic leukemia (T-ALL) is an aggressive hematological malignancy of the lymphoid progenitor cells, contributing to ~ 20% of the total ALL cases, with a higher prevalence in adults than children. Despite the important role of human T-ALL cell lines in understanding the pathobiology of the disease, a detailed comparison of the tumorigenic potentials of two commonly used T-ALL cell lines, MOLT4 and JURKAT cells, is still lacking.

Methodology: In the present study, NOD-*Prkdc*^{scid}*IL2rgd*^{ull} (NTG) mice were intravenously injected with MOLT4, JURKAT cells, and PBS as a control. The leukemiac cell homing/infiltration into the bone marrow, blood, liver and spleen was investigated for bioluminescence imaging, flow cytometry, and immunohistochemistry staining. Gene expression profiling of the two cell lines was performed via RNA-seq to identify the differentially expressed genes (DEGs). CCR9 identified as a DEG, was further screened for its role in invasion and metastasis in both cell lines *in vitro*. Moreover, a JURKAT cell line with overexpressed CCR9 (Jurkat-OeCCR9) was investigated for T-ALL formation in the NTG mice as compared to the GFP control. Jurkat-OeCCR9 cells were then subjected to transcriptome analysis to identify the genes and pathways associated with the upregulation of CCR9 leading to enhanced tumirogenesis. The DEGs of the CCR9-associated upregulation were validated both at mRNA and protein levels. Simvastatin was used to assess the effect of cholesterol biosynthesis inhibition on the aggressiveness of T-ALL cells.

Results: Comparison of the leukemogenic potentials of the two T-ALL cell lines showed the relatively higher leukemogenic potential of MOLT4 cells, characterized by their enhanced tissue infiltration in NOD-*PrkdcscidIL2rgdull*

Abbreviations: BM, bone marrow; CCR9, CC chemokine receptor 9; CCL25, CC chemokine ligand 25l; DEGs, Differentially expressed genes; DO, Disease ontology; GEO, Gene Expression Omnibus; GO, Gene ontology; HE, hematoxylin and eosin; HMGCS1, 3-hydroxy-3-methylglutaryl-CoA synthase 1; HMGCR, 3-hydroxy-3-methylglutaryl-CoA reductase; IHC, Immunohistochemistry; KEGG, Kyoto encyclopedia of gene and genome; MVD, Mevalonate Pyrophosphate decarboxylase; MSMO1, Methyl sterol monooxygenase 1; PB, peripheral blood; PBS, Phosphate-buffered sa-line; qRT-PCR, Quantitative real-time PCR; SREBF2, Sterol regulatory element-binding factor 2; STRING, Search Tool for the Retrieval of Interacting Genes/Proteins; shRNA, short hairpin RNA; siRNA, Small interfering RNA; NTG, NOD-PrkdcscidIL2rgdull; T-ALL, T-cell acute lymphoblastic leukemia.

(NTG) mice. Transcriptmoe analysis of the two cell lines revealed numerous DEGs, including CCR9, enriched in vital signaling pathways associated with growth and proliferation. Notably, the upregulation of CCR9 also promoted the tissue infiltration of JURKAT cells *in vitro* and in NTG mice. Transcriptome analysis revealed that CCR9 overexpression facilitated cholesterol production by upregulating the expression of the transcriptional factor SREBF2, and the downstream genes: MSMO1, MVD, HMGCS1, and HMGCR, which was then corroborated at the protein levels. Notably, simvastatin treatment reduced the migration of the CCR9-overexpressing JURKAT cells, suggesting the importance of cholesterol in T-ALL progression.

Conclusions: This study highlights the distinct tumorigenic potentials of two T-ALL cell lines and reveals CCR9-regulated enhanced cholesterol biosynthesis in T-ALL.

KEYWORDS

T-ALL, tissue infiltration, RNA-sequencing, CCR9, SREBF2, cholesterol biosynthesis, simvastatin

1 Introduction

Acute lymphoblastic leukemia (ALL) is an aggressive hematological cancer characterized by the malignant transformation and proliferation of lymphoblasts in bone marrow, blood, and extramedullary tissues (Litzow and Ferrando, 2015; Terwilliger and Abdul-Hay, 2017). Based on the morphology and cytogenetic profiling of the lymphoblast, ALL is classified into B-cell ALL (B-ALL), T-cell ALL (T-ALL). Almost 75% of ALL cases correspond to B-ALL, compared to 10%–15% of T-ALL clinical representation (Wenzinger et al., 2018). Compared to B-ALL, T-ALL is associated with several unfavorable characteristics and a worse prognosis, which generally requires aggressive therapy. Moreover, relapse in clinical T-ALL patients can only be treated with a high dose of chemotherapy along with radiotherapy and bone transplantation (Barrett and Battiwalla, 2010). Although the survival rate of T-ALL patients has significantly improved over the last decades due to advancements in the development of chemotherapies (Pui et al., 2008). However, drug resistance and disease relapse and recurrence offer hindrances to the proper management of T-ALL patients (Follini et al., 2019). This dismal outcome has been associated with the complex nature of the disease, involving the interaction of both genetic and environmental factors to support disease progression and antileukemic drug resistance (Passaro et al., 2016). Therefore, understanding the molecular mechanism underlying T-ALL progression is necessary for the classification of the disease and the development of effective personalized therapeutic strategies against T-ALL.

Cancer cell lines are widely utilized as *in vitro* model systems in biomedical research to investigate disease mechanisms and as a platform for drug discovery (Barretina et al., 2012). Identification of factors associated with T-ALL subtypes and differential clinical outcomes has updated our understanding of the molecular mechanism of T-ALL pathogenesis and target-specific therapeutics (Cordó et al., 2021). In a recent study, single-cell RNA sequencing of thousands of cells isolated from the bone marrow of pediatric T-ALL patients as compared to the healthy pediatric bone marrow revealed deregulated expression of genes associated with cellular growth, proliferation, and metabolic pathways, implicating these genes as oncogenic mediators in T-ALL blasts (Bhasin et al., 2020). Moreover, the molecular characterization of T-ALL genomes based on gene expression pattern, mutation, or copy number variation disclosed additional genomic mutations in the T-cell progenitor impacting the JAK/STAT signaling pathway, protein translation, and epigenetic regulation, thus expanding the current therapeutic option against T-ALL (Girardi et al., 2017). MOLT4 and JURKAT cell lines derived from human T-ALL patients (Minowada et al., 1972; Schneider et al., 1977) are widely utilized models to study the molecular mechanisms underlying T-ALL and develop targeted therapeutic strategies (Dos Santos et al., 2009; Chiarini et al., 2010; Youns et al., 2010; Mezencev and Mcdonald, 2011). Particularly, the MOLT4 cell line, due to its earliest establishment and harboring gene expression patterns, genetic abnormalities, and cellular phenotypes of T-ALL, offers potential to study T-ALL biology and drug development. Likewise, the JURKAT cell line is also important in advancing our understanding of T-ALL pathogenesis as these cells carry several genetic anomalies, including the rearrangement of the T-cell receptor (TCR) and activation of the NOTCH1 signaling pathway, which are common characteristics of T-ALL pathogenesis (Abraham and Weiss, 2004; Gioia et al., 2018). However, cancer cells differ from the primary tumor in a biologically significant manner, and not all the tumor cell lines may recapitulate their annotated cancer type. Earlier studies of multiple cancers have documented discrete molecular profiles of cell lines extracted from the same tumor type, suggesting their dissimilar ability to represent the primary tumors (Jiang et al., 2016; Yu et al., 2019). Notably, analysis of the phosphorylation status of ten signaling pathway proteins with phosopho-specific flow cytometry revealed a higher variability in these proteins across three different T-ALL cell lines under both basal and modulated conditions (Perbellini et al., 2022). Subsequently, T-ALL cell lines, despite their widespread use in cancer biology, differ in their tumorigenic potentials. Moreover, differences between the tumorigenic potentials of MOLT4 and JURKAT cells have not been documented before.

Chemokines and their receptors exhibit great potential in tumor-targeted therapy owing to their active roles in remodeling the tumor microenvironment. The involvement of the CCL25/CCR9 axis in T-ALL is comprehensively summarized by Hong et al. (Hong et al., 2021). Lipid homeostasis is crucial for membrane production and

TABLE 1 Primers sequences of genes.

Gene	Forward sequences	Reverse sequences
CCR9	TCGTGGTCATGGCTTGCTGCTA	AAGACGGTCAGGACAGTGATGG
HMGCS1	AAGTCACACAAGATGCTACACCG	TCAGCGAAGACATCTGGTGCCA
MVD	AAGCGCGATGAAGAGCTGGTTC	TCCTCGGTGAAGTCCTTGCTGA
MSMO1	GCTGCCTTTGATTTGTGGAACCT	CTGCACAACCAAAGCATCTTGCC
HMGCR	GACGTGAACCTATGCTGGTCAG	GGTATCTGTTTCAGCCACTAAGG
SREBF2	CTCCATTGACTCTGAGCCAGGA	GAATCCGTGAGCGGTCTACCAT
ACTB	CACCATTGGCAATGAGCGGTTC	AGGTCTTTGCGGATGTCCACGT
GAPDH	CTGGGCTACACTGAGCACC	AAGTGGTCGTTGAGGGCAATG

shRNA-plasmid	Target sequence information
CCR9-shRNA-1	CCAGAAATCTTATACAGCCAA
CCR9-shRNA-2	GTGCCGTTTCCACCAACATTG
Negative control	GTTCTCCGAACGTGTCACGTT

lipid-based protein posttranslational modifications in rapidly proliferating tumor cells to maintain the rapid proliferation rate. Accordingly, leukemia cells reprogram their metabolism by enhancing the *de novo* biosynthesis of cholesterol using different strategies (Ding et al., 2019; Zhao et al., 2019). Studies have shown that chemokines may modulate cholesterol biosynthesis in cancers. A recent study documented the chemokines-induced enhanced cholesterol biosynthesis in the pulmonary tropism of breast cancer cells (Han et al., 2022). However, the role of chemokines in metabolic reshaping in T-ALL remains largely unknown. In this study, we characterized the tumorigenic potentials of both cell lines *in vivo* using NOD PrkdcscidIL2rgdull (NTG) mice. Further, gene expression profiling was carried out to decipher the distinguished transcriptome and signaling pathways and identify several DEGs, including CCR9. Functional genetic studies were conducted to test the role of CCR9 in JURKAT and MOLT4 cells *in vitro*, as well as *in vivo*. In addition, RNA-sequencing of the JURKAT cells overexpressing CCR9 was performed to determine the aberrantly expressed genes and their associated pathways that could contribute to the increased T-ALL tissue infiltration. Inhibition of the cholesterol biosynthesis pathway with simvastatin was carried out to test the antileukemic effect of statin.

2 Materials and methods

2.1 Cell culture

HEK293T cells and T-ALL cell lines; MOLT-4, and JURKAT cells, were purchased from the American Type Culture Collection, (ATCC, Manassas, VA). HEK293T cells were cultured in DMEM supplemented with 10% fetal bovine serum (FBS, Biological Industries, Israel) and 1% penicillin/streptomycin (Beyotime Biotechnology, China). MOLT-4 and JURKAT cells were cultured in RPMI-1460 media (Biological Industries, Israel) supplemented with 10% fetal bovine serum (FBS, Biological Industries, Israel), 1% L-glutamine (Hyclone, United States), and 1% penicillin/streptomycin (Beyotime Biotechnology, China). The cells in the culture were maintained at 37°C in a humidified atmosphere with 5% CO2.

2.2 Lentivirus transduction for stable cell line generation

The plasmid constructs for the overexpression of CCR9, knockdown of CCR9, and a control plasmid were acquired from the Public Protein/Plasmid Library Company. Stable cell line construction was performed following the procedure described in our published study (Zeng et al., 2023). The stable transgenic cell lines obtained after the screening were utilized for subsequent experiments. The efficiency of silencing was verified by RT-qPCR, flow cytometry, and Western blot.

2.3 Total cholesterol detection assay

The cells were starved in RPMI media with only 1% FBS for 12 h, followed by seeding of 1×10^6 cells per well in a 12-well plate. To assess the effect of the CCR9 ligand on the total cholesterol (TC) level, the cells were treated with 100 $ng.mL^{-1}$ of CCL25. After incubation of the cells for 0 h, 24 h, and 48 h, culture medium was collected at the respective time points. The TC in the culture medium was determined according to the total cholesterol assay kit (Abbkine, catalog number KTB2220, China). First, TC working solution was preheated at 37 °C for ~ 30 min, from which 150 μL was added to each well in a 96-well plate, followed by the addition of 50 μL of measuring standard solution, or RIPA blank solution. After mixing, the reaction was incubated at room temperature for 15 min, and the absorbance was measured at 500 nm wavelength using a microplate reader (TECAN, Switzerland). Finally, a standard curve was generated, and the corresponding total cholesterol concentration of each well was calculated according to the standard curve.

2.4 RNA isolation and real-time quantitative PCR (RT-qPCR)

The total cellular RNA was isolated using the TRIzol reagent (Thermo Fisher Scientific, United States) following the manufacturer's instructions. The mRNA was reverse transcribed into cDNA using the RT-kit following the manufacturer's guidelines (R323-01; Vazyme, China). The cDNA was amplified with ChamQ SYBR qPCR Master Mix (Q311-02; Vazyme, China) using the Quant Studio 6 Flex Real-Time PCR System (Life Technologies, United States). The expression values of the target gene were normalized according to the reference genes GAPDH and ACTB. The gene expression quantification was evaluated using the $2^{-\Delta\Delta CT}$ method. The sequence information of the primers used in this study is listed in Table 1.

2.5 Protein isolation and Western blotting

Isolated cells were lysed with RIPA lysis buffer supplemented with the protease inhibitor PMSF (Beyotime Biotechnology, China) after washing the cells with PBS. The protein content in the cellular lysate was quantified using the BCA kit (Beyotime Biotechnology, China). The lysate samples were separated on SDS-PAGE after boiling at 100°C for 5 min. The proteins on the gel were cold transferred to a polyvinylidene difluoride membrane (Millipore, United States) for 2 h. After transfer, membrane blocking was done with 5% milk dissolved in PBST, followed by incubation with the target primary antibody for overnight at 4°C with gentle shaking. The membrane was washed and probed with secondary antibodies (Proteintech, China) for 1 h. The protein signal in the membrane was detected using an ultra-high-sensitivity ECL kit (MedChemExpress, United States). Antibodies: CCR9 (Abcam, ab32556), HMGCS1 (Proteintech, 17643-1-AP), MSMO1 (Immunoway, YT7443), HMGCR (HUABIO ET1702-41), MVD (Proteintech, 15331-1-AP), ACTIN (HUABIO, ET1702-52), GAPDH (ABclonal, AC002), HRP-conjugated anti-mouse IgG secondary antibodies (Proteintech, SA00001-1), HRP-conjugated anti-rabbit IgG secondary antibodies (Proteintech, SA00001-2).

2.6 Transwell migration/chemotaxis, and invasion assay

Transwell migration/chemotaxis and invasion assay were carried out in 24-well transwell chambers (Corning) using 5 μm pore size polycarbonate insets (Corning, United States). For transwell migration assay, culture with 1×10^5 suspended in cells in 1% FBS medium was seeded in the upper chamber. 600 μL culture medium with 10% FBS was added into the lower chamber. For chemotaxis assay, 100 ng/mL CCL25 in RPMI 1640 with 1% FBS was placed in the lower well, and cell suspension containing 1×10^5 in 1% FBS was added to the upper well of the chamber. For the invasion assay, the transwell chamber was coated with 100 μL of 1: 7 diluted Matrigel (BD Biosciences, United States). Cells ($1–2 \times 10^5$) suspended in 2% FBS medium were seeded onto the upper chambers followed by addition of either 10% FBS medium or 2% FBS medium with CCL25 to the bottom chambers. The cells were allowed to migration for 24 h at 37°C. The metastatic cells were counted using an inverted microscope with a hemacytometer. The results of migration/invasion assays are expressed as fold values.

For the chemotaxis assay after simvastatin treatment, cells were treated with different concentrations of simvastatin 3 μM, 6 μM, 12 μM and 24 μM, (Sigma, S6196) for 24 h. Subsequently, 1×10^5 cells in 1% FBS medium were seeded in the upper chamber, and 600 μL medium with 10% FBS was added to the lower chambers. After 12 h, the cells in the lower well were recovered and counted using a Neubauer chamber.

2.7 Flow cytometry

Cells were washed and resuspended at a concentration of 1×10^6 cells per 100 μL in PBS. Cells were stained with the corresponding monoclonal antibodies as per the manufacturer's instructions, then washed and analyzed with FACS Aria III flow cytometer (BD, United States). The FACS data were analyzed with FlowJo (BD Bio, United States). CCR9 (BD Pharmingen, United States), Hu CD45 APC HI30 100Tst (BD Pharmingen, United States), and DAPI (BD Pharmingen, United States).

2.8 RNA sequencing (RNA-Seq) and bioinformatics analysis

MOLT4 cells, JURKAT cells, JURKAT cells overexpressing CCR9 (Oe-CCR9-JURKAT) cells, and the GFP control were used for the RNA-sequencing. We performed all the RNA-seq in biological replicates. The total RNA of the corresponding cells was extracted following the aforementioned protocol. The integrity of RNA was assessed by 1% agarose gel electrophoresis, and integrity was validated by running the RNA Nano 6000 Assay Kit of the Bioanalyzer 2100 system (Agilent Technologies, United States). A total of 1 μg of RNA per sample was used as input material to generate the RNA-sequencing library using the Illumina NEBNext® UltraTM RNA Library Prep Kit following the manufacturer's protocol. The library was sequenced on an Illumina Novaseq platform and 150 bp paired-end reads were generated. After pretreatment of the raw reads (filtering and QC), clean reads were aligned to the human reference genome using Hisat2 v2.0.5. After mapping to the reference genome, the read numbers mapped to each gene were initially counted with FeatureCounts (v 1.5.0-p3), followed by the calculation of FPKM values for each gene based on the length of the gene and the read counts mapping to it. The read counts were adjusted by the edgeR program package through one scaling normalized factor. Next, the edgeR R package (version 3.22.5) was used to perform differential expression analysis between the conditions. Adjacent *p*-values were calculated following Benjamini and Hochberg's approach. The corrected *p*-values of <0.05 and log2FC > 1 were set as the threshold for defining a significant differential gene expression.

The enrichment of the DEGs in the Gene Ontology (GO), KEGG pathway, Reactome pathway, DisGeNET pathway, and disease ontology (DO) pathway was implemented by the clusterProfiler R package (3.8.1) in R-studio. Pathways associated with the DEGs with *p*-values ≤ 0.05 were regarded as significant. STRING database was used to construct the network of genes and was visualized with Cytoscape (v.3.9.1).

GSE48558 and GSE26713 datasets used in this study were retrieved from the Gene Expression Omnibus (http://www.ncbi.nlm.nih.gov/geo). GSE48558 dataset contains gene expression data obtained from normal and malignant hematopoietic cells. GSE26713 dataset contains the gene expression data of 117 human T-ALL bone marrow samples and 7 normal individual bone marrow samples. Additionally, GEO2R (https://www.ncbi.nlm.nih.gov/geo/geo2r/) was used to compare the expression of the genes between leukemia and normal conditions. UALCAN database (http://ualcan.path.uab.edu/index.html), containing the cancer genome atlas (TCGA) gene expression data, was utilized to determine the expression of genes in various cancers.

2.9 Xenotransplantation experiments

NTG mice (female, 4–6 weeks old, Institute of Model Animals, Wuhan University, China) were reared in a sterile animal facility on a 12-h light and dark cycle. The mice were treated in accordance with European Union guidelines and with the approval of the Medical Ethics Committee of Wuhan University School of Medicine (Permit Number: WP20220022). MOLT-4 and JURKAT cells constitutively expressing the luciferase gene under a ubiquitous promoter were tail injected into NTG immunocompromised mice (1×10^7 cells per mouse). Simultaneously, PBS was used as a control. Next, JURKAT cell line overexpressing CCR9 (OeCCR9-JURKAT) was injected into the NTG. For comparison GFP expressing–JURKAT cells (GFP-JURKAT) was used. The imaging system Xtreme BI (Bruker, United States) was used to image bioluminescence *in vivo*. Mice were intraperitoneally injected with 150 mg/kg D-Luciferin and Potassium Salt (Yeason, China). Engraftment and disease progression were analyzed by the assessment of body weight, peripheral blood smear, flow cytometry, IHC staining, bioluminescence imaging, and mouse organ examination.

2.10 Wright's Giemsa (WG) staining

The slides of bone marrow (BM) and peripheral blood (PB) from mice were stained with Wright's Giemsa stain solution (Solarbio, G1020) according to the manufacturer's instructions and were then observed or photographed under the microscope (Nikon, Japan).

2.11 Hematoxylin-eosin (HE) staining

The tissue samples from the brain, liver, and spleen of mice were fixed with 4% paraformaldehyde and then embedded in paraffin. The paraffinized tissues were sliced into sections. The preserved tissue sections were deparaffinized, rehydrated, and finally stained with hematoxylin and eosin using the HE Staining Kit (Servicebio, G1003). All the procedures were performed according to the manufacturer's instructions. All the finished sections were observed and photographed under the microscope (Nikon, Japan).

2.12 Immunohistochemical (IHC) staining

The IHC staining assay was performed as described in the previous study (Lei et al., 2022). Briefly, the microarray tissue samples were dewaxed with xylene twice for 15 min and rehydrated with an increased concentration of ethanol for 5 min each. Sodium citrate buffer was used for antigen retrieval, and the samples were heated at 100°C followed by inhibition of the endogenous peroxidase activity with 3% H2O2. Then the sections were blotted with the primary antibodies against CD45 (Servicebio, GB113885) and SREBF2 (Proteintech 14508-1-AP). After washing with PBS, the tissue sections were incubated with a secondary antibody (Servicebio, G1215). The histochemistry score (H-score) was calculated to assess the IHC results. H-score = (percentage of cells of weak intensity × 1) + (percentage of cells of moderate intensity × 2) + (percentage of cells of strong intensity × 3).

2.13 Statistical analysis

The statistical analysis and data visualization was performed with GraphPad Prism (v. 8.0). Unpaired *t*-test and one-way ANOVA followed by Dunnett's test were employed. A p-value < 0.05 was considered statistically significant.

3 Results

3.1 MOLT4 cells exhibit remarkably increased tumorigenic potential *in vivo*

To characterize the tumorigenic potentials of the two T-ALL cell lines, an *in vivo* investigation with the NTG mice model was performed following the workflow outlined in Figure 1A. To this end, JURKAT and MOLT4 cells expressing the luciferase gene and PBS were injected intravenously (i.v.) into the immunodeficient NTG mice. The mice were maintained for 26 days, imaged, and sacrificed for subsequent pathogenic examinations. A significant body weight reduction was observed in mice bearing MOLT4 cells (MOLT4-NTG), represented by the red line, as compared to the group of mice injected with JURKAT cells (JURKAT-NTG) and the PBS control (PBS-NTG) (Figure 1B). Likewise, the bioluminescence imaging presented a significantly increased expansion of the cells in MOLT4-NTG, as shown by the enhanced luciferase signal, compared to JURKAT-NTG and PBS-NTG mice (Figure 1C). Next, we determined the organ weight of the mice in three groups and found a robust increase in liver and spleen weight of MOLT4-NTG mice as compared to JURKAT-NTG and PBS-NTG mice (Supplementary Figures S1A, B), showing a robust increased tumor formation ability of MOLT4 cells. We used flow cytometry to detect the dissemination of JURKAT and MOLT4 cells in multiple organs, respectively, by gating on human CD45. Consistently, a profound increase in the percentage of $CD45^+$ cells was observed not only in BM and PB but also in the liver and spleen of MOLT4-NTG mice, showing a remarkably increased organ infiltration of MOLT4 cells as compared to JURKAT cells (Figures 1D–H). Moreover, HE and WG staining of the tumor sections displayed an increased tumor infiltration of the

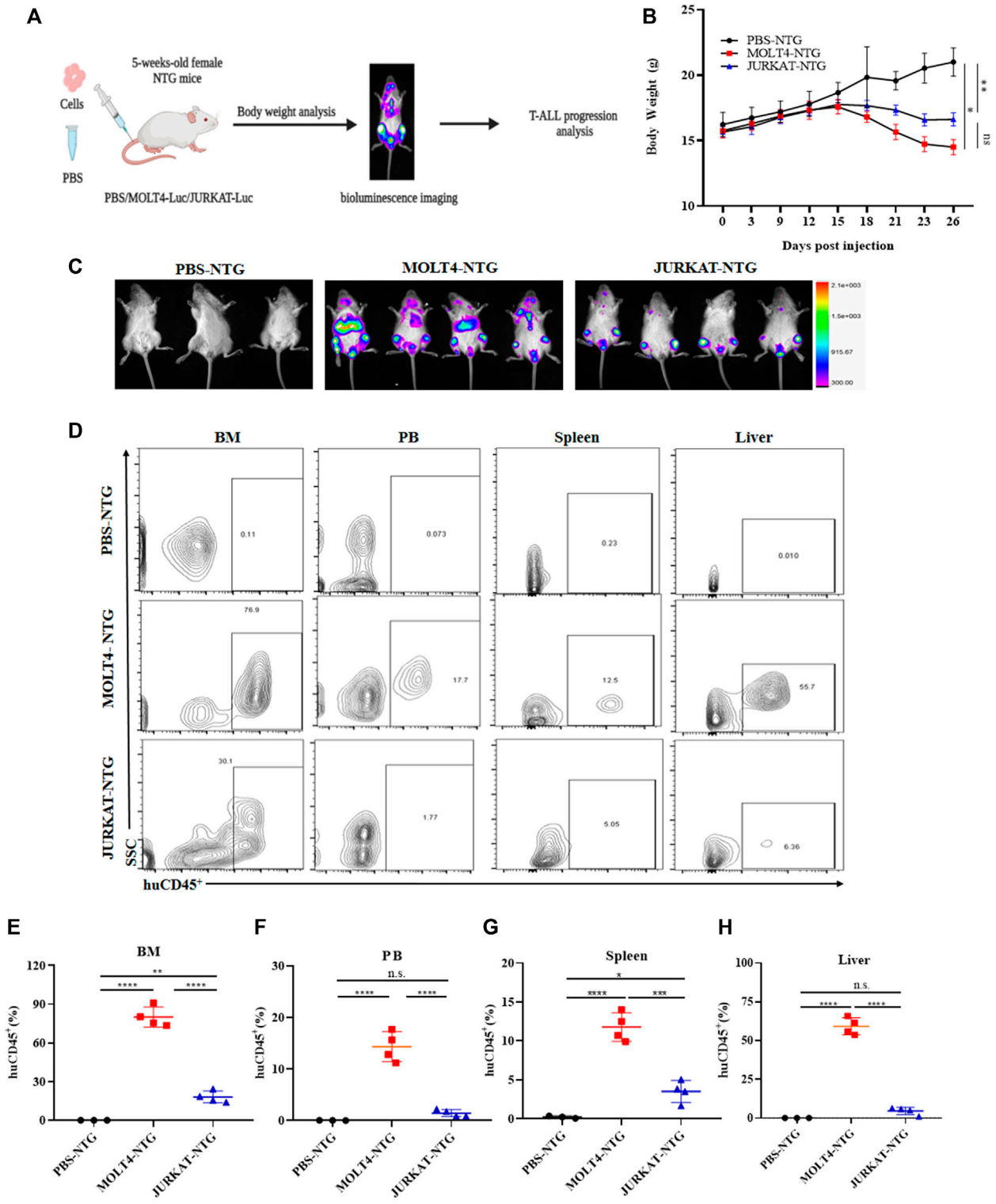

FIGURE 1
MOLT4 exhibits remarkably increased tumorigenic potential ***in vivo***. **(A)** Schematic representation of the strategy used in this study, NTG mice (n = 5) in each group were injected with MOLT4 and JURKAT cells expressing the luciferase gene as compared to the PBS control **(B)** curve representing the actual average weight of the mice during the course of 26 days of incubation. **(C)** Bioluminescence imaging was conducted 26 days after the injection. **(D)** Flow cytometry analysis of MOLT4 and JURKAT cells in peripheral blood, bone marrow, spleen, or liver of NTG mice gated on human CD45. **(E–H)** The percentage of cells represents MOLT4 and JURKAT cells over total gated cells, respectively. Each symbol represents data for an individual mouse. Data represent the mean ± SD. $*p < 0.05$, $**p < 0.01$, $***p < 0.0001$ by 1-way ANOVA. A representative experiment from three independent experiments is shown.

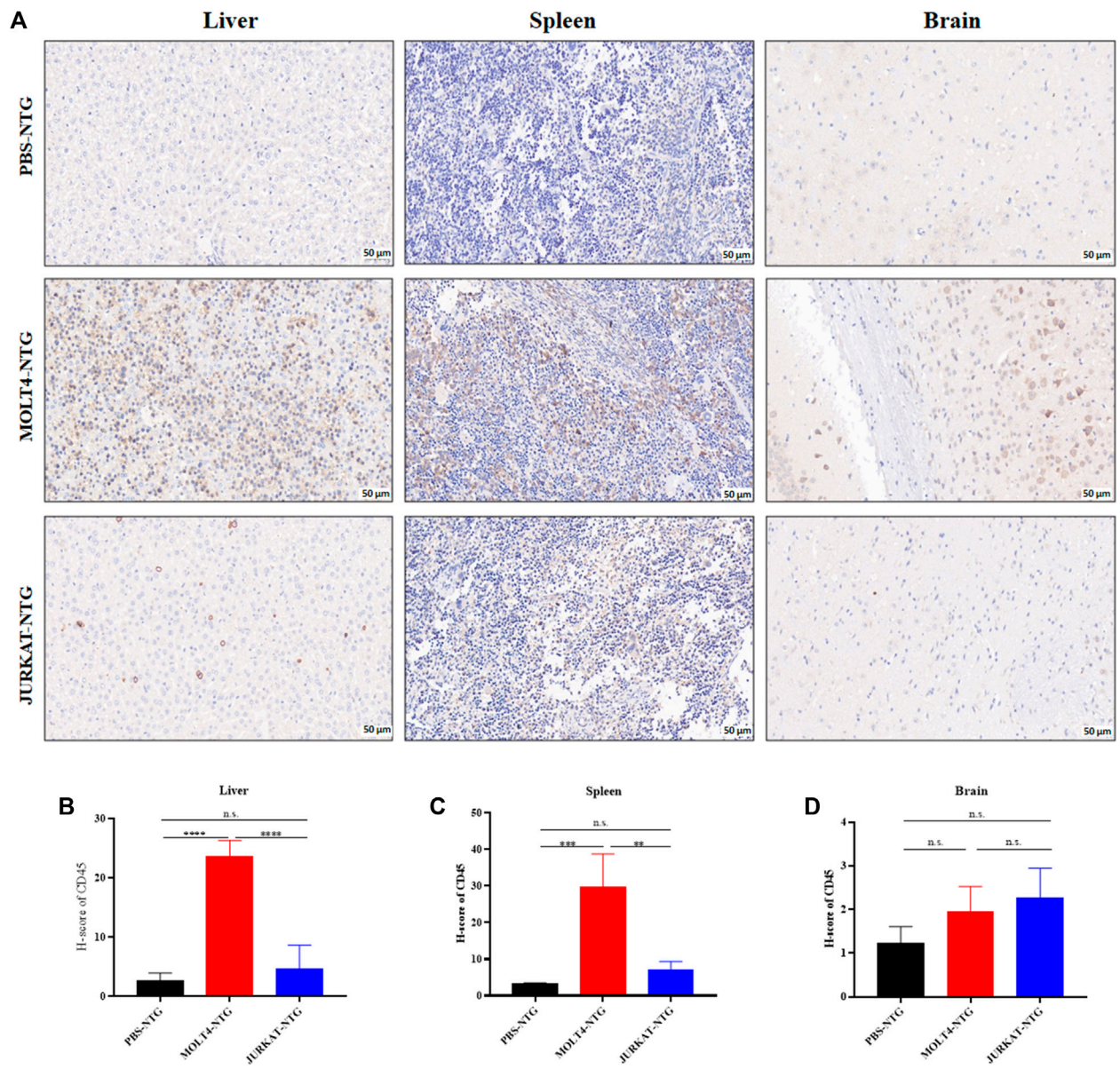

FIGURE 2
MOLT4 cells exhibit an increased pattern of organ infiltration compared to JURKAT cells. **(A)** Representative images of the IHC analysis of CD45$^+$ cells in liver, spleen, and brain tissue sections of mice injected with PBS, MOLT4, and JURKAT, respectively. **(B)** H-scores of the CD45$^+$ cells in the liver of PBS-NTG, MOLT-NTG, and JURKAT-NTG mice. **(C)** H-scores of the CD45$^+$ cells in the spleen of PBS-NTG, MOLT-NTG, and JURKAT-NTG mice. **(D)** H-scores of the CD45$^+$ cells in the brain of PBS-NTG, MOLT-NTG, and JURKAT-NTG mice. Data represent the mean ± SD. $*p < 0.05$, $**p < 0.01$, $***p < 0.0001$ by 1-way ANOVA.

MOLT4 cells to the liver, spleen, brain, bone marrow, and peripheral blood as compared to the JURKAT cells (Supplementary Figure S1C). To corroborate these findings, we performed IHC of the brain, liver, and spleen tissue sections acquired from NTG mice of the two groups and found an elevated number of CD45$^+$ cells in the liver of MOLT4-NTG mice as compared to liver obtained from JURKAT-NTG and PBS-NTG mice (Figures 2A, B). We observed a similar trend in the spleen (Figures 2A, C). However, no striking difference in the number of CD45$^+$ cells in brain of the different mice groups was observed (Figures 2A, D). Taken together, these results support the notion that MOLT4 cells display a relatively higher tissue infiltration ability as compared to JURKAT cells.

3.2 Transcriptome profiling of T-ALL cell lines revealed different DEGs involved in vital cellular pathways

We performed RNA-sequencing of MOLT4 and JURKAT cell lines to characterize the differences in the gene expression profiles and the associated pathways that cause the differences in the tumorigenic potential of the two cell types. We identified 4414 DEGs, including 2076 upregulated genes using the criteria DESeq2, padj = < 0.05, and Log2 FC > 1 (Supplementary Table S1) and 2338 downregulated genes using the criteria DESeq2, padj = < 0.05, and log2 FC > −1 in the R program (Supplementary Table S2).

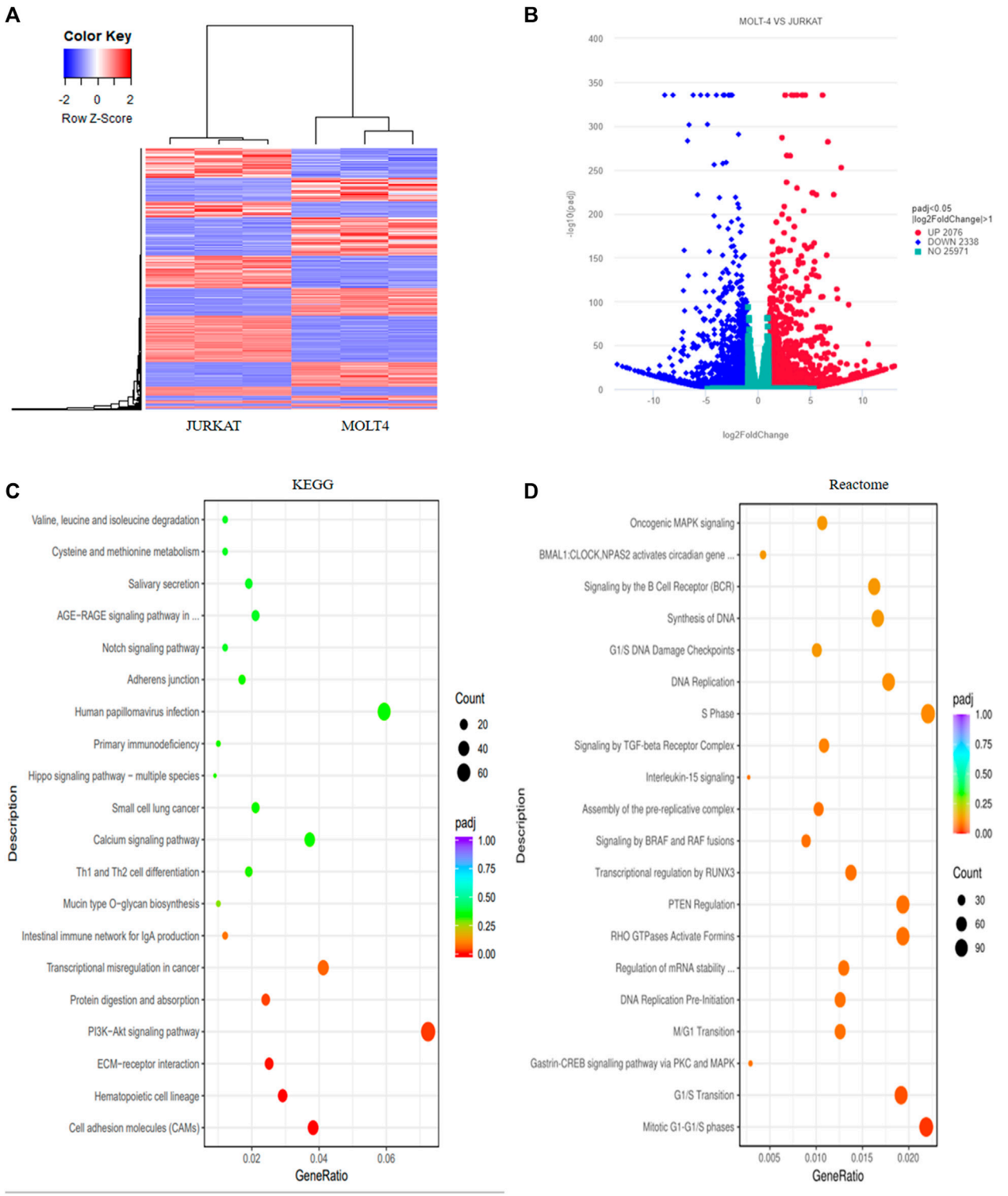

FIGURE 3
Transcriptome profiling of T-ALL cell lines revealed different differentially expressed genes involved in vital cellular pathways. **(A)** The heatmap represents the expression pattern of the differentially expressed genes (DEGs) between the MOLT4 and JURKAT cells. Red and blue represent upregulated and downregulated genes, respectively. **(B)** The volcano plot represents the distribution of DEGs obtained between MOLT4 and JURKAT cells following the criteria (log2FC > 1, padj < 0.05). Red and blue dots refer to upregulated and downregulated genes, respectively. **(C)** KEGG pathway enrichment analysis of the DEGs: the dot represents the number of DEGs count enriched in a particular pathway, whereas the color represents the *p*-value. **(D)** Enrichment of the DEGs in the GO in the Reactome pathway enrichment database.

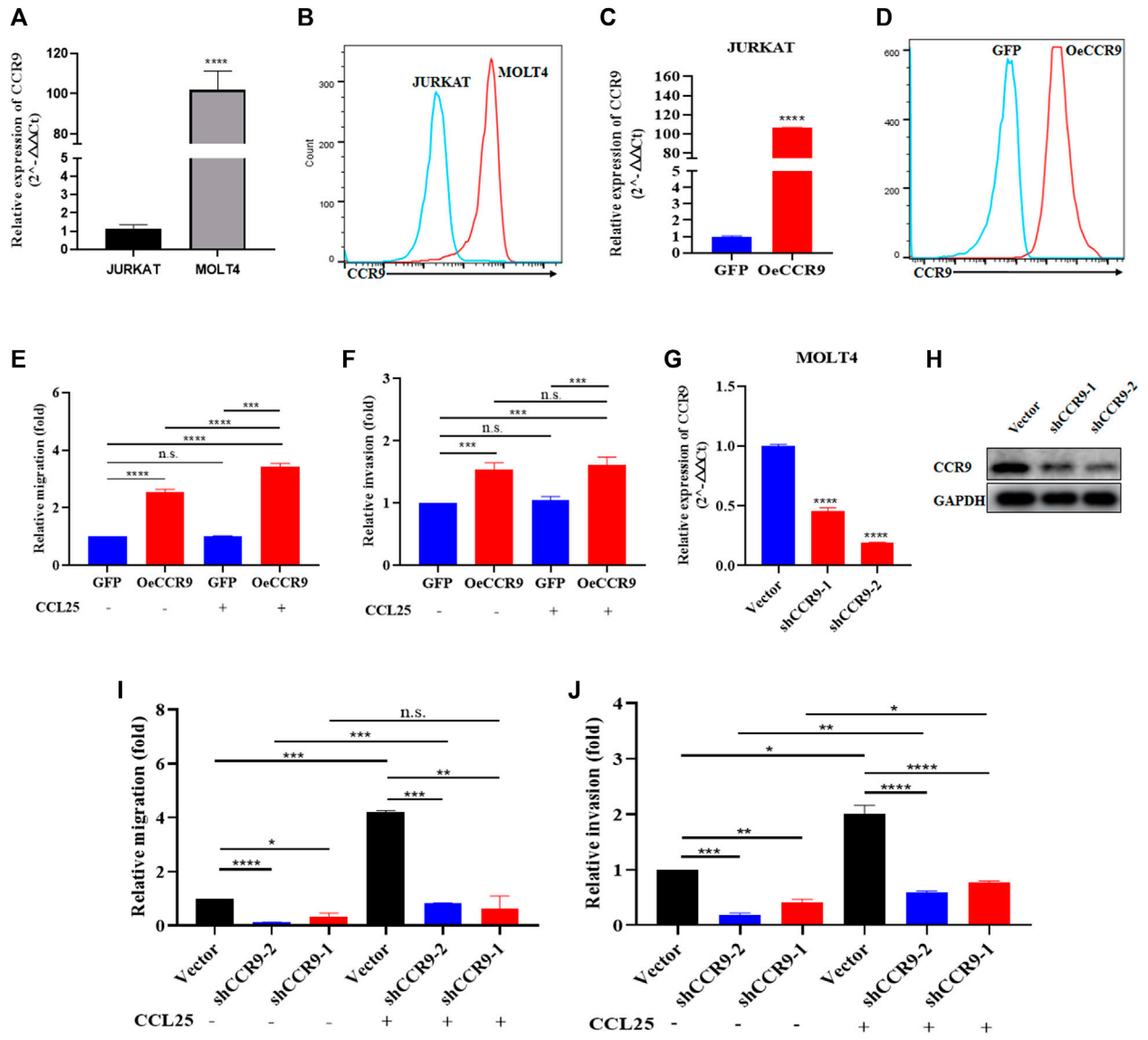

FIGURE 4
The aberrant expression of CCR9 affected the metastasis and invasion of T-ALL cell lines. **(A)** Quantification of CCR9 expression in MOLT4 and JURKAT cell lines on the mRNA level. **(B)** Comparative expression analysis of CCR9 between MOLT4 and JURKAT cell lines using flow cytometry. **(C)** Confirmation of CCR9 overexpression in JURKAT cells via qRT-PCR. **(D)** Confirmation of CCR9 overexpression in JURKAT cells via flow cytometry. **(E)** The relative migration of JURKAT with overexpressed CCR9 as compared to the vector control with and without stimulation with CCL25. Cells in suspended in 1% FBS were added to the upper chamber. Transwell chambers containing either 10% FBS medium or 2% FBS medium with CCL25 (100 ng/mL) in the bottom chambers were used for cell migration and chemotaxis assays, respectively. Migrated cells in the bottom chamber were quantified after 24 h. **(F)** Transwell chambers coated with Matrigel (1:7 ratio) and FBS medium with and without CCL25 (100 ng/mL) in the bottom chambers were used for cell invasion assays. Invaded cells in the bottom chamber were quantified after 24 h. The results of assays are expressed as fold value. The relative invasion of JURKAT cells overexpressing CCR9 as compared to the vector control with and without stimulation with CCL25. **(G, H)** shRNA-mediated stable silencing of CCR9 in MOLT4 cells, two different shRNAs with different silencing effects are shown. **(I)** ShRNA-2-mediated CCR9 silencing yielded a reduction in the migration of MOLT4 cells. **(J)** A similar repressing effect of the shRNA2-mediated silencing of CCR9 on the invasion of MOLT4 is evident. Data represent the mean ± SD. $*p < 0.05$, $**p < 0.01$, $***p < 0.0001$ by 2-tailed Student's *t*-test or 1-way ANOVA. A representative experiment from three independent experiments is shown.

The differential expression of genes between the two cell lines is represented as a heatmap (Figure 3A), and the distribution of the DEGs between the cells is illustrated in the volcano plot (Figure 3B). KEGG pathway enrichment analysis displayed the involvement of the DEGs in the PI3K-Akt signaling pathway, cell adhesion molecules, and hematopoietic cell lineage (Supplementary Table S3, Figure 3C). The Reactome database integrates the biological and molecular pathways of model organisms, including humans (Croft et al., 2010). The Reactome pathway enrichment analysis with a padj > 0.05 as a threshold displayed the association of the DEGs with various vital cell cycle-related pathways, including mitotic G1-G1/S phases, G1/S transition, M/G1 transition, and tumor suppressor pathways, including PTEN regulation and signaling by the TGF-beta receptor complex (Figure 3D). The DisGeNET database is a

collection of resources providing information about the gene and its variants in human diseases (Piñero et al., 2020). The DisGeNET gene ontology (GO) analysis showed the abundance of genes in leukemic pathways such as precursor cell lymphoblastic leukemia, leukemia-T cell, and adult T-cell lymphoma/leukemia (Supplementary Figure S2A). The gene ontology function of the DEGs revealed the enrichment of these genes in various important biological pathways such as T-cell activation, actin cytoskeleton, transcription factor activity, DNA binding, and axon development (Supplementary Table S4 and Supplementary Figure S2B). Moreover, the biological function (BF) category of the GO analysis revealed the enrichment of the DEGs in T-cell activation, axon development, and embryonic organ morphogenesis. Regarding the cellular component, DEGs were enriched in the actin cytoskeleton, receptor complex, and extracellular matrix component. Whereas the DEGs were associated with various enzymatic activities, including protein tyrosine kinase, transcriptional activation, enzyme inhibition, and signal transduction, in the molecular function (MF) category of the GO analysis (Supplementary Figure S2C).

These findings highlight the distinct gene expression profiles and high signaling variability across the two cell lines. Moreover, enrichment in various important biological pathways, such as T-cell development and activation, may lead to the distinct developmental fates and subsequent tumorigenic potentials of the two cell lines.

3.3 The aberrant expression of CCR9 affected the metastasis and invasion of T-ALL cell lines

In order to get crucial candidate genes in T-ALL, we set a stringent criterion (log2FC > 5 and padj value = <0.05) to get significantly upregulated genes. We found C-C chemokine receptor 9 (CCR9) with a log2FC = 7.941006 and padj = 2.58E-253 as one of the crucial genes with clinical relevance in T-ALL (Supplementary Table S5). To explore the role of CCR9 in T-ALL, we analyzed published T-ALL GSE datasets (GSE33315, GSE48558, and GSE13159) and observed an elevated expression of CCR9 in clinical samples and T-ALL cell lines (Supplementary Figure S3). Next, we determined the expression of CCR9 in both cells and noted that MOLT4 cells displayed an increased expression of CCR9 (Figures 4A, B). We then investigated the role of CCR9 in T-ALL by upregulating CCR9 in JURKAT cells (OeCCR9-JURKAT) (Figures 4C, D). Next, to assess whether the upregulation of CCR9 influences the migration and invasion, and chemotaxis abilities of the T-ALL cells, *in vitro* transwell migration/chemotaxis and invasion assays were performed. A pictorial representation of the mechanism of these assays is given in Supplementary Figure S4. We found that migration of the JURKAT cells through the chamber increased when CCR9 was upregulated as compared to the GFP control (Figure 4E). C-C chemokine ligand 25 (CCL25) a ligand for CCR9, orchestrates the trafficking of lymphocytes and induces migration of $CCR9^{high}$ T-ALL cells, polarization, and microvilli absorption, enhancing T-ALL cell infiltration (Tu et al., 2016). To check whether CCR9 ligand impact cell migration and invasion, CCL25 was added to the cell culture media in the bottom chambers to stimulate the cells. We observed a synergistic effect of CCL25 addition on the migration of CCR9-overexpressing JURKAT cells (Figure 4E). Next, the CCR9 overexpressing JURKAT cells were checked for their invasive properties by assessing their migration through a Matrigel-coated transwell chamber. Notably, the invasive capacity of the JURKAT cell was increased with the overexpression of CCR9 as compared to GFP. (Figure 4F), whereas no remarkable difference in the invasion of OeCCR9-JURKAT cells was observed with the addition of CCL25 (Figure 4F). Since MOLT4 cells constitutively express CCR9, we aimed to ascertain its role in MOLT4 cells by repressing its expression. To this end, we stably silenced CCR9 by using two different short hairpin RNAs (shRNAs) (Table 1) (Figures 4G, H) and analyzed their influence on the migration and invasion of MOLT4 cells. Of note, reduced migration and invasion of MOLT4 cells upon the silencing of CCR9 with shRNA-2 were observed (Figures 4I, J). We observed that the addition of CCL25 facilitated the migration and invasion of the MOLT4 cells in the control (vector) group, suggesting the dependence of CCL25 on its cognate receptor, CCR9. These findings highlight the functional role of CCR9 in the aggressiveness of the leukemic cells and support the notion that the aberrant expression of CCR9 in turn could potentially contribute to distinct T-ALL outcomes.

3.4 The overexpression of CCR9 increased the tumorigenic potential of JURKAT cells *in vivo*

To corroborate the *in vitro* findings of the oncogenic function of CCR9, we tested its role *in vivo* by xenotransplanting the OeCCR9-JURKAT into NTG mice. To this end, 5-week-old NTG mice were subjected to i.v. injection of OeCCR9-JURKAT cells (OeCCR9-JURKAT-NTG) as compared to JURKAT cells expressing GFP (GFP-JURKAT-NTG). The mice were reared for 25 days before tumor imaging for luciferase signal intensity and disease progression analysis (Figure 5A). Consequently, a robust decline in body weight was observed in OeCCR9-JURKAT-NTG mice as compared to GFP-JURKAT-NTG mice (Figure 5B). We observed an enhanced luciferase signal in mice harboring OeCCR9-JURKAT, showing the abundance of CCR9-overexpressing JURKAT cells compared to the GFP-JURKAT cells (Figure 5C). Moreover, analysis of the organ weight showed a remarkable increase in spleen (Supplementary Figure S5A) and liver weight (Supplementary Figure S5B), marking increased organ infiltration of OeCCR9-JURKAT cells. To assess the increased infiltration of OeCCR9-JURKAT cells that could lead to enhanced disease progression, the absolute number of $CD45^+$ cells in BM and PB was quantified with flow cytometry. Consistently, we observed a noticeable increase in the number of $CD45^+$ cells in the BM and PB of OeCCR9-JURKAT-NTG mice as compared to the GFP-JURKAT-NTG group (Figures 5D–F). HE and WG staining also portrayed elevated T-ALL formation in the PB, BM, spleen, and liver (Supplementary Figure S5C). Next, we performed IHC of $CD45^+$ cells in the liver, spleen, and brain tissue sections obtained from mice in the two groups. We observed an elevated number of $CD45^+$ cells in the liver and spleen of OeCCR9-JURKAT-NTG mice as compared to the liver tissue section obtained from GFP-JURKAT-NTG mice (Figures 6A–C). However, no striking difference in the number of $CD45^+$ cells infiltrating the brain was observed (Figures 6A, D). Based on these findings from our *in vitro* and *in vivo* investigations, CCR9 promotes the infiltration of T-ALL cells into the liver and spleen.

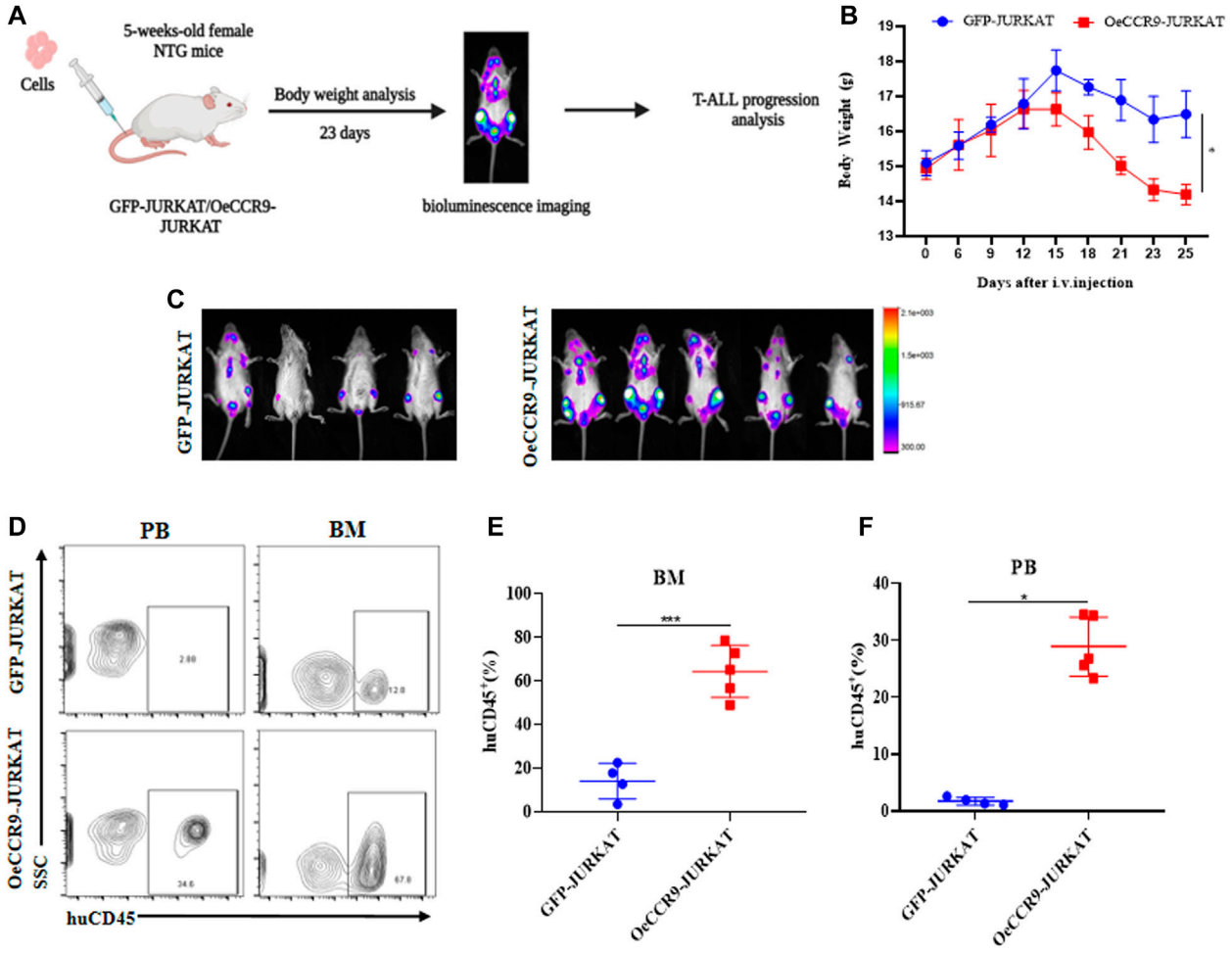

FIGURE 5
Overexpression of CCR9 increased the tumorigenic potential of JURKAT cells *in vivo*. **(A)** Schematic representation of the strategy used in this study, mice were divided into two groups, and NTG mice (n = 5) in each group were injected with OeCCR9-JURKAT cells and GFP-JURKAT cells as controls. The mice were maintained for 23 days, imaged for luciferase signaling, sacrificed, and subsequently analyzed for T-ALL progression. **(B)** Body weight analysis of the NTG mice in the two groups. The data is represented as the actual average weight measured at different days **(C)** Bioluminescence imaging of the OeCCR9-JURKAT-NTG and GFP-JURKAT-NTG mice was performed 23 days post-injection. **(D–F)** Flow cytometry analysis of CD45$^+$ cells in peripheral blood and bone marrow.

3.5 The overexpression of CCR9 was associated with increased cholesterol biosynthesis in T-ALL

To gain insights into the molecular mechanism governing the aggressive T-ALL phenotype conferred as a result of the overexpression of CCR9, we performed RNA-sequencing of the OeCCR9-JURKAT and GFP-JURKAT cells. Using the criteria DESeq2, padj = < 0.05, and log2 FC > 1, we obtained a total of 18 DEGs, including 17 upregulated genes and 1 downregulated gene (Table 2) (Figure 7A). A 4-fold overexpression of CCR9 is shown in the volcano plot, thus confirming the reliability of our RNA sequencing data (Figure 7B). We performed the DisGeNET GO enrichment analysis to get the disease phenotype associated with CCR9 overexpression and found its enrichment in leukemic pathways including precursor cell lymphoblastic leukemia, acute promyelocytic leukemia, and acute lymphocytic leukemia (Supplementary Figure S6A). The KEGG function revealed the association of DEGs with metabolic pathways including carbon metabolism, biosynthesis of amino acids, and biosynthesis of steroids (Supplementary Figure S6B). Moreover, when investigated in GO function, DEGs were found supplemented in the lipid biosynthesis pathways, including the steroid biosynthetic process, cholesterol biosynthetic process, steroid metabolic process, and regulation of the steroid metabolic process (Supplementary Table S6; Figures 7C, D).

Next, we assessed the role of these DEGs in the cholesterol biosynthesis pathway. The genes belonging to the cholesterol biosynthesis pathway that are upregulated with CCR9 overexpression are represented in a heatmap (Figure 8A). A protein-protein interaction (PPI) network of the DEGs associated with the cholesterol biosynthesis pathway was retrieved from the online resource STRING and visualized with Cytoscape (Figure 8B). The network shows a closer association of these genes with each

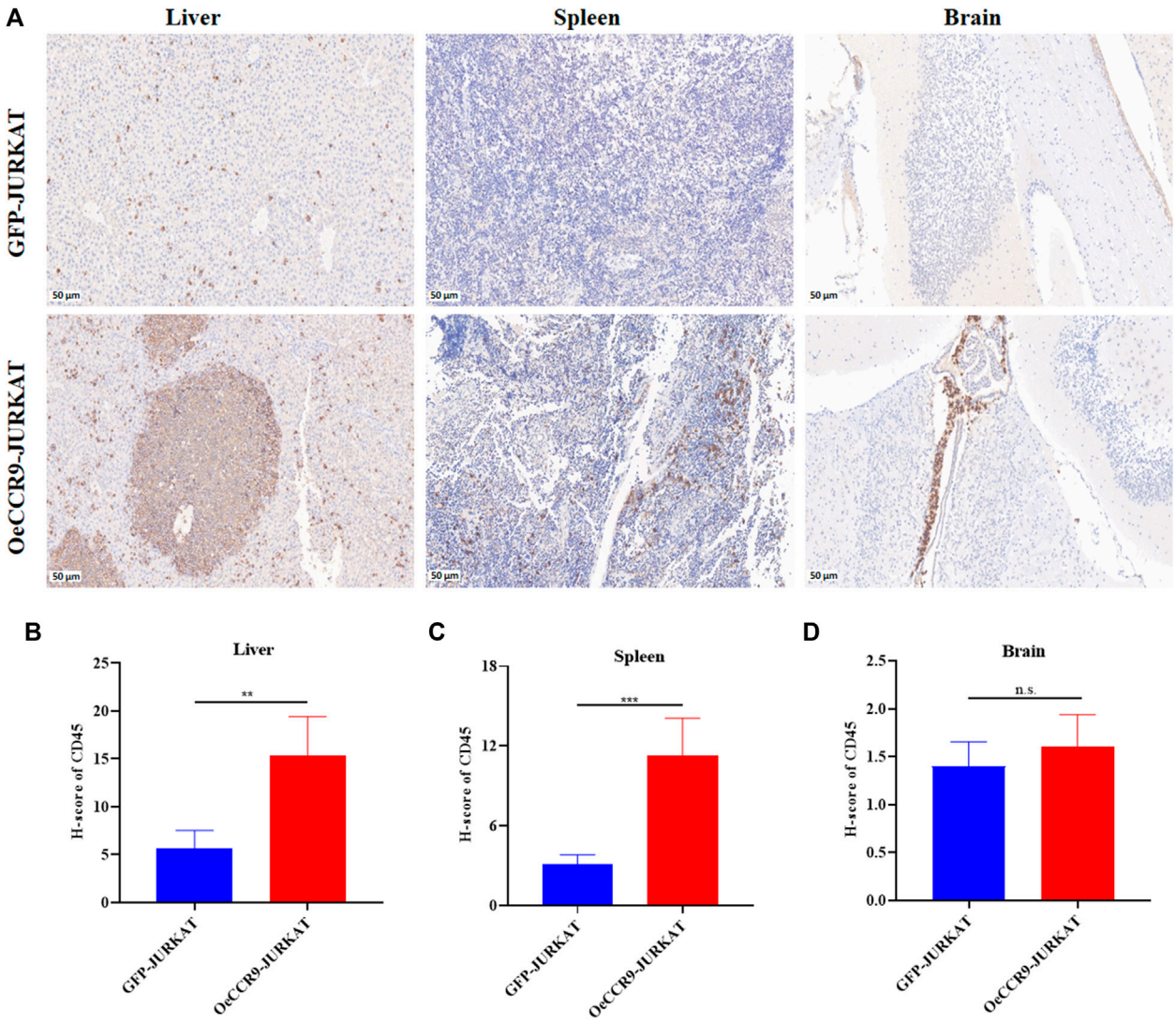

FIGURE 6
OeCCR9-JURKAT cells exhibit an increased pattern of organ infiltration. **(A)** Representative images of the IHC analysis of CD45$^+$ cells in liver, spleen, and brain tissue sections of OeCCR9-JURKAT-NTG and GFP-JURKAT-NTG mice, respectively. **(B)** H-scores of the CD45$^+$ cells in the liver of OeCCR9-JURKAT-NTG and GFP-JURKAT-NTG mice. **(C)** H-scores of the CD45$^+$ cells in the spleen of OeCCR9-JURKAT-NTG and GFP-JURKAT-NTG mice. **(D)** H-scores of the CD45$^+$ cells in the brain of OeCCR9-JURKAT-NTG and GFP-JURKAT-NTG mice. Data represent the mean ± SD. $*p < 0.05$, $**p < 0.01$, $***p < 0.0001$ by 1-way ANOVA.

other. To corroborate the elevated expression of the cholesterol biosynthesis pathway genes in our genome-wide transcriptome data, we checked the expression of the rate limiting enzyme, HMGCR, and three main genes, including MSMO1, HMGCS1, and MVD at mRNA level, which showed a significant upregulation of these genes (Figure 8C). Notably, we also verified the elevated expression of the master regulator of the cholesterol biosynthesis pathway, SREBF2 (Madison, 2016) (Figure 8C). To assess the expression of these genes at protein level, Western blotting was performed. We confirmed the overexpression of these genes with CCR9 upregulation as compared to GFP control (Figure 8D). Furthermore, we screened the expression of these genes in GSE48558 (Cramer-Morales et al., 2013) and found a relatively higher expression of MSMO1, HMGCS1, MVD,SREBF2, and HMGCR in T-ALL cell lines and patients (Supplementary Figure S7A). Moreover, the analysis of GSE26713 (Homminga et al., 2011) also showed an increased expression of MSMO1,HMGCS1, SREBF2, and HMGCR in T-ALL cell lines and patients (Supplementary Figures S7A, B), but MVD showed no significant difference (Supplementary Figure S6B). In addition, the increased expression of MSMO1, HMGCS1, MVD, and SREBF2 across solid tumors vs. normal tissues based on the analysis of TCGA datasets (Supplementary Figures S8A–D) further signifies the crucial role of these metabolic genes in multiple cancers.

To check whether CCR9-induced upregulation of the cholesterol biosynthesis genes has an impact on the total cellular cholesterol level, we detected the total cholesterol level in the OeCCR9-JURKAT and GFP-JURKAT cells. Notably, we found a slight increase in the cholesterol concentration of the OeCCR9-JURKAT cells (46.35 μmol/L) as compared to the GFP-JURKAT cells (43.46 μmol/L) (Figure 8E).

TABLE 2 DEGs of OeCCR9.

Gene_Id	Log2FC	p-value	p-adj	Gene name
ENSG00000112972	1.272596	0	0	HMGCS1
ENSG00000064886	1.21112	$7.77E^{-301}$	$3.03E^{-297}$	CHI3L2
ENSG00000052802	1.101884	$1.75E^{-149}$	$2.91E^{-146}$	MSMO1
ENSG00000181577	1.084427	$6.27E^{-94}$	$6.65E^{-91}$	C6orf223
ENSG00000167508	1.005813	$1.19E^{-87}$	$1.16E^{-84}$	MVD
ENSG00000173585	4.004182	$1.82E^{-75}$	$1.25E^{-72}$	CCR9
ENSG00000130707	1.082549	$3.59E^{-43}$	$1.68E^{-40}$	ASS1
ENSG00000225855	1.164233	$4.23E^{-38}$	$1.70E^{-35}$	RUSC1-AS1
ENSG00000120738	1.295977	$5.11E^{-21}$	$1.17E^{-18}$	EGR1
ENSG00000134594	1.170273	$1.65E^{-18}$	$3.15E^{-16}$	RAB33A
ENSG00000131069	1.142529	$1.06E^{-14}$	$1.50E^{-12}$	ACSS2
ENSG00000110848	1.016023	$4.57E^{-11}$	$4.56E^{-09}$	CD69
ENSG00000183604	1.076263	$2.93E^{-09}$	$2.14E^{-07}$	SMG1P5
ENSG00000223901	1.267168	$2.12E^{-08}$	$1.30E^{-06}$	AP001469.1
ENSG00000274536	1.131767	$3.17E^{-07}$	$1.39E^{-05}$	AL034397.3
ENSG00000131044	1.007419	$1.36E^{-06}$	$4.94E^{-05}$	TTLL9
ENSG00000132854	−1.07934	$8.30E^{-06}$	0.000244	KANK4
ENSG00000170390	1.136976	$2.34E^{-05}$	0.000606	DCLK2

Notably, TC levels were increased further (50.71 μmol/L) when CCL25 was added to stimulate CCR9-overexpressing JURKAT cells. These findings support the notion that the upregulation of CCR9 could enhance total cellular cholesterol production in T-ALL cells, and this effect is further potentiated with the addition of CCL25.

To investigate the effect of increased cholesterol biosynthesis on the aggressiveness of the JURKAT cells, we inhibited the total cholesterol biosynthesis by treating the cells with varying concentrations of simvastatin (3 μM, 6 μM, 12 μM, and 24 μM), a hypocholesterolemic drug that blocks the activity of HMGCR receptor (Corsini et al., 1995). We observed that a concentration above 10 μM compromised the viability of the cells leading to cell death (data not shown). Subsequently, we selected a 6 μM concentration of treatment for the chemotaxis assay and observed a notable decrease in the migration of OeCCR9-JURKAT cells with simvastatin as compared to the mock treatment (Figure 8F). Moreover, immunohistochemical analysis of the main transcription factor, SREBF2, in the mice tissues xenografted with OeCCR9-JURKAT cells and GFP-JURKAT cells revealed a relatively increased expression of SREBF2 in the liver tissue of the OeCCR9-JURKAT mice as compared to the GFP counterpart (Supplementary Figures S9A, B). However, no distinction in the expression of SREBF2 was observed in the spleen tissue (Supplementary Figures S9C, D) between the two groups, suggesting enhanced cholesterol production in the liver, the organ primarily responsible for cholesterol production. In addition to these experiments, we used the https://tnmplot.com/analysis/ database, which contains ChIP-seq and RNA-seq data of various tumors vs. normal tissue, to check the correlation between CCR9 and SREBF2. A significant positive correlation (R = 0.43, p value = 0.00) between CCR9 and SREBF2 in ALL was observed (Supplementary Figure S9D).

Taken together, these results suggest that CCR9 overexpression promotes cholesterol biosynthesis in JURKAT cells by upregulating the candidate genes, and blocking the cholesterol biosynthesis pathway with simvastatin reduces the aggressiveness of the CCR9-overexpressing JURKAT cells.

4 Discussion

T-ALL is a hematological malignancy characterized by the abnormal expansion of immature lymphoid cells (Vadillo et al., 2018). The molecular mechanism of the leukemic cells' infiltration into distant organs is a complex process that remains largely unknown. The *in vitro* and *in vivo* application of T-ALL cells remains a standard toolkit in cancer biology to understand the molecular mechanism of T-ALL. But these cell lines differ in their tumorigenic potentials and often demonstrate dissimilar T-ALL-inducing potentials when utilized in murine models.

This study reports the distinct T-ALL initiation and progression patterns of MOLT4 and JURKAT cell lines. Our findings suggest that MOLT4 cells show a more aggressive T-ALL phenotype as compared to JURKAT cells in the NTG mice, characterized by increased tumor tissue infiltration as indicated by FC, HE staining, and IHC analyses. Unlike the liver and spleen, the difference in T-ALL cell infiltration into the brain was not remarkable between the groups. The central nervous system is one of the sanctuary sites of ALL, with 5%–8% of the patients possessing CNS pathology causing damage to the cranial nerves and infiltration into the meninges (Jabbour et al., 2005; Jabbour et al., 2015), suggesting that not all the ALL patients present with CNS involvement. Gene expression profiling revealed enrichment of DEGs in vital cancer-associated signaling pathways such as PI3K-Akt and MAPK-ERK, extracellular matrix reorganization, DNA replication and cell cycle regulation, PTEN regulation, and RHO GTPases formins. These signaling pathways have been previously reported in the pathogenesis of leukemia (Steelman et al., 2011). Particularly, PI3K-Akt is the most predominant activated signaling pathway in more than 70% of T-ALL patients (Silva et al., 2008). In T-ALL, activation of the PI3K/AKT pathway is commonly observed and contributes to the survival and proliferation of leukemic cells. Inhibition of the PI3K/AKT pathway has been shown to be an effective therapeutic strategy for T-ALL.

CCR9, an upregulated gene in the list of DEGs, belongs to the G protein-coupled receptor family and is of great clinical relevance in T-ALL, particularly because of its relevance to tumor infiltration and metastasis (Tu et al., 2016; Li et al., 2021). The CCL25/CCR9-mediated RhoA-ROCK-MLC/ezrin axis has been reported to promote T-ALL metastasis mainly in MOLT4 cells (Zhang et al., 2011). Remarkably, the aberrant expression of CCR9 impacted the invasion and migration of T-ALL cells in our functional genetic analysis *in vitro*. Further, the overexpression of CCR9 led to a drastic increase in tumorigenic activity in the NTG mice characterized by a surge in JURKAT cell infiltration to the spleen and liver, as well as marked cell expansion in BM and PB.

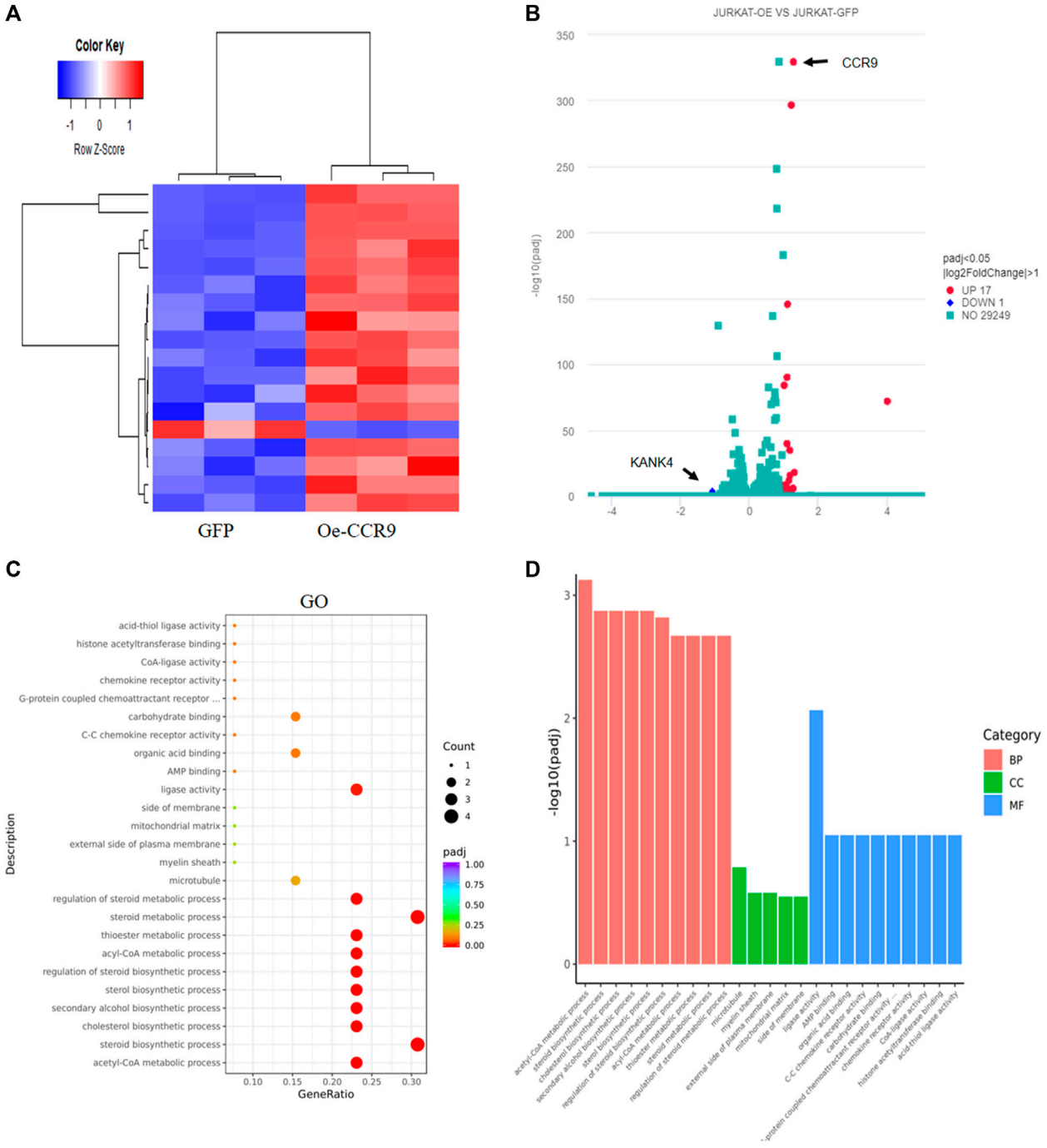

FIGURE 7
Transcriptome profiling of the Oe-CCR9-JURKAT cells revealed differentially expressed genes associated with metabolic pathways. **(A)** A heatmap representing the expression pattern of the DEGs between OeCCR9-JURKAT and GFP-JURKAT cells. Red and blue represent upregulated and downregulated genes, respectively. **(B)** The volcano plot represents the distribution of DEGs obtained between OeCCR9-JURKAT and GFP-JURKA cells following the criteria (log2FC > 1, padj<0.05). Red and blue dots refer to upregulated and downregulated genes, respectively. **(C)** GO pathway enrichment analysis of the DEGs, the dot represents the number of DEGs count enriched in a particular pathway, whereas the color represents the *p*-value. **(D)** The enrichment of DEGs in a cellular component, molecular function, and biological process categories in GO function.

T-ALL, being a highly proliferative malignancy, requires the rewiring of cholesterol biosynthesis metabolic pathways to sustain the rapid growth and proliferation of the leukemic cells (Zhao et al., 2019). In addition, the role of cholesterol biosynthesis is widely appreciated for promoting the aggressiveness of multiple cancer types (Ding et al., 2019). Among the common mechanisms used by cancer cells to alter intracellular cholesterol are the upregulation of the cholesterol biosynthesis pathway genes and the repression of the cholesterol efflux protein (Luo et al., 2020). In this study, gene expression profiling of OeCCR9-JURKAT cells showed the

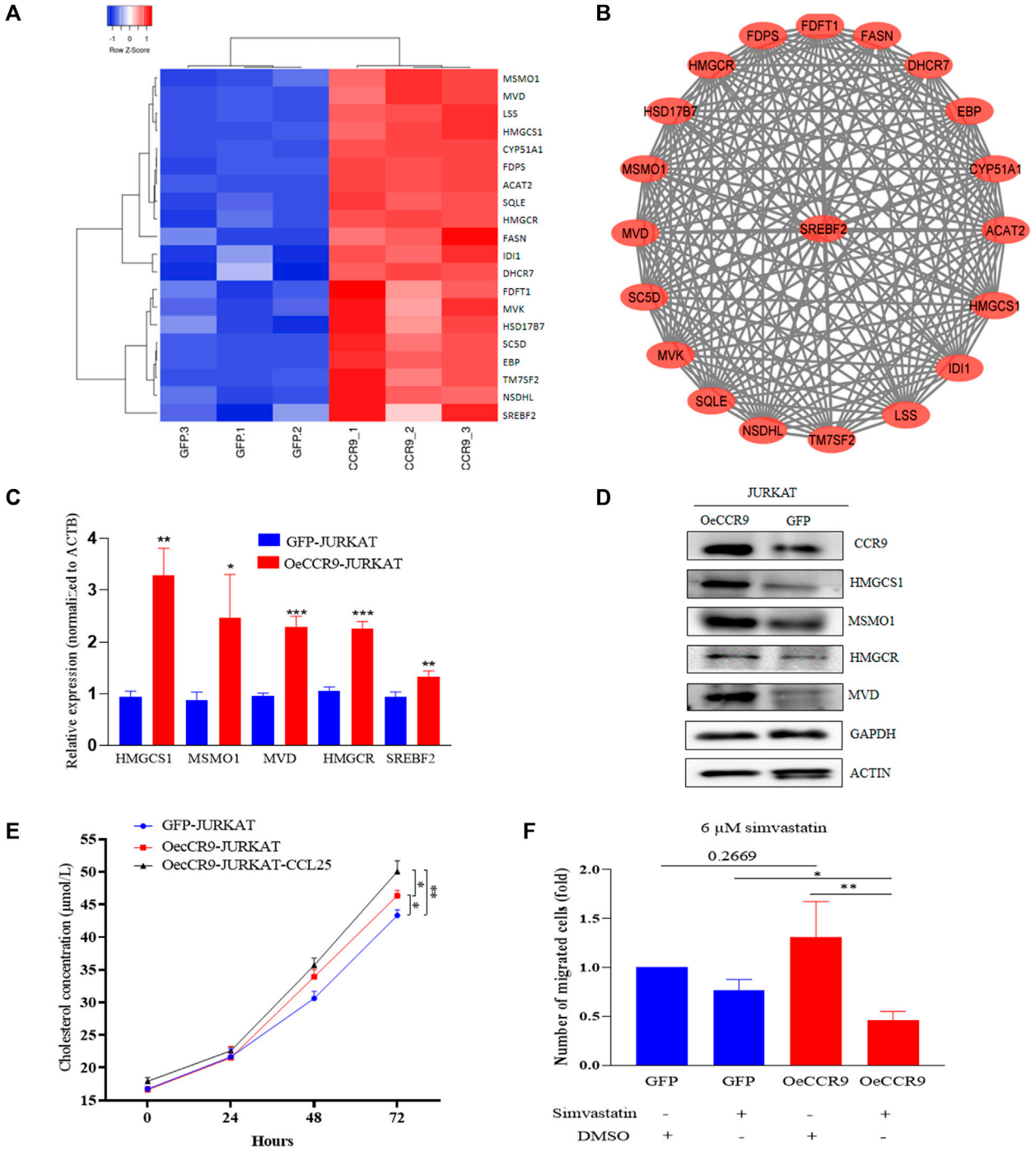

FIGURE 8
The overexpression of CCR9 is associated with increased cholesterol biosynthesis in T-ALL. **(A)** A heatmap of the DEGs associated with cholesterol biosynthesis pathways. **(B)** The protein-protein interaction network of the cholesterol biosynthesis pathway genes visualized with Cytoscape shows a strong interaction among these genes. **(C)** Quantification of the expression of MSMO1, HMGCS1, MVD, HMGCR and SREBF2 in OeCCR9-JURKAT cells vs. GFP-JURKAT cells on mRNA level **(D)** The protein expression of CCR9, HMGCS1, MSMO1, HMGCR and MVD was analyzed by Western blot. GAPDH and ACTIN were used as loading control. The corresponding antibodies for CCR9, HMGCS1, and MSMO1 were diluted in (1:1000). Antibodies for MVD and HMGCR were diluted at 1:200 and 1:500 ratios, respectively. GAPDH and ACTIN antibodies were diluted at 1:3000 dilutions. Blots were incubated with their corresponding primary antibodies overnight at 4 C. The secondary antibodies used were diluted at 1:3000 followed by incubation for 2 h at room temperature. **(E)** Total cholesterol concentration detected at different time points between OeCCR9-JURKAT cells, OeCCR9-JURKAT cells supplemented with CCL25, and GFP-JURKAT control cells. **(F)** Assessment of cell migration of OeCCR9-JURKAT cells vs. GFP-JURKAT cells post simvastatin treatment as compared to mock. $*p < 0.05$, $**p < 0.01$, $***p < 0.0001$ by 2-tailed Student's *t*-test.

upregulation of several genes belonging to the cholesterol biosynthesis family, including SREBF2 and the rate limiting enzyme HMGCR, and other genes including HMGCS1, HMGCR, MVK, and MVD. The potential significance of these cholesterol biogenesis-related genes in various malignancies has been illustrated by (Ershov et al., 2021). The clinical relevance of these genes was further verified in T-ALL, showing enhanced expression in T-ALL cell lines and T-ALL patients. However, the precise oncogenic function of these genes in T-ALL remains mysterious. In a recent study, characterization of the metabolome and transcriptome in ETP-ALLs, a discrete group of T-cell leukemia associated with relapse and poor prognosis, revealed an elevated biosynthesis of phospholipids and sphingolipids in ETP-ALL as compared to T-ALL (Rashkovan et al., 2022). Moreover, Following HMGCR inhibition with pitavastatin treatment, an attenuated oncogenic AKT1 signaling was evident along with the suppression of MYC signaling pathway expression via the loss of chromatin accessibility at the leukemia stem cell-specific long-range MYC enhancer. HMGCR inhibition blocked cell proliferation, dampened cell viability, and compromised cell growth *in vitro* (Rashkovan et al., 2022). This is consistent with our results showing reduced migration of the OeCCR9-JURKAT cells following simvastatin treatment.

The existing data shown in this study lacks *in vivo* confirmation of the antileukemic effect of statin treatment. Several lines of investigation confirm the notion that inhibiting the rate-limiting enzymes of the cholesterol production pathway with statin exhibits profound antileukemic functions (Rashkovan et al., 2022). For instance, statin treatment induced selective autophagy in the leukemic cell lines by attenuating the phosphorylation of Akt levels in the lipid rafts along with a reduction in the activation of the vital autophagy suppressor mTOR pathway and its associated substrate, ribosomal p70S6 (Vilimanovich et al., 2015). Apart from these preclinical studies, several clinical trials have suggested the anti-leukemic activities of statins (Minden et al., 2001; Li et al., 2003; van der Weide et al., 2009). In addition, statin administration has been documented to improve the efficacy of standard therapy in acute myeloid leukemia (Kornblau et al., 2006; Advani et al., 2014). Sheen et al. investigated the *in vitro* effects of six different statins on ALL cells and showed that simvastatin resulted in ALL cell death by inducing apoptosis and exerted a synergistic effect in combination with other cytotoxic drugs, including vincristine, doxorubicin, and dexamethasone (Sheen et al., 2011). The similar antitumor function of statin on ALL cells, characterized by cell-cycle arrest, and induction of apoptosis mainly by upregulating BAX, p21, and p27 cells and downregulating cyclin D1, BCL-2, and p-Akt expression, has also been documented in another study (Wang et al., 2018). Dysregulated cholesterol biosynthesis has been associated with T-ALL drug resistance. Subsequently, inhibition of this pathway with simvastatin displayed a strong combined cytotoxic effect with gluocorticoids in resistant cells (Samuels et al., 2014b). In a preclinical setting, a T-ALL *in vivo* model developed from patient-derived T-ALL xenografts showed aberrant lipid and cholesterol metabolism as potential drivers of drug resistance and suggested simvastatin as a potential treatment regimen to overcome drug resistance (Samuels et al., 2014a).

The cholesterol biosynthesis pathway is under the strict regulation of SREBP2 and liver X receptors (LXRs). In other instances, metabolic reprograming involves the synergistic interaction of SREBF2 with other transcription factors such as early growth response element 1 (EGR1) (Gokey et al., 2011) and the nuclear receptor RAR-related receptor gamma (RORγ) to promote cholesterol biosynthesis, particularly in cancer (Cai et al., 2019). The precise mechanism by which chemokines induces cholesterol biosynthesis pathway remains largely unknown. Chemokines can either directly act on SREBP2 to activate the pathway, as evident in the tropism of breast cancer to the lungs, where CCL2/CCL7 produced from the lung fibroblast stimulates the synthesis of cholesterol by activating SREBF2 in lung-colonizing breast cancer cells to fuel the metastatic niche (Han et al., 2022). Consistently, we observe an increase in SREBF2 expression with CCR9-upregulation not only on the transcript level *in vitro* but also on the protein level in NTG mice liver tissue, suggesting the potential activation of SREBF2 to facilitate *de novo* cholesterol biosynthesis. Gaining mechanistic insights into the molecular mechanism of CCR9-SREBF2 in boosting cholesterol biosynthesis would be an exciting future research avenue in the relatively new era of T-ALL cholesterol metabolism.

5 Conclusion

In summary, we found that MOLT4 cells possess relatively higher aggressive tumorigenic potentials, characterized by their robust organ infiltration, as compared to JURKAT cells. Transcriptome profiling revealed several DEGs with enrichment in vital oncogenic pathways. Particularly, CCR9 not only facilitated the migration and invasion of cells *in vitro* but also promoted organ infiltration in the mouse model. CCR9 overexpression was associated with increased cellular cholesterol production, mainly due to the increased expression of the core regulatory genes of the cholesterol biosynthesis pathway. The enhanced cholesterol biosynthesis rate in turn promoted the aggressiveness of the JURKAT cells, which was markedly repressed with simvastatin administration. The findings in the current study reveal a novel mechanism for cholesterol biosynthesis that supports T-ALL cell migration and invasion. These findings propose that inhibiting the CCR9-induced cholesterol biosynthesis pathway with statin may pave the way for the development of effective therapeutic strategies to treat T-ALL progression.

Summary

T-ALL is a form of hematological cancer derived from the early T-cell progenitor. The disease arises as a result of the accumulation of genomic lesions affecting signaling pathways involved in cell growth, proliferation, survival, and differentiation of thymocytes. In order to understand the biological mechanism of T-ALL, *in vitro* T-ALL cell lines are commonly employed. However, a comprehensive comparison of two common T-ALL cell lines, MOLT4 and JURKAT cells, for T-ALL development is not yet available. We compared MOLT4 and JURKAT cells for their T-ALL inducing potentials and found that MOLT4 cells exhibited a relatively increased aggressive leukemic phenotype in mice as compared to JURKAT cells. We examined the molecular

characteristics of two cell lines that could lead to differences in cancer development. Transcriptional profiling of MOLT4 and JURKAT cells revealed significant changes in the expression of several genes involved in important signaling pathways, including CCR9. Notably, the aberrant expression of CCR9 impacted the migration and invasion of the T-ALL cell lines *in vitro*. In addition, higher expression levels of CCR9 also promoted T-ALL progression *in vivo*. Transcriptome analysis revealed that the overexpression of CCR9 promoted cholesterol biosynthesis in JURKAT cells. The altered lipid biosynthesis facilitates fatty acid synthesis, which is crucial to maintaining lipid homeostasis for membrane production and lipid-based protein posttranslational modifications in the rapidly proliferating tumor cells.

Data availability statement

The transcriptome raw data generated in this study have been deposited to NCBI SRA database (BioProject ID PRJNA897746) and can be accessed through https://www.ncbi.nlm.nih.gov/bioproject/?term=PRJNA897746.

Ethics statement

Ethical approval was not required for the studies on humans in accordance with the local legislation and institutional requirements because only commercially available established cell lines were used. The animal study was approved by Medical Ethics Committee of Wuhan University School of Medicine (Permit Number: WP20220022). The study was conducted in accordance with the local legislation and institutional requirements.

Author contributions

MJ: Conceptualization, Formal Analysis, Methodology, Writing–original draft, Writing–review and editing. YL: Investigation, Methodology, Validation, Writing–original draft, Writing–review and editing. HH: Data curation, Formal Analysis, Software, Writing–review and editing. XZ: Data curation, Formal Analysis, Visualization, Writing–review and editing. HB: Data curation, Formal Analysis, Methodology, Writing–review and editing. DX: Data curation, Methodology, Software, Writing–review and editing. LS: Funding acquisition, Supervision, Writing–review and editing, Writing–original draft. FZ: Funding acquisition, Supervision, Writing–review and editing, Conceptualization. QZ: Conceptualization, Formal Analysis, Funding acquisition, Project administration, Supervision, Writing–original draft, Writing–review and editing.

Funding

The authors declare financial support was received for the research, authorship, and/or publication of this article. This work was supported by the National Natural Science Foundation of China (Nos 81770180 and 81500151), the Hubei Provincial Natural Science Fund for Creative Research Groups (2018CFA018), and the Innovation and Cultivation Fund of Zhongnan Hospital (ZNLH201902).

Acknowledgments

The authors are grateful to the members of the laboratory and collaborators for their assistance in experiments and manuscript preparation. The authors are thankful to Dr. Mudassar Niaz Mughal at the Department for Dermatology and Allergology, Philipps University Marburg, Germany, and Dr. Philip G. Penketh at the Department of Pharmacology, Yale University School of Medicine, for critically revising and improving the language of the manuscript.

Conflict of interest

The authors declare that the research was conducted in the absence of any commercial or financial relationships that could be construed as a potential conflict of interest.

Publisher's note

Supplementary material

The Supplementary Material for this article can be found online at: https://www.frontiersin.org/articles/10.3389/fphar.2023.1257289/full#supplementary-material

SUPPLEMENTARY FIGURE S1
Analysis of the organ weight and tissue infiltration in mice in each group **(A)** Comparison of the size of the spleen organ obtained from mice in three groups. The spleen weight of the mice in each group was also calculated. **(B)** Representation of the size and weight of the liver in each group. **(C)** H.E. staining of the tissue sections derived from the liver and spleen of mice injected with PBS, MOLT4, and JURKAT, respectively.

SUPPLEMENTARY FIGURE S2
Pathway analysis of the DEGs between MOLT4 and JURKAT **(A)** DisGeNET gene ontology (GO) analysis of the DEGs **(B)** The GO shows the enrichment of the DEGs in various pathways. **(C)** The enrichment of DEGs in a cellular component, molecular function, and biological process categories in GO function.

SUPPLEMENTARY FIGURE S3
Distribution of the DEGs across the GSE datasets **(A)** Volcano plot representing the DEGs in the GSE33315 dataset **(B)** Volcano plot representing the DEGs in the GSE48558 dataset **(C)** Volcano plot representing the DEGs in GSE13159. The red and blue dots refer to the upregulated and downregulated genes, respectively. The log2FC value > 1 of CCR9 is mentioned in each dataset.

SUPPLEMENTARY FIGURE S4
Pictorial representation of the migration and invasion assays **(A)** Schematic illustration of the different parts of the transwell system used to assess the

migration of the cells. Cells are seeded on the upper side of the transwell membrane in 1% FBS. To allow the migration of the cells, 10% FBS containing media or chemoattractant is added. **(B)** To allow the distinction between migration and invasion, an extracellular matrix component like matrigel coated matrix is added, which mimics a more complex physiological environment, to allow the invasion of the cells.

SUPPLEMENTARY FIGURE S5
Organ weight and HE staining analysis **(A)** a representative picture of the spleen size and weight between OeCCR9 and GFP-JURKAT cells. **(B)** A representative picture of the liver size and weight between OeCCR9 and GFP-JURKAT cells. **(C)** HE staining of the section obtained from the bone marrow, peripheral blood, liver, brain, and spleen of the mice in the two groups.

SUPPLEMENTARY FIGURE S6
Pathway analysis of the DEGs between OeCCR9- and GFP-JURKAT cells **(A)** The DisGeNET functional enrichment analysis of the DEGs shows the involvement of the DEGs in various diseases. **(B)** The KEGG functional enrichment analysis of the DEGs in metabolic pathways.

SUPPLEMENTARY FIGURE S7
Expression analysis of the MSMO1, HMGCS1, MVD, and SREBF2 across GSE datasets **(A)** Relative expression of MSMO1, HMGCS1, MVD, SREBF2, and HMGCR in T-cells vs. T-ALL cell lines and T-ALL patients across the GSE48558 dataset as compared to healthy bone marrow in the GSE13159 dataset samples, respectively. **(B)** Analysis of the GSE26713 for the relative expression of MSMO1, HMGCS1, MVD, SREBF2, and HMGCR in normal bone marrow samples vs. T-ALL. $*p < 0.05$, $**p < 0.01$, $***p < 0.0001$ by 2-tailed Student's t-test.

SUPPLEMENTARY FIGURE S8
Expression analysis of the MSMO1, HMGCS1, MVD, and SREBF2 across the TCGA database **(A-D)** relative expression of MSMO1, HMGCS1, MVD, and SREBF2 in various solid tumors as compared to the corresponding normal tissue. The expression analysis is done using TCGA datasets.

SUPPLEMENTARY FIGURE S9
IHC of SREFBF2 in the liver and spleen tissue of mice transplanted with OeCCR9-JURKAT cells vs. GFP-JURKAT. IHC analysis of SREBF2 expression in liver and spleen tissue sections. **(B)** Representative images of the SREBF2 expression in liver of OeCCR9-JURKAT-NTG and GFP-JURKAT-NTG mice. **(B)** H-scores of the SREBF2+ cells in the liver of OeCCR9-JURKAT-NTG and GFP-JURKAT-NTG mice. **(C)** Representative images of the SREBF2 expression in spleen of OeCCR9-JURKAT-NTG and GFP-JURKAT-NTG mice. **(D)** H-scores of the SREBF2+ cells in the liver of OeCCR9-JURKAT-NTG and GFP-JURKAT-NTG mice. **(E)** TNMplot database was used to screen the correlation between CCR9 and SREBF2 in T-ALL. We selected CCR9: gene **(A)** vs. SREBF2: gene **(B)**, T-ALL: tissue, Tumor: sample type, and Spearman: correlation method analysis.

SUPPLEMENTARY TABLE S1
List of upregulated genes.

SUPPLEMENTARY TABLE S2
List of downregulated genes.

SUPPLEMENTARY TABLE S3
KEGG pathway enrichment analysis of the DEGs.

SUPPLEMENTARY TABLE S4
GO enrichment analysis of the DEGs.

SUPPLEMENTARY TABLE S5
list of selective DEGs following log2FC < 7, *p*-value = smallest.

SUPPLEMENTARY TABLE S6
GO enrichment analysis of the DEGs between the GFP-JURKAT and OeCCR9-JURKAT cells.

References

Abraham, R. T., and Weiss, A. (2004). Jurkat T cells and development of the T-cell receptor signalling paradigm. *Nat. Rev. Immunol.* 4, 301–308. doi:10.1038/nri1330

Advani, A. S., Mcdonough, S., Copelan, E., Willman, C., Mulford, D. A., List, A. F., et al. (2014). Swog 0919: A phase 2 study of idarubicin and cytarabine in combination with pravastatin for relapsed acute myeloid leukaemia. *Br. J. Haematol.* 167, 233–237. doi:10.1111/bjh.13035

Barretina, J., Caponigro, G., Stransky, N., Venkatesan, K., Margolin, A. A., Kim, S., et al. (2012). The Cancer Cell Line Encyclopedia enables predictive modelling of anticancer drug sensitivity. *Nature* 483, 603–607. doi:10.1038/nature11003

Barrett, A. J., and Battiwalla, M. (2010). Relapse after allogeneic stem cell transplantation. *Expert Rev. Hematol.* 3, 429–441. doi:10.1586/ehm.10.32

Bhasin, S. S., Summers, R. J., Thomas, B. E., Sarkar, D., Dwivedi, B., Park, S. I., et al. (2020). Characterization of T-ALL-specific heterogenous blast populations using high resolution single cell profiling. *Blood* 136, 11–12. doi:10.1182/blood-2020-143017

Cai, D., Wang, J., Gao, B., Li, J., Wu, F., Zou, J. X., et al. (2019). RORγ is a targetable master regulator of cholesterol biosynthesis in a cancer subtype. *Nat. Commun.* 10, 4621. doi:10.1038/s41467-019-12529-3

Chiarini, F., Grimaldi, C., Ricci, F., Tazzari, P. L., Evangelisti, C., Ognibene, A., et al. (2010). Activity of the novel dual phosphatidylinositol 3-kinase/mammalian target of rapamycin inhibitor NVP-BEZ235 against T-cell acute lymphoblastic leukemia. *Cancer Res.* 70, 8097–8107. doi:10.1158/0008-5472.CAN-10-1814

Cordó, V., Van Der Zwet, J. C., Canté-Barrett, K., Pieters, R., and Meijerink, J. P. (2021). T-Cell acute lymphoblastic leukemia: A roadmap to targeted therapies. *Blood cancer Discov.* 2, 19–31. doi:10.1158/2643-3230.BCD-20-0093

Corsini, A., Maggi, F. M., and Catapano, A. L. (1995). Pharmacology of competitive inhibitors of HMG-CoA reductase. *Pharmacol. Res.* 31, 9–27. doi:10.1016/1043-6618(95)80042-5

Cramer-Morales, K., Nieborowska-Skorska, M., Scheibner, K., Padget, M., Irvine, D. A., Sliwinski, T., et al. (2013). Personalized synthetic lethality induced by targeting RAD52 in leukemias identified by gene mutation and expression profile. *Blood, J. Am. Soc. Hematol.* 122, 1293–1304. doi:10.1182/blood-2013-05-501072

Croft, D., O'kelly, G., Wu, G., Haw, R., Gillespie, M., Matthews, L., et al. (2010). Reactome: A database of reactions, pathways and biological processes. *Nucleic acids Res.* 39, D691–D697. doi:10.1093/nar/gkq1018

Ding, X., Zhang, W., Li, S., and Yang, H. (2019). The role of cholesterol metabolism in cancer. *Am. J. cancer Res.* 9, 219–227.

Dos Santos, M., Schwartsmann, G., Roesler, R., Brunetto, A., and Abujamra, A. (2009). Sodium butyrate enhances the cytotoxic effect of antineoplastic drugs in human lymphoblastic T-cells. *Leukemia Res.* 33, 218–221. doi:10.1016/j.leukres.2008.07.003

Ershov, P., Kaluzhskiy, L., Mezentsev, Y., Yablokov, E., Gnedenko, O., and Ivanov, A. (2021). Enzymes in the cholesterol synthesis pathway: interactomics in the cancer context. *Biomedicines* 9, 895. doi:10.3390/biomedicines9080895

Follini, E., Marchesini, M., and Roti, G. (2019). Strategies to overcome resistance mechanisms in T-cell acute lymphoblastic leukemia. *Int. J. Mol. Sci.* 20, 3021. doi:10.3390/ijms20123021

Gioia, L., Siddique, A., Head, S. R., Salomon, D. R., and Su, A. I. (2018). A genome-wide survey of mutations in the Jurkat cell line. *BMC genomics* 19, 334. doi:10.1186/s12864-018-4718-6

Girardi, T., Vicente, C., Cools, J., and De Keersmaecker, K. (2017). The genetics and molecular biology of T-ALL. *Blood, J. Am. Soc. Hematol.* 129, 1113–1123. doi:10.1182/blood-2016-10-706465

Gokey, N. G., Lopez-Anido, C., Gillian-Daniel, A. L., and Svaren, J. (2011). Early growth response 1 (Egr1) regulates cholesterol biosynthetic gene expression. *J. Biol. Chem.* 286, 29501–29510. doi:10.1074/jbc.M111.263509

Han, B., Alonso-Valenteen, F., Wang, Z., Deng, N., Lee, T.-Y., Gao, B., et al. (2022). A chemokine regulatory loop induces cholesterol synthesis in lung-colonizing triple-negative breast cancer cells to fuel metastatic growth. *Mol. Ther.* 30, 672–687. doi:10.1016/j.ymthe.2021.07.003

Homminga, I., Pieters, R., Langerak, A. w., De rooi, J. J., Stubbs, A., Verstegen, M., et al. (2011). Integrated transcript and genome analyses reveal NKX2-1 and MEF2C as potential oncogenes in T cell acute lymphoblastic leukemia. *Cancer Cell* 19, 484–497. doi:10.1016/j.ccr.2011.02.008

Hong, Z., Wei, Z., Xie, T., Fu, L., Sun, J., Zhou, F., et al. (2021). Targeting chemokines for acute lymphoblastic leukemia therapy. *J. Hematol. Oncol.* 14, 48. doi:10.1186/s13045-021-01060-y

Jabbour, E. J., Faderl, S., and Kantarjian, H. M. (2005). "Adult acute lymphoblastic leukemia," in *Mayo clinic proceedings* (Elsevier), 1517–1527. doi:10.4065/80.11.1517

Jabbour, E., O'brien, S., Konopleva, M., and Kantarjian, H. (2015). New insights into the pathophysiology and therapy of adult acute lymphoblastic leukemia. *Cancer* 121, 2517–2528. doi:10.1002/cncr.29383

Jiang, G., Zhang, S., Yazdanparast, A., Li, M., Pawar, A. V., Liu, Y., et al. (2016). Comprehensive comparison of molecular portraits between cell lines and tumors in breast cancer. *BMC genomics* 17 (7), 525. doi:10.1186/s12864-016-2911-z

Kornblau, S. M., Banker, D. E., Stirewalt, D., Shen, D., Lemker, E., Verstovsek, S., et al. (2006). Blockade of adaptive defensive changes in cholesterol uptake and synthesis in AML by the addition of pravastatin to idarubicin + high-dose ara-C: A phase 1 study. *Blood* 109, 2999–3006. doi:10.1182/blood-2006-08-044446

Lei, Y., Jamal, M., Zeng, X., He, H., Xiao, D., Zhang, C., et al. (2022). Insulin receptor substrate 1 (IRS1) is related with lymph node metastases and prognosis in esophageal squamous cell carcinoma. *Gene* 835, 146651. doi:10.1016/j.gene.2022.146651

Li, H. Y., Appelbaum, F. R., Willman, C. L., Zager, R. A., and Banker, D. E. (2003). Cholesterol-modulating agents kill acute myeloid leukemia cells and sensitize them to therapeutics by blocking adaptive cholesterol responses. *Blood* 101, 3628–3634. doi:10.1182/blood-2002-07-2283

Li, J., Muhammad, J., Xie, T., Sun, J., Lei, Y., Wei, Z., et al. (2021). LINC00853 restrains T cell acute lymphoblastic leukemia invasion and infiltration by regulating CCR9/CCL25. *Mol. Immunol.* 140, 267–275. doi:10.1016/j.molimm.2021.10.016

Litzow, M. R., and Ferrando, A. A. (2015). How I treat T-cell acute lymphoblastic leukemia in adults. *Blood* 126, 833–841. doi:10.1182/blood-2014-10-551895

Luo, J., Yang, H., and Song, B.-L. (2020). Mechanisms and regulation of cholesterol homeostasis. *Nat. Rev. Mol. Cell Biol.* 21, 225–245. doi:10.1038/s41580-019-0190-7

Madison, B. B. (2016). Srebp2: A master regulator of sterol and fatty acid synthesis[1]. *J. Lipid Res.* 57, 333–335. doi:10.1194/jlr.C066712

Mezencev, R., and Mcdonald, J. F. (2011). Subcutenous xenografts of human T-lineage acute lymphoblastic leukemia Jurkat cells in nude mice. *vivo* 25, 603–607.

Minden, M. D., Dimitroulakos, J., Nohynek, D., and Penn, L. Z. (2001). Lovastatin induced control of blast cell growth in an elderly patient with acute myeloblastic leukemia. *Leukemia Lymphoma* 40, 659–662. doi:10.3109/10428190109097663

Minowada, J., Ohnuma, T., and Moore, G. (1972). Rosette-forming human lymphoid cell lines. I. Establishment and evidence for origin of thymus-derived lymphocytes. *J. Natl. Cancer Inst.* 49, 891–895.

Passaro, D., Quang, C. T., and Ghysdael, J. (2016). Microenvironmental cues for T-cell acute lymphoblastic leukemia development. *Immunol. Rev.* 271, 156–172. doi:10.1111/imr.12402

Perbellini, O., Cavallini, C., Chignola, R., Galasso, M., and Scupoli, M. T. (2022). Phospho-specific flow cytometry reveals signaling heterogeneity in T-cell acute lymphoblastic leukemia cell lines. *Cells* 11, 2072. doi:10.3390/cells11132072

Piñero, J., Ramírez-Anguita, J. M., Saüch-Pitarch, J., Ronzano, F., Centeno, E., Sanz, F., et al. (2020). The DisGeNET knowledge platform for disease genomics: 2019 update. *Nucleic acids Res.* 48, D845–D855. doi:10.1093/nar/gkz1021

Pui, C.-H., Robison, L. L., and Look, A. T. (2008). Acute lymphoblastic leukaemia. *Lancet* 371, 1030–1043. doi:10.1016/S0140-6736(08)60457-2

Rashkovan, M., Albero, R., Gianni, F., Perez-Duran, P., Miller, H. I., Mackey, A. L., et al. (2022). Intracellular cholesterol pools regulate oncogenic signaling and epigenetic circuitries in Early T-cell Precursor Acute Lymphoblastic Leukemia. *Cancer Discov.* 12, 856–871. doi:10.1158/2159-8290.CD-21-0551

Samuels, A. L., Beesley, A. H., Yadav, B. D., Papa, R. A., Sutton, R., Anderson, D., et al. (2014a). A pre-clinical model of resistance to induction therapy in pediatric acute lymphoblastic leukemia. *Blood Cancer J.* 4, e232. doi:10.1038/bcj.2014.52

Samuels, A. L., Heng, J. Y., Beesley, A. H., and Kees, U. R. (2014b). Bioenergetic modulation overcomes glucocorticoid resistance in T-lineage acute lymphoblastic leukaemia. *Br. J. Haematol.* 165, 57–66. doi:10.1111/bjh.12727

Schneider, U., Schwenk, H. U., and Bornkamm, G. (1977). Characterization of EBV-genome negative "null" and "T" cell lines derived from children with acute lymphoblastic leukemia and leukemic transformed non-Hodgkin lymphoma. *Int. J. cancer* 19, 621–626. doi:10.1002/ijc.2910190505

Sheen, C., Vincent, T., Barrett, D., Horwitz, E. M., Hulitt, J., Strong, E., et al. (2011). Statins are active in acute lymphoblastic leukaemia (ALL): A therapy that may treat ALL and prevent avascular necrosis. *Br. J. Haematol.* 155, 403–407. doi:10.1111/j.1365-2141.2011.08696.x

Silva, A., Yunes, J. A., Cardoso, B. A., Martins, L. R., Jotta, P. Y., Abecasis, M., et al. (2008). PTEN posttranslational inactivation and hyperactivation of the PI3K/Akt pathway sustain primary T cell leukemia viability. *J. Clin. investigation* 118, 3762–3774. doi:10.1172/JCI34616

Steelman, L., Franklin, R., Abrams, S., Chappell, W., Kempf, C., Bäsecke, J., et al. (2011). Roles of the Ras/Raf/MEK/ERK pathway in leukemia therapy. *Leukemia* 25, 1080–1094. doi:10.1038/leu.2011.66

Terwilliger, T., and Abdul-Hay, M. (2017). Acute lymphoblastic leukemia: A comprehensive review and 2017 update. *Blood cancer J.* 7, e577. doi:10.1038/bcj.2017.53

Tu, Z., Xiao, R., Xiong, J., Tembo, K. M., Deng, X., Xiong, M., et al. (2016). CCR9 in cancer: oncogenic role and therapeutic targeting. *J. Hematol. Oncol.* 9, 10–19. doi:10.1186/s13045-016-0236-7

Vadillo, E., Dorantes-Acosta, E., Pelayo, R., and Schnoor, M. (2018). T cell acute lymphoblastic leukemia (T-ALL): new insights into the cellular origins and infiltration mechanisms common and unique among hematologic malignancies. *Blood Rev.* 32, 36–51. doi:10.1016/j.blre.2017.08.006

Van Der Weide, K., De Jonge-Peeters, S. D. P. W. M., Kuipers, F., De Vries, E. G. E., and Vellenga, E. (2009). Combining simvastatin with the farnesyltransferase inhibitor tipifarnib results in an enhanced cytotoxic effect in a subset of primary CD34+ acute myeloid leukemia samples. *Clin. Cancer Res.* 15, 3076–3083. doi:10.1158/1078-0432.CCR-08-3004

Vilimanovich, U., Bosnjak, M., Bogdanovic, A., Markovic, I., Isakovic, A., Kravic-Stevovic, T., et al. (2015). Statin-mediated inhibition of cholesterol synthesis induces cytoprotective autophagy in human leukemic cells. *Eur. J. Pharmacol.* 765, 415–428. doi:10.1016/j.ejphar.2015.09.004

Wang, J.-J., Tian, Y., Xu, K.-L., Fu, R.-X., Niu, M.-S., and Zhao, K. (2018). Statins regulate the proliferation and apoptosis of T-ALL cells through the inhibition of Akt pathway. *Zhongguo shi yan xue ye xue za zhi* 26, 359–367. doi:10.7534/j.issn.1009-2137.2018.02.009

Wenzinger, C., Williams, E., and Gru, A. A. (2018). Updates in the pathology of precursor lymphoid neoplasms in the revised fourth edition of the WHO classification of tumors of hematopoietic and lymphoid tissues. *Curr. Hematol. malignancy Rep.* 13, 275–288. doi:10.1007/s11899-018-0456-8

Youns, M., Fu, Y.-J., Zu, Y.-G., Kramer, A., Konkimalla, V. B., Radlwimmer, B., et al. (2010). Sensitivity and resistance towards isoliquiritigenin, doxorubicin and methotrexate in T cell acute lymphoblastic leukaemia cell lines by pharmacogenomics. *Naunyn-Schmiedeberg's archives Pharmacol.* 382, 221–234. doi:10.1007/s00210-010-0541-6

Yu, K., Chen, B., Aran, D., Charalel, J., Yau, C., Wolf, D. M., et al. (2019). Comprehensive transcriptomic analysis of cell lines as models of primary tumors across 22 tumor types. *Nat. Commun.* 10, 3574. doi:10.1038/s41467-019-11415-2

Zeng, X., Lei, Y., Pan, S., Sun, J., He, H., Xiao, D., et al. (2023). LncRNA15691 promotes T-ALL infiltration by upregulating CCR9 via increased MATR3 stability. *J. Leukoc. Biol.* 113, 203–215. doi:10.1093/jleuko/qiac010

Zhang, L., Yu, B., Hu, M., Wang, Z., Liu, D., Tong, X., et al. (2011). Role of Rho-ROCK signaling in MOLT4 cells metastasis induced by CCL25. *Leukemia Res.* 35, 103–109. doi:10.1016/j.leukres.2010.07.039

Zhao, L., Zhan, H., Jiang, X., Li, Y., and Zeng, H. (2019). The role of cholesterol metabolism in leukemia. *Blood Sci. Baltim. Md* 1, 44–49. doi:10.1097/BS9.0000000000000016

frontiers | Frontiers in Pharmacology

TYPE Original Research
PUBLISHED 06 September 2023
DOI 10.3389/fphar.2023.1265440

OPEN ACCESS

EDITED BY
Pranav Kumar Prabhakar,
Lovely Professional University, India

REVIEWED BY
Bhupinder Kumar,
Hemwati Nandan Bahuguna Garhwal University, India
Farhat Parween,
National Institutes of Health (NIH), United States
Mohammad Zafaryab,
Alabama State University, United States

*CORRESPONDENCE
Muhammad Zaheer,
muhammad.zaheer@lums.edu.pk
Muhammad Badar,
mbadar@gu.edu.pk

RECEIVED 22 July 2023
ACCEPTED 22 August 2023
PUBLISHED 06 September 2023

CITATION
Akbar MU, Khattak S, Khan MI, Saddozai UAK, Ali N, AlAsmari AF, Zaheer M and Badar M (2023), A pH-responsive bi-MIL-88B MOF coated with folic acid-conjugated chitosan as a promising nanocarrier for targeted drug delivery of 5-Fluorouracil.
Front. Pharmacol. 14:1265440.
doi: 10.3389/fphar.2023.1265440

A pH-responsive bi-MIL-88B MOF coated with folic acid-conjugated chitosan as a promising nanocarrier for targeted drug delivery of 5-Fluorouracil

Muhammad Usman Akbar[1], Saadullah Khattak[2], Malik Ihsanullah Khan[3], Umair Ali Khan Saddozai[4], Nemat Ali[5], Abdullah F. AlAsmari[5], Muhammad Zaheer[6]* and Muhammad Badar[1]*

[1]Gomal Center of Biochemistry and Biotechnology, Gomal University, Dera Ismail Khan, Pakistan, [2]Henan International Joint Laboratory of Nuclear Protein Regulation, School of Basic Medical Sciences, Henan University, Kaifeng, China, [3]Institute of Molecular Biology and Biotechnology, The University of Lahore, Lahore, Pakistan, [4]Department of Preventive Medicine, Institute of Bioinformatics, Henan Provincial Engineering Center for Tumor Molecular Medicine, School of Basic Medical Sciences, Henan University, Kaifeng, China, [5]Department of Pharmacology and Toxicology, College of Pharmacy, King Saud University, Riyadh, Saudi Arabia, [6]Department of Chemistry and Chemical Engineering, Syed Babar Ali School of Science and Engineering, Lahore University of Management Sciences (LUMS), Lahore, Pakistan

Cancer has remained one of the leading causes of death worldwide, with a lack of effective treatment. The intrinsic shortcomings of conventional therapeutics regarding tumor specificity and non-specific toxicity prompt us to look for alternative therapeutics to mitigate these limitations. In this regard, we developed multifunctional bimetallic (FeCo) bi-MIL-88B-FC MOFs modified with folic acid—conjugated chitosan (FC) as drug delivery systems (DDS) for targeted delivery of 5-Fluorouracil (5-FU). The bi-MIL-88B nanocarriers were characterized through various techniques, including powder X-ray diffraction, scanning electron microscopy, energy-dispersive X-ray, thermogravimetric analysis, and Fourier transform infrared spectroscopy. Interestingly, 5-FU@bi-MIL-88B-FC showed slower release of 5-FU due to a gated effect phenomenon endowed by FC surface coating compared to un-modified 5-FU@bi-MIL-88B. The pH-responsive drug release was observed, with 58% of the loaded 5-FU released in cancer cells mimicking pH (5.2) compared to only 24.9% released under physiological pH (5.4). The *in vitro* cytotoxicity and cellular internalization experiments revealed the superiority of 5-FU@bi-MIL-88B-FC as a highly potent targeted DDS against folate receptor (FR) positive SW480 cancer cells. Moreover, due to the presence of Fe and Co in the structure, bi-MIL-88B exhibited peroxidase-like activity for chemodynamic therapy. Based on the results, 5-FU@bi-MIL-88B-FC could serve as promising candidate for smart DDS by sustained drug release and selective targeting.

KEYWORDS

metal-organic framework, folic acid -chitosan, stimuli responsive, drug delivery, targeted therapy, anticancer

1 Introduction

The emergence of nanomedicine as a next-generation technology has brought a revolution in battling diseases, particularly cancer (van der Meel et al., 2019). Cancer, for decades, has remained the leading cause of death worldwide after cardiovascular disease (Dibden et al., 2020). Despite advances in early diagnosis and associated treatments, current anticancer therapies rely heavily on invasive surgical procedures, radiotherapy, and chemotherapy (Das et al., 2020). These procedures are endemic to the problems of unwanted toxicity, insufficient drug delivery, premature drug degradation, and cancer recurrence due to incomplete eradication (Ulldemolins et al., 2021). The field of nanomedicine tries to mitigate such limitations by using smart nanodevices to transport therapeutic molecules specifically to cancer cells reducing off-target side effects (Akbarzadeh et al., 2021; Manzari et al., 2021; Surekha et al., 2021; Bäumer et al., 2022). Drug delivery systems based on nanodevices have become increasingly popular due to their advantages of improved drug loading, stable transfer of drugs to the target site, and reduced dosage requirement (Li Y. et al., 2022; Wang et al., 2022a; Yu et al., 2022; Rana et al., 2023). In this regard, various nanomaterials have been explored as drug delivery systems comprising carbon nanotubes (CNTs), liposomes, hydrogels, Layered double hydroxides (LDHs), dendrimers and metal-organic frameworks (MOFs) (Hesse et al., 2013; Chen et al., 2020; Zhang et al., 2020; Anisimov et al., 2022; Yang et al., 2022; Zhao et al., 2023). Among others, MOFs, due to their exceptional characteristics, have recently gained much attention for their potential in gas sorption, catalysis, sensing, and drug delivery (Okur et al., 2021; Abbas et al., 2023; Oh et al., 2023; Ye et al., 2023). MOFs are crystalline materials formed by self-assembling inorganic (metal ion/clusters) and organic linkers through coordination chemistry (Vodyashkin et al., 2023). They are highly diverse structures with tunable surface chemistry, adjustable pores, and high surface areas reaching up to 10,000 m^2/g (Adegoke and Maxakato, 2021; Altintas et al., 2022; Yin et al., 2022). Moreover, through pre or post-synthetic modifications, MOFs can respond to various stimuli (pH, temperature, redox reaction, and ATP) (Wang et al., 2020; Sun and Davis, 2021). Upon encountering such stimuli, MOFs undergo structural alterations allowing them to release their encapsulated drug molecules (Zhao et al., 2021). Various MOFs such as MIL-101 (MIL = Material Institute Lavoisier), UiO-66 (UiO = University of Oslo), and ZIF-8 (ZIF = Zeolite Imidazolate Framework) have been successfully deployed in the past as stimuli-responsive smart DDS for chemotherapy (Abánades Lázaro et al., 2020; Karimi Alavijeh and Akhbari, 2020; Yan et al., 2020). The metal nodes in MOFs also act as catalytic centers performing peroxidase-like (POD) reactions to induce reactive oxygen species (ROS) mediated stress in cancer cells for chemodynamic therapy (Di et al., 2023). In this regard, mixed-metal MOFs have shown higher POD performance than mono-metallic MOFs due to the excellent M^{III}/M^{II} cycling frequency and efficient electron transfer capability (Lyu et al., 2017; Wen et al., 2021). The performance of MOFs for drug delivery applications could also be improved by making MOFs-composites through surface modification or encapsulating MOFs in biodegradable materials (e.g., Biopolymers) (Ge et al., 2022).

Compared to other polymers used for biodegradable coatings in targeted DDS, chitosan (CS) has recently attracted much attention due to its cationic character, biodegradable nature, pH sensitivity, efflux pump inhibition, and higher cellular permeability (Aibani et al., 2021; Sathiyaseelan et al., 2021). The repeated amine groups found in the structure of CS are responsive towards tumor microenvironment mimicking acidic media and cause swelling of the system to release loaded cargo (Lv et al., 2016; Chen et al., 2017). The tumor specificity of the DDS modified with CS could further be improved by functionalizing it with active targeting ligands like folic acid (FA) (Nemati et al., 2021). Since FA receptors are exclusively overexpressed in most tumor cells, CS functionalization with FA could help DDS internalize into the cells through receptor-mediated endocytosis (İnce et al., 2020). However, the application of CS-based DDS as stand-alone nanocarriers is limited due to their rapid degradation and higher swelling degree leading towards premature drug release (Peers et al., 2020). Thus, making a composite of CS with other materials is termed beneficial to improve the system's overall efficiency (El Leithy et al., 2019).

5-Fluorouracil (5-FU) is a pyrimidine analog anticancer drug that exerts its cytotoxic effects through DNA/RNA incorporation, causing apoptosis in cancer cells (Guo et al., 2020). However, it has a rapid degradation rate (5–10 min) which hampers its broad clinical efficacy (Longley et al., 2003). The non-specific nature of the 5-FU and lack of suitable carriers further aggravate the situation by causing side effects such as diarrhea, cardiac toxicity, mucositis, dermatitis, and myelosuppression (Chang et al., 2012). Therefore, encapsulation of 5-FU in suitable carriers to avoid unnecessary side effects has been in focus (Valencia-Lazcano et al., 2023). For this, FeCo based bi-MIL-88B nanocarriers were synthesized in the current study due to their flexible structure, high surface area, and biocompatible nature of the components (Horcajada et al., 2012). The bi-MIL-88B nanocarriers exhibited a higher 5-FU loading capacity of 29.8wt%. After loading, these nanocarriers were coated with FA-conjugated CS (FC) to endow them with an extra-gated obstruction in premature drug release and folate receptor-associated cellular uptake. The pH-responsive 5-FU release was realized against the tumor-mimicking environment (pH = 5.2) and a normal physiological environment (pH = 7.4). The *in vitro* cytotoxicity and cellular uptake of the FC-coated bi-MIL-88B were checked against HEK-293 (FR negative) and SW480 (FR positive) cell lines. Moreover, the Fe^{III} and Co^{II} based trinuclear clusters in MIL-88B act as catalytic centers for *in situ* peroxidase-like activity.

2 Materials and methods

All the chemicals used in the study were of analytical grade and used as received. Iron (III) nitrate nonahydrate ($Fe(NO_3)_3{\cdot}9H_2O$), Cobalt (II) nitrate hexahydrate ($Co(NO_3)_3{\cdot}6H_2O$), Sodium acetate trihydrate ($CH_3COONa{\cdot}3H_2O$), Terephthalic acid, 5-Fluorouracil (5-FU), N, N-dimethylformamide (DMF), 3,3′,5,5′-Tetramethylbenzidine (TMB), Phosphate buffer saline (PBS) tablets, Chitosan (CS), Folic Acid (FA), 1,1′-Dioctadecyl-3,3,3′,3′tetramethyl indocarbocyanine perchlorate (Dil), N-hydroxysuccinimide (NHS), 1-ethyl-3-(3-dimethyl aminopropyl) carbodiimide (EDC), dimethyl sulfoxide (DMSO),

and Glacial acetic acid used were manufactured of Sigma-Aldrich. Roswell park memorial institute (RMPI-1640) medium, 3-(4,5-Dimethylthiazol-2-yl)-2,5-Diphenyltetrazolium Bromide (MTT), L-glutamine, Penicillin-Streptomycin (pen-strep), Alexa fluor™ 488 Phalloidin and Fetal bovine serum (FBS), were manufactured of Gibco, Invitrogen.

2.1 Characterization

A powder X-ray diffraction (PXRD) pattern was obtained to perform crystal structure analysis using BRUKER (D2 Phaser) with Ni-filtered Cu-Kα irradiation (λ = 1.5406 Å) over 2θ range from 5° to 50°. FEI NOVA Nano 450 scanning electron microscope (SEM) equipped with an energy dispersive X-ray spectroscope (EDX) was used to analyze the morphology of the samples. The samples' Zeta potential (ZP) was obtained through Zetasizer (Nano ZS, Malvern) at room temperature in water. N_2 adsorption-desorption isotherm was obtained to Brunauer-Emmett-Teller (BET) surface area and porous makeup of the samples using Quantachrome Nova 2200e. Infrared studies were performed using Bruker Alpha Platinum ATR between the 500–4,500 cm^{-1} range. Thermogravimetric analysis (TGA) was obtained through the TA instrument under an N_2 atmosphere in a temperature ranging from 10°C to 600°C with a heat ramp of 10°/min. UV-Vis spectrophotometry was used to characterize drug loading/release and TMB oxidation studies by Shimadzu UV-1800 spectrophotometer. The cellular uptake fluorescence studies were performed through confocal laser scanning microscope (CLSM) model ZEISS LSM—880, Jena, Germany.

2.2 Synthesis of bi-metallic cluster

The synthesis of bi-metallic acetate cluster FeCo(μ_3-O) was performed using a previously reported method with slight modifications (Sanchez-Lievanos et al., 2020). Briefly, 0.022 mol (3 g) of $CH_3COONa.3H_2O$ were dissolved in 5 mL of deionized water and was called solution-A. On the other hand, a solution-B of Fe and Co was prepared by dissolving 0.0014 mol (0.571 g) of $Fe(NO_3)_3.9H_2O$ and 0.007 mol (2.07 g) of $Co(NO_3)_3.6H_2O$ in 5 mL of deionized water and was kept on stirring after filtration. Later, solution-A was added dropwise into the thoroughly stirred solution-B, and the mother mix was kept on stirring for 24 h at room temperature. After 24 h of stirring, the light brown precipitates were collected through filtration and washed thrice with small amounts of water and ethanol. After washing, the collected product was kept to air dry at room temperature.

2.3 Synthesis of bi-MIL-88B

To synthesize bi-MIL-88B MOFs from pre-synthesized FeCo-μ_3O clusters, equimass of Terephthalic acid (100 mg) and FeCo-μ_3O (100 mg) were separately dissolved in vials containing 9 mL of DMF each through sonication. After dissolution, the terephthalic acid solution was added into the FeCo-μ_3O containing solution under stirring. An additional 1 mL of the glacial acetic acid as a modulating agent was added to the mother solution. The whole mixture was homogenously dissolved and inserted into a Teflon-lined autoclave for incubation at 120°C for 24 h. After 24 h of reaction, bi-MIL-88B MOF precipitates were isolated through centrifugation and later washed thrice with DMF and distilled ethanol to remove any unreacted linker present in the structure.

2.4 Preparation of folic acid-conjugated chitosan (FC)

The folic acid conjugated chitosan (FC) was synthesized using a previously reported method (Hu et al., 2017). In this method, amine groups of CS were conjugated to the FA by NHS-EDC chemistry. Briefly, a solution of FA (0.16 mmol, 7, 150 mg) was prepared through dissolution in 40 mL of anhydrous DMSO at room temperature. After that, NHS (3.36 mmol, 380 mg) and EDC (3.36 mmol, 645 mg) were added to the solution and stirred for 2 hours at room temperature. The solution turned into red brown colored ester solution of DMSO containing activated FA. In the second step, a solution of CS was prepared by dissolving 60 mg of CS in 15 mL of sodium acetate buffer (pH = 7.4) containing 0.1 M acetic acid. Later, the activated FA solution of DMSO was added dropwise into the CS solution at room temperature under dark conditions. The solution was allowed to stir for 24 h. After this time, the pH of the solution was adjusted to 9.0 through the slow addition of 0.1 M sodium hydroxide. In the end, the obtained mixed solution was dialyzed in PBS for 3 days to remove phosphoric acid salt, and finally, FC conjugates were obtained through freeze drying.

2.5 Drug loading

Before drug loading, bi-MIL-88B nanocarriers were activated under vacuum for 24 h at 100°C to eliminate some of the coordinated solvent molecules occupying the pores. Briefly, 100 mg of bi-MIL-88B were dispersed into a 30 mL concentrated 5-FU (6,000 ppm) solution in ethanol. The solution was put on an orbital shaker at room temperature for 48 h. After that, the drug-loaded 5-FU@bi-MIL-88B MOFs were isolated through centrifugation and the supernatant was analyzed for the remaining drug. The drug loading capacity (DLC) and drug loading efficiency (DLE) of the nanocarriers were determined using a calibration curve of 5-FU in ethanol (λ_{max} = 265 nm) (Supplementary Figure S8) according to the following formulas (Parsaei and Akhbari, 2022a);

$$DLC\ (wt\%) = \frac{weight\ of\ loaded\ drug}{weight\ of\ drug\ loaded\ MOFs} \times 100 \quad (1)$$

$$DLE\ (wt\%) = \frac{weight\ of\ loaded\ drug}{total\ weight\ of\ feeded\ drug} \times 100 \quad (2)$$

2.6 Fabrication of 5-FU@bi-MIL-88B-FC

To prepare the final composite, FC (20 mg) was dissolved in 4 mL of an acetic acid solution (pH 6.0) under stirring for 24 h to

form a homogenous solution. After that, the homogenous FC solution was added to the saturated ethanolic solution of 5-FU (20 mL) containing 100 mg 5-FU@bi-MIL-88B dispersed nanocarriers. Finally, the master mix was stirred at room temperature for 24 h. Later, the resultant FC-coated drug carriers were collected through centrifugation and rinsed twice with ethanol and ultrapure water. After rinsing, the final products were allowed to dry at room temperature under a vacuum for 24 h.

2.7 Drug release

The pH-responsive drug release from samples was realized against TME (pH 5.2) and physiological environment (pH 7.4) mimicking PBS solutions. Briefly, 60 mg of 5-FU@bi-MIL-88B and 5-FU@bi-MIL-88B-FC were dispersed in a dialysis bag (3.5 kDa MWCO) containing a small amount of PBS. Later, the dialysis bag containing drug-loaded nanocarriers was placed in a beaker containing 60 mL of PBS (pH 5.2 and 7.4). The drug release was performed through dialysis at 37°C under mild stirring. At predetermined intervals, 1 mL of the dialysate solution was pipetted out and replaced with the same amount of fresh PBS to maintain the total volume constant. The withdrawn samples were analyzed through a UV-Vis spectrophotometer, and the concentration of the released drug was determined according to the calibration curve of 5-FU in PBS (Supplementary Figure S9). The experiments were performed in duplicate and the final results were plotted through averaging. The following equations were used to obtain the cumulative 5-FU release percentage:

$$Drug\ release\ (cumulative\ \%) = \frac{Rt}{Rf} \times 100$$

Where Rt denotes the 5-FU concentration released at time t and Rf represents the total amount of 5-FU loaded on the nanocarriers.

2.8 Cell culture

Human embryonic kidney cells (HEK-293 cells) and human colon cancer (SW480 cells) were obtained from The University of Lahore (UOL) Cell Culture Collection (UCCC). The cells were cultured in RMPI-1640 media supplemented with 1% Pen-strep (100 IU/ml penicillin and 100 µg/mL streptomycin), 10% Hi-FBS, and 2 mM L-glutamine in a humidified incubator with 5% CO_2 at 37°C.

2.9 Cell cytotoxicity assay

The *in vitro* cytotoxicity of the 5-FU, bi-MIL-88B, 5-FU@bi-MIL-88B and 5-FU@bi-MIL-88B-CS was evaluated by the MTT assay. Briefly, the HEK293 and SW480 cells were seeded in a 96-well plate at a 1×10^4 density and incubated for 24 h in a CO_2 incubator at 37°C. After 24 h, the cell culture medium was removed and different concentrations of the test samples (7.81—500 µg/mL) dissolved in the culture medium supplied to the cells and allowed for 48 h of incubation. After incubation, 10 µL of MTT (12 mM) reagent was further supplied to each well and the cells were further incubated for another 4 h. Later, the medium was removed and DMSO (100 µL) was added to each well. The absorbance was recorded by PerkinElmer Enspire 2300 multimode reader at 570 nm. The experiments were conducted in triplicated and the final results were presented through averaging. The IC_{50} values were calculated by a non-linear regression model using GraphPad Prism 8 (San Diego, United States).

2.10 Cellular uptake studies

Confocal laser scanning microscopy was used to study the cellular uptake of nanocarriers. For CLSM imaging, SW480 cells at a density of 3×10^4 were seeded and grown on a glass coverslip in a 24-well plate for 24 h. After incubation for a predetermined time, the original medium was replaced with fresh medium containing Dil@bi-MIL-88B and Dil@bi-MIL-88B-CS (80 µg/mL) and incubated for an additional 12 h. Dil was used as a fluorescent probe to detect the internalization of the nanocarriers. Later, cells were washed twice with PBS and fixed through 4% formalin. The DAPI and Alexa flour 488 phalloidine were used to stain the nuclei and cytoskeleton of the cells. Finally, the cells were visualized under CLSM.

2.11 Peroxidase-like activity

The peroxidase-like property of synthesized nanocarriers was studied through the TMB oxidation methodology. Briefly, 5 mL of PBS (pH 5.2) was prepared by adding different amounts of bi-MIL-88B (0, 10, 20, 40, 60, and 80 µg/mL), H_2O_2 (1 mM) and TMB (0.25 mM) and allowed to incubate for 10 min at 37 °C. After that, samples were analyzed through a UV-Vis spectrophotometer at 652 nm wavelength related to the oxidized form of the TMB. Moreover, mechanistic studies on the performance of bi-MIL-88B nanocarriers were performed by varying the temperature (30°C—60°C) and pH (4—8) of the solution with concentrations of TMB (0.25 mM), H_2O_2 (1 mM) and bi-MIL-88B (50 µg/mL) kept constant.

2.12 Statistical analysis

The statistical analysis carried out in the study was performed through GraphPad Prism 8.0. The MTT data were shown as mean ± standard deviation. The statistically significant values of different groups were obtained through the Kruskal-Wallis test, followed by Dunn's multiple comparison analysis. The degree of significance of the treated groups against the control is represented as $^{****}p \leq 0.0001$, $^{***}p \leq 0.001$, $^{**}p \leq 0.01$, and $^{*}p \leq 0.05$.

3 Results and discussions

3.1 Synthesis and characterization of bi-MIL-88B

The bi-metallic (FeCo) bi-MIL-88B MOFs were synthesized using a previously published two-step secondary building unit (SBU) approach (Iqbal et al., 2021). A FeCo-μ_3O trinuclear

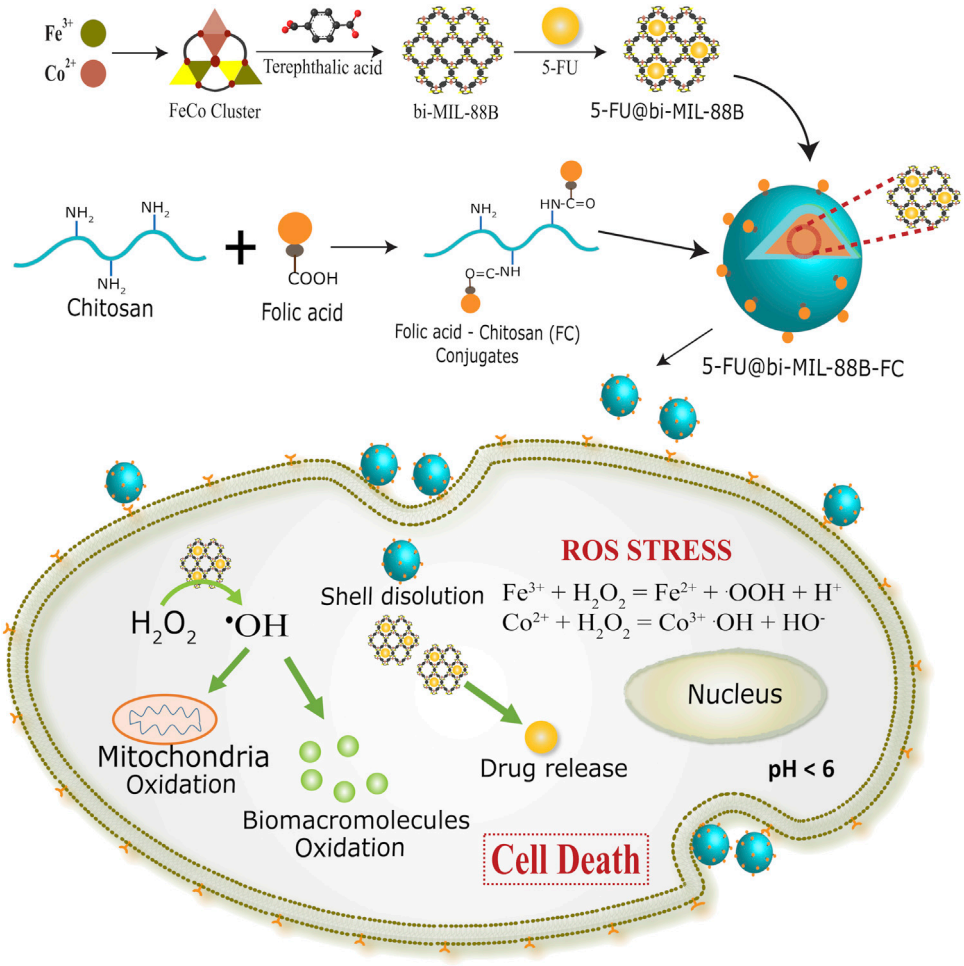

SCHEME 1
Synthetic scheme of 5-FU@bi-MIL-88B and folate receptor (FR) mediated endocytosis in SW480 (FR positive) cells.

cluster with metal ions connected to central oxygen (μ_3-O) in a trinuclear fashion was synthesized in the first step (Akbar et al., 2022). These metal ions are stabilized through the coordinated acetate ligands and solvent molecules at their terminal positions. In the second step, FeCo-μ_3O cluster is reacted with the terephthalic acid as the organic ligand. During the reaction, the terephthalic acid attaches to the metal ions by replacing the acetate ligands in a dissociative manner to form a bi-MIL-88B MOFs (Liu et al., 2016). Compared to SBU route, mixed-metal MOF synthesis through conventional one-pot synthesis or postsynthetic modifications (PSMs) method is tricky and results in mixed phase MOFs with unwanted altered physico-chemical properties (Li et al., 2013). Moreover, these methodologies provide less control over the reproducibility of the same MOFs and often generate unwanted metal oxides or even amorphous structures (Wongsakulphasatch et al., 2015). While, the SBU route exhibits certain advantages over others as the concentration of metals in the final MOFs can be precisely controlled avoiding the generation of unwanted metal oxides. Moreover, stable incorporation of the pre-synthesized mixed-metal SBU into the final MOF allows excellent reproducibility with predictable incorporation of the second metal (Co) with stoichiometric ratio of Fe and Co (2 : 1) (Peng et al., 2017). The synthetic approach of bi-MIL-88B, drug loading, FC coating, and mechanism of action are illustrated in Scheme 1.

The SEM analysis was performed to observe the morphological features of the synthesized samples. As seen in Supplementary Figures S1A, B, the FeCo clusters exhibited a jumble of rocks type appearance having undefined morphology. However, upon reaction with the organic linker, the resulting bi-MIL-88B MOFs revealed hexagonal rod-like morphology resembling the pure MIL-88B MOFs reported in the literature (Figures 1A, B) (Cai et al., 2016). The average size of the bi-MIL-88B was around 338 ± 30 nm, evaluated through average aspect ratio and size distribution analysis by DLS method (Figure 1D; Supplementary Figure S5). The EDX, elemental map and ICP-OES analysis was performed to analyze the elemental composition of the FeCo-cluster and bi-MIL-88B. The EDX spectra and elemental maps showed the homogenous distribution of Fe and Co ions having a stoichiometric ratio of Fe to Co (2 : 1) in the synthesized cluster (Supplementary Figures S1D, S2A) and bi-MIL-88B (Figure 1C; Supplementary Figure S2B).

Moreover, the ICP-OES analysis also revealed the homogenous distribution of Fe and Co in both samples with a ratio of 2:1 (Supplementary Figure S1). The presence of a similar

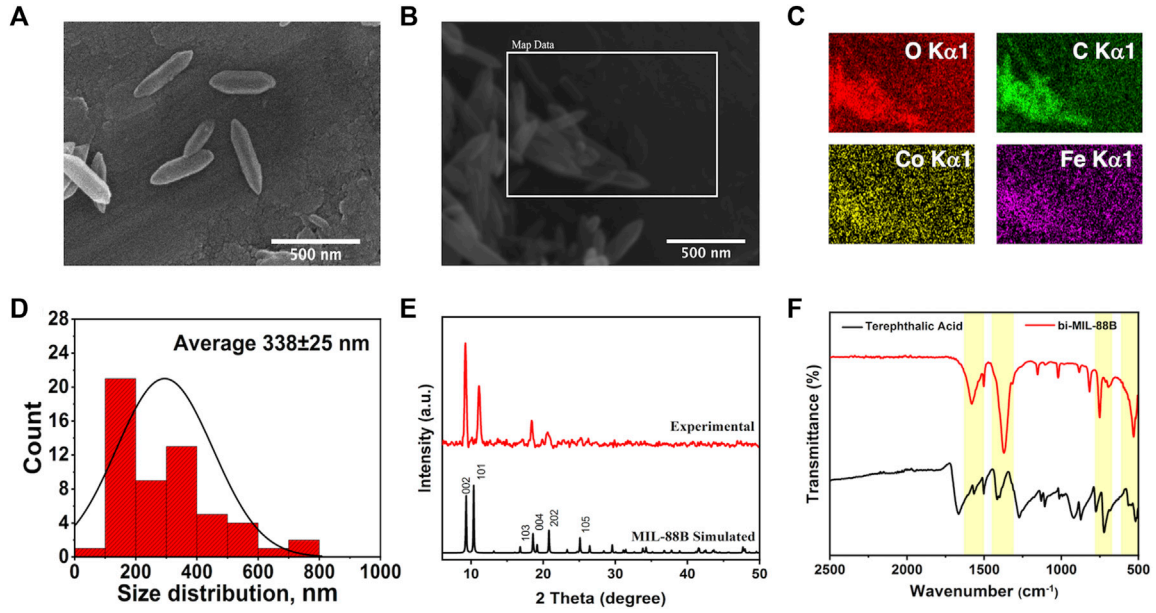

FIGURE 1
(A–B) SEM images; **(C)** Elemental Maps; **(D)** Size distribution chart of bi-MIL-88B nanocarriers; **(E)** PXRD pattern of simulated and experiment bi-MIL-88B; **(F)** FT-IR spectra of terephthalic acid and bi-MIL-88B.

stoichiometric ratio of both metals in the bi-MIL-88B indicates that the FeCo clusters retained their structural traits in the final product without any deformities. FT-IR analysis was performed to evaluate the major linkages in the samples. In the case of monometallic Fe-based MIL-88B, the Fe_3O trinuclear cluster in the structure exhibits metal-oxygen bond vibrations around 600 cm^{-1}. However, when one Co is incorporated into the cluster, the D_{3h} symmetry of Fe_3O breaks into C_{2v}, evident by the emergence of two new vibrational stretching around 734 cm^{-1} and 528 cm^{-1} related to FeCo-O bonds in the cluster (Supplementary Figure S3) (Iqbal et al., 2019). The vibrational bands found around 1,590 cm and 1,420 cm^{-1} in the cluster are related to the carboxyl groups of the coordinated acetate ligands (Zhang et al., 2012). The vibrational stretching in bi-MIL-88B MOFs found at 1,592 cm^{-1} and 1,386 cm^{-1} were related to -COO stretching of the coordinated linker (Liu et al., 2013).

The PXRD analysis revealed the crystal structure and phase purity of the samples. The characteristic peaks of the synthesized FeCo cluster's PXRD pattern matched well with the simulated one (Supplementary Figure S1C) (Sanchez-Lievanos et al., 2020). The bi-MIL-88B exhibited highly crystalline phase purity with distinctive peaks at 9.3°, 10.2°, and 11.6° related to 002, 100, and 101 planes also found in the simulated MIL-88B MOF (Figure 1F) (Horcajada et al., 2008). The porous makeup of the bi-MIL-88B nanocarriers was studied by N_2 adsorption-desorption analysis at 77K (Supplementary Figure S4A). The BET-specific surface area of the bi-MIL-88B was 86 m^2/g with an average pore diameter and volume of 1.9 nm and 0.21 cc/g (Supplementary Figure S4B). The lower surface area of the nanocarriers could be due to shrinkage of the structure upon solvent removal during thermal activation (Ma et al., 2013). The bi-MIL-88B MOFs have a flexible structure and tend to shrink/expand on the removal/addition of the guest molecules, known as a reversible breathing effect (Cao et al., 2022).

3.2 Fabrication of 5-FU@bi-MIL-88B-FC

SEM analysis was used to study the morphological changes after the drug impregnation and subsequent FC coating. As shown in Figure 2, bi-MIL-88B, 5-FU@bi-MIL-88B, and 5-FU@bi-MIL-88B-FC, the drug-loaded and FC-coated nanocarriers exhibited similar morphology to the unmodified MOFs. However, 5-FU@bi-MIL-88B reflects some swelling crystals due to the drug impregnation and reversible expansion. After FC coating, 5-FU@bi-MIL-88B-FC showed less aggregation than 5-FU@bi-MIL-88B, which aggregated upon drug impregnation (Figure 2).

The FT-IR studies further confirmed the incorporation of the 5-FU and the final synthesis of the FC-coated composite. As seen in the FT-IR spectra of 5-FU (Supplementary Figure S6), the vibrational peaks around 1,245 cm^{-1} and 1740 cm^{-1} are related to the C—N and C—O stretching, and the peaks between 800 cm^{-1} to 540 cm^{-1} represent C—F deformations (Chowdhuri et al., 2016). The characteristic peaks of 5-FU, when compared with bi-MIL-88B, can also be seen in the drug-loaded 5-FU@bi-MIL-88B samples confirming the successful drug incorporation. After the drug encapsulation, the second step involved the synthesis of folic acid–conjugated chitosan (FC) and subsequent composite 5-FU@bi-MIL-88B-FC. The synthesis of FC can be verified by comparing the FT-IR spectra of CS, FA and final conjugated FC. As seen in Supplementary Figure S7, in the FT-IR spectrum of CS, the peaks at 3,360 cm^{-1}, 2922 cm^{-1} and 2875 cm^{-1} are attributed to the N—H and asymmetric/symmetric vibrations of C—H groups. The peaks around 1,060 cm^{-1} represent C—O stretching, and vibrational bands around 1,322 cm^{-1} and 1,650 cm^{-1} are related to C—N and C=O bonds in the CS. While the peak at 1,154 cm^{-1} represents asymmetric stretching modes of C—O—C in the CS spectrum (Chen et al., 2011; Al-Nemrawi et al., 2022). Whereas the

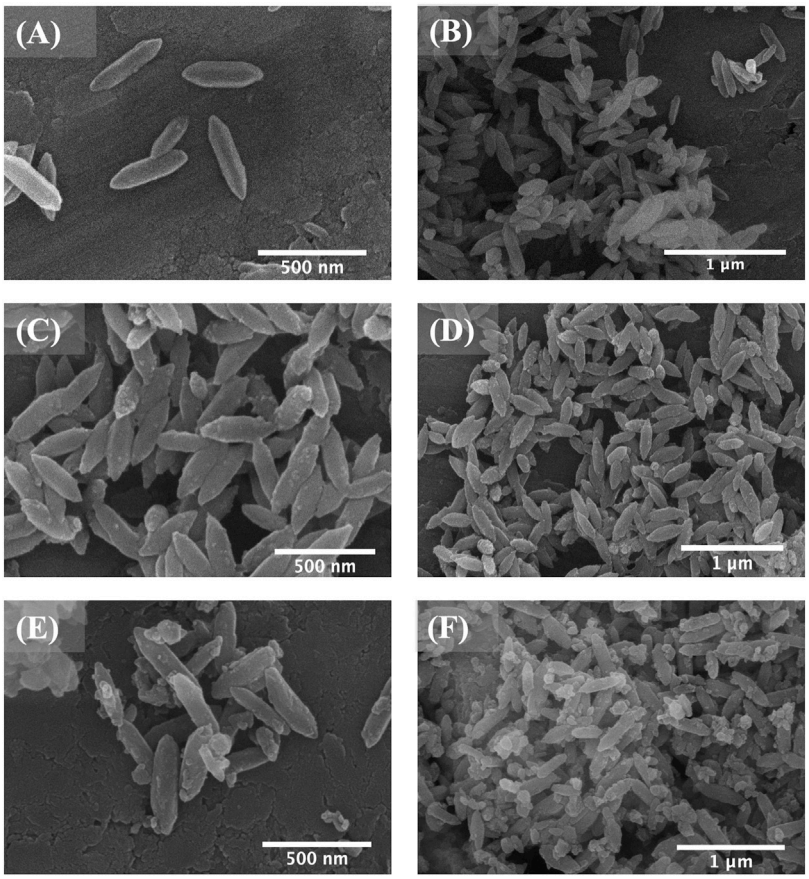

FIGURE 2
SEM images of bi-MIL-88B **(A, B)**; 5-FU@bi-MIL-88B **(C, D)**; and 5-FU@bi-MIL-88B-FC **(E, F)**.

characteristic peaks at 1,695 cm^{-1}, 1,480 cm^{-1}, 1,230 cm^{-1} and 1,170 cm^{-1} in the FT-IR spectra of FA are attributed to C=O, C=C, C—O, and C-N vibrational stretching. The 830 cm^{-1} and 750 cm^{-1} bands represent aromatic rings' out-of-plane C—H bond stretching (Parsaei and Akhbari, 2022b). Most of the characteristic peaks of CS and FA are observed in the FT-IR spectra of FC, which confirms the conjugation of FA to the CS in the final product (Supplementary Figure S7) (Chanphai et al., 2017). Moreover, the characteristic peaks of FC conjugates are also visible in the 5-FU@bi-MIL-88B composite confirming the successful coating of the 5-FU@bi-MIL-88B nanocarriers with the FC (Figure 3A). The influence of the 5-FU encapsulation and FC coating on the structural properties of the bi-MIL-88B was observed through the PXRD analysis. According to Figure 3B, no significant alteration in the PXRD patterns of the 5-FU@bi-MIL-88B and 5-FU@bi-MIL-88B-FC was observed compared to the pure bi-MIL-88B. A minor decrease in the diffraction angle of the peak related to the 101 plane from 11.6 to 11.2 can be attributed to the pore expansion by 5-FU loading due to the reversible breathing effect (Horcajada et al., 2011). The reduction in the overall peak intensities of the 5-FU@bi-MIL-88B-FC nanocarriers could be due to the external coating by the FC (Shi et al., 2018).

The ZP of the nanocarriers plays an essential role in deciding the stability and adhesion to the cells (Ishihara et al., 2015). The ZPs of the CS, FA, FC, 5-FU, bi-MIL-88B, 5-FU@bi-MIL-88B, and 5-FU@bi-MIL-88B were 0.47, −22.1, −9.83, −10.7, −3.52, −19.9 and −30.5 respectively (Figure 3C). The positive ZP of CS is due to the cationic amino groups, and the negative ZP of the FA can be ascribed to the anionic carboxyl groups of FA (Song et al., 2013). The shift to the higher negative ZP value after the FC coating of 5-FU@bi-MIL-88B can be related to the anionic properties of the FC conjugates. The higher ZP values for nanocarriers are beneficial as the highly charged particles tend to repulse each other limiting agglomeration. A lower ZP value results in coagulation due to the weaker repulsion force being overtaken by the attraction force between the charged particles. Moreover, nanoparticles are found in stabilized dispersions with an optimal ZP value of −30 mV (Samimi et al., 2019). The surface charge of the nanocarriers also plays a significant role in the cellular uptake of the nanocarriers. The nanocarriers with cationic character are usually internalized into the cell via caveolae-mediated endocytosis and micropinocytosis. While the nanocarriers with anionic features mainly tend to internalize through clathrin/caveolae-mediated endocytosis pathways (Foroozandeh and Aziz, 2018; Mazumdar et al., 2021). The TGA analysis further provided insights into the degradation patterns of the samples. As shown in Figure 3D, the bi-MIL-88B nanocarriers before the 5-FU incorporation exhibited two significant weight loss regions. The first weight loss below 280°C is attributed to the removal of coordinated solvent molecules in the structure (Gandara-Loe et al., 2020). The second considerable weight loss from 320°C to 480°C represents the decomposition of the organic linker and structural disintegration (Rojas et al., 2018).

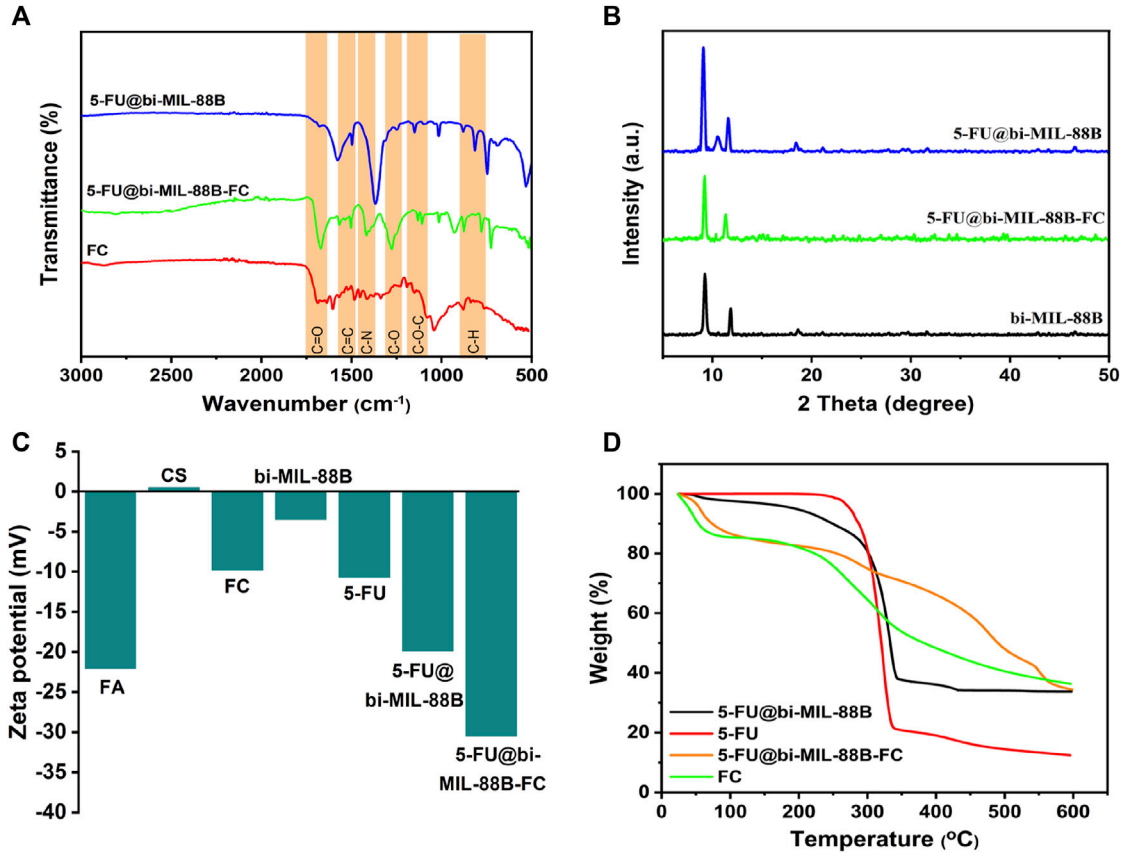

FIGURE 3
(A) FT-IR spectra; **(B)** PXRD patterns; **(C)** Zeta potential values; and **(D)** TGA patterns of the samples.

The drug-loaded 5-FU@bi-MIL-88B nanocarriers exhibited a weight loss pattern similar to the TGA of both 5-FU and bi-MIL-88B. The initial weight loss regions found in unloaded MOFs related to solvent molecules were not observed in the TGA of 5-FU@bi-MIL-88B, indicative of the pores filed with 5-FU molecules (Sheta et al., 2018). The initial weight loss till 320°C in the 5-FU@bi-MIL-88B is related to the decomposition of 5-FU molecules. In contrast, the second significant weight loss follows the pattern of linker decomposition similar to the unloaded MOFs. The 5-FU loaded nanocarriers coated with the FC exhibited a mixture of weight loss patterns identical to the TGA pattern of FC and 5-FU@bi-MIL-88B, which indicates the synthesis of FC-coated 5-FU@bi-MIL-88B composites (Nejadshafiee et al., 2019). Through the characterizations of SEM, FT-IR, PXRD, ZP, and TGA, the incorporation of the 5-FU and the subsequent coating by FC over the bi-MIL-88B nanocarriers was verified. Through the UV-Vis spectrophotometry analysis, the DLC and DLE of the nanocarriers were found to be 29.8% and 18.2%.

3.3 Drug release

The *in vitro* 5-FU release was investigated in two PBS mediums with variable pH mimicking the cancer cell environment (pH 5.2) and typical physiological environment (pH 7.4). The concentration of the 5-FU released from the nanocarriers was calculated by correlating the results with the 5-FU calibration curve in PBS (Supplementary Figure S9). The drug release behavior of 5-FU@bi-MIL-88B was compared with the FC-coated 5-FU@bi-MIL-88B-FC to examine the influence of the external coating on the release properties.

The 5-FU release profiles of uncoated and coated bi-MIL-88B are shown in Figure 4. Generally, MOF-based drug delivery systems follow a two-step drug release pattern (Li et al., 2020). The first stage, rapid/burst release, is due to the drug molecules loosely bound to the surface of the nanocarriers. The quick release stage is followed by more sustained release related to nanocarriers' structural modifications and departure of the drug molecules from the pores (Oh et al., 2015; Jiang et al., 2016). The 5-FU@bi-MIL-88B and 5-FU@bi-MIL-88B-FC followed a similar two-phase drug release kinetics pattern. A typical parabola of burst release during the first stage can be observed in all samples, with slight changes in both PBS (5.2 and 7.4). In the first 4 hours, 5-FU@bi-MIL-88B showed 23.8% and 37.9% of the 5-FU release in pH 5.2 and 7.4 (PBS). The drug release amounts reached 86.7% and 46.4% after 48 h in the second stage.

In contrast to the uncoated 5-FU@bi-MIL-88B, the FC-coated 5-FU@bi-MIL-88B-FC exhibited a much-controlled release kinetics of 5-FU in both PBS mediums simulating cancer microenvironment (pH = 5.2) and physiological environment (7.4). The FC-coated nanocarriers showed only 24.9% of drug release even after 48 h in

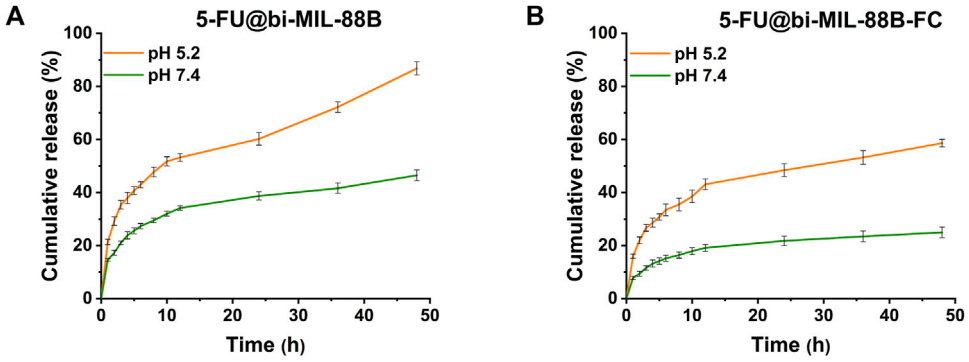

FIGURE 4
5-FU release pattern from **(A)** 5-FU@bi-MIL-88B; and **(B)** 5-FU@bi-MIL-88B-FC at different pHs (5.2 and 7.4).

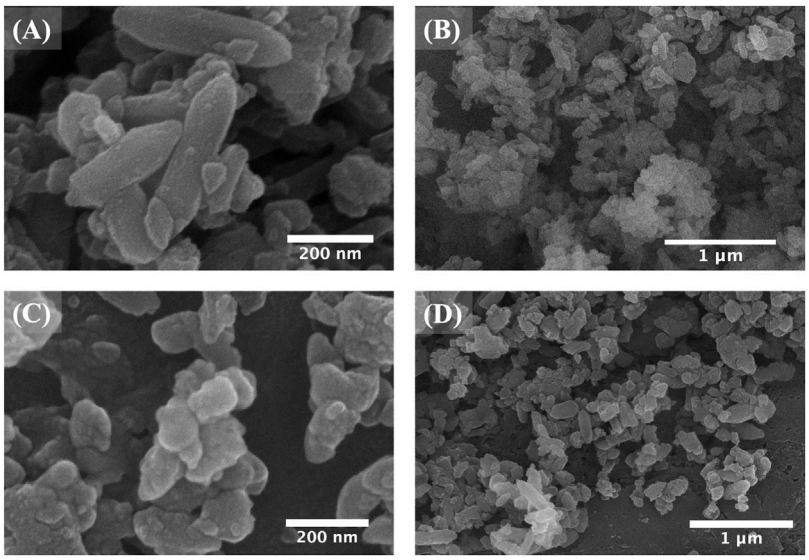

FIGURE 5
SEM images of 5-FU@bi-MIL-88B-FC after 4 days of immersion in PBS **(A, B)** of pH 7.4 and **(C, D)** pH 5.2.

the PBS of pH = 7.4, which could be beneficial to mitigate the unwanted toxicity of the drug to the normal cells. The lower release of the 5-FU from the 5-FU@bi-MIL-88B-FC nanocarriers under a physiological environment can be ascribed to the lower pKa (6.5) of the free amino groups in the CS. These groups lose their charge due to deprotonation at higher pHs and turn CS into an insoluble biopolymer shell. The insoluble coating act as a barrier to the premature release of the drug molecules. Moreover, the higher 5-FU release from the FC-coated nanocarriers in acidic PBS (pH = 5.2) compared to the physiological pH (7.4) is due to the protonation of the amine groups making the CS more soluble (Taghavi et al., 2017; Lu et al., 2019). Interestingly, the 5-FU@bi-MIL-88B-FC showed much sustained and slower release than their counterparts (5-FU@bi-MIL-88B) in the acidic pH (5.2). Only 58% of the 5-FU was released from the FC-coated nanocarriers compared to the uncoated ones, with 86% of the drug released during the same period. Due to the rapid degradation rate, chemotherapies based on free 5-FU administration lead to many issues, such as rapid cancer progression, metastasis and drug resistance (Leelakanok et al., 2018). Therefore, sustained release from the FC-coated 5-FU@bi-MIL-88B-FC could be helpful to overcome these challenges by a prolonged drug presence at the tumor site with target specificity of the carriers (Ali et al., 2023).

The structural stability of 5-FU@bi-MIL-88B-FC was examined by immersing the samples in PBS of pH (5.2 and 7.4) for 4 days. According to the SEM images (Figures 5A, B), the nanocarriers immersed at a pH of 7.4 showed little or no difference in morphology, consistent with CS's insoluble character at pHs above 6.5 (Liu et al., 2012). However, 5-FU@bi-MIL-88B-FC immersed in acidic media (pH = 5.2) showed complete degradation of the morphological traits resulting in distorted shape, indicating the drug release in acidic media due to structural breakdown (Figures 5C, D).

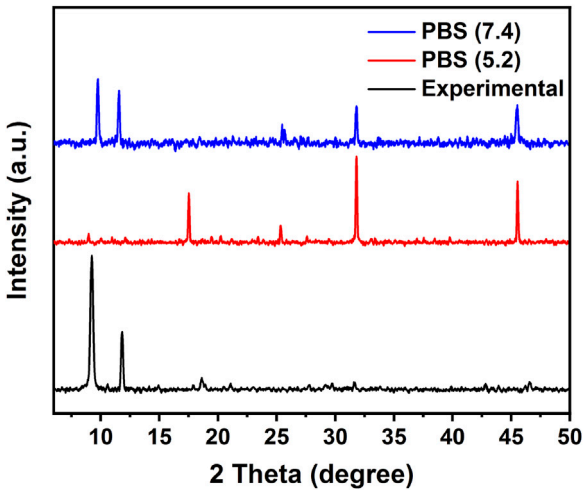

FIGURE 6
PXRD pattern of experimental bi-MIL-88B and immersed samples in PBS (pH 7.4 and 5.2).

PXRD analysis was obtained from these PBS (5.2 and 7.4) immersed samples further to analyze the structural alterations of nanocarriers under different pH. Figure 6., compares the PXRD pattern of PBS-immersed nanocarriers with the pure bi-MIL-88B. The nanocarriers soaked in PBS of pH 7.4 maintained most of the characteristic peaks reflected in the PXRD pattern of the pure bi-MIL-88B, supporting the good stability of MOF under physiological conditions also observed in SEM analysi. However, the PXRD pattern of the samples immersed under acidic pH (5.2) exhibited a loss of characteristic peaks of the parent MOFs indicating structural decomposition and instability. Moreover, the degradation of MOF in PBS could also be attributed to the strong affinity of phosphate ions present in the PBS towards the exposed metal sites in the MOF's structure (Li et al., 2017). Evident from the pxrd pattern of samples immersed in acidic pH, the extra peaks found arround 17, 26, 32° and 46° (2theta) indicate the presence of Fe and Co phosphates due to their strong interaction (Beale and Sankar, 2002; Yuan et al., 2016).

3.4 *In Vitro* cytotoxicity and cellular uptake studies

In vitro, the cytotoxicity profile of the samples was investigated to evaluate the efficacy of the FC-conjugated system for targeted 5-FU delivery. For this purpose, different concentrations (7.81–500 μg/mL) of 5-FU, bi-MIL-88B, 5-FU@bi-MIL-88B and 5-FU@bi-MIL-88B-FC were administered to the HEK-293 (FR-negative) and SW480 (FR-positive) cell lines. As seen in Figure 7A, 5-FU showed higher cytotoxic effects towards both

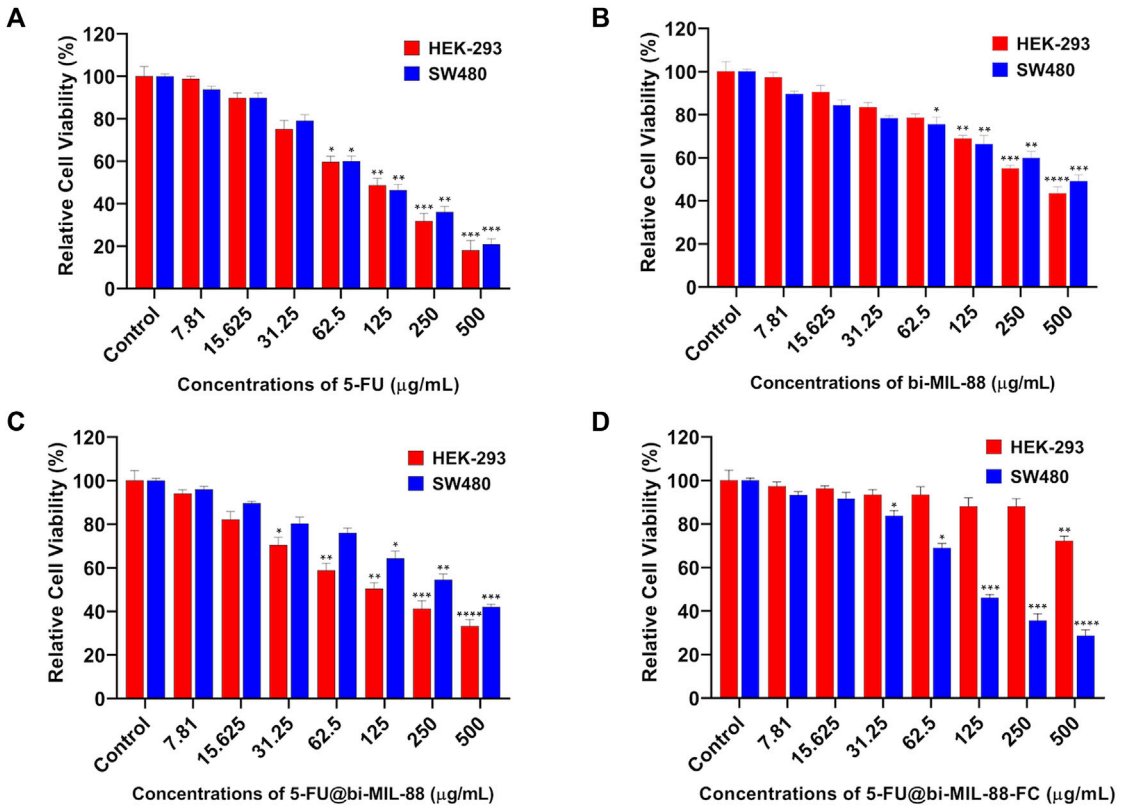

FIGURE 7
Cell viability results of HEK-293 and SW480 against different concentrations (7.81–500) of **(A)** 5-FU; **(B)** bi-MIL-88; **(C)** 5-FU@bi-MIL-88B and **(D)** 5-FU@bi-MIL-88B-FC. The degree of significance between the control and treatment groups for each cell line is denoted by ****$p \leq 0.0001$, ***$p \leq 0.001$, **$p \leq 0.01$, and *$p \leq 0.05$.

TABLE 1 Estimated IC_{50} values of different treatment groups against HEK-293 and SW480 cells.

Treatment groups (μg/mL)				
Cell line	5-FU	bi-MIL-88B	5-FU@bi-MIL-88B	5-FU@bi-MIL-88B-FC
HEK-293	108	342	184	N.A
SW480	113	482	301	136

N.A: not accountable.

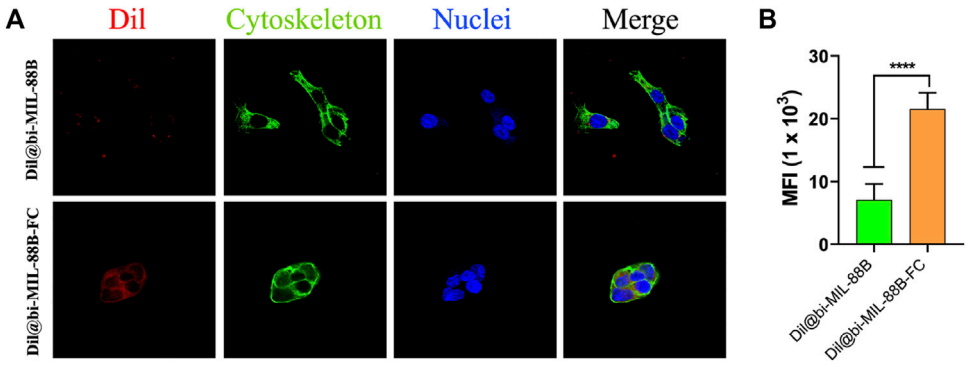

FIGURE 8
(A) Cellular internalization results of Dil@bi-MIL-88B (top) and Dil@bi-MIL-88B-FC (bottom) against SW480 cells visualized through CLSM. Red fluorescence (Dil), Green (Alexa fluor 488 stained cytoplasm), Blue (DAPI stained nuclei) and Merge (Overlay image); **(B)** Quantification of the MFI of Dil per cell via ImageJ. Data is shown in mean ± SD (n = 10). *****p* < *0.0001*.

cell lines due to its non-specific nature (Alvarez et al., 2012). The IC_{50} value of 5-FU and other treated agents are mentioned in Table 1. The unloaded and uncoated bi-MIL-88B MOFs showed considerable biocompatibility against HEK-293 cell lines with an IC_{50} value calculated at 342 μg/mL (Figure 7B). Moreover, 5-FU-loaded 5-FU@bi-MIL-88B nanocarriers exhibited concentration-dependent toxicity in HEK-293 and SW480 cells. The non-selective cytotoxicity behavior of 5-FU@bi-MIL-88B, if applied without FC coating, could lead to unwanted cytotoxicity against normal cells (Figure 7C) and cause failure of the whole system. The FC-coated 5-FU@bi-MIL-88B-FC exhibited selective toxicity against the FR-positive SW480 cells only with an IC_{50} of 136 μg/mL. A slightly higher IC_{50} value of FC-coated nanocarriers was observed compared to the free 5-FU against SW480 cells. It is because the free drug is readily available to the system to exert its effects during a short incubation time. In contrast, the encapsulated drug molecules are released slowly into the system and require more time to show their full efficacy (Gu et al., 2012). Moreover, 5-FU@bi-MIL-88B-FC showed very low toxicity towards the FR-negative cell lines (HEK-293), demonstrating the potential of the synthesized DDS to be effectively applied for targeted drug delivery against FR-positive cancer cell lines (Figure 7D).

To further support the observation of enhanced and selective toxicity of FC-coated nanocarriers against FR-positive SW480 cancer cells, the carbocyanine dye (Dil) labeled Dil@bi-MIL-88B and Dil@bi-MIL-88B-FC MOFs were used as a fluorescent probe. The Dil fluorescence intensity was measured using the excitation wavelength of 550 nm and an emission peak at 564 nm. The cellular uptake based on the Dil fluorescence intensity is shown in Figure 8A. The higher fluorescence intensity in cells treated with Dil@bi-MIL-88B-FC, compared to non-FC conjugated Dil@bi-MIL-88B, indicates the enhanced cellular uptake due to the FC shell. The cytoplasm was stained with alexa fluor 488 phalloidin, and the nucleus was stained with DAPI. Moreover, the increaed in the mean fluorescence intensity (MFI) by 1.8 to 2.4- fold for cells treated with Dil@bi-MIL-88B-FC compared to Dil@bi-MIL-88B further corroborated to the excellent cellular uptake of FC functionalized nanocarriers. These results suggest that the FC coating facilitates folate receptor-mediated cellular uptake and is essential in developing targeted DDS (Stella et al., 2000; Song et al., 2013).

3.5 Peroxidase-like activity

Inspired by the peroxidase (POD) like activity of the different transition metals such as Fe, Mn, Cu, and Co, and their use in chemodynamic therapy, we examined the POD activity of our nanocarriers through the TMB oxidation test (Scheme 2) (Bokare and Choi, 2014). Due to their altered metabolic pathways, the cancer cells are known to have higher levels of reactive oxygen species (H_2O_2, $^1O_2$, $^{\bullet}OH$) production (Giacosa et al., 2021). This over-expressed ROS production is utilized by cancer cells for various purposes, such as drug resistance, tumor pathogenesis, and metastasis (Ishikawa et al., 2008; Chun et al., 2021). The bi-MIL-88B MOFs, due to their trinuclear oxo cluster with terminal

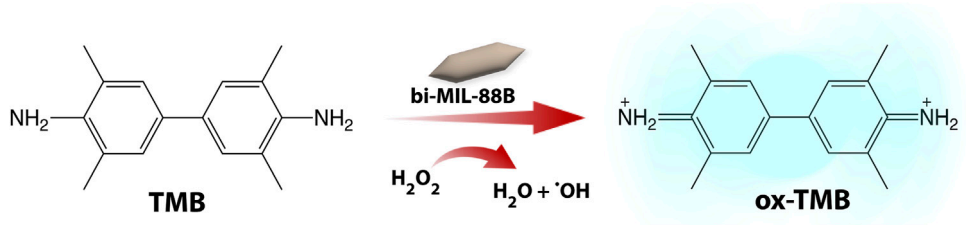

SCHEME 2
The peroxidase-like activity of bi-MIL-88B nanocarriers.

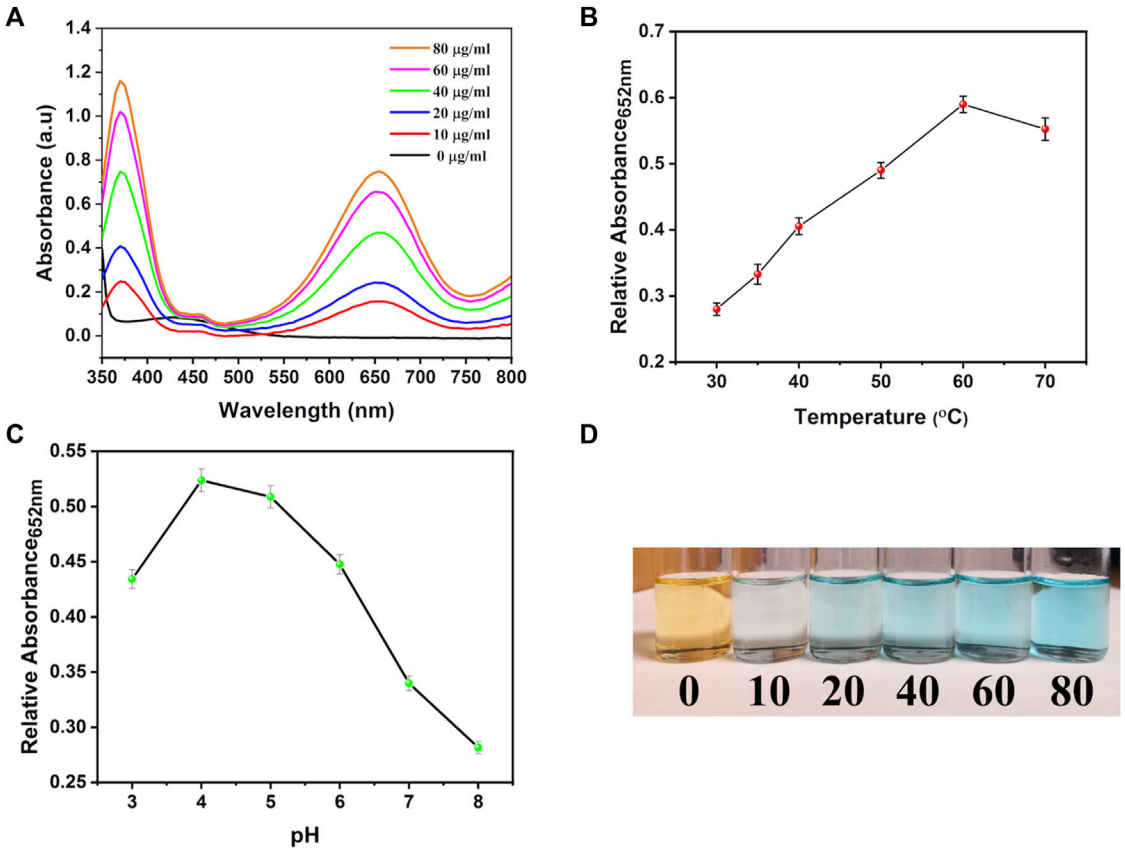

FIGURE 9
(A) TMB oxidation with different concentrations of bi-MIL-88B; **(B)** Effect of temperature and **(C)** pH on the POD activity of bi-MIL-88B; **(D)** Digital photograph of TMB color change during the oxidation process.

coordinatively unsaturated sites (CUS), are capable of decomposing H_2O into highly toxic $^{\bullet}OH$ radicals (Xiao et al., 2023). These $^{\bullet}OH$ radicals are highly potent and can oxidize any macromolecules that come in contact with them (Li H. et al., 2022).

Similar results were observed in the current study; when the system contained only H_2O_2 and TMB, no catalytic reaction was observed regarding TMB oxidation (Figure 9A). However, by adding different concentrations of the bi-MIL-88B, the colorless TMB started to convert into a blue-colored oxidized form (detected at 652 nm wavelength), indicating the POD potential. Furthermore, mechanistic studies were performed to evaluate the performance of bi-MIL-88B nanocarriers under variable pH and temperature. As seen in Figure 9B, an increase in the pH from 4 to 8 reduced the production of oxidized TMB, indicating our nanocarriers' safety at physiological pH (7.4). Higher catalytic activity in the samples in an acidic pH medium suggested the cancer cell-specific POD performance. The catalytic performance also increased by increasing the system's temperature (Figure 9C). The increased activity with higher temperatures benefits our

TABLE 2 List of reported MOF based nanocarriers functionalized with folic acid for targeted therapy.

MOF	Functionalization	Drug	Loading capacity	Stimuli	Therapy	Reference
ZIF-67@ZIF-8	Iron oxide, FA	Quercetin	50 wt%	pH	CT, CDT	Pandit et al. (2022)
BioMOF-101	FA	Curcumin	99.42 wt%	pH	CT	Alves et al. (2023)
MOF-808	FA - CS	Quercetin	43 wt%	pH	CT	Parsaei and Akhbari (2022b)
Zr-MOF	FA	Bufalin	17.4 wt%	pH, GSH	CT	Zeng et al. (2022)
PCN-224	FA	Camptothecin, Doxorubicin	10,7 and 6.8 wt%	pH	CT	Xie et al. (2022)
Fe-MIL-88@ZIF-8	FA	Doxorubicin, MnOx	43.2 wt%	pH	CT, CDT	Zeng et al. (2021)
Zn-MOF	FA - CS	Methotrexate	78 wt%	pH	CT	Khatibi et al. (2022)
UiO-66-NH2	FA	Oxaliplatin	29.3 wt%	pH	CT	Hashemzadeh et al. (2021)
ZIF-8	FA	miR-491–59		pH	Gene regulation	Ju et al. (2021)
UiO-66	FA– Pluronic F127 and SiO_2	Doxorubicin	5.6 wt%	pH	CT	Trushina et al. (2022)
Fe-MOF-5-NH2	FA, 5-FAM	5-FU	35 wt%	pH	CT	Gao et al. (2019)
Bi-MIL-88B	FA—CS	5-FU	29.8 wt%	pH	CT, CDT	This study

developed DDS, as cancer cells usually have higher internal temperatures than normal cells (Vahed et al., 2017). The enhanced POD performance under rising temperature can be related to the altered entropy of the reaction constant and reduced activation energy needed for the catalytic reaction (Åqvist et al., 2017). Based on the multidimensional therapeutic ability, 5-FU@bi-MIL-88B-FC present excellent potential in the field of multifaceted targeted therapies. Some of the MOF based carriers functionalized through FA for targeted therapies are mentioned in Table 2.

As it is crucial for the effectiveness of any therapy that drug accumulation should be in the target sites rather off-target (Farooq et al., 2019; Saddozai et al., 2020). In case of leakage to healthy tissue, adverse effects in terms of cellular cytotoxicity could be observed, leading to severe complications (Torchilin, 2010; He et al., 2020). Several factors, such as the physicochemical properties of drug molecules and tumor biology, can affect passive targeting. Therefore, these issues can be addressed by functionalizing drug-loaded nanocarriers with targeting ligands (Attia et al., 2019; Tesauro et al., 2019). FA is the most commonly used ligand for MOFs' surface functionalization to obtain FR-receptor targeting (Muhamad et al., 2018). In addition to active targeting, MOF-based nanocarriers utilizing intrinsic components of TME to generate ROS stress for a synergistic therapeutic effect along with chemotherapy present a new class of intelligent nanomaterials for efficient anticancer properties (Wang C. et al., 2022; Wang et al., 2022c; Liang et al., 2023). In this regard, bi-MIL-88B-FC can be effectively utilized as a potential DDS for multidimensional targeted chemotherapy and chemodynamic therapy based on mechanistic insights into the catalytic performance and drug release kinetics.

4 Conclusion

In this study, 5-FU@bi-MIL-88B-FC nanocarriers were synthesized for tumor-specific targeted drug delivery. The nanocarriers presented a higher 5-FU loading capacity of 29.8 wt%. Moreover, surface modification through the FA conjugated CS (FC) endowed these carriers with exceptional cell targeting and sustained drug release properties. The presence of an extra polymer coating provided a gated effect in improving the controlled release of the loaded drug and evasion of premature leakage. The 5-FU@bi-MIL-88B-FC exhibited pH-responsive drug release with higher concentrations of the 5-FU released under the tumor-mimicking environment (pH 5.2). The cytotoxicity profile and folate receptor-mediated cellular uptake was investigated against HEK-293 (FR-negative) and cancer SW480 (FR-positive). The results showed FR-positive cancer cell-specific cytotoxic effects of 5-FU@bi-MIL-88B-FC against the SW480 cells with sufficient internalization efficacy. Moreover, the peroxidase-like activity due to the catalytic sites provides these nanocarriers an extra feature to be tested for a full-fledged multidimensional anticancer therapy. The sufficient short-time stability, stimuli-responsive drug release, POD mimicking character and active targeting of FR-positive tumor cells with FA binding make these nanocarriers promising DDS for multifunctional tumor therapy.

Data availability statement

The original contributions presented in the study are included in the article/Supplementary Material, further inquiries can be directed to the corresponding authors.

Ethics statement

Ethical approval was not required for the studies on humans cell lines in accordance with the local legislation and institutional requirements because only commercially available established cell lines were used. No potentially identifiable images or data are presented in this study.

Author contributions

MA: Data curation, Formal Analysis, Investigation, Methodology, Writing–original draft. SK: Writing–review and editing. MK: Writing–review and editing. US: Writing–review and editing. NA: Funding acquisition, Writing–review and editing. AA: Funding acquisition, Writing–review and editing. MZ: Investigation, Project administration, Supervision, Writing–review and editing. MB: Conceptualization, Formal Analysis, Funding acquisition, Methodology, Project administration, Supervision, Writing–review and editing.

Acknowledgments

The authors acknowledge LUMS and Gomal University for providing technical support for the investigations into the project. The authors also extend their gratitude to The University of Lahore and Henan University for providing technical assistance in the project. And the authors acknowledge and extend their appreciation to the Researchers Supporting Project Number (RSPD2023R940), King Saud University, Riyadh, Saudi Arabia for funding this study.

Conflict of interest

The authors declare that the research was conducted in the absence of any commercial or financial relationships that could be construed as a potential conflict of interest.

Publisher's note

All claims expressed in this article are solely those of the authors and do not necessarily represent those of their affiliated organizations, or those of the publisher, the editors and the reviewers. Any product that may be evaluated in this article, or claim that may be made by its manufacturer, is not guaranteed or endorsed by the publisher.

Supplementary material

The Supplementary Material for this article can be found online at: https://www.frontiersin.org/articles/10.3389/fphar.2023.1265440/full#supplementary-material

References

Abánades Lázaro, I., Wells, C. J., and Forgan, R. S. (2020). Multivariate modulation of the Zr MOF UiO-66 for defect-controlled combination anticancer drug delivery. *Angew. Chem.* 132, 5211–5217. doi:10.1002/anie.201915848

Abbas, M., Maceda, A. M., Xiao, Z., Zhou, H.-C., and Balkus, K. J. (2023). Transformation of a copper-based metal–organic polyhedron into a mixed linker MOF for CO 2 capture. *Dalton Trans.* 52, 4415–4422. doi:10.1039/d2dt04162f

Adegoke, K. A., and Maxakato, N. W. (2021). Porous metal-organic framework (MOF)-based and MOF-derived electrocatalytic materials for energy conversion. *Mater. Today Energy* 21, 100816. doi:10.1016/j.mtener.2021.100816

Aibani, N., Rai, R., Patel, P., Cuddihy, G., and Wasan, E. K. (2021). Chitosan nanoparticles at the biological interface: implications for drug delivery. *Pharmaceutics* 13, 1686. doi:10.3390/pharmaceutics13101686

Akbar, M. U., Badar, M., and Zaheer, M. (2022). Programmable drug release from a dual-stimuli responsive magnetic metal–organic framework. *ACS omega* 7, 32588–32598. doi:10.1021/acsomega.2c04144

Akbarzadeh, I., Shayan, M., Bourbour, M., Moghtaderi, M., Noorbazargan, H., Eshrati Yeganeh, F., et al. (2021). Preparation, optimization and *in-vitro* evaluation of curcumin-loaded niosome@ calcium alginate nanocarrier as a new approach for breast cancer treatment. *Biology* 10, 173. doi:10.3390/biology10030173

Ali, A., Madni, A., Shah, H., Jamshaid, T., Jan, N., Khan, S., et al. (2023). Solid lipid-based nanoparticulate system for sustained release and enhanced *in-vitro* cytotoxic effect of 5-fluorouracil on skin Melanoma and squamous cell carcinoma. *Plos one* 18, e0281004. doi:10.1371/journal.pone.0281004

Al-Nemrawi, N. K., Altawabeyeh, R. M., and Darweesh, R. S. (2022). Preparation and characterization of docetaxel-PLGA nanoparticles coated with folic acid-chitosan conjugate for cancer treatment. *J. Pharm. Sci.* 111, 485–494. doi:10.1016/j.xphs.2021.10.034

Altintas, C., Erucar, I., and Keskin, S. (2022). MOF/COF hybrids as next generation materials for energy and biomedical applications. *CrystEngComm* 24, 7360–7371. doi:10.1039/d2ce01296k

Alvarez, P., Marchal, J. A., Boulaiz, H., Carrillo, E., Vélez, C., Rodríguez-Serrano, F., et al. (2012). 5-Fluorouracil derivatives: A patent review. *Expert Opin. Ther. Pat.* 22, 107–123. doi:10.1517/13543776.2012.661413

Alves, R. C., Quijia, C. R., da Silva, P. B., Faria, R. S., Morais, A. A. C., Morais, J. A. V., et al. (2023). Folic acid-conjugated curcumin-loaded bioMOF-101 for breast cancer therapy. *J. Drug Deliv. Sci. Technol.* 86, 104702. doi:10.1016/j.jddst.2023.104702

Anisimov, R. A., Gorin, D. A., and Abalymov, A. A. (2022). 3D cell spheroids as A tool for evaluating the effectiveness of carbon nanotubes as A drug delivery and photothermal therapy agents. *C* 8, 56. doi:10.3390/c8040056

Åqvist, J., Kazemi, M., Isaksen, G. V., and Brandsdal, B. O. (2017). Entropy and enzyme catalysis. *Accounts Chem. Res.* 50, 199–207. doi:10.1021/acs.accounts.6b00321

Attia, M. F., Anton, N., Wallyn, J., Omran, Z., and Vandamme, T. F. (2019). An overview of active and passive targeting strategies to improve the nanocarriers efficiency to tumour sites. *J. Pharm. Pharmacol.* 71, 1185–1198. doi:10.1111/jphp.13098

Bäumer, N., Tiemann, J., Scheller, A., Meyer, T., Wittmann, L., Suburu, M. E. G., et al. (2022). Targeted siRNA nanocarrier: a platform technology for cancer treatment. *Oncogene* 41, 2210–2224. doi:10.1038/s41388-022-02241-w

Beale, A. M., and Sankar, G. (2002). Following the structural changes in iron phosphate catalysts by *in situ* combined XRD/QuEXAFS technique. *J. Mater. Chem.* 12, 3064–3072. doi:10.1039/b204059j

Bokare, A. D., and Choi, W. (2014). Review of iron-free Fenton-like systems for activating H2O2 in advanced oxidation processes. *J. Hazard. Mater.* 275, 121–135. doi:10.1016/j.jhazmat.2014.04.054

Cai, X., Lin, J., and Pang, M. (2016). Facile synthesis of highly uniform Fe-MIL-88B particles. *Cryst. Growth Des.* 16, 3565–3568. doi:10.1021/acs.cgd.6b00313

Cao, D., Sha, Q., Wang, J., Li, J., Ren, J., Shen, T., et al. (2022). Advanced anode materials for sodium-ion batteries: confining polyoxometalates in flexible metal–organic frameworks by the "breathing effect". *ACS Appl. Mater. Interfaces* 14, 22186–22196. doi:10.1021/acsami.2c04077

Chang, C.-T., Ho, T.-Y., Lin, H., Liang, J.-A., Huang, H.-C., Li, C.-C., et al. (2012). 5-Fluorouracil induced intestinal mucositis via nuclear factor-κB activation by transcriptomic analysis and *in vivo* bioluminescence imaging. *PloS one* 7, e31808. doi:10.1371/journal.pone.0031808

Chanphai, P., Konka, V., and Tajmir-Riahi, H. (2017). Folic acid–chitosan conjugation: A new drug delivery tool. *J. Mol. Liq.* 238, 155–159. doi:10.1016/j.molliq.2017.04.132

Chen, Q., Wang, X., Chen, F., Zhang, Q., Dong, B., Yang, H., et al. (2011). Functionalization of upconverted luminescent NaYF4: Yb/Er nanocrystals by folic acid–chitosan conjugates for targeted lung cancer cell imaging. *J. Mater. Chem.* 21, 7661–7667. doi:10.1039/c0jm04468g

Chen, C., Yu, Y., Wang, X., Shi, P., Wang, Y., and Wang, P. (2017). Manipulation of pH-Sensitive interactions between podophyllotoxin-chitosan for enhanced controlled drug release. *Int. J. Biol. Macromol.* 95, 451–461. doi:10.1016/j.ijbiomac.2016.11.053

Chen, Z.-J., Yang, S.-C., Liu, X.-L., Gao, Y., Dong, X., Lai, X., et al. (2020). Nanobowl-supported liposomes improve drug loading and delivery. *Nano Lett.* 20, 4177–4187. doi:10.1021/acs.nanolett.0c00495

Chowdhuri, A. R., Laha, D., Pal, S., Karmakar, P., and Sahu, S. K. (2016). One-pot synthesis of folic acid encapsulated upconversion nanoscale metal organic frameworks

for targeting, imaging and pH responsive drug release. *Dalton Trans.* 45, 18120–18132. doi:10.1039/c6dt03237k

Chun, K.-S., Kim, D.-H., and Surh, Y.-J. (2021). Role of reductive versus oxidative stress in tumor progression and anticancer drug resistance. *Cells* 10, 758. doi:10.3390/cells10040758

Das, P. K., Islam, F., and Lam, A. K. (2020). The roles of cancer stem cells and therapy resistance in colorectal carcinoma. *Cells* 9, 1392. doi:10.3390/cells9061392

Di, X., Pei, Z., Pei, Y., and James, T. D. (2023). Tumor microenvironment-oriented MOFs for chemodynamic therapy. *Coord. Chem. Rev.* 484, 215098. doi:10.1016/j.ccr.2023.215098

Dibden, A., Offman, J., Duffy, S. W., and Gabe, R. (2020). Worldwide review and meta-analysis of cohort studies measuring the effect of mammography screening programmes on incidence-based breast cancer mortality. *Cancers* 12, 976. doi:10.3390/cancers12040976

El Leithy, E. S., Abdel-Bar, H. M., and Ali, R. A.-M. (2019). Folate-chitosan nanoparticles triggered insulin cellular uptake and improved *in vivo* hypoglycemic activity. *Int. J. Pharm.* 571, 118708. doi:10.1016/j.ijpharm.2019.118708

Farooq, M. A., Aquib, M., Farooq, A., Haleem Khan, D., Joelle Maviah, M. B., Sied Filli, M., et al. (2019). Recent progress in nanotechnology-based novel drug delivery systems in designing of cisplatin for cancer therapy: an overview. *Artif. Cells, Nanomed. Biotechnol.* 47, 1674–1692. doi:10.1080/21691401.2019.1604535

Foroozandeh, P., and Aziz, A. A. (2018). Insight into cellular uptake and intracellular trafficking of nanoparticles. *Nanoscale Res. Lett.* 13, 1–12. doi:10.1186/s11671-018-2728-6

Gandara-Loe, J., Souza, B. E., Missyul, A., Giraldo, G., Tan, J.-C., and Silvestre-Albero, J. (2020). MOF-based polymeric nanocomposite films as potential materials for drug delivery devices in ocular therapeutics. *ACS Appl. Mater. Interfaces* 12, 30189–30197. doi:10.1021/acsami.0c07517

Gao, X., Cui, R., Song, L., and Liu, Z. (2019). Hollow structural metal–organic frameworks exhibit high drug loading capacity, targeted delivery and magnetic resonance/optical multimodal imaging. *Dalton Trans.* 48, 17291–17297. doi:10.1039/c9dt03287h

Ge, X., Wong, R., Anisa, A., and Ma, S. (2022). Recent development of metal-organic framework nanocomposites for biomedical applications. *Biomaterials* 281, 121322. doi:10.1016/j.biomaterials.2021.121322

Giacosa, S., Pillet, C., Séraudie, I., Guyon, L., Wallez, Y., Roelants, C., et al. (2021). Cooperative blockade of CK2 and ATM kinases drives apoptosis in VHL-deficient renal carcinoma cells through ROS overproduction. *Cancers* 13, 576. doi:10.3390/cancers13030576

Gu, P. F., Xu, H., Sui, B. W., Gou, J. X., Meng, L. K., Sun, F., et al. (2012). Polymeric micelles based on poly (ethylene glycol) block poly (racemic amino acids) hybrid polypeptides: conformation-facilitated drug-loading behavior and potential application as effective anticancer drug carriers. *Int. J. Nanomed.* 7, 109–122. doi:10.2147/IJN.S27475

Guo, J., Yu, Z., Das, M., and Huang, L. (2020). Nano codelivery of oxaliplatin and folinic acid achieves synergistic chemo-immunotherapy with 5-fluorouracil for colorectal cancer and liver metastasis. *ACS Nano* 14, 5075–5089. doi:10.1021/acsnano.0c01676

Hashemzadeh, A., Amerizadeh, F., Asgharzadeh, F., Darroudi, M., Avan, A., Hassanian, S. M., et al. (2021). Delivery of oxaliplatin to colorectal cancer cells by folate-targeted UiO-66-NH2. *Toxicol. Appl. Pharmacol.* 423, 115573. doi:10.1016/j.taap.2021.115573

He, Z., Zhang, Y., and Feng, N. (2020). Cell membrane-coated nanosized active targeted drug delivery systems homing to tumor cells: A review. *Mater. Sci. Eng. C* 106, 110298. doi:10.1016/j.msec.2019.110298

Hesse, D., Badar, M., Bleich, A., Smoczek, A., Glage, S., Kieke, M., et al. (2013). Layered double hydroxides as efficient drug delivery system of ciprofloxacin in the middle ear: an animal study in rabbits. *J. Mater. Sci. Mater. Med.* 24, 129–136. doi:10.1007/s10856-012-4769-1

Horcajada, P., Serre, C., Maurin, G., Ramsahye, N. A., Balas, F., Vallet-Regi, M., et al. (2008). Flexible porous metal-organic frameworks for a controlled drug delivery. *J. Am. Chem. Soc.* 130, 6774–6780. doi:10.1021/ja710973k

Horcajada, P., Salles, F., Wuttke, S., Devic, T., Heurtaux, D., Maurin, G., et al. (2011). How linker's modification controls swelling properties of highly flexible iron (III) dicarboxylates MIL-88. *J. Am. Chem. Soc.* 133, 17839–17847. doi:10.1021/ja206936e

Horcajada, P., Gref, R., Baati, T., Allan, P. K., Maurin, G., Couvreur, P., et al. (2012). Metal–organic frameworks in biomedicine. *Chem. Rev.* 112, 1232–1268. doi:10.1021/cr200256v

Hu, Y., Ke, L., Chen, H., Zhuo, M., Yang, X., Zhao, D., et al. (2017). Natural material-decorated mesoporous silica nanoparticle container for multifunctional membrane-controlled targeted drug delivery. *Int. J. Nanomed.* 12, 8411–8426. doi:10.2147/IJN.S148438

İnce, İ., Yıldırım, Y., Güler, G., Medine, E. İ., Ballıca, G., Kuşdemir, B. C., et al. (2020). Synthesis and characterization of folic acid-chitosan nanoparticles loaded with thymoquinone to target ovarian cancer cells. *J. Radioanal. Nucl. Chem.* 324, 71–85. doi:10.1007/s10967-020-07058-z

Iqbal, B., Saleem, M., Arshad, S. N., Rashid, J., Hussain, N., and Zaheer, M. (2019). One-pot synthesis of heterobimetallic metal–organic frameworks (MOFs) for multifunctional catalysis. *Chemistry–A Eur. J.* 25, 10490–10498. doi:10.1002/chem.201901939

Iqbal, B., Laybourn, A., and Zaheer, M. (2021). Size-controlled synthesis of spinel nickel ferrite nanorods by thermal decomposition of a bimetallic Fe/Ni-MOF. *Ceram. Int.* 47, 12433–12441. doi:10.1016/j.ceramint.2021.01.100

Ishihara, K., Kitagawa, T., and Inoue, Y. (2015). Initial cell adhesion on well-defined surface by polymer brush layers with varying chemical structures. *ACS Biomaterials Sci. Eng.* 1, 103–109. doi:10.1021/ab500048w

Ishikawa, K., Takenaga, K., Akimoto, M., Koshikawa, N., Yamaguchi, A., Imanishi, H., et al. (2008). ROS-generating mitochondrial DNA mutations can regulate tumor cell metastasis. *Science* 320, 661–664. doi:10.1126/science.1156906

Jiang, K., Zhang, L., Hu, Q., Zhao, D., Xia, T., Lin, W., et al. (2016). Pressure controlled drug release in a Zr-cluster-based MOF. *J. Mater. Chem. B* 4, 6398–6401. doi:10.1039/c6tb01756h

Ju, G., Liu, B., Ji, M., Jin, R., Xu, X., Xiao, Y., et al. (2021). Folic acid–modified miR-491-5p–Loaded ZIF-8 nanoparticles inhibit castration-resistant prostate cancer by regulating the expression of EPHX1. *Front. Bioeng. Biotechnol.* 9, 706536. doi:10.3389/fbioe.2021.706536

Karimi Alavijeh, R., and Akhbari, K. (2020). Biocompatible MIL-101 (Fe) as a smart carrier with high loading potential and sustained release of curcumin. *Inorg. Chem.* 59, 3570–3578. doi:10.1021/acs.inorgchem.9b02756

Khatibi, Z., Kazemi, N. M., and Khaleghi, S. (2022). Targeted and biocompatible NMOF as efficient nanocomposite for delivery of methotrexate to colon cancer cells. *J. Drug Deliv. Sci. Technol.* 73, 103441. doi:10.1016/j.jddst.2022.103441

Leelakanok, N., Geary, S., and Salem, A. (2018). Fabrication and use of poly (d, l-lactide-co-glycolide)-based formulations designed for modified release of 5-fluorouracil. *Journal of pharmaceutical sciences* 107 (2), 513–528.

Li, L., Xiang, S., Cao, S., Zhang, J., Ouyang, G., Chen, L., et al. (2013). A synthetic route to ultralight hierarchically micro/mesoporous Al (III)-carboxylate metal-organic aerogels. *Nat. Commun.* 4, 1774. doi:10.1038/ncomms2757

Li, X., Lachmanski, L., Safi, S., Sene, S., Serre, C., Grenèche, J.-M., et al. (2017). New insights into the degradation mechanism of metal-organic frameworks drug carriers. *Sci. Rep.* 7, 13142. doi:10.1038/s41598-017-13323-1

Li, L., Han, S., Zhao, S., Li, X., Liu, B., and Liu, Y. (2020). Chitosan modified metal–organic frameworks as a promising carrier for oral drug delivery. *RSC Adv.* 10, 45130–45138. doi:10.1039/d0ra08459j

Li, Y., Jiang, Y., Zheng, Z., Du, N., Guan, S., Guo, W., et al. (2022a). Co-Delivery of precisely prescribed multi-prodrug combination by an engineered nanocarrier enables efficient individualized cancer chemotherapy. *Adv. Mater.* 34, 2110490. doi:10.1002/adma.202110490

Li, H., Zhang, Y., Liang, L., Song, J., Wei, Z., Yang, S., et al. (2022b). Doxorubicin-loaded metal-organic framework nanoparticles as acid-activatable hydroxyl radical nanogenerators for enhanced chemo/chemodynamic synergistic therapy. *Materials* 15, 1096. doi:10.3390/ma15031096

Liang, J., Zhang, W., Wang, J., Li, W., Ge, F., Jin, W., et al. (2023). Development of the Cu/ZIF-8 MOF acid-sensitive nanocatalytic platform capable of chemo/chemodynamic therapy with improved anti-tumor efficacy. *ACS Omega* 8, 19402–19412. doi:10.1021/acsomega.3c00269

Liu, H., Wang, C., Zou, S., Wei, Z., and Tong, Z. (2012). Simple, reversible emulsion system switched by pH on the basis of chitosan without any hydrophobic modification. *Langmuir* 28, 11017–11024. doi:10.1021/la3021113

Liu, Y. L., Zhao, X. J., Yang, X. X., and Li, Y. F. (2013). A nanosized metal-organic framework of Fe-MIL-88NH₂ as a novel peroxidase mimic used for colorimetric detection of glucose. *Analyst* 138, 4526–4531. doi:10.1039/c3an00560g

Liu, Q., Cong, H., and Deng, H. (2016). Deciphering the spatial arrangement of metals and correlation to reactivity in multivariate metal–organic frameworks. *J. Am. Chem. Soc.* 138, 13822–13825. doi:10.1021/jacs.6b08724

Longley, D. B., Harkin, D. P., and Johnston, P. G. (2003). 5-fluorouracil: mechanisms of action and clinical strategies. *Nat. Rev. cancer* 3, 330–338. doi:10.1038/nrc1074

Lu, B., Lv, X., and Le, Y. (2019). Chitosan-modified PLGA nanoparticles for control-released drug delivery. *Polymers* 11, 304. doi:10.3390/polym11020304

Lv, G., Qiu, L., Liu, G., Wang, W., Li, K., Zhao, X., et al. (2016). pH sensitive chitosan-mesoporous silica nanoparticles for targeted delivery of a ruthenium complex with enhanced anticancer effects. *Dalton Trans.* 45, 18147–18155. doi:10.1039/c6dt03783f

Lyu, L., Zhang, L., He, G., He, H., and Hu, C. (2017). Selective H 2 O 2 conversion to hydroxyl radicals in the electron-rich area of hydroxylated CgC 3 N 4/CuCo–Al 2 O 3. *J. Mater. Chem. A* 5, 7153–7164. doi:10.1039/c7ta01583f

Ma, M., Bétard, A., Weber, I., Al-Hokbany, N. S., Fischer, R. A., and Metzler-Nolte, N. (2013). Iron-based metal–organic frameworks MIL-88B and NH2-MIL-88B: high quality microwave synthesis and solvent-induced lattice "breathing". *Cryst. Growth Des.* 13, 2286–2291. doi:10.1021/cg301738p

Manzari, M. T., Shamay, Y., Kiguchi, H., Rosen, N., Scaltriti, M., and Heller, D. A. (2021). Targeted drug delivery strategies for precision medicines. *Nat. Rev. Mater.* 6, 351–370. doi:10.1038/s41578-020-00269-6

Mazumdar, S., Chitkara, D., and Mittal, A. (2021). Exploration and insights into the cellular internalization and intracellular fate of amphiphilic polymeric nanocarriers. *Acta Pharm. Sin. B* 11, 903–924. doi:10.1016/j.apsb.2021.02.019

Muhamad, N., Plengsuriyakarn, T., and Na-Bangchang, K. (2018). Application of active targeting nanoparticle delivery system for chemotherapeutic drugs and traditional/herbal medicines in cancer therapy: A systematic review. *Int. J. nanomedicine* 13, 3921–3935. doi:10.2147/IJN.S165210

Nejadshafiee, V., Naeimi, H., Goliaei, B., Bigdeli, B., Sadighi, A., Dehghani, S., et al. (2019). Magnetic bio-metal–organic framework nanocomposites decorated with folic acid conjugated chitosan as a promising biocompatible targeted theranostic system for cancer treatment. *Mater. Sci. Eng. C* 99, 805–815. doi:10.1016/j.msec.2019.02.017

Nemati, M., Bani, F., Sepasi, T., Zamiri, R. E., Rasmi, Y., Kahroba, H., et al. (2021). Unraveling the effect of breast cancer patients' plasma on the targeting ability of folic acid-modified chitosan nanoparticles. *Mol. Pharm.* 18, 4341–4353. doi:10.1021/acs.molpharmaceut.1c00525

Oh, H., Li, T., and An, J. (2015). Drug release properties of a series of adenine-based metal–organic frameworks. *Chemistry–A Eur. J.* 21, 17010–17015. doi:10.1002/chem.201501560

Oh, J. Y., Choi, E., Jana, B., Go, E. M., Jin, E., Jin, S., et al. (2023). Protein-precoated surface of metal-organic framework nanoparticles for targeted delivery. *Small* 2023, 2300218. doi:10.1002/smll.202300218

Okur, S., Qin, P., Chandresh, A., Li, C., Zhang, Z., Lemmer, U., et al. (2021). An enantioselective e-nose: an array of nanoporous homochiral MOF films for stereospecific sensing of chiral odors. *Angew. Chem. Int. Ed.* 60, 3566–3571. doi:10.1002/anie.202013227

Pandit, P., Bhagat, S., Rananaware, P., Mohanta, Z., Kumar, M., Tiwari, V., et al. (2022). Iron oxide nanoparticle encapsulated; folic acid tethered dual metal organic framework-based nanocomposite for MRI and selective targeting of folate receptor expressing breast cancer cells. *Microporous Mesoporous Mater.* 340, 112008. doi:10.1016/j.micromeso.2022.112008

Parsaei, M., and Akhbari, K. (2022a). Smart multifunctional UiO-66 metal–organic framework nanoparticles with outstanding drug-loading/release potential for the targeted delivery of quercetin. *Inorg. Chem.* 61, 14528–14543. doi:10.1021/acs.inorgchem.2c00743

Parsaei, M., and Akhbari, K. (2022b). Synthesis and application of MOF-808 decorated with folic acid-conjugated chitosan as a strong nanocarrier for the targeted drug delivery of quercetin. *Inorg. Chem.* 61, 19354–19368. doi:10.1021/acs.inorgchem.2c03138

Peers, S., Montembault, A., and Ladavière, C. (2020). Chitosan hydrogels for sustained drug delivery. *J. Control. Release* 326, 150–163. doi:10.1016/j.jconrel.2020.06.012

Peng, L., Asgari, M., Mieville, P., Schouwink, P., Bulut, S., Sun, D. T., et al. (2017). Using predefined M3 (μ3-O) clusters as building blocks for an isostructural series of metal–organic frameworks. *ACS Appl. Mater. Interfaces* 9, 23957–23966. doi:10.1021/acsami.7b06041

Rana, I., Oh, J., Baig, J., Moon, J. H., Son, S., and Nam, J. (2023). Nanocarriers for cancer nano-immunotherapy. *Drug Deliv. Transl. Res.* 13, 1936–1954. doi:10.1007/s13346-022-01241-3

Rojas, S., Colinet, I., Cunha, D., Hidalgo, T., Salles, F., Serre, C., et al. (2018). Toward understanding drug incorporation and delivery from biocompatible metal–organic frameworks in view of cutaneous administration. *ACS Omega* 3, 2994–3003. doi:10.1021/acsomega.8b00185

Saddozai, U. A. K., Wang, F., Cheng, Y., Lu, Z., Akbar, M. U., Zhu, W., et al. (2020). Gene expression profile identifies distinct molecular subtypes and potential therapeutic genes in Merkel cell carcinoma. *Transl. Oncol.* 13, 100816. doi:10.1016/j.tranon.2020.100816

Samimi, S., Maghsoudnia, N., Eftekhari, R. B., and Dorkoosh, F. (2019). Lipid-based nanoparticles for drug delivery systems. *Charact. Biol. Nanomater. drug Deliv.*, 47–76. doi:10.1016/b978-0-12-814031-4.00003-9

Sanchez-Lievanos, K. R., Tariq, M., Brennessel, W. W., and Knowles, K. E. (2020). Heterometallic trinuclear oxo-centered clusters as single-source precursors for synthesis of stoichiometric monodisperse transition metal ferrite nanocrystals. *Dalton Trans.* 49, 16348–16358. doi:10.1039/d0dt01369b

Sathiyaseelan, A., Saravanakumar, K., Mariadoss, A. V. A., and Wang, M.-H. (2021). pH-controlled nucleolin targeted release of dual drug from chitosan-gold based aptamer functionalized nano drug delivery system for improved glioblastoma treatment. *Carbohydr. Polym.* 262, 117907. doi:10.1016/j.carbpol.2021.117907

Sheta, S. M., El-Sheikh, S. M., and Abd-Elzaher, M. M. (2018). Simple synthesis of novel copper metal–organic framework nanoparticles: biosensing and biological applications. *Dalton Trans.* 47, 4847–4855. doi:10.1039/c8dt00371h

Shi, Z., Chen, X., Zhang, L., Ding, S., Wang, X., Lei, Q., et al. (2018). FA-PEG decorated MOF nanoparticles as a targeted drug delivery system for controlled release of an autophagy inhibitor. *Biomaterials Sci.* 6, 2582–2590. doi:10.1039/c8bm00625c

Song, H., Su, C., Cui, W., Zhu, B., Liu, L., Chen, Z., et al. (2013). Folic acid-chitosan conjugated nanoparticles for improving tumor-targeted drug delivery. *BioMed Res. Int.* 2013, 723158. doi:10.1155/2013/723158

Stella, B., Arpicco, S., Peracchia, M. T., Desmaële, D., Hoebeke, J., Renoir, M., et al. (2000). Design of folic acid-conjugated nanoparticles for drug targeting. *J. Pharm. Sci.* 89, 1452–1464. doi:10.1002/1520-6017(200011)89:11<1452::aid-jps8>3.0.co;2-p

Sun, Y., and Davis, E. (2021). Nanoplatforms for targeted stimuli-responsive drug delivery: A review of platform materials and stimuli-responsive release and targeting mechanisms. *Nanomaterials* 11, 746. doi:10.3390/nano11030746

Surekha, B., Kommana, N. S., Dubey, S. K., Kumar, A. P., Shukla, R., and Kesharwani, P. (2021). PAMAM dendrimer as a talented multifunctional biomimetic nanocarrier for cancer diagnosis and therapy. *Colloids Surfaces B Biointerfaces* 204, 111837. doi:10.1016/j.colsurfb.2021.111837

Taghavi, S., Ramezani, M., Alibolandi, M., Abnous, K., and Taghdisi, S. M. (2017). Chitosan-modified PLGA nanoparticles tagged with 5TR1 aptamer for *in vivo* tumor-targeted drug delivery. *Cancer Lett.* 400, 1–8. doi:10.1016/j.canlet.2017.04.008

Tesauro, D., Accardo, A., Diaferia, C., Milano, V., Guillon, J., Ronga, L., et al. (2019). Peptide-based drug-delivery systems in biotechnological applications: recent advances and perspectives. *Molecules* 24, 351. doi:10.3390/molecules24020351

Torchilin, V. P. (2010). Passive and active drug targeting: drug delivery to tumors as an example. *Drug Deliv.*, 3–53. doi:10.1007/978-3-642-00477-3_1

Trushina, D. B., Sapach, A. Y., Burachevskaia, O. A., Medvedev, P. V., Khmelenin, D. N., Borodina, T. N., et al. (2022). Doxorubicin-loaded core–shell UiO-66@SiO2 metal–organic frameworks for targeted cellular uptake and cancer treatment. *Pharmaceutics* 14, 1325. doi:10.3390/pharmaceutics14071325

Ulldemolins, A., Seras-Franzoso, J., Andrade, F., Rafael, D., Abasolo, I., Gener, P., et al. (2021). Perspectives of nano-carrier drug delivery systems to overcome cancer drug resistance in the clinics. *Cancer Drug Resist.* 4, 44–68. doi:10.20517/cdr.2020.59

Vahed, S. Z., Salehi, R., Davaran, S., and Sharifi, S. (2017). Liposome-based drug co-delivery systems in cancer cells. *Mater. Sci. Eng. C* 71, 1327–1341. doi:10.1016/j.msec.2016.11.073

Valencia-Lazcano, A. A., Hassan, D., Pourmadadi, M., Behzadmehr, R., Rahdar, A., Medina, D. I., et al. (2023). 5-Fluorouracil nano-delivery systems as a cutting-edge for cancer therapy. *Eur. J. Med. Chem.* 246, 114995. doi:10.1016/j.ejmech.2022.114995

van der Meel, R., Sulheim, E., Shi, Y., Kiessling, F., Mulder, W. J., and Lammers, T. (2019). Smart cancer nanomedicine. *Nat. Nanotechnol.* 14, 1007–1017. doi:10.1038/s41565-019-0567-y

Vodyashkin, A. A., Sergorodceva, A. V., Kezimana, P., and Stanishevskiy, Y. M. (2023). Metal-organic framework (MOF)—a universal material for biomedicine. *Int. J. Mol. Sci.* 24, 7819. doi:10.3390/ijms24097819

Wang, Y., Yan, J., Wen, N., Xiong, H., Cai, S., He, Q., et al. (2020). Metal-organic frameworks for stimuli-responsive drug delivery. *Biomaterials* 230, 119619. doi:10.1016/j.biomaterials.2019.119619

Wang, L., You, X., Dai, C., Fang, Y., and Wu, J. (2022a). Development of poly (p-coumaric acid) as a self-anticancer nanocarrier for efficient and biosafe cancer therapy. *Biomaterials Sci.* 10, 2263–2274. doi:10.1039/d2bm00027j

Wang, C., Xue, F., Wang, M., An, L., Wu, D., and Tian, Q. (2022b). 2D Cu-bipyridine MOF nanosheet as an agent for colon cancer therapy: A three-in-one approach for enhancing chemodynamic therapy. *ACS Appl. Mater. Interfaces* 14, 38604–38616. doi:10.1021/acsami.2c11999

Wang, L., Xu, Y., Liu, C., Si, W., Wang, W., Zhang, Y., et al. (2022c). Copper-doped MOF-based nanocomposite for GSH depleted chemo/photothermal/chemodynamic combination therapy. *Chem. Eng. J.* 438, 135567. doi:10.1016/j.cej.2022.135567

Wen, J., Liu, X., Liu, L., Ma, X., Fakhri, A., and Gupta, V. K. (2021). Bimetal cobalt-Iron based organic frameworks with coordinated sites as synergistic catalyst for fenton catalysis study and antibacterial efficiency. *Colloids Surfaces A Physicochem. Eng. Aspects* 610, 125683. doi:10.1016/j.colsurfa.2020.125683

Wongsakulphasatch, S., Nouar, F., Rodriguez, J., Scott, L., Le Guillouzer, C., Devic, T., et al. (2015). Direct accessibility of mixed-metal (III/II) acid sites through the rational synthesis of porous metal carboxylates. *Chem. Commun.* 51, 10194–10197. doi:10.1039/c5cc02550h

Xiao, K., Shu, B., Lv, K., Huang, P., Chang, Q., Wu, L., et al. (2023). Recent progress of MIL MOF materials in degradation of organic pollutants by fenton reaction. *Catalysts* 13, 734. doi:10.3390/catal13040734

Xie, B.-X., Shu, W., Wang, H.-S., Chen, L., Xu, J., Zhang, F.-Z., et al. (2022). Folic acid-modified metal-organic framework carries CPT and DOX for cancer treatment. *J. Solid State Chem.* 306, 122803. doi:10.1016/j.jssc.2021.122803

Yan, J., Liu, C., Wu, Q., Zhou, J., Xu, X., Zhang, L., et al. (2020). Mineralization of pH-sensitive doxorubicin prodrug in ZIF-8 to enable targeted delivery to solid tumors. *Anal. Chem.* 92, 11453–11461. doi:10.1021/acs.analchem.0c02599

Yang, X., Zhang, C., Deng, D., Gu, Y., Wang, H., and Zhong, Q. (2022). Multiple stimuli-responsive MXene-based hydrogel as intelligent drug delivery carriers for deep chronic wound healing. *Small* 18, 2104368. doi:10.1002/smll.202104368

Ye, G., Wan, L., Zhang, Q., Liu, H., Zhou, J., Wu, L., et al. (2023). Boosting catalytic performance of MOF-808 (Zr) by direct generation of rich defective Zr nodes via a solvent-free approach. *Inorg. Chem.* 62, 4248–4259. doi:10.1021/acs.inorgchem.2c04364

Yin, X., Alsuwaidi, A., and Zhang, X. (2022). Hierarchical metal-organic framework (MOF) pore engineering. *Microporous Mesoporous Mater.* 330, 111633. doi:10.1016/j.micromeso.2021.111633

Yu, C., Zhang, Y., Wang, N., Wei, W., Cao, K., Zhang, Q., et al. (2022). Treatment of bladder cancer by geoinspired synthetic chrysotile nanocarrier-delivered circPRMT5 siRNA. *Biomaterials Res.* 26, 6–20. doi:10.1186/s40824-022-00251-z

Yuan, C.-Z., Jiang, Y.-F., Wang, Z., Xie, X., Yang, Z.-K., Yousaf, A. B., et al. (2016). Cobalt phosphate nanoparticles decorated with nitrogen-doped carbon layers as highly active and stable electrocatalysts for the oxygen evolution reaction. *J. Mater. Chem. A* 4, 8155–8160. doi:10.1039/c6ta01929c

Zeng, X., Chen, B., Song, Y., Lin, X., Zhou, S.-F., and Zhan, G. (2021). Fabrication of versatile hollow metal–organic framework nanoplatforms for folate-targeted and combined cancer imaging and therapy. *ACS Appl. Bio Mater.* 4, 6417–6429. doi:10.1021/acsabm.1c00603

Zeng, H., Xia, C., Zhao, B., Zhu, M., Zhang, H., Zhang, D., et al. (2022). Folic acid–functionalized metal-organic framework nanoparticles as drug carriers improved bufalin antitumor activity against breast cancer. *Front. Pharmacol.* 12, 747992. doi:10.3389/fphar.2021.747992

Zhang, T.-z., Lu, Y., Li, Y.-g., Zhang, Z., Chen, W.-l., Fu, H., et al. (2012). Metal–organic frameworks constructed from three kinds of new Fe-containing secondary building units. *Inorganica Chim. Acta* 384, 219–224. doi:10.1016/j.ica.2011.12.006

Zhang, H.-J., Zhao, X., Chen, L.-J., Yang, C.-X., and Yan, X.-P. (2020). Dendrimer grafted persistent luminescent nanoplatform for aptamer guided tumor imaging and acid-responsive drug delivery. *Talanta* 219, 121209. doi:10.1016/j.talanta.2020.121209

Zhao, H., Zhao, Y., and Liu, D. (2021). pH and H2S dual-responsive magnetic metal–organic frameworks for controlling the release of 5-fluorouracil. *ACS Appl. Bio Mater.* 4, 7103–7110. doi:10.1021/acsabm.1c00710

Zhao, X., He, S., Li, B., Liu, B., Shi, Y., Cong, W., et al. (2023). DUCNP@ Mn–MOF/FOE as a highly selective and bioavailable drug delivery system for synergistic combination cancer therapy. *Nano Lett.* 23, 863–871. doi:10.1021/acs.nanolett.2c04042

frontiers | Frontiers in Pharmacology

TYPE Review
PUBLISHED 18 September 2023
DOI 10.3389/fphar.2023.1274088

OPEN ACCESS

EDITED BY
Ayaz Shahid,
Western University of Health Sciences, United States

REVIEWED BY
Jifa Zhang,
Sutro Biopharma, Inc., United States
Marco Cavaco,
Universidade de Lisboa, Portugal

*CORRESPONDENCE
Paolo Macor,
pmacor@units.it

RECEIVED 07 August 2023
ACCEPTED 07 September 2023
PUBLISHED 18 September 2023

CITATION
Riccardi F, Dal Bo M, Macor P and Toffoli G (2023), A comprehensive overview on antibody-drug conjugates: from the conceptualization to cancer therapy.
Front. Pharmacol. 14:1274088.
doi: 10.3389/fphar.2023.1274088

A comprehensive overview on antibody-drug conjugates: from the conceptualization to cancer therapy

Federico Riccardi[1], Michele Dal Bo[1], Paolo Macor[2]* and Giuseppe Toffoli[1]

[1]Experimental and Clinical Pharmacology Unit, Centro di Riferimento Oncologico (CRO), IRCCS, Aviano, Italy, [2]Department of Life Sciences, University of Trieste, Trieste, Italy

Antibody-Drug Conjugates (ADCs) represent an innovative class of potent anti-cancer compounds that are widely used in the treatment of hematologic malignancies and solid tumors. Unlike conventional chemotherapeutic drug-based therapies, that are mainly associated with modest specificity and therapeutic benefit, the three key components that form an ADC (a monoclonal antibody bound to a cytotoxic drug via a chemical linker moiety) achieve remarkable improvement in terms of targeted killing of cancer cells and, while sparing healthy tissues, a reduction in systemic side effects caused by off-tumor toxicity. Based on their beneficial mechanism of action, 15 ADCs have been approved to date by the market approval by the Food and Drug Administration (FDA), the European Medicines Agency (EMA) and/or other international governmental agencies for use in clinical oncology, and hundreds are undergoing evaluation in the preclinical and clinical phases. Here, our aim is to provide a comprehensive overview of the key features revolving around ADC therapeutic strategy including their structural and targeting properties, mechanism of action, the role of the tumor microenvironment and review the approved ADCs in clinical oncology, providing discussion regarding their toxicity profile, clinical manifestations and use in novel combination therapies. Finally, we briefly review ADCs in other pathological contexts and provide key information regarding ADC manufacturing and analytical characterization.

KEYWORDS

antibody-drug conjugate, antibodies, linkers, payloads, target therapy, cancer treatment

1 Introduction

Cancer is a multi-stage progression that transforms normal healthy cells into malignant lesions (Cooper, 2000). It is the leading cause of death worldwide, accounting for nearly 10 million deaths in 2020, and one of the most challenging diseases to treat (Sung et al., 2021). Conventional therapeutic strategies are grouped into chemotherapy, radiotherapy, immunotherapy and surgery, with the former being the main approach for treating various cancers (Dan et al., 2018). Although most remarkable goals have been achieved with small cytotoxic drugs, they had several drawbacks that limited their efficacy, including a low therapeutic index and a high off-tumor effect (Senapati et al., 2018). Usually, the low effectiveness of chemotherapy provoked a high incidence of severe side effects in patients, mainly caused by the non-specific action of

chemotherapeutic drugs on rapidly dividing normal cells (Senapati et al., 2018). Therefore, one of the hot topics in the field concerns the discovery of new chemical agents with enhanced therapeutic efficacy and that preferentially ablate tumor-derived cells, without harming the body itself (Casi and Neri, 2012). In the field of immunotherapy, several monoclonal antibodies (mAbs) have been clinically approved as they showed therapeutic benefits in both hematologic malignancies and solid tumors by selectively targeting cancer cells and by activating direct and/or indirect killing mechanisms (Weiner et al., 2009; Kimiz-Gebologlu et al., 2018; Castelli et al., 2019). However, issues including tissue accessibility, poor pharmacokinetics and lame interactions with the immune system have led to the need to exploit newer, safer and more effective targeted therapies (Chames et al., 2009; Talotta et al., 2019). In 1907, German nobel laureate Paul Erlich postulated that there could exist compounds that would selectively target pathogenic microbes, such as bacteria, while sparing normal cells, a concept gone down in history as "zauberkugel" (magic bullet) (Schwartz, 2004). From his hypothesis, an innovative therapeutic approach, known as Antibody-Drug Conjugate (ADC), has arisen in the oncology field and was firstly 40 used years ago to treat patients with advanced cancer (Ford et al., 1983). ADCs are an emerging class of pharmacological compounds that combine the potency of anti-cancer drugs (often called payloads) with the specificity of mAbs to the tumor site, thus combining chemotherapy and immunotherapy. They are composed of three portions, a mAb, an organic spacer and a cytotoxic drug. Ideally, they use the mAb targeting ability to take the cytotoxic agent, which is bound to the mAb via a stable linker, to the cancerous cells or to the cellular components of the tumor microenvironment (TME) where it can exert its anti-tumor activity and lead to cell death (Baah et al., 2021; Mckertish and Kayser, 2021; Fu et al., 2022). Compared with standard chemotherapy, this strategy offers several advantages including better drug tolerability, cytotoxicity even at low concentrations, drug stability in the bloodstream and in lysosomes, reduced off-target effects, and systemic toxicity, all features that contribute to the expansion of its therapeutic potential (Khongorzul et al., 2020; Drago et al., 2021; Mckertish and Kayser, 2021; Fu et al., 2022). Beginning with the first ADC, which was approved by the Food and Drug Administration (FDA) in 2000 (Norsworthy et al., 2018), and given the ever-evolving technology of mAbs, linkers, and payloads, by April 2023 13 different ADCs have been FDA-approved for clinical use for both solid and hematologic malignancies, setting the stage for a new era of targeted cancer therapy (Dumontet et al., 2023). In addition, a few studies have already addressed the potential use of ADCs in non-oncologic context, including infections (O'Leary et al., 2023; Tvilum et al., 2023) and autoimmune disorders (Lee et al., 2017; Yasunaga et al., 2017), with promising results showing the possibility of expanding the use of ADCs in various diseases. In this review, we aim to summarize the current knowledge of ADCs and address some key points about their molecular properties, their interaction with tumor mass and TME, their clinical use, toxicities and combinate regimens in cancer treatment. Finally, we will provide an overview on current research on ADCs in other diseases and address the main challenges and limitations in their production and characterization.

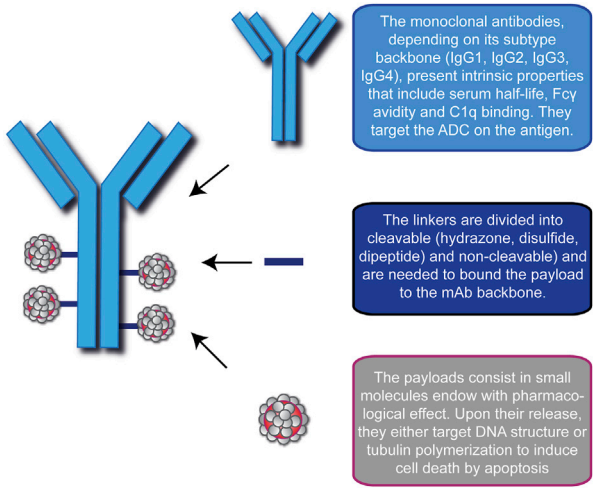

FIGURE 1
Schematic representation of the modular components of an Antibody-Drug Conjugate (ADC). ADC consists of a monoclonal antibody (blue), a linker (blue lines) and the cytotoxic drugs (gray/red). In this picture, the representative ADC on the left has a Drug-to-Antibody ratio equal to 4. A brief description of the basic function of each module is indicated on the right.

2 ADCs consist of antibodies linked to cytotoxic payloads via a linker

2.1 Antibodies form the scaffold that guides ADCs to target cells

An ADC is a synthetic molecule with pharmacological activity comprising three blocks: a selective mAb, a stable linker, and a potent cytotoxic drug (Figure 1). Together, they ensure tumor-specific targeting and efficient ablation of malignant cells by creating a "new" compound with enhanced therapeutic efficacy.

2.1.1 Full size antibodies are the most used as ADCs scaffolds

An antibody (Ab) or immunoglobulin (Ig) is a Y-shaped glycoprotein produced by plasma cells that presents an intrinsic selective ability to bind to its target (Baah et al., 2021; Pettinato, 2021). Several Abs used in oncology, upon interaction with their target antigens, possess the capacity to influence the biological activity of the tumor mass by modulating survival-related pathways and/or activating potent immune effector functions through three main mechanisms: antibody-dependent cell-mediated cytotoxicity (ADCC), in which the Fc portion of bound Ab is recognized by Natural Killer (NK) cell Fc-receptor and activates the release of lytic factors, complement-dependent cytotoxicity (CDC), in which the interaction between the Fc region and C1q triggers the classic pathway of the complement system leading to cell lysis (Macor and Tedesco, 2007; Macor et al., 2018) and antibody-dependent cellular phagocytosis (ADCP), a mechanism that relies on active macrophages to engulf tumor cells (Peters and Brown, 2015; Chen et al., 2020; Vozella et al., 2021). Similarly, tumor-targeting

Abs in ADCs shall be monoclonal and ensure high target specificity and binding affinity, long half-life in plasma, minimal immunogenicity combined with low cross-reactivity, and allow efficient internalization as well as induce direct/indirect killing effects (Peters and Brown, 2015; Dean et al., 2021; Liu and Chen, 2022). According to the amino acid sequence of their heavy chain constant regions, human Igs are classified into 5 isotypes or classes (IgM, IgG, IgA, IgE, and IgD), with IgG being the most abundant in serum. Based on further amino acid variations, this isotype can be subdivided into 4 subtypes (IgG1, IgG2, IgG3, and IgG4). IgG1 consists of the variable heavy (VH) and light (VL) domains in the N-terminal portion of the antibody, the C-domains of the light chains constant region (CL) and the heavy chain constant regions (CH1, CH2, CH3) and the hinge region between the CH1 and CH2 domains (Chiu et al., 2019). To date, its backbone is the most used in ADC preparations because of its serum half-life (~21 days), high Fcγ receptors avidity, thereby having strong immune activation of Fc-dependent pathways, and more potent complement activation (Yu et al., 2020). Beside these indirect cytotoxic mechanisms, upon the interaction with specific antigens on malignant cells, IgG1-based mAb can also exert direct killing effects by blocking pathways associated to cancer cell proliferation, metastasis and invasiveness (Natsume et al., 2009; Drago et al., 2021). As for the other subclasses, IgG2 plays a role in the response against bacterial capsular polysaccharides but exhibits low Fcγ receptor avidity, low plasma concentration and tends to form covalent dimers that likely lead to aggregation and ADC inefficacy (Zhang et al., 2018). IgG3 protects the body from a range of intracellular bacteria, parasites, and viruses. They are potent mediators of effector functions, including enhanced ADCC and CDC responses, but they are also the subtype with the shortest circulating half-life (Stapleton et al., 2011; Hoffmann et al., 2018), limiting their suitability for ADCs. The IgG4 subtype has a similar half-life to IgG1 and IgG2 but is less efficient at triggering the C1q-related pathway because it has only intermediate affinity for the Fc receptor on phagocytic cells (Spiess et al., 2013; Fu et al., 2022). However, the ability to induce a poor immune response results in a more favorable safety profile compared to the IgG1 backbone, making IgG4 ADCs suitable in cases where antibody-mediated cytotoxicity is not desired (Herbener et al., 2018).

2.1.2 Antibody-fragments represent a new and innovative approach in ADC strategy

A growing number of studies raises questions regarding the usage of full-size IgG moiety in the treatment of solid cancers and points to some critical limitations, particularly on its size (Deonarain et al., 2018; Richards, 2018). As IgG1, which is the most used in ADC synthesis, is quite large (150 kDa) it may hinder the distribution of the drug in the tumor mass and consequently affect in a negative manner ADC pharmacokinetics and the therapeutic outcome. Although this issue may find a partial solution in the tumor-associated leaky vasculature, which shall still allow sufficient pharmacological benefit due to the retention and permeability effect (EPR) (Ferl et al., 2006), its efficiency and the microdistribution of the compound in the tumor depend on many factors, such as ADC preparations and molecular and cellular signatures of the mass (Deonarain et al., 2018; Richards, 2018). Other problems related to scaffold size include systemic accumulation and slowed target-independent clearance rate (Adams et al., 2001; Jain, 2001; Thurber and Dane Wittrup, 2012). Because of these limitations, researchers are seeking new "miniaturized" versions of natural antibodies (also known as antibody-fragments) as a new and smaller drug-conjugatable alternative to expand the ADC therapeutic benefits. These fragments are produced either by proteolytic cleavage of full-size antibodies or by recombinant protein engineering and primarily retain the binding capacity of full-size IgG through the VH and VL regions (Brinkmann and Kontermann, 2017; Kholodenko et al., 2019). They present engineered scaffolds that lack the CH2 domain and Fc region and include three different formulations: the Fab format, a ~50 kDa structure in which VL and VH are bound to CL and CH1, respectively, and linked by a disulfide bond between the chains, the single-chain variable fragment (scFv), a ~27 kDa structure in which VH is linked to VL by a short peptide linker, and the diabody, a non-covalent ~55 kDa dimer scFv consisting of the VH and VL regions linked by a small peptide linker (Xenaki et al., 2017; Deonarain et al., 2018; Kholodenko et al., 2019). In addition, small immunoproteins (SIPs) composed of dimerized scFvs through a CHε4 domain are a fragmentated format developed against fibronectin and other vascular antigens (Perrino et al., 2014). By preserving the targeting capacity of the full-size antibody and combining it with smaller and dynamic formats, antibody-fragments have the potential to overcome some of the major drawbacks of full-size Ig moieties and may represent an innovation in the treatment of solid tumors. To date, promising data showed a remarkable improvement in stability, tumor targeting and penetration and epitope accessibility, particularly in cancers that are still difficult to reach via conventional IgG-based ADCs (Dennis et al., 2007; Thurber et al., 2008). In addition, smaller formats should be better tolerated by the body and produce fewer adverse effects mainly because they do not show cross-reactivity caused by the interaction with Fc receptor and targeted immune cells (Cilliers et al., 2018; Gogesch et al., 2021). If these benefits should be assessed to a greater extent, significant weaknesses can be identified. For example, because of their smaller size and the absence of the Fc domain, without which they cannot trigger the neonatal Fc receptor rescue pathway, antibody-fragments are degraded more rapidly and potentially do not remain in the body long enough to exert sufficient anti-tumor activity. From this perspective, one solution might be to control the dosing regimen by administering higher and/or more frequent doses to achieve a therapeutic effect, but too little is known about the behavior of these formats in the clinic and extensive efforts are underway to improve their feasibility (Deonarain et al., 2018; Deonarain and Xue, 2020). Moreover, the absence of the Fc domain severely limits the possibility of activating the immune system, thus losing an important partner in the fight against the tumor progression. Besides these formulations, scaffolds not based on antibodies are currently being explored (Luo et al., 2022; Kaplon et al., 2023). Nevertheless, though the Ab moiety properties must be carefully considered, the choice of linker and payload are equally important to create the most suitable therapeutic ADC.

2.2 Linkers are sequences that connect antibodies to payloads by a chemical bond

In the development of the ADC strategy, linkers represent the technology that ensures a bridge between the mAb and the cytotoxic payload. They are the most modifiable part of an ADC and influence its biophysical and functional properties such as stability, potency, efficacy, and toxicity. The two main purposes of linkers are to prevent the premature release of the cytotoxic drug in the blood circulation and to ensure its efficient release at the target site (Lu et al., 2016; Bargh et al., 2019). Depending on the release mechanisms of the payloads, linkers can be broadly classified into two classes: cleavable and non-cleavable. Recent advances in linker chemistry, including formulations not currently used in clinical ADCs, such as biorthogonal, photo-responsive and Fe(II)-cleavable linkers, are discussed in Su et al., 2021.

2.2.1 Cleavable linkers are versatile and widely employed in ADCs

Cleavable linkers are most commonly used in the synthesis of ADCs and are designed to disengage the cytotoxic drug in response to changes in environmental conditions (pH, redox potential, GSH concentration, or enzymatic activity) that occur between the bloodstream, the tumor cells and the TME niche. They are stable under physiological conditions and, following the internalization of the ADC into the tumor cell, they are rapidly cleaved to ensure selective release of the cytotoxic preparation (Peters and Brown, 2015; Tsuchikama and An, 2018). In addition, these linkers are often cleaved in the TME because of its higher acidity and oxidative stress, making them the most used preparation to affect large solid masses barely impenetrable to full-size antibodies (Ponziani et al., 2020). Cleavable linkers are commonly divided into chemical (hydrazone and disulfide bonds) and enzyme (peptide bonds and glucuronide) cleavage linkers (Bargh et al., 2019). Hydrazone linkers are an example of acid-labile linkers used mainly in hematologic malignancies. They are usually stable in the physiological pH range of the blood circulation and undergo hydrolysis within the acidic microenvironment of the endosomes and lysosomes (pH 4.8–6.2) of the tumor cell (Jain et al., 2015). Similarly, linkers based on disulfide bonds are stable in the bloodstream alkaline environment, but payload release is sensitive to glutathione (GSH), a metabolite whose concentration is much higher in the cytoplasm of cancer cells (Balendiran et al., 2004; Estrela et al., 2006). However, both linkers raised concerns about their non-targeted cytotoxicity (Baah et al., 2021; Fu et al., 2022). Peptide bonds ensure that ADC remains integral in the circulation and enable the release of the cytotoxic drug upon interaction with lysosomal proteases (Tsuchikama and An, 2018), such as cathepsin B, which is generally overexpressed in several tumor cell types (Gondi and Rao, 2013). Peptide linkers are associated with improved serum stability and anticancer activity compared chemical linkers (Lu et al., 2016; Tang et al., 2019; Khongorzul et al., 2020). In addition, linkers based on glucuronide bonds, another type of enzyme-sensitive chemical bridge, are commonly used in ADCs design and rely on cleavage by β-glucuronidase, the level of which is often high in the tumor cellular microenvironment (Kostova et al., 2021).

2.2.2 Non-cleavable linkers avoid non-specific payloads release

Non-cleavable linkers include maleimidocaproyl (MC) and 4-maleimidomethyl cyclohexane-1-carboxylate (MCC) structures and consist of chemical structures that are not fragmented by enzymatic degradation. They are inert to conventional chemicals but allow the release of the cytotoxic drug once the mAb has been completely catabolized by the lysosome. In this way, they release their toxic payload into the tumor target cells without harming normal healthy cells. Due to their chemical synthesis, these linkers offer some advantages over the cleavable alternative, including lower toxicity and longer half-life in plasma (Baah et al., 2021; Fu et al., 2022). On the other hand, their limitations are mainly related to their mechanism of action as they are strongly dependent on an efficient intracellular trafficking and on cellular components with high-expression and internalizing antigens (Lu et al., 2016; Tsuchikama and An, 2018).

2.3 Payloads consist of potent cytotoxic agents against tumor cells

As described above, the linker serves as a spacer to connect the mAb to the payload, a cytotoxic drug that must be released in the tumor site to properly exert its pharmacological effects. To be suitable as payloads in ADCs, chemicals shall ideally have low molecular weight and immunogenicity, high stability in the blood circulation and endosomal/lysosomal pathways, and high cytotoxicity (Peters and Brown, 2015; Khongorzul et al., 2020; Baah et al., 2021; Mckertish and Kayser, 2021). Because intravenous administration has shown that only a very small fraction of ADC reaches the tumor (0.1%–2%) (Chari, 2008; Hughes, 2010; Beck et al., 2017), their payloads must be 100- to 1000-fold more effective than the drugs used in chemotherapeutics as free small molecules (Baah et al., 2021). Given that the goal of the ADC strategy is to achieve potent cytotoxic activity, an important attribute to consider in the design process of these compounds is the Drug-to-antibody ratio (DAR), a value that indicates the average number of chemical molecules conjugated to the mAb. For current conjugation methods based on lysine side-chain amidation or mainly on the reduction of cysteine intermediate-chain disulfide bonds, the common DAR values range from 0 (lowest value) to 8 (highest value) (Dan et al., 2018; Wagh et al., 2018; Sun Kang et al., 2021). Nevertheless, *in vivo* experiments have demonstrated that a high DAR value negatively correlates with Ab pharmacokinetics. Although a low DAR implies the loading of poor number of drug molecules and consequently lower therapeutic efficacy, it is worth noting that an average DAR of 2 to 4 results in an ADC with greater anti-cancer activity/efficacy compared to an ADC with higher DAR, likely because the latter is more rapidly cleared from the body when compared to the corresponding average-conjugated counterparts (Hamblett et al., 2004; Strop et al., 2015). Nowadays, cytotoxic payloads usually act as DNA-damaging agents or tubulin inhibitors, but novel potential drugs under investigation include inhibitors of B-cell lymphoma-extra large (Bcl-xL) anti-apoptotic protein, RNA and Niacinamide phosphate ribose transferase (NAMPT) inhibitors, and carmaphycins, inhibitors of proteasome activity (Wang et al., 2023).

2.3.1 DNA-damaging drugs act as crosslinkers, alkylators and topoisomerase inhibitors

The available agents that induce cell death by damaging DNA can act up to picomolar concentrations (Hartley, 2011) and affect both proliferating and non-proliferating cells, so they can potentially contribute to the ablation of the tumor mass by affecting tumor-initiating cells (Cheung-Ong et al., 2013; Bornstein, 2015). From a mechanistic point of view, these chemicals alter the double helix in different ways, e.g., by inducing single/double strand breaks, alkylation and cross-linking of the DNA minor groove, or by inhibiting Topoisomerase I/II and thus replication. Some of them include amanitins (naturally byciclic octapeptides that inhibit RNA Polymerase II action and disrupt RNA and protein synthesis), calicheamicins (DNA-interactive antitumor antibiotics, that cause DNA double-strand breaks and inhibit replication), duocarmycins (natural DNA minor groove alkylating molecules), and pyrrolobenzodiazepines (highly potent DNA minor groove crosslinking agents). Two other compounds that have been used in first-generation ADCs that are worth mentioning are camptothecin (DNA topoisomerase I inhibitor at the replication bubble) and doxorubicin (antibiotic molecule that damages DNA by intercalating into it and generating free radicals) (Sau et al., 2017; Fu and Ho, 2018; Baah et al., 2021; Mckertish and Kayser, 2021).

2.3.2 Tubulin-targeting agents block the mitotic fuse formation and the cell cycle

Tubulin inhibitors block the rapid proliferation of tumor cells at the G2/M cell cycle stage by binding tubulin subunits, leading to cell death by apoptosis. This class includes maytansinoids and auristatins, a family of tubulin-inhibiting cytotoxins that arrest cells in metaphase. The auristatin derivatives monomethyl auristatin E (MMAE) and the less toxic F (MMAF) (Park et al., 2019) are commonly used as payloads in ADC design and exert their function by blocking tubulin polymerization, thereby perturbing microtubule growth and causing cell cycle arrest (Sau et al., 2017; Baah et al., 2021; Mckertish and Kayser, 2021). Looking at the mechanism in detail, microtubule formation involves either nucleation or assembly of the αβ-tubulin heterodimer into a microtubule seed in the cytoplasm (Francisco et al., 2003; Goodson and Jonasson, 2018). As auristatin, by interfering with GTP hydrolysis on the β subunit, causes an excessive and sustained growth of microtubules, they lose the ability to shorten and separate sister chromatids in anaphase, causing cells to freeze in metaphase of mitosis (Waight et al., 2016).

2.4 The development of ADC therapeutic strategy goes through three generations of compounds

In the last years the ADC development path brought into the marketplace a dozen ADCs against various hematologic and solid malignancies. Generally, these ADCs have been divided into three generations (first, second, and third) according to the type of mAb, the chemistry of the linker, the mechanism of action as well as the relationship between DAR and the conjugation method (Sau et al., 2017; Fu et al., 2022). Representing the first attempt at a novel therapeutic strategy, the first-generation ADCs caused acute adverse effects, such as hematotoxicity, and morbidity in patients, mainly due to the mAbs backbone, linker chemistry, and target non-specificity rather than the drug itself (Sau et al., 2017). Originally, these biologics utilized mouse-derived and then chimeric mAbs conjugated via unstable linkers to the few weakly potent drugs available in chemotherapy. Unfortunately, after administration, these mAbs were recognized as non-self from the body and inevitably triggered an immune response through the formation of human anti-mouse antibodies (HAMA), often leading to serious immunogenicity problems (Kim and Kim, 2015). In addition, the chemistry of acid-labile linkers, which are quite unstable at bloodstream pH, led to uncontrolled release of payloads (Beck et al., 2017), such as calicheamicin, duocarmycin, and doxorubicin, whose potency was in any case too low to cause cancer cell death. In this context, stochastic conjugation to random lysines did not allow to control DAR and resulted in heterogeneous mAbs mixtures containing unconjugated, partially conjugated, and overconjugated mAbs in unknown proportions, which negatively affected ADC efficacy, limited tumor penetration, and resulted in a narrow therapeutic window (Lucas et al., 2018). Furthermore, antigens were selected even though they lacked tumor-specific expression, resulting in severe systemic off-target effects (Sau et al., 2017; Fu et al., 2022). As expected, based on the limitations of the first-generation ADCs, the second-generation ADCs offered some implementations aimed at improving compound efficacy and largely reducing off-target toxicity. To limit potential side effects associated with the mAb backbone as much as possible, humanized mAbs were preferred over mouse-derived or chimeric mAbs due to the lower immunological response upon administration (Lambert and Chari, 2014). Cleavable linkers have been replaced by the non-cleavable alternative to ensure the stability of ADCs in the blood and to reduce the premature and dangerous release of drugs (Sau et al., 2017; Tsuchikama and An, 2018). In addition, far more potent cytotoxic chemicals have been discovered and selected to induce cell death by attacking DNA structure (disrupting its double helix conformation) and tubulin polymerization (disrupting mitotic fusion formation) (Carter and Senter, 2008; Senter, 2009). Due to the low amount of ADC *in situ*, the IgG1 subtype was preferred over IgG4 because it has better targeting abilities and better conjugation capabilities (Lambert and Chari, 2014). However, despite the introduction of improvements in linker stability and higher drug cytotoxicity, the main weaknesses of this generation of ADCs were still heterogeneous DAR (4–8), rapid clearance for high DAR drugs, off-target toxicity, and drug resistance effects (Sau et al., 2017). What makes the third generation of ADCs the best (so far) is based on fully human mAbs, avoiding the disadvantage of immunogenicity, and optimization in terms of linker stability, payload cytotoxicity, and site-specific conjugation. This new method consists in an evolution of previous ones and was introduced to address heterogeneous DARs and consequently improve ADC pharmacokinetics and utility (Fu et al., 2022). To this end, the synthesis of recombinant Abs bearing engineered cysteine residues enabled the precise bioconjugation of various drugs, resulting in the so-called THIOMAB drug conjugates (TDCs). The THIOMAB antibody technology platform results in a highly stable and effective ADC, whose DAR value is almost uniform (from 2 to 4) and is associated with fewer systemic side effects, improved drug activity, toxicity, and

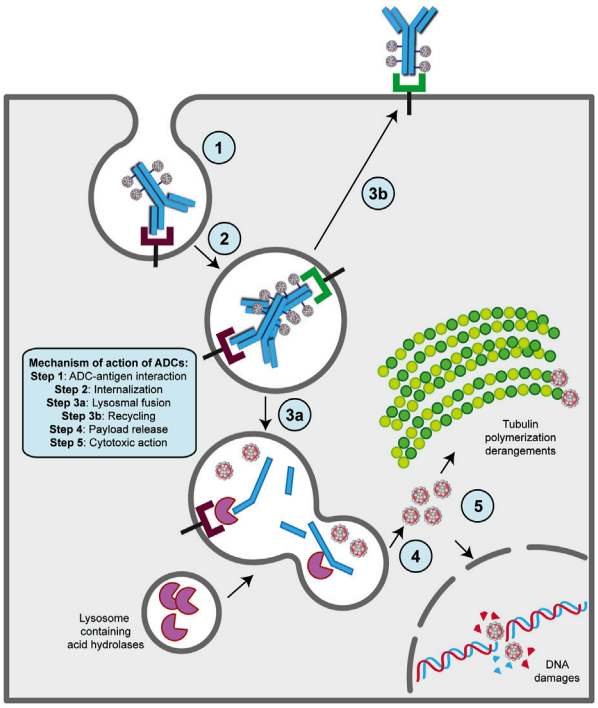

FIGURE 2
Mechanism of action of ADC strategy. The major steps of the process are indicated on the figure. Basically, following ADC-target interaction on the surface of cancer cell (step 1), this complex undergoes receptor-mediated endocytosis and enters the endosomal/lysosomal pathway until the payload is released in the cytoplasm (steps 2, 3a and 4). Then, the drug can exert its killing activity either damaging DNA structure in the nucles or derange mitotic fuse polymerization (step 5), leading to cell death by apoptosis. A fraction of ADCs binds to FcRn receptors in the early step on endosomal/lysosomal pathway and get transported out of the cell (step 2a and 3b).

efficacy (Junutula et al., 2008). In addition, despite the potential toxicity due to the high potency of the payloads, these ADCs have lower immunogenicity and hydrophilic linkers, giving patients a more chance to counteract cancer progression (Baah et al., 2021; Fu et al., 2022).

2.5 Binding to specific tumor-related targets triggers internalization and cytotoxicity of ADCs

2.5.1 Choosing the right targeting antigen is critical for ADCs killing

Considering that one of the advantages of ADC is that a potent cytotoxic drug can be delivered specifically to cancer cells, the choice of target antigen must be the first consideration in developing this strategy. To take advantage of the maximal therapeutic index of ADCs, the ideal antigen should be a cell surface structure (such as proteins, glycoproteins, or aberrant gangliosides) that is highly or predominantly expressed on tumor cells compared to healthy, normal cells, or at least abundant on malignant, disease-associated cells (Damelin et al., 2015; Peters and Brown, 2015). Ideally, the target proteins should be tumor-specific antigens (TSAs), which are present only on cancer cell types, and/or tumor-associated antigens (TAAs), which are proteins that are highly overexpressed in tumors but rare or sparsely present in normal tissue. In conjunction with this feature, the epitope of the antigen should ideally face the extracellular matrix (rather than the internal site) to ensure easier accessibility and interaction with ADC after diffusing from blood vessels (Tipton et al., 2015; Zhao et al., 2020). In addition, to avoid undesirable systemic side effects and safety issues, the target antigen should be a protein that is anchored to the membrane and not secreted into the blood circulation. If this were the case, ADC would promote unwanted binding outside the tumor and thus reduce the anticancer effect on malignant cells (Ritchie et al., 2013; Zhao et al., 2020). Nevertheless, after the ADC interaction, the optimal antigen should ensure proper internalization of the antigen- ADC complex into the endosomal/lysosomal pathway, leading to drug release and ultimately cytotoxicity. It should be noted that the speed and efficiency of the internalization process strictly depend on the nature of the target, the type of the epitope, and the payload conjugated to ADC (Carter and Senter, 2008; Donaghy, 2016; Fu et al., 2022). Finally, since the tumor mass and its surrounding microenvironment (TME) are tightly coupled and constantly communicate with each other, TME components have been targeted as novel potential ADC targets (see below in the text) (Andersen, 2023).

2.5.2 The mechanism of action of ADCs requires internalization to exert antitumor cytotoxicity

The presence of a mAb targeting an antigen that is either specifically present on cancer cell types or highly overexpressed during carcinogenesis is a fundamental requirement for the ADC strategy (Alley et al., 2010; Damelin et al., 2015). With this in mind, the mechanism of action of ADCs is quite simple and allows for therapeutic action against the disease as well as potent on-target cytotoxicity (Figure 2) (Peters and Brown, 2015; Khongorzul et al., 2020; Drago et al., 2021; Samantasinghar et al., 2023). After administration, usually by intravenous injection to preserve drug functionality (Nolting, 2013), the mAb portion of the ADC binds to the target antigen on cancer cells, and after internalization of the antigen- ADC complex by receptor-mediated endocytosis, the newly formed early endosome matures into a late endosome that ultimately fuses with the lysosome. In this cellular compartment, acidic or redox conditions combined with the presence of proteases (cathepsin B, plasmin, etc.) allow the detachment of the cytotoxic payload from its mAb carrier, whereupon the drug diffuses into the cell and leads to cell death by attacking DNA structure or microtubule polymerization (Peters and Brown, 2015; Khongorzul et al., 2020; Drago et al., 2021; Samantasinghar et al., 2023). Of note, the IgG subtype that is widely employed in ADC synthesis can be rescued from the endosomal/lysosomal degradation pathway and recycled outside cells through interaction with the neonatal Fc receptor (FcRn), an IgG receptor involved in the regulation of IgG turnover. Therefore, this FcRn-mediated transcytosis into the extracellular space, although involving only a small percentage of the internalized ADC -complex, can potentially enhance the clearance of ADC and thus reduce its therapeutic index (Xu, 2015). On the other hand, if the small molecule is permeable to the cell membrane, it can partially

diffuse back into the extracellular matrix and enter neighboring cells regardless of the expression level of the antigen, causing a "bystander effect" (Staudacher and Brown, 2017). This phenomenon, by altering components of the TME, such as neovascular endothelial cells and/or cancer-associated fibroblasts (CAFs), could further enhance the killing effect of ADC, especially in cancer lesions with high heterogeneous target expression (Gerber et al., 2009; Purcell et al., 2018; Szot et al., 2018). Moreover, the therapeutic strategy of ADCs involves other killing mechanisms to ensure efficacy against cancer. In several contexts, it has been shown that the interaction of the mAb with its specific target can directly cause potent inhibition of downstream signaling pathways triggered by antigen receptor stimulation (Albanell et al., 2003; Vu and Claret, 2012; Marei et al., 2022). While the Fab fragment of the carrier is bound to the target epitope on the malignant cell, the Fc portion of the same mAb can interact with the FcR on NK cells and macrophages, triggering ADCC and ADCP, respectively, as well as the C1q component of the complement system, triggering CDC (Junttila et al., 2011; Tai et al., 2014; Redman et al., 2015).

2.6 The TME offers new potential targets to ADCs strategy

Most of the ADCs in preclinical and clinical development target TAAs or TSAs localized mainly on the cancer mass (Sau et al., 2017; Tong et al., 2021). Compared to hematologic malignancies, solid tumors thrive in a complex and dynamic entity called the TME, whose composition can vary widely depending on the tumor type. Key features of the TME generally include abundant extracellular matrix, stromal cells (e.g., cancer-associated fibroblasts, CAFs), new and abnormal blood vessels, and immune cells, the latter capable of infiltrating the tumor mass and exerting pro- and anti-tumor functions (Anderson and Simon, 2020; Baghban et al., 2020). Particularly in the early stages of tumor growth, a bidirectional and complex interaction exists between cancer cells and the TME components through the release of soluble factors that promote the survival of the tumor mass, its local invasion and subsequent metastatic spread (Visser and Joyce, 2023). In this sense, the TME supports the basic needs of the tumor through a neo-angiogenesis program that removes metabolic waste and, most importantly, restores oxygen and nutrient supply to the mass (Anderson and Simon, 2020; Visser and Joyce, 2023; Wang et al., 2023). Given the close relationship between these two entities, TME-associated antigens (TMAs), i.e., proteins that are dysregulated on non-malignant cells within the TME, offer new potential targets for the treatment of solid tumors as they differentiate from more traditional tumor antigens (Andersen, 2023). Major TMAs include chemokines and cytokines, transcription factors, metabolic enzymes, and checkpoint molecules. Some of their advantages lie in their overexpression on endothelial, stromal, and immune cells, whereas they are rare or very low in healthy tissues, and in their easier accessibility to ADCs when administered into the bloodstream, especially to antigens present on neo-vessels or stromal cells. Furthermore, because TME components are distinct from cancer cells, they are less susceptible to resistance mechanisms caused by inefficient DNA repair mechanisms (Agrafiotis et al., 2022; Ceci et al., 2022; Andersen, 2023). The development of agents against these antigens not only weakens the tumor mass but also provides the opportunity to modulate the TME itself, making it less immunotolerant and more susceptible to tumor ablation (Andersen, 2023). Preclinical and clinical evidence suggest that cell types/factors belonging to the tumor extracellular matrix and neo-blood vessels may be valuable choices for new ADC target antigens (Peters and Brown, 2015; Xiao and Yu, 2021). For instance, an ADC targeting stromal cells may cause cell death by altering the concentration of growth factors in the tumor niche or induce hypoxia and nutrient deprivation by binding to an antigen on the neo-vasculature (Jain, 2005; Mahadevan and Von Hoff, 2007; Xiao and Yu, 2021). In this regard, it is worth mentioning the effect of the "binding site barrier" (BSB), a phenomenon that occurs between mAb and cell populations near blood vessels and retains part of the ADC near them, reducing the penetration of Ab into the tumor mass (van Dongen, 2021). However, most TMAs have been identified on cells of the immune system and targeting them offers an innovative anti-cancer therapeutic approach achieved by promoting effector cell proliferation, the anti-cancer cytokine/chemokine production, and overall survival to create a new immune-hostile tumor niche with reduced neo angiogenesis (Gajewski et al., 2006; Labani-Motlagh et al., 2020; Andersen, 2023; Del Prete et al., 2023). To date, some TMAs targeted by novel ADCs include CD74, an MHC class chaperone II targeted by the ADC STRO-001, currently in phase I in the treatment of B-cell malignancies (NCT03424603) (Le et al., 2023) and CCR7, a chemokine receptor targeted by the novel ADC JBH492 in non-Hodgkin lymhoma and chronic lymphocytic leukemia patients (NCT04240704). In addition, Camidanlumab tesirine, also known as ADCT-301, is an ADC in phase 1/2 for the treatment of classical Hodgkin's lymphoma (cHL) and non-HL (NCT02432235) (Hamadani et al., 2021), and CD276, an immune checkpoint overexpressed during pathologic angiogenesis and an interesting candidate target of different ADCs in advanced solid tumors (NCT04145622, NCT03729596 and NCT03595059) (Ceci et al., 2022; Ziogas et al., 2023).

2.7 Cancer creates different ways to escape the effectiveness of ADCs

A well-known feature of cancers is their ability to overcome the efficacy of therapeutic approaches, making them susceptible to various mechanisms of resistance. The evasion mechanisms developed by malignant cells can be divided into down-/high-regulation of antigen, the presence of drug efflux pumps, defects in lysosomal functions, and deregulation of signaling pathways involved in cell cycle progression and apoptotic dysregulation (Shefet-Carasso and Benhar, 2015; Loganzo et al., 2016; García-Alonso et al., 2018). In this context, an association between antigen levels and the efficacy of ADC treatment with brentuximab vedotin was observed, whose multiple treatment cycles correlated with CD30 downregulation and consequently stronger tumor resistance to MMAE (Chen et al., 2015). In another study, the cancer cell line JIMT1-TM showed long-term resistance to the drug after repeated administration of anti-human epidermal growth factor receptor 2 (anti-HER2) transtuzumab maytansinoid, as the level of HER2 protein decreased (Loganzo et al., 2015). Nevertheless,

upregulation of CD33 antigen in the blood limited gemtuzumab ozogamicin penetration into the bone marrow, suggesting that elevated CD33 levels still negatively affect treatment and likely reduce drug exposure (van der Velden et al., 2004). Another non-negligible mechanism of resistance relies on a family of transmembrane proteins called ABC transporters (Zheng et al., 2021). These transmembrane proteins act as drug efflux pumps, causing various chemicals, including those used as payloads, to be excreted from the cancer cell, making it resistant or at least less susceptible to treatment (Zheng et al., 2021). This mechanism has been observed in AML cells, in which overexpression of the ABC-family member MDR1 made them resistant to gemtuzumab ozogamicin (Matsumoto et al., 2012; Senter and Sievers, 2012) and in breast carcinoma cells, in which cyclic dosing of TDM-1 induced an increase in ABCC1 transporter levels (Loganzo et al., 2015). Another escape mechanism involves lysosomal acidification. After administration of ADC and internalization, linkers are cleaved by lysosomal acid hydrolases to subsequently release the cytotoxic agent into the cytoplasm of cancer cells. However, upon persistent treatments malignant cells may acquire the ability to disrupt this process by altering the pH of the lysosomal compartment to slow the catabolic activity of their proteases, a process that has been demonstrated in HER2-positive breast cancer clones resistant to long-term T-DM1 (Ríos-Luci et al., 2017; García-Alonso et al., 2018). Nevertheless, perturbations in signaling pathways involved in cell cycle regulation and alterations in apoptotic regulation may also modulate tumor cell sensitivity to ADC (Collins et al., 2019). In T-DM1-resistant HER2-positive breast cancer cells, an increase in cyclin B levels, a protein required for the G2/M cell cycle transition, has been observed. This upregulation at the protein level could affect cell cycle dynamics by altering sensitivity to treatment with ADC (Sabbaghi et al., 2017). Moreover, in AML cells, activation of a related pathway (PI3K/Akt) was associated with lower efficacy of gemtuzumab ozogamicin and a deletion in the PTEN pathway was associated with trastuzumab low effectiveness (García-Alonso et al., 2018). Of note, in the same hematologic tumor, overexpression of members of the anti-apoptotic BCL-2 and BCL-X families plays a role in sensitivity to gemtuzumab ozogamicin (Godwin et al., 2020).

2.8 Clinically approved ADCs for the treatment of hematologic and solid malignancies

The ADC strategy represents a highly successful therapeutic alternative in cancer treatment. The excellent ability to deliver a pharmacological compound *in situ* by drawing the mAb of choice along with various linkers and chemical alternatives represented an innovative development compared to mAb-only based therapy and traditional chemotherapy. As mentioned earlier, although the development of ADC remains challenging in terms of drug safety, efficacy, and targeting, the development of new and more precise technologies, as well as the identification of new targets and components, has led to an explosion in the use of ADC in clinical oncology (Drago et al., 2021; Dumontet et al., 2023; Fuentes-Antrás et al., 2023). To date, hundreds of ADCs are in clinical trials, and 15 of them have been approved by the FDA, the European Medicines Agency (EMA), and/or other government agencies and launched into the marketplace for the treatment of hematologic malignancies and solid tumors. Over the past 23 years, the following ADCs have been developed for the treatment of hematologic tumors: Gemtuzumab ozogamicin (Mylotarg®), Brentuximab vedotin (Adcetris®), Inotuzumab ozogamicin (Besponsa®), Polatuzumab vedotin (Polivy®), Belantamab mafodotin (Blenrep®), Loncastuximab tesirine (Zynlonta®) and Moxetumomab pasudotox (Lumoxiti®), an ADC, which uses an immunotoxin rather than a chemotherapeutic agent as a payload. The ADCs currently approved for solid tumor therapy are Ado-trastuzumab emtansine (Kadcyla®), Fam-trastuzumab deruxtecan (Enhertu®), Enfortumab vedotin (Padcev®), Sacituzumab govitecan (Trodelvy®), Tisotumab vedotin-tftv (Tivdak®), Mirvetuximab soravtansine (ELAHERE®), Disitamab vedotin (Aidixi®), and Cetuximab sarotalocan (Akalux®) (Fu et al., 2022; Kaplon et al., 2023; Yao et al., 2023). A brief description of each agent is provided below and key characteristics are listed in Table 1. In addition, Supplementary Table 1 provides the recruiting clinical trials on the use of novel ADCs being investigated for the treatment of cancer.

2.8.1 Hematologic malignancies

2.8.1.1 Gemtuzumab ozogamicin

Gemtuzumab ozogamicin (Mylotarg®; Pfizer) was the first ADC ever developed and clinically approved by the FDA in 2000 and by the EMA in 2018. As a first-generation ADC, it was based on a humanized anti-CD33 IgG4 antibody linked to the DNA-interactive agent calicheamicin (or ozogamicin) via a hydrazone-cleavable linker bound to surface lysines (average DAR 2–3). It was indicated for the treatment of relapsed/refractory acute myeloid leukemia (AML) though it was withdrawn in 2010, but reapproved at a lower dose in 2017, because patients suffered severe toxicity problems likely due to the higher dose (Fu et al., 2022). Following administration, Mylotarg binds to the CD33 transmembrane glycoprotein on AML cells, and upon internalization, a precursor of calicheamicin is released through hydrolysis of its linker. The active form of the drug then exerts a cytotoxic activity by binding to DNA and breaking its conformation to cause cell cycle arrest and cell death. Of note, the hydrophobic nature of calicheamicin enables a bystander killing of cells in the TME that are negative for the CD33 target antigen (Coats et al., 2019; Kayser and Levis, 2022).

2.8.1.2 Brentuximab vedotin

Brentuximab vedotin (Adcetris®; Seagen, Takeda Pharma) was approved by the FDA in 2011 and by the EMA in 2012 as monotherapy for the treatment of systemic anaplastic large cell lymphoma (sALCL) and in 2018 in combination with chemotherapy for relapsed/refractory Hodgkin lymphoma (HL). It consists of a chimeric IgG1 targeting CD30, a cell membrane protein of the tumor necrosis factor receptor family, on cancer cells and is cysteine conjugated to MMAE (DAR equals 4) through a protease-cleavable linker (Mckertish and Kayser, 2021). After interacting with its target, Adcetris enters the endosomal/lysosomal pathway via clathrin-dependent endocytosis, where its linker is cleaved by acid hydrolases to release MMAE in the cytoplasm. The drug interferes with microtubule polymerization and induces apoptosis and cell death. Like calicheamicin, MMAE exerts its cytotoxic effect on neighboring CD30-negative cells using the bystander killing effect, suggesting that the efficacy of Adcetris in heterogeneous

TABLE 1 FDA/EMA approved ADCs in clinical oncology. e early; m metastatic; AML acute myeloid leukemia; HL Hodgkin lymphoma; sALCL systemic Anaplastic Large Cell Lymphoma; B-cell prec. L B-cell precursor leukemia; DLBCL diffuse large B-cell lymphoma; MM multiple myeloma; HCL hairy cell leukemia; BC breast cancer; UC urothelial cancer; NSCLC non-small-cell lung cancer; GC gastric cancer; GOJ gastro-oesophageal junction cancer; TNBC triple negative breast cancer; CC cervical cancer; OC ovarian cancer; HNSCC Head and neck squamous cell carcinoma. The detailed description of the treatment for each disease is described in the text. *: withdraw from market in 2022. **: Aidixi® and Akalux® have not received FDA/EMA approval yet but Akalux® is approved by PMDA (Pharmaceuticals and Medical Devices Agency of Japan) and Aidixi® by NMPA (National Medical Products Administration of China).

ADC	Manufacturer	Trade name®	Target	FDA/EMA approval	Cancer
Gemtuzumab ozogamicin	Pfizer	Mylotarg	CD33	2000(2017)/2018	AML
Brentuximab vedotin	Seagen, Takeda Pharma	Adcetris	CD30	2011/2012	HL; sALCL
Inotuzumab ozogamicin	Pfizer	Besponsa	CD22	2017	B-cell prec. ALL
Polatuzumab vedotin	Genentech	Polivy	CD79b	2019/2020	DLBCL
Belantamab mafodotin	GlaxoSmithKline	Blenrep	BCMA	2020*	MM
Loncastuximab tesirine	ADC Therapeutics	Zynlonta	CD19	2021/2022	large B-cell prec. L
Moxetumomab pasudotox	AstraZeneca	Lumoxiti	PE38	2018	HCL
Ado-Trastuzumab Emtansine	Genentech	Kadcyla	HER2	2013	HER2+ e/m BC
Enfortumab vedotin	Astellas Pharma US, Seagen	Padcev	NECTIN4	2019/2022	mUC
Fam-trastuzumab Deruxtecan	Daichii Sankyo	Enhertu	HER2	2019/2021	HER2+ BC; NSCLC; GC/GOJ
Sacituzumab govitecan	Gilead Sciences	Trodelvy	TROP2	2020/2021	TNBC; mUC
Tisotumab vedotin-tftv	Seagen	Tivdak	TF	2021 (only FDA)	CC
Mirvetuximab Soravtansine	ImmunoGen	ELAHERE	FRα	2022 (only FDA)	OC
Disitamab Vedotin	Remegen	Aidixi**	HER2	—	UC; GC
Cetuximab Sarotalocan	Rakuten Medical	Akalux**	EGFR	—	HNSCC

lymphomas *in vivo* may be related to this effect (Katz et al., 2011; Scott, 2017).

2.8.1.3 Inotuzumab ozogamicin

Inotuzumab ozogamicin (Besponsa®; Pfizer) was approved by the FDA and EMA in 2017. It targets CD22, an antigen expressed on relapsed/refractory B-cell precursors in acute lymphoblastic leukemia (ALL). It consists of a humanized IgG4 mAb linked to calicheamicin via an acid-cleavable linker attached to lysine residues. It has a DAR, ranging from 5 to 7. From a mechanistic perspective, it acts similarly to gemtuzumab ozogamicin in that it is based on the same Ab backbone and loaded with the same drug (Dahl et al., 2016; Garrett et al., 2019; Lanza et al., 2020).

2.8.1.4 Polatuzumab vedotin

Polatuzumab vedotin (Polivy®; Genentech) contains a humanized IgG1 anti-CD79b, a component of the B-cell receptor conjugated to MMAE via the same organic bridge used in the synthesis of brentuximab vedotin. The conjugation method was via engineered cysteines utilizing the THIOMAB system and has a DAR of 3.5. The clinical use of Polivy has been approved by the FDA in 2019 and by the EMA in 2020 for the treatment of adult patients with relapsed/refractory diffuse large B-cell lymphoma (DLBCL) in combination with bendamustine and rituximab (anti-CD20 mAb) (Sehn et al., 2022; Varma et al., 2022). Upon administration, this agent is internalized into cancer cells and proteolytically cleaved to release MMAE, which causes apoptotic cell death by inhibiting tubulin polymerization (Deeks, 2019; Kaplon et al., 2020).

2.8.1.5 Belantamab mafodotin

Belantamab mafodotin (Blenrep®; GlaxoSmithKline) was approved by the FDA and EMA for the treatment of refractory/relapsed multiple myeloma in 2020 (MM) but was withdrawn in 2022 because it did not meet FDA standards (https://www.myeloma.org/news-events/withdrawal-blenrep-us-market). The mAb portion of this ADC is unique in that it consists of a humanized Fc-afucosylated IgG1, a modification that enhances binding and cytotoxicity of the ADC. From the mAb backbone, a cysteine-bound, non-cleavable linker bridges the mAb with the cytotoxic payload MMAF. Its DAR is 4. The target of Blenrep is B cell maturation antigen (BCMA), a member of the tumor necrosis factor receptor family that is overexpressed in mature B lymphocytes and plasma cells (Chen et al., 2020; Yu et al., 2020). As with other ADCs, BCMA targeting internalizes ADC and degrades mAb to release MMAF, a tubulin inhibitor, into the cytoplasm, where it blocks cancer cell cycle progression and leads them to death through apoptosis (Seckinger et al., 2017; Kaplon et al., 2020).

2.8.1.6 Loncastuximab tesirine

Loncastuximab tesirine (Zynlonta®; ADC Therapeutics) targets CD19 and received accelerated approval from the FDA in 2021 and from the EMA in 2022 for relapsed/refractory B-cell lymphoma after two or more lines of systemic therapy, including DLBCL not otherwise specified, DLBCL from low-grade lymphoma, and high-grade B-cell lymphoma. Zynlonta targets CD19, a transmembrane protein commonly expressed in all B cell lineages, and consists of a humanized IgG1 mAb linked to SG3199 (a dimeric PBD alkylating agent) via an enzymatically

cleavable linker (DAR of 2–3) (Lee, 2021). The payload exerts its pharmacological benefit by irreversibly binding to DNA and generating a strong adduct that inhibits DNA synthesis and causes cell death. Because SG3199 exhibits cytotoxicity in the picomolar range, it is the most toxic drug currently available on the market ADC. Currently, Zynlonta is the only anti-CD19 drug approved ADC for relapsed/refractory DLBCL as a single agent (Zammarchi et al., 2018; Fu et al., 2022).

2.8.1.7 Moxetumomab pasudotox

Moxetumomab pasudotox (Lumoxiti®; AstraZeneca) is not widely considered an ADC because its payload consists of a fragment of *Pseudomonas aeruginosa* exotoxin A called PE38. However, since it uses the same targeting mechanism based on mAb, we would still like to consider it as part of the ADC biocompound family. It was approved by the FDA in 2018 for patients with refractory/relapsed hairy cell leukemia (HCL) who have not received at least two systemic therapies. It was granted marketing authorization in the EU in 2021. Lumoxiti is based on an anti-CD22 mouse IgG1 mAb carrying a cleavable linker bound to the immunotoxin PE38. After interaction, internalization, and cleavage, PE38 is released into the cell cytoplasm and acts by blocking translation and inducing cell apoptosis (Kreitman and Pastan, 2011; Kreitman, 2019; Kang, 2021).

2.8.2 Solid tumors

2.8.2.1 Trastuzumab-based ADCs

Since FDA approval of rituximab for the treatment of non-HL in 1997 (Leget and Czuczman, 1998), several mAbs have been investigated and achieved approval in clinical oncology. Considering the mAbs that form the scaffold of approved ADCs, trastuzumab is an example of an anti-cancer molecule used in combination therapy or alone, and also represents the carrier motif in two preparations ADC. Trastuzumab (Herceptin®) is a humanized IgG1mAb that binds to the extracellular domain of HER2, a tyrosine kinase receptor that is upregulated in 20% of breast cancer (BC) patients, preventing its homodimerization and thereby blocking its intracellular signaling (Greenblatt and Khaddour, 2023). Because of its role in cell growth, survival, and differentiation, HER2+ breast cancers tend to grow and spread more aggressively than HER2 negative tumors (Iqbal and Iqbal, 2014). Trastuzumab was approved by the FDA in 1998 for the treatment of HER2+ BC. It improved overall survival (OS) and progression-free survival (PFS) (Albanell and Baselga, 1999; Goldenberg, 1999), but its administration was also associated with risk of cardiac toxicities, such as left ventricular ejection fraction (LVEF) decline and congestive heart failure (Bouwer et al., 2020). In the U.S. it is approved for HER2+ BC in adjuvant therapy (with anthracyclines and taxane) and for metastatic HER2+ BC in monotherapy or in combination with chemotherapeutics, tyrosine kinase inhibitors (TKIs), and immunotherapy. It is also used in a combination regimen for HER2+ gastric cancer (Dumontet et al., 2023). Trastuzumab is administered by intravenous infusion, and the dosing regimen can be adjusted depending on the stage of tumor growth (Greenblatt and Khaddour, 2023). Nowadays, the trastuzumab backbone has been used for the synthesis of two FDA- and EMA-approved ADCs, ado-trastuzumab emtansine (T-DM1, Kadcyla®; Genentech) and fam-trastuzumab deruxtecan (T-Dxd, Enhertu®, Daiichi Sankyo, Astrazeneca), which have improved the OS in the second and third-line settings and are currently used for the treatment of HER2+ early/metastatic and HER2+ low BC, respectively (Ferraro et al., 2021; Rassy et al., 2022).

2.8.2.1.1 Ado-trastuzumab emtansine

Ado-trastuzumab emtansine (Kadcyla®; Genentech) is based on a humanized IgG1 linked to emtansine via a non-cleavable linker attached to the lysine residues. Its average DAR is 3.5 (Mckertish and Kayser, 2021). After interaction with HER2 antigen, Kadcyla is internalized by endocytosis and reaches the lysosome, where IgG1 is completely proteolytically degraded. Subsequently, lysine-MCC-DM1, a DM1-containing metabolite, is released into the cytosol, where it disrupts the microtubule network and causes cell death. Interestingly, lysine-MCC-DM1 has similar toxicity to DM1 but cannot exert its pharmacological effect via the bystander killing effect due to its charge at neutral pH (Barok et al., 2014; Lambert and Chari, 2014). T-DM1 received FDA approval in 2013 for the treatment of advanced HER2+ BC based on data from the EMILIA clinical trial (Phase III). This study evaluated the efficacy of T-DM1 compared to capecitabine and lapatinib in patients with HER2+ BC previously treated with transtuzumab and taxane chemotherapy. Results based on 911 included patients were favorable for T-DM1, whose administration resulted in an improvement in objective response rate (ORR) (43.6% vs. 30.8%), median PFS (9.6 months vs. 6.4 months; $p < 0.001$), and median OS (29.9 vs. 25.9 months, $p < 0.001$) after a median follow-up of 47.8 months (Blackwell et al., 2012; Diéras et al., 2017). A few years later, positive results from the KATHERINE clinical trial (phase III) established the novel use of T-DM1 as adjuvant therapy for patients with early-stage HER2+ BC with residual disease after neoadjuvant treatment (taxane and trastuzumab). Among the 1,486 patients who met criteria, those who received T-DM1 showed a significant 50% improvement in invasive disease-free survival (IDFS) at 3 years compared with patients treated with trastuzumab alone in the control arm (88.3% vs. 77%, $p < 0.001$) (von Minckwitz et al., 2019; Wedam et al., 2020; Mamounas et al., 2021). From the data collected in these two studies, T-DM1 exhibits stronger therapeutic efficacy compared to chemotherapeutic agents and trastuzumab alone in HER2+ early or metastatic BC, likely because this ADC preserves the antineoplastic functions of trastuzumab and adds a novel cytotoxic effect (Ferraro et al., 2021). Remarkably, the superior benefit of T-DM1 was associated with manageable side effects, mostly grade 1 or 2, as only a small percentage of included patients reported elevations in liver enzymes aspartate transaminase (AST) and alanine transaminase (ALT) and thrombocytopenia (Diéras et al., 2017).

2.8.2.1.2 Fam-trastuzumab deruxtecan

Fam-trastuzumab Deruxtecan (Enhertu®; Daiichi Sankyo) is the second ADC HER2-targeting drug approved by the FDA. T-Dxd was approved by the FDA in 2019 and by the EMA in 2021 for the treatment of unresectable or metastatic HER2+ breast cancer (after patients have received two or more anti-HER2 therapies), non-small cell lung cancer, and for locally advanced or metastatic HER2+ gastric or gastroesophageal junction adenocarcinoma, after a trastuzumab-based therapy. It consists of a humanized IgG1-mAb carrying Dxd, a more potent DNA topoisomerase I inhibitor than SN-38, as a

cytotoxic payload via an enzymatically cleavable linker. It has a DAR of 7 or 8 (Mckertish and Kayser, 2021; Fu et al., 2022; Dumontet et al., 2023). After internalization of the HER2-Enhertu complex and cleavage, Dxd blocks DNA topoisomerase I, an enzyme that controls and alters the topological state of DNA during transcription, leading to cell death. Compared to Kadcyla, which has the same target, Enhertu has several improvements related to the novel cysteine-conjugated peptide linker, higher DAR and cytotoxicity of the drug, which is more potent and hydrophobic to increase the bystander killing effect on neighboring cells (Kaplon et al., 2020; Shitara et al., 2021). This is essential for extending cytotoxic activity to cells with low or heterogeneous HER2 levels. In this sense, the bystander-killing effect achieved by T-Dxd allows for a better therapeutic response and thus greater cytotoxicity in tumors refractory to its T-DM1 counterpart (Ferraro et al., 2021). In 2019, T-Dxd received accelerated FDA approval based on positive results from the single-arm DESTINY -Breast01 trial (Phase II). In this study, a cohort of 184 female patients with HER2+ metastatic BC who had received two or more prior lines of therapy, including T-DM1, was enrolled to test the efficacy of T-Dxd. Interestingly, 60.9% of patients showed an objective response, and the median duration and median response were 16.4 months and 14.8 months, respectively, with a median time response of 1.6 months (95% CI) (Modi et al., 2020; 2021). In addition, the efficacy of T-Dxd and T-DM1 was evaluated in the DESTINY -Breast 03 trial (phase III), which enrolled 524 patients with HER2+ metastatic BC previously treated with trastuzumab and taxane. Randomization data showed superior efficacy of T-Dxd in terms of ORR (79.9% vs. 34.2%), PFS (not reached vs. 6.8 months, $p < 0.001$), and OS (94.1% vs. 85.9%) (Cortés et al., 2021; 2022). In general, hematotoxicity, nausea, and fatigue were the most common grade ≥3 adverse effects observed in patients treated with T-Dxd. Of note, treatment with T-Dxd was also associated with pulmonary toxicity and, in particular, interstitial lung disease (ILD), a group of respiratory diseases that require careful management and may lead to treatment discontinuation (Diéras et al., 2017; Cardoso et al., 2020). Finally, the DESTINY-Breast04 trial evaluated the use of T-Dxd *versus* physician's choice chemotherapy in 577 patients with low HER2+ metastatic BC who had received prior chemotherapy in the metastatic setting or developed a recurrence within 6 months of completing adjuvant chemotherapy. The results of this study showed that administration of T-Dxd resulted in significantly longer median progression-free (9.9 months *versus* 5.1 months) and overall survival (23.4 months *versus* 16.8 months) than pharmacologic therapy in enrolled patients (Modi et al., 2022).

2.8.2.2 Enfortumab vedotin

Enfortumab vedotin (Padcev®; Astellas Pharma US, Seagen) is a fully human IgG1 conjugated to the microtubule inhibitor MMAE via a protease-cleavable linker on cysteine residues and has a DAR of 3.8 (Joubert et al., 2020). It targets nectin-4, a transmembrane protein involved in multiple cellular signaling pathways, including cell adhesion, proliferation, and migration, and is overexpressed in several malignancies. in 2019, Padcev was approved by the FDA for locally advanced or metastatic urothelial carcinoma following Pt-containing therapy and a PD -1 or PD -L1 inhibitor (Alt et al., 2020; Chang et al., 2021) and received EU-wide marketing approval in 2022.

2.8.2.3 Sacituzumab govitecan

Sacituzumab govitecan (Trodelvy®; Gilead Sciences) is an ADC consisting of a humanized IgG1 mAb targeting Tumor-associated calcium signal transducer 2 (TROP2), a transmembrane glycoprotein involved in cell self-renewal, proliferation, invasion, and survival, and plays an important role in intracellular calcium signaling. It is generally overexpressed in most solid tumors, including triple negative breast cancer (TNBC) (Furlanetto et al., 2022). The mAb harnesses to malignant cells SN-38, a DNA topoisomerase I inhibitor that causes DNA breaks and ultimately cell death. IgG1 and payload are connected via an acid-cleavable linker bound to cysteine residues with a DAR between 7 and 8 (Tong et al., 2021). Trodelvy was approved by the FDA in 2020 and by the EMA in 2021 for the treatment of locally advanced or metastatic TNBC in patients who have received at least two prior therapies and in locally advanced or metastatic urothelial carcinoma following Pt-containing therapy and a PD -1 or PD -L1 inhibitor (Mehanna et al., 2019; Bardia et al., 2021; Tong et al., 2021).

2.8.2.4 Tisotumab vedotin-tftv

Tisotumab vedotin-tftv (Tivdak®; Seagen) consists of a fully human IgG1, an enzymatically cleavable linker, MMAE as a payload, and a DAR equal to 4. It targets tissue factor (TF), a membrane protein related to cancer metastasis and invasiveness that is highly expressed in various solid tumors. Being the last ADC on the market, it was approved by the FDA in 2021 for the treatment of relapsed/refractory metastatic cervical cancer with disease progression during or after chemotherapy (Liu et al., 2011; Alley et al., 2019; Heitz et al., 2023).

2.8.2.5 Mirvetuximab soravtansine

Mirvetuximab soravtansine (ELAHERE®; ImmunoGen) was approved by the FDA in 2022 for the treatment of adult patients with Folate Receptor α (FRα)-positive, platinum-resistant epithelial ovarian cancer who have previously received 1–3 systemic therapies. It targets FRα, a member of the folate receptor family that is overexpressed on several epithelial-derived cancer cells (Macor et al., 2006). It consists of a chimeric mAb bound via a cleavable linker to DM4, a potent tubulin targeting agent that belongs to the maytansinoids. Like other ADC, the drug exerts its cytotoxic effect after internalization into cancer cells, leading to their death by blocking their mitotic fuse formation (Dilawari et al., 2023; Heo, 2023; Kaplon et al., 2023).

2.8.2.6 Disitamab vedotin

Disitamab vedotin (Aidixi®; RemeGen) was approved by the NMPA (National Medical Products Administration of China) in 2021 as a second-line treatment for patients with HER2-expressing, locally advanced or metastatic urothelial carcinoma (mUC) who have previously received Pt-containing chemotherapy (Fu et al., 2022), and approved for patients with HER2-overexpressing locally advanced or metastatic gastric cancer who have received at least two systemic chemotherapy regimens (Deeks, 2021). It delivers HER2+ cancer cell MMAE (DAR equals 4) via a cleavable linker bound to a humanized mAb. Interestingly, Aidixi showed high specific antigenic activity and stronger tumor activity compared to other HER2+-targeted ADCs in preclinical experiments and in animal models (Shi et al., 2022).

2.8.2.7 Cetuximab sarotalocan

Cetuximab sarotalocan (Akalux®; Rakuten Medical) received PMDA (Pharmaceuticals and Medical Devices Agency of Japan) approval in 2020 (Gomes-da-Silva et al., 2020). It is comprised of a chimeric IgG1 mAb specifically targeting epidermal growth factor receptor (EGFR), the triggering of which is involved in cell proliferation, angiogenesis, and invasion/metastasis. The conjugation of Akalux is not with a small molecule, but with a light-activatable near-infrared dye called 700DX (DAR 1.3–3.8) (Fu et al., 2022). In this case, we would also like to consider it as ADC given its mechanism of action against cancer cells. After interaction with ADC-EGFR, this ADC inhibits EGFR signaling pathway and achieves high anticancer effect by laser activation of 700DX dye. In this way, malignant cells are targeted and rapidly eliminated while healthy cells surrounding the tumor mass are spared. It has been approved for the treatment of unresectable locally advanced or recurrent head and neck squamous cell carcinoma (HNSCC) (Kitamura et al., 2020; Omura et al., 2023).

2.9 The therapeutic strategy of ADC reveals challenges and limitations and can be combined in combinatorial regimens

2.9.1 Payloads are the main cause of ADCs toxicity

In 2 decades, ADCs have achieved remarkable results in the treatment of hematologic malignancies and solid tumors and represent a valid alternative in the field of clinical oncology. Although they have been designed to release cytotoxic agents by targeting selective cell populations, a striking number of clinical trials have shown that ADCs are not free of adverse effects, sometimes leading to toxicities commonly observed with conventional chemotherapy (Dumontet et al., 2023; Tarantino et al., 2023). In general, a significant proportion of patients suffered various toxicities, sometimes so severe (or fatal) to require dose reduction or interruption, treatment delays, and supportive medications (Dumontet et al., 2023; Tarantino et al., 2023). Each of the blocks that form an ADC can result in significant side effects when these compounds are administered to the human body. Even if the nature of mAbs is responsible for moderate/severe immunogenic side effects, especially in ADCs preparations using murine and chimeric mAb scaffolds (Kim and Kim, 2015), the primary manifestation of a toxicity profile is highly dependent on the type of payload (Zahavi and Weiner, 2020). Most ADCs used in the clinic are loaded with tubulin inhibitors or DNA-interacting agents that exert their cytotoxic effects in the range of nano- or picomolar concentrations and are highly toxic when used in unconjugated form (Mecklenburg, 2018). Unfortunately, because only a very small percentage of ADCs reach their targets and a part of the payload is released prematurely, a significant portion of the dose is virtually free to interact with numerous non-target healthy cells and cause unconventional systemic or local side effects (Dahlgren and Lennernäs, 2020). The out-of-target toxicities are closely related to the linker. Non-cleavable linkers exhibit greater stability in plasma and the ADCs are better tolerated by the body. However, in the majority of ADCs used in the clinic and foremost to the ones use in solid tumors, cleavable linkers are preferred as they have shown more benefits, probably due to the bystander side effect. This out-of-cell toxicity has two sides. On the one hand, it may extend the efficacy of treatment to antigen-negative cells found in the tumor niche, to cells that form the core of the tumor mass being less accessible to the ADC (Jain, 2005; Mahadevan and Von Hoff, 2007; Xiao and Yu, 2021), and to cells that have low/heterogeneous expression of the antigen. On the other hand, due to the non-specific effect of the conventional small drugs, normal cells can also suffer severe damages with potential unpredictable consequences (Donaghy, 2016; Staudacher and Brown, 2017). Other limitations relate to the pharmacokinetic properties of ADCs. Rapid clearance and aggregation represent two important aspects that may negatively impact the therapeutic activity of these compounds (Lucas et al., 2018; Mahmood, 2021; Pettinato, 2021). To solve complications and improve the body compatibility of ADC, the mAb component and linker can be chemically modified by glycosylation or PEGylation (Mahmood, 2021; Edwards et al., 2022). While the former has not been studied in detail within this platform, the latter allows overcoming some drawbacks (Pettinato, 2021). PEGylation involves the addition of polyethylene glycol (PEG) to specific amino acid residues. In general, it has been shown that the use of PEG as a linker can improve the solubility of ADCs and reduce aggregation, improving their pharmacokinetic by enhancing stability and distribution in the body (Verhoef and Anchordoquy, 2013; Mahmood, 2021).

2.9.2 Clinical manifestations of ADCs include major toxicities

As ADCs are developed to limit their exposure to healthy tissues, they are associated with quite manageable toxicities, with nausea, vomiting, diarrhea and fatigue being among the most frequent ones. Unfortunately, the large amount of data provided by several clinical trials also highlights the presence of severe toxicities (grade 3 or higher) that include peripheral neuropathy and hematotoxicity, often dose-limiting (Masters et al., 2018; Professional Committee on Clinical Research of Oncology Drugs et al., 2022). Peripheral neuropathy includes tingling, pain in the extremities, numbness, and rarely muscle weakness and is commonly associated with ADCs carrying cleavable linkers bound to tubulin inhibitors (i.e., all ADCs loaded with MMAE) and Mirvetuximab soravtansine, carrying DM4 (Nguyen et al., 2023). As cleavable linkers are associated to the premature drug release and that these compounds block tubulin polymerization, this common side effect is not unexpected as microtubules are deeply involved in the axonal transport, an essential process to the growth and maturation of neurons (Yogev et al., 2016). Hematologic side effects include anemia, neutropenia, thrombocytopenia, leukopenia and are mainly due to the off-target Fc receptor-mediated uptake of ADCs into immune cells, with neutropenia being the most prominent toxicity in ADC-based monotherapy (Mahalingaiah et al., 2019). Besides, major toxicities responsible for dose limitations are related to drug classes and mainly include hepatotoxicity (for MMAF, DM1, and calicheamicin), skin toxicity (for MMAE and PBD), and ocular toxicity (for MMAF and DM4) (Zhao et al., 2020; Hurwitz et al., 2023). Of note, the mechanism underlying corneal toxicity has not been solved yet but occurred in a relevant percentage of patients treated with Belantamab mafotodin, Trastuzumab emtansine and Mirvetuximab soravtansine, all loaded with tubulin inhibitors (Aschauer et al., 2022; Domínguez-Llamas et al., 2023). Other

relevant clinical manifestations include gastrointestinal side effects upon administration of Sacituzumab govitecan and Trastuzumab deruxtecan, two ADC used in the treatment of breast cancer and loaded with Topoisomerase inhibitors and serosal effusion for duocarmycin and PBD, the latter responsible of nephrotic toxicity in Loncastuzimab tesirine preparation (Nguyen et al., 2023). In addition, Trastuzumab emtansine and Trastuzumab deruxtecan, both targeting HER2+ breast cancer, are associated with an increased risk of interstitial lung disease (ILD)/pneumonitis, which must be carefully managed with dose adjustment and supportive care recommendations to avoid fatal outcomes (Ma et al., 2018; Hackshaw et al., 2020). Like other strategies based on small molecules and immunotherapy, ADCs show some challenges that need to be carefully addressed to improve their efficacy and reduce systemic side effects. A variety of approaches is being taken into consideration in clinics to deeply counteract the manifestation of side effects, and many of them focus on an individual basis. Extensive efforts are being made to identify patients who have potentially life-threatening toxicities at an early stage and offer them supportive measures, such as dose and schedule adjustments. The investigation of patients' history and data on previous treatments, comorbidities, or genetic profiles, including pharmacogenetic analysis to identify SNPs or potential mutations in key genes, will undoubtedly play a critical role in the determination of the best strategy to improve the tolerability and efficacy of ADCs (Lambert and Morris, 2017; Dumontet et al., 2023; Tarantino et al., 2023).

2.9.1 ADCs can be used in combination therapies

In addition to the use of ADCs as monotherapy, recent preclinical and clinical studies have also focused on ADCs combinations with chemo-immunotherapics. Ideally, concomitant administration of ADCs with antiangiogenic agents, i.e., agents that damage neo-blood vessels to facilitate ADC penetration into the tumor niche, or immunomodulatory drugs that promote immune surveillance should amplify the body's anti-neoplastic response to the tumor mass and its TME, without or with limited severe toxicities and safety issues (Dumontet et al., 2023; Fuentes-Antrás et al., 2023). Regarding ADC combination with chemotherapy, promising data include the combination of Brentuximab vedotin and CHP (cyclophosphamide, doxorubicin, and prednisone) and Polatuzumab vedotin and Rituximab-CHP in $CD30^{+}$ peripheral T cell lymphoma (Herrera et al., 2021) and in DLBCL (Tilly et al., 2022), respectively. Similarly, the combination therapy based on Trastuzumab emtansine and the selective anti-HER2 tyrosine kinase inhibitor (TKI) tucatinib achieved remarkable benefits in metastatic breast cancer (Nader-Marta et al., 2022) and the administration of bevacizumab, the mAb targeting the Vascular-Endothelial Growth Factor (VEGF), with Mirvetuximab soravtansine obtained similar benefits in preclinal models of ovarian cancer (Ponte et al., 2016). Combinatorial approaches using ADCs and immunotherapeutic agents have been recently explored in several types of cancers (Fuentes-Antrás et al., 2023). Immune checkpoint inhibitors (ICIs) are immunotherapy that enhance antineoplastic immune responses by converting exhausted T-cells into activated ones and bypassing the pathways that cause the tumor escape from the immune system (Shiravand et al., 2022; von Arx et al., 2023). ICIs targeting Cytotoxic T-Lymphocyte Antigen 4 (CTLA-4) and the Programmed Cell Death Protein 1/its ligand (PD-1/PD-L1) axis have demonstrated robust clinical activity in several malignancies but only a fraction of patients experience long-term benefits with monotherapy (Wojtukiewicz et al., 2021). From this perspective, an effort could come from ADCs, capable to enhance antitumor immune responses by inducing tumor-specific adaptive immunity through increasing T cell infiltration into the TME, while ICIs revitalize exhausted T cells (Nicolò et al., 2022). Accordingly, encouraging results come from the combination of ICIs and HER2-targeted trastuzumab emtansine in the treatment of PD-L1+, HER2+ advanced breast cancer (Emens et al., 2020).

2.10 ADC strategy shows application in non-oncology indications

In recent years, research groups have investigated the use of ADCs in non-oncologic contexts, mainly focusing on the treatment of bacterial infections and autoimmune diseases. Tvilum et al. achieved antimicrobial efficacy by developing an Antibody-Antibiotic Conjugate (AAC), an antibody directed against bacteria conjugated to the antimicrobial molecule mitomycin C, for the treatment of implant-associated biofilm infections caused by *Staphylococcus aureus*, the most common causative agent in prosthetic joint infections (Tvilum et al., 2023). In another study, O-Leary et al. proposed the development of an Antibody-Bactericide Conjugate (ABC), an antibody conjugated to an antimicrobial peptide that exerts its effect by binding to the cell surface of *P. aeruginosa*, providing another interesting example of ADC activity against bacterial infections (O'Leary et al., 2023). Regarding inflammatory diseases, Yasunaga et al. developed an ADC targeting IL-7 receptor (IL-7R) conjugated with MMAE and showed that ADC-mediated immunoregulation of the IL-7R, the upregulation of which is a common mechanism in the pathogenesis of autoimmunity, specifically depleted IL-7R-positive cells in the inflammation site of a mouse model of autoimmune arthritis and abrogated disease progression (Yasunaga et al., 2017). In the same year, Lee et al. demonstrated in a model of rheumatoid arthritis (RA) the immunosuppressive efficacy of TCZ-ALD, an ADC that targets the IL-6 receptor (IL-6R) and is conjugated to the small molecule alendronate. TCZ-ALD blocks the IL-6R activity and macrophages activity in the manifestation of RA symptoms and joint inflammation (Lee et al., 2017). A few years later, Gillard et al. achieved immune reset of disease-causing reactive T cells by a single administration of CD45-ADC and bone marrow transplantation, resulting in significant disease-modifying effect in mouse models of autoimmune disease (Gillard et al., 2020). In addition, a few studies also addressed the use of ADCs in cardiovascular (Lim et al., 2015) and renal diseases (Kvirkvelia et al., 2015), highlighting the potential application of this therapeutic strategy in other pathological conditions.

2.11 Challenges and solutions in the manufacturing of ADCs

2.11.1 Process development consists of several steps

The main goal in the manufacture of ADCs by companies is to produce a pure and bioburden-free compound that is safe for the

human body for clinical use. Since the preparations of ADC consist of mixtures of mAbs with multiple conjugation sites and small organic molecules, several analytical steps are required in the development of these compounds, and several challenges must be overcome. Overall, the production of ADCs can be divided into three steps: production of the antibody, synthesis of the drug-linker complex, and conjugation to form the final ADC (Hutchinson et al., 2018; Bulger et al., 2023). The conjugation step is of fundamental importance as it determines the therapeutic efficacy of the biomolecule. Conventional conjugation methods based on lysine side-chains or reduced cysteines result in heterogeneous ADC preparations whose safety and therapeutic efficacy are difficult to predict. To overcome this crucial limitation, site-selective conjugation methods have recently been developed. In this way, a known number of drug molecules are constantly bound to selected sites on mAbs, resulting in a more homogeneous mixture with improved batch-to-batch consistency and therapeutic efficacy (Cao et al., 2019; Nejadmoghaddam et al., 2019). After the conjugation step, ADC proceeds to purification and filling into aseptic vials, all following the sterile pipeline of current Good Manufacturing Practices (cGMP). Quality is controlled throughout the development process. Production requires a biological manufacturing environment that allows for the safe handling of sensitive structures, such as various powders and chemicals, purified mAbs, and high potency drugs, to minimize potential pollution and losses that may occur at various stages of production. To ensure product purity and sterility, synthesis and bioconjugation reactions are performed in aseptic rooms and conditions, with regular documentation of instrument accuracy in accordance with cGMP standards. To reduce potential contamination and exposure from the use of hazardous substances, each step of the experimental process is achieved by providing in-depth expertise and specialized equipment to personnel and operators (Hutchinson et al., 2018; Schmidhalter et al., 2019). In addition, the production of ADC usually involves several departments/services and, in this sense, an extremely low temperature supply chain and secure packaging must be ensured to reduce possible variations, damage and leakage during long-term storage and transportation (Ducry, 2012). Considering the complexity and number of processes involved, the production of ADCs is quite laborious, time-consuming and economically expensive. Large capital investments are required to cover a multitude of steps ranging from the design of the experiment, the invention and development of new drugs to product innovation, differentiation, and safety monitoring, all at a cost that must make the finished drug marketable (www.cbo.gov). To overcome these barriers, contract development and manufacturing organizations (CDMOs), companies that provide drug development and manufacturing services to the pharmaceutical industry, are turning to single-use technologies (SUTs) and automated end-to-end systems (Schmidhalter et al., 2019). SUTs are sterile, single-use items made of various plastics, most of which can be used in the same way as their stainless-steel counterparts without the need for sterilization and recycling after use. As a result, these technologies offer significant advantages over traditional reusable systems by reducing the risk of cross-contamination, better ensuring sterility, allowing more flexibility throughout the process and, most importantly, improving cost efficiency and reducing time to market (Schmidhalter et al., 2019). In these terms, continuous improvement in technology and investments by major biopharmaceutical companies in extensive research programs will drive the growth of the ADC market (valued at approximately $7 billion in June 2022 but expected to reach $22.4 billion in 2030 (www.researchandmarkets.com) and increase the number of available ADC-based therapies in new medical areas.

2.11.2 Analytical characterization startegies

Another challenge in the production of ADCs is the evaluation of their biochemical attributes to obtain a safe and effective product. Critical quality attributes of ADCs that must be carefully controlled during the manufacturing process include determination of DAR and distribution of drug, residual non-conjugated species, especially in terms of mAb and payload, and evaluation of size and charge variants in the final preparations. Nowadays, various *in vitro* instruments and techniques are used either alone or in combination to perform comprehensive analytical characterization of ADCs, including spectroscopic, chromatographic, and mass spectrometric methods (Wagh et al., 2018; Liu et al., 2022).

2.11.2.1 Determination of purity

Purity of compound is a fundamental goal in any biopharmaceutical manufacturing process. One of the techniques used to evaluate the purity of ADC preparations is size exclusion chromatography followed by ultraviolet detection (SEC-UV), a method that separates molecules by size and, in some cases, molecular weight, and is used to fractionate large macromolecules such as proteins (e.g., mAbs) or protein complexes (de Mel et al., 2019). In ADC synthesis, separation of macromolecules by size allows purification of the mAb from potential fragments, aggregates, and particles, three examples of undesirable species that affect the efficacy of the final ADC as well as its safety when administered to patients (Jiang et al., 2019). In general, coupling SEC with multi-angle laser light scattering (SEC-MALS) offers some advantages for biopharmaceutical applications. In MALS detection, a laser beam passes through a sample solution containing the target molecule, and depending on the size of the molecules, the intensity of the scattered light is measured at specific angles (Some et al., 2019). Compared to SEC itself, SEC-MALS requires high-purity columns but provides additional information by increasing the sensitivity for detecting impurities in the preparation (Beck et al., 2019). Other techniques for determining the presence of aggregation or fragmentation include dynamic light scattering (DLS), sedimentation velocity analytical ultracentrifugation (SV-AUC) (Ducry, 2012), and capillary electrophoresis followed by sodium dodecyl sulfate analysis (CE-SDS), a valuable method commonly used in the biopharmaceutical industry for mAbs and ADC preparations to determine batch consistency and overall protein purity (Wagner et al., 2020). In addition, various residual species in ADC preparations may pose a potential safety risk to patients and are a critical quality attribute that must be carefully evaluated. The levels of these unconjugated forms can be monitored by measuring the charge on the molecules (Wakanar, 2011). Since the bioconjugation reaction between the mAb and the payload can significantly alter the electrostatic profile of the newly formed ADC, charge-based separation techniques such as ion exchange chromatography (IEC), isoelectric focusing gel

electrophoresis (IEF), and capillary isoelectric focusing (cIEF) can provide information on charge heterogeneity, drug distribution pattern, and overall preparation quality (Ducry, 2012). To date, imaged capillary isoelectric focusing (iCIEF) is considered a robust method in biopharmaceutical quality control because it can quantitatively separate samples based on the isoelectric point (pI) of individual variants (Wagh et al., 2018; Abbood, 2023). Therefore, iCIEF can be used to rapidly measure the content of free mAb in an ADC mixture according to the different pI of the mAb and its conjugated form. However, the drawbacks of this assay are that conjugates cannot be distinguished from reaction intermediates and other impurities, and it can only be used for conjugation chemistries that result in significant changes in charge and net pI (Wagh et al., 2018).

2.11.2.2 Determination of DAR and drug distribution

Probably the hottest topic in the ADC manufacturing process is the ability to achieve bioconjugation reactions that lead to the synthesis of a homogeneous mixture and thus a controlled DAR and payload. Various analytical methods have been used to determine these parameters, including ultraviolet/visible spectroscopy (UV/Vis) (Andris et al., 2018), hydrophobic interaction chromatography (HIC) (Andris and Hubbuch, 2020), reversed-phase liquid chromatography (RPLC) (Chen et al., 2019), and mass spectrometry (MS). As for MS, its extended use in characterization of ADCs is discussed in other works (Debaene et al., 2014; Zmolek et al., 2016; Liu and Chen, 2022; Barbero et al., 2023). UV/Vis spectrometry is relatively easy to measure DAR compared to the other techniques, although it requires sufficiently different absorption profiles between the mAb and the payload and a UV/Vis chromophore on the payload (Wagh et al., 2018). Among liquid chromatographic methods, HIC and RPLC are routinely used to measure average DAR and drug distribution (Ouyang, 2013; D'atri et al., 2019). HIC is a method that allows determination of species distribution based on differences in their hydrophobic properties and uniquely preserves the native structures and activity of ADCs. Because the analysis is performed under mild, non-denaturing conditions, ADCs can be studied in their native conformation, which is an advantage because isolation of chromatographically pure species allows their further characterization in subsequent analysis. This method is commonly used to analyze cysteine-conjugated ADCs and other site-specific conjugations but cannot be applied to ADCs obtained by lysine conjugation because the greater heterogeneity of these preparations complicates chromatographic separation (D'atri et al., 2019; Liu and Chen, 2022). Nevertheless, HIC requires a large amount of starting material, shows low efficiency for randomly conjugated ADCs, and cannot separate positional isomers from cysteine-conjugated ADCs or determine the chain, H or L, to which the drug was conjugated (Becker et al., 2020; Fleming, 2020; Liu and Chen, 2022). The RPLC method also separates the components of a mixture according to their hydrophobicity, but this approach requires denaturation of the proteins, resulting in the loss of some information about the distribution of some ADCs and the loss of certain DAR species (Liu and Chen, 2022).

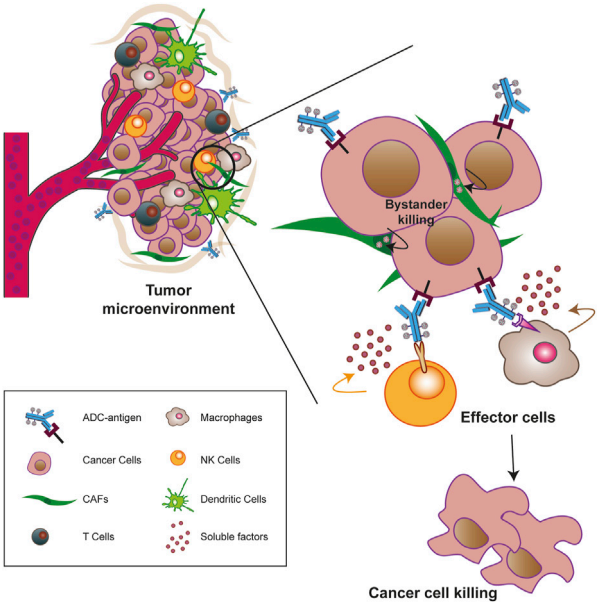

FIGURE 3
Overview on the tumor-targeting ADCs. Taking advantage of blood circulation, ADCs reach the tumor microenvironment (TME), which is composed by cancer-associated fibroblasts (CAFs) and other cell types and interact with malignant cells that exposed the tumor associated/specific antigen on their surface. In addition to their canonical mechanism of action, ADCs can potentiate their positive response against the tumor mass. To this aim, ADCs hydrophobic payloads may diffuse through the cell membrane inducing the killing of neighborhood antigen-negative cells via bystander killing effect (black arrows) and/or the ADCs antibody Fc fragment may elicit anti-tumor immunity (ADCC, CDC, and ADCP) by engaging immune effector mechanisms, such as complement system, macrophages and NK cells. All together, these mechanisms aim to induce the death of the cellular component of the tumor mass via apoptosis.

2.12 Conclusion and perspectives

Nowadays, ADC represents a solid strategy to treat different types of malignancies. The design of ADCs provides an exceptional opportunity to selectively deliver an effective anti-tumor chemical to the target cell and eliminate it without severe toxic off-target effects. The main advantage of ADC lies in its mechanism of action, as it offers the potential to overcome some major limitations of conventional small molecule-based therapies, such as low therapeutic index and high off-tumor toxicity The possibility of killing neighboring antigen-negative cells, through the bystander effect, in the mass and in the TME and the potential activation of direct and indirect anti-cancer mechanisms via mAb-antigen interaction and immune cell activation, respectively, argue for their use in the clinic (Figure 3). In this context, it is worth noting that the benefits associated with the activity of ADCs when administered as monotherapy may encounter consistent clinical limitations due to the presence of tumor-derived resistance mechanisms and several manageable and few severe adverse effects mainly caused by the payload of the ADC (Fuentes-Antrás et al., 2023). Despite the promising results obtained so far, the ADC technology is still under investigation and has some limitations in terms of its pharmacokinetic properties

and biological efficacy in different tumor contexts. To develop a more suitable generation of ADCs, future prospects in this field are based on the optimization of available technologies and especially on the discovery of new methodologies. Accordingly, profound improvements in the validation of newly developed mAbs, in the synthesis of less immunogenic and more stable linkers, and in the discovery of more effective payloads are being actively explored by scientists in this field, and similar advance are also focused on the development of more appropriate formulations as well as on the identification of new target antigens. Given the central role of the TME in solid tumor progression and spread, targeting novel candidates upregulated in stromal cells, blood vessels and most importantly immune cells within the TME could lead to greater inhibition of tumor escape mechanisms and metabolic dysfunctions to achieve long-lasting therapeutic effects. Moreover, combinatorial therapies with different drug classes have already shown synergistic and promising results in the treatment of hematologic and solid tumors by enhancing the anticancer efficacy and therapeutic index of ADCs. Based on these observations, all these efforts are aimed at developing a new generation of ADCs that will undoubtedly show significant improvements in terms of pharmacological properties, therapeutic efficacy and safety in the field of oncology and in other pathological conditions.

Author contributions

FR: Writing–original draft. MDB: Writing–review and editing. PM: Writing–review and editing. GT: Writing–review and editing.

Funding

The authors declare financial support was received for the research, authorship, and/or publication of this article. The research leading to these results has received funding from the European Union—NextGenerationEU through the Italian Ministry of University and Research under PNRR—M4C2-I1.3 Project PE_00000019 "HEAL ITALIA" to MDB (Spoke 5) and GT (Spoke 6) (CUP J33C22002930006 of Centro di Riferimento Oncologico di Aviano, IRCCS). This research was supported in part by the Italian Ministry of Health (Ricerca Corrente).

Conflict of interest

The authors declare that the research was conducted in the absence of any commercial or financial relationships that could be construed as a potential conflict of interest.

Publisher's note

All claims expressed in this article are solely those of the authors and do not necessarily represent those of their affiliated organizations, or those of the publisher, the editors and the reviewers. Any product that may be evaluated in this article, or claim that may be made by its manufacturer, is not guaranteed or endorsed by the publisher.

Author disclaimer

The views and opinions expressed are those of the authors only and do not necessarily reflect those of the European Union or the European Commission. Neither the European Union nor the European Commission can be held responsible for them.

Supplementary material

The Supplementary Material for this article can be found online at: https://www.frontiersin.org/articles/10.3389/fphar.2023.1274088/full#supplementary-material

References

Abbood, A. (2023). Optimization of the imaged cIEF method for monitoring the charge heterogeneity of antibody-maytansine conjugate. *J. Anal. Methods Chem.* 2023, 8150143. doi:10.1155/2023/8150143

Abrahams, C. L., Li, X., Embry, M., Yu, A., Krimm, S., Krueger, S., et al. (2018). Targeting CD74 in multiple myeloma with the novel, site-specific antibody-drug conjugate STRO-001. *Oncotarget* 9, 37700–37714. doi:10.18632/oncotarget.26491

Adams, G. P., Schier, R., McCall, A. M., Simmons, H. H., Horak, E. M., Alpaugh, R. K., et al. (2001). High affinity restricts the localization and tumor penetration of single-chain fv antibody molecules. *Cancer Res.* 61, 4750–4755.

Agrafiotis, A. C., Siozopoulou, V., Hendriks, J. M. H., Pauwels, P., Koljenovic, S., and Van Schil, P. E. (2022). Tumor microenvironment in thymic epithelial tumors: A narrative review. *Cancers (Basel)* 14, 6082. doi:10.3390/cancers14246082

Albanell, J., and Baselga, J. (1999). Trastuzumab, a humanized anti-HER2 monoclonal antibody, for the treatment of breast cancer. *Drugs Today (Barc)* 35, 931–946. doi:10.1358/dot.1999.35.12.564040

Albanell, J., Codony, J., Rovira, A., Mellado, B., and Gascón, P. (2003). Mechanism of action of anti-HER2 monoclonal antibodies: scientific update on trastuzumab and 2C4. *Adv. Exp. Med. Biol.* 532, 253–268. doi:10.1007/978-1-4615-0081-0_21

Alley, S. C., Harris, J. R., Cao, A., Heuvel, E. G., Velayudhan, J., Satijn, D., et al. (2019). Abstract 221: Tisotumab vedotin induces anti-tumor activity through MMAE-mediated, Fc-mediated, and Fab-mediated effector functions *in vitro*. *Cancer Res.* 79, 221. doi:10.1158/1538-7445.AM2019-221

Alley, S. C., Okeley, N. M., and Senter, P. D. (2010). Antibody-drug conjugates: targeted drug delivery for cancer. *Curr. Opin. Chem. Biol.* 14, 529–537. doi:10.1016/j.cbpa.2010.06.170

Alt, M., Stecca, C., Tobin, S., Jiang, D. M., and Sridhar, S. S. (2020). Enfortumab Vedotin in urothelial cancer. *Ther. Adv. Urol.* 12, 1756287220980192. doi:10.1177/1756287220980192

Andersen, M. H. (2023). Tumor microenvironment antigens. *Semin. Immunopathol.* 45, 253–264. doi:10.1007/s00281-022-00966-0

Anderson, N. M., and Simon, M. C. (2020). The tumor microenvironment. *Curr. Biol.* 30, R921–R925. doi:10.1016/j.cub.2020.06.081

Andris, S., and Hubbuch, J. (2020). Modeling of hydrophobic interaction chromatography for the separation of antibody-drug conjugates and its application towards quality by design. *J. Biotechnol.* 317, 48–58. doi:10.1016/j.jbiotec.2020.04.018

Andris, S., Rüdt, M., Rogalla, J., Wendeler, M., and Hubbuch, J. (2018). Monitoring of antibody-drug conjugation reactions with UV/Vis spectroscopy. *J. Biotechnol.* 288, 15–22. doi:10.1016/j.jbiotec.2018.10.003

Aschauer, J., Donner, R., Lammer, J., Roberts, P., Funk, M., Agis, H., et al. (2022). Corneal toxicity associated with Belantamab mafodotin is not restricted to the epithelium: Neuropathy studied with confocal microscopy. *Am. J. Ophthalmol.* 242, 116–124. doi:10.1016/j.ajo.2022.06.009

Baah, S., Laws, M., and Rahman, K. M. (2021). Antibody–drug conjugates—a tutorial review. *Molecules* 26, 2943. doi:10.3390/molecules26102943

Baghban, R., Roshangar, L., Jahanban-Esfahlan, R., Seidi, K., Ebrahimi-Kalan, A., Jaymand, M., et al. (2020). Tumor microenvironment complexity and therapeutic implications at a glance. *Cell Commun. Signal.* 18, 59. doi:10.1186/s12964-020-0530-4

Balendiran, G. K., Dabur, R., and Fraser, D. (2004). The role of glutathione in cancer. *Cell Biochem. Funct.* 22, 343–352. doi:10.1002/cbf.1149

Barbero, L. M., Ianni, A. D., Molinaro, F., Cowan, K. J., and Sirtori, F. R. (2023). Hybrid liquid chromatography high resolution and accuracy mass spectrometry approach for quantification of antibody-drug conjugates at the intact protein level in biological samples. *Eur. J. Pharm. Sci.* 188, 106502. doi:10.1016/j.ejps.2023.106502

Bardia, A., Hurvitz, S. A., Tolaney, S. M., Loirat, D., Punie, K., Oliveira, M., et al. (2021). Sacituzumab govitecan in metastatic triple-negative breast cancer. *N. Engl. J. Med.* 384, 1529–1541. doi:10.1056/NEJMoa2028485

Bargh, J. D., Isidro-Llobet, A., Parker, J. S., and Spring, D. R. (2019). Cleavable linkers in antibody-drug conjugates. *Chem. Soc. Rev.* 48, 4361–4374. doi:10.1039/c8cs00676h

Barok, M., Joensuu, H., and Isola, J. (2014). Trastuzumab emtansine: mechanisms of action and drug resistance. *Breast Cancer Res.* 16, 209. doi:10.1186/bcr3621

Beck, A., D'Atri, V., Ehkirch, A., Fekete, S., Hernandez-Alba, O., Gahoual, R., et al. (2019). Cutting-edge multi-level analytical and structural characterization of antibody-drug conjugates: present and future. *Expert Rev. Proteomics* 16, 337–362. doi:10.1080/14789450.2019.1578215

Beck, A., Goetsch, L., Dumontet, C., and Corvaïa, N. (2017). Strategies and challenges for the next generation of antibody-drug conjugates. *Nat. Rev. Drug Discov.* 16, 315–337. doi:10.1038/nrd.2016.268

Becker, C. L., Duffy, R. J., Gandarilla, J., and Richter, S. M. (2020). Purification of ADCs by hydrophobic interaction chromatography. *Methods Mol. Biol.* 2078, 273–290. doi:10.1007/978-1-4939-9929-3_19

Blackwell, K. L., Miles, D., Gianni, L., Krop, I. E., Welslau, M., Baselga, J., et al. (2012). Primary results from EMILIA, a phase III study of trastuzumab emtansine (T-DM1) versus capecitabine (X) and lapatinib (L) in HER2-positive locally advanced or metastatic breast cancer (MBC) previously treated with trastuzumab (T) and a taxane. *JCO* 30, LBA1. doi:10.1200/jco.2012.30.18_suppl.lba1

Bornstein, G. G. (2015). Antibody drug conjugates: Preclinical considerations. *AAPS J.* 17, 525–534. doi:10.1208/s12248-015-9738-4

Bouwer, N. I., Jager, A., Liesting, C., Kofflard, M. J. M., Brugts, J. J., Kitzen, J. J. E. M., et al. (2020). Cardiac monitoring in HER2-positive patients on trastuzumab treatment: A review and implications for clinical practice. *Breast* 52, 33–44. doi:10.1016/j.breast.2020.04.005

Brinkmann, U., and Kontermann, R. E. (2017). The making of bispecific antibodies. *MAbs* 9, 182–212. doi:10.1080/19420862.2016.1268307

Bulger, P. G., Conlon, D. A., Cink, R. D., Fernandez-Cerezo, L., Zhang, Q., Thirumalairajan, S., et al. (2023). Drug-linkers in antibody–drug conjugates: Perspective on current industry Practices. *Org. Process Res. Dev.* 27, 1248–1257. doi:10.1021/acs.oprd.3c00136

Cao, M., De Mel, N., Jiao, Y., Howard, J., Parthemore, C., Korman, S., et al. (2019). Site-specific antibody-drug conjugate heterogeneity characterization and heterogeneity root cause analysis. *MAbs* 11, 1064–1076. doi:10.1080/19420862.2019.1624127

Cardoso, F., Paluch-Shimon, S., Senkus, E., Curigliano, G., Aapro, M. S., André, F., et al. (2020). 5th ESO-ESMO international consensus guidelines for advanced breast cancer (ABC 5). *Ann. Oncol.* 31, 1623–1649. doi:10.1016/j.annonc.2020.09.010

Carter, P. J., and Senter, P. D. (2008). Antibody-drug conjugates for cancer therapy. *Cancer J.* 14, 154–169. doi:10.1097/PPO.0b013e318172d704

Casi, G., and Neri, D. (2012). Antibody-drug conjugates: basic concepts, examples and future perspectives. *J. Control Release* 161, 422–428. doi:10.1016/j.jconrel.2012.01.026

Castelli, M. S., McGonigle, P., and Hornby, P. J. (2019). The pharmacology and therapeutic applications of monoclonal antibodies. *Pharmacol. Res. Perspect.* 7, e00535. doi:10.1002/prp2.535

Ceci, C., Lacal, P. M., and Graziani, G. (2022). Antibody-drug conjugates: Resurgent anticancer agents with multi-targeted therapeutic potential. *Pharmacol. Ther.* 236, 108106. doi:10.1016/j.pharmthera.2021.108106

Chames, P., Van Regenmortel, M., Weiss, E., and Baty, D. (2009). Therapeutic antibodies: successes, limitations and hopes for the future. *Br. J. Pharmacol.* 157, 220–233. doi:10.1111/j.1476-5381.2009.00190.x

Chang, E., Weinstock, C., Zhang, L., Charlab, R., Dorff, S. E., Gong, Y., et al. (2021). FDA approval summary: Enfortumab vedotin for locally advanced or metastatic urothelial carcinoma. *Clin. Cancer Res.* 27, 922–927. doi:10.1158/1078-0432.CCR-20-2275

Chari, R. V. J. (2008). Targeted cancer therapy: conferring specificity to cytotoxic drugs. *Acc. Chem. Res.* 41, 98–107. doi:10.1021/ar700108g

Chen, R., Hou, J., Newman, E., Kim, Y., Donohue, C., Liu, X., et al. (2015). CD30 downregulation, MMAE resistance, and MDR1 upregulation are all associated with resistance to brentuximab vedotin. *Mol. Cancer Ther.* 14, 1376–1384. doi:10.1158/1535-7163.MCT-15-0036

Chen, T.-H., Yang, Y., Zhang, Z., Fu, C., Zhang, Q., Williams, J. D., et al. (2019). Native reversed-phase liquid chromatography: A technique for lcms of intact antibody-drug conjugates. *Anal. Chem.* 91, 2805–2812. doi:10.1021/acs.analchem.8b04699

Chen, T., Chen, Y., Stella, C., Medley, C. D., Gruenhagen, J. A., and Zhang, K. (2016). Antibody-drug conjugate characterization by chromatographic and electrophoretic techniques. *J. Chromatogr. B* 1032, 39–50. doi:10.1016/j.jchromb.2016.07.023

Chen, W., Yuan, Y., and Jiang, X. (2020). Antibody and antibody fragments for cancer immunotherapy. *J. Control Release* 328, 395–406. doi:10.1016/j.jconrel.2020.08.021

Cheung-Ong, K., Giaever, G., and Nislow, C. (2013). DNA-Damaging agents in cancer chemotherapy: serendipity and chemical biology. *Chem. Biol.* 20, 648–659. doi:10.1016/j.chembiol.2013.04.007

Cilliers, C., Menezes, B., Nessler, I., Linderman, J., and Thurber, G. M. (2018). Improved tumor penetration and single-cell targeting of antibody drug conjugates increases anticancer efficacy and host survival. *Cancer Res.* 78, 758–768. doi:10.1158/0008-5472.CAN-17-1638

Coats, S., Williams, M., Kebble, B., Dixit, R., Tseng, L., Yao, N.-S., et al. (2019). Antibody-drug conjugates: Future directions in clinical and translational strategies to improve the therapeutic index. *Clin. Cancer Res.* 25, 5441–5448. doi:10.1158/1078-0432.CCR-19-0272

Collins, D. M., Bossenmaier, B., Kollmorgen, G., and Niederfellner, G. (2019). Acquired resistance to antibody-drug conjugates. *Cancers (Basel)* 11, 394. doi:10.3390/cancers11030394

Cooper, G. M. (2000). "The development and causes of cancer," in *The cell: A molecular approach*. 2nd edition (Sunderland: Sinauer Associates). Available at: https://www.ncbi.nlm.nih.gov/books/NBK9963/ (Accessed July 12, 2023).

Cortés, J., Kim, S.-B., Chung, W.-P., Im, S.-A., Park, Y. H., Hegg, R., et al. (2021). LBA1 Trastuzumab deruxtecan (T-DXd) vs trastuzumab emtansine (T-DM1) in patients (Pts) with HER2+ metastatic breast cancer (mBC): Results of the randomized phase III DESTINY-Breast03 study. *Ann. Oncol.* 32, S1287–S1288. doi:10.1016/j.annonc.2021.08.2087

Cortés, J., Kim, S.-B., Chung, W.-P., Im, S.-A., Park, Y. H., Hegg, R., et al. (2022). Trastuzumab deruxtecan versus trastuzumab emtansine for breast cancer. *N. Engl. J. Med.* 386, 1143–1154. doi:10.1056/NEJMoa2115022

Dahl, J., Marx, K., and Jabbour, E. (2016). Inotuzumab ozogamicin in the treatment of acute lymphoblastic leukemia. *Expert Rev. Hematol.* 9, 329–334. doi:10.1586/17474086.2016.1143771

Dahlgren, D., and Lennernäs, H. (2020). Antibody-drug conjugates and targeted treatment strategies for hepatocellular carcinoma: A drug-delivery perspective. *Molecules* 25, 2861. doi:10.3390/molecules25122861

Damelin, M., Zhong, W., Myers, J., and Sapra, P. (2015). Evolving strategies for target selection for antibody-drug conjugates. *Pharm. Res.* 32, 3494–3507. doi:10.1007/s11095-015-1624-3

Dan, N., Setua, S., Kashyap, V. K., Khan, S., Jaggi, M., Yallapu, M. M., et al. (2018). Antibody-drug conjugates for cancer therapy: Chemistry to clinical implications. *Pharm. (Basel)* 11, 32. doi:10.3390/ph11020032

D'Atri, V., Pell, R., Clarke, A., Guillarme, D., and Fekete, S. (2019). Is hydrophobic interaction chromatography the most suitable technique to characterize site-specific antibody-drug conjugates? *J. Chromatogr. A* 1586, 149–153. doi:10.1016/j.chroma.2018.12.020

de Mel, N., Mulagapati, S. H. R., Cao, M., and Liu, D. (2019). A method to directly analyze free-drug–related species in antibody-drug conjugates without sample preparation. *J. Chromatogr. B* 1116, 51–59. doi:10.1016/j.jchromb.2019.04.012

Dean, A. Q., Luo, S., Twomey, J. D., and Zhang, B. (2021). Targeting cancer with antibody-drug conjugates: Promises and challenges. *MAbs* 13, 1951427. doi:10.1080/19420862.2021.1951427

Debaene, F., Boeuf, A., Wagner-Rousset, E., Colas, O., Ayoub, D., Corvaïa, N., et al. (2014). Innovative native MS methodologies for antibody drug conjugate characterization: High resolution native MS and IM-MS for average DAR and DAR distribution assessment. *Anal. Chem.* 86, 10674–10683. doi:10.1021/ac502593n

Deeks, E. D. (2021). Disitamab vedotin: First approval. *Drugs* 81, 1929–1935. doi:10.1007/s40265-021-01614-x

Deeks, E. D. (2019). Polatuzumab vedotin: First global approval. *Drugs* 79, 1467–1475. doi:10.1007/s40265-019-01175-0

Del Prete, A., Salvi, V., Soriani, A., Laffranchi, M., Sozio, F., Bosisio, D., et al. (2023). Dendritic cell subsets in cancer immunity and tumor antigen sensing. *Cell Mol. Immunol.* 20, 432–447. doi:10.1038/s41423-023-00990-6

Dennis, M. S., Jin, H., Dugger, D., Yang, R., McFarland, L., Ogasawara, A., et al. (2007). Imaging tumors with an albumin-binding Fab, a novel tumor-targeting agent. *Cancer Res.* 67, 254–261. doi:10.1158/0008-5472.CAN-06-2531

Deonarain, M. P., and Xue, Q. (2020). Tackling solid tumour therapy with small-format drug conjugates. *Antib. Ther.* 3, 237–245. doi:10.1093/abt/tbaa024

Deonarain, M. P., Yahioglu, G., Stamati, I., Pomowski, A., Clarke, J., Edwards, B. M., et al. (2018). Small-format drug conjugates: A viable alternative to ADCs for solid tumours? *Antibodies (Basel)* 7, 16. doi:10.3390/antib7020016

Diéras, V., Miles, D., Verma, S., Pegram, M., Welslau, M., Baselga, J., et al. (2017). Trastuzumab emtansine versus capecitabine plus lapatinib in patients with previously treated HER2-positive advanced breast cancer (EMILIA): a descriptive analysis of final

overall survival results from a randomised, open-label, phase 3 trial. *Lancet Oncol.* 18, 732–742. doi:10.1016/S1470-2045(17)30312-1

Dilawari, A., Shah, M., Ison, G., Gittleman, H., Fiero, M. H., Shah, A., et al. (2023). FDA approval summary: Mirvetuximab soravtansine-gynx for FRα-positive, platinum-resistant ovarian cancer. *Clin. Cancer Res.* 22, OF1–OF6. CCR-23-0991. doi:10.1158/1078-0432.CCR-23-0991

Domínguez-Llamas, S., Caro-Magdaleno, M., Mataix-Albert, B., Avilés-Prieto, J., Romero-Barranca, I., and Rodríguez-de-la-Rúa, E. (2023). Adverse events of antibody–drug conjugates on the ocular surface in cancer therapy. *Clin. Transl. Oncol.* 2023, 03261. doi:10.1007/s12094-023-03261-y

Donaghy, H. (2016). Effects of antibody, drug and linker on the preclinical and clinical toxicities of antibody-drug conjugates. *MAbs* 8, 659–671. doi:10.1080/19420862.2016.1156829

Drago, J. Z., Modi, S., and Chandarlapaty, S. (2021). Unlocking the potential of antibody–drug conjugates for cancer therapy. *Nat. Rev. Clin. Oncol.* 18, 327–344. doi:10.1038/s41571-021-00470-8

Ducry, L. (2012). Challenges in the development and manufacturing of antibody-drug conjugates. *Methods Mol. Biol.* 899, 489–497. doi:10.1007/978-1-61779-921-1_29

Dumontet, C., Reichert, J. M., Senter, P. D., Lambert, J. M., and Beck, A. (2023). Antibody–drug conjugates come of age in oncology. *Nat. Rev. Drug Discov.* 22, 641–661. doi:10.1038/s41573-023-00709-2

Edwards, E., Livanos, M., Krueger, A., Dell, A., Haslam, S. M., Mark Smales, C., et al. (2022). Strategies to control therapeutic antibody glycosylation during bioprocessing: Synthesis and separation. *Biotechnol. Bioeng.* 119, 1343–1358. doi:10.1002/bit.28066

Emens, L. A., Esteva, F. J., Beresford, M., Saura, C., Laurentiis, M. D., Kim, S.-B., et al. (2020). Trastuzumab emtansine plus atezolizumab versus trastuzumab emtansine plus placebo in previously treated, HER2-positive advanced breast cancer (KATE2): a phase 2, multicentre, randomised, double-blind trial. *Lancet Oncol.* 21, 1283–1295. doi:10.1016/S1470-2045(20)30465-4

Estrela, J. M., Ortega, A., and Obrador, E. (2006). Glutathione in cancer biology and therapy. *Crit. Rev. Clin. Lab. Sci.* 43, 143–181. doi:10.1080/10408360500523878

Fleming, R. (2020). ADC analysis by hydrophobic interaction chromatography. *Methods Mol. Biol.* 2078, 147–161. doi:10.1007/978-1-4939-9929-3_10

Ferl, G. Z., Kenanova, V., Wu, A. M., and DiStefano, J. J. (2006). A two-tiered physiologically based model for dually labeled single-chain Fv-Fc antibody fragments. *Mol. Cancer Ther.* 5, 1550–1558. doi:10.1158/1535-7163.MCT-06-0072

Ferraro, E., Drago, J. Z., and Modi, S. (2021). Implementing antibody-drug conjugates (ADCs) in HER2-positive breast cancer: state of the art and future directions. *Breast Cancer Res.* 23, 84. doi:10.1186/s13058-021-01459-y

Flynn, M. J., Zammarchi, F., Tyrer, P. C., Akarca, A. U., Janghra, N., Britten, C. E., et al. (2016). ADCT-301, a pyrrolobenzodiazepine (PBD) dimer-containing antibody-drug conjugate (ADC) targeting CD25-expressing hematological malignancies. *Mol. Cancer Ther.* 15, 2709–2721. doi:10.1158/1535-7163.MCT-16-0233

Ford, C. H., Newman, C. E., Johnson, J. R., Woodhouse, C. S., Reeder, T. A., Rowland, G. F., et al. (1983). Localisation and toxicity study of a vindesine-anti-CEA conjugate in patients with advanced cancer. *Br. J. Cancer* 47, 35–42. doi:10.1038/bjc.1983.4

Francisco, J. A., Cerveny, C. G., Meyer, D. L., Mixan, B. J., Klussman, K., Chace, D. F., et al. (2003). cAC10-vcMMAE, an anti-CD30-monomethyl auristatin E conjugate with potent and selective antitumor activity. *Blood* 102, 1458–1465. doi:10.1182/blood-2003-01-0039

Fu, Y., and Ho, M. (2018). DNA damaging agent-based antibody-drug conjugates for cancer therapy. *Antib. Ther.* 1, 33–43. doi:10.1093/abt/tby007

Fu, Z., Li, S., Han, S., Shi, C., and Zhang, Y. (2022). Antibody drug conjugate: the "biological missile" for targeted cancer therapy. *Sig Transduct. Target Ther.* 7, 93. doi:10.1038/s41392-022-00947-7

Fuentes-Antrás, J., Genta, S., Vijenthira, A., and Siu, L. L. (2023). Antibody–drug conjugates: in search of partners of choice. *Trends Cancer* 9, 339–354. doi:10.1016/j.trecan.2023.01.003

Fukuda, Y., Bustos, M. A., Cho, S.-N., Roszik, J., Ryu, S., Lopez, V. M., et al. (2022). Interplay between soluble CD74 and macrophage-migration inhibitory factor drives tumor growth and influences patient survival in melanoma. *Cell Death Dis.* 13, 117. doi:10.1038/s41419-022-04552-y

Furlanetto, J., Marmé, F., and Loibl, S. (2022). Sacituzumab govitecan: past, present and future of a new antibody-drug conjugate and future horizon. *Future Oncol.* 18, 3199–3215. doi:10.2217/fon-2022-0407

Gajewski, T. F., Meng, Y., and Harlin, H. (2006). Immune suppression in the tumor microenvironment. *J. Immunother.* 29, 233–240. doi:10.1097/01.cji.0000199193.29048.56

García-Alonso, S., Ocaña, A., and Pandiella, A. (2018). Resistance to antibody–drug conjugates. *Cancer Res.* 78, 2159–2165. doi:10.1158/0008-5472.CAN-17-3671

Garrett, M., Ruiz-Garcia, A., Parivar, K., Hee, B., and Boni, J. (2019). Population pharmacokinetics of inotuzumab ozogamicin in relapsed/refractory acute lymphoblastic leukemia and non-Hodgkin lymphoma. *J. Pharmacokinet. Pharmacodyn.* 46, 211–222. doi:10.1007/s10928-018-9614-9

Gerber, H.-P., Senter, P. D., and Grewal, I. S. (2009). Antibody drug-conjugates targeting the tumor vasculature: Current and future developments. *MAbs* 1, 247–253. doi:10.4161/mabs.1.3.8515

Gillard, G. O., Proctor, J. L., Brooks, M. L., Lamothe, T. L., Hyzy, S. L., McDonough, S. M., et al. (2020). A novel targeted approach to achieve immune system reset: CD45-Targeted antibody drug conjugates enable autologous HSCT and ameliorate disease in preclinical autoimmune disease models. *Biol. Blood Marrow Transplant.* 26, S307–S308. doi:10.1016/j.bbmt.2019.12.407

Godwin, C. D., Bates, O. M., Jean, S. R., Laszlo, G. S., Garling, E. E., Beddoe, M. E., et al. (2020). Anti-apoptotic BCL-2 family proteins confer resistance to calicheamicin-based antibody-drug conjugate therapy of acute leukemia. *Leuk. Lymphoma* 61, 2990–2994. doi:10.1080/10428194.2020.1786553

Gogesch, P., Dudek, S., van Zandbergen, G., Waibler, Z., and Anzaghe, M. (2021). The role of Fc receptors on the effectiveness of therapeutic monoclonal antibodies. *Int. J. Mol. Sci.* 22, 8947. doi:10.3390/ijms22168947

Goldenberg, M. M. (1999). Trastuzumab, a recombinant DNA-derived humanized monoclonal antibody, a novel agent for the treatment of metastatic breast cancer. *Clin. Ther.* 21, 309–318. doi:10.1016/S0149-2918(00)88288-0

Gomes-da-Silva, L. C., Kepp, O., and Kroemer, G. (2020). Regulatory approval of photoimmunotherapy: photodynamic therapy that induces immunogenic cell death. *Oncoimmunology* 9, 1841393. doi:10.1080/2162402X.2020.1841393

Gondi, C. S., and Rao, J. S. (2013). Cathepsin B as a cancer target. *Expert Opin. Ther. Targets* 17, 281–291. doi:10.1517/14728222.2013.740461

Goodson, H. V., and Jonasson, E. M. (2018). Microtubules and microtubule-associated proteins. *Cold Spring Harb. Perspect. Biol.* 10, a022608. doi:10.1101/cshperspect.a022608

Greenblatt, K., and Khaddour, K. (2023). Trastuzumab, in StatPearls (treasure island (FL): StatPearls publishing). Available at: http://www.ncbi.nlm.nih.gov/books/NBK532246/ [Accessed August 29, 2023].

Hackshaw, M. D., Danysh, H. E., Singh, J., Ritchey, M. E., Ladner, A., Taitt, C., et al. (2020). Incidence of pneumonitis/interstitial lung disease induced by HER2-targeting therapy for HER2-positive metastatic breast cancer. *Breast Cancer Res. Treat.* 183, 23–39. doi:10.1007/s10549-020-05754-8

Hamadani, M., Collins, G. P., Caimi, P. F., Samaniego, F., Spira, A., Davies, A., et al. (2021). Camidanlumab tesirine in patients with relapsed or refractory lymphoma: a phase 1, open-label, multicentre, dose-escalation, dose-expansion study. *Lancet Haematol.* 8, e433–e445. doi:10.1016/S2352-3026(21)00103-4

Hamblett, K. J., Senter, P. D., Chace, D. F., Sun, M. M. C., Lenox, J., Cerveny, C. G., et al. (2004). Effects of drug loading on the antitumor activity of a monoclonal antibody drug conjugate. *Clin. Cancer Res.* 10, 7063–7070. doi:10.1158/1078-0432.CCR-04-0789

Hartley, J. A. (2011). The development of pyrrolobenzodiazepines as antitumour agents. *Expert Opin. Investig. Drugs* 20, 733–744. doi:10.1517/13543784.2011.573477

Herbener, P., Schönfeld, K., König, M., Germer, M., Przyborski, J. M., Bernöster, K., et al. (2018). Functional relevance of *in vivo* half antibody exchange of an IgG4 therapeutic antibody-drug conjugate. *PLoS One* 13, e0195823. doi:10.1371/journal.pone.0195823

Heitz, N., Greer, S. C., and Halford, Z. (2023). A review of Tisotumab vedotin-tftv in recurrent or metastatic cervical cancer. *Ann. Pharmacother.* 57, 585–596. doi:10.1177/10600280221118370

Heo, Y.-A. (2023). Mirvetuximab soravtansine: First approval. *Drugs* 83, 265–273. doi:10.1007/s40265-023-01834-3

Herrera, A. F., Zain, J., Savage, K. J., Feldman, T. A., Brammer, J. E., Chen, L., et al. (2021). Brentuximab vedotin plus cyclophosphamide, doxorubicin, etoposide, and prednisone (CHEP-BV) followed by BV consolidation in patients with CD30-expressing peripheral T-cell lymphomas. *Blood* 138, 133. doi:10.1182/blood-2021-151105

Hoffmann, R. M., Coumbe, B. G. T., Josephs, D. H., Mele, S., Ilieva, K. M., Cheung, A., et al. (2018). Antibody structure and engineering considerations for the design and function of Antibody Drug Conjugates (ADCs). *Oncoimmunology* 7, e1395127. doi:10.1080/2162402X.2017.1395127

Hughes, B. (2010). Antibody-drug conjugates for cancer: poised to deliver? *Nat. Rev. Drug Discov.* 9, 665–667. doi:10.1038/nrd3270

Hurwitz, J., Haggstrom, L. R., and Lim, E. (2023). Antibody–drug conjugates: Ushering in a new era of cancer therapy. *Pharmaceutics* 15, 2017. doi:10.3390/pharmaceutics15082017

Hutchinson, M. H., Hendricks, R. S., Lin, X. X., and Olson, D. A. (2018). "Chapter 40 - process development and manufacturing of antibody-drug conjugates," in *Biopharmaceutical processing*. Editors G. Jagschies, E. Lindskog, K. Łącki, and P. Galliher (Amsterdam: Elsevier), 813–836. doi:10.1016/B978-0-08-100623-8.00041-4

Iqbal, N., and Iqbal, N. (2014). Human epidermal growth factor receptor 2 (HER2) in cancers: Overexpression and therapeutic implications. *Mol. Biol. Int.* 2014, 852748. doi:10.1155/2014/852748

Jain, N., Smith, S. W., Ghone, S., and Tomczuk, B. (2015). Current ADC linker chemistry. *Pharm. Res.* 32, 3526–3540. doi:10.1007/s11095-015-1657-7

Jain, R. K. (2001). Delivery of molecular and cellular medicine to solid tumors. *Adv. Drug Deliv. Rev.* 46, 149–168. doi:10.1016/s0169-409x(00)00131-9

Jain, R. K. (2005). Normalization of tumor vasculature: an emerging concept in antiangiogenic therapy. *Science* 307, 58–62. doi:10.1126/science.1104819

Jiang, Q., Patel, B., Jin, X., Di Grandi, D., Bortell, E., Czapkowski, B., et al. (2019). Structural characterization of the aggregates of gemtuzumab ozogamicin. *ACS Omega* 4, 6468–6475. doi:10.1021/acsomega.8b03627

Joubert, N., Beck, A., Dumontet, C., and Denevault-Sabourin, C. (2020). Antibody–drug conjugates: The last decade. *Pharmaceuticals* 13, 245. doi:10.3390/ph13090245

Junttila, T. T., Li, G., Parsons, K., Phillips, G. L., and Sliwkowski, M. X. (2011). Trastuzumab-DM1 (T-DM1) retains all the mechanisms of action of trastuzumab and efficiently inhibits growth of lapatinib insensitive breast cancer. *Breast Cancer Res. Treat.* 128, 347–356. doi:10.1007/s10549-010-1090-x

Junutula, J. R., Raab, H., Clark, S., Bhakta, S., Leipold, D. D., Weir, S., et al. (2008). Site-specific conjugation of a cytotoxic drug to an antibody improves the therapeutic index. *Nat. Biotechnol.* 26, 925–932. doi:10.1038/nbt.1480

Kang, C. (2021). Moxetumomab pasudotox in hairy cell leukaemia: A profile of its use. *Clin. Drug Investig.* 41, 829–834. doi:10.1007/s40261-021-01069-8

Kaplon, H., Crescioli, S., Chenoweth, A., Visweswaraiah, J., and Reichert, J. M. (2023). Antibodies to watch in 2023. *MAbs* 15, 2153410. doi:10.1080/19420862.2022.2153410

Kaplon, H., Muralidharan, M., Schneider, Z., and Reichert, J. M. (2020). Antibodies to watch in 2020. *MAbs* 12, 1703531. doi:10.1080/19420862.2019.1703531

Katz, J., Janik, J. E., and Younes, A. (2011). Brentuximab vedotin (SGN-35). *Clin. Cancer Res.* 17, 6428–6436. doi:10.1158/1078-0432.CCR-11-0488

Kayser, S., and Levis, M. J. (2022). Updates on targeted therapies for acute myeloid leukaemia. *Br. J. Haematol.* 196, 316–328. doi:10.1111/bjh.17746

Kholodenko, R. V., Kalinovsky, D. V., Doronin, I. I., Ponomarev, E. D., and Kholodenko, I. V. (2019). Antibody fragments as potential biopharmaceuticals for cancer therapy: Success and limitations. *CMC* 26, 396–426. doi:10.2174/0929867324666170817152554

Khongorzul, P., Ling, C. J., Khan, F. U., Ihsan, A. U., and Zhang, J. (2020). Antibody–drug conjugates: A comprehensive review. *Mol. Cancer Res.* 18, 3–19. doi:10.1158/1541-7786.MCR-19-0582

Kim, E. G., and Kim, K. M. (2015). Strategies and advancement in antibody-drug conjugate optimization for targeted cancer therapeutics. *Biomol. Ther. Seoul.* 23, 493–509. doi:10.4062/biomolther.2015.116

Kimiz-Gebologlu, I., Gulce-Iz, S., and Biray-Avci, C. (2018). Monoclonal antibodies in cancer immunotherapy. *Mol. Biol. Rep.* 45, 2935–2940. doi:10.1007/s11033-018-4427-x

Kitamura, N., Sento, S., Yoshizawa, Y., Sasabe, E., Kudo, Y., and Yamamoto, T. (2020). Current trends and future prospects of molecular targeted therapy in head and neck squamous cell carcinoma. *Int. J. Mol. Sci.* 22, 240. doi:10.3390/ijms22010240

Kostova, V., Désos, P., Starck, J.-B., and Kotschy, A. (2021). The chemistry behind ADCs. *Pharm. (Basel)* 14, 442. doi:10.3390/ph14050442

Kreitman, R. J. (2019). Hairy cell leukemia: present and future directions. *Leuk. Lymphoma* 60, 2869–2879. doi:10.1080/10428194.2019.1608536

Kreitman, R. J., and Pastan, I. (2011). Antibody fusion proteins: anti-CD22 recombinant immunotoxin moxetumomab pasudotox. *Clin. Cancer Res.* 17, 6398–6405. doi:10.1158/1078-0432.CCR-11-0487

Kvirkvelia, N., McMenamin, M., Gutierrez, V. I., Lasareishvili, B., and Madaio, M. P. (2015). Human anti-α3(IV)NC1 antibody drug conjugates target glomeruli to resolve nephritis. *Am. J. Physiol. Ren. Physiol.* 309, F680–F684. doi:10.1152/ajprenal.00289.2015

Labani-Motlagh, A., Ashja-Mahdavi, M., and Loskog, A. (2020). The tumor microenvironment: A milieu hindering and obstructing antitumor immune responses. *Front. Immunol.* 11, 940. doi:10.3389/fimmu.2020.00940

Lambert, J. M., and Chari, R. V. J. (2014). Ado-trastuzumab emtansine (T-DM1): an antibody-drug conjugate (ADC) for HER2-positive breast cancer. *J. Med. Chem.* 57, 6949–6964. doi:10.1021/jm500766w

Lambert, J. M., and Morris, C. Q. (2017). Antibody–drug conjugates (ADCs) for personalized treatment of solid tumors: A review. *Adv. Ther.* 34, 1015–1035. doi:10.1007/s12325-017-0519-6

Lanza, F., Maffini, E., Rondoni, M., Massari, E., Faini, A. C., and Malavasi, F. (2020). CD22 expression in B-cell acute lymphoblastic leukemia: Biological significance and implications for inotuzumab therapy in adults. *Cancers (Basel)* 12, 303. doi:10.3390/cancers12020303

Le, Q., Tang, T., Leonti, A., Castro, S., McKay, C. N., Perkins, L., et al. (2023). Preclinical studies targeting CD74 with STRO-001 antibody-drug conjugate in acute leukemia. *Blood Adv.* 7, 1666–1670. doi:10.1182/bloodadvances.2022008303

Lee, A. (2021). Loncastuximab tesirine: First approval. *Drugs* 81, 1229–1233. doi:10.1007/s40265-021-01550-w

Lee, H., Bhang, S. H., Lee, J. H., Kim, H., and Hahn, S. K. (2017). Tocilizumab-alendronate conjugate for treatment of rheumatoid arthritis. *Bioconjug Chem.* 28, 1084–1092. doi:10.1021/acs.bioconjchem.7b00008

Leget, G. A., and Czuczman, M. S. (1998). Use of rituximab, the new FDA-approved antibody. *Curr. Opin. Oncol.* 10, 548–551. doi:10.1097/00001622-199811000-00012

Lim, R. K. V., Yu, S., Cheng, B., Li, S., Kim, N.-J., Cao, Y., et al. (2015). Targeted delivery of LXR agonist using a site-specific antibody-drug conjugate. *Bioconjug Chem.* 26, 2216–2222. doi:10.1021/acs.bioconjchem.5b00203

Lin, J., and Lazar, A. C. (2013). Determination of charge heterogeneity and level of unconjugated antibody by imaged cIEF. *Methods Mol. Biol.* 1045, 295–302. doi:10.1007/978-1-62703-541-5_19

Lindley, C., McCune, J. S., Thomason, T. E., Lauder, D., Sauls, A., Adkins, S., et al. (1999). Perception of chemotherapy side effects cancer versus noncancer patients. *Cancer Pract.* 7, 59–65. doi:10.1046/j.1523-5394.1999.07205.x

Liu, L., and Chen, J. (2022). Therapeutic antibodies for precise cancer immunotherapy: current and future perspectives. *Med. Rev.* 2, 555–569. doi:10.1515/mr-2022-0033

Liu, Y., Jiang, P., Capkova, K., Xue, D., Ye, L., Sinha, S. C., et al. (2011). Tissue factor-activated coagulation cascade in the tumor microenvironment is critical for tumor progression and an effective target for therapy. *Cancer Res.* 71, 6492–6502. doi:10.1158/0008-5472.CAN-11-1145

Loganzo, F., Sung, M., and Gerber, H.-P. (2016). Mechanisms of resistance to antibody–drug conjugates. *Mol. Cancer Ther.* 15, 2825–2834. doi:10.1158/1535-7163.MCT-16-0408

Loganzo, F., Tan, X., Sung, M., Jin, G., Myers, J. S., Melamud, E., et al. (2015). Tumor cells chronically treated with a trastuzumab-maytansinoid antibody-drug conjugate develop varied resistance mechanisms but respond to alternate treatments. *Mol. Cancer Ther.* 14, 952–963. doi:10.1158/1535-7163.MCT-14-0862

Lu, J., Jiang, F., Lu, A., and Zhang, G. (2016). Linkers having a crucial role in antibody-drug conjugates. *Int. J. Mol. Sci.* 17, 561. doi:10.3390/ijms17040561

Lucas, A. T., Price, L. S. L., Schorzman, A. N., Storrie, M., Piscitelli, J. A., Razo, J., et al. (2018). Factors affecting the pharmacology of antibody-drug conjugates. *Antibodies (Basel)* 7, 10. doi:10.3390/antib7010010

Luo, R., Liu, H., and Cheng, Z. (2022). Protein scaffolds: antibody alternatives for cancer diagnosis and therapy. *RSC Chem. Biol.* 3, 830–847. doi:10.1039/D2CB00094F

Ma, Z., Wang, H., Cai, Y., Wang, H., Niu, K., Wu, X., et al. (2018). Epigenetic drift of H3K27me3 in aging links glycolysis to healthy longevity in Drosophila. *eLife* 7, e35368. doi:10.7554/eLife.35368

Macor, P., Capolla, S., and Tedesco, F. (2018). Complement as a biological tool to control tumor growth. *Front. Immunol.* 9, 2203. doi:10.3389/fimmu.2018.02203

Macor, P., Mezzanzanica, D., Cossetti, C., Alberti, P., Figini, M., Canevari, S., et al. (2006). Complement activated by chimeric anti-folate receptor antibodies is an efficient effector system to control ovarian carcinoma. *Cancer Res.* 66, 3876–3883. doi:10.1158/0008-5472.CAN-05-3434

Macor, P., and Tedesco, F. (2007). Complement as effector system in cancer immunotherapy. *Immunol. Lett.* 111, 6–13. doi:10.1016/j.imlet.2007.04.014

Mahadevan, D., and Von Hoff, D. D. (2007). Tumor-stroma interactions in pancreatic ductal adenocarcinoma. *Mol. Cancer Ther.* 6, 1186–1197. doi:10.1158/1535-7163.MCT-06-0686

Mahalingaiah, P. K., Ciurlionis, R., Durbin, K. R., Yeager, R. L., Philip, B. K., Bawa, B., et al. (2019). Potential mechanisms of target-independent uptake and toxicity of antibody-drug conjugates. *Pharmacol. Ther.* 200, 110–125. doi:10.1016/j.pharmthera.2019.04.008

Mahmood, I. (2021). Clinical pharmacology of antibody-drug conjugates. *Antibodies (Basel)* 10, 20. doi:10.3390/antib10020020

Malhotra, V., and Perry, M. C. (2003). Classical chemotherapy: mechanisms, toxicities and the therapeutic window. *Cancer Biol. Ther.* 2, S2–S4.

Mamounas, E. P., Untch, M., Mano, M. S., Huang, C.-S., Geyer, C. E., von Minckwitz, G., et al. (2021). Adjuvant T-DM1 versus trastuzumab in patients with residual invasive disease after neoadjuvant therapy for HER2-positive breast cancer: subgroup analyses from KATHERINE. *Ann. Oncol.* 32, 1005–1014. doi:10.1016/j.annonc.2021.04.011

Marei, H. E., Cenciarelli, C., and Hasan, A. (2022). Potential of antibody–drug conjugates (ADCs) for cancer therapy. *Cancer Cell Int.* 22, 255. doi:10.1186/s12935-022-02679-8

Masters, J. C., Nickens, D. J., Xuan, D., Shazer, R. L., and Amantea, M. (2018). Clinical toxicity of antibody drug conjugates: a meta-analysis of payloads. *Invest. New Drugs* 36, 121–135. doi:10.1007/s10637-017-0520-6

Matsumoto, T., Jimi, S., Hara, S., Takamatsu, Y., Suzumiya, J., and Tamura, K. (2012). Importance of inducible multidrug resistance 1 expression in HL-60 cells resistant to gemtuzumab ozogamicin. *Leuk. Lymphoma* 53, 1399–1405. doi:10.3109/10428194.2012.656102

Mckertish, C. M., and Kayser, V. (2021). Advances and limitations of antibody drug conjugates for cancer. *Biomedicines* 9, 872. doi:10.3390/biomedicines9080872

Mecklenburg, L. (2018). A brief introduction to antibody-drug conjugates for toxicologic pathologists. *Toxicol. Pathol.* 46, 746–752. doi:10.1177/0192623318803059

Mehanna, J., Haddad, F. G., Eid, R., Lambertini, M., and Kourie, H. R. (2019). Triple-negative breast cancer: current perspective on the evolving therapeutic landscape. *Int. J. Womens Health* 11, 431–437. doi:10.2147/IJWH.S178349

Modi, S., Jacot, W., Yamashita, T., Sohn, J., Vidal, M., Tokunaga, E., et al. (2022). Trastuzumab deruxtecan in previously treated HER2-low advanced breast cancer. *N. Engl. J. Med.* 387, 9–20. doi:10.1056/NEJMoa2203690

Modi, S., Saura, C., Yamashita, T., Park, Y. H., Kim, S.-B., Tamura, K., et al. (2021). Abstract PD3-06: Updated results from DESTINY-breast01, a phase 2 trial of trastuzumab deruxtecan (T-DXd) in HER2 positive metastatic breast cancer. *Cancer Res.* 81, PD3–06. doi:10.1158/1538-7445.SABCS20-PD3-06

Modi, S., Saura, C., Yamashita, T., Park, Y. H., Kim, S.-B., Tamura, K., et al. (2020). Trastuzumab deruxtecan in previously treated HER2-positive breast cancer. *N. Engl. J. Med.* 382, 610–621. doi:10.1056/NEJMoa1914510

Nader-Marta, G., Martins-Branco, D., Agostinetto, E., Bruzzone, M., Ceppi, M., Danielli, L., et al. (2022). Efficacy of tyrosine kinase inhibitors for the treatment of patients with HER2-positive breast cancer with brain metastases: a systematic review and meta-analysis. *ESMO Open* 7, 100501. doi:10.1016/j.esmoop.2022.100501

Natsume, A., Niwa, R., and Satoh, M. (2009). Improving effector functions of antibodies for cancer treatment: Enhancing ADCC and CDC. *Drug Des. Devel Ther.* 3, 7–16. doi:10.2147/dddt.s4378

Nejadmoghaddam, M.-R., Minai-Tehrani, A., Ghahremanzadeh, R., Mahmoudi, M., Dinarvand, R., and Zarnani, A.-H. (2019). Antibody-drug conjugates: Possibilities and challenges. *Avicenna J. Med. Biotechnol.* 11, 3–23.

Nguyen, T. D., Bordeau, B. M., and Balthasar, J. P. (2023). Mechanisms of ADC toxicity and strategies to increase ADC tolerability. *Cancers (Basel)* 15, 713. doi:10.3390/cancers15030713

Nicolò, E., Giugliano, F., Ascione, L., Tarantino, P., Corti, C., Tolaney, S. M., et al. (2022). Combining antibody-drug conjugates with immunotherapy in solid tumors: current landscape and future perspectives. *Cancer Treat. Rev.* 106, 102395. doi:10.1016/j.ctrv.2022.102395

Nolting, B. (2013). Linker technologies for antibody-drug conjugates. *Methods Mol. Biol.* 1045, 71–100. doi:10.1007/978-1-62703-541-5_5

Norsworthy, K. J., Ko, C.-W., Lee, J. E., Liu, J., John, C. S., Przepiorka, D., et al. (2018). FDA approval summary: Mylotarg for treatment of patients with relapsed or refractory CD33-positive acute myeloid leukemia. *Oncologist* 23, 1103–1108. doi:10.1634/theoncologist.2017-0604

Ouyang, J. (2013). Drug-to-antibody ratio (DAR) and drug load distribution by hydrophobic interaction chromatography and reversed phase high-performance liquid chromatography. *Methods Mol. Biol.* 1045, 275–283. doi:10.1007/978-1-62703-541-5_17

O'Leary, M. K., Ahmed, A., and Alabi, C. A. (2023). Development of host-cleavable antibody-bactericide conjugates against extracellular pathogens. *ACS Infect. Dis.* 9, 322–329. doi:10.1021/acsinfecdis.2c00492

Omura, G., Honma, Y., Matsumoto, Y., Shinozaki, T., Itoyama, M., Eguchi, K., et al. (2023). Transnasal photoimmunotherapy with cetuximab sarotalocan sodium: Outcomes on the local recurrence of nasopharyngeal squamous cell carcinoma. *Auris Nasus Larynx* 50, 641–645. doi:10.1016/j.anl.2022.06.004

Park, M.-H., Lee, B. I., Byeon, J.-J., Shin, S.-H., Choi, J., Park, Y., et al. (2019). Pharmacokinetic and metabolism studies of monomethyl auristatin F via liquid chromatography-quadrupole-time-of-flight mass spectrometry. *Molecules* 24, 2754. doi:10.3390/molecules24152754

Perrino, E., Steiner, M., Krall, N., Bernardes, G. J. L., Pretto, F., Casi, G., et al. (2014). Curative properties of noninternalizing antibody-drug conjugates based on maytansinoids. *Cancer Res.* 74, 2569–2578. doi:10.1158/0008-5472.CAN-13-2990

Peters, C., and Brown, S. (2015). Antibody–drug conjugates as novel anti-cancer chemotherapeutics. *Biosci. Rep.* 35, e00225. doi:10.1042/BSR20150089

Pettinato, M. C. (2021). Introduction to antibody-drug conjugates. *Antibodies* 10, 42. doi:10.3390/antib10040042

Ponte, J. F., Ab, O., Lanieri, L., Lee, J., Coccia, J., Bartle, L. M., et al. (2016). Mirvetuximab soravtansine (IMGN853), a folate receptor alpha-targeting antibody-drug conjugate, potentiates the activity of standard of care therapeutics in ovarian cancer models. *Neoplasia* 18, 775–784. doi:10.1016/j.neo.2016.11.002

Ponziani, S., Di Vittorio, G., Pitari, G., Cimini, A. M., Ardini, M., Gentile, R., et al. (2020). Antibody-drug conjugates: The new frontier of chemotherapy. *Int. J. Mol. Sci.* 21, 5510. doi:10.3390/ijms21155510

Professional Committee on Clinical Research of Oncology Drugs, Expert Committee for Monitoring the Clinical Application of Antitumor Drugs, Chinese Anti-Cancer Association, and Cancer Chemotherapy Quality Control Expert Committee of Beijing Cancer Treatment Quality Control and Improvement Center (2022). Expert consensus on the clinical application of antibody-drug conjugates in the treatment of malignant tumors (2021 edition). *Cancer Innov.* 1, 3–24. doi:10.1002/cai2.8

Purcell, J. W., Tanlimco, S. G., Hickson, J., Fox, M., Sho, M., Durkin, L., et al. (2018). LRRC15 is a novel mesenchymal protein and stromal target for antibody–drug conjugates. *Cancer Res.* 78, 4059–4072. doi:10.1158/0008-5472.CAN-18-0327

Ritchie, M., Tchistiakova, L., and Scott, N. (2013). Implications of receptor-mediated endocytosis and intracellular trafficking dynamics in the development of antibody drug conjugates. *MAbs* 5, 13–21. doi:10.4161/mabs.22854

Rassy, E., Rached, L., and Pistilli, B. (2022). Antibody drug conjugates targeting HER2: Clinical development in metastatic breast cancer. *Breast* 66, 217–226. doi:10.1016/j.breast.2022.10.016

Redman, J. M., Hill, E. M., AlDeghaither, D., and Weiner, L. M. (2015). Mechanisms of action of therapeutic antibodies for cancer. *Mol. Immunol.* 67, 28–45. doi:10.1016/j.molimm.2015.04.002

Richards, D. A. (2018). Exploring alternative antibody scaffolds: Antibody fragments and antibody mimics for targeted drug delivery. *Drug Discov. Today Technol.* 30, 35–46. doi:10.1016/j.ddtec.2018.10.005

Ríos-Luci, C., García-Alonso, S., Díaz-Rodríguez, E., Nadal-Serrano, M., Arribas, J., Ocaña, A., et al. (2017). Resistance to the antibody-drug conjugate T-DM1 is based in a reduction in lysosomal proteolytic activity. *Cancer Res.* 77, 4639–4651. doi:10.1158/0008-5472.CAN-16-3127

Sabbaghi, M., Gil-Gómez, G., Guardia, C., Servitja, S., Arpí, O., García-Alonso, S., et al. (2017). Defective cyclin B1 induction in trastuzumab-emtansine (T-DM1) acquired resistance in HER2-positive breast cancer. *Clin. Cancer Res.* 23, 7006–7019. doi:10.1158/1078-0432.CCR-17-0696

Salem, A., Alotaibi, M., Mroueh, R., Basheer, H. A., and Afarinkia, K. (2021). CCR7 as a therapeutic target in Cancer. *Biochim. Biophys. Acta Rev. Cancer* 1875, 188499. doi:10.1016/j.bbcan.2020.188499

Samantasinghar, A., Sunildutt, N. P., Ahmed, F., Soomro, A. M., Salih, A. R. C., Parihar, P., et al. (2023). A comprehensive review of key factors affecting the efficacy of antibody drug conjugate. *Biomed. Pharmacother.* 161, 114408. doi:10.1016/j.biopha.2023.114408

Sau, S., Alsaab, H. O., Kashaw, S. K., Tatiparti, K., and Iyer, A. K. (2017). Advances in antibody-drug conjugates: A new era of targeted cancer therapy. *Drug Discov. Today* 22, 1547–1556. doi:10.1016/j.drudis.2017.05.011

Schmidhalter, D. R., Elzner, S., and Schmid, R. (2019). "Progress in the development of single-use solutions in antibody–drug conjugate (ADC) manufacturing," in *Single-use technology in biopharmaceutical manufacture* (New Jersey: John Wiley & Sons, Ltd), 303–310. doi:10.1002/9781119477891.ch27

Schwartz, R. S. (2004). Paul Ehrlich's magic bullets. *N. Engl. J. Med.* 350, 1079–1080. doi:10.1056/NEJMp048021

Scott, L. J. (2017). Brentuximab vedotin: A review in CD30-positive Hodgkin lymphoma. *Drugs* 77, 435–445. doi:10.1007/s40265-017-0705-5

Seaman, S., Zhu, Z., Saha, S., Zhang, X. M., Yang, M. Y., Hilton, M. B., et al. (2017). Eradication of tumors through simultaneous ablation of CD276/B7-H3-positive tumor cells and tumor vasculature. *Cancer Cell* 31, 501–515. doi:10.1016/j.ccell.2017.03.005

Seckinger, A., Delgado, J. A., Moser, S., Moreno, L., Neuber, B., Grab, A., et al. (2017). Target expression, generation, preclinical activity, and pharmacokinetics of the BCMA-T cell bispecific antibody EM801 for multiple myeloma treatment. *Cancer Cell* 31, 396–410. doi:10.1016/j.ccell.2017.02.002

Sehn, L. H., Hertzberg, M., Opat, S., Herrera, A. F., Assouline, S., Flowers, C. R., et al. (2022). Polatuzumab vedotin plus bendamustine and rituximab in relapsed/refractory DLBCL: survival update and new extension cohort data. *Blood Adv.* 6, 533–543. doi:10.1182/bloodadvances.2021005794

Senapati, S., Mahanta, A. K., Kumar, S., and Maiti, P. (2018). Controlled drug delivery vehicles for cancer treatment and their performance. *Signal Transduct. Target Ther.* 3, 7. doi:10.1038/s41392-017-0004-3

Senter, P. D. (2009). Potent antibody drug conjugates for cancer therapy. *Curr. Opin. Chem. Biol.* 13, 235–244. doi:10.1016/j.cbpa.2009.03.023

Senter, P. D., and Sievers, E. L. (2012). The discovery and development of brentuximab vedotin for use in relapsed Hodgkin lymphoma and systemic anaplastic large cell lymphoma. *Nat. Biotechnol.* 30, 631–637. doi:10.1038/nbt.2289

Shefet-Carasso, L., and Benhar, I. (2015). Antibody-targeted drugs and drug resistance--challenges and solutions. *Drug Resist Updat* 18, 36–46. doi:10.1016/j.drup.2014.11.001

Shi, F., Liu, Y., Zhou, X., Shen, P., Xue, R., and Zhang, M. (2022). Disitamab vedotin: a novel antibody-drug conjugates for cancer therapy. *Drug Deliv.* 29, 1335–1344. doi:10.1080/10717544.2022.2069883

Shiravand, Y., Khodadadi, F., Kashani, S. M. A., Hosseini-Fard, S. R., Hosseini, S., Sadeghirad, H., et al. (2022). Immune checkpoint inhibitors in cancer therapy. *Curr. Oncol.* 29, 3044–3060. doi:10.3390/curroncol29050247

Shitara, K., Baba, E., Fujitani, K., Oki, E., Fujii, S., and Yamaguchi, K. (2021). Discovery and development of trastuzumab deruxtecan and safety management for patients with HER2-positive gastric cancer. *Gastric Cancer* 24, 780–789. doi:10.1007/s10120-021-01196-3

Some, D., Amartely, H., Tsadok, A., and Lebendiker, M. (2019). Characterization of proteins by size-exclusion chromatography coupled to multi-angle light scattering (SEC-MALS). *J. Vis. Exp.* 2019, 59615. doi:10.3791/59615

Spiess, C., Bevers, J., Jackman, J., Chiang, N., Nakamura, G., Dillon, M., et al. (2013). Development of a human IgG4 bispecific antibody for dual targeting of interleukin-4 (IL-4) and interleukin-13 (IL-13) cytokines. *J. Biol. Chem.* 288, 26583–26593. doi:10.1074/jbc.M113.480483

Staudacher, A. H., and Brown, M. P. (2017). Antibody drug conjugates and bystander killing: is antigen-dependent internalisation required? *Br. J. Cancer* 117, 1736–1742. doi:10.1038/bjc.2017.367

Stapleton, N. M., Andersen, J. T., Stemerding, A. M., Bjarnarson, S. P., Verheul, R. C., Gerritsen, J., et al. (2011). Competition for FcRn-mediated transport gives rise to short half-life of human IgG3 and offers therapeutic potential. *Nat. Commun.* 2, 599. doi:10.1038/ncomms1608

Strop, P., Delaria, K., Foletti, D., Witt, J. M., Hasa-Moreno, A., Poulsen, K., et al. (2015). Site-specific conjugation improves therapeutic index of antibody drug conjugates with high drug loading. *Nat. Biotechnol.* 33, 694–696. doi:10.1038/nbt.3274

Su, Z., Xiao, D., Xie, F., Liu, L., Wang, Y., Fan, S., et al. (2021). Antibody–drug conjugates: Recent advances in linker chemistry. *Acta Pharm. Sin. B* 11, 3889–3907. doi:10.1016/j.apsb.2021.03.042

Sun Kang, M., See Kong, T. W., Xin Khoo, J. Y., and Loh, T.-P. (2021). Recent developments in chemical conjugation strategies targeting native amino acids in proteins and their applications in antibody–drug conjugates. *Chem. Sci.* 12, 13613–13647. doi:10.1039/D1SC02973H

Sung, H., Ferlay, J., Siegel, R. L., Laversanne, M., Soerjomataram, I., Jemal, A., et al. (2021). Global cancer statistics 2020: GLOBOCAN estimates of incidence and mortality worldwide for 36 cancers in 185 countries. *CA Cancer J. Clin.* 71, 209–249. doi:10.3322/caac.21660

Szot, C., Saha, S., Zhang, X. M., Zhu, Z., Hilton, M. B., Morris, K., et al. (2018). Tumor stroma–targeted antibody-drug conjugate triggers localized anticancer drug release. *J. Clin. Invest.* 128, 2927–2943. doi:10.1172/JCI120481

Tai, Y.-T., Mayes, P. A., Acharya, C., Zhong, M. Y., Cea, M., Cagnetta, A., et al. (2014). Novel anti-B-cell maturation antigen antibody-drug conjugate (GSK2857916) selectively induces killing of multiple myeloma. *Blood* 123, 3128–3138. doi:10.1182/blood-2013-10-535088

Talotta, R., Rucci, F., Canti, G., and Scaglione, F. (2019). Pros and cons of the immunogenicity of monoclonal antibodies in cancer treatment: a lesson from autoimmune diseases. *Immunotherapy* 11, 241–254. doi:10.2217/imt-2018-0081

Tang, H., Liu, Y., Yu, Z., Sun, M., Lin, L., Liu, W., et al. (2019). The analysis of key factors related to ADCs structural design. *Front. Pharmacol.* 10, 373. doi:10.3389/fphar.2019.00373

Tarantino, P., Ricciuti, B., Pradhan, S. M., and Tolaney, S. M. (2023). Optimizing the safety of antibody–drug conjugates for patients with solid tumours. *Nat. Rev. Clin. Oncol.* 20, 558–576. doi:10.1038/s41571-023-00783-w

Thurber, G. M., and Dane Wittrup, K. (2012). A mechanistic compartmental model for total antibody uptake in tumors. *J. Theor. Biol.* 314, 57–68. doi:10.1016/j.jtbi.2012.08.034

Thurber, G. M., Schmidt, M. M., and Wittrup, K. D. (2008). Antibody tumor penetration: transport opposed by systemic and antigen-mediated clearance. *Adv. Drug Deliv. Rev.* 60, 1421–1434. doi:10.1016/j.addr.2008.04.012

Tilly, H., Morschhauser, F., Sehn, L. H., Friedberg, J. W., Trněný, M., Sharman, J. P., et al. (2022). Polatuzumab vedotin in previously untreated diffuse large B-cell lymphoma. *N. Engl. J. Med.* 386, 351–363. doi:10.1056/NEJMoa2115304

Tipton, T. R. W., Roghanian, A., Oldham, R. J., Carter, M. J., Cox, K. L., Mockridge, C. I., et al. (2015). Antigenic modulation limits the effector cell mechanisms employed by type I anti-CD20 monoclonal antibodies. *Blood* 125, 1901–1909. doi:10.1182/blood-2014-07-588376

Tong, J. T. W., Harris, P. W. R., Brimble, M. A., and Kavianinia, I. (2021). An insight into FDA approved antibody-drug conjugates for cancer therapy. *Molecules* 26, 5847. doi:10.3390/molecules26195847

Tsuchikama, K., and An, Z. (2018). Antibody-drug conjugates: recent advances in conjugation and linker chemistries. *Protein Cell* 9, 33–46. doi:10.1007/s13238-016-0323-0

Tvilum, A., Johansen, M. I., Glud, L. N., Ivarsen, D. M., Khamas, A. B., Carmali, S., et al. (2023). Antibody-drug conjugates to treat bacterial biofilms via targeting and extracellular drug release. *Adv. Sci. (Weinh)* 10, e2301340. doi:10.1002/advs.202301340

van der Velden, V. H. J., Boeckx, N., Jedema, I., te Marvelde, J. G., Hoogeveen, P. G., Boogaerts, M., et al. (2004). High CD33-antigen loads in peripheral blood limit the efficacy of gemtuzumab ozogamicin (Mylotarg) treatment in acute myeloid leukemia patients. *Leukemia* 18, 983–988. doi:10.1038/sj.leu.2403350

van Dongen, G. A. M. S. (2021). Improving tumor penetration of antibodies and antibody-drug conjugates: Taking away the barriers for trojan horses. *Cancer Res.* 81, 3956–3957. doi:10.1158/0008-5472.CAN-21-0952

Varma, G., Wang, J., and Diefenbach, C. (2022). Polatuzumab vedotin in relapsed/refractory aggressive B-cell lymphoma. *Expert Rev. Anticancer Ther.* 22, 795–803. doi:10.1080/14737140.2022.2093191

Verhoef, J. J. F., and Anchordoquy, T. J. (2013). Questioning the use of PEGylation for drug delivery. *Drug Deliv. Transl. Res.* 3, 499–503. doi:10.1007/s13346-013-0176-5

Vidarsson, G., Dekkers, G., and Rispens, T. (2014). IgG subclasses and allotypes: from structure to effector functions. *Front. Immunol.* 5, 520. doi:10.3389/fimmu.2014.00520

Visser, K. E. de, and Joyce, J. A. (2023). The evolving tumor microenvironment: From cancer initiation to metastatic outgrowth. *Cancer Cell* 41, 374–403. doi:10.1016/j.ccell.2023.02.016

von Arx, C., De Placido, P., Caltavituro, A., Di Rienzo, R., Buonaiuto, R., De Laurentiis, M., et al. (2023). The evolving therapeutic landscape of trastuzumab-drug conjugates: Future perspectives beyond HER2-positive breast cancer. *Cancer Treat. Rev.* 113, 102500. doi:10.1016/j.ctrv.2022.102500

von Minckwitz, G., Huang, C.-S., Mano, M. S., Loibl, S., Mamounas, E. P., Untch, M., et al. (2019). Trastuzumab emtansine for residual invasive HER2-positive breast cancer. *N. Engl. J. Med.* 380, 617–628. doi:10.1056/NEJMoa1814017

Vozella, F., Fazio, F., Lapietra, G., Petrucci, M. T., Martinelli, G., and Cerchione, C. (2021). Monoclonal antibodies in multiple myeloma. *Panminerva Med.* 63, 21–27. doi:10.23736/S0031-0808.20.04149-X

Vu, T., and Claret, F. X. (2012). Trastuzumab: updated mechanisms of action and resistance in breast cancer. *Front. Oncol.* 2, 62. doi:10.3389/fonc.2012.00062

Wagh, A., Song, H., Zeng, M., Tao, L., and Das, T. K. (2018). Challenges and new frontiers in analytical characterization of antibody-drug conjugates. *MAbs* 10, 222–243. doi:10.1080/19420862.2017.1412025

Wagner, E., Colas, O., Chenu, S., Goyon, A., Murisier, A., Cianferani, S., et al. (2020). Determination of size variants by CE-SDS for approved therapeutic antibodies: Key implications of subclasses and light chain specificities. *J. Pharm. Biomed. Anal.* 184, 113166. doi:10.1016/j.jpba.2020.113166

Waight, A. B., Bargsten, K., Doronina, S., Steinmetz, M. O., Sussman, D., and Prota, A. E. (2016). Structural basis of microtubule destabilization by potent auristatin anti-mitotics. *PLoS One* 11, e0160890. doi:10.1371/journal.pone.0160890

Wang, Q., Shao, X., Zhang, Y., Zhu, M., Wang, F. X. C., Mu, J., et al. (2023). Role of tumor microenvironment in cancer progression and therapeutic strategy. *Cancer Med.* 12, 11149–11165. doi:10.1002/cam4.5698

Wang, Z., Li, H., Gou, L., Li, W., and Wang, Y. (2023). Antibody–drug conjugates: Recent advances in payloads. *Acta Pharm. Sin. B* 2023, 15. doi:10.1016/j.apsb.2023.06.015

Wedam, S., Fashoyin-Aje, L., Gao, X., Bloomquist, E., Tang, S., Sridhara, R., et al. (2020). FDA approval summary: Ado-trastuzumab emtansine for the adjuvant treatment of HER2-positive early breast cancer. *Clin. Cancer Res.* 26, 4180–4185. doi:10.1158/1078-0432.CCR-19-3980

Weiner, L. M., Dhodapkar, M. V., and Ferrone, S. (2009). Monoclonal antibodies for cancer immunotherapy. *Lancet* 373, 1033–1040. doi:10.1016/S0140-6736(09)60251-8

Wojtukiewicz, M. Z., Rek, M. M., Karpowicz, K., Górska, M., Polityńska, B., Wojtukiewicz, A. M., et al. (2021). Inhibitors of immune checkpoints—PD-1, PD-L1, CTLA-4—New opportunities for cancer patients and a new challenge for internists and general practitioners. *Cancer Metastasis Rev.* 40, 949–982. doi:10.1007/s10555-021-09976-0

Xiao, Y., and Yu, D. (2021). Tumor microenvironment as a therapeutic target in cancer. *Pharmacol. Ther.* 221, 107753. doi:10.1016/j.pharmthera.2020.107753

Xu, S. (2015). Internalization, trafficking, intracellular processing and actions of antibody-drug conjugates. *Pharm. Res.* 32, 3577–3583. doi:10.1007/s11095-015-1729-8

Yao, P., Zhang, Y., Zhang, S., Wei, X., Liu, Y., Du, C., et al. (2023). Knowledge atlas of antibody-drug conjugates on CiteSpace and clinical trial visualization analysis. *Front. Oncol.* 12, 1039882. doi:10.3389/fonc.2022.1039882

Yasunaga, M., Manabe, S., and Matsumura, Y. (2017). Immunoregulation by IL-7R-targeting antibody-drug conjugates: overcoming steroid-resistance in cancer and autoimmune disease. *Sci. Rep.* 7, 10735. doi:10.1038/s41598-017-11255-4

Yogev, S., Cooper, R., Fetter, R., Horowitz, M., and Shen, K. (2016). Microtubule organization determines axonal transport dynamics. *Neuron* 92, 449–460. doi:10.1016/j.neuron.2016.09.036

Yu, J., Song, Y., and Tian, W. (2020). How to select IgG subclasses in developing anti-tumor therapeutic antibodies. *J. Hematol. Oncol.* 13, 45. doi:10.1186/s13045-020-00876-4

Zahavi, D., and Weiner, L. (2020). Monoclonal antibodies in cancer therapy. *Antibodies (Basel)* 9, 34. doi:10.3390/antib9030034

Zammarchi, F., Corbett, S., Adams, L., Tyrer, P. C., Kiakos, K., Janghra, N., et al. (2018). ADCT-402, a PBD dimer-containing antibody drug conjugate targeting CD19-expressing malignancies. *Blood* 131, 1094–1105. doi:10.1182/blood-2017-10-813493

Zhang, J., Woods, C., He, F., Han, M., Treuheit, M. J., and Volkin, D. B. (2018). Structural changes and aggregation mechanisms of two different dimers of an IgG2 monoclonal antibody. *Biochemistry* 57, 5466–5479. doi:10.1021/acs.biochem.8b00575

Zhao, P., Zhang, Y., Li, W., Jeanty, C., Xiang, G., and Dong, Y. (2020). Recent advances of antibody drug conjugates for clinical applications. *Acta Pharm. Sin. B* 10, 1589–1600. doi:10.1016/j.apsb.2020.04.012

Zheng, Y., Ma, L., Sun, Q., and Tian, L. (2021). Clinically-relevant ABC transporter for anti-cancer drug resistance. *Front. Pharmacol.* 12, 648407. doi:10.3389/fphar.2021.648407

Ziogas, D. C., Theocharopoulos, C., Lialios, P.-P., Foteinou, D., Koumprentziotis, I.-A., Xynos, G., et al. (2023). Beyond CTLA-4 and PD-1 inhibition: Novel immune checkpoint molecules for melanoma treatment. *Cancers (Basel)* 15, 2718. doi:10.3390/cancers15102718

Zmolek, W., Bañas, S., Barfield, R. M., Rabuka, D., and Drake, P. M. (2016). A simple LC/MRM-MS-based method to quantify free linker-payload in antibody-drug conjugate preparations. *J. Chromatogr. B Anal. Technol. Biomed. Life Sci.* 1032, 144–148. doi:10.1016/j.jchromb.2016.05.055

frontiers | Frontiers in Pharmacology

TYPE Original Research
PUBLISHED 21 September 2023
DOI 10.3389/fphar.2023.1258387

OPEN ACCESS

EDITED BY
Ayaz Shahid,
Western University of Health Sciences, United States

REVIEWED BY
Aiswarya Chaudhuri,
Indian Institute of Technology (BHU), India
Mohamed Ali,
Zagazig University, Egypt

*CORRESPONDENCE
Sara F. Gaafar,
sarafekri111088@gmail.com

RECEIVED 13 July 2023
ACCEPTED 08 September 2023
PUBLISHED 21 September 2023

CITATION
Hussein MMA, Abdelfattah-Hassan A, Eldoumani H, Essawi WM, Alsahli TG, Alharbi KS, Alzarea SI, Al-Hejaili HY and Gaafar SF (2023), Evaluation of anti-cancer effects of carnosine and melittin-loaded niosomes in MCF-7 and MDA-MB-231 breast cancer cells. *Front. Pharmacol.* 14:1258387. doi: 10.3389/fphar.2023.1258387

Evaluation of anti-cancer effects of carnosine and melittin-loaded niosomes in MCF-7 and MDA-MB-231 breast cancer cells

Mohamed M. A. Hussein[1], Ahmed Abdelfattah-Hassan[2,3], Haitham Eldoumani[4], Walaa M. Essawi[5], Tariq G. Alsahli[6], Khalid Saad Alharbi[7], Sami I. Alzarea[6], Hassan Y. Al-Hejaili[8] and Sara F. Gaafar[1]*

[1]Biochemistry Department, Faculty of Veterinary Medicine, Zagazig University, Zagazig, Egypt, [2]Department of Anatomy and Embryology, Faculty of Veterinary Medicine, Zagazig University, Zagazig, Egypt, [3]Biomedical Sciences Program, University of Science and Technology, Zewail City of Science and Technology, Giza, Egypt, [4]Department of Anatomy and Embryology, Faculty of Veterinary Medicine, Mansoura University, Mansoura, Egypt, [5]Department of Theriogenology, Faculty of Veterinary Medicine, Aswan University, Aswan, Egypt, [6]Department of Pharmacology, College of Pharmacy, Jouf University, Sakaka, Saudi Arabia, [7]Department of Pharmacology and Toxicology, Unaizah College of Pharmacy, Qassim University, Qassim, Saudi Arabia, [8]Pharmaceutical Care Department, King Salman Bin Abdulaziz Medical City, Ministry of Health, Medina, Saudi Arabia

Background: We investigated the anti-cancer effect of carnosine-loaded niosomes (Car-NIO) and melittin-loaded niosomes (Mel-NIO) with olaparib in breast cancer cell lines (MCF-7 and MDA-MB-231).

Methods: The thin film method was used for preparing the niosomes and characterized in terms of morphology, size, and polydispersity index (PDI). We further evaluated the impact of these peptides on breast cancer cells viability, RT-qPCR assays, malondialdehyde (MDA) activity, and cell cycle progression, to determine if these are linked to carnosine and melittin's anti-proliferative properties.

Results: Car-NIO and Mel-NIO *in vitro* study inhibited cancer cell viability. They have also upregulated the expression of protein 53 (P53), BCL2-Associated X Protein (Bax), caspase-9, caspase-3, programmed cell death 4 (PDCD4), and Forkhead box O3 (FOXO3), while downregulated the expression of B-cell lymphoma 2 (Bcl2), poly (ADP-ribose) polymerase (PARP 1), and MicroRNA-183 (miRNA-183). The MCF-7 cells were arrested at the G2/M phase in Car-NIO, on the other hand, the MDA-MB-231 cells were arrested at the S phase. While the Mel-NIO and olaparib arrested the MCF-7 and MDA-MB-231 cells at the G0/1 phase.

Conclusion: Our study successfully declared that Mel-NIO had more anti-cancer effects than Car-NIO in both MCF-7 and MDA-MB-231 breast cancer cells.

KEYWORDS

carnosine, melittin, niosome, breast cancer cells, cell cycle analysis, miRNA-183

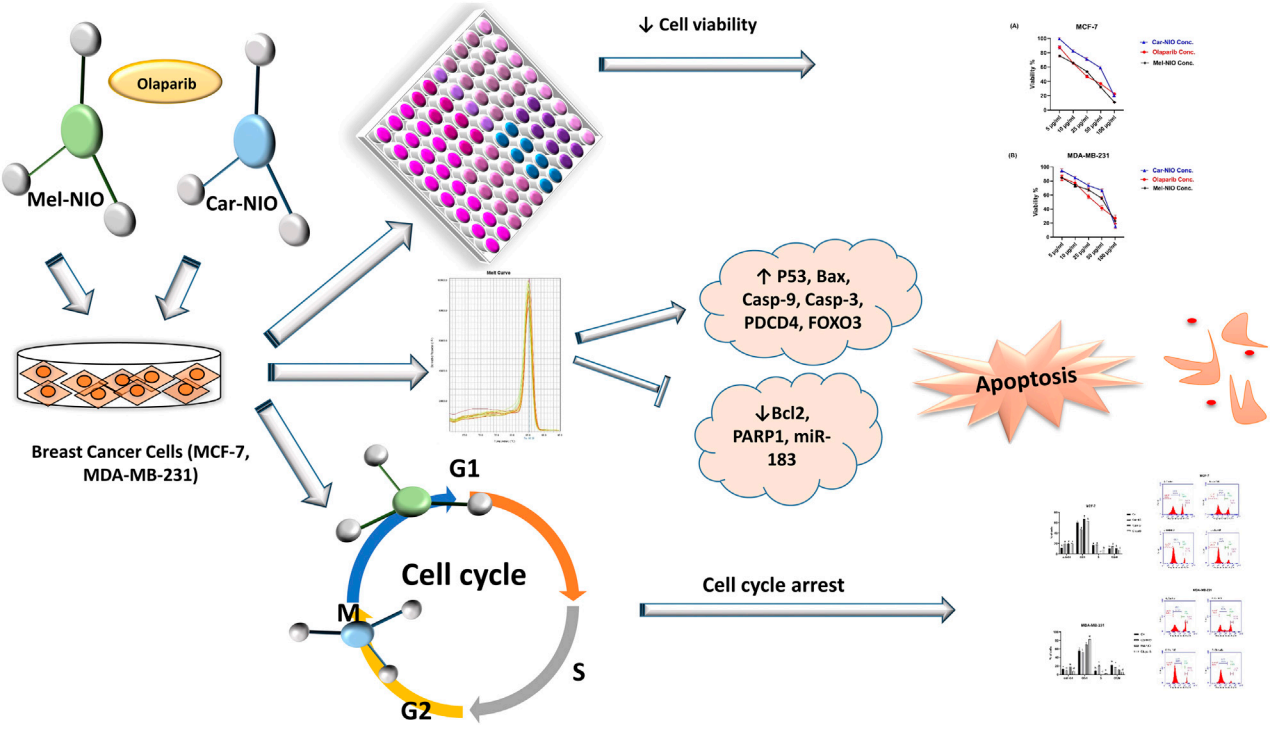

GRAPHICAL ABSTRACT

1 Introduction

A series of disorders known as cancer disrupt the genome, causes aberrant cell development and expands or encroaches on different body regions. Anticancer therapeutic peptide (ACP) medicines have distinct characteristics. Peptides have been thought to target and eliminate cancer cells. It has been established over time that ACPs have a variety of biological targets via which they act, including cell membranes (necrosis), mitochondrial membranes (apoptosis), and non-membrane action (Bakare et al., 2021). In actuality, the majority of ACPs work when they become internalized by cancer cells, although their ability to penetrate cancer cells is limited. To enable impactive therapy, it is crucial to increase the penetrability of ACPs. Numerous studies have already been conducted on various methods to improve ACPs' ability to penetrate cancer cells (Ghaly et al., 2023).

Carnosine is a dipeptide molecule (β-alanyl-L-histidine) that occurs naturally and has anti-inflammatory, anti-oxidant, anti-glycosylation, and chelating impacts. Endogenous concentrations in humans can reach 20 mM, mostly found in the brain and skeletal muscle. The field of exercise physiology has long made use of this dietary supplement to boost performance (Hussein and Gaafar, 2022). However, there was limited *in vitro* proof that carnosine could specifically stop cancer cells from proliferating. The quick metabolism of carnosine by serum and kidney carnosinases is thought to be one of the factors limiting its impactiveness as a medication. These enzymes rapidly lower the serum level of carnosine, blocking its long-lasting impacts (Prakash et al., 2021).

Melittin (Mel), separated from bee venom, is an amphipathic peptide that is water soluble, contains 26 amino acids, and 6 favourable charges. It is the primary active ingredient in bees. Mel was used due to its wide bioactivity, which includes antibacterial, antiviral, anti-inflammatory, and anti-cancer activities. Mel has demonstrated great impactiveness in producing cell cycle arrest, apoptosis, necrosis, mitochondrial disruption, and stopping the angiogenesis of cancer cells (Tiwari et al., 2022). The injection of Mel, on the other hand, is linked to irritating reactions at the injection site, erythema, discomfort, and finally edema, as well as the necrosis of vascular endothelial cells. So, while the application of Mel therapy has been relatively constrained, strong prospects for continuous, regulated, and targeted medication administration to enhance therapeutic impacts and lessen side impacts are micro-or nanoparticle-based drug delivery systems. These methods allow therapeutic compounds to be encapsulated to prevent contact with their environment (Wang et al., 2022).

Nanotechnology is a cutting-edge scientific discipline that takes into account oddities at the nanoscale. Therapeutic alternatives that require precision administration have nanoparticles as a potential delivery mechanism. Niosomes are one-of-a-kind drug carriers synthesized by a combination of cholesterol and non-ionic surfactants. Niosomes can stand in for phospholipid vesicles since they provide the same stability for both hydrophobic and hydrophilic drugs while also being biocompatible, biodegradable, inexpensive to prepare, and so on. Noisome lessens the drug's negative side impacts, namely, toxicity, and hemolysis (Bhardwaj et al., 2020).

The most significant tumor suppressor gene is protein 53 (P53). P53 is a key marker for cancer, and a higher level of P53 expression may improve the prognosis of the patient. Bcl2-Associated X Protein (Bax) is a member of the B-cell lymphoma 2 (Bcl2) protein family, which is crucial for either cell death or life (Kaloni et al., 2022). Overexpression of Bax causes cells to undergo apoptosis, indicating that Bax must be tightly regulated from transcription to post-

translational processing for cells to survive. Bcl2 is an essential apoptosis-regulating protein. Protection from cell death caused by oncogenic and environmental stressors is provided by its extremely variable expression in several haematological cancers (Wolf et al., 2022). Important steps in initiating and concluding apoptosis are facilitated by members of the caspase family (Boice and Bouchier-Hayes, 2020).

Numerous cancer treatments enhance apoptosis by indirectly activating these caspases, killing the cancer cells. Apoptosis, regulation of cell proliferation, replication, and DNA damage repair are only a few of the many important biological processes in which poly (ADP-ribose) polymerase-1 (PARP-1) plays a role (Kumar et al., 2020). Multiple types of cancer cells have been found to express higher levels of PARP-1, and this upregulation has been linked to tumour progression (Boice and Bouchier-Hayes, 2020).

MicroRNAs (miRNAs) are a subclass of non-coding oligonucleotides that control gene expression in cancer cells. These modifications frequently result in alterations to cellular properties like proliferation, differentiation, and programmed cell death. In numerous cancer types, miRNA-183 has been demonstrated to have both tumor-suppressive and oncolytic functions (Hussein et al., 2021). miRNA-183 targets programmed cell death 4 (PDCD4) and Fork-head box O3 (FOXO3) to increase proliferation and invasion in human carcinoma (Cao et al., 2020; Rani et al., 2023).

Olaparib is a small molecule inhibitor of PARP that counteracts the effects of ionizing radiation and alkylating chemicals on DNA when taken orally. The FDA has approved the PARP inhibitor olaparib (Lynparza) to treat adult patients with deleterious or suspected deleterious gBRCAm, HER2-negative metastatic breast cancer who have been treated with chemotherapy in the neoadjuvant, adjuvant, or metastatic setting (Andreidesz et al., 2021).

This study aimed to reveal the chemoprotective impact of Car-NIO and Mel-NIO against *in vitro* cancer models by testing their ability to induce apoptosis on the MCF-7 and MDA-MB-231 breast cancer cells and investigating the mechanisms underlying this effect.

2 Materials and methods

2.1 Chemicals

Carnosine and melittin were purchased from Sigma Aldrich (St. Louis, MO, United States). Car-NIO and Mel-NIO were prepared at the Nanomaterials Research and Synthesis Unit, Animal Health Research Institute (ARC, Giza, Egypt). Olaparib was purchased from LKT Laboratories (St. Paul, MN, United States). The cell lines were purchased from the National Research Centre, Giza, Egypt. Other chemicals in the experiment were purchased from Sigma Aldrich (St. Louis, MO, United States).

2.2 Preparation of Car-NIO and Mel-NIO

2.2.1 Preparation of Car-NIO

The thin film approach (Moulahoum et al., 2019) was used to prepare the niosomes, in a nutshell, 20 mg of cholesterol in 10 ML chloroform and 100 mg of Span 60 were mixed together. The solvent was removed using a rotary evaporator (Buchi R-3, Switzerland). Niosomes (Car-NIO) loaded with carnosine were created by hydrating the resultant thin film with a carnosine solution. To achieve a final concentration of 50 mg/mL, carnosine was dissolved in 10 mL of phosphate buffered saline (PBS) at Ph 7.4, 60°C. An ultrasonic bath (Sonics and Materials Inc., United States) was used to sonicate the aqueous solution and disperse the lipid layer at 60 HTz and room temperature for 15 min.

2.2.2 Preparation of Mel-NIO

The thin-film approach was utilized in the creation of the Mel-NIO. A thin lipid film (120 rpm, 60°C, 1 h) was made by dissolving Span 60 (100 mg) and cholesterol (20 mg) in chloroform (10 mL) and then evaporating off the solvent with a rotary evaporator (Buchi R-3, Switzerland). The resultant thin film was then hydrated with a melittin solution to produce Mel-NIO. To achieve the desired final concentration, 10 mL of phosphate-buffered saline was added to separate solutions of melittin (50 mg/mL) at pH 7.4 at 60°C. The niosomal formulation was achieved by dispersing the lipid layer with the aqueous solution and sonicating it in an ultrasonic bath (Sonics and Materials Inc., United States) at 60 HTz and room temperature for 15 min (Moulahoum et al., 2019).

2.3 Characterization of Car-NIO and Mel-NIO

2.3.1 Zeta potential, polydispersity index, and morphology

Dynamic light scattering (DLS) analysis was used to ascertain the niosomes size, polydispersity index (PDI) testing, and zeta potential (ZP) values (DLS, Malvern Zetasizer, Nano ZS model, Malvern Instruments Ltd., United Kingdom). Triplicate analyses were performed on each sample. The morphology of Car-NIO and Mel-NIO formulations was analyzed with the help of a digital micrograph and soft image viewer software using a transmission electron microscope (TEM) (JEOL JEM-2100; JEOL Ltd., Tokyo, Japan). One drop of drug-loaded niosomal dispersion was diluted 10 times with deionized water and then put on a carbon-coated copper grid for 1 min to help niosomes stick. Once the samples were dry at room temperature, they were examined with TEM without being stained (Darwesh et al., 2021).

2.3.2 Entrapment efficiency (EE)

At 4,000 g for 30 min, the Car-NIO and Mel-NIO formulations were ultra-filtered over an Amicon Ultra-15 membrane (MWCO 30,000 Da). The drug-carrying niosomes awaited filtration in the upper chamber, while the free medicines were allowed to flow beyond the filter membrane. UV-visible spectroscopy (JASCO, V-530, Tokyo, Japan) was used to determine the drug's concentration at its highest absorbance wavelength (420 nm for Mel-NIO and 205 nm for Car-NIO). Each drug concentration was compared to a standard curve. The following equation was then used to determine the efficiency of encapsulation (Yadavar-Nikravesh et al., 2021):

$$\text{Efficiency of Enclosure (\%)} = \left[(A - B)/A\right] X\, 100$$

where A is the initial concentration of the drug in the niosomal preparations and B is the amount of free drug in the filtrate.

TABLE 1 Primers sequences used in this study.

Gene	Primers	Accession number
P_{53}	F 5′- CCTCAGCATCTTATCCGAGTGG-3′	NM_000546
	R 5′-TGGATGGTGGTACAGTCAGAGC-3′	
Bax	F 5′- TCAGGATGCGTCCACCAAGAAG -3′	NM_001291428
	R 5′- TGTGTCCACGGCGGCAATCATC -3′	
Bcl2	F 5′- ATCGCCCTGTGGATGACTGAGT-3′	NM_000633
	R 5′- GCCAGGAGAAATCAAACAGAGGC-3′	
Caspase-9	F 5′-GTTTGAGGACCTTCGACCAGCT-3′	NM_001229
	R 5′-CAACGTACCAGGAGCCACTCTT-3′	
Caspase-3	F 5′- GGAAGCGAATCAATGGACTCTGG-3′	NM_004346
	R 5′-GCATCGACATCTGTACCAGACC-3′	
PARP 1	F 5′- CCAAGCCAGTTCAGGACCTCAT-3′	NM_001618
	R 5′- GGATCTGCCTTTTGCTCAGCTTC-3′	
PDCD4	F 5′- ACTGTGCCAACCAGTCCAAAGG-3′	NM_001199492
	R 5′- CCTCCACATCATACACCTGTCC-3′	
FOXO3	F 5′- TCTACGAGTGGATGGTGCGTTG-3′	NM_001455
	R 5′- CTCTTGCCAGTTCCCTCATTCTG-3′	
GAPDH	F 5′- GTCTCCTCTGACTTCAACAGCG -3′	NM_001256799
	R 5′- ACCACCCTGTTGCTGTAGCCAA -3′	
MiRNA-183	F 5′- ATGGCACTGGTAGAATTC-3′	MIMAT0000261
	R 5′- GAACATGTCTGCGTATCTC-3′	
U6	F 5′- CTCGCTTCGGCAGCACAT-3′	NR_004394.1
	R 5′- TTTGCGTGTCATCCTTGCG-3′	

2.3.3 Drug release study

A dialysis bag (MWCO = 12 kDa) was used to compare 2 mL of free drugs, Car-NIO and Mel-NIO for drug release (*in vitro*). This bag was placed in a phosphate buffered saline (PBS) solution (50 mL, 1X, pH = 5.4) with slow stirring (50 rpm) at 37°C. At certain intervals, a portion of the PBS solution was removed and replaced with a new aliquot.

2.3.4 Stability studies

To test the Car-NIO and Mel-NIO's stability, we kept them in two distinct environments. Both 25 ± 1°C and 4 ± 1 C were used to keep the formulation for a month. After that, measurements were taken of its physical parameters (such as mean particle size (nm) and entrapment efficiency (EE)) at zero, fourteen, and 30 days.

2.4 Cell culture

Culture of MCF-7 and MDA-MB-231 cells were maintained at sub-confluence in 37°C, 5% CO2, and complete Roswell Park Memorial Institute-1640 medium added (catalog number: 11875093, Sigma-Aldrich, St. Louis, MO, United States), with 10% fetal bovine serum (catalog number:16000044, Sigma-Aldrich, St. Louis, MO, United States), penicillin/streptomycin (catalog number: 15140122, Sigma-Aldrich, St. Louis, MO, United States), and L-glutamine (catalog number: 25030081, Sigma-Aldrich, St. Louis, MO, United States).

2.5 *In vitro* cytotoxicity

The 3-(4,5-dimethylthiazol-2-yl)-2,5-diphenyl-2H-tetrazolium bromide (MTT) assay is a colorimetric method that uses the transformation of yellow MTT into purple formazan. The following procedures were carried out in a clean environment using MTT Assay Kit (Cell Proliferation) (catalog number: ab211091, Abcam, United Kingdom), with the use of a Laminar flow cabinet meeting biosafety standard II (Baker, SG403INT, Sanford, ME, United States), $l0^4$ cells/well were subjected to varying doses of Car-NIO (5, 10, 25, 50, and 100 μM) (Tehrani et al., 2018) and Mel-NIO (5, 10, 25, 50, and 100 μM) (Yaacoub et al., 2021) and olaparib (5, 10, 25, 50, and 100 μM) (Ashmawy et al., 2017). After 48 h, we added 2.5 μg/mL of MTT to each well and

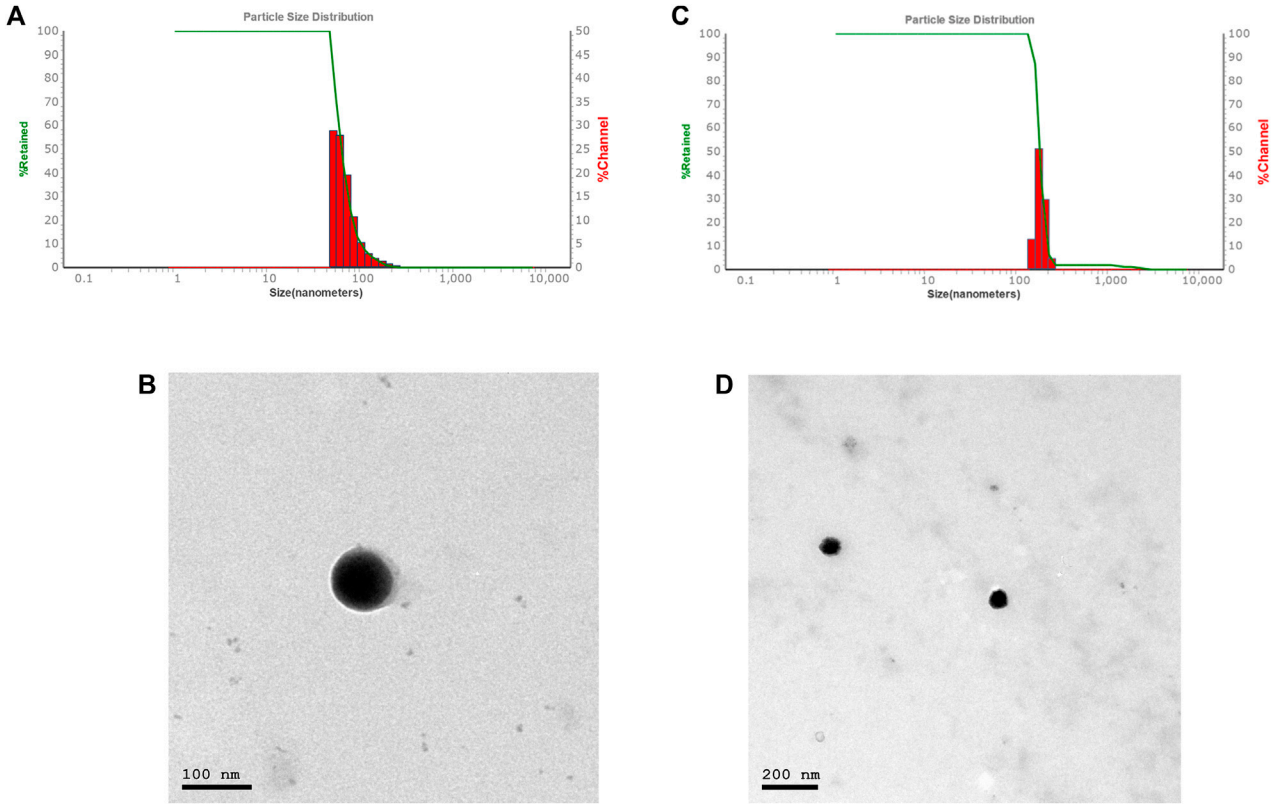

FIGURE 1
Characterization of Car-NIO and Mel-NIO. Dynamic light scattering size measurement of Car-NIO **(A)**. TEM image of the Car-NIO **(B)**. Mel-NIO dynamic light scattering size measurement **(C)**. TEM image of the Mel-NIO **(D)**.

incubated the plates at 37°C for another 4 h. After the formation of formazan crystals, 10% sodium dodecyl sulfate (200 µL/well) was used to dissolve the crystals. We measured the absorbance at 595 nm, and a positive control that causes 100% mortality under the same conditions was utilized. Using the following formula, the change in viability was given as a percentage was calculated:

$$\text{Cytotoxicity \%} = (\text{Extract reading}/\text{Negative control reading})\ \text{x}100$$

Viability % = 100- Cytotoxicity%, The impact of each treatment is measured by its IC50 (the concentration at which 50% of the viability is inhibited).

2.6 Quantitative RT-PCR analysis

The cells' total RNA was extracted with the help of the RNA Mini Kit from Ambion by Life Technologies by Thermo Scientific (catalog number: 12183018A). To ensure the integrity of the RNA samples, we used a NanoDrop® ND-1000 Spectrophotometer from NanoDrop Technologies in Wilmington, Delaware, United States A High Capacity cDNA Reverse Transcription Kit (catalog number: 4374966) from Thermo Scientific was then used to amplify the cDNA. The Maxima SYBR Green qPCR Master Mix (2X) kit from Thermo Scientific, (catalog number: K0251), was used for real-time PCR amplification (Shehata et al., 2018). The housekeeping GADPH (for mRNA) or U6 (for miRNA) were used as a standard. The $2^{-\Delta\Delta ct}$ formula was used to calculate the levels of target gene expression (Livak and Schmittgen, 2001). Table 1 contains the sequences of the desired gene primers.

2.7 Detection of lipid peroxidation

For this assay, the cells (2×10^6 cells/mL) were seeded onto 96-well culture plates to determine lipid peroxidation levels. Following a 48-h incubation with Car-NIO (48.83, 51.4 µM), Mel-NIO (21.23, 43.65 µM), and olaparib (23.31, 32.55 µM), cells were collected and washed twice with phosphate-buffered saline. The cells were harvested with a sonicator probe (VCX-130 W, Newtown, United States) on ice, and then disrupted by ultra-sonication for 5 s. Following the manufacturer's guidelines for best results, the malondialdehyde (MDA) was detected in the cell extract using the MDA test kit (catalog number: ab287797, Abcam, United Kingdom). The microplate reader was used to determine the MDA concentration at a wavelength of 532 nm (Tecan, Mannedorf, Switzerland) (Gérard-Monnier et al., 1998).

2.8 Detection of the cell cycle stage

Overnight, the cells were cultured in 100-mm plates at a density of 2×10^6 cells/mL per well using fresh culture media. Treatment

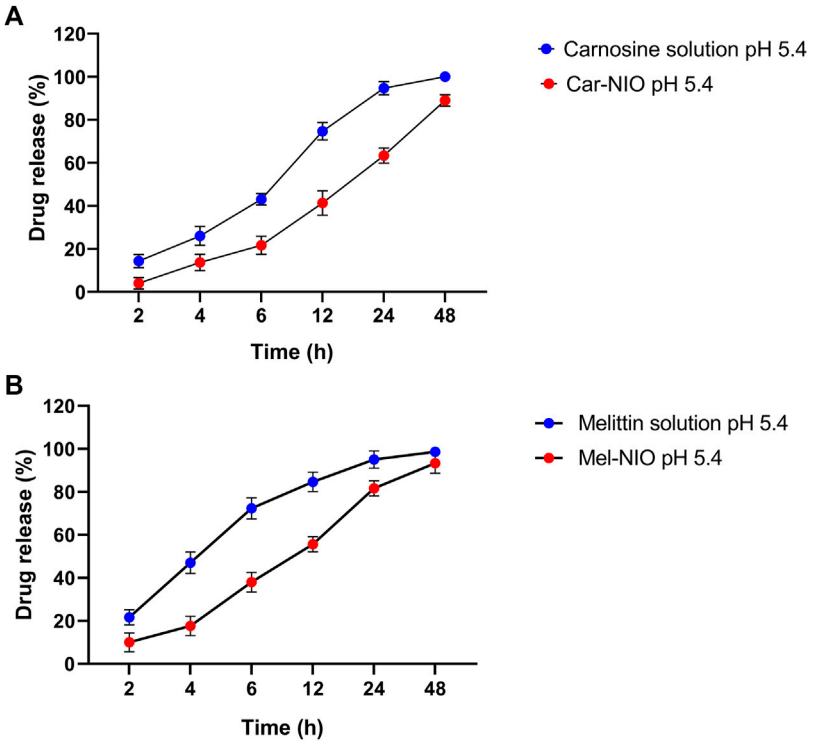

FIGURE 2
In vitro drug release profile of carnosine and Car-NIO **(A)**, melittin and Mel-NIO **(B)** from the dialysis bag in pH 5.4 at 37°C. Results are represented by mean ± SD (n = 3). *p < 0.05, **p < 0.001.

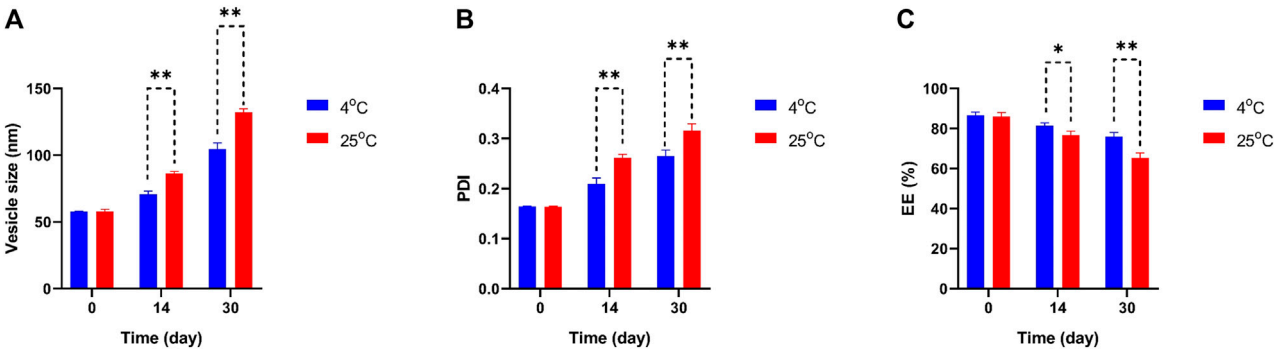

FIGURE 3
Comparing stability of optimum formulation at 4°C and 25°C of Car-NIO. Mean particle size **(A)**, PDI **(B)** and EE % **(C)** were studied as stability parameters. Results are represented by mean ± SD (n = 3). *p < 0.05, **p < 0.001.

with Car-NIO (48.83, 51.4 μM), Mel-NIO (21.23, 43.65 μM), and olaparib (23.31, 32.55 μM) for 48 h began the next day. After harvesting, the cells were fixed in 70% ethanol at 20°C for 12 h. After that, the cells were exposed to RNase (10 mg/mL) and propidium iodide (50 μg/mL) for 30 min. The cell cycle distribution was analyzed using flow cytometry, and the data were analyzed using FlowJo (TreeStar, Ashland, OR, United States) (Mei et al., 2019).

2.9. Statistical analysis

Graph Pad Prism 5 (Graph Pad Software, La Jolla, CA, United States) was used for the statistical analysis. Multiple group comparisons were made using one-way analysis of variance (ANOVA) and Tukey's *post hoc* test for statistical significance. All figures are reported as the average standard error of at least three independent measurements. The level of significance chosen was less than 0.05.

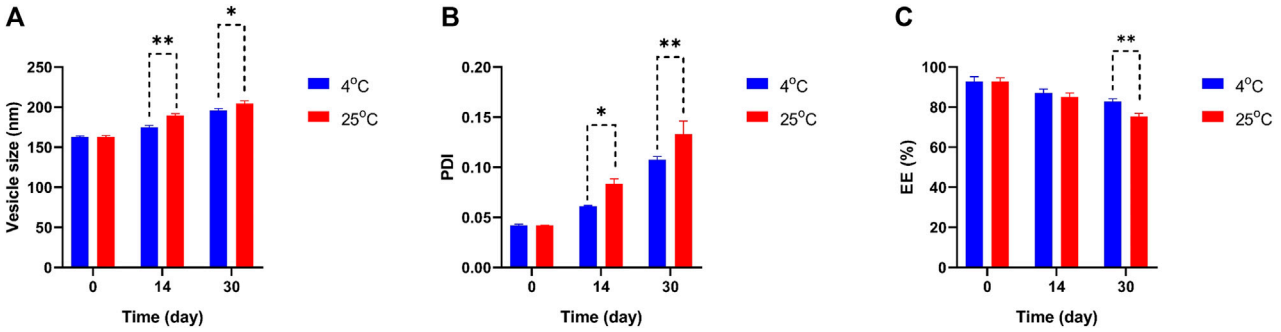

FIGURE 4
Comparing stability of optimum formulation at 4°C and 25°C of Mel-NIO. Mean particle size **(A)**, PDI **(B)** and EE % **(C)** were studied as stability parameters. Results are represented by mean ± SD (n = 3). *p < 0.05, **p < 0.001.

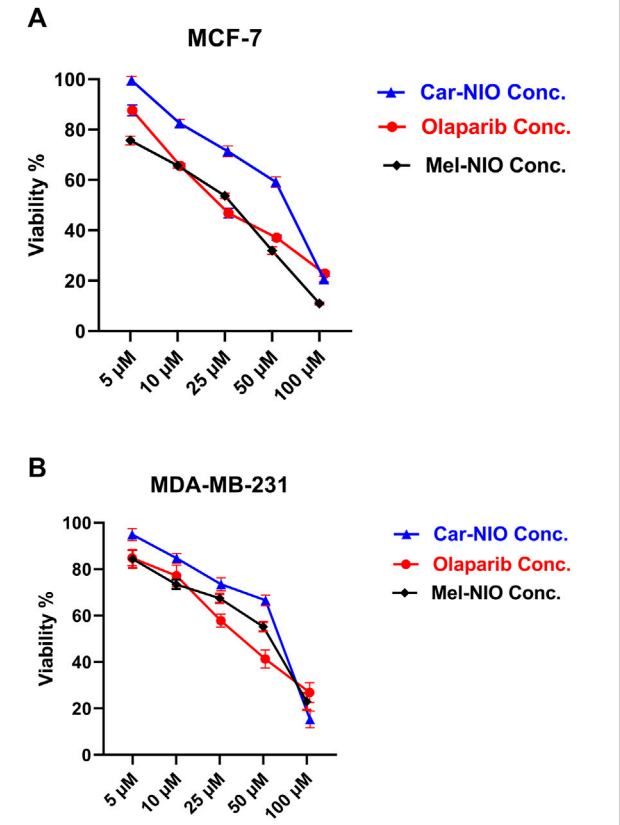

FIGURE 5
The impact of different concentrations of Car-NIO, Mel-NIO, and olaparib on the viability of MCF-7 **(A)**, and MDA-MB-231 **(B)** cells by using the MTT assay after 48 h of incubation. Data are shown as mean ± SEM, and p < 0.05.

3 Results

3.1 Car-NIO and Mel-NIO characterization

3.1.1 Morphological characterization

The average particle size, PDI, and zeta potential were measured by dynamic scattering light analysis using the Malvern Zetasizer. In Car-NIO the average size was 58 ± 0.50 nm. The PDI value was 0.16441 ± 0.04, which is considered in the acceptable range. The ZP value of Car-NIO was −20 ± 0.3 mV (Figures 1A, B). While in Mel-NIO the average size was 163 ± 1.3 nm. The PDI value was 0.0424 ± 0.1, which is considered in the acceptable range. The ZP value of Mel-NIO was −86.6 ± 0.9 Mv (Figures 1C, D).

3.1.2 Drug release studies of carnosine and melittin from niosomes

Each carnosine and melittin formulation's drug release profile was studied for 48 h at 5.4 pH at 37°C to learn more about *in vitro* drug release. As can be observed in the "Release" plot (Figure 2), the free medications first saw a rapid increase in release (43%, 72.3% over the first 6 h); after 24 h, the rate of release slowed to a steady state. According to the monitoring of the Car-NIO and Mel-NIO release profile, after 6 h, 21.6%, and 38% of the drug had infiltrated cells at a pH of 5.4. According to research by Rinaldi et al. (Rinaldi et al., 2017), the expanding structure of niosomes in an acidic environment results in 89%, and 93.3% of the medications being released into the bloodstream after 48 h at pH 5.4, respectively. The acidic shift of niosomes has been linked to electrophilic addition processes. The release rate of the drugs inside the niosomes was carefully calculated. Tumour wards typically contain acidic conditions, which crushed the niosomes' structure, accelerating the release rate and increasing the toxicity (Naderinezhad et al., 2017). More cytotoxicity is induced by an acidic environment because of changes in carnosine and melittin and an increase in osmotic pressure. Release statistics for melittin were calculated for 72 h at body temperature over 5.4 pH. Carnosine and melittin, as free drugs, were released at a rate, with an R2 value of 0.951 suggesting a release proportional to drug concentration.

3.1.3 Physical stability study of Car-NIO and Mel-NIO

To determine the physical stability and effectivity of Car-NIO and Mel-NIO, the vesicle size, PDI, and EE were measured at 4°C and 25°C, and on days 0, 14, and 30 following manufacture. Interestingly, the measurements showed that neither the particle size nor the PDI nor the EE percentage was impacted by the temperature and that the formulation recently generated possessed the least size of Car-NIO with a mean of 58 nm, the

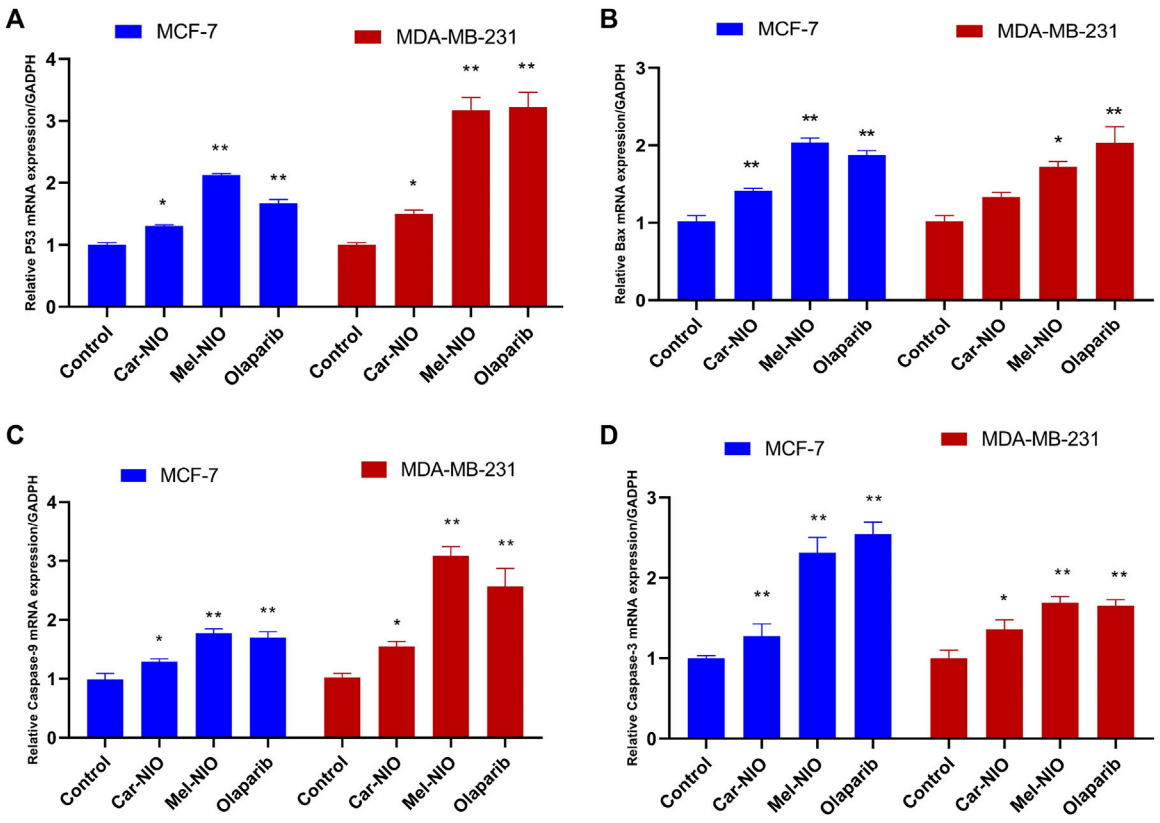

FIGURE 6
The impact of Car-NIO, Mel-NIO and olaparib on the genes expressions levels of P53 **(A)**, Bax **(B)**, caspase-9 **(C)**, and caspase-3 **(D)** (relative gene mRNA expressions/GADPH) in the MCF-7 and MDA-MB-231 cell lines. * Significant difference between control and treated group ($p < 0.05$), ** highly significant difference between control and treated group ($p < 0.01$).

maximum PDI (0.316), and the EE (86.67%). The stability diagram (Figure 3) shows that the temperature had an effect on all the parameters from day 0 to day 30. Size growth, increased PDI, and diminished EE were all brought on by a rise in temperature. Increases in drug release as temperatures rise are responsible for the EE decrease (Nasseri, 2005). Growing the pores of the niosomes; could be beneficial on the particle size and PDI, increasing either of them and decreasing the EE to the lowest amount (76%), as the temperature can affect rigidity and elasticity. In contrast, at 25°C, the developed pores caused larger size, more PDI, and less EE (65.3%), suggesting that the niosomes are more stiff and elastomeric at lower temperatures.

In Figure 4 the particle size, PDI, and EE percentage of Mel-NIO across a wide range of temperatures revealed some interesting trends. The Mel-NIO formulation had the smallest particles (mean size of 162.9 nm), highest PDI (0.133), and highest EE (92.6%). Temperature had an impact on all parameters from day 0 to day 30 as demonstrated by the stability diagram (Figure 4). A temperature rise led to an increase in size, PDI, and EE, and a decrease in EE. Temperature-induced increases in drug release explain the observed decline in EE. Increasing the niosomes' pore size may improve the particle size and PDI, while decreasing the EE to its minimum value (82.6%) due to the temperature's effect on the niosomes' rigidity and elasticity. However, at 25 °C, the niosomes were found to be more rigid and elastomeric, with larger sizes, higher PDI, and lower EE (75.3%).

3.2 Cytotoxic impact on MCF-7 and MDA-MB-231 cells

Our results in Figure 5 referred to a dose-dependent basis, the viability% of MCF-7 and MDA-MB-231 cells were significantly reduced when the cells were incubated for 48 h with different concentrations of Car-NIO, Mel-NIO, and olaparib, respectively. Moreover, Car-NIO produced a cytotoxic effect on both cell types with an IC50 of 48.83, 51.4 μM, also in Mel-NIO with an IC50 of 21.23, 43.65 μM, and olaparib with IC50 of 23.31, 32.55 μM concentrations (Figures 5A, B).

3.3 Assessment of the mRNA expression levels of marker genes on MCF-7 and MDA-MB-231 cells

Results showed a significant upregulation in the levels of mRNA expression of P53, Bax, caspase-9, and caspase-3 in MCF-7 and MDA-MB-231 cells treated with Car-NIO, Mel-NIO, and olaparib in comparison with untreated cancer cells. In MCF-7 cells treated with Mel-NIO and olaparib showed non-significant differences between each other in mRNA expression levels of caspase-9 and caspase-3, also non-significant differences in the expression level of caspase-3 between untreated cancer cells and Car-NIO treated cell

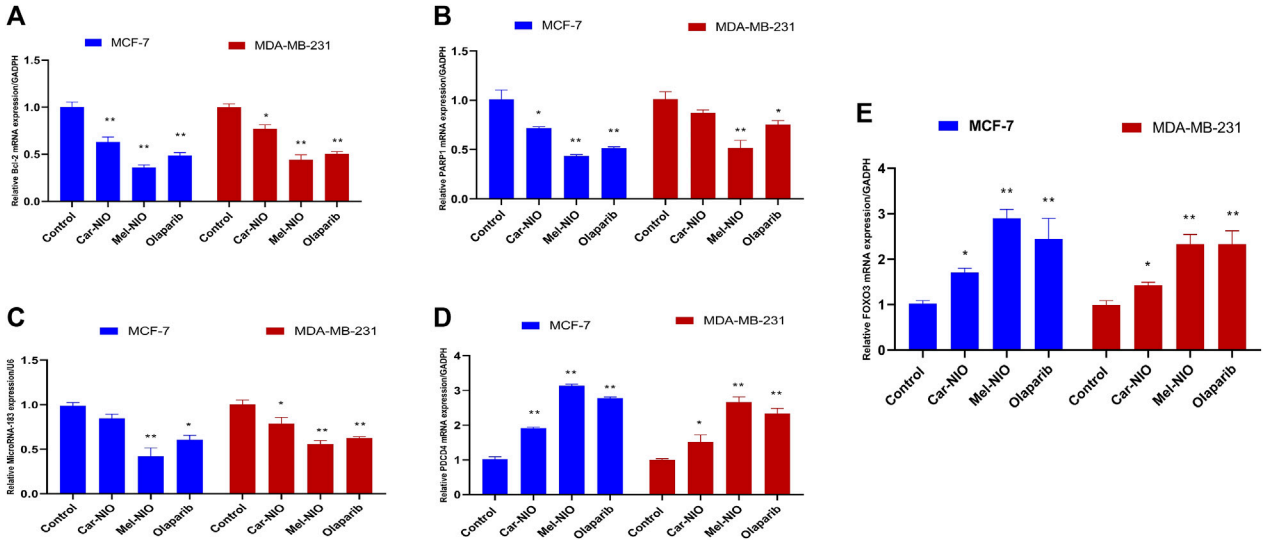

FIGURE 7
The impact of Car-NIO, Mel-NIO and olaparib on the genes expressions levels of Bcl2 **(A)**, PARP 1 **(B)**, MicroRNA-183 **(C)**, PDCD4 **(D)** and FOXO3 **(E)** (Relative gene mRNA expressions/GADPH) in the MCF-7 and MDA-MB-231 cell lines. * Significant difference between control and treated group ($p < 0.05$), ** highly significant difference between control and treated group ($p < 0.01$).

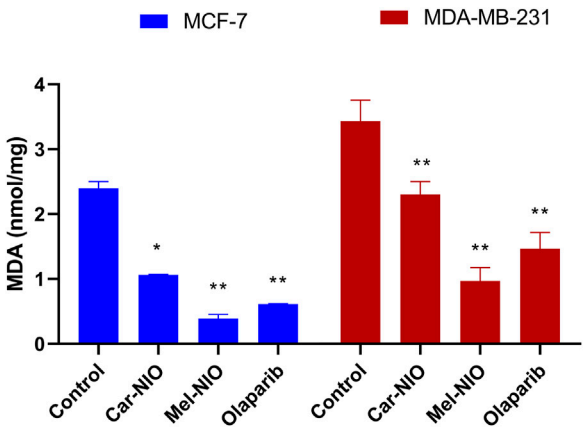

FIGURE 8
The impact of Car-NIO, Mel-NIO, and olaparib on the level of MDA (nmol/mg) in the MCF-7 and MDA-MB-231 cell lines. * Significant difference between control and treated group ($p < 0.05$), ** highly significant difference between control and treated group ($p < 0.01$).

were detected. While in MDA-MB-231 cells treated with Mel-NIO and olaparib showed non-significant differences between each other in the expression levels of P53 and caspase-3, on the other hand, the expression level of Bax showed non-significant differences between untreated cancer cells and Car-NIO treated cell (Figure 6).

In contrast to our previous results, the expression levels of anti-apoptotic Bcl2, PARP 1, and miRNA-183 were significantly the highest transcriptional level in untreated cancer cells, while the cells treated with Car-NIO, Mel-NIO, and olaparib revealed significant downregulation in Bcl2, PARP 1, and miRNA-183 in MCF-7 and MDA-MB-231 cells in comparison with the untreated cancer cells. While, the expression levels of PDCD4 and FOXO3 were significantly upregulated in both cell types treated with Car-NIO, Mel-NIO, and olaparib in comparison with untreated cancer cells. Also, the FOXO3 expression level showed non-significant differences between Mel-NIO and olaparib-treated cells in both cell types. The expression levels of Bcl2, PDCD4, and miRNA-183 showed non-significant differences between Mel-NIO and olaparib-treated cells in MDA-MB-231 cells (Figure 7).

3.4 Assessment of lipid peroxidation marker (MDA)

The MDA levels were significantly higher in the untreated cancer cells, while the cells treated with Car-NIO, Mel-NIO, and olaparib showed significant downregulation in MCF-7 and MDA-MB-231 cells in comparison with the untreated cancer cells. On the other hand, in MDA-MB-231 cells the Mel-NIO, and olaparib-treated cells demonstrated non-significant differences in MDA levels (Figure 8).

3.5 Analysis of the cell cycle

We hypothesized that Car-NIO and Mel-NIO induced apoptosis involved cell cycle interruption, and thus evaluated the cell cycle distribution upon Car-NIO and Mel-NIO treatment. Breast cancer MCF-7 cells treated with Car-NIO for 48 h revealed a significant ($p < 0.05$) increase in the number of cells arrested at the G2/M (15.3%) phase, and the proportion of cells in the G0/1 phase (47.0%) was decreased in comparison with untreated cancer cells as well as cells treated with Mel-NIO showed a significant increase in the number of cells arrested at the G0/1 (67.5%) phase, and the proportion of cells in the S phase (1.0%) was decreased in comparison with untreated

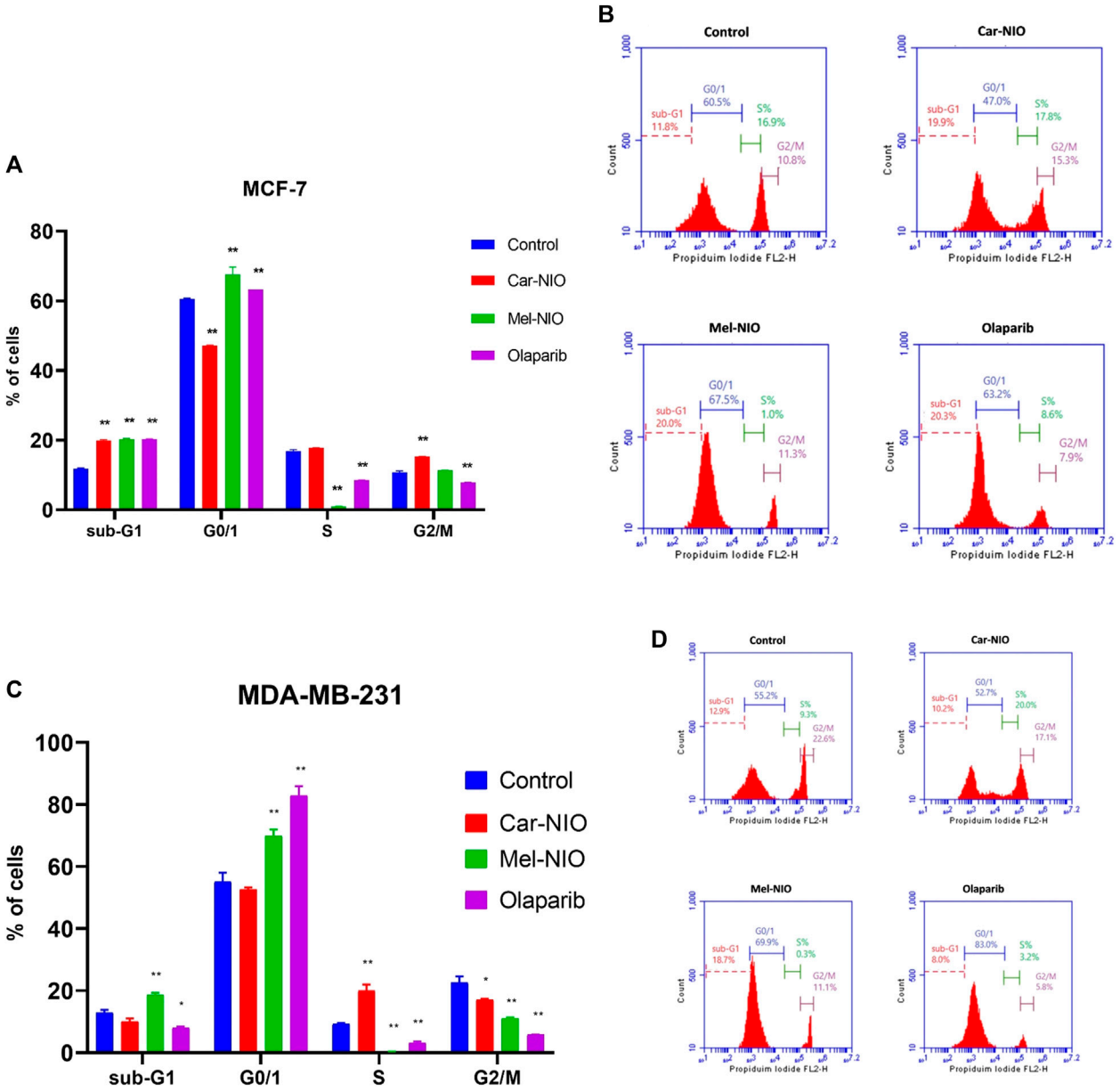

FIGURE 9
The impact of Car-NIO, Mel-NIO, and olaparib on cell cycle progression of breast cancer MCF-7 **(A, B)**, and MDA-MB-231 **(C, D)** cell lines. * Significant difference between control and treated group ($p < 0.05$), ** highly significant difference between control and treated group ($p < 0.01$).

cancer cells. In the cells treated with olaparib, our data showed a significant increase in the number of cells arrested at G0/1 (63.2%), and the proportion of cells in the S phase (8.6%) was decreased in comparison with untreated cancer cells (Figures 9A, B).

Breast cancer MDA-MB-231 cells treated with Car-NIO for 48 h showed a significant increase in the number of arrested cells at S (20.0%) phase, and the proportion of cells in G2/M phase (17.8%) was decreased in comparison with untreated cancer cells as well as the cells treated with Mel-NIO showed a significant increase in the number of cells arrested at the Sub-G1 population (18.7%), and G0/1 (69.9%) phases and the proportion of cells in the S phase (0.3%) was decreased in comparison with untreated cancer cells. In the cells treated with olaparib, there was a significant increase in the number of cells arrested at the G0/1 (83.0%), and the proportion of cells in the S phase (3.2%) was decreased in comparison with untreated cancer cells. These findings in MCF-7 and MDA-MB-231 cells point to a block in the cell cycle at G1, and a decrease in the percentage of cells in S phase suggests fewer cells are entering the DNA-synthesis phase (Figures 9C, D).

4 Discussion

Finding a powerful anticancer medicine without harmful side impacts is still very much in demand. Bioactive peptides are abundant in a variety of food sources and are produced from

food proteins by fermentation, enzymatic, chemical hydrolysis, or gastrointestinal digestive processes. In recent years, there has been a significant increase in the number of articles highlighting their potential benefits on blood pressure and lipid metabolism, in addition to their anticancer, immunomodulatory, antibacterial, analgesic, anti-oxidant, and anti-inflammatory actions (Komarov et al., 2022).

Even if the advantages of bioactive peptides are well known, there is still an opportunity for advancement because science is an area that is constantly evolving. Some chemicals degrade before they reach their targets or are unable to reach particular organs. Engineered carriers are an appealing strategy, especially when trying to treat cancer cells (Liu and Zhang, 2022). As an alternative to liposomes, niosomes are biodegradable, non-toxic, more stable, and less expensive vesicles made from non-ionic surfactants. Having a structure comparable to that of a liposome, they can stand in for liposomes as an alternate vesicular system. Niosomes have a propensity for loading many medications. One of their main advantages is that they can encapsulate chemicals of different physicochemical properties and modify the impacts these compounds have on the body (Alqosaibi, 2022).

Carnosine has long been recommended for usage as an antioxidant and antiglycating agent. There have also been indications of carnosine's anti-proliferative activities, which may help prevent the emergence of a variety of malignancies. However, because serum and tissue carnosinase enzymes are present in the body, carnosine turns over quickly, necessitating repeated daily dosages for usage as a dietary supplement (Turner et al., 2021).

According to several reports, carnosine, for instance, slowed the formation of tumors in the fibroblast cells and hepatocellular carcinoma cells implanted in BALB/c nude mice model. When carnosine was administered concurrently with the subcutaneous injection of cancer cells into the dorsal skin of female nude mice, it has been shown to have a significant ability to inhibit the proliferation of malignant cells *in vivo*. Carnosine has been touted as having the advantage of slowing tumor growth, nevertheless (Horii et al., 2012).

Our findings demonstrated that Car-NIO and Mel-NIO had a protective impact against *in vitro* cancer trials, in which our treatments demonstrated a significant cytotoxic impact in MCF-7 and MDA-MB-231 breast cancer cells and upregulated the mRNA expression levels of P53, Bax, caspase-9, caspase-3, PDCD4, FOXO3 and downregulated the expression levels of Bcl2, PARP 1 and miRNA-183 in comparison with untreated cancer cells. This is the first publication we're aware of that compares the chemo-protective effects of Car-NIO with Mel-NIO in many breast cancer cell lines together.

The carnosine derivative was combined with various concentrations of phosphatidyl-choline and cholesterol to create liposomal/carnosine conjugates, which were subsequently used to create liposomes. The resulting immunoliposomes, which had a size of about 100 nm, were subsequently examined *in vitro* in different cancer models. The liposomal/carnosine had higher IC50 values than the reference drug 5-Fluororuracil for all cell lines. Carnosine encapsulated in these liposomes is better protected from the impacts of carnosinase (Zoppo et al., 2016).

Gaafar et al. (Gaafar et al., 2021), coupled liquid crystalline nanoparticles (NPs) that are PEGylated with L-carnosine (P-LCNPs), and proved that P-Liquisomes were successful in maximizing the therapeutic impact of carnosine without changing its activity and may be employed as a delivery strategy for additional encouraging hydrophilic anticancer drugs. By *in vitro* analysis, spherical, light-colored vesicles encased in the liquid crystals were discovered, demonstrating the P-LCNPs were nanosized (149.3 nm) with high ZP. After 24 h of incubation, *in vitro* cytotoxicity testing showed that P-Liquisomes had a superior cytotoxic impact. Also, compared to carnosine solution, P-Liquisomes had a stronger chemopreventive impact, as shown by a decrease in tumor growth, an increase in the ratio of tumor growth inhibition %, vascular endothelial growth factor levels, cyclin D1 levels, and caspase-3 levels, and a decrease in tumor size.

Reactive oxygen species (ROS) are a form of oxidative stress that has been linked to carcinogenesis. It plays a role in DNA damage, cell proliferation, adhesion, survival, and apoptosis, among other physiological and pathological processes. MDA is commonly utilized as a biomarker of oxidative stress during severe health problems like cancer, etc., due to its status as a lipid peroxidation marker caused by ROS that is both extremely cytotoxic and carcinogenic. MDA, or lipid peroxidation, is elevated in several types of tumours. There is evidence that it encourages cellular senescence and death. During times of oxidative stress, MDA is a functional intermediate that contributes to cellular growth. Since MDA interactions with amino groups are a naturally occurring metabolic process, it has been hypothesized that these changes may be responsible for proliferation. Excessive ROS generation was linked to DNA damage, heritable mutations, mitochondrial dysfunction, and cell death. Moreover, a differential redox control in proliferation and viability between normal and malignant cells suggests that tumour cells are more vulnerable to oxidative stress than healthy cells. One potential therapeutic strategy involves exploiting the redox fragility of cancer cells. Increased metabolic stress combined with strong proliferative capacity causes these cells to lose their ability to effectively regulate high levels of induced cellular oxidative stress, leading to elevated levels of reactive oxygen species-associated DNA damage and ultimately compromising cell viability. The cells treated with Car-NIO and Mel-NIO especially Mel-NIO showed non-significant differences in some parameters in comparison with cells treated with olaparib. The cell cycle progression results suggested that the cells treated with Car-NIO and Mel-NIO arrested a high proportion of cells in the G1 phase as well as the reduction of cells in the S phase indicating the reduction of the number of cells entering the phase of DNA synthesis in both cell lines.

Our results are in line with preceding reports suggesting that carnosine prohibits the G1-S stage progress in both HeLa (adenocarcinoma) and SiHa (squamous cell carcinoma) cells, causing G1 arrest. Based on all the evidence, it looks like carnosine stopped the growth of human cervical gland carcinoma cells (Bao et al., 2018).

In murine bone marrow cells, carnosine attenuated cyclophosphamide-induced G2/M arrest, which was associated with decreased phosphorylated-checkpoint kinase 1/checkpoint kinase 1 and phosphorylated-P53/P53 ratios as well as decreased protein 21 expressions. Carnosine therapy also prevented cell death brought on by cyclophosphamide (Deng et al., 2018).

Melittin is the leading active ingredient in bee venom and has a wide range of biological functions. However, because of substantial side

impacts, the researchers created melittin loaded on nanocarriers to reduce toxicity and investigate the inhibitory actions on liver cancer along with biological safety. It was suggested that melittin nano-liposomes are a bright new drug for treating hepatocellular carcinoma (Mao et al., 2017).

In the past, Melittin has been encapsulated using a wide variety of nanocarrier delivery technologies, such as liposomes, polymeric or solid lipid nanoparticles, lipid or albumin nanocapsules, micelles, etc. Niosome-based drug delivery systems have been developed as an alternative to liposome-based systems because of the instability of liposome structures, which can result in drug leakage. Despite their structural differences, niosomes (also known as non-ionic surfactant vesicles) share many of the same activities and physicochemical properties as liposomes. Since subsequent studies confirmed that the melittin and carnosine-loaded nanocarrier demonstrated greater efficacy, bioavailability, fewer side effects, and a more potent anticancer effect than the free form, we decided against using the free form as a comparison and instead used two different kinds of peptides and a new standard drug in our experiment (Tian et al., 2011; Huang et al., 2013; Mao et al., 2017).

Tian et al. (2011) examined the anti-cancer impact and vascular stimulation of melittin liposomes and a poloxame with melittin solution. Results showed that melittin liposomes with a poloxamer-modified surface had greater bioavailability, more effective anticancer action, and fewer adverse effects than melittin solution. The melittin may accumulate in the tumor location as a result of the prolonged circulation period and enhanced permeability and retention action of liposomes, increasing its anti-tumor efficacy.

To mitigate the toxicity, allergic responses, and pain caused by free melittin, Mao et al. (2017) developed melittin nano-liposomes by encapsulating melittin with poloxamer. They looked into the biological safety and the inhibitory effects on liver cancer. They found that melittin nano-liposomes significantly reduced tumour formation following orthotopic and subcutaneous hepatocellular carcinoma (HCC) transplantation *in vivo* and suppressed HCC cell survival *in vitro*, in comparison to free melittin. An important finding was that it reduced inflammation and allergy symptoms in mice compared to melittin. When compared to free melittin, melittin nano-liposomes have higher anti-tumor efficacy and enhanced biological safety, making them a promising candidate for use in HCC therapy.

Huang et al. (2013), explained that the melittin-based lipid nanoparticle had a prospective clinical use in solid tumor therapies through intravenous injection due to its good characteristics. This melittin-based lipid nanoparticle hides the positive charge of melittin within the phospholipid monolayer, generating a neutral nanoparticle with lower cytotoxicity and a wider safe dose range. Finally, melanoma-carrying mice were intravenously injected with melittin-NPs. The melittin-NPs inhibited the proliferation of the melanoma cells in comparison with a control group. In addition, the core-shell spherical morphology of melittin-NPs allows for the synergistic loading of chemical agents, their perfect bio-compatibility and monodispersity give them superior utility as synergistic therapeutics, and their ultrasmall size makes it possible for them to efficiently penetrate solid tumours.

The melittin-encoded lipid-coated polymeric nanoparticle complex significantly inhibited tumor development without causing hemolysis or tissue damage. The outcome showed that the core-shell-structured melittin nanoparticle that was made may be able to solve the main problems melittin faces in clinical applications and has a lot of potential to be used to treat cancer (Ye et al., 2021).

Asfour et al. (2022), suggested that in diabetic rats, the nanoconjugate of gabapentin and melittin demonstrated remarkable wound healing properties. The size of the complex was 156.9 nm. The results of the *in vivo* investigation declared that mice treated with gabapentin-melittin had faster wound healing. The complex formula demonstrated antioxidant properties by increasing the levels of glutathione peroxidase and superoxide dismutase while inhibiting the accumulation of MDA.

Consistent with previous research, another study found that melittin significantly upregulates the caspase-2 and Bax, and depresses Bcl2 protein expression in comparison with untreated cancer cell line tests and *in vivo* model of lung cancer, by activating caspase-2 by suppressing miRNA-183 expression. When patients with lung cancer were given an injection under the skin, the size and weight of their tumors were much smaller in the melittin group than in the vehicle group (Gao et al., 2018).

The oral PARP inhibitor olaparib is therapeutically impactive in patients with recurrent ovarian cancer and a breast cancer gene (BRCA) mutation. People who have human epidermal growth factor receptor 2-negative, metastatic breast cancer and a hereditary BRCA mutation benefited greatly from switching to olaparib monotherapy rather than the standard treatment, with olaparib monotherapy extending median progression-free survival by 2.8 months and reducing the risk of death (Tutt et al., 2021).

Moskwa et al. (2011), suggested that the miRNA-182 overexpression was sensitive to the PARP inhibitor *in vitro* and *in vivo*. A clinical-grade PARP1 inhibitor affected the development of cancers in animal models that express miRNA-182. Together, these results show that the downregulation of BRCA1 by miRNA-182 stops DNA repair and may affect how breast cancer is treated.

Ashmawy et al. (2017), proved that miRNAs-181a/b were suppressed by their inhibitors followed by treatment with olaparib. The MDA-MB-231 cells revealed a large increase in cell survival, cell proliferation, and ATM protein as well as a significant decrease in Bcl2 activity. Their results demonstrated that miRNA-181a and miRNA-181b are essential for determining the olaparib sensitivity of triple-negative breast cancer cells. Additionally, miRNAs181a/b may be employed as a potential predictive biomarker for olaparib response.

According to research, miRNA-183 can restrict PDCD4 expression and hence prevent the apoptosis of transforming growth factor beta 1-induced human hepatocellular carcinoma cells, also miRNA-183 is suggested to restrict FOXO expression in lung cancer (Li et al., 2010; Zhang et al., 2015). Based on another study, it was concluded that miRNA-183 played a crucial role in the advancement of cancer cells by promoting oesophageal squamous cell carcinoma cell proliferation and invasion via binding to the PDCD4 mRNA (Ren et al., 2015) and this was in parallel with our results.

The carnosine and melittin nanoformulations for the treatment of breast cancer utilizing a stimulus-responsive system are promising and provide fresh information on the chemotherapeutic usage of carnosine and melittin. This study also highlights the potential of natural medicines with specific nanoformulation to replace costly and potentially harmful conventional cancer chemotherapeutics. Last but not least, even though our formulation's potential as a diagnostic tool needs further work, it is still a fascinating future project with considerable potential therapeutic consequences.

5 Conclusion

In this study, we observed that Car-NIO and Mel-NIO significantly inhibited the proliferation of MCF-7 and MDA-MB-231 breast cancer cell lines, but the Mel-NIO showed significantly greater anti-cancer activity on these breast cancer cells compared to Car-NIO. Our data revealed additional impacts of Car-NIO and Mel-NIO by upregulating the levels of P53, Bax, caspase-9, caspase-3, PDCD4, FOXO3 and downregulating the expression of Bcl2, PARP 1, and miRNA-183, which also decreased MDA levels, Car-NIO inhibited the cells at the G2/M phase transition in MCF-7 cells and S phase at MDA-MB-231 cells, while Mel-NIO and olaparib inhibited both cells at the G0/1 phase transition and occur inhibition of cells at S phase. All these implications indicate the anti-proliferative properties of Car-NIO and Mel-NIO, which could be useful on MCF-7 and MDA-MB-231 breast cancer cells.

Data availability statement

The original contributions presented in the study are included in the article/Supplementary material, further inquiries can be directed to the corresponding author.

Author contributions

MH: Conceptualization, Methodology, Supervision, Writing–original draft, Writing–review and editing. AA-H: Writing–original draft. HE: Conceptualization, Resources, Writing–original draft. WE: Investigation, Writing–original draft. TA: Writing–original draft. KA: Investigation, Writing–original draft. SA: Conceptualization, Resources, Writing–original draft. HA-H: Writing–original draft. SG: Conceptualization, Methodology, Supervision, Writing–original draft, Writing–review and editing.

Funding

The author(s) declare that no financial support was received for the research, authorship, and/or publication of this article.

Conflict of interest

The authors declare that the research was conducted in the absence of any commercial or financial relationships that could be construed as a potential conflict of interest.

Publisher's note

References

Alqosaibi, A. I. (2022). Nanocarriers for anticancer drugs: Challenges and perspectives. *Saudi J. Biol. Sci.* 29, 103298. doi:10.1016/j.sjbs.2022.103298

Andreidesz, K., Koszegi, B., Kovacs, D., Bagone Vantus, V., Gallyas, F., and Kovacs, K. (2021). Effect of oxaliplatin, olaparib and LY294002 in combination on triple-negative breast cancer cells. *Int. J. Mol. Sci.* 22, 2056. doi:10.3390/ijms22042056

Asfour, H. Z., Alhakamy, N. A., Ahmed, O. A., Fahmy, U. A., El-Moselhy, M. A., Rizg, W. Y., et al. (2022). Enhanced healing efficacy of an optimized gabapentin-melittin nanoconjugate gel-loaded formulation in excised wounds of diabetic rats. *Drug Deliv.* 29, 1892–1902. doi:10.1080/10717544.2022.2086943

Ashmawy, A. M., Sheta, M. A., Zahran, F., and Abdel Wahab, A. H. (2017). MiRNAs-181a/b as Predictive biomarkers for olaparib sensitivity in triple-negative breast cancer cells. *BLJ* 13, 221–229. doi:10.21608/blj.2017.47612

Bakare, O. O., Gokul, A., Wu, R., Niekerk, L. A., Klein, A., and Keyster, M. (2021). Biomedical relevance of novel anticancer peptides in the sensitive treatment of cancer. *Biomolecules* 11, 1120. doi:10.3390/biom11081120

Bao, Y., Ding, S., Cheng, J., Liu, Y., Wang, B., Xu, H., et al. (2018). Carnosine inhibits the proliferation of human cervical gland carcinoma cells through inhibiting both mitochondrial bioenergetics and glycolysis pathways and retarding cell cycle progression. *Integr. Cancer Ther.* 17, 80–91. doi:10.1177/1534735416684551

Bhardwaj, P., Tripathi, P., Gupta, R., and Niosomes, P. S. (2020). Niosomes: A review on niosomal research in the last decade. *J. Drug Deliv. Sci. Technol.* 56, 101581. doi:10.1016/j.jddst.2020.101581

Boice, A., and Bouchier-Hayes, L. (2020). Targeting apoptotic caspases in cancer. *Biochim. Biophys. Acta - Mol. Cell. Res.* 1867, 118688. doi:10.1016/j.bbamcr.2020.118688

Cao, D., Di, M., Liang, J., Shi, S., Tan, Q., and Wang, Z. (2020). MicroRNA-183 in cancer progression. *J. Cancer* 11, 1315–1324. doi:10.7150/jca.39044

Darwesh, A. Y., El-Dahhan, M. S., and Meshali, M. M. (2021). A new dual function orodissolvable/dispersible meclizine HCL tablet to challenge patient inconvenience: *In vitro* evaluation and *in vivo* assessment in human volunteers. *Drug deli. Transl. Res.* 11, 2209–2223. doi:10.1007/s13346-020-00889-z

Deng, J., Zhong, Y. F., Wu, Y. P., Luo, Z., Sun, Y. M., Wang, G. E., et al. (2018). Carnosine attenuates cyclophosphamide-induced bone marrow suppression by reducing oxidative DNA damage. *Redox Biol.* 14, 1–6. doi:10.1016/j.redox.2017.08.003

Gaafar, P. M., El-Salamouni, N. S., Farid, R. M., Hazzah, H. A., Helmy, M. W., and Abdallah, O. Y. (2021). Pegylated liquisomes: A novel combined passive targeting nanoplatform of L-carnosine for breast cancer. *Int. J. Pharm.* 602, 120666. doi:10.1016/j.ijpharm.2021.120666

Gao, D., Zhang, J., Bai, L., Li, F., Dong, Y., and Li, Q. (2018). Melittin induces NSCLC apoptosis via inhibition of miR-183. *Onco Targets Ther.* 1, 4511–4523. doi:10.2147/OTT.S169806

Gérard-Monnier, D., Erdelmeier, I., Régnard, K., Moze-Henry, N., Yadan, J. C., and Chaudiere, J. (1998). Reactions of 1-methyl-2-phenylindole with malondialdehyde and 4-hydroxyalkenals. Analytical applications to a colorimetric assay of lipid peroxidation. *Chem. Res. Toxicol.* 11, 1176–1183. doi:10.1021/tx9701790

Ghaly, G., Tallima, H., Dabbish, E., Badr ElDin, N., Abd El-Rahman, M. K., Ibrahim, M. A., et al. (2023). Anti-cancer peptides: Status and future prospects. *Molecules* 28, 1148. doi:10.3390/molecules28031148

Horii, Y., Shen, J., Fujisaki, Y., Yoshida, K., and Nagai, K. (2012). Effects of l-carnosine on splenic sympathetic nerve activity and tumor proliferation. *Neurosci. Lett.* 510, 1–5. doi:10.1016/j.neulet.2011.12.058

Huang, C., Jin, H., Qian, Y., Qi, S., Luo, H., Luo, Q., et al. (2013). Hybrid melittin cytolytic peptide-driven ultrasmall lipid nanoparticles block melanoma growth *in vivo*. *ACS Nano* 7, 5791–5800. doi:10.1021/nn400683s

Hussein, M., Arisha, A., Mahmoud, E., and Abdo, S. (2021). Mir-140 and Mir-34a as molecular markers for apoptotic brain in sunset yellow and carmoisine intoxicated mice. *Zagazig Vet. J.* 49, 37–49.þ doi:10.21608/zvjz.2021.66481.1141

Hussein, M. M. A., and Gaafar, S. F. (2022). Histidine-dipeptides in relation to diabetes and obesity. *Int. J. Vet. Sci.* 11, 221–228. doi:10.47278/journal.ijvs/2021.093

Kaloni, D., Diepstraten, S. T., Strasser, A., and Kelly, G. L. (2022). BCL-2 protein family: Attractive targets for cancer therapy. *Apoptosis* 28, 20–38. doi:10.1007/s10495-022-01780-7

Komarov, I. V., Tolstanova, G., Kuznietsova, H., Dziubenko, N., Yanchuk, P. I., Shtanova, L. Y., et al. (2022). Towards *in vivo* photomediated delivery of anticancer peptides: Insights from pharmacokinetic and-dynamic data. *J. Photochem Photobiol. B, Biol.* 233, 112479. doi:10.1016/j.jphotobiol.2022.112479

Kumar, M., Jaiswal, R. K., Yadava, P. K., and Singh, R. P. (2020). An assessment of poly (ADP-ribose) polymerase-1 role in normal and cancer cells. *BioFactors* 46, 894–905. doi:10.1002/biof.1688

Li, J., Fu, H., Xu, C., Tie, Y., Xing, R., Zhu, J., et al. (2010). miR-183 inhibits TGF-beta1-induced apoptosis by downregulation of PDCD4 expression in human hepatocellular carcinoma cells. *BMC cancer* 10, 354–360. doi:10.1186/1471-2407-10-354

Liu, L. H., and Zhang, X. Z. (2022). Carrier-free nanomedicines for cancer treatment. *Prog. Mater Sci.* 125, 100919. doi:10.1016/j.pmatsci.2021.100919

Livak, K. J., and Schmittgen, T. D. (2001). Analysis of relative gene expression data using real-time quantitative PCR and the 2(-Delta Delta C(T)) Method. *Methods* 25, 402–408. doi:10.1006/meth.2001.1262

Mao, J., Liu, S., Ai, M., Wang, Z., Wang, D., Li, X., et al. (2017). A novel melittin nano-liposome exerted excellent anti-hepatocellular carcinoma efficacy with better biological safety. *J. Hematol. Oncol.* 10, 71–74. doi:10.1186/s13045-017-0442-y

Mei, L., Sang, W., Cui, K., Zhang, Y., Chen, F., and Li, X. (2019). Norcantharidin inhibits proliferation and promotes apoptosis via c-Met/Akt/mTOR pathway in human osteosarcoma cells. *Cancer Sci.* 10, 582–595. doi:10.1111/cas.13900

Moskwa, P., Buffa, F. M., Pan, Y., Panchakshari, R., Gottipati, P., Muschel, R. J., et al. (2011). miR-182-mediated downregulation of BRCA1 impacts DNA repair and sensitivity to PARP inhibitors. *Mol. Cell.* 41, 210–220. doi:10.1016/j.molcel.2010.12.005

Moulahoum, H., Sanli, S., Timur, S., and Zihnioglu, F. (2019). Potential effect of carnosine encapsulated niosomes in bovine serum albumin modifications. *Int. J. Biol. Macromol.* 137, 583–591. doi:10.1016/j.ijbiomac.2019.07.003

Naderinezhad, S., Amoabediny, G., and Haghiralsadat, F. (2017). Co-delivery of hydrophilic and hydrophobic anticancer drugs using biocompatible pH-sensitive lipid-based nano-carriers for multidrug-resistant cancers. *RSC Adv.* 7, 30008–30019. doi:10.1039/C7RA01736G

Nasseri, B. (2005). Effect of cholesterol and temperature on the elastic properties of niosomal membranes. *Int. J. Pharm.* 300, 95–101. doi:10.1016/j.ijpharm.2005.05.009

Prakash, M. D., Fraser, S., Boer, J. C., Plebanski, M., de Courten, B., and Apostolopoulos, V. (2021). Anti-cancer effects of carnosine—A dipeptide molecule. *Molecules* 26, 1644. doi:10.3390/molecules26061644

Rani, M., Kumari, R., Singh, S. P., Devi, A., Bansal, P., Siddiqi, A., et al. (2023). MicroRNAs as master regulators of FOXO transcription factors in cancer management. *Life Sci.* 321, 121535. doi:10.1016/j.lfs.2023.121535

Ren, L. H., Chen, W. X., Li, S., He, X. Y., Zhang, Z. M., Li, M., et al. (2015). MicroRNA-183 promotes proliferation and invasion in oesophageal squamous cell carcinoma by targeting programmed cell death 4. *BJC* 111, 2003–2013. doi:10.1038/bjc.2014.485

Rinaldi, F., Del Favero, E., Rondelli, V., Pieretti, S., Bogni, A., Ponti, J., et al. (2017). pH-sensitive niosomes: Effects on cytotoxicity and on inflammation and pain in murine models. *J. Enzyme Inhib. Med. Chem.* 32, 538–546. doi:10.1080/14756366.2016.1268607

Shehata, Y., Rafaat, N., Gaafar, S., and F. Gaafar, S. (2018). Selective Cytotoxic and Chemoprotective effect of nanocurcumin against human HCT-116 cell line. *BLJ* 14, 85–93. doi:10.21608/blj.2018.47586

Tehrani, M. H., Bamoniri, A., and Gholibeikian, M. (2018). The toxicity study of synthesized inverse carnosine peptide analogues on HepG2 and HT-29 cells. *IJBMS* 21, 39–46. doi:10.22038/IJBMS.2017.23153.5852

Tian, J. L., Ke, X., Chen, Z., Wang, C. J., Zhang, Y., and Zhong, T. C. (2011). Melittin liposomes surface modified with poloxamer 188: *In vitro* characterization and *in vivo* evaluation. *Pharmazie* 66, 362–367. doi:10.1691/ph.2011.0327

Tiwari, R., Tiwari, G., Lahiri, A., Ramachandran, V., and Rai, A. (2022). Melittin: A natural peptide with expanded therapeutic applications. *J. Nat. Prod.* 12, 13–29. doi:10.2174/2210315510999201210143035

Turner, M. D., Sale, C., Garner, A. C., and Hipkiss, A. R. (2021). Anti-cancer actions of carnosine and the restoration of normal cellular homeostasis. *Biochim. Biophys. Acta Mol. Cell. Res.* 1868, 119117. doi:10.1016/j.bbamcr.2021.119117

Tutt, A. N., Garber, J. E., Kaufman, B., Viale, G., Fumagalli, D., Rastogi, P., et al. (2021). Adjuvant olaparib for patients with BRCA1-or BRCA2-mutated breast cancer. *NEJM* 384, 2394–2405. doi:10.1056/NEJMoa2105215

Wang, A., Zheng, Y., Zhu, W., Yang, L., Yang, Y., and Peng, J. (2022). Melittin-based nano-delivery systems for cancer therapy. *Biomolecules* 12, 118. doi:10.3390/biom12010118

Wolf, P., Schoeniger, A., and Edlich, F. (2022). Pro-apoptotic complexes of BAX and BAK on the outer mitochondrial membrane. *Biochim. Biophys. Acta - Mol. Cell. Res.* 1869, 119317. doi:10.1016/j.bbamcr.2022.119317

Yaacoub, C., Rifi, M., El-Obeid, D., Mawlawi, H., Sabatier, J. M., Coutard, B., et al. (2021). The cytotoxic effect of *Apis mellifera* venom with a synergistic potential of its two main components—melittin and PLA2—on colon cancer HCT116 cell lines. *Molecules* 26, 2264. doi:10.3390/molecules26082264

Yadavar-Nikravesh, M. S., Ahmadi, S., Milani, A., Akbarzadeh, I., Khoobi, M., Vahabpour, R., et al. (2021). Construction and characterization of a novel Tenofovir-loaded PEGylated niosome conjugated with TAT peptide for evaluation of its cytotoxicity and anti-HIV effects. *Adv. Powder Technol.* 32, 3161–3173. doi:10.1016/j.apt.2021.05.047

Ye, R., Zheng, Y., Chen, Y., Wei, X., Shi, S., Chen, Y., et al. (2021). Stable loading and delivery of melittin with lipid-coated polymeric nanoparticles for effective tumor therapy with negligible systemic toxicity. *ACS Appl. Mater Interfaces* 13, 55902–55912. doi:10.1021/acsami.1c17618

Zhang, L., Quan, H., Wang, S., Li, X., and Che, X. (2015). MiR-183 promotes growth of non-small cell lung cancer cells through FoxO1 inhibition. *Tumor Biol.* 36, 8121–8126. doi:10.1007/s13277-015-3550-8

Zoppo, L., Del Zoppo, L., Morelli, G., Condorelli, D. F., Barresi, V., Musso, N., et al. (2016). Liposome antibody–ionophore conjugate antiproliferative activity increases by cellular metallostasis alteration. *MedChemComm* 7, 2364–2367. doi:10.1039/C6MD00461J

frontiers | Frontiers in Pharmacology

TYPE Review
PUBLISHED 25 September 2023
DOI 10.3389/fphar.2023.1272546

OPEN ACCESS

EDITED BY
Pranav Kumar Prabhakar,
Lovely Professional University, India

REVIEWED BY
Peizheng Yan,
Shandong University of Traditional Chinese Medicine, China
Jian Chen,
Peking University, China
Lei Xia,
Shandong University of Traditional Chinese Medicine, China

*CORRESPONDENCE
Xufeng Huang,
huangxufeng@mailbox.unideb.hu
Ronggao Qin,
20130240@kust.edu.cn
Guangzhu Cao,
caoguangzhu@kust.edu.cn

†These authors have contributed equally to this work

RECEIVED 04 August 2023
ACCEPTED 08 September 2023
PUBLISHED 25 September 2023

CITATION
Cao Q, Wang Q, Wu X, Zhang Q, Huang J, Chen Y, You Y, Qiang Y, Huang X, Qin R and Cao G (2023), A literature review: mechanisms of antitumor pharmacological action of leonurine alkaloid.
Front. Pharmacol. 14:1272546.
doi: 10.3389/fphar.2023.1272546

A literature review: mechanisms of antitumor pharmacological action of leonurine alkaloid

Qiang Cao[1,2†], Qi Wang[3†], Xinyan Wu[4†], Qi Zhang[5†], Jinghan Huang[6†], Yuquan Chen[7], Yanwei You[8], Yi Qiang[1], Xufeng Huang[9*], Ronggao Qin[1*] and Guangzhu Cao[1*]

[1]Department of Earth Sciences, Kunming University of Science and Technology, Kunming, China, [2]School of Medicine, Macau University of Science and Technology, Taipa, China, [3]Department of Gastroenterology, Affiliated Hospital of Jiangsu University, Jiangsu University, Zhenjiang, China, [4]College of Veterinary Medicine, Sichuan Agricultural University, Chengdu, China, [5]Undergraduate Department, Taishan University, Taian, China, [6]Undergraduate Department, Sichuan Conservatory of Music, Chengdu, China, [7]Institute of Medical Information/Library, Chinese Academy of Medical Sciences, Beijing, China, [8]Division of Sports Science and Physical Education, Tsinghua University, Beijing, China, [9]Faculty of Dentistry, University of Debrecen, Debrecen, Hungary

Leonurine refers to the desiccated aerial portion of a plant in the Labiatae family. The primary bioactive constituent of Leonurine is an alkaloid, Leonurine alkaloid (Leo), renowned for its substantial therapeutic efficacy in the treatment of gynecological disorders, in addition to its broad-spectrum antineoplastic capabilities. Over recent years, the pharmacodynamic mechanisms of Leo have garnered escalating scholarly interest. Leo exhibits its anticancer potential by means of an array of mechanisms, encompassing the inhibition of neoplastic cell proliferation, induction of both apoptosis and autophagy, and the containment of oncogenic cell invasion and migration. The key signal transduction pathways implicated in these processes include the Tumor Necrosis Factor-Related Apoptosis-Inducing Ligand (TRAIL), the Phosphoinositide3-Kinase/Serine/Threonine Protein Kinase (PI3K/AKT), the Signal Transducer and Activator of Transcription 3 (STAT3), and the Mitogen-Activated Protein/Extracellular Signal-Regulated Kinase (MAP/ERK). This paper commences with an exploration of the principal oncogenic cellular behaviors influenced by Leo and the associated signal transduction pathways, thereby scrutinizing the mechanisms of Leo in the antineoplastic sequence of events. The intention is to offer theoretical reinforcement for the elucidation of more profound mechanisms underpinning Leo's anticancer potential and correlating pharmaceutical development.

KEYWORDS

leonurine, anti-tumor mechanisms, signal transduction pathways, apoptosis and autophagy, tumor cell proliferation and migration

1 Introduction

At present, the global escalation of both incidence and mortality rates of cancer is swiftly becoming a substantial menace to human health. A multitude of natural products, particularly small natural molecules, often exhibit potent anticancer activities whilst maintaining low toxicological side-effects. These qualities render them paramount in the process of antitumor drug screening, thus prompting an upsurge of interest from the scientific community (Dehelean et al., 2021; Hashem et al., 2022; Liang et al., 2020; Majolo et al., 2019; Zhu et al., 2022). Leonurine, a biologically active alkaloid with diverse

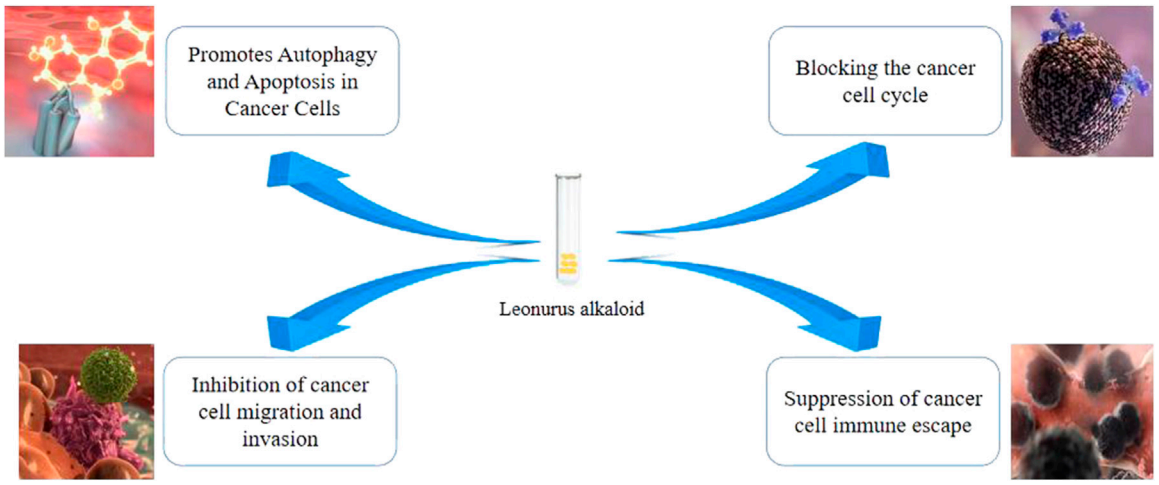

FIGURE 1
Mechanism of antitumour action of Leonurine alkaloid.

pharmacological properties, is derived from the desiccated aerial portion of plants belonging to the Labiatae family, commonly known as the mint family. These plants, including species like Leonurus cardiaca (Motherwort), serve as the primary source of leonurine alkaloid.

Leonurine alkaloid, the primary active biological alkaloid contained within Motherwort, has been acknowledged for its extensive array of biological functions and its exceptional antitumor properties (Zhu et al., 2018; Leorita et al., 2020; Liu et al., 2021; Liang et al., 2022). The cornerstone of Leo's antitumor actions primarily hinge upon its anti-inflammatory and antioxidant activities (Lin et al., 2020; Chen et al., 2023; Tian et al., 2023). Additionally, Leonurine exhibits capacity to impede tumor cell cycles, induce apoptosis in tumor cells, and stimulate the immune system.

Emerging from Zhang et al.'s study (Zhang et al., 2019), it has been posited that Leonurine alkaloid moderates the progression of hepatocellular carcinoma in murine models via the AMPK/SREBP-1c signaling pathway. In addition to its role in moderating hepatocellular carcinoma, Leo's impact on oxidative stress and cancer risk reduction is noteworthy. Leo's antioxidative properties are underpinned by its ability to enhance cellular oxidative stress responses and bolster superoxide dismutase (SOD) activity. Oxidative stress is a critical factor in cancer development, as it contributes to DNA damage and genomic instability, potentially leading to tumorigenesis. Leo's capacity to enhance SOD activity, which is essential for mitigating cellular oxidative damage, has significant implications for reducing the risk of cancer initiation and progression. By bolstering the cellular defense against oxidative stress, Leo showcases its potential not only in impeding cancer progression but also in preemptively reducing the chances of cancer development. Shen et al.'s study (Shen et al., 2023) posits that the Leonurine alkaloid can mitigate lung cancer through the NF-κB signaling pathway, decrease phosphorylation and nuclear translocation in myocardial cells' P65, and subsequently attenuate the expression of inflammatory factors such as IL-6, TNF-α, and MCP-1. Deng et al.'s study (Deng et al., 2022) unveils that Leonurine alkaloid can ameliorate cellular oxidative stress, enhance SOD activity, thus diminishing the risk of cancer.

There are myriad studies suggesting that Leo can halt cancer progression or manifest anticancer effects (Chen et al., 2021; Qiang et al., 2022; Raza et al., 2022; Ajzashokouhi et al., 2023; Chi et al., 2023). This article undertakes a review of the research concerning the anticancer pharmacological mechanisms of Leo, thereby facilitating further insights for pharmacological research and novel drug development.

2 Main antitumor mechanisms of leo

Leo displays antitumor effects both *in vivo* and *in vitro*, with physiological effects as shown in Figure 1. It exerts its antitumor actions by inducing tumor cell apoptosis and inhibiting tumor cell proliferation, invasion, and migration (Liu et al., 2018; Hu et al., 2019; Zhuang et al., 2021).

2.1 Leo promotes tumor cell cycle arrest

The complex orchestration of cellular cycle modulation is effectuated through a sophisticated and intricate network of interdependencies, which encompass an assortment of proteins, enzymes, cytokines, and cell cycle signaling pathways. These components are fundamentally pivotal to the execution of cellular proliferation, growth, and regeneration processes. The cell cycle itself is partitioned into four cardinal phases, namely the first interphase gap (G1), the DNA synthesis phase (S), the second interphase gap (G2), and the mitotic phase (M) (Zou and Lin, 2021; You et al., 2023a; Yuan et al., 2023). Deviations in the precision of this cellular cycle regulation demonstrate a close association with the onset, advancement, and distant metastasis of tumorous growths (Wang, 2021; Zou and Lin, 2021; You et al., 2023b). As a result, modulating cell cycle distribution and inducing

cellular cycle arrest are perceived as potent methodologies for anticancer interventions (Bonelli et al., 2019; Guan and Guan, 2020; Cao et al., 2022a). Leo can exert its antiproliferative impact on malignant cells by mediating the regulation of cell cycle and cellular proliferation processes. Leo can induce a state of cellular cycle arrest in cancerous cells, either at the G0/G1 or G2/M phase, which effectively inhibits cellular expansion. It negatively regulates the expression of cyclins D1 and D2, along with their partner proteins, Cyclin-Dependent Kinases 2 (CDK2), CDK4, and CDK6. Simultaneously, it increases the expression of p21WAE1/CIP1 and p27, thereby inhibiting the transition from G0 to G1 phase and the preparatory activities leading to the S phase, primarily through the control of protein levels (Chen et al., 2015; Chen et al., 2019; Xu et al., 2020; Cao et al., 2022b). Yu et al.'s study (Yu et al., 2023) found that Leo can maintain the Cyclin D1-CDK4 complex at lower levels by reducing the expression of CDK4, thereby stalling the cell cycle. In studies using Leo-treated breast cancer cell lines, it was found that the expression levels of Cyclins A1, B1, and CDK1 decreased in the treated cells, while p53 and BAX were upregulated, resulting in a significant cell cycle arrest at the G2/M phase, which subsequently leads to cell apoptosis (Chen et al., 2013a; Sitarek et al., 2021; Cao et al., 2022c; Xi et al., 2023).

Li et al.'s study (Li et al., 2020) showed that Leo has anti-inflammatory effects, can inhibit the transformation of lung adenocarcinoma, and ultimately inhibit the proliferation of lung adenocarcinoma cells.

2.2 Leo promotes cancer cell apoptosis

Apoptosis, delineated as a genetically-regulated mechanism of cellular demise, functions as a vital biological process within the human body, mediating the systematic removal of damaged and aberrant cells (Darcy, 2019; Kornepati et al., 2022; You et al., 2023c). This intrinsic cellular mechanism operates as a natural impediment, restraining the endurance and propagation of malignant cellular entities (Cheung and Vousden, 2022; Matthews et al., 2022; You et al., 2023d). Notwithstanding, cancer cells ingeniously circumvent the apoptosis pathway, by inducing genetic mutations or eliciting epigenetic alterations therein, thereby accentuating the significance of harnessing the apoptosis pathway for the eradication of cancer cells in therapeutic oncology (Chen et al., 2013b; Ozyerli-Goknar and Bagci-Onder, 2021; Karami Fath et al., 2022; Jin and Jeong, 2023).

Apoptotic signal transduction fundamentally encompasses both exogenous and endogenous mechanisms. Intracellular triggers, such as DNA damage, deficiency of growth factors, and oxidative stress predominantly activate the endogenous apoptosis pathway (Rezatabar et al., 2019; Souliotis et al., 2019; Wenqi et al., 2023). Conversely, exogenous apoptosis is principally prompted by the interaction between Fas ligand and Fas receptor or Tumor Necrosis Factor (TNF) ligand and its receptor. Experimental findings suggest that the compound "Leo" has the potential to instigate both these apoptosis pathways in cancer cells. Leo's impact on the exogenous apoptotic mechanism is a significant aspect to consider. Exogenous apoptosis is mainly initiated by the interaction between death ligands and their corresponding death receptors, such as Fas ligand and Fas receptor or Tumor Necrosis Factor (TNF) ligand and its receptor. Studies have shown that Leo can sensitize cancer cells to the exogenous apoptotic pathway by increasing the expression of death receptors on the cell surface. Leo has been found to upregulate the expression of Death Receptor 4 (DR4) and Death Receptor 5 (DR5), both of which are involved in the initiation of the extrinsic apoptotic pathway. This enhancement in death receptor expression can render cancer cells more susceptible to death ligand-induced apoptosis, further contributing to Leo's antitumor effects (Huang et al., 2021; Wu et al., 2021; You et al., 2023e; Schramm et al., 2023). Thus, Leo's influence on both endogenous and exogenous apoptotic pathways underscores its potential as a multifaceted agent for promoting apoptosis in cancer cells. (Zhao et al., 2021; Zhang et al., 2022; Zhou et al., 2022).

2.3 Leo promotes autophagy in cancer cells

Autophagy represents a universal metabolic degradation mechanism that encompasses the inclusion of intracellular cytoplasmic proteins or organelles within vesicular structures. These subsequently amalgamate with lysosomes to form autolysosomes, which serve the function of degrading the sequestered material (Brennand et al., 2011; Joshi et al., 2020; Vargas et al., 2023). The byproducts of this degradation process are repurposed to facilitate metabolic adaptation and uphold energy equilibrium, hence ensuring cellular metabolic processes and rejuvenation. In certain circumstances, autophagy within the cells can precipitate cell death. Atg12, an instrumental gene implicated in autophagy, governs the generation of autophagy precursors and the establishment of autophagosomes, thereby modulating cellular autophagy. A multitude of studies have demonstrated an inhibition of Atg12 in an array of cancer cells.

Post the administration of Leo to hepatocellular carcinoma cell lines, evidence of autophagosome formation and heightened levels of LC3-II were documented within the cells, corroborating the induction of autophagy in the Leo-treated hepatocellular carcinoma cells. In addition, various investigations have indicated the dual capability of Leo to trigger both autophagy and apoptosis concurrently in diverse cancer cells. It is noteworthy that the Leo concentration bears an impact on the incidence rates of both apoptosis and autophagy. When the concentration of Leo is less than 150 μmol·L-1, the rate of autophagy induction is superior to that of apoptosis. However, at Leo concentrations surpassing 150 μmol·L-1, the apoptosis incidence rate surpasses that of autophagy (Zhao et al., 2021; Meng et al., 2023; Zhou et al., 2023).

2.4 Leo inhibits immune evasion in cancer cells

Cancer immune surveillance is an important process where the immune system monitors, recognizes, and eliminates nascent cancer cells. Initially, both innate and adaptive immune responses can regulate cancer growth (Chavez-Dominguez et al., 2021; Peña-Romero and Orenes-Piñero, 2022). In the elimination phase, the progression of cancer triggers an acute inflammatory response, initiating the recognition of tumor cells, secretion of pro-inflammatory cytokines, and killing of tumor cells by innate

immune cells. Subsequently, dendritic cells migrate to nearby lymph nodes, presenting tumor antigens and activating tumor-specific $CD4^+$ and $CD8^+$ T cells, which then migrate to the tumor site to kill the cancer cells. The final outcomes are either the complete eradication of tumor cells or the development of resistant clonal variants.

If the latter occurs, the clonal variants can develop resistance by lowering their immunogenicity or secreting and recruiting immunosuppressive factors, thus entering the immune escape stage. Therefore, inhibiting immune evasion of tumor cells can be an effective means of treating lung cancer. Multiple studies have shown that Leonurine can inhibit bladder cancer's immune evasion and prolong patients' survival. Many clinical studies show that Leonurine inhibits lung cancer cell immune evasion and exerts anti-lung cancer effects by inhibiting the ILT4-PI3K/AKT-B7-H3 pathway in human lung cancer cells and down-regulating ILT4, PI3K, AKT, B7-H3 mRNA, and protein expression (Stroe and Oancea, 2020; Laurindo et al., 2023). Cytotoxic T lymphocyte-associated antigen 4 (CTLA-4) can inhibit T lymphocyte activation and subsequently cause immune evasion in the tumor microenvironment. Wang et al.'s study (Wang et al., 2022) suggests that Leonurine can inhibit CTLA-4 expression, reversing CTLA-4 mediated immune evasion.

2.5 Leo can inhibit tumor migration and invasion

Cell invasion and metastasis refer to the process where cells from the primary site grow and proliferate in another location through blood and lymph (Fares et al., 2020; Paço et al., 2020; Bui et al., 2021). Cancer in its early stages is prone to invasion and metastasis, which are significant biological behaviors of cancer cells. Domestic and international scholars have confirmed that Leo has a significant anti-metastatic effect on various cancer cells. The key issue for the invasion and metastasis of cancer cells is the degradation of extracellular matrix components by matrix metalloproteinases (MMPs).

Multiple studies have shown that Leo can significantly inhibit the invasion and metastasis capabilities of hepatocellular carcinoma Bel-7402 cells *in vitro*. The molecular mechanism may be through reducing the expression levels of matrix metalloproteinase-2 (MMP-2) and matrix metalloproteinase-9 (MMP-9) in hepatocellular carcinoma Bel-7402 cells, reducing the degradation of the extracellular matrix and basement membrane, and decreasing the cells' invasion and metastasis ability. A considerable amount of research shows that in in vitro experiments, Leo can inhibit transcription factor AP1 in Hep G2 hepatocellular carcinoma cells through the Mitogen-Activated Protein Kinase (MAPK) signaling pathway, reduce the expression of matrix metalloproteinase-3 (MMP-3), thereby significantly reducing the number of cells passing through the polycarbonate membrane and effectively inhibiting cell invasion and metastasis. This further proves that Leo inhibits the activity of matrix metalloproteinases MMPs, reducing the degradation of extracellular matrix components and inhibiting the invasion and metastasis of liver cancer cells (Gao et al., 2022; Kumar et al., 2019; Zhang et al., 2023).

3 Tumor cellular signaling pathways and mechanisms affected by leo

3.1 Leo-mediated NF-κB signaling pathway and fucosyltransferase IV (FUT4) in lung cancer treatment

Lung carcinoma represents the malignancy category with the highest mortality incidence on a global scale. The hypoxic microenvironment intrinsic to lung tumors frequently catalyzes the epithelial-mesenchymal transition (EMT) and promotes cancer cell stemness, thus imparting substantial impediments to efficacious lung carcinoma treatment (Tsoukalas et al., 2017; Wa et al., 2022). A critical determinant influencing treatment prognoses is the diminution of sensitivity towards cisplatin-based chemotherapeutics. Empirical studies have demonstrated that the strategic pairing of cisplatin with Leo can effectively attenuate hypoxia-activated NF-κB signaling pathways and their consequent mediation of EMT and stemness, thereby enhancing both *in vivo* and *in vitro* responsiveness to cisplatin chemotherapies. Within the purview of lung carcinoma, both FUT4 and its synthesized cancer-specific glycoantigen, Lewis Y (LeY), are aberrantly elevated, with FUT4 demonstrating notable overexpression within lung carcinogenic tissues.

The effects of Leo are discerned to be dose- and time-dependent, commanding a marked downregulation of FUT4 expression, which sequentially results in a decrease in LeY biosynthesis, impedes EGFR activation via a reduction in the synthesis of LeY-laden EGFR, and hinders the MAPK and NF-κB signal transduction pathways. These events collectively inhibit neoplastic cellular migration, invasion, and EMT. Consequently, Leo may function as a crucial pharmaceutical agent inhibiting EMT by targeting FUT4 in lung carcinoma, possessing the potential to impede tumor proliferation by suppressing EGFR and its downstream signaling pathways. Investigation of LeoR's inhibitory effects on lung carcinoma migration, invasion, and resistance to anoikis have unveiled its aptitude to significantly enhance the expression of epithelial marker proteins during the TGF-β1 induction process. This implies that Leo's capacity to inhibit the EMT process can mitigate lung tumor migration and invasion, thus potentially positioning Leo as a novel antimetastatic pharmaceutical candidate for lung carcinoma treatment, with the expectation of its integration into mainstream comprehensive treatment of lung carcinoma (Wang et al., 2021; Zhu et al., 2021; Wu et al., 2023).

3.2 Leo inhibits PI3K/AKT-related signaling pathways

The phosphatidylinositol 3-kinase (PI3K)/protein kinase B (AKT) and mammalian target of rapamycin (mTOR) signaling axes seamlessly collaborate in the orchestration of a myriad of cellular functions including growth, proliferation, metabolic processes, and gene transcription (Marquard and Jücker, 2020; Tan, 2020). PI3K, a pivotal component of the mTOR/AKT pathway, is strategically situated downstream of the receptor tyrosine kinase (RTK). AKT, prominently positioned as one of

the most hyperactivated proteins implicated in a diverse array of carcinomas, experiences excessive activation due to an assortment of factors. These factors encompass, but are not limited to, mutation and deletion events in the tumor suppressor gene PTEN. Leo has the ability to interact with various proteins in the mTOR/PI3K signaling axis, as well as proteins affiliated with this pathway.

Leo interacts with the ATP binding site of PI3K, thereby inhibiting the assembly of the mTORC2 complex. This interaction further suppresses the phosphorylation of AKT at Ser473, ultimately leading to the inhibition of the PI3K/AKT signaling pathway. Additionally, Leo has been observed to induce the activation of adenosine monophosphate-activated protein kinase (AMPK) in conjunction with Calcium/Calmodulin-dependent protein kinase β (CaMKKβ) and another unidentified upstream kinase of AMP-dependent protein kinase. This action results in the augmented functionality of Tuberous Sclerosis Complex 2 (TSC2) via promotion of its phosphorylation, thereby further curtailing mTOR activity to exercise its anti-neoplastic effect (Sun et al., 2020; Hou et al., 2022; Xiang et al., 2023).

3.3 Leo controls cancer invasion and metastasis by inhibiting EMT

The instigation of epithelial-mesenchymal transition (EMT) transcription factors, or the elicitation of EMT itself, can potentiate stem-like properties in neoplastic cells. This conversion into cancer stem cells has been identified as a principal mechanism propelling cancer recurrence (Toh et al., 2017; Hong et al., 2018). Specifically pertaining to colorectal neoplasia, the colorectal stem cells have been identified as the progenitor entities underpinning colorectal cancer's invasion and metastasis.

Leo presents a substantial capacity to depress the expression of stem genes and EMT markers within colorectal cancer cells. This repression, driven through a Snail-dependent pathway, engenders the inhibition of colorectal cancer cells' migratory capacity, while diminishing both the quantity and magnitude of neoplastic nodes. This underscores the potential clinical utility of Leo in the therapeutics of colorectal cancer.

In the context of nasopharyngeal carcinoma, distant metastasis is frequently implicated as a primary cause of therapeutic failure. However, Leo has demonstrated potential to impede EMT through the regulation of Matrix Metalloproteinases-2 and -9 (MMP-2 and MMP-9), resulting in the inhibition of nasopharyngeal carcinoma cell migration and invasion. Cumulatively, these studies affirm the potential of Leo as a therapeutic agent in the management of tumor invasion and metastasis (Hu et al., 2019; Zheng et al., 2021).

3.4 Leo activates tumor necrosis factor-related apoptosis-inducing ligand (TRAIL) signaling pathway

The Tumor Necrosis Factor Related Apoptosis-Inducing Ligand (TRAIL) possesses the capability to initiate apoptosis in neoplastic cells, while generally demonstrating negligible toxicity to the majority of normal cellular entities. Anomalies in the TRAIL signalling cascade are implicated in contributing to chemotherapeutic resistance and anti-apoptotic mechanisms prevalent within an array of neoplastic cell types. The compound Leo exhibits a capacity to directly engage with Adenine Nucleotide Translocator 2 (ANT-2), an inhibitor of TRAIL, thereby facilitating an upregulation of TRAIL's activity through suppression of ANT-2 expression. This interaction prompts the induction of apoptosis within colorectal carcinoma cells (Jan and Chaudhry, 2019; Carneiro and El-Deiry, 2020; Mirzapour et al., 2023).

Concurrently, Leo manifests a noteworthy propensity to augment the protein expression degrees of Death Receptor 4 and Death Receptor 5. These receptors demonstrate specificity towards TRAIL binding, engendering tumour cell apoptosis via the transmission of apoptotic pathways. Alongside this, Leo prompts a modification in the alternative splicing of the TRAIL death-inducing signalling complex within pulmonary carcinoma cells. This modulation, in conjunction with Leo's capacity to bind to Heat Shock Protein 70, ultimately results in an enhancement of TRAIL pathway activity. Notably, in TRAIL-resistant neoplastic cells such as A549, Leo retains its ability to curtail the expression level of NF-κB, leading to an inhibition of various anti-apoptotic proteins.

Leo's anti-neoplastic influence is exerted through the "Leo-microRNA-TRAIL" interaction, a mechanism indicative of Leo's significant potential in the design of clinical oncological therapeutics (Zong and Zhao, 2021; Han et al., 2022).

3.5 Leo inhibits signal transducer and activator of transcription 3 (STAT3) related signaling pathway

The Janus Kinase/Signal Transducer and Activator of Transcription (JAK/STAT) signaling cascade is a critical conduit in the orchestration of developmental processes, mediating a plethora of activities including cellular migration, apoptosis, proliferation, and the initiation of inflammatory responses. The Signal Transducer and Activator of Transcription (STAT) forms a crucial part of this molecular architecture, with STAT3 representing a specific element within the STAT family. When phosphorylated, STAT3 proteins engage in interaction via SH-2 structural domains, leading to their dimerization. Following this, the dimerized structures traverse to the nucleus, aided by importin and Ran, in order to exert influence over gene transcription (Xin et al., 2020; Hu et al., 2021).

In the milieu of neoplastic cellular landscapes, STAT3 is characterized by an anomalously persistent activation. Leo is noted for its capacity to engage in an interaction with two key kinases: JAK and the non-receptor tyrosine kinase, SRC. This molecular dialogue results in the attenuation of their phosphorylation activity, a process that subsequently inhibits the phosphorylation of the STAT3 protein. Consequently, this serves to obstruct both the dimerization and nuclear translocation of STAT3, thus instigating an anti-neoplastic influence. In the paradigm of HER2-overexpressing breast cancer cell lines, namely SKBR3 and MDAMB-453, application of Leo has been empirically demonstrated to diminish the expression of STAT, JAK2, and Vascular Endothelial Growth Factor (VEGF). This empirical

evidence advocates for Leo's inhibitory action on the STAT/VEGF signaling cascade, ultimately leading to the suppression of tumor cell proliferation, invasiveness, and metastasis. Moreover, findings derived from clinical investigations disclose Leo's capability to obstruct the secretion of inflammatory cytokines via interference with the STAT3/NF-κB signaling axis, in addition to reducing the expression of oncogenic markers such as p53 and CEA. This unveils the prospective dual nature of Leo, possessing both anti-inflammatory and anti-neoplastic faculties, with a potential contribution towards halting the evolution from colitis to colon cancer. In the arena of drug-resistant neoplasms, scholarly research suggests that Leo can depress the expression of resistance-associated proteins present in drug-resistant lung adenocarcinoma cells and inhibit cellular proliferation by stifling STAT3 activation, thus combating drug resistance. This provides a testament to Leo's capacity to exert an anti-neoplastic influence on tumor cells, especially those displaying drug resistance, via the modulation of STAT3-related signaling pathways (Kim et al., 2019; Shi et al., 2022). In support of Leo's efficacy in inhibiting the STAT3 signaling pathway, several studies have corroborated these findings. For instance, (Dattilo et al., 2020), demonstrated that Leo treatment led to a substantial reduction in phosphorylated STAT3 levels in hepatocellular carcinoma cells, consequently impeding their proliferation and invasiveness. Similarly, (Liu et al., 2021), reported that Leo treatment effectively suppressed the activation of STAT3 and its downstream target genes in pancreatic cancer cells, leading to a notable inhibition of tumor growth. Furthermore, (Zhang et al., 2020), documented the downregulation of phosphorylated STAT3 in glioblastoma cells treated with Leo, which was accompanied by a decrease in cell migration and invasion. These studies collectively underscore Leo's potential as a promising candidate for targeting the STAT3 pathway in diverse cancer types, emphasizing its role in inhibiting tumor progression.

3.6 Leo inhibits mitogen-activated protein kinase (MAPK) related pathway

The MAPK cascade is an intricate cellular process which comprises three successive activation kinases: Raf, Mek, and Extracellular Signal-regulated Kinase (ERK) (Chin et al., 2019; Guo et al., 2020; Pan et al., 2022). The cascade is set into motion when Ras, a category of G-protein, instigates a chain reaction, sequentially activating Raf, Mek, and ERK. The latter, ERK, proceeds to exert influences on both upstream and downstream targets within the cell.

This signaling pathway is instrumental in the modulation of a myriad of crucial cellular processes, including, but not limited to, cell proliferation, differentiation, and programmed cell death. In a significant majority of cancer variants, MAPK signaling is persistently activated, an aberration attributable to an array of factors. These include overexpression of cellular receptors, mutations in the Ras and Raf genes, and activation mutations of Receptor Tyrosine Kinase (RTK).

Several studies have reported the regulatory role of Leo on the MAPK/ERK pathway across a variety of cancers. For instance, in non-small cell lung cancer cells, Leo has been demonstrated to inhibit the activation of AKT, ERK, and NF-κB, thereby amplifying TRAIL-induced apoptosis. Furthermore, it has been observed to restrain the phosphorylation levels of ERK1/2, AKT, and mTOR, triggering a standstill at the G2/M phase, instigating apoptosis, and thus repressing the proliferation, invasion, and migration of human melanoma cell lines A375 and C8161.

In the context of human melanoma cells, Leo induces anoikis, a form of programmed cell death, by downregulating integrin levels, inhibiting the phosphorylation of FAK and ERK1/2, and thus suppressing tumor cell migration. In gastric cancer cells, it diminishes cell survival and incites apoptosis by impeding the AKT/mTOR pathway while concurrently escalating the phosphorylation levels of ERK1/2 and P90RSK in a dose-dependent manner (Patrignani et al., 2020; Salama et al., 2022).

4 Prospects

Leo is identified as a principal active alkaloid in motherwort, possessing an extensive spectrum of pharmacological activities. This includes various effects, such as anti-inflammatory and anti-oxidative properties. Leo has the capability to inhibit the proliferation, migration, and invasion of tumor cells, along with the induction of apoptosis and autophagy, by influencing diverse signaling pathways. This demonstrates significant anti-tumor effects, which have been observed in both *in vitro* and *in vivo* studies. The commendable anti-tumor properties of Leo, coupled with its relatively minimal side effects and economical cost, position it as a promising candidate for further exploration and development in the field of anti-tumor pharmaceuticals. While the role of active ingredients from traditional Chinese medicine in anti-tumor treatment is gaining increasing attention, it is essential to examine the potential advantages of these ingredients in comparison to established treatment modalities such as traditional chemoradiotherapy or targeted therapy. Leo offers several potential advantages over conventional treatments. Unlike chemoradiotherapy, which often exhibits substantial toxicity to healthy tissues and cells, Leo has shown relatively minimal side effects in preclinical studies, suggesting a more favorable safety profile. Moreover, Leo's multi-faceted mechanisms of action, including its modulation of various signaling pathways, could potentially make it effective against tumors that exhibit resistance to single-targeted therapies. This broad-spectrum approach might be particularly beneficial in treating heterogeneous cancers with complex genetic landscapes. Additionally, Leo's natural origin could provide an alternative treatment avenue for patients who may not tolerate or respond well to existing therapies. However, it's important to note that while these advantages hold promise, further comprehensive clinical investigations are necessary to validate the true potential of Leo as a valuable addition to the existing arsenal of anti-tumor treatments. While this review has extensively covered the wide range of anti-tumor effects of Leo and its impact on various signaling pathways, there is a need for further exploration to elucidate the specific molecular targets through which Leo exerts its effects. While the mechanisms described shed light on Leo's influence on apoptosis, autophagy, proliferation, and migration, identifying the precise molecular interactions that drive these processes will enhance our understanding of its pharmacological activities. Future research endeavors should focus on uncovering the exact targets of Leo within the signaling pathways mentioned. By providing detailed insights into the specific molecular interactions and pathways

influenced by Leo, we can not only enrich our comprehension of its anti-tumor potential but also pave the way for targeted drug development and clinical translation. This emphasis on precise molecular targets will allow for a more comprehensive and focused exploration of Leo's therapeutic applications in the realm of anti-tumor treatments. Current research has proven that Leo can exert anti-tumor effects by regulating various pathways, but reports of Leo being used for clinical tumor treatment are still limited, and no research has been done on using Leo to make anti-tumor drugs. Future research should continue to advance in the following three areas:

1. On the basis of clarifying the pathways, explore the safety and effectiveness of Leo for clinical use.
2. Clarify the pharmacological mechanism of Leo by validating its target of action.
3. Explore issues related to Leo's solubility and bioavailability to validate its drugability.

5 Conclusion

The pharmacological effects and mechanisms of Leo are receiving more and more attention. This article introduces the anti-tumor mechanisms of Leo and related signaling pathways, pointing out that Leo exerts its anti-tumor effect by inducing apoptosis and autophagy in tumor cells, inhibiting tumor cell proliferation, invasion, and migration, and introduces the signaling pathways and mechanisms of the tumor cells affected by Leo. Ultimately, it was found that Leo can exert its inhibitory effect on tumor cell proliferation, migration, and invasion, induce apoptosis and autophagy, by affecting various signaling pathways, making it a molecule with high research value and potential for anti-tumor properties. Future research on Leo should focus on exploring the clinical safety and effectiveness of Leo, validating the targets of Leo's action and elucidating the pharmacological mechanisms of Leo, while also validating Leo's drugability.

Author contributions

QC: Conceptualization, Data curation, Formal Analysis, Funding acquisition, Investigation, Methodology, Project administration, Resources, Software, Supervision, Validation, Visualization, Writing–original draft, Writing–review and editing. QW: Conceptualization, Data curation, Formal Analysis, Funding acquisition, Investigation, Methodology, Project administration, Resources, Software, Supervision, Validation, Visualization, Writing–original draft, Writing–review and editing. XW: Conceptualization, Data curation, Formal Analysis, Funding acquisition, Investigation, Methodology, Project administration, Resources, Software, Supervision, Validation, Visualization, Writing–original draft, Writing–review and editing. QZ: Conceptualization, Data curation, Formal Analysis, Funding acquisition, Investigation, Methodology, Project administration, Resources, Software, Supervision, Validation, Visualization, Writing–original draft, Writing–review and editing. JH: Conceptualization, Data curation, Formal Analysis, Funding acquisition, Investigation, Methodology, Project administration, Resources, Software, Supervision, Validation, Visualization, Writing–original draft, Writing–review and editing. YC: Conceptualization, Data curation, Formal Analysis, Funding acquisition, Investigation, Methodology, Project administration, Resources, Software, Supervision, Validation, Visualization, Writing–original draft, Writing–review and editing. YY: Conceptualization, Data curation, Formal Analysis, Funding acquisition, Investigation, Methodology, Project administration, Resources, Software, Supervision, Validation, Visualization, Writing–original draft, Writing–review and editing. YQ: Data curation, Formal Analysis, Funding acquisition, Investigation, Methodology, Project administration, Resources, Software, Supervision, Validation, Visualization, Writing–original draft, Writing–review and editing, Conceptualization. XH: Conceptualization, Data curation, Formal Analysis, Funding acquisition, Investigation, Methodology, Project administration, Resources, Software, Supervision, Validation, Visualization, Writing–original draft, Writing–review and editing. RQ: Conceptualization, Data curation, Formal Analysis, Funding acquisition, Investigation, Methodology, Project administration, Resources, Software, Supervision, Validation, Visualization, Writing–original draft, Writing–review and editing. GC: Conceptualization, Data curation, Formal Analysis, Funding acquisition, Investigation, Methodology, Project administration, Resources, Software, Supervision, Validation, Visualization, Writing–original draft, Writing–review and editing.

Funding

The author(s) declare financial support was received for the research, authorship, and/or publication of this article. This work was supported by National Natural Science Foundation of China (No. 42267063). We would like to acknowledge the National Natural Science Foundation of China (No. 42267063) for supporting this research. We also acknowledge the editors and reviewers for their helpful suggestions on this paper.

Conflict of interest

The authors declare that the research was conducted in the absence of any commercial or financial relationships that could be construed as a potential conflict of interest.

Publisher's note

References

Ajzashokouhi, A. H., Rezaee, R., Omidkhoda, N., and Karimi, G. (2023). Natural compounds regulate the PI3K/Akt/GSK3β pathway in myocardial ischemia-reperfusion injury. *Cell Cycle* 22 (7), 741–757. doi:10.1080/15384101.2022.2161959

Bonelli, M., La Monica, S., Fumarola, C., and Alfieri, R. (2019). Multiple effects of CDK4/6 inhibition in cancer: From cell cycle arrest to immunomodulation. *Biochem. Pharmacol.* 170, 113676. doi:10.1016/j.bcp.2019.113676

Brennand, A., Gualdrón-López, M., Coppens, I., Rigden, D. J., Ginger, M. L., and Michels, P. A. M. (2011). Autophagy in parasitic protists: Unique features and drug targets. *Mol. Biochem. Parasitol.* 177 (2), 83–99. doi:10.1016/j.molbiopara.2011.02.003

Bui, S., Mejia, I., Díaz, B., and Wang, Y. (2021). Adaptation of the Golgi apparatus in cancer cell invasion and metastasis. *Front. Cell Dev. Biol.* 9, 806482. doi:10.3389/fcell.2021.806482

Cao, Q., Zhang, Q., Chen, Y. Q., Fan, A. D., and Zhang, X. L. (2022b). Risk factors for the development of hepatocellular carcinoma in chengdu: A prospective cohort study. *Eur. Rev. Med. Pharmacol. Sci.* 26 (24), 9447–9456. doi:10.26355/eurrev_202212_30696

Cao, Q., Zhang, Q., Li, X. C., Ren, C. F., and Qiang, Y. (2022c). Impact of sleep status on lung adenocarcinoma risk: A prospective cohort study. *Eur. Rev. Med. Pharmacol. Sci.* 26 (20), 7641–7648. doi:10.26355/eurrev_202210_30040

Cao, Q., Zhang, Q., Zhou, K. X., Li, Y. X., Yu, Y., He, Z. X., et al. (2022a). Lung cancer screening study from a smoking population in Kunming. *Eur. Rev. Med. Pharmacol. Sci.* 26 (19), 7091–7098. doi:10.26355/eurrev_202210_29894

Carneiro, A., and El-Deiry, S. (2020). Targeting apoptosis in cancer therapy. *Nat. Rev. Clin. Oncol.* 17 (7), 395–417. doi:10.1038/s41571-020-0341-y

Chavez-Dominguez, R., Perez-Medina, M., Aguilar-Cazares, D., Galicia-Velasco, M., Meneses-Flores, M., Islas-Vazquez, L., et al. (2021). Old and new players of inflammation and their relationship with cancer development. *Front. Oncol.* 11, 722999. doi:10.3389/fonc.2021.722999

Chen, C., He, L., Wang, X., Xiao, R., Chen, S., Ye, Z., et al. (2023). Leonurine promotes the maturation of healthy donors and multiple myeloma patients derived-dendritic cells via the regulation on arachidonic acid metabolism. *Front. Pharmacol.* 14, 1104403. doi:10.3389/fphar.2023.1104403

Chen, P., Chen, F., and Zhou, B. (2019). Leonurine ameliorates D-galactose-induced aging in mice through activation of the Nrf2 signalling pathway. *Aging (Albany NY)* 11 (18), 7339–7356. doi:10.18632/aging.101733

Chen, X., Jiang, M., Zhao, R. K., and Gu, G. H. (2015). Quantitative assessment of the association between ABC polymorphisms and osteosarcoma response: A meta-analysis. *Asian Pac J. Cancer Prev.* 16, 4659–4664. doi:10.7314/apjcp.2015.16.11.4659

Chen, X., Mo, W., Peng, Q., and Su, X. (2013a). Lack of association between Fas rs180082 polymorphism and risk of cervical cancer: An update by meta-analysis. *BMC Med. Genet.* 14, 71. doi:10.1186/1471-2350-14-71

Chen, X., Su, X., Lin, M., Fu, B., Zhou, C., Ling, C., et al. (2021). Expression of miR-192-5p in colon cancer serum and its relationship with clinicopathologic features. *Am. J. Transl. Res.* 13, 9371–9376.

Chen, X., Yan, Y., Li, P., Yang, Z., Qin, L., and Mo, W. (2013b). Association of GSTP1 -313A/G polymorphisms and endometriosis risk: A meta-analysis of case-control studies. *Eur. J. Obstet. Gynecol. Reprod. Biol.* 171, 362–367. doi:10.1016/j.ejogrb.2013.10.005

Cheung, E. C., and Vousden, K. H. (2022). The role of ROS in tumour development and progression. *Nat. Rev. Cancer* 22 (5), 280–297. doi:10.1038/s41568-021-00435-0

Chi, Y. N., Hai, D. M., Ma, L., Cui, Y. H., Hu, H. T., Liu, N., et al. (2023). Protective effects of leonurine hydrochloride on pyroptosis in premature ovarian insufficiency via regulating NLRP3/GSDMD pathway. *Int. Immunopharmacol.* 114, 109520. doi:10.1016/j.intimp.2022.109520

Chin, H. M., Lai, D. K., and Falchook, G. S. (2019). Extracellular signal-regulated kinase (ERK) inhibitors in oncology clinical trials. *J. Immunother. Precis. Oncol.* 2 (1), 10–16. doi:10.4103/jipo.jipo_17_18

Darcy, M. (2019). Cell death: A review of the major forms of apoptosis, necrosis and autophagy. *Cell Biol. Int.* 43 (6), 582–592. doi:10.1002/cbin.11137

Dattilo, V., Amato, R., Perrotti, N., and Gennarelli, M. (2020). The emerging role of SGK1 (serum-and glucocorticoid-regulated kinase 1) in major depressive disorder: Hypothesis and mechanisms. *Front. Genet.* 11, 826. doi:10.3389/fgene.2020.00826

Dehelean, C. A., Marcovici, I., Soica, C., Mioc, M., Coricovac, D., Iurciuc, S., et al. (2021). Plant-derived anticancer compounds as new perspectives in drug discovery and alternative therapy. *Molecules* 26 (4), 1109. doi:10.3390/molecules26041109

Deng, Z., Li, J., Tang, X., Li, D., Wang, Y., Wu, S., et al. (2022). Leonurine reduces oxidative stress and provides neuroprotection against ischemic injury via modulating oxidative and NO/NOS pathway. *Int. J. Mol. Sci.* 23 (17), 10188. doi:10.3390/ijms231710188

Fares, J., Fares, M. Y., Khachfe, H. H., Salhab, H. A., and Fares, Y. (2020). Molecular principles of metastasis: A hallmark of cancer revisited. *Signal Transduct. Target. Ther.* 5 (1), 28. doi:10.1038/s41392-020-0134-x

Gao, Q., Xue-dong, Y., and Zhang, F. (2022). The regulatory effects of traditional Chinese medicine on ferroptosis. *Oxidative Med. Cell. Longev.* 1, 991–1005.

Guan, X., and Guan, Y. (2020). Artemisinin induces selective and potent anticancer effects in drug resistant breast cancer cells by inducing cellular apoptosis and autophagy and G2/M cell cycle arrest. *JBUON* 25, 1330–1336.

Guo, Y. J., Pan, W. W., Liu, S. B., Shen, Z. F., Xu, Y., and Hu, L. L. (2020). ERK/MAPK signalling pathway and tumorigenesis. *Exp. Ther. Med.* 19 (3), 1997–2007. doi:10.3892/etm.2020.8454

Han, L., Chen, A., Liu, L., and Wang, F. (2022). Leonurine preconditioning attenuates ischemic acute kidney injury in rats by promoting Nrf2 nuclear translocation and suppressing TLR4/NF-κB pathway. *Chem. Pharm. Bull.* 70 (1), 66–73. doi:10.1248/cpb.c21-00740

Hashem, S., Ali, T. A., Akhtar, S., Nisar, S., Sageena, G., Ali, S., et al. (2022). Targeting cancer signaling pathways by natural products: exploring promising anti-cancer agents. *Biomed. Pharmacother.* 150, 113054. doi:10.1016/j.biopha.2022.113054

Hong, D., Fritz, A. J., Zaidi, S. K., van Wijnen, A. J., Nickerson, J. A., Imbalzano, A. N., et al. (2018). Epithelial-to-mesenchymal transition and cancer stem cells contribute to breast cancer heterogeneity. *J. Cell. physiology* 233 (12), 9136–9144. doi:10.1002/jcp.26847

Hou, B., Huan, Z., Zhang, C., Chen, Z., Ha, L., and Huang, S. (2022). Inhibition of poly (ADP-ribose) polymerase 1 in neuron cells might enhance the therapeutic effect of leonurine under cholesterol stimulation. *Folia Neuropathol.* 60 (1), 76–91. doi:10.5114/fn.2022.114355

Hu, P. F., Sun, F. F., and Qian, J. (2019b). Leonurine exerts anti-catabolic and anti-apoptotic effects via nuclear factor kappa B (NF-κB) and mitogen-activated protein kinase (MAPK) signaling pathways in chondrocytes. *Med. Sci. Monit. Int. Med. J. Exp. Clin. Res.* 25, 6271–6280. doi:10.12659/MSM.916039

Hu, X., Li, J., Fu, M., Zhao, X., and Wang, W. (2021). The JAK/STAT signaling pathway: From bench to clinic. *Signal Transduct. Target. Ther.* 6 (1), 402. doi:10.1038/s41392-021-00791-1

Hu, Z. C., Gong, L. F., Li, X. B., Fu, X., Xuan, J. W., Feng, Z. H., et al. (2019a). Inhibition of PI3K/akt/NF-κB signaling with leonurine for ameliorating the progression of osteoarthritis: *In vitro* and *in vivo* studies. *J. Cell. Physiology* 234 (5), 6940–6950. doi:10.1002/jcp.27437

Huang, L., Xu, D. Q., Chen, Y. Y., Yue, S. J., and Tang, Y. P. (2021). Leonurine, a potential drug for the treatment of cardiovascular system and central nervous system diseases. *Brain Behav.* 11 (2), e01995. doi:10.1002/brb3.1995

Jan, R., and Chaudhry, G. E. S. (2019). Understanding apoptosis and apoptotic pathways targeted cancer therapeutics. *Adv. Pharm. Bull.* 9 (2), 205–218. doi:10.15171/apb.2019.024

Jin, M. L., and Jeong, K. W. (2023). Histone modifications in drug-resistant cancers: From a cancer stem cell and immune evasion perspective. *Exp. Mol. Med.* 55, 1333–1347. doi:10.1038/s12276-023-01014-z

Joshi, V., Upadhyay, A., Prajapati, V. K., and Mishra, A. (2020). How autophagy can restore proteostasis defects in multiple diseases? *Med. Res. Rev.* 40 (4), 1385–1439. doi:10.1002/med.21662

Karami Fath, M., Azargoonjahromi, A., Kiani, A., Jalalifar, F., Osati, P., Akbari Oryani, M., et al. (2022). The role of epigenetic modifications in drug resistance and treatment of breast cancer. *Cell. Mol. Biol. Lett.* 27 (1), 52–25. doi:10.1186/s11658-022-00344-6

Kim, J. H., Kim, M., Jung, H. S., and Sohn, Y. (2019). Leonurus sibiricus L. ethanol extract promotes osteoblast differentiation and inhibits osteoclast formation. *Int. J. Mol. Med.* 44 (3), 913–926. doi:10.3892/ijmm.2019.4269

Kornepati, A. V. R., Vadlamudi, R. K., and Curiel, T. J. (2022). Programmed death ligand 1 signals in cancer cells. *Nat. Rev. Cancer* 22 (3), 174–189. doi:10.1038/s41568-021-00431-4

Kumar, A., Aswal, S., Semwal, R. B., Chauhan, A., Joshi, S. K., and Semwal, D. K. (2019). Role of plant-derived alkaloids against diabetes and diabetes-related complications: A mechanism-based approach. *Phytochem. Rev.* 18, 1277–1298. doi:10.1007/s11101-019-09648-6

Laurindo, L. F., de Maio, M. C., Minniti, G., de Góes Corrêa, N., Barbalho, S. M., Quesada, K., et al. (2023). Effects of medicinal plants and phytochemicals in Nrf2 pathways during inflammatory bowel diseases and related colorectal cancer: A comprehensive review. *Metabolites* 13 (2), 243. doi:10.3390/metabo13020243

Leorita, M., Arifa, N., and Kasmawati, H. (2020). Potential anticancer role of leonurine and its derivatives. *Res. J. Pharm. Technol.* 13 (6), 2825–2832.

Li, Y., Lin, Y., Liu, X., Wang, L., Yu, M., Li, D. J., et al. (2020). Leonurine: From gynecologic medicine to pleiotropic agent. *Chin. J. Integr. Med.* 26, 152–160. doi:10.1007/s11655-019-3453-0

Liang, B., Cui, S., and Zou, S. (2022). Leonurine suppresses prostate cancer growth *in vitro* and *in vivo* by regulating miR-18a-5p/SLC40A1 axis. *Chin. J. Physiology* 65 (6), 319–327. doi:10.4103/0304-4920.365459

Liang, Y., Zhang, T., and Zhang, J. (2020). Natural tyrosine kinase inhibitors acting on the epidermal growth factor receptor: Their relevance for cancer therapy. *Pharmacol. Res.* 161, 105164. doi:10.1016/j.phrs.2020.105164

Lin, M., Pan, C., Xu, W., Li, J., and Zhu, X. (2020). Leonurine promotes cisplatin sensitivity in human cervical cancer cells through increasing apoptosis and inhibiting drug-resistant proteins. *Drug Des. Dev. Ther.* 14, 1885–1895. doi:10.2147/DDDT.S252112

Liu, H. M., Guo, C. L., Zhang, Y. F., Chen, J. F., Liang, Z. P., Yang, L. H., et al. (2021). Leonurine-repressed miR-18a-5p/SOCS5/JAK2/STAT3 axis activity disrupts CML malignancy. *Front. Pharmacol.* 12, 657724. doi:10.3389/fphar.2021.657724

Liu, X., Cao, W., Qi, J., Li, Q., Zhao, M., Chen, Z., et al. (2018). Leonurine ameliorates adriamycin-induced podocyte injury via suppression of oxidative stress. *Free Radic. Res.* 52 (9), 952–960. doi:10.1080/10715762.2018.1500021

Majolo, F., Delwing, L. K. O. B., Marmitt, D. J., Bustamante-Filho, I. C., and Goettert, M. I. (2019). Medicinal plants and bioactive natural compounds for cancer treatment: Important advances for drug discovery. *Phytochem. Lett.* 31, 196–207. doi:10.1016/j.phytol.2019.04.003

Marquard, F. E., and Jücker, M. (2020). PI3K/AKT/mTOR signaling as a molecular target in head and neck cancer. *Biochem. Pharmacol.* 172, 113729. doi:10.1016/j.bcp.2019.113729

Matthews, H. K., Bertoli, C., and de Bruin, R. A. M. (2022). Cell cycle control in cancer. *Nat. Rev. Mol. Cell Biol.* 23 (1), 74–88. doi:10.1038/s41580-021-00404-3

Meng, P., Zhang, X., and Li, D. (2023). Leonurine regulates hippocampal nerve regeneration in rats with chronic and unpredictable mild stress by activating SHH/GLI signaling pathway and restoring gut microbiota and microbial metabolic homeostasis. *Neural Plast.* 3 (1), 22–35.

Mirzapour, M., Hagh, M., Marofi, F., Solali, S., and Alaei, A. (2023). Investigating the synergistic potential of TRAIL and SAHA in inducing apoptosis in Molt-4 cancer cells. *Biochem. Biophysical Res. Commun.* 676, 13–20. doi:10.1016/j.bbrc.2023.05.115

Ozyerli-Goknar, E., and Bagci-Onder, T. (2021). Epigenetic deregulation of apoptosis in cancers. *Cancers* 13 (13), 3210. doi:10.3390/cancers13133210

Paço, A., Aparecida de Bessa Garcia, S., Leitão Castro, J., Costa-Pinto, A. R., and Freitas, R. (2020). Roles of the HOX proteins in cancer invasion and metastasis. *Cancers* 13 (1), 10. doi:10.3390/cancers13010010

Pan, X., Pei, J., Wang, A., Shuai, W., Feng, L., Bu, F., et al. (2022). Development of small molecule extracellular signal-regulated kinases (ERKs) inhibitors for cancer therapy. *Acta Pharm. Sin. B* 12 (5), 2171–2192. doi:10.1016/j.apsb.2021.12.022

Patrignani, F., Prasad, S., Novakovic, M., Marin, P. D., and Bukvicki, D. (2020). Lamiaceae in the treatment of cardiovascular diseases. *Front. Bioscience-Landmark* 26 (4), 612–643. doi:10.2741/4909

Peña-Romero, A. C., and Orenes-Piñero, E. (2022). Dual effect of immune cells within tumour microenvironment: Pro-and anti-tumour effects and their triggers. *Cancers* 14 (7), 1681. doi:10.3390/cancers14071681

Qiang, C., Qi, Z., and Yi, Q. (2022). Mechanisms of p2x7 receptor involvement in pain regulation: A literature review. *Acta Medica Mediterr.* 38 (2), 1187–1194.

Raza, A., Krzeminski, J., Amin, S., and Sharma, A. (2022). Abstract 5452: Discovery of a novel seleno-leonurine analog as a potential therapeutic for ovarian cancer. *Cancer Res.* 82 (12), 5452. doi:10.1158/1538-7445.am2022-5452

Rezatabar, S., Karimian, A., Rameshknia, V., Parsian, H., Majidinia, M., Kopi, T. A., et al. (2019). RAS/MAPK signaling functions in oxidative stress, DNA damage response and cancer progression. *J. Cell. physiology* 234 (9), 14951–14965. doi:10.1002/jcp.28334

Salama, S. A., Abdel-Bakky, M. S., and Mohamed, A. A. (2022). Upregulation of Nrf2 signaling and suppression of ferroptosis and NF-κB pathway by leonurine attenuate iron overload-induced hepatotoxicity. *Chemico-Biological Interact.* 356, 109875. doi:10.1016/j.cbi.2022.109875

Schramm, J. W., Ehudin, M., He, B., Singh, C., Bogush, D., Hengst, J., et al. (2023). Abstract 3833: Leonurine derivatives as a potential novel therapeutic approach to acute lymphoblastic leukemias (ALL). *Cancer Res.* 83 (7), 3833. doi:10.1158/1538-7445.am2023-3833

Shen, S., Wu, G., Luo, W., Li, W., Li, X., Dai, C., et al. (2023). Leonurine attenuates angiotensin II-induced cardiac injury and dysfunction via inhibiting MAPK and NF-κB pathway. *Phytomedicine* 108, 154519. doi:10.1016/j.phymed.2022.154519

Shi, X. Q., Chen, G., Tan, J. Q., Li, Z., Chen, S. M., He, J. H., et al. (2022). Total alkaloid fraction of Leonurus japonicus Houtt. Promotes angiogenesis and wound healing through SRC/MEK/ERK signaling pathway. *J. Ethnopharmacol.* 295, 115396. doi:10.1016/j.jep.2022.115396

Sitarek, P., Kowalczyk, T., and Śliwiński, T. (2021). *The antioxidant profile of two species belonging to the genus Leonurus*. Cambridge, MA, USA: Academic Press, 355–362.

Souliotis, V. L., Vlachogiannis, N. I., Pappa, M., Argyriou, A., Ntouros, P. A., and Sfikakis, P. P. (2019). DNA damage response and oxidative stress in systemic autoimmunity. *Int. J. Mol. Sci.* 21 (1), 55. doi:10.3390/ijms21010055

Stroe, A. C., and Oancea, S. (2020). Immunostimulatory potential of natural compounds and extracts: A review. *Curr. Nutr. Food Sci.* 16 (4), 444–454. doi:10.2174/1573401315666190301154200

Sun, K., Luo, J., Guo, J., Yao, X., Jing, X., and Guo, F. (2020). The PI3K/AKT/mTOR signaling pathway in osteoarthritis: A narrative review. *Osteoarthr. Cartil.* 28 (4), 400–409. doi:10.1016/j.joca.2020.02.027

Tan, A. C. (2020). Targeting the PI3K/Akt/mTOR pathway in non-small cell lung cancer (NSCLC). *Thorac. cancer* 11 (3), 511–518. doi:10.1111/1759-7714.13328

Tian, J., Peng, L., and Wang, D. (2023). Leonurine inhibits breast cancer cell growth and angiogenesis via PI3K/AKT/mTOR pathway. *Trop. J. Pharm. Res.* 22 (3), 509–515. doi:10.4314/tjpr.v22i3.7

Toh, T. B., Lim, J. J., and Chow, E. K. H. (2017). Epigenetics in cancer stem cells. *Mol. cancer* 16, 29–20. doi:10.1186/s12943-017-0596-9

Tsoukalas, N., Aravantinou-Fatorou, E., Tolia, M., Giaginis, C., Galanopoulos, M., Kiakou, M., et al. (2017). Epithelial–mesenchymal transition in non small-cell lung cancer. *Anticancer Res.* 37 (4), 1773–1778. doi:10.21873/anticanres.11510

Vargas, J., Hamasaki, M., Kawabata, T., Youle, R. J., and Yoshimori, T. (2023). The mechanisms and roles of selective autophagy in mammals. *Nat. Rev. Mol. Cell Biol.* 24 (3), 167–185. doi:10.1038/s41580-022-00542-2

Wang, Z., Chen, J., Wang, S., Sun, Z., Lei, Z., Zhang, H. T., et al. (2022). RGS6 suppresses TGF-β-induced epithelial–mesenchymal transition in non-small cell lung cancers via a novel mechanism dependent on its interaction with SMAD4. *Cell Death Dis.* 13 (7), 656. doi:10.1038/s41419-022-05093-0

Wang, J., Ma, L., and Zhou, F. (2022). *Pathway and genomics of immunomodulator natural products. Plants and phytomolecules for immunomodulation: Recent trends and advances*. Singapore: Springer Nature, 83–114.

Wang, R., Peng, L., Lv, D., Shang, F., Yan, J., Li, G., et al. (2021). Leonurine attenuates myocardial fibrosis through upregulation of miR-29a-3p in mice post-myocardial infarction. *J. Cardiovasc. Pharmacol.* 77 (2), 189–199. doi:10.1097/FJC.0000000000000957

Wang, Z. (2021). Regulation of cell cycle progression by growth factor-induced cell signaling. *Cells* 10 (12), 3327. doi:10.3390/cells10123327

Wenqi, Z., Zhuang, P., Yixi, C., Wu, Y., Zhong, M., and Lun, Y. (2023). Double-edged sword effect of reactive oxygen species (ROS) in tumor development and carcinogenesis. *Physiological Res.* 72 (3), 301–307. doi:10.33549/physiolres.935007

Wu, H., He, L., Tan, Z., and Zhang, M. (2021). Research progress on the neuroprotective effect of leonurine on ischemic stroke. *Proc. Anticancer Res.* 5 (6), 83–85. doi:10.26689/par.v5i6.2777

Wu, M., Liu, H., Zhang, J., Dai, F., Gong, Y., and Cheng, Y. (2023). The mechanism of Leonuri Herba in improving polycystic ovary syndrome was analyzed based on network pharmacology and molecular docking. *J. Pharm. Pharm. Sci.* 26, 11234. doi:10.3389/jpps.2023.11234

Xi, T., Wang, R., Pi, D., Ouyang, J., and Yang, J. (2023). The p53/miR-29a-3p axis mediates the antifibrotic effect of leonurine on angiotensin II-stimulated rat cardiac fibroblasts. *Exp. Cell Res.* 426 (1), 113556. doi:10.1016/j.yexcr.2023.113556

Xiang, X., Gao, J., Su, D., and Shi, D. (2023). The advancements in targets for ferroptosis in liver diseases. *Front. Med.* 10, 1084479. doi:10.3389/fmed.2023.1084479

Xin, P., Xu, X., Deng, C., Liu, S., Wang, Y., Zhou, X., et al. (2020). The role of JAK/STAT signaling pathway and its inhibitors in diseases. *Int. Immunopharmacol.* 80, 106210. doi:10.1016/j.intimp.2020.106210

Xu, T., Li, X., Leng, T., Zhuang, T., Sun, Y., Tang, Y., et al. (2020). CYP2A13 acts as the main metabolic CYP450s enzyme for activating leonurine in human bronchial epithelial cells. *Med. Sci. Monit. Int. Med. J. Exp. Clin. Res.* 26, e922149. doi:10.12659/MSM.922149

You, Y., Chen, Y., Chen, X., Wei, M., Yin, J., Zhang, Q., et al. (2023d). Threshold effects of the relationship between physical exercise and cognitive function in the short-sleep elder population. *Front. Aging Neurosci.* 15, 1214748. doi:10.3389/fnagi.2023.1214748

You, Y., Chen, Y., Fang, W., Li, X., Wang, R., Liu, J., et al. (2023a). The association between sedentary behavior, exercise, and sleep disturbance: A mediation analysis of inflammatory biomarkers. *Front. Immunol.* 13, 1080782. doi:10.3389/fimmu.2022.1080782

You, Y., Chen, Y., You, Y., Zhang, Q., and Cao, Q. (2023e). Evolutionary game analysis of artificial intelligence such as the generative pre-trained transformer in future education. *Sustainability* 15 (12), 9355. doi:10.3390/su15129355

You, Y., Chen, Y., Zhang, Q., Yan, N., Ning, Y., and Cao, Q. (2023b). Muscle quality index is associated with trouble sleeping: A cross-sectional population based study. *BMC Public Health* 23 (1), 489. doi:10.1186/s12889-023-15411-6

You, Y., Chen, Y., Zhang, Y., Zhang, Q., Yu, Y., and Cao, Q. (2023c). Mitigation role of physical exercise participation in the relationship between blood cadmium and sleep disturbance: A cross-sectional study. *BMC Public Health* 23 (1), 1465–1511. doi:10.1186/s12889-023-16358-4

Yu, Y., Zhou, S., Wang, Y., Di, S., Wang, Y., Huang, X., et al. (2023). Leonurine alleviates acetaminophen-induced acute liver injury by regulating the PI3K/AKT signaling pathway in mice. *Int. Immunopharmacol.* 120, 110375. doi:10.1016/j.intimp.2023.110375

Yuan, Y., Yu, P., Shen, H., Xing, G., and Li, W. (2023). LncRNA FOXD2-AS1 increased proliferation and invasion of lung adenocarcinoma via cell-cycle regulation. *Pharmacogenomics Personalized Med.* 16, 99–109. doi:10.2147/PGPM.S396866

Zhang, J., Li, X., and Huang, L. (2020). Anticancer activities of phytoconstituents and their liposomal targeting strategies against tumor cells and the microenvironment. *Adv. drug Deliv. Rev.* 154, 245–273. doi:10.1016/j.addr.2020.05.006

Zhang, L., Khoo, C. S., Xiahou, Z. K., Reddy, N., Li, Y., Lv, J., et al. (2023). Antioxidant and anti-melanogenesis activities of extracts from Leonurus japonicus Houtt. *Biotechnol. Genet. Eng. Rev.*, 1–22. doi:10.1080/02648725.2023.2202544

Zhang, L., Li, H. X., Pan, W. S., Khan, F. U., Qian, C., Qi-Li, F. R., et al. (2019). Novel hepatoprotective role of Leonurine hydrochloride against experimental non-alcoholic steatohepatitis mediated via AMPK/SREBP1 signaling pathway. *Biomed. Pharmacother.* 110, 571–581. doi:10.1016/j.biopha.2018.12.003

Zhang, Q., Sun, Q., Tong, Y., Bi, X., Chen, L., Lu, J., et al. (2022). Leonurine attenuates cisplatin nephrotoxicity by suppressing the NLRP3 inflammasome, mitochondrial dysfunction, and endoplasmic reticulum stress. *Int. Urology Nephrol.* 54 (9), 2275–2284. doi:10.1007/s11255-021-03093-1

Zhao, B., Peng, Q., Poon, E. H. L., Chen, F., Zhou, R., Shang, G., et al. (2021b). Leonurine promotes the osteoblast differentiation of rat BMSCs by activation of autophagy via the PI3K/Akt/mTOR pathway. *Front. Bioeng. Biotechnol.* 9, 615191. doi:10.3389/fbioe.2021.615191

Zhao, H., Xue, S., Meng, Q., and Zhou, C. (2021a). *In vitro* study on the effect of leonurine hydrochloride on the enzyme activity of cytochrome P450 enzymes in human liver microsomes. *Xenobiotica* 51 (9), 977–982. doi:10.1080/00498254.2021.1947544

Zheng, S., Zhuang, T., Tang, Y., Wu, R., Xu, T., Leng, T., et al. (2021). Leonurine protects against ulcerative colitis by alleviating inflammation and modulating intestinal microflora in mouse models. *Exp. Ther. Med.* 22 (5), 1199–1210. doi:10.3892/etm.2021.10633

Zhou, T., Fang, Q., Cai, J., Wu, X., and Lv, X. (2022). Leonurine alleviates alcoholic steatohepatitis through the TLR4/NF-κB signalling pathway. *Rev. Bras. Farmacogn.* 32 (4), 593–607. doi:10.1007/s43450-022-00284-4

Zhou, Y., Li, X., Chen, Y., Zhou, M., Wang, M., Cheng, X., et al. (2023). KCNMA1 promotes obesity-related hypertension: Integrated analysis based on genome-wide association studies. *Tradit. Med. Res.* 8 (10), 58–61. doi:10.1016/j.gendis.2022.04.025

Zhu, Y., Lin, B., Ding, F., Ma, F., Zhou, X., Zong, H., et al. (2021). Leonurine negatively modulates T cells activity by suppressing recombination activation gene protein 2 in pulmonary fibrosis. *Eur. J. Inflamm.* 19, 205873922110359. doi:10.1177/20587392211035907

Zhu, Y., Ouyang, Z., Du, H., Wang, M., Wang, J., Sun, H., et al. (2022). New opportunities and challenges of natural products research: When target identification meets single-cell multiomics. *Acta Pharm. Sin. B* 12, 4011–4039. doi:10.1016/j.apsb.2022.08.022

Zhu, Y. Z., Wu, W., Zhu, Q., and Liu, X. (2018). Discovery of leonuri and therapeutical applications: From bench to bedside. *Pharmacol. Ther.* 188, 26–35. doi:10.1016/j.pharmthera.2018.01.006

Zhuang, Q., Ruan, L., Jin, T., Zheng, X., and Jin, Z. (2021). Anti-leukaemia effects of leonurine *in vitro* and *in vivo*. *General Physiology Biophysics* 40 (5), 397–407. doi:10.4149/gpb_2021018

Zong, F., and Zhao, Y. (2021). Alkaloid leonurine exerts anti-inflammatory effects via modulating MST1 expression in trophoblast cells. *Immun. Inflamm. Dis.* 9 (4), 1439–1446. doi:10.1002/iid3.493

Zou, T., and Lin, Z. (2021). The involvement of ubiquitination machinery in cell cycle regulation and cancer progression. *Int. J. Mol. Sci.* 22 (11), 5754. doi:10.3390/ijms22115754

frontiers | Frontiers in Pharmacology

TYPE Review
PUBLISHED 17 November 2023
DOI 10.3389/fphar.2023.1293130

OPEN ACCESS

EDITED BY
Pranav Kumar Prabhakar,
Lovely Professional University, India

REVIEWED BY
Lixing Feng,
East China Normal University, China
Yujuan Zhan,
Guangzhou University of Chinese Medicine, China
Fujun Dai,
Henan University, China

*CORRESPONDENCE
Shu-Yan Han,
shuyanhan@bjmu.edu.cn
Xiao-Hong Li,
xh@bucm.edu.cn

†These authors have contributed equally to this work and share first authorship

‡These authors have contributed equally to this work

RECEIVED 12 September 2023
ACCEPTED 27 October 2023
PUBLISHED 17 November 2023

CITATION
Zhang J-X, Yuan W-C, Li C-G, Zhang H-Y, Han S-Y and Li X-H (2023), A review on the mechanisms underlying the antitumor effects of natural products by targeting the endoplasmic reticulum stress apoptosis pathway.
Front. Pharmacol. 14:1293130.
doi: 10.3389/fphar.2023.1293130

A review on the mechanisms underlying the antitumor effects of natural products by targeting the endoplasmic reticulum stress apoptosis pathway

Jie-Xiang Zhang[1†], Wei-Chen Yuan[2,3†], Cheng-Gang Li[4], Hai-Yan Zhang[4], Shu-Yan Han[5*‡] and Xiao-Hong Li[4*‡]

[1]The First Clinical College of Shandong University of Traditional Chinese Medicine, Jinan, China, [2]Jiangsu Collaborative Innovation Center of Traditional Chinese Medicine in Prevention and Treatment of Tumor, The First Clinical College of Nanjing University of Chinese Medicine, Nanjing, China, [3]The College of Traditional Chinese Medicine, Shandong University of Traditional Chinese Medicine, Jinan, China, [4]Shandong University of Traditional Chinese Medicine, Jinan, China, [5]Key Laboratory of Carcinogenesis and Translational Research (Ministry of Education), Department of Integration of Chinese and Western Medicine, Peking University Cancer Hospital and Institute, Beijing, China

Cancer poses a substantial risk to human life and wellbeing as a result of its elevated incidence and fatality rates. Endoplasmic reticulum stress (ERS) is an important pathway that regulates cellular homeostasis. When ERS is under- or overexpressed, it activates the protein kinase R (PKR)-like endoplasmic reticulum kinase (PERK)-, inositol-requiring enzyme 1 (IRE1)- and activating transcription Factor 6 (ATF6)-related apoptotic pathways to induce apoptosis. Tumor cells and microenvironment are susceptible to ERS, making the modulation of ERS a potential therapeutic approach for treating tumors. The use of natural products to treat tumors has substantially progressed, with various extracts demonstrating antitumor effects. Nevertheless, there are few reports on the effectiveness of natural products in inducing apoptosis by specifically targeting and regulating the ERS pathway. Further investigation and elaboration of its mechanism of action are still needed. This paper examines the antitumor mechanism of action by which natural products exert antitumor effects from the perspective of ERS regulation to provide a theoretical basis and new research directions for tumor therapy.

KEYWORDS

endoplasmic reticulum stress, natural products, antitumor, apoptosis, review

1 Introduction

Cancer is a large threat to human health, resulting in 19.29 million cancer diagnoses and 9.96 million fatalities across the globe in 2020, with 49.3% of new cases and 58.3% of deaths occurring in Asia, among the highest in the world; in addition, 28.4 million new cancer cases are expected to occur by 2040, a 47% increase from 2020 (Sung et al., 2021). According to a single estimate, China is approximately 4,820,000 individuals diagnosed with cancer and 3,210,000 fatalities due to cancer in 2022 (Xia C. et al., 2022). In addition, according to the U.S. Cancer Database, as of 1 January 2022, there are more than 18 million Americans with a history of cancer (8.3 million males and 9.7 million females) of which the most common cancer for males is prostate cancer (3,523,230) and for females is breast cancer (4,055,770)

(Miller et al., 2022). Hence, tackling this problem and decreasing the occurrence and death rates related to cancer is crucial. The mechanisms and development of cancer are not completely understood. These factors could include smoking, drinking alcohol, genetic predisposition, dietary habits, and nutritional intake. Early cancer detection is rare, and there are limited radical treatment options. Contemporary cancer treatments primarily consist of surgical procedures, radiation therapy, chemotherapy, targeted therapy, and immunotherapy. However, these methods may be accompanied by distinct toxic side effects and adverse reactions, leading to less-than-anticipated outcomes. Therefore, the ability to effectively treat or even eradicate cancer and reduce the accompanying toxic side effects has been a pressing issue. To this end, we have tried various approaches and found that natural products seem to be an effective way.

Natural products are compounds or substances found in living organisms in nature. Natural products are widespread around the world for their suitable antitumor properties, and more than 100 products have demonstrated ideal anticancer effects, mostly from plants and to a lesser extent from ore-based drugs, animals and microorganisms (Fabiani, 2020; Sauter, 2020; Zhou et al., 2022). Natural products have the advantages of stable efficacy, multitargeting and multiple routes of action, as well as a high safety profile due to less irritation to the gastrointestinal tract and less damage to liver and kidney function. Studies have found that many natural products, such as dihydroartemisinin, celastrol, and resveratrol, possess the ability to hinder the spread and growth of tumor cells, promote cancer cell death, improve cancer cell metabolism and regulate oncogenes (Luo et al., 2019; Xiang et al., 2019; Wang et al., 2021). Turmeric extract β-elemene inhibits cancer cell proliferation and promotes apoptosis by regulating vascular endothelial growth factor (VEGF), matrix metalloproteinase, E-cadherin, N-cadherin and vimentin, which are factors related to tumor angiogenesis and metastasis, while enhancing the sensitivity of tumor cells to radiotherapy (Zhai et al., 2019). Amygdalin, which is widely found in the seed kernels of apricot, peach, plum and prune plants, has been demonstrated to trigger the internal mitochondrial apoptotic pathway in HepG2 cells, a type of liver cancer cell, and block cells in the G2/M period to induce apoptosis (El-Desouky et al., 2020). A clinical trial concerning 75 patients with advanced stomach cancer shows that after two cycles of treatment with Javanica oil emulsion injection combined with chemotherapy, the total effective rate of treatment was 85.3%, which indicates its good anti-tumor effect (Liu et al., 2013). Although long-term experiments have been conducted on the antitumor mechanism of action of many natural products, their specific mechanisms of action remain unclear, necessitating additional research.

The endoplasmic reticulum stress (ERS)-induced apoptosis pathway has recently gained increasing recognition in the field of tumor therapy. The endoplasmic reticulum is an essential organelle for synthesizing, folding and modifying proteins in the cell. It is also involved in intracellular material transportation, lipid synthesis and metabolism, and storing Ca^{2+}. Under nonstress conditions, three endoplasmic reticulum proteins, protein kinase R (PKR)-like endoplasmic reticulum kinase (PERK), inositol-requiring enzyme 1 (IRE1) and activating transcription Factor 6 (ATF6), specifically bind to the regulatory protein heavy-chain binding protein/glucose-regulated protein 78 (Bip/GRP78), forming a homeostatic complex and remaining in an inactive state. However, if the cell is altered internally as a result of changes in its environment, the aggregation of unfolded and misfolded proteins and Ca^{2+} homeostasis disruption activate the protective ERS pathway. As a result, PERK, IRE1, and ATF6 separate from the GRP78 protein and activate the unfolded protein response (UPR). The UPR helps return misfolded or unfolded proteins to normal, relieving the endoplasmic reticulum load to maintain cellular homeostasis (Oakes and Papa, 2015; Marciniak et al., 2022). However, under- or overactivation of ERS can induce cell death (Walter and Ron, 2011). Tumor cells substantially differ from normal cells and are often exposed to an ischaemic, hypoxic and nutrient-deficient tumor microenvironment (Chen and Cubillos-Ruiz, 2021; Groenendyk et al., 2021), predisposing them to ERS (Oakes, 2020). Thus, regulating the ERS of tumor cells may be a tumor treatment strategy (Kim and Kim, 2018). There is also growing evidence that the modulation of endoplasmic reticulum pressure sensors or UPR-related factors significantly increases the sensitivity of aggressive tumors to cytotoxic drugs, targeted therapies and immunotherapy (Chen and Cubillos-Ruiz, 2021). The effectiveness of standard chemotherapy and cancer immunotherapy can be improved by implementing targeted ERS responses (Cubillos-Ruiz et al., 2017). However, the mechanism of action of natural products that regulate ERS-related apoptotic pathways still needs to be clarified and requires further integration of various reports and pieces of information. Previous studies have described that natural products and traditional Chinese medicines inhibit tumor progression through ERS (Kim and Kim, 2018; Xia F. et al., 2022), but they involve fewer cancer types and fail to summarize the antitumor mechanism of the ERS-meditated apoptosis pathway fully. In this paper, we searched PubMed to collect as much recent literature as possible on the antitumor effects by which natural products exert through the modulation of ERS apoptotic pathway to describe better the mechanism of ERS-related effects and their relationship with antitumor therapy to provide new research ideas for tumor treatment.

2 The mechanism of apoptosis induced by ERS

PERK, IRE1 and ATF6 bind to the GRP78 protein in a nonactivated state under physiological conditions (Zhao and Ackerman, 2006). ERS triggers the release of PERK, which then phosphorylates its catalytic substrate eukaryotic translation initiation Factor 2 α (eIF2α) through autophosphorylation. Phosphorylated eIF2α can quickly hinder protein synthesis and decrease the burden on the endoplasmic reticulum. Nevertheless, as the stress reaction escalates, excessively stimulated eIF2α stimulates the production of initiating transcription Factor 4 (ATF4), leading to the upregulated expression of the apoptotic signaling molecule C/EBP homologous protein (CHOP)/growth arrest and DNA damage-inducible 153 (GADD153). CHOP can trigger oxidative damage by activating growth arrest and DNA damage protein 34 (GADD34) or suppressing the level of the antiapoptotic protein B-cell lymphoma-2 (Bcl-2), thereby facilitating apoptosis (Boyce and Yuan, 2006; Bobrovnikova-Marjon et al., 2010; Rozpedek et al., 2016).

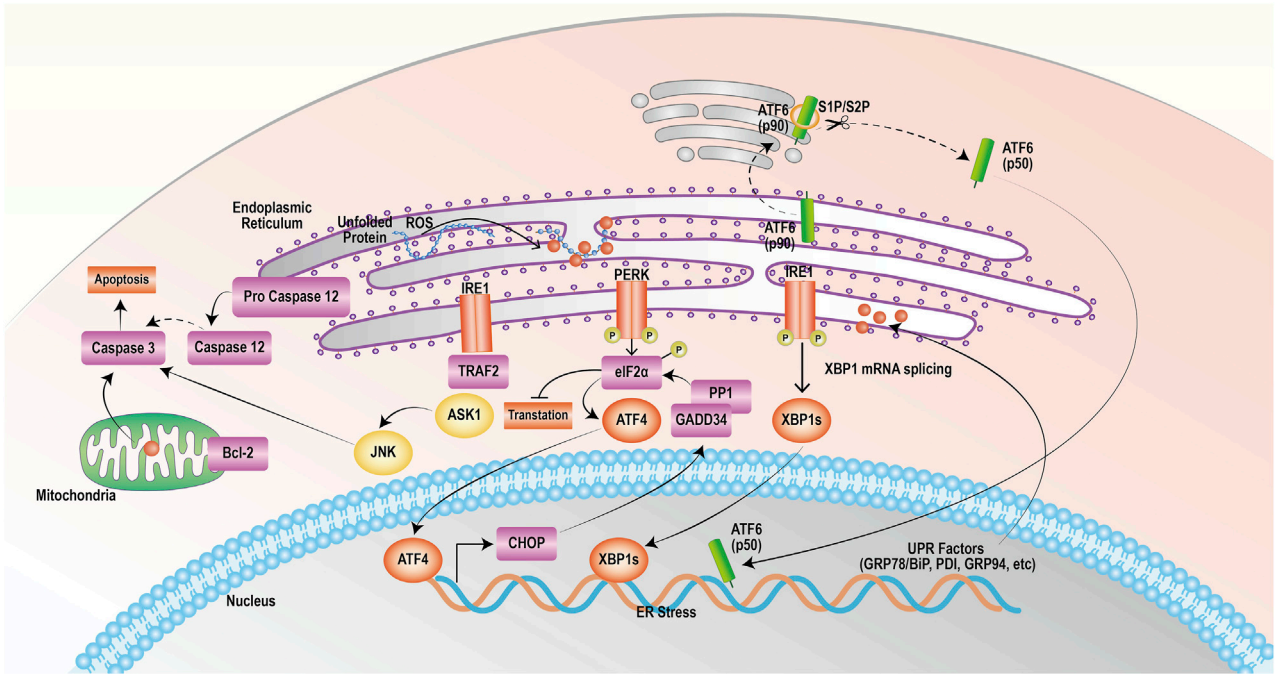

FIGURE 1
Endoplasmic reticulum stress exerts a mechanism that promotes apoptosis. The onset of the unfolded protein response activates endoplasmic reticulum stress, which mediates the PERK, IRE1, and ATF6 pathways that all induce apoptosis.

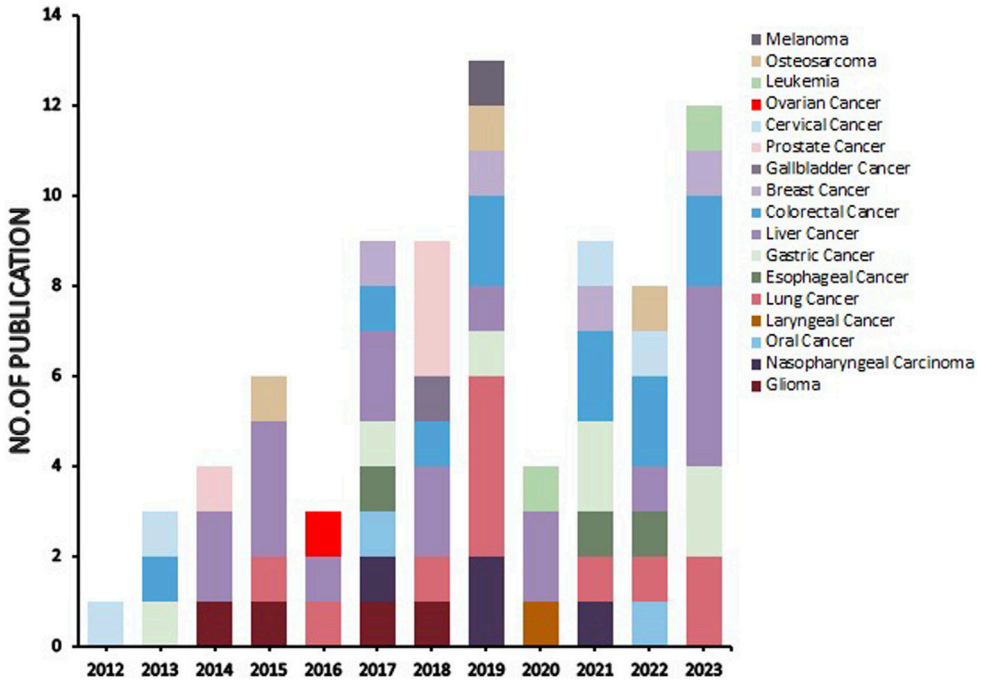

FIGURE 2
Literature on studies related to natural products targeting endoplasmic reticulum stress for antitumor effects (stacked diagram). The period is set from 1 January 2012 to 20 July 2023. As can be seen from the graph, there is an upward trend in its research heat.

TABLE 1 Mechanism of action of natural products targeting ERS to promote apoptosis in tumor cells and structural formulae of some natural products.

Natural products	Source	Types of natural products	Types of cancer	Cellular/animal models	Mechanism of action of ERS	References
Fatsioside A	Fatsia japonica	Triterpene glycoside	Glioma	U87MG cells	PERK, eIF2α, CHOP↑, cleavage of caspase-4	Pan et al. (2015)
Sinomenine Hydrochloride 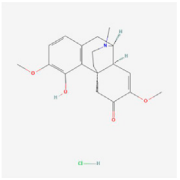	Sinomenium acutum	Morphinans	Glioblastoma	U87 and SF767 cells	Ca2+, GRP78, PERK, IRE1 and CHOP↑	Jiang et al. (2018)
Bufalin 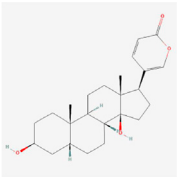	Bufonis Venenum	Glycosides	Glioma	U87MG and LN229 cells	CHOP, ATF6, GRP78 ↑, p-PERK and p-eIF2α↑, cleavage of caspase-4	Shen et al. (2014)
Isochaihulactone (K8) 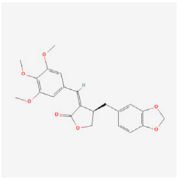	Bupleurum scorzonerifolium Willd.	Benzodioxoles	Glioblastoma multiform	GBM cells /xenograft mice	DDIT3, nag1↑	Tsai et al. (2017b)
Guangsangon E	Leaves of Morus alba L	Diels-Alder adduct	Nasopharyngeal Cancer	CNE1 cells	GRP78, IRE1α, ATF4 and ROS↑	Shu et al. (2021)
Gambogenic acid 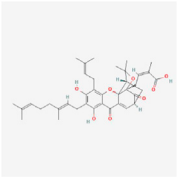	Gamboge	Flavonoid	Nasopharyngeal Cancer	CNE-2Z cells	CHOP, ATF4↑	Su et al. (2019)
PP-22	P.polyphylla var. yunnanensis	Monomers	Nasopharyngeal Cancer	CNE-2 cells	PERK↑, phosphorylation and upregulation of CHOP, BIP, PDI, EROL-LA and IRE-LA	Tan et al. (2019)

(Continued on following page)

10.3389/fphar.2023.1293130

TABLE 1 (*Continued*) Mechanism of action of natural products targeting ERS to promote apoptosis in tumor cells and structural formulae of some natural products.

Natural products	Source	Types of natural products	Types of cancer	Cellular/animal models	Mechanism of action of ERS	References
Tetrandrine 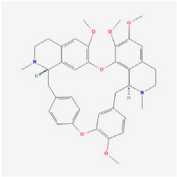	Stephania tetrandra	Alkaloids	Nasopharyngeal Cancer	NPC-TW 039 cells	ROS, Ca2+, GADD153 and GRP78↑	Liu et al. (2017a)
Glaucocalyxin A 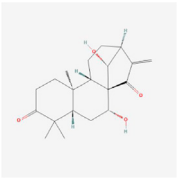	Rabdosia japonica	Terpenoids	Human oral squamous cell cancer	SCC25 and CAL27 cells	PERK-ATF4-CHOP pathway, CHAC1, ROS↑	Wang et al. (2022)
Arsenic-Trioxide (As2O3) 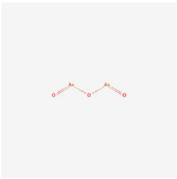	Arsenic-Trioxide	Arsenicals	Oral cancer	Oral cancer cells	GRP78, calpain 1/2 and caspase-3/9/12↑	Tsai et al. (2017a)
Oridonin 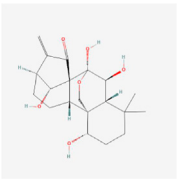	Rabdosia rubescens	Terpenes	Throat cancer	LSCC cells	ROS, CHOP and GRP78↑	Kang et al. (2020)
Guangsangon E	Leaves of Morus alba L	Diels-Alder adduct	Lung Cancer	A549 cells /female Balb/c nude mice	GRP78, IRE1α, ATF4 and ROS↑	Shu et al. (2021)
Fucoidan 	Brown seaweed	Polysaccharide	Lung Cancer	A549 and H1975 cells	GRP78 and its mediated caspase-3/PARP apoptosis pathway↑	Hsu et al. (2018)

(Continued on following page)

10.3389/fphar.2023.1293130

TABLE 1 (*Continued*) Mechanism of action of natural products targeting ERS to promote apoptosis in tumor cells and structural formulae of some natural products.

Natural products	Source	Types of natural products	Types of cancer	Cellular/animal models	Mechanism of action of ERS	References
Lathyrol 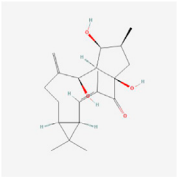	Semen Euphorbiae	Terpenes	Lung Cancer	A549, H460 cells and H460 cells were established as a subcutaneous lung cancer model in BALB/c nude mice	SERCA2↓,Ca2+ and GRP78↑, PERK-eIF2α-ATF4-CHOP signal pathway↑	Chen et al. (2023)
Dendrobium denneanum	*Dendrobium denneanum Kerr*	Ether	Lung Cancer	A549 cells	disturbed the metabolic process of proteins and other substances, ERS↓	Zhang et al. (2019)
Kushenol Z	Sophora flavescens	Alcohols	Lung Cancer	A549 and NCI-H226 cells	CHOP, caspase-7/12↑	Chen et al. (2019)
Glycyrrhetinic acid 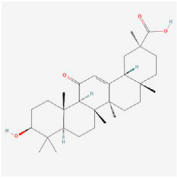	Liquorice	Terpenes	Lung Cancer	A549 and NCI-H460 cells	Bip, PERK and ERP72↑	Zhu et al. (2015)
Arisema heterophyllum Blume	Rhizoma Arisaematis	Agglutinin	Lung Cancer	A549 cells	p-eIF2α, CHOP, IRE1α and p-JNK↑	Feng et al. (2016)
Ginsenosides 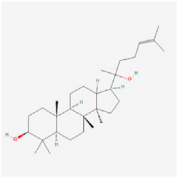	Ginseng (Panax ginseng C. A. Mey)	Glycosides	Lung Cancer	A549 cells	ATF4, CHOP, BIP↑, AKT-1 and p70 S6 kinase↓, ATG7↑	Zhao et al. (2019)
Evodiamine 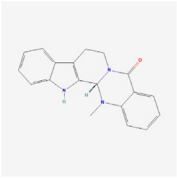	Evodia rutaecarpa (Juss.)	Quinazolines	Lung Cancer	Lewis lung cancer tumor-bearing mouse model/A549 and LLC cells	TRAF2, ASK1, p-JNK, caspase-12/9/3 and Bax↑,Bcl-2 ↓, mRNA expression of Grp78 and Ire1↑	Li et al. (2022b)
Flavonoid components in Astragali Radix	Astragali Radix	Flavonoid	Lung Cancer	Lewis lung cancer model in C57BL/6 mice	XBP1, IRE1 and GRP78↓, CHOP↑	Yang et al. (2019)
Marsdenia tenacissima extract	*Marsdenia tenacissima*	-	Lung Cancer	PC-9 and H1975 cells	ATF6, GRP-78, ATF4, xbp1, CHOP and ROS↑	Yuan et al. (2023a)

(Continued on following page)

10.3389/fphar.2023.1293130

TABLE 1 (*Continued*) Mechanism of action of natural products targeting ERS to promote apoptosis in tumor cells and structural formulae of some natural products.

Natural products	Source	Types of natural products	Types of cancer	Cellular/animal models	Mechanism of action of ERS	References
Corilagin 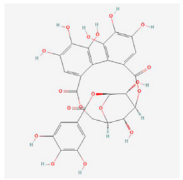	Phmllanthi Fructus	Phenol	Oesophagal cancer	ECA109 cells and KYSE150 cells	GRP78, ERS-induced cellular homeostasis↓, caspase-12/7 apoptotic signal pathways↑	Wu et al. (2021)
Daurisoline 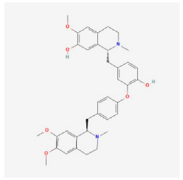	Menispermi	Alkaloids	oesophagal squamous cell carcinoma	EC1 and ECA109 cells	ROS and PERK-peIF2α-ATF4 signal pathway↑	Yuan et al. (2022b)
Tanshinone IIA 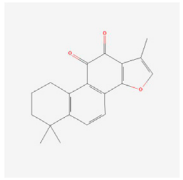	Salvia miltiorrhiza Bunge	Terpenes	Oesophagal cancer	Eca-109 cells	CHOP pathway↑	Zhang et al. (2017)
Betulinic Acid 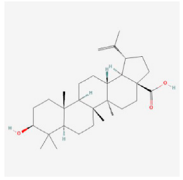	Birch bark	Terpenes	Breast cancer	MDA-MB-231 and BT-549 cells	GRP78↑, block GRP78 binding to PERK pathway, β-catenin/c-Myc pathway and glycolysis ↓	Zheng et al. (2019)
Dihydrotanshinone I 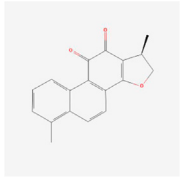	Salvia miltiorrhiza Bunge	Quinones	Breast cancer	MDA-MB-231 cells	ERp57↑, PERK-eIF2α-ATF4 apoptotic pathway↑	Shi et al. (2021)

(Continued on following page)

10.3389/fphar.2023.1293130

TABLE 1 (*Continued*) Mechanism of action of natural products targeting ERS to promote apoptosis in tumor cells and structural formulae of some natural products.

Natural products	Source	Types of natural products	Types of cancer	Cellular/animal models	Mechanism of action of ERS	References
Matrine 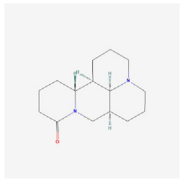	Sophora f lavescens	Alkaloids	Breast cancer	ER-7-positive MCF-7 cells	GRP78, eIF2α and CHOP↑	Xiao et al. (2017)
Peimine 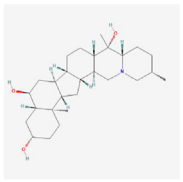	Fritillaria	Alkaloids	Breast cancer	MCF-7 cells	PERK, eIF2α and CHOP↓, ERS and NLRP3 inflammatory vesicles↓	Sun et al. (2023)
Schizandrin A 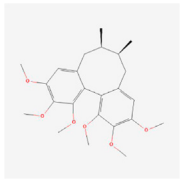	Fructus Schisandra	Benzene Derivatives	Stomach Cancer	AGS cells	GRP78, eIF2α, PERK and CHOP↑	Pu et al. (2021)
Curcumin 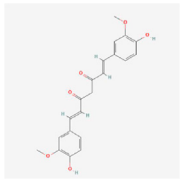	Rhizomes of Curcuma longa	Curdione	Stomach Cancer	AGS cells	CHOP and JNK pathways↑	Cao et al. (2013)
Wogonoside 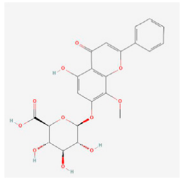	Scutellaria baicalensis	Sugar Acids	Stomach Cancer	AGS and MKN - 45 cells	GRP78, GRP94, IRE1α pathway, TRAF2, ASK1, JNK signaling pathway↑, Bax↑, Bcl-2↓	Gu et al. (2021)

(Continued on following page)

10.3389/fphar.2023.1293130

TABLE 1 (*Continued*) Mechanism of action of natural products targeting ERS to promote apoptosis in tumor cells and structural formulae of some natural products.

Natural products	Source	Types of natural products	Types of cancer	Cellular/animal models	Mechanism of action of ERS	References
Myristicin 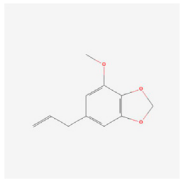	Myristica fragrans	Benzene Derivatives	Stomach Cancer	AGS and MKN - 45 cells	GRP78, phosphorylated IRE1α, PERK and ATF6↑, caspase-12↑	Song et al. (2023)
Isoquercitrin 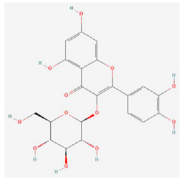	Hypericum perforatum L	Flavonols	Stomach Cancer	AGS and HGC-27 cells	p-PERK, p-eIF2α, GRP78 and CHOP↑, BCL-2↓, BAX↑, cleaved caspase-3/12↑	Liu et al. (2023)
KangFuXin	Periplaneta americana	Alcohols	Stomach Cancer	SGC-7901 cells	GRP78, CHOP and caspase-12↑	Chen et al. (2017)
The ethanolic extract of C. cicadae	Cordyceps cicadae	Ethanolic	Stomach Cancer	SGC-7901 cells	Ca2+, calpain-1, caspase-12/9↑	Xie et al. (2019)
Cytisine 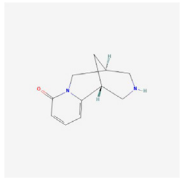	Sophora Alopecuraides L.	Alkaloids	Liver cancer	HepG2 cells	Ca2+, CHOP/GADD153, JNK and caspase-4↑	Yu et al. (2018)
Gecko polypeptide mixture	Gekko japonicus	polypeptide	Liver cancer	HepG2 cells	GRP78, ROS, PERK, ATF4, DDIT3, CHOP, PARP and caspase-3↑	Duan et al. (2018)
Muscone 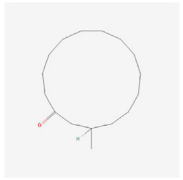	Musk	Cycloparaffins	Liver cancer	HepG2 cells	TRIB3, PERK, eIF2α, ATF4, DDIT3, caspase-3 and Bax ↑, Bcl-2↓	Qi et al. (2020)

(Continued on following page)

10.3389/fphar.2023.1293130

TABLE 1 (*Continued*) Mechanism of action of natural products targeting ERS to promote apoptosis in tumor cells and structural formulae of some natural products.

Natural products	Source	Types of natural products	Types of cancer	Cellular/animal models	Mechanism of action of ERS	References
Alisol B 23-acetate 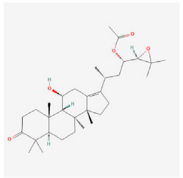	Alisma orientalis (Sam.) Juzep.	Steroids	Liver cancer	HepG2 cells	BIP, CHOP and intracellular Ca2+ ↑	Xu et al. (2015)
Realgar quantum dots	Realgar (As4S4)	-	Liver cancer	HepG2 cells	mRNA of Chop10 and GRP78↑	Qin et al. (2015)
Cryptomeridiol 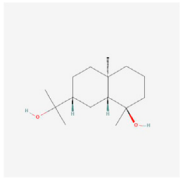	Magnolia Officinalis	Naphthalenes	Liver cancer	HepG2 cells /subcutaneous HepG2 xenografts in male BALB/c nude mice	IRE1α, ASK1, Bip, CHOP, Bkh126, JNK and p38↑	Li et al. (2022a)
Bufalin 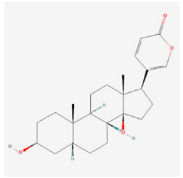	Bufonis Venenum	Glycosides	Liver cancer	HepG2 and Huh7 cells	IRE1-JNK pathway↑	Hu et al. (2014)
Bufalin 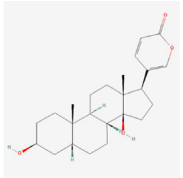	Bufonis Venenum	Glycosides	Liver cancer	HepG2 and Huh7 cells	eIF2α, CHOP and IRE1↑, p-Akt↓	Zhai et al. (2015)
Celastrol 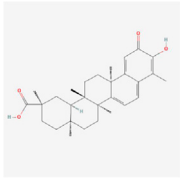	Tripterygium wilfordii and Celastrus regelii	Terpenes	Liver cancer	HepG2, Bel7402 cells /H22 tumor-bearing mice	GRP78/BiP, ATF4, CHOP, IRE1α and XBP1s↑	Ren et al. (2017)

(Continued on following page)

10.3389/fphar.2023.1293130

TABLE 1 (*Continued*) Mechanism of action of natural products targeting ERS to promote apoptosis in tumor cells and structural formulae of some natural products.

Natural products	Source	Types of natural products	Types of cancer	Cellular/animal models	Mechanism of action of ERS	References
Konjac glucomannan	Amorphophallus konjac K. Koch	Polysaccharide	Liver cancer	HepG2 and Bel-7402 cells	TLR4↓, PERK/ATF4/CHOP signaling pathway↑	Shi et al. (2022)
5,2',4'-trihydroxy-6,7,5'-trimethoxyflavone-nps	Sorbaria sorbifolia	Flavonoid	Liver cancer	HepG2, Hep3B, and PLC/PRF/5 cells	GRP78, PERK, IRE1α, ATF6 pathways, CHOP and caspase4 ↑	Xiao et al. (2016)
Fisetin 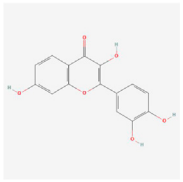	Traditional medicines, plants, vegetables, and fruits	Flavonols	Liver cancer	HepG2, Hep3B and Huh7 cells /HepG2 xenograft mouse models	Ca2+, CHOP, p-eIF2α, p-PERK, cleaved caspase-3, ATF4 and induction of GRP78 exosomes↑	Kim (2023)
Aqueous extract of *polygonum bistorta*	*Polygonum bistorta*	-	Liver cancer	Hep3B cells	ROS, DAPK3, caspase 8/9/3 and PARP 1 activity↑	Liu et al. (2017b)
Astragalus Polysaccharide 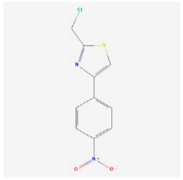	Astragalus membranaceus	Polysaccharide	Liver cancer	Hep3B cells	PERK/eIF2α/CHOP signaling pathway, caspase-3, Bax and Bim↑	Li et al. (2023)
Caudatin 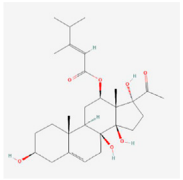	The roots of Cynanchum bungei Decne	Glycosides	Liver cancer	Diethylnitrosamine-induced hepatocellular carcinoma in a rat model	ATF6 and PERK-eIF2α-ATF4 pathways↓	Song et al. (2020)
Psoralen 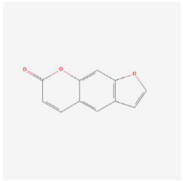	Psoralea corylifolia (L.)	Pyrans	Liver cancer	SMMC7721 cells	GRP78, GRP94, IRE1 and ATF6 pathways, DDIT3↑, caused endoplasmic reticulum Ca2+ disruption and Bcl-2↓	Wang et al. (2019)

(Continued on following page)

10.3389/fphar.2023.1293130

TABLE 1 (*Continued*) Mechanism of action of natural products targeting ERS to promote apoptosis in tumor cells and structural formulae of some natural products.

Natural products	Source	Types of natural products	Types of cancer	Cellular/animal models	Mechanism of action of ERS	References
Baicalein 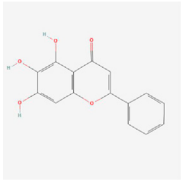	Scutellaria baicalensis Georgi	Flavonoid	Liver cancer	SMMC-7721 and Bel-7402 cells	PERK, IRE1 pathway, BiP, eIF2α and CHOP↑, Bcl-2, Bcl-xL and Mcl-1↓, caspase-9/3↑ and PARP↓	Wang et al. (2014)
Notopterol 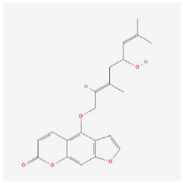	Notopterygium incisum	Pyrans	Liver cancer	HepJ5, Mahlavu cell line and female BALB/c nude mice	cancer stemness↓, PERK, CHOP and oxidative stress↑	Huang et al. (2023)
Lupeol 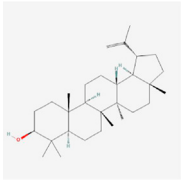	Edible fruits and vegetables	Terpenes	Colorectal cancer	LoVo Cells	eIF2α and caspase-3 phosphorylation↑	Chen et al. (2018)
Oridonin 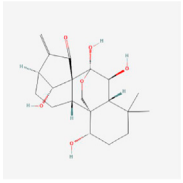	Rabdosia rubescens	Terpenes	Colorectal cancer	LoVo and RKO cells	TCF4↓, TP53, ATF4 and CHOP↑	Zhou et al. (2023)
Curcumin 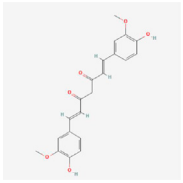	Rhizomes of Curcuma longa	Curdione	Colorectal cancer	LoVo and HT-29 cells	ROS, BIP, PDI and CHOP↑	Huang et al. (2017)

(Continued on following page)

10.3389/fphar.2023.1293130

TABLE 1 (*Continued*) Mechanism of action of natural products targeting ERS to promote apoptosis in tumor cells and structural formulae of some natural products.

Natural products	Source	Types of natural products	Types of cancer	Cellular/animal models	Mechanism of action of ERS	References
Curcumin 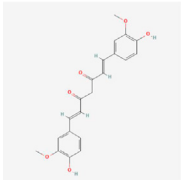	Rhizomes of Curcuma longa	Curdione	Colorectal cancer	HT-29 cells	CHOP and JNK pathways↑	Cao et al. (2013)
Osthole 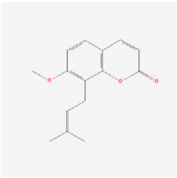	Cnidium monnieri	Pyrans	Colorectal cancer	HT-29 cells	GRP78, PERK, eIF2α and CHOP↑	Zhou et al. (2021)
Artemisianins A	Artemisia argyi	Sesquiterpenoid dimers	Colorectal cancer	HT-29 cells	IRE1α, XBP1s, ATF6 ,CHOP, p-PERK and p-eIF2α↑, and disrupted intracellular Ca2+ homeostasis	Xue et al. (2019)
Palmitic acid 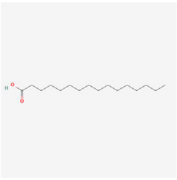	Palm oil and some animal products	Monounsaturated fatty acid	Colorectal cancer	HT-29 and HCT-116 cells	p-PERK, p-eIF2α, ATF4, Ca2+↑	Kuang et al. (2023)
A Purified Resin Glycoside Fraction	Pharbitidis Semen	Resin glycoside	Colorectal cancer	HT-29 and HCT-116 cells	BIP/GRP78, CHOP, IRE1α, XBP1s and ubiquitinated protein expression↑, proteasome-dependent degradation↓, MAPK signaling pathway↑, JNKs and ERKs↑	Zhu et al. (2019)
Periplogenin 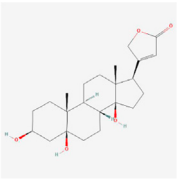	Periplocae	Glycosides	Colorectal cancer	HCT-116 cells	ROS, BIP, p-eIF2α, CHOP, IRE1α, p-JNK↑, p-ASK1↓, Bax↑, cleavage of caspase-3 and PARP↑, Bcl-2↓	Yang et al. (2021)

(Continued on following page)

10.3389/fphar.2023.1293130

TABLE 1 (*Continued*) Mechanism of action of natural products targeting ERS to promote apoptosis in tumor cells and structural formulae of some natural products.

Natural products	Source	Types of natural products	Types of cancer	Cellular/animal models	Mechanism of action of ERS	References
Shikonin 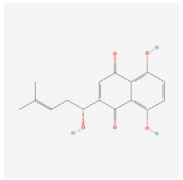	Lithospermum erythrorhizon	Quinones	Colorectal cancer	HCT-116 and HCT-15 cells /BALB/c nude mice	BiP, PERK/elF2α/ATF4/CHOP and IRE1α/JNK signaling pathways↑, Bcl-2 ↓, caspase-3/9↑	Qi et al. (2022)
Artesunate 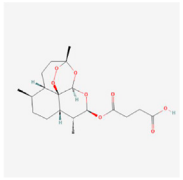	Artemisinin	Terpenes	Colorectal cancer	HCT-116, SW480 cells /BALB/c mice grown on CT-26 cells	BIP, IRE1 and p-IRE1α-CHOP-DR5 signaling pathway↑	Huang et al. (2022)
Ginsenoside Rg3 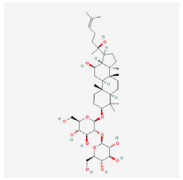	Ginseng	Glycosides	Gallbladder cancer	GBC-SD cells/ transplanted tumor-bearing mice	PERK, eIF2α, ATF4, CHOP, Lipocalin 2, ROS, lincRNA-p21↑	Wu et al. (2018)
Matrine 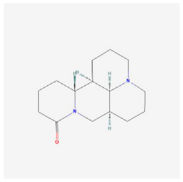	Sophora f lavescens	Alkaloids	Prostate cancer	DU145, PC-3 cells / DU145 cell xenografts in mice	Bip, PERK, eIF2α, ATF4, CHOP and Bax↑, Bcl-2↓	Chang et al. (2018)
Astragaloside 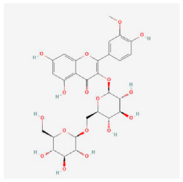	Astragalus membranaceus	Flavonoid	Prostate cancer	DU145 cells	BiP, IRE1, p-PERK, AFT6, AFT4, CHOP and caspase-12-related apoptotic pathways↑	Tan et al. (2018)

(Continued on following page)

10.3389/fphar.2023.1293130

TABLE 1 (*Continued*) Mechanism of action of natural products targeting ERS to promote apoptosis in tumor cells and structural formulae of some natural products.

Natural products	Source	Types of natural products	Types of cancer	Cellular/animal models	Mechanism of action of ERS	References
Isobavachalcone 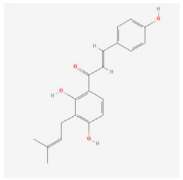	Psoralea corylifolia Linn.	Flavonoid	Prostate cancer	PC-3 cells	XBP-1, ATF4, GRP78, Chop and p-eIF2α proteins↑, TrxR1 protein↓, ROS ↑, and produced oxidative stress	Li et al. (2018)
Quercetin 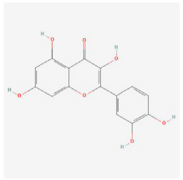	Many plants are found in stems, flowers, leaves, buds, seeds, fruits	Flavonols	Prostate cancer	PC-3 cells	Facilitate the transport of AIF protein released from mitochondria to the nucleus, ATF, GRP78 and GADD153↑	Liu et al. (2014)
Tanshinone IIA 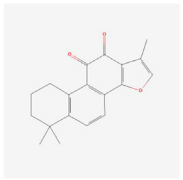	Salvia miltiorrhiza Bunge	Terpenes	Cervical cancer	CaSki cells	ROS, PERK, IRE1, eIF2α, ATF4 and CHOP levels ↑, led to PARP degradation, p38 and ASK signaling pathway↑	Pan et al. (2013)
Saikosaponin-A 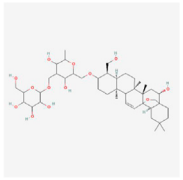	Bupleurum falcatum	Triterpenoids	Cervical cancer	HeLa cells /nude mice	GRP78, CHOP and caspase12↑	Du et al. (2021)
Celastrol 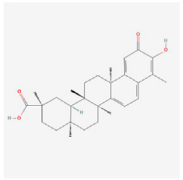	Tripterygium wilfordii and Celastrus regelii	Terpenes	Cervical cancer	HeLa cells	Bip, PERK and IRE1↑, and caused cytoplasmic vacuolization	Wang et al. (2012)

(Continued on following page)

10.3389/fphar.2023.1293130

TABLE 1 (*Continued*) Mechanism of action of natural products targeting ERS to promote apoptosis in tumor cells and structural formulae of some natural products.

Natural products	Source	Types of natural products	Types of cancer	Cellular/animal models	Mechanism of action of ERS	References
20(S)-Ginsenoside Rh2 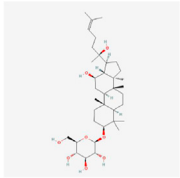	CelastrolGinseng	Glycosides	Cervical cancer	HeLa cells	ATF4, DDIT3, JUN, FOS, BBC3 and PMAIP1↑, DDIT3 heterodimer↓	Liu et al. (2022)
Myricetin 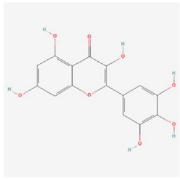	Walnuts, vegetables and fruits	Flavonoid	Ovarian cancer	SKOV3 cells	GRP78 and CHOP ↑	Xu et al. (2016)
Asperuloside 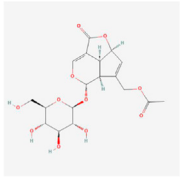	Herba Paederiae	Glycosides	Leukemia	U937 and HL-60 cells /primary leukemia cells (AML); tumor model for U937 cells xenograft in nude mice	GRP78, PERK, eIF2α, CHOP, p-IRE1, XBP1, ATF6 and cleaved caspase-12↑	Rong et al. (2020)
Shikonin 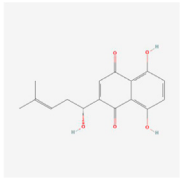	Lithospermum erythrorhizo	Quinones	Leukemia	ATLL cells	ROS, p-eIF2α, ATF4, XBP-1, p-JNK, and CHOP↑	Boonnate et al. (2023)
Polyphyllin I	Paris polyphylla Smith var.yunnanensis (Franch.) Hand.-Mazz	Glycosides	Osteosarcoma	MG-63, Saos-2 and U2OS cells	BiP, PERK-eIF2α-ATF4-GADD153 (CHOP) pathway↑, Bcl-2 and Bcl-xL↓, Bax and Bak↑, caspase-3 and PARP ↑	Chang et al. (2015)

(Continued on following page)

10.3389/fphar.2023.1293130

TABLE 1 (*Continued*) Mechanism of action of natural products targeting ERS to promote apoptosis in tumor cells and structural formulae of some natural products.

Natural products	Source	Types of natural products	Types of cancer	Cellular/animal models	Mechanism of action of ERS	References
(3R)-5,6,7-trihydroxy-3-isopropyl-3-methylisochroman-1-one 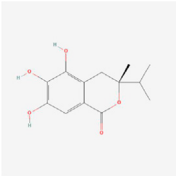	Selaginella moellendorffii Hieron.	Antioxidants	Osteosarcoma	U2OS cells and mice	IRE1, ATF6 and GRP78↑	Song et al. (2019)
Psoralen 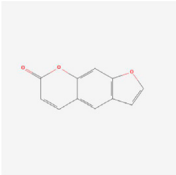	Psoralea corylifolia Linn. (Leguminosae)	Pyrans	Osteosarcoma	MG-63 and U2OS cells	GRP78, DDIT3, GADD34, EDEM1, GDF15 and S1P mRNA, CHOP, IRE1, XBP-1s, GRP78, PERK and ATF-6 ↑	Li and Tu (2022)
Shikonin 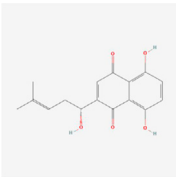	Lithospermum erythrorhizon	Quinones	Melanoma	A375 cells	ROS, p-eIF2α, CHOP and caspase-3↑	Liu et al. (2019)

10.3389/fphar.2023.1293130

Activation of IRE1 induces its phosphorylation and the formation of dimeric IRE1α, which leads to apoptosis through three pathways. First, IRE1α exhibits nucleic acid endonuclease activity, causing cleavage and maturation of X-box binding protein 1 (XBP1) mRNA and upregulating CHOP transcriptional expression, thereby promoting apoptosis (Li et al., 2019; Jaud et al., 2020). Second, IRE1 interacts with TNF receptor-associated Factor 2 (TRAF2) and recruits apoptosis signal-regulating kinase 1 (ASK1), composing the IRE1-TRAF2-ASK1 complex and activating c-Jun N-terminal kinase (JNK) to induce the JNK apoptotic pathway (Urano et al., 2000a; Urano et al., 2000b). Finally, IRE1 activates caspase-12 by binding to TRAF2, initiating the caspase cascade reaction and inducing apoptosis. ATF6 is dissociated from the GRP78 protein and transferred to the Golgi apparatus, which becomes active through the cleavage of Golgi proteases S1P and S2P; activated ATF6 promotes CHOP transcription and expression, which inhibits Bcl-2 and leads to apoptosis (Wang et al., 2000; Chen et al., 2022). The mechanism of action of targeting ERS to promote apoptosis in tumor cells is shown in Figure 1.

3 Application of natural products in inducing apoptosis in tumor cells

Natural products can target ERS to exert apoptotic effects on tumor cells and have inhibitory effects on various cancers listed below. Figure 2 is demonstrated. A total of 69 natural products promoting apoptosis in tumor cells through the ERS pathway were collected, of which 51 could be searched for structural formulae from Pubchem. The mechanisms of action and structural formulae of the natural products are shown in Table 1.

4 Natural products target ERS-mediated apoptosis in Neuroglioma

Fatsioside A at 80 nM induced ERS in malignant glioma U87MG cells, causing apoptosis by enhancing the phosphorylation of PERK and eIF2α, upregulating CHOP protein level and promoting caspase-4 cleavage (Pan et al., 2015). The application of sinomenine hydrochloride at concentrations of 0.125 and 0.25 mM to human glioblastoma U87 and SF767 cells, respectively, led to a rise in the cytoplasmic levels of free Ca^{2+} and upregulated the expression of GRP78, PERK, IRE1, and CHOP; additionally, it suppressed the mesenchymal markers vimentin, Snail, and Slug, indicating that sinomenine hydrochloride reduces the invasive capacity of tumor cells by activating ERS and reversing epithelial-mesenchymal transition (EMT) (Jiang et al., 2018). In glioma U87MG cells and LN229 cells, bufalin triggered apoptosis via the mitochondrial and ERS pathways, and the mechanisms of ERS-mediated apoptosis included the upregulation of CHOP, ATF6 and GRP78, enhanced phosphorylation of PERK and eIF2α, and cleavage of caspase-4; bufalin also played a cytoprotective role through initiating the AMP-activated protein kinase (AMPK)/mammalian target of rapamycin (mTOR) pathway and PERK/eIF2α/CHOP pathway, forming acidic vesicular organelles, increasing autophagic lysosomes and accumulating LC3-II to induce cellular autophagy and thereby alleviating ERS, which suggested that ERS preceded bufalin-induced autophagy, that inhibition of autophagy strengthened its proapoptotic effect and that ERS could be engaged in apoptosis and autophagy simultaneously (Shen et al., 2014). In glioblastoma multiforme (GBM) cell lines and xenograft mouse models, isochaihulactone (K8) directly induced DNA damage inducible transcript 3 (DDIT3) activation and increased nonsteroidal anti-inflammatory drug-activated gene 1 expression, which was not dependent on GRP78 and PERK expression, and activated the caspase signaling pathway to upregulate caspase 3 expression, thereby disrupting endoplasmic reticulum homeostasis in GBM cell lines and inducing G2/M period cell cycle arrest and apoptosis (Tsai S. F. et al., 2017). In summary, the mechanism by which fatsioside A, sinomenine hydrochloride, and bufalin induce apoptosis in glioma cells is predominantly the PERK pathway, with U87MG cells being the primary cell line studied.

5 Natural products target ERS-mediated apoptosis in nasopharyngeal cancer

Guangsangon E at a concentration of 20 μM enhanced the expression of GRP78, IRE1α and ATF4 and reactive oxygen species (ROS) in the CNE1 human nasopharyngeal carcinoma cell line, activated the ERS pathway, along with boosted the level of cleaved caspase-3 and autophagy-related protein 5 (Atg5), thereby inducing apoptosis, and similar results were obtained *in vivo* using female BALB/c nude mice as a model (Shu et al., 2021). Gambogenic acid opened chloride channels and activated VSOR Cl^- channels, leading to the efflux of VSOR Cl^- currents, a decrease in the levels of ERS-related protein GRP78 and an increase in CHOP and ATF4 expression levels; the primary mechanism behind these processes was the overexpression of CHOP, which repressed the anti-apoptotic impact of the UPR and triggered apoptosis in the CNE-2Z cell line of nasopharyngeal carcinoma (Su et al., 2019). PP-22 triggered apoptosis by activating the ERS sensor PERK, which upregulated CHOP protein expression and upregulated BIP, protein disulfide isomerase (PDI), EROL-LA, and IRE-LA levels; additionally, PP-22 promoted apoptosis through the mitochondrial signaling apoptosis pathway, inhibited the extracellular regulated protein kinases (ERK) pathway, activated the p38-mitogen-activated protein kinase (MAPK) signaling pathway and downregulated the signal transducer and activator of transcription 3 pathway to trigger apoptosis in nasopharyngeal cancer CNE-2 cells; interestingly, PP-22 hindered apoptosis by promoting autophagy through ERK pathway inhibition (Tan et al., 2019). In nasopharyngeal cancer NPC-TW 039 cells, a concentration of 8 μM tetrandrine hindered cell viability and rendered G0/G1 period cell cycle arrest; it also induced apoptosis through a pathway involving calcium-mediated ERS and caspase, the mechanism of which was mainly due to the production of ROS and Ca^{2+} caused by powdered antibiotics, leading to intracytoplasmic Ca^{2+} release, ERS promotion, and enhanced expression levels of relevant proteins such as GADD153 and GRP78 (Liu K. C. et al., 2017). In summary, the mechanisms by which guangsangon E, gambogenic acid, PP-22, and tetrandrine induce apoptosis in nasopharyngeal cancer cells are predominantly

the PERK and IRE1 pathways, with CNE cells being the primary cell line studied.

6 Natural products target ERS-mediated apoptosis in oral cancer

Glaucocalyxin A, at concentrations of 4 and 8 μM, activated the ERS-mediated PERK pathway in human oral squamous cell carcinoma SCC25 and CAL27 cells, promoted the ATF4-CHOP pathway and its downstream signal cation transport regulator-like protein 1 (CHAC1) expression, and increased ROS accumulation through degradation of glutathione, thereby promoting oxidative stress and inducing apoptosis (Wang et al., 2022). Arsenic-Trioxide at 0.5 μM in combination with 20 μM dithiothreitol caused apoptosis in oral cancer cells by the mechanism that arsenic-Trioxide in combination with dithiothreitol upregulated cytochrome c (Cyt C), BCL2-associated X (Bax) and Bak and decreased Bcl-2 and p53 levels, resulting in the loss of mitochondrial membrane potential (MMP), generated ROS-induced DNA strand breaks, and triggered apoptosis through the mitochondrial apoptotic pathway; additionally, it also caused ERS, increased GRP78, calpain 1 and calpain 2 levels and increased expression levels of the cysteine proteases caspase-3, -9 and -12 (Tsai C. W. et al., 2017). In summary, glaucocalyxin A and arsenic trioxide promoted apoptosis in oral cancer cells by modulating ERS.

7 Natural products target ERS-mediated apoptosis in throat cancer

Oridonin combined with cetuximab suppressed the proliferation of laryngeal squamous cell carcinoma (LSCC) cells with high expression of epidermal growth factor receptor (EGFR) through the phosphatidylinositol 3-kinase (PI3K)/protein kinase B (Akt) and Janus kinase/signal transducer and activator of transcription (STAT) pathway-regulated nuclear factor kappa-B (NF-κB) pathways while downregulating MMP and Bcl-2 expression, increasing Bax, caspase 9 cleavage and Cyt C levels, and triggering mitochondria-dependent apoptosis, while oridonin induced ROS production and upregulation of CHOP and GRP78 to trigger the ERS apoptotic pathway (Kang et al., 2020). It was evident that oridonin caused the death of laryngeal cancer cells by stimulating ERS.

8 Natural products target ERS-mediated apoptosis in lung cancer

Guangsangon E triggered apoptosis in non-small cell lung cancer (NSCLC) A549 cells through the ERS pathway, a finding also confirmed by *in vivo* experiments, and the mechanism of action was consistent with the anti-nasopharyngeal carcinoma pathway described above (Shu et al., 2021). Fucoidan promoted tunicamycin expression and activated the ERS pathway in lung cancer A549 and H1975 cells, which promoted apoptosis by upregulating the GRP78 protein and its mediated caspase-3/poly ADP-ribose polymerase (PARP) apoptotic pathway; additionally, fucoidan has been synergized with cisplatin to induce apoptosis and decrease the toxic effects of cisplatin by enhancing the viability of cisplatin-treated cells (Hsu et al., 2018). Lathyrol (30, 60 and 120 μg/mL) induced ERS and activated its mediated PERK-eIF2α-ATF4-CHOP signaling pathway by downregulating Ca^{2+}-ATPase 2 (SERCA2) activity in lung cancer A549 and H460 cells, increasing Ca^{2+} levels and GRP78 protein expression levels in the endoplasmic reticulum lumen, and inducing apoptosis by upregulating Bax, caspase-3 and Cyt C expression and downregulating anti-apoptotic Bcl-2 protein level; tumors were markedly inhibited by treatment with 10, 20 or 40 mg/kg lathyrol in a subcutaneous tumor model established in BALB/c nude mice with H460 cells (Chen et al., 2023). In NSCLC A549 cells, the ether extract of *Dendrobium denneanum* disrupted the metabolic processes of proteins and other substances, induced ERS reactions, disrupted cell self-repair mechanisms, and impaired cell adhesion and proliferation; moreover, *D. denneanum* notably elevated ROS levels in lung cancer cells and disturbed the intracellular redox system, causing lung cancer cells to initiate various processes, such as apoptosis and autophagy, to facilitate cell death (Zhang et al., 2019). In NSCLC A549 and NCI-H226 cells, kushenol Z exerted tumor suppressive effects by enhancing the Bax/Bcl-2 ratio and activating caspase-3/9, resulting in mitochondrial apoptosis while upregulating CHOP and activating caspase-7/12 expression to trigger the ERS apoptotic pathway; additionally, kushenol Z exerted anti-proliferative activity by inhibiting cAMP-phosphodiesterases and Akt expression from suppressing the mTOR pathway (Chen et al., 2019). Glycyrrhetinic acid did not trigger apoptosis in NSCLC A549 and NCI-H460 cells but stimulated cell cycle arrest in the G0/G1 period by enhancing cyclin-dependent kinase inhibitors (p18, p16, p27 and p21), suppressing cyclin (cyclin-D1, -D3 and -E) and cyclin-dependent kinases (CDK4, 6 and 2), maintaining retinoblastoma protein phosphorylation and suppressing E2F Transcription Factor 1 (E2F1) in both cell lines, and significantly increasing the expression levels of Bip, PERK, and endoplasmic reticulum resident protein 72 (ERP72), regulatory proteins associated with ERS, which might be the mechanism by which glycyrrhetinic acid inhibits NSCLC cell proliferation (Zhu et al., 2015). *Arisema heterophyllum* Blume (AHA) curbed the propagation of lung cancer A549 cells, caused cell cycle arrest in the G1 period, and affected apoptosis by restraining the PI3K/Akt pathway and inducing ERS through the mechanism of enhancement of Bax, reduction of Bcl-2, and initiation of caspase-9/3; additionally, AHA elevated the levels of p-eIF2α, CHOP, IRE1α and p-JNK to promote ERS, and increased LC3-II and Autophagy Related Protein 7 (ATG7) expression to induce autophagy (Feng et al., 2016). In NSCLC A549 cells, extracts of total ginsenosides upregulated the protein expression of ATF4, CHOP and BIP, inhibited AKT-1 and p70 S6 kinase phosphorylation, increased ATG7 expression levels, activated ERS, promoted LC3-II levels and autophagosome formation, and increased autophagic flux, thereby inducing cell autophagic death, a process that is mediated via the ATF4-CHOP-AKT1-mTOR axis (Zhao et al., 2019). Evodiamine upregulated GRP78 protein expression in NSCLC LLC and A549 cell lines and LLC tumor-bearing mouse models, activated ERS pathway-mediated autophosphorylation of IRE1, which then bound to TRAF2 and attracted ASK1 to constitute the IRE1-TRAF2-ASK1 compound, activated the JNK pathway, upregulated caspase-12/9/3 and Bax expression and downregulated Bcl-2 levels to induce associated apoptosis (Li Y. et al., 2022). In the Lewis lung cancer model in C57BL/6 mice, flavonoid components in Astragali Radix showed significant inhibition of tumor growth in both the low (5 g/kg/d) and high (10 g/kg/d) dose groups, while the high dose group lowered the expression of XBP1, IRE1 and GRP78 and enhanced the expression of CHOP, which subsequently promoted the ERS apoptotic pathway and

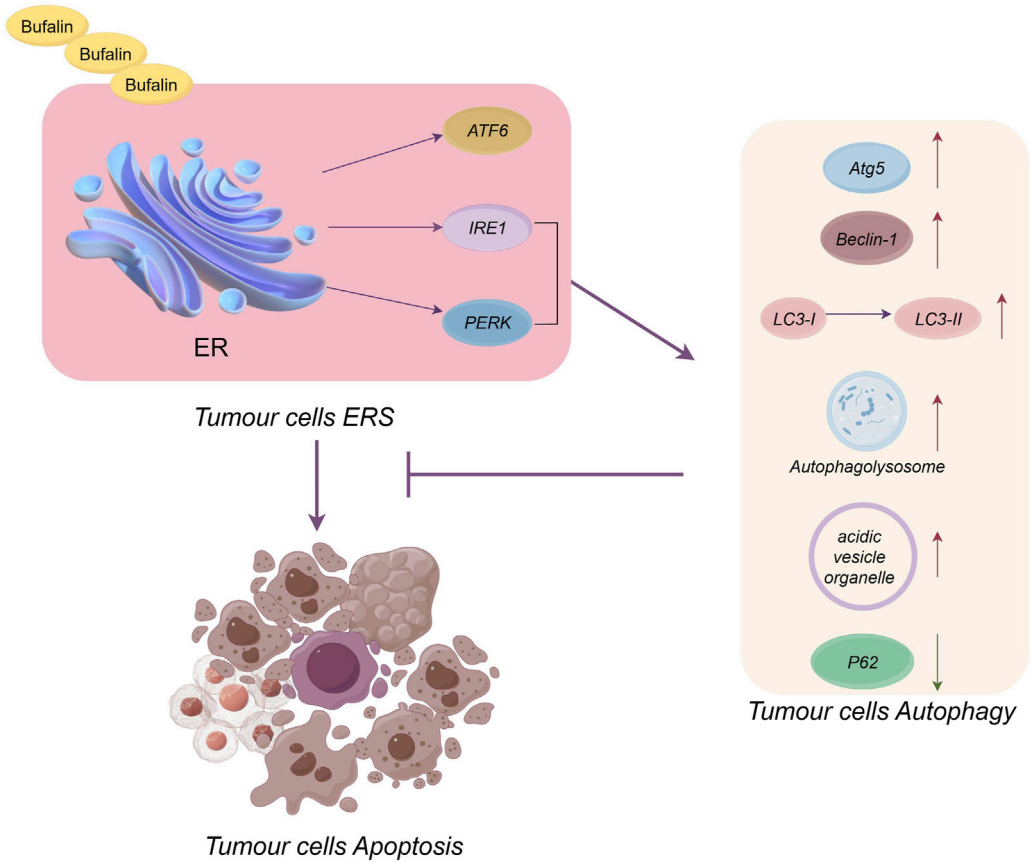

FIGURE 3
Plot of the relationship between ERS, autophagy and tumour cell apoptosis (in the case of bufalin). Bufalin promotes tumour cell apoptosis via the ERS pathway, but ERS also promotes autophagy to inhibit ERS-induced tumour cell apoptosis.

mediated the apoptosis of tumor cells (Yang et al., 2019). *Marsdenia tenacissima* extract (MTE) at a concentration of 40 mg crude/mL notably upregulated the expression of ATF6, GRP-78, ATF4, xbp1, and CHOP in NSCLC PC-9 and H1975 cells, activated ERS while increasing ROS production, and upregulated immunogenic cell expression of death-related markers (ATP, HMGB1) and reduced MMP, thereby inducing apoptosis; in addition, MTE was shown to trigger ERS and immunogenic cell death by inhibiting tyrosine protein kinase receptor AXL activity (Yuan et al., 2023a). In summary, the mechanisms by which guangsangon E, fucoidan, lathyrol, and others induce apoptosis in lung cancer cells are predominantly the PERK and IRE1 pathways, with A549 cells being the primary cell line studied.

9 Natural products target ERS-mediated apoptosis in oesophageal cancer

Corilagin caused programmed cell death in ECA109 and KYSE150 oesophageal cancer cells, which occurred by reducing the levels of GRP78 and disrupting the cellular balance induced by ERS; simultaneously, corilagin enhanced the initiation of the cleaved caspase-12/7 pathways to evoke apoptosis; in addition, corilagin also promoted apoptosis and cell migration by activating the mitochondria-associated apoptotic signaling pathway (Wu et al., 2021). Daurisoline induced cell death in EC1 and ECA109 cells of oesophageal squamous cell carcinoma, mainly because daurisoline resulted in the aggregation of ROS in the cells and induced the initiation of the ERS-mediated PERK-peIF2α-ATF4 signaling pathway, and when Noxa was activated as one of the downstream targets of ATF4, it bound to myeloid cell leukemia-1 (Mcl-1), an anti-apoptotic protein in the Bcl-2 family, triggered the expression of cleaved caspases 9, 3 and 7 and activated the endogenous apoptotic pathway to promote apoptosis; in contrast, ATF4 upregulated CHOP expression and activated the death receptor 5 (DR5) recombinant protein, followed by the upregulation of the exogenous apoptosis-related marker cleaved caspase 8 and its downstream-mediated truncated bid gene to activate the exogenous apoptotic pathway to promote apoptosis (Yuan S. et al., 2022). Apoptosis was observed in Eca-109 cells of human oesophageal cancer when exposed to tanshinone IIA at a concentration of 60 μg/mL, which was achieved in two primary ways: first, by promoting the level of Cyt C and initiating caspase-9/3, thereby cleaving PARP and leading to apoptosis; second, by activating the ERS-mediated CHOP pathway after downregulating the expression of binding immunoglobulin protein, thereby inducing apoptosis in Eca-109 cells (Zhang et al., 2017). In summary, corilagin, daurisoline, and tanshinone IIA could regulate ERS to promote apoptosis in oesophageal cancer cells, and they worked primarily through the ECA109 cell line.

10 Natural products target ERS-mediated apoptosis in breast cancer

Betulinic acid at 20 and 40 μM upregulated the expression of GRP78 in breast cancer MDA-MB-231 and BT-549 cells, triggered the ERS apoptotic pathway, induced cell mortality, blocked the binding of GRP78 to the PERK pathway and suppressed the β-catenin/c-Myc pathway to suppress cell metastasis and aggression; moreover, betulinic acid decreased the levels of N-cadherin and vimentin, which are mesenchymal markers, and upregulated the epithelial marker E-cadherin, which demonstrated that betulinic acid inhibited EMT and significantly reduced the release of matrix metalloproteinase-2 and matrix metalloproteinase-9, thereby attenuating the metastasis and aggression of breast cancer cells (Zheng et al., 2019). Dihydrotanshinone I significantly inhibited endoplasmic reticulum resident protein 57 (ERP57), a chaperone protein that mediates the correct folding of endoplasmic reticulum glycoproteins in MDA-MB-231 cells, which activated ERS; the unfolded protein bound to BiP and separated it from PERK, which initiated PERK and drove eIF2α phosphorylation, leading to the upregulated expression of ATF4 and ultimately to apoptosis (Shi et al., 2021). Matrine induced apoptosis in breast cancer ER-7-positive MCF-7 cells via two main pathways: firstly, matrine enhanced the levels of GRP78, eIF2α, and CHOP, activating ERS and facilitating apoptosis; secondly, matrine downregulated the expression of intracellular hexokinase-II, reduced mitochondrial ATP production and inhibited energy metabolism, thus promoting apoptosis (Xiao et al., 2017). ERS is actively expressed in breast cancer cells and is involved in the initiation of NOD-like receptor pyrin domain-containing protein 3 (NLRP3), and 10 μM peiminine markedly reduces the expression levels of PERK, eIF2α and CHOP in breast cancer MCF-7 cells, suggesting that ERS is inhibited while blocking the activation of NOD-like receptor pyrindomain-containing protein3 (NLRP3) inflammatory vesicles, thereby inhibiting cell growth and inducing apoptosis (Sun et al., 2023). In summary, betulinic acid and dihydrotanshinone I mainly affected the MDA-MB-231 cells, and matrine and peiminine could affect the MCF-7 cells; they primarily promoted the apoptosis of breast cancer cells through the PERK pathway.

11 Natural products target ERS-mediated apoptosis in stomach cancer

Schizandrin A at 30 μM notably enhanced the level of the ERS receptor GRP78 protein in AGS gastric cancer cells and caused apoptosis by inducing phosphorylation of the eIF2α and PERK signaling pathways, along with upregulating the level of CHOP and promoting the ERS-mediated apoptosis pathway (Pu et al., 2021). In AGS gastric cancer cells, curcumin initiated ERS and enhanced the activation of the CHOP and Jnk pathways; moreover, curcumin increased the Ca^{2+} concentration in cells, stimulated the release of mitochondrial Cyt C, and caused apoptosis by downregulating MMP and Bcl-2 expression in cells; the half maximal inhibitory concentration (IC_{50}) was 21.9 ± 0.1 μM in AGS cell lines (Cao et al., 2013). Wogonoside at 50 μM resulted in the activation of ERS in gastric cancer AGS and MKN-45 cells, increased levels of GRP78 and glucose regulated protein 94 (GRP94) proteins and activated the IRE1α pathway and its mediated TRAF2 and ASK1-related complexes, thereby activating the JNK signaling pathway and inducing apoptosis by enhancing Bax expression and reducing Bcl-2 expression (Gu et al., 2021). MKN-45 and AGS gastric cancer cell lines were treated with 7.8125, 15.625 and 31.25 μM myristicin, and the findings indicated that the expression of GRP78, the connector protein of ERS, phosphorylated IRE1α and PERK, and ATF6 were increased, while Myristicin upregulated caspase-12, the executor protein of ERS-triggered cell death, and triggered apoptosis (Song et al., 2023). Isoquercitrin at concentrations of 20–80 μM significantly elevated the levels of p-PERK, p-eIF2α, GRP78 and CHOP in gastric cancer HGC-27 and AGS cells while downregulating BCL-2 expression, upregulating BAX expression and cleaved caspase-3/12, and activating the ERS pathway; moreover, isoquercitrin enhanced the level of the immunogenic cell death (ICD) markers ATP, high-mobility group Box 1 (HMGB1), HSP70 and HSP90, promoting ICD and disrupting the immunosuppression of gastric cancer cells, thereby inducing cell death (Liu et al., 2023). Kangfuxin at 1 μg/mL was able to promote GRP78 protein expression, accelerate ERS, upregulate CHOP and caspase-12 protein concentration, and increase the release of autophagy-related proteins Beclin-1 and LC3-II/LC3-I in gastric cancer SGC-7901 cells; the trend of ERS-induced apoptosis and cellular autophagy was the same, and cellular autophagy could not be activated even after ERS was inhibited, so it can be concluded that Kangfuxin promotes apoptosis by activating autophagy, which was carried out after promoting ERS (Chen et al., 2017). The ethanolic extract of *C. cicadae* (EEC), on the one hand, upregulated the expression of Bax, AIF, caspase-8/6/3, decreased Bcl-2 and MMP levels in gastric cancer SGC-7901 cells, promoted the release of Cyt C from mitochondria, activated the cell surface receptors Fas and cleaved PARP, causing mitochondrial dysfunction and inducing the mitochondrial apoptosis pathway; otherwise, EEC upregulated the expression of the transcription factors E2F1, cyclin A2, cyclin E and p53 and downregulated CDK2 expression to block the cell cycle in S phase; additionally, EEC enhanced the intracellular Ca^{2+} concentration, promoted Ca^{2+} release from the endoplasmic reticulum and upregulated the expression of the ERS apoptosis pathway-related proteins calpain-1 and caspase-12/9 (Xie et al., 2019). In summary, the mechanisms by which schizandrin A, curcumin, wogonoside, and others induce apoptosis in stomach cancer cells are mainly the PERK and IRE1 pathways, and the AGS cells are the primary cell line that has been studied.

12 Natural products target ERS-mediated apoptosis in liver cancer

Cytisine at a concentration of 10 mmol/L significantly increased the Ca^{2+} concentration in liver cancer HepG2 cells, disrupted endoplasmic reticulum Ca^{2+} homeostasis and caused ERS, upregulated CHOP/GADD153, JNK and caspase-4, and finally activated the corresponding pathway to trigger apoptosis (Yu et al., 2018). Gecko polypeptide mixture at 0.3 mg/mL upregulated GRP78 protein expression and induced ROS production in hepatocellular carcinoma HepG2 cells, activated the ERS-mediated PERK signaling pathway and upregulated ATF4 expression to promote DDIT3 and CHOP expression in

the cells, ultimately inducing apoptosis through starting of the apoptosis-associated proteins PARP and caspase-3 (Duan et al., 2018). Muscone notably elevated the expression of Tribbles pseudokinase 3 (TRIB3) in hepatocellular carcinoma HepG2 cells with an IC_{50} of 0.663 μM; Muscone activated the ERS-mediated PERK pathway and subsequently induced eIF2α phosphorylation and complex formation with ATF4, induced DDIT3 expression, upregulated caspase-3 and Bax expression and lowered Bcl-2 expression to induce apoptosis; additionally, muscone activated Sestrin 2, an autophagy-related gene, and AMPK to inhibit intracellular mTOR expression, thereby inducing cellular autophagy (Qi et al., 2020). The IC_{50} of alisol B 23-acetate isolated from *Alisma orientalis* (Sam.) Juzep. was 18.01 μM, and alisol B 23-acetate upregulated the expression of ERS markers BIP and CHOP in HepG2 cells in a concentration-dependent manner while increasing the intracellular calcium concentration and activating ERS to suppress cell growth and promote apoptosis; additionally, alisol B 23-acetate also upregulated the expression of LC3II to promote autophagy (Xu et al., 2015). Realgar quantum dots (RQDs) at 30 μg/mL declined Bcl-2 expression and elevated Bax expression in hepatocellular carcinoma HepG2 cells, promoted Cyt C release with complete loss of MMP and triggered an apoptotic enzyme cascade effect, together with the upregulated mRNA expression of Chop10 and GRP78, which suggested that RQDs induced apoptosis and necrosis probably via ERS, loss of MMP, and an elevated Bax/Bcl-2 ratio (Qin et al., 2015). In liver cancer cells and male BALB/c nude mice xenografted with subcutaneous HepG2 cells, cryptomeridiol stimulated the IRE1α-ASK1-JNK signaling pathway and induced MMP loss by translocating the orphan nuclear receptor Nur77 to mitochondria, resulting in mitochondrial dysfunction, while cryptomeridiol activated IRE1α and ASK1, stimulated IRE1α and PERK phosphorylation, and significantly upregulated Bip and CHOP expression; since ASK1 mediates IRE1α signaling, Bkh126 could promote ASK1 activity and subsequently increase the phosphorylation of JNK and p38 (both substrates and effectors of ASK1) to stimulate the ERS signaling pathway; ERS exacerbation and mitochondrial dysfunction led to increased ROS cytotoxic products and induced apoptosis, suggesting that Bkh126 induced Nur77 to link ERS to mitochondria-mediated cell killing (Li X. et al., 2022). Bufalin at 80 nmol/L activated the ERS-mediated IRE1-JNK pathway in HCC Huh-7 and HepG-2 cells and induced apoptosis, but subsequent studies showed that IRE1 upregulated Beclin-1 and autophagy-associated protein Atg5 levels, promoted the transformation of LC3-I to LC3-II, inhibited p62 expression, and triggered cytoprotective autophagy to counteract apoptosis (Hu et al., 2014). The administration of bufalin to HepG2 and Huh7 hepatocellular carcinoma cells exhibited a synergistic inhibition of tumor cell growth and triggered apoptosis when combined with sorafenib, which effectively reversed both intrinsic and acquired resistance to sorafenib through various mechanisms; specifically, the activation of Akt by sorafenib and subsequent resistance were counteracted by bufalin's time-dependent upregulation of eIF2α, CHOP, and IRE1 expression; moreover, bufalin induced Akt inactivation by reducing phosphorylated Akt levels through the IRE1 pathway in an ERS-dependent manner (Zhai et al., 2015). Celastrol inhibited the reproduction of liver cancer HepG2 and Bel7402 cells, causing G2/M cell cycle arrest; following a 24-h treatment of HepG2 cells with 0.625–10 μM celastrol, GRP78/BiP, ATF4, CHOP, IRE1α and XBP1 splice forms (XBP1s) in the cells were significantly increased, and immunoblotting results showed that celastrol enhanced phosphorylation of IRE1α and xbp1, particularly at 2.5 μM, which suggested that celastrol caused ERS in hepatocellular carcinoma cells (HCC); in a homozygous model study of H22 tumor-bearing mice, GRP78/BiP expression was upregulated, and caspase-3 was activated in celastrol-treated mice, suggesting that celastrol enhanced ERS and caspase activity inhibition of tumor growth (Ren et al., 2017). Compared with Konjac glucomannan (KGM) or 5-Fluorouracil (5-FU) alone, KGM combined with 5-FU notably induced apoptosis and suppressed cell proliferation and migration with inhibition of Toll-like receptor 4 (TLR4) expression to activate ERS and its mediated PERK/ATF4/CHOP signaling pathway in HCC HepG2 and Bel-7402 cells; moreover, KGM reversed the resistance of HCC to 5-FU by decreasing TLR4 *in vivo* experiments (Shi et al., 2022). Nanoparticles (TTF1-nps) of TTF1 (5,2′,4′-trihydroxy-6,7,5′-trimethoxyflavone) upregulated the expression of GRP78 in liver cancer lines (HepG2, Hep3B, PLC/PRF/5), activated three main pathways involved in ERS, namely, PERK, IRE1α, and ATF6, and upregulated the expression of CHOP and caspase4, thereby inducing apoptosis, and TTF1-nps at 5, 10 and 20 μmol/kg doses treated with nude mouse HepG2 xenograft models for 16, 18 and 20 days, respectively, were also shown to suppress the proliferation of tumor cells (Xiao et al., 2016). Fisetin (3,7,3′,4′-tetrahydroxyflavone), in HCC HepG2, Hep3B and Huh7 cells and HepG2 xenograft mouse models, promoted apoptosis by releasing Ca^{2+}, increasing CHOP, p-eIF2α, p-PERK, cleaved caspase-3, ATF4 and induction of GRP78 exosomes to activate the ERS-mediated PERK-ATF4-CHOP signaling pathway; moreover, ERS inhibited the EMT phenomenon under radiation conditions and reversed radiotherapy resistance (Kim, 2023). Aqueous extract of *Polygonum bistorta* (PB) at 240 μg/mL upregulated the expression of LC3B-II protein, GFP-LC3B puncta and p62/Sequestosome 1, a marker of autophagosome formation in hepatocellular carcinoma Hep3B cells, suggesting that PB enhanced the aggregation of cellular autophagosomes, and some studies claim that excessive accumulation of autophagy can induce apoptosis; moreover, PB accelerated the creation of ROS and upregulated the expression of death-associated protein kinase 3 (DAPK3), an upstream integrator of ERS-mediated apoptosis, and the expression of caspase 8/9/3 and PARP 1 activity was notably upregulated, confirming the pro-apoptotic effect of ERS in Hep3B cells; similar results were obtained in Hep3B and HepG2 xenograft mouse models after 276 mg/kg PB treatment (Liu Y. H. et al., 2017). Treatment with 50 mg/L Astragalus polysaccharide combined with 1 μM doxorubicin lowered the expression of O-GlcNAc transferase and enhanced the expression of O-GlcNAcase in hepatocellular carcinoma Hep3B cells, which ultimately inhibited O-GlcNAcylation in Hep3B cells, thereby promoting doxorubicin-induced ERS expression, activating the PERK/eIF2α/CHOP signaling pathway, and upregulating cleaved caspase-3, Bax and Bcl-2 interacting mediator of cell death (Bim) expression by inhibiting Bcl-2 expression, thus inducing Hep3B cell apoptosis; similar experimental results were obtained *in vivo* with 50 mg/kg

Astragalus polysaccharide and/or 2 mg/kg doxorubicin treatment in Hep3B mouse xenograft tumor models (Li et al., 2023). In a rat model of diethylnitrosamine (DEN)-induced hepatocellular carcinoma, caudatin at 50 mg/kg modulated ERS in rat cells and triggered apoptosis in hepatocellular carcinoma cells by suppressing the ATF6 and PERK-eIF2α-ATF4 pathways, while caudatin reduced interleukin-6, macrophage chemoattractant protein-1 and interleukin-1β levels and biomarkers of liver inflammation, which were effective in the prevention of liver cancer (Song et al., 2020). Psoralen at 40 μM promoted apoptosis in liver cancer SMMC7721 cells by enhancing GRP78 and GRP94 protein expression, activating the IRE1 and ATF6 pathways, and improving the gene expression of DDIT3, resulting in disruption of endoplasmic reticulum Ca^{2+} homeostasis and downregulating the expression of Bcl-2 (Wang et al., 2019). Baicalein at a concentration of 200 μM upregulated BiP expression in hepatoma SMMC-7721 and Bel-7402 cells, activated PERK and IRE1 pathways and the phosphorylation of UPR downstream molecules CHOP and eIF2α, decreased the expression of Bcl-2, Bcl-xL and Mcl-1, activated caspase-9/3 and inhibited the DNA repair enzyme PARP to induce apoptosis; moreover, baicalein increased the conversion of LC-3I to LC-3II and promoted apoptosis by increasing cellular autophagy (Wang et al., 2014). Notopterol, which exerted antitumor effects through inhibition of cancer stemness, upregulation of PERK and CHOP, enhancement of ERS and increased oxidative stress in HCC HepJ5, Mahlavu cell line and female BALB/c nude mice (Huang et al., 2023). In summary, the mechanisms by which cytisine, gecko polypeptide mixture, muscone, and others induce apoptosis in liver cancer cells are mainly the PERK, IRE1, and ATF6 pathways, and HepG2 cells are the primary cell line that has been studied.

13 Natural products target ERS-mediated apoptosis in colorectal cancer

Overexpression of ATP-binding cassette, subfamily G (WHITE), member 2 (ABCG2/BCRP) led to resistance of tumor cells to multiple chemotherapeutic agents; after lupeol treatment, ABCG2 expression was downregulated in the LoVo colorectal cancer cell and the oxaliplatin-resistant OXA-R LoVo cell, but ERS marker levels as well as eIF2α (P-eIF2α) and caspase-3 phosphorylation levels were significantly increased, suggesting that lupeol might induce apoptosis by inhibiting ABCG2 and subsequently activating the ERS pathway, as was the case in the tumor-bearing mice; moreover, cell viability of the OXA-R LoVo cell line was significantly reduced after 50 and 100 μM lupeol treatment compared to that of the parental LoVo cell line, and apoptosis was increased after 24 h of 50 μM lupeol treatment in the OXA-R LoVo cell line, thus lupeol has the prospective to be a valid treatment for chemotherapy multidrug resistant cancers, particularly in oxaliplatin-resistant LoVo CRC cells (Chen et al., 2018). Transcription factor 4 (TCF4) was a key regulator of ERS, and tumor protein p53 (TP53) could inhibit TCF4 activity; in CRC LoVo and RKO cells, oridonin upregulated the expression of TP53 in a concentration-dependent manner, which inhibited the activity of TCF4 and caused the cellular ROS aggregation and disrupting Ca^{2+} homeostasis, and elevating the expression levels of ATF4 and CHOP, which ultimately led to apoptosis; this suggested that Oridonin exerts its antitumor effects by regulating ERS induced via the TP53/TCF4 axis (Zhou et al., 2023). Curcumin triggered apoptosis and G0/G1 cycle arrest by heightening intracellular calcium levels in CRC LoVo and HT-29 cells, while curcumin and/or irinotecan produced ROS and elevated the expression levels of ERS-related proteins BIP, PDI and CHOP to activate the apoptotic pathway of the endoplasmic reticulum, which large amounts of ROS can further activate; thus, curcumin improved the ability of irinotecan to facilitate apoptosis in CRC cells by producing ROS and activating the ERS pathway (Huang et al., 2017). Curcumin exhibited an IC_{50} value of 40.7 ± 0.5 μM, which led to the initiation of the ERS pathway and upregulated the expression of CHOP and jnk pathways in CRC HT-29 cells; moreover, curcumin could increase the concentration of Ca^{2+} in cells, facilitating the liberation of mitochondrial Cyt C and ultimately decreasing MMP and Bcl-2 expression levels and upregulating bax expression to induce apoptosis (Cao et al., 2013). Osthole effectively upregulated the expression of GRP78, PERK, elF2α and CHOP proteins in colorectal cancer HT-29 cells at both 25 and 50 μM concentrations, activating ERS and promoting apoptosis, inducing autophagy and thus promoting apoptosis by upregulating the LC3-II/LC3-I ratio and downregulating p62 protein expression (Zhou et al., 2021). Artemisianins A exhibited a strong repressive effect on CRC HT-29 cells with an IC_{50} value of 7.2 μM, and it increased the expression of IRE1α and XBP1s, upregulated autophosphorylated p-PERK and PERK-mediated p-eIF2α phosphorylation, and upregulated the expression of ATF6 and CHOP, suggesting that artemisinin A triggered apoptosis in HT-29 cells and activated ERS apoptotic signaling for tumor suppression by upregulating the UPR pathway of IRE1α, p-PERK, ATF6 and CHOP and by disrupting intracellular Ca^{2+} homeostasis (Xue et al., 2019). Palmitic acid at a dose of 120 μmol/L upregulated the expression of p-PERK, p-eIF2α and ATF4 in CRC HT29 and HCT116 cell lines, which promoted the translocation of transferrin by activating Ca^{2+} release from ERS, thereby inducing ferroptosis caused by iron accumulation and eventually cell death, while high expression of fatty acid translocase (FAT/CD36) facilitated the enhancement of palmitic acid-induced ferroptosis; BALB/c-nu mouse models of HT29 cells, SW620 cells and SW620 cells with high CD36 expression were established, and after treatment with 10 mg/kg palmitic acid in an *in vitro* experiment, the effects were in general agreement with the *in vivo* experiment (Kuang et al., 2023). A purified resin glycoside fraction from Pharbitidis Semen (RFP)-induced apoptosis was mediated by the coexistence of caspase independence and autophagy protection and characterised by cytoplasmic vacuole accumulation and mitochondrial swelling; this compound triggered paraptosis-like apoptosis by upregulating the ERS markers BIP/GRP78, CHOP, IRE1α, XBP1s and ubiquitinated proteins, activating the IRE1 branch of UPR signaling, suppressing proteasome-dependent degradation and activating the MAPK signaling pathway, and RFP-induced cytoplasmic vacuolisation and apoptosis were positively modulated by JNKs and ERKs, which were not associated with ROS generation or intracellular calcium stabilisation; furthermore, RFP was found to arouse intracellular Chloride Intracellular Channel Protein 1 (CLIC1) and increase intracellular Cl^- concentrations, as blocking CLIC1 attenuated cell death, cytoplasmic vacuolation and ERS, and therefore the cytotoxic effect of RFP on CRC HT-29 and HCT-116 cells was caused by

CLIC1-mediated apoptosis (Zhu et al., 2019). ROS are an upstream regulator of ERS, and ROS-ERS is an important pathway for apoptosis induction by natural products; the IC_{50} values of 10.5 and 2.8 μM after 24 and 48 h of treatment with periplogenin produced ROS, increased BIP, p-eIF2α, CHOP, IRE1α, and p-JNK protein levels and decreased p-ASK1 protein levels, suggesting that periplogenin simultaneously activated two signaling pathways in ROS-mediated ERS, BIP-eIF2α-CHOP and IRE1α-ASK1-JNK; moreover, this compound upregulated Bax expression and downregulated Bcl-2 expression, lowered the cleavage of caspase-3 and PARP, and promoted cell apoptosis, while periplogenin exhibited dose- and time-dependent inhibition of the viability of CRC HCT116 cells (Yang et al., 2021). Shikonin at 1.5 μM significantly upregulated BiP protein expression in CRC HCT-116 and HCT-15 cells, activated the ERS-mediated PERK/elF2α/ATF4/CHOP and IRE1α/JNK signaling pathways, lowered the expression of Bcl-2 and enhanced the expression of caspase-3/9 to trigger apoptosis in relevant cells; the same results were obtained after 3 mg/kg shikonin in HCT-116 and HCT-15 cell-grown rhabdoid mice (Qi et al., 2022). Artesunate at concentrations of 1–4 μM promoted the accumulation of ROS in CRC SW480 and HCT116 cells and enhanced the expression of the cellular senescence-associated proteins p16, p21, IL-6 and MMP3, leading to cellular senescence and cell cycle arrest; the upregulated expression of BIP and IRE1 showed that artesunate promoted the expression of the ERS mechanism, which mediated the activation of the p-IRE1α-CHOP-DR5 signaling pathway; similarly, *in vivo* experiments showed that the growth of tumors was inhibited after artesunate treatment in tumor-bearing mice grown with CRC CT26 cells (Huang et al., 2022). In summary, the mechanisms by which lupeol, oridonin, curcumin, and others induce apoptosis in colorectal cancer cells are predominantly the PERK and IRE1 pathways, with HT-29 and HCT-116 cells being the main cell lines studied.

14 Natural products target ERS-mediated apoptosis in gallbladder cancer

Ginsenoside Rg3 stimulated the ERS-mediated PERK pathway, leading to the increased phosphorylation of eIF2α, ATF4, CHOP, and Lipocalin 2 in GBC-SD gallbladder cancer cells and transplanted tumor-bearing mice; this activation also induced ROS production and significantly upregulated the expression of lincRNA-p21, which suggested that Rg3 suppressed propagation and enhanced apoptosis by promoting the apoptotic signaling pathway mediated by ERS (Wu et al., 2018). It was shown that ginsenoside Rg3 induced the apoptosis of gallbladder cancer cells via the ERS pathway.

15 Natural products target ERS-mediated apoptosis in prostate cancer

Matrine at a concentration of 4 mM inhibited proteasomal CT-like activity in prostate cancer DU145 and PC-3 cells and suppressed EMT by enhancing E-cadherin and lowering Vimentin and N-cadherin expression; moreover, matrine activated the ubiquitin–proteasome system, promoted the UPR, released Bip, activated the ERS-mediated PERK pathway, phosphorylated eIF2α, upregulated ATF4 and CHOP expression, and triggered apoptosis by suppressing Bcl-2 and upregulating Bax; *in vivo*, similar results were achieved in DU145 xenograft mice treated with 50 mg/kg matrine, with inhibition of tumor proliferation and Ki-67 expression in tumor-bearing nude mice (Chang et al., 2018). Astragaloside (100 nmol/L) significantly upregulated the protein expression of the ERS factor BiP in prostate cancer DU145 cells and promoted ERS-mediated protein expression of IRE1, p-PERK and AFT6 without affecting the total level of PERK, thereby activating AFT4, CHOP and caspase-12-related apoptotic pathways and inducing apoptosis in prostate cancer cells (Tan et al., 2018). Excessive ROS production disrupted the pro-oxidant/antioxidant balance by exceeding the number of available intracellular antioxidants, which triggered mitochondrial dysfunction and the pro-apoptotic ERS signaling pathway, leading to apoptosis; isobavachalcone significantly decreased pro-caspase-3 levels, enhanced cleaved caspase-3 levels and activated the caspase apoptotic pathway, while isobavachalcone upregulated the expression of ERS markers XBP-1, ATF4, GRP78, Chop and p-eIF2α proteins and inhibited the enzymatic activity of the antioxidant enzyme thioredoxin reductase 1 (TrxR1) protein in a concentration-dependent manner; silencing of TrxR1 elevated the level of isobavachalcone-induced ROS, generated oxidative stress, induced lethal ERS in prostate cancer PC-3 cells and promoted apoptosis (Li et al., 2018). Quercetin lowered the protein levels of CDK2 and cyclins E and D and induced G0/G1 phase block, reduced Bcl-2 protein levels and MMP, generated Ca^{2+} and released Cyt C, upregulated Bax and caspase-3/8/9, facilitated the transportation of AIF proteins from mitochondria to the nucleus and upregulated the protein expression of ATF, GRP78 and GADD153; these data suggested that quercetin might stimulate apoptosis utilizing the mitochondrial pathway and direct activation of the caspase cascade by ERS (Liu et al., 2014). In summary, the mechanisms by which matrine, astragaloside, isobavachalcone, and quercetin induce apoptosis in prostate cancer cells are mainly the PERK and IRE1 pathways, with DU145 and PC-3 cells being the primary cell lines studied.

16 Natural products target ERS-mediated apoptosis in cervical cancer

Tanshinone IIA significantly enhanced the degradation of PARP, caspase-3/9, upregulated the Bax/Bcl-2 ratio, released Cyt C into the cytoplasm, upregulated the phosphorylation of p38 and JNK signaling, and hindered the cell cycle in the G2/M period in advanced cervical cancer CaSki cells, resulting in a potent growth suppression and pro-apoptotic effect on CaSki cells, suggesting that 7.5 μM tanshinone IIA induced mitochondria-associated apoptosis by stimulating the JNK and p38/Bax/caspase signaling pathways; furthermore, tanshinone IIA increased the levels of PERK, IRE1, and phosphorylated eIF2α, ATF4 and CHOP, leading to PARP degradation, and activated the p38 and ASK1 signaling pathway to promote cell death, suggesting that tanshinone IIA might induce apoptosis, at least partially, through the ERS pathway via eIF2α phosphorylation and IRE1-ASK1 activation (Pan et al., 2013). Saikosaponin-A at 15 μM notably upregulated the expression of GRP78, CHOP and caspase12 in HeLa cells, induced activation of the ERS pathway, and thus promoted apoptosis; moreover, Saikosaponin-A enhanced Bax expression, downregulated Bcl-2 expression, stimulated the expression of caspase-3, an important

mediator of apoptosis, and suppressed the PI3K/AKT signaling pathway to induce apoptosis; these findings with HeLa nude mice as a model were also confirmed *in vivo* (Du et al., 2021). In cervical cancer HeLa cells, celastrol induced G2/M cell cycle arrest and caused apoptosis, parapoptosis and autophagy via various pathways, including proteasome, ERS and Hsp90 inhibition; apoptosis and parapoptosis promoted cell death, while autophagy was a cytoprotective mechanism in which endoplasmic reticulum apoptosis was caused by celastrol treatment, resulting in the significant upregulation of ERS markers Bip, PERK and IRE1 and causing cytoplasmic vacuolization that was associated with endoplasmic reticulum expansion rather than autophagy (Wang et al., 2012). In addition, 45 μM 20(S)-ginsenoside Rh2 elevated caspase 3 activity and phosphatidylserine (PS) ectopia to inhibit cervical cancer HeLa cell proliferation and promote apoptosis, and 20(S)-ginsenoside Rh2 enhanced ATF4, DDIT3, JUN, FOS, Bcl- 2-binding component 3 (BBC3) and phorbol-12-myristate-13-acetate-induced protein 1 (PMAIP1) gene expression and significantly suppressed the heterodimer of transcript DDIT3 for induction of ERS-related apoptosis in HeLa cells (Liu et al., 2022). In summary, the mechanisms by which tanshinone IIA, saikosaponin-A, celastrol, and 20(S)-ginsenoside Rh2 induce apoptosis in cervical cancer cells are predominantly the PERK and IRE1 pathways, with HeLa cells being the primary cell line studied.

17 Natural products target ERS-mediated apoptosis in ovarian cancer

Myricetin suppressed the viability of ovarian cancer SKOV3 cells, induced nuclear fragmentation, enhanced caspase 3 activity levels and thus induced apoptosis in SKOV3 cells; in addition, myricetin also upregulated the ERS-related proteins GRP78 and CHOP in SKOV3 cells and boosted the phosphorylation of the DNA double-strand break (DNA DSB) marker H2AX, indicating that myricetin induced DNA DSBs and ERS, promoting apoptosis in SKOV3 cells (Xu et al., 2016). It was evident that myricetin promoted apoptosis in ovarian cancer cells by stimulating ERS.

18 Natural products target ERS-mediated apoptosis in leukemia

In the leukemia cell lines U937 and HL-60 and primary leukemia cells (AML), asperuloside stimulated the cleavage of caspase-9/3 and PARP and facilitated the loss of MMP and the release of Cyto-c from mitochondria, inducing cell death; in addition, in U937 cells and heterozygous nude mice, asperuloside significantly induced ERS by increasing the expression levels of GRP78, PERK, eIF2α, CHOP, p-IRE1, XBP1, ATF6 and cleaved caspase-12, further showing that asperuloside regulated the interaction between GRP78 and PERK and subsequently mediated apoptosis (Rong et al., 2020). Shikonin increased ROS accumulation in Adult T cell leukemia/lymphoma (ATLL) cells, stimulated ERS and promoted the expression of p-eIF2α, ATF4, XBP-1, p-JNK, and CHOP, which induced apoptosis; moreover, shikonin suppressed the growth of ATLL cells in xenograft mice (Boonnate et al., 2023). In summary, asperuloside and shikonin promoted apoptosis in leukemia cells by regulating the ERS pathway.

19 Natural products target ERS-mediated apoptosis in osteosarcoma

Polyphyllin I at a dose of 1.25 mM inhibited proteasomal CT-like activity in osteosarcoma MG-63, Saos-2 and U-2 OS cells and induced cellular ERS to active the UPR and dispose of accumulated undegraded proteins; BiP expression was upregulated and its mediated PERK-eIF2α-ATF4-GADD153 (CHOP) pathway was activated, and Polyphyllin I inhibited the activity of Bcl-2 and Bcl-xL and promoted the activity of Bax and Bak, which subsequently upregulated caspase-3 and PARP protein expression and triggered apoptosis (Chang et al., 2015). In osteosarcoma U2OS cells and hormonal mice, (3R)-5,6,7-trihydroxy-3-isopropyl-3-methylisochroman-1-one (TIM) decreased MMP, promoted Cyt C release, increased DNA fragmentation, enhanced caspase-3/9 and Bax activity and lowered Bcl-2 expression, suggesting that TIM suppressed cell growth and triggered apoptosis by the process of mitochondrial death regulation; TIM also elevated the expression of the proapoptotic protein NOXA and decreased the expression of the antiapoptotic protein Mcl-1 in the apoptotic pathway, suggesting that TIM induced intracellular mitochondria through NOXA/Mcl-1 axis apoptosis; moreover, TIM upregulated the protein expression of IRE1, ATF6 and GRP78, indicating that TIM activated the ERS apoptotic pathway (Song et al., 2019). In osteosarcoma MG-63 and U2OS cells, psoralen triggered G0/G1 cell cycle arrest by reducing the levels of cyclin A1, cyclin B1, cyclin D1 and cyclin k2 and promoted apoptosis by elevating cleaved caspase 3 and Bax protein levels and declining the levels of Bcl-2 protein; additionally, psoralen upregulated the expression of DDIT3, GADD34, ER degradation-enhancing alpha-mannosidase-like 1 (EDEM1), Growth Differentiation Factor 15 (GDF15), and S1P mRNA and enhanced the levels of CHOP, IRE1, XBP1s, GRP78, PERK, and ATF-6, indicating the activation of ERS and suppression of cell proliferation, and finally psoralen-induced apoptosis (Li and Tu, 2022). In summary, Polyphyllin I, TIM, and psoralen primarily worked on U2OS cell lines and promoted apoptosis in osteosarcoma cells by activating the PERK and IRE1 pathways.

20 Natural products target ERS-mediated apoptosis in melanoma

Shikonin suppressed the proliferation of human melanoma A375 cells by arresting cells at the G2/M stage, inducing apoptosis and regulating autophagy in the ROS/ERS apoptotic pathway and the ROS/p38 signaling pathway, which the specific mechanism was that shikonin increased p21 levels and decreased cyclin B1 levels, leading to G2/M phase block; Shikonin produced ROS, induced ERS and upregulated p-eIF2α, CHOP and cleaved caspase-3 expression, which significantly triggered ERS-mediated apoptosis; moreover, Shikonin initiated protective autophagy by the activation of the p38 pathway, leading to increased levels of p-p38, LC3B-II and Beclin 1, suggesting that blocking autophagy could promote apoptosis (Liu et al., 2019). Shikonin triggered apoptosis in melanoma cells via the ERS pathway.

21 Discussion

The effects of natural products on tumors are evident, and mainly include inhibiting tumor cell growth, enhancing cell death, regulating cell autophagy, arresting the cell cycle, and reducing drug resistance in tumor cells. Our review indicates that natural products exert their antitumor effects mainly by stimulating the ERS pathway to promote the apoptosis of tumor cells. Inhibiting cell proliferation, regulating autophagy, blocking the cell cycle and alleviating drug resistance of tumor cells do not require ERS-related processes to occur. We have summarised the literature on natural products that promote tumor cell apoptosis by targeting ERS and have drawn the following conclusions:

In terms of cancer types, the stacked plot in Figure 2 revealed that the natural products targeting the ERS apoptotic pathway were predominantly studied in liver, lung, and colorectal cancers, followed by substantial research in gastric cancer, breast cancer, nasopharyngeal cancer, glioma, cervical cancer, prostate cancer, oesophageal cancer, and osteosarcoma. Conversely, studies on other cancer types were scarce, and no studies investigated pancreatic and bladder cancer. The reasons for this absence are twofold. First, since tumors with high morbidity and mortality are more dangerous and more urgently in need of specific drugs to alleviate them, experimental studies are of greater clinical significance (Li et al., 2017; Islam et al., 2022). Second, the maturity of experimental techniques for different tumors influences the extent of research, and tumors with higher morbidity and mortality possess more cell types and mature experiments (Yuan et al., 2023b). A total of 69 natural products are reviewed in this paper. However, research on various natural products is sporadic, lacking consistency, and no single product has been tested on a large scale to target their mechanism of action, and a potent natural product has yet to be selected for standardized and quantitative experiments. In the present study, bufalin, curcumin, ginsenoside, tanshinone and artemisianin were tested more frequently but only twice or thrice. Therefore, the next step is to select a more effective natural product extract, such as bufalin or curcumin, and select more experimental cancer types, such as liver and lung cancer, for ERS apoptosis pathway-related experiments. Furthermore, it is essential to include untested cancer types such as pancreatic and bladder cancer in ERS experiments to bridge the existing knowledge gap.

Regarding the tumor death mechanism, we found that tumor cells achieve death mainly through a combination of the mitochondrial apoptosis pathway, ERS apoptosis pathway, autophagy pathway and cell cycle inhibition pathway but through the ERS apoptosis pathway alone (Yuan M. et al., 2022; Kooshki et al., 2022; Tewari et al., 2022). This does not mean that the ERS apoptotic pathway is a concomitant pathway; on the contrary, the ERS apoptotic pathway is a key pathway for the antitumour effects of natural products, a fact that has been well demonstrated by the fact that all 69 natural products reviewed here promote tumour cell apoptosis via ERS. However, at this stage, when researchers conduct experiments on natural products, they usually measure the ERS apoptosis pathway, mitochondrial apoptosis pathway and autophagy pathway at the same time in order to have a comprehensive understanding of the anti-tumour effects of natural products. So there are fewer studies targeting the ERS apoptotic pathway alone, but this does not mean that the ERS apoptotic pathway is not critical. Given the above background, the conclusions we have drawn also confirm that the ERS apoptotic pathway, the mitochondrial apoptotic pathway and autophagy most often function simultaneously, and that natural product-induced tumour cell death is mainly achieved through these combined pathways, and that related studies have focused on these three pathways. Regarding the link between the autophagic and apoptotic pathways, a study claimed that inhibition of ERS-mediated autophagy in ATF4-associated cells could play an anticancer role (Yang et al., 2023). The results of this paper show that natural products promote ERS in order to promote apoptosis in tumour cells, and in the process ERS also mediates autophagy, which is primarily a protective pathway whose mechanism of action is to inhibit apoptosis by mitigating ERS and promoting the restoration of endoplasmic reticulum homeostasis. We explained the relationship between autophagy, ERS and tumour cell apoptosis using the most frequently occurring bufalin as an example, see Figure 3. From the figure, it can be seen that bufalin induces ERS through ATF6, PERK and IRE1 pathways, immediately followed by apoptosis of tumour cells. Whereas IRE1 and PERK pathways can induce changes in autophagy-related markers such as increased Atg5, LC3-II, *etc.*, to promote autophagy, which inhibits ERS-induced apoptosis in tumour cells. It can be seen that autophagy and ERS apoptosis are antagonistic to each other. However, there are relatively few studies on the interaction between autophagy and ERS apoptosis, and at the same time autophagy is one of the important pathways of tumour cell death. Influenced by the above reasons, the next step needs to continue the interaction study between autophagy and ERS apoptosis to determine whether autophagy only unilaterally inhibits ERS apoptosis, and whether it can promote ERS apoptosis. Therefore, it is imperative to investigate the interactions between autophagy and ERS to understand their intrinsic mechanisms, and it is crucial to study how autophagy promotes ERS-induced apoptosis. At the same time, the next step should be to conduct studies on the apoptosis-promoting pathway of ERS alone, and it is also worthwhile to explore how the combination of mitochondrial apoptosis, autophagy death and ERS apoptosis can better promote apoptosis. It can also be seen from this paper that both underexpression and overexpression of ERS can cause apoptosis. Natural products regulate apoptosis mainly by upregulating the expression of GPR78 or CHOP-related proteins. However, inhibiting ERS by methods such as reducing the expression levels of PERK, eIF2α and CHOP, has rarely been studied, with only three cases mentioned in this paper. Meanwhile for the ERS-related apoptosis pathway, most of the experimental proteins and pathways studied at this stage are two related pathways mediated by PERK and IRE1. In contrast, the ATF6 pathway, also an ERS apoptotic pathway, has rarely been studied, especially since the studies related to natural products were close to zero. Therefore, further research is needed to identify the mechanisms by which natural products inhibit ERS and promote apoptosis under inadequate ERS expression. Additionally, studies on promoting apoptosis by ATF6-related pathways and proteins under the condition of ERS overexpression are required to improve the understanding of the ERS apoptosis pathway. Finally, studies on the relationship between ERS, ROS levels and calcium are insufficient and should be conducted.

In terms of experimental techniques, it mainly rely on cell and mouse experiments (Voskoglou-Nomikos et al., 2003), as no clinical studies involving humans have yet been conducted. We believe that the lack of clinical trial evidence may be due to the following reasons: 1. Since the antitumor pathway of natural product-targeted ERS is not yet completely clear and the mechanism is still controversial, the relevant drugs have not been developed or are still in the beginning stage of research and development, and cannot be subjected to clinical trials for the time being. 2. Due to the lack of efficacy or safety issues, as well as differences in the control of clinical trials in different countries, it is not possible to ensure the smooth progress of the trials, and not every trial will achieve the expected results. 3. The threat of cancer is too great, and patients are often unable to overcome the psychological pressure to face the clinical trials, which is a great obstacle to the development of the trials and the collection of data in later stages. Therefore, a commonly used natural product targeting the ERS apoptotic pathway, such as bufalin, first needs to be selected for drug development. The next crucial step is conducting large-scale clinical studies and evidence-based medical research to identify drugs that effectively treat malignant tumors. Additionally, there have been limited safety studies on natural products, likely due to the small number of experimental studies on natural products targeting ERS (Atanasov et al., 2021). Therefore, the next step is to perform safety studies and pharmacokinetic and pharmacological analyses of natural products to ensure the safety of natural products.

In summary, natural products have the ability to modulate the ERS pathway to promote apoptosis in various cancer cells. Nevertheless, the relevant research content is insufficient, the mechanism is unelucidated, no relevant clinical studies have been performed, and safety studies are inadequate. The next step is to identify an effective natural product that targets ERS and to conduct quantitative cellular or animal experiments on one type of tumor cell from common cancer types or many different types of tumor cells from various cancer types to clarify the three ERS apoptotic pathways, focusing on the ATF6-related apoptotic pathway. Then, evidence-based medical research, clinical trials, safety testing, and pharmacokinetic and pharmacological analyses of natural products can be executed to develop novel drugs and optimize the antitumor effects of natural products.

Author contributions

J-XZ: Investigation, Writing–original draft, Writing–review and editing. W-CY: Investigation, Writing–original draft, Writing–review and editing. C-GL: Investigation, Supervision, Writing–review and editing. H-YZ: Investigation, Supervision, Writing–review and editing. S-YH: Conceptualization, Methodology, Supervision, Writing–review and editing. X-HL: Conceptualization, Methodology, Supervision, Writing–review and editing.

Funding

The authors declare that no financial support was received for the research, authorship, and/or publication of this article.

Conflict of interest

The authors declare that the research was conducted in the absence of any commercial or financial relationships that could be construed as a potential conflict of interest.

Publisher's note

All claims expressed in this article are solely those of the authors and do not necessarily represent those of their affiliated organizations, or those of the publisher, the editors and the reviewers. Any product that may be evaluated in this article, or claim that may be made by its manufacturer, is not guaranteed or endorsed by the publisher.

References

Atanasov, A. G., Zotchev, S. B., Dirsch, V. M., International Natural Product Sciences, T., and Supuran, C. T. (2021). Natural products in drug discovery: advances and opportunities. *Nat. Rev. Drug Discov.* 20 (3), 200–216. doi:10.1038/s41573-020-00114-z

Bobrovnikova-Marjon, E., Grigoriadou, C., Pytel, D., Zhang, F., Ye, J., Koumenis, C., et al. (2010). PERK promotes cancer cell proliferation and tumor growth by limiting oxidative DNA damage. *Oncogene* 29 (27), 3881–3895. doi:10.1038/onc.2010.153

Boonnate, P., Kariya, R., and Okada, S. (2023). Shikonin induces ROS-dependent apoptosis via mitochondria depolarization and ER stress in Adult T cell leukemia/lymphoma. *Antioxidants (Basel)* 12 (4), 864. doi:10.3390/antiox12040864

Boyce, M., and Yuan, J. (2006). Cellular response to endoplasmic reticulum stress: a matter of life or death. *Cell Death Differ.* 13 (3), 363–373. doi:10.1038/sj.cdd.4401817

Cao, A., Li, Q., Yin, P., Dong, Y., Shi, H., Wang, L., et al. (2013). Curcumin induces apoptosis in human gastric carcinoma AGS cells and colon carcinoma HT-29 cells through mitochondrial dysfunction and endoplasmic reticulum stress. *Apoptosis* 18 (11), 1391–1402. doi:10.1007/s10495-013-0871-1

Chang, J., Hu, S., Wang, W., Li, Y., Zhi, W., Lu, S., et al. (2018). Matrine inhibits prostate cancer via activation of the unfolded protein response/endoplasmic reticulum stress signaling and reversal of epithelial to mesenchymal transition. *Mol. Med. Rep.* 18 (1), 945–957. doi:10.3892/mmr.2018.9061

Chang, J., Wang, H., Wang, X., Zhao, Y., Zhao, D., Wang, C., et al. (2015). Molecular mechanisms of Polyphyllin I-induced apoptosis and reversal of the epithelial-mesenchymal transition in human osteosarcoma cells. *J. Ethnopharmacol.* 170, 117–127. doi:10.1016/j.jep.2015.05.006

Chen, H., Yang, J., Hao, J., Lv, Y., Chen, L., Lin, Q., et al. (2019). A novel flavonoid kushenol Z from Sophora flavescens mediates mTOR pathway by inhibiting phosphodiesterase and Akt activity to induce apoptosis in non-small-cell lung cancer cells. *Molecules* 24 (24), 4425. doi:10.3390/molecules24244425

Chen, M., Liu, Y., Yang, Y., Qiu, Y., Wang, Z., Li, X., et al. (2022). Emerging roles of activating transcription factor (ATF) family members in tumourigenesis and immunity: implications in cancer immunotherapy. *Genes Dis.* 9 (4), 981–999. doi:10.1016/j.gendis.2021.04.008

Chen, M. C., Hsu, H. H., Chu, Y. Y., Cheng, S. F., Shen, C. Y., Lin, Y. J., et al. (2018). Lupeol alters ER stress-signaling pathway by downregulating ABCG2 expression to induce Oxaliplatin-resistant LoVo colorectal cancer cell apoptosis. *Environ. Toxicol.* 33 (5), 587–593. doi:10.1002/tox.22544

Chen, P., Li, Y., Zhou, Z., Pan, C., and Zeng, L. (2023). Lathyrol promotes ER stress-induced apoptosis and proliferation inhibition in lung cancer cells by targeting SERCA2. *Biomed. Pharmacother.* 158, 114123. doi:10.1016/j.biopha.2022.114123

Chen, P. P., Ma, X. Y., Lin, Q., Xu, H. L., Shi, H. X., Zhang, H. Y., et al. (2017). Kangfuxin promotes apoptosis of gastric cancer cells through activating ER-stress and autophagy. *Mol. Med. Rep.* 16 (6), 9043–9050. doi:10.3892/mmr.2017.7716

Chen, X., and Cubillos-Ruiz, J. R. (2021). Endoplasmic reticulum stress signals in the tumour and its microenvironment. *Nat. Rev. Cancer* 21 (2), 71–88. doi:10.1038/s41568-020-00312-2

Cubillos-Ruiz, J. R., Bettigole, S. E., and Glimcher, L. H. (2017). Tumorigenic and immunosuppressive effects of endoplasmic reticulum stress in cancer. *Cell* 168 (4), 692–706. doi:10.1016/j.cell.2016.12.004

Du, J., Song, D., Cao, T., Li, Y., Liu, J., Li, B., et al. (2021). Saikosaponin-A induces apoptosis of cervical cancer through mitochondria- and endoplasmic reticulum stress-dependent pathway *in vitro* and *in vivo*: involvement of PI3K/AKT signaling pathway. *Cell Cycle* 20 (21), 2221–2232. doi:10.1080/15384101.2021.1974791

Duan, Y. M., Jin, Y., Guo, M. L., Duan, L. X., and Wang, J. G. (2018). Differentially expressed genes of HepG2 cells treated with gecko polypeptide mixture. *J. Cancer* 9 (15), 2723–2733. doi:10.7150/jca.26339

El-Desouky, M. A., Fahmi, A. A., Abdelkader, I. Y., and Nasraldin, K. M. (2020). Anticancer effect of amygdalin (vitamin B-17) on hepatocellular carcinoma cell line (HepG2) in the presence and absence of zinc. *Anticancer Agents Med. Chem.* 20 (4), 486–494. doi:10.2174/1871520620666200120095525

Fabiani, R. (2020). Antitumoral properties of natural products. *Molecules* 25 (3), 650. doi:10.3390/molecules25030650

Feng, L. X., Sun, P., Mi, T., Liu, M., Liu, W., Yao, S., et al. (2016). Agglutinin isolated from Arisema heterophyllum Blume induces apoptosis and autophagy in A549 cells through inhibiting PI3K/Akt pathway and inducing ER stress. *Chin. J. Nat. Med.* 14 (11), 856–864. doi:10.1016/S1875-5364(16)30102-9

Groenendyk, J., Agellon, L. B., and Michalak, M. (2021). Calcium signaling and endoplasmic reticulum stress. *Int. Rev. Cell Mol. Biol.* 363, 1–20. doi:10.1016/bs.ircmb.2021.03.003

Gu, Q., Zhu, C., Wu, X., Peng, L., Huang, G., and Hu, R. (2021). Wogonoside promotes apoptosis and ER stress in human gastric cancer cells by regulating the IRE1α pathway. *Exp. Ther. Med.* 21 (4), 411. doi:10.3892/etm.2021.9842

Hsu, H. Y., Lin, T. Y., Hu, C. H., Shu, D. T. F., and Lu, M. K. (2018). Fucoidan upregulates TLR4/CHOP-mediated caspase-3 and PARP activation to enhance cisplatin-induced cytotoxicity in human lung cancer cells. *Cancer Lett.* 432, 112–120. doi:10.1016/j.canlet.2018.05.006

Hu, F., Han, J., Zhai, B., Ming, X., Zhuang, L., Liu, Y., et al. (2014). Blocking autophagy enhances the apoptosis effect of bufalin on human hepatocellular carcinoma cells through endoplasmic reticulum stress and JNK activation. *Apoptosis* 19 (1), 210–223. doi:10.1007/s10495-013-0914-7

Huang, T. Y., Yang, C. K., Chen, M. Y., Yadav, V. K., Fong, I. H., Yeh, C. T., et al. (2023). Furanocoumarin notopterol: inhibition of hepatocellular carcinogenesis through suppression of cancer stemness signaling and induction of oxidative stress-associated cell death. *Nutrients* 15 (11), 2447. doi:10.3390/nu15112447

Huang, Y. F., Zhu, D. J., Chen, X. W., Chen, Q. K., Luo, Z. T., Liu, C. C., et al. (2017). Curcumin enhances the effects of irinotecan on colorectal cancer cells through the generation of reactive oxygen species and activation of the endoplasmic reticulum stress pathway. *Oncotarget* 8 (25), 40264–40275. doi:10.18632/oncotarget.16828

Huang, Z., Gan, S., Zhuang, X., Chen, Y., Lu, L., Wang, Y., et al. (2022). Artesunate inhibits the cell growth in colorectal cancer by promoting ROS-dependent cell senescence and autophagy. *Cells* 11 (16), 2472. doi:10.3390/cells11162472

Islam, M. R., Akash, S., Rahman, M. M., Nowrin, F. T., Akter, T., Shohag, S., et al. (2022). Colon cancer and colorectal cancer: prevention and treatment by potential natural products. *Chem. Biol. Interact.* 368, 110170. doi:10.1016/j.cbi.2022.110170

Jaud, M., Philippe, C., Di Bella, D., Tang, W., Pyronnet, S., Laurell, H., et al. (2020). Translational regulations in response to endoplasmic reticulum stress in cancers. *Cells* 9 (3), 540. doi:10.3390/cells9030540

Jiang, Y., Jiao, Y., Liu, Y., Zhang, M., Wang, Z., Li, Y., et al. (2018). Sinomenine hydrochloride inhibits the metastasis of human glioblastoma cells by suppressing the expression of matrix metalloproteinase-2/-9 and reversing the endogenous and exogenous epithelial-mesenchymal transition. *Int. J. Mol. Sci.* 19 (3), 844. doi:10.3390/ijms19030844

Kang, N., Cao, S., Jiang, B., Zhang, Q., Donkor, P. O., Zhu, Y., et al. (2020). Cetuximab enhances oridonin-induced apoptosis through mitochondrial pathway and endoplasmic reticulum stress in laryngeal squamous cell carcinoma cells. *Toxicol Vitro* 67, 104885. doi:10.1016/j.tiv.2020.104885

Kim, C., and Kim, B. (2018). Anti-cancer natural products and their bioactive compounds inducing ER stress-mediated apoptosis: a review. *Nutrients* 10 (8), 1021. doi:10.3390/nu10081021

Kim, T. W. (2023). Fisetin, an anti-inflammatory agent, overcomes radioresistance by activating the PERK-ATF4-CHOP Axis in liver cancer. *Int. J. Mol. Sci.* 24 (10), 9076. doi:10.3390/ijms24109076

Kooshki, L., Mahdavi, P., Fakhri, S., Akkol, E. K., and Khan, H. (2022). Targeting lactate metabolism and glycolytic pathways in the tumor microenvironment by natural products: a promising strategy in combating cancer. *Biofactors* 48 (2), 359–383. doi:10.1002/biof.1799

Kuang, H., Sun, X., Liu, Y., Tang, M., Wei, Y., Shi, Y., et al. (2023). Palmitic acid-induced ferroptosis via CD36 activates ER stress to break calcium-iron balance in colon cancer cells. *FEBS J.* 290, 3664–3687. doi:10.1111/febs.16772

Li, K., Zheng, Q., Chen, X., Wang, Y., Wang, D., and Wang, J. (2018). Isobavachalcone induces ROS-mediated apoptosis via targeting thioredoxin reductase 1 in human prostate cancer PC-3 cells. *Oxid. Med. Cell Longev.* 2018, 1915828. doi:10.1155/2018/1915828

Li, M., Duan, F., Pan, Z., Liu, X., Lu, W., Liang, C., et al. (2023). Astragalus polysaccharide promotes doxorubicin-induced apoptosis by reducing O-GlcNAcylation in hepatocellular carcinoma. *Cells* 12 (6), 866. doi:10.3390/cells12060866

Li, S., and Tu, H. (2022). Psoralen inhibits the proliferation and promotes apoptosis through endoplasmic reticulum stress in human osteosarcoma cells. *Folia Histochem Cytobiol.* 60 (1), 101–109. doi:10.5603/FHC.a2022.0010

Li, X., Chen, Q., Liu, J., Lai, S., Zhang, M., Zhen, T., et al. (2022a). Orphan nuclear receptor Nur77 mediates the lethal endoplasmic reticulum stress and therapeutic efficacy of cryptomeridiol in hepatocellular carcinoma. *Cells* 11 (23), 3870. doi:10.3390/cells11233870

Li, Y., Jiang, W., Niu, Q., Sun, Y., Meng, C., Tan, L., et al. (2019). eIF2α-CHOP-BCl-2/JNK and IRE1α-XBP1/JNK signaling promote apoptosis and inflammation and support the proliferation of Newcastle disease virus. *Cell Death Dis.* 10 (12), 891. doi:10.1038/s41419-019-2128-6

Li, Y., Li, S., Meng, X., Gan, R. Y., Zhang, J. J., and Li, H. B. (2017). Dietary natural products for prevention and treatment of breast cancer. *Nutrients* 9 (7), 728. doi:10.3390/nu9070728

Li, Y., Wang, Y., Wang, X., Jin, L., Yang, L., Zhu, J., et al. (2022b). Evodiamine suppresses the progression of non-small cell lung carcinoma via endoplasmic reticulum stress-mediated apoptosis pathway *in vivo* and *in vitro*. *Int. J. Immunopathol. Pharmacol.* 36, 3946320221086079. doi:10.1177/03946320221086079

Liu, J., Huang, X. E., Tian, G. Y., Cao, J., Lu, Y. Y., Wu, X. Y., et al. (2013). Phase II study on safety and efficacy of Yadanzi® (Javanica oil emulsion injection) combined with chemotherapy for patients with gastric cancer. *Asian Pac J. Cancer Prev.* 14 (3), 2009–2012. doi:10.7314/apjcp.2013.14.3.2009

Liu, J., Ren, L., Wang, H., and Li, Z. (2023). Isoquercitrin induces endoplasmic reticulum stress and immunogenic cell death in gastric cancer cells. *Biochem. Genet.* 61 (3), 1128–1142. doi:10.1007/s10528-022-10309-1

Liu, K. C., Lin, Y. J., Hsiao, Y. T., Lin, M. L., Yang, J. L., Huang, Y. P., et al. (2017a). Tetrandrine induces apoptosis in human nasopharyngeal carcinoma NPC-tw 039 cells by endoplasmic reticulum stress and Ca(2+)/calpain pathways. *Anticancer Res.* 37 (11), 6107–6118. doi:10.21873/anticanres.12059

Liu, K. C., Yen, C. Y., Wu, R. S., Yang, J. S., Lu, H. F., Lu, K. W., et al. (2014). The roles of endoplasmic reticulum stress and mitochondrial apoptotic signaling pathway in quercetin-mediated cell death of human prostate cancer PC-3 cells. *Environ. Toxicol.* 29 (4), 428–439. doi:10.1002/tox.21769

Liu, Y., Kang, X., Niu, G., He, S., Zhang, T., Bai, Y., et al. (2019). Shikonin induces apoptosis and prosurvival autophagy in human melanoma A375 cells via ROS-mediated ER stress and p38 pathways. *Artif. Cells Nanomed Biotechnol.* 47 (1), 626–635. doi:10.1080/21691401.2019.1575229

Liu, Y., Wang, X., Qiao, J., Wang, J., Jiang, L., Wang, C., et al. (2022). Ginsenoside Rh2 induces HeLa apoptosis through upregulating endoplasmic reticulum stress-related and downstream apoptotic gene expression. *Molecules* 27 (22), 7865. doi:10.3390/molecules27227865

Liu, Y. H., Weng, Y. P., Lin, H. Y., Tang, S. W., Chen, C. J., Liang, C. J., et al. (2017b). Aqueous extract of Polygonum bistorta modulates proteostasis by ROS-induced ER stress in human hepatoma cells. *Sci. Rep.* 7, 41437. doi:10.1038/srep41437

Luo, H., Vong, C. T., Chen, H., Gao, Y., Lyu, P., Qiu, L., et al. (2019). Naturally occurring anti-cancer compounds: shining from Chinese herbal medicine. *Chin. Med.* 14, 48. doi:10.1186/s13020-019-0270-9

Marciniak, S. J., Chambers, J. E., and Ron, D. (2022). Pharmacological targeting of endoplasmic reticulum stress in disease. *Nat. Rev. Drug Discov.* 21 (2), 115–140. doi:10.1038/s41573-021-00320-3

Miller, K. D., Nogueira, L., Devasia, T., Mariotto, A. B., Yabroff, K. R., Jemal, A., et al. (2022). Cancer treatment and survivorship statistics, 2022. *CA Cancer J. Clin.* 72 (5), 409–436. doi:10.3322/caac.21731

Oakes, S. A. (2020). Endoplasmic reticulum stress signaling in cancer cells. *Am. J. Pathol.* 190 (5), 934–946. doi:10.1016/j.ajpath.2020.01.010

Oakes, S. A., and Papa, F. R. (2015). The role of endoplasmic reticulum stress in human pathology. *Annu. Rev. Pathol.* 10, 173–194. doi:10.1146/annurev-pathol-012513-104649

Pan, J. M., Zhou, L., Wang, G. B., Xia, G. W., Xue, K., Cui, X. G., et al. (2015). Fatsioside A inhibits the growth of glioma cells via the induction of endoplasmic reticulum stress-mediated apoptosis. *Mol. Med. Rep.* 11 (5), 3493–3498. doi:10.3892/mmr.2015.3213

Pan, T. L., Wang, P. W., Hung, Y. C., Huang, C. H., and Rau, K. M. (2013). Proteomic analysis reveals tanshinone IIA enhances apoptosis of advanced cervix carcinoma CaSki cells through mitochondria intrinsic and endoplasmic reticulum stress pathways. *Proteomics* 13 (23-24), 3411–3423. doi:10.1002/pmic.201300274

Pu, H., Qian, Q., Wang, F., Gong, M., and Ge, X. (2021). Schizandrin A induces the apoptosis and suppresses the proliferation, invasion and migration of gastric cancer cells by activating endoplasmic reticulum stress. *Mol. Med. Rep.* 24 (5), 787. doi:10.3892/mmr.2021.12427

Qi, H., Zhang, X., Liu, H., Han, M., Tang, X., Qu, S., et al. (2022). Shikonin induced apoptosis mediated by endoplasmic reticulum stress in colorectal cancer cells. *J. Cancer* 13 (1), 243–252. doi:10.7150/jca.65297

Qi, W., Li, Z., Yang, C., Jiangshan Dai, J., Zhang, Q., Wang, D., et al. (2020). Inhibitory mechanism of muscone in liver cancer involves the induction of apoptosis and autophagy. *Oncol. Rep.* 43 (3), 839–850. doi:10.3892/or.2020.7484

Qin, Y. U., Wang, H., Liu, Z. Y., Liu, J., and Wu, J. Z. (2015). Realgar quantum dots induce apoptosis and necrosis in HepG2 cells through endoplasmic reticulum stress. *Biomed. Rep.* 3 (5), 657–662. doi:10.3892/br.2015.489

Ren, B., Liu, H., Gao, H., Liu, S., Zhang, Z., Fribley, A. M., et al. (2017). Celastrol induces apoptosis in hepatocellular carcinoma cells via targeting ER-stress/UPR. *Oncotarget* 8 (54), 93039–93050. doi:10.18632/oncotarget.21750

Rong, C., Wei, W., and Yu-Hong, T. (2020). Asperuloside exhibits a novel anti-leukemic activity by triggering ER stress-regulated apoptosis via targeting GRP78. *Biomed. Pharmacother.* 125, 109819. doi:10.1016/j.biopha.2020.109819

Rozpedek, W., Pytel, D., Mucha, B., Leszczynska, H., Diehl, J. A., and Majsterek, I. (2016). The role of the PERK/eIF2α/ATF4/CHOP signaling pathway in tumor progression during endoplasmic reticulum stress. *Curr. Mol. Med.* 16 (6), 533–544. doi:10.2174/1566524016666160523143937

Sauter, E. R. (2020). Cancer prevention and treatment using combination therapy with natural compounds. *Expert Rev. Clin. Pharmacol.* 13 (3), 265–285. doi:10.1080/17512433.2020.1738218

Shen, S., Zhang, Y., Wang, Z., Liu, R., and Gong, X. (2014). Bufalin induces the interplay between apoptosis and autophagy in glioma cells through endoplasmic reticulum stress. *Int. J. Biol. Sci.* 10 (2), 212–224. doi:10.7150/ijbs.8056

Shi, W., Han, H., Zou, J., Zhang, Y., Li, H., Zhou, H., et al. (2021). Identification of dihydrotanshinone I as an ERp57 inhibitor with anti-breast cancer properties via the UPR pathway. *Biochem. Pharmacol.* 190, 114637. doi:10.1016/j.bcp.2021.114637

Shi, Y., Ma, J., Chen, K. E., and Chen, B. (2022). Konjac glucomannan enhances 5-FU-induced cytotoxicity of hepatocellular carcinoma cells via TLR4/PERK/CHOP signaling to induce endoplasmic reticulum stress. *Oncol. Res.* 30 (4), 201–210. doi:10.32604/or.2022.027584

Shu, Y. H., Yuan, H. H., Xu, M. T., Hong, Y. T., Gao, C. C., Wu, Z. P., et al. (2021). A novel Diels-Alder adduct of mulberry leaves exerts anticancer effect through autophagy-mediated cell death. *Acta Pharmacol. Sin.* 42 (5), 780–790. doi:10.1038/s41401-020-0492-5

Song, J., Ding, W., Liu, B., Liu, D., Xia, Z., Zhang, L., et al. (2020). Anticancer effect of caudatin in diethylnitrosamine-induced hepatocarcinogenesis in rats. *Mol. Med. Rep.* 22 (2), 697–706. doi:10.3892/mmr.2020.11135

Song, J., Xu, X., He, S., Wang, N., Bai, Y., Chen, Z., et al. (2023). Myristicin suppresses gastric cancer growth via targeting the EGFR/ERK signaling pathway. *Curr. Mol. Pharmacol.* 16 (7), 712–724. doi:10.2174/1874467216666230103104600

Song, M. Z., Zhang, F. L., and Lin, L. J. (2019). (3R)-5,6,7-trihydroxy-3-isopropyl-3-methylisochroman-1-one inhibited osteosarcoma growth by inducing apoptosis. *Exp. Ther. Med.* 18 (2), 1107–1114. doi:10.3892/etm.2019.7681

Su, J., Xu, T., Jiang, G., Hou, M., Liang, M., Cheng, H., et al. (2019). Gambogenic acid triggers apoptosis in human nasopharyngeal carcinoma CNE-2Z cells by activating volume-sensitive outwardly rectifying chloride channel. *Fitoterapia* 133, 150–158. doi:10.1016/j.fitote.2019.01.002

Sun, J., Li, J., Kong, X., and Guo, Q. (2023). Peimine inhibits MCF-7 breast cancer cell growth by modulating inflammasome activation: critical roles of MAPK and NF-κB signaling. *Anticancer Agents Med. Chem.* 23 (3), 317–327. doi:10.2174/1871520622666220324100510

Sung, H., Ferlay, J., Siegel, R. L., Laversanne, M., Soerjomataram, I., Jemal, A., et al. (2021). Global cancer statistics 2020: GLOBOCAN estimates of incidence and mortality worldwide for 36 cancers in 185 countries. *CA Cancer J. Clin.* 71 (3), 209–249. doi:10.3322/caac.21660

Tan, B., Jia, R., Wang, G., and Yang, J. (2018). Astragaloside attenuates the progression of prostate cancer cells through endoplasmic reticulum stress pathways. *Oncol. Lett.* 16 (3), 3901–3906. doi:10.3892/ol.2018.9071

Tan, G. X., Wang, X. N., Tang, Y. Y., Cen, W. J., Li, Z. H., Wang, G. C., et al. (2019). PP-22 promotes autophagy and apoptosis in the nasopharyngeal carcinoma cell line CNE-2 by inducing endoplasmic reticulum stress, downregulating STAT3 signaling, and modulating the MAPK pathway. *J. Cell Physiol.* 234 (3), 2618–2630. doi:10.1002/jcp.27076

Tewari, D., Patni, P., Bishayee, A., Sah, A. N., and Bishayee, A. (2022). Natural products targeting the PI3K-Akt-mTOR signaling pathway in cancer: a novel therapeutic strategy. *Semin. Cancer Biol.* 80, 1–17. doi:10.1016/j.semcancer.2019.12.008

Tsai, C. W., Yang, M. D., Hsia, T. C., Chang, W. S., Hsu, C. M., Hsieh, Y. H., et al. (2017a). Dithiothreitol enhanced arsenic-trioxide-induced cell apoptosis in cultured oral cancer cells via mitochondrial dysfunction and endoplasmic reticulum stress. *Environ. Toxicol.* 32 (1), 17–27. doi:10.1002/tox.22208

Tsai, S. F., Tao, M., Ho, L. I., Chiou, T. W., Lin, S. Z., Su, H. L., et al. (2017b). Isochaihulactone-induced DDIT3 causes ER stress-PERK independent apoptosis in glioblastoma multiforme cells. *Oncotarget* 8 (3), 4051–4061. doi:10.18632/oncotarget.13266

Urano, F., Bertolotti, A., and Ron, D. (2000a). IRE1 and efferent signaling from the endoplasmic reticulum. *J. Cell Sci.* 113 Pt 21, 3697–3702. doi:10.1242/jcs.113.21.3697

Urano, F., Wang, X., Bertolotti, A., Zhang, Y., Chung, P., Harding, H. P., et al. (2000b). Coupling of stress in the ER to activation of JNK protein kinases by transmembrane protein kinase IRE1. *Science* 287 (5453), 664–666. doi:10.1126/science.287.5453.664

Voskoglou-Nomikos, T., Pater, J. L., and Seymour, L. (2003). Clinical predictive value of the *in vitro* cell line, human xenograft, and mouse allograft preclinical cancer models. *Clin. Cancer Res.* 9 (11), 4227–4239.

Walter, P., and Ron, D. (2011). The unfolded protein response: from stress pathway to homeostatic regulation. *Science* 334 (6059), 1081–1086. doi:10.1126/science.1209038

Wang, S., Fu, J. L., Hao, H. F., Jiao, Y. N., Li, P. P., and Han, S. Y. (2021). Metabolic reprogramming by traditional Chinese medicine and its role in effective cancer therapy. *Pharmacol. Res.* 170, 105728. doi:10.1016/j.phrs.2021.105728

Wang, W. B., Feng, L. X., Yue, Q. X., Wu, W. Y., Guan, S. H., Jiang, B. H., et al. (2012). Paraptosis accompanied by autophagy and apoptosis was induced by celastrol, a natural compound with influence on proteasome, ER stress and Hsp90. *J. Cell Physiol.* 227 (5), 2196–2206. doi:10.1002/jcp.22956

Wang, X., He, M. J., Chen, X. J., Bai, Y. T., and Zhou, G. (2022). Glaucocalyxin A impairs tumor growth via amplification of the ATF4/CHOP/CHAC1 cascade in human oral squamous cell carcinoma. *J. Ethnopharmacol.* 290, 115100. doi:10.1016/j.jep.2022.115100

Wang, X., Peng, P., Pan, Z., Fang, Z., Lu, W., and Liu, X. (2019). Psoralen inhibits malignant proliferation and induces apoptosis through triggering endoplasmic reticulum stress in human SMMC7721 hepatoma cells. *Biol. Res.* 52 (1), 34. doi:10.1186/s40659-019-0241-8

Wang, Y., Shen, J., Arenzana, N., Tirasophon, W., Kaufman, R. J., and Prywes, R. (2000). Activation of ATF6 and an ATF6 DNA binding site by the endoplasmic reticulum stress response. *J. Biol. Chem.* 275 (35), 27013–27020. doi:10.1074/jbc.M003322200

Wang, Z., Jiang, C., Chen, W., Zhang, G., Luo, D., Cao, Y., et al. (2014). Baicalein induces apoptosis and autophagy via endoplasmic reticulum stress in hepatocellular carcinoma cells. *Biomed. Res. Int.* 2014, 732516. doi:10.1155/2014/732516

Wu, C., Huang, H., Choi, H. Y., Ma, Y., Zhou, T., Peng, Y., et al. (2021). Anti-esophageal cancer effect of corilagin extracted from phmllanthi fructus via the mitochondrial and endoplasmic reticulum stress pathways. *J. Ethnopharmacol.* 269, 113700. doi:10.1016/j.jep.2020.113700

Wu, K., Huang, J., Li, N., Xu, T., Cai, W., and Ye, Z. (2018). Antitumor effect of ginsenoside Rg3 on gallbladder cancer by inducing endoplasmic reticulum stress-mediated apoptosis *in vitro* and *in vivo*. *Oncol. Lett.* 16 (5), 5687–5696. doi:10.3892/ol.2018.9331

Xia, C., Dong, X., Li, H., Cao, M., Sun, D., He, S., et al. (2022a). Cancer statistics in China and United States, 2022: profiles, trends, and determinants. *Chin. Med. J. Engl.* 135 (5), 584–590. doi:10.1097/CM9.0000000000002108

Xia, F., Sun, S., Xia, L., Xu, X., Hu, G., Wang, H., et al. (2022b). Traditional Chinese medicine suppressed cancer progression by targeting endoplasmic reticulum stress responses: a review. *Med. Baltim.* 101 (51), e32394. doi:10.1097/MD.0000000000032394

Xiang, Y., Guo, Z., Zhu, P., Chen, J., and Huang, Y. (2019). Traditional Chinese medicine as a cancer treatment: modern perspectives of ancient but advanced science. *Cancer Med.* 8 (5), 1958–1975. doi:10.1002/cam4.2108

Xiao, B., Liu, C., Liu, B. T., Zhang, X., Liu, R. R., and Zhang, X. W. (2016). TTF1-NPs induce ERS-mediated apoptosis and inhibit human hepatoma cell growth *in vitro* and *in vivo*. *Oncol. Res.* 23 (6), 311–320. doi:10.3727/096504016X14567549091341

Xiao, Y., Ma, D., Wang, H., Wu, D., Chen, Y., Ji, K., et al. (2017). Matrine suppresses the ER-positive MCF cells by regulating energy metabolism and endoplasmic reticulum stress signaling pathway. *Phytother. Res.* 31 (4), 671–679. doi:10.1002/ptr.5785

Xie, H., Li, X., Chen, Y., Lang, M., Shen, Z., and Shi, L. (2019). Ethanolic extract of Cordyceps cicadae exerts antitumor effect on human gastric cancer SGC-7901 cells by inducing apoptosis, cell cycle arrest and endoplasmic reticulum stress. *J. Ethnopharmacol.* 231, 230–240. doi:10.1016/j.jep.2018.11.028

Xu, W., Li, T., Qiu, J. F., Wu, S. S., Huang, M. Q., Lin, L. G., et al. (2015). Anti-proliferative activities of terpenoids isolated from Alisma orientalis and their structure-activity relationships. *Anticancer Agents Med. Chem.* 15 (2), 228–235. doi:10.2174/1871520614666140601213514

Xu, Y., Xie, Q., Wu, S., Yi, D., Yu, Y., Liu, S., et al. (2016). Myricetin induces apoptosis via endoplasmic reticulum stress and DNA double-strand breaks in human ovarian cancer cells. *Mol. Med. Rep.* 13 (3), 2094–2100. doi:10.3892/mmr.2016.4763

Xue, G. M., Zhu, D. R., Han, C., Wang, X. B., Luo, J. G., and Kong, L. Y. (2019). Artemisianins A-D, new stereoisomers of seco-guaianolide involved heterodimeric [4+2] adducts from Artemisia argyi induce apoptosis via enhancement of endoplasmic reticulum stress. *Bioorg Chem.* 84, 295–301. doi:10.1016/j.bioorg.2018.11.013

Yang, B., Yu, G. H., Li, M. Y., Gu, H. M., Chen, Y. P., Feng, L., et al. (2019). Mechanism of flavonoid components in Astragali Radix in inhibiting tumor growth and immunoregulation in C57BL/6 tumor bearing mice based on "invigorating Qi for consolidation of exterior". *Zhongguo Zhong Yao Za Zhi* 44 (23), 5184–5190. doi:10.19540/j.cnki.cjcmm.20191104.401

Yang, J., Hasenbilige, Bao, S., Luo, S., Jiang, L., Li, Q., et al. (2023). Inhibition of ATF4-mediated elevation of both autophagy and AKT/mTOR was involved in antitumorigenic activity of curcumin. *Food Chem. Toxicol.* 173, 113609. doi:10.1016/j.fct.2023.113609

Yang, Y., Liu, Y., Zhang, Y., Ji, W., Wang, L., and Lee, S. C. (2021). Periplogenin activates ROS-ER stress pathway to trigger apoptosis via BIP-eIF2α- CHOP and ire1α-ASK1-JNK signaling routes. *Anticancer Agents Med. Chem.* 21 (1), 61–70. doi:10.2174/1871520620666200708104559

Yu, L., Jiang, B., Chen, Z., Wang, X., Shang, D., Zhang, X., et al. (2018). Cytisine induces endoplasmic reticulum stress caused by calcium overload in HepG2 cells. *Oncol. Rep.* 39 (3), 1475–1484. doi:10.3892/or.2018.6200

Yuan, M., Zhang, G., Bai, W., Han, X., Li, C., and Bian, S. (2022a). The role of bioactive compounds in natural products extracted from plants in cancer treatment and their mechanisms related to anticancer effects. *Oxid. Med. Cell Longev.* 2022, 1429869. doi:10.1155/2022/1429869

Yuan, S., Pan, Y., Xu, T., Zhang, L., Chen, X., Wang, F., et al. (2022b). Daurisoline inhibits ESCC by inducing G1 cell cycle arrest and activating ER stress to trigger noxa-dependent intrinsic and CHOP-DR5-Dependent extrinsic apoptosis via p-eIF2α-ATF4 Axis. *Oxid. Med. Cell Longev.* 2022, 5382263. doi:10.1155/2022/5382263

Yuan, Y., Guo, Y., Guo, Z. W., Hao, H. F., Jiao, Y. N., Deng, X. X., et al. (2023a). Marsdenia tenacissima extract induces endoplasmic reticulum stress-associated immunogenic cell death in non-small cell lung cancer cells through targeting AXL. *J. Ethnopharmacol.* 314, 116620. doi:10.1016/j.jep.2023.116620

Yuan, Y., Long, H., Zhou, Z., Fu, Y., and Jiang, B. (2023b). PI3K-AKT-Targeting breast cancer treatments: natural products and synthetic compounds. *Biomolecules* 13 (1), 93. doi:10.3390/biom13010093

Zhai, B., Hu, F., Yan, H., Zhao, D., Jin, X., Fang, T., et al. (2015). Bufalin reverses resistance to sorafenib by inhibiting Akt activation in hepatocellular carcinoma: the role of endoplasmic reticulum stress. *PLoS One* 10 (9), e0138485. doi:10.1371/journal.pone.0138485

Zhai, B., Zhang, N., Han, X., Li, Q., Zhang, M., Chen, X., et al. (2019). Molecular targets of beta-elemene, a herbal extract used in traditional Chinese medicine, and its potential role in cancer therapy: a review. *Biomed. Pharmacother.* 114, 108812. doi:10.1016/j.biopha.2019.108812

Zhang, X. Q., Li, Y., Liu, J., Zhao, T. M., Zhao, R. X., Zheng, S. G., et al. (2019). Quantitative proteomics of inhibitory mechanism of Dendrobium denneanum ether extract on lung cancer cells. *Zhongguo Zhong Yao Za Zhi* 44 (4), 765–773. doi:10.19540/j.cnki.cjcmm.20181031.004

Zhang, Y., Li, S., He, H., Han, Q., Wang, B., and Zhu, Y. (2017). Influence of Tanshinone IIA on apoptosis of human esophageal carcinoma Eca-109 cells and its molecular mechanism. *Thorac. Cancer* 8 (4), 296–303. doi:10.1111/1759-7714.12441

Zhao, L., and Ackerman, S. L. (2006). Endoplasmic reticulum stress in health and disease. *Curr. Opin. Cell Biol.* 18 (4), 444–452. doi:10.1016/j.ceb.2006.06.005

Zhao, M., Chen, Q., Xu, W., Wang, H., Che, Y., Wu, M., et al. (2019). Total ginsenosides extract induce autophagic cell death in NSCLC cells through activation of endoplasmic reticulum stress. *J. Ethnopharmacol.* 243, 112093. doi:10.1016/j.jep.2019.112093

Zheng, Y., Liu, P., Wang, N., Wang, S., Yang, B., Li, M., et al. (2019). Betulinic acid suppresses breast cancer metastasis by targeting GRP78-mediated glycolysis and ER stress apoptotic pathway. *Oxid. Med. Cell Longev.* 2019, 8781690. doi:10.1155/2019/8781690

Zhou, F., Gao, H., Shang, L., Li, J., Zhang, M., Wang, S., et al. (2023). Oridonin promotes endoplasmic reticulum stress via TP53-repressed TCF4 transactivation in colorectal cancer. *J. Exp. Clin. Cancer Res.* 42 (1), 150. doi:10.1186/s13046-023-02702-4

Zhou, X., Wang, X., Sun, Q., Zhang, W., Liu, C., Ma, W., et al. (2022). Natural compounds: a new perspective on targeting polarization and infiltration of tumor-associated macrophages in lung cancer. *Biomed. Pharmacother.* 151, 113096. doi:10.1016/j.biopha.2022.113096

Zhou, X. H., Kang, J., Zhong, Z. D., and Cheng, Y. (2021). Osthole induces apoptosis of the HT-29 cells via endoplasmic reticulum stress and autophagy. *Oncol. Lett.* 22 (4), 726. doi:10.3892/ol.2021.12987

Zhu, D., Chen, C., Xia, Y., Kong, L. Y., and Luo, J. (2019). A purified resin glycoside fraction from Pharbitidis semen induces paraptosis by activating chloride Intracellular Channel-1 in human colon cancer cells. *Integr. Cancer Ther.* 18, 1534735418822120. doi:10.1177/1534735418822120

Zhu, J., Chen, M., Chen, N., Ma, A., Zhu, C., Zhao, R., et al. (2015). Glycyrrhetinic acid induces G1-phase cell cycle arrest in human non-small cell lung cancer cells through endoplasmic reticulum stress pathway. *Int. J. Oncol.* 46 (3), 981–988. doi:10.3892/ijo.2015.2819

Glossary

5-FU	5-Fluorouracil
ABCG2	ATP-binding cassette, subfamily G (WHITE), member 2
AIF	Apoptosis Inducing Factor
Akt	protein kinase B
AMPK	AMP-activated protein kinase
ASK1	apoptosis signal-regulating kinase 1
ATF4	activating transcription Factor 4
ATF6	activating transcription Factor 6
Atg5	autophagy-related protein 5
ATG7	Autophagy Related Protein 7
ATLL	Adult T cell leukaemia/lymphoma
Bax	BCL2-associated X
BBC3	Bcl-2-binding component 3
Bcl-2	B-cell lymphoma-2
BiP	heavy-chain binding protein
Caspase	cysteinyl aspartate specific proteinase
CDK	cyclin-dependent kinases
CDK2	cyclin-dependent kinases 2
CDK4	cyclin-dependent kinases 4
CDK6	cyclin-dependent kinases 6
CHAC1	cation transport regulator-like protein 1
CHOP	C/EBP homologous protein
CLIC1	Chloride Intracellular Channel Protein 1
Cyt C	cytochrome c
DAPK3	death-associated protein kinase 3
DDIT3	DNA damage inducible transcript 3
DNA DSB	DNA double-strand break
DR5	death receptor 5
E2F1	E2F Transcription Factor 1
EDEM1	ER degradation-enhancing alpha-mannosidase-like 1
EEC	ethanolic extract of *C. cicadae*
eIF2α	eukaryotic translation initiation Factor 2 α
EMT	epithelial-mesenchymal transition
ERK	extracellular regulated protein kinases
ERP57	endoplasmic reticulum resident protein 57
ERP72	endoplasmic reticulum resident protein 72
ERS	endoplasmic reticulum stress
FOS	Fos proto-oncogene
GADD34	growth arrest and DNA damage protein 34
GADD153	growth arrest and DNA damage-inducible 153
GBM	glioblastoma multiforme; GDF15, Growth Differentiation Factor 15
GRh2	Ginsenoside Rh2
GRP78	glucose regulated protein 78
GRP94	glucose regulated protein 94
HCC	hepatocellular carcinoma cells
IC_{50}	half maximal inhibitory concentration
IRE1	inositol-requiring enzyme 1
IRE1α	inositol-requiring enzyme 1 α
JNK	c-Jun N-terminal kinase
KGM	Konjac glucomannan
MAPK	mitogen-activated protein kinase
Mcl-1	myeloid cell leukemia-1
MMP	Mitochondrial membrane potential
mTOR	mammalian target of rapamycin
NF-κB	nuclear factor kappa-B
NLRP3	NOD-like receptor pyrindomain-containing protein3
NSCLC	non-small cell lung cancer
PARP	poly ADP-ribose polymerase
PDI	protein disulfide isomerase
PERK	protein kinase R (PKR)-like endoplasmic reticulum kinase
PI3K	phosphatidylinositol 3-kinase
PMAIP	phorbol-12-myristate-13-acetate-induced protein 1
ROS	reactive oxygen species
SERCA2	Ca^{2+}-ATPase 2
TCF4	Transcription factor 4
TLR4	Toll-like receptor 4
TNF	tumor necrosis factor
TP53	Tumor protein p53
TRAF2	TNF receptor-associated Factor 2
TRIB3	Tribbles pseudokinase 3
TrxR1	thioredoxin reductase 1
TTF1-NPs	5,2′,4′-trihydroxy-6,7,5′-trimethoxyflavone nanoparticles
UPR	unfolded protein response
VEGF	vascular endothelial growth factor
VSOR	volume-sensitive outwardly rectifying
XBP1	X-box binding protein 1

frontiers | Frontiers in Oncology

TYPE Original Research
PUBLISHED 06 December 2023
DOI 10.3389/fonc.2023.1322875

OPEN ACCESS

EDITED BY
Pranav Kumar Prabhakar,
Lovely Professional University, India

REVIEWED BY
Ankita Leekha,
University of Houston, United States
Fnu Wahiduzzaman,
St. Jude Children's Research Hospital, United States
Shadab Kazmi,
University of Missouri, United States

*CORRESPONDENCE
Haoli Jiang
alexkeung@sina.com
Rajkuberan Chandrasekaran
kuberan87@gmail.com

RECEIVED 17 October 2023
ACCEPTED 09 November 2023
PUBLISHED 06 December 2023

CITATION
Chandrasekaran R, Krishnan M, Chacko S, Gawade O, Hasan S, Joseph J, George E, Ali N, AlAsmari AF, Patil S and Jiang H (2023) Assessment of anticancer properties of cumin seed (*Cuminum cyminum*) against bone cancer.
Front. Oncol. 13:1322875.
doi: 10.3389/fonc.2023.1322875

Assessment of anticancer properties of cumin seed (*Cuminum cyminum*) against bone cancer

Rajkuberan Chandrasekaran[1]*, Muthukumar Krishnan[2], Sonu Chacko[1], Omkar Gawade[1], Sheik Hasan[1], John Joseph[1], Evelin George[3], Nemat Ali[4], Abdullah F. AlAsmari[4], Sandip Patil[5] and Haoli Jiang[6]*

[1]Department of Biotechnology, Karpagam Academy of Higher Education, Coimbatore, India, [2]Department of Petrochemical Technology, Anna University, Tiruchirappalli, India, [3]Department of Biochemistry, JSS Academy of Higher Education, Mysuru, India, [4]Department of Pharmacology and Toxicology, College of Pharmacy, King Saud University, Riyadh, Saudi Arabia, [5]Department of Haematology and Oncology, Shenzhen Children's Hospital, Shenzhen, China, [6]Department of Orthopedics, the Third People's Hospital of Shenzhen, Shenzhen, China

Introduction: Early-life osteosarcoma is associated with severe morbidity and mortality, particularly affecting young children and adults. The present cancer treatment regimen is exceedingly costly, and medications like ifosfamide, doxorubicin, and cisplatin have unneeded negative effects on the body. With the introduction of hyphenated technology to create medications based on plant molecules, the application of ayurvedic medicine as a new dimension (formulation, active ingredients, and nanoparticles) in the modern period is rapidly growing. The primary source of lead compounds for the development of medications for avariety of ailments is plants and their products. Traditionally, *Cuminum cyminum* (cumin) has been used as medication to treat a variety of illnesses and conditions.

Methods: The cumin seed was successfully extracted with solvents Hexane, Chloroform, Methanol, Ethanol and Acetone. Following the solvent extraction, the extract residue was assayed in MG63 cells for their anti-proliferative properties.

Results: First, we used the [3-(4,5-Dimethylthiazol-2-yl)-2,5-Diphenyltetrazolium Bromide] (MTT) assay to test the extracted residue's cytotoxicity. The results show that hexane extract Half-maximal inhibitory concentration (IC50 86 µG/mL) efficiently inhibits cells by causing programmed cell death. Furthermore, using the Acridine orange/ethidium bromide (AO/EB) staining method, the lactate dehydrogenase assay, and the reactive oxygen species assay using the Dichloro-

dihydro-fluorescein diacetate (DCHFDA) staining method, we have demonstrated that the hexane extract causes apoptosis in MG63 cells. Furthermore, flow cytometry research revealed that the hexane extract stops the cell cycle in the S phase. In addition, the hexane extract limits colony formation and the migration potential as shown by the scratch wound healing assay. Furthermore, the extract from cumin seeds exhibits remarkable bactericidal properties against infections that are resistant to drugs. Gas chromatography analysis was used to quantitatively determine the hexane and methanolic extract based on the experimental data. The primary chemical components of the extract are revealed by the study, and these help the malignant cells heal. The present study finds that there is scientific validity in using cumin seeds as a novel method of anticancer therapy after undergoing both intrinsic and extrinsic research.

KEYWORDS

cumin seed, anticancer, bone, cancer, bacteria, MDR strains

1 Introduction

Osteosarcoma is a bone cancer arising at the ages of 10–14, specifically in children and adolescents, and, even at the age of 50, there is a high risk of suffering osteosarcoma (1). The primary change in the metaphysis of the long bones, followed by accelerated cell division, is responsible for osteosarcoma (2). At this stage, the loss of functionality of the tumor suppressor gene will eventually develop into cancer. In India, the incidence of these cancers varied from 4.7% to 11.6%, with significant morbidity and mortality. However, in recent 5-year reports, the occurrence of these cancers rose to 44% in India compared with that in other countries (3). Henceforth, the demographic data suggest that it is indeed to initiate modernized chemotherapies to counteract the diseases intensively.

Osteosarcoma is now treated with chemotherapy and surgery, as well as medication such as methotrexate, doxorubicin, ifosfamide, and cisplatin (4). However, 70% of patients now have a survival of up to 5 years because of this medication. In addition, acquired chemoresistance has been linked in certain instances to poor prognosis, with a survival rate of only 20 years (5). Creating medications with significant long-term effects and lower toxicity is indeed required to overcome these obstacles and other related side effects.

Many purgative qualities are available for a range of illnesses and disorders through plants and their products. In the past, Ayurveda, an indigenous medical system, was widely utilized throughout the nation (6). All infectious and non-infectious disorders were treated with great efficacy and zero toxicity by Ayurvedic medicine (7). Undeniably, plants are versatile resources that can be developed as lead molecules for treating cancers. For instance, camptothecins (irinotecan and topotecan), taxanes (paclitaxel), epipodophyllotoxins (etoposide), and *Vinca alkaloids* (vincristine and vinblastine) were the drugs derived from the plants that are widely in various types of cancer chemotherapy (8). Plants contain phenols, alkaloids, terpenoids, tannins, proteins, and other biomolecules involving antiproliferative properties (9). Henceforth, understanding the plant's chemical entities and exploring its prospective applications in cancer therapy will eventually develop new drugs with high efficacy and efficiency.

Indian spices are fragrant and have a wide range of purgative qualities that can be used to treat anything from tumors to the common cold (10). Indians use spices as a food element in a variety of culinary preparations. Curcumin, derived from *Curcuma longa*, is a traditional example of Indian spice and an essential anticancer agent against a variety of cancers (11). Similarly, antiproliferative qualities were discovered for capsicum, ginger, garlic, fenugreek, bay leaves, cinnamon, and cumin (12).

Cumin seeds (*Cuminumcyminum* L.) belong to the family of *Apiaceae*; the seeds are an aromatic spice that imparts taste, color, and flavor to food preparations (13). Apart from food preparations, the seed has distinctive medicinal properties due to the rich content of phenols, flavanoids, and terpenes (14). The cumin exhibited strong antagonistic activity against bacterial and fungal pathogens, viral, anticarcinogenic, wound healing, antioxidant, ovicidal, and hypoglycemic activities (15). At the present epoch, microbes tend to acquire resistance against antibiotics, which is a serious concern to the research fraternities (16). The drug-resistant microbes cause severe morbidity in patient's compliance with existing chronic diseases. Therefore, the development of plant-based chemical moieties as a drug will be sustainable for the management of infectious diseases (17). The choice of cumin seed against bone cancer is the incidence of bone cancer in Indians, whereas the cumin seed is used in the food preparations. Henceforth, the clinical relevance of cumin seeds must be critically investigated. With the above rationale, the current studies manifest the anticancer activities of cumin seeds in the MG63 cell line. Although there are consistent reports of cumin seed extracts in various cancers, our study is the first instance to outcome the anticancer activity of cumin seed extract in the osteoblastic model MG63 cell line.

2 Materials and methods

Cell line, chemicals, and reagents were purchased from the authorized agency National Centre for Cell Science (NCCS) Pune India and Sigma-Aldrich Pvt Ltd. Cumin seeds were purchased from local markets in Coimbatore, India.

2.1 Preparation of cumin seed extract

Fresh cumin seeds, free from infection, were purchased and transferred immediately to the laboratory. The seeds were rinsed in deionized water and incubated at 50°C for 24 h and macerated in a blender to obtain fine powder formation. A simple infusion technique is used in the present study to prepare the extracts. Solvents such as ethanol (E), methanol (M), acetone (A), ethyl acetate (EA), and n-hexane (NH) were used in the present study. The rationale for using the solvents was based on the polarity: polar solvents (alcohol), intermediate solvent (A); non-polar solvents (chloroform, hexane). For extract preparation, 100 gm of cumin seed is mixed with 250 mL of respective solvents individually. After the extract preparation, using the rotary vacuum evaporator, the extracts were concentrated to form crude extracts. The obtained extracts were stored in a refrigerator and proceeded for further activities.

2.2 Antibacterial activity of the crude extract

Multidrug-resistant (MDR) strains—*Bacillus flexus* (*B. flexus*) (NCBI accession number MN045189), *Bacillus filamentosus* (*B. filamentosus*) (MN045186), *Pseudomonas stutzeri* (*P. stutzeri*) (MN045185), and *Acinetobacter baumannii* (*A. baumannii*) (MN045188)—were gifts from the Department of Marine Sciences, Bharathidasan University, Tiruchirappalli, India. The disc diffusion method evaluated the cumin seed extracts against the MDR strains (18). Briefly, a sterile nutrient agar plate was inoculated with 1.5×10^8 colony-forming units (CFU/mL) MDR strains, and different concentrations of cumin seed extracts (25 µg mL^{-1}, 50 µg mL^{-1}, 75 µg mL^{-1}, and 100 µg mL^{-1}) were loaded onto the well and incubated at room temperature at 37°C. After the incubation, the zone of inhibition (ZOI) was measured.

2.3 Anticancer activity of cumin seed extract

2.3.1 MTT assay

After the collection of MG63 cells from the NCCS, the cells were maintained in Dulbecco's modified Eagle's medium (DMEM) and kept in a humidified 5% CO_2 incubator at 37°C. After 2 days, the monolayer culture cells were trypsinized and suspended in a 10% growth medium; 100 µL of cell suspension was added to a multi-well plate and incubated in a CO_2 incubator.

By using cyclomixer, 1 mg of cumin seed extract was suspended in Dimethyl sulfoxide (DMSO). A 0.22-µm Millipore syringe filter was used to filter the cumin seed extract to ensure sterility. In the 96-well plates, to the cells, different concentrations of the cumin seed extract (6.25 µg/mL, 12.5 µg/mL, 25 µg/mL, 50 µg/mL, and 100 µg/mL) were added and kept in the incubation. After the incubation, 30 µL of MTT solution was added to all the wells and incubated in a CO_2 incubator for 5 h at 38°C. After the time, to the multi-well plate, 100 µL of Dimethyl sulfoxide (DMSO) was added to solubilize the formazan crystals. At 540-nm wavelength, the absorbance values were measured by using a spectrophotometer (19).

On the basis of the results of the crude extracts, the best solvent extract with a significant Lethal Concentration 50 (LC_{50}) value was chosen and proceeded further for other activities.

2.3.2 AO/EB staining

The cell line cultured in an animal tissue culture flask supplemented with DMEM was maintained in a CO_2 incubator. After attaining 80% confluence, cells were exposed to Lethal Dose 50% (LD_{50}) concentration of cumin extract (NH, 86.13 µg/mL) and incubated for 24 h. The cells were bathed with cold Phosphate-buffered saline (PBS) and stained with Ethidium Bromide (EtBr) (100 µg/mL) and AO (100 µg/mL) at 37°C for 20 min (20). Furthermore, the stained cells were washed and subjected to fluorescence microscopic study by using an Olympus fluorescence microscope.

2.3.3 Lactate dehydrogenase assay

The cultured cells supplemented with DMEM were maintained in a CO_2 incubator. The test was performed with supernatant collected from tissue culture plates which were exposed to different concentrations of hexane extract (6.25 µg/mL, 12.5 µg/mL, 25 µg/mL, 50 µg/mL, and 100 µg/mL). For Optical Density (OD) analysis, a 50-µL sample was added to 1 mL of working reagent and recorded at 340 nm in a spectrophotometer after 1 min of incubation (21).

The activity of lactate dehydrogenase was calculated by using the following formula:

$$\text{lactate dehydrogenase assay(LDH)activity(U/mL)} = ((\Delta OD)/\text{min} \,.\, X3333) \,.$$

2.3.4 *In vitro* ROS measurement using DCFDA staining

The cultured cells supplemented with DMEM were maintained in a CO_2 incubator. The cells were washed and stained with DCFDA, and a 50-µL sample was added and incubated for 35 min (22). After incubation, the unbound dye was washed with PBS, and the fluorescence was captured by Olympus fluorescence. At 470-nm excitation and 635-nm emission, the intensity of fluorescence was measured and expressed in arbitrary units (AU).

2.4 Cell cycle analysis

The MG63 cells at 1×10^6 were cultured in six-well plates and incubated with NH extract of 86.13 µg/mL for 24 h. After the period, the cells were washed, centrifuged, resuspended in E, and kept incubated at −20°C. After incubation, the cells were centrifuged, and, to the pellet, PBS and cell cycle reagent of 250 µL were added and incubated in the dark for 30 min (23). A flow cytometer was used to analyze the treated and untreated cells.

2.5 Scratch assay

For the assay, MG63 cells at a density of 300,000 cells per well were seeded into a multi-well plate for 24 h of incubation (24). Using a sterile pipette tip, a wound was made by scratching the cells. After scratches, the debris was removed and the cell was washed with PBS, followed by incubation with NH extract of 86.13 µg/mL at varying time intervals (0 h–24 h–48 h–72 h–96 h). The wound areas were annotated by capturing the images, and the effect of the hexane extract on wound closure was determined microscopically (×4 magnification, Olympus CKX41) and calculated using MRI-ImageJ analysis software.

2.6 Clonogenic assay

The cells at a density of 1×10^3 cells were treated with the hexane extract and kept in a CO_2 incubator for 24 h. After that time, the medium was replenished with the new medium and again incubated for 5 days. After the period, the medium was changed and washed with PBS buffer, and the cells were fixed with fixative formaldehyde for 2 h at 37°C and stained with crystal violet for 30 min. The assay was made in triplicate, and colonies with 50 cells were counted (25).

2.7 GC-MS analysis

The Gas chromatography-Mass spectrometry (GC-MS) analysis was done for the extracts of M and NH. The analysis was performed with the instrument GC-MS QP 2010 (Shimadzu) with the standard operating conditions and analyzed with the previously reported methodology (26). The results were compared, and the compounds were identified using the Spectral Library search program of the National Institute of Standards and Technology (NIST).

3 Results and discussion

Humans underuse, overuse, and misuse antibiotics, which pave the way for developing resistance in microbes (27). In general, MDR strains cannot be controlled with standard drugs, increasing the risk of infection to others (28). The globally emerging MDR strains make the treatment difficult to control and speed up the infection persistency (29). Henceforth, the emergence of these superbugs should be controlled with the development of novel antimicrobial drugs from natural bioresources. Plants with diverse, unique natural secondary metabolites possess various therapeutic properties. MDR strains can be substantially controlled by phytochemicals derived from plant resources effectively.

3.1 Antimicrobial activity

The present study evaluated the cumin seed extracts against the MDR pathogen B. *flexus* (MN045189), *B. filamentosus* (MN045186), *P. stutzeri* (MN045185), and *A. baumannii* (MN045188) by the disc diffusion method. As a result, the cumin extracts displayed strong antagonistic activity against the MDR pathogens. As illustrated in Figure 1, at varying dosage levels (25 µg/mL to 100 µg/mL), the cumin extracts performed concentration-dependent activity against the bacterium. The order of efficacy was observed to be high in M extract > ethanol extract > hexane extract > A extract > EA. The M extract performed superior activity against all the tested pathogens. In particular, the M extract displayed stupendous activity in *P. stutzeri* > *B. filamentosus* > *A. baumannii* > *B. flexus*. In our observation, the M extract performed effectively inhibitory against the tested pathogens. This is due to the presence of biomolecules trapped in the M solvent. The reason for the elevated bactericidal activity is M is a polar solvent that can efficiently trap the low–molecular weight polyphenols from the cumin seed. Therefore, the active constituents in the M extract interact with various biomolecules (DNA/RNA/proteins) of bacterial cells and inhibit the functions, which lead to cell death (30) A similar kind of pattern of observations was noticed in the bactericidal activity of Cuminumcyminum oil against MDR *S. aureus* (31). Likewise, consistent reports documented *C. cyminum* oils as strong bactericidal agents in variant pathogens (32). Still, our study is the first to demonstrate cumin seed extract's antibacterial activity against MDR pathogens.

3.2 Anticancer activity of cumin seed extract

3.2.1 Cytotoxicity assay

The cytotoxicity of cumin seed (E, M, EA, NH, and A) extracts was evaluated by MTT assay against the MG63 cell line. The MTT assay is a preliminary assay to intrigue the toxic potential of the extracted solvent residue against the cell line. The cumin seed (E, M, EA, NH, and A) extracts at the respective concentrations (6.25 µg/mL to 100 µg/mL) were evaluated, and the result is displayed in Figures 2A–E. The cumin seed extract performed significant inhibitory activity against the MG63 cells to dose concentration.

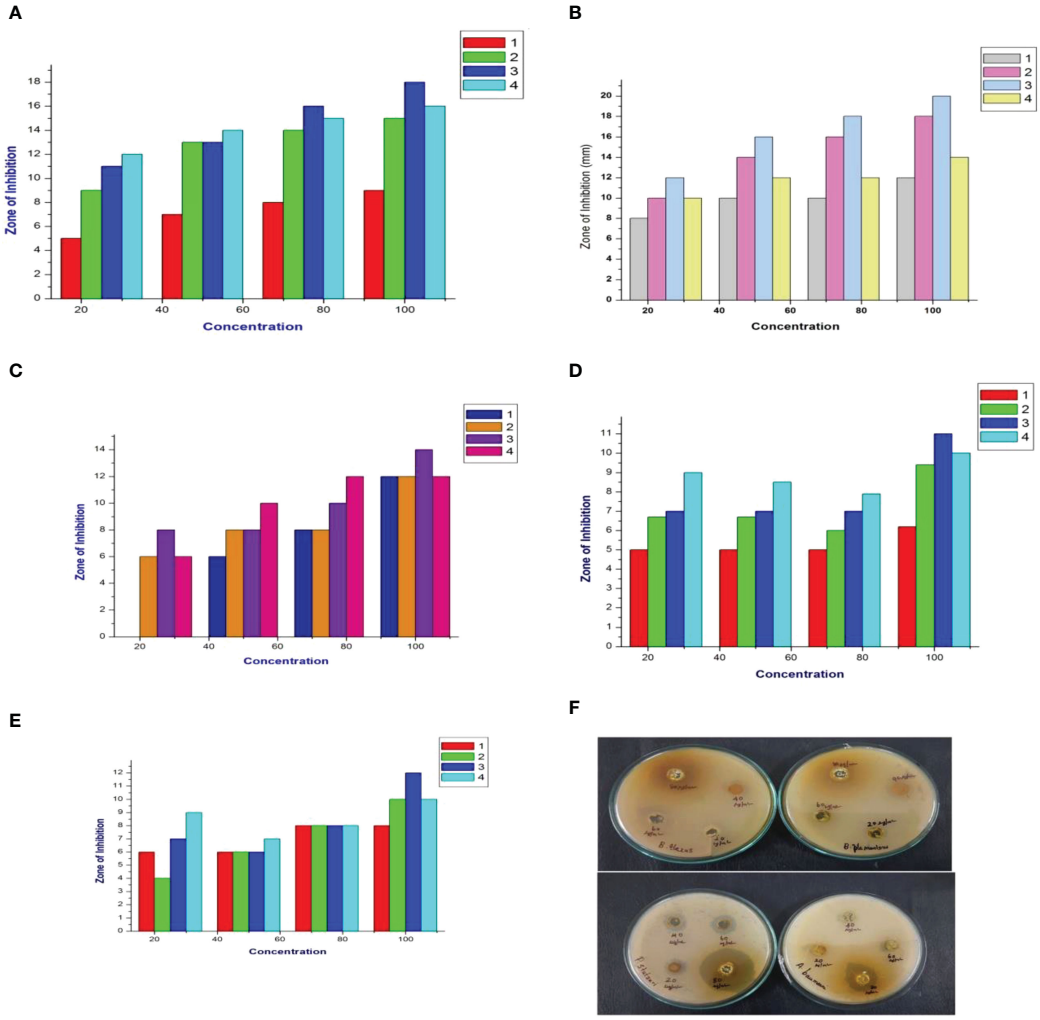

FIGURE 1
Antimicrobial activity of cumin seed extracts against MDR strains. **(A)** Graphical representation of the hexane extract (ZOI) in mm. **(B)** Graphical representation of the methanol extract (ZOI) in mm. **(C)** Graphical representation of the ethyl acetate extract (ZOI) in mm. **(D)** Graphical representation of the ethanol extract (ZOI) in mm. **(E)** Graphical representation of the acetone extract (ZOI) in mm. (1) *Bacillus flexus* (MN045189), (2) *Bacillus filamentosus* (MN045186), (3) *Pseudomonas stutzeri* (MN045185), and (4) *Acinetobacter baumannii* (MN045188). **(F)** Photograph of the methanol extract against MDR strains.

Table 1 determines the cytotoxicity analysis of the crude extracts. Among the extracts, NH extract accelerated the inhibitory activity effectively with a noticeable LC_{50} value. This is due to the synergistic interaction of phytoconstituents in the NH extract, and the NH solvent traps the oil constituents very effectively from the cumin seed. Due to the presence of volatile and non volatile oils and lipophillic compounds the anticancer activity was escalated in the present study. The NH extract interacts with the cell membrane and induces reactive oxygen species (ROS), which substantially interacts with DNA/RNA/proteins and induces apoptosis (33).

The anticancer activity of solvent extract residue is directly related to the nature of phytochemicals, cell lines, and other factors. Prakash et al. (34) studied the anticancer activity of cumin seeds against seven cell lines, including OVCAR-5, PC-5, SF-295, and Colon 502713, to justify the cell lines Colo-205, Hep-2, and A-549. The ethanolic extract was assayed against the cell line at 100 µg/mL. The ethanolic extract performed effective growth inhibitory activity in different cell lines with significant percentage growth inhibition; the percentage inhibition was high in Colon 502713 cell line at 61% and least in the SF-295 cell line at 25%. Likewise, the benzene extract of cumin seed was tested for cytotoxicity against the six cell lines: HEPG2, HELA, HCT116, MCF7, HEP2, and CACO2 (35). The assay outcome showed a higher growth inhibition in MCF7, followed by HEPG2, HEP2, CACO2, HCT116, and HELA cell lines. The benzene extract does not infer cytotoxic properties against the normal fibroblast cell line BHK. In the present study, we have observed that non-polar NH extract performed superior activity than E, A, EA, and M

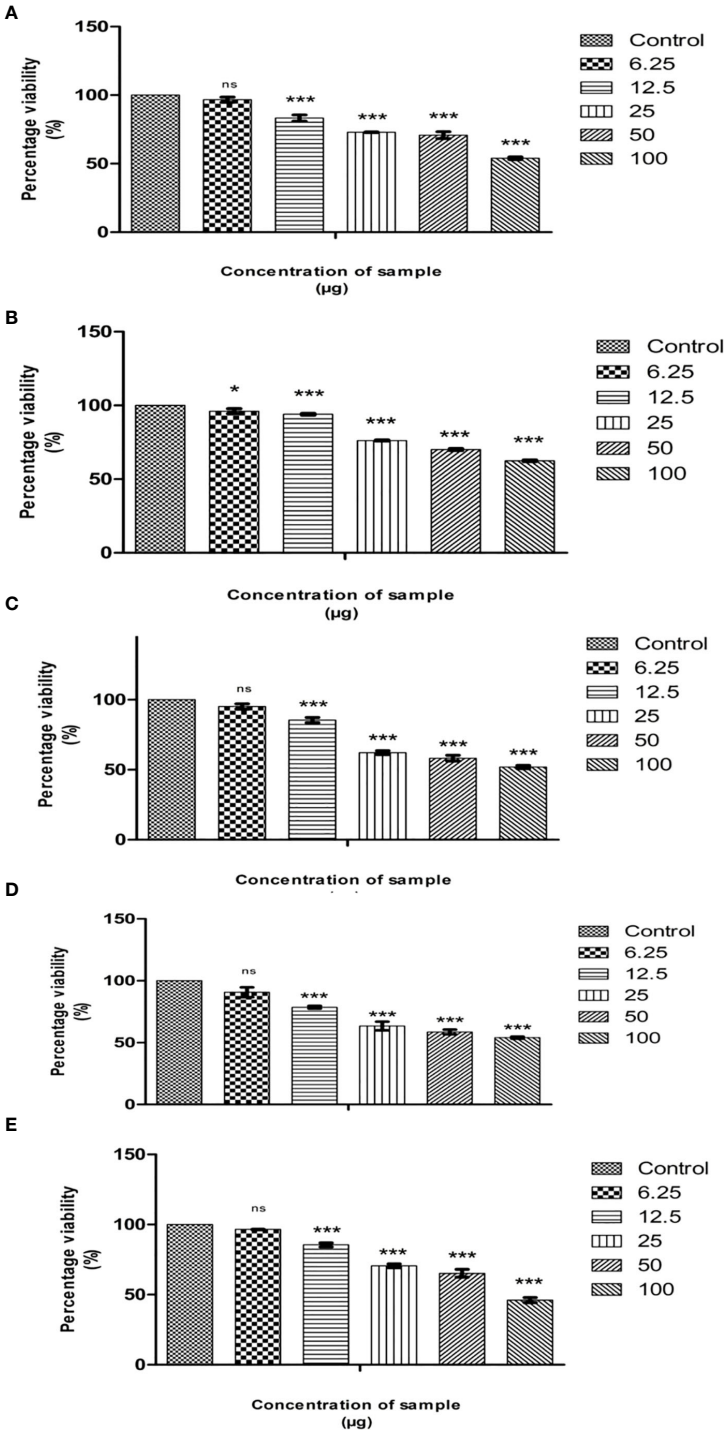

FIGURE 2
Cytotoxic effects of Cumin seed extract in MG63 cells by MTT assay. **(A)** Hexane extract; **(B)** Methanol extract; **(C)** Ethyl acetate extract; **(D)** Ethanol extract; **(E)** acetone extract Different concentrations (6.25µg, 12,5µg, 25µg, 50 µg and 100 µg) of n hexane extracts were assessed in MG63 cells. The X axis is percentage viability and Y represents the concentration of the sample. All experiments were done in triplicates and results represented as Mean+/- SE. One-way ANOVA and Dunnets test were performed to analyse data. *p< 0.05, ***p< 0.001 compared to control group, ns – non significant

TABLE 1 Cytotoxicity analysis of cumin seed extracts against MG63 cells.

S. no	Name of the extract	LC_{50} value
1.	Ethanol	113 µg/mL
2.	Acetone	118 µg/mL
3.	Ethyl acetate	130 µg/mL
4.	Methanol	166 µg/mL
5.	n-Hexane	86 µg/mL

extracts in the MG63 cell line. Our study is the first to encounter the anticancer activity of cumin seed extract against the MG63 cell line.

3.2.2 AO/EB staining

The most promising effect of herbal therapeutics in cancer cells is to induce apoptosis (36). Chemotherapeutic drugs exert their anticancer activity by activating the apoptosis process. The degree of apoptosis is strongly associated with drug sensitivity; to detect the cell death caused by apoptosis, various techniques like terminal deoxynucleotidyl, propidium iodide, *in situ* nick translation, thermal denaturation assays, and acidic denaturation were employed (37). However, the techniques have limits and delimit, restricting the detection of apoptotic cells. Dual AO/EB staining is a method to determine apoptotic cells (38). The staining method utilizes fluorescent dyes to identify the cell membrane changes associated with apoptosis precisely.

In the present study, the effect of NH extract on the MG63 cell line was subjected to AO/EB staining. On illumination with a fluorescent microscope, the images were captured and presented as Figure 3. The left side of the image depicts the control group; green-colored cells indicate that a circular nucleus is uniformly distributed in the center of the cell. The right side of the image denotes the apoptotic, late apoptotic, and necrotic cells. Early apoptotic cells were denoted by orange-green fluorescence, whereas orange fluorescence implies late apoptotic cells; red fluorescence denotes the necrotic cells. AO can easily penetrate the live cells, whereas EB will penetrate only to the dead cells where the cell membrane is ruptured (39). From the image, it is assumed that NH extracts trigger apoptosis in the MG63 cells and cause cell death.

3.2.3 Lactate dehydrogenase assay

LDH assay is a sensitive and reliable assay to detect the extent of cell damage in the treated cells indicated by the release of lactate dehydrogenase enzyme into the medium. These enzymes catalyze pyruvate conversion to lactate in the presence of NADH (40). The cell membrane damage of MG63 cells was assessed by the method of DGKC upon the treatment of NH extract. After incubation for 24 h, the culture supernatant of 50 µL was collected and mixed with 1 mL of working reagent, and OD was recorded at 340nm. The result is presented in Figure 4. The result denotes that the extent of cell damage was increased in response to dose concentrations. At higher concentrations, the cell damage was high, indirectly reflecting the leakage of the high level of LDH into the medium. This indicates the phenomenon of cell death by apoptosis induced by NH extract.

3.2.4 *In vitro* ROS measurement using DCFDA staining

Excessive cellular-level production of ROS damages the cell molecules (DNA/RNA/protein), eventually leading to cell death (41). To confirm that NH extract induces apoptosis in the MG63 cells by the ROS production upon the treatment, we investigated the intracellular production of ROS in the MG63 cells by the DCFDA staining method. Cellular esterases deacetylated the DCFDA to a non-fluorescent compound, which ROS later oxidizes into 2′,7′-

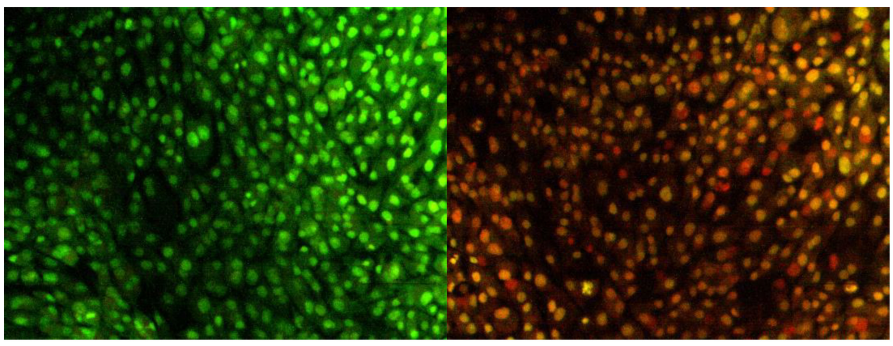

FIGURE 3
Apoptosis determination by AO/EB staining. Image captured by a fluorescence microscope. The left slide denotes the live cells bright green color (control); right slide denotes the treatment of hexane extract in the cells; green-colored cells, early apoptotic cells; orange-colored cells, late apoptotic cells.

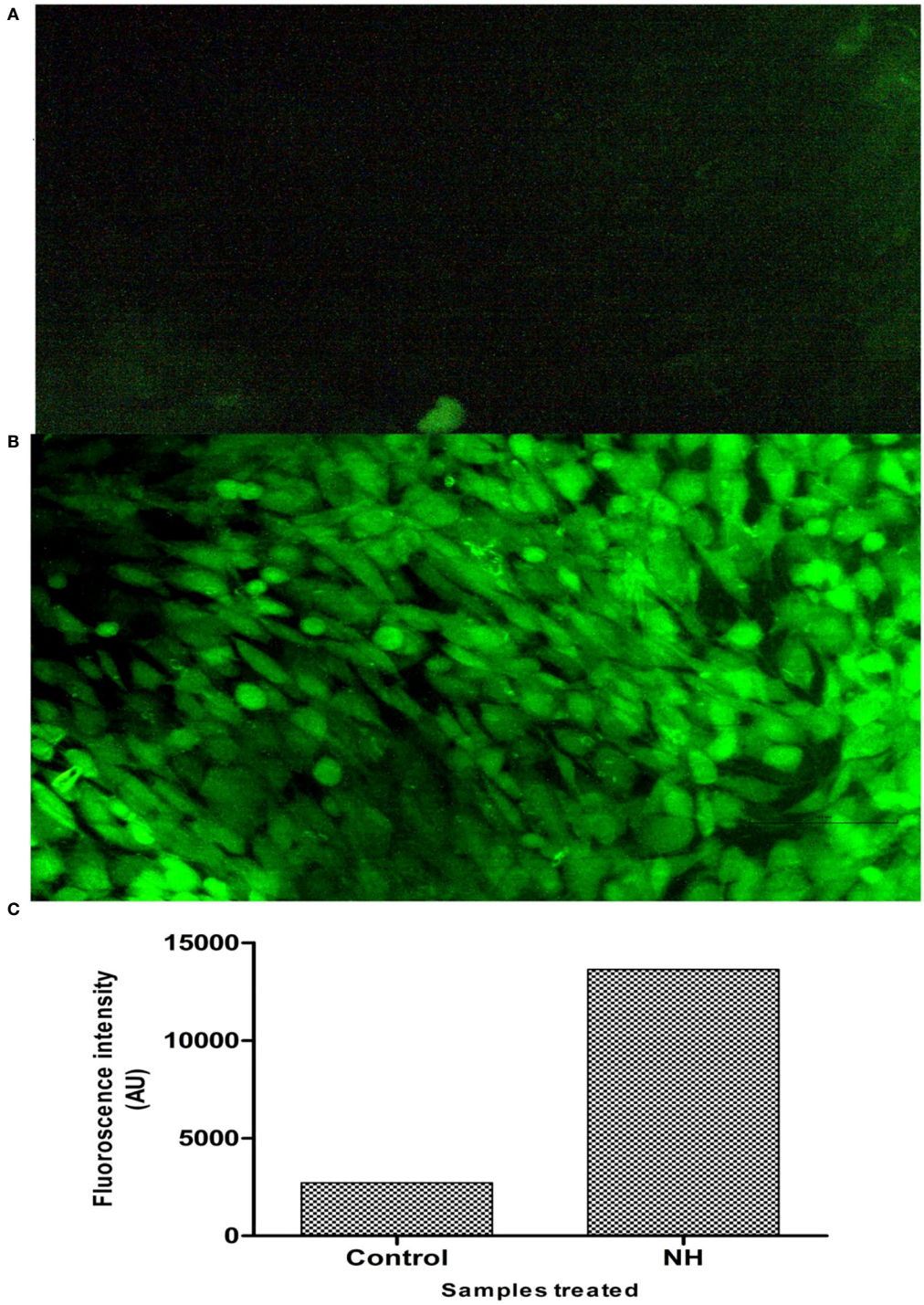

FIGURE 4
Deduction of cellular ROS by DCFDA staining assay. **(A)** Fluorescence image of control MG63 cells. **(B)** Fluorescence image of hexane extract treated MG63 cells. **(C)** Spectroscopic fluorescence intensity measurement of n-hexane–treated MG63 cells compared with control.

dichlorofluorescein (DCF), emitting green fluorescence (42). Carboxy-H_2DCFDA is non-fluorescent, but, in the presence of ROS, it becomes green fluorescent when this reagent is oxidized. The result is presented in Figure 5. The images denote that NH extracts induce the production of ROS by which the cells undergo the apoptosis process. The intensity of ROS production in control and treated cells was expressed in AU: control, 2,722.13; and treated cells, 13,363.12. It is thereby certain that NH extract induces apoptosis by the intracellular production of ROS in the MG63 cells.

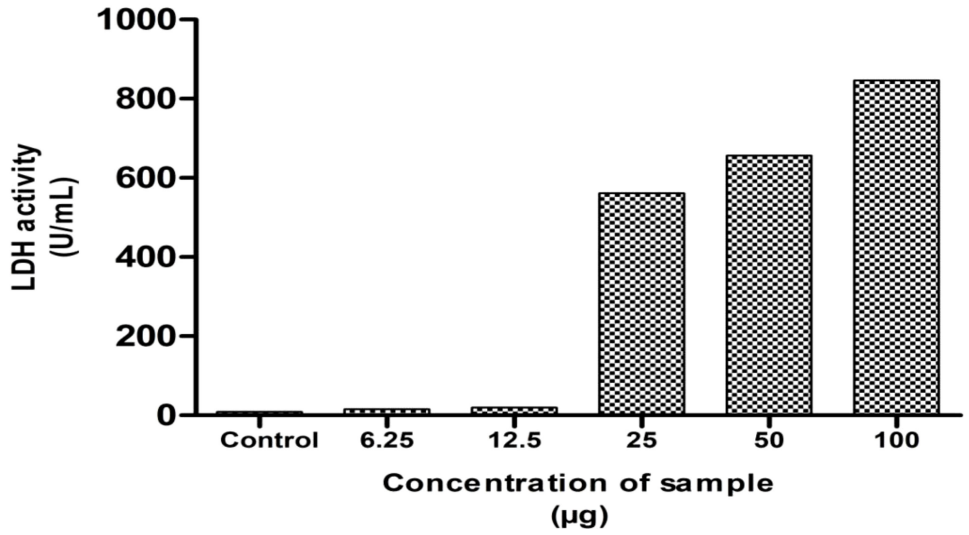

FIGURE 5
Lactate dehydrogenase assay (LDH) of the hexane extract against the MG63 cell line. The results showed the significant cytotoxicity at various concentrations.

3.3 Cell cycle analysis

Using flow cytometry analysis, the inhibitory effect of NH extract in the MG63 cell cycle phases was investigated. Figures 6A–E show a definite change in the cellular DNA of MG63 cells. The G0/G1 phase (52.5%) showed a significant buildup of the cell population in the control cells, followed by the S phase (24%). By contrast, the cell population of the treated cells decreased significantly in the G0/G1 phase (47%) and the S phase (21%). In addition, we saw a significant alteration in the G2 cell cycle. To explain the above observation, we infer that the NH extract residue underwent apoptosis in the MG63 cells. By inducing apoptosis and cell cycle arrest, respectively, plant extract kills cells. Separating apoptotic cells with fragmented DNA from those that have lost cellular DNA can be done using flow cytometry (43).

3.4 Scratch wound healing assay

According to Krakmal et al. (44), invasion and migration of cancer are critical stages in the malignancy of cancer. In this work, we evaluated the MG63 cells' ability to repair wounds *in vitro*. The activity outcomes are shown in Figure 7. As anticipated, the hexane extract successfully and slowly prevented MG63 cells from migrating. The control cells moved more quickly than the hexane-treated cells in comparison to the control. The influence of wound closure rate at various time intervals is shown by the graph plotted from the image (Figure 8). On the basis of the investigation, it can be concluded that hexane extract causes the MG63 to become immobile, disturb cells and, ultimately, induces apoptosis.

3.5 Clonogenic assay

Another important parameter to assess the therapeutic efficacy of the drug is the clonogenic assay. This assay determines the drug's ability to retain the cell from forming colonies, thus reducing the survival of the cancer cell line. The present study employed hexane extract at a concentration of 86 µg/mL for the clonogenic assay. The assay result is presented in Figure 9; the image conferred that the extract after the incubation reduced the colonies' growth significantly. These results indicate that the hexane extract of cumin seed has antiproliferative activity against bone cancer.

3.6 Identification of phytoconstituents

On the basis of the above findings from the antibacterial and anticancer activities, it is deemed that methanolic and hexane extracts performed superior activities in bacterial and cancer cells. Hence, we qualitatively identified the chemical constituents present in the extract (Figure 10). The identified molecules were compared with the NIST database and tabulated the compounds (Tables 2A, B). From the GC-MS analysis, the M extract contains abundantly phthalic acid (21%), whereas, in hexane extract, the major compound is propanal, 2-methyl-3-phenyl- (23%). Phthalic acid is reportedly present in various plants and possesses strong antibacterial properties (45). 2-Methyl-3-phenyl- is a derivative of methyl esters reportedly present in plants with various biological properties (46). The GC-MS analysis postulates that M and hexane extract contains

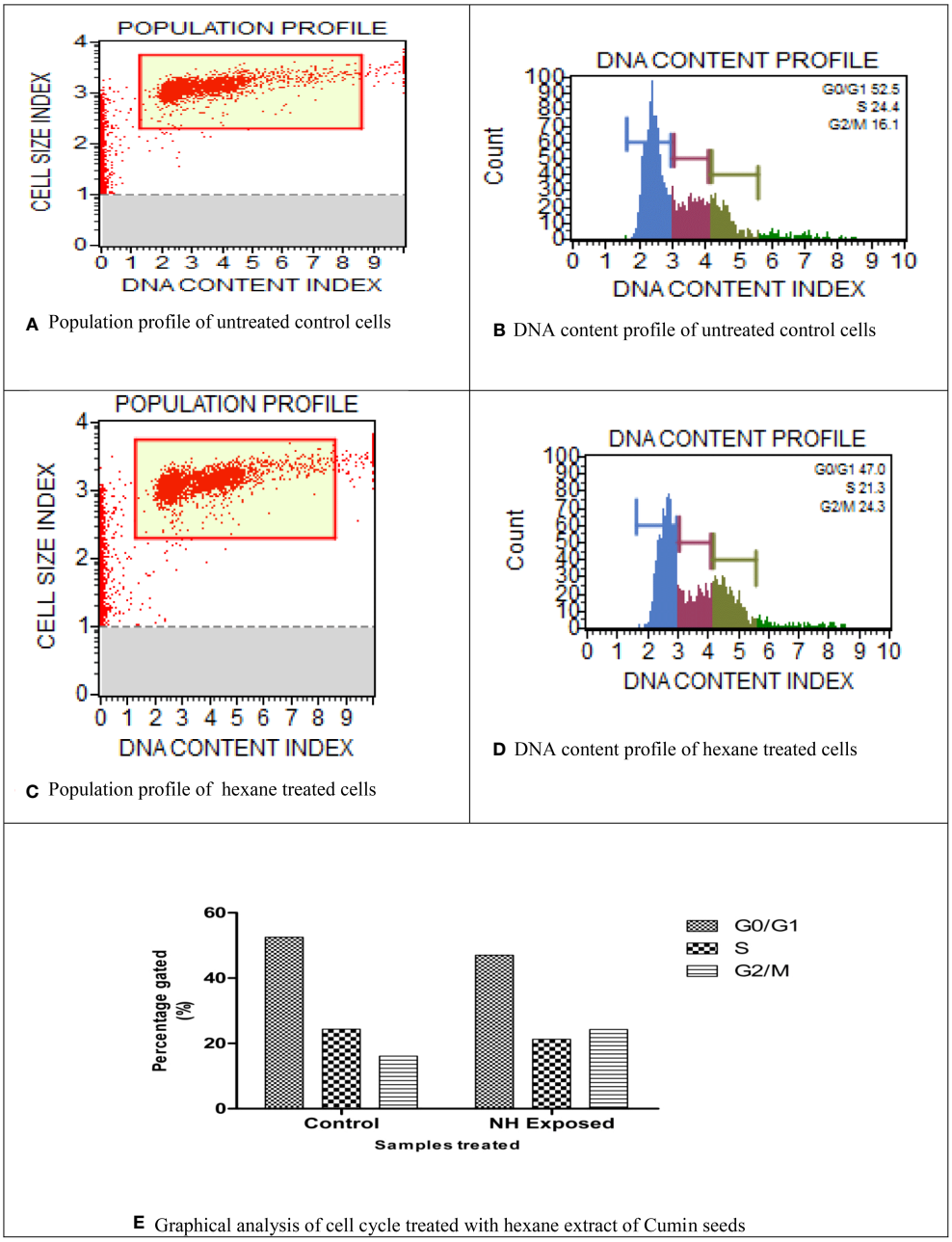

FIGURE 6
Cell cycle analysis of n-hexane–treated MG63 cells. **(A)** Population profile of untreated control cells. **(B)** DNA content profile of untreated control cells. **(C)** Population profile of hexane-treated cells. **(D)** DNA content profile of hexane-treated cells. **(E)** Graphical analysis of cell cycle treated with hexane extract of cumin seeds.

various bioactive molecules that claim to be antimicrobial, anticancer, arthritis, immunosuppressants, and others (47–52). Thus, from the analysis, it is inferred that the chemical constituents actively synergistically spur the bactericidal and anticancer effects (53). However, the isolation of important abundance compounds in the extract must be studied to investigate the cancerous activity.

4 Conclusion

The present study manifests the therapeutic properties of cumin seed extract against MDR strains and bone cancer cells. Upon the solvent extraction of the cumin seed, the extracted residue was assayed against the MDR pathogen *B. flexus*, *B. filamentosus*, *P. stutzeri*, and *A. baumannii*. As a result, the methanolic extract

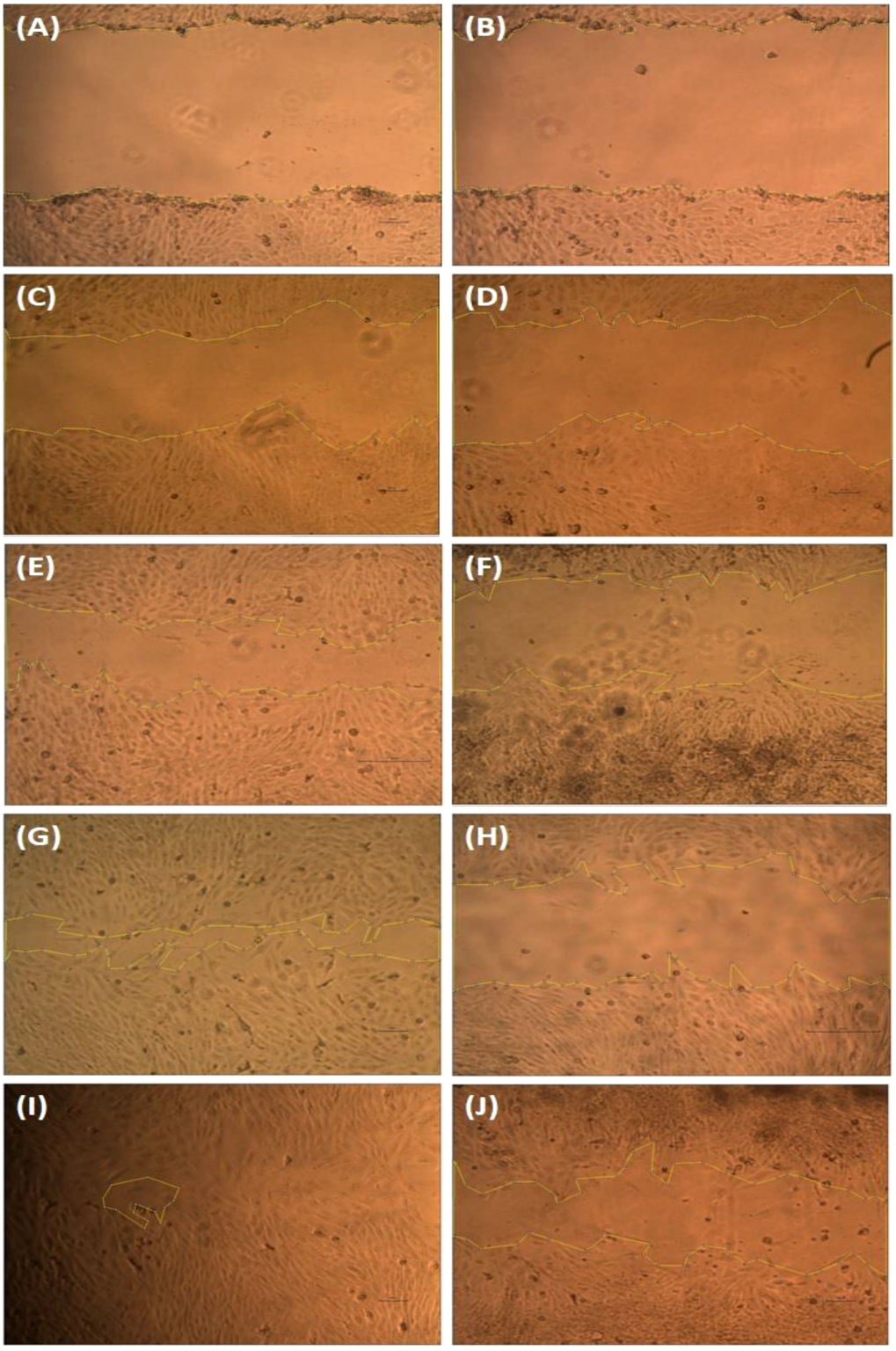

FIGURE 7
Wound healing assay. The MG63 cells were scratched and treated with hexane extract. After 24 h, the images were captured using an Olympus CKX41 microscope with ×4 magnification. Control images **(A, C, E, G, I)** and treatment cells **(B, D, F, H, J)**.

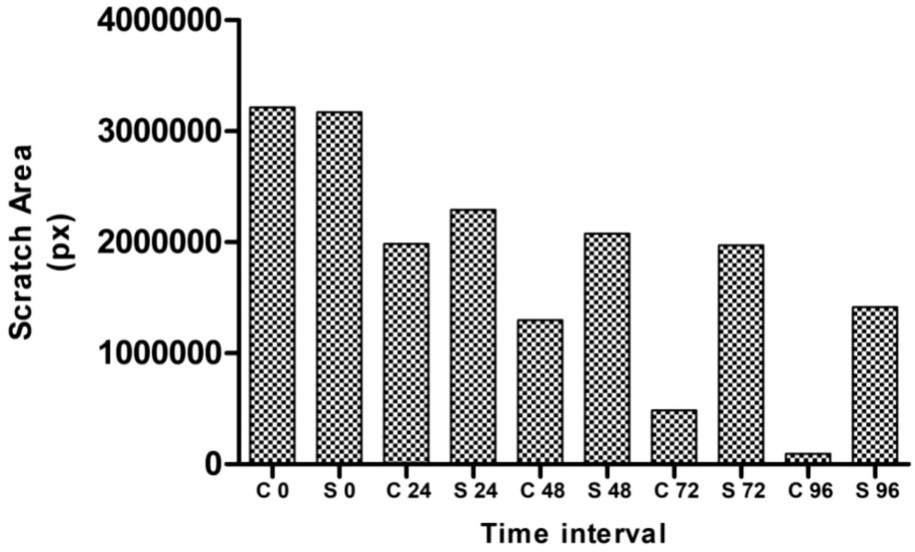

FIGURE 8
Graphical representation depicting the migration assay (C, control; S, hexane extract).

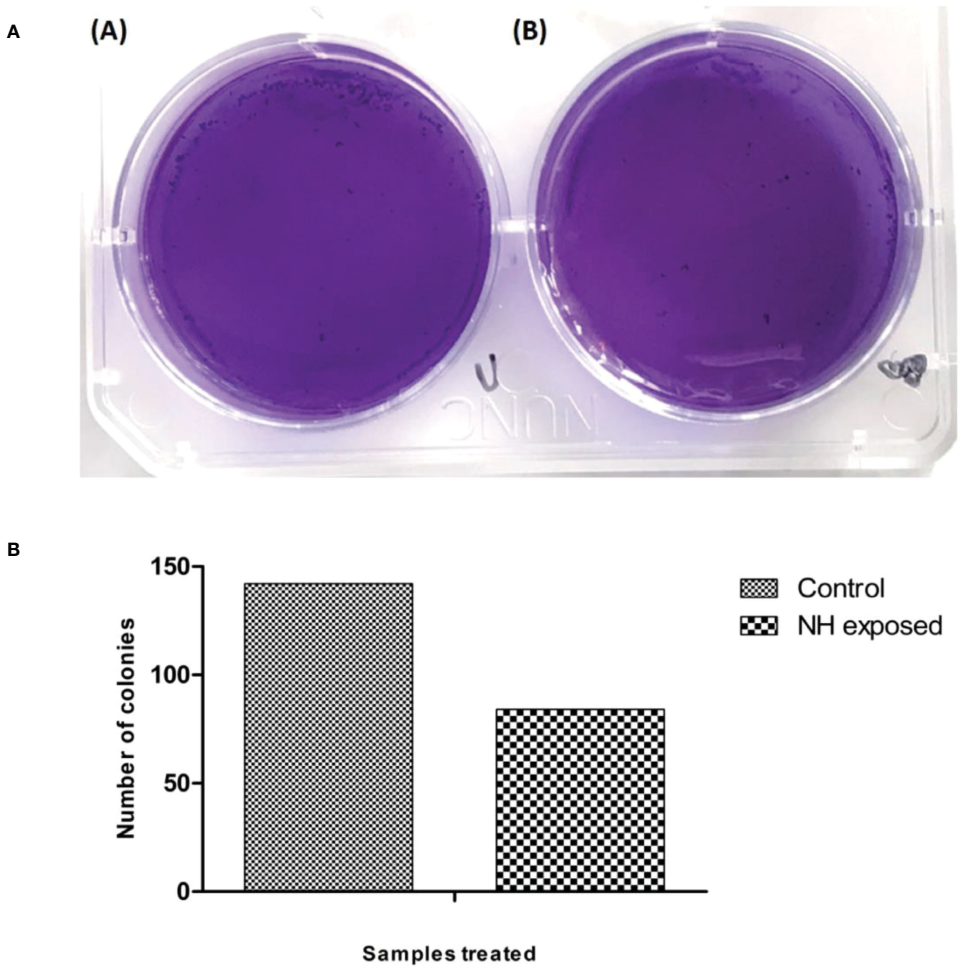

FIGURE 9
(A) Clonogenic assay of MG63 cells treated with n-hexane extract: (i) control; (ii) treated cells. **(B)** Graphical representation of clonogenic assay in hexane-treated MG63 cells.

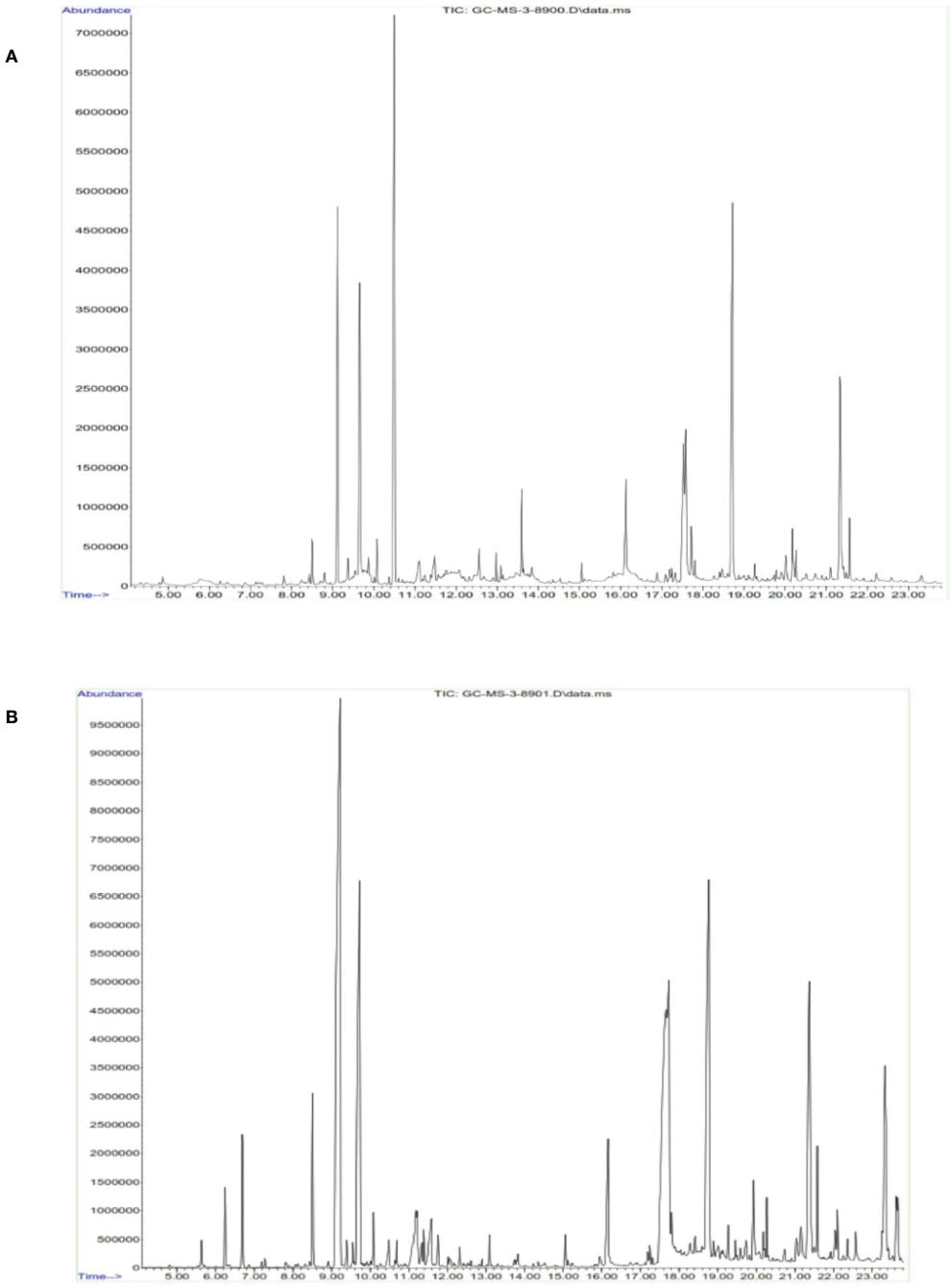

FIGURE 10
Identification of functional chemical constituents present in cumin seed extract using GC-MS. **(A)** Methanol extract. **(B)** n-Hexane extract.

performed better bactericidal activity against the MDR strains. Furthermore, we substantially evaluated cumin seed extract's anticancer and antiproliferative activities in MG63 cell line. The MTT assay was investigated in MG63 cell line. Among the solvent extracts, hexane triggers stupendous cytotoxic properties in MG63 cells. Moreover, hexane extract was sequentially assessed in AO/EB staining; the findings portrayed that hexane extract induced apoptosis in the MG63 cells. The LDH assay and DCFDA staining results also confirm the induction of apoptosis in the MG63 cells. The hexane extract arrests the S phase of the cell cycle revealed by flow cytometry analysis. In addition, we have studied the scratch wound healing assay in the MG63 cells. The hexane extract prevents the migration of the cells when compared with the control. The hexane extracts also inhibit the formation of colonies assessed by clonogenic assay. On the basis of the above results and interpretation, we have qualitatively determined the chemical constituents present in the methanolic and hexane extract using GC-MS. The analysis reveals the chemical constituents that

TABLE 2A Qualitative GC-MS analysis of methanol extract.

Peak number	Name of the compound	Time (in min)	Percentage (%)	Abundance
1	d-Galactitol	5.787	1.28	16
2	Pulegone	8.497	1.09	53
3	Propanal, 2-methyl-3-phenyl-	9.120	10.59	98
4	Cyclohexene, 3-methyl-6-(1-methylethylidene)-	9.375	0.65	91
5	2-Methoxy-4-vinylphenol	9.653	8.45	76
6	2-Methoxy-4-vinylphenol	9.864	1.11	93
7	1,4-Cyclohexadiene-1-methanol, 4-(1-methylethyl)-	10.075	1.01	72
8	Phthalic acid	10.497	21.73	50
9	Benzoic acid, 4-(1-methylethyl)-	11.108	1.37	93
10	Hepta-2,6-dienoic acid	11.486	1.13	56
11	.beta.-D-Glucopyranose	12.075	0.44	53
12	1,4-Anhydro-d-galactitol	12.441	0.48	64
13	3-Methylsalicylhydrazide	12.564	1.09	76
14	Methanol	12.975	0.55	50
15	Ethanone, 1,1′,1″-(1,3,5-benzene…	13.597	1.90	49
16	4-Isopropylcinnamic acid	13.841	0.63	98
17	Cyclooctane	15.052	0.43	91
18	n-Hexadecanoic acid	16.130	3.28	87
19	9,12-Octadecadienoic acid (Z,Z)	17.530	6.68	99
20	6-Octadecenoic acid	17.585	5.33	99
21	Octadecanoic acid	17.719	1.39	99
22	1H-Indene, 2,3,3a,4,7,7a-hexahyd.	18.718	15.23	35
23	4-Amino-5-imidazolecarboxamide hydrochloride	20.018	1.03	38
24	Hexadecanoic acid 2-hydroxy-1-(hydroxymethyl) ethyl ester	20.174	1.57	62
25	Propanedinitrile, dicyclohexyl-	20.263	0.62	59
26	Cyclohexene, 5-methyl-3-(1-methylethenyl)-	21.096	0.47	46
27	Z,E-7,11-Hexadecadien-1-yl acetate	21.329	8.20	83
28	3-Methylbut-2-enoic acid	21.562	1.41	35
29	trans-2-Dodecen-1-ol, pentafluoropropionate	22.218	0.44	56
30	1H-Benzimidazol-2-amine	23.318	0.44	46

TABLE 2B Qualitative GC-MS analysis of n-hexane extract. The compounds were identified using NIST library.

Peak number	Name of the compound	Time (in min)	Percentage (%)	Abundance
1	.beta.-Pinene	5.631	0.38	97
2	Benzene, 1-methyl-3-(1-methylethyl)-	6.242	0.94	95
3	1,4-Cyclohexadiene	6.686	1.57	94
4	1,3,3-Trimethylcyclohex-1-ene-4-carboxaldehyde, (+,-)-	8.508	2.11	60
5	Propanal, 2-methyl-3-phenyl-	9.231	23.80	97

(Continued)

10.3389/fonc.2023.1322875

TABLE 2B Continued

Peak number	Name of the compound	Time (in min)	Percentage (%)	Abundance
6	p-Menth-2-en-7-ol	9.397	0.36	87
7	1-Cyclohexene-1-carboxaldehyde	9.553	0.32	94
8	1,5,6,7-Tetrahydro-4-indolone	9.719	10.77	62
9	1,4-Cyclohexadiene-1-methanol, 4-(1-methylethyl)-	10.086	0.60	49
10	3,3-Dimethyl-6-methylenecyclohexene	10.486	0.48	60
11	Benzoic acid, 4-(1-methylethyl)-	11.186	2.65	94
12	Cycloprop-2-enecarbonic acid	11.341	0.45	38
13	1,6,10-Dodecatriene, 7,11-dimethyl-3-methylene-	11.386	0.35	96
14	2,4-Cyclohexadiene-1-carboxylic acid	11.586	1.41	35
15	Tricyclo[5.4.0.0(2,8)]undec-9-ene, 2,6,6,9-tetramethyl-, (1R,2S,7R,8R)-	11.764	0.47	52
16	Carotol	13.097	0.35	91
17	4-Isopropylcinnamic acid	13.830	0.26	98
18	Pyrene, hexadecahydro-	15.052	0.35	46
19	n-Hexadecanoic acid	16.163	2.63	99
20	9,12-Octadecadienoic acid (Z,Z)-	17.663	14.57	99
21	cis-Vaccenic acid	17.807	0.56	97
22	Ethyl 2-(O-nitrophenylhydrazono).	18.774	11.30	41
23	2-Cyclohexen-1-ol, 2-methyl-5-(1-methylethenyl)-, cis-	19.018	0.35	55
24	Benzene, 2-methoxy-4-methyl-1-(1-methylethyl)-	19.129	0.31	43
25	Phthalic acid, hexyl tridec-2-yn-1-yl ester	19.274	0.49	35
26	2-Pentenoic acid, 2-methyl-, (E)	19.740	0.40	64
27	9,17-Octadecadienal, (Z)-	19.929	1.40	76
28	Hexadecanoic acid 2-hydroxy-1-(hydroxymethyl) ethyl ester	20.185	0.43	86
29	3-Methylbut-2-enoic acid	20.274	0.65	42
30	2-Methyl-4,5-diphenyl-4,5-dihydro	21.029	0.55	38
31	Stigmasterol	21.151	0.86	94
32	2,3-Dihydroxypropyl elaidate	21.373	7.32	90
33	6-Octadecenoic acid	21.496	0.28	49
34	3-Methylbut-2-enoic acid, 3,5-di.	21.585	1.22	35
35	.gamma.-Sitosterol	22.040	0.59	97
36	Hydrazine	22.096	0.54	49
37	Benzene, octyl-	22.362	0.28	47
38	Hexadecane, 1-iodo-	22.573	0.47	96
39	Benzene, 1,1′-(1,1,2,2-tetramethyl-1,2-ethanediyl)bis[4-methyl-	23.329	5.46	53
40	Benzene, (2-methylpropyl)-	23.629	1.75	53

The compounds were identified using NIST library.

proclaim to have various therapeutic properties. Thus, we can conclude that cumin seed extract has stringent cancerous activity in the MG63 cells and can be formulated as a chemotherapeutic agent in the near future.

Data availability statement

The original contributions presented in the study are included in the article/supplementary material. Further inquiries can be directed to the corresponding authors.

Author contributions

RC: Conceptualization, Writing – original draft. KM: Resources, Writing – review & editing. SC: Investigation, Writing – review & editing. OG: Methodology, Writing – review & editing. SH: Methodology, Writing – review & editing. JJ: Methodology, Writing – review & editing. EG: Methodology, Writing – review & editing. NA: Validation, Writing – review & editing. AA: Supervision, Writing – review & editing. SP: Supervision, Writing – review & editing. HJ: Conceptualization, Writing – original draft.

Funding

The author(s) declare financial support was received for the research, authorship, and/or publication of this article. This research was funded through the Researchers Supporting Project Number (RSPD2023R940) King Saud University, Riyadh, Saudi Arabia.

Acknowledgments

The authors express their gratitude to the management of Karpagam Academy of Higher Education, Coimbatore, India, and Researchers Supporting Project Number (RSPD2023R940), King Saud University, Riyadh, Saudi Arabia.

Conflict of interest

The authors declare that the research was conducted in the absence of any commercial or financial relationships that could be construed as a potential conflict of interest.

Publisher's note

References

1. Izadpanah S, Shabani P, Aghebati-Maleki A, Baghbanzadeh A, Fotouhi A, Bisadi A, et al. Prospects for the involvement of cancer stem cells in the pathogenesis of osteosarcoma. *J Cell Physiol* (2020) 235(5):4167–82. doi: 10.1002/jcp.29344

2. Simpson E, Brown HL. Understanding osteosarcomas. *Jaapa* (2018) 31(8):15–9. doi: 10.1097/01.JAA.0000541477.24116.8d

3. Komaranchath AS, Appaji L, Lakshmaiah KC, Kamath M, Kumar RV. Demographic profile of pediatric osteosarcoma in south India: a single institution experience. *Int J Med Res Health Sci* (2015) 4(3):551–4. doi: 10.5958/2319-5886.2015.00106.X

4. Zhang B, Zhang Y, Li R, Li J, Lu X, Zhang Y. The efficacy and safety comparison of first-line chemotherapeutic agents (high-dose methotrexate, doxorubicin, cisplatin, and ifosfamide) for osteosarcoma: a network meta-analysis. *J Orthopaedic Surg Res* (2020) 15(1):1–10. doi: 10.1186/s13018-020-1576-0

5. Longhi A, Errani C, De Paolis M, Mercuri M, Bacci G. Primary bone osteosarcoma in the pediatric age: state of the art. *Cancer Treat Rev* (2006) 32 (6):423–36. doi: 10.1016/j.ctrv.2006.05.005

6. Mukherjee PK, Nema NK, Venkatesh P, Debnath PK. Changing scenario for promotion and development of Ayurveda–way forward. *J ethnopharmacology* (2012) 143(2):424–34. doi: 10.1016/j.jep.2012.07.036

7. Patil S, Chandrasekaran R. Biogenic nanoparticles: A comprehensive perspective in synthesis, characterization, application and its challenges. *J Genet Eng Biotechnol* (2020) 18(1):1–23. doi: 10.1186/s43141-020-00081-3

8. Cragg GM, Newman DJ. Plants as a source of anticancer agents. *J ethnopharmacology* (2005) 100(1-2):72–9. doi: 10.1016/j.jep.2005.05.011

9. Lin D, Xiao M, Zhao J, Li Z, Xing B, Li X, et al. An overview of plant phenolic compounds and their importance in human nutrition and management of type 2 diabetes. *Molecules* (2016) 21(10):1374. doi: 10.3390/molecules21101374

10. Kumar KS, Yadav A, Srivastava S, Paswan S, sankar Dutta A. Recent trends in Indian traditional herbs Syzygiumaromaticum and its health benefits. *J Pharmacognosy Phytochem* (2012) 1(1):13–22.

11. Nisar T, Iqbal M, Raza A, Safdar M, Iftikhar F, Waheed M. Turmeric: A promising spice for phytochemical and antimicrobial activities. *AmEur J Agric Environ Sci* (2015) 15(7):1278–88. doi: 10.5829/idosi.aejaes.2015.15.7.9528

12. Oluwole O, Fernando WB, Lumanlan J, Ademuyiwa O, Jayasena V. Role of phenolic acid, tannins, stilbenes, lignans and flavonoids in human health–a review. *Int J Food Sci Tech* (2022) 57(10):6326–35.

13. Singh RK, Pandey KB, Rizvi SI. Medicinal properties of some Indian spices. *Ann Phytomedicine* (2012) 1(1):29–33.

14. Mnif S, Aifa S. Cumin (Cuminumcyminum L.) from traditional uses to potential biomedical applications. *Chem biodiversity* (2015) 12(5):733–42. doi: 10.1002/cbdv.201400305

15. Al-Snafi AE. The pharmacological activities of Cuminumcyminum-A review. *IOSR J Pharm* (2016) 6(6):46–65.

16. Prabukumar S, Rajkuberan C, Sathishkumar G, Illaiyaraja M, Sivaramakrishnan S. One pot green fabrication of metallic silver nanoscale materials using Crescentia cujete L. *Assess their bactericidal activity. IET nanobiotechnology* (2018) 12(4):505–8. doi: 10.1049/iet-nbt.2017.0209

17. Sangilimuthu AY, Sivaraman T, Chandrasekaran R, Sundaram KM, Ekambaram G. Screening chemical inhibitors for alpha-amylase from leaves extracts of Murraya koenigii (Linn.) and Aegle marmelos L. *J Complementary Integr Med* (2020) 18(1):51–7. doi: 10.1515/jcim-2019-0345

18. Adwan G, Abu-Shanab B, Adwan K. Antibacterial activities of some plant extracts alone and in combination with different antimicrobials against multidrug–resistant Pseudomonas aeruginosa strains. *Asian Pacific J Trop Med* (2010) 3(4):266–9. doi: 10.1016/S1995-7645(10)60064-8

19. Sharif A, Akhtar MF, Akhtar B, Saleem A, Manan M, Shabbir M, et al. Genotoxic and cytotoxic potential of whole plant extracts of Kalanchoelaciniata by Ames and MTT assay. *EXCLI J* (2017) 16:593. doi: 10.17179%2Fexcli2016-748

20. Varalakshmi B, Anand AV, Karpagam T, Bai JS, Manikandan R. *In vitro* antimicrobial and anticancer activity of Cinnamomumzeylanicum Linn bark extracts. *Int J Pharm PharmSci* (2014) 6(1):12–8.

21. Specian AFL, Serpeloni JM, Tuttis K, Ribeiro DL, Cilião HL, Varanda EA, et al. LDH, proliferation curves and cell cycle analysis are the most suitable assays to identify and characterize new phytotherapeutic compounds. *Cytotechnology* (2016) 68(6):2729–44. doi: 10.1007/s10616-016-9998-6

22. Choi W, Lee JB, Cui L, Li Y, Li Z, Choi JS, et al. Therapeutic efficacy of topically applied antioxidant medicinal plant extracts in a mouse model of experimental dry eye. *Oxid Med Cell Longevity* (2016) 2016:4727415. doi: 10.1155/2016/4727415

23. González-Sarrías A, Li L, Seeram NP. Effects of maple (Acer) plant part extracts on proliferation, apoptosis and cell cycle arrest of human tumorigenic and non-tumorigenic colon cells. *Phytotherapy Res* (2012) 26(7):995–1002. doi: 10.1002/ptr.3677

24. Nayak D, Ashe S, Rauta PR, Nayak B. Assessment of antioxidant, antimicrobial and anti-osteosarcoma potential of four traditionally used Indian medicinal plants. *J Appl Biomedicine* (2017) 15(2):119–32. doi: 10.1016/j.jab.2016.10.005

25. Lee CM, Lee J, Nam MJ, Choi YS, Park SH. Tomentosin displays anticarcinogenic effect in human osteosarcoma MG-63 cells via the induction of intracellular reactive oxygen species. *Int J Mol Sci* (2019) 20(6):1508. doi: 10.3390/ijms20061508

26. Chandrasekaran R, Gnanasekar S, Seetharaman P, Krishnan M, Sivaperumal S. Intrinsic studies of Euphorbia antiquorum L. latex extracts against human bacterial pathogens and mosquito vector AedesaEgypti, Culexquinquefasciatus (Diptera: Culicidae). *Biocatalysis Agric Biotechnol* (2017) 10:75–82. doi: 10.1016/j.bcab.2017.02.008

27. Laxminarayan R, Duse A, Wattal C, Zaidi AK, Wertheim HF, Sumpradit N, et al. Antibiotic resistance—the need for global solutions. *Lancet Infect Dis* (2013) 13 (12):1057–98. doi: 10.1016/S1473-3099(13)70318-9

28. Chang KC, Yew WW. Management of difficult multidrug-resistant tuberculosis and extensively drug-resistant tuberculosis: update 2012. *Respirology* (2013) 18(1):8–21. doi: 10.1111/j.1440-1843.2012.02257.x

29. Huemer M, MairpadyShambat S, Brugger SD, Zinkernagel AS. Antibiotic resistance and persistence—Implications for human health and treatment perspectives. *EMBO Rep* (2020) 21(12):e51034. doi: 10.15252/embr.202051034

30. Kohanski MA, Dwyer DJ, Collins JJ. How antibiotics kill bacteria: from targets to networks. *Nat Rev Microbiol* (2010) 8(6):423–35. doi: 10.1038/nrmicro2333

31. Sharifi A, Mohammadzadeh A, Salehi TZ, Mahmoodi P, Nourian A. Cuminumcyminum L. essential oil: A promising antibacterial and antivirulence agent against multidrug-resistant Staphylococcus aureus. *Front Microbiol* (2021) 12. doi: 10.3389/fmicb.2021.667833

32. Gachkar L, Yadegari D, Rezaei MB, Taghizadeh M, Astaneh SA, Rasooli I. Chemical and biological characteristics of Cuminumcyminum and Rosmarinus officinalis essential oils. *Food Chem* (2007) 102(3):898–904. doi: 10.1016/j.foodchem.2006.06.035

33. Ahmed B, Dwivedi S, Abdin MZ, Azam A, Al-Shaeri M, Khan MS, et al. Mitochondrial and chromosomal damage induced by oxidative stress in Zn2+ ions, ZnO-bulk and ZnO-NPs treated Allium cepa roots. *Sci Rep* (2017) 7(1):1–14. doi: 10.1038/srep40685

34. Prakash E, Gupta DK. Cytotoxic activity of ethanolic extract of Cuminumcyminum Linn against seven human cancer cell line. *Universal J Agric Res* (2014) 2(1):27–30. doi: 10.13189/ujar.2014.020104

35. Mekawey AA, Mokhtar MM, Farrag RM. Antitumor and antibacterial activities of [1-(2-Ethyl, 6-Heptyl) Phenol] from Cuminumcyminum seeds. *J Appl Sci Res* (2009) 5(11):1881–8.

36. Qi F, Li A, Inagaki Y, Gao J, Li J, Kokudo N, et al. Chinese herbal medicines as adjuvant treatment during chemoor radio-therapy for cancer. *Bioscience Trends* (2010) 4(6):297–307.

37. Darzynkiewicz Z, Juan G, Li X, Gorczyca W, Murakami T, Traganos F. Cytometry in cell necrobiology: analysis of apoptosis and accidental cell death (necrosis). *Cytometry: J Int Soc Analytical Cytology* (1997) 27(1):1–20. doi: 10.1002/(SICI)1097-0320(19970101)27:1<1::AID-CYTO2>3.0.CO;2-L

38. Liu K, Liu PC, Liu R, Wu X. Dual AO/EB staining to detect apoptosis in osteosarcoma cells compared with flow cytometry. *Med Sci monitor basic Res* (2015) 21:15. doi: 10.12659/MSMBR.893327

39. Squier MK, Cohen JJ. Standard quantitative assays for apoptosis. *Mol Biotechnol* (2001) 19(3):305–12. doi: 10.1385/MB:19:3:305

40. Fotakis G, Timbrell JA. *In vitro* cytotoxicity assays: comparison of LDH, neutral red, MTT and protein assay in hepatoma cell lines following exposure to cadmium chloride. *Toxicol Lett* (2006) 160(2):171–7. doi: 10.1016/j.toxlet.2005.07.001

41. Majumder D, Nath P, Debnath R, Maiti D. Understanding the complicated relationship between antioxidants and carcinogenesis. *J Biochem Mol Toxicol* (2021) 35 (2):e22643. doi: 10.1002/jbt.22643

42. Szychowski KA, Binduga UE, Rybczyńska-Tkaczyk K, Leja ML, Gmiński J. Cytotoxic effects of two extracts from garlic (Allium sativum L.) cultivars on the human squamous carcinoma cell line SCC-15. *Saudi J Biol Sci* (2018) 25(8):1703–12. doi: 10.1016/j.sjbs.2016.10.005

43. Darzynkiewicz Z, Bedner E, Smolewski P. Flow cytometry in analysis of cell cycle and apoptosis. In: *Seminars in hematology*. WB Saunders (2001). 38(2):179–93.

44. Krakhmal NV, Zavyalova MV, Denisov EV, Vtorushin SV, Perelmuter VM. Cancer invasion: patterns and mechanisms. *ActaNaturae* (2015) 7(2):17–28. doi: 10.32607/20758251-2015-7-2-17-28

45. Manayi A, Kurepaz-Mahmoodabadi M, Gohari AR, Ajani Y, Saeidnia S. Presence of phthalate derivatives in the essential oils of a medicinal plant Achillea tenuifolia. *DARU J Pharm Sci* (2014) 22:1–6. doi: 10.1186/s40199-014-0078-1

46. Nasrabadi M, Halimi Khalilabad M, Soorgi H, Nadaf M. Isolation and structure elucidation of methylphenyLindole alkaloid from crucianella sintenisii growing in Iran. *Journal of Medicinal and Chemical Sciences* (2023) 6(4):771–7. doi: 10.26655/JMCHEMSCI.2023.4.8

47. Beis SH, Azcan N, Ozek T, Kara M, Baser KHC. production of essential oil from cumin seeds. *Chem Natural compounds* (2000) 36(3):265–8. doi: 10.1007/BF02238331

48. Ravi R, Prakash M, Bhat KK. Characterization of aroma active compounds of cumin (Cuminumcyminum L.) by GC-MS, e-Nose, and sensory techniques. *Int J Food Properties* (2013) 16(5):1048–58. doi: 10.1080/10942912.2011.576356

49. Ali N, Rashid S, Nafees S, Hasan SK, Sultana S. Beneficial effects of Chrysin against Methotrexate-induced hepatotoxicity via attenuation of oxidative stress and apoptosis. *Mol Cell Biochem* (2014) 385:215–23. doi: 10.1007/s11010-013-1830-4

50. AlAsmari AF, Alharbi M, Alqahtani F, Alasmari F, AlSwayyed M, Alzarea SI, et al. Diosmin alleviates doxorubicin-induced liver injury via modulation of oxidative stress-mediated hepatic inflammation and apoptosis via NfkB and MAPK pathway: A preclinical study. *Antioxidants* (2021) 10(12):1998. doi: 10.3390/antiox10121998

51. Ali N, AlAsmari AF, Imam F, Ahmed MZ, Alqahtani F, Alharbi M, et al. Protective effect of diosmin against doxorubicin-induced nephrotoxicity. *Saudi J Biol Sci* (2021) 28(8):4375–83. doi: 10.1016/j.sjbs.2021.04.030

52. Ashokkumar K, Vellaikumar S, Murugan M, Dhanya MK, Karthikeyan A, Ariharasutharsan G, et al. GC/MS analysis of essential oil composition from selected seed spices. *Natl Acad Sci Lett* (2021) 44(6):503–6. doi: 10.1007/s40009-021-01066-7

53. Pourmortazavi SM, Hajimirsadeghi SS. Supercritical fluid extraction in plant essential and volatile oil analysis. *J Chromatogr A* (2007) 1163(1-2):2–24. doi: 10.1016/j.chroma.2007.06.021

frontiers | Frontiers in Pharmacology

TYPE Original Research
PUBLISHED 11 December 2023
DOI 10.3389/fphar.2023.1260683

OPEN ACCESS

EDITED BY
Ayaz Shahid,
Western University of Health Sciences, United States

REVIEWED BY
Yan Ren Lin,
Changhua Christian Hospital, Taiwan
Chun-Yu Chen,
Tungs' Taichung MetroHarbor Hospital, Taiwan

*CORRESPONDENCE
Han-Ping Wu,
arthur1226@gmail.com

RECEIVED 18 July 2023
ACCEPTED 25 September 2023
PUBLISHED 11 December 2023

CITATION
Chen Y-H, Chen C-T and Wu H-P (2023), Effect of Danshen for improving clinical outcomes in patients with bladder cancer: a retrospective, population-based study.
Front. Pharmacol. 14:1260683.
doi: 10.3389/fphar.2023.1260683

Effect of Danshen for improving clinical outcomes in patients with bladder cancer: a retrospective, population-based study

Yi-Hsin Chen[1,2,3], Chih-Tsung Chen[1] and Han-Ping Wu[4,5]*

[1]Department of Nephrology, Taichung Tzu Chi Hospital, Taichung, Taiwan, [2]School of Medicine, Tzu Chi University, Hualien, Taiwan, [3]Department of Artificial Intelligence and Data Science, National Chung Hsing University, Taichung, Taiwan, [4]College of Medicine, Chang Gung University, Taoyuan, Taiwan, [5]Department of Pediatrics, Chiayi Chang Gung Memorial Hospital, Chiayi, Taiwan

Introduction: Traditional Chinese Medicine (TCM) has a broad application in healthcare, with Danshen being a notable herb used in Eastern medicine for cancer treatment. This study aims to explore the relationship between Danshen use and cardiovascular risks among bladder cancer patients.

Methods: Patients were selected based on a confirmed diagnosis of bladder cancer with specific inclusion and exclusion criteria to control for certain comorbidities and treatments. Utilizing Taiwan's National Health Insurance data from 2003 to 2013, this retrospective, population-based study identified three groups: 525 patients treated with Danshen, 6,419 patients not treated with TCM, and 4,356 patients treated with TCM but not with Danshen. The Cox proportional hazard model was employed to estimate the risks of Major Adverse Cardiovascular Events (MACE) and mortality while accounting for various confounders.

Results: The overall incidence of MACEs was significantly lower in the Danshen group (5%) compared to the TCM (8.1%) and non-TCM (9.9%) groups ($p < 0.001$). The Cox model revealed that bladder cancer patients treated with Danshen had the lowest risk of MACE (adjusted hazard ratio, 0.56; 95% confidence interval, 0.38–0.84) and all-cause mortality (adjusted hazard ratio, 0.60; 95% confidence interval, 0.44–0.82).

Discussion: The findings suggest that Danshen reduces the risk of MACE and all-cause mortality in bladder cancer patients, highlighting its potential benefits. This underpins the necessity for further research to substantiate the cardiovascular benefits of Danshen in bladder cancer patients and potentially broaden its application in oncology healthcare.

KEYWORDS

Danshen therapy, bladder cancer, cardiovascular outcomes, traditional Chinese medicine, TCM

Abbreviations: aHR, adjusted hazard ratio; CCIS, Charlson Comorbidity Index Score; CCL2, C-C motif ligand 2; DT, di-hydroisotanshinone I; HR, hazard ratio; ICD-9, International Classification of Diseases, ninth revision; MACE, major adverse cardiac events; NHI, National Health Insurance; NHIRD, National Health Insurance Research Database; STAT3, signal transducer and activator of transcription 3; TCM, traditional Chinese medicine; TSN IIA, sodium tanshinone IIA.

1 Introduction

Bladder cancer is one of the 10 most prevalent malignancies worldwide, with approximately 550,000 new cases diagnosed annually (Richters et al., 2020). Although only 5% of patients initially have metastatic bladder cancer, many patients treated for localized illness relapse or develop advanced stages, with a 5-year relative survival rate of 4.6% (Flaig et al., 2020). Cisplatin-based chemotherapy, which often causes nephrotoxicity, remains the standard treatment for eligible patients with bladder cancer, despite the emergence of immunotherapy (Flaig et al., 2020).

The use of traditional Chinese medicine (TCM) in healthcare is widespread in many Asian and Western countries. Owing to the quality of finished herbal products and their ease of use, TCM doctors often prescribe contemporary forms of decoctions, in which herbal formulas and single herbs are condensed in granulated compounds. Taiwan's National Health Insurance (NHI) program pays claims for finished herbal products, including individual herbs and formulas. As both clinical pharmaceuticals and TCM are often used to explore their clinical effects on patients in Taiwan, the NHI Research Database (NHIRD) of Taiwan provides a wealth of information about the prescriptions, procedures, and diagnoses of patients (Chang et al., 2015; Fleischer et al., 2017; Hung et al., 2017; Lin et al., 2017).

The association between cancer and excess risk of heart disease has received particular attention in recent years (Cardinale et al., 2008; Stoltzfus et al., 2011; Herrmann et al., 2014). Although the mechanism underlying this link is complex, both conditions are speculated to share similar pathophysiological pathways of chronic inflammation and oxidative stress (Johnson et al., 2016). The cardiovascular risk in patients with cancer is further increased by the possible cardiotoxicity associated with cancer therapy. Thus, healthcare professionals are now aware of the common risk factors and are paying specific attention to the cardiovascular health of oncology patients receiving cardiotoxic anticancer medications.

Danshen, derived from the dried root of Salvia miltiorrhiza Bunge, is a traditional Chinese medicine (TCM) agent used predominantly for various endocrine and cardiovascular ailments, encompassing menstrual irregularities, hepatitis, and coronary artery disease. In the context of this study, Danshen was employed as a singular agent. Its bioactive components, notably TSN IIA, have been recognized for their cardioprotective and potential anti-cancer attributes. The influence of Danshen on the progression or therapeutic approach to bladder cancer remains an active area of scholarly investigation. (Han et al., 2002; Liu et al., 2016; Wang et al., 2017; Li et al., 2018; Yuan et al., 2019). Danshen improved the biochemical indicators in 126 patients at a 3-month follow-up, demonstrating a decreased risk of coronary heart disease (Liu et al., 2016). In addition to improving the ejection fraction and fractional shortening, Danshen injections also improved heart function. In a mouse model of heart failure caused by ligation of the left anterior descending coronary artery, intramuscular Danshen injections at a dose of 1.5 mL/kg/d for 14 days prevented left ventricular remodeling (Wang et al., 2017). Therefore, this study aimed to analyze the effects of Danshen on survival and major adverse cardiac events (MACE) in patients with bladder cancer.

2 Materials and methods

2.1 Ethics

This study was approved by the Institutional Review Board of Buddhist Taichung Tzu Chi General Hospital in Taiwan (REC111-14) and was conducted in accordance with the tenets of the Declaration of Helsinki. Before the analysis, the NHIRD identification numbers of individuals were removed from the dataset. The review board waived the requirement for patient consent because of the retrospective nature of the study.

2.2 NHI Research Database

The NHI, a single-payer system managed by the government, was established in Taiwan in 1995. Currently, 99% of Taiwanese residents participate in the NHI program (Chiang, 1997). The National Health Research Institutes collect data related to these services and input them into the NHIRD. It includes inpatient records, outpatient records, medication records, and registration files. The National Health Research Institutes of Taiwan released NHIRD data from 1 January 2003, to 31 December 2013, which were utilized in this investigation. The International Classification of Diseases, Ninth Revision (ICD-9) codes were used in this study, along with records of admissions and outpatient visits, which included patient characteristics such as sex, date of birth, date of admission, date of discharge, date of visit, and up to three diagnoses made during an outpatient visit. The names of the prescribed medications (both Western medicine and TCM), their dosages, durations, total costs, and additional treatments were obtained from the patient prescriptions for this study.

2.3 Danshen exposure and control group selection

The participants were selected from the Registry for Catastrophic Illness Patients of the NHIRD (Figure 1). Patients with bladder cancer were considered eligible if the diagnosis was registered in the Catastrophic Illness database. First, we included patients newly diagnosed with bladder cancer (ICD-9-CM 188) between 1 January 2003, and 31 December 2013 (n = 48,873). Individuals utilizing Danshen for a duration exceeding 30 days, while adhering to a typical clinical dosage of 3 g per day—a standard in clinical Chinese medicine practices, referenced from (Lin et al., 2019) and who received a bladder cancer diagnosis (confirmed through the application for the cancer catastrophic illness certificate) were categorized as Danshen users. In contrast, those employing TCM without incorporating Danshen were identified as TCM users, while those who underwent treatment for a period less than 30 days or abstained from any TCM were classified as non-TCM users. We excluded patients with a follow-up of <3 months and those with MACE that occurred before the index date. The presence of at least three outpatient visits by the same person was confirmed to support these diagnoses. Figure 1 illustrates the inclusion of a matched cohort of 11,300 individuals from an initial sample of 48,875 patients, based on these criteria. From

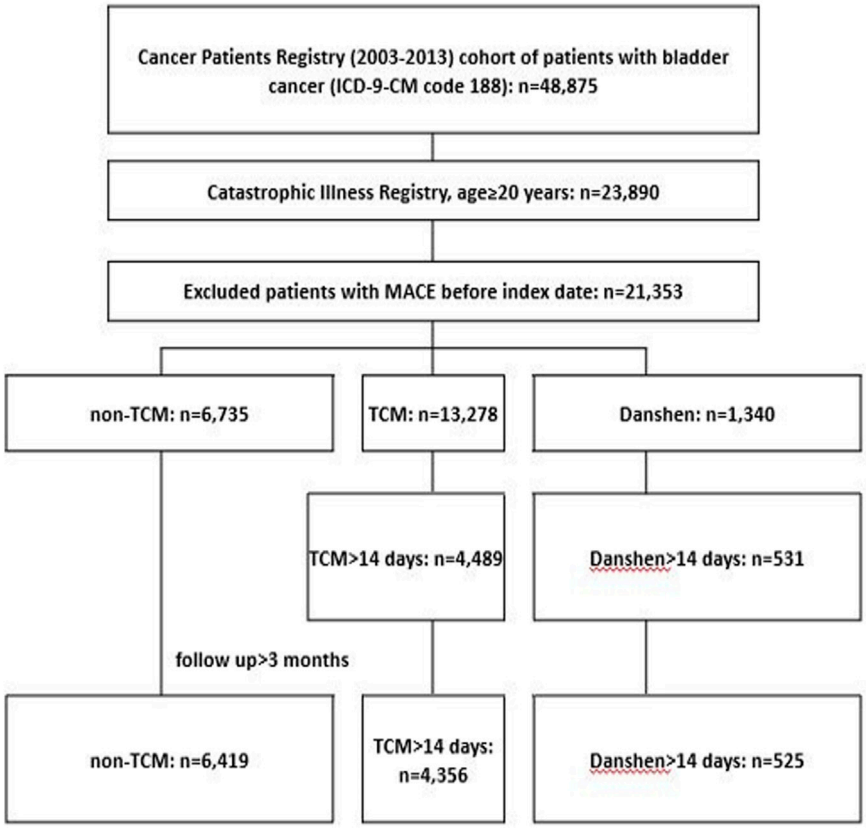

FIGURE 1
Study design flow chart. Danshen, patients who used Danshen; ICD-9-CM, International Classification of Diseases, ninth revision; MACE, major adverse cardiac events; non-TCM, patients who did not use any traditional Chinese medicine; TCM, patients who used traditional Chinese medicine other than Danshen.

1 January 2003, to the date of death, date of removal from the registry, or 31 December 2013, the enrolled patients accrued the follow-up time.

2.4 Covariates

The sociodemographic factors included age and sex. Baseline comorbidities were considered if the following ICD-9-CM codes appeared at least once in patients or inpatients before the initial bladder cancer diagnosis: diabetes mellitus (ICD-9-CM: 250) and hypertension (ICD-9-CM: 401–405). Charlson Comorbidity Index Score (CCIS)-related diagnoses were considered in the analysis, including myocardial infarction (ICD-9-CM: 410, 412), congestive heart failure (ICD-9-CM: 42, 785.4), peripheral vascular disease (ICD-9-CM: 44x), cerebrovascular disease (ICD-9-CM: 43x), dementia (ICD-9-CM: 290), chronic obstructive pulmonary disease (ICD-9-CM: 49x, 500–506), connective tissue disease (ICD-9-CM: 710.x), peptic ulcer disease (ICD-9-CM: 533.xx), chronic kidney disease (ICD-9-CM: 582, 583, 585, 586, 588), hemiplegia (ICD-9-CM: 342, 344.1), leukemia (ICD-9-CM: 204, 206, 207, 208), malignant lymphoma (ICD-9-CM: 200, 201, 202, 203, 205), solid tumor (ICD-9-CM: 196–199), and liver disease (ICD-9-CM: 571.2, 571.4, 571.5, 571.6).

2.5 Statistical analysis

SAS 9.4 (SAS Institute Inc., Cary, NC, United States) was used for all analyses. Baseline attributes are reported as number and percentage for categorical data and as mean and standard deviation for continuous data. For categorical data, the $\chi 2$ and Fisher's exact tests were used. Analysis of variance was used for continuous variables. The threshold for statistical significance was set at a confidence level of alpha = 0.05. The life table technique (SAS LIFETEST program) was used to estimate the Kaplan–Meier survival curves for all-cause mortality and MACE, and the log-rank test was used to analyze the differences among the Danshen, TCM, and non-TCM groups. Sex, diabetes, hypertension, myocardial infarction, congestive heart failure, peripheral vascular disease, dementia, connective tissue disease, peptic ulcer disease, chronic kidney disease, hemiplegia, leukemia, malignant lymphoma, solid tumors, and liver disease were adjusted for in all Cox proportional hazard models.

3 Results

3.1 Patient characteristics

A total of 4,881 patients (3,389 males and 1,492 females) with bladder cancer who were prescribed Chinese medicine in Taiwan

TABLE 1 Comparison of demographic characteristics among patients in the tress groups.

	Non-TCM *n* = 6,419	TCM *n* = 4,356	Danshen *n* = 525	*p*-value
Age	68.6 ± 12.9	64.2 ± 12.2	63.1 ± 11.4	<0.001
Sex male	5,128 (79.9)	3,031 (69.6)	358 (68.2)	<0.001
CCIS	1.3 ± 1.9	1.2 ± 1.8	1.3 ± 1.9	0.017
Myocardial infarction	19 (0.3)	12 (0.3)	2 (0.4)	0.911
Congestive heart failure	679 (10.6)	385 (8.8)	59 (11.2)	0.007
Peripheral vascular disease	130 (2.0)	98 (2.2)	8 (1.5)	0.473
Cerebrovascular disease	318 (5.0)	162 (3.7)	14 (2.7)	0.001
Dementia	80 (1.2)	29 (0.7)	7 (1.3)	0.010
COPD	685 (10.7)	409 (9.4)	47 (9.0)	0.064
Connective tissue disease	47 (0.7)	56 (1.3)	3 (0.6)	0.009
Peptic ulcer disease	677 (10.5)	590 (13.5)	68 (13.0)	<0.001
Chronic kidney disease	868 (13.5)	546 (12.5)	73 (13.9)	0.289
Hemiplegia	14 (0.2)	5 (0.1)	0 (0)	0.276
Leukemia	5 (0.1)	4 (0.1)	0 (0)	0.778
Malignant lymphoma	24 (0.4)	15 (0.3)	1 (0.2)	0.786
Solid tumor	380 (5.9)	211 (4.8)	33 (6.3)	0.041
Liver disease	277 (4.3)	240 (5.5)	32 (6.1)	0.007
Diabetes mellitus	1,210 (18.9)	766 (17.6)	82 (15.6)	0.072
Hypertension	2,889 (45.0)	1,788 (41.0)	222 (42.3)	<0.001
Event				<0.001
None	5,014 (78.1)	3,654 (83.9)	462 (88.0)	
MACE	638 (9.9)	353 (8.1)	26 (5.0)	
Death	767 (11.9)	349 (8.0)	37 (7.0)	
Event F/u (year)	4.3 ± 3.1	3.8 ± 2.7	4.9 ± 2.8	<0.001
Overall death	935 (14.6)	407 (9.3)	42 (8.0)	<0.001
Overall death F/u (year)	5.0 ± 3.2	4.4 ± 2.7	5.4 ± 2.8	<0.001
First hospitalization	5,249 (81.8)	2,966 (68.1)	368 (70.1)	<0.001
Time to first hospitalization, median (month) (Q1, Q3)	2.7 (0.7, 8.1)	6.5 (1.9, 19.3)	9.9 (2.5, 26.8)	<0.001
Socioeconomic status				<0.001
Low SES	2,232 (34.8)	1,345 (30.9)	163 (31.0)	
Moderate and high SES	4,187 (65.2)	3,011 (69.1)	362 (69.0)	
Geographic region				0.079
Northern/Central	3,791 (59.1)	2,527 (58.0)	285 (54.3)	
Southern/Eastern	2,628 (40.9)	1,829 (42.0)	240 (45.7)	

CCIS, charlson comorbidity index score; COPD, chronic obstructive pulmonary disease; F/u, follow-up; MACE, major adverse cardiac events; Q, quartile; SES, socioeconomic status; TCM, traditional Chinese medicine.

were included in our study cohort, which was obtained from the NHIRD. Another 6,419 patients with bladder cancer who did not use Chinese medicine were included in the control group, consisting of 5,128 male and 1,291 female patients. Among the student population, we identified 525 patients treated with Danshen, 4,356 patients treated with TCM but not Danshen, and 6,419 patients not treated with TCM. A comparison of the demographic characteristics, CCIS-related comorbidities, MACE, mortality rates, length of stay in the first hospitalization, socioeconomic status, and geographic regions among patients in the stress groups is shown in Table 1. Patients in the non-TCM group were significantly older than those in the other two groups ($p < 0.001$). CCISs of patients in the Danshen and non-TCM groups were higher than those of patients in the TCM group ($p < 0.05$). The proportion of myocardial infarction was not significantly different among the three groups, although the Danshen group had the highest proportion (11.2%), followed by the non-TCM group (10.6%) and the TCM group (8.8%). For cerebrovascular diseases, the non-TCM group had the highest proportion (5.0%) compared with the other two groups (3.7% for TCM and 2.7% for Danshen) ($p < 0.01$). The frequency of hypertension was higher in the non-TCM group (45.0%) than in the TCM (41.0%) and Danshen (42.3%) groups ($p < 0.001$). In addition, the Danshen group had the lowest MACE rate during the short-term follow-up compared with the TCM and non-TCM groups ($p < 0.001$). The Danshen group had the lowest overall mortality rate (8.0%), whereas the non-TCM group had the highest mortality rate (14.6%). During the first hospitalization, the TCM group had the lowest rate (68.1%), followed by the Danshen group (70.1%). During the first hospitalization, the patients in the Danshen group had the

TABLE 2 Cox's proportional hazard model in patients of the Danshen group.

	MACE				Death			
	Crude HR (95%CI)	*p*-value	Adjusted HR (95%CI)	*p*-value	Crude HR (95%CI)	*p*-value	Adjusted HR (95%CI)	*p*-value
Drug Group								
Non-TCM	Ref.		Ref.		Ref.		Ref.	
TCM	0.91 (0.80–1.04)	0.172	1.12 (0.98–1.28)	0.106	0.69 (0.62–0.78)	<.001	0.81 (0.72–0.91)	<.001
Danshen	0.44 (0.30–0.65)	<.001	0.56 (0.38–0.84)	0.004	0.51 (0.37–0.69)	<.001	0.60 (0.44–0.82)	<.001
Age	1.04 (1.03–1.05)	<.001	1.04 (1.03–1.04)	<.001	1.03 (1.02–1.03)	<.001	1.02 (1.02–1.03)	<.001
Male sex	1.14 (0.98–1.33)	0.074			1.16 (1.02–1.31)	0.026	1.16 (1.02–1.32)	0.025
CCIS	1.07 (1.04–1.11)	<.001	0.96 (0.92–1.00)	0.059	1.18 (1.16–1.21)	<.001	1.17 (1.14–1.2)	<.001
Diabetes mellitus	1.76 (1.53–2.02)	<.001	1.50 (1.28–1.74)	<.001	1.29 (1.14–1.47)	<.001	0.99 (0.86–1.13)	0.854
Hypertension	2.10 (1.85–2.38)	<.001	1.56 (1.37–1.78)	<.001	1.34 (1.20–1.49)	<.001	1.02 (0.91–1.14)	0.765
COPD	1.66 (1.39–1.97)	<.001	1.25 (1.04–1.50)	0.019	1.70 (1.47–1.96)	<.001	1.12 (0.96–1.31)	0.138
Chronic kidney disease	1.51 (1.29–1.78)	<.001	1.71 (1.41–2.07)	<.001	1.51 (1.32–1.74)	<.001	1.09 (0.94–1.28)	0.252
Socioeconomic status								
Low SES	Ref.		Ref.		Ref.		Ref.	
Moderate and high SES	0.77 (0.68–0.88)	<.001	0.91 (0.80–1.04)	0.166	0.50 (0.45–0.55)	<.001	0.56 (0.5–0.62)	<.001
Geographic region								
Northern/Central	Ref.				Ref.		Ref.	
Southern/Eastern	1.03 (0.91–1.17)	0.603			0.80 (0.72–0.89)	<.001	0.83 (0.74–0.92)	<.001

CI, confidence interval; CCIS, charlson comorbidity index score; COPD, chronic obstructive pulmonary disease; HR, hazard ratio; MACE, major adverse cardiac events; Ref., reference; SES, socioeconomic status; TCM, traditional Chinese medicine.

longest length of stay (9.9 months) compared with those in the non-TCM (2.7 months) and TCM (6.5 months) groups. No significant differences were noted between patients from different geographic regions.

3.2 Association between Danshen use and clinical outcomes

The patients in the Danshen group had the lowest crude hazard ratio (HR) for all-cause mortality [HR: 0.51 (0.37–0.69)] and MACE [HR: 0.44 (0.30–0.65)] in the Cox proportional model (Table 2). Age was a significant risk factor for MACE and mortality in the adjusted model [adjusted HR (aHR): 1.04 (1.03–1.04) for MACE and aHR: 1.02 (1.02–1.03) for all-cause mortality]. While sex was a risk factor for MACE in the model, male sex posed a greater risk for all-cause mortality, with an aHR of 1.16 (1.02–1.32). A higher CCIS posed a greater risk for all-cause mortality, with an aHR of 1.17 (1.14–1.2), but not for MACE. Diabetes mellitus, hypertension, chronic obstructive pulmonary disease, and chronic kidney disease were risk factors for MACE but not for all-cause mortality. However, a higher socioeconomic status lowered the risk of all-cause mortality, although not MACE, with an aHR of 0.56 (0.5–0.62). Kaplan–Meier survival curves yielded similar results; the Danshen group showed better survival and lower MACE rates than the other groups (all $p < 0.001$) (Figure 2).

4 Discussion

In this study, we found that Danshen use was associated with a 40% decrease in mortality and a 44% reduction in MACE compared with those in the TCM and non-TCM groups. Compared to previous studies on Danshen's effects on cardiovascular outcomes in cancer patients, our findings provide a more comprehensive understanding, especially in the context of bladder cancer. Patients with bladder cancer treated with Danshen showed a significantly lower incidence of MACE and improved survival rates. A meta-analysis of 20 randomized controlled trials including 2,574 patients with coronary heart disease showed that Danshen decreased the MACE risk ratio by 47% (Li et al., 2020). Notably, sodium tanshinone IIA (TSN IIA) sulfonate isolated from Danshen exerted a cardioprotective effect by reducing myocardial infarct size in a rabbit model, suggesting beneficial effects on the clinically crucial vascular endothelium (Wu et al., 1993).

Cardiovascular toxicity caused by cancer treatments has attracted the attention of both cardiologists and oncologists. Chemotherapeutic drugs, cancer-targeting agents, and irradiation can cause cardiovascular damage, leading to plaque formation, thrombosis, arrhythmia, or cardiomyopathy (Weaver et al., 2013). Left ventricular dysfunction and congestive heart failure caused by accumulated anthracycline doses are among the most well-established cardiotoxic side effects (Volkova and Russell, 2011). Emotional stress in patients with cancer may also cause Takotsubo (stress-induced) cardiomyopathy (Haugnes et al., 2010). Moreover, cardiovascular risk factors such as hypertension,

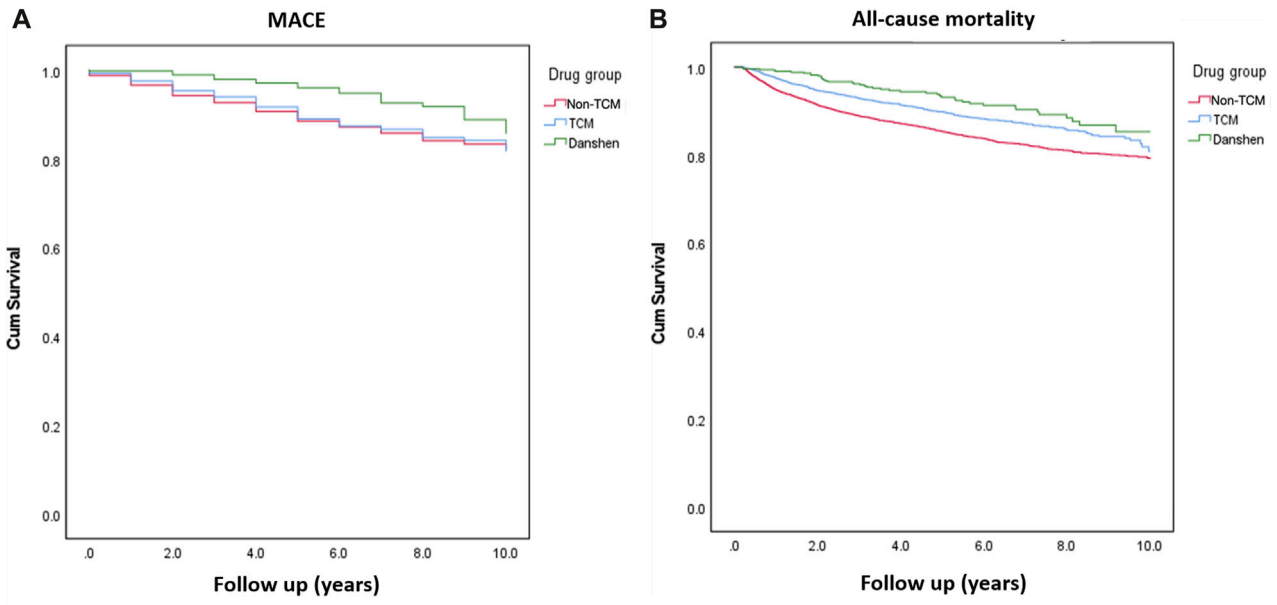

FIGURE 2
Kaplan–Meier curves of the cumulative incidence of MACE **(A)** and all-cause mortality **(B)** in patients with bladder cancer who were treated with Danshen, traditional Chinese medicine without Danshen (TCM), or therapies other than TCM (non-TCM). The log-rank test was used to compare the Kaplan–Meier curves. Both parameters had significant group differences with $p < 0.001$. MACE, major adverse cardiac events.

diabetes mellitus, obesity, smoking, and inactivity are common among cancer survivors (Weaver et al., 2013). Additionally, epidemiological data have identified similar risk factors, such as smoking, obesity, an imbalanced diet, and insufficient physical exercise, for both cancer and cardiovascular diseases (Johnson et al., 2016). Notably, cardiotoxicity is a known side effect of numerous anticancer treatments that increases the risk of cardiovascular disease in patients with cancer (Weaver et al., 2013). For instance, patients with testicular cancer treated with the chemotherapeutic drug cisplatin, which is frequently used to treat bladder cancer, have an increased risk of coronary artery disease (Huddart et al., 2003; Haugnes et al., 2010). The long-term side effects of cancer therapies such as cisplatin administration also include hypertension (Sagstuen et al., 2005).

TCM offers an alternative method for treating cardiovascular damage caused by cancer treatment. According to the TCM theory, Danshen is highly efficient in promoting circulation, removing blood stasis, and blood thinning (Cheng, 2006). Purified S. miltiorrhiza extracted from Danshen was evaluated for myocardial ischemia/reperfusion injury in isolated rat hearts, and post-ischemic contractile function recovered significantly better in the hearts of the Danshen-treated group (Chang et al., 2006). By preventing the expression of profibrotic molecules, inflammation, and cell death, Danshen dripping pill has been shown to protect against myocardial damage caused by doxorubicin or isoprenaline in C57BL/6 mice in a heart failure model (Feng et al., 2021). Danshen contains the pharmacologically active ingredient TSN IIA, which exerts cardioprotective effects. TSN IIA prevents Leu27 insulin-like growth factor II-enhanced insulin-like growth factor II receptor-mediated cardiac apoptosis (Chou et al., 2022). In the current study, Danshen therapy offered better cardiac protection and decreased the risk of MACEs compared with other TCM and non-TCM treatments in patients with bladder cancer. While our study is based on data from Taiwan, the findings may have implications for broader populations. However, cultural, genetic, or healthcare system factors in Taiwan might influence the results.

Several studies have explored the relationship between Danshen and its effects on cardiovascular and cancer outcomes. Our findings align with some of these studies and provide a unique perspective on bladder cancer patients. In recent years, research on the mechanisms underlying the antitumor properties of active Danshen ingredients has progressed, and Danshen has been used as an anticancer treatment. Studies have identified numerous key anticancer components in Danshen, including di-hydroisotanshinone I (DT), which has been demonstrated to cause cell death. In a rat model of head and neck squamous cell carcinoma, p38 signaling was shown to partially control DT-induced cell death and reduce tumor growth (Hsu et al., 2021). Another study revealed that DT prevents prostate cancer cells from attracting macrophages and inhibits the expression of signal transducer and activator of transcription 3 (STAT3), which causes cancer cells to secrete chemokine ligand 2 (Hsu et al., 2021). Another active Danshen component, cryptotanshinone, influences the Janus kinase-2/STAT3 signaling pathway, causing esophageal cancer cells to undergo apoptosis (Ji et al., 2019). Additionally, cryptotanshinone diminishes the effects of dynamin-related protein 1 and fragments mitochondria (Yen et al., 2019). In addition to safeguarding the cardiovascular system, TSN IIA exhibits anticancer properties. TSN IIA controls the STAT3/chemokine ligand 2 signaling pathway to prevent epithelial-mesenchymal transition in bladder cancer cells (Huang et al., 2017). By encouraging the activation of anti-protein kinase RNA-like endoplasmic reticulum kinase, anti-activating transcription factor 6, caspase-12, caspase-3, inositol-requiring enzyme 1, and anti-CCAAT enhancer-binding protein homologous protein, TSN IIA can cause endoplasmic reticulum stress in pan-cancerous cells (Chiu and Su, 2017).

This study used the NHIRD, which is frequently evaluated for diagnostic accuracy by the NHI Bureau of Taiwan, as a nationwide population database. Approximately 99% of Taiwan's population and hospitals are represented in the database, which contains all ambulatory and inpatient treatment records (Hsieh et al., 2019). Taiwan also offers equitable access to healthcare for all citizens, creating excellent circumstances for epidemiological research. A recent study based on the Taiwan NHIRD found that the highest usage rate of Danshen was 9.48% for menstrual disorders and abnormal bleeding from the female genital tract, whereas usage for cardiovascular symptoms was the third most common application at 4.18% (Tseng et al., 2021). After considering comorbidities, our population-based study found that Danshen dramatically reduced the incidence of MACEs in patients with bladder cancer. Moreover, the mortality rate was lower in the Danshen group than in the non-TCM group. Building on our findings, a prospective study or randomized controlled trial would be a valuable next step. Investigating the relationship between Danshen and cardiovascular outcomes in other populations or settings would also be beneficial.

4.1 Limitations

This study had some limitations, including potential biases due to its retrospective nature. Limitations in data sources and the categorization of variables might also influence the results., in which two or more experts reviewed the data upon confirmation of the diagnosis, we were unable to fully verify these data. While we adjusted for several potential confounders in our analysis, we acknowledge that information on certain confounders, like alcohol consumption and smoking status, is not included in the NHIRD. Additionally, it is crucial to note that we are unable to ascertain the specific staging of bladder cancer in this study. This lack of granularity in the data may mask potential variances in the effects of Danshen across different cancer stages. In future research, a more detailed, stage-specific analysis would indeed be beneficial to provide more nuanced insights. Future research would benefit from a more detailed, stage-specific analysis to provide nuanced insights. Further studies are also warranted to explore the mechanism of action of Danshen in patients with bladder cancer.

An additional limitation to note is that TCM treatments are typically personalized, based on individual patient conditions. Due to the limitations of the NHIRD, detailed consultation data, including specific treatments for various reasons, is not available. Nonetheless, we have endeavored to control for potential variability in complex conditions using Cox's proportional hazard model in Table 2. Regarding conventional drug treatments for the non-TCM group, the NHIRD does not provide specific details about the medications prescribed to the patients in our study.

5 Conclusion

Danshen may be useful in reducing the risks of MACE and all-cause mortality in patients with bladder cancer. The observed benefits suggest its potential integration into standard care protocols, especially for patients at risk of cardiovascular events. In conclusion, our study highlights the potential benefits of Danshen in reducing cardiovascular risks in bladder cancer patients. These findings pave the way for further research and potential clinical applications.

Data availability statement

The original contributions presented in the study are included in the article/Supplementary Material, further inquiries can be directed to the corresponding author.

Ethics statement

The studies involving humans were approved by the institutional review board of the Buddhist Taichung Tzu Chi General Hospital in Taiwan (REC111-14). The studies were conducted in accordance with the local legislation and institutional requirements. The ethics committee/institutional review board waived the requirement of written informed consent for participation from the participants or the participants' legal guardians/next of kin because the review board waived the requirement for patient written informed consent due to the nature of this retrospective study.

Author contributions

Y-HC: Investigation, Writing–original draft, Data curation. C-TC: Supervision, Writing–original draft, Investigation. H-PW: Writing–review and editing, Conceptualization, Data curation, Visualization.

Funding

The authors declare that no financial support was received for the research, authorship, and/or publication of this article.

Conflict of interest

The authors declare that the research was conducted in the absence of any commercial or financial relationships that could be construed as a potential conflict of interest.

Publisher's note

References

Cardinale, D., Colombo, A., Lamantia, G., Colombo, N., Civelli, M., De Giacomi, G., et al. (2008). Cardio-oncology: a new medical issue. *Ecancermedicalscience* 2, 126. doi:10.3332/ecancer.2008.126

Chang, C. M., Chu, H. T., Wei, Y. H., Chen, F. P., Wang, S., Wu, P. C., et al. (2015). Corrigendum: the core pattern analysis on Chinese herbal medicine for Sjögren's syndrome: a nationwide population-based study. *Sci. Rep.* 5, 14887. doi:10.1038/srep14887

Chang, P. N., Mao, J. C., Huang, S. H., Ning, L., Wang, Z. J., On, T., et al. (2006). Analysis of cardioprotective effects using purified Salvia miltiorrhiza extract on isolated rat hearts. *J. Pharmacol. Sci.* 101, 245–249. doi:10.1254/jphs.fpj05034x

Cheng, T. O. (2006). Danshen: a versatile Chinese herbal drug for the treatment of coronary heart disease. *Int. J. Cardiol.* 113, 437–438. doi:10.1016/j.ijcard.2005.10.026

Chiang, T. L. (1997). Taiwan's 1995 health care reform. *Health Policy* 39, 225–239. doi:10.1016/s0168-8510(96)00877-9

Chiu, T. L., and Su, C. C. (2017). Tanshinone IIA increases protein expression levels of PERK, ATF6, IRE1α, CHOP, caspase-3 and caspase-12 in pancreatic cancer BxPC-3 cell-derived xenograft tumors. *Mol. Med. Rep.* 15, 3259–3263. doi:10.3892/mmr.2017.6359

Chou, S. L., Ramesh, S., Kuo, C. H., Ali, A., Ho, T. J., Chang, K. P., et al. (2022). Tanshinone IIA inhibits Leu27IGF-II-induced insulin-like growth factor receptor II signaling and myocardial apoptosis via estrogen receptor-mediated Akt activation. *Environ. Toxicol.* 37, 142–150. doi:10.1002/tox.23385

Feng, K., Liu, Y., Sun, J., Zhao, C., Duan, Y., Wang, W., et al. (2021). Compound Danshen dripping pill inhibits doxorubicin or isoproterenol-induced cardiotoxicity. *Biomed. Pharmacother.* 138, 111531. doi:10.1016/j.biopha.2021.111531

Flaig, T. W., Spiess, P. E., Agarwal, N., Bangs, R., Boorjian, S. A., Buyyounouski, M. K., et al. (2020). Bladder cancer, version 3.2020, NCCN clinical practice guidelines in oncology. *J. Natl. Compr. Canc Netw.* 18, 329–354. doi:10.6004/jnccn.2020.0011

Fleischer, T., Chang, T. T., Chiang, J. H., Sun, M. F., and Yen, H. R. (2017). Improved survival with integration of Chinese herbal medicine therapy in patients with acute myeloid leukemia: a nationwide population-based cohort study. *Integr. Cancer Ther.* 16, 156–164. doi:10.1177/1534735416664171

Han, S., Zheng, Z., and Ren, D. (2002). Effect of Salvia miltiorrhiza on left ventricular hypertrophy and cardiac aldosterone in spontaneously hypertensive rats. *J. Huazhong Univ. Sci. Technol. Med. Sci.* 22, 302–304. doi:10.1007/BF02896770

Haugnes, H. S., Wethal, T., Aass, N., Dahl, O., Klepp, O., Langberg, C. W., et al. (2010). Cardiovascular risk factors and morbidity in long-term survivors of testicular cancer: a 20-year follow-up study. *J. Clin. Oncol.* 28, 4649–4657. doi:10.1200/JCO.2010.29.9362

Herrmann, J., Lerman, A., Sandhu, N. P., Villarraga, H. R., Mulvagh, S. L., and Kohli, M. (2014). Evaluation and management of patients with heart disease and cancer: cardio-oncology. *Mayo Clin. Proc.* 89, 1287–1306. doi:10.1016/j.mayocp.2014.05.013

Hsieh, C. Y., Su, C. C., Shao, S. C., Sung, S. F., Lin, S. J., Kao Yang, Y. H., et al. (2019). Taiwan's national health insurance research database: past and future. *Clin. Epidemiol.* 11, 349–358. doi:10.2147/CLEP.S196293

Hsu, C. M., Yang, M. Y., Tsai, M. S., Chang, G. H., Yang, Y. H., Tsai, Y. T., et al. (2021). Dihydroisotanshinone I as a treatment option for head and neck squamous cell carcinomas. *Int. J. Mol.* 22, 8881. doi:10.3390/ijms22168881

Huang, S. Y., Chang, S. F., Liao, K. F., and Chiu, S. C. (2017). Tanshinone IIA inhibits Epithelial-Mesenchymal transition in bladder cancer cells via modulation of STAT3-CCL2 signaling. *Int. J. Mol. Sci.* 18, 1616. doi:10.3390/ijms18081616

Huddart, R. A., Norman, A., Shahidi, M., Horwich, A., Coward, D., Nicholls, J., et al. (2003). Cardiovascular disease as a long-term complication of treatment for testicular cancer. *J. Clin. Oncol.* 21, 1513–1523. doi:10.1200/JCO.2003.04.173

Hung, K. F., Hsu, C. P., Chiang, J. H., Lin, H. J., Kuo, Y. T., Sun, M. F., et al. (2017). Complementary Chinese herbal medicine therapy improves survival of patients with gastric cancer in Taiwan: a nationwide retrospective matched-cohort study. *J. Ethnopharmacol.* 199, 168–174. doi:10.1016/j.jep.2017.02.004

Ji, Y., Liu, Y., Xue, N., Du, T., Wang, L., Huang, R., et al. (2019). Cryptotanshinone inhibits esophageal squamous-cell carcinoma *in vitro* and *in vivo* through the suppression of STAT3 activation. *Onco Targets Ther.* 12, 883–896. doi:10.2147/OTT.S187777

Johnson, C. B., Davis, M. K., Law, A., and Sulpher, J. (2016). Shared risk factors for cardiovascular disease and cancer: implications for preventive health and clinical care in oncology patients. *Can. J. Cardiol.* 32, 900–907. doi:10.1016/j.cjca.2016.04.008

Li, C., Li, Q., Xu, J., Wu, W., Wu, Y., Xie, J., et al. (2020). The efficacy and safety of compound Danshen dripping pill combined with percutaneous coronary intervention for coronary heart disease. *Evid. Based Complement. Altern. Med.* 2020, 5067137. doi:10.1155/2020/5067137

Li, Z. M., Xu, S. W., and Liu, P. Q. (2018). Salvia miltiorrhizaBurge (Danshen): a golden herbal medicine in cardiovascular therapeutics. *Acta Pharmacol. Sin.* 39, 802–824. doi:10.1038/aps.2017.193

Lin, T. H., Yen, H. R., Chiang, J. H., Sun, M. F., Chang, H. H., and Huang, S. T. (2017). The use of Chinese herbal medicine as an adjuvant therapy to reduce incidence of chronic hepatitis in colon cancer patients: a Taiwanese population-based cohort study. *J. Ethnopharmacol.* 202, 225–233. doi:10.1016/j.jep.2017.03.027

Lin, Y. S., Shen, Y. C., Wu, C. Y., Tsai, Y. Y., Yang, Y. H., Kuan, F. C., et al. (2019). Danshen improves survival of patients with breast cancer and dihydroisotanshinone I induces ferroptosis and apoptosis of breast cancer cells. *Front. Pharmacol.* 10, 1226. doi:10.3389/fphar.2019.01226

Liu, B., Du, Y., Cong, L., Jia, X., and Yang, G. (2016). Danshen (Salvia miltiorrhiza) compounds improve the biochemical indices of the patients with coronary heart disease. *Evid. Based Complement. Altern. Med.* 2016, 9781715. doi:10.1155/2016/9781715

Richters, A., Aben, K. K. H., and Kiemeney, LALM (2020). The global burden of urinary bladder cancer: an update. *World J. Urol.* 38, 1895–1904. doi:10.1007/s00345-019-02984-4

Sagstuen, H., Aass, N., Fosså, S. D., Dahl, O., Klepp, O., Wist, E. A., et al. (2005). Blood pressure and body mass index in long-term survivors of testicular cancer. *J. Clin. Oncol.* 23, 4980–4990. doi:10.1200/JCO.2005.06.882

Stoltzfus, K. C., Zhang, Y., Sturgeon, K., Sinoway, L. I., Trifiletti, D. M., Chinchilli, V. M., et al. (2011). Fatal heart disease among cancer patients. *Nat. Commun.* 11, 2011. doi:10.1038/s41467-020-15639-5

Tseng, Y. J., Hung, Y. C., Kuo, C. E., Chung, C. J., Hsu, C. Y., Muo, C. H., et al. (2021). Prescription of radix Salvia miltiorrhiza in Taiwan: a Population-Based study using the national health insurance research database. *Front. Pharmacol.* 12, 719519. doi:10.3389/fphar.2021.719519

Volkova, M., and Russell, R., 3rd (2011). Anthracycline cardiotoxicity: prevalence, pathogenesis and treatment. *Curr. Cardiol. Rev.* 7, 214–220. doi:10.2174/157340311799960645

Wang, L., Yu, J., Fordjour, P. A., Xing, X., Gao, H., Li, Y., et al. (2017). Danshen injection prevents heart failure by attenuating post-infarct remodeling. *J. Ethnopharmacol.* 205, 22–32. doi:10.1016/j.jep.2017.04.027

Weaver, K. E., Foraker, R. E., Alfano, C. M., Rowland, J. H., Arora, N. K., Bellizzi, K. M., et al. (2013). Cardiovascular risk factors among long-term survivors of breast, prostate, colorectal, and gynecologic cancers: a gap in survivorship care? *J. Cancer Surviv* 7, 253–261. doi:10.1007/s11764-013-0267-9

Wu, T. W., Zeng, L. H., Fung, K. P., Wu, J., Pang, H., Grey, A. A., et al. (1993). Effect of sodium tanshinone IIA sulfonate in the rabbit myocardium and on human cardiomyocytes and vascular endothelial cells. *Biochem. Pharmacol.* 46, 2327–2332. doi:10.1016/0006-2952(93)90624-6

Yen, J. H., Huang, H. S., Chuang, C. J., and Huang, S. T. (2019). Activation of dynamin-related protein 1 - dependent mitochondria fragmentation and suppression of osteosarcoma by cryptotanshinone. *J. Exp. Clin. Cancer Res.* 38, 42. doi:10.1186/s13046-018-1008-8

Yuan, T., Chen, Y., Zhou, X., Lin, X., and Zhang, Q. (2019). Effectiveness and safety of danshen injection on heart failure: protocol for a systematic review and meta-analysis. *Medicine* 98, e15636. doi:10.1097/MD.0000000000015636

frontiers | Frontiers in Pharmacology

TYPE Review
PUBLISHED 16 January 2024
DOI 10.3389/fphar.2024.1323083

OPEN ACCESS

EDITED BY
Pranav Kumar Prabhakar,
Lovely Professional University, India

REVIEWED BY
Yong Zhi Lun,
Putian University, China

*CORRESPONDENCE
Angelika Buczyńska,
angelika.buczynska@umb.edu.pl
Anna Popławska-Kita,
annapoplawskakita@op.pl

†These authors have contributed equally to this work

RECEIVED 17 October 2023
ACCEPTED 02 January 2024
PUBLISHED 16 January 2024

CITATION
Buczyńska A, Kościuszko M, Krętowski AJ and Popławska-Kita A (2024), Exploring the clinical utility of DPP-IV and SGLT2 inhibitors in papillary thyroid cancer: a literature review. *Front. Pharmacol.* 15:1323083. doi: 10.3389/fphar.2024.1323083

Exploring the clinical utility of DPP-IV and SGLT2 inhibitors in papillary thyroid cancer: a literature review

Angelika Buczyńska[1]*, Maria Kościuszko[2], Adam Jacek Krętowski[1,2†] and Anna Popławska-Kita[2*†]

[1]Clinical Research Centre, Medical University of Bialystok, Bialystok, Poland, [2]Department of Endocrinology, Diabetology and Internal Medicine, Medical University of Bialystok, Bialystok, Poland

In the realm of clinical management, Papillary Thyroid Cancer (PTC) stands out as a prevalent thyroid malignancy, characterized by significant metabolic challenges, particularly in the context of carbohydrate metabolism. Recent studies have unveiled promising applications of Dipeptidyl Peptidase-IV (DPP-IV) and Sodium-Glucose Cotransporter 2 (SGLT2) inhibitors, which are conventionally employed in the treatment of type 2 diabetes mellitus (T2DM), as potential adjuncts in anticancer therapy. DPP-IV and SGLT2 inhibitors can be imply to counteract the Warburg effect in cancer, with a specific focus on PTC, owing to their potential metabolic advantages and their influence on the tumor microenvironment, achieved by imposing restrictions on glucose accessibility. Consequently, a comprehensive review has been undertaken, involving meticulous examination of the existing body of evidence pertaining to the utilization of DPP-IV and SGLT2 inhibitors in the context of PTC. The mechanisms of action inherent to these inhibitors have been thoroughly explored, drawing upon insights derived from preclinical investigations. Furthermore, this review initiates discussions concerning the implications for future research directions and the formulation of innovative therapeutic strategies for PTC. As the intricate interplay between carbohydrate metabolism, the Warburg effect, and cancer progression garners increasing attention, attaining a comprehensive understanding of the roles played by DPP-IV and SGLT2 inhibitors in PTC management may serve as the cornerstone for novel approaches aimed at enhancing patient care and broadening the spectrum of available therapeutic modalities.

KEYWORDS

papillary thyroid cancer, DPP-IV, lsglt2, adjuvant therapy, thyroid cancer

1 Introduction

Papillary Thyroid Cancer (PTC) is the most prevalent subtype of thyroid malignancy, accounting for approximately 80% of all thyroid cancer cases (Rego-Iraeta et al., 2009; Li et al., 2022). According to data from the Surveillance, Epidemiology, and End Results (SEER) database spanning from 1975 to 2012, the rate of PTC diagnoses rose from 4.8 to 14.9 per 100,000 individuals (K et al., 2020; Davies and Welch, 2006). It typically exhibits relatively favorable prognosis; however, the clinical management of PTC remains a complex and evolving challenge (Gorgone et al., 2009). Nevertheless, the clinical management of

thyroid cancer depends on the specific risk of cancer progression and encompasses various approaches, such as total thyroidectomy, lobectomy, radioiodine therapy (RAI), laser ablation, or active surveillance based on 2015 American Thyroid Association guidance (Haugen et al., 2016). Currently, there is a lack of non-invasive pharmacological interventions that could potentially confer additional anti-cancer effects. This limitation restricts the utilization of non-invasive treatment options, necessitating reliance on invasive methods (Haugen et al., 2016; Cho et al., 2019). The latest literature data highlights that the regulation of carbohydrate metabolism constitutes an important and modern focal point in many anticancer therapies. Accordingly, the Warburg effect represents a significant area of research as the basis for anticancer action in various types of cancers, including thyroid cancer (Tran et al., 2016). Thus, recent research has shed light on the potential role of novel pharmacological medicaments, such as antihyperglycemic agents, in the treatment of PTC (Li et al., 2020). Among these agents, Dipeptidyl Peptidase-IV (DPP-IV) inhibitors and Sodium-Glucose Cotransporter 2 (SGLT2) inhibitors have emerged as promising candidates (Busek et al., 2022; Basak et al., 2023). DPP-IV and SGLT2 inhibitors are primarily known for their applications in the management of type 2 diabetes mellitus (T2DM). DPP-IV inhibitors prevent the degradation of incretin hormones, such as glucagon-like peptide-1 (GLP-1) and glucose-dependent insulinotropic polypeptide (GIP), resulting in improved glycemic control (Golightly et al., 2012). On the other hand, SGLT2 inhibitors reduce glucose reabsorption in the renal tubules, leading to glycosuria and lower blood glucose levels (Scheen, 2015). The link between T2DM and cancer has long been a subject of investigation, and recent studies have demonstrated that individuals with T2DM implicated in antihyperglycemic agents are characterized by decreased risk of certain malignancies, including PTC (Bea et al., 2023). Given the established roles of DPP-IV and SGLT2 inhibitors in diabetes management and their potential impact on cancer pathways, it is essential to explore their potential clinical utility in PTC.

This literature review aims to comprehensively explore the existing evidence regarding the use of DPP-IV and SGLT2 inhibitors in the context of PTC. By examining the mechanisms of action, preclinical studies, and clinical trials, we aim to elucidate the potential benefits and limitations of these pharmacological agents in the management of PTC. Additionally, we will address the implications of these findings for future research directions and potential therapeutic strategies for PTC patients. As the field of thyroid cancer research continues to advance, understanding the role of DPP-IV and SGLT2 inhibitors in potential PTC management may offer new avenues for improving patient outcomes and expanding the therapeutic armamentarium for this prevalent malignancy.

2 Materials and methods

To conduct this comprehensive literature review, a systematic approach encompassing several key steps was employed. Initially, a meticulous selection of pertinent scientific literature related to PTC and DPP-IV SGLT2 inhibitors was undertaken. This encompassed articles, reviews, and clinical studies available in databases such as PubMed, MEDLINE, and Google Scholar. Subsequently, inclusion and exclusion criteria were defined. Only peer-reviewed articles published in the English language were included, and studies encompassing both human and animal models, as well as preclinical and clinical investigations examining the impact of DPP-IV and SGLT2 inhibitors on cancer, especially PTC development, were considered. Conversely, studies not directly relevant to the topic, publications in languages other than English, and those inaccessible via reputable scientific databases were excluded from the review. The search strategy was constructed using a combination of keywords and Medical Subject Headings (MeSH), including terms such as "Papillary Thyroid Cancer," "Thyroid Neoplasms," "DPP-IV inhibitors," "SGLT2 inhibitors," and their variations. Boolean operators (AND, OR) were deployed to formulate precise search queries. Additionally, manual scrutiny of reference lists within selected articles was conducted to identify supplementary sources.

Data extraction involved the retrieval and structured organization of information from the chosen articles. This encompassed details pertaining to study design, patient characteristics, interventions (DPP-IV and SGLT2 inhibitors), outcomes, and conclusions. Particular emphasis was placed on comprehending the mechanisms of action of these inhibitors and their potential influence on PTC development. Qualitative synthesis of the literature was subsequently conducted, focusing on key findings, trends, and novel insights concerning the clinical potential of DPP-IV and SGLT2 inhibitors in the management of PTC. A critical appraisal of the included studies was also performed to assess methodological quality and identify potential sources of bias. Results and interpretations from the selected sources were synthesized and discussed within the context of the research objectives. Implications for future research directions and innovative therapeutic strategies were considered, underscoring the importance of exploring unconventional therapies to optimize outcomes in PTC treatment. The review concluded with a summary of the current state of knowledge in this field.

3 Papillary thyroid cancer risk factors

The incidence of PTC has been steadily increasing over the past few decades worldwide (Sung et al., 2021; Pizzato et al., 2022). PTC displays a significant gender bias, with females being roughly three times as susceptible to its development as males (Arroyo et al., 2022). The consistent gender disparity in PTC incidence has been a recurring observation in various populations and geographical contexts. Numerous investigations have explored plausible factors, including hormonal influences (notably, the presence of estrogen receptors in thyroid tissue, and estrogen's potential role in stimulating thyroid cell growth and proliferation) and genetic factors, such as the BRAF mutation, as well as other genetic alterations like RET/PTC rearrangements and RAS mutations, which may underlie this gender difference (Leclair et al., 2021). Furthermore, PTC can impact individuals across all age brackets, although it is most frequently identified in adults ranging from 30 to 50 years old (Arroyo et al., 2022). Nonetheless, the occurrence of PTC demonstrates substantial variation among various nations and geographic areas. Elevated incidence rates have been documented in

regions characterized by increased iodine consumption, particularly in areas with a high prevalence of goiter (Zhang et al., 2022). Current research endeavors to elucidate the influence of environmental factors, genetic predisposition, and disparities in healthcare practices as contributing factors to these geographical discrepancies (Miranda-Filho et al., 2021). Notably, there is a well-established association between exposure to ionizing radiation, particularly during childhood, and an increased risk of developing PTC (Su et al., 2016). Individuals who have received radiation therapy as a treatment for medical conditions, such as Hodgkin's lymphoma or head and neck cancers, face an elevated likelihood of PTC occurrence (Albi et al., 2017; Buczyńska et al., 2023a). Numerous studies have consistently demonstrated a dose-response relationship between radiation exposure and the risk of PTC. A study conducted by Baloch et al. identified several noteworthy prognostic factors associated with PTC prognosis. These factors encompassed age, tumor size, the presence of lymph node metastasis, extrathyroidal extension, and distant metastasis. The findings indicated that older age, larger tumor size, the presence of lymph node metastasis, and extrathyroidal extension were correlated with a less favorable prognosis, whereas the presence of distant metastasis signified a notably worse outcome. This study provided valuable insights into prognostic factors, including the measurement of angioinvasion, which can aid in predicting the outcomes of patients diagnosed with well-differentiated follicular-derived carcinoma, specifically PTC (Baloch and LiVolsi, 2001; Buczyńska et al., 2023b; Buczyńska et al., 2023c). In light of the above findings, there is a need to continue exploring new, minimally invasive therapeutic approaches that will be well-tolerated within the PTC patient population.

4 Warburg effect–the novel target in PTC clinical management

Literature data has indicated that molecular alterations within signaling pathways, such as RAS, RAF, and mitogen-activated protein kinase (MAPK), play a role in the development of thyroid neoplasms (Soares et al., 2003). Additionally, previous investigations have revealed that thyroid cancer is characterized by enhanced glucose uptake, as detected by 18F-fluorodeoxyglucose positron emission tomography (18F-FDG PET), along with reduced radioiodine uptake capability (Lang and Law, 2011; Larg et al., 2019). In general, transformed cells exhibit modified energy metabolism, as they do not inhibit glycolysis in the presence of oxygen. Nearly a century ago, Warburg observed that cancer cells can convert glucose into lactate even when oxygen is available, a phenomenon termed aerobic glycolysis or the "Warburg effect" (Liberti et al., 2016). Subsequent research has demonstrated increased expression of glucose transporters (GLUTs) alongside decreased oxidative metabolism in cancer cells (Tran et al., 2016; Kościuszko et al., 2023). While the Warburg hypothesis is well-established, the precise adaptive mechanisms responsible for reduced oxidative metabolism in cancer cells remain unclear in many carcinoma models (Schiliro et al., 2021). These characteristics underscore the necessity of investigating the metabolic profile of thyroid tumors (Lee et al., 2015). Despite their representing an intriguing spectrum of tumors with varying prognoses, few studies have directly assessed energy metabolism in relation to tumorigenesis (Martínez-Reyes and Chandel, 2021). Skorupa et al. recently demonstrated that thyroid iodide and glucose uptake are influenced by the AMP-activated protein kinase (AMPK) signaling pathway, often referred to as the cellular energy "fuel gauge" (Skorupa et al., 2021). However, the unique metabolic characteristics of thyroid cancer cells do not merely represent a passive alteration but rather constitute an active change in genetic expression, leading to a shift in metabolic pathways that promote the development and invasiveness of tumors (Heydarzadeh et al., 2020). The study performed by Matsuzu et al. showed that in all thyroid parenchymal cells, there was uniform expression of GLUT1, GLUT3, GLUT4, and GLUT10. GLUT1 exhibited heightened expression in carcinoma cases, as well as when compared to corresponding normal tissue samples from the same patient. The expression levels of other GLUTs remained statistically unchanged in pathological tissues. These findings support the hypothesis that during the development of cancer in the thyroid, GLUT1 becomes overexpressed and could have a significant impact on increased glucose absorption by thyroid cancer cells (Matsuzu et al., 2004). Therefore, high expression of GLUT1, positively correlate with the proliferative index and equates to the malignant characteristic (Morani et al., 2014). Thus, targeting tumor metabolism holds promise as a potential approach for treating thyroid cancer. Additionally, molecules associated with tumor metabolism may serve as prognostic markers for thyroid cancer outcomes (Rogucki et al., 2021; Rogucki et al., 2022). Prior research has linked thyroid cancer progression to increased glucose uptake. These findings suggest that pivotal molecules involved in tumor Warburg effect and metabolism could play a role in predicting the prognosis of thyroid cancer simultaneously defining novel medical targets. The pathomechanism of the Warburg effect, along with the identification of potential medical targets, has been delineated in Figure 1 (Figure 1).

5 Antihyperglycemic agents in the treatment of thyroid cancer

Metformin is a commonly prescribed medication for diabetes management, and it is known for its excellent safety record. Over the past decade, several studies have indicated that metformin can lower thyroid-stimulating hormone (TSH) levels in individuals with diabetes. Most research suggests that metformin can reduce TSH levels in individuals who have either overt or subclinical thyroid issues, but this effect is not observed in people with normal thyroid function (Pappa and Alevizaki, 2013; Adamska et al., 2021; Buczyńska et al., 2021; Buczyńska et al., 2022). Additionally, metformin seems to possess anti-growth properties against various types of thyroid cancer (Wang et al., 2022a). However, there is experimental evidence suggesting that metformin may reduce the effectiveness of radioactive iodine treatment in individuals with differentiated thyroid cancer. This limitation might restrict its use in the management of such cancer cases (Pappa and Alevizaki, 2013). Consequently, exploring alternative antihyperglycemic drugs like DPP-IV and SGLT2 inhibitors is of significant interest for PTC patients. To succinctly encapsulate the key findings of the most significant studies, Table 1 has been generated (Table 1).

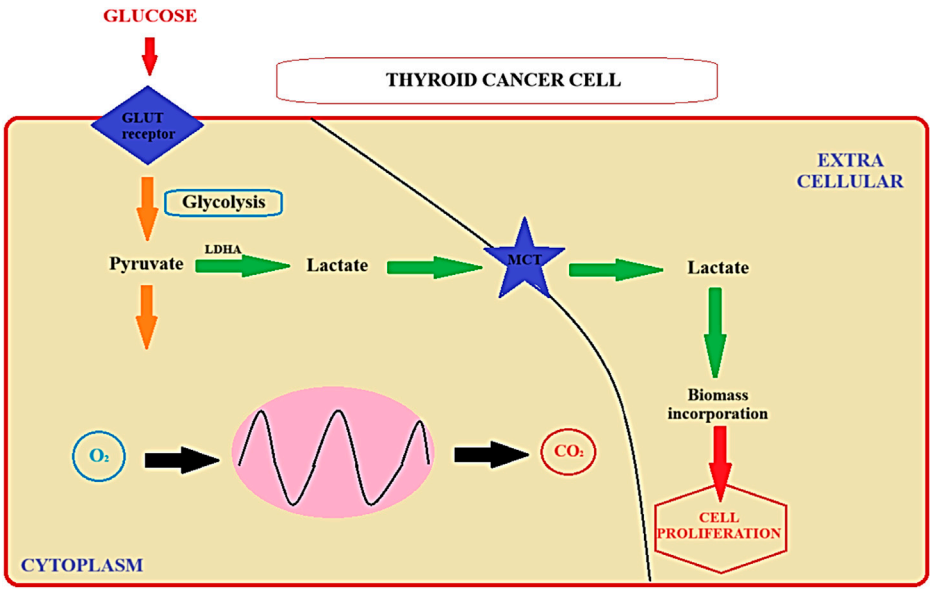

FIGURE 1
The Warburg effect (Liberti et al., 2016). LDHA - Lactate Dehydrogenase A; MCT-Medium-Chain Triglycerides; GLUT Receptor - Glucose Transporter Receptor.

5.1 DPP-IV inhibitors

The scientific basis for their therapeutic utility in the context of cancer treatment lies in their multifaceted actions on various physiological processes. DPP-IV is an enzyme responsible for the degradation of incretin hormones such as glucagon-like peptide-1 (GLP-1) and glucose-dependent insulinotropic peptide (GIP). These hormones play pivotal roles in regulating glucose homeostasis and insulin secretion. DPP-IV inhibitors, by virtue of their mechanism of action, increase the bioavailability of GLP-1 and GIP, leading to enhanced insulin secretion, improved glycemic control, and reduced insulin resistance in diabetes. Beyond their antidiabetic effects, DPP-IV inhibitors have exhibited additional properties that make them potentially valuable in oncology. During DPP-IV inhibition by substance P inhibition of synthesis the expression of GLUT4 in thyroid cancer cells would be reduced (Barchetta et al., 2022). Moreover, DPP-IV is expressed on various immune cells, including T lymphocytes. Inhibition of DPP-IV has been associated with immunomodulatory effects, resulting in enhanced T-cell function and immune responses. This aspect is of particular interest in cancer therapy, where a robust immune response against tumor cells is crucial for effective eradication (Shao et al., 2020). Inflammation is a recognized contributor to cancer progression and metastasis, making the anti-inflammatory potential of DPP-IV inhibitors a valuable asset in cancer treatment. Additionally, DPP-IV has been implicated in angiogenesis, a process pivotal for tumor growth and metastasis. Inhibition of DPP-IV may impede angiogenesis by altering the availability of angiogenic factors, further contributing to its potential antitumor effects. In preclinical studies and some clinical trials, DPP-IV inhibitors have exhibited promise in reducing tumor growth and enhancing the efficacy of conventional cancer therapies (Enz et al., 2019).

5.1.1 Potential implication in PTC clinical management

Preclinical studies and emerging clinical evidence suggest that DPP-IV inhibitors may exert direct anti-tumor effects in PTC (Lee et al., 2017). The schematic depiction of the DPP-IV inhibitor's mechanism, coupled with the identification of potential targets within differentiated thyroid cancer, has been incorporated in Figure 2 (Figure 2).

Gao et al. conducted a study on DPP-IV in thyroid carcinoma (THCA) and its links to prognosis and antitumor immunity. They analyzed data from The Cancer Genome Atlas (TCGA), Genotype-Tissue Expression (GTEx), and Gene Expression Omnibus (GEO) databases to explore DPP-IV expression, its impact on THCA prognosis, and its connection to immune response. Additionally, they validated DPP-IV mRNA levels in 18 THCA tissues and paracancerous tissues and confirmed DPP-IV protein levels in 12 medullary thyroid carcinoma (MTC) tissues using immunohistochemistry. Their bioinformatics analysis revealed that DPP-IV mRNA expression was significantly higher in THCA than in paracancerous tissues, with the highest expression in MTC. They observed differences in DPP-IV expression based on clinical characteristics. Higher DPP-IV expression in THCA was linked to lower disease-free survival (HR = 1.8). The study also showed a substantial connection between DPP-IV, immune cell infiltration, immune response, and 21 immune checkpoint genes (ICGs) in THCA. Laboratory results demonstrated significant upregulation of DPP-IV mRNA in 18 THCA tissues compared to paracancerous tissues. Immunohistochemistry indicated higher DPP-IV protein levels in 12 MTC tissues compared to paracancerous tissues. These effects might involve tumor cell proliferation suppression, apoptosis induction, or interference with PTC progression signaling pathways. DPP-IV inhibitors have shown promise in modulating the immune response,

TABLE 1 The sSummary of kKey fFindings from rRelevant PTC sStudies.

Study type of intervention examination	Participants	Method of detection	Outcomes	Reference
DPP-IV	18 thyroid carcinoma tissues and paracancerous tissues and 12 medullary thyroid carcinoma tissues	immunohistochemistry	DPP-IV mRNA expression was significantly higher in MTC thyroid carcinoma tissues vs. thyroid carcinoma tisues	Gao et al. (2022)
			Higher DPP-IV expression was linked with poorer prognosis	
	N/D	bioinformatics analysis	overexpression of the DPP4/CTNNB1/MET gene is associated with immuno-invasive phenotypes, cancer progression, metastasis, resistance to treatment, and unfavorable clinical outcomes	Cheng et al. (2022)
			DPP-IV inhibitors were designated for these patients	
	mouse xenograft model	immunohistochemistry	high DPP-IV expression was significantly linked to extrathyroidal extension, BRAF mutations, and advanced tumor stages	Lee et al. (2017)
			silencing DPP-IV or using DPP-IV inhibitors significantly reduced colony formation, cell migration, and invasion	
			sitagliptin treatment reduced tumor growth and the expression of transforming growth factor-β receptor I in xenografts mouses	
	GLAG-66 and TPC-1 PTC tissues	silencing the DPP-IV gene using siRNA/DPP-IV inhibitor	Using siRNA or the DPP-IV inhibitor sitagliptin led to a substantial reduction in the expression of key factors associated with PTC pathogenesis; reduced expression and phosphorylation of ERK1/2, JNK1, and P38 MAPK were observed, indicating modulation of the MAPK pathway; Decreased expression of pro-angiogenic factors such as VEGF, along with downregulation of fibroblast growth factor receptors (FGFR-1), TGF-β1, Snail, and HIF-1α, suggests an anti-angiogenic effect; an increase in the expression of cell adhesion protein E-cadherin and apoptosis-related protein Bax was noted, indicating a potential influence on cellular processes	Hu et al. (2021)
SGLT2	thyroid cancer cells both *in vitro* and *in vivo*	immunohistochemistry and clinical dataset analysis	Inhibition of SGLT2 mitigates thyroid cancer cell proliferation *in vitro* and *in vivo*	Wang et al. (2022b)
			Canagliflozin, an SGLT2 inhibitor, suppresses glucose uptake and glycolysis in thyroid cancer cells	
			Canagliflozin inhibits the AKT/mTOR signaling pathway and enhances AMPK activation	
			Canagliflozin hinders the G1 to S phase transition in the cell cycle, downregulating cyclin D1, cyclin D3, cyclin E1, cyclin E2, and E2F1	
			Canagliflozin induces apoptosis in thyroid cancer cells	
			Canagliflozin activates the DNA damage response pathway ATM/CHK2 and increases γ-H2AX expression	
			Elevated SGLT2 levels observed in thyroid cancer tissues of patients	

(Continued on following page)

TABLE 1 (*Continued*) The sSummary of kKey fFindings from rRelevant PTC sStudies.

Study type of intervention examination	Participants	Method of detection	Outcomes	Reference
			Positive correlation between SGLT2 expression and cyclin D3 levels in thyroid cancer patients	
			Inhibition of SGLT2 may restrict PTC development by reducing cyclin D1 and D3 expression, inhibiting excessive cell proliferation	

AKT/mTOR, serine/threonine protein kinase/Mammalian Target of Rapamycin; AMPK - AMP-Activated Protein Kinase; ATM/CHK2 - Ataxia Telangiectasia Mutated/Checkpoint Kinase 2; Bax - Bcl-2-associated X protein; Canagliflozin - SGLT2, inhibitor; DPP-IV, Dipeptidyl Peptidase IV; E-cadherin - Epithelial Cadherin; ERK1/2 - Extracellular Signal-Regulated Kinase 1/2; FGFR-1, Fibroblast Growth Factor Receptor 1; G1 to S phase - Transition from the Gap 1 phase to the Synthesis phase; GLAG-66, type of PTC, tissue; HIF-1α - Hypoxia-Inducible Factor 1 Alpha; JNK1 - c-Jun N-terminal Kinase 1; MAPK, Mitogen-Activated Protein Kinase; MTC, Medullary Thyroid Carcinoma; P38 MAPK, p38 Mitogen-Activated Protein Kinase; N/D–No data; PTC, Papillary Thyroid Carcinoma; SGLT2 - Sodium-Glucose Co-Transporter 2; siRNA, Small Interfering RNA; TPC-1 PTC, Thyroid Papillary Carcinoma; TPC-1, cell line; TGF-β1, Transforming Growth Factor Beta 1; VEGF, Vascular Endothelial Growth Factor; γ-H2AX, Phosphorylated form of Histone H2AX.

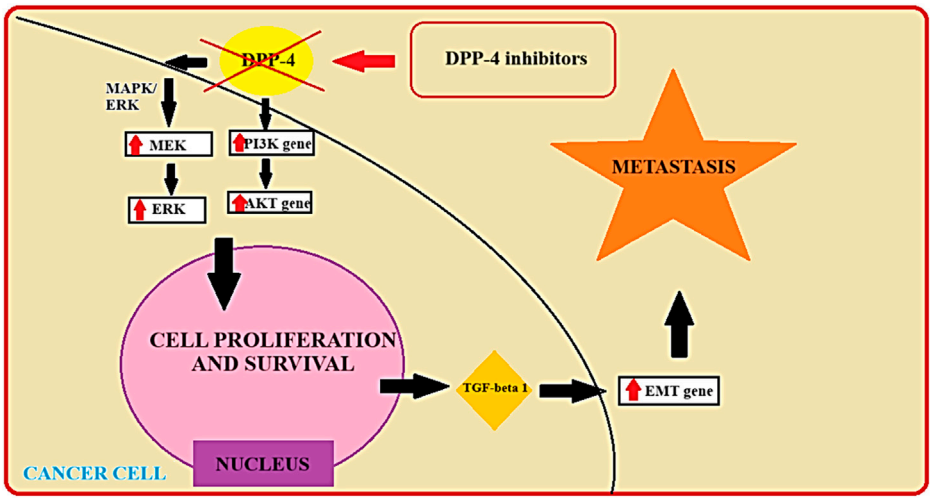

FIGURE 2
The potential targets of DPP-IV among PTC cells (Deacon, 2018). AKT - serine/threonine protein kinase; DPP-4 - Dipeptidyl Peptidase-4; EMT - Epithelial-Mesenchymal Transition Gene; ERK - Extracellular Signal-Regulated Kinase; MAPK/ERK - Mitogen-Activated Protein Kinase/Extracellular Signal-Regulated Kinase; MEK - Mitogen-Activated Protein Kinase; PI3K Gene - Phosphoinositide 3-Kinase Gene; TGF-beta 1 - Transforming Growth Factor-beta 1.

particularly by enhancing T-cell function. This immunomodulatory property is crucial in cancer therapy, potentially enhancing treatment efficacy when combined with conventional treatments like surgery, radioactive iodine therapy, or targeted therapies. Research on the safety and efficacy of such combinations is a critical area of study (Gao et al., 2022). In the similar study performed by Cheng et al., a bioinformatics analysis was employed to identify crucial theragnostic markers for thyroid carcinoma (THCA). Remarkably, the analysis revealed the overexpression of the DPP4/CTNNB1/MET gene signature in PTCa. These findings suggest that this signature is associated with immuno-invasive phenotypes, cancer progression, metastasis, resistance to treatment, and unfavorable clinical outcomes in thyroid cancer patients. Given the limitations of conventional cancer drugs, which can be cytotoxic and non-specific, decided to investigate the potential anticancer effects of the antidiabetic drug sitagliptin, which has recently shown promise as an anticancer agent and is known for its good tolerability and efficacy. Interestingly, their *in silico* molecular docking results indicated that sitagliptin may exhibit putative binding affinities with the DPP4/CTNNB1/MET signatures, surpassing those of standard inhibitors for these genes. This suggests that sitagliptin holds promise as a potential therapeutic option for THCA, warranting further investigation in both *in vitro* and *in vivo* studies, as well as in clinical settings (Cheng et al., 2022).

Therefore, Jie-Jen et al. conducted a study to investigate the role of DPP-IV in thyroid cancer and its underlying mechanisms. Previous research had suggested that DPP-IV could be a marker for thyroid cancer, but its prognostic significance was unclear. They used immunohistochemistry to assess DPP-IV expression in thyroid cancer tissue microarrays. In addition, they conducted *in vitro* studies with genetic and pharmacological DPP-IV inhibition. Gene expression and pathway analyses were used to identify molecular targets affected by DPP-IV. They also evaluated the

therapeutic potential of DPP-IV inhibition using a mouse xenograft model. The study found that high DPP-IV expression was significantly linked to extrathyroidal extension, BRAF mutations, and advanced tumor stages in PTC. Individuals with high DPP-IV expression were less likely to achieve a "no evidence of disease" status during follow-up. *In vitro* experiments showed that silencing DPP-IV or using DPP-IV inhibitors significantly reduced colony formation, cell migration, and invasion. Analysis of gene expression changes after DPP-IV knockdown suggested involvement of the transforming growth factor-β signaling pathway. *In vivo* experiments demonstrated that sitagliptin treatment reduced tumor growth and the expression of transforming growth factor-β receptor I in xenografts (Lee et al., 2017).

In the following study performed by Hu et al. aimed to comprehensively examine the role of the DPP-IV gene in PTC tissues and its potential association with the MAPK pathway the significant increase in DPP-IV gene expression in PTC tissues were observed. Experiments conducted on PTC cell lines (GLAG-66 and TPC-1) demonstrated that silencing the DPP-IV gene using siRNA or employing the DPP-IV inhibitor, sitagliptin, resulted in a substantial reduction in the expression of key factors related to PTC pathogenesis. Specifically, reduced expression and phosphorylation of ERK1/2, JNK1, and P38 MAPK were observed, along with decreased expression of pro-angiogenic factors (VEGF), fibroblast growth factor receptors (FGFR-1), transforming growth factor β1 (TGF-β1), Snail, and hypoxia-inducible factor 1α (HIF-1α). Simultaneously, an increase in the expression of cell adhesion (E-cadherin) and apoptosis-related (Bax) proteins was noted. Furthermore, DPP-IV gene silencing inhibited PTC cell proliferation and enhanced apoptosis. The findings from this study suggest that the silencing of the DPP-IV gene exerts a significant impact on the molecular and cellular processes associated with PTC progression, primarily through modulation of the MAPK pathway and the expression of key regulatory factors. These discoveries may open new avenues for understanding and treating PTC (Hu et al., 2021).

5.1.2 Future perspectives

Identifying predictive biomarkers that can stratify PTC patients who are likely to benefit from DPP-IV inhibitor therapy is essential. These biomarkers may encompass molecular signatures, genetic profiles, or immunological markers that can guide patient selection and personalized treatment strategies. Conducting well-designed clinical trials specifically focused on the use of DPP-IV inhibitors in PTC is imperative. These trials should assess the safety, efficacy, and long-term outcomes of DPP-IV inhibitor-based regimens in PTC patients. Robust clinical data are essential to establish their role in routine clinical practice.

5.2 SGLT2 inhibitors

The exploration of SGLT2 inhibitors in the context of antitumor treatment represents an intriguing avenue of investigation with several scientific implications. Originally developed for their glucose-lowering properties in diabetes management, SGLT2 inhibitors have displayed multifaceted effects that may have relevance in the broader field of cancer therapy (Dutka et al., 2022).

SGLT2 inhibitors have been associated with significant metabolic alterations, including reductions in blood glucose levels, insulin resistance, and body weight. These metabolic changes could potentially impact the tumor microenvironment, affecting factors such as nutrient availability and oxidative stress, which are crucial for tumor cell survival and proliferation (Wright, 2021). Emerging evidence suggests that SGLT2 inhibitors may influence various cellular signaling pathways that are implicated in cancer progression (Benedetti et al., 2022; L et al., 2014). This modulation could potentially lead to the inhibition of tumor growth or the sensitization of tumor cells to other antitumor agents. The tumor microenvironment plays a pivotal role in cancer development and progression. SGLT2 inhibitors may affect the tumor microenvironment by altering the composition of immune cells, cytokine profiles, and angiogenesis. Investigating these potential effects in the context of antitumor treatment is crucial (Basak et al., 2023; L et al., 2014; Bose et al., 2021). Given their metabolic and signaling effects, SGLT2 inhibitors may have synergy with existing cancer therapies, such as chemotherapy, immunotherapy, or targeted therapies. In the study performed by Xie et al. identified that SGLT2 inhibitor possesses the ability to inhibit the advancement and progression of cervical cancer. This inhibitory effect is attributed to the activation of the adenosine monophosphate (AMP)-activated protein kinase (AMPK) signaling pathway and the concurrent downregulation of forkhead Box A1 (FOXA1) and sonic hedgehog (SHH) expression (Xie et al., 2020). *In vitro*, SGLT2 exhibited antitumor activity by augmenting caspase 3 cleavage activity and modulating the expression of Bax/Bcl-2 (Xie et al., 2020). The following study performed by Faridi et al. investigated SGLT2 inhibitors impact on the human lung cancer cell line A549, revealing a significant inhibitory effect. A computer simulation study using molecular docking software identified apoptosis-related proteins, including Bcl-2, p53, and Caspase-3, as potential targets for SGLT2 inhibitor. The study indicated favorable binding with apoptotic protein receptors 1GJH, 1TUP, and 2XYG, suggesting a potential binding affinity between SGLT2 inhibitors and these receptors (Faridi et al., 2020). Furthermore, SGLT2 inhibitors may be used as adjuvant cancer treatment leading to better treatment outcomes. The study performed by focuses on overcoming challenges in treating triple-negative breast cancer (TNBC), a highly aggressive and drug-resistant subtype. Researchers explore the potential of the PI3K/AKT/mTOR pathway as a target for TNBC, finding improved prognosis with AKT inhibitors combined with paclitaxel. Doxorubicin (DOX), a common TNBC chemotherapy, faces resistance issues. SGLT2 inhibitors emerges as a promising candidate to sensitize tumor cells to DOX, offering cardioprotective effects and promoting apoptosis. Combining SGLT2 inhibitor with DOX synergistically inhibits TNBC cell survival by interfering with the mTOR pathway and inhibiting calmodulin. SGLT2 inhibitor significance lies in its ability to sensitize TNBC cells to DOX, offering a potential strategy to enhance chemotherapy efficacy and overcome drug resistance in this challenging cancer subtype. Combining SGLT2 inhibitors with conventional treatments could enhance treatment efficacy and improve patient outcomes (Basak et al., 2023). The diagram illustrating the operational dynamics of the SGLT2 inhibitor, alongside the identification of prospective targets

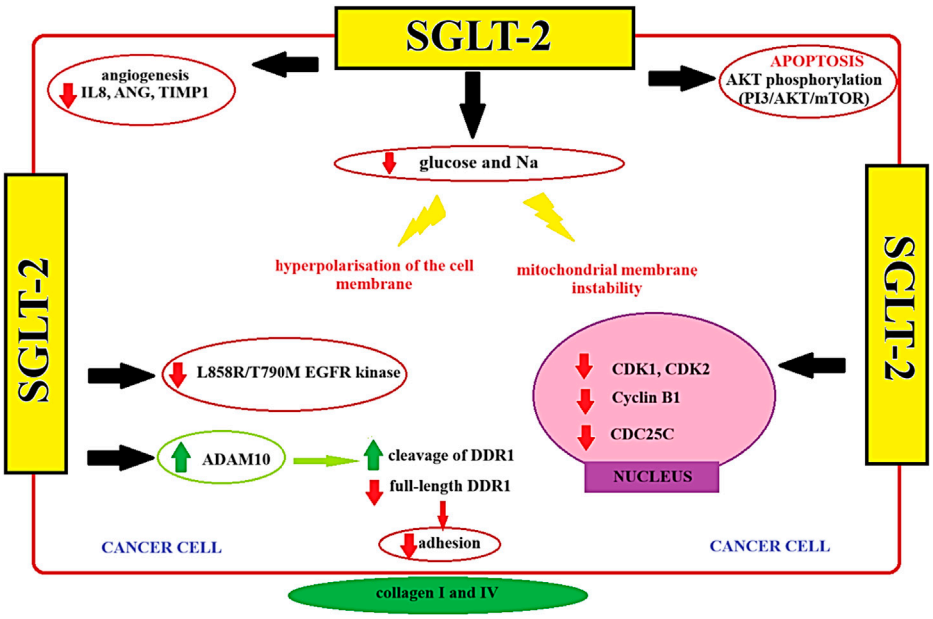

FIGURE 3
The potential targets of SGLT-2 among PTC cells (Wang et al., 2022b). AKT - serine/threonine protein kinase; ADAM10 - A Disintegrin and Metalloproteinase 10; ANG–Angiopoietin; CDC25C - Cell Division Cycle 25C; CDK1 - Cyclin-Dependent Kinase 1 CDK2 - Cyclin-Dependent Kinase 2; Cyclin B1 - Cyclin B1; DDR1 - Discoidin Domain Receptor 1 IL8 - Interleukin 8; L858R/T790M EGFR Kinase - Leucine 858 to Arginine/Threonine 790 to Methionine Epidermal Growth Factor Receptor Kinase; mTOR - Mechanistic Target of Rapamycin; PI3 - Phosphoinositide 3-Kinase; SGLT2 - Sodium-Glucose Transporter 2; TIMP1 - Tissue Inhibitor of Metalloproteinases 1.

in differentiated thyroid cancer, has been presented in Figure 3 (Figure 3).

5.2.1 Potential implication in PTC clinical management

The study performed by Wang et al. employed a multifaceted approach to investigate the impact of SGLT2 levels and the potential anticancer effects of canagliflozin in the context of PTC. Inhibition of SGLT2 demonstrated a mitigating effect on the proliferation of thyroid cancer cells both *in vitro* and *in vivo*. Canagliflozin, an SGLT2 inhibitor, exhibited several notable effects on thyroid cancer cells. It suppressed glucose uptake, glycolysis, and the activation of the AKT/mTOR signaling pathway while concurrently enhancing AMPK activation within the thyroid cancer cells. Moreover, canagliflozin hindered the transition from the G1 to S phase in the cell cycle and downregulated the expression levels of key cell cycle regulators, including cyclin D1, cyclin D3, cyclin E1, cyclin E2, and E2F1. Additionally, canagliflozin induced apoptosis in thyroid cancer cells. Further exploration uncovered that canagliflozin had the capability to increase the expression of γ-H2AX, a marker of DNA damage, and activated the DNA damage response signaling pathway ATM/CHK2. In thyroid cancer patients, elevated levels of SGLT2 were observed in thyroid cancer tissues, and there was a positive correlation between SGLT2 expression and cyclin D3 levels (Wang et al., 2022b). Elevated levels of cyclin D3 may be indicative of increased cell proliferation in PTC (Romitti et al., 2016). Therefore, the inhibition of SGLT2 may potentially lead to the restriction of the development of PTC by reducing the expression levels of cyclin D1 and D3, thus inhibiting excessive cancer cell proliferation (Romitti et al., 2016; Wang et al., 2022b; Cai et al., 2023).

5.2.2 Future perspectives

Conducting well-designed multiple clinical trials specifically focused on the use of SGLT2 inhibitors in cancer treatment is imperative. These trials should evaluate the safety, efficacy, and long-term outcomes of SGLT2 inhibitor-based regimens in PTC and different stages. SGLT2 inhibitors have shown cardiovascular benefits in patients with diabetes. Since cardiovascular disease often coexists with cancer, the cardiovascular effects of SGLT2 inhibitors may have additional relevance in cancer patients, especially those undergoing cancer treatments with potential cardiovascular risks. Identifying specific patient populations within the realm of oncology who may derive the most benefit from SGLT2 inhibitor therapy is a crucial consideration. This may involve identifying biomarkers, genetic profiles, or tumor characteristics that can guide treatment decisions.

6 Exploring limitations in the use of DPP-IV and SGLT2 inhibitors

These inhibitors, while holding promise in various therapeutic applications, are not without constraints. One notable limitation involves the need for a more comprehensive understanding of their long-term effects, particularly in populations with pre-existing conditions. Additionally, issues related to cost, patient adherence, and potential side effects contribute to the nuanced landscape of their practical implementation (Ahrén, 2010).

DPP-IV inhibitors demonstrate favorable safety and tolerability in extensive phase III clinical studies, with nasopharyngitis and cutaneous lesions as primary adverse events (Scheen, 2018; Sesti

et al., 2019). Notably, these events rarely lead to treatment discontinuation. The efficacy and safety of DPP-IV inhibitors prove advantageous for individuals with renal impairment and elderly subjects with type 2 diabetes. Post-marketing surveillance and long-term cardiovascular safety studies reveal no significant safety imbalances (Gallwitz, 2016). Concerns about pancreatic safety prompted thorough evaluations by regulatory agencies, including the European Medicines Agency (EMA) and the US Food and Drug Administration (FDA) (Elashoff et al., 2011; Pinto et al., 2018). No causal link was found between incretin-based therapies, such as DPP-IV inhibitors, and pancreatic safety. Despite an acknowledged twofold risk of acute pancreatitis in type 2 diabetes, inclusion of an acute pancreatitis risk label, and low risk in retrospective studies, large cardiovascular safety studies did not confirm significant signals. An analysis estimated a number needed to harm of 1,066 for DPP-IV inhibitor therapy (Abbas et al., 2016). Recent reviews found no elevated cancer risk, including pancreatic cancer (Abbas et al., 2016). Concerning cutaneous manifestations, specifically bullous pemphigoid, retrospective analysis of over 9,000 patients treated in Japan (2009–2017) associated it with DPP-IV inhibitors, particularly vildagliptin (Kawaguchi et al., 2019). Regulatory agencies (EMA and FDA) imposed relevant labels (Kawaguchi et al., 2019). However, large cardiovascular safety studies did not confirm this association, warranting further investigation. Pathophysiologically, these skin lesions may be an "indirect target" effect of DPP-IV inhibitors.

Concerning SGLT2 inhibitors evaluation, the findings indicate that when compared to a placebo, the use of SGLT2 inhibitors did not demonstrate a significant difference in the risks associated with various adverse events. Specifically, there were similar incidences of hypoglycemia, urinary tract infections (UTI), genital infections, hypovolemia, and fractures observed between individuals treated with SGLT2 inhibitors and those administered a placebo (Mukai et al., 2021). The following study, incorporating data from six trials with 49,875 participants assessing four SGLT2 inhibitors, revealed a reduction in serious hyperkalemia risk (1754 cases) with a hazard ratio of 0.84 (95% CI, 0.76-0.93). This effect remained consistent across diverse studies (Pheterogeneity = 0.71). Investigator-reported hyperkalemia events (1,119 cases) also showed a lower incidence with SGLT2 inhibitors (hazard ratio, 0.80 [95% CI, 0.68-0.93]; Pheterogeneity = 0.21). This risk reduction extended across subgroups, including various baseline factors and medication use. Importantly, SGLT2 inhibitors did not increase the risk of hypokalemia (hazard ratio, 1.04 [95% CI, 0.94-1.15]; Pheterogeneity = 0.42). In conclusion, SGLT2 inhibitors mitigate serious hyperkalemia risk without elevating the risk of hypokalemia in individuals with type 2 diabetes, high cardiovascular risk, or chronic kidney disease (Neuen et al., 2022).

7 Conclusion

This literature review has illuminated the potential roles of DPP-IV and SGLT2 inhibitors in the management of PTC, albeit with limited exploration thus far. While promising mechanistic connections have been identified, their clinical utility remains uncertain in the absence of robust clinical trials. Of particular significance, both SGLT2 and DPP-IV inhibitors exhibit promise in cancer therapy, potentially disrupting critical cancer-related processes such as the Warburg effect. The modulation of glycolytic pathways and the tumor microenvironment underscores their anticancer potential. To advance our understanding of the therapeutic potential of these inhibitors, meticulous clinical trials are imperative. These trials should comprehensively assess safety, efficacy, and personalized applicability in PTC patients. Furthermore, such efforts may lead to innovative therapeutic strategies that could significantly enhance PTC management. This review highlights the promising yet untapped potential of DPP-IV and SGLT2 inhibitors in the context of PTC. While mechanistic links to cancer pathophysiology are evident, realizing their clinical benefits necessitates rigorous clinical validation. Moving forward, a collaborative, multicenter, research-driven approach will be crucial to unlock the therapeutic potential of these agents, potentially revolutionizing PTC treatment.

Data availability statement

The original contributions presented in the study are included in the article/Supplementary material, further inquiries can be directed to the corresponding authors.

Author contributions

AB: Conceptualization, Investigation, Software, Validation, Visualization, Writing–original draft. MK: Formal Analysis, Investigation, Writing–original draft. AK: Methodology, Supervision, Writing–review and editing. AP-K: Data curation, Formal Analysis, Funding acquisition, Methodology, Project administration, Supervision, Validation, Writing–review and editing.

Funding

The author(s) declare financial support was received for the research, authorship, and/or publication of this article. Internal Financing of Medical University of Bialystok (B.SUB.23.547).

Conflict of interest

The authors declare that the research was conducted in the absence of any commercial or financial relationships that could be construed as a potential conflict of interest.

Publisher's note

References

Abbas, A. S., Dehbi, H. M., and Ray, K. K. (2016). Cardiovascular and non-cardiovascular safety of dipeptidyl peptidase-4 inhibition: a meta-analysis of randomized controlled cardiovascular outcome trials. *Diabetes. Obes. Metab.* 18, 295–299. doi:10.1111/DOM.12595

Adamska, A., Tomczuk-Bobik, P., Popławska-Kita, A. B., Siewko, K., Buczyńska, A., Szumowski, P., et al. (2021). Assessment of different markers of ovarian reserve in women with papillary thyroid cancer treated with radioactive iodine. *Endocr. Connect.* 10, 1283–1290. doi:10.1530/EC-21-0187

Ahrén, B. (2010). Use of DPP-4 inhibitors in type 2 diabetes: focus on sitagliptin. *Diabetes. Metab. Syndr. Obes.* 3, 31–41. doi:10.2147/DMSOTT.S7327

Albi, E., Cataldi, S., Lazzarini, A., Codini, M., Beccari, T., Ambesi-Impiombato, F. S., et al. (2017). Radiation and thyroid cancer. *Int. J. Mol. Sci.* 18, 911. doi:10.3390/ijms18050911

Arroyo, N., Bell, K. J. L., Hsiao, V., Fernandes-Taylor, S., Alagoz, O., Zhang, Y., et al. (2022). Prevalence of subclinical papillary thyroid cancer by age: meta-analysis of autopsy studies. *J. Clin. Endocrinol. Metab.* 107, 2945–2952. doi:10.1210/CLINEM/DGAC468

Baloch, Z. W., and LiVolsi, V. A. (2001). Prognostic factors in well-differentiated follicular-derived carcinoma and medullary thyroid carcinoma. *Thyroid* 11, 637–645. doi:10.1089/105072501750362709

Barchetta, I., Cimini, F. A., Dule, S., and Cavallo, M. G. (2022). Dipeptidyl peptidase 4 (DPP4) as A novel adipokine: role in metabolism and fat homeostasis. *Biomed* 10, 2306. doi:10.3390/BIOMEDICINES10092306

Basak, D., Gamez, D., and Deb, S. (2023). SGLT2 inhibitors as potential anticancer agents. *Anticancer Agents* 11, 1867. doi:10.3390/BIOMEDICINES11071867

Bea, S., Son, H., Bae, J. H., Cho, S. W., Shin, J. Y., and Cho, Y. M. (2023). Risk of thyroid cancer associated with glucagon-like peptide-1 receptor agonists and dipeptidyl peptidase-4 inhibitors in patients with type 2 diabetes: a population-based cohort study. *Diabetes. Obes. Metab.* 26, 108–117. doi:10.1111/DOM.15292

Benedetti, R., Benincasa, G., Glass, K., Chianese, U., Vietri, M. T., Congi, R., et al. (2022). Effects of novel SGLT2 inhibitors on cancer incidence in hyperglycemic patients: a meta-analysis of randomized clinical trials. *Pharmacol. Res.* 175, 106039. doi:10.1016/J.PHRS.2021.106039

Bose, S., Zhang, C., and Le, A. (2021). Glucose metabolism in cancer: the Warburg effect and beyond. *Adv. Exp. Med. Biol.* 1311, 3–15. doi:10.1007/978-3-030-65768-0_1

Buczyńska, A., Kościuszko, M., Krętowski, A. J., and Popławska-Kita, A. (2023b). Exploring the clinical utility of angioinvasion markers in papillary thyroid cancer: a literature review. *Front. Endocrinol. (Lausanne).* 14, 1261860. doi:10.3389/FENDO.2023.1261860

Buczyńska, A., Sidorkiewicz, I., Kościuszko, M., Adamska, A., Siewko, K., Dzięcioł, J., et al. (2023a). The relationship between oxidative status and radioiodine treatment qualification among papillary thyroid cancer patients. *Cancers* 15, 2436. doi:10.3390/CANCERS15092436

Buczyńska, A., Sidorkiewicz, I., Kościuszko, M., Adamska, A., Siewko, K., Dzięcioł, J., et al. (2023c). Clinical significance of oxidative stress markers as angioinvasion and metastasis indicators in papillary thyroid cancer. *Sci. Rep.* 13, 13711. doi:10.1038/s41598-023-40898-9

Buczyńska, A., Sidorkiewicz, I., Krętowski, A. J., Zbucka-Krętowska, M., and Adamska, A. (2022). Metformin intervention-A panacea for cancer treatment? *Cancers (Basel)* 14, 1336. doi:10.3390/CANCERS14051336

Buczyńska, A., Sidorkiewicz, I., Rogucki, M., Siewko, K., Adamska, A., Kościuszko, M., et al. (2021). Oxidative stress and radioiodine treatment of differentiated thyroid cancer. *Sci. Rep.* 11, 17126. doi:10.1038/s41598-021-96637-5

Busek, P., Duke-Cohan, J. S., and Sedo, A. (2022). Does DPP-IV inhibition offer new avenues for therapeutic intervention in malignant disease? *Cancers (Basel)* 14, 2072. doi:10.3390/CANCERS14092072

Cai, W., Shu, L. Z., Liu, D. J., Zhou, L., Wang, M. M., and Deng, H. (2023). Targeting cyclin D1 as a therapeutic approach for papillary thyroid carcinoma. *Front. Oncol.* 13, 1145082. doi:10.3389/FONC.2023.1145082

Cheng, S. Y., Wu, A. T. H., Batiha, G. E. S., Ho, C. L., Lee, J. C., Lukman, H. Y., et al. (2022). Identification of DPP4/CTNNB1/MET as a theranostic signature of thyroid cancer and evaluation of the therapeutic potential of sitagliptin. *Biol. (Basel)* 11, 324. doi:10.3390/BIOLOGY11020324

Cho, S. J., Suh, C. H., Baek, J. H., Chung, S. R., Choi, Y. J., Chung, K. W., et al. (2019). Active surveillance for Small papillary thyroid cancer: a systematic review and meta-analysis. *Thyroid* 29, 1399–1408. doi:10.1089/THY.2019.0159

Davies, L., and Welch, H. G. (2006). Increasing incidence of thyroid cancer in the United States, 1973-2002. *JAMA* 295, 2164–2167. doi:10.1001/JAMA.295.18.2164

Deacon, C. F. (2018). A review of dipeptidyl peptidase-4 inhibitors. Hot topics from randomized controlled trials. *Diabetes. Obes. Metab.* 20 (1), 34–46. doi:10.1111/DOM.13135

Dutka, M., Bobiński, R., Francuz, T., Garczorz, W., Zimmer, K., Ilczak, T., et al. (2022). SGLT-2 inhibitors in cancer treatment—mechanisms of action and emerging new perspectives. *Cancers (Basel)* 14, 5811. doi:10.3390/CANCERS14235811

Elashoff, M., Matveyenko, A. V., Gier, B., Elashoff, R., and Butler, P. C. (2011). Pancreatitis, pancreatic, and thyroid cancer with glucagon-like peptide-1-based therapies. *Gastroenterology* 141, 150–156. doi:10.1053/J.GASTRO.2011.02.018

Enz, N., Vliegen, G., De Meester, I., and Jungraithmayr, W. (2019). CD26/DPP4 - a potential biomarker and target for cancer therapy. *Pharmacol. Ther.* 198, 135–159. doi:10.1016/J.PHARMTHERA.2019.02.015

Faridi, U., Al-Mutairi, F., Humaira, P., and Sahar, K. (2020). An in-vitro and *in silico* anticancer study of FDA approved antidiabetic drugs glimepiride and empagliflozin. *Int. J. Life Sci. Pharma Res.* 10, 52–57. doi:10.22376/IJPBS/LPR.2020.10.2.L52-57

Gallwitz, B. (2016). Novel therapeutic approaches in diabetes. *Endocr. Dev.* 31, 43–56. doi:10.1159/000439372

Gao, X., Le, Y., Geng, C., Jiang, Z., Zhao, G., and Zhang, P. (2022). DPP4 is a potential prognostic marker of thyroid carcinoma and a target for immunotherapy. *Int. J. Endocrinol.* 2022, 5181386. doi:10.1155/2022/5181386

Golightly, L. K., Drayna, C. C., and McDermott, M. T. (2012). Comparative clinical pharmacokinetics of dipeptidyl peptidase-4 inhibitors. *Clin. Pharmacokinet.* 51, 501–514. doi:10.1007/BF03261927

Gorgone, S., Campennì, A., Calbo, E., Catalfamo, A., Sciglitano, P., Sofia, L., et al. (2009). Differentiated thyroid cancers. *G. Chir.* 30, 26–29. doi:10.26442/18151434.2020.4.200507

Haugen, B. R., Alexander, E. K., Bible, K. C., Doherty, G. M., Mandel, S. J., Nikiforov, Y. E., et al. (2016). 2015 American thyroid association management guidelines for adult patients with thyroid nodules and differentiated thyroid cancer: the American thyroid association guidelines task force on thyroid nodules and differentiated thyroid cancer. *Thyroid* 26, 1–133. doi:10.1089/THY.2015.0020

Heydarzadeh, S., Moshtaghie, A. A., Daneshpoor, M., and Hedayati, M. (2020). Regulators of glucose uptake in thyroid cancer cell lines. *Cell Commun. Signal.* 18, 83. doi:10.1186/S12964-020-00586-X

Hu, X., Chen, S., Xie, C., Li, Z., Wu, Z., and You, Z. (2021). DPP4 gene silencing inhibits proliferation and epithelial-mesenchymal transition of papillary thyroid carcinoma cells through suppression of the MAPK pathway. *J. Endocrinol. Invest.* 44, 1609–1623. doi:10.1007/S40618-020-01455-7

Kawaguchi, Y., Shimauchi, R., Nishibori, N., Kawashima, K., Oshitani, S., Fujiya, A., et al. (2019). Dipeptidyl peptidase-4 inhibitors-associated bullous pemphigoid: a retrospective study of 168 pemphigoid and 9,304 diabetes mellitus patients. *J. Diabetes Investig.* 10, 392–398. doi:10.1111/JDI.12877

Kitahara, C. M., Sosa, J. A., and Shiels, M. S. (2020). Influence of nomenclature changes on trends in papillary thyroid cancer incidence in the United States, 2000 to 2017. *J. Clin. Endocrinol. Metab.* 105, e4823–e4830. doi:10.1210/CLINEM/DGAA690

Kościuszko, M., Buczyńska, A., Krętowski, A. J., and Popławska-Kita, A. (2023). Could oxidative stress play a role in the development and clinical management of differentiated thyroid cancer? *Cancers (Basel)* 15, 3182. doi:10.3390/CANCERS15123182

Lang, B.H.-H., and Law, T. T. (2011). The role of 18F-fluorodeoxyglucose positron emission tomography in thyroid neoplasms. *Oncologist* 16, 458–466. doi:10.1634/THEONCOLOGIST.2010-0256

Larg, M. I., Barbus, E., Gabora, K., Pestean, C., Cheptea, M., and Piciu, D. (2019). 18F-FDG PET/CT in differentiated thyroid carcinoma. *Acta Endocrinol.* 15, 203–208. doi:10.4183/AEB.2019.203

Leclair, K., Bell, K. J. L., Furuya-Kanamori, L., Doi, S. A., Francis, D. O., and Davies, L. (2021). Evaluation of gender inequity in thyroid cancer diagnosis: differences by sex in US thyroid cancer incidence compared with a meta-analysis of subclinical thyroid cancer rates at autopsy. *JAMA Intern. Med.* 181, 1351–1358. doi:10.1001/jamainternmed.2021.4804

Lee, J., Chang, J. Y., Kang, Y. E., Yi, S., Lee, M. H., Joung, K. H., et al. (2015). Mitochondrial energy metabolism and thyroid cancers. *Endocrinol. Metab.* 30, 117–123. doi:10.3803/ENM.2015.30.2.117

Lee, J. J., Wang, T. Y., Liu, C. L., Chien, M. N., Chen, M. J., Hsu, Y. C., et al. (2017). Dipeptidyl peptidase IV as a prognostic marker and therapeutic target in papillary thyroid carcinoma. *J. Clin. Endocrinol. Metab.* 102, 2930–2940. doi:10.1210/JC.2017-00346

Li, C., Kuang, J., Zhao, Y., Sun, H., and Guan, H. (2020). Effect of type 2 diabetes and antihyperglycemic drug therapy on signs of tumor invasion in papillary thyroid cancer. *Endocrine* 69, 92–99. doi:10.1007/S12020-020-02291-8

Li, Y., Che, W., Yu, Z., Zheng, S., Xie, S., Chen, C., et al. (2022). The incidence trend of papillary thyroid carcinoma in the United States during 2003–2017. *Cancer Control.* 29, 10732748221135447. doi:10.1177/10732748221135447

Liberti, M. V., and Locasale, J. W. (2016). The Warburg effect: how does it benefit cancer cells? *Trends biochem. Sci.* 41, 211–218. doi:10.1016/J.TIBS.2015.12.001

Lin, H. W., and Tseng, C. H. (2014). A review on the relationship between SGLT2 inhibitors and cancer. *Int. J. Endocrinol.* 2014, 719578. doi:10.1155/2014/719578

Martínez-Reyes, I., and Chandel, N. S. (2021). Cancer metabolism: looking forward. *Nat. Rev. Cancer* 21, 669–680. doi:10.1038/S41568-021-00378-6

Matsuzu, K., Segade, F., Matsuzu, U., Carter, A., Bowden, D. W., and Perrier, N. D. (2004). Differential expression of glucose transporters in normal and pathologic thyroid tissue. *Thyroid* 14, 806–812. doi:10.1089/THY.2004.14.806

Miranda-Filho, A., Lortet-Tieulent, J., Bray, F., Cao, B., Franceschi, S., Vaccarella, S., et al. (2021). Thyroid cancer incidence trends by histology in 25 countries: a population-based study. *Lancet. Diabetes Endocrinol.* 9, 225–234. doi:10.1016/S2213-8587(21)00027-9

Morani, F., Phadngam, S., Follo, C., Titone, R., Aimaretti, G., Galetto, A., et al. (2014). PTEN regulates plasma membrane expression of glucose transporter 1 and glucose uptake in thyroid cancer cells. *J. Mol. Endocrinol.* 53, 247–258. doi:10.1530/JME-14-0118

Mukai, J., Kanno, S., and Kubota, R. (2021). A literature review and meta-analysis of safety profiles of SGLT2 inhibitors in Japanese patients with diabetes mellitus. *Sci. Rep.* 11, 13472. doi:10.1038/S41598-021-92925-2

Neuen, B. L., Oshima, M., Agarwal, R., Arnott, C., Cherney, D. Z., Edwards, R., et al. (2022). Sodium-glucose cotransporter 2 inhibitors and risk of hyperkalemia in people with type 2 diabetes: a meta-analysis of individual participant data from randomized, controlled trials. *Circulation* 145, 1460–1470. doi:10.1161/CIRCULATIONAHA.121.057736

Pappa, T., and Alevizaki, M. (2013). Metformin and thyroid: an update. *Eur. Thyroid. J.* 2, 22–28. doi:10.1159/000346248

Pinto, L. C., Rados, D. V., Barkan, S. S., Leitão, C. B., and Gross, J. L. (2018). Dipeptidyl peptidase-4 inhibitors, pancreatic cancer and acute pancreatitis: a meta-analysis with trial sequential analysis. *Sci. Rep.* 8, 782. doi:10.1038/S41598-017-19055-6

Pizzato, M., Li, M., Vignat, J., Laversanne, M., Singh, D., La Vecchia, C., et al. (2022). The epidemiological landscape of thyroid cancer worldwide: GLOBOCAN estimates for incidence and mortality rates in 2020. *Lancet Diabetes Endocrinol.* 10, 264–272. doi:10.1016/S2213-8587(22)00035-3

Rego-Iraeta, A., Pérez-Méndez, L. F., Mantinan, B., and Garcia-Mayor, R. V. (2009). Time trends for thyroid cancer in northwestern Spain: true rise in the incidence of micro and larger forms of papillary thyroid carcinoma. *Thyroid* 19, 333–340. doi:10.1089/thy.2008.0210

Rogucki, M., Buczyńska, A., Krętowski, A. J., and Popławska-Kita, A. (2021). The importance of miRNA in the diagnosis and prognosis of papillary thyroid cancer. *Thyroid. Cancer* 10, 4738. doi:10.3390/JCM10204738

Rogucki, M., Sidorkiewicz, I., Niemira, M., Dzięcioł, J. B., Buczyńska, A., Adamska, A., et al. (2022). Expression profile and diagnostic significance of MicroRNAs in papillary thyroid cancer. *Cancers (Basel)* 14, 2679. doi:10.3390/CANCERS14112679

Romitti, M., Wajner, S. M., Ceolin, L., Vaz Ferreira, C., Ribeiro, R. V. P., Rohenkohl, H. C., et al. (2016). MAPK and SHH pathways modulate type 3 deiodinase expression in papillary thyroid carcinoma. *Endocr. Relat. Cancer* 23, 135–146. doi:10.1530/ERC-15-0162

Scheen, A. J. (2015). Pharmacokinetics, pharmacodynamics and clinical use of SGLT2 inhibitors in patients with type 2 diabetes mellitus and chronic kidney disease. *Clin. Pharmacokinet.* 54, 691–708. doi:10.1007/S40262-015-0264-4

Scheen, A. J. (2018). The safety of gliptins: updated data in 2018. *Expert Opin. Drug Saf.* 17, 387–405. doi:10.1080/14740338.2018.1444027

Schiliro, C., and Firestein, B. L. (2021). Mechanisms of metabolic reprogramming in cancer cells supporting enhanced growth and proliferation. *Cells* 10, 1056. doi:10.3390/CELLS10051056

Sesti, G., Avogaro, A., Belcastro, S., Bonora, B. M., Croci, M., Daniele, G., et al. (2019). Ten years of experience with DPP-4 inhibitors for the treatment of type 2 diabetes mellitus. *Acta Diabetol.* 56, 605–617. doi:10.1007/S00592-018-1271-3

Shao, S., Xu, Q. Q., Yu, X., Pan, R., and Chen, Y. (2020). Dipeptidyl peptidase 4 inhibitors and their potential immune modulatory functions. *Pharmacol. Ther.* 209, 107503. doi:10.1016/J.PHARMTHERA.2020.107503

Skorupa, A., Ciszek, M., Chmielik, E., Boguszewicz, Ł., Oczko-Wojciechowska, M., Kowalska, M., et al. (2021). Shared and unique metabolic features of the malignant and benign thyroid lesions determined with use of 1H HR MAS NMR spectroscopy. *Sci. Rep.* 11, 1344. doi:10.1038/S41598-020-79565-8

Soares, P., Trovisco, V., Rocha, A. S., Lima, J., Castro, P., Preto, A., et al. (2003). BRAF mutations and RET/PTC rearrangements are alternative events in the etiopathogenesis of PTC. *Oncogene* 22, 4578–4580. doi:10.1038/sj.onc.1206706

Su, X., Li, Z., He, C., Chen, W., Fu, X., and Yang, A. (2016). Radiation exposure, young age, and female gender are associated with high prevalence of RET/PTC1 and RET/PTC3 in papillary thyroid cancer: a meta-analysis. *Oncotarget* 7, 16716–16730. doi:10.18632/oncotarget.7574

Sung, H., Ferlay, J., Siegel, R. L., Laversanne, M., Soerjomataram, I., Jemal, A., et al. (2021). Global cancer statistics 2020: GLOBOCAN estimates of incidence and mortality worldwide for 36 cancers in 185 countries. *Ca. Cancer J. Clin.* 71, 209–249. doi:10.3322/CAAC.21660

Tran, Q., Lee, H., Park, J., Kim, S. H., and Park, J. (2016). Targeting cancer metabolism - revisiting the Warburg effects. *Toxicol. Res.* 32, 177–193. doi:10.5487/TR.2016.32.3.177

Wang, Y., Yang, L., Mao, L., Zhang, L., Zhu, Y., Xu, Y., et al. (2022b). SGLT2 inhibition restrains thyroid cancer growth via G1/S phase transition arrest and apoptosis mediated by DNA damage response signaling pathways. *Cancer Cell Int.* 22, 74. doi:10.1186/S12935-022-02496-Z

Wang, Z., Luo, J., Zhang, Y., Xun, P., and Chen, Z. (2022a). Metformin and thyroid carcinoma incidence and prognosis: a systematic review and meta-analysis. *PLoS One* 17, e0271038. doi:10.1371/JOURNAL.PONE.0271038

Wright, E. M. (2021). SGLT2 inhibitors: physiology and Pharmacology. *Kidney360* 2, 2027–2037. doi:10.34067/KID.0002772021

Xie, Z., Wang, F., Lin, L., Duan, S., Liu, X., Li, X., et al. (2020). An SGLT2 inhibitor modulates SHH expression by activating AMPK to inhibit the migration and induce the apoptosis of cervical carcinoma cells. *Cancer Lett.* 495, 200–210. doi:10.1016/J.CANLET.2020.09.005

Zhang, X., Zhang, F., Li, Q., Feng, C., and Teng, W. (2022). Iodine nutrition and papillary thyroid cancer. *Front. Nutr.* 9, 1022650. doi:10.3389/FNUT.2022.1022650

frontiers | Frontiers in Pharmacology

TYPE Review
PUBLISHED 01 February 2024
DOI 10.3389/fphar.2024.1324140

OPEN ACCESS

EDITED BY
Ayaz Shahid,
Western University of Health Sciences, United States

REVIEWED BY
Andrew David Redfern,
University of Western Australia, Australia
Demin Cai,
Yangzhou University, China

*CORRESPONDENCE
Licheng Wu,
wulicheng@ncmc.edu.cn
Chuanzhou Li,
chuanzhouli@hust.edu.cn

†These authors have contributed equally to this work

RECEIVED 19 October 2023
ACCEPTED 23 January 2024
PUBLISHED 01 February 2024

CITATION
Wang J, Liu C, Hu R, Wu L and Li C (2024), Statin therapy: a potential adjuvant to immunotherapies in hepatocellular carcinoma. *Front. Pharmacol.* 15:1324140. doi: 10.3389/fphar.2024.1324140

Statin therapy: a potential adjuvant to immunotherapies in hepatocellular carcinoma

Jiao Wang[1†], Chengyu Liu[2†], Ronghua Hu[2], Licheng Wu[3*] and Chuanzhou Li[4*]

[1]Department of Laboratory Medicine, Wuhan Hospital of Traditional Chinese and Western Medicine, Tongji Medical College, Huazhong University of Science and Technology, Wuhan, China, [2]Department of Transfusion Medicine, Wuhan Hospital of Traditional Chinese and Western Medicine, Tongji Medical College, Huazhong University of Science and Technology, Wuhan, China, [3]School of Clinical Medicine, Nanchang Medical College, Nanchang, China, [4]Department of Medical Genetics, School of Basic Medicine, Tongji Medical College, Huazhong University of Science and Technology, Wuhan, China

Hepatocellular carcinoma (HCC) is one of the most prevalent cancers worldwide and accounts for more than 90% of primary liver cancer. The advent of immune checkpoint inhibitor (ICI)-related therapies combined with angiogenesis inhibition has revolutionized the treatment of HCC in late-stage and unresectable HCC, as ICIs alone were disappointing in treating HCC. In addition to the altered immune microenvironment, abnormal lipid metabolism in the liver has been extensively characterized in various types of HCC. Stains are known for their cholesterol-lowering properties and their long history of treating hypercholesterolemia and reducing cardiovascular disease risk. Apart from ICI and other conventional therapies, statins are frequently used by advanced HCC patients with dyslipidemia, which is often marked by the abnormal accumulation of cholesterol and fatty acids in the liver. Supported by a body of preclinical and clinical studies, statins may unexpectedly enhance the efficacy of ICI therapy in HCC patients through the regulation of inflammatory responses and the immune microenvironment. This review discusses the abnormal changes in lipid metabolism in HCC, summarizes the clinical evidence and benefits of stain use in HCC, and prospects the possible mechanistic actions of statins in transforming the immune microenvironment in HCC when combined with immunotherapies. Consequently, the use of statin therapy may emerge as a novel and valuable adjuvant for immunotherapies in HCC.

KEYWORDS

HCC, immunotherapy, statins, cholesterol, ICI, inflammation

1 Introduction

Hepatocellular carcinoma (HCC) accounts for 90% of primary liver cancer, and its incidence, along with associated morbidity and mortality, is increasing globally (Podlasek et al., 2023). The majority of HCCs are secondary to chronic Hepatitis B or C infections (Coffin and He, 2023), which mostly lead to cirrhosis, a chronic stage of liver lesion before HCC where scar tissue replaces liver cells (Omar et al., 2023). Accumulating findings indicate that cellular and acellular components in the tumor microenvironment (TME) can reprogram tumor initiation, growth, invasion, metastasis, and response to therapies (Jin and Jin, 2020), through interactions among various cell types, including the tumor cells, immune cells, stromal cells, and blood vessels (Sangro et al., 2021; Llovet et al., 2022;

Hosonuma and Yoshimura, 2023). In recent years, a more comprehensive understanding of the TME has facilitated the development of immunotherapies for various cancers (Hosonuma and Yoshimura, 2023). Compared to conventional therapies such as chemotherapy and radiation therapy, immunotherapies have demonstrated striking efficacy and much less adverse effects (Kamrani et al., 2023). Major immunotherapy strategies include immune checkpoint blockers or inhibitors (ICB/ICIs) and adoptive cell transfer (ACT), in addition to vaccines and virotherapy, the clinical value of which has not yet been fully validated. Despite promising and often unprecedented response rates with ICI therapy, a substantial portion of patients fail to benefit from this therapy. Consequently, applications of combinational therapies or precision medicine, biomarker discoveries, and efforts in overcoming drug resistance and reducing adverse effects also emerge endlessly (Kamrani et al., 2023).

Key nutrients such as glucose and amino acids maintain metabolic homeostasis within immune cells and tumor cells present in the TME (Zou and Green, 2023). Metabolic reprogramming in the TME alters tumor immunity leading to changes in immunotherapeutic response observed in tumor-bearing mice and patients with cancer (Zou and Green, 2023). Recently, the importance of lipid accumulation has been particularly underscored in different immune cell subsets and tumor cells in the TME; for instance: tumor-associated macrophages (TAMs) show increased levels of the scavenger receptor CD36, leading to accumulated intracellular lipid and elevated fatty acid oxidation (FAO), which in return contributes to pro-tumor TAM polarization (Su et al., 2020). Similarly, high expression of fatty acid transporter protein 2 in tumor-associated neutrophils causes augmented uptake of arachidonic acid and synthesis of immunosuppressive molecule prostaglandin E2 (PGE2) (Veglia et al., 2019). In addition, cholesterol metabolism has also been involved in regulating $CD8^+$ T cells in the TME. Suppression of acetyl-CoA acetyltransferase 1 (ACAT1) responsible for cholesterol esterification or cholesterol transporter proprotein convertase subtilisin/kexin type 9 (PCSK9) improves the anti-tumor performance of $CD8^+$ T cells and potentiates ICB therapy (Yang et al., 2016; Liu et al., 2020).

Statins are widely used as cholesterol-lowering drugs in clinical practice and were originally discovered as potent inhibitors of the rate-limiting enzyme 3-hydroxy-3-methylglutaryl coenzyme A (HMG-CoA) reductase (HMGCR) in the mevalonate pathway (Lee et al., 2014). Besides the canonical effects on cholesterol levels, statins show pleiotropic effects on various cellular activities, such as proliferation, cell adhesion and migration, immune regulation, and endothelial functions (Pedersen, 2010). Concerning the synthesis of sterols and isoprenoids resulting from the mevalonate pathway are shown to be crucial for tumor growth, statins are proven to reduce the risk of HCC in plenty of meta-analyses and observational studies (Zhong et al., 2016; Wong et al., 2021). A recent meta-analysis including 24 studies demonstrated a 46% decrease in HCC risk among statin users, which indicate the high potential effects of statins as an alternative option in chemoprophylaxis of high-risk HCC population (Islam et al., 2020). The underlying mechanisms of the protective effects of statins may involve inhibition of oncogene MYC, protein kinase B (AKT), and NF-κB pathways by statins, leading to the enhanced cytokine production of interleukin-6 (IL-6), tumor necrosis factor-α (TNF−α), and transforming growth factor-β1(TGF-β1) (Li et al., 2020a). Therefore, modulation of the tumor immune microenvironment (TIME) through cytokines or chemokines by statins now has been extensively recognized. Statins inhibit chemokine (C-C motif) ligand 3 (CCL3) secretion by primary lung cancer cells and suppress IL-6 and CCL2 production by mesenchymal stromal cells (MSCs), and disrupt the communication between lung cancer cells and MSCs (Galland et al., 2020). As a result, statins negatively affect the proliferation of primary lung cancer cells, inspiring the reuse of statins in targeting the TIME (Galland et al., 2020). In addition, statin therapy has surprisingly increased the sensitivity and function of natural killer (NK) cells, enhancing the spontaneous killing of tumor cells in colon cancer and melanoma (Janakiram et al., 2016; Zhu et al., 2021). More recently, immune-based therapeutic mechanisms of simvastatin in HCC are offering broad opportunities for its applications in HCC patients (Yu et al., 2022). These findings together have highlighted the beneficial role of statins in cancer therapy.

Most of cancers progress from the chronic diseases or symptoms, and in this context, initially prescribed drugs against the chronic disease such as statin and metformin might be continually administrated during cancer treatment. Emerging studies have reported the impacts of adjunct use of commonly prescribed drugs on the outcome of ICI therapy (Vos et al., 2022). For example, in a multicenter observational retrospective study, statins were being used by 19.4% of the patients with various types of cancer following PD/PD-L1 therapy, and the baseline use of statins was independently related to an increased objective response rate (ORS), but not with progression-free survival (PFS) and overall survival (OS) (Cortellini et al., 2020). In two cohorts of patients with non-small-cell lung cancer (NSCLC) and malignant pleural mesothelioma, the concomitant use of statins was significantly related to improved OS and PFS in patients received ICIs (Zhang et al., 2021). Similarly, a recent study also showed improved OS with statin use in PD/PD-L1 inhibitor-treated patients with NSCLC (Singh et al., 2022). To date, these conclusions have mostly been drawn from retrospective studies and meta-analyses, and prospective studies are warranted to validate these findings. In this review, we introduce advances in immune microenvironment-driven immunotherapies for HCC, describe varieties of aberrant lipid metabolism in the liver that guide the application of statin as a cholesterol-lowering agent in HCC treatment, and discuss the potential use of stain in future immune therapy strategies for combinational treatment, based on observations mostly from long-term population studies and clinical trials.

2 Lipid metabolism in HCC

2.1 Tumor microenvironment in HCC

The complexity and homeostasis in TME during the tumor occurrence and development have now been well recognized, and cancer cells evolve to escape from immune surveillance by establishing a TME, which manifests remarkable immune

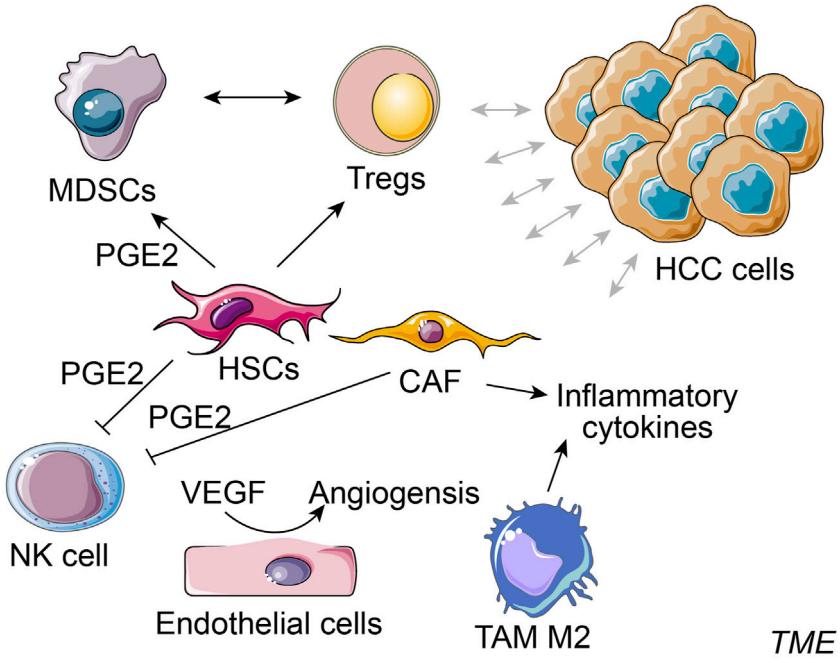

FIGURE 1
Simplified cellular components in TME of HCC. Typical cellular components in the tumor microenvironment (TME) of HCC consist of hepatocellular carcinoma (HCC) cells, hepatic stellate cells (HSCs), cancer-associated fibroblasts (CAFs), NK cell, regulatory T cells (Tregs), myeloid-derived suppressor cell (MDSCs), endothelial cells and tumor-associated macrophages (TAMs) M2, etc.

suppression and promotion on tumor progression and metastasis. The architecture of a characteristic TME consists of the extracellular matrix (ECM) elements, fibroblasts, myofibroblasts, adipose cells, immune and inflammatory cells, endothelial cells, and pericytes, supplemented with secreted cytokines, chemokines and enzymes (Yang et al., 2011; Chen et al., 2015a). In a such milieu, interactive crosstalk among these components together determines how the tumor mass grows (Yang et al., 2011). The recent advent of ICI therapy for cancer has revolutionized the treatment of HCC and led to new therapeutic standards, as well as a more profound understanding of tumorigenesis, indicating that cancer treatment should not only target cancer cells but also the surrounding TME. It is noted that all components in TME are not independently existed, and their intrinsic interconnections are usually way more complex than described. Many reviews have also comprehensively discussed the architecture of TME in HCC (Sangro et al., 2021; Llovet et al., 2022; Sas et al., 2022). In particular, recent studies using single-cell profiling and multiomic techniques have greatly advanced our knowledge of the ecosystem in primary, metastatic, and early-relapse HCC, as well as how immune system and tumor cells respond to HCC status, immune evasion, and immunotherapies (Zheng et al., 2017; Sun et al., 2021; Lu et al., 2022; Liu et al., 2023; Murai et al., 2023).

2.1.1 Cellular components in TME of HCC

Typical cellular components in TME of HCC consist of hepatic stellate cells (HSCs), cancer-associated fibroblasts (CAFs), endothelial cells, NKs, regulatory T cells (Tregs), myeloid-derived suppressor cell (MDSCs) and TAMs (Figure 1) (Tahmasebi Birgani and Carloni, 2017). HSCs are a significant component in HCC-TME and are pivotal mediators of immunosuppression and pathogenesis of cirrhosis and HCC. HSCs provide an immunosuppressive niche for HCC by promoting the infiltration of Tregs and MDSCs (Zhao et al., 2014). MDSCs are important in immune suppression induced by inflammatory cytokines (e.g., PGE2), and MDSCs could affect the induction and function of Tregs. The inhibition of HSCs-derived PGE2 suppresses MDSCs accumulation induced by HSCs and HCC growth (Xu et al., 2016). CAFs secrete a higher amount of hepatocyte growth factor than the normal fibroblasts, and the secretion capacity of CAFs around HCC is positively correlated with the tumor size (Jia et al., 2013). CAFs-secreted C-C motif chemokine ligand proteins, CCL2, CCL5, CCL7, and CXCL16, promote the migration and invasion of HCC cells and enhance their metastasis to other organs by activation of the TGF signaling pathway (Liu et al., 2016). Alternatively, CAFs in TME also secrete PGE2 to suppress the NK cell function in HCC (Li et al., 2012). Tumor endothelial cells promote tumor angiogenesis and regulate cytotoxic T cells in the TME (Sakano et al., 2022; Feng et al., 2023b). In HCC, tumor endothelial cells could induce tumor-infiltrating T-cell exhaustion and induce the suppression of tumor growth via silencing glycoprotein non-metastatic melanoma protein B expression (Sakano et al., 2022). Like other cancers, liver malignancies and HCC progression are also facilitated by TAMs at TME of HCC (Shirabe et al., 2012). A high abundance of M2 macrophage has been shown to correlate with aggressive phenotypes of HCC (Dong et al., 2016). These alternatively activated macrophages release high levels of pro-metastatic cytokines in the circulation of HCC patients, such as IL-6, IL-1, and TNF-α (Ataseven et al., 2006). TAMs, by activating the STAT3 signaling in HCC cells, are associated with large tumor size, intrahepatic metastasis, and a high rate of HCC recurrence

(Peng et al., 2005; Mano et al., 2013). Taken together, the complex cellular components in TME of HCC dynamically interact through cell-cell contacts and cytokine signaling and exhibit considerable influences on tumor immune responses (Chen et al., 2023a).

2.1.2 Non-cellular components in TME of HCC

ECM containing extracellular substances, tumor vasculature system, exosomes, and cytokines are major non-cellular components in TME of HCC (Tahmasebi Birgani and Carloni, 2017). Matrix metalloproteinases (MMPs) are remodeler enzymes responsible for the degradation and remodeling of the ECM. Increased expression of MMP-9 was detected around the tumor capsule in HCC and was strongly correlated with tumor size, capsule status, tumor stage, and HCC recurrence risk (Arii et al., 1996; Sun et al., 2005). An upregulated level of pro-inflammatory cytokine IL-6 was found in the serum of HCC patients (Xu et al., 2021), and the IL-6/STAT3 signaling pathway has been frequently shown to be constitutively activated in HCC patients, which is associated with poor prognosis (Li et al., 2023a), affecting activities of anti-apoptosis, angiogenesis, proliferation, invasion, metastasis, and drug resistance of HCC cells (Xu et al., 2021). IFN-γ produced by mucosa-associated invariant T (MAIT) cells was reduced in the peripheral blood and liver of HCC patients than in the controls (Huang et al., 2021). Moreover, increased vascular endothelial growth factor (VEGF) in the serum of HCC patients strongly dictates the severities of tumor invasiveness, metastasis, and poor prognosis of patients (Li et al., 1999; Poon et al., 2004; Lacin and Yalcin, 2020), while suppression of VEGF mitigates the angiogenesis and prevents the proliferation and growth of HCC cells (Raskopf et al., 2008).

2.2 Abnormal lipid metabolism (dyslipidemia) in HCC

As another critical target for cancer therapy, cancer metabolism is regulated by cell-intrinsic factors and metabolite availability in the TME. Key modulations are dependent on tumor cell metabolism, cell interactions in TME, tumor heterogeneity, and whole-body metabolism homeostasis (Elia and Haigis, 2021). Consequently, specific metabolic adaptations by TMEs drive further cancer progression. Aberrant lipid metabolism in HCC generally manifests as alternations in lipid uptake and efflux, dysregulated endogenous lipid synthesis, elevated cholesterol esterification, and disruptions in lipid oxidation. These alterations are intimately linked with tumor activities in HCC (Feng et al., 2023a).

2.2.1 Lipid metabolism in the normal liver

The liver is the second largest organ in the body where a variety of metabolic activities take place. In this review, other than protein metabolism and glucose metabolism, we briefly discuss lipid metabolism in normal liver and HCC. Lipids in the body include triglycerides, phospholipids, and cholesterol, and the first two are composed of fatty acids. Triglycerides are mainly used as an energy store in case of high energy demand, whereas cholesterol and phospholipids are the source materials for the synthesis of the cell membrane and steroid hormones, respectively (Borén and Taskinen, 2022). Lipogenesis occurs in the fat cells and hepatocytes by converting excess acetyl CoA generated by glycolysis into fatty acids, triglycerides, cholesterol, steroids, and bile salts (Desoye and Herrera, 2021). When energy is needed from the fat stored in adipose tissue, the process of lipolysis initiates by hydrolyzing triglycerides into fatty acids and glycerol which further enter the circulation to be transported to tissues such as the liver. Then in the liver, glycerol enters the glycolysis pathway after converted into glycerol-3-phosphate and fatty acids undergo β-oxidation and enter the tricarboxylic acid cycle to release ATP (Feng et al., 2023a).

2.2.2 Fatty acid metabolism in HCC

Increased uptake of extracellular fatty acids promotes epithelial-mesenchymal transition, cell growth, and proliferation in HCC by mechanisms that induction of CD36/fatty acid translocase is strongly engaged (Nath et al., 2015; Pascual et al., 2017). In line with this, the synthesis of fatty acids in HCC cells is atypically higher, due to the disrupted expression or activities of key enzymes involved during the synthesis process, including malonyl-CoA, acetyl-CoA, and fatty acid synthase (FASN). Overexpression of FASN was evidenced to promote the carcinogenesis of HCC (Wang et al., 2022). Inactivation of FASN impairs hepatocarcinogenesis driven by AKT and pharmacological blockade of FASN might be highly useful in the treatment of human HCC (Li et al., 2016). β-oxidation of fatty acids (FAO), a process of lipolysis taking place at the mitochondria, is found deficient in HCC (Fujiwara et al., 2018). Peroxisome-proliferator-activated receptors (PPARs) are transcription factors that are activated by endogenous fatty acids and fatty acid derivatives. PPARα is a major transcriptional regulator of fatty acid oxidation and extended PPARα activation causes HCC in rodent mice by mechanisms that involve perturbation of the cell cycle and production of ROS [reviewed by Michalik et al. (2004)]. Overall, the extracellular uptake, biosynthesis, and degradation of fatty acids are reinforced in HCC progression.

2.2.3 Cholesterol metabolism in HCC

Given the low expression of low-density lipoprotein receptor (LDLR), the transmembrane receptor for cholesterol, facilitates upregulated cholesterol synthesis, the expression of LDLR seems to be notably lower than that in normal cells surrounding the tumor in HCC (Chen et al., 2021). In addition to the LDLR-mediated cholesterol uptake, the efflux of cholesterol has also been shown to be downregulated in HCC (Cui et al., 2020). Upregulated cholesterol esterification is another indication of HCC-associated cholesterol metabolism. Cholesterols are stored as cholesterol esters after cholesterol esterification and provide a critical energy supply for tumor cells (Tosi and Tugnoli, 2005). Alternatively, cholesterol can be oxidized into oxysterols which later impact the TME by promoting immunosuppression and assist tumor metastasis (Xia et al., 2021).

3 Lipid-targeting statins in HCC

HMG-CoA inhibitors statins are a class of small bioactive molecules designed decades ago to reduce cholesterol levels and therefore are routinely used to tackle many cardiovascular diseases (CVD). Accumulating evidence has demonstrated the multifaceted

TABLE 1 Representative observational studies regarding statins use in HCC and other cancers.

Study	Therapy	Cancer type	Study type	Patient number	Findings
Zeng et al. (2023)	Statins	HCC	Meta-analysis	1,774,476	Statin use was associated with reduced HCC risk (HR: 0.52; 95% CI, 0.37–0.72)
Khazaaleh et al. (2022)	Statins	HCC	Meta-analysis	2,668,497	Significant risk reduction of HCC among all statin users with a pooled OR of 0.573 (95% CI: 0.491–0.668, $p < 0.05$) compared to non-statin users
Vahedian-Azimi et al. (2021)	Statins	HCC	Meta-analysis	195,602	Statin use was associated with lower risk of mortality in people with HCC or cirrhosis, but it was not significant due to the large confidence interval [OR (95% CI) = 0.32 (0.09, 1.15), $p = 0.210$]
Islam et al. (2020)	Statins	HCC	Meta-analysis	59,703	Statin use was associated with a reduced risk of HCC development (risk ratio, 0.54; 95% CI, 0.47–0.61) compared with non-statin users, supporting the beneficial inhibitory effect of statins on HCC incidence
Li et al. (2020b)	Statins	HCC	Meta-analysis	62,273	Statin use was associated with a reduced all-cause mortality in HCC patients [risk ratio (RR): 0.81, 95% CI: 0.74–0.88, $p < 0.001$]
Santoni et al. (2022)	Statins	Kidney cancer	Retrospective cohort study	219	Statin use was associated with an apparently longer median OS (34.4 *versus* 18.6 months, $p = 0.017$) and PFS (11.7 *versus* 4.6 months, $p = 0.013$)
Nayan et al. (2017)	Statins	Kidney cancer	Meta-analysis	18,105	Statin use was not significantly associated with PFS (pooled HR 0.92, 95% CI, 0.51–1.65); however, statin use was associated with marked improvements in cancer-specific survival (pooled HR 0.67, 95% CI, 0.47–0.94) and overall survival (pooled HR 0.74, 95% CI, 0.63–0.88) in patients with kidney cancer
Allott et al. (2020)	Statins	Prostate cancer	Prospective cohort study	44,126	Current statin use was associated with lower risk of PTEN-null and lethal prostate cancer (HR, 0.40; 95% CI, 0.19–0.87; and HR, 0.76; 95% CI, 0.60–0.96; respectively)
Jespersen et al. (2014)	Statins	Prostate cancer	Case-control study	42,480	The use of statins was associated with a risk reduction of overall prostate cancer (adjusted OR, 0.94; 95% CI, 0.91–0.97) and specifically with advanced prostate cancer (adjusted OR, 0.90; 95% CI, 0.85–0.96)
Cardwell et al. (2015)	Statins (after cancer diagnosis)	Breast cancer	Retrospective cohort study	17,880	Statin use after a diagnosis of breast cancer reduced mortality due to breast cancer (adjusted HR, 0.84; 95% CI, 0.68–1.04)
Ahern et al. (2011)	Statins (simvastatin being the mostly prescribed lipophilic statin)	Breast cancer	Prospective cohort study	18,769	Simvastatin was associated with a reduced risk of breast cancer recurrence among Danish women diagnosed with stage I–III breast carcinoma (adjusted HR = 0.70, 95% CI, 0.57–0.86)
Takada et al. (2022)	Statins	Lung cancer	Propensity score-matched analysis	390	Statin use was associated with a significantly longer in the OS ($p = 0.0433$), but not the PFS ($p = 0.2251$) than those who did not receive statin therapy
Rossi et al. (2021)	Statins	Lung cancer	Retrospective cohort study	162	Statin use was associated with an apparently longer Median PFS (17.57 vs. 9.57 months, $p = <0.001$) and median OS was superior in the statin-users group, with a statistically significant difference (19.94 vs. 10.94 months, $p = <0.001$)
Ung et al. (2018)		Lung cancer	Retrospective cohort study	19,974	Overall baseline statin exposure was associated with a decrease in mortality risk for squamous-

(Continued on following page)

TABLE 1 (*Continued*) Representative observational studies regarding statins use in HCC and other cancers.

Study	Therapy	Cancer type	Study type	Patient number	Findings
	Atorvastatin, simvastatin, lovastatin, pravastatin, and rosuvastatin (both pre- and post- cancer diagnosis)				cell carcinoma patients (HR, 0.89; 95% CI, 0.82–0.96) and adenocarcinoma patients (HR, 0.87; 95% CI, 0.82–0.94), but not among those with SCLC. Post-diagnostic statin exposure was associated with prolonged survival in squamous-cell carcinoma patients (HR, 0.68; 95% CI, 0.59–0.79) and adenocarcinoma patients (HR, 0.78; 95% CI, 0.68–0.89). Baseline or post-diagnostic exposure to simvastatin and atorvastatin was associated with extended survival in NSCLC cancer subtypes
Cho et al. (2015)	Statins (before cancer diagnosis)	Non-Hodgkin lymphoma	Case-control study	18,657	Previous statin administration was associated with a reduced risk of subsequent non-Hodgkin lymphoma (adjusted OR, 0.52; 95% CI, 0.43–0.62)
Cote et al. (2019)	Statins (before cancer diagnosis)	Glioblastoma	Prospective cohort study	280,455	Ever statin use (HR, 1.43, 95% CI, 1.10–1.86) was significantly associated with increased glioma risk
Sperling et al. (2017)	Statins (before cancer diagnosis)	Endometrial cancer	Case-control study	77,509	The use of statins was not associated with the risk of endometrial cancer (OR, 1.03; 95% CI, 0.94–1.14). In addition, endometrial cancer risk did not vary substantially with duration or intensity of statin use
Li et al. (2021)	Statins	Colorectal cancer	Meta-analysis	387,518	The use of statins was significantly associated with a decrease in overall mortality (HR, 0.81; 95% CI, 0.76–0.86) and cancer-specific mortality (HR, 0.78; 95% CI, 0.72–0.85) of colorectal cancer
Cho et al. (2021)	Statins	Gastric cancer	Retrospective cohort study	80,271	Statin use was associated with a reduction of gastric cancer mortality in the general population but not with gastric cancer incidence
Nielsen et al. (2012)	Statins (before cancer diagnosis)	13 cancer types	Retrospective cohort study	295,925	Statin use in patients with cancer was associated with reduced cancer-related mortality. Multivariable-adjusted HR for statin users, as compared with patients who had never used statins, were 0.85 (95% CI, 0.83–0.87) for death from any cause and 0.85 (95% CI, 0.82–0.87) for death from cancer
Mei et al. (2017)	Statins	Miscellaneous	Meta-analysis	1,111,407	Statin use was significantly associated with decreased risk of all-cause mortality (HR, 0.70; 95% CI, 0.66–0.74) compared with non-statin users. The observed pooled estimates were retained for cancer-specific mortality (HR, 0.60; 95% CI, 0.47–0.77), PFS (HR, 0.67; 95% CI, 0.56–0.81), recurrence-free survival (HR, 0.74; 95% CI, 0.65–0.83) and disease-free survival (HR, 0.53; 95% Cl, 0.40–0.72)
Wang et al. (2016)	Statins	Miscellaneous	Prospective cohort study	146,326	In a cohort of postmenopausal women, regular use of statins or other lipid-lowering medications was associated with decreased cancer death (HR, 0.78; 95% CI, 0.71–0.86), regardless of the type, duration, or potency of statin medications used
Emberson et al. (2012)	Statins	Miscellaneous	Meta-analysis	175,000	A median of 5 years of statin therapy had no effect on the incidence of, or mortality from, any type of cancer (or the aggregate of all cancer)

Abbreviations: HCC, hepatocellular carcinoma; HR, hazard ratio; OR, odds ratio; OS, overall survival; PC, placebo-controlled; PFS, progression-free survival; RR, response rate.

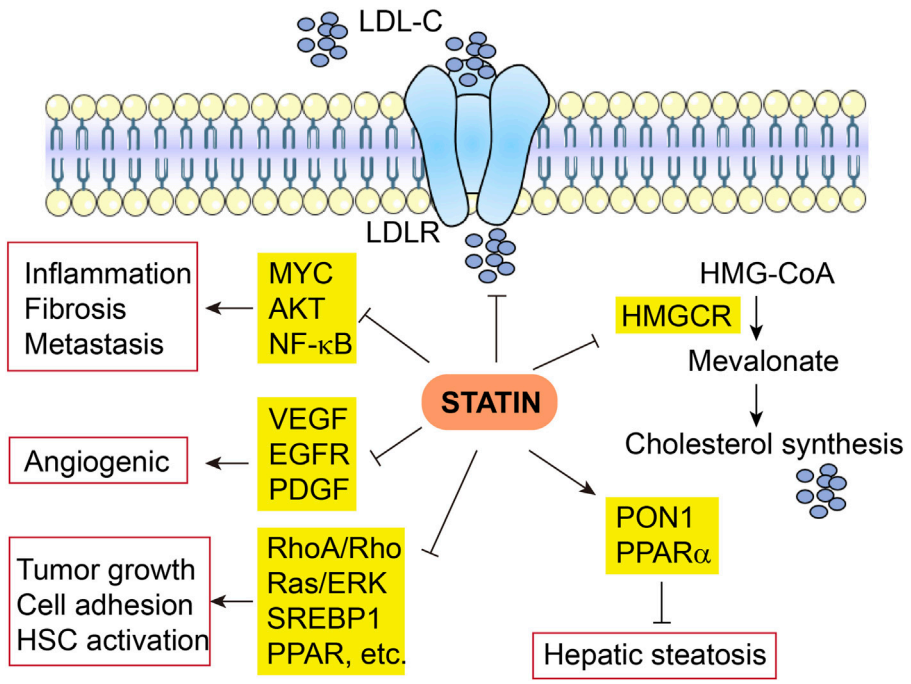

FIGURE 2
Multifaceted mechanisms of actin of statin in HCC. LDL-C, low-density lipoprotein cholesterol; LDLR, low-density lipoprotein receptor; HMGCR, 3-Hydroxy-3-Methylglutaryl-CoA reductase.

impacts of statins on the metabolism of lipoproteins, such as chylomicrons and high-density lipoproteins (HDLs) (Lamon-Fava, 2013).

Notably, the development and application of statins have ushered in a new era in the prevention and treatment of CVDs such as coronary heart disease and hypertension. For the primary and secondary prevention of coronary heart disease, statins have been identified as the first choice for hypercholesterolemia. Statins include lovastatin (Altoprev), pravastatin, simvastatin (Zocor), fluvastatin (Lescol XL), atorvastatin (Lipitor), cerivastatin, bervastatin, niavastatin, pitavastatin (Livalo) and rosuvastatin (Crestor), etc. The first six statins have been approved by the Food and Drug Administration (FDA), and the benefits and advantages of statins have now been extensively recognized (Pedersen, 2010; Adhyaru and Jacobson, 2018).

3.1 Anti-tumor effects of statins in HCC

A promising role of statins in the prevention and relapse protection of HCC has been suggested by several retrospective observational trials showing the efficacy of statins in reducing the risk and recurrence of HCC and other cancers (Goh and Sinn, 2022) (Table 1). The mechanisms of action are broadly categorized below into inflammation and non-inflammation related functions (Figure 2).

3.1.1 Inflammation related mechanisms

The anti-tumor effects of statins in HCC have been attributed to the inhibition of MYC oncogene (Cao et al., 2011), protein kinase B (AKT) (Roudier et al., 2006; Ghalali et al., 2017), and NF-κB pathways, as well as decreased production of pro-inflammatory cytokines (Wang et al., 2006; Li et al., 2020a). Fluvastatin blocked the activation and hepatic fibrogenesis of steatosis-induced HSCs by suppressing the generation of reactive oxygen species (ROS), NF-κB activity, and expression of pro-inflammatory genes (Chong et al., 2015). Rosuvastatin also decreases hepatic inflammation through downregulated expression of pro-inflammatory cytokines such as TNF-α, IL-6, and TGF-β1 and other tumor-associated growth factors (Yokohama et al., 2016). Nonalcoholic fatty liver disease (NAFLD) and non-alcoholic steatohepatitis (NASH) could be treated and prevented with statins owing to the diverse properties of statins via prevention of the liver from inflammation and fibrosis (Ahsan et al., 2020). Some animal studies indicate that statins significantly improve NASH-associated hepatic lipotoxicity, oxidative stress, inflammatory responses, and fibrosis (Park et al., 2016; Schierwagen et al., 2016; Ahsan et al., 2020). In NAFLD/NASH patients, the pleiotropic effects of statins are elaborated by decreased inflammation and fibrosis via modulation of cell proliferation, anti-oxidant, and anti-thrombotic activities (Chong et al., 2015).

3.1.2 Non-inflammation related mechanisms

The anti-angiogenic effects of statins have been widely disclosed. Statins show a protective role against HCC as they decrease hepatic expression of angiogenic factors like VEGF receptor, epidermal growth factor receptor (EGFR), and platelet-derived growth factor (PDGF) (Dulak and Józkowicz, 2005; Yokohama et al., 2016). Simvastatin has been found to lessen tumor cell growth and impair tumor cell adhesion and invasion (Relja et al., 2011). Hepatic fibrosis is blocked by simvastatin via RhoA/Rho kinase and Ras/ERK pathways (Schierwagen et al., 2016). Atorvastatin use also

TABLE 2 Representative intervention clinical studies regarding statins use in HCC.

Intervention	Cancer type	Trial ID	Study type	Patient number	Overall benefits	Findings
Pravastatin (40 mg/day) plus TAE and 5-FU	HCC	NR	Randomized trial	91	Positive	Pravastatin prolonged the survival of patients with advanced HCC (median survival, pravastatin group vs. controls, 18 months vs. 9 months, $p = 0.006$) (Kawata et al. (2001))
Pravastatin (20–40 mg/day) plus TACE	HCC	NR	Randomized trial	183	Positive	Pravastatin plus TACE prolonged the survival of patients with advanced HCC (median survival, pravastatin plus TACE group vs. TACE alone group, 20.9 months vs. 12.0 months, $p = 0.003$) (Graf et al. (2008))
Atorvastatin (A, 10 mg/day) and metformin (M) in combination (SAM) with Sorafenib (S)	HCC	CTRI/2018/07/014,865	Phase I, sequential cohorts	40	Positive regarding the adverse effects	The SAM combination in HCC patients with predominantly unfavorable baseline disease characteristics showed a marked reduction in sorafenib-related side effects. The median OS for patients without early hepatic decompensation ($n = 31$) was 8.9 months (95% CI: 3.2–14.5 months) (Ostwal et al. (2022))
Pravastatin (40 mg/day) plus sorafenib	HCC	NCT01075555	Phase III, randomized trial	312	Negative	Addition of pravastatin to sorafenib did not improve survival in patients with advanced HCC, with no difference in median OS between sorafenib-pravastatin and sorafenib groups (10.7 months vs. 10.5 months; HR = 1.00; $p = 0.975$) (Jouve et al. (2019))
Pravastatin (40 mg/day), sorafenib, their combination or supportive care	HCC	NCT01357486	Phase II, randomized trial	160	Negative	In the overall Child–Pugh B population, neither sorafenib nor pravastatin seemed to provide benefit. Median OS was similar between the four arms: 3.8 (95% CI: 2.4–6.5), 3.1 (95% CI: 1.9–4.3), 4.0 (95% CI: 3.2–5.5) and 3.5 months (95% CI: 2.2–5.4) in four arms, respectively (Blanc et al. (2021))
Pravastatin (40 mg/day) plus sorafenib	HCC	NCT01418729	Phase II, Randomized, Double-Blind, PC trial	216	No results posted	The purpose of this study was to evaluate the OS in order to assess the efficacy and safety of pravastatin as adjuvant treatment to sorafenib
Atorvastatin (10 mg/day) plus sorafenib	HCC	NCT03275376	Phase II, Randomized	34	No results posted	The aim of this study was to evaluate whether statins improve the tumor responses and overall survival for patients who receive sorafenib therapy for advanced HCC by a prospective randomized controlled study
Atorvastatin (10 mg/day)	HCC	NCT03024684	Phase IV, double-blind, randomized PC trial	Recruiting	No results posted	The aim of this study was to evaluate the effect of atorvastatin for preventing HCC recurrence after curative treatment. The primary endpoint was to compare the 3-year cumulative incidence of recurrent HCC between the intervention group and control counterpart
Pravastatin (40 mg/day) plus sorafenib	HCC	NCT01903694	Phase III, Randomized	474	No results posted	The aim of this study was to evaluate the effect of the combination pravastatin—sorafenib *versus* sorafenib alone on overall survival in patients with hepatocellular carcinoma developing on Child-Pugh A cirrhosis who are unsuitable for curative treatment
Pravastatin plus sorafenib	HCC	NCT01075555	Phase III, Randomized	323	No results posted	The aim of this study was to investigate sorafenib tosylate given together with pravastatin to see how well it works

(Continued on following page)

TABLE 2 (*Continued*) Representative intervention clinical studies regarding statins use in HCC.

Intervention	Cancer type	Trial ID	Study type	Patient number	Overall benefits	Findings
						compared with giving sorafenib tosylate alone in treating patients with liver cancer and cirrhosis
Simvastatin (40 mg/day)	High-Risk Compensated Cirrhosis	NCT03654053	Phase III, randomized, double-blind, PC trial	Recruiting	No results posted	The aim of this study was to test whether simvastatin can lower the risk of hepatic decompensation (developing symptoms of cirrhosis) in United States

Abbreviations: HCC, hepatocellular carcinoma; HR, hazard ratio; NR, not reported; OS, overall survival; PC, placebo-controlled; CI, confidence interval; SAM, Sorafenib (S) + Atorvastatin (A) + metformin (M); TAE, transcatheter arterial embolization; TACE, transarterial chemoembolization.

reduces HSC activation via the production of sterol regulatory element-binding protein 1 (SREBP1) and peroxisomal proliferator-activated receptor (PPAR) (Marinho et al., 2017), in addition to the reduction in fibrosis and portal hypertension via non-canonical Hedgehog signaling (Uschner et al., 2015). In addition, statins also decrease isoprenoid biogenesis that is essential for cell survival (Schierwagen et al., 2016), resolve crown-like cholesterol crystals (Ioannou et al., 2015), and inactivate HSCs (Wang et al., 2013). In line with these findings, by downregulating the oxidative stress, statins decrease hepatic steatosis through increased hepatic antioxidant paraoxonase 1 (PON1) activity (Samy and Hassanian, 2011), and increase mitochondrial and peroxisomal oxidation, as well as expression of an FAO regulator PPAR-alpha (Park et al., 2016). Furthermore, statins ameliorate fibrogenesis in NASH through reestablishment of liver sinusoidal endothelial cell and HSCs phenotype and increasing endothelial nitric oxide synthase (eNOS) activity (Abraldes et al., 2007; Marrone et al., 2013; Rodríguez et al., 2017).

In summary, the pleiotropic anti-tumor effects of statin in HCC are not exclusively dependent on its impacts on HMGCR and downstream cholesterol biosynthesis, instead, via complex crosstalk, they interact frequently. For instance, cholesterol synthesis is not only directly downregulated by statin via the mevalonate pathway, but also modulated by SREBP1 and PPAR which are also suppressed by statin, in addition, NF-kB-induced inflammation can be ameliorated by direct effects of statin, as well indirect effects due to reduced cholesterol synthesis.

3.2 Clinical use of statins in HCC

3.2.1 Monotherapy use of statins in HCC

Intriguingly but somehow disappointingly, indications from prospective interventional trials and studies remain inconclusive, although association of statin use with a decreased risk of HCC carcinogenesis and recurrence has been described (Table 2) (Chiu et al., 2011; Tsan et al., 2012; Butt et al., 2015; Kawaguchi et al., 2017; Khazaaleh et al., 2022). In virus-independent liver lesions, atorvastatin use (10 mg/day) in NASH patients indicated an improvement in liver functions by 74%, along with a rise in serum protein and lipid metabolism regulator adiponectin (Hyogo et al., 2008; Athyros et al., 2017). Sustained virologic response and lower risk of cirrhosis progression were consistently found among statin users (Butt et al., 2015). These evidences together indicate a general liver protective function of statin use.

A case-control study using the Taiwan National Health Insurance Research Database has suggested that statins may reduce the risk of liver cancer (Chiu et al., 2011). Later, using the same database, a study has shown that statin use may dose-dependently decrease the risk of HCC in hepatitis B virus (HBV)-infected patients (Tsan et al., 2012); moreover, a similar conclusion with protective effects of statin use was drawn with hepatitis C virus (HCV)-infected patients in this cohort (Tsan et al., 2013). Despite the strong associative indications, further mechanistic evaluation is required. Consistently, statin users with each yearly increment of cumulative defined daily doses (cDDDs) reported a dose-dependent response and reduced HCC risk by 23.6% (Pinyopornpanish et al., 2021). Furthermore, a meta-analysis combining data from 24 studies also demonstrated that statin users showed a 46% decrease in HCC risk, indicative of the potential use of statins as chemoprophylaxis (Islam et al., 2020; Lange et al., 2021). Multiple clinical centers consistently and independently reported the chemo-preventive effects of statins use in HCC among the general population, regardless of the locations of those studies (Björkhem-Bergman et al., 2014; McGlynn et al., 2015; Tran et al., 2020). Statin users have also shown suppressed HCC development in addition to improved liver function and lower cirrhosis risk (Butt et al., 2015). Another study enrolling 1,072 patients with NASH-related advanced liver fibrosis also reported a notable effect of statin in preventing HCC from deterioration (Pinyopornpanish et al., 2021). In summary, the above studies strongly demonstrate the role of statin use in protecting both the general population and HCC risk cohort from HCC occurrence and HCC progression.

Ongoing efforts are driven to further understand the direct effects of statins on the earlier stage of HCC and the prognosis of HCC. The secondary protective effects of simvastatin in cirrhosis are being evaluated in a Phase II clinical trial (NCT02968810). Combined treatment of simvastatin and atorvastatin has decreased the comorbidities for HCC in an Asian cohort (OR = 0.31 and 0.29; 95% CI = 0.14–0.67 and 0.15–0.57, respectively) (Chen et al., 2015b). At present, a multi-center double-blinded randomized trial (Phase IV) has been initiated attempting to determine the potential prevention of atorvastatin for HCC recurrence after curative treatment (SHOT trial; NCT03024684).

3.2.2 Combination of statins with other therapies in HCC

Owing to the comorbidities and other chronic conditions in HCC patients, statins are not used alone but often prescribed together with other frequently or even daily used medications such as aspirin and metformin. A retrospective study of

521 patients demonstrated that the combination use of aspirin and statin is associated with a lower incidence of HCC and this association remained significant in the multivariable model (Singh et al., 2022). Simvastatin, atorvastatin, or rosuvastatin, in combination with metformin, also showed decreased HCC risk among diabetic patients in an Asian cohort; in addition, as for HCC, in particular, only the metformin and simvastatin combination among these combos suggested significantly decreased comorbidities of HCC (Chen et al., 2015b). NAFLD is known to develop liver inflammation and progress to NASH, fibrosis, cirrhosis or HCC. For the treatment of NAFLD/NASH at high risk of CVD or HCC, statins alone or together with anti-diabetic PPAR-gamma agonist pioglitazone and other drugs, were primarily recommended for the primary or secondary prevention of CVD, in addition to cirrhosis avoidance, liver transplantation, and HCC, according to a statement from official guidelines (Athyros et al., 2017).

For intermediate-stage HCC, transarterial chemoembolization (TACE) is the most common bridging therapy as a standard local-regional treatment before liver transplantation. Compared to chemoembolization alone, combination therapy of chemoembolization and pravastatin greatly improves survival of advanced HCC (Graf et al., 2008). During the 5-year observation of HCC patients, 23.7% of patients treated by TACE alone and 36.5% of patients treated by TACE plus pravastatin survived, and median survival was significantly longer in HCC patients treated by the combination than in patients treated by TACE alone (Graf et al., 2008).

Currently, a body of clinical trials addressing the interventional impacts of statins alone or with non-immunotherapy treatment in HCC have been initiated (Table 2). So far, 6 of the 11 trials have not reported any results, and one trial has indicated benefits of atorvastatin in reducing sorafenib-related side effects. In the rest 4 trials, all trials used pravastatin as treatment for advanced HCC, and pravastatin plus conventional transcatheter arterial embolization (TAE) (plus 5-FU) or TACE in 2 of the trials have observed prolonged survival of patients with advanced HCC (Kawata et al., 2001; Graf et al., 2008); however, the other 2 trials concluded more recently (2019 and 2021) using pravastatin in combination with sorafenib showed no benefits in OS, and even the protective effects of sorafenib seem to disappear or be very subtle (Jouve et al., 2019; Blanc et al., 2021), which is difficult to interpret as a whole. Treatment strategies among these trials differ, and the sample size for conclusion and the subpopulation at various disease stages or with varying liver function, even though all patients at advanced HCC, could contribute to the unexpected ineffectiveness. More results from the rest ongoing trials are being anticipated.

3.3 Adverse effects of statins in HCC

Statin-associated cardiovascular benefits, including declined risks of major coronary events and revascularization as well as the risk of stroke, far outweigh the potential risks. However, after statins have been prescribed for clinical use for several decades, statin is shown to be not all good. Statin-associated muscle symptoms (SAMS) are the most common toxicity of statins, as shown by manifestations of myalgia, myopathy, myositis with increased creatine kinase (CK), or rhabdomyolysis (Ward et al., 2019), and SAMS risk appears to link with systemic exposure to higher doses of statins (Armitage et al., 2010). As reported in a randomized controlled trial, two patients with advanced liver disease, out of 69 patients in the simvastatin group, receiving simvastatin 40 mg/day experienced rhabdomyolysis, with no such sign found in the placebo group (Abraldes et al., 2016).

Although the statins-induced liver injury is relatively uncommon (<1.2/100,000 users) and likely idiosyncratic in nature (Björnsson et al., 2012), the risk of hepatotoxicity has been reported from time to time in statin users, therefore physicians should be cautious when prescribing statins to patients with liver diseases (Rzouq et al., 2010; Blais et al., 2016). An earlier assessment indicates that decompensated cirrhosis or acute liver failure, rather than chronic liver disease or compensated cirrhosis, are contraindications for statin use (Bays et al., 2014). Mechanistically, individuals with advanced cirrhosis are challenged with elevated drug exposure resulting from delayed statin clearance, deficiency of cytochrome P450 3A4 which is responsible for drug metabolism in the liver, and disrupted transporter activity (Pose et al., 2019), therefore facing a higher risk of SAMS.

Despite the harmful impacts on muscle and liver with statin therapy, concerns have emerged regarding statin-related risk of new-onset diabetes mellitus, cognitive impairment, and hemorrhagic stroke, as well as the risk of extremely low levels of LDL cholesterol (LDL-C) (Adhyaru and Jacobson, 2018). For instance, the incidence of new-onset diabetes mellitus is approximately 0.1% per year and 0.2% per year with moderate-intensity and high-intensity statin therapy, respectively. Consequently, balancing the clinical benefits and potential risks, statins should be provided diligently and wisely to patients to ensure that they adhere to therapy regimens (Adhyaru and Jacobson, 2018).

4 TIME and targeted therapies in HCC

4.1 The TIME of HCC

When the liver lesions develop from liver cirrhosis to HCC, numerous immune cells progress to dysfunction, in a manner of being either abnormally inactivated or overactivated. As a result, TIME is formed as a key component of TME, bridging the interplay between tumor cells and immune cells, which is crucial for HCC development and somehow dictates the immunotherapy outcomes. Characterizing the immunological networks present in the TIME of HCC will facilitate the understanding of liver immunity and the principal mechanisms of both spontaneous and therapy-induced immune responses.

The activation of dendritic cells (DCs) contributes to the activation of $CD8^+$ T-cells, while regulatory B-cells (Bregs) inactivate $CD8^+$ T-cells (Kotsari et al., 2023). In HCC, decreased antigen presentation is found in DCs (Hilligan and Ronchese, 2020; Kotsari et al., 2023). In primary HCC patients, TAM density predicts poor prognosis related to vascular invasion, tumor multiplicity, and fibrous capsule formation (Oura et al., 2021). Pro-inflammatory cytokines induced by toll-like receptor (TLR) ligand and Th1 response index, such as IFN-α/β, and IFN-γ, could activate M1 macrophages to differentiate into M2 macrophages (Oura et al., 2021), which enhances the recruitment and growth of Tregs, resulting in an aggressive phenotype, poor OS, and rapid recurrence (Dong et al.,

2016), by downregulating $CD8^+$ T cells, DCs, and NK cells HCC (Langhans et al., 2019). Tumor-associated neutrophils (TANs) produced chemokines such as CCL2 and CCL17, which later recruited TAMs and Tregs and promoted tumor growth in HCC (Zhou et al., 2016). CAFs could produce inflammatory cytokines, growth factors, and chemokines to promote HCC development and metastasis (Foerster et al., 2022; Xu et al., 2022); moreover, CAFs activate TANs and promote the differentiation of monocytes into MDSCs (Kotsari et al., 2023). The number of B-cells in HBV-positive HCC correlates with smaller tumor size, compromised vascular invasion, and augmented infiltration of $CD8^+$ T lymphocytes, furthermore, an increased population of B-cell subsets notably prolonged HCC patients' survival (Zhang et al., 2019; Kotsari et al., 2023), suggestive of protective benefits of B cell in HCC. These above-described immunocomponents, alongside the tumor cells, and a variety of inflammatory molecules compose a complex microenvironment for immune response and regulation, advances of which have greatly facilitated the immunoregulation directed therapies, certainly not limited to HCC. In recent years, immunotherapies in combination with conventional treatments such as anti-angiogenic drugs in HCC have achieved extraordinary success, although the effects of immunotherapy alone as treatment have been of relatively infrequent benefit. Here we only briefly introduce the most popular and well-accepted immunotherapies [reviewed elsewhere (Oura et al., 2021; Li et al., 2023a)] in HCC.

4.2 Immunotherapies in HCC

After tumors escape from immune control, immunotherapies pioneered by ICIs and related applications are aiming to activate the immune system to recognize, target, and eliminate cancer cells. In addition to ICIs, other immunotherapies such as ACT and cancer vaccines also demonstrate promising efficacy in HCC.

4.2.1 Immune checkpoint inhibitor (ICI) therapies in HCC

In recent years, ICI therapies have been well recognized as a main component in systemic first-line treatment of HCC due to considerably less systemic side effects and more durable responses compared with other conventional therapies (He and Xu, 2020). Programmed cell death protein-1 (PD-1), programmed death ligand-1 (PD-L1) and cytotoxic T lymphocyte-associated protein 4 (CTLA-4) signaling represent the most prominent and well-studied immune checkpoints. By inhibiting these immunoreceptors, ICIs boost the antitumor activities of host immune cells to prevent the metastasis of cancer cells (He and Xu, 2020). PD-1 on the surface of immune cells binds to PD-L1 in tumor cells, leading to tumor immune evasion (Chen et al., 2023b). Blocking the PD1/PD-L1 interaction so far appears to be one of the most effective immunologic treatments for cancers (Llovet et al., 2022; Zhang et al., 2023). The immune checkpoint regulator CTLA-4 is exclusively expressed in T cells and impedes the effector functions of these T cells (Bulaon et al., 2023). Although the response to immunotherapy in HCC is limited due to several reasons, the safety and efficacy of these ICI-based therapies have been widely confirmed in HCC-relevant trials (Borghaei et al., 2015; Ribas and Wolchok, 2018; Li et al., 2023a). Major inhibitors relating these immunoreceptors, in the format of monoclonal antibodies, include PD-1 inhibitors nivolumab, pembrolizumab and sintilimab, PD-L1 inhibitor atezolizumab and durvalumab, and CTLA-4 blocker tremelimumab and ipilimumab, etc. (Li et al., 2023a; Shannon et al., 2023).

The effects of ICI monotherapy were first investigated in HCC and have been approved by the FDA. The efficacy of anti-PD-1 monoclonal antibody nivolumab in advanced HCC has been assessed in a phase I/II study, which showed an objective response rate (ORR) of 20%, a disease control rate (DCR) of 64% and a median OS of 13.2 months (El-Khoueiry et al., 2017). Another phase II trial showed that in patients with advanced HCC who had been previously treated with a multi-target kinase inhibitor sorafenib for HCC, PD-1 inhibitors pembrolizumab suggested an ORR rate of 17% and 77% of patients demonstrated sustained response for more than 9 months (Zhu et al., 2018).

Conventional treatments such as VEGF inhibitors and multi-kinase inhibitors are usually offered as a foundational treatment when the efficacy of additional ICI therapies is evaluated. A phase II/III study assessed the efficacy of PD-1 inhibitor sintilimab plus IBI305, a bevacizumab (VEGF monoclonal antibody) biosimilar, *versus* sorafenib, as a first-line therapy for unresectable HBV-associated HCC. As a result, patients in the sintilimab and IBI305 combination group indicated a significantly longer median PFS (4.6 months) than sorafenib group patients (2.8 months) (Rossi et al., 2021). Similarly, the IMbrave 150 clinical trial demonstrated that PD-L1 inhibitor atezolizumab combined with bevacizumab had improved PFS and OS *versus* sorafenib treatment in HCC patients (Finn et al., 2020; Roy, 2022). It is worth noting that these updated results from this key study confirm the combination as the first-line standard of care for advanced HCC (Finn et al., 2020; Roy, 2022).

Combined ICI immunotherapies have also been widely explored in HCC. PD-1 inhibitor nivolumab monotherapy has been provento improve prognosis in HCC, and the addition of CTLA-4 inhibitor ipilimumab seemed to augment the impact, suggested by elevated ORR and OS in the combination group (Yau et al., 2022). In line with that, another CheckMate 040 clinical trial also suggested nivolumab plus ipilimumab had manageable safety, promising ORS, and durable responses (Yau et al., 2020). A phase III HIMALAYA clinical trial has also shown that combination therapy of PD-L1 inhibitor durvalumab and CTLA-4 blocker tremlimumab correlates with improved ORR and OS compared with sorafenib treatment (Abou-Alfa et al., 2022).

4.2.2 Non-ICI therapies

Chimeric antigen receptor (CAR)-T cells and T cell receptor (TCR) engineered T cells are 2 cell types of ACT therapy that are applied in the therapy of HCC. Currently, about 24 clinical trials related to CAR-T cell therapy for HCC are in phase I/II (Gao and Zuo, 2023). Among these, glypican-3 (GPC3) is the main target. In addition, other targets include alpha-fetoprotein (AFP), NK group 2, member D ligand, mucin 1 glycoprotein 1, claudin18.2, CD147, CD133, etc. Efficient multi-epitope peptide vaccines against HCC have started to be designed. As the main target of adoptive T cell therapy for HCC, GPC3, and AFP have been employed in designing HCC vaccines. A phase I trial in advanced HCC has demonstrated that GPC3 peptide vaccine-induced GPC3-specific CTLs that could infiltrate into the HCC tissues, leading to improved OS induced by GPC3-based vaccine in advanced HCC (Tsuchiya et al., 2017). Besides, an AFP-based vaccine has been designed for the treatment of AFP-positive HCC (Lu et al., 2023). Recently, most

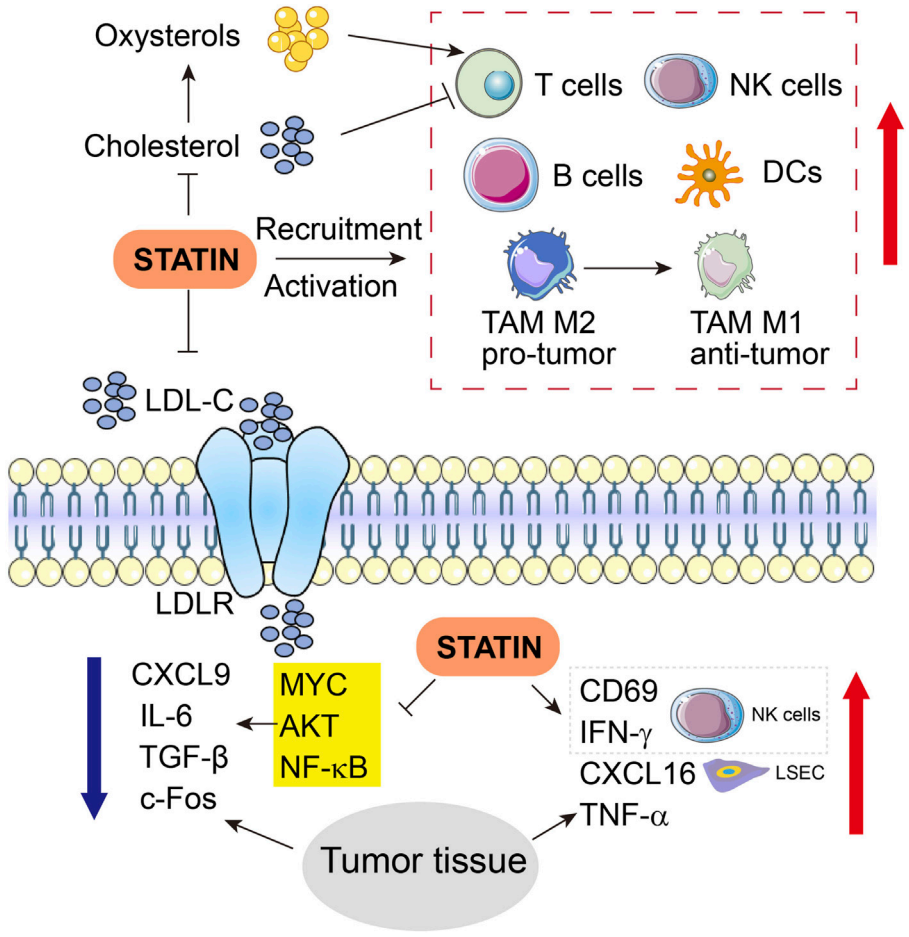

FIGURE 3
Engagement of immune cells and related molecules and cytokines in anti-tumor functions of statins in HCC. Upward red arrows indicate activation or increased expression, whereas downward blue arrow indicates inhibition or suppressed expression. LSEC, liver sinusoidal endothelial cells.

of cancer vaccines were generated against HCC, such as the VEGF vaccine, the DC-based nano-vaccine, as well as a combination of vaccines and ICIs, and all applications have demonstrated the capacity to halt HCC progression (Gao and Zuo, 2023; Lu et al., 2023). Virotherapy presents a novel immunotherapy modality for HCC. Oncolytic virotherapy (OVT) effectively induces antitumor responses through selective replication of oncolytic virus in cancerous tissues and killing HCC cells (Li et al., 2023b).

5 Interaction of statin treatment and immunotherapy in HCC

5.1 Crosstalk of TIME and lipid metabolism in HCC

In TIME, molecules related to lipid metabolism and their metabolites may directly or indirectly impact the state of tumor immune responses. Low expression of transmembrane protein coiled-coil domain containing 25 (CCDC25) on HCC cells leads to metabolic disorders such as dysregulation of FA, and CCDC25is shown to affect the sensitivity of HCC to targeted therapy, infiltration of immune cells as well as expression of immune checkpoints. Moreover, CCDC25 abundance positively correlates with the infiltration of $CD8^+$ T cells, macrophages, and DCs, but is negatively associated with infiltration of Tregs and expression levels of immune checkpoints such as CTLA4 (Dickson, 2020; Yang et al., 2020; Deng et al., 2022). Blockade of immune escape of tumors also involves CCDC25 via recruiting more tumor killer cells, inactivating immunosuppressive cells, and direct inhibition of immune checkpoints (Dickson, 2020; Oura et al., 2021; Deng et al., 2022; Liang et al., 2023a). As a significant component of membrane lipids, cholesterol plays a vital part in the formation of immune synapses of T cells and thereby regulates the functions of the T cell receptor (Molnár et al., 2012). In contrast, the upregulated production of oxysterols that are oxidized from cholesterols in turn inhibits the T cell functions through the liver X receptor signaling (Figure 3) (Huang et al., 2020).

5.2 Effects of statins on immune microenvironment in HCC

Apart from the above-mentioned anti-tumor effects of statins in HCC involving inflammation and non-inflammation pathways, the

impacts of statins on the immune microenvironment would guide the delicate interplays between immune cells and tumor cells; furthermore, this knowledge may also provide mechanistic insights and clues if statins could favor or boost the development of future immunotherapy in HCC.

Simvastatin has been shown to indirectly regulate the recruitment and activation of dozens of relevant immune cells (Figure 3). Transcript expression and protein expression of chemokine CXCL16 are augmented by simvastatin in liver sinusoidal endothelial cells (LSEC) SK-Hep1 in a dose-dependent manner. However, although simvastatin alone fails to alter the activity of natural killer T (NKT) cells, CXCL16 overexpression induced by simvastatin recruits and potentiates NKT cells to the liver, and later simvastatin upregulates CD69 and IFN-γ expression in the NKT cells when SK-Hep1 and NKT cells are co-cultured, and thoroughly activates NKT cells (Yu et al., 2022). Further evidence shows that simvastatin treatment increased the production of the immunostimulatory cytokines such as CXCL16, IFN-γ, and TNF-α, while suppressing the expression of immunosuppressive cytokines including CXCL9, IL-6, and TGF-β in HCC tumor tissues (Yu et al., 2022). Pitavastatin treatment can change the cytokine microenvironment by inhibiting the cytokine production in HCC, partially due to NF-κB activation and subsequent downstream IL-6 expression triggered by TNF-α in HCC cells (Figure 3) (Wang et al., 2006).

Fos-dependent inflammation contributes to HCC progression. Knockout of c-Fos in hepatocytes protects the liver against HCC initiation, while overexpression of c-Fos in the liver accelerates the malignant transformation of HCC, as manifested by necrotic foci, accumulated $CD45^+$ cells, reduced NK and B cells, increased circulating leukocytes, infiltration of immune cells and accumulated lesions in hepatocytes. In this manner, c-Fos-dependent HCC progression is blocked by statin treatment, which has also modulated the components of the immune system in the TIME of HCC (Figure 3) (Bakiri et al., 2017).

5.3 Combinational effects of statins and immunotherapies in non-HCC cancers

Dyslipidemia often takes place either before the onset of cancer in chronic condition or as a concomitant outcome as metabolic dysfunction after cancer initiation, therefore, cholesterol-lowering statins are a regularly prescribed medication that has to be continuously used (Lamon-Fava, 2013; Adhyaru and Jacobson, 2018; Ward et al., 2019). In this respect, the association of statin treatment with available immunotherapies in cancers such as lung cancer, breast cancer, advanced renal cell carcinoma, head and neck cancer, etc., has been broadly investigated.

Takada et al. (2022) examined 390 patients with advanced or recurrent non-small-cell lung cancer (NSCLC) who were treated with anti-PD-1 therapy in clinical practice and found that patients receiving anti-PD-1 therapy combined with statin treatment have much longer OS than those without statin treatment. However, another study showed that when the two groups of PD-L1 treatment with or without statin were compared, median PFS was 17.57 months and 9.57 months in the statin group and non-statin group, respectively ($p < 0.001$); median OS was significantly ($p < 0.001$) higher in the statin group than the non-statin group 19.94 and 10.94 months, respectively (Rossi et al., 2021). Although further prospective randomized trials are required, these strong associations together confirm that ICI treatment combined with statins in NSCLC patients may remarkably improve survival and prognosis, suggesting that the antitumor functions of statins synergize the benefits of ICI therapy in prevalent lung cancer.

In a cohort of metastatic renal cell carcinoma receiving PD-1 inhibitor nivolumab, 27% were statin users and 73% were non-statin users. The median OS and PFS were longer in the statin user group than in the non-statin users. Interestingly, in both patients aged ≥70 years and <70 years, the longer median OS and PFS were associated with longer statin exposure (Santoni et al., 2022). In conclusion, overall clinical benefits were greater in the statin user group than non-statin user group (71% and 54%), again strongly supporting the benefit of statin in PD-1-directed immunotherapy (Santoni et al., 2022).

Furthermore, in breast cancer, atorvastatin promotes cytotoxic T-cell activity, inhibits the immune evasion of T cells, and enhances antitumor immune response, thereby boosting the efficacy of anti-PD-L1 therapy (Choe et al., 2022). In addition, daily oral simvastatin or lovastatin combined with PD-1 blockade in mice promoted tumor control and extended survival, notably, lovastatin plus anti-PD-1 treatment leads to rejection of oral cancer tumors of the head and neck cancer in 30% of mice. The underlying protective effects are likely owing to that combination therapy enhances T cell activation and promotes predominant shifts of macrophage from M2 to M1 status, therefore, exerting resistance against head and neck cancer (Kansal et al., 2023) (Figure 3). In summary, these evidences together imply a consistent advantage of statin use in improving the therapeutic response of immunotherapy in multiple cancer types, via interacting with a range of immune cells, although detailed mechanisms are still lacking.

5.4 Combination of systemic therapy and immunotherapy in HCC

Before ICI immunotherapy had modified the management of HCC in the past few years, around 50% of patients with HCC received systemic therapies, generally, sorafenib or lenvatinib in the first line, followed by regorafenib, cabozantinib or ramucirumab as the second. Combinational regimens have been widely shown to yield significantly improved OS and superior PFS, thereby receiving rapid FDA approval (Llovet et al., 2022). For instance, generally used tyrosine kinase inhibitors (TKIs) for systemic treatment including sorafenib and lenvatinib, in combination with ICIs including nivolumab and pembrolizumab have been approved for the treatment of advanced HCC because of their noteworthy antitumor efficacy (Lee et al., 2022). Advances and benefits of immunotherapies along with other conventional treatment strategies have been well discussed in a broad therapeutic view in cancers including but not limited to HCC (Llovet et al., 2022).

Typical TKI, sorafenib, combined with PD-1-based ICIs for advanced HCC has been proven to be safe and effective, as the median PFS of combination treatment was greatly longer than the PD-1 monotherapy, The median OS of the combination treatment

group (21.63 months) was also longer than the PD-1 group (16.43 months) (Qin et al., 2022). Another TKI Lenvatinib, also an angiogenesis inhibitor, in combination with ICI therapy has demonstrated a synergistic antitumor effect, as VEGFA inhibition promotes the infiltration and survival of CTLs, and the meantime mitigates recruitment of Treg lymphocytes, leading to the more advantageous immune microenvironment for antitumor activity of ICI therapy (Hilmi et al., 2019). Lenvatinib was also found to be superior to sorafenib as the first-line treatment of HCC in regard to OS improvement (Kudo et al., 2018). Lenvatinib and anti-PD-1 antibody together robustly suppressed tumor growth, induced vascular normalization, and improved anti-PD-1 therapeutic efficacy in HCC (Yang et al., 2023). In a cohort of 139 male Chinese patients with advanced HCC, the median OS in the combined treatment group (PD-1 inhibitor sintilimab plus Lenvatinib) and Lenvatinib monotherapy group were 21.7 months and 12.8 months, and the median PFS were 11.3 months and 6.6 months, respectively. This combination regimen has shown acceptable efficacy and safety in practice and obviously improved long-term outcomes than monotherapy with either Lenvatinib or PD-1inhibitor (Zhao et al., 2022). Novel TKI regorafenib also augments the effects of ICI therapy against HCC (Xie et al., 2023). Afatinib, a second-generation EGFR-TKI, exhibits considerable inhibitory impacts on liver cancer cells and enhances the PD-L1 presentation in tumor cells. Afatinib combined with anti-PD1 treatment also notably enhances the immunotherapeutic effect in HCC (Yu et al., 2023).

Besides TKI-based therapies for HCC, there are many preclinical studies showing other non-TKI compounds are also potential candidates for adjuncts of immunotherapy in HCC. In particular, many of these drugs, similar to statins, are regularly seen and prescribed for chronic metabolic syndromes. The effect of metformin plus anti-PD-1 is enhanced than anti-PD-1 therapy against liver tumors in NASH-HCC murine models (Wabitsch et al., 2022). Aspirin enhanced the anti-PD-L1 immunotherapeutic efficacy, and combination therapy significantly induced HCC tumor regression and extended the lifespan of tumor-bearing mice (Lin et al., 2023). Moreover, abrine, a specific inhibitor of indoleamine-2,3-dioxygenase 1 (IDO1) and also a major player in immunosuppression in tumors, exerts profound liver-protective functions in immunotherapy. The combination of abrine and anti-PD-1 antibody treatment synergistically repressed the tumor growth in HCC by inducing $CD4^+$ or $CD8^+$ T cells, decreasing $Foxp3^+$ Treg cells, and inhibiting immune-suppressive molecules such as IDO1, CD47, and PD-L1(Liang et al., 2023b). Taken together, notable successes have been obtained in clinical trials when HCC is treated with immunotherapies combined with systemic monotherapy that has been used alone in the past.

5.5 Effects of statins on immunotherapies in HCC

Recently, although statins have already been applied in other non-HCC cancers as adjuncts of immunotherapy, and obvious benefits have been attained, such applications in the clinical treatment of HCC are still lacking. Preclinical studies in HCC mice revealed that either simvastatin or PD-L1 antibody alone indicated a slight but significant influence in tumor suppression ($p < 0.01$), whereas the combination of simvastatin and PD-L1 antibody significantly inhibited HCC tumor progression ($p < 0.001$), and the OS in the combination therapy were prolonged almost 2 times compared with the non-drug control ($p < 0.001$) (Yu et al., 2022). Furthermore, simvastatin treatment combined with PD-L1 antibody could not only improve the prognosis of the intrahepatic inoculation HCC model but also achieve satisfactory therapeutic efficacy in model of advanced HCC (Yu et al., 2022). Inspired by other combinations of statin use with immunotherapy in other cancer types, data from this study, although from a preliminary study, has underlined the great potential of statins as adjuncts for immunotherapy in HCC.

Furthermore, a prospective observational trial designed to evaluate the safety and efficacy of ICI therapy in combination with statins in treating NSCLC is now recruiting patients. We anticipate that preclinical and clinical explorations of statin/ICI therapy regimens for both HCC and non-HCC cancers will soon, embrace unprecedented new opportunities, certainly facing concomitant challenges ahead.

In addition to statins, other lipid-lowering drugs, such as PCSK9 inhibitors, fibrates, and ezetimide, may also impact or potentiate ICI therapy. In particular, immunomodulatory effects of PCSK9 inhibition are being studied shortly in cardiovascular disease and inflammation-related conditions, in addition to a phase II trial in NSCLC aiming to evaluate the anti-tumor activity of the combination of anti-PCSK9 and anti-PD-1 antibody therapy.

6 Conclusion and future perspectives

In the past decades, statins, traditionally used because of their cholesterol-lowering properties, have demonstrated multifaceted effects on the immune system in general cellular homeostasis, including modulation of T cell responses and anti-inflammatory properties. The exploration of statins as potential adjuncts in immunotherapies for HCC and other cancer types has yielded promising results. By enhancing immune responses via cytokine stimulation, statins can enhance the efficacy of immunotherapies such as ICIs in HCC. Such a combination approach, by incorporating statins into the existing immunotherapeutic regimens, may the hold key to improving treatment outcomes in HCC. However, it's crucial to acknowledge that more extensive preclinical investigations are prerequisites to provide more mechanistic basis for future clinical trials, before adding statins into immunotherapy regimens in HCC.

Such an integration strategy for HCC represents an exciting avenue from several future perspectives. First, future trials should assess the safety and efficacy of combining statins with various immunotherapeutic agents, with a focus on patient stratification to identify those who might benefit most. In addition, mechanistic studies should delve deeper into the immunomodulatory effects of statins in HCC, to resolve the precise pathways and cellular interactions that contribute to enhanced outcomes of immunotherapies. Furthermore, the development of novel statin derivatives with improved bioavailability and reduced side effects could broaden the feasibility of combination therapy. Lastly,

predictive biomarkers to identify HCC patients who are most likely to respond favorably to statin-immunotherapy combinations could be a priority to investigate. In conclusion, the future of statins in immunotherapies for HCC holds great promise, likely to refine the treatment landscape for this challenging malignancy and improve the treatment outcomes in patients.

Author contributions

JW: Funding acquisition, Resources, Visualization, Writing–original draft, Writing–review and editing. CeL: Funding acquisition, Visualization, Writing–original draft, Writing–review and editing. RH: Writing–original draft. LW: Visualization, Writing–review and editing. CuL: Funding acquisition, Supervision, Visualization, Writing–original draft, Writing–review and editing.

Funding

The authors declare financial support was received for the research, authorship, and/or publication of this article. This work was supported by Wuhan Science and Technology Bureau Innovation Project (2022020801020526, 2023020201020529) to JW and CeL, Science and Technology Project of Jiangxi Traditional Chinese Medicine Administration to LW (2023B1242), and grants from the National Natural Science Foundation of China (32070961) to CuL.

Conflict of interest

The authors declare that the research was conducted in the absence of any commercial or financial relationships that could be construed as a potential conflict of interest.

Publisher's note

References

Abou-Alfa, G. K., Chan, S. L., Kudo, M., Lau, G., Kelley, R. K., Furuse, J., et al. (2022). Phase 3 randomized, open-label, multicenter study of tremelimumab (T) and durvalumab (D) as first-line therapy in patients (pts) with unresectable hepatocellular carcinoma (uHCC): HIMALAYA. *J. Clin. Oncol.* 40 (4), 379. doi:10.1200/JCO.2022.40.4_suppl.379

Abraldes, J. G., Rodríguez-Vilarrupla, A., Graupera, M., Zafra, C., García-Calderó, H., García-Pagán, J. C., et al. (2007). Simvastatin treatment improves liver sinusoidal endothelial dysfunction in CCl4 cirrhotic rats. *J. Hepatol.* 46 (6), 1040–1046. doi:10.1016/j.jhep.2007.01.020

Abraldes, J. G., Villanueva, C., Aracil, C., Turnes, J., Hernandez-Guerra, M., Genesca, J., et al. (2016). Addition of simvastatin to standard therapy for the prevention of variceal rebleeding does not reduce rebleeding but increases survival in patients with cirrhosis. *Gastroenterology* 150 (5), 1160–1170. doi:10.1053/j.gastro.2016.01.004

Adhyaru, B. B., and Jacobson, T. A. (2018). Safety and efficacy of statin therapy. *Nat. Rev. Cardiol.* 15 (12), 757–769. doi:10.1038/s41569-018-0098-5

Ahern, T. P., Pedersen, L., Tarp, M., Cronin-Fenton, D. P., Garne, J. P., Silliman, R. A., et al. (2011). Statin prescriptions and breast cancer recurrence risk: a Danish nationwide prospective cohort study. *J. Natl. Cancer Inst.* 103 (19), 1461–1468. doi:10.1093/jnci/djr291

Ahsan, F., Oliveri, F., Goud, H. K., Mehkari, Z., Mohammed, L., Javed, M., et al. (2020). Pleiotropic effects of statins in the light of non-alcoholic fatty liver disease and non-alcoholic steatohepatitis. *Cureus* 12 (9), e10446. doi:10.7759/cureus.10446

Allott, E. H., Ebot, E. M., Stopsack, K. H., Gonzalez-Feliciano, A. G., Markt, S. C., Wilson, K. M., et al. (2020). Statin use is associated with lower risk of PTEN-null and lethal prostate cancer. *Clin. Cancer Res.* 26 (5), 1086–1093. doi:10.1158/1078-0432.Ccr-19-2853

Arii, S., Mise, M., Harada, T., Furutani, M., Ishigami, S., Niwano, M., et al. (1996). Overexpression of matrix metalloproteinase 9 gene in hepatocellular carcinoma with invasive potential. *Hepatology* 24 (2), 316–322. doi:10.1053/jhep.1996.v24.pm0008690399

Armitage, J., Bowman, L., Wallendszus, K., Bulbulia, R., Rahimi, K., Haynes, R., et al. (2010). Intensive lowering of LDL cholesterol with 80 mg versus 20 mg simvastatin daily in 12,064 survivors of myocardial infarction: a double-blind randomised trial. *Lancet* 376 (9753), 1658–1669. doi:10.1016/s0140-6736(10)60310-8

Ataseven, H., Bahcecioglu, I. H., Kuzu, N., Yalniz, M., Celebi, S., Erensoy, A., et al. (2006). The levels of ghrelin, leptin, TNF-alpha, and IL-6 in liver cirrhosis and hepatocellular carcinoma due to HBV and HDV infection. *Mediat. Inflamm.* 2006 (4), 78380. doi:10.1155/mi/2006/78380

Athyros, V. G., Alexandrides, T. K., Bilianou, H., Cholongitas, E., Doumas, M., Ganotakis, E. S., et al. (2017). The use of statins alone, or in combination with pioglitazone and other drugs, for the treatment of non-alcoholic fatty liver disease/non-alcoholic steatohepatitis and related cardiovascular risk. An Expert Panel Statement. *Metabolism* 71, 17–32. doi:10.1016/j.metabol.2017.02.014

Bakiri, L., Hamacher, R., Graña, O., Guío-Carrión, A., Campos-Olivas, R., Martinez, L., et al. (2017). Liver carcinogenesis by FOS-dependent inflammation and cholesterol dysregulation. *J. Exp. Med.* 214 (5), 1387–1409. doi:10.1084/jem.20160935

Bays, H., Cohen, D. E., Chalasani, N., and Harrison, S. A. (2014). An assessment by the statin liver safety task force: 2014 update. *J. Clin. Lipidol.* 8 (3), S47–S57. doi:10.1016/j.jacl.2014.02.011

Björkhem-Bergman, L., Backheden, M., and Söderberg Löfdal, K. (2014). Statin treatment reduces the risk of hepatocellular carcinoma but not colon cancer-results from a nationwide case-control study in Sweden. *Pharmacoepidemiol Drug Saf.* 23 (10), 1101–1106. doi:10.1002/pds.3685

Björnsson, E., Jacobsen, E. I., and Kalaitzakis, E. (2012). Hepatotoxicity associated with statins: reports of idiosyncratic liver injury post-marketing. *J. Hepatol.* 56 (2), 374–380. doi:10.1016/j.jhep.2011.07.023

Blais, P., Lin, M., Kramer, J. R., El-Serag, H. B., and Kanwal, F. (2016). Statins are underutilized in patients with nonalcoholic fatty liver disease and dyslipidemia. *Dig. Dis. Sci.* 61 (6), 1714–1720. doi:10.1007/s10620-015-4000-6

Blanc, J. F., Khemissa, F., Bronowicki, J. P., Monterymard, C., Perarnau, J. M., Bourgeois, V., et al. (2021). Phase 2 trial comparing sorafenib, pravastatin, their combination or supportive care in HCC with Child-Pugh B cirrhosis. *Hepatol. Int.* 15 (1), 93–104. doi:10.1007/s12072-020-10120-3

Borén, J., and Taskinen, M. R. (2022). "Metabolism of triglyceride-rich lipoproteins," in *Prevention and treatment of atherosclerosis: improving state-of-the-art management and search for novel targets*. Editors A. von Eckardstein, and C. J. Binder (Cham (CH): Springer), 133–156.

Borghaei, H., Paz-Ares, L., Horn, L., Spigel, D. R., Steins, M., Ready, N. E., et al. (2015). Nivolumab versus docetaxel in advanced nonsquamous non-small-cell lung cancer. *N. Engl. J. Med.* 373 (17), 1627–1639. doi:10.1056/NEJMoa1507643

Bulaon, C. J. I., Khorattanakulchai, N., Rattanapisit, K., Sun, H., Pisuttinusart, N., Strasser, R., et al. (2023). Antitumor effect of plant-produced anti-CTLA-4 monoclonal antibody in a murine model of colon cancer. *Front. Plant Sci.* 14, 1149455. doi:10.3389/fpls.2023.1149455

Butt, A. A., Yan, P., Bonilla, H., Abou-Samra, A. B., Shaikh, O. S., Simon, T. G., et al. (2015). Effect of addition of statins to antiviral therapy in hepatitis C virus-infected persons: results from ERCHIVES. *Hepatology* 62 (2), 365–374. doi:10.1002/hep.27835

Cao, Z., Fan-Minogue, H., Bellovin, D. I., Yevtodiyenko, A., Arzeno, J., Yang, Q., et al. (2011). MYC phosphorylation, activation, and tumorigenic potential in hepatocellular carcinoma are regulated by HMG-CoA reductase. *Cancer Res.* 71 (6), 2286–2297. doi:10.1158/0008-5472.Can-10-3367

Cardwell, C. R., Hicks, B. M., Hughes, C., and Murray, L. J. (2015). Statin use after diagnosis of breast cancer and survival: a population-based cohort study. *Epidemiology* 26 (1), 68–78. doi:10.1097/ede.0000000000000189

Chen, C., Wang, Z., Ding, Y., and Qin, Y. (2023a). Tumor microenvironment-mediated immune evasion in hepatocellular carcinoma. *Front. Immunol.* 14, 1133308. doi:10.3389/fimmu.2023.1133308

Chen, F., Zhuang, X., Lin, L., Yu, P., Wang, Y., Shi, Y., et al. (2015a). New horizons in tumor microenvironment biology: challenges and opportunities. *BMC Med.* 13, 45. doi:10.1186/s12916-015-0278-7

Chen, H. H., Lin, M. C., Muo, C. H., Yeh, S. Y., Sung, F. C., and Kao, C. H. (2015b). Combination therapy of metformin and statin may decrease hepatocellular carcinoma among diabetic patients in asia. *Med. Baltim.* 94 (24), e1013. doi:10.1097/md.0000000000001013

Chen, M., Bie, L., and Ying, J. (2023b). Cancer cell-intrinsic PD-1: its role in malignant progression and immunotherapy. *Biomed. Pharmacother.* 167, 115514. doi:10.1016/j.biopha.2023.115514

Chen, Z., Chen, L., Sun, B., Liu, D., He, Y., Qi, L., et al. (2021). LDLR inhibition promotes hepatocellular carcinoma proliferation and metastasis by elevating intracellular cholesterol synthesis through the MEK/ERK signaling pathway. *Mol. Metab.* 51, 101230. doi:10.1016/j.molmet.2021.101230

Chiu, H. F., Ho, S. C., Chen, C. C., and Yang, C. Y. (2011). Statin use and the risk of liver cancer: a population-based case–control study. *Am. J. Gastroenterol.* 106 (5), 894–898. doi:10.1038/ajg.2010.475

Cho, M. H., Yoo, T. G., Jeong, S. M., and Shin, D. W. (2021). Association of aspirin, metformin, and statin use with gastric cancer incidence and mortality: a nationwide cohort study. *Cancer Prev. Res. (Phila)* 14 (1), 95–104. doi:10.1158/1940-6207.Capr-20-0123

Cho, S. F., Yang, Y. H., Liu, Y. C., Hsiao, H. H., Huang, C. T., Wu, C. H., et al. (2015). Previous exposure to statin may reduce the risk of subsequent non-hodgkin lymphoma: a nationwide population-based case-control study. *PLoS One* 10 (10), e0139289. doi:10.1371/journal.pone.0139289

Choe, E. J., Lee, C. H., Bae, J. H., Park, J. M., Park, S. S., and Baek, M. C. (2022). Atorvastatin enhances the efficacy of immune checkpoint therapy and suppresses the cellular and extracellular vesicle PD-L1. *Pharmaceutics* 14 (8), 1660. doi:10.3390/pharmaceutics14081660

Chong, L. W., Hsu, Y. C., Lee, T. F., Lin, Y., Chiu, Y. T., Yang, K. C., et al. (2015). Fluvastatin attenuates hepatic steatosis-induced fibrogenesis in rats through inhibiting paracrine effect of hepatocyte on hepatic stellate cells. *BMC Gastroenterol.* 15, 22. doi:10.1186/s12876-015-0248-8

Coffin, P., and He, A. (2023). Hepatocellular carcinoma: past and present challenges and progress in molecular classification and precision oncology. *Int. J. Mol. Sci.* 24 (17), 13274. doi:10.3390/ijms241713274

Cortellini, A., Tucci, M., Adamo, V., Stucci, L. S., Russo, A., Tanda, E. T., et al. (2020). Integrated analysis of concomitant medications and oncological outcomes from PD-1/PD-L1 checkpoint inhibitors in clinical practice. *J. Immunother. Cancer* 8 (2), e001361. doi:10.1136/jitc-2020-001361

Cote, D. J., Rosner, B. A., Smith-Warner, S. A., Egan, K. M., and Stampfer, M. J. (2019). Statin use, hyperlipidemia, and risk of glioma. *Eur. J. Epidemiol.* 34 (11), 997–1011. doi:10.1007/s10654-019-00565-8

Cui, Y., Liang, S., Zhang, S., Zhang, C., Zhao, Y., Wu, D., et al. (2020). ABCA8 is regulated by miR-374b-5p and inhibits proliferation and metastasis of hepatocellular carcinoma through the ERK/ZEB1 pathway. *J. Exp. Clin. Cancer Res.* 39 (1), 90. doi:10.1186/s13046-020-01591-1

Deng, H., Zhang, J., Zheng, Y., Li, J., Xiao, Q., Wei, F., et al. (2022). CCDC25 may be a potential diagnostic and prognostic marker of hepatocellular carcinoma: results from microarray analysis. *Front. Surg.* 9, 878648. doi:10.3389/fsurg.2022.878648

Desoye, G., and Herrera, E. (2021). Adipose tissue development and lipid metabolism in the human fetus: the 2020 perspective focusing on maternal diabetes and obesity. *Prog. Lipid Res.* 81, 101082. doi:10.1016/j.plipres.2020.101082

Dickson, I. (2020). NETs promote liver metastasis via CCDC25. *Nat. Rev. Gastroenterology Hepatology* 17 (8), 451. doi:10.1038/s41575-020-0345-1

Dong, P., Ma, L., Liu, L., Zhao, G., Zhang, S., Dong, L., et al. (2016). $CD86^+$/$CD206^+$, diametrically polarized tumor-associated macrophages, predict hepatocellular carcinoma patient prognosis. *Int. J. Mol. Sci.* 17 (3), 320. doi:10.3390/ijms17030320

Dulak, J., and Józkowicz, A. (2005). Anti-angiogenic and anti-inflammatory effects of statins: relevance to anti-cancer therapy. *Curr. Cancer Drug Targets* 5 (8), 579–594. doi:10.2174/156800905774932824

Elia, I., and Haigis, M. C. (2021). Metabolites and the tumour microenvironment: from cellular mechanisms to systemic metabolism. *Nat. Metab.* 3 (1), 21–32. doi:10.1038/s42255-020-00317-z

El-Khoueiry, A. B., Sangro, B., Yau, T., Crocenzi, T. S., Kudo, M., Hsu, C., et al. (2017). Nivolumab in patients with advanced hepatocellular carcinoma (CheckMate 040): an open-label, non-comparative, phase 1/2 dose escalation and expansion trial. *Lancet* 389 (10088), 2492–2502. doi:10.1016/s0140-6736(17)31046-2

Emberson, J. R., Kearney, P. M., Blackwell, L., Newman, C., Reith, C., Bhala, N., et al. (2012). Lack of effect of lowering LDL cholesterol on cancer: meta-analysis of individual data from 175,000 people in 27 randomised trials of statin therapy. *PLoS One* 7 (1), e29849. doi:10.1371/journal.pone.0029849

Feng, X. C., Liu, F. C., Chen, W. Y., Du, J., and Liu, H. (2023a). Lipid metabolism of hepatocellular carcinoma impacts targeted therapy and immunotherapy. *World J. Gastrointest. Oncol.* 15 (4), 617–631. doi:10.4251/wjgo.v15.i4.617

Feng, Y., Luo, S., Fan, D., Guo, X., and Ma, S. (2023b). The role of vascular endothelial cells in tumor metastasis. *Acta histochem.* 125 (6), 152070. doi:10.1016/j.acthis.2023.152070

Finn, R. S., Qin, S. K., Ikeda, M., Galle, P. R., Ducreux, M., Kim, T. Y., et al. (2020). Atezolizumab plus bevacizumab in unresectable hepatocellular carcinoma. *N. Engl. J. Med.* 382 (20), 1894–1905. doi:10.1056/NEJMoa1915745

Foerster, F., Gairing, S. J., Ilyas, S. I., and Galle, P. R. (2022). Emerging immunotherapy for HCC: a guide for hepatologists. *Hepatology* 75 (6), 1604–1626. doi:10.1002/hep.32447

Fujiwara, N., Nakagawa, H., Enooku, K., Kudo, Y., Hayata, Y., Nakatsuka, T., et al. (2018). CPT2 downregulation adapts HCC to lipid-rich environment and promotes carcinogenesis via acylcarnitine accumulation in obesity. *Gut* 67 (8), 1493–1504. doi:10.1136/gutjnl-2017-315193

Galland, S., Martin, P., Fregni, G., Letovanec, I., and Stamenkovic, I. (2020). Attenuation of the pro-inflammatory signature of lung cancer-derived mesenchymal stromal cells by statins. *Cancer Lett.* 484, 50–64. doi:10.1016/j.canlet.2020.05.005

Gao, X., and Zuo, S. (2023). Immune landscape and immunotherapy of hepatocellular carcinoma: focus on innate and adaptive immune cells. *Clin. Exp. Med.* 23, 1881–1899. doi:10.1007/s10238-023-01015-2

Ghalali, A., Martin-Renedo, J., Högberg, J., and Stenius, U. (2017). Atorvastatin decreases HBx-induced phospho-akt in hepatocytes via P2X receptors. *Mol. Cancer Res.* 15 (6), 714–722. doi:10.1158/1541-7786.Mcr-16-0373

Goh, M. J., and Sinn, D. H. (2022). Statin and aspirin for chemoprevention of hepatocellular carcinoma: time to use or wait further? *Clin. Mol. Hepatol.* 28 (3), 380–395. doi:10.3350/cmh.2021.0366

Graf, H., Jüngst, C., Straub, G., Dogan, S., Hoffmann, R. T., Jakobs, T., et al. (2008). Chemoembolization combined with pravastatin improves survival in patients with hepatocellular carcinoma. *Digestion* 78 (1), 34–38. doi:10.1159/000156702

He, X., and Xu, C. (2020). Immune checkpoint signaling and cancer immunotherapy. *Cell Res.* 30 (8), 660–669. doi:10.1038/s41422-020-0343-4

Hilligan, K. L., and Ronchese, F. (2020). Antigen presentation by dendritic cells and their instruction of CD4+ T helper cell responses. *Cell Mol. Immunol.* 17 (6), 587–599. doi:10.1038/s41423-020-0465-0

Hilmi, M., Neuzillet, C., Calderaro, J., Lafdil, F., Pawlotsky, J. M., and Rousseau, B. (2019). Angiogenesis and immune checkpoint inhibitors as therapies for hepatocellular carcinoma: current knowledge and future research directions. *J. Immunother. Cancer* 7 (1), 333. doi:10.1186/s40425-019-0824-5

Hosonuma, M., and Yoshimura, K. (2023). Association between pH regulation of the tumor microenvironment and immunological state. *Front. Oncol.* 13, 1175563. doi:10.3389/fonc.2023.1175563

Huang, B., Song, B. L., and Xu, C. (2020). Cholesterol metabolism in cancer: mechanisms and therapeutic opportunities. *Nat. Metab.* 2 (2), 132–141. doi:10.1038/s42255-020-0174-0

Huang, W., Ye, D., He, W., He, X., Shi, X., and Gao, Y. (2021). Activated but impaired IFN-γ production of mucosal-associated invariant T cells in patients with hepatocellular carcinoma. *J. Immunother. Cancer* 9 (11), e003685. doi:10.1136/jitc-2021-003685

Hyogo, H., Tazuma, S., Arihiro, K., Iwamoto, K., Nabeshima, Y., Inoue, M., et al. (2008). Efficacy of atorvastatin for the treatment of nonalcoholic steatohepatitis with dyslipidemia. *Metabolism* 57 (12), 1711–1718. doi:10.1016/j.metabol.2008.07.030

Ioannou, G. N., Van Rooyen, D. M., Savard, C., Haigh, W. G., Yeh, M. M., Teoh, N. C., et al. (2015). Cholesterol-lowering drugs cause dissolution of cholesterol crystals and disperse Kupffer cell crown-like structures during resolution of NASH. *J. Lipid Res.* 56 (2), 277–285. doi:10.1194/jlr.M053785

Islam, M. M., Poly, T. N., Walther, B. A., Yang, H. C., and Jack Li, Y. C. (2020). Statin use and the risk of hepatocellular carcinoma: a meta-analysis of observational studies. *Cancers (Basel)* 12 (3), 671. doi:10.3390/cancers12030671

Janakiram, N. B., Mohammed, A., Bryant, T., Zhang, Y., Brewer, M., Duff, A., et al. (2016). Potentiating NK cell activity by combination of Rosuvastatin and Difluoromethylornithine for effective chemopreventive efficacy against Colon Cancer. *Sci. Rep.* 6, 37046. doi:10.1038/srep37046

Jespersen, C. G., Nørgaard, M., Friis, S., Skriver, C., and Borre, M. (2014). Statin use and risk of prostate cancer: a Danish population-based case-control study, 1997-2010. *Cancer Epidemiol.* 38 (1), 42–47. doi:10.1016/j.canep.2013.10.010

Jia, C. C., Wang, T. T., Liu, W., Fu, B. S., Hua, X., Wang, G. Y., et al. (2013). Cancer-associated fibroblasts from hepatocellular carcinoma promote malignant cell proliferation by HGF secretion. *PLoS One* 8 (5), e63243. doi:10.1371/journal.pone.0063243

Jin, M. Z., and Jin, W. L. (2020). The updated landscape of tumor microenvironment and drug repurposing. *Signal Transduct. Target Ther.* 5 (1), 166. doi:10.1038/s41392-020-00280-x

Jouve, J. L., Lecomte, T., Bouché, O., Barbier, E., Khemissa Akouz, F., Riachi, G., et al. (2019). Pravastatin combination with sorafenib does not improve survival in advanced hepatocellular carcinoma. *J. Hepatol.* 71 (3), 516–522. doi:10.1016/j.jhep.2019.04.021

Kamrani, A., Hosseinzadeh, R., Shomali, N., Heris, J. A., Shahabi, P., Mohammadinasab, R., et al. (2023). New immunotherapeutic approaches for cancer treatment. *Pathol. Res. Pract.* 248, 154632. doi:10.1016/j.prp.2023.154632

Kansal, V., Burnham, A. J., Kinney, B. L. C., Saba, N. F., Paulos, C., Lesinski, G. B., et al. (2023). Statin drugs enhance responses to immune checkpoint blockade in head and neck cancer models. *J. Immunother. Cancer* 11 (1), e005940. doi:10.1136/jitc-2022-005940

Kawaguchi, Y., Sakamoto, Y., Ito, D., Ito, K., Arita, J., Akamatsu, N., et al. (2017). Statin use is associated with a reduced risk of hepatocellular carcinoma recurrence after initial liver resection. *Biosci. Trends* 11 (5), 574–580. doi:10.5582/bst.2017.01191

Kawata, S., Yamasaki, E., Nagase, T., Inui, Y., Ito, N., Matsuda, Y., et al. (2001). Effect of pravastatin on survival in patients with advanced hepatocellular carcinoma. A randomized controlled trial. *Br. J. Cancer* 84 (7), 886–891. doi:10.1054/bjoc.2000.1716

Khazaaleh, S., Sarmini, M. T., Alomari, M., Al Momani, L., El Kurdi, B., Asfari, M., et al. (2022). Statin use reduces the risk of hepatocellular carcinoma: an updated meta-analysis and systematic review. *Cureus* 14 (7), e27032. doi:10.7759/cureus.27032

Kotsari, M., Dimopoulou, V., Koskinas, J., and Armakolas, A. (2023). Immune system and hepatocellular carcinoma (HCC): new insights into HCC progression. *Int. J. Mol. Sci.* 24 (14), 11471. doi:10.3390/ijms241411471

Kudo, M., Finn, R. S., Qin, S., Han, K. H., Ikeda, K., Piscaglia, F., et al. (2018). Lenvatinib versus sorafenib in first-line treatment of patients with unresectable hepatocellular carcinoma: a randomised phase 3 non-inferiority trial. *Lancet* 391 (10126), 1163–1173. doi:10.1016/s0140-6736(18)30207-1

Lacin, S., and Yalcin, S. (2020). The prognostic value of circulating VEGF-A level in patients with hepatocellular cancer. *Technol. Cancer Res. Treat.* 19, 1533033820971677. doi:10.1177/1533033820971677

Lamon-Fava, S. (2013). Statins and lipid metabolism: an update. *Curr. Opin. Lipidol.* 24 (3), 221–226. doi:10.1097/MOL.0b013e3283613b8b

Lange, N. F., Radu, P., and Dufour, J. F. (2021). Prevention of NAFLD-associated HCC: role of lifestyle and chemoprevention. *J. Hepatol.* 75 (5), 1217–1227. doi:10.1016/j.jhep.2021.07.025

Langhans, B., Nischalke, H. D., Krämer, B., Dold, L., Lutz, P., Mohr, R., et al. (2019). Role of regulatory T cells and checkpoint inhibition in hepatocellular carcinoma. *Cancer Immunol. Immunother.* 68 (12), 2055–2066. doi:10.1007/s00262-019-02427-4

Lee, S. J., Lee, I., Lee, J., Park, C., and Kang, W. K. (2014). Statins, 3-hydroxy-3-methylglutaryl coenzyme A reductase inhibitors, potentiate the anti-angiogenic effects of bevacizumab by suppressing angiopoietin2, BiP, and Hsp90α in human colorectal cancer. *Br. J. Cancer* 111 (3), 497–505. doi:10.1038/bjc.2014.283

Lee, S. W., Yang, S. S., Lien, H. C., Peng, Y. C., Tung, C. F., and Lee, T. Y. (2022). The combining of tyrosine kinase inhibitors and immune checkpoint inhibitors as first-line treatment for advanced stage hepatocellular carcinoma. *J. Clin. Med.* 11 (16), 4874. doi:10.3390/jcm11164874

Li, J., Xuan, S., Dong, P., Xiang, Z., Gao, C., Li, M., et al. (2023a). Immunotherapy of hepatocellular carcinoma: recent progress and new strategy. *Front. Immunol.* 14, 1192506. doi:10.3389/fimmu.2023.1192506

Li, L., Cui, N., Hao, T., Zou, J., Jiao, W., Yi, K., et al. (2021). Statins use and the prognosis of colorectal cancer: a meta-analysis. *Clin. Res. Hepatol. Gastroenterol.* 45 (5), 101588. doi:10.1016/j.clinre.2020.101588

Li, L., Pilo, G. M., Li, X. L., Cigliano, A., Latte, G., Che, L., et al. (2016). Inactivation of fatty acid synthase impairs hepatocarcinogenesis driven by AKT in mice and humans. *J. Hepatology* 64 (2), 333–341. doi:10.1016/j.jhep.2015.10.004

Li, S., Saviano, A., Erstad, D. J., Hoshida, Y., Fuchs, B. C., Baumert, T., et al. (2020a). Risk factors, pathogenesis, and strategies for hepatocellular carcinoma prevention: emphasis on secondary prevention and its translational challenges. *J. Clin. Med.* 9 (12), 3817. doi:10.3390/jcm9123817

Li, T., Yang, Y., Hua, X., Wang, G., Liu, W., Jia, C., et al. (2012). Hepatocellular carcinoma-associated fibroblasts trigger NK cell dysfunction via PGE2 and Ido. *Cancer Lett.* 318 (2), 154–161. doi:10.1016/j.canlet.2011.12.020

Li, X., Liu, L., and Hu, Y. (2020b). Statin use and the prognosis of patients with hepatocellular carcinoma: a meta-analysis. *Biosci. Rep.* 40 (4). doi:10.1042/bsr20200232

Li, X., Sun, X., Wang, B., Li, Y., and Tong, J. (2023b). Oncolytic virus-based hepatocellular carcinoma treatment: current status, intravenous delivery strategies, and emerging combination therapeutic solutions. *Asian J. Pharm. Sci.* 18 (1), 100771. doi:10.1016/j.ajps.2022.100771

Li, X. M., Tang, Z. Y., Qin, L. X., Zhou, J., and Sun, H. C. (1999). Serum vascular endothelial growth factor is a predictor of invasion and metastasis in hepatocellular carcinoma. *J. Exp. Clin. Cancer Res.* 18 (4), 511–517.

Liang, H., Du, Y., Zhu, C., Zhang, Z., Liao, G., Liu, L., et al. (2023a). Nanoparticulate cationic poly(amino acid)s block cancer metastases by destructing neutrophil extracellular traps. *ACS Nano* 17 (3), 2868–2880. doi:10.1021/acsnano.2c11280

Liang, X., Gao, H., Xiao, J., Han, S., He, J., Yuan, R., et al. (2023b). Abrine, an Ido1 inhibitor, suppresses the immune escape and enhances the immunotherapy of anti-PD-1 antibody in hepatocellular carcinoma. *Front. Immunol.* 14, 1185985. doi:10.3389/fimmu.2023.1185985

Lin, M., He, J., Zhang, X., Sun, X., Dong, W., Zhang, R., et al. (2023). Targeting fibrinogen-like protein 1 enhances immunotherapy in hepatocellular carcinoma. *J. Clin. Invest.* 133 (9), e164528. doi:10.1172/jci164528

Liu, J., Chen, S., Wang, W., Ning, B. F., Chen, F., Shen, W., et al. (2016). Cancer-associated fibroblasts promote hepatocellular carcinoma metastasis through chemokine-activated hedgehog and TGF-β pathways. *Cancer Lett.* 379 (1), 49–59. doi:10.1016/j.canlet.2016.05.022

Liu, X., Bao, X., Hu, M., Chang, H., Jiao, M., Cheng, J., et al. (2020). Inhibition of PCSK9 potentiates immune checkpoint therapy for cancer. *Nature* 588 (7839), 693–698. doi:10.1038/s41586-020-2911-7

Liu, Y., Xun, Z. Z., Ma, K., Liang, S. H., Li, X. Y., Zhou, S., et al. (2023). Identification of a tumour immune barrier in the HCC microenvironment that determines the efficacy of immunotherapy. *J. Hepatology* 78 (4), 770–782. doi:10.1016/j.jhep.2023.01.011

Llovet, J. M., Castet, F., Heikenwalder, M., Maini, M. K., Mazzaferro, V., Pinato, D. J., et al. (2022). Immunotherapies for hepatocellular carcinoma. *Nat. Rev. Clin. Oncol.* 19 (3), 151–172. doi:10.1038/s41571-021-00573-2

Lu, X., Deng, S., Xu, J., Green, B. L., Zhang, H., Cui, G., et al. (2023). Combination of AFP vaccine and immune checkpoint inhibitors slows hepatocellular carcinoma progression in preclinical models. *J. Clin. Invest.* 133 (11), e163291. doi:10.1172/jci163291

Lu, Y. M., Yang, A. Q., Quan, C., Pan, Y. W., Zhang, H. Y., Li, Y. F., et al. (2022). A single-cell atlas of the multicellular ecosystem of primary and metastatic hepatocellular carcinoma. *Nat. Commun.* 13 (1), 4594. doi:10.1038/s41467-022-32283-3

Mano, Y., Aishima, S., Fujita, N., Tanaka, Y., Kubo, Y., Motomura, T., et al. (2013). Tumor-associated macrophage promotes tumor progression via STAT3 signaling in hepatocellular carcinoma. *Pathobiology* 80 (3), 146–154. doi:10.1159/000346196

Marinho, T. S., Kawasaki, A., Bryntesson, M., Souza-Mello, V., Barbosa-da-Silva, S., Aguila, M. B., et al. (2017). Rosuvastatin limits the activation of hepatic stellate cells in diet-induced obese mice. *Hepatol. Res.* 47 (9), 928–940. doi:10.1111/hepr.12821

Marrone, G., Russo, L., Rosado, E., Hide, D., García-Cardeña, G., García-Pagán, J. C., et al. (2013). The transcription factor KLF2 mediates hepatic endothelial protection and paracrine endothelial-stellate cell deactivation induced by statins. *J. Hepatol.* 58 (1), 98–103. doi:10.1016/j.jhep.2012.08.026

McGlynn, K. A., Hagberg, K., Chen, J., Graubard, B. I., London, W. T., Jick, S., et al. (2015). Statin use and risk of primary liver cancer in the Clinical Practice Research Datalink. *J. Natl. Cancer Inst.* 107 (4), djv009. doi:10.1093/jnci/djv009

Mei, Z., Liang, M., Li, L., Zhang, Y., Wang, Q., and Yang, W. (2017). Effects of statins on cancer mortality and progression: a systematic review and meta-analysis of 95 cohorts including 1,111,407 individuals. *Int. J. Cancer* 140 (5), 1068–1081. doi:10.1002/ijc.30526

Michalik, L., Desvergne, B., and Wahli, W. (2004). Peroxisome-proliferator-activated receptors and cancers: complex stories. *Nat. Rev. Cancer* 4 (1), 61–70. doi:10.1038/nrc1254

Molnár, E., Swamy, M., Holzer, M., Beck-García, K., Worch, R., Thiele, C., et al. (2012). Cholesterol and sphingomyelin drive ligand-independent T-cell antigen receptor nanoclustering. *J. Biol. Chem.* 287 (51), 42664–42674. doi:10.1074/jbc.M112.386045

Murai, H., Kodama, T., Maesaka, K., Tange, S., Motooka, D., Suzuki, Y., et al. (2023). Multiomics identifies the link between intratumor steatosis and the exhausted tumor immune microenvironment in hepatocellular carcinoma. *Hepatology* 77 (1), 77–91. doi:10.1002/hep.32573

Nath, A., Li, I., Roberts, L. R., and Chan, C. (2015). Elevated free fatty acid uptake via CD36 promotes epithelial-mesenchymal transition in hepatocellular carcinoma. *Sci. Rep.* 5, 14752. doi:10.1038/srep14752

Nayan, M., Punjani, N., Juurlink, D. N., Finelli, A., Austin, P. C., Kulkarni, G. S., et al. (2017). Statin use and kidney cancer survival outcomes: a systematic review and meta-analysis. *Cancer Treat. Rev.* 52, 105–116. doi:10.1016/j.ctrv.2016.11.009

Nielsen, S. F., Nordestgaard, B. G., and Bojesen, S. E. (2012). Statin use and reduced cancer-related mortality. *N. Engl. J. Med.* 367 (19), 1792–1802. doi:10.1056/NEJMoa1201735

Omar, M. A., Omran, M. M., Farid, K., Tabll, A. A., Shahein, Y. E., Emran, T. M., et al. (2023). Biomarkers for hepatocellular carcinoma: from origin to clinical diagnosis. *Biomedicines* 11 (7), 1852. doi:10.3390/biomedicines11071852

Ostwal, V., Ramaswamy, A., Gota, V., Bhargava, P. G., Srinivas, S., Shriyan, B., et al. (2022). Phase I study evaluating dose de-escalation of sorafenib with metformin and atorvastatin in hepatocellular carcinoma (SMASH). *Oncologist* 27 (3), 165–e222. doi:10.1093/oncolo/oyab008

Oura, K., Morishita, A., Tani, J., and Masaki, T. (2021). Tumor immune microenvironment and immunosuppressive therapy in hepatocellular carcinoma: a review. *Int. J. Mol. Sci.* 22 (11), 5801. doi:10.3390/ijms22115801

Park, H. S., Jang, J. E., Ko, M. S., Woo, S. H., Kim, B. J., Kim, H. S., et al. (2016). Statins increase mitochondrial and peroxisomal fatty acid oxidation in the liver and prevent non-alcoholic steatohepatitis in mice. *Diabetes Metab. J.* 40 (5), 376–385. doi:10.4093/dmj.2016.40.5.376

Pascual, G., Avgustinova, A., Mejetta, S., Martín, M., Castellanos, A., Attolini, C. S., et al. (2017). Targeting metastasis-initiating cells through the fatty acid receptor CD36. *Nature* 541 (7635), 41–45. doi:10.1038/nature20791

Pedersen, T. R. (2010). Pleiotropic effects of statins: evidence against benefits beyond LDL-cholesterol lowering. *Am. J. Cardiovasc Drugs* 10 (1), 10–17. doi:10.2165/1158822-s0-000000000-00000

Peng, S. H., Deng, H., Yang, J. F., Xie, P. P., Li, C., Li, H., et al. (2005). Significance and relationship between infiltrating inflammatory cell and tumor angiogenesis in hepatocellular carcinoma tissues. *World J. Gastroenterol.* 11 (41), 6521–6524. doi:10.3748/wjg.v11.i41.6521

Pinyopornpanish, K., Al-Yaman, W., Butler, R. S., Carey, W., McCullough, A., and Romero-Marrero, C. (2021). Chemopreventive effect of statin on hepatocellular carcinoma in patients with nonalcoholic steatohepatitis cirrhosis. *Am. J. Gastroenterol.* 116 (11), 2258–2269. doi:10.14309/ajg.0000000000001347

Podlasek, A., Abdulla, M., Broering, D., and Bzeizi, K. (2023). Recent advances in locoregional therapy of hepatocellular carcinoma. *Cancers (Basel)* 15 (13), 3347. doi:10.3390/cancers15133347

Poon, R. T., Ho, J. W., Tong, C. S., Lau, C., Ng, I. O., and Fan, S. T. (2004). Prognostic significance of serum vascular endothelial growth factor and endostatin in patients with hepatocellular carcinoma. *Br. J. Surg.* 91 (10), 1354–1360. doi:10.1002/bjs.4594

Pose, E., Trebicka, J., Mookerjee, R. P., Angeli, P., and Ginès, P. (2019). Statins: old drugs as new therapy for liver diseases? *J. Hepatol.* 70 (1), 194–202. doi:10.1016/j.jhep.2018.07.019

Qin, J., Huang, Y., Zhou, H., and Yi, S. (2022). Efficacy of sorafenib combined with immunotherapy following transarterial chemoembolization for advanced hepatocellular carcinoma: a propensity score analysis. *Front. Oncol.* 12, 807102. doi:10.3389/fonc.2022.807102

Raskopf, E., Vogt, A., Sauerbruch, T., and Schmitz, V. (2008). siRNA targeting VEGF inhibits hepatocellular carcinoma growth and tumor angiogenesis *in vivo*. *J. Hepatol.* 49 (6), 977–984. doi:10.1016/j.jhep.2008.07.022

Relja, B., Meder, F., Wang, M., Blaheta, R., Henrich, D., Marzi, I., et al. (2011). Simvastatin modulates the adhesion and growth of hepatocellular carcinoma cells via decrease of integrin expression and ROCK. *Int. J. Oncol.* 38 (3), 879–885. doi:10.3892/ijo.2010.892

Ribas, A., and Wolchok, J. D. (2018). Cancer immunotherapy using checkpoint blockade. *Science* 359 (6382), 1350–1355. doi:10.1126/science.aar4060

Rodríguez, S., Raurell, I., Torres-Arauz, M., García-Lezana, T., Genescà, J., and Martell, M. (2017). A nitric oxide-donating statin decreases portal pressure with a better toxicity profile than conventional statins in cirrhotic rats. *Sci. Rep.* 7, 40461. doi:10.1038/srep40461

Rossi, A., Filetti, M., Taurelli Salimbeni, B., Piras, M., Rizzo, F., Giusti, R., et al. (2021). Statins and immunotherapy: togetherness makes strength the potential effect of statins on immunotherapy for NSCLC. *Cancer Rep. Hob.* 4 (4), e1368. doi:10.1002/cnr2.1368

Roudier, E., Mistafa, O., and Stenius, U. (2006). Statins induce mammalian target of rapamycin (mTOR)-mediated inhibition of Akt signaling and sensitize p53-deficient cells to cytostatic drugs. *Mol. Cancer Ther.* 5 (11), 2706–2715. doi:10.1158/1535-7163.Mct-06-0352

Roy, A. (2022). Updated efficacy and safety data from IMbrave150: atezolizumab plus bevacizumab vs. Sorafenib for unresectable hepatocellular carcinoma. *J. Clin. Exp. Hepatol.* 12 (6), 1575–1576. doi:10.1016/j.jceh.2022.07.003

Rzouq, F. S., Volk, M. L., Hatoum, H. H., Talluri, S. K., Mummadi, R. R., and Sood, G. K. (2010). Hepatotoxicity fears contribute to underutilization of statin medications by primary care physicians. *Am. J. Med. Sci.* 340 (2), 89–93. doi:10.1097/MAJ.0b013e3181e15da8

Sakano, Y., Noda, T., Kobayashi, S., Sasaki, K., Iwagami, Y., Yamada, D., et al. (2022). Tumor endothelial cell-induced CD8(+) T-cell exhaustion via GPNMB in hepatocellular carcinoma. *Cancer Sci.* 113 (5), 1625–1638. doi:10.1111/cas.15331

Samy, W., and Hassanian, M. A. (2011). Paraoxonase-1 activity, malondialdehyde and glutathione peroxidase in non-alcoholic fatty liver disease and the effect of atorvastatin. *Arab. J. Gastroenterol.* 12 (2), 80–85. doi:10.1016/j.ajg.2011.04.008

Sangro, B., Sarobe, P., Hervás-Stubbs, S., and Melero, I. (2021). Advances in immunotherapy for hepatocellular carcinoma. *Nat. Rev. Gastroenterology Hepatology* 18 (8), 525–543. doi:10.1038/s41575-021-00438-0

Santoni, M., Massari, F., Matrana, M. R., Basso, U., De Giorgi, U., Aurilio, G., et al. (2022). Statin use improves the efficacy of nivolumab in patients with advanced renal cell carcinoma. *Eur. J. Cancer* 172, 191–198. doi:10.1016/j.ejca.2022.04.035

Sas, Z., Cendrowicz, E., Weinhäuser, I., and Rygiel, T. P. (2022). Tumor microenvironment of hepatocellular carcinoma: challenges and opportunities for new treatment options. *Int. J. Mol. Sci.* 23 (7), 3778. doi:10.3390/ijms23073778

Schierwagen, R., Maybüchen, L., Hittatiya, K., Klein, S., Uschner, F. E., Braga, T. T., et al. (2016). Statins improve NASH via inhibition of RhoA and Ras. *Am. J. Physiol. Gastrointest. Liver Physiol.* 311 (4), G724–g733. doi:10.1152/ajpgi.00063.2016

Shannon, A. H., Manne, A., Diaz Pardo, D. A., and Pawlik, T. M. (2023). Combined radiotherapy and immune checkpoint inhibition for the treatment of advanced hepatocellular carcinoma. *Front. Oncol.* 13, 1193762. doi:10.3389/fonc.2023.1193762

Shirabe, K., Mano, Y., Muto, J., Matono, R., Motomura, T., Toshima, T., et al. (2012). Role of tumor-associated macrophages in the progression of hepatocellular carcinoma. *Surg. Today* 42 (1), 1–7. doi:10.1007/s00595-011-0058-8

Singh, J., Wozniak, A., Cotler, S. J., Dhanarajan, A., Aldrich, D., Park, D., et al. (2022). Combined use of aspirin and statin is associated with a decreased incidence of hepatocellular carcinoma. *J. Clin. Gastroenterol.* 56 (4), 369–373. doi:10.1097/mcg.0000000000001546

Sperling, C. D., Verdoodt, F., Friis, S., Dehlendorff, C., and Kjaer, S. K. (2017). Statin use and risk of endometrial cancer: a nationwide registry-based case-control study. *Acta Obstet. Gynecol. Scand.* 96 (2), 144–149. doi:10.1111/aogs.13069

Su, P., Wang, Q., Bi, E., Ma, X., Liu, L., Yang, M., et al. (2020). Enhanced lipid accumulation and metabolism are required for the differentiation and activation of tumor-associated macrophages. *Cancer Res.* 80 (7), 1438–1450. doi:10.1158/0008-5472.Can-19-2994

Sun, M. H., Han, X. C., Jia, M. K., Jiang, W. D., Wang, M., Zhang, H., et al. (2005). Expressions of inducible nitric oxide synthase and matrix metalloproteinase-9 and their effects on angiogenesis and progression of hepatocellular carcinoma. *World J. Gastroenterol.* 11 (38), 5931–5937. doi:10.3748/wjg.v11.i38.5931

Sun, Y. F., Wu, L., Zhong, Y., Zhou, K. Q., Hou, Y., Wang, Z. F., et al. (2021). Single-cell landscape of the ecosystem in early-relapse hepatocellular carcinoma. *Cell* 184 (2), 404–421. doi:10.1016/j.cell.2020.11.041

Tahmasebi Birgani, M., and Carloni, V. (2017). Tumor microenvironment, a paradigm in hepatocellular carcinoma progression and therapy. *Int. J. Mol. Sci.* 18 (2), 405. doi:10.3390/ijms18020405

Takada, K., Shimokawa, M., Takamori, S., Shimamatsu, S., Hirai, F., Tagawa, T., et al. (2022). A propensity score-matched analysis of the impact of statin therapy on the outcomes of patients with non-small-cell lung cancer receiving anti-PD-1 monotherapy: a multicenter retrospective study. *BMC Cancer* 22 (1), 503. doi:10.1186/s12885-022-09385-8

Tosi, M. R., and Tugnoli, V. (2005). Cholesteryl esters in malignancy. *Clin. Chim. Acta* 359 (1-2), 27–45. doi:10.1016/j.cccn.2005.04.003

Tran, K. T., McMenamin Ú, C., Coleman, H. G., Cardwell, C. R., Murchie, P., Iversen, L., et al. (2020). Statin use and risk of liver cancer: evidence from two population-based studies. *Int. J. Cancer* 146 (5), 1250–1260. doi:10.1002/ijc.32426

Tsan, Y. T., Lee, C. H., Ho, W. C., Lin, M. H., Wang, J. D., and Chen, P. C. (2013). Statins and the risk of hepatocellular carcinoma in patients with hepatitis C virus infection. *J. Clin. Oncol.* 31 (12), 1514–1521. doi:10.1200/jco.2012.44.6831

Tsan, Y. T., Lee, C. H., Wang, J. D., and Chen, P. C. (2012). Statins and the risk of hepatocellular carcinoma in patients with hepatitis B virus infection. *J. Clin. Oncol.* 30 (6), 623–630. doi:10.1200/jco.2011.36.0917

Tsuchiya, N., Yoshikawa, T., Fujinami, N., Saito, K., Mizuno, S., Sawada, Y., et al. (2017). Immunological efficacy of glypican-3 peptide vaccine in patients with advanced hepatocellular carcinoma. *Oncoimmunology* 6 (10), e1346764. doi:10.1080/2162402x.2017.1346764

Ung, M. H., MacKenzie, T. A., Onega, T. L., Amos, C. I., and Cheng, C. (2018). Statins associate with improved mortality among patients with certain histological subtypes of lung cancer. *Lung Cancer* 126, 89–96. doi:10.1016/j.lungcan.2018.10.022

Uschner, F. E., Ranabhat, G., Choi, S. S., Granzow, M., Klein, S., Schierwagen, R., et al. (2015). Statins activate the canonical hedgehog-signaling and aggravate non-cirrhotic portal hypertension, but inhibit the non-canonical hedgehog signaling and cirrhotic portal hypertension. *Sci. Rep.* 5, 14573. doi:10.1038/srep14573

Vahedian-Azimi, A., Shojaie, S., Banach, M., Heidari, F., Cicero, A. F. G., Khoshfetrat, M., et al. (2021). Statin therapy in chronic viral hepatitis: a systematic review and meta-analysis of nine studies with 195,602 participants. *Ann. Med.* 53 (1), 1227–1242. doi:10.1080/07853890.2021.1956686

Veglia, F., Tyurin, V. A., Blasi, M., De Leo, A., Kossenkov, A. V., Donthireddy, L., et al. (2019). Fatty acid transport protein 2 reprograms neutrophils in cancer. *Nature* 569 (7754), 73–78. doi:10.1038/s41586-019-1118-2

Vos, W. G., Lutgens, E., and Seijkens, T. T. P. (2022). Statins and immune checkpoint inhibitors: a strategy to improve the efficacy of immunotherapy for cancer? *J. Immunother. Cancer* 10 (9), e005611. doi:10.1136/jitc-2022-005611

Wabitsch, S., McCallen, J. D., Kamenyeva, O., Ruf, B., McVey, J. C., Kabat, J., et al. (2022). Metformin treatment rescues CD8(+) T-cell response to immune checkpoint inhibitor therapy in mice with NAFLD. *J. Hepatol.* 77 (3), 748–760. doi:10.1016/j.jhep.2022.03.010

Wang, A., Aragaki, A. K., Tang, J. Y., Kurian, A. W., Manson, J. E., Chlebowski, R. T., et al. (2016). Statin use and all-cancer survival: prospective results from the Women's Health Initiative. *Br. J. Cancer* 115 (1), 129–135. doi:10.1038/bjc.2016.149

Wang, H., Zhou, Y., Xu, H., Wang, X., Zhang, Y., Shang, R., et al. (2022). Therapeutic efficacy of FASN inhibition in preclinical models of HCC. *Hepatology* 76 (4), 951–966. doi:10.1002/hep.32359

Wang, J., Tokoro, T., Higa, S., and Kitajima, I. (2006). Anti-inflammatory effect of pitavastatin on NF-kappaB activated by TNF-alpha in hepatocellular carcinoma cells. *Biol. Pharm. Bull.* 29 (4), 634–639. doi:10.1248/bpb.29.634

Wang, W., Zhao, C., Zhou, J., Zhen, Z., Wang, Y., and Shen, C. (2013). Simvastatin ameliorates liver fibrosis via mediating nitric oxide synthase in rats with non-alcoholic steatohepatitis-related liver fibrosis. *PLoS One* 8 (10), e76538. doi:10.1371/journal.pone.0076538

Ward, N. C., Watts, G. F., and Eckel, R. H. (2019). Statin toxicity. *Circ. Res.* 124 (2), 328–350. doi:10.1161/circresaha.118.312782

Wong, Y. J., Qiu, T. Y., Ng, G. K., Zheng, Q., and Teo, E. K. (2021). Efficacy and safety of statin for hepatocellular carcinoma prevention among chronic liver disease patients: a systematic review and meta-analysis. *J. Clin. Gastroenterol.* 55 (7), 615–623. doi:10.1097/mcg.0000000000001478

Xia, L., Oyang, L., Lin, J., Tan, S., Han, Y., Wu, N., et al. (2021). The cancer metabolic reprogramming and immune response. *Mol. Cancer* 20 (1), 28. doi:10.1186/s12943-021-01316-8

Xie, L., Liu, M., Cai, M., Huang, W., Guo, Y., Liang, L., et al. (2023). Regorafenib enhances anti-tumor efficacy of immune checkpoint inhibitor by regulating IFN-γ/NSDHL/SREBP1/TGF-β1 axis in hepatocellular carcinoma. *Biomed. Pharmacother.* 159, 114254. doi:10.1016/j.biopha.2023.114254

Xu, H., Zhao, J., Li, J., Zhu, Z., Cui, Z., Liu, R., et al. (2022). Cancer associated fibroblast-derived CCL5 promotes hepatocellular carcinoma metastasis through activating HIF1α/ZEB1 axis. *Cell Death Dis.* 13 (5), 478. doi:10.1038/s41419-022-04935-1

Xu, J., Lin, H., Wu, G., Zhu, M., and Li, M. (2021). IL-6/STAT3 is a promising therapeutic target for hepatocellular carcinoma. *Front. Oncol.* 11, 760971. doi:10.3389/fonc.2021.760971

Xu, Y., Zhao, W., Xu, J., Li, J., Hong, Z., Yin, Z., et al. (2016). Activated hepatic stellate cells promote liver cancer by induction of myeloid-derived suppressor cells through cyclooxygenase-2. *Oncotarget* 7 (8), 8866–8878. doi:10.18632/oncotarget.6839

Yang, J., Guo, Z., Song, M., Pan, Q., Zhao, J., Huang, Y., et al. (2023). Lenvatinib improves anti-PD-1 therapeutic efficacy by promoting vascular normalization via the NRP-1-PDGFRβ complex in hepatocellular carcinoma. *Front. Immunol.* 14, 1212577. doi:10.3389/fimmu.2023.1212577

Yang, J. D., Nakamura, I., and Roberts, L. R. (2011). The tumor microenvironment in hepatocellular carcinoma: current status and therapeutic targets. *Semin. Cancer Biol.* 21 (1), 35–43. doi:10.1016/j.semcancer.2010.10.007

Yang, L. B., Liu, Q., Zhang, X. Q., Liu, X. W., Zhou, B. X., Chen, J. N., et al. (2020). DNA of neutrophil extracellular traps promotes cancer metastasis via CCDC25. *Nature* 583 (7814), 133–138. doi:10.1038/s41586-020-2394-6

Yang, W., Bai, Y., Xiong, Y., Zhang, J., Chen, S., Zheng, X., et al. (2016). Potentiating the antitumour response of CD8(+) T cells by modulating cholesterol metabolism. *Nature* 531 (7596), 651–655. doi:10.1038/nature17412

Yau, T., Kang, Y. K., Kim, T. Y., El-Khoueiry, A. B., Santoro, A., Sangro, B., et al. (2020). Efficacy and safety of nivolumab plus ipilimumab in patients with advanced hepatocellular carcinoma previously treated with sorafenib: the CheckMate 040 randomized clinical trial. *JAMA Oncol.* 6 (11), e204564. doi:10.1001/jamaoncol.2020.4564

Yau, T., Park, J. W., Finn, R. S., Cheng, A. L., Mathurin, P., Edeline, J., et al. (2022). Nivolumab versus sorafenib in advanced hepatocellular carcinoma (CheckMate 459): a randomised, multicentre, open-label, phase 3 trial. *Lancet Oncol.* 23 (1), 77–90. doi:10.1016/s1470-2045(21)00604-5

Yokohama, K., Fukunishi, S., Ii, M., Nakamura, K., Ohama, H., Tsuchimoto, Y., et al. (2016). Rosuvastatin as a potential preventive drug for the development of hepatocellular carcinoma associated with non-alcoholic fatty liver disease in mice. *Int. J. Mol. Med.* 38 (5), 1499–1506. doi:10.3892/ijmm.2016.2766

Yu, C., Zhang, X., Wang, M., Xu, G., Zhao, S., Feng, Y., et al. (2023). Afatinib combined with anti-PD1 enhances immunotherapy of hepatocellular carcinoma via ERBB2/STAT3/PD-L1 signaling. *Front. Oncol.* 13, 1198118. doi:10.3389/fonc.2023.1198118

Yu, Z., Guo, J., Liu, Y., Wang, M., Liu, Z., Gao, Y., et al. (2022). Nano delivery of simvastatin targets liver sinusoidal endothelial cells to remodel tumor microenvironment for hepatocellular carcinoma. *J. Nanobiotechnology* 20 (1), 9. doi:10.1186/s12951-021-01205-8

Zeng, R. W., Yong, J. N., Tan, D. J. H., Fu, C. E., Lim, W. H., Xiao, J., et al. (2023). Meta-analysis: chemoprevention of hepatocellular carcinoma with statins, aspirin and metformin. *Aliment. Pharmacol. Ther.* 57 (6), 600–609. doi:10.1111/apt.17371

Zhang, J., Hu, C., Xie, X., Qi, L., Li, C., and Li, S. (2023). Immune checkpoint inhibitors in HBV-caused hepatocellular carcinoma therapy. *Vaccines (Basel)* 11 (3), 614. doi:10.3390/vaccines11030614

Zhang, Y., Chen, H., Chen, S., Li, Z., Chen, J., and Li, W. (2021). The effect of concomitant use of statins, NSAIDs, low-dose aspirin, metformin and beta-blockers on outcomes in patients receiving immune checkpoint inhibitors: a systematic review and meta-analysis. *Oncoimmunology* 10 (1), 1957605. doi:10.1080/2162402x.2021.1957605

Zhang, Z., Ma, L., Goswami, S., Ma, J., Zheng, B., Duan, M., et al. (2019). Landscape of infiltrating B cells and their clinical significance in human hepatocellular carcinoma. *Oncoimmunology* 8 (4), e1571388. doi:10.1080/2162402x.2019.1571388

Zhao, L., Chang, N., Shi, L., Li, F., Meng, F., Xie, X., et al. (2022). Lenvatinib plus sintilimab versus lenvatinib monotherapy as first-line treatment for advanced HBV-related hepatocellular carcinoma: a retrospective, real-world study. *Heliyon* 8 (6), e09538. doi:10.1016/j.heliyon.2022.e09538

Zhao, W., Zhang, L., Xu, Y., Zhang, Z., Ren, G., Tang, K., et al. (2014). Hepatic stellate cells promote tumor progression by enhancement of immunosuppressive cells in an orthotopic liver tumor mouse model. *Lab. Invest.* 94 (2), 182–191. doi:10.1038/labinvest.2013.139

Zheng, C. H., Zheng, L. T., Yoo, J. K., Guo, H. H., Zhang, Y. Y., Guo, X. Y., et al. (2017). Landscape of infiltrating T cells in liver cancer revealed by single-cell sequencing. *Cell* 169 (7), 1342–1356. doi:10.1016/j.cell.2017.05.035

Zhong, G. C., Liu, Y., Ye, Y. Y., Hao, F. B., Wang, K., and Gong, J. P. (2016). Meta-analysis of studies using statins as a reducer for primary liver cancer risk. *Sci. Rep.* 6, 26256. doi:10.1038/srep26256

Zhou, S. L., Zhou, Z. J., Hu, Z. Q., Huang, X. W., Wang, Z., Chen, E. B., et al. (2016). Tumor-associated neutrophils recruit macrophages and T-regulatory cells to promote progression of hepatocellular carcinoma and resistance to sorafenib. *Gastroenterology* 150 (7), 1646–1658. doi:10.1053/j.gastro.2016.02.040

Zhu, A. X., Finn, R. S., Edeline, J., Cattan, S., Ogasawara, S., Palmer, D., et al. (2018). Pembrolizumab in patients with advanced hepatocellular carcinoma previously treated with sorafenib (KEYNOTE-224): a non-randomised, open-label phase 2 trial. *Lancet Oncol.* 19 (7), 940–952. doi:10.1016/s1470-2045(18)30351-6

Zhu, P. F., Wang, M. X., Chen, Z. L., and Yang, L. (2021). Targeting the tumor microenvironment: a literature review of the novel anti-tumor mechanism of statins. *Front. Oncol.* 11, 761107. doi:10.3389/fonc.2021.761107

Zou, W., and Green, D. R. (2023). Beggars banquet: metabolism in the tumor immune microenvironment and cancer therapy. *Cell Metab.* 35 (7), 1101–1113. doi:10.1016/j.cmet.2023.06.003

frontiers | Frontiers in Pharmacology

TYPE Review
PUBLISHED 26 March 2024
DOI 10.3389/fphar.2023.1273993

OPEN ACCESS

EDITED BY
Daiqing Liao,
University of Florida, United States

REVIEWED BY
Lei Huang,
University of Massachusetts Medical School, United States
Salvador F. Aliño,
University of Valencia, Spain

*CORRESPONDENCE
Syed A. Husain,
shusain@jmi.ac.in
Anas Shamsi,
anas.shamsi18@gmail.com

†PRESENT ADDRESS
Asifa Khan,
Department of Molecular, Cell and Cancer Biology, University of Massachusetts Chan Medical School, Worcester, MA, United States

‡These authors have contributed equally to this work

RECEIVED 07 August 2023
ACCEPTED 09 November 2023
PUBLISHED 26 March 2024

CITATION
Khan A, Khan A, Khan MA, Malik Z, Massey S, Parveen R, Mustafa S, Shamsi A and Husain SA (2024), Phytocompounds targeting epigenetic modulations: an assessment in cancer.
Front. Pharmacol. 14:1273993.
doi: 10.3389/fphar.2023.1273993

Phytocompounds targeting epigenetic modulations: an assessment in cancer

Aqsa Khan[1‡], Asifa Khan[1†‡], Mohammad Aasif Khan[1,2], Zoya Malik[1], Sheersh Massey[1], Rabea Parveen[1], Saad Mustafa[1], Anas Shamsi[3]* and Syed A. Husain[1]*

[1]Department of Bioscience, Faculty of Natural Sciences, Jamia Millia Islamia (A Central University), New Delhi, India, [2]Department of Radiation Oncology, The University of Texas Health Science Centre at San Antonio, San Antonio, TX, United States, [3]Center for Medical and Bio-Allied Health Sciences Research, Ajman University, Ajman, United Arab Emirates

For centuries, plants have been serving as sources of potential therapeutic agents. In recent years, there has been a growing interest in investigating the effects of plant-derived compounds on epigenetic processes, a novel and captivating Frontier in the field of epigenetics research. Epigenetic changes encompass modifications to DNA, histones, and microRNAs that can influence gene expression. Aberrant epigenetic changes can perturb key cellular processes, including cell cycle control, intercellular communication, DNA repair, inflammation, stress response, and apoptosis. Such disruptions can contribute to cancer development by altering the expression of genes involved in tumorigenesis. However, these modifications are reversible, offering a unique avenue for therapeutic intervention. Plant secondary compounds, including terpenes, phenolics, terpenoids, and sulfur-containing compounds are widely found in grains, vegetables, spices, fruits, and medicinal plants. Numerous plant-derived compounds have demonstrated the potential to target these abnormal epigenetic modifications, including apigenin (histone acetylation), berberine (DNA methylation), curcumin (histone acetylation and epi-miRs), genistein (histone acetylation and DNA methylation), lycopene (epi-miRs), quercetin (DNA methylation and epi-miRs), *etc.* This comprehensive review highlights these abnormal epigenetic alterations and discusses the promising efficacy of plant-derived compounds in mitigating these deleterious epigenetic signatures in human cancer. Furthermore, it addresses ongoing clinical investigations to evaluate the therapeutic potential of these phytocompounds in cancer treatment, along with their limitations and challenges.

KEYWORDS

cancer, cancer epigenetics, DNMTs, HDACs, miRNAs, phytocompounds, bioactive compounds, cancer prevention

1 Introduction

Despite modern advances and therapeutics, cancer remains one of the most dreaded diseases globally. According to the GLOBOCAN cancer statistics 2020, female breast cancer incidence superseded lung cancer globally. Around 19.3 million new cancer cases have been reported worldwide, with 10 million cancer deaths. With a record of 2.3 million new diagnoses, female breast cancer has surpassed lung cancer as the most frequently diagnosed cancer, followed by colorectal (10.0%), prostate (7.3%), and abdominal (5.6%) cancers

respectively. In 2040, the global cancer incidence is predicted to increase to 28.4 million cases, increasing 47% from 2020 (Sung et al., 2021). This creates an alarming situation towards the increasing number of cancer cases and calls for better and safer treatment options.

Cancer is a multifaceted disease with genetic mutations and abnormal epigenetic modifications (Baylin et al., 2001). According to Conrad Hal Waddington, epigenetics refers to heritable and reversible modifications in gene expression or changes in a chromosome without any alterations in DNA sequence (Henikoff and Matzke, 1997). The epigenetic regulation includes DNA methylation, posttranslational histone protein modifications such as acetylation, methylation, and phosphorylation, and microRNAs (noncoding RNA) that can inhibit translation or degrade mRNAs by modulating gene expression (Dehan et al., 2009). Epigenetic control plays a crucial role during early embryonic development, such as X-inactivation in females, genomic imprinting, development, and differentiation like the formation of long-term memory and behavior (Payer and Lee, 2008; Lubin et al., 2011). In addition to this, research studies suggest that epigenetic DNA modifications on uniparental disomy also serves as an underlying mechanism for developmental disorders, neurological diseases and tumorigenesis (Zoghbi and Beaudet, 2016; Tuna et al., 2009). A study on colorectal cancer showed several tumor suppressor genes (*VCAN*, *FLT4*, *SFRP1* and *GAS7*) in the uniparental disomy and polysomy regions displaying elevated levels of DNA methylation (Torabi et al., 2015).

Deregulation of epigenetic modifications has critical implications on human health, such as cancer, metabolic syndrome, and neurodegenerative disorders like Alzheimer's disease, Huntington's disease, and amyotrophic lateral sclerosis (Berson et al., 2018; Smith and Ryckman, 2015). Recent studies highlighted that maternal behavioral patterns, diet choice, and exposure to other intrinsic or extrinsic factors have dramatically altered gene expression patterns and are implicated with epigenetic mechanisms (Chung and Herceg, 2020; Safi-Stibler and Gabory, 2020).

Since epigenetic modifications are reversible, a significant number of studies are now focused on the identification and development of pharmaceuticals that target these modulations (Singh et al., 2016; Liu Z. et al., 2019). In recent years, Food and Drug Administration, United States, approved several small synthetic molecule inhibitors that target distinct epigenetic modulations to treat several solid tumors and hematological malignancies. These clinically approved conventional drugs include Azacytidine and Decitabine (DNA methyltransferases (DNMT) inhibitors). Four histone deacetylases inhibitors (HDACi) are approved for the treatment of lymphomas, including vorinostat (SAHA), romidepsin (FK-228), belinostat (PXD-101), and tucidinostat (chidamide) (previous conditional approvals for panobinostat [LBH-589] for multiple myeloma [in combination with bortezomib] and romidepsin for peripheral T-cell lymphoma [PTCL] were recently withdrawn by the FDA) (Liu Z. et al., 2019; Xiao et al., 2023). On the contrary, several studies have found phytocompounds as potential regulators that can reverse these aberrant epigenetic modifications that induce tumor progression and eventually lead to cancer (Aggarwal et al., 2015; Montgomery and Srinivasan, 2019).

Drug development using naturally derived bioactive compounds has drawn a lot of interest in recent years as they are safe and economical. In contrast, present-day chemotherapeutic drugs are not only expensive but also toxic. One significant side effect of conventional medications is their ability to target normal cells in the body undergoing rapid proliferation, such as bone marrow cells, along with proliferating tumor cells. However, phytocompounds are nontoxic to normal cells and hence better tolerated (Singh et al., 2016). Phytocompounds are bioactive compounds, obtained from a wide variety of herbs, spices, vegetables, and fruits (Table 1), that possess anti-inflammatory, antioxidant, antimicrobial, anticancer, and anti-diabetic properties (Verma, 2016; Altaf et al., 2018; Gonelimali et al., 2018; Salehi et al., 2019). Furthermore, phytocompounds can target multiple cell cycle proteins, transcription factors, cell adhesion molecules, protein kinases, and anti-apoptotic factors (Aggarwal and Shishodia, 2006; Kundu and Surh, 2009; Bailon-Moscoso et al., 2017; Malik et al., 2021). Besides this, plant-based compounds possess the ability to target deregulated metabolic proteins and pathways in cancer, such as glycolysis, pentose phosphate pathway, lipid metabolism, amino acid metabolism, *etc.* (Pani et al., 2020; Khan et al., 2021a; Khan et al., 2021b). These multipronged functions of phytocompounds, targeted at various cellular pathways implicated epigenetically in cancer, can be a promising solution in the treatment of this deadliest disease.

This review highlights the prospective use of distinct phytocompounds to counteract epigenetic abnormalities that promote tumor development and progression in humans as well as their potential in anticancer therapeutics as summarized in Figure 1. Therefore, a comprehensive explanation of the most studied dietary compounds that critically modulate the epigenetic landscape in human cancer along with the latest developments, is provided extensively. In addition, list of all the phytocompounds that are discussed in this review and that are known to control epigenetic alterations are listed below in Table 1, along with their classification and sources.

2 Method

Research articles, reviews, and abstracts were pulled for a literature survey from a variety of databases, including PubMed, Google Scholar, Springer, Wiley Online Library, ScienceDirect, *etc.*, From the year 1998 and to 2022. Information from research articles, review articles, abstracts were used for this review. The literature search was conducted against the terminology "Bioactive compounds in cancer epigenetics" while other terminologies such as phytocompounds targeting DNA methylation, histone modification and epi-miRNAs were also included in this search as illustrated in Figure 2. Data was processed to find out general information about phytocompounds, with a strong focus on how they affect epigenetics modifications. Inclusion criteria was based on the topics that include phytocompounds targeting epigenetic modifications (DNA methylation, Histone modifications and miRNAs) in cancer. While the exclusion criteria, was based on studies demonstrating information duplication, such as reviews, material available in languages other than English, information unrelated to the subjects included in this analysis, insufficient information, and data older than 1998.

TABLE 1 List of phytocompounds, their source and types.

Dietary phytocompound	Source	Type	Structure
Allicin	Allium sativum (Garlic)	Organosulfur compound	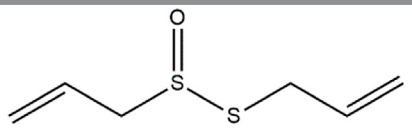
Allyl isothiocyanate	Garlic, broccoli, wasabi	Organosulfur compound	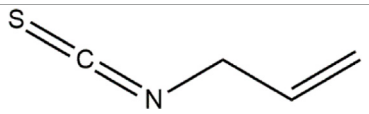
Apigenin	Fruits, vegetables, herbs (Parsley and chamomile)	Polyphenol (Flavonoid)	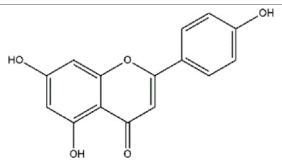
Berberine	*Berberis vulgaris* (barberry), *Berberis aristata* (tree turmeric)	Alkaloid	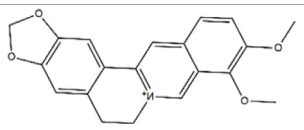
Celastrol	*Tripterygium wilfordii*, *Tripterygium regelii*	Triterpenoid	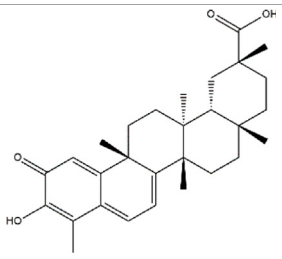
Cucurbitacin B	Cucumis sativus (Cucumber)	Triterpenoid	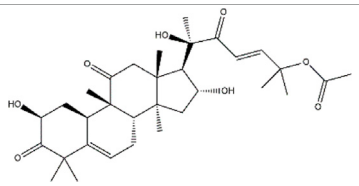
Curcumin	*Curcumin longa* (Turmeric)	Polyphenol (Flavonoid)	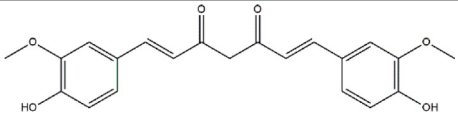
Daidzein	Soya beans and legumes	Polyphenol (Isoflavone)	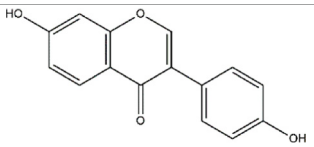
Diallyl disulfide	*Allium* genus	Organosulfur compound	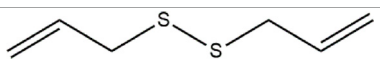

(Continued on following page)

TABLE 1 (*Continued*) List of phytocompounds, their source and types.

Dietary phytocompound	Source	Type	Structure
Demethylzeylasteral	*Tripterygium wilfordii* (three wingnut root)	Triterpenoid	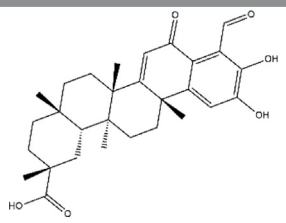
3,3′- Diindolylmethane	Cruciferous vegetables	Glucosinolates	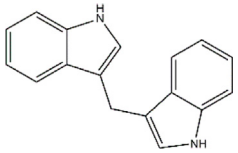
Ellagitannin	*Punica granatum* (Pomegranate) berries	Polyphenol	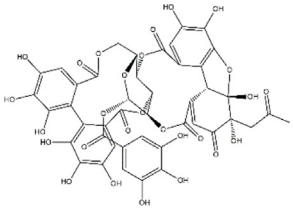
Epigallocatechin 3-gallate	*Camellia sinensis* (Green Tea)	Polyphenol (Catechol)	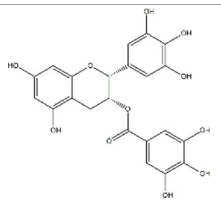
Garcinol	*Garcinia indica* (kokum)	Benzophenone	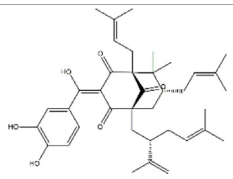
Genistein	*Glycine* max (soya beans)	Polyphenol (Isoflavone)	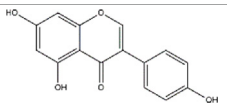
Ginsenoside Rh2	Panax ginseng (Korean ginseng)	Ginsenoside	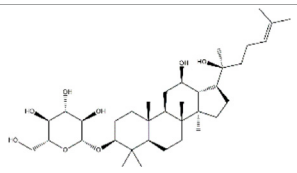
Glabridin	*Glycyrrhiza glabra* (Licorice)	Polyphenol (Isoflavone)	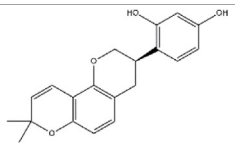

(Continued on following page)

TABLE 1 (*Continued*) List of phytocompounds, their source and types.

Dietary phytocompound	Source	Type	Structure
Gossypol	*Gossypium hirsutum* (cotton plant)	Phenol	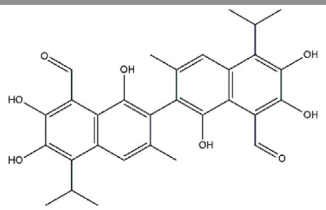
Icariin	*Herba epimedii* (Yin-yang-huo)	Polyphenol (Flavonoid)	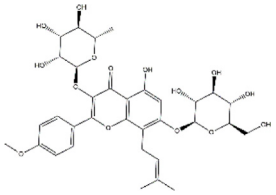
Indole-3-carbinol	Cruciferous vegetables	Glucosinolates	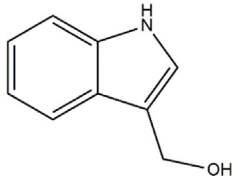
Kaempferol	Fruits, vegetables and herbs	Polyphenol (Flavonoid)	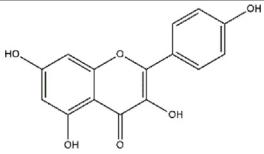
Luteolin	Parsley, broccoli, carrots, peppers, cabbage	Polyphenol (Flavonoid)	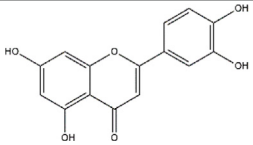
Lycopene	Tomato, papaya, watermelon	Carotenoid	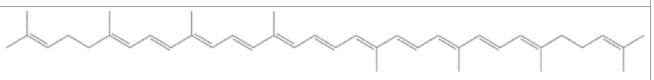
Methyl jasmonate	*Jasminum grandiflorum* (Spanish Jasmine)	Methyl ester	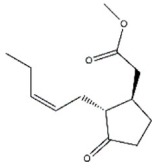
Parthenolide	*Tanacetum parthenium* (Feverfew)	Sesquiterpene lactone	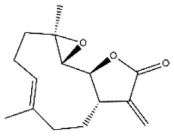
Phenethyl isothiocyanate	Cruciferous vegetables	Isothiocyanate	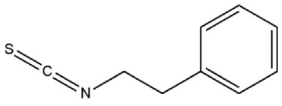

(Continued on following page)

TABLE 1 (*Continued*) List of phytocompounds, their source and types.

Dietary phytocompound	Source	Type	Structure
Piceatannol	Red wine, grapes, passion fruit	Stilbene	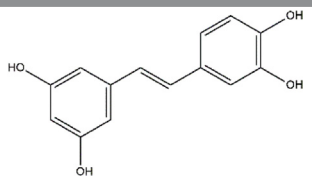
Quercetin	Fruits, vegetables, tea, red wine, nuts, propolis	Polyphenol (Flavonoid)	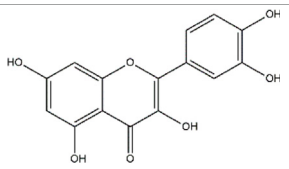
Resveratrol	Grapes, berries	Polyphenol	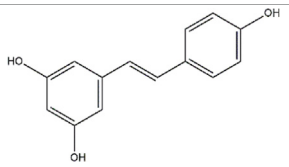
Rosmarinic acid	*Rosmarinus officinalis* (rosemary)	Polyphenol	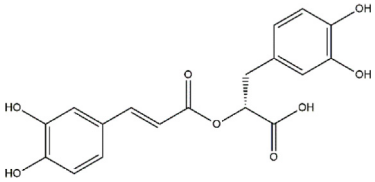
Shikonin	*Lithospermum erythrorhizon* (purple gromwell)	Naphthoquinone	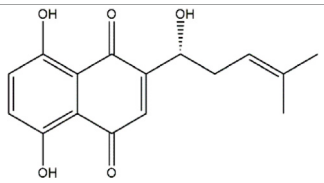
Sulforaphane	Cruciferous vegetables	Isothiocyanate	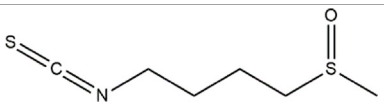
Thymoquinone	*Monarda fistulosa* (wild bergamot), *Nigella sativa* (black cumin)	Terpenoid	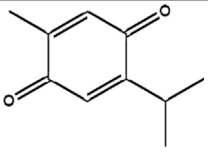
Triptolide	*Tripterygium wilfordii* (Three wingnut Root)	Terpenoid	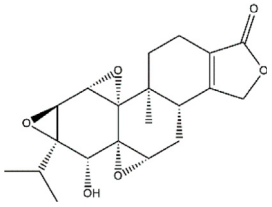

(Continued on following page)

TABLE 1 (*Continued*) **List of phytocompounds, their source and types.**

Dietary phytocompound	Source	Type	Structure
Ursolic acid	*Oldenlandia diffusa* (Snake-needle grass), *Radix actinidiae* (kiwi root)	Terpenoid	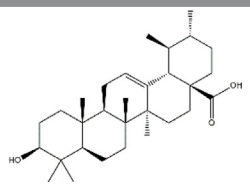
Withaferin A	*Withania somnifera* (ashwagandha)	Lactone	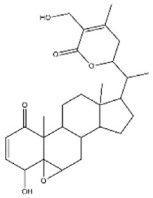

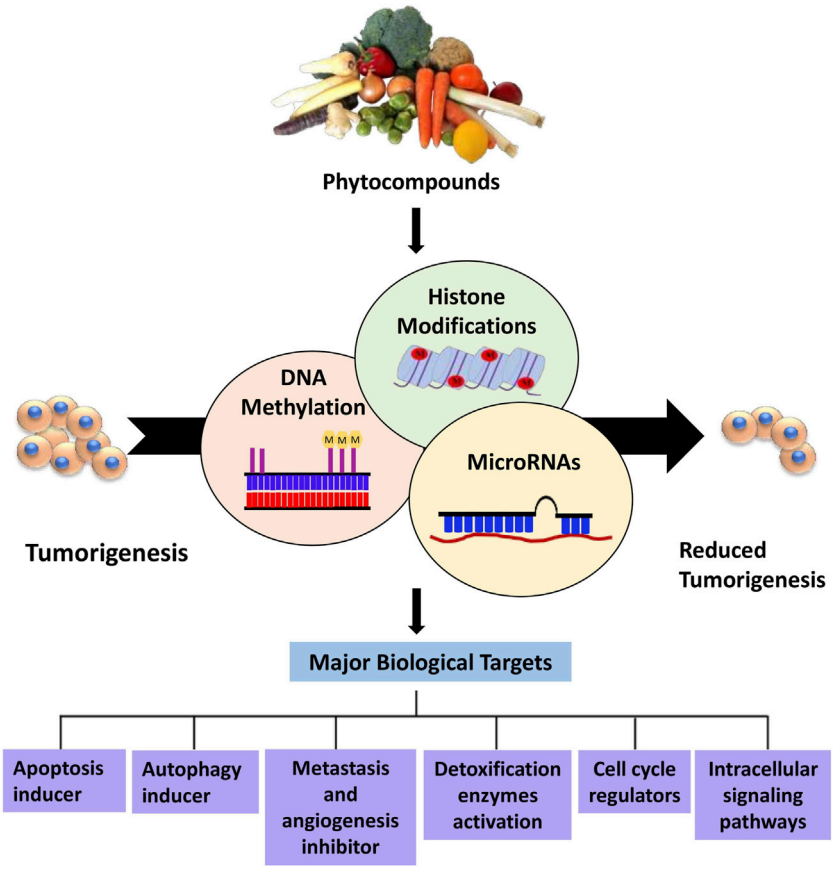

FIGURE 1
Overview of phytocompounds regulating major epigenetic modifications that involve regulation of key biological targets to reduce tumorigenesis.

2.1 DNA methylation

DNA methylation is responsible for controlling gene expression and interacting with the nucleosomes that control DNA packaging, and it can influence entire DNA domains. It is a chemical, biological modification where cytosine residues are methylated at a 5′position. This modification mainly occurs at cytosine residues present in GC dinucleotide-rich regions clustered together to form the CpG islands spanned the 5′end region of several genes (Issa and Kantarjian, 2009).

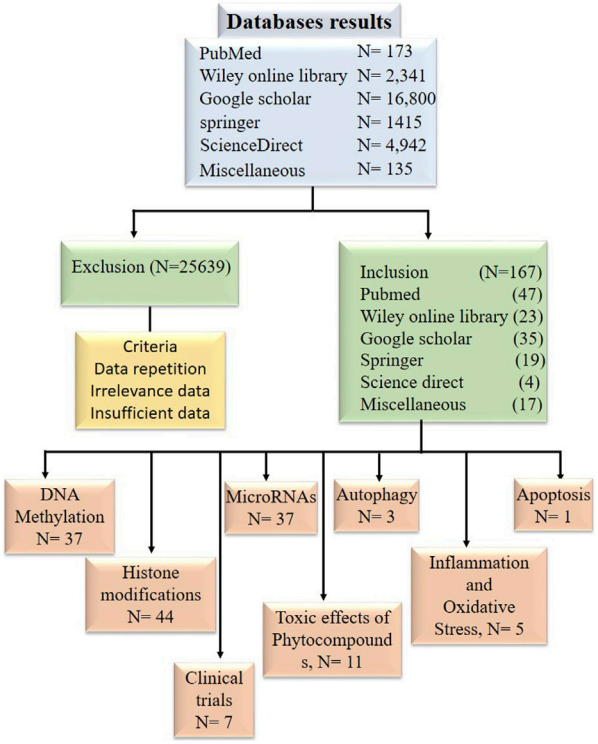

FIGURE 2
Diagram in block form illustrating the inclusion and exclusion of research publications in data tabulation.

2.2 DNA methyltransferases

The human genome contains approximately 28 million CpG sites. Under normal circumstances, most CpG islands, especially within the promoter region, are unmethylated except in the case of X-inactivation, genome imprinting, and repression of transposons. DNA methylation occurs during the early embryonic stages by a set of distinct enzymes called DNA methyltransferases (DNMTs) (Bird, 2002). DNA methyltransferases catalyze the formation of 5-methyl cytosine that involves the transfer of a methyl group from S-adenosyl-L- methionine (SAM) to the 5′position of the cytosine residue in CG dinucleotide (Santi et al., 1983). DNMT1, DNMT3A, and DNMT3B are the three major DNMTs involved in DNA methylation in mammals. Maintenance of methylation patterns during replication is one of the critical functions of DNMT1. During replication, DNMT1 adds a methyl group to hemi methylated CpG dinucleotides in the daughter strand as it shows 5–30 times greater affinity for hemi methylated substrates. In contrast, DNMT3A and DNMT3B are *de novo* methyltransferases exclusively involved in the methylation of previously unmethylated DNA sequences (Okano et al., 1999; Bestor, 2000). To ensure methylation, DNMTs must have access to the DNA that can be gained via perturbation of chromatin structure by specific chromatin remodeling proteins (As shown in Figure 3) (Baylin et al., 2001).

In cancer, hypermethylation of CpG islands in the promoter sequence of some genes results in gene silencing by suppressing the transcriptional activity of tumor suppressor genes (Dehan et al., 2009). For instance, promoter hypermethylation of CpG sites of tumor suppressor genes like *RARβ* and *RASSF1A* can induce breast cancer development (Van Hoesel et al., 2013). Certain studies of malignant and tumor cells have shown hypomethylation of DNA sequences at CpG sites that can cause conformational and functional alterations in chromosomes (Gama-Sosa et al., 1983). In cancer there are several natural compounds known to influence the DNA methylation as listed in Table 2 in most of the cases by a single publication.

2.3 Phytocompounds targeting DNA methylation

An increasing list of different phytocompounds targeting DNA methylation at distinct genes in various cancer cell lines has been discovered in the last two decades. This section summarizes the phytocompounds that have the potential to act as DNA methylation inhibitors and activators altering the tumor suppressor gene expression.

Apigenin, a polyphenol, has been shown to reduce the methylation of CpG sites in the *Nrf2* promoter region, which contributed to increased mRNA levels of downstream genes. *Nrf2* codes a transcription factor that regulates antioxidant enzymes. Furthermore, apigenin also decreased DNMT expression in mouse skin cancer cell line (Paredes-Gonzalez et al., 2014).

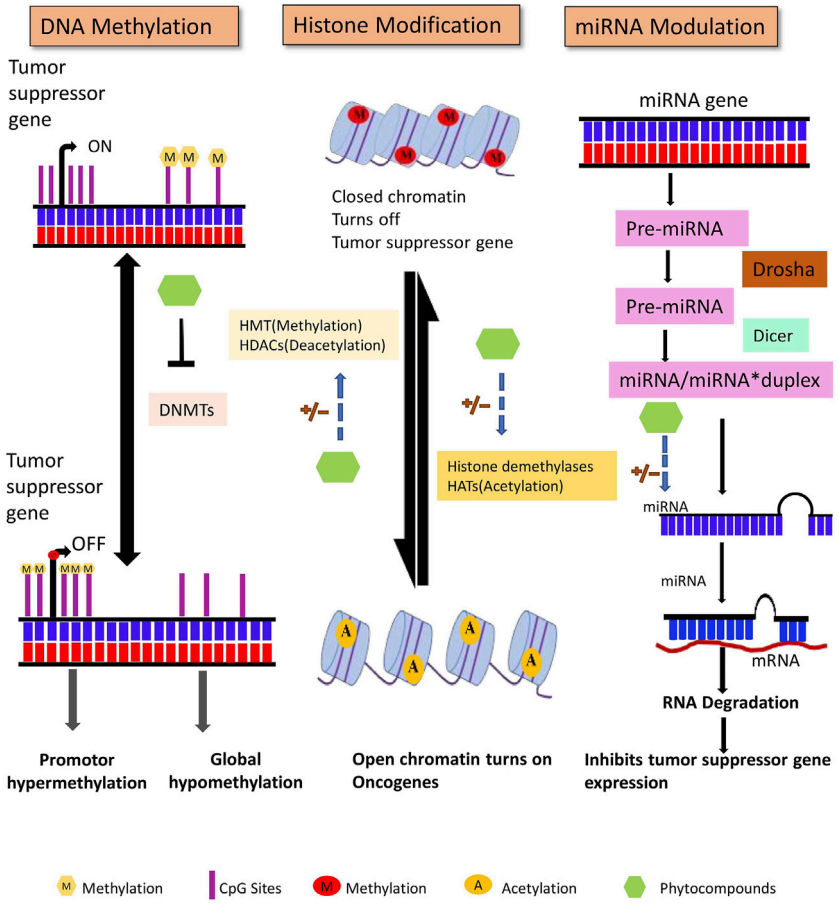

FIGURE 3
DNA methylation, posttranslational histone modifications, and microRNAs are all major epigenetic processes that regulate gene expression. These pathways are found to be dysregulated in cancer. Phytocompounds have shown to modulate abnormal epigenetic modifications.

Neurog-1 gene plays a critical role in neuronal differentiation. Curcumin-induced treatment reported demethylation of 14 CpG sites of *Neurog-1* promoter and downstream gene reactivation in prostate cancer cell line (Shu et al., 2011). *BRCA1*, a DNA repair gene, critically regulates cell cycle checkpoints and transcription. Triple-negative breast cancer (TNBC) cell lines were treated with curcumin, which caused the upregulation of the TET1 gene that promoted the *BRCA1* promoter's hypomethylation. Furthermore, it induced upregulation of DNMT3 that resulted in suppressed expression of proto-oncogene *SNCG* (Al-Yousef et al., 2020). Curcumin treatment reactivated *RARβ* by causing promoter hypomethylation in lung cancer cells. The treatment further resulted in increased RARβ protein and mRNA expression. Curcumin treatment also induced downregulation of DNMT3b, resulting in decreased expression of DNMT3b mRNA levels (Jiang et al., 2015).

Epigallocatechin 3-gallate (EGCG), a polyphenol obtained from green tea, is one of the most studied chemo preventive agents. Besides EGCG, epigallocatechin and epicatechin are also among the major constituents of green tea. Several studies have documented numerous medical benefits of EGCG; regulation of cancer cell growth is one of them (Shankar et al., 2007). According to an *in vitro* study, catechol inhibits DNMT activity by directly inhibiting DNMTs or by causing o-methylation of SAM by methyltransferases that result in increased SAM levels. Treatment of esophageal cancer cell lines with EGCG exhibited unmethylation specific bands for tumor suppressor *p16INK4a*, retinoic acid receptor *β* (*RARβ*), *MGMT*, and DNA repair *hMLH1* genes. Furthermore, it demonstrated that EGCG reactivated the *RARβ* gene in prostate cancer and esophageal cancer cell lines (Fang et al., 2007). In another study, breast cancer cell lines reported downregulation of DNMT expression and restoration of the tumor suppressor gene *SCUBE 2* expression, when treated with EGCG, that resulted in increased E-cadherin expression and suppression of cell migration and invasion (Sheng et al., 2019).

Genistein-induced treatment of HeLa cells reduced promoter 5′CpG methylation levels of various tumor suppressor genes involved in PI3K and MAPK signaling. The restoration of transcription levels of earlier hypermethylated genes (mentioned in Table 2) can be correlated to a decrease in methylation levels (Sundaram et al., 2019). In a triple-negative breast cancer cell, silencing of *BRCA1* is often a result of overexpression of the aryl hydrocarbon receptor. *In vivo* study of the mammary gland of adult mice demonstrated that lifelong treatment with genistein reduced *BRCA1* CpG methylation in the offspring's mammary tissue (Donovan et al., 2019). Treatment with genistein and daidzein

TABLE 2 List of phytocompounds modulating DNA methylation.

Dietary phytocompound	Mechanism	Genes targeted	Cancer type (cancer cell line)	References
Apigenin	DNMT inhibitor, Promoter demethylation	*Nrf2*	Skin (JB6 P + -mouse cell line)	Paredes-Gonzalez et al. (2014)
Berberine	DNMT inhibitor	*p53*	Hepatocellular carcinoma (Hep3B)	Kim et al. (2020)
Cucurbitacin B	Promoter hypermethylation	*c-Myc, cyclin D1, survivin*	Breast (MDA-MB-231, MCF-7)	Dittharot et al. (2019)
Curcumin	DNMT inhibitor, promoter demethylation	*BRCA1, SNCG, TET1*	Breast (HCC-38, UACC-3199, T47D)	Al-Yousef et al. (2020)
		Neurog-1	Prostate (LNCaP)	Shu et al. (2011)
	Promoter hypomethylation	*RARβ*	Lung (A549, H460)	Jiang et al. (2015)
Daidzein	DNMT inhibitor, Promoter demethylation	*BRCA1, EPHB2 and GSTP1*	Prostate (DU-145, PC-3)	Adjakly et al. (2011)
Epigallocatechin 3-gallate (EGCG)	DNMT inhibitor	*p16INK4a, RARβ, MGMT, hMLH1*	Esophageal (KYSE 150, KYSE 510), Prostate (PC-3), Colon (HT-29)	Fang et al. (2007)
		SCUBE 2	Breast (MCF-7, MDA-MB-231)	Sheng et al. (2019)
Genistein	DNMT inhibitor, Promoter demethylation	*EPHB2, GSTP1, BRCA1*	Prostate (DU-145, PC-3)	Adjakly et al. (2011)
		TP53, PTEN, CDH1, DAPK1, FHIT, RUNX3, SOCS1	Cervix (HeLa)	Sundaram et al. (2019)
Luteolin	DNMT inhibitor, Promoter demethylation	*P16INK4a*	Colorectal (BE)	Krifa et al. (2014)
		Nrf2	Colorectal (HCT116)	Zuo et al. (2018)
		Nrf2, p53	Colon (HT-29, SNU-407)	Kang et al. (2019)
Lycopene	DNMT inhibitor, Promoter demethylation	*GSTP1*	Prostate (PC3)	Fu et al. (2014)
Phenethyl isothiocyanate (PEITC)	DNMT inhibitor, Promoter demethylation	*RASSF1A*	Prostate (LNCaP)	Boyanapalli et al. (2016)
		GSTP1		Wang et al. (2007)
Quercetin	DNMT inhibitor, Promoter demethylation	*P16INK4a, Er-beta, RASSF1A*	Bladder (EJ, J28, T24)	Ma et al. (2006)
		DAPK1, BCL2L11, BAX, BNIP3, BNIP3L, APAF1	Leukemia (HL60, U937)	Alvarez et al. (2018)
		APC, CDH1, CDH13, DAPK1, FHIT, GSTP1, MGMT, MLH1, PTEN, RARB, RASSF1, SOC51, TIMP3, VHL	Cervix (HeLa)	Kedhari Sundaram et al. (2019)
Resveratrol	DNMT inhibitor Promoter demethylation	*CRABP2*	Thyroid (THJ-11T, UW228-2)	Liu et al. (2019b)
Rosmarinic acid	DNMT inhibitor	-	Breast (MCF7)	Paluszczak et al. (2010)
Shikonin	DNMT inhibitor	-	Breast (MCF-7), Cervix (HeLa)	Jang et al. (2015)
Sulforaphane	DNMT inhibitor, Promoter demethylation	-	Prostate (PC-3, LNCaP)	Wong et al. (2014)
		Nrf2	Colon (Caco-2)	Zhou et al. (2019a)
Triptolide	Promoter demethylation	*WIF-1*	Lung (A549, H460)	Nardi et al. (2018)
Withaferin A	CpG hypermethylation	*ADAM8, PLAU, TNFSF12, ME3, GSTM1*	Breast (MCF-7, MDA-MB-231)	vel Szic et al. (2017)
	CpG hypomethylation	*GLRX2, GFPT2, STX11 and VGF*		

resulted in re-expression of *BRCA1, EPHB2,* and Glutathione S-transferase pi 1 (*GSTP1*) in prostate cancer cells, suggesting a preventive effect of soy phytoestrogens against prostate cancer (Adjakly et al., 2011).

GSTP1 encodes for a detoxifying enzyme that protects cells from genome-damaging stresses caused by reactive chemical species. Lycopene induced promoter demethylation of *GSTP1* in prostate cancer cells, increasing the mRNA and protein levels. Further

treatment with lycopene also decreased the protein levels of DNMT3a. Fu et al. (2014).

The hypermethylated *RASSF1A* promoter in prostate cancer cell line, when treated with phenethyl isothiocyanate (PEITC), reported a decrease in methylation of CpG sites by an average of 90% compared to untreated cells with 98% of methylation at 16 CpG sites. Promoter demethylation of the tumor suppressor gene *RASSF1A* correlated with decreased mRNA expression of DNMT1 and DNMT3A when treated with PEITC (Boyanapalli et al., 2016). PEITC induced CpG demethylation in *GSTP1* promoter of LNCAP cells in a concentration-dependent manner and was almost similar or higher than the commonly used DNMT inhibitor 5-Aza-2′-deoxycytidine. On further analysis by pyrosequencing tool, it was revealed that PEITC treatment significantly reduced CpG methylation at positions 1 and 3 from 89.5% to 73.2% and 61.8%–6.5%, respectively, that was higher than the demethylating activity of 5′-Aza (Wang et al., 2007).

Quercetin inhibited the DNMT activity and resulted in the restoration of various tumor suppressor genes that were earlier hypermethylated at 5′CpG promoter sites in cervical cancer cells (mentioned in Table 2). Furthermore, *in silico* studies revealed that quercetin competitively inhibit DNMTs by binding to its catalytic active sites (Kedhari Sundaram et al., 2019). Quercetin treatment decreases the methylation levels of *P16INK4a, Er-beta,* and *RASSF1A* genes in bladder cancer cell lines. Furthermore, quercetin treatment inhibited the expression of mutant p53 and survivin proteins. P53 maintains cell cycle regulation, DNA repair, and apoptosis, and any alteration in p53 happens to decrease genomic stability and DNA repair. While Survivin acts as antagonists by inhibiting antiapoptotic pathways and promoting mitotic progression (Ma et al., 2006). *In vitro* and *in vivo* studies revealed that quercetin induced demethylation of highly methylated promoter sites of apoptosis-related genes *BCL2L11* and *DAPKlin,* leukemia cell lines (Alvarez et al., 2018).

A study on rodent's mammary tumor treated with resveratrol indicated a decrease in DNMT 3b expression. The study further reported that 26% of rats developed tumors when treated with a low dose of resveratrol, while only 18% developed tumors with high dose compared to 33% in the control group (Qin et al., 2014). Resveratrol upregulated the expression of cellular retinoic acid binding protein 2 (*CRABP2*) that mediates retinoic acid anticancer pathways in thyroid cancer cell lines by partial demethylation of CpG promoter sites. In addition, resveratrol significantly decreased DNMT1 and DNMT3A expression (Liu X. et al., 2019).

Sulforaphane treatment downregulated DNMT expression and can mediate promoter demethylation in prostate cancer cells (Wong et al., 2014). In colon cancer cells, sulforaphane inhibited the expression of DNMT1 and increased Nrf2 protein expression by decreasing the methylation of Nrf2 promoter region (Zhou J. W. et al., 2019).

In TNBC cells, withaferin A induced hypermethylation of tumor-promoting genes *ADAM8, PLAU, TNFSF12, GSTM1, ME3,* and hypomethylation of *GLRX2, GFPT2, STX11,* and *VGF* (vel Szic et al., 2017).

The reversible epigenetic process of DNA methylation regulates chromosomal integrity, tissue differentiation, and gene expression throughout embryogenesis. However, any aberrant epigenetic modifications during these processes can lead to tumorigenesis. As extensively discussed above, numerous studies provide evidence that these abnormal modifications can be undone by a plethora of phytocompound treatment. Phytocompounds targeting DNA methylation are listed below in Table 2.

3 Histone modifications

The eukaryotic DNA is condensed in the form of chromatin. A nucleosome, the basic unit of chromatin, comprises of three parts, i.e., a core nucleosome, linker DNA, and histone H1. Each nucleosome core contains 2 copies of each histone H2A, H2B, H3, and H4, and approximately ~147bp of DNA wrapped around it, in the form of a histone octamer. Core histone proteins comprise of three structural motifs, i.e., the histone fold regions, their diverse extensions, and histone tails. Histone tails are sites of posttranslational modifications and are extremely basic, which consists mainly of lysine and arginine amino acids (Luger and Richmond, 1998; Kornberg and Lorch, 1999). Histone modifications influence the regulation of chromatin dynamics in processes such as gene regulation, DNA repair, cell proliferation, and apoptosis. In cancer, deregulation of genes involved in these pathways may lead to unwarranted activation of oncogenes or inactivation of tumor suppressor genes (Audia and Campbell, 2016).

3.1 Histone acetylation

Histone acetyltransferases (HATs) catalyze the transfer of an acetyl group to the ε-amino group of the lysine side chains utilizing the cofactor acetyl CoA, thereby weakening the DNA and histone interactions. HATs have been classified into two- Type-A and Type-B. Further, HATs can be divided into three major categories- GNAT, MYST, and p300/CBP (Bannister and Kouzarides, 2011). Acetylation at K5 and K12 of newly synthesized H4 histones is catalyzed by type-B HAT (HAT1), along with specific sites at H3 histone (Kouzarides, 2007). Predominant transcriptional repressors, histone deacetylases (HDACs), catalyze the reverse lysine acetylation, thus restoring the positive charge of lysine and stabilizing the chromatin structure. The HDACs have been categorized into four major classes: classes I, II, III, and IV. HDACs 1, 2, 3 and belongs to class I HDACs, while class II comprises of HDACs 4, 5, 6, 7, 9, and 10; and only HDAC11 belongs to class IV HDACs. Sirtuins, another name for class III HDACs, are structurally distinct from the other classes and require a cofactor (NAD^+) for its activity (Mottet and Castronovo, 2008).

3.2 Histone methylation

Lysine and arginine residues are mostly favored for histone methylation. Lysine methyltransferases catalyze the transfer of a methyl group from SAM to a ε-amino group of lysine, whereas arginine methyltransferases catalyze the transfer of a methyl group from SAM to arginine's ω-amino group. Histone demethylases have the opposite effect to histone methylases, both can activate or repress the transcriptional activity (Bannister et al., 2002). For example,

methylation of histone H3 at K9 and K36 may negatively affect the promoter region while a positive one in the coding region (Kouzarides, 2007). Additionally, decreased levels of acetylation of histones H3 and H4 and elevated levels of DNA methyltransferases are usually found in prostate cancer cells (Baumgart and Haendler, 2017).

3.3 Histone phosphorylation

Histone phosphorylation is highly versatile and occurs predominantly at serine, threonine, and tyrosine residues. Phosphorylation results from the transfer of a phosphate group from ATP to the hydroxyl group of the amino acid side chain that is catalyzed by histone kinases (Xhemalce et al., 2011).

3.4 Histone lactylation

A recent study also revealed that lactate, produced by the incomplete oxidation of glucose through the Warburg effect in cancer cells, can regulate gene expression in macrophages by functioning as a new histone modification, i.e., lactylation. Excessive lactate production, i.e., Warburg effect benefits cancer in number of ways-promotes metastasis, angiogenesis, activation of T cells, polarization of macrophages. Now it is well documented that lactic acid also contributed in epigenetic modifications by adding the lactyl group on the ε-amino group of a lysine residue (Zhang et al., 2019).

In addition, there are diverse sets of posttranslational histone modifications that include deamination, ADP ribosylation, ubiquitylation, and sumoylation but are beyond the scope of this review.

3.5 Phytocompounds inhibiting histone modifications

In the last two decades, several dietary compounds have been confirmed to play a substantial role in the reversal of histone onco-modification and a few of the most important of them are discussed in detail below.

In prostate cancer cells, apigenin induced a decrease in HDAC activity, downregulated HDAC1 and 3 expression, and increased acetylation of histones H3 and H4. *In vivo* studies reveled that apigenin treatment reduced tumor growth and a significant decrease in HDAC activity that correlated with increased levels of p21/waf1and Bax protein along with a reduction in protein levels of bcl2 that favored apoptosis in tumor cells of the mice (Pandey et al., 2012). Another *in vivo* study on the breast cancer cell line of athymic nude mice revealed a decrease in HDAC activity on treatment with apigenin in a dose-dependent manner. Acetylation of histone H3 was shown to increase after treatment with apigenin correlated with transcriptional activation of $p21^{WAF1/CIP1}$ gene (Tseng et al., 2017). Apigenin treatment lowered the protein expression levels of HDAC1, 3, 4, 5, 6, and 8 in the mouse skin cancer cell line in a dose-dependent manner (Paredes-Gonzalez et al., 2014).

Curcumin treatment resulted in inhibition of cell proliferation in Raji cells of B-NHL cancer. The protein expression levels of HDAC1, 3, and 8 were also found to be downregulated and acetylation of H4 histone increased after treatment with curcumin in a dose- and time-dependent manner (Liu et al., 2005). In HeLa nuclear extracts, curcumin decreases the HDAC activity. Docking studies suggested curcumin as a potent inhibitor of HDAC8 than its carboxylic acid-derived pharmacological counterparts (Bora-Tatar et al., 2009). In human hepatoma Hep3B cells, curcumin induced a decrease in H3 and H4 histone acetylation. Further *in vitro* studies showed curcumin treatment decreased core histone acetylation catalyzed by HAT extracted from Hep3B cancer cell line that suggested the role of HAT in curcumin-induced histone hypoacetylation (Kang et al., 2005).

In a recent study, demethylzeylasteral treatment promoted decrease in tumor progression in liver stem cells by inhibiting H3 lactylation (H3K9la and H3K56la) (Pan et al., 2022).

Green tea polyphenol (GTP) treatment decreased a maximum of 43% HDAC activity in a time-dependent manner in prostate cancer cells, which was similar to Trichostatin A (TSA) that caused 45% inhibition in 24 h. Furthermore, a decrease in protein expression of HDAC1 and 3 was also observed. GTP treatment decreased the mRNA levels of HDAC1, 2, and 3 in a gradual time course, whereas no such changes were observed with TSA. Exposure to GTP further resulted in a 22-fold and 2.2-fold increase in H3 and H4 acetylation, respectively, in a gradual-time course (Pandey et al., 2010). EGCG treatment significantly reduced HDAC activity in skin cancer cell line A431. Acetylation and methylation levels of H3K9 were found to be increased and decreased, respectively, when treated with EGCG. Furthermore, acetylation of H3K4 and H4K5, 12, and 16 were shown to be increased after EGCG treatment, thus reactivating tumor suppressor genes (Nandakumar et al., 2011). In prostate cancer cells, GTP and its major constituent EGCG induced treatment caused a substantial decrease in the expression and activity of HDAC 1, 2, 3, and 8. On further investigation, EGCG acetylated the *p53* gene at K373 and K382, which was found to be diminished when the EGCG treatment was withdrawn after a certain time period (Thakur et al., 2012).

Genistein treatment increased acetylation at H3, H4, and H3 dimethylated at K4 near the transcription start sites of tumor suppressor genes *p21* and *p16* in prostate cancer cell lines. ChIP analysis revealed an elevation in HAT activity, suggesting an increase in transcription level and gene activation after treatment with genistein (Majid et al., 2008). Genistein, eqoul, and AglyMax induced ER-mediated core histone acetylation via modulating the activity of HATs, and daidzein stimulated Erβ mediated histone acetylation (Hong et al., 2004).

Triple-negative breast cancer is considered the most aggressive subtype of breast cancer. An *in vitro* study on the effect of indole-3-carbinol on HCC70 triple-negative breast cancer cell lines has shown to inhibit the overall HDAC activity (Nouriemamzaden et al., 2020).

PEITC treatment of LNCaP prostate cancer cell line significantly reduced the protein levels of HDAC1, 2, 4, and 6 that correlated with promoter demethylation and activation of a tumor suppressor gene, *RASSF1A* (Boyanapalli et al., 2016). Histone hypoacetylation due to excessive HDAC activity is one of the hallmarks of leukemia. Mononuclear extracts from the bone marrow of acute myeloid leukemia patients showed limited or no H3 and H4 histone

TABLE 3 List of phytocompounds modulating histone modifications.

Dietary phytocompound	Mechanism	Genes targeted	Cancer type (cancer cell line)	References
Allicin	H4 acetylation↑	-	Mouse erythroleukemia (DS19)	Link et al. (2013)
Allyl isothiocyanate	H4 acetylation↑	-	Mouse erythroleukemia (DS19)	Lea et al. (2001)
Apigenin	HDAC activity↓	-	Prostate (PC-3, 22Rv)	Pandey et al. (2012)
	HDAC expression↓	*p21/waf1*	Breast (MDA-MB-231)	Tseng et al. (2017)
	H3 and H4 acetylation↑			
Curcumin	HDAC activity↓	-	Cervix (HeLa)	Bora-Tatar et al. (2009)
	HDAC expression↓		Hepatoma (Hep3B)	Kang et al. (2005)
	H4 acetylation↑		Lymphoma (Raji)	Liu et al. (2005)
	H3 and H4 acetylation↓			
Diallyl disulfide	HDAC activity↓	*p21(waf1/cip1)*	Colon (Caco-2, HT-29)	Druesne et al. (2004)
	H3 and H4 acetylation↑			
Demethylzeylasteral	H3 lactylation↓	*Cyclin D, CDK2, Cyclin E*	Hepatoma (Hep3B, HCCLM3)	Pan et al. (2022)
EGCG	HDAC activity↓	*GSTP1*	Prostate (LNCaP)	Pandey et al. (2010)
	HDAC expression↓	*p16INK4a, Cip1/p21, p53*	Skin (A431)	Nandakumar et al. (2011)
	H3 and H4 acetylation↑			
	H3 methylation↓			
Garcinol	HAT expression ↓	-	Esophageal (KYSE150, KYSE450)	Wang et al. (2020)
Genistein	HAT activity↑	*p21WAF1/CIP1, p16INK4a*	Prostate (LNCaP, DuPro, RWPE)	Majid et al. (2008)
	H3 and H4 acetylation↑			
	H3 methylation↑			
Ginsenoside Rh2	HDAC activity↑	*MMP3*	Hepatocellular (HepG2)	Shi et al. (2014)
Indole-3-carbinol	HDAC activity↓	-	Breast (HCC70)	Nouriemamzaden et al. (2020)
Kaempferol	HDAC activity↓	-	Hepatocellular (HepG2, Hep3B) and Colorectal (HCT-116)	Berger et al. (2013)
Luteolin	HDAC activity ↓	-	Colorectal (HCT-116)	Zuo et al. (2018)
Parthenolide	HDAC activity ↓	-	Colorectal (HCT-116)	Dawood et al. (2019)
Phenethyl isothiocyanate (PEITC)	HDAC activity↓	*RASSF1A*	Prostate (LNCaP)	Boyanapalli et al. (2016)
Phenylhexyl isothiocyanate	H3 and H4 acetylation↑	-	Leukemia (mononuclear extract)	Xiao et al. (2010)
Quercetin	HAT activity↑	*DAPK1, BCL2L11, BAX, APAF1, BNIP3, BNIP3L*	Leukemia (HL-60)	Alvarez et al. (2018)
	HDAC activity↓	-	Cervix (HeLa)	Kedhari Sundaram et al. (2019)
	H3and H4 acetylation↑			
	HMT activity↓			
Resveratrol	HMT activity↓	*BRCA1, p53, p21*	Breast (MCF-7, MDA-MB-231)	Chatterjee et al. (2019)
	HMT expression↓	-	Renal (ACHN)	Dai et al. (2020)

(Continued on following page)

TABLE 3 (*Continued*) List of phytocompounds modulating histone modifications.

Dietary phytocompound	Mechanism	Genes targeted	Cancer type (cancer cell line)	References
	HDAC activity↓			
	H3 and H4 acetylation↑			
Rosmarinic acid	HDAC expression↓	*p53, Bax, Bcl-2, PARP-1*	Prostate (PC-3, DU145)	Jang et al. (2018)
Sulforaphane	HMT activity↓	*hTERT*	Prostate (LNCaP)	Abbas et al. (2015)
	HDAC activity↓	-	Melanoma (A375)	Mitsiogianni et al. (2020)
	HAT activity↓			
	H3 and H4 acetylation↓			
Thymoquinone	HDAC activity↓	*p21, Maspin, Bax and Bcl-2*	Breast (MCF-7)	Parbin et al. (2016)
Triptolide	HMT activity↓	-	Lung (A549, H460)	Nardi et al. (2018)

acetylation. However, after treatment with phenylhexyl isothiocyanate (PHI), there was a significant elevation in H3 and H4 histone acetylation compared to the control cultures (Xiao et al., 2010).

In HL-60 leukemia cancer cell lines, quercetin treatment induced FasL expression that triggered extrinsic apoptotic pathway, protein activation and conformational changes, and activation of ERK and JNK signaling pathways. Furthermore, H3 acetylation was found to be increased in quercetin treated HL-60 cells, and upregulated HAT activity and downregulated HDAC activity together resulted in stimulation of FasL expression (Lee et al., 2011). Leukemia cancer cell lines when treated with quercetin showed an increase in global histone acetylation of H3 and H4 histones. Promoter regions of proapoptotic genes experienced a three-to ten-fold increase in H3 and H4 acetylation in HL-60 and U937 cancer cells. *In vitro* and *in vivo* studies of two human xenograft myeloid leukemia models exhibited a decrease in HDAC1 and 2 activity after treatment with quercetin (Alvarez et al., 2018). Quercetin treatment significantly reduced the HDAC activity in a dose-dependent manner and HMT activity at H3 histone, which may methylate and trimethylate the ninth lysine residue in HeLa cancer cell lines. Molecular docking results of quercetin reported a decline in HDAC activity, suggesting that quercetin can competitively inhibit HDAC2, HDAC4, HDAC7, and HDAC8 by binding to the catalytic residue sites (Kedhari Sundaram et al., 2019).

In breast cancer cell lines, resveratrol decreases the protein levels of arginine methyltransferase PRMT5, lysine methyltransferase EZH2, and lysine deacetylase KDAC in a dose- and time-dependent manner that correlated with an increase in protein levels of *BRAC1, p21,* and *p53* genes. After treatment with resveratrol, near to the proximity of the transcription start site of the mentioned genes, the levels of H4R3me2s and H3K27me3 were found to be decreased while that of H3K9ac and H3K27ac increased (Chatterjee et al., 2019). In human carcinoma cell line, resveratrol treatment increase the protein levels of acH3K9, acH3K14, acH3K12, acH4K5, and acH4K16, suggesting anti-tumor effects of resveratrol (Dai et al., 2020).

In human malignant melanoma cells, sulforaphane, decreases the protein expression levels of HDAC1, 2, 4, and 6. Sulforaphane also decreases the total HDAC activity and protein expression levels of CBP, CBP/p300, and PCAF. Furthermore, the protein expression levels of acH3K9, 14, and 27, and acH3K8 and 12 were significantly reduced after treatment with sulforaphane. The study also revealed a decrease HMT activity of SET7/9, further affecting the methylation at K9, 36, and 79 when treated with sulforaphane (Mitsiogianni et al., 2020). TERT (Telomerase Reverse Transcriptase) is associated with processes such as cell proliferation, senescence, cell differentiation, *etc.*, and any alteration in it contributes to immortality and carcinogenesis. Sulforaphane treatment suppressed HDAC activity in prostate cancer cells and induced an increase in pan-acetylation of H3 and H4 histones of the hTERT promoter (Abbas et al., 2015).

Furthermore, the histone modulation activity of various phytocompounds like diallyl disulfide, garcinol, ginsenoside Rh2, phenyl hexyl isothiocyanate, rosmarinic acid, *etc.*, in distinct cancer types is mentioned in Table 3.

Based on the studies mentioned above, it is evident that a wide range of phytocompounds (apigenin, curcumin, sulforaphane, resveratrol, genistein, quercetin, *etc.*) possess the ability to target major histone modifications that regulate gene expression of apoptosis, cell proliferation and inflammatory pathways (extensively discussed in section 6), all of which, when dysregulated can lead to carcinogenesis.

4 MicroRNAs

Non-coding RNAs without protein or peptide-coding potential are classified into two major categories: long ncRNA (200 nucleotides long) and short ncRNA that consists of miRNAs, siRNA, piwiRNA, *etc.* Non-coding RNAs, initially assumed to be junk in the transcriptome, have now been discovered to play a crucial role in cellular signaling pathways, including those that regulate cancer initiation and progression (Setoyama et al., 2011). miRNAs are single-stranded and 18–20 nucleotides in length that are formed after undergoing

TABLE 4 List of phytocompounds modulating MicroRNA.

Dietary phytocompound	Mechanism	Genes targeted	Cancer type (cancer cell line)	References
Apigenin	miR-16↑	*MMP-9*	Glioma (U87)	Chen et al. (2016)
Celastrol	miR-17–92a↓	*ATG7*	Prostate (LNCaP)	Guo et al. (2016)
Cucurbitacin B	miR- 146-5p↑	-	Pancreas (BxPC-3, MiaPaCa-2, HPAC, ASPC-1)	Zhou et al. (2019b)
Curcumin	miR-99a↑	-	Retinoblastoma (SO-Rb50, Y-79)	Li et al. (2018)
	miR-34a↑, let-7b↑, miR-200a↑	*Axl, Slug, CD24, Rho-A*	Breast (MDA-MB-231, MCF-10F)	Gallardo et al. (2020)
3,3′- Diindolylmethane	miR-30e↓	*ATG5, LC3*	Gastric (BGC-823, SGC-7901)	Ye et al. (2016)
Ellagitannins	let-7a↓, let-7c↓, let-7d↓, let-7e↑, miR-370↑, miR-373*↑, miR-526b↑	-	Hepatocarcinoma ($HepG_2$)	Wen et al. (2009)
EGCG	miR-18a↓, miR-34b↓, miR-193b↓, miR-222↓ miR-342↓, miR-16↑, miR-221↑, let-7b↑	*Bcl-2*	Hepatocarcinoma (HepG2)	Tsang and Kwok (2010)
Genistein	miR-574-3p↑	-	Prostate (PC3, DU145)	Chiyomaru et al. (2013)
	miR-145↑	*ABCE1*	Retinoblastoma (Y79)	Wei et al. (2017)
Glabridin	miR-148a↑	-	Breast (MDA-MB-231, Hs-578T)	Mu et al. (2017)
Gossypol	miR-15a↑	*Bcl-2*	Pituitary (GH3, MMQ)	Tang et al. (2015)
Icariin	miR-625-3p↓	-	Thyroid (SW579, TPC1)	Fang et al. (2019)
Kaempferol	miR-340↑	-	Lung (A549)	Han et al. (2018)
Lycopene	miR-let-7f-1↑	-	Prostate (PC3)	Li et al. (2016)
Methyl jasmonate	miR-101↑	-	Colorectal (SW670)	Peng and Zhang (2017)
PEITC	miR-194↑	-	Prostate (LNCaP)	Zhang et al. (2016)
Piceatannol	miR-21↓	*PTEN*	Osteosarcoma (MG-63, Saos-2) Colorectal (HCT-116, HT29)	Zheng and Wu (2020)
	miR-129↑	-		Zhang et al. (2014)
Quercetin	miR-16↑	*HOXA 10*	Oral (HSC-16, SCC-9)	Zhao et al. (2019)
	miR-146a↑	-	Breast (MCF-7, MDA-MB-231)	Tao et al. (2015)
Resveratrol	miR-200c↑	-	Colorectal (HCT-116)	Karimi Dermani et al. (2017)
Rosmarinic acid	miR-506↑	-	Pancreas (Panc-1, SW 1990)	Han et al. (2019)
Sulforaphane	miR-135b-3p↑	*RASAL2*	Pancreas (BxPC-3, PANC-1, AsPC-1)	Yin et al. (2019)
	miR-21↓	-	Colorectal (RKO)	Martin et al. (2017)
Thymoquinone	miR-16↑, miR-375↑	*BCL-2, Caspase-3*	Hepatocellular carcinoma (HepG2, Huh7)	Bashir et al. (2020)
Triptolide	miR-193b-3p↑	*KLF4*	Nephroblastoma (G-401, WiT49)	Hang et al. (2019)
Ursolic acid	miR-21↓	-	Glioblastoma (U251)	Wang et al. (2012)
Withaferin A	miR-let-7c-5p↑	*CCND1, c-MYC*	Breast (MCF-7)	Prajapati et al. (2022)

complex maturation steps (Figure 3). With the assistance of Drosha (RNase III enzyme) and Pasha (ds-RNA binding endonuclease), the primary miRNA stem-loop structure undergoes numerous modifications, which leaves a 70 nucleotide long pre-miRNA. This pre-miRNA is then transported to the cytoplasm from the nucleus and is subjected to further processing with DICER and TRBP (transactivating response RNA-binding protein) that generates a 22-nucleotide extended miRNA duplex. The duplex

associates with the RISC (RNA inducing silencing complex) complex that targets the mRNA for gene regulation (Zhang et al., 2007; Shruti et al., 2011). Several studies have suggested that miRNA can influence cell signaling, regulation, proliferation, and apoptosis by controlling oncogenes and tumor suppressor gene expression (Mishra et al., 2016).

4.1 Epi-miRNA

Any alterations during the biogenesis of miRNA or mutation of the factors can have profound implications. A category of miRNAs, termed as epi-miRNAs (epi-miRs), has recently been discovered to modulate the expression of genes encoding epigenetic reader proteins (Dai et al., 2014). Aberrant modulation of epi-miRs can induce epigenetic silencing of tumor suppressor genes or activation of oncogenes, resulting in carcinogenesis. MicroRNAs have been classically categorized as two distinct epi-miRs, namely, OncomiRs and tumor-suppressor miRs that play distinctive roles in tumorigenesis. OncomiRs are generally upregulated, resulting in enhanced cancer cell proliferation and metastasis, whereas tumor-suppressor miRs are downregulated leading to carcinogenesis (Svoronos et al., 2016; Sadakierska-Chudy, 2020). Phytocompounds that are known to alter the epi-miRNAs is the entire effect of the each phytocomponents is supported by a single publication are listed in Table 4.

4.2 Phytocompounds modulating the epi-miRNAs expression

A significant proportion of studies have demonstrated the potential role of phytocompounds in the regulation of epi-miRs in carcinogenesis. For instance, the apigenin-treated glioma cancer cell line U87 exhibited increased miR-16 expression, decreased BCL2 protein expression, and decreased expression of the *MMP-9* gene. Anti-miR-16 transfection inhibited apigenin-induced miR-16 gene expression. Furthermore, anti-miR-16 transfection inhibited apigenin-induced miR-16 gene expression, increased BCL2 protein expression and NF-κB/MMP-9 levels (Chen et al., 2016).

Curcumin induced upregulation of miR-99a in retinoblastoma cancer cell line, SO-Rb50, and Y-79. When the cells were transfected with miR-99a inhibitor, the miR-99a expression decreased that correlated with anti-tumor activity of curcumin through enhancement of miR-99a expression. Phosphorylation levels of JAK1, STAT1, and STAT3 were significantly reduced when treated with curcumin, although no such effect was observed when miR-99a was knocked down (Li et al., 2018). Curcumin-treated breast cancer cell line MCF-10F resulted in decreased gene transcript and protein levels of *Axl, Slug, CD24, and Rho-A*, which are associated with epithelial-mesenchymal transition (EMT). An increased expression of miR-200a, let-7b, and miR-34a was found in the MCF-10F cancer cell line, while only miR-34a expression increased in the MDA-MB-231 cancer cell line after exposure to curcumin. An increase in expression of the examined genes occurred after the knockdown of miR-34a, while the genes were found downregulated when treated with curcumin and transfected with anti-miR-34a. The invasive and migrating capabilities of MCF-10F decreased when cells were transfected with anti-miR-34a and treated with curcumin (Gallardo et al., 2020).

Ellagitannin treated hepatocarcinoma cells showed a decrease in cell proliferation. The treatment further downregulated and upregulated the expression of various mi-RNAs (Table 4) (Wen et al., 2009).

Hepatocarcinoma cell line HepG2 exhibited decreased growth when treated with EGCG in a dose-dependent manner. miR-18a, miR-34b, miR-193b, miR-222, and miR-342 were found to be downregulated, while miR-16, miR-221, and let-7b were found to be upregulated after treatment with EGCG. *Bcl-2* expression was suppressed after transfection with miR-16. Furthermore, transfection with miR-16 enhanced the activity of EGCG in *Bcl-2* suppression and induction of apoptosis (Tsang and Kwok, 2010). Nasopharyngeal cancer cell line CNE2 was treated with EGCG where 32 miRNAs exhibited > 2-fold changes that have been shown to modulate cancer development, out of which 29 miRNAs were found to be upregulated and 1 miRNA was downregulated in a dose-dependent manner (Li et al., 2017).

Genistein-treated prostate cancer cell lines, exhibited an increase in miR-574-3p expression compared to the control. Transfection with pre-miR-574-3p miRNA precursors into PCa cell lines led to a significant increase in miR-574-3p expression and decreased cell invasion. In an *in vivo* study, the transfection of DU145 cells with miR-574-3p subcutaneously into nude mice resulted in tumor suppression due to overexpression of miR-574-3p (Chiyomaru et al., 2013). A significant increase in miR-145 expression was observed in genistein-treated retinoblastoma cancer cell line (Y79). Genistein treatment also reduced cancer cell proliferation and induced apoptosis. Y79 cells transfected with miR-145 specific siRNA resulted in the restoration of colony formation capacity and suppression of cell apoptosis that was induced due to genistein treatment. In silico studies suggested *ABCE1* gene to be a potential target of miR-145. Furthermore, an *in vivo* study on the xenograft nude mice model revealed the suppression of tumor growth in Y79 cells administered with genistein (Wei et al., 2017).

Treatment with lycopene induced upregulation of miR-let-7f-1 in a dose and time-dependent manner in prostate cancer cells. Furthermore, transfection with miR mimics led to inhibition of cell proliferation and apoptosis induction (Li et al., 2016).

PEITC treated prostate cancer cell lines exhibited an increase in the expression of miR-194. Furthermore, the expression of the two matrix metalloproteinase, *MMP2 and MMP9*, which significantly contributes to tumor progression in terms of migration, invasion, and metastasis, decreased when treated with PEITC. An *in silico* study revealed *BMP1* is a potential target of miR-194 and its inhibition tends to downregulate MMP2 and MMP9 levels (Zhang et al., 2016).

Quercetin-treated oral cancer cells exhibited an increase in miR-16 expression. Cell viability, migration, and invasive capabilities of oral cancer cells were found to be repressed when transfected with miR-16. HomeboxA10 (*HOXA10*) was found to be targeted by miR-16 after the bioinformatics analysis of the binding sites of HOXA10 and miR-16. *HOXA10* is generally involved in the proliferation, invasion, and migration of cancer cells and is one of the potential biomarkers in oral cancer. Overexpressed miR-16 downregulated the protein levels of *HOXA10*, while the opposite was

observed in miR-16 knockdown cells (Zhao et al., 2019). In breast cancer cells, miR-146a expression increased after treatment with quercetin in a dose-dependent manner. Furthermore, growth of the cells was inhibited after transfection with miR-146a mimic and treatment with quercetin. A substantial elevation in the expression of *Bax* and cleaved caspases was observed when transfected with miR-146a. Quercetin treatment for 8 weeks increased miR-146a expression and reduced tumor growth in a nude mouse orthotopic xenograft model (Tao et al., 2015).

Colorectal cancer cell line HCT-116 exhibited a decrease in cell viability in a dose-and-time-dependent manner when treated with resveratrol. HCT-116 cells transfected with LNA miR inhibitor showed a dramatic decline in miR-200c expression compared with the un-transfected and scrambled groups. After treatment with resveratrol, miR-200c expression increased significantly in both transfected and un-transfected cells. Resveratrol treatment reduced the mRNA and protein expression of vimentin and ZEB1, while that of E-cadherin increased in both groups that correlated with EMT induction (Karimi Dermani et al., 2017).

Rosmarinic acid decreased cell viability, cell proliferation, invasion, and migration and suppressed EMT while promoting apoptosis in pancreatic cancer cell lines. Further treatment resulted in increased miR-506 levels that correlated with suppression of MMP2 and MMP16 proteins. The xenograft mouse model also exhibited a reduction in tumor growth after treatment with rosmarinic acid (Han et al., 2019).

Sulforaphane-treated pancreatic cancer cell lines showed a substantial increase in miR135b-5p. Cells transfected with liposomes of miR-135b-5p mimics exhibited overexpression of miR-135b-3p that resulted in reduced cell viability, migration, and colony-forming capacity. *In silico* analysis revealed *RASAL2* to be a potential target of miR-135b-3p. Furthermore, an *in vivo* studies on tumor xenografts, where BxPC-3 cells were transfected with miR-135b-3p mimics, resulted in decreased tumor size that correlated with overexpression of miR-135b-3p and *RASAL2* (Yin et al., 2019). In colorectal cancer cell, sulforaphane treatment inhibited oncogenic miR-21, decreased cell viability, induced apoptosis, and downregulated the expression of *hTERT* (Martin et al., 2017).

In human glioblastoma cells, miR-21 levels were increased that has been shown to target a positive regulator of apoptosis, the *PDCD4* gene. Ursolic acid treatment decreased cell proliferation and induced apoptosis while suppressing the levels of miR-21 that eventually led to enhanced expression of *PDCD4* (Wang et al., 2012).

All these studies discuss the therapeutic effect of phytocompounds targeting epi-miRs that either decreases or increases miRNA level to eventually reduce tumorigenesis. An elaborate list of phytocompounds modulating miRNA in specific cancer cell types is provided in Table 4.

5 Plant-based compounds as epigenetic modulator of genes involved in apoptosis, autophagy, inflammation and oxidative stress

As discussed above, aberrant epigenetic modulation can alter the function and activity of typical genes and transcriptional factors involved in various essential pathways like autophagy, apoptosis inflammation, *etc.*, that can lead to cancer.

5.1 Autophagy

Autophagy plays a dual role in cancer by promoting tumorigenesis or suppressing tumor progression. To satisfy the high metabolic requirements of proliferating tumor cells, autophagy recycles the cells' intracellular constituents to supply nutrients, while suppression or inhibition of autophagy genes may result in cancer cell death. Autophagy also promotes inflammation in tumor cells, which eventually results in tumor progression (Yun and Lee, 2018). Post-translational modifications like acetylation, phosphorylation, ubiquitination, nitrosylation can influence autophagy by regulating the activity of ATG proteins and the expression of genes involved in autophagy (Botti-Millet et al., 2016). As described above, many studies have shown that deregulation of ATG genes through different epigenetic modulations can cause tumor progression. For instance, curcumin treatment inhibited DNMT1 and DNMT3B expression in prostate cancer cells that resulted in promoter hypomethylation of miR-143 and miR-145. This restoration of miRNAs further downregulated *ATG2B* expression, thus inhibiting autophagy (Liu et al., 2017).

5.2 Apoptosis

Dysregulation of apoptosis is one of the hallmarks of cancer. Cancer cells tend to survive longer and accumulate mutations due to deregulation of apoptosis over a period of time. Furthermore, deviations from normal apoptotic pathways can enhance the invasiveness of cancer cells and promote angiogenesis. In most cancer cells, BCL-2 is generally overexpressed while the function of caspases is found to be disabled (Pfeffer and Singh, 2018). As mentioned above, emerging studies have shown that phytocompounds can correct epigenetic modulations that interfere with apoptotic pathways that result in cancer progression.

5.3 Inflammation and oxidative stress

Excessive aggregation of reactive oxygen species (ROS) has been observed in cancer. ROS is involved in inflammation, cell transformation, tumor cell survival, proliferation, invasion, angiogenesis, and metastasis, mediated through transcription factors such as NF-κB, AP-1, STAT3, *etc.* (Gupta et al., 2012; Prasad et al., 2017). Furthermore, the overexpression of MMPs can be correlated with enhanced invasiveness and angiogenesis in distinct cancer types (Reunanen and Kähäri, 2013). Besides this, ROS can also regulate the expression of multiple tumor suppressor genes like *p53, Nrf2, PTEN, and Rb* (Gupta et al., 2012). Nrf2 plays a crucial role in homeostasis maintenance and regulation of genes that produce anti-inflammatory and anti-cancer effects (Wu et al., 2019). Additionally, it is evident from the studies mentioned that abnormal epigenetic modulation can alter the function and activity of transcription factors and genes involved in the production of

ROS in cancer. However, distinct phytocompounds (curcumin, resveratrol, berberine, luteolin, *etc.*) as mentioned above, possess the ability to reverse the activity of all these transcription factors and genes involved in the accumulation of ROS back to normal, which have been implicated in abnormal epigenetic modulation.

Therefore, it is evident from all these studies and observations that autophagy, apoptosis, inflammation, and oxidative stress play a crucial role in cancer. This warrants additional studies to understand the underlying mechanisms of genes, transcription factors, and pathways implicated in cancer. Furthermore, these implications can also be used as biomarkers in the diagnosis of distinct cancer types.

6 Toxic effects of phytocompounds

Most *in vitro* and *in vivo* studies suggested the use of high concentrations of phytocompounds for tumor growth suppression and chemoprevention. However, in humans, certain elevated levels of these phytocompounds may not be reached due to their poor bioavailability and may lack therapeutic efficacy. Studies also show that such high doses of phytocompounds over a prolonged duration may exhibit high toxicity. For instance, resveratrol was administered to rats for 4 weeks in a dose-dependent manner. Serious side effects such as increased kidney weight, increased plasma BUN, and creatinine levels, which gradually contributed to nephrotoxicity, were observed at a concentration of 3,000 mg resveratrol per kg body weight of rats (Crowell et al., 2004). In another study on rat thymocytes, resveratrol at 10 μM concentration raised the shrunken cell population and exerted cytotoxic effects on normal cells by inducing apoptosis (Fujimoto et al., 2009). Despite evidence indicating the antioxidant activity of curcumin, several studies also demonstrated the pro-oxidant activity of curcumin, increasing ROS levels in cells (Yoshino et al., 2004; Su et al., 2006). The pro-oxidant nature of curcumin would increase cellular ROS levels at higher doses, potentially contributing to carcinogenesis (López-Lázaro, 2008). Furthermore, excessive quercetin intake exacerbates tumorigenicity induced by a chemical carcinogen N-ethyl-N′-nitro-N-nitrosoguanidine (ENNG), in the duodenum of mice (Matsukawa et al., 2002). While the immense health-promoting benefits of epigallocatechin-3-gallate, a study demonstrated that high dose administration of EGCG in mice resulted in hepatotoxicity correlated with inhibition of antioxidant enzymes and Nrf2 targeted genes (Wang et al., 2015). Treatment of female CD-1 mice with genistein at environmentally appropriate doses resulted in irregular estrous cycles, early reproductive senescence, impaired ovarian activity, diminished fertility, while at higher doses, the number of stillbirths increased (Jefferson et al., 2005). In an *in vivo* study on Swiss mice, administration of higher doses (100 and 200 mg/kg) of apigenin resulted in elevated serum levels of alanine aminotransferase, aspartate aminotransferase, alkaline phosphatase, and reactive oxygen species that eventually contributed to liver damage (Singh et al., 2012).

In addition to this, a variety of phytocompounds that humans have consumed for decades have been shown to possess carcinogenic properties. For example, capsaicin, cycasin, phytoestrogens, safrole, amygdalin, phorbol esters, pyrrolizidine alkaloids, obtained from different dietary sources, may serve as potential carcinogens or promoters of tumors (Bode and Dong, 2015; Guldiken et al., 2018).

Several experiments have been performed with numerous phytocompounds to examine their possible positive and detrimental biological effects. However, all natural substances should not be considered healthy and attention should also be given to their toxic dose-related effects. Furthermore, all these observations warrant additional studies and humanized clinical trials regarding the adverse and chronic effects of high toxic doses of distinct phytocompounds.

7 Clinical trials

Phytocompounds disrupt the process of epigenetic transformation in cancer by directly inhibiting epigenetic modulations and also by modulating epigenetic regulators. As more evidence emerges highlighting the therapeutic importance of epigenetic modifications of cancer and the ability of phytocompounds to target these modifications further endorses their clinical relevance. The potential of phytocompounds already known to have anticancer effects to target epigenetics should be thoroughly assessed and may be used as a criterion for inclusion of compounds for further clinical evaluation. For this context, we review a few plant-based compounds known to suppress epigenetic modifications that are currently in various phases of clinical studies below.

Several preclinical studies have demonstrated the efficacy of phytocompounds in regulating epigenetic changes for chemotherapeutic purposes, there have been insufficient clinical trials to back this up. For instance, curcumin regulated the activity of MMP-2, Bcl-2, Nrf-2, Bax, and PIK3/AkT signaling in a randomized clinical trial to study the effects of paclitaxel and curcumin combined in breast cancer to mitigate multidrug resistance. In patients with advanced breast cancer, curcumin is under investigation as monotherapy (NCT03980509) or in combination with paclitaxel in phase II clinical trial (NCT03072992). The main object of these clinical studies is to determine the effect of curcumin on the development of advanced breast cancer and to estimate the risk of adverse effects. In a phase II study of the effect of sulforaphane-rich extracts in men with recurrent cancer, 20 subjects were treated with 200 μmoles/day of sulforaphane extract for 20 weeks. Out of the 20 subjects, six showed an increase in histone acetylation following sulforaphane treatment (Alumkal et al., 2015). In an ongoing randomized pilot study in phase I clinical trial investigating the impact of quercetin on EGCG uptake in prostate cancer, the downregulating effects of quercetin on enzyme function and protein and gene expression of COMT (catechol-O-methyltransferase) and DNMT1 are being assessed (NCT01912820). Treatment with 3,3′-Diindolylmethane enhanced the expression of let-7, miR-27b, miR-34a, miR-124, miR-200, and miR-320, which led to downregulation of androgen receptor activity, EMT, and stem cell markers, all of which were associated with enzalutamide resistance in Castration-resistant prostate cancer (Li and Sarkar, 2016).

Additionally, these natural compounds can be categorized in to 3 different phases as per their success in treating cancer are

compounds under preclinical trials, clinical trials and those are used in current cancer therapy. Phytocompounds those are in pre-clinical trials are ursolic acid (Prasad et al., 2012; Zhang et al., 2018), withaferin A (Choi and Kim, 2015; Suman et al., 2016; Kuppusamy et al., 2017), curcumin (Kunnumakkara et al., 2017), baicalein (Dou et al., 2018; Tao et al., 2018), EGCG (Thangapazham et al., 2007), apigenin (Chang et al., 2018; Yan et al., 2018), genistein (Zhang et al., 2013; Hsiao et al., 2019), resveratrol (Banerjee et al., 2002), sulphorane (Qazi et al., 2010), thymoquinone (Zhu et al., 2016), *etc.* Phytocompounds that go for clinical trial focus on three major aspects of cancer research: 1) improving the response of cancer cells towards standard chemo- and radiotherapy, 2) reducing the severe adverse effects of standard cancer therapy, and 3) looking for unwanted interactions with standard therapy. Preclinical studies have shown the effectiveness of various phytochemicals as mentioned above. The phytochemicals which are currently under clinical trials against various cancers are Berberine (NCT03281096), curcumin (NCT03072992), EGCG (NCT02891538), lycopene (NCT03167268), quercetin (NCT01912820), resveratrol (NCT01476592) and sulphorane (NCT03232138). Several compounds are in clinical use are vincristine, vinblastine, paclitaxel, etoposide to name a few. This underscores the significance of natural chemicals and the imperative to further investigate their potential in developing the most efficacious and secure pharmaceutical interventions for cancer therapy.

Research on cancer-fighting phytocompounds is still in their infancy since only a small number of phytocompounds (such as paclitaxel, docetaxel, and vinblastine) have been granted clinical use licenses. With an increasing understanding of the range of anticancer effects of plant-based compounds, such as inhibition of cancer epigenetics, there is an urgent need to screen more therapeutically effective phytocompounds. In addition, no clinical investigation has been conducted to date to assess how phytocompounds modify micro RNAs in the context of cancer epigenetics therapy. In the majority of related clinical studies, methodological flaws such as the absence of a control or placebo group, small sample sizes, and brief trial duration are observed. Therefore, for many phytochemicals, it is too early to conclude their anticancer actions and hence large-scale and well-controlled clinical trials are required to validate their efficacies, adverse effects, and safeties before their use for the treatment of cancer. To achieve the international standard, promising phytochemicals require extensive standardization in terms of methods for evaluating their bioavailability, efficacy, safety, quality, composition, manufacturing processes, regulatory and approval practices. In order to enhance the clinical assessment of phytocompounds, we must establish an evaluation pipeline. A methodology that takes into account drug optimization, effectiveness assessment, tissue toxicity and distribution, chemical accessibility, pharmacokinetics, absorption, and most importantly bioavailability should be created for an enhanced evaluation of phytocompounds. The stability and availability of phytocompounds in blood can be improved by using stable synthetic analogues, chemically modified derivatives, micelle-coated medications, liposomal conjugates, phospholipid complexes, adjuvants, and nanoparticles. The effectiveness of plant-based medicines can also be augmented by using other techniques including structure-activity relationship, directed optimization, and pharmacophore-oriented molecular design (Xiao et al., 2016; Atanasov et al., 2021; Mohammadi et al., 2022).

8 Conclusion and future prospects

Epigenetic aberrations remarkably contribute to cancer incidence. As mentioned above, distinct studies highlighted the potential of phytocompounds in preventing tumorigenesis through regulation of epigenetic modulation by targeting the activity and expression of DNMTs, HDACs, HMTs, epi-miRNAs. The dietary phytocompounds analyzed tend to modulate epigenetic modifications *in vitro* and in some *in vivo* cancer models, thus inhibiting or suppressing cancer cell viability, proliferation, and growth. However, the limited number of studies and insufficient preclinical and clinical data on the effect of phytocompounds on the epigenetic landscape still remains a challenge. Future research should focus on clinical studies regarding the optimal dose and duration of phytocompounds as epidrugs. One of the studies exhibited that a low dietary dose of resveratrol compared with a 200-fold higher dose tends to suppress colorectal cancer development in human and mice tissues (Cai et al., 2015). This result indicates that a low dose of phytocompounds can inhibit tumor progression, thus making it essential to analyze the optimal dose and toxicity of the phytocompounds. To develop anticancer therapeutics, the issue of poor bioavailability of phytocompounds needs to be addressed. Furthermore, significant epidemiological studies revealed that phytocompounds interact with other bioactive compounds that may interfere with their intestinal absorption (Phan et al., 2018). A promising approach to overcome these challenges is the utilization of modern drug delivery systems such as nanoparticles, micelles, liposomes, *etc.*, to enhance bioavailability and overcome systemic toxicity (Aqil et al., 2013). Accumulating shreds of evidence have also demonstrated the synergistic effects of various phytochemicals with chemotherapeutic drugs to be more effective in chemoprevention and cure (Tan and Norhaizan, 2019). However, research regarding the mechanism and course of action of these combined phytocompounds and drugs is still in their infancy. More studies are essential to fully comprehend the mode of action of phytocompounds that have been shown to target a single cell type or are tissue/organ-specific. Besides *in vivo* and *in vitro* studies, mechanistic studies using bioinformatics and high-throughput sequencing methods can help us to better understand and target altered epigenetic modifications in cancer. Dietary phytocompounds (as listed in Tables 2–4) may offer a cost-effective method for chemoprevention, hence improving global health by decreasing the incidence of cancer. Numerous shreds of evidence point to the potential of phytocompounds to target aberrant epigenetic alterations in different forms of cancer. As was already established, genistein functions as a DNMT inhibitor, promotes histone acetylation, and increases levels of miRNAs, all of which contribute to therapeutic impact on prostate cancer. Such phytochemicals need to undergo a thorough evaluation for preclinical and clinical investigations taking into consideration their therapeutic potential in the treatment of cancer. Our study concludes by highlighting the potential of natural compounds in addressing the epigenetic vulnerabilities of cancer, as well as the possible therapeutic benefits that can be identified by advancing our knowledge in this field.

Author contributions

AqK: Writing–review and editing, Conceptualization, Investigation, Writing–original draft. AsK: Conceptualization, Investigation, Writing–original draft, Writing–review and editing. MK: Conceptualization, Investigation, Writing–review and editing, Formal Analysis. ZM: Conceptualization, Formal Analysis, Investigation, Writing–review and editing. SM: Conceptualization, Formal Analysis, Writing–review and editing. RP: Conceptualization, Formal Analysis, Writing–review and editing, Investigation. SM: Conceptualization, Formal Analysis, Investigation, Writing–review and editing. SH: Writing–review and editing, Supervision.

Funding

The author(s) declare financial support was received for the research, authorship, and/or publication of this article. AK acknowledges the support provided by Department of Bioscience, Jamia Millia Islamia. SH acknowledges the support provided by the Department of Bioscience, Faculty of Natural Sciences, Jamia Millia Islamia. AS is grateful to Ajman University, UAE for supporting this publication.

Conflict of interest

The authors declare that the research was conducted in the absence of any commercial or financial relationships that could be construed as a potential conflict of interest.

Publisher's note

References

Abbas, A., Hall, J. A., Patterson, W. L., Ho, E., Hsu, A., Al-Mulla, F., et al. (2015). Sulforaphane modulates telomerase activity via epigenetic regulation in prostate cancer cell lines. *Biochem. Cell Biol.* 94 (1), 71–81. doi:10.1139/bcb-2015-0038

Adjakly, M., Bosviel, R., Rabiau, N., Boiteux, J. P., Bignon, Y. J., Guy, L., et al. (2011). DNA methylation and soy phytoestrogens: quantitative study in DU-145 and PC-3 human prostate cancer cell lines. *Epigenomics* 3, 795–803. doi:10.2217/epi.11.103

Aggarwal, B. B., and Shishodia, S. (2006). Molecular targets of dietary agents for prevention and therapy of cancer. *Biochem. Pharmacol.* 71, 1397–1421. doi:10.1016/j.bcp.2006.02.009

Aggarwal, R., Jha, M., Shrivastava, A., and Jha, A. K. (2015). Natural compounds: role in reversal of epigenetic changes. *Biochem.* 80 (8), 972–989. doi:10.1134/S0006297915080027

Altaf, M. M., Ahmad Khan, M. S., and Ahmad, I. (2018). "Diversity of bioactive compounds and their therapeutic potential," in *New look to phytomedicine: advancements in herbal products as novel drug leads* (Elsevier), 15–34.

Alumkal, J. J., Slottke, R., Schwartzman, J., Cherala, G., Munar, M., Graff, J. N., et al. (2015). A phase II study of sulforaphane-rich broccoli sprout extracts in men with recurrent prostate cancer. *Invest. New Drugs* 33 (2), 480–489. doi:10.1007/s10637-014-0189-z

Alvarez, M. C., Maso, V., Torello, C. O., Ferro, K. P., and Saad, S. T. O. (2018). The polyphenol quercetin induces cell death in leukemia by targeting epigenetic regulators of pro-apoptotic genes. *Clin. Epigenetics* 10 (1), 139. doi:10.1186/s13148-018-0563-3

Al-Yousef, N., Shinwari, Z., Al-Shahrani, B., Al-Showimi, M., and Al-Moghrabi, N. (2020). Curcumin induces Re-expression of BRCA1 and suppression of γ synuclein by modulating DNA promoter methylation in breast cancer cell lines. *Oncol. Rep.* 43 (3), 827–838. doi:10.3892/or.2020.7473

Aqil, F., Munagala, R., Jeyabalan, J., and Vadhanam, M. V. (2013). Bioavailability of phytochemicals and its enhancement by drug delivery systems. *Cancer Lett.* 28, 133–141. doi:10.1016/j.canlet.2013.02.032

Atanasov, A. G., Zotchev, S. B., Dirsch, V. M., Orhan, I. E., Banach, M., Rollinger, J. M., et al. (2021). Natural products in drug discovery: advances and opportunities. *Nat. Rev. Drug Discov.* 20, 200–216. doi:10.1038/s41573-020-00114-z

Audia, J. E., and Campbell, R. M. (2016). Histone modifications and cancer. *Cold Spring Harb. Perspect. Biol.* 8 (4), a019521. doi:10.1101/cshperspect.a019521

Bailon-Moscoso, N., Cevallos-Solorzano, G., Romero-Benavides, J., and Ramirez Orellana, M. (2017). Natural compounds as modulators of cell cycle arrest: application for anticancer chemotherapies. *Curr. Genomics* 18, 106–131. doi:10.2174/1389202917666160808125645

Banerjee, S., Bueso-Ramos, C., and Aggarwal, B. B. (2002). Suppression of 7,12-dimethylbenz(a)anthracene-induced mammary carcinogenesis in rats by resveratrol: role of nuclear factor-kappaB, cyclooxygenase 2, and matrix metalloprotease 9. *Cancer Res.* 62 (17), 4945–4954.

Bannister, A. J., and Kouzarides, T. (2011). Regulation of chromatin by histone modifications. *Cell Res.* 21, 381–395. doi:10.1038/cr.2011.22

Bannister, A. J., Schneider, R., and Kouzarides, T. (2002). Histone methylation: dynamic or static? *Cell* 109 (7), 801–806. doi:10.1016/s0092-8674(02)00798-5

Bashir, A. O., El-Mesery, M. E., Anwer, R., and Eissa, L. A. (2020). Thymoquinone potentiates MiR-16 and MiR-375 expressions in hepatocellular carcinoma. *Life Sci.*, 254. doi:10.1016/j.lfs.2020.117794

Baumgart, S. J., and Haendler, B. (2017). Exploiting epigenetic alterations in prostate cancer. *Int. J. Mol. Sci.* 18, 1017. doi:10.3390/ijms18051017

Baylin, S. B., Esteller, M., Rountree, M. R., Bachman, K. E., Schuebel, K., and Herman, J. G. (2001). Abberant patterns of DNA methylation, chromatin formation and gene expression in cancer. *Human molecular genetics. Hum. Mol. Genet.* 10, 687–692. doi:10.1093/hmg/10.7.687

Berger, A., Venturelli, S., Kallnischkies, M., Böcker, A., Busch, C., Weiland, T., et al. (2013). Kaempferol, a new nutrition-derived pan-inhibitor of human histone deacetylases. *J. Nutr. Biochem.* 24 (6), 977–985. doi:10.1016/j.jnutbio.2012.07.001

Berson, A., Nativio, R., Berger, S. L., and Bonini, N. M. (2018). Epigenetic regulation in neurodegenerative diseases. *Trends Neurosci.* 41, 587–598. doi:10.1016/j.tins.2018.05.005

Bestor, T. H. (2000). The DNA methyltransferases of mammals. *Hum. Mol. Genet.* 9 (16), 2395–2402. doi:10.1093/hmg/9.16.2395

Bird, A. (2002). DNA methylation patterns and epigenetic memory. *Genes Dev.* 16 (1), 6–21. doi:10.1101/gad.947102

Bode, A. M., and Dong, Z. (2015). Toxic phytochemicals and their potential risks for human cancer. *Cancer Prev. Res.* 1, 1–8. doi:10.1158/1940-6207.CAPR-14-0160

Bora-Tatar, G., Dayangaç-Erden, D., Demir, A. S., Dalkara, S., Yelekçi, K., and Erdem-Yurter, H. (2009). Molecular modifications on carboxylic acid derivatives as potent histone deacetylase inhibitors: activity and docking studies. *Bioorg. Med. Chem.* 17 (14), 5219–5228. doi:10.1016/j.bmc.2009.05.042

Botti-Millet, J., Nascimbeni, A. C., Dupont, N., Morel, E., and Codogno, P. (2016). Fine-tuning autophagy: from transcriptional to posttranslational regulation. *Am. J. Physiol. Physiol.* 311 (3), C351–C362. doi:10.1152/ajpcell.00129.2016

Boyanapalli, S. S. S., Li, W., Fuentes, F., Guo, Y., Ramirez, C. N., Gonzalez, X. P., et al. (2016). Epigenetic reactivation of RASSF1A by phenethyl isothiocyanate (PEITC) and promotion of apoptosis in LNCaP cells. *Pharmacol. Res.* 114, 175–184. doi:10.1016/j.phrs.2016.10.021

Cai, H., Scott, E., Kholghi, A., Andreadi, C., Rufini, A., Karmokar, A., et al. (2015). Cancer chemoprevention: evidence of a nonlinear dose response for the protective effects of resveratrol in humans and mice. *Sci. Transl. Med.* 7 (298), 298ra117. doi:10.1126/scitranslmed.aaa7619

Chang, J. H., Cheng, C. W., Yang, Y. C., Chen, W. S., Hung, W. Y., Chow, J. M., et al. (2018). Downregulating CD26/DPPIV by apigenin modulates the interplay between akt and snail/slug signaling to restrain metastasis of lung cancer with multiple EGFR statuses. *J. Exp. Clin. Cancer Res.* 37 (1), 199. doi:10.1186/s13046-018-0869-1

Chatterjee, B., Ghosh, K., and Kanade, S. R. (2019). Resveratrol modulates epigenetic regulators of promoter histone methylation and acetylation that restores BRCA1, P53,

P21CIP1 in human breast cancer cell lines. *BioFactors* 45 (5), 818–829. doi:10.1002/biof.1544

Chen, X. J., Wu, M. Y., Li, D. H., and You, J. (2016). Apigenin inhibits glioma cell growth through promoting MicroRNA-16 and suppression of BCL-2 and nuclear factor-KB/MMP-9. *Mol. Med. Rep.* 14 (3), 2352–2358. doi:10.3892/mmr.2016.5460

Chiyomaru, T., Yamamura, S., Fukuhara, S., Hidaka, H., Majid, S., Saini, S., et al. (2013). Genistein up-regulates tumor suppressor MicroRNA-574-3p in prostate cancer. *PLoS One* 8 (3), e58929. doi:10.1371/journal.pone.0058929

Choi, B. Y., and Kim, B.-W. (2015). Withaferin-A inhibits colon cancer cell growth by blocking STAT3 transcriptional activity. *J. Cancer Prev.* 20 (3), 185–192. doi:10.15430/JCP.2015.20.3.185

Chung, F. F. L., and Herceg, Z. (2020). The promises and challenges of toxico-epigenomics: environmental chemicals and their impacts on the epigenome. *Environ. Health Perspect.* 128, 15001. doi:10.1289/EHP6104

Crowell, J. A., Korytko, P. J., Morrissey, R. L., Booth, T. D., and Levine, B. S. (2004). Resveratrol-associated renal toxicity. *Toxicol. Sci.* 82 (2), 614–619. doi:10.1093/toxsci/kfh263

Dai, E., Yu, X., Zhang, Y., Meng, F., Wang, S., Liu, X., et al. (2014). EpimiR: a database of curated mutual regulation between MiRNAs and epigenetic modifications. *Database* 2014, bau023. doi:10.1093/database/bau023

Dai, L., Chen, L., Wang, W., and Lin, P. (2020). Resveratrol inhibits ACHN cells via regulation of histone acetylation. *Pharm. Biol.* 58 (1), 231–238. doi:10.1080/13880209.2020.1738503

Dawood, M., Ooko, E., and Efferth, T. (2019). Collateral sensitivity of parthenolide via NF-κB and HIF-α inhibition and epigenetic changes in drug-resistant cancer cell lines. *Front. Pharmacol.* 10, 542. doi:10.3389/fphar.2019.00542

Dehan, P., Kustermans, G., Guenin, S., Horion, J., Boniver, J., and Delvenne, P. (2009). DNA methylation and cancer diagnosis: new methods and applications. *Expert Rev. Mol. Diagnostics* 9, 651–657. doi:10.1586/erm.09.53

Dittharot, K., Dakeng, S., Suebsakwong, P., Suksamrarn, A., Patmasiriwat, P., and Promkan, M. (2019). Cucurbitacin B induces hypermethylation of oncogenes in breast cancer cells. *Planta Med.* 85 (5), 370–378. doi:10.1055/a-0791-1591

Donovan, M. G., Selmin, O. I., Doetschman, T. C., and Romagnolo, D. F. (2019). Epigenetic activation of BRCA1 by genistein *in vivo* and triple negative breast cancer cells linked to antagonism toward aryl hydrocarbon receptor. *Nutrients* 11 (11), 2559. doi:10.3390/nu11112559

Dou, J., Wang, Z., Ma, L., Peng, B., Mao, K., Li, C., et al. (2018). Baicalein and baicalin inhibit colon cancer using two distinct fashions of apoptosis and senescence. *Oncotarget* 9 (28), 20089–20102. doi:10.18632/oncotarget.24015

Druesne, N., Pagniez, A., Mayeur, C., Thomas, M., Cherbuy, C., Duée, P. H., et al. (2004). Diallyl disulfide (DADS) increases histone acetylation and P21waf1/cip1 expression in human colon tumor cell lines. *Carcinogenesis* 25, 1227–1236. doi:10.1093/carcin/bgh123

Fang, L., Xu, W., and Kong, D. (2019). Icariin inhibits cell proliferation, migration and invasion by down-regulation of MicroRNA-625-3p in thyroid cancer cells. *Biomed. Pharmacother.* 109, 2456–2463. doi:10.1016/j.biopha.2018.04.012

Fang, M., Chen, D., and Yang, C. S. (2007). Dietary polyphenols may affect DNA methylation. *J. Nutr.* 137 (1), 223S-228S–228S. doi:10.1093/jn/137.1.223S

Fu, L. J., Ding, Y. B., Wu, L. X., Wen, C. J., Qu, Q., Zhang, X., et al. (2014). The effects of lycopene on the methylation of the GSTP1 promoter and global methylation in prostatic cancer cell lines PC3 and LNCaP. *Int. J. Endocrinol.* 2014, 620165. doi:10.1155/2014/620165

Fujimoto, A., Sakanashi, Y., Matsui, H., Oyama, T., Nishimura, Y., Masuda, T., et al. (2009). Cytometric analysis of cytotoxicity of polyphenols and related phenolics to rat thymocytes: potent cytotoxicity of resveratrol to normal cells. *Basic Clin. Pharmacol. Toxicol.* 104 (6), 455–462. doi:10.1111/j.1742-7843.2009.00386.x

Gallardo, M., Kemmerling, U., Aguayo, F., Bleak, T. C., Muñoz, J. P., and Calaf, G. M. (2020). Curcumin rescues breast cells from epithelial-mesenchymal transition and invasion induced by anti-miR-34a. *Int. J. Oncol.* 56, 480–493. doi:10.3892/ijo.2019.4939

Gama-Sosa, M. A., Slagel, V. A., Trewyn, R. W., Oxenhandler, R., Kuo, K. C., Gehrke, C. W., et al. (1983). The 5-methylcytosine content of DNA from human tumors. *Nucleic Acids Res.* 11 (19), 6883–6894. doi:10.1093/nar/11.19.6883

Gonelimali, F. D., Lin, J., Miao, W., Xuan, J., Charles, F., Chen, M., et al. (2018). Antimicrobial properties and mechanism of action of some plant extracts against Food pathogens and spoilage microorganisms. *Front. Microbiol.* 9, 1639. doi:10.3389/fmicb.2018.01639

Guldiken, B., Ozkan, G., Catalkaya, G., Ceylan, F. D., Ekin Yalcinkaya, I., and Capanoglu, E. (2018). Phytochemicals of herbs and spices: health versus toxicological effects. *Food Chem. Toxicol.* 119, 37–49. doi:10.1016/j.fct.2018.05.050

Guo, J., Mei, Y., Li, K., Huang, X., and Yang, H. (2016). Downregulation of MiR-17-92a cluster promotes autophagy induction in response to celastrol treatment in prostate cancer cells. *Biochem. Biophys. Res. Commun.* 478 (2), 804–810. doi:10.1016/j.bbrc.2016.08.029

Gupta, S. C., Hevia, D., Patchva, S., Park, B., Koh, W., and Aggarwal, B. B. (2012). Upsides and downsides of reactive oxygen species for cancer: the roles of reactive oxygen species in tumorigenesis, prevention, and therapy. *Antioxidants Redox Signal.* 1, 1295–1322. doi:10.1089/ars.2011.4414

Han, X., Liu, C. F., Gao, N., Zhao, J., and Xu, J. (2018). RETRACTED: kaempferol suppresses proliferation but increases apoptosis and autophagy by up-regulating microRNA-340 in human lung cancer cells. *Biomed. Pharmacother.* 108, 809–816. doi:10.1016/j.biopha.2018.09.087

Han, Y., Ma, L., Zhao, L., Feng, W., and Zheng, X. (2019). Rosmarinic inhibits cell proliferation, invasion and migration via up-regulating MiR-506 and suppressing MMP2/16 expression in pancreatic cancer. *Biomed. Pharmacother.* 115, 108878. doi:10.1016/j.biopha.2019.108878

Hang, S., Wang, X., and Li, H. (2019). Triptolide inhibits viability and migration while promotes apoptosis in nephroblastoma cells by regulation of MiR-193b-3p. *Exp. Mol. Pathol.* 108, 80–88. doi:10.1016/j.yexmp.2019.04.006

Henikoff, S., and Matzke, M. A. (1997). Exploring and explaining epigenetic effects. *Trends Genet.* 13 (8), 293–295. doi:10.1016/s0168-9525(97)01219-5

Hong, T., Nakagawa, T., Pan, W. J., Kim, M. Y., Kraus, W. L., Ikehara, T., et al. (2004). Isoflavones stimulate estrogen receptor-mediated core histone acetylation. *Biochem. Biophys. Res. Commun.* 317 (1), 259–264. doi:10.1016/j.bbrc.2004.03.041

Hsiao, Y. C., Peng, S. F., Lai, K. C., Liao, C. L., Huang, Y. P., Lin, C. C., et al. (2019). Genistein induces apoptosis *in vitro* and has antitumor activity against human leukemia HL-60 cancer cell xenograft growth *in vivo*. *Environ. Toxicol.* 34 (4), 443–456. doi:10.1002/tox.22698

Issa, J. P. J., and Kantarjian, H. M. (2009). Targeting DNA methylation. *Clin. Cancer Res.* 15 (12), 3938–3946. doi:10.1158/1078-0432.CCR-08-2783

Jang, S. Y., Hong, D., Jeong, S. Y., and Kim, J. H. (2015). Shikonin causes apoptosis by up-regulating P73 and down-regulating ICBP90 in human cancer cells. *Biochem. Biophys. Res. Commun.* 465 (1), 71–76. doi:10.1016/j.bbrc.2015.07.131

Jang, Y. G., Hwang, K. A., and Choi, K. C. (2018). Rosmarinic acid, a component of rosemary tea, induced the cell cycle arrest and apoptosis through modulation of HDAC2 expression in prostate cancer cell lines. *Nutrients* 10, 1784. doi:10.3390/nu10111784

Jefferson, W. N., Padilla-Banks, E., and Newbold, R. R. (2005). Adverse effects on female development and reproduction in CD-1 mice following neonatal exposure to the phytoestrogen genistein at environmentally relevant doses. *Biol. Reprod.* 73 (4), 798–806. doi:10.1095/biolreprod.105.041277

Jiang, A., Wang, X., Shan, X., Li, Y., Wang, P., Jiang, P., et al. (2015). Curcumin reactivates silenced tumor suppressor gene RARβ by reducing DNA methylation. *Phyther. Res.* 29, 1237–1245. doi:10.1002/ptr.5373

Kang, J., Chen, J., Shi, Y., Jia, J., and Zhang, Y. (2005). Curcumin-induced histone hypoacetylation: the role of reactive oxygen species. *Biochem. Pharmacol.* 69 (8), 1205–1213. doi:10.1016/j.bcp.2005.01.014

Kang, K. A., Piao, M. J., Hyun, Y. J., Zhen, A. X., Cho, S. J., Ahn, M. J., et al. (2019). Luteolin promotes apoptotic cell death via upregulation of Nrf2 expression by DNA demethylase and the interaction of Nrf2 with P53 in human colon cancer cells. *Exp. Mol. Med.* 51 (4), 1–14. doi:10.1038/s12276-019-0238-y

Karimi Dermani, F., Saidijam, M., Amini, R., Mahdavinezhad, A., Heydari, K., and Najafi, R. (2017). Resveratrol inhibits proliferation, invasion, and epithelial–mesenchymal transition by increasing MiR-200c expression in HCT-116 colorectal cancer cells. *J. Cell. Biochem.* 118 (6), 1547–1555. doi:10.1002/jcb.25816

Kedhari Sundaram, M., Hussain, A., Haque, S., Raina, R., and Afroze, N. (2019). Quercetin modifies 5′CpG promoter methylation and reactivates various tumor suppressor genes by modulating epigenetic marks in human cervical cancer cells. *J. Cell. Biochem.* 120 (10), 18357–18369. doi:10.1002/jcb.29147

Khan, A., Mohammad, T., Shamsi, A., Hussain, A., Alajmi, M. F., Husain, S. A., et al. (2021b). Identification of plant-based hexokinase 2 inhibitors: combined molecular docking and dynamics simulation studies. *J. Biomol. Struct. Dyn.* 40, 10319–10331. doi:10.1080/07391102.2021.1942217

Khan, A., Siddiqui, S., Husain, S. A., Mazurek, S., and Iqbal, M. A. (2021a). Phytocompounds targeting metabolic reprogramming in cancer: an assessment of role, mechanisms, pathways, and therapeutic relevance. *J. Agric. Food Chem.* 16, 6897–6928. doi:10.1021/acs.jafc.1c01173

Kim, D.-Y., Kim, S.-H., Cheong, H.-T., Ra, C.-S., Rhee, K.-J., and Jung, B. D. (2020). Berberine induces P53-dependent apoptosis through inhibition of DNA Methyltransferase3b in Hep3B cells. *Korean J. Clin. Lab. Sci.* 52 (1), 69–77. doi:10.15324/kjcls.2020.52.1.69

Kornberg, R. D., and Lorch, Y. (1999). Twenty-five years of the nucleosome, fundamental particle of the eukaryote chromosome. *Cell* 98, 285–294. doi:10.1016/s0092-8674(00)81958-3

Kouzarides, T. (2007). Chromatin modifications and their function. *Cell* 23, 693–705. doi:10.1016/j.cell.2007.02.005

Krifa, M., Leloup, L., Ghedira, K., Mousli, M., and Chekir-Ghedira, L. (2014). Luteolin induces apoptosis in BE colorectal cancer cells by downregulating calpain, UHRF1, and DNMT1 expressions. *Nutr. Cancer* 66 (7), 1220–1227. doi:10.1080/01635581.2014.951729

Kundu, J. K., and Surh, Y. J. (2009). Molecular basis of chemoprevention with dietary phytochemicals: redox-regulated transcription factors as relevant targets. *Phytochem. Rev.* 8 (2), 333–347. doi:10.1007/s11101-009-9132-x

Kunnumakkara, A. B., Bordoloi, D., Harsha, C., Banik, K., Gupta, S. C., and Aggarwal, B. B. (2017). Curcumin mediates anticancer effects by modulating multiple cell signaling pathways. *Clin. Sci.* 1, 1781–1799. doi:10.1042/CS20160935

Kuppusamy, P., Nagalingam, A., Muniraj, N., Saxena, N. K., and Sharma, D. (2017). Concomitant activation of ETS-like transcription factor-1 and death receptor-5 via extracellular signal-regulated kinase in withaferin A-mediated inhibition of hepatocarcinogenesis in mice. *Sci. Rep.* 7 (1), 17943. doi:10.1038/s41598-017-18190-4

Lea, M. A., Randolph, V. M., Lee, J. E., and DesBordes, C. (2001). Induction of histone acetylation in mouse erythroleukemia cells by some organosulfur compounds including allyl isothiocyanate. *Int. J. Cancer* 92 (6), 784–789. doi:10.1002/ijc.1277

Lee, W. J., Chen, Y. R., and Tseng, T. H. (2011). Quercetin induces FasL-related apoptosis, in part, through promotion of histone H3 acetylation in human leukemia HL-60 cells. *Oncol. Rep.* 25 (2), 583–591. doi:10.3892/or.2010.1097

Li, B. B., Huang, G. L., Li, H. H., Kong, X., and He, Z. W. (2017). Epigallocatechin-3-Gallate modulates MicroRNA expression profiles in human nasopharyngeal carcinoma CNE2 cells. *Chin. Med. J. Engl.* 130 (1), 93–99. doi:10.4103/0366-6999.196586

Li, D., Chen, L., Zhao, W., Hao, J., and An, R. (2016). MicroRNA-Let-7f-1 is induced by lycopene and inhibits cell proliferation and triggers apoptosis in prostate cancer. *Mol. Med. Rep.* 13 (3), 2708–2714. doi:10.3892/mmr.2016.4841

Li, Y., and Sarkar, F. H. (2016). Role of BioResponse 3,3′-diindolylmethane in the treatment of human prostate cancer: clinical experience. *Med. Princ. Pract.* 25 (2), 11–17. doi:10.1159/000439307

Li, Y., Sun, W., Han, N., Zou, Y., and Yin, D. (2018). Curcumin inhibits proliferation, migration, invasion and promotes apoptosis of retinoblastoma cell lines through modulation of MiR-99a and JAK/STAT pathway. *BMC Cancer* 18 (1), 1230. doi:10.1186/s12885-018-5130-y

Link, A., Balaguer, F., Shen, Y., Lozano, J. J., Leung, H. C. E., Boland, C. R., et al. (2013). Curcumin modulates DNA methylation in colorectal cancer cells. *PLoS One* 8 (2), e57709. doi:10.1371/journal.pone.0057709

Liu, H. L., Chen, Y., Cui, G. H., and Zhou, J. F. (2005). Curcumin, a potent anti-tumor reagent, is a novel histone deacetylase inhibitor regulating B-nhl cell line Raji proliferation. *Acta Pharmacol. Sin.* 26 (5), 603–609. doi:10.1111/j.1745-7254.2005.00081.x

Liu, J., Li, M., Wang, Y., and Luo, J. (2017). Curcumin sensitizes prostate cancer cells to radiation partly via epigenetic activation of MiR-143 and MiR-143 mediated autophagy inhibition. *J. Drug Target.* 25 (7), 645–652. doi:10.1080/1061186X.2017.1315686

Liu, X., Li, H., Wu, M. L., Wu, J., Sun, Y., Zhang, K. L., et al. (2019b). Resveratrol reverses retinoic acid resistance of anaplastic thyroid cancer cells via demethylating CRABP2 gene. *Front. Endocrinol. (Lausanne).* 10, 734. doi:10.3389/fendo.2019.00734

Liu, Z., Gao, Y., and Li, X. (2019a). Cancer epigenetics and the potential of epigenetic drugs for treating solid tumors. *Expert Rev. Anticancer Ther.* 19, 139–149. doi:10.1080/14737140.2019.1552139

López-Lázaro, M. (2008). Anticancer and carcinogenic properties of curcumin: considerations for its clinical development as a cancer chemopreventive and chemotherapeutic agent. *Mol. Nutr. Food Res.* 52, S103–S127. doi:10.1002/mnfr.200700238

Lubin, F. D., Gupta, S., Parrish, R. R., Grissom, N. M., and Davis, R. L. (2011). Epigenetic mechanisms: critical contributors to long-term memory formation. *Neurosci* 17 (6), 616–632. doi:10.1177/1073858411386967

Luger, K., and Richmond, T. J. (1998). The histone tails of the nucleosome. *Curr. Opin. Genet. Dev.* 8, 140–146. doi:10.1016/s0959-437x(98)80134-2

Ma, L., Feugang, J. M., Konarski, P., Wang, J., Lu, J., Fu, S., et al. (2006). Growth inhibitory effects of quercetin on bladder cancer cell. *Front. Biosci.* 11 (Suppl. 1), 2275–2285. doi:10.2741/1970

Majid, S., Kikuno, N., Nelles, J., Noonan, E., Tanaka, Y., Kawamoto, K., et al. (2008). Genistein induces the P21WAF1/CIP1 and P16INK4a tumor suppressor genes in prostate cancer cells by epigenetic mechanisms involving active chromatin modification. *Cancer Res.* 68 (8), 2736–2744. doi:10.1158/0008-5472.CAN-07-2290

Malik, Z., Parveen, R., Parveen, B., Zahiruddin, S., Aasif Khan, M., Khan, A., et al. (2021). Anticancer potential of andrographolide from andrographis paniculata (Burm.f.) nees and its mechanisms of action. *J. Ethnopharmacol.* 272, 113936. doi:10.1016/j.jep.2021.113936

Martin, S. L., Kala, R., and Tollefsbol, T. O. (2017). Mechanisms for the inhibition of colon cancer cells by sulforaphane through epigenetic modulation of MicroRNA-21 and human telomerase reverse Transcriptase (HTERT) down-regulation. *Curr. Cancer Drug Targets* 18 (1), 97–106. doi:10.2174/1568009617666170206104032

Matsukawa, Y., Nishino, H., Yoshida, M., Sugihara, H., Katsura, K., Takamatsu, T., et al. (2002). Quercetin enhances tumorigenicity induced by N-ethyl-N'-Nitro-N-nitrosoguanidine in the duodenum of mice. *Environ. Health Prev. Med.* 6 (4), 235–239. doi:10.1007/BF02897975

Mishra, S., Yadav, T., and Rani, V. (2016). Exploring MiRNA based approaches in cancer diagnostics and therapeutics. *Crit. Rev. Oncology/Hematology* 98, 12–23. doi:10.1016/j.critrevonc.2015.10.003

Mitsiogianni, M., Trafalis, D. T., Franco, R., Zoumpourlis, V., Pappa, A., and Panayiotidis, M. I. (2020). Sulforaphane and iberin are potent epigenetic modulators of histone acetylation and methylation in malignant melanoma. *Eur. J. Nutr.* 60, 147–158. doi:10.1007/s00394-020-02227-y

Mohammadi, K., Sani, M. A., Azizi-Lalabadi, M., and McClements, D. J. (2022). Recent progress in the application of plant-based colloidal drug delivery systems in the pharmaceutical Sciences. *Adv. Colloid Interface Sci.* 307, 102734. doi:10.1016/j.cis.2022.102734

Montgomery, M., and Srinivasan, A. (2019). Epigenetic gene regulation by dietary compounds in cancer prevention. *Adv. Nutr.* 10, 1012–1028. doi:10.1093/advances/nmz046

Mottet, D., and Castronovo, V. (2008). Histone deacetylases: target enzymes for cancer therapy. *Clin. Exp. Metastasis* 25, 183–189. doi:10.1007/s10585-007-9131-5

Mu, J., Zhu, D., Shen, Z., Ning, S., Liu, Y., Chen, J., et al. (2017). The repressive effect of MiR-148a on wnt/β-catenin signaling involved in glabridin-induced anti-angiogenesis in human breast cancer cells. *BMC Cancer* 17 (1), 307. doi:10.1186/s12885-017-3298-1

Nandakumar, V., Vaid, M., and Katiyar, S. K. (2011). (-)-Epigallocatechin-3-Gallate reactivates silenced tumor suppressor genes, Cip1/P21 and P16INK4a, by reducing DNA methylation and increasing histones acetylation in human skin cancer cells. *Carcinogenesis* 32, 537–544. doi:10.1093/carcin/bgq285

Nardi, I., Reno, T., Yun, X., Sztain, T., Wang, J., Dai, H., et al. (2018). Triptolide inhibits wnt signaling in NSCLC through upregulation of multiple wnt inhibitory factors via epigenetic modifications to histone H3. *Int. J. Cancer* 143 (10), 2470–2478. doi:10.1002/ijc.31756

Nouriemamzaden, F., Word, B., Cotton, E., Hawkins, A., Littlejohn, K., Moore, R., et al. (2020). Modulation of estrogen α and progesterone receptors in triple negative breast cancer cell lines: the effects of vorinostat and indole-3-carbinol *in vitro*. *Anticancer Res.* 40 (7), 3669–3683. doi:10.21873/anticanres.14356

Okano, M., Bell, D. W., Haber, D. A., and Li, E. (1999). DNA methyltransferases Dnmt3a and Dnmt3b are essential for *de novo* methylation and mammalian development. *Cell* 99 (3), 247–257. doi:10.1016/s0092-8674(00)81656-6

Paluszczak, J., Krajka-Kuźniak, V., and Baer-Dubowska, W. (2010). The effect of dietary polyphenols on the epigenetic regulation of gene expression in MCF7 breast cancer cells. *Toxicol. Lett.* 192, 119–125. doi:10.1016/j.toxlet.2009.10.010

Pan, L., Feng, F., Wu, J., Fan, S., Han, J., Wang, S., et al. (2022). Demethylzeylasteral targets lactate by inhibiting histone lactylation to suppress the tumorigenicity of liver cancer stem cells. *Pharmacol. Res.* 181, 106270. doi:10.1016/j.phrs.2022.106270

Pandey, M., Kaur, P., Shukla, S., Abbas, A., Fu, P., and Gupta, S. (2012). Plant flavone apigenin inhibits HDAC and remodels chromatin to induce growth arrest and apoptosis in human prostate cancer cells: *in vitro* and *in vivo* study. *Mol. Carcinog.* 51 (12), 952–962. doi:10.1002/mc.20866

Pandey, M., Shukla, S., and Gupta, S. (2010). Promoter demethylation and chromatin remodeling by green tea polyphenols leads to Re-expression of GSTP1 in human prostate cancer cells. *Int. J. Cancer* 126 (11), 2520–2533. doi:10.1002/ijc.24988

Pani, S., Sahoo, A., Patra, A., and Debata, P. R. (2020). Phytocompounds curcumin, quercetin, indole-3-carbinol, and resveratrol modulate lactate–pyruvate level along with cytotoxic activity in HeLa cervical cancer cells. *Biotechnol. Appl. Biochem.* 68, 1396–1402. doi:10.1002/bab.2061

Parbin, S., Shilpi, A., Kar, S., Pradhan, N., Sengupta, D., Deb, M., et al. (2016). Insights into the molecular interactions of thymoquinone with histone deacetylase: evaluation of the therapeutic intervention potential against breast cancer. *Mol. Biosyst.* 12 (1), 48–58. doi:10.1039/c5mb00412h

Paredes-Gonzalez, X., Fuentes, F., Su, Z. Y., and Kong, A. N. T. (2014). Apigenin reactivates Nrf2 anti-oxidative stress signaling in mouse skin epidermal JB6 P + cells through epigenetics modifications. *AAPS J.* 16 (4), 727–735. doi:10.1208/s12248-014-9613-8

Payer, B., and Lee, J. T. (2008). X chromosome dosage compensation: how mammals keep the balance. *Annu. Rev. Genet.* 42, 733–772. doi:10.1146/annurev.genet.42.110807.091711

Peng, Z., and Zhang, Y. (2017). Methyl jasmonate induces the apoptosis of human colorectal cancer cells via downregulation of EZH2 expression by MicroRNA-101. *Mol. Med. Rep.* 15 (2), 957–962. doi:10.3892/mmr.2016.6061

Pfeffer, C. M., and Singh, A. T. K. (2018). Apoptosis: a target for anticancer therapy. *Int. J. Mol. Sci.* 2, 448. doi:10.3390/ijms19020448

Phan, M. A. T., Paterson, J., Bucknall, M., and Arcot, J. (2018). Interactions between phytochemicals from fruits and vegetables: effects on bioactivities and bioavailability. *Crit. Rev. Food Sci. Nutr.* 58 (8), 1310–1329. doi:10.1080/10408398.2016.1254595

Prajapati, K. S., Shuaib, M., Gupta, S., and Kumar, S. (2022). Withaferin A mediated changes of MiRNA expression in breast cancer-derived mammospheres. *Mol. Carcinog.* 61 (9), 876–889. doi:10.1002/mc.23440

Prasad, S., Gupta, S. C., and Tyagi, A. K. (2017). Reactive oxygen species (ROS) and cancer: role of antioxidative nutraceuticals. *Cancer Lett.* 28, 95–105. doi:10.1016/j.canlet.2016.03.042

Prasad, S., Yadav, V. R., Sung, B., Reuter, S., Kannappan, R., Deorukhkar, A., et al. (2012). Ursolic acid inhibits growth and metastasis of human, colorectal cancer in an orthotopic nude mouse model by targeting multiple cell signaling pathways: chemosensitization with capecitabine. *Clin. Cancer Res.* 18 (18), 4942–4953. doi:10.1158/1078-0432.CCR-11-2805

Qazi, A., Pal, J., Maitah, M., Fulciniti, M., Pelluru, D., Nanjappa, P., et al. (2010). Anticancer activity of a broccoli derivative, sulforaphane, in barrett adenocarcinoma: potential use in chemoprevention and as adjuvant in chemotherapy. *Transl. Oncol.* 3 (6), 389–399. doi:10.1593/tlo.10235

Qin, W., Zhang, K., Clarke, K., Weiland, T., and Sauter, E. R. (2014). Methylation and MiRNA effects of resveratrol on mammary tumors vs. Normal tissue. *Nutr. Cancer* 66 (2), 270–277. doi:10.1080/01635581.2014.868910

Reunanen, N., and Kähäri, V. (2013). "Matrix metalloproteinases in cancer cell invasion," in *Madame curie bioscience database* (Austin, TX: Landes Bioscience).

Sadakierska-Chudy, A. (2020). Micrornas: diverse mechanisms of action and their potential applications as cancer epi-therapeutics. *Biomolecules* 10, 1285. doi:10.3390/biom10091285

Safi-Stibler, S., and Gabory, A. (2020). Epigenetics and the developmental origins of health and disease: parental environment signalling to the epigenome, critical time windows and sculpting the adult phenotype. *Seminars Cell Dev. Biol.* 97, 172–180. doi:10.1016/j.semcdb.2019.09.008

Salehi, B., Ata, A., Kumar, N. V. A., Sharopov, F., Ramírez-Alarcón, K., Ruiz-Ortega, A., et al. (2019). Antidiabetic potential of medicinal plants and their active components. *Biomolecules* 9, 551. doi:10.3390/biom9100551

Santi, D. V., Garrett, C. E., and Barr, P. J. (1983). On the mechanism of inhibition of DNA-cytosine methyltransferases by cytosine analogs. *Cell* 33, 9–10. doi:10.1016/0092-8674(83)90327-6

Setoyama, T., Ling, H., Natsugoe, S., and Calin, G. A. (2011). Non-coding RNAs for medical practice in oncology. *Keio J. Med.* 60 (4), 106–113. doi:10.2302/kjm.60.106

Shankar, S., Ganapathy, S., and Srivastava, R. K. (2007). Green tea polyphenols: biology and therapeutic implications in cancer. *Front. Biosci.* 12, 4881–4899. doi:10.2741/2435

Sheng, J., Shi, W., Guo, H., Long, W., Wang, Y., Qi, J., et al. (2019). The inhibitory effect of (-)-Epigallocatechin-3 -gallate on breast cancer progression via reducing SCUBE2 methylation and DNMT activity. *Molecules* 24 (16), 2899. doi:10.3390/molecules24162899

Shi, Q., Li, J., Feng, Z., Zhao, L., Luo, L., You, Z., et al. (2014). Effect of ginsenoside Rh2 on the migratory ability of HepG2 liver carcinoma cells: recruiting histone deacetylase and inhibiting activator protein 1 transcription factors. *Mol. Med. Rep.* 10 (4), 1779–1785. doi:10.3892/mmr.2014.2392

Shruti, K., Shrey, K., and Vibha, R. (2011). Micro RNAs: tiny sequences with enormous potential. *Biochem. Biophys. Res. Commun.* 15, 445–449. doi:10.1016/j.bbrc.2011.03.058

Shu, L., Khor, T. O., Lee, J. H., Boyanapalli, S. S. S., Huang, Y., Wu, T. Y., et al. (2011). Epigenetic CpG demethylation of the promoter and reactivation of the expression of Neurog1 by curcumin in prostate LNCaP cells. *AAPS J.* 13 (4), 606–614. doi:10.1208/s12248-011-9300-y

Singh, P., Mishra, S. K., Noel, S., Sharma, S., and Rath, S. K. (2012). Acute exposure of apigenin induces hepatotoxicity in Swiss mice. *PLoS One* 7, e31964. doi:10.1371/journal.pone.0031964

Singh, S., Sharma, B., Kanwar, S. S., and Kumar, A. (2016). Lead phytochemicals for anticancer drug development. *Front. Plant Sci.* 7, 1667. doi:10.3389/fpls.2016.01667

Smith, C. J., and Ryckman, K. K. (2015). Epigenetic and developmental influences on the risk of obesity, diabetes, and metabolic syndrome. *Diabetes, Metabolic Syndrome Obes.* 8, 295–302. doi:10.2147/DMSO.S61296

Su, C. C., Lin, J. G., Li, T. M., Chung, J. G., Yang, J. S., Ip, S. W., et al. (2006). Curcumin-induced apoptosis of human colon cancer colo 205 cells through the production of ROS, Ca2+ and the activation of caspase-3. *Anticancer Res.* 26, 4379–4389.

Suman, S., Das, T. P., Sirimulla, S., Alatassi, H., Ankem, M. K., and Damodaran, C. (2016). Withaferin-A suppress AKT induced tumor growth in colorectal cancer cells. *Oncotarget* 7 (12), 13854–13864. doi:10.18632/oncotarget.7351

Sundaram, M. K., Unni, S., Somvanshi, P., Bhardwaj, T., Mandal, R. K., Hussain, A., et al. (2019). Genistein modulates signaling pathways and targets several epigenetic markers in hela cells. *Genes (Basel).* 10 (12), 955. doi:10.3390/genes10120955

Sung, H., Ferlay, J., Siegel, R. L., Laversanne, M., Soerjomataram, I., Jemal, A., et al. (2021). Global cancer statistics 2020: GLOBOCAN estimates of incidence and mortality worldwide for 36 cancers in 185 countries. *Ca. Cancer J. Clin.* 71, 209–249. doi:10.3322/caac.21660

Svoronos, A. A., Engelman, D. M., and Slack, F. J. (2016). OncomiR or tumor suppressor? The duplicity of MicroRNAs in cancer. *Cancer Res.* 1, 3666–3670. doi:10.1158/0008-5472.CAN-16-0359

Tan, B. L., and Norhaizan, M. E. (2019). Curcumin combination chemotherapy: the implication and efficacy in cancer. *Molecules* 24, 2527. doi:10.3390/molecules24142527

Tang, J., Wang, Z., Chen, L., Huang, G., and Hu, X. (2015). Gossypol acetate induced apoptosis of pituitary tumor cells by targeting the BCL-2 via the upregulated MicroRNA MiR-15a. *Int. J. Clin. Exp. Med.* 8 (6), 9079–9085.

Tao, S. F., He, H. F., and Chen, Q. (2015). Quercetin inhibits proliferation and invasion acts by up-regulating MiR-146a in human breast cancer cells. *Mol. Cell. Biochem.* 402 (1–2), 93–100. doi:10.1007/s11010-014-2317-7

Tao, Y., Zhan, S., Wang, Y., Zhou, G., Liang, H., Chen, X., et al. (2018). Baicalin, the major component of traditional Chinese medicine scutellaria baicalensis induces colon cancer cell apoptosis through inhibition of OncomiRNAs. *Sci. Rep.* 8 (1), 14477. doi:10.1038/s41598-018-32734-2

Thakur, V. S., Gupta, K., and Gupta, S. (2012). Green tea polyphenols increase P53 transcriptional activity and acetylation by suppressing class I histone deacetylases. *Int. J. Oncol.* 41 (1), 353–361. doi:10.3892/ijo.2012.1449

Thangapazham, R. L., Singh, A. K., Sharma, A., Warren, J., Gaddipati, J. P., and Maheshwari, R. K. (2007). Green tea polyphenols and its constituent epigallocatechin gallate inhibits proliferation of human breast cancer cells *in vitro* and *in vivo*. *Cancer Lett.* 245 (1–2), 232–241. doi:10.1016/j.canlet.2006.01.027

Torabi, K., Miró, R., Fernández-Jiménez, N., Quintanilla, I., Ramos, L., Prat, E., et al. (2015). Patterns of somatic uniparental disomy identify novel tumor suppressor genes in colorectal cancer. *Carcinogenesis* 36 (10), 1103–1110. doi:10.1093/carcin/bgv115

Tsang, W. P., and Kwok, T. T. (2010). Epigallocatechin gallate up-regulation of MiR-16 and induction of apoptosis in human cancer cells. *J. Nutr. Biochem.* 21 (2), 140–146. doi:10.1016/j.jnutbio.2008.12.003

Tseng, T. H., Chien, M. H., Lin, W. L., Wen, Y. C., Chow, J. M., Chen, C. K., et al. (2017). Inhibition of MDA-MB-231 breast cancer cell proliferation and tumor growth by apigenin through induction of G2/M arrest and histone H3 acetylation-mediated P21WAF1/CIP1 expression. *Environ. Toxicol.* 32 (2), 434–444. doi:10.1002/tox.22247

Tuna, M., Knuutila, S., and Mills, G. B. (2009). Uniparental disomy in cancer. *Trends Mol. Med.* 15, 120–128. doi:10.1016/j.molmed.2009.01.005

Van Hoesel, A. Q., Sato, Y., Elashoff, D. A., Turner, R. R., Giuliano, A. E., Shamonki, J. M., et al. (2013). Assessment of DNA methylation status in early stages of breast cancer development. *Br. J. Cancer* 108 (10), 2033–2038. doi:10.1038/bjc.2013.136

vel Szic, K. S., Declerck, K., Crans, R. A. J., Diddens, J., Scherf, D. B., Gerhäuser, C., et al. (2017). Epigenetic silencing of triple negative breast cancer hallmarks by withaferin A. *Oncotarget* 8, 40434–40453. doi:10.18632/oncotarget.17107

Verma, S. (2016). Medicinal plants with anti-inflammatory activity. *J. Phytopharm.* 5 (4), 157–159. doi:10.31254/phyto.2016.5407

Wang, D., Wang, Y., Wan, X., Yang, C. S., and Zhang, J. (2015). Green tea polyphenol (-)-Epigallocatechin-3-Gallate triggered hepatotoxicity in mice: responses of major antioxidant enzymes and the Nrf2 rescue pathway. *Toxicol. Appl. Pharmacol.* 283 (1), 65–74. doi:10.1016/j.taap.2014.12.018

Wang, J., Li, Y., Wang, X., and Jiang, C. (2012). Ursolic acid inhibits proliferation and induces apoptosis in human glioblastoma cell lines U251 by suppressing TGF-β1/MiR-21/PDCD4 pathway. *Basic Clin. Pharmacol. Toxicol.* 111, 106–112. doi:10.1111/j.1742-7843.2012.00870.x

Wang, J., Wu, M., Zheng, D., Zhang, H., Lv, Y., Zhang, L., et al. (2020). Garcinol inhibits esophageal cancer metastasis by suppressing the P300 and TGF-β1 signaling pathways. *Acta Pharmacol. Sin.* 41 (1), 82–92. doi:10.1038/s41401-019-0271-3

Wang, L. G., Beklemisheva, A., Liu, X. M., Ferrari, A. C., Feng, J., and Chiao, J. W. (2007). Dual action on promoter demethylation and chromatin by an isothiocyanate restored GSTP1 silenced in prostate cancer. *Mol. Carcinog.* 46 (1), 24–31. doi:10.1002/mc.20258

Wei, D., Yang, L., Lv, B., and Chen, L. (2017). Genistein suppresses retinoblastoma cell viability and growth and induces apoptosis by upregulating MiR-145 and inhibiting its target ABCE1. *Mol. Vis.* 23, 385–394.

Wen, X. Y., Wu, S. Y., Li, Z. Q., Liu, Z. Q., Zhang, J. J., Wang, G. F., et al. (2009). Ellagitannin (BJA3121), an anti-proliferative natural polyphenol compound, can regulate the expression of MiRNAs in HepG2 cancer cells. *Phyther. Res.* 23, 778–784. doi:10.1002/ptr.2616

Wong, C. P., Hsu, A., Buchanan, A., Palomera-Sanchez, Z., Beaver, L. M., Houseman, E. A., et al. (2014). Effects of sulforaphane and 3,3′-diindolylmethane on genome-wide promoter methylation in normal prostate epithelial cells and prostate cancer cells. *PLoS One* 9 (1), e86787. doi:10.1371/journal.pone.0086787

Wu, S., Lu, H., and Bai, Y. (2019). Nrf2 in cancers: a double-edged sword. *Cancer Med.* 8, 2252–2267. doi:10.1002/cam4.2101

Xhemalce, B., Dawson, M. A., and Bannister, A. J. (2011). "Histone modifications," in *Encyclopedia of molecular cell biology and molecular medicine* (American Cancer Society).

Xiao, L., Huang, Y., Zhen, R., Chiao, J. W., Liu, D., and Ma, X. (2010). Deficient histone acetylation in acute leukemia and the correction by an isothiocyanate. *Acta Haematol.* 123 (2), 71–76. doi:10.1159/000264628

Xiao, Y., Hale, S., Awasthee, N., Meng, C., Zhang, X., Liu, Y., et al. (2023). HDAC3 and HDAC8 PROTAC dual degrader reveals roles of histone acetylation in gene regulation. *Cell Chem. Biol.* doi:10.1016/j.chembiol.2023.07.010

Xiao, Z., Morris-Natschke, S. L., and Lee, K. H. (2016). Strategies for the optimization of natural leads to anticancer drugs or drug candidates. *Med. Res. Rev.* 36 (1), 32–91. doi:10.1002/med.21377

Yan, X., Xie, T., Wang, S., Wang, Z., Li, H. Y., and Ye, Z. M. (2018). Apigenin inhibits proliferation of human chondrosarcoma cells via cell cycle arrest and mitochondrial apoptosis induced by ROS generation-an *in vitro* and *in vivo* study. *J. Clin. Exp. Med.* 11 (3), 1615–1631.

Ye, Y., Fang, Y., Xu, W., Wang, Q., Zhou, J., and Lu, R. (2016). 3,3′-Diindolylmethane induces anti-human gastric cancer cells by the MiR-30e-ATG5 modulating autophagy. *Biochem. Pharmacol.* 115, 77–84. doi:10.1016/j.bcp.2016.06.018

Yin, L., Xiao, X., Georgikou, C., Luo, Y., Liu, L., Gladkich, J., et al. (2019). Sulforaphane induces MiR135b-5p and its target gene, RASAL2, thereby inhibiting the progression of pancreatic cancer. *Mol. Ther. - Oncolytics* 14, 74–81. doi:10.1016/j.omto.2019.03.011

Yoshino, M., Haneda, M., Naruse, M., Htay, H. H., Tsubouchi, R., Qiao, S. L., et al. (2004). Prooxidant activity of curcumin: copper-dependent formation of 8-hydroxy-2′-deoxyguanosine in DNA and induction of apoptotic cell death. *Toxicol. Vitr.* 18 (6), 783–789. doi:10.1016/j.tiv.2004.03.009

Yun, C. W., and Lee, S. H. (2018). The roles of autophagy in cancer. *Int. J. Mol. Sci.* 19, 3466. doi:10.3390/ijms19113466

Zhang, B., Wang, Q., and Pan, X. (2007). MicroRNAs and their regulatory roles in animals and plants. *J. Cell. Physiology* 210, 279–289. doi:10.1002/jcp.20869

Zhang, C., Shu, L., Kim, H., Khor, T. O., Wu, R., Li, W., et al. (2016). Phenethyl isothiocyanate (PEITC) suppresses prostate cancer cell invasion epigenetically through regulating MicroRNA-194. *Mol. Nutr. Food Res.* 60 (6), 1427–1436. doi:10.1002/mnfr.201500918

Zhang, D., Tang, Z., Huang, H., Zhou, G., Cui, C., Weng, Y., et al. (2019). Metabolic regulation of gene expression by histone lactylation. *Nature* 574 (7779), 575–580. doi:10.1038/s41586-019-1678-1

Zhang, H., Jia, R., Wang, C., Hu, T., and Wang, F. (2014). Piceatannol promotes apoptosis via up-regulation of MicroRNA-129 expression in colorectal cancer cell lines. *Biochem. Biophys. Res. Commun.* 452 (3), 775–781. doi:10.1016/j.bbrc.2014.08.150

Zhang, Y., Huang, L., Shi, H., Chen, H., Tao, J., Shen, R., et al. (2018). Ursolic acid enhances the therapeutic effects of oxaliplatin in colorectal cancer by inhibition of drug resistance. *Cancer Sci.* 109 (1), 94–102. doi:10.1111/cas.13425

Zhang, Y., Li, Q., Zhou, D., and Chen, H. (2013). Genistein, a soya isoflavone, prevents azoxymethane-induced up-regulation of WNT/β-Catenin signalling and reduces colon pre-neoplasia in rats. *Br. J. Nutr.* 109 (1), 33–42. doi:10.1017/S0007114512000876

Zhao, J., Fang, Z., Zha, Z., Sun, Q., Wang, H., Sun, M., et al. (2019). Quercetin inhibits cell viability, migration and invasion by regulating MiR-16/HOXA10 Axis in oral cancer. *Eur. J. Pharmacol.* 847, 11–18. doi:10.1016/j.ejphar.2019.01.006

Zheng, M., and Wu, Y. (2020). Piceatannol suppresses proliferation and induces apoptosis by regulation of the MicroRNA-21/phosphatase and tensin homolog/protein kinase B signaling pathway in osteosarcoma cells. *Mol. Med. Rep.* 22 (5), 3985–3993. doi:10.3892/mmr.2020.11484

Zhou, J., Liu, M., Chen, Y., Xu, S., Guo, Y., and Zhao, L. (2019b). Cucurbitacin B suppresses proliferation of pancreatic cancer cells by CeRNA: effect of MiR-146b-5p and LncRNA-AFAP1-AS1. *J. Cell. Physiol.* 234 (4), 4655–4667. doi:10.1002/jcp.27264

Zhou, J. W., Wang, M., Sun, N. X., Qing, Y., Yin, T. F., Li, C., et al. (2019a). Sulforaphane-induced epigenetic regulation of Nrf2 expression by DNA methyltransferase in human caco-2 cells. *Oncol. Lett.* 18 (3), 2639–2647. doi:10.3892/ol.2019.10569

Zhu, W. Q., Wang, J., Guo, X. F., Liu, Z., and Dong, W. G. (2016). Thymoquinone inhibits proliferation in gastric cancer via the STAT3 pathway *in vivo* and *in vitro*. *World J. Gastroenterol.* 22 (16), 4149–4159. doi:10.3748/wjg.v22.i16.4149

Zoghbi, H. Y., and Beaudet, A. L. (2016). Epigenetics and human disease. *Cold Spring Harb. Perspect. Biol.* 8 (2), a019497. doi:10.1101/cshperspect.a019497

Zuo, Q., Wu, R., Xiao, X., Yang, C., Yang, Y., Wang, C., et al. (2018). The dietary flavone luteolin epigenetically activates the Nrf2 pathway and blocks cell transformation in human colorectal cancer HCT116 cells. *J. Cell. Biochem.* 119 (11), 9573–9582. doi:10.1002/jcb.27275

Glossary

ABCE1	ATP-binding cassette subfamily E, member 1
ADAM8	ADAM Metallopeptidase Domain 8
ATG5	Autophagy related 5
BAX	BCL2 Associated X
BCL2L11	Bcl-2-like protein 11
BMP1	Bone Morphogenetic Protein 1
BNIP3	BCL2 Interacting Protein 3
BRCA-1	Breast Cancer gene 1
CCND1	Cyclin D1
CDH1	Cadherin-1
CRABP2	Cellular retinoic acid-binding protein 2
DAPK1	Death-Associated Protein Kinase 1
DNMT	DNA methyl transferases
EGCG	Epigallocatechin-3-gallate
EPHB2	Ephrin type-B receptor 2
FHIT	Fragile Histidine Triad Diadenosine Triphosphatase
GFPT2	glutamine-fructose-6-phosphate transaminase 2
GLRX2	glutaredoxin 2
GNAT	Gcn5-related N-acetyltransferase
GSTM1	glutathione S-transferase mu 1
GSTP1	Glutathione S-transferase pi 1
HAT	Histone acetyltransferases
HDAC	Histone deacetylases
hMLH1	mutL homolog 1
HMT	Histone methyltransferases
JAK1	Janus Kinase1
MAPK	mitogen-activated protein kinase
ME3	malic enzyme 3
MGMT	O-6-Methylguanine-DNA Methyltransferase
MMP	Matrix metalloproteinases
Neurog-1	Neurogenin 1
Nrf2	nuclear factor erythroid 2–related factor 2
PDCD4	Programmed cell death protein 4
PI3K	Phosphatidylinositol-3-kinase
PLAU	Plasminogen Activator, Urokinase
PTEN	Phosphatase and tensin homolog
RARβ	retinoic acid receptor beta
RASSF1A	Ras association domain family 1 isoform A
Rho-A	ras homolog family member A
RISC	RNA-induced silencing complex
RUNX3	runt-related transcription factor 3
SAM	S-adenosylmethionine synthase
SCUBE 2	Signal Peptide, CUB Domain And EGF Like Domain Containing 2
SNCG	Synuclein Gamma
SOCS1	Suppressor of Cytokine Signaling 1
STAT1	Signal transducer and activator of transcription 1
STX11	syntaxin 11
TET1	Ten-eleven translocation methylcytosine dioxygenase 1
TNBC	Triple-negative breast cancer
TNFSF12	Tumor necrosis factor ligand superfamily member 12
TRBP	transactivation response element RNA-binding protein
TERT	Telomerase Reverse Transcriptase
VGF	VGF nerve growth factor inducible

Frontiers in Pharmacology

Explores the interactions between chemicals and living beings

The most cited journal in its field, which advances access to pharmacological discoveries to prevent and treat human disease.

Discover the latest Research Topics

See more →

Frontiers

Avenue du Tribunal-Fédéral 34
1005 Lausanne, Switzerland
frontiersin.org

Contact us

+41 (0)21 510 17 00
frontiersin.org/about/contact